



biomolecules

Mitochondrial Transport Proteins

Edited by

Ferdinando Palmieri

Printed Edition of the Special Issue Published in *Biomolecules*

Mitochondrial Transport Proteins

Mitochondrial Transport Proteins

Editor

Ferdinando Palmieri

MDPI • Basel • Beijing • Wuhan • Barcelona • Belgrade • Manchester • Tokyo • Cluj • Tianjin



Editor

Ferdinando Palmieri
Campus universitario
University of Bari
Bari
Italy

Editorial Office

MDPI
St. Alban-Anlage 66
4052 Basel, Switzerland

This is a reprint of articles from the Special Issue published online in the open access journal *Biomolecules* (ISSN 2218-273X) (available at: www.mdpi.com/journal/biomolecules/special_issues/mitochondrial_transport_protein).

For citation purposes, cite each article independently as indicated on the article page online and as indicated below:

LastName, A.A.; LastName, B.B.; LastName, C.C. Article Title. <i>Journal Name</i> Year , Volume Number, Page Range.

ISBN 978-3-0365-3410-7 (Hbk)

ISBN 978-3-0365-3409-1 (PDF)

© 2022 by the authors. Articles in this book are Open Access and distributed under the Creative Commons Attribution (CC BY) license, which allows users to download, copy and build upon published articles, as long as the author and publisher are properly credited, which ensures maximum dissemination and a wider impact of our publications.

The book as a whole is distributed by MDPI under the terms and conditions of the Creative Commons license CC BY-NC-ND.

Contents

Cecilia Jimenez-Sánchez, Thierry Brun and Pierre Maechler Mitochondrial Carriers Regulating Insulin Secretion Profiled in Human Islets upon Metabolic Stress Reprinted from: <i>Biomolecules</i> 2020 , <i>10</i> , 1543, doi:10.3390/biom10111543	1
Alberto Leguina-Ruzzi, Anežka Vodičková, Blanka Holendová, Vojtěch Pavluch, Jan Tauber and Hana Engstová et al. Glucose-Induced Expression of DAPIT in Pancreatic β -Cells Reprinted from: <i>Biomolecules</i> 2020 , <i>10</i> , 1026, doi:10.3390/biom10071026	23
Konstantin N. Belosludtsev, Mikhail V. Dubinin, Eugeny Yu. Talanov, Vlada S. Starinets, Kirill S. Tenkov and Nadezhda M. Zakharova et al. Transport of Ca^{2+} and Ca^{2+} -Dependent Permeability Transition in the Liver and Heart Mitochondria of Rats with Different Tolerance to Acute Hypoxia Reprinted from: <i>Biomolecules</i> 2020 , <i>10</i> , 114, doi:10.3390/biom10010114	47
Yevheniia Kravenska, Vanessa Checchetto and Ildiko Szabo Routes for Potassium Ions across Mitochondrial Membranes: A Biophysical Point of View with Special Focus on the ATP-Sensitive K^+ Channel Reprinted from: <i>Biomolecules</i> 2021 , <i>11</i> , 1172, doi:10.3390/biom11081172	61
Mathias Ziegler, Magnus Monné, Andrey Nikiforov, Gennaro Agrimi, Ines Heiland and Ferdinando Palmieri Welcome to the Family: Identification of the NAD^+ Transporter of Animal Mitochondria as Member of the Solute Carrier Family SLC25 Reprinted from: <i>Biomolecules</i> 2021 , <i>11</i> , 880, doi:10.3390/biom11060880	79
Giorgia Pallafacchina, Sofia Zanin and Rosario Rizzuto From the Identification to the Dissection of the Physiological Role of the Mitochondrial Calcium Uniporter: An Ongoing Story Reprinted from: <i>Biomolecules</i> 2021 , <i>11</i> , 786, doi:10.3390/biom11060786	95
Annamaria Tonazzi, Nicola Giangregorio, Lara Console, Ferdinando Palmieri and Cesare Indiveri The Mitochondrial Carnitine Acyl-carnitine Carrier (SLC25A20): Molecular Mechanisms of Transport, Role in Redox Sensing and Interaction with Drugs Reprinted from: <i>Biomolecules</i> 2021 , <i>11</i> , 521, doi:10.3390/biom11040521	119
Rami Mosaoa, Anna Kasprzyk-Pawelec, Harvey R. Fernandez and Maria Laura Avantaggiati The Mitochondrial Citrate Carrier SLC25A1/CIC and the Fundamental Role of Citrate in Cancer, Inflammation and Beyond Reprinted from: <i>Biomolecules</i> 2021 , <i>11</i> , 141, doi:10.3390/biom11020141	139
Vito De Pinto Renaissance of VDAC: New Insights on a Protein Family at the Interface between Mitochondria and Cytosol Reprinted from: <i>Biomolecules</i> 2021 , <i>11</i> , 107, doi:10.3390/biom11010107	157
Gergely Gyimesi and Matthias A. Hediger Sequence Features of Mitochondrial Transporter Protein Families Reprinted from: <i>Biomolecules</i> 2020 , <i>10</i> , 1611, doi:10.3390/biom10121611	169

Varda Shoshan-Barmatz, Anna Shteinfer-Kuzmine and Ankit Verma VDAC1 at the Intersection of Cell Metabolism, Apoptosis, and Diseases Reprinted from: <i>Biomolecules</i> 2020 , <i>10</i> , 1485, doi:10.3390/biom10111485	187
Adriano Nunes-Nesi, João Henrique F. Cavalcanti and Alisdair R. Fernie Characterization of In Vivo Function(s) of Members of the Plant Mitochondrial Carrier Family Reprinted from: <i>Biomolecules</i> 2020 , <i>10</i> , 1226, doi:10.3390/biom10091226	227
Antoni Wrzosek, Bartłomiej Augustynek, Monika Żochowska and Adam Szewczyk Mitochondrial Potassium Channels as Druggable Targets Reprinted from: <i>Biomolecules</i> 2020 , <i>10</i> , 1200, doi:10.3390/biom10081200	247
Ian Max Møller, R. Shyama Prasad Rao, Yuexu Jiang, Jay J. Thelen and Dong Xu Proteomic and Bioinformatic Profiling of Transporters in Higher Plant Mitochondria Reprinted from: <i>Biomolecules</i> 2020 , <i>10</i> , 1190, doi:10.3390/biom10081190	267
Anastasija Plett, Lennart Charton and Nicole Linka Peroxisomal Cofactor Transport Reprinted from: <i>Biomolecules</i> 2020 , <i>10</i> , 1174, doi:10.3390/biom10081174	281
Jane L. Buchanan and Eric B. Taylor Mitochondrial Pyruvate Carrier Function in Health and Disease across the Lifespan Reprinted from: <i>Biomolecules</i> 2020 , <i>10</i> , 1162, doi:10.3390/biom10081162	297
Youjun Zhang and Alisdair R. Fernie On the Detection and Functional Significance of the Protein–Protein Interactions of Mitochondrial Transport Proteins Reprinted from: <i>Biomolecules</i> 2020 , <i>10</i> , 1107, doi:10.3390/biom10081107	317
Takeyori Saheki, Mitsuaki Moriyama, Aki Funahashi and Eishi Kuroda AGC2 (Citrin) Deficiency—From Recognition of the Disease till Construction of Therapeutic Procedures Reprinted from: <i>Biomolecules</i> 2020 , <i>10</i> , 1100, doi:10.3390/biom10081100	337
Joséphine Zangari, Francesco Petrelli, Benoît Maillot and Jean-Claude Martinou The Multifaceted Pyruvate Metabolism: Role of the Mitochondrial Pyruvate Carrier Reprinted from: <i>Biomolecules</i> 2020 , <i>10</i> , 1068, doi:10.3390/biom10071068	355
Alisdair R. Fernie, João Henrique F. Cavalcanti and Adriano Nunes-Nesi Metabolic Roles of Plant Mitochondrial Carriers Reprinted from: <i>Biomolecules</i> 2020 , <i>10</i> , 1013, doi:10.3390/biom10071013	373
Patrick Horten, Lilia Colina-Tenorio and Heike Rampelt Biogenesis of Mitochondrial Metabolite Carriers Reprinted from: <i>Biomolecules</i> 2020 , <i>10</i> , 1008, doi:10.3390/biom10071008	397
Massimo Bonora, Simone Patergnani, Daniela Ramaccini, Giampaolo Morciano, Gaia Pedriali and Asrat Endrias Kahsay et al. Physiopathology of the Permeability Transition Pore: Molecular Mechanisms in Human Pathology Reprinted from: <i>Biomolecules</i> 2020 , <i>10</i> , 998, doi:10.3390/biom10070998	411
Ferdinando Palmieri, Pasquale Scarcia and Magnus Monné Diseases Caused by Mutations in Mitochondrial Carrier Genes <i>SLC25</i> : A Review Reprinted from: <i>Biomolecules</i> 2020 , <i>10</i> , 655, doi:10.3390/biom10040655	437



Article

Mitochondrial Carriers Regulating Insulin Secretion Profiled in Human Islets upon Metabolic Stress

Cecilia Jimenez-Sánchez, Thierry Brun and Pierre Maechler *

Department of Cell Physiology and Metabolism & Faculty Diabetes Center, University of Geneva Medical Center, 1206 Geneva, Switzerland; Cecilia.Jimenez-Sanchez@unige.ch (C.J.-S.); thierry.brun@unige.ch (T.B.)

* Correspondence: pierre.maechler@unige.ch

Received: 31 July 2020; Accepted: 10 November 2020; Published: 12 November 2020

Abstract: Chronic exposure of β -cells to nutrient-rich metabolic stress impairs mitochondrial metabolism and its coupling to insulin secretion. We exposed isolated human islets to different metabolic stresses for 3 days: 0.4 mM oleate or 0.4 mM palmitate at physiological 5.5 mM glucose (lipotoxicity), high 25 mM glucose (glucotoxicity), and high 25 mM glucose combined with 0.4 mM oleate and/or palmitate (glucolipotoxicity). Then, we profiled the mitochondrial carriers and associated genes with RNA-Seq. Diabetogenic conditions, and in particular glucotoxicity, increased expression of several mitochondrial solute carriers in human islets, such as the malate carrier DIC, the α -ketoglutarate-malate exchanger OGC, and the glutamate carrier GC1. Glucotoxicity also induced a general upregulation of the electron transport chain machinery, while palmitate largely counteracted this effect. Expression of different components of the TOM/TIM mitochondrial protein import system was increased by glucotoxicity, whereas glucolipotoxicity strongly upregulated its receptor subunit TOM70. Expression of the mitochondrial calcium uniporter MCU was essentially preserved by metabolic stresses. However, glucotoxicity altered expression of regulatory elements of calcium influx as well as the $\text{Na}^+/\text{Ca}^{2+}$ exchanger NCLX, which mediates calcium efflux. Overall, the expression profile of mitochondrial carriers and associated genes was modified by the different metabolic stresses exhibiting nutrient-specific signatures.

Keywords: pancreatic islets; β -cell; mitochondria; diabetes; glucotoxicity; glucolipotoxicity; lipotoxicity

1. Introduction

Pancreatic β -cells secrete insulin in response to the elevation of circulating glucose, thereby maintaining euglycemia. Once in the β -cell, glucose is processed through glycolysis and the thus formed pyruvate enters the mitochondria where it is transformed into intracellular signals leading to the stimulation of insulin exocytosis. This metabolism–secretion coupling requires efficient mitochondrial metabolism, primarily implicating pyruvate import and ATP production. The latter induces cell membrane depolarization that promotes a rise in cytosolic Ca^{2+} concentration (Figure 1). Elevation of cytosolic Ca^{2+} is rapidly transferred into mitochondria, which results in further activation of mitochondrial metabolism. While cytosolic Ca^{2+} is an obligatory signal, this ion is not sufficient to promote the full secretory response. Accordingly, metabolism in general and mitochondria in particular produce additive factors, which participate in the amplifying pathway of the Ca^{2+} signal [1]. Collectively, these mechanisms require optimal function of the mitochondrial components, i.e., the solute carriers of various metabolites and associated enzymes, the electron transport chain machinery, the TOM/TIM mitochondrial protein import system, and proteins for iron and calcium homeostasis.

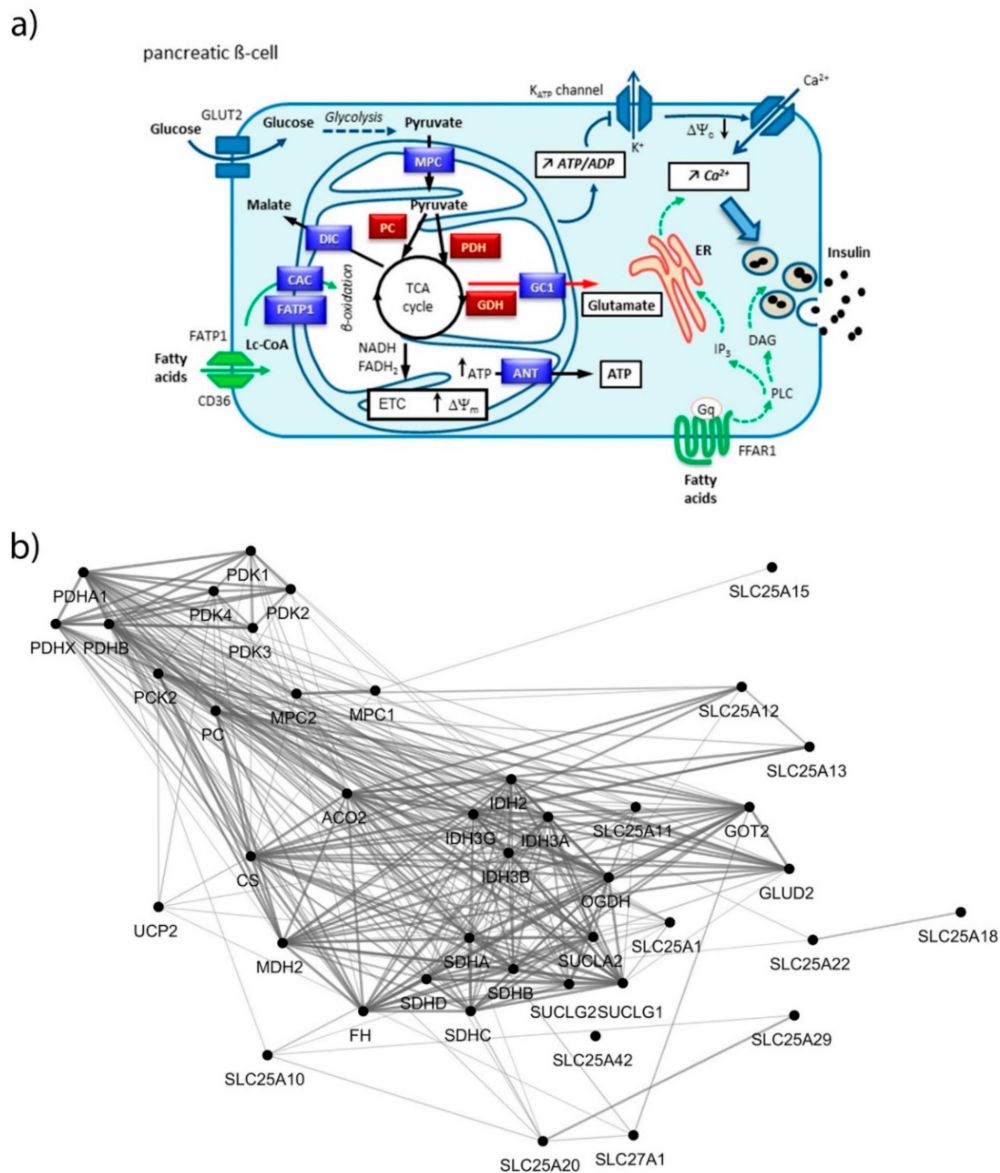


Figure 1. (a) Coupling of glucose metabolism with insulin secretion in pancreatic β -cell. Glucose is metabolized through glycolysis that produces pyruvate. Pyruvate enters into mitochondria through the mitochondrial pyruvate carrier (MPC) and fuels the TCA cycle by the action of both pyruvate carboxylase (PC) and pyruvate dehydrogenase (PDH). The TCA cycle generates reducing equivalents transferred by NADH and FADH₂ to the electron transport chain (ETC), leading to the hyperpolarization of the mitochondrial membrane ($\Delta\Psi_m$) and generation of ATP. Then, ANT transfers ATP to the cytosol, raising the ATP/ADP ratio that induces the closure of the K-ATP channels promoting plasma membrane depolarization ($\Delta\Psi_c$). This opens voltage sensitive Ca²⁺ channels, increasing cytosolic Ca²⁺ concentration ([Ca²⁺]_c), which triggers insulin exocytosis (triggering pathway, blue arrows). The amplifying pathway of metabolism–secretion coupling is contributed to by additive coupling factors, e.g., glutamate produced by glutamate dehydrogenase (GDH) and transported by GC1 (red arrow). Free fatty acids potentiate glucose-stimulated insulin secretion through long-chain acyl-coenzyme A (Lc-CoA), glycerolipid/free fatty acid cycle (not shown), import into mitochondria through the fatty acid transport protein (FATP1) and the carnitine/acylcarnitine carrier (CAC), β -oxidation; or through FFAR1 signaling (green arrows). G α_q activates phospholipase C (PLC) producing both inositol trisphosphate (IP₃), which triggers calcium release from the endoplasmic reticulum (ER) stores, and raises diacylglycerol (DAG), an activator of the phosphokinase C (PKC) involved in insulin exocytosis. (b) Functional interaction network of mitochondrial metabolite carriers and associated genes, i.e., pyruvate metabolism, TCA cycle, amino acid metabolism and fatty acid transport. Nodes were connected using the STRING interaction knowledgebase with a confidence score > 0.4.

Using RNA-Seq analysis on isolated human islets, we have delineated the changes of such mitochondrial components following chronic exposure to different metabolic stresses hypothesized to participate to the etiology of type 2 diabetes, i.e., glucotoxicity, lipotoxicity, and glucolipotoxicity. This profiling, evaluated in light of previous studies, uncovered specific signatures of the different nutrients.

2. Materials and Methods

2.1. Reagents

Culture media, D-glucose, fatty acids, and other basic reagents were obtained from Sigma-Aldrich (St. Louis, MO, USA).

2.2. Human Islets and Treatments

Human islets were isolated from pancreases of deceased multiorgan donors ($n = 8$), who had provided written informed consent (ECIT consortium, <http://ecit.dri-sanraffaele.org/>, 2009). None of the donors were diagnosed with diabetes nor metabolic syndrome (clinical data are provided in Supplementary Table S1). Donors had an average BMI of 25.5 ± 2.2 kg/m² and were aged 51.5 ± 7.6 years. Islets were maintained for a standard recovery period of time (between 1 to 4 days) in CMRL-1066 medium containing 5.5 mM glucose supplemented with 10% (vol./vol.) fetal calf serum and used for experiments straight away without shipping maneuver (isolation and experiments being performed in the same institution at the Hôpitaux Universitaires de Genève, Switzerland). Isolated islets were hand-picked, washed twice and further maintained for 3 days at physiological 5.5 mM glucose (G5.5 control) with either 0.4 mM oleate (unsaturated fatty acid C18:1, Olea) or 0.4 mM palmitate (saturated fatty acid C16:0, Palm). Islets were also exposed to high 25 mM glucose (G25) with 0.4 mM oleate (G25 + Olea), 0.4 mM palmitate (G25 + Palm), or the combination of both fatty acids at 0.4 mM (G25+Olea+Palm, 0.2 mM each); all conditions with 0.5% BSA in the culture medium [2]. Stock solutions of fatty acids were adjusted to 8 mM in 11% fatty acid-free BSA solution, without organic solvent, and stored at -20 °C as previously described [3]. This resulted in the addition of 0.55% BSA in the culture media supplemented with the tested fatty acids. The physiological 5.5 mM glucose in CMRL-1066 medium served as control. The different treatments were systematically performed in parallel cultures. Islet batches from different donors were used for transcript quantification using different techniques, those corresponding to donors #1–5 were used for RNA-Seq analyses, those of donors #1, 2, 4, 6–8 were used for quantitative RT-PCR, while those of donors #1, 2, and 6 were used for previously published NanoString[®] (nCounter system, Seattle, WA, USA) technology analysis [4]; see Supplementary Table S1.

2.3. RNA-Sequencing

Total RNA was extracted from cultured isolated human islets with Trizol reagent (Invitrogen, Carlsbad, CA, USA) [4]. RNA sequencing was performed in Susanne Mandrup's laboratory (University of Southern Denmark, Odense, Denmark) as detailed previously [2,5]. Accession numbers for each transcript in NCBI reference sequence format are provided in Supplementary Tables S2–S6.

2.4. Quantitative RT-PCR

An amount of 2 µg of isolated RNA was converted into cDNA as previously described [6]. Primers for SLC25A10, SLC25A11, SLC25A22, SLC8B1, TIMM13, and cyclophilin A (PPIA) were designed using the Primer Express Software (Applied Biosystems, Rotkreutz, Switzerland); see list of primers in Supplementary Table S7. Quantitative RT-PCR was performed for human islets from donors #1, #2, #4, #6, #7, #8 using a StepOnePlus[™] Real-Time PCR system (Thermo Fisher Scientific, Waltham, MA, USA). PCR products were quantified fluorometrically using the SYBR Green Master kit (Roche,

Mannheim, Germany). Experiments were performed in duplicate for each transcript, and mean values were normalized to those of the reference mRNA cyclophilin A (PPIA).

2.5. Network Analysis

We selected specific human genes with a direct or indirect role in mitochondrial transport for network analysis (full transcriptome data not shown). Functional interaction networks were built using stringApp (v 1.4.2) in Cytoscape (v 3.6.1), which includes both physical interactions from experimental data and functional associations from curated pathways, automatic text mining, and prediction methods; with a confidence score cutoff of 0.4 [7]. Finally, transcriptomic data were assembled into a functional network using Omics Visualizer (v 1.3.0) in Cytoscape (3.8.1) [8]. To avoid inference of interdependence between gene expression levels and their functional links, the edges from the networks including transcriptomic data were removed.

2.6. Statistical Analysis

Significant changes were considered when two or more independent islet batches (donors) exhibited down or upregulation with a \log_2 fold change (\log_2 FC) threshold of 0.5 associated with at least one or more adjusted $p < 0.05$; highlighted in bold in the figures. For quantitative RT-PCR results, a mixed model approach for repeated measures was applied with a significance threshold of 0.05.

3. Results

Exposure of β -cells to chronic fuel surfeit triggers adaptive responses to cope with the increased insulin demand and also as a protective mechanism. When the adaptive mechanism fails, toxicity occurs with nutrient surplus, leading to β -cell dysfunction, dedifferentiation, and ultimately cell death. Although still debated, the terms lipotoxicity, glucotoxicity, and glucolipotoxicity are used to describe potentially nutrient-rich toxic conditions responsible for those pathogenic mechanisms in the context of type-2 diabetes. Of note, these terms may not only include potential toxic effects of nutrient excess, but also the beneficial adaptive mechanisms resulting from these conditions [9]. In previous reports, we characterized mitochondrion-associated genes in INS-1E β -cells using TaqMan Micro Fluidic Cards RT-PCR system (Thermo Fisher Scientific, Waltham, MA, USA) [10] and in human islets using NanoString[®] targeted transcriptomic technology [4], revealing stress-specific signatures in response to chronic exposure to high glucose or fatty acids. Based on these studies and using an untargeted transcriptomic technology (RNA-Seq), we are now reporting the expression profile of mitochondrion transport-associated genes in response to specific metabolic stresses, i.e., to high glucose or fatty acids and also to their combination. This *in vitro* approach aims at mimicking, respectively, glucotoxic, lipotoxic, and glucolipotoxic conditions, potentially uncovering the specific contributions of the different stressors. We previously reported that such treatments induce marginal caspase-3 cleavage and essentially preserve β -cell differentiation, documented through the expression of the transcription factor IPF-1 [11]. Here, we provide a snapshot of the regulation of the mitochondrial carriers and associated genes from a whole-transcriptome data set (full data set not shown). We delineated a functional interaction network of selected genes using the STRING knowledgebase [7,12] (Figure 1b and Supplementary Figure S1). In particular, we selected mitochondrial metabolite carriers and associated genes involved in pyruvate metabolism, the tricarboxylic acid (TCA) cycle, amino acid metabolism and fatty acid transport; in the electron transport chain and related carriers; in the outer and inner mitochondrial membrane translocases TOM/TIM; in iron transport; and in calcium transport. Then, transcriptomic data were added into the functional gene network for visualization of each islet batch corresponding to the individual donors #1–5 (Figures 2–5, Supplementary Figures S2 and S3, Supplementary Tables S2–S6). The main changes are summarized in Figure 7.

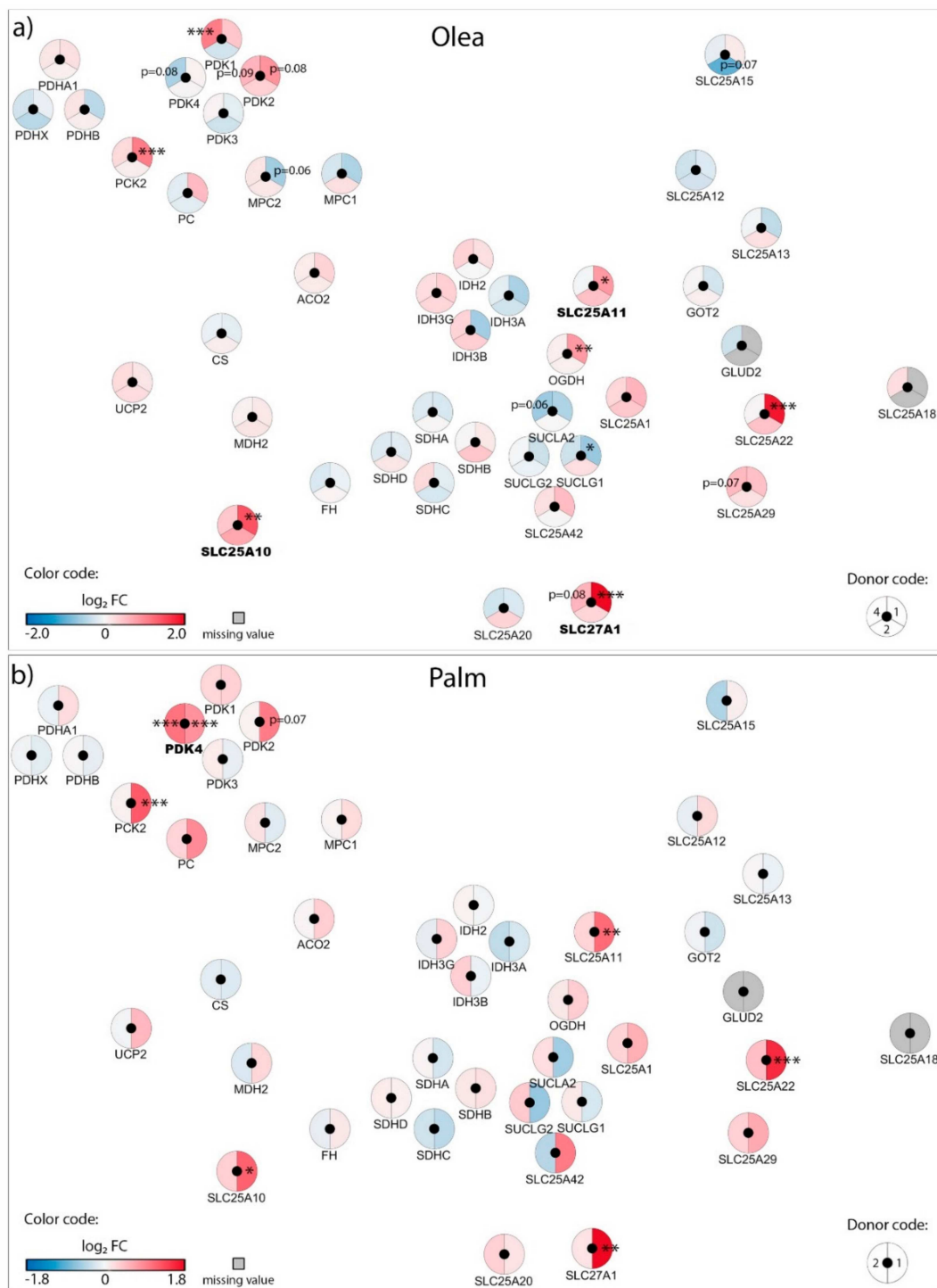


Figure 2. Effects of oleate (Olea) and palmitate (Palm) on the transcriptional regulation of mitochondrial solute carriers and associated genes: pyruvate metabolism, TCA cycle enzymes, amino acid metabolism and fatty acid transport. Human islets were exposed to 0.4 mM (a) Olea or (b) Palm at standard glucose concentration (G5.5) for 3 days before RNA-Seq analysis. Effects of lipotoxic culture conditions on transcript levels are compared to standard G5.5 medium and shown as upregulated (red), downregulated (blue), or unchanged (white). Missing values are represented in grey. Each disk is split into individual changes for the different islet donors. Color code reflects the transcriptional changes in \log_2 fold changes ($\log_2 FC$) for that particular gene in individual donors. Clinical data from individual donors are shown in Supplementary Table S1, while quantitative transcriptional data are shown in Supplementary Table S2. * adjusted $p < 0.05$, ** adjusted $p < 0.01$, *** adjusted $p < 0.001$ between control 5.5 mM glucose and the specific culture condition.

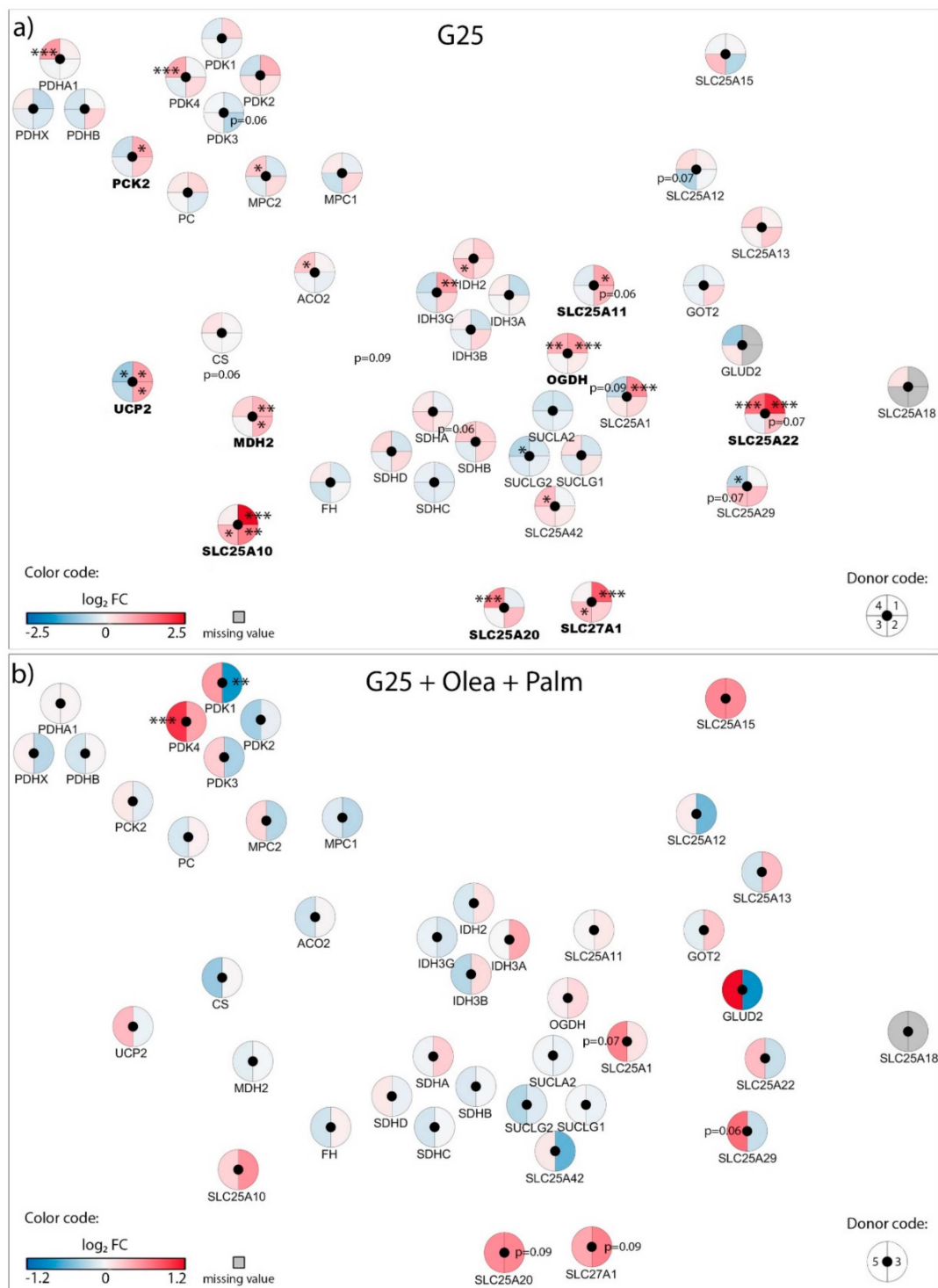


Figure 3. Effects of high 25 mM glucose (G25) and G25 plus 0.4 mM oleate and palmitate (G25 + Olea + Palm) on the transcriptional regulation of mitochondrial solute carriers and associated genes. Human islets were exposed to (a) G25 glucotoxic condition or (b) G25 + Olea + Palm glucolipotoxic condition for 3 days before RNA-Seq analysis. Effects of culture conditions on transcript levels are compared to standard G5.5 medium and shown as upregulated (red), downregulated (blue), or unchanged (white). Missing values are represented in grey. Each disk is split into individual changes for the different donors. Color code reflects the transcriptional changes in \log_2 fold changes ($\log_2 FC$) for that particular gene in individual donors. Clinical data from individual donors are shown in Supplementary Table S1, while quantitative transcriptional data are shown in Supplementary Table S2. * adjusted $p < 0.05$, ** adjusted $p < 0.01$, *** adjusted $p < 0.001$ between control 5.5 mM glucose and the specific culture condition.

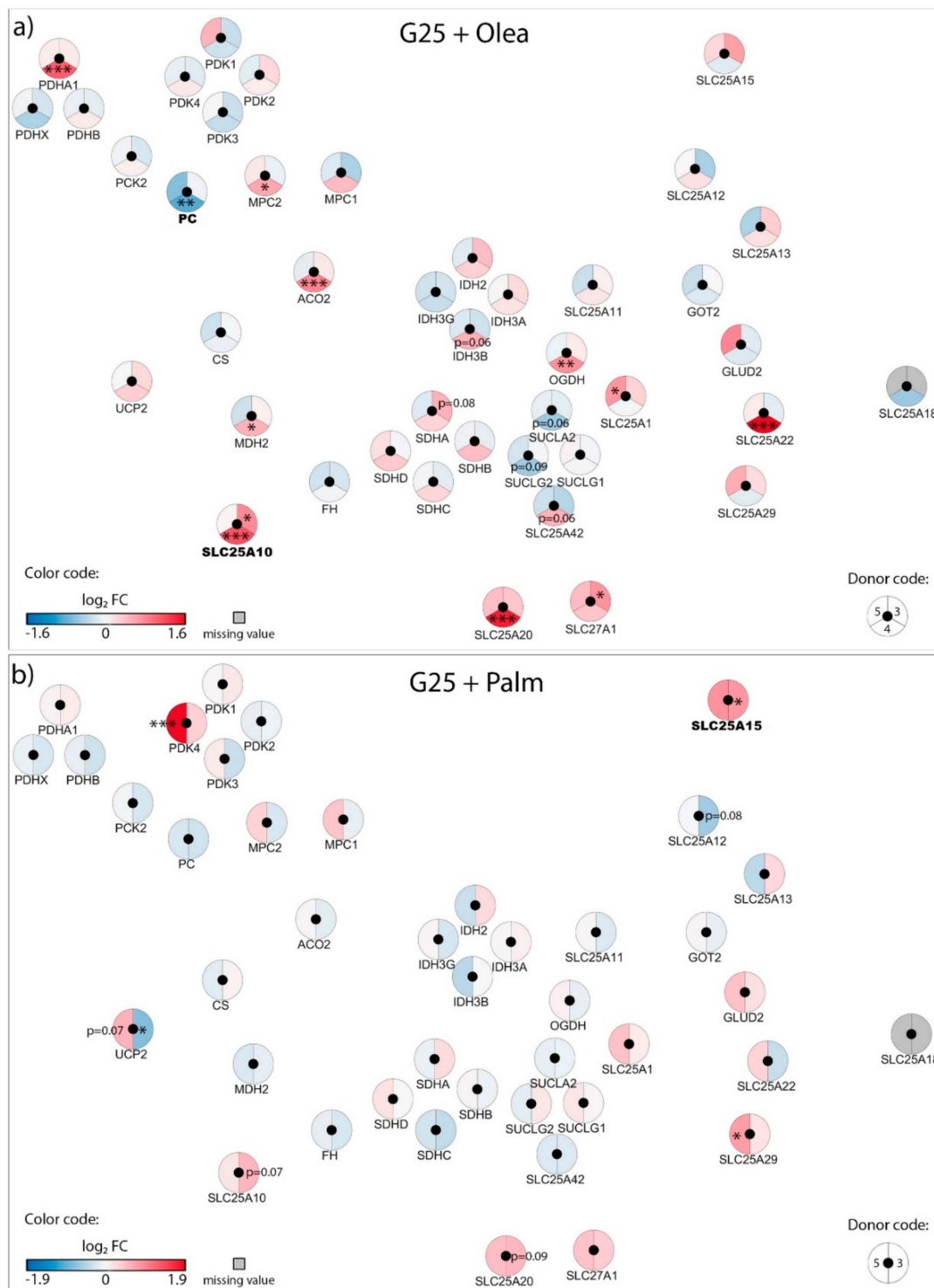


Figure 4. Effects of high 25 mM glucose (G25) plus 0.4 mM oleate (G25 + Olea) or palmitate (G25 + Palm) on the transcriptional regulation of mitochondrial solute carriers and associated genes. Human islets were exposed to (a) G25 + Olea or (b) G25 + Palm glucolipotoxic conditions for 3 days before RNA-Seq analysis. Effects of culture conditions on transcript levels are compared to standard G5.5 medium and shown as upregulated (red), downregulated (blue), or unchanged (white). Missing values are represented in grey. Each disk is split into individual changes for the different donors. Color code reflects the transcriptional changes in \log_2 fold changes ($\log_2 FC$) for that particular gene in individual donors. Clinical data from individual donors are shown in Supplementary Table S1, while quantitative transcriptional data are shown in Supplementary Table S2. * adjusted $p < 0.05$, ** adjusted $p < 0.01$, *** adjusted $p < 0.001$ between control 5.5 mM glucose and the specific culture condition.

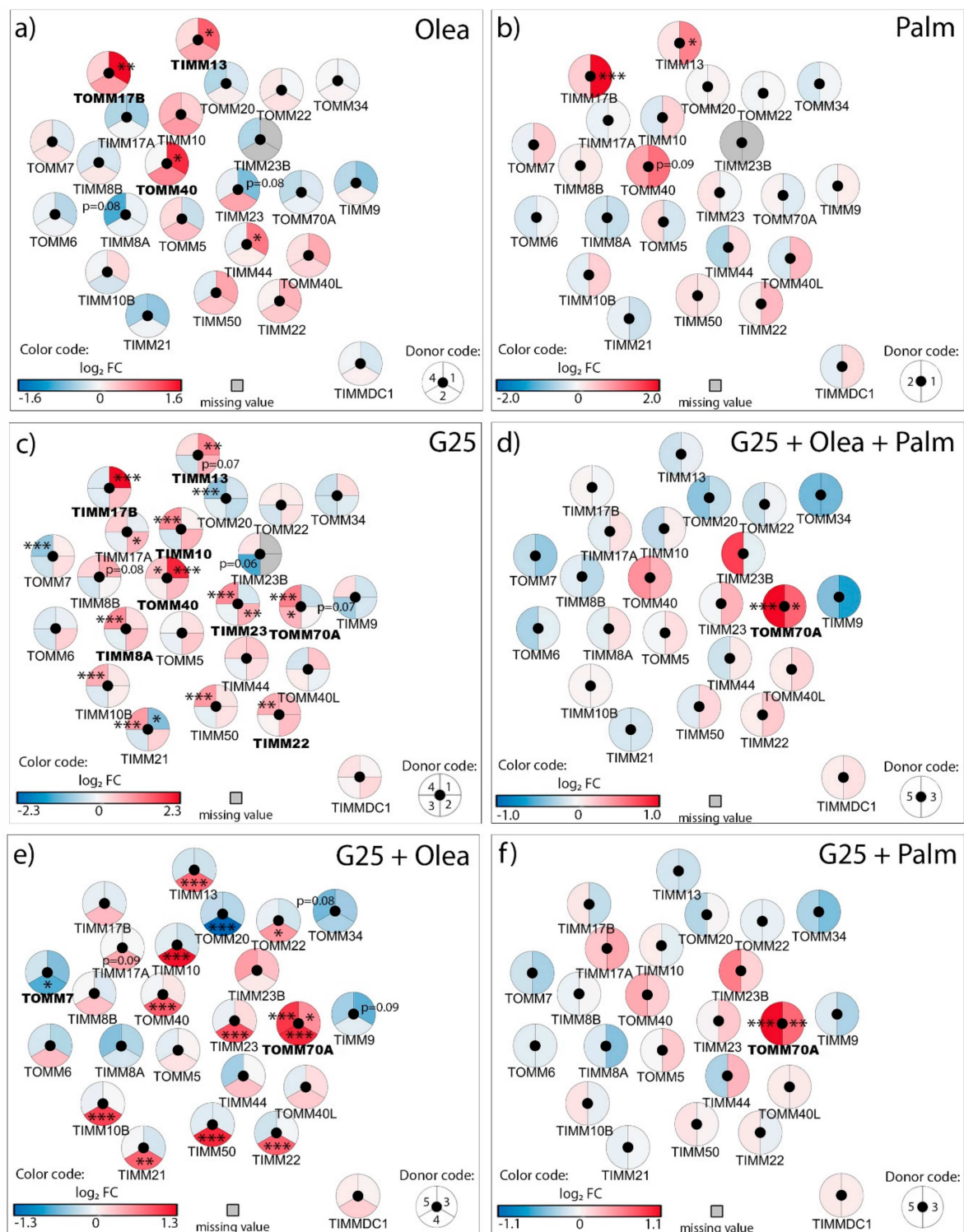


Figure 5. Effects of high 25 mM glucose (G25) and 0.4 mM oleate (Olea) or palmitate (Palm) on the transcriptional regulation of the outer and inner mitochondrial membrane translocases TOM/TIM. Human islets were exposed to (a) Olea at G5.5, (b) Palm at G5.5, (c) G25, (d) G25 + Olea + Palm, (e) G25 + Olea, and (f) G25 + Palm for 3 days before RNA-Seq analysis. Effects of culture conditions on transcript levels are compared to standard G5.5 medium and shown as upregulated (red), downregulated (blue), or unchanged (white). Missing values are represented in grey. Each disk is split into individual changes for the different donors. Color code reflects the transcriptional changes in \log_2 fold changes ($\log_2 FC$) for that particular gene in individual donors. * adjusted $p < 0.05$, ** adjusted $p < 0.01$, *** adjusted $p < 0.001$ between control 5.5 mM glucose and the specific culture condition.

In order to compare alternative technologies commonly used for the assessment of mRNA levels, we measured some genes of interest with qRT-PCR (Supplementary Figure S4). This was performed on some of the islet batches used for the present RNA-Seq analysis (donors #1, #2, #4) and also on additional independent islet batches (donors #6–8). In addition to RNA-Seq and qRT-PCR, NanoString® targeted transcriptomic technology was previously applied for delineation of mitochondrial transcriptome using material extracted from shared islet batches (donors #1, #2, #6); see Supplementary Table S1 and [4]. Collectively, this cross-comparison reveals important differences regarding relative mRNA levels, in particular for RNA-Seq versus qRT-PCR data. The latter requires amplification of a target sequence and use of an internal control, which confer limitations when measurements are performed on samples of various origins, such as islets isolated from different donors and not pooled for experimental in vitro treatments. This approach also shows that changes in gene expression in isolated human islets are highly batch specific.

3.1. Adaptation of Mitochondrial Solute Carriers Responsible for Metabolite Transport

Chronic effects of nutrient-rich metabolic stresses on mitochondrial carriers involved in the transport of pyruvate, TCA cycle intermediates, amino acids, fatty acids and associated genes were determined in isolated human islets at the end of a three-day exposure to the different diabetogenic milieus using RNA-Seq (Figures 2–4, Supplementary Table S2).

In human islets cultured with physiological glucose G5.5, neither oleate nor palmitate modified expression of the pyruvate carrier (*MPC1* and *MPC2*) and the pyruvate dehydrogenase complex (*PDH*), see Figure 2a,b. However, treatment of islets with palmitate at G5.5 for 3 days increased the pyruvate dehydrogenase kinase 4 (*PDK4*) mRNA levels (Figure 2b), while a similar trend was observed for *PDK1* with oleate (Figure 2a). Oleate upregulated the dicarboxylate/malate carrier DIC (*SLC25A10*), the 2-oxoglutarate/malate carrier OGC (*SLC25A11*), and the fatty acid transport protein FATP1 (*SLC27A1*); while palmitate exhibited a similar pattern (Figure 2a,b), as observed previously using microarray analysis [13]. Quantitative RT-PCR analyses were performed on shared islet batches (donors #1, #2, and #4) as well as on additional batches (donors #6–8) for *SLC25A10*, *SLC25A11*, and *SLC25A22* (Supplementary Figure S4); confirming that variations in transcript levels are batch-specific. Overall, chronic exposure of islets to palmitate and oleate induced limited changes in the expression of genes of the mitochondrial solute carrier family.

High glucose (G25) increased expression of pyruvate dehydrogenase E1 subunit alpha 1 (*PDHA1*), pyruvate dehydrogenase kinase 4 (*PDK4*), and the pyruvate carrier (*MPC2*) in only one donor out of four (Figure 3a), suggesting that mitochondrial pyruvate handling should be preserved in these conditions. However, high glucose consistently upregulated the expression of the malate carrier DIC (*SLC25A10*), the 2-oxoglutarate/malate carrier OGC (*SLC25A11*), and the glutamate carrier GC1 (*SLC25A22*), along with the associated enzymes malate dehydrogenase 2 (*MDH2*) and 2-oxoglutarate dehydrogenase (*OGDH*). Of note, the uncoupling protein 2 (*UCP2*) was diversely modified in the different donors (Figure 3a). G25 also increased expression of the fatty acid transport protein FATP1 (*SLC27A1*) and the carnitine/acylcarnitine carrier CAC (*SLC25A20*). Such a profile suggests that glucotoxic conditions induce important mitochondrial anaplerotic/cataplerotic and NADPH-generating shuttle activities, as well as increased fatty acid import into mitochondria.

Regarding the glucolipotoxic conditions, expression of *PDK4* was unchanged at G25 plus oleate (Figure 4a), although significantly upregulated in one donor at G25 plus palmitate (Figure 4b) as well as G25 plus both saturated and unsaturated fatty acids (Figure 3b). This points to palmitate having a specific effect on *PDK4* expression, consistent with the increase in *PDK4* we observed with palmitate alone at standard G5.5 (Figure 2a). Similar to G25 alone, G25 plus oleate upregulated the malate carrier DIC (*SLC25A10*) (Figure 4a). However, palmitate at G25, even combined with oleate, restored expression of DIC (*SLC25A10*) to nearly control levels (Figures 3b and 4b, respectively). The expression of enzymes participating in the TCA cycle was marginally affected by glucolipotoxic conditions (Figures 3b and 4a,b). Overall, chronic exposure of islets to high glucose plus palmitate and

oleate induced moderate changes in the expression of genes of the mitochondrial solute carrier family, although exhibiting specific fatty acid signatures.

3.2. Adaptation of the Electron Transport Chain Machinery

Chronic effects of metabolic stress on the electron transport chain (ETC) machinery were then investigated in human islets at the end of the three-day exposure to the different diabetogenic milieus using RNA-Seq (Supplementary Figure S2, Supplementary Table S3). Treatment of islets with oleate at G5.5 for 3 days increased expression of the nuclear-encoded respiratory chain subunits of complex I (*NDUFS7*, *NDUFB7*, *NDUFS8*) and complex IV (*COX8A*, *COX5B*). Palmitate treatment, while inducing a similar trend, significantly upregulated complex V (*ATP5D*, *ATP5G1*). Expression of the phosphate carrier PiC (*SLC25A3*), the ADP/ATP translocases ANT1 and ANT2 (*SLC25A4* and *SLC25A5*) and the uncoupling proteins (*UCP2*, *SLC25A27* and *SLC25A14*) was preserved (Supplementary Figure S2a,b).

With respect to the other stressors, high glucose by itself caused the strongest expression changes in mitochondrial ETC subunits, inducing upregulation of the nuclear-encoded subunits of complex I (*NDUFS7*, *NDUFS8*, *NDUFB2*, *NDUFB9*, *NDUFB10*), complex III (*UQCRCQ*, *UQCRC1*, *UQCRCFS1*, *UQCRC10*), complex IV (*COX5B*), complex V (*ATPIF1*, *ATP5J2*, *ATP5D*, *ATP5G1*), and downregulation of complex IV subunit (*COX7B*, *COX6C*), see Supplementary Figure S2c. High glucose also altered the expression of uncoupling proteins (*UCP2*, *SLC25A14*).

Addition of palmitate (alone or combined with oleate) at G25 elicited a general shift towards decreased expression of ETC subunits (Supplementary Figure S2d,f). This reduction in the overall G25 effect was less pronounced in the presence of oleate (Supplementary Figure S2e). In particular, islets from donor #4 exhibited strong changes in the expression of the different subunits of complexes I, III, IV and V, along with cytochrome C oxidase assembly components (Supplementary Figure S2e).

These results point to glucotoxic condition as the main effector for changes in the ETC machinery, while palmitate prevented most of the upregulations associated with high glucose.

3.3. Adaptation of the Translocases of the Outer and Inner Mitochondrial Membrane TOM/TIM

Next, we investigated mitochondrial membrane translocases responsible for preprotein import. Exposure of human islets to oleate, and to a lesser extent palmitate, at standard G5.5 for 3 days increased expression of the transmembrane channel of the outer membrane TOM complex *TOMM40*, the component of the intermembrane space TIM8–TIM13 complex *TIMM13*, and the component of the inner membrane TIM23 complex *TIMM17B* (Figure 5a,b; Supplementary Table S4).

Consistent with the changes observed in the ETC, high glucose caused the strongest transcriptional modifications in the translocases of the outer and inner mitochondrial membranes with respect to the other metabolic stresses. Similar to fatty acids at G5.5, G25 also per se upregulated *TOMM40*, *TIMM13*, and *TIMM17B*, while compared to fatty acids at G5.5 high glucose specifically upregulated the TOM70 receptor (*TOMM70A*) of the TOM complex, among other components of the inner membrane (*TIMM8A*, *TIMM10*, *TIMM22*, *TIMM23*), see Figure 5c. Some of the G25 effects were reinforced by the presence of fatty acids, in particular regarding the upregulation of the TOM70 receptor (Figure 5d–f). Complementary qRT-PCR analyses indicated that the upregulation of *TIMM13* by G25 is highly donor-dependent (Supplementary Figure S4). To our knowledge, this is the first description of transcriptional changes in the mitochondrial protein import machinery upon glucotoxic and lipotoxic conditions in pancreatic islets. Essentially, lipotoxicity and glucotoxicity increased expression of components of the outer membrane TOM complex, the intermembrane space TIM8–TIM13 complex and of the inner membrane TIM23 complex, while glucolipotoxicity strongly upregulated the *TOMM70A* receptor of the TOM complex.

3.4. Adaptation of the Mitochondrial Iron Transport

Iron is essential for mitochondrial redox activity through the heme synthesis pathway and, as a consequence, for the function of the ETC. Culture with oleate at G5.5 increased expression of the

translocator *TSPO* and the ATP-binding cassette MITOSUR (*ABCB8*), while palmitate exhibited a similar pattern but additionally repressed expression of frataxin (*FXN*), see Supplementary Figure S3a,b and Supplementary Table S5. Interestingly, disruption of the frataxin gene in mice causes the loss of β -cell mass and then diabetes [14]. Similar to fatty acids, high glucose increased expression of *TSPO* and *ABCB8*, as well as the carrier CGI-69 (*SLC25A39*), which was marginally upregulated by oleate and palmitate. These results suggest shared responses between lipotoxic and glucotoxic conditions (Supplementary Figure S3c). Combination of G25 with oleate showed upregulation of mitoferrin-2 (*SLC25A28*), see Supplementary Figure S3E. Conversely, apoptosin (*SLC25A38*) was downregulated by the presence of fatty acids at G25 (Supplementary Figure S3e,f). Of note, mitochondrial ferritin (*FTMT*) was not detected in any of the donors upon any conditions. Overall, mitochondrial iron transport components exhibited moderate responses with high inter-individual variability upon diabetogenic conditions.

3.5. Adaptation of the Mitochondrial Calcium Transport

The next group of mitochondrial components we analyzed mediates calcium transport across the mitochondrial membrane. At G5.5, neither oleate nor palmitate modified expression of the Ca^{2+} uniporter *MCU*, while both fatty acids exhibited a trend for increased expression of the essential MCU regulator *SMDT1* (Figure 6a,b), an effect significantly induced by G25 alone (Figure 6c, Supplementary Table S6). Interestingly, the combination of high glucose with fatty acids counteracted the upregulation of *SMDT1* observed with individual stressors (Figure 6d–f). Oleate and G25 by themselves decreased expression of the MCU regulatory partners *MICU3*, while the combination of both nutrient-rich conditions blunted such effects (Figure 6a,c–e). High glucose also upregulated the $\text{Na}^+/\text{Ca}^{2+}$ exchanger *NCLX* (*SLC8B1*) (Figure 6c), an effect not revealed by qRT-PCR (Supplementary Figure S4).

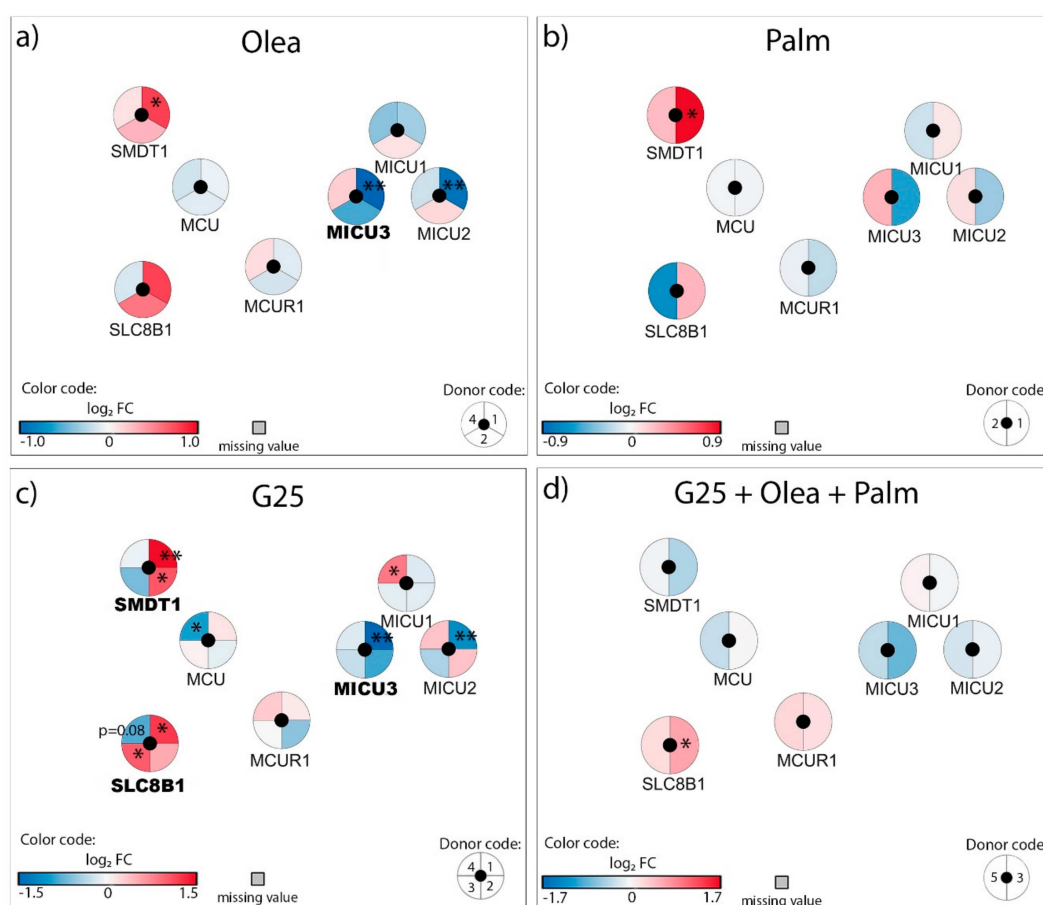


Figure 6. Cont.

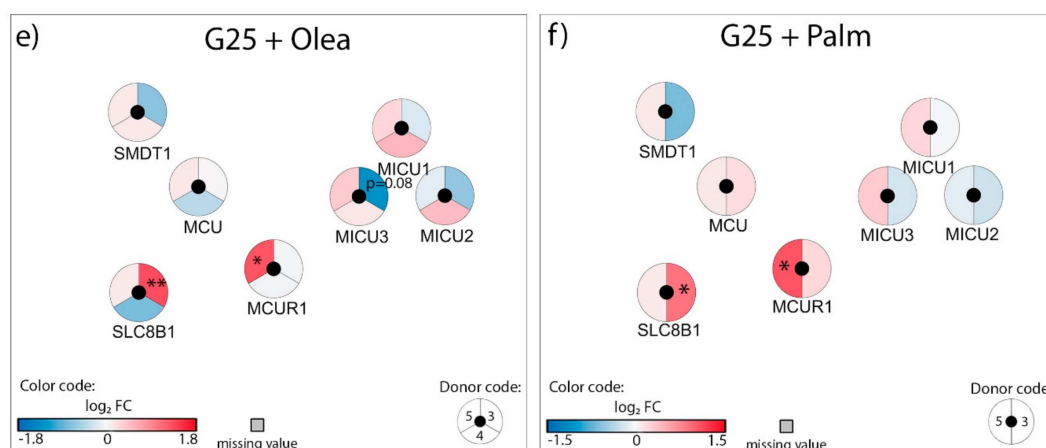


Figure 6. Effects of high 25 mM glucose (G25) and 0.4 mM oleate (Olea) or palmitate (Palm) on the transcriptional regulation of mitochondrial calcium transport genes. Human islets were exposed to (a) Olea at G5.5, (b) Palm at G5.5, (c) G25, (d) G25 + Olea + Palm, (e) G25 + Olea, and (f) G25 + Palm for 3 days before RNA-Seq analysis. Effects of culture conditions on transcript levels are compared to standard G5.5 medium and shown as upregulated (red), downregulated (blue), or unchanged (white). Missing values are represented in grey. Each disk is split into individual changes for the different donors. Color code reflects the transcriptional changes in \log_2 fold changes (\log_2 FC) for that particular gene in individual donors. * adjusted $p < 0.05$, ** adjusted $p < 0.01$ between control 5.5 mM glucose and the specific culture condition.

Overall, some changes induced by either lipotoxic or glucotoxic conditions disappeared when glucolipotoxicity was applied, in particular the upregulation of *SMDT1* and the downregulation of MCU regulatory partners.

4. Discussion

4.1. Adaptation of Mitochondrial Solute Carriers Responsible for Metabolite Transport

We first analyzed the carriers and associated genes involved in mitochondrial metabolic fluxes. Of primary importance, pyruvate is the link between glycolysis and mitochondrial activation, allowing TCA cycle fueling. Upon diabetogenic conditions, the machinery for pyruvate entry and oxidation in mitochondria was essentially preserved, although palmitate increased the expression of pyruvate dehydrogenase kinase *PDK4*. In islets of non-obese β V59M diabetic mice, *PDK1* is strongly upregulated, at both RNA and protein levels, while TCA cycle enzymes are essentially downregulated [15]. Increased *PDK* expression may account for reduced PDH activity reported in β -cells and pancreatic islets exposed to elevated fatty acids [16,17]. However, knockdown of both isoforms one and three of *PDK* in INS-1E β -cells does not affect metabolism–secretion coupling [18]. Interestingly, *PDK4* expression was specifically upregulated by the saturated fatty acid palmitate. Increased *PDK4* activity inhibits PDH and rapidly suppresses mitochondrial pyruvate utilization. In mice fed a high-fat diet, upregulation of *PDK4* precedes diet-induced alteration of glucose oxidation in the heart [19], although we lack similar data on insulin-producing cells. These results suggest a specific fatty acid signature, resulting in lower pyruvate oxidation in the presence of saturated fat.

Downstream of pyruvate metabolism, intermediates of the TCA cycle are recruited to serve as substrates leading to the formation of coupling factors for metabolism–secretion coupling in β -cells [20]. Some of the diabetogenic conditions upregulated several mitochondrial carriers in human islets, i.e., the malate carrier DIC (*SLC25A10*), the α -ketoglutarate-malate exchanger OGC (*SLC25A11*), and the glutamate carrier GC1 (*SLC25A22*). Despite some discrepancies between studies as well as mRNA versus protein levels [21], this observation suggests important mitochondrial anaplerotic/cataplerotic pathways and NAD(P)H-generating shuttle activities, thereby generating

factors supporting glucose-stimulated insulin secretion [1,22–25]. Interestingly, the fatty acid transporter FATP1 was also upregulated by metabolic stresses, potentially promoting β -oxidation. In several models of obese type-2 diabetes, oxidation of fatty acids in β -cells is enhanced along with reduced glucose-stimulated insulin secretion [26–28], favoring detoxification of intracellular lipids. Consequently, channeling fatty acids towards β -oxidation in mitochondria would divert cytosolic fatty acids from the generation of lipid-derived amplifying signals for insulin exocytosis [22,29,30], possibly compensated by the glycerolipid/free fatty acid cycle [26].

Overall, nutrient-rich metabolic stresses induced (i) anaplerotic/cataplerotic machinery that preserves glucose oxidation and metabolism–secretion coupling, pointing to a mitohormetic response [31,32] and (ii) fatty acid import into mitochondria, diverting cytosolic fatty acids from the generation of amplification signals.

4.2. Adaptation of the Electron Transport Chain Machinery

The TCA cycle generates reducing equivalents transferred to the ETC by NADH and FADH₂, promoting hyperpolarization of the mitochondrial membrane ($\Delta\Psi_m$) and ATP production, which is necessary for distal events on the plasma membrane inducing insulin exocytosis (Figure 1a).

Our results uncover increased expression of components of the ETC upon glucotoxic conditions, to a lesser extent upon lipotoxic conditions, and towards normalization with combined glucolipotoxicity. Regarding genes encoded by the mitochondrial genome, i.e., 13 ETC subunits, we previously reported that their expression is reduced in human islets upon high glucose with moderate effects upon oleate exposure [4,10]. Experiments with β -cell lines exposed to chronic high glucose or palmitate showed impaired mitochondrial hyperpolarization in response to glucose notwithstanding preserved mitochondrial respiration [11,33], pointing to changes in the mitochondrial inner membrane current–voltage relationship [33,34]. Conversely, and consistent with the present data, exposure of a clonal β -cell line to chronic high glucose results in elevated mitochondrial respiration, although glucose-stimulated insulin secretion is impaired [4,33]. These discrepancies between studies related to glucotoxicity could be explained by differences in the experimental conditions, such as the duration of the treatments (24/48/72 h). For the β -cell, glucose holds this apparent paradox of being its primary stimulus for metabolism–secretion coupling and becoming toxic when chronically reaching stimulatory concentrations. Palmitate combined with elevated glucose consistently reduces mitochondrial respiration and metabolism–secretion coupling [35]. This is in agreement with the notion that accumulation of glucose-derived malonyl-CoA accounts for adaptation to glucolipotoxicity [30], and is consistent with the blunted upregulation of ETC components we observed upon glucolipotoxic conditions.

When exploring the ETC machinery of pancreatic islets from type-2 diabetic donors, the observations are also variable. Anello et al. observed increased expression of complex I and complex V of the ETC with impaired hyperpolarization of $\Delta\Psi_m$ and lower ATP production upon glucose stimulation [36]. Conversely, other studies have reported decreased expression of genes involved in the ETC [37,38], including isolated human islets exposed for 2 days to palmitate [39]. Rodent and cell culture studies support the finding that reduced expression of ETC components lowers oxidative phosphorylation (OXPHOS) enzyme activity and hence impairs glucose-stimulated ATP production and insulin exocytosis [40]. However, OXPHOS is the main upregulated set of genes in islets of a prediabetic mouse model in response to diabetogenic high-fat diet [41]. This observation could explain the high variability observed between the different studies [13,39] including ours, in the prediabetic state, enhanced OXPHOS by upregulation of the ETC could be a compensatory mechanism to increase ATP production and insulin exocytosis, while this mechanism is lost as diabetes progresses. Hence, different donors at different stages of diabetes with distinct β -cell functionality could show distinct responses.

4.3. Adaptation of the Translocases of the Outer and Inner Mitochondrial Membrane TOM/TIM

The concerted actions of TOM and TIM are responsible for the post-translational import of nuclear-encoded mitochondrial proteins [42]. Our unprecedented analysis of the TOM/TIM system by diabetogenic conditions in insulin-producing cells reveals upregulation of the TOM/TIM import machinery upon glucotoxic and lipotoxic conditions, potentially accounting for increased mitochondrial activity. Of note, glucolipotoxicity robustly and consistently upregulated *TOMM70A*. This receptor (TOM70) plays a key role in the import of mitochondrial carrier precursors [43]. Independently of its protein import function, TOM70 also sustains cell bioenergetics by mediating Ca^{2+} transfer from the endoplasmic reticulum (ER) to the mitochondria [44]. Elevation of mitochondrial Ca^{2+} concentrations favors the activity of Ca^{2+} -sensitive mitochondrial dehydrogenases [45] and ATP synthase-dependent respiration in β -cells [46]. This observation is consistent with the increased ER–mitochondria contact sites in human islets and INS-1E cells exposed to glucotoxic conditions [47]. Despite the numerous ER–mitochondria contact sites, Ca^{2+} transfer into the mitochondria is impaired in these conditions [47], suggesting a possible compensatory mechanism by TOM70. Upregulated by glucotoxic conditions, *TIMM13* and *TIMM8A* form the Tom8–Tom13 complex that is involved in the import of the mitochondrial aspartate/glutamate carriers AGC1 (or aralar1) and AGC2 (or citrin) [48]. AGC1 is an important component of NADH shuttle activity in insulin-secreting cells, particularly solicited upon robust glycolytic flux [24,49]. In summary, chronic nutrient-rich metabolic stress increased transcription of key components of the TOM/TIM import machinery, potentially enhancing the mitochondrial oxidative phosphorylation activity.

4.4. Adaptation of the Mitochondrial Iron Transport

An increasing body of evidence suggests that iron accumulation is associated with elevated risk of type-2 diabetes and might be directly implicated in its pathophysiology [50–55]. In vitro, cellular iron import through the divalent metal transporter DMT1 is increased by diabetogenic conditions, such as exposure to cytokines [56] and glucolipotoxicity [57]. As a consequence, the cytosolic labile iron pool (LIP) is enlarged, favoring the production of reactive oxygen species (ROS) and impairing mitochondrial function [57]. Dietary iron restriction, or iron chelation, protects obese mice from alteration of β -cell function and diabetes [58]. Apart from its role in cytoplasmic and nuclear functions, iron is necessary in mitochondria for the synthesis of heme and the associated iron sulfur cluster (ISC)-containing proteins of the ETC [59]. Iron is imported into mitochondria through mitoferrin 1 or 2 (*SLC25A37* or *SLC25A28*), stored by mitochondrial-ferritin (*FTMT*), and assembled into ISC with the help of frataxin (*FXN*) [60]. In contrast with one report documenting expression of *FTMT* in rodent islets [61], our RNA-Seq analysis did not detect mitochondrial ferritin in human islets. One can speculate that mitochondrial iron homeostasis in human islets is highly dynamic, with active frataxin-mediated ISC assembly and transfer to the ETC limiting its mitochondrial matrix storage [62,63]. We observed that palmitate repressed frataxin, favoring uncontrolled accumulation of mitochondrial iron. The role of *FXN* in the β -cell is illustrated by patients with Friedreich's ataxia. These patients have reduced expression of *FXN* associated with β -cell demise secondary to oxidative stress-induced apoptosis [64] and with defects in insulin secretion and action [39]. Loss of frataxin impacts mitochondrial ATP production in vivo [65], consistent with its role in the building of the ETC. Of note, islets from type-2 diabetic donors have lower *FXN* expression levels [66].

Lipotoxicity and glucotoxicity increased expression of the ATP-binding cassette subfamily B member 8 (*ABCB8*) located in the inner mitochondrial membrane. There are no reports on the regulation of *ABCB8* upon such conditions, although its role in the export of mitochondrial iron and in the defense against oxidative stress has been documented [67,68]. *ABCB8* forms a complex with other mitochondrial proteins, including succinate dehydrogenase, inorganic phosphate carrier, adenine nucleotide translocator, and ATP synthase [69]. As the mitochondrial respiratory chain is a major source of ROS in β -cells and other cell types [70–72], upregulation of *ABCB8* could represent a defense mechanism in β -cells. Finally, *SLC25A39* was significantly upregulated by high glucose and marginally

by fatty acids. The function of *SLC25A39* is not yet well defined, although it is probably not directly implicated in iron transport. Indeed, its silencing does affect mitochondrial iron levels, while it impairs iron incorporation into heme [73], demonstrating a role for this gene in mitochondrial iron homeostasis.

Overall, past and present data show that diabetogenic conditions alter the expression of genes involved in mitochondrial iron homeostasis, with possible implications in the pathophysiology of diabetes and β -cell function.

4.5. Adaptation of the Mitochondrial Calcium Transport

When β -cells are stimulated with elevated glucose, mitochondrial ATP generation promotes plasma membrane depolarization and a subsequent rise in cytosolic Ca^{2+} concentration, thereby triggering insulin secretion. Part of the Ca^{2+} peak is transferred into mitochondria [74], as well as in the ER [75]. Increased mitochondrial Ca^{2+} enhances the activity of some dehydrogenases [76–78], promoting the generation of additive coupling factors for insulin exocytosis [79–81].

The channel responsible for mitochondrial Ca^{2+} uptake is the uniporter MCU and its expression is required in β -cells for proper in vitro glucose-stimulated insulin secretion [82]. Consistent with previous reports [47], none of the tested conditions significantly modified MCU expression, in agreement with its complex post-translational regulation [83]. However, we show here that glucotoxicity upregulated *SMDT1* (essential MCU regulator, EMRE), which is indispensable for MCU activity [84]. Silencing of MCU in β -cells impairs the rise in mitochondrial Ca^{2+} evoked by cell depolarization and reduces the plateau phase of ATP/ADP ratio upon glucose stimulation without affecting mitochondrial membrane potential [85]. Accordingly, knockdown of MCU in mouse β -cells inhibits glucose-evoked insulin exocytosis [86]. At the in vivo level, mice lacking MCU in β -cells display normal glycemia despite impaired glucose-stimulated insulin secretion, which was tested on isolated islets [82]. Surprisingly, whole-body MCU knockout mice exhibit a mild phenotype without noticeable impact on oxidative phosphorylation [87]. It has been proposed that cytosolic Ca^{2+} , more than mitochondrial matrix Ca^{2+} , may adapt OXPHOS to workload by adjusting the rate of pyruvate supply from the cytosol to the mitochondria [88]. Regarding Ca^{2+} efflux out of mitochondria, this is mediated by the $\text{Na}^+/\text{Ca}^{2+}$ exchanger NCLX (*SLC8B1*) [89] and its inhibition increases both mitochondrial Ca^{2+} concentration and glucose-stimulated insulin secretion [90]. In insulinoma cells, it was reported that high glucose abolishes the allosteric inhibition of NCLX, favoring Ca^{2+} efflux [91]. Here, we show that the glucotoxic condition upregulated *SLC8B1* (NCLX) in human islets. Therefore, NCLX could serve as a glucose sensor linking mitochondrial metabolism and Ca^{2+} signaling.

Overall, in human islets, a high glucose condition alters transcription of MCU regulatory partners and NCLX-mediated mitochondrial Ca^{2+} efflux, with a potential impact on mitochondrial activity and the generation of coupling factors.

5. Conclusions

Lipotoxic, glucotoxic, and glucolipotoxic conditions applied to human islets induced specific expression changes in solute mitochondrial carriers and associated genes, TOM/TIM protein import machinery, ETC components, and iron and calcium transport. Glucotoxicity was the condition that altered the expression of the largest number of genes. Interestingly, the addition of fatty acids to the high glucose culture counteracted several of the changes, in particular regarding the ETC components and the TOM/TIM machinery (Figure 7). The specificities of changes could also discriminate between saturated and unsaturated fatty acids. Delineation of nutrient-specific signatures in human islets may provide novel insights for the management of type-2 diabetes.

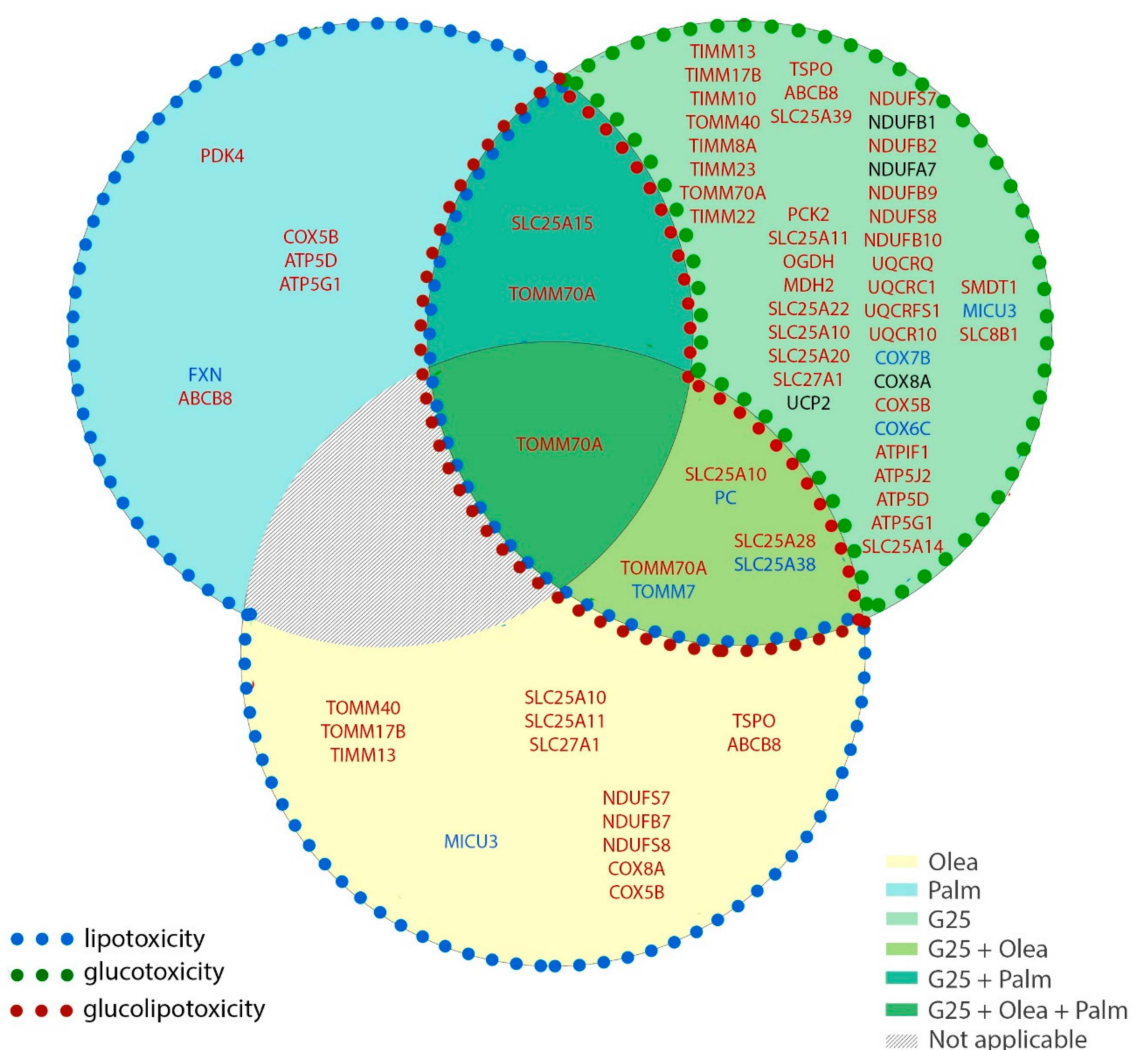


Figure 7. Stress-specific mitochondrial transcriptome profile of human islets upon lipotoxic, glucotoxic, and glucolipotoxic conditions. Isolated human islets were exposed for 3 days to different culture conditions: 25 mM glucose (G25) in the green circle, 0.4 mM oleate (Olea) in the yellow circle, and 0.4 mM palmitate (Palm) in the blue circle. The superimposition of the circles represents the mix of the corresponding conditions: G25 + Olea in the superimposition of the green and yellow circles, G25 + Palm in the superimposition of the green and blue circles, and G25 + Palm + Olea in the superimposition of the three conditions. The condition corresponding to Palm + Olea at G5.5 was not tested (not applicable). The circle sections contain the genes whose expression is modified upon that specific stress condition. Colors reflect positive (red), negative (blue) or variable (black) changes in mRNA. Significant changes were considered when two or more independent islet batches (donors) exhibited down or upregulation with a \log_2 FC threshold of 0.5 associated with one or more adjusted $p < 0.05$.

Supplementary Materials: The following are available online at <http://www.mdpi.com/2218-273X/10/11/1543/s1>; Supplementary Figure S1. Functional interaction network; Supplementary Figure S2. Transcriptional regulation of the electron transport chain machinery and related mitochondrial carriers in human islets; Supplementary Figure S3. Transcriptional regulation of mitochondrial iron transport genes in human islets; Supplementary Figure S4: Effects of high 25 mM glucose (G25) and 0.4 mM palmitate (Palm) or oleate (Olea) on mRNA levels of selected genes in human islets measured by quantitative RT-PCR, normalized to cyclophilin A (PPIA). See Supplementary Table S1 for details on the donors. Supplementary Table S1: Clinical data of the human donors of pancreatic islets; Supplementary Table S2. Quantitative data related to the transcriptomic profiles of mitochondrial solute carriers and associated genes in human islets upon metabolic stress; Supplementary Table S3. Quantitative data related to the transcriptomic profiles of the electron transport chain machinery and related mitochondrial carriers in

human islets upon metabolic stress; Supplementary Table S4. Quantitative data related to the transcriptomic profiles of the outer and inner mitochondrial membrane translocases TOM/TIM machinery in human islets upon metabolic stress; Supplementary Table S5. Quantitative data related to the transcriptomic profiles of mitochondrial iron transport genes in human islets under metabolic stress; Supplementary Table S6. Quantitative data related to the transcriptomic profiles of mitochondrial calcium transport genes in human islets upon metabolic stress. Supplementary Table S7: Primers used for quantitative RT-PCR analysis.

Author Contributions: C.J.-S. designed the research and analyzed the data; P.M. designed and supervised the research; C.J.-S., T.B., and P.M. wrote the manuscript. All authors have read and agreed to the published version of the manuscript.

Funding: The research was funded by the Swiss National Science Foundation (#166625 to P.M.), the Bo & Kerstin Hjelt Diabetes Foundation and Fundación Alfonso Martín Escudero (to C.J.-S.), and the State of Geneva.

Acknowledgments: We are grateful to Lucie Oberhauser (University of Geneva) for islet cultures, to Jesper Grud Skat Madsen (University of Southern Denmark) for RNA-Seq processing, and to Dominique Duhamel (University of Geneva) for quantitative RT-PCR analyses. The most precious contribution of present and past members of the laboratory is acknowledged.

Conflicts of Interest: The authors declare no conflict of interest.

References

1. Maechler, P. Mitochondrial function and insulin secretion. *Mol. Cell. Endocrinol.* **2013**, *379*, 12–18. [CrossRef]
2. Brun, T.; Jiménez-Sánchez, C.; Madsen, J.G.S.; Hadadi, N.; Duhamel, D.; Bartley, C.; Oberhauser, L.; Trajkovski, M.; Mandrup, S.; Maechler, P. AMPK Profiling in Rodent and Human Pancreatic Beta-Cells under Nutrient-Rich Metabolic Stress. *Int. J. Mol. Sci.* **2020**, *21*, 3982. [CrossRef] [PubMed]
3. Frigerio, F.; Brun, T.; Bartley, C.; Usardi, A.; Bosco, D.; Ravnskjaer, K.; Mandrup, S.; Maechler, P. Peroxisome proliferator-activated receptor α (PPAR α) protects against oleate-induced INS-1E beta cell dysfunction by preserving carbohydrate metabolism. *Diabetologia* **2009**, *53*, 331–340. [CrossRef] [PubMed]
4. Brun, T.; Li, N.; Jourdain, A.A.; Gaudet, P.; Duhamel, D.; Meyer, J.; Bosco, D.; Maechler, P. Diabetogenic milieu induce specific changes in mitochondrial transcriptome and differentiation of human pancreatic islets. *Hum. Mol. Genet.* **2015**, *24*, 5270–5284. [CrossRef] [PubMed]
5. Schmidt, S.F.; Madsen, J.G.S.; Frafjord, K.Ø.; la Cour Poulsen, L.; Salö, S.; Boergesen, M.; Loft, A.; Larsen, B.D.; Madsen, M.S.; Holst, J.J.; et al. Integrative Genomics Outlines a Biphasic Glucose Response and a ChREBP-RORgamma Axis Regulating Proliferation in beta Cells. *Cell Rep.* **2016**, *16*, 2359–2372. [CrossRef] [PubMed]
6. Bartley, C.; Brun, T.; Oberhauser, L.; Grimaldi, M.; Molica, F.; Kwak, B.R.; Bosco, D.; Chanson, M.; Maechler, P. Chronic fructose renders pancreatic beta-cells hyper-responsive to glucose-stimulated insulin secretion through extracellular ATP signaling. *Am. J. Physiol. Endocrinol. Metab.* **2019**, *317*, E25–E41. [CrossRef]
7. Doncheva, N.T.; Morris, J.H.; Gorodkin, J.; Jensen, L.J. Cytoscape StringApp: Network Analysis and Visualization of Proteomics Data. *J. Proteome Res.* **2019**, *18*, 623–632. [CrossRef]
8. Legeay, M.; Doncheva, N.T.; Morris, J.H.; Jensen, L.J. Visualize omics data on networks with Omics Visualizer, a Cytoscape App. *F1000Res* **2020**, *9*, 157. [CrossRef] [PubMed]
9. Prentki, M.; Peyot, M.L.; Masiello, P.; Madiraju, S.M. Nutrient-Induced Metabolic Stress, Adaptation, Detoxification, and Toxicity in the Pancreatic beta-Cell. *Diabetes* **2020**, *69*, 279–290. [CrossRef]
10. Brun, T.; Scarcia, P.; Li, N.; Gaudet, P.; Duhamel, D.; Palmieri, F.; Maechler, P. Changes in mitochondrial carriers exhibit stress-specific signatures in INS-1E beta-cells exposed to glucose versus fatty acids. *PLoS ONE* **2013**, *8*, e82364. [CrossRef]
11. Oberhauser, L.; Granziera, S.; Colom, A.; Goujon, A.; Lavallard, V.; Matile, S.; Roux, A.; Brun, T.; Maechler, P. Palmitate and oleate modify membrane fluidity and kinase activities of INS-1E β -cells alongside altered metabolism-secretion coupling. *Biochim. Biophys. Acta Mol. Cell Res.* **2020**, *1867*, 118619. [CrossRef] [PubMed]
12. Szklarczyk, D.; Gable, A.L.; Lyon, D.; Junge, A.; Wyder, S.; Huerta-Cepas, J.; Simonovic, M.; Doncheva, N.T.; Morris, J.H.; Bork, P.; et al. STRING v11: Protein–protein association networks with increased coverage, supporting functional discovery in genome-wide experimental datasets. *Nucleic Acids Res.* **2018**, *47*, D607–D613. [CrossRef] [PubMed]
13. Sargsyan, E.; Cen, J.; Roomp, K.; Schneider, R.; Bergsten, P. Identification of early biological changes in palmitate-treated isolated human islets. *BMC Genom.* **2018**, *19*, 629. [CrossRef]

14. Ristow, M.; Mulder, H.; Pomplun, D.; Schulz, T.J.; Müller-Schmehl, K.; Krause, A.; Fex, M.; Puccio, H.; Müller, J.; Isken, F.; et al. Frataxin deficiency in pancreatic islets causes diabetes due to loss of beta cell mass. *J. Clin. Investig.* **2003**, *112*, 527–534. [CrossRef]
15. Haythorne, E.; Rohm, M.; Van De Bunt, M.; Brereton, M.F.; Tarasov, A.I.; Blacker, T.S.; Sachse, G.; Dos Santos, M.S.; Exposito, R.T.; Davis, S.; et al. Diabetes causes marked inhibition of mitochondrial metabolism in pancreatic β -cells. *Nat. Commun.* **2019**, *10*, 1–17. [CrossRef]
16. Zhou, Y.P.; Berggren, P.O.; Grill, V. A fatty acid-induced decrease in pyruvate dehydrogenase activity is an important determinant of beta-cell dysfunction in the obese diabetic db/db mouse. *Diabetes* **1996**, *45*, 580–586. [CrossRef] [PubMed]
17. Zhou, Y.P.; Grill, V. Long term exposure to fatty acids and ketones inhibits B-cell functions in human pancreatic islets of Langerhans. *J. Clin. Endocrinol. Metab.* **1995**, *80*, 1584–1590. [PubMed]
18. Rutter, G.A.; Burnett, P.; Rizzuto, R.; Brini, M.; Murgia, M.; Pozzan, T.; Tavare, J.M.; Denton, R.M. Subcellular imaging of intramitochondrial Ca^{2+} with recombinant targeted aequorin: Significance for the regulation of pyruvate dehydrogenase activity. *Proc. Natl. Acad. Sci. USA* **1996**, *93*, 5489–5494. [CrossRef] [PubMed]
19. Crewe, C.; Kinter, M.; Szweda, L.I. Rapid Inhibition of Pyruvate Dehydrogenase: An Initiating Event in High Dietary Fat-Induced Loss of Metabolic Flexibility in the Heart. *PLoS ONE* **2013**, *8*, e77280. [CrossRef]
20. Maechler, P.; Carobbio, S.; Rubi, B. In beta-cells, mitochondria integrate and generate metabolic signals controlling insulin secretion. *Int. J. Biochem. Cell Biol.* **2006**, *38*, 696–709. [CrossRef]
21. Brun, T.; Maechler, P. Beta-cell mitochondrial carriers and the diabetogenic stress response. *Biochim. Biophys. Acta (BBA) Bioenerg.* **2016**, *1863*, 2540–2549. [CrossRef] [PubMed]
22. Roduit, R.; Nolan, C.J.; Alarcon, C.; Moore, P.; Barbeau, A.; Delghingaro-Augusto, V.; Przybykowski, E.; Morin, J.; Massé, F.; Massie, B.; et al. A role for the malonyl-CoA/long-chain acyl-CoA pathway of lipid signaling in the regulation of insulin secretion in response to both fuel and nonfuel stimuli. *Diabetes* **2004**, *53*, 1007–1019. [CrossRef] [PubMed]
23. Macdonald, M.J. Feasibility of a mitochondrial pyruvate malate shuttle in pancreatic islets. Further implication of cytosolic NADPH in insulin secretion. *J. Biol. Chem.* **1995**, *270*, 20051–20058. [PubMed]
24. Rubí, B.; Del Arco, A.; Bartley, C.; Satrustegui, J.; Maechler, P. The Malate-Aspartate NADH Shuttle Member Aralar1 Determines Glucose Metabolic Fate, Mitochondrial Activity, and Insulin Secretion in Beta Cells. *J. Biol. Chem.* **2004**, *279*, 55659–55666. [CrossRef]
25. Casimir, M.; Lasorsa, F.M.; Rubi, B.; Caille, D.; Palmieri, F.; Meda, P.; Maechler, P. Mitochondrial Glutamate Carrier GC1 as a Newly Identified Player in the Control of Glucose-stimulated Insulin Secretion. *J. Biol. Chem.* **2009**, *284*, 25004–25014. [CrossRef]
26. Prentki, M.; Madiraju, S.R. Glycerolipid/free fatty acid cycle and islet beta-cell function in health, obesity and diabetes. *Mol. Cell Endocrinol.* **2012**, *353*, 88–100. [CrossRef]
27. Delghingaro-Augusto, V.; Nolan, C.J.; Gupta, D.; Jetton, T.L.; Latour, M.G.; Peshavaria, M.; Madiraju, S.R.M.; Joly, E.; Peyot, M.-L.; Prentki, M.; et al. Islet beta cell failure in the 60% pancreatectomised obese hyperlipidaemic Zucker fatty rat: Severe dysfunction with altered glycerolipid metabolism without steatosis or a falling beta cell mass. *Diabetologia* **2009**, *52*, 1122–1132. [CrossRef]
28. Nolan, C.J.; Madiraju, M.S.; Delghingaro-Augusto, V.; Peyot, M.L.; Prentki, M. Fatty acid signaling in the beta-cell and insulin secretion. *Diabetes* **2006**, *55* (Suppl. 2), S16–S23. [CrossRef]
29. Zhao, S.; Mugabo, Y.; Iglesias, J.; Xie, L.; Delghingaro-Augusto, V.; Lussier, R.; Peyot, M.-L.; Joly, E.; Taib, B.; Davis, M.A.; et al. α/β -Hydrolase Domain-6-Accessible Monoacylglycerol Controls Glucose-Stimulated Insulin Secretion. *Cell Metab.* **2014**, *19*, 993–1007. [CrossRef]
30. Prentki, M.; Joly, E.; El-Assaad, W.; Roduit, R. Malonyl-CoA Signaling, Lipid Partitioning, and Glucolipototoxicity: Role in β -Cell Adaptation and Failure in the Etiology of Diabetes. *Diabetes* **2002**, *51*, 405–413. [CrossRef]
31. El-Assaad, W.; Buteau, J.; Peyot, M.-L.; Nolan, C.; Roduit, R.; Hardy, S.; Joly, E.; Dbaibo, G.; Rosenberg, L.; Prentki, M. Saturated Fatty Acids Synergize with Elevated Glucose to Cause Pancreatic β -Cell Death. *Endocrinology* **2003**, *144*, 4154–4163. [CrossRef] [PubMed]
32. Li, N.; Stojanovski, S.; Maechler, P. Mitochondrial Hormesis in Pancreatic beta Cells: Does Uncoupling Protein 2 Play a Role? *Oxid. Med. Cell Longev.* **2012**, *2012*, 740849. [CrossRef] [PubMed]

33. Göhring, I.; Sharoyko, V.V.; Malmgren, S.; Andersson, L.E.; Spégel, P.; Nicholls, D.G.; Mulder, H. Chronic high glucose and pyruvate levels differentially affect mitochondrial bioenergetics and fuel-stimulated insulin secretion from clonal INS-1 832/13 cells. *J. Biol. Chem.* **2014**, *289*, 3786–3798. [CrossRef] [PubMed]
34. Rial, E.; Poustie, A.; Nicholls, D.G. Brown-adipose-tissue mitochondria: The regulation of the 32 000-Mr uncoupling protein by fatty acids and purine nucleotides. *JBIC J. Biol. Inorg. Chem.* **1983**, *137*, 197–203. [CrossRef] [PubMed]
35. Barlow, J.P.; Affourtit, C. Novel insights into pancreatic β -cell glucolipotoxicity from real-time functional analysis of mitochondrial energy metabolism in INS-1E insulinoma cells. *Biochem. J.* **2013**, *456*, 417–426. [CrossRef]
36. Anello, M.; Lupi, R.; Spampinato, D.; Piro, S.; Masini, M.; Boggi, U.; Del Prato, S.; Rabuazzo, A.M.; Purrello, F.; Marchetti, P. Functional and morphological alterations of mitochondria in pancreatic beta cells from type 2 diabetic patients. *Diabetology* **2005**, *48*, 282–289. [CrossRef]
37. Olsson, A.H.; Yang, B.T.; Hall, E.; Taneera, J.; Salehi, A.; Nitert, M.D.; Ling, C. Decreased expression of genes involved in oxidative phosphorylation in human pancreatic islets from patients with type 2 diabetes. *Eur. J. Endocrinol.* **2011**, *165*, 589–595. [CrossRef]
38. Segerstolpe, Å.; Palasantza, A.; Eliasson, P.; Andersson, E.-M.; Andréasson, A.-C.; Sun, X.; Picelli, S.; Sabirsh, A.; Clausen, M.; Bjursell, M.K.; et al. Single-Cell Transcriptome Profiling of Human Pancreatic Islets in Health and Type 2 Diabetes. *Cell Metab.* **2016**, *24*, 593–607. [CrossRef]
39. Cnop, M.; Abdulkarim, B.; Bottu, G.; Da Cunha, D.A.; Igoillo-Esteve, M.; Masini, M.; Turatsinze, J.-V.; Griebel, T.; Villate, O.; Santin, I.; et al. RNA Sequencing Identifies Dysregulation of the Human Pancreatic Islet Transcriptome by the Saturated Fatty Acid Palmitate. *Diabetes* **2013**, *63*, 1978–1993. [CrossRef]
40. Koeck, T.; Olsson, A.H.; Nitert, M.D.; Sharoyko, V.V.; Ladvall, C.; Kotova, O.; Reiling, E.; Rönn, T.; Parikh, H.; Taneera, J.; et al. A Common Variant in TFB1M Is Associated with Reduced Insulin Secretion and Increased Future Risk of Type 2 Diabetes. *Cell Metab.* **2011**, *13*, 80–91. [CrossRef]
41. Dreja, T.; Jovanovic, Z.; Rasche, A.; Kluge, R.; Herwig, R.; Joost, H.G.; Yeo, G.; Al-Hasani, H. Diet-induced gene expression of isolated pancreatic islets from a polygenic mouse model for the metabolic syndrome. *Diabetol. Stoffwechs.* **2008**, *3*, 71. [CrossRef]
42. Chacinska, A.; Koehler, C.M.; Milenkovic, D.; Lithgow, T.; Pfanner, N. Importing Mitochondrial Proteins: Machineries and Mechanisms. *Cell* **2009**, *138*, 628–644. [CrossRef] [PubMed]
43. Wiedemann, N.; Pfanner, N. Mitochondrial Machineries for Protein Import and Assembly. *Annu. Rev. Biochem.* **2017**, *86*, 685–714. [CrossRef]
44. Filadi, R.; Leal, N.S.; Schreiner, B.; Rossi, A.; Dentoni, G.; Pinho, C.M.; Wiehager, B.; Cieri, D.; Cali, T.; Pizzo, P.; et al. TOM70 Sustains Cell Bioenergetics by Promoting IP3R3-Mediated ER to Mitochondria Ca^{2+} Transfer. *Curr. Biol.* **2018**, *28*, 369–382.e6. [CrossRef]
45. Denton, R.M. Regulation of mitochondrial dehydrogenases by calcium ions. *Biochim. et Biophys. Acta (BBA) Bioenerg.* **2009**, *1787*, 1309–1316. [CrossRef] [PubMed]
46. De Marchi, U.; Thevenet, J.; Hermant, A.; Dioum, E.; Wiederkehr, A. Calcium Co-regulates Oxidative Metabolism and ATP Synthase-dependent Respiration in Pancreatic Beta Cells. *J. Biol. Chem.* **2014**, *289*, 9182–9194. [CrossRef] [PubMed]
47. Dingreville, F.; Panthu, B.; Thivolet, C.; Ducreux, S.; Gouriou, Y.; Pesenti, S.; Chauvin, M.-A.; Chikh, K.; Errazuriz-Cerda, E.; Van Coppenolle, F.; et al. Differential Effect of Glucose on ER-Mitochondria Ca^{2+} Exchange Participates in Insulin Secretion and Glucotoxicity-Mediated Dysfunction of β -Cells. *Diabetes* **2019**, *68*, 1778–1794. [CrossRef]
48. Roesch, K.; Hynds, P.J.; Varga, R.; Tranebjaerg, L.; Koehler, C.M. The calcium-binding aspartate/glutamate carriers, citrin and aralar1, are new substrates for the DDP1/TIMM8a-TIMM13 complex. *Hum. Mol. Genet.* **2004**, *13*, 2101–2111. [CrossRef]
49. Casimir, M.; Rubi, B.; Frigerio, F.; Chaffard, G.; Maechler, P. Silencing of the mitochondrial NADH shuttle component aspartate-glutamate carrier AGC1/Aralar1 in INS-1E cells and rat islets. *Biochem. J.* **2009**, *424*, 459–466. [CrossRef]
50. Thomas, M.C.; MacIsaac, R.J.; Tsalamandris, C.; Jerums, G. Elevated iron indices in patients with diabetes. *Diabet. Med.* **2004**, *21*, 798–802. [CrossRef]
51. Rajpathak, S.N.; Crandall, J.P.; Wylie-Rosett, J.; Kabat, G.C.; Rohan, T.E.; Hu, F.B. The role of iron in type 2 diabetes in humans. *Biochim. Biophys. Acta (BBA) Gen. Subj.* **2009**, *1790*, 671–681. [CrossRef] [PubMed]

52. Ellervik, C.; Mandrup-Poulsen, T.; Andersen, H.U.; Tybjaerg-Hansen, A.; Frandsen, M.; Birgens, H.; Nordestgaard, B.G. Elevated transferrin saturation and risk of diabetes: Three population-based studies. *Diabetes Care* **2011**, *34*, 2256–2258. [CrossRef]
53. Huang, J.; Jones, D.; Luo, B.; Sanderson, M.; Soto, J.; Abel, E.D.; Cooksey, R.C.; McClain, D.A. Iron Overload and Diabetes Risk: A Shift From Glucose to Fatty Acid Oxidation and Increased Hepatic Glucose Production in a Mouse Model of Hereditary Hemochromatosis. *Diabetes* **2010**, *60*, 80–87. [CrossRef] [PubMed]
54. Montonen, J.; Boeing, H.; Steffen, A.; Lehmann, R.; Fritsche, A.E.; Joost, H.-G.; Schulze, M.B.; Pischon, T. Body iron stores and risk of type 2 diabetes: Results from the European Prospective Investigation into Cancer and Nutrition (EPIC)-Potsdam study. *Diabetologia* **2012**, *55*, 2613–2621. [CrossRef] [PubMed]
55. Fernández-Real, J.M.; McClain, D.; Manco, M. Mechanisms Linking Glucose Homeostasis and Iron Metabolism Toward the Onset and Progression of Type 2 Diabetes. *Diabetes Care* **2015**, *38*, 2169–2176. [CrossRef] [PubMed]
56. Hansen, J.B.; Tonnesen, M.F.; Madsen, A.N.; Hagedorn, P.H.; Friberg, J.; Grunnet, L.G.; Heller, R.S.; Nielsen, A.Ø.; Størling, J.; Baeyens, L.; et al. Divalent metal transporter 1 regulates iron-mediated ROS and pancreatic beta cell fate in response to cytokines. *Cell Metab.* **2012**, *16*, 449–461. [CrossRef]
57. Hansen, J.B.; Dos Santos, L.R.B.; Liu, Y.; Prentice, K.J.; Teudt, F.; Tonnesen, M.; Jonas, J.-C.; Wheeler, M.B.; Mandrup-Poulsen, T. Glucolipotoxic conditions induce β -cell iron import, cytosolic ROS formation and apoptosis. *J. Mol. Endocrinol.* **2018**, *61*, 69–77. [CrossRef]
58. Cooksey, R.C.; Jones, D.; Gabrielsen, S.; Huang, J.; Simcox, J.A.; Luo, B.; Soesanto, Y.; Rienhoff, H.; Dale Abel, E.; McClain, D.A. Dietary iron restriction or iron chelation protects from diabetes and loss of beta-cell function in the obese (ob/ob lep^{-/-}) mouse. *Am. J. Physiol. Endocrinol. Metab.* **2010**, *298*, E1236–E1243. [CrossRef]
59. Richardson, D.R.; Lane, D.J.R.; Becker, E.M.; Huang, M.L.-H.; Whitnall, M.; Rahmanto, Y.S.; Sheftel, A.D.; Ponka, P. Mitochondrial iron trafficking and the integration of iron metabolism between the mitochondrion and cytosol. *Proc. Natl. Acad. Sci. USA* **2010**, *107*, 10775–10782. [CrossRef]
60. Hansen, J.B.; Moen, I.W.; Mandrup-Poulsen, T. Iron: The hard player in diabetes pathophysiology. *Acta Physiol.* **2014**, *210*, 717–732. [CrossRef]
61. Santambrogio, P.; Biasiotto, G.; Sanvito, F.; Olivieri, S.; Arosio, P.; Levi, S. Mitochondrial Ferritin Expression in Adult Mouse Tissues. *J. Histochem. Cytochem.* **2007**, *55*, 1129–1137. [CrossRef] [PubMed]
62. Stemmler, T.L.; Lesuisse, E.; Pain, D.; Dancis, A. Frataxin and Mitochondrial FeS Cluster Biogenesis. *J. Biol. Chem.* **2010**, *285*, 26737–26743. [CrossRef] [PubMed]
63. Gonzalez-Cabo, P.; Vázquez-Manrique, R.P.; Garcia-Gimeno, M.A.; Sanz, P.; Palau, F. Frataxin interacts functionally with mitochondrial electron transport chain proteins. *Hum. Mol. Genet.* **2005**, *14*, 2091–2098. [CrossRef] [PubMed]
64. Igoillo-Esteve, M.; Gurgul-Convey, E.; Hu, A.; Dos Santos, L.R.B.; Abdulkarim, B.; Chintawar, S.; Marselli, L.; Marchetti, P.; Jonas, J.-C.; Eizirik, D.L.; et al. Unveiling a common mechanism of apoptosis in β -cells and neurons in Friedreich’s ataxia. *Hum. Mol. Genet.* **2014**, *24*, 2274–2286. [CrossRef] [PubMed]
65. Lodi, R.; Cooper, J.M.; Bradley, J.L.; Manners, D.N.; Styles, P.; Taylor, D.J.; Schapira, A.H.V. Deficit of in vivo mitochondrial ATP production in patients with Friedreich ataxia. *Proc. Natl. Acad. Sci. USA* **1999**, *96*, 11492–11495. [CrossRef] [PubMed]
66. Del Guerra, S.; D’Aleo, V.; Gualtierotti, G.; Pandolfi, R.; Boggi, U.; Vistoli, F.; Barnini, S.; Filipponi, F.; Del Prato, S.; Lupi, R. Evidence for a Role of Frataxin in Pancreatic Islets Isolated from Multi-Organ Donors with and Without Type 2 Diabetes Mellitus. *Horm. Metab. Res.* **2012**, *44*, 471–475. [CrossRef]
67. Ichikawa, Y.; Ghanefar, M.; Bayeva, M.; Wu, R.; Khechaduri, A.; Prasad, S.V.N.; Mutharasan, R.K.; Naik, T.J.; Ardehali, H. Cardiotoxicity of doxorubicin is mediated through mitochondrial iron accumulation. *J. Clin. Investig.* **2014**, *124*, 617–630. [CrossRef]
68. Ardehali, H.; O’Rourke, B.; Marbán, E. Cardioprotective Role of the Mitochondrial ATP-Binding Cassette Protein 1. *Circ. Res.* **2005**, *97*, 740–742. [CrossRef]
69. Ardehali, H.; Chen, Z.; Ko, Y.; Mejía-Alvarez, R.; Marbán, E. Multiprotein complex containing succinate dehydrogenase confers mitochondrial ATP-sensitive K⁺ channel activity. *Proc. Natl. Acad. Sci. USA* **2004**, *101*, 11880–11885. [CrossRef]
70. Turrens, J.F. Mitochondrial formation of reactive oxygen species. *J. Physiol.* **2003**, *552*, 335–344. [CrossRef]

71. Lenaz, G. The Mitochondrial Production of Reactive Oxygen Species: Mechanisms and Implications in Human Pathology. *IUBMB Life* **2001**, *52*, 159–164. [CrossRef] [PubMed]
72. Newsholme, P.; Haber, E.P.; Hirabara, S.M.; Rebelato, E.L.O.; Procopio, J.; Morgan, D.; Oliveira-Emilio, H.C.; Carpinelli, A.R.; Curi, R. Diabetes associated cell stress and dysfunction: Role of mitochondrial and non-mitochondrial ROS production and activity. *J. Physiol.* **2007**, *583*, 9–24. [CrossRef] [PubMed]
73. Nilsson, R.; Schultz, I.J.; Pierce, E.L.; Soltis, K.A.; Naranuntarat, A.; Ward, D.M.; Baughman, J.M.; Paradkar, P.N.; Kingsley, P.D.; Culotta, V.C.; et al. Discovery of Genes Essential for Heme Biosynthesis through Large-Scale Gene Expression Analysis. *Cell Metab.* **2009**, *10*, 119–130. [CrossRef] [PubMed]
74. Kennedy, E.D.; Rizzuto, R.; Theler, J.M.; Pralong, W.F.; Bastianutto, C.; Pozzan, T.; Wollheim, C.B. Glucose-stimulated insulin secretion correlates with changes in mitochondrial and cytosolic Ca²⁺ in aequorin-expressing INS-1 cells. *J. Clin. Investig.* **1996**, *98*, 2524–2538. [CrossRef] [PubMed]
75. Maechler, P.; Kennedy, E.D.; Sebö, E.; Valeva, A.; Pozzan, T.; Wollheim, C.B. Secretagogues modulate the calcium concentration in the endoplasmic reticulum of insulin-secreting cells. Studies in aequorin-expressing intact and permeabilized ins-1 cells. *J. Biol. Chem.* **1999**, *274*, 12583–12592. [CrossRef] [PubMed]
76. Maechler, P.; Kennedy, E.D.; Wang, H.; Wollheim, C.B. Desensitization of Mitochondrial Ca²⁺ and Insulin Secretion Responses in the Beta Cell. *J. Biol. Chem.* **1998**, *273*, 20770–20778. [CrossRef]
77. Denton, R.M.; McCormack, J.G. Ca²⁺ as a second messenger within mitochondria of the heart and other tissues. *Annu. Rev. Physiol.* **1990**, *52*, 451–466. [CrossRef]
78. McCormack, J.G.; Halestrap, A.P.; Denton, R.M. Role of calcium ions in regulation of mammalian intramitochondrial metabolism. *Physiol. Rev.* **1990**, *70*, 391–425. [CrossRef]
79. Maechler, P.; Kennedy, E.D.; Pozzan, T.; Wollheim, C.B. Mitochondrial activation directly triggers the exocytosis of insulin in permeabilized pancreatic beta-cells. *EMBO J.* **1997**, *16*, 3833–3841. [CrossRef]
80. Wiederkehr, A.; Wollheim, C.B. Impact of mitochondrial calcium on the coupling of metabolism to insulin secretion in the pancreatic beta-cell. *Cell Calcium* **2008**, *44*, 64–76. [CrossRef]
81. Alam, M.R.; Groschner, L.N.; Parichatikanond, W.; Kuo, L.; Bondarenko, A.I.; Rost, R.; Waldeck-Weiermair, M.; Malli, R.; Graier, W.F. Mitochondrial Ca²⁺ Uptake 1 (MICU1) and Mitochondrial Ca²⁺ Uniporter (MCU) Contribute to Metabolism-Secretion Coupling in Clonal Pancreatic β -Cells. *J. Biol. Chem.* **2012**, *287*, 34445–34454. [CrossRef] [PubMed]
82. Georgiadou, E.; Haythorne, E.; Dickerson, M.T.; Lopez-Noriega, L.; Pullen, T.J.; Xavier, G.D.S.; Davis, S.P.X.; Martinez-Sanchez, A.; Semplici, F.; Rizzuto, R.; et al. The pore-forming subunit MCU of the mitochondrial Ca²⁺ uniporter is required for normal glucose-stimulated insulin secretion in vitro and in vivo in mice. *Diabetologia* **2020**, *63*, 1368–1381. [CrossRef] [PubMed]
83. Pendin, D.; Greotti, E.; Pozzan, T. The elusive importance of being a mitochondrial Ca²⁺ uniporter. *Cell Calcium* **2014**, *55*, 139–145. [CrossRef]
84. Sancak, Y.; Markhard, A.L.; Kitami, T.; Kovács-Bogdán, E.; Kamer, K.J.; Udeshi, N.D.; Carr, S.A.; Chaudhuri, D.; Clapham, D.E.; Li, A.A.; et al. EMRE Is an Essential Component of the Mitochondrial Calcium Uniporter Complex. *Science* **2013**, *342*, 1379–1382. [CrossRef] [PubMed]
85. Tarasov, A.I.; Semplici, F.; Ravier, M.A.; Bellomo, E.A.; Pullen, T.J.; Gilon, P.; Sekler, I.; Rizzuto, R.; Rutter, G.A. The mitochondrial Ca²⁺ uniporter MCU is essential for glucose-induced ATP increases in pancreatic beta-cells. *PLoS ONE* **2012**, *7*, e39722. [CrossRef] [PubMed]
86. Tarasov, A.I.; Semplici, F.; Li, D.; Rizzuto, R.; Ravier, M.A.; Gilon, P.; Rutter, G.A. Frequency-dependent mitochondrial Ca²⁺ accumulation regulates ATP synthesis in pancreatic beta cells. *Pflugers Arch.* **2013**, *465*, 543–554. [CrossRef]
87. Pan, X.; Liu, J.; Nguyen, T.; Liu, C.; Sun, J.; Teng, Y.; Fergusson, M.M.; Rovira, I.I.; Allen, M.; Springer, D.A.; et al. The physiological role of mitochondrial calcium revealed by mice lacking the mitochondrial calcium uniporter. *Nat. Cell Biol.* **2013**, *15*, 1464–1472. [CrossRef]
88. Szibor, M.; Gizatullina, Z.; Gainutdinov, T.; Endres, T.; Debska-Vielhaber, G.; Kunz, M.; Karavasili, N.; Hallmann, K.; Schreiber, F.; Bamberger, A.; et al. Cytosolic, but not matrix, calcium is essential for adjustment of mitochondrial pyruvate supply. *J. Biol. Chem.* **2020**, *295*, 4383–4397. [CrossRef]
89. Palty, R.; Silverman, W.F.; Hershinkel, M.; Caporale, T.; Sensi, S.L.; Parnis, J.; Nolte, C.; Fishman, D.; Shoshan-Barmatz, V.; Herrmann, S.; et al. NCLX is an essential component of mitochondrial Na⁺/Ca²⁺ exchange. *Proc. Natl. Acad. Sci. USA* **2010**, *107*, 436–441. [CrossRef]

90. Lee, B.; Miles, P.D.; Vargas, L.; Luan, P.; Glasco, S.; Kushnareva, Y.; Kornbrust, E.S.; Grako, K.A.; Wollheim, C.B.; Maechler, P.; et al. Inhibition of mitochondrial Na⁺-Ca²⁺ exchanger increases mitochondrial metabolism and potentiates glucose-stimulated insulin secretion in rat pancreatic islets. *Diabetes* **2003**, *52*, 965–973. [CrossRef]
91. Kostic, M.; Katoshevski, T.; Sekler, I. Allosteric Regulation of NCLX by Mitochondrial Membrane Potential Links the Metabolic State and Ca²⁺ Signaling in Mitochondria. *Cell Rep.* **2018**, *25*, 3465–3475. [CrossRef] [PubMed]

Publisher’s Note: MDPI stays neutral with regard to jurisdictional claims in published maps and institutional affiliations.



© 2020 by the authors. Licensee MDPI, Basel, Switzerland. This article is an open access article distributed under the terms and conditions of the Creative Commons Attribution (CC BY) license (<http://creativecommons.org/licenses/by/4.0/>).

Article

Glucose-Induced Expression of DAPIT in Pancreatic β -Cells

Alberto Leguina-Ruzzi , Anežka Vodičková, Blanka Holendová , Vojtěch Pavluch, Jan Tauber, Hana Engstová, Andrea Dlasková and Petr Ježek * 

Department of Mitochondrial Physiology, No.75, Institute of Physiology of the Czech Academy of Sciences, 142 20 Prague, Czech Republic; AlbertoAndres.LeguinaRuzzi@fgu.cas.cz (A.L.-R.); anezka.kahancova@fgu.cas.cz (A.V.); blanka.holendova@fgu.cas.cz (B.H.); vojtech.pavluch@fgu.cas.cz (V.P.); jan.tauber@fgu.cas.cz (J.T.); hana.engstova@fgu.cas.cz (H.E.); andrea.dlaskova@fgu.cas.cz (A.D.)

* Correspondence: jezek@biomed.cas.cz; Tel.: +420-296442760

Received: 20 April 2020; Accepted: 8 July 2020; Published: 10 July 2020

Abstract: Transcript levels for selected ATP synthase membrane F_0 -subunits—including DAPIT—in INS-1E cells were found to be sensitive to lowering glucose down from 11 mM, in which these cells are routinely cultured. Depending on conditions, the diminished mRNA levels recovered when glucose was restored to 11 mM; or were elevated during further 120 min incubations with 20-mM glucose. Asking whether DAPIT expression may be elevated by hyperglycemia in vivo, we studied mice with hyaluronic acid implants delivering glucose for up to 14 days. Such continuous two-week glucose stimulations in mice increased DAPIT mRNA by >5-fold in isolated pancreatic islets (ATP synthase $F_1\alpha$ mRNA by 1.5-fold). In INS-1E cells, the glucose-induced ATP increment vanished with DAPIT silencing (6% of ATP rise), likewise a portion of the mtDNA-copy number increment. With 20 and 11-mM glucose the phosphorylating/non-phosphorylating respiration rate ratio diminished to ~70% and 96%, respectively, upon DAPIT silencing, whereas net GSIS rates accounted for 80% and 90% in USMG5/DAPIT-deficient cells. Consequently, the sufficient DAPIT expression and complete ATP synthase assembly is required for maximum ATP synthesis and mitochondrial biogenesis, but not for insulin secretion as such. Elevated DAPIT expression at high glucose further increases the ATP synthesis efficiency.

Keywords: mitochondria; USMG5/DAPIT; glucose-stimulated insulin secretion; glucose-induced expression; membrane subunits of ATP synthase; ATP synthase oligomers mitochondrial cristae morphology

1. Introduction

Pancreatic β -cells sense glucose and respond to its elevated concentration in rich capillaries of the pancreatic islets by exocytosis of insulin granules [1–7]. The increased mitochondrial ATP synthesis due to the elevated oxidative phosphorylation (OXPHOS) represented a consensual canonical mechanism of glucose-stimulated insulin secretion (GSIS). We recently demonstrated that also NADPH-oxidase-4 (NOX4-) mediated H_2O_2 release is fundamentally required for GSIS in addition to ATP [8]. The elevated OXPHOS is transformed to the increased ATP/ADP ratio at the peri-plasma membrane loci proximal to the ATP-sensitive K^+ channel. The channel closes when both conditions are fulfilled, i.e., elevated ATP and elevated H_2O_2 [8], which results in the depolarization of the plasma membrane. This activates voltage-gated L-type Ca^{2+} channels (Ca_L). The subsequent Ca^{2+} entry to the cytosol initiates the insulin exocytosis of insulin granules.

To match physiological postprandial glucose concentrations with the sensitivity range of the glucose sensor, numerous factors delicately tune glucose-concentration dependence for the insulin

release mechanism. The insulin-independent glucose transporter GLUT-2 (GLUT-1 in humans) rapidly equilibrates blood glucose with the cytosolic glucose in β -cells [9]. The glucokinase (hexokinase IV) is insensitive to the inhibition by glucose-6-phosphate [10]. Moreover, low activities of lactate dehydrogenase and pyruvate dehydrogenase kinase enable a nearly 100% utilization of pyruvate by OXPHOS [1–6].

We found that also the inhibitory factor IF1 of the mitochondrial ATP synthase belongs to the key proteins, ensuring the physiological range of the glucose sensor [11,12]. The IF1 slightly inhibits synthesis of ATP, thus setting the range for elevation of phosphorylating respiration and insulin release above 3-mM glucose [11,13], with half-activation between 3.5 and 4-mM and saturation above 8-mM glucose [11,12]. When such a slight *in vivo* inhibition was largely cancelled using the silencing of IF1, the elevation of respiration and OXPHOS occurred at very low glucose concentration approaching to zero [9]. Simultaneously, the half-activation for the insulin release dose–response was shifted to the range of 0–2-mM glucose in INS-1E cells [9]. In contrast, overexpression of IF1 substantially blocked GSIS [13].

Another peculiar aspect of the pancreatic β -cell glucose sensor is the steepness of the related dose–response, i.e., insulin release dependence vs. glucose concentration [11,12,14–16]. The revealed narrowing of mitochondrial cristae may hypothetically contribute to this steepness, such as observed in INS-1E cells during GSIS [17] or upon the increased load of cell-permeant Krebs cycle substrate [18,19]. Moreover, the ATP synthase dimers, tetramers [20] or speculatively higher oligomers are associated within the rows along the crista rims [21–26].

The stabilization within the rims may depend on the presence and correct assembly of the membrane embedded subunits *e*, *f*, *g* of the membrane F_0 -sector [20,26]; or DAPIT, which is the peripheral outmost subunit of the ATP synthase (Figure 1), added lastly upon the assembly [26]. DAPIT is a product of the rat *Usmg5* gene [27–31]. Similarly, Mic10 was suggested to be inserted between the neighbor dimers or tetramers of the ATP synthase [32,33]. Likewise, crosslinking of two F_1 moieties from the neighbor ATP synthase dimers by the un-phosphorylated dimeric inhibitory factor IF1 can stabilize the rim [20], but at the expense of ATP synthesis, since this interaction is inhibitory [13]. The inner mitochondrial membrane (IMM) bending itself may be ensured by subunits *e* and *g* [20]. In porcine ATP synthase a self-standing subunit *k* belongs to those outmost subunits [14], whereas a yeast subunit *k* was originally annotated as a DAPIT ortholog [26].

DAPIT is bound to the (mtDNA-) mitochondria-encoded subunit *a* (Figure 1). DAPIT may also interact with the second mtDNA-encoded subunit ATP8 [20,26]. However, a tetramer formation may be facilitated by an interaction of DAPIT with the subunit *g* within an interface between all four monomers [20]. Such interface was termed site three among altogether six sites determining the tetramer structure. Since DAPIT was found to be assembled as the last subunit into the F_0 -sector structure [26], we may speculate that its stoichiometry to the F_0 moiety may be variable.

Moreover, a fraction of Mic10 was found to be associated with the ATP synthase and hypothetically can crosslink the neighbor dimers [32,33]. Mic10 otherwise ensures 90° curvature of the IMM at the crista outlets being a part of the MICOS complex [32,33]. Besides Mic10 [32,33], also DAPIT has been suggested to crosslink rows of ATP synthase dimers at crista rims and thus stabilize them [26].

The DAPIT was originally termed diabetes-associated protein in insulin-sensitive tissue. At a complete stoichiometry, the physiologically established dimers and tetramers of the ATP synthase possess two and four F_0 -sectors, respectively, each containing a single DAPIT subunit, embedded into IMM, actually spanning from its intracristal surface to the matrix IMM surface (Figure 1). DAPIT-knockdown in He–La cells reportedly led to a slightly decreased ATP synthesis activity and slower cell growth, while transcripts for the F_1 -sector subunits α and β did not change [29]. Moreover, a homozygous splice-site mutation (c.87 + 1G > C) in *Dapit/Usmg5* gene reportedly determines suppression of ATP synthase dimers and inhibition of ATP synthesis in patient’s fibroblasts [34]. This particular DAPIT mutation causes altered mitochondrial cristae in fibroblasts of Leigh syndrome

patients [35]. Possibly similar or related mechanisms as caused by the DAPIT mutation are involved in sensitizing of pancreatic cancer cells to inhibitors impairing their survival [36].

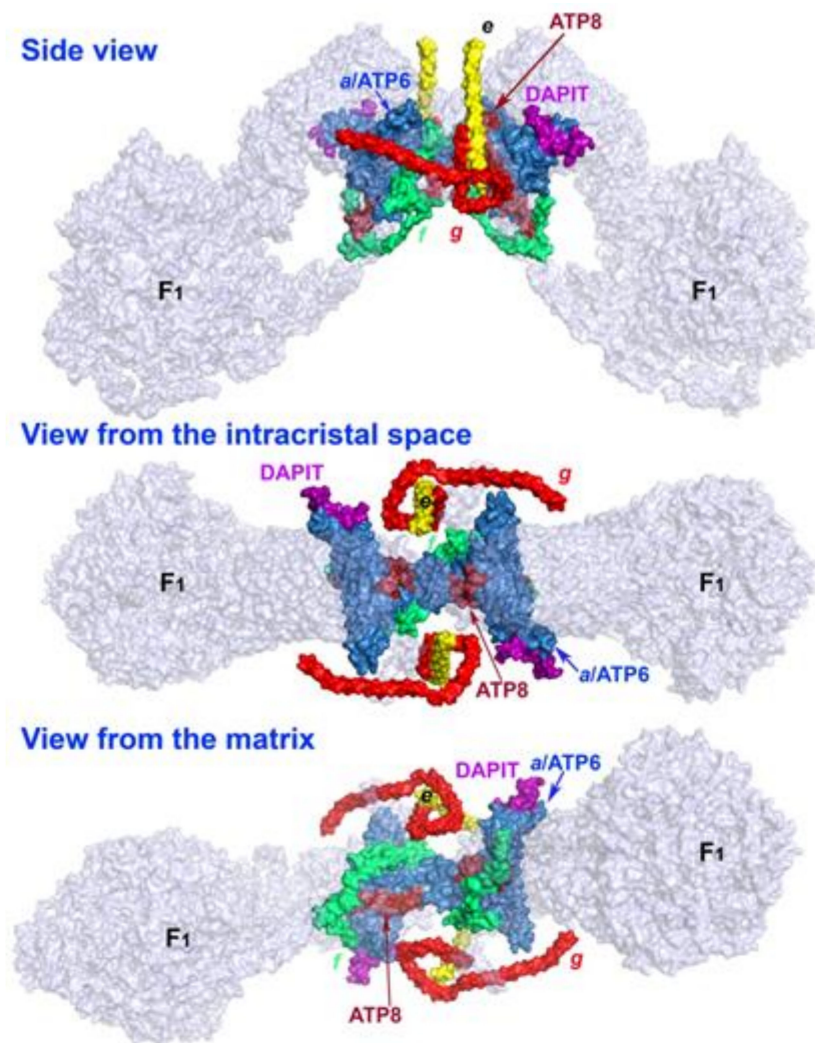


Figure 1. DAPIT location within the ATP synthase structure. Neighbor subunits of DAPIT are shown within the structure of membrane F₀-sector of the ATP synthase. DAPIT and the surrounding subunits are depicted in color, the remaining subunits are transparent. A side view represents a transversal section of the crista rim; a “bottom” view is from the intracristal space directly viewing the inner sharpest IMM bend, when one considers the F₁ moiety being positioned at the top. A top view is also the top view for the crista rim and the top of the sharp edge of the IMM bent. The ATP synthase structure was derived from the atomic model for the dimeric F₀ region of mitochondrial ATP synthase published by Guo H. et al. [37], pdb code 6b8 h. The structure was visualized using the PyMOL Molecular Graphics System, Version 1.8 Schrödinger, LLC.

Despite its name pointing to diabetes (alternatively to *upregulated in skeletal muscle gene 5*, *Usmg5* in the rat genome), the DAPIT protein has not been studied in pancreatic β -cells and there is no knowledge concerning its effect on the regulation of the ATP synthase efficiency and its role in GSIS. Consequently, we attempted to study possible DAPIT role, using the rat pancreatic β -cell line INS-1E.

2. Materials and Methods

2.1. Model Cells

2.1.1. Cell Culturing

Rat insulinoma INS-1E cells were kindly provided by Prof. Maechler, University of Geneva or purchased from AddexBio (San Diego, CA, USA; cat. No. C0018009). The results were invariant of the source as documented in previous reports [8,11,12,38,39]. Cells were cultivated with 11-mM glucose in RPMI 1640 medium with L-glutamine, supplemented with 10-mM HEPES, 1-mM pyruvate, 5% (*v/v*) fetal calf serum, 50- μ mol/L mercaptoethanol, 50 IU/mL penicillin and 50- μ g/mL streptomycin [38,39]. Prior to each experiment, cells were preincubated for 30 min (two washes of 15 min each) in cultivation medium containing 3-mM glucose and 2.5% of fetal calf serum.

2.1.2. Silencing

Silencing of *Usmg5/Dapit* expression was performed with two database-registered siRNAs (#HA13041841, #HA13041842 by Sigma-Aldrich, St. Louis, MO, USA) at final concentration of 50 nM, transfected with Lipofectamine™ RNAiMAX Reagent (13778150, Thermo Fisher, Life Technologies Waltham, MA, USA), following the manufacturer protocol. Effects of siRNA silencing were tested by individual western blots and qPCR to ensure specificity of the silencing. Scrambled-sequence containing siRNA, nonspecific to any *Rattus norvegicus* gene (Scr siRNA), was used as a control.

2.2. qRT-PCR

2.2.1. qRT-PCR Protocol

Total RNA was extracted from cells by the acid guanidinium thiocyanate–phenol–chloroform extraction using Trizol reagent (15596-018; ThermoFisher, Waltham, MA, USA). The reverse transcription was performed using QuantiTect Reverse Transcription Kit (QiaGen, Venlo, The Netherlands; cat. No. 205310), using 1000 ng of RNA previously quantified by NanoDrop 2000 (Thermo Fisher). Real-time polymerase chain reaction was performed with FastStart Essential DNA Green Master Mix (Roche, Basel, Switzerland). The PCR amplification was carried out with initial denaturation at 95 °C for 20 s, followed by 45 cycles of 95 °C for 3 s and 60 °C for 30 s in a LightCycler 96 (Roche). The primers used were as indicated in Table 1. All of them led to a single amplicon product, when the described qRT-PCR procedure was performed. Data were calculated by the $2^{-\Delta\Delta CT}$ method (where CT is cycle threshold and $\Delta\Delta CT$ is CT for the gene of interest minus CT of the internal control), having β -actin ("*Actb*") as an internal control for each experimental condition.

Table 1. Primers used to identify individual transcripts.

	Protein	Sequence
<i>Usmg5</i>	DAPIT	Fw: GATGCCCAATTCCAGTTCAC Rev: CCAGGACACATCCATTCTACC
<i>Atp5i</i>	subunit F _O <i>e</i>	Fw: CACCGTGGCGCCGATGCCATGCCG Rev: AAACCGGCATGGCATAACGGCGGCGCACAC
<i>Atp5j2</i>	subunit F _O <i>f</i>	Fw: GAGAGCTGCCAAGCTGGATA Rev: GTCGCCGTTTCGTGTTTGAG
<i>Atp5l</i>	subunit F _O <i>g</i>	Fw: CACCGCATCCGTAACCTCGCGGACA Rev: AAAGTGTCCGCGAGGTTACGGATGC
<i>Atp6</i>	subunit F _O <i>a</i>	Fw: CGCCACCCTAGCAATATCAA Rev: TTAAGGCGACAGCGATTCT

Table 1. Cont.

	Protein	Sequence
<i>Minos1</i>	Mic10	Fw: GAACATCCCAGCGGGAGAAA Rev: ACTGATGGCACTGTCACAGGA
<i>Atp5f1a</i>	subunit F ₁ α	Fw: TCCAAGCAGGCT GTTGCTTAC Rev: TGT AGGCGGACACATCACCA
<i>Pgc1a</i>	PGC-1 α	Fw: GGAGTGACATAGAGTGTGCTG Rev: CGCGGGCT ATT GTTGTACT
<i>Actb</i>	Actin	Fw: ATCTGGCACCACACCTTC Rev: AGCCAGGTCCAGACGCA
<i>Nd5</i> of mtDNA	ND5	Fw: AACTCCCGTCTCTGCCCTAC Rev: GGCCTAGTTGGCTGGATGTT
<i>Slco2a1</i>	SLCO2A1	Fw: GCAAACCTGGGTCATTGCCT Rev: CCCTCCAAGAGCCGTTTCC

2.2.2. Estimation of mtDNA Copy Number

The mtDNA from model β -cells, INS-1E cells, was isolated by phenol–chloroform extraction. This was followed by SYBR Green qPCR amplification with primers annealing on the *Slco2a1* nuclear gene (encoding solute carrier organic anion transporter family member 2A1) and the *Nd5* mitochondrial gene (bp 11,092 to 11,191 according to GenBank sequences from The National Center for Biotechnology Information, Bethesda, MD, USA) [40]. For primers see Table 1. The ratio between *Nd5* amplicon and half of the nuclear amplicon amounts was taken as the mtDNA copy number per cell.

2.3. Protein Separation Methods and Western Blotting

2.3.1. SDS-Electrophoresis and Western Blotting

To determine relative levels of DAPI/USMG5, ATP synthase α -subunit, PGC-1 α and β -actin proteins, cells were lysed in RIPA buffer (Tris-HCl 20 mM, NaCl 150 mM, Na₂EDTA 1 mM, EGTA 1-mM and NP-40 1%) containing protease inhibitors (1-mg/mL aminocaproic acid, 1-mg/mL benzamidine, 0.2-mg/mL SBTI and 3-mM PMSF) and phosphatase inhibitors (0.012-mg/mL sodium orthovanadate, 4.46-mg/mL sodium pyrophosphate and 4.2-mg/mL sodium fluoride). Total protein concentration was determined by the bicinchoninic acid protein assay (Pierce, Waltham, MA, USA).

Proteins (30 μ g) from lysates were separated by electrophoresis in 12% SDS–polyacrylamide gel (SDS-PAGE). Proteins were transferred to a 0.45 μ m PVDF membrane, which was blocked with 5% non-fat milk in TTBS containing 0.05% Tween-20 at room temperature. Then, the PVDF membrane was incubated overnight at 4 °C with the primary antibody anti-ATPA (Abcam, Cambridge, MA, USA, ab110273), PGC1 (ThermoFisher, PA5–38021), DAPI/USMG5 (Abcam, ab108225) or anti- β -actin mAb (Sigma–Aldrich, A2228) at 1:2000 of dilution, followed by incubation with secondary antibody conjugated to peroxidase at 1:10,000 of dilution (Santa Cruz Biotechnology, Dallas, TX, USA) for one hour at room temperature. Immunoreactive bands were visualized using a chemiluminescent reagent (Western Lightning, PerkinElmer, Waltham, MA, USA) according to the procedure described by the manufacturer. Chemiluminescence was detected by the Chemidoc-IT Imaging System (UVP, LLC) and immunoreactive bands were analyzed by densitometry analysis using the ImageJ software (National Institutes of Health).

2.3.2. Isolation of Mitochondria from INS-1E Cells

Mitochondria were isolated by differential centrifugation in ice-cold medium (180-mM KCl, 5-mM MOPS-K buffer, pH 7.2, 2-mM EGTA and 0.5% bovine serum albumin, BSA) according to a published

procedure [41]. Final mitochondrial pellets were washed by resuspension/centrifugation in the isolation medium lacking BSA. The protein content was determined by the BCA method (Sigma).

2.3.3. Blue-Native and Clear-Native Electrophoresis

ATP synthase oligomerization was analyzed by one-dimensional blue native (BN-) and clear native (CN-) polyacrylamide gel electrophoresis (PAGE). Protein complexes were extracted from INS-1E cells or INS-1E cell mitochondria using digitonin (Thermo Fisher; 2.5:1, *w:w*, protein:digitonin ratio). The obtained lysates were separated on bis-Tris 3%–13% gels. Following BN/CN PAGE proteins were transferred by wet electroblotting onto PVDF membranes. ATP synthase and DAPIT were immunodetected with monoclonal antibodies against the ATP synthase F₁ α -subunit (Abcam, ab110273) and DAPIT/USMG5 (Abcam, ab108225) after acidic membrane-stripping.

2.4. ATP Assay

Before the experiment, siRNA-transfected cells were preincubated for 2 h in the KRH buffer with 0.1% fatty acid-free BSA and indicated glucose concentrations. Quantification of ATP was performed using the ATP Assay bioluminescence kit HSII (Roche). Cells were mixed with boiling lysis buffer (100-mM Tris, 4-mM EDTA, pH 7.75) and further boiled for 2 min. Samples were centrifuged at 10,000× *g* for 1 min. Diluted supernatants were mixed with luciferase reagent and a Synergy HT luminometer was used to read the bioluminescence. To confirm that the assay procedure does not interfere with the ATP concentration determination, internal ATP standards were added to the samples during the initial experiments.

2.5. High Resolution Respirometry

Routinely, an oxygraph 2k (Oroboros Instruments GmbH, Innsbruck, Austria) has been used for experiments checking respiration of INS-1E cells as described elsewhere [11,12].

2.6. Transmission Electron Microscopy

Cells were cultured on poly-L-lysine-coated petri dishes. For transmission electron microscopy (TEM), cells were fixed for 24 h in 0.1-M cacodylate buffer (pH 7.2) containing 2.5% glutaraldehyde and postfixed in 2% OsO₄ in the same buffer. For visualization of conspicuous membranes of mitochondria, post fixation was performed with 2% OsO₄ plus 0.8% K₄Fe(CN)₆ in a PBS buffer. Fixed samples were dehydrated through an ascending ethanol and acetone series and embedded in araldite–Poly/Bed[®] 812 mixture (ThermoFisher, Waltham, MA, USA). Thin sections were cut on a Reichert-Jung Ultracut E ultramicrotome and stained using uranyl acetate and lead citrate. Sections were examined and photographed using JEOL JEM-1011 electron microscope. Fine structure measurements were performed using a Veleta camera and iTEM 5.1 software (Olympus Soft Imaging Solution GmbH, Hamburg, Germany).

2.7. Experiment with Mice

2.7.1. Mice

C57BL/6 mice were obtained from The Jackson Laboratory, Bar Harbor, MN. Experiments were approved by the Animal Care and Use Committee (Inst. Molecular Genetics, ASCR) in accordance with the European Union Directive 2010/63/EU for animal experiments, U.K. Animals (Scientific Procedures) Act, 1986 and the Guide for the Care and Use of Laboratory Animals (NIH Publication No. 85–23, revised 1996) and the ARRIVE guidelines (www.nc3rs.org.uk/ARRIVE).

2.7.2. Experiments with Hyaluronic Acid Implants

Our protocol was adopted from Praveen et al. [42,43]. Hyaluronic acid implants were a kind gift from Dr. Semira Kwabi from Skin Clinic UK. A Juvederm Ultra 4 hyaluronic acid filler was

mixed with D-glucose to a final concentration of 10 M. Such preparation (either 100 μ L or 200 μ L) was subcutaneously implanted to mice. Typically, two weeks of treatment with hyaluronic acid implants of the designated volumes were performed. Pancreases were removed from three mice and mRNA was isolated using an RNA isolation kit (Qiagen). This was followed by qRT-PCR as described above. Alternatively pancreatic islets were isolated from three pooled pancreases as described elsewhere [40].

2.8. Statistical Analysis

Results are presented as mean \pm standard deviation (SD) for N number of biologic replicates or total number of estimates (n). Graphs were plotted and statistical analyses were performed using SigmaPlot 6.0 and SigmaStat 3.1 (Systat Software, San Jose, CA, USA) and ANOVA followed by the Tukey's test on the pre-validated data; or, alternatively using a Prism (GraphPad Software, San Diego, CA, USA) and an unpaired Student's t -test (when comparing two groups) or one-way nonparametric ANOVA (Tukey's test) followed by Bonferroni post hoc analysis (for the comparison of more than two groups) or correlation analysis. Statistical significance was set at *** $p < 0.001$; ** $p < 0.05$; * $p < 0.1$.

3. Results

3.1. Expression of DAPIT and Other F_0 Subunits Varies according to Metabolic State in INS-1E Cells

INS-1E cells are routinely cultured with 11-mM glucose, thus keeping optimum autocrine factors and *Ins* gene expression [39,41]. Hence, we attempted to study dependencies on glucose for selected subunits of the membrane F_0 moiety of the ATP synthase, starting with DAPIT. To do this, glucose was first depleted from INS-1E cells, using short prewashing in PBS followed by two 15-min washings in the culturing medium with 3-mM glucose and a half-content of the fetal calf serum. Cells were subsequently incubated at 3 mM, 11-mM and 20-mM glucose in the KRH buffer for up to 120 min. The *Usmg5/Dapit* transcript frequently decreased after the two consequent 15 min preincubations with 3-mM glucose (Supplementary File 1; Figure S1a) and for some cell passages we have encountered decreased DAPIT mRNA even after the initial PBS wash. One may regard these conditions as simulating fasting state in vivo, when a slower rate of metabolism is established; nevertheless, for cultured cells this treatment represents a certain form of shock.

Further incubation in KRH containing 11 mM or 20-mM glucose led frequently to restoring the initial levels of DAPIT mRNA already after 30 min (Supplementary File 1; Figure S1a). With further incubations at 20-mM glucose up to 120 min, DAPIT transcript increased up to the ratio to β -actin about 2.5 for some cell passages (Supplementary File 1; Figure S1b). The extent of such elevation was variable, most probably depending on the variability in the initial pretreatment. Nevertheless, specificity of this qRT-PCR assessment was checked in conjunction with pre-transfection by DAPIT siRNA. Indeed, if elevations of DAPIT transcript occurred in control INS-1E^{Scr1} cells (transfected with siRNA containing the scrambled sequence), they vanished when cells were silenced for DAPIT (Supplementary File 1; Figure S1b). Moreover, when cells were left in the medium with 11-mM glucose up to 120 min, DAPIT mRNA started to rise around 60 min (Supplementary File 1; Figure S1c). When glucose was initially set to 20 mM, the elevations of DAPIT mRNA levels were higher around and after 30 min (Supplementary File 1; Figure S1c). We may interpret these elevations as responses to the elevated metabolism and beginning at 60 min even some biogenesis could take place. Investigations of these aspects are reported below.

Dealing with the other three selected subunits of the ATP synthase membrane F_0 sector, i.e., subunits *e*, *f* and *g*, their transcripts were less sensitive to pretreatments in the medium containing 3-mM glucose, except of *g* (Supplementary File 1; Figure S2a–c). As expected, DAPIT silencing had no effect to the mRNA recovery of these subunits due to the accelerated metabolism (Supplementary File 1; Figure S2d–f). Their recoveries/elevations were nearly synchronous with those found for DAPIT mRNA.

3.2. Upregulation of DAPIT in Pancreatic β -Cells in Mice

Next, we investigated, whether any glucose-induced upregulation of DAPIT exists in vivo in mice (Figure 2a–e; Figure 3a–h; Figure 4). The transcript of mouse *Usmg/Dapit* was estimated in whole pancreases (Figure 2a,b,d), as well as in the isolated pancreatic islets (Figure 2c). Up to 2 weeks of diffusion of glucose was allowed from the hyaluronic acid implants inserted into the omentum of Black6/J mice (Figure 2a). Attained fasting blood glucose levels reached on average to 7.5 and 9-mM for 100 μ L and 200 μ L volumes of implants, respectively (Figure 2e). The observed increases relatively to β -actin in whole pancreases (Figure 2b) and isolated islets (Figure 2c) support the existence of the glucose-induced expression of DAPIT in vivo. Similarly, an increase in F₁ subunit α mRNA was pronounced in mice having glucose delivery by the implants (Figure 3e), as well as increases in mRNA of the other selected membrane F_O sector ATP synthase subunits (Figure 3a,b,d,f–h), except of subunit g (Figure 3c). In conclusion, two-week glucose delivery induced expression of the ATP synthase subunits of the membrane F_O sector and subunit α , as a major subunit of the F₁ moiety.

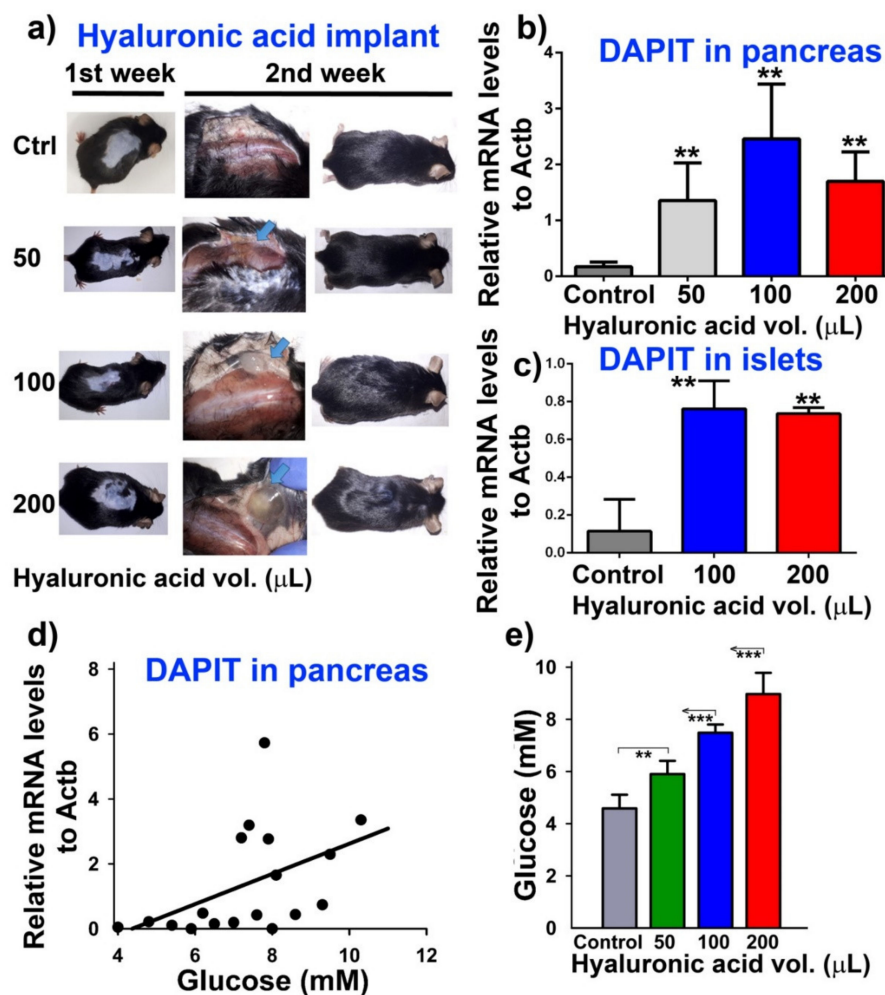


Figure 2. Upregulation of DAPIT in pancreas and pancreatic islets in mice. (a) typical experiment, (b,d) DAPIT mRNA in pancreas (c) in isolated pancreatic islets after two weeks of treatment with hyaluronic acid implants of the designated volumes. Data were mutually significantly different ($N = n = 5$ mice per group): ** $p < 0.05$ (except 50 vs. 200 μ L) as well as data vs. control in (c); (d) dependence of DAPIT transcript in pancreas vs. glucose; resulting from fasting glucose levels in mice, calibrated relatively to volume of hyaluronic acid (see panel (e); *** $p < 0.05$). Spearman coefficient for obtained fit is 0.56; $p = 0.015$.

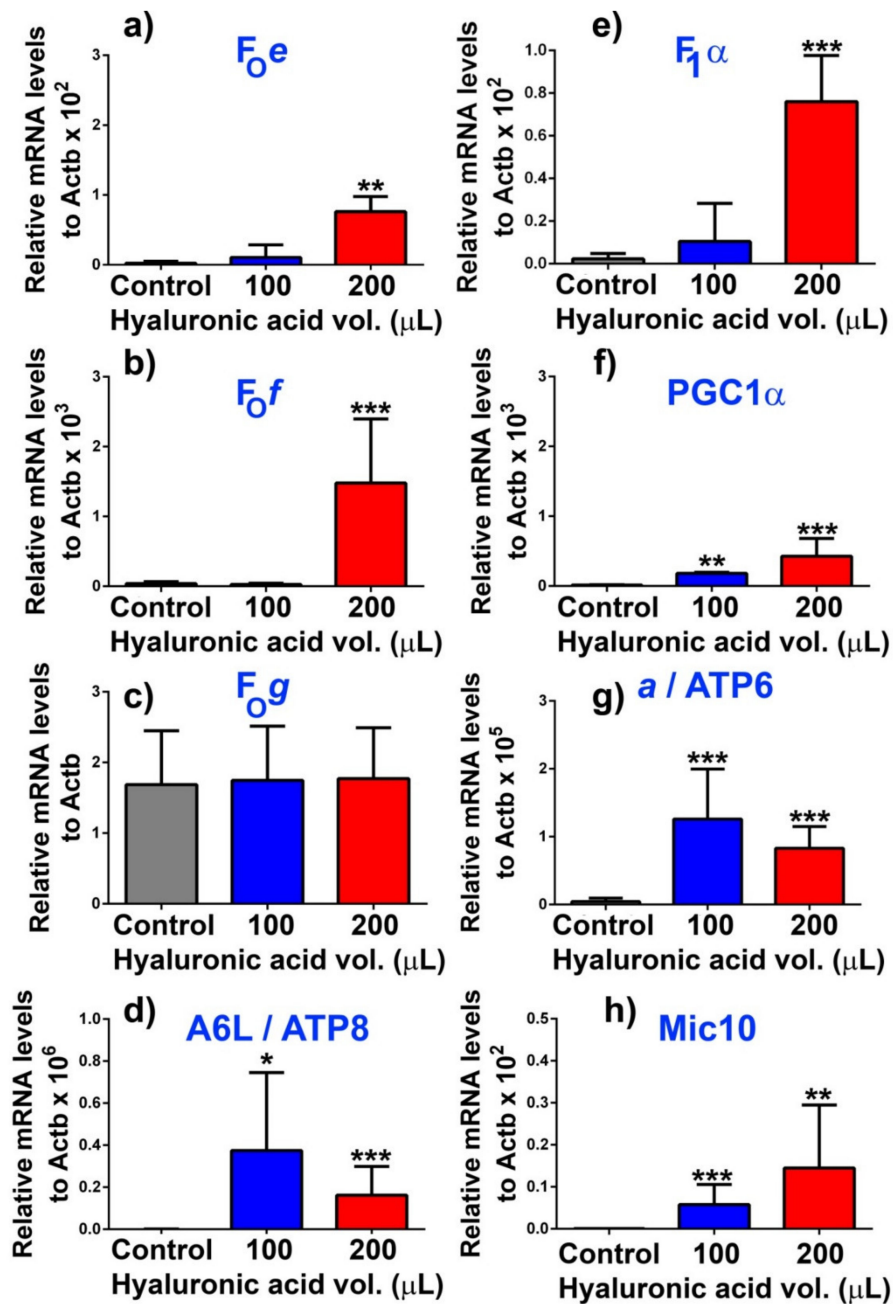


Figure 3. Upregulation of transcripts of other ATP synthase subunits (a) F_{Oe} , (b) F_{Of} , (c) F_{Og} , (d) A6L/ATP8, (e) $F_1\alpha$, and (g) ATP6 and (f) PGC1 α and (h) and Mic10 in pancreatic islets in mice—after two weeks of treatment with hyaluronic acid implants of the designated volumes. Data except in panel (c) are mutually significantly different ($N = n = 5$ mice per group): *** $p < 0.001$; ** $p < 0.05$; * $p < 0.1$ (with exception of controls vs. 100 μ l in panels (a,b,e).

Note that the applied procedure did not induce any glucose intolerance as documented by the time courses of insulin release after glucose injection (Figure 4) and concomitantly performed glucose tolerance tests (Figure 4). With higher implant volumes, mice had rather exhausted fasting insulin levels, possibly reflecting starting hypoinsulinemia. Nevertheless, insulin release time course was identical to sham-operated controls (Figure 4).

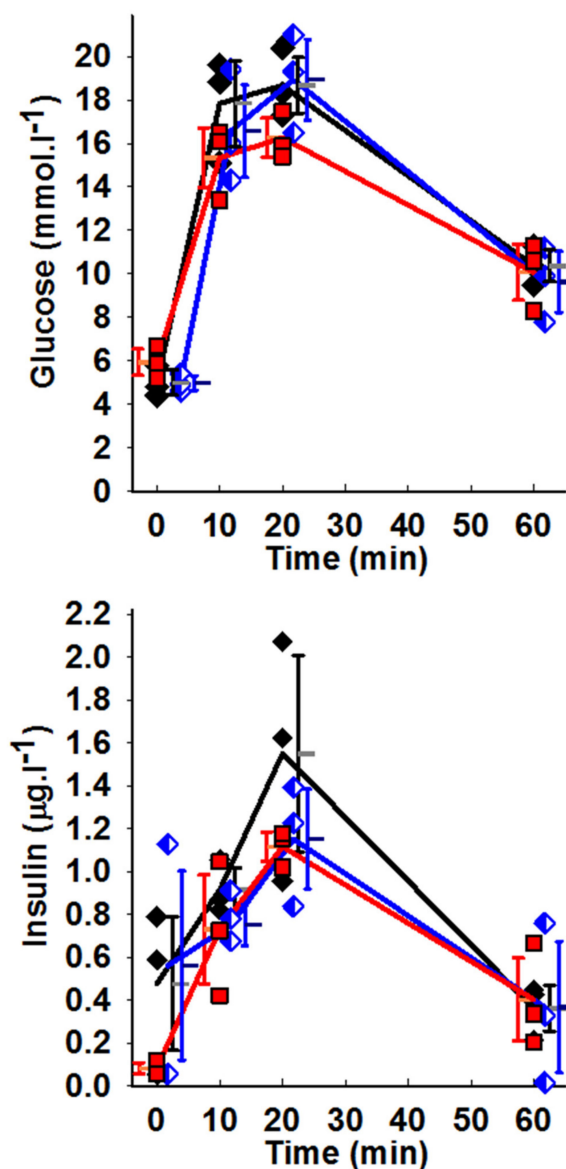


Figure 4. Time course of glycemia and insulin release —i.e., intraperitoneal glucose tolerance test and insulin time course, performed as described in Ref. [8], after a single glucose dose. Mice were treated for two-weeks with hyaluronic-acid implants with no glucose (black symbols represent sham operation); 100 μ L (blue symbols) and 200 μ L of implants (red symbols). $N = 3$ mice at each time point. Note for rather exhausted fasting insulin levels (at time zero) for treatment with 200 μ L of implants.

3.3. Glucose Independent but DAPIT-Dependent Mitochondrial Biogenesis in INS-1E Cells

Turning attention back to INS-1E cells, we further investigated possible glucose-induced mitochondrial biogenesis, to answer a question whether any glucose-induced replication of mitochondrial DNA (mtDNA) and/or PGC-1 α expression exists. Both, when elevated, reflect the initiation of mitochondrial biogenesis. We found that the mtDNA copy number and PGC-1 α (mRNA and protein) were not enhanced until 60 min and 120 min, respectively, lasting from the end of pretreatment (from the two 15-min preincubations with 3-mM glucose) (Figure 5a–g). Elevations of mtDNA copy number became significantly ~ 1.5 higher after 60 min and 3-fold higher after 120 min with all tested glucose concentrations but zero (Figure 5a). For these experiments, INS-1E cells were transfected with siRNA containing the scrambled sequence (i.e., INS-1E^{Scrl} cells were used).

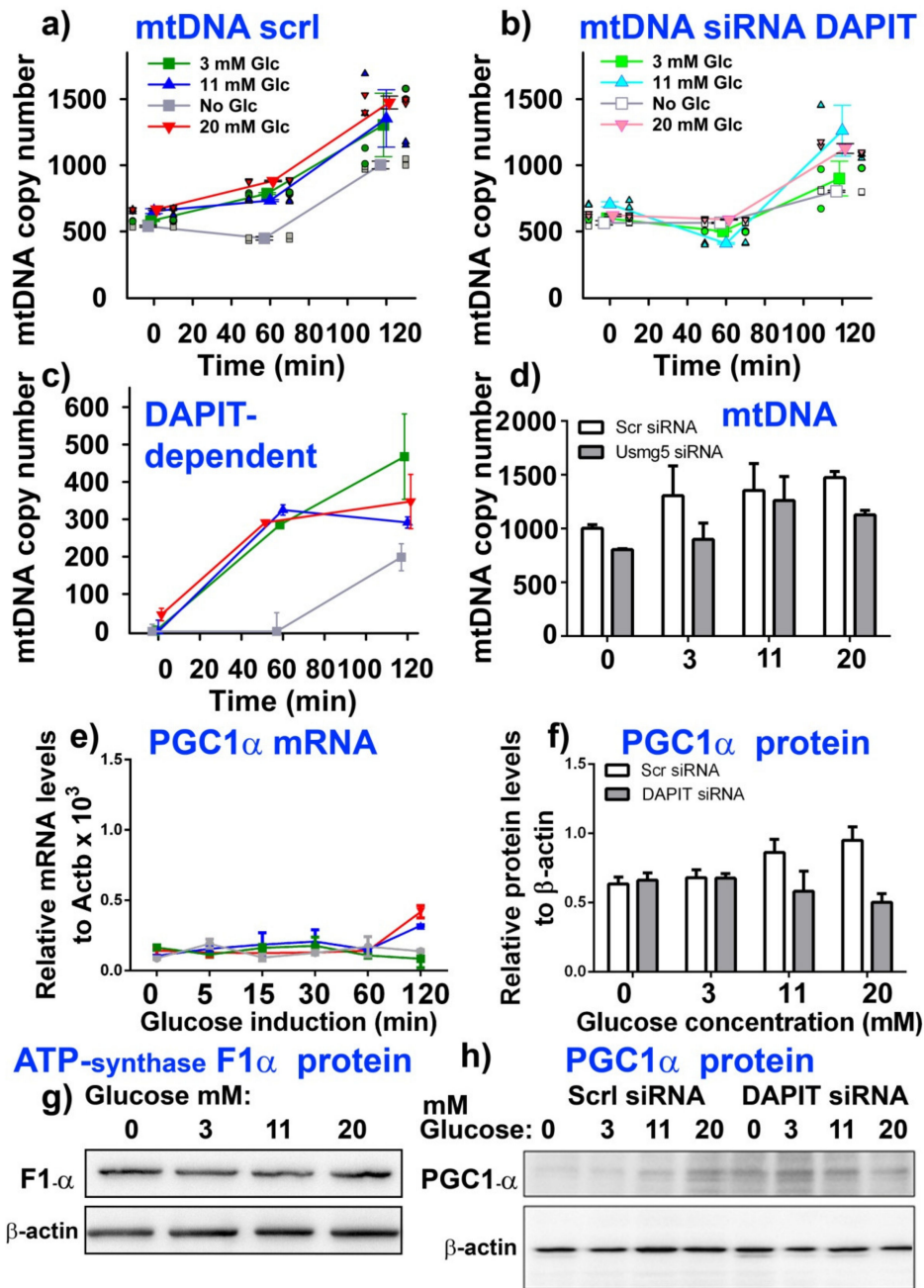


Figure 5. Glucose-induced expression of mitochondrial biogenesis. Time course (a–c) and glucose concentration dependence (d) for DAPIT-dependent increase in mitochondrial DNA copy number. Panels (a,b) show individual data plus their averages, while (c) shows the DAPIT-dependent increase in copy number. Changes in transcript of PGC-1 α (e) and PGC-1 α protein (N = 3) (f,h) and F₁ α protein (g) are shown. ANOVA (N = 4): (a,b) vs. zero glucose: ** p < 0.05; *** p < 0.001. Full size western blot of panel (g) and F₁ α mRNA see Supplementary File 1, Figure S4. For (e), thresholds yielded by RT-PCR concerning the PGC-1 α amplicon were in triplicates as follows: 24.6; 24.4 and 24.5 for samples of zero glucose, whereas samples treated with 20-mM glucose yielded 22.76; 23.06 and 22.9.

No increase at 60 min, but a smaller increase at 120 min, was recognized for INS-1E cells silenced for DAPIT (Figure 5b; see Supplementary File 1, Figure S3 for silencing efficiency). As a result, only a portion of increases in mtDNA copy number was DAPIT dependent (Figure 5c); however, even this portion did not depend on glucose. Rather permanent mtDNA replication proceeded, as recognized

also when no glucose was added while estimating the time course. Thus, the initial effective mtDNA replication was dependent on DAPIT, i.e., on a complete ATP synthase expression/assembly.

PGC-1 α mRNA increased apparently only at 120 min (Figure 5e), similarly to protein levels (Figure 5f,h). In INS-1E silenced for DAPIT, the levels of PGC-1 α protein were nearly equal to those in controls for zero and 3-mM glucose but with 20-mM glucose the PGC-1 α protein decreased by 25% relative to zero glucose, which was about 50% relative to INS-1E cells transfected with the scrambled siRNA (Figure 5f,h). Levels of PGC-1 α were not affected by the pretreatment with 3-mM glucose (not shown). Furthermore, F₁ α subunit mRNA and protein did not change (Figure 5g; Supplementary File 1; Figure S4).

3.4. ATP Levels Correlate with DAPIT Expression Induced by Glucose in INS-1E Cells

Seeking for consequences of DAPIT deficiency, we estimated elevations in the total cellular ATP levels during parallel incubations of INS-1E cells with different glucose concentrations and timing, comparing cells transfected with DAPIT siRNA vs. those transfected with siRNA containing scrambled sequence. Cells were again routinely pretreated by two 15 min pre-incubations with 3-mM glucose. The initial increase was apparent during the 120-min time course for absolute total ATP levels (Figure 6a), despite the constant levels of subunits F₁ α (Figure 5g). Since mitochondrial biogenesis was beginning at around 60 min, as documented above, the initial increases in the total ATP content must originate exclusively from the elevated ATP synthesis by the existing and probably constant number of ATP synthase molecules. This is due to the enhanced metabolism initiated by the added glucose. Such an increase is retarded after 15 min (Figure 6a). Then biogenesis may contribute to the second phase of the observed increase in the total ATP. These two phases are better recognized when the incremental ATP increases were calculated, i.e., when values of the total ATP content was subtracted for samples when no glucose is added (Supplementary File 1; Figure S5).

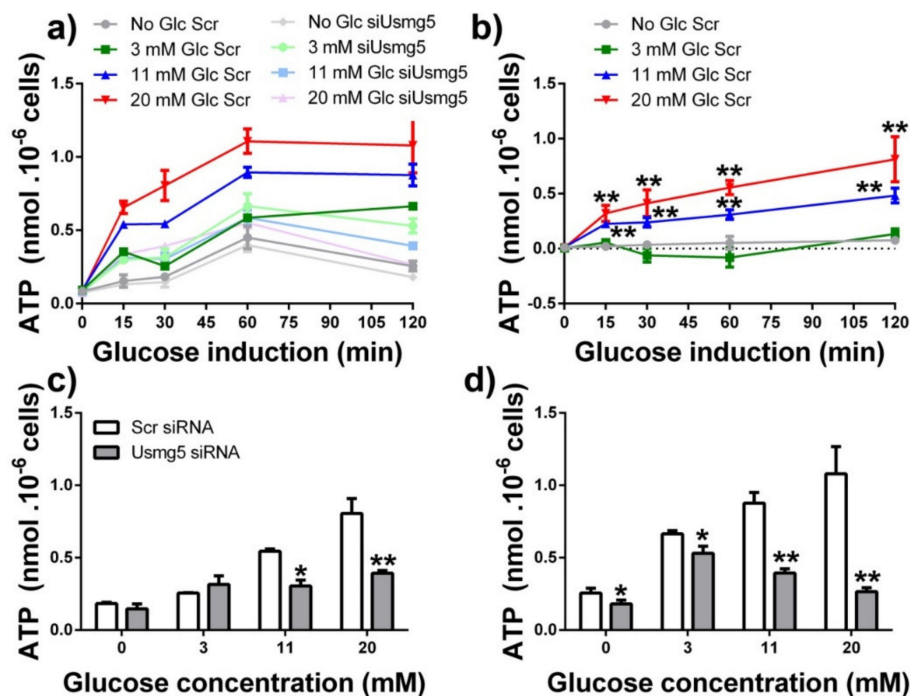


Figure 6. ATP levels in INS-1E cells. (a) Time course of the total ATP levels upon glucose induction in INS-1E cells transfected with scrambled siRNA (color coding as in Figure 1) or *Dapit/Usmg5* siRNA as indicated; (b) DAPIT-dependent part of the total ATP levels (data for *Dapit* siRNA were subtracted from data of scrambled sequence containing siRNA) after glucose induction; (c,d) Glucose dependencies constructed from the data of panel (a). $p < 0.001$ for 11 and 20-mM glucose in (c,d). Data were significantly different from zero (3 mM) glucose data as indicated ($N = 3$): ** $p < 0.05$; * $p < 0.1$.

When induced with 11 and 20-mM glucose, at least half of the incremental ATP increase was dependent on expression of DAPIT, since only about less than half and ~30% of the incremental ATP increase was reached at 30 min and 120 min, respectively, upon DAPIT silencing (Figure 6a). Thus, when induced with 3-mM glucose, the rise of total ATP with time was independent of DAPIT since data were equal to those upon DAPIT silencing (Figure 6a).

Estimating the total ATP content which would be related to the DAPIT presence, we subtracted the time courses measured in INS-1E cells transfected with DAPIT siRNA from controls transfected with siRNA having scrambled sequence (Figure 6b). Clearly, no ATP increase related to DAPIT exists without the induction by glucose and when induced only with 3-mM glucose. In contrast, when induced with 11 and 20-mM glucose, the revealed biphasic DAPIT-dependent accumulation was similar as the net ATP surplus but reaching about 50% of ATP elevations and about 50% initial rate (Figure 6b). If we anticipate that the ablation of DAPIT using siRNA was incomplete, one may expect even higher inhibition of the ATP surplus at completed DAPIT ablation. The glucose concentration dependence at 15 min and 120 min (Figure 6c,d) again indicated a substantial increase in ATP. In DAPIT-deficient INS-1E cells, absolute ATP levels were insignificantly different with 3-mM glucose, but with 11 and 20-mM glucose the total ATP went drastically down. All these results show that the DAPIT, and therefore the complete ATP synthase, is required for the maximum synthesis of ATP.

3.5. Phosphorylating Respiration of INS-1E Cells at High Glucose Partially Depends on DAPIT

To estimate independently whether a direct correlation exists between ATP synthesis and DAPIT levels, we evaluated INS-1E cell respiration by standard bioenergetics tests using an oxygraph after 120-min incubations with different glucose concentrations in the KRH buffer, after two previous washings in KRH only (Figure 7a–d). The ratios between phosphorylating vs. non-phosphorylating rates of respiration (V_3/V_4) were derived (Figure 7e). In control INS-1E^{Scr1} cells, these ratios physiologically increased from 1.1 to 2.6 and 2.9, when glucose was raised from 3 mM (representing the insulin non-stimulating levels) to 11 mM and 20 mM, respectively (Figure 7e). The latter two concentrations of glucose are stimulating the release of insulin (see below). The V_3/V_4 ratios with 11-mM glucose upon DAPIT silencing were statistically insignificantly different from those in controls (siRNA with scrambled sequence) but at 20 mM, the V_3/V_4 ratio was significantly lower by ~30%. This perfectly matches the DAPIT contribution to the ATP accumulation (Figure 6a,b).

The total capacity of the respiratory chain can be expressed as the maximum respiration rate V_{max} , evaluated by titration with an uncoupler FCCP, to reach maximum and saturated respiration. With increasing glucose from 3 to 11 mM, values of V_{max} respiration increased 1.5-fold and stayed nearly the same at 20-mM glucose, independently of DAPIT silencing (Figure 7d). We can derive an alternative parameter $R_{ATP\ synthesis}$, expressing the portion of the total respiratory chain capacity required for ATP synthesis, as $(V_3 - V_4)/V_{max}$. The calculated values of $R_{ATP\ synthesis}$ reached only 5% at 3-mM glucose for INS-1E^{Scr1} cells or cells transfected with DAPIT siRNA. Independently of DAPIT silencing, the $R_{ATP\ synthesis}$ ratios increased to about 40% with 11-mM and 20-mM glucose (Figure 7f).

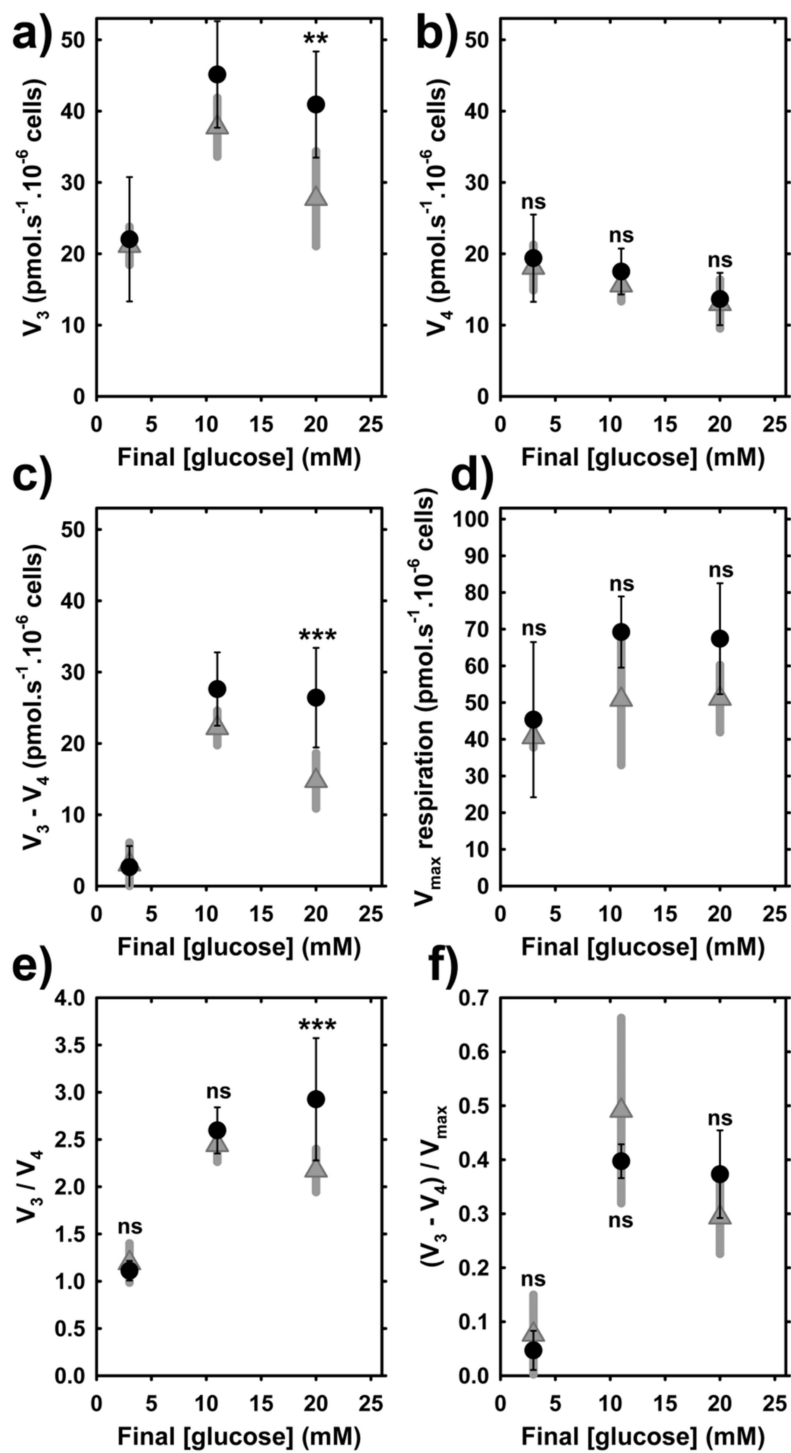


Figure 7. Respiration of control and DAPIT-silenced INS-1E cells. Glucose concentration dependencies for 120 min induction ($N = 4$, $n = 6-8$), after which respiration of was estimated in INS-1E cells transfected with scrambled sequence containing siRNA (black) or *Dapit/Usmg5* siRNA (gray) (data, SDs) such as: (a) phosphorylating (basal) respiration rates (V_3); (b) non-phosphorylating respiration rates (V_4); (c) ATP synthase-related respiration rates ($V_3 - V_4$); (d) maximum respiration rates V_{max} (derived from titration with an uncoupler FCCP); (e) Ratios V_3/V_4 , i.e., between phosphorylating vs. non-phosphorylating respiration rates; and (f) $R_{ATP\ synthesis}$, i.e., portion of total respiratory chain capacity required for the ATP synthesis calculated as $(V_3 - V_4)/V_{max}$. *** $p < 0.001$, ** $p < 0.05$ for significant differences of DAPIT-silenced vs. cells transfected with scrambled siRNA.

3.6. Insulin Release Is Insignificantly Affected by the Profoundly Decreased DAPIT Expression in INS-1E Cells

Next, we estimated time courses of secreted insulin during 120-min incubations of INS-1E cells while using different glucose concentrations added initially (Figure 8a,b). At no glucose addition a small basal rate of insulin release was found (Figure 8a). A similar low linearized rate occurred after the initial addition of 3-mM glucose (Figure 8b). When induced with 11-mM (Figure 8b) and 20-mM glucose (Figure 8a), a nearly linear dependence of the released insulin vs. time up to 120 min reflected the established high rate of insulin secretion at these two stimulating concentrations. Differences between these rates and the basal rate at zero glucose addition represent the net GSIS rate. Surprisingly, the net GSIS rate did not vanish upon DAPIT silencing (Figure 8a,b). When induced with 11 and 20-mM glucose, the net GSIS rate in DAPIT-silenced INS-1E cells accounted for 90% and 80%, respectively, of the mean net GSIS rate for control INS-1E^{Scr1} cells. The effect after around 100 min may contain a contribution of mitochondrial biogenesis occurring during the time course of this experiment, since the PGC-1 α transcript 1.5-fold increased during the same period as well as mtDNA copy number.

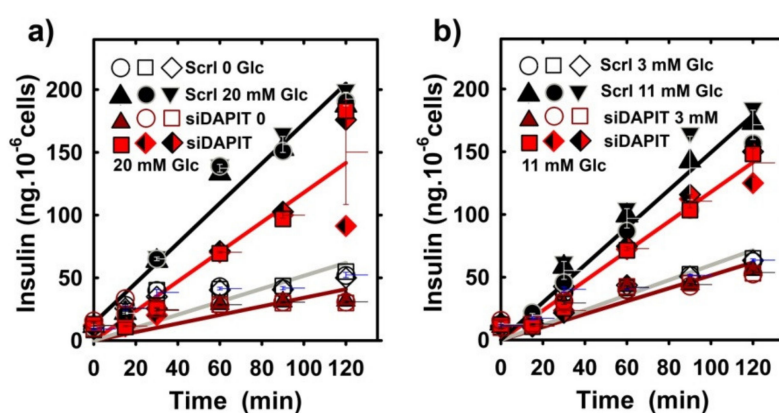


Figure 8. Insulin release in INS-1E^{Scr1} cells vs. DAPIT-silenced cells. Time course of the accumulated insulin with no addition (a) and after the addition of 3-mM (b), 11-mM (b) and 20-mM glucose (a). Data originate from $N = 3$ time courses for each condition. Legend: “Scr1”, INS-1E^{Scr1} cells; “siDAPIT”, DAPIT-silenced INS-1E cells.

3.7. Morphology of Mitochondrial Cristae Does Not Change with DAPIT Deficiency

Next, we evaluated possible changes in morphology of mitochondrial cristae as consequences of the DAPIT deficiency. We were unable to reach substantial changes in cristae morphology, such as those reported elsewhere [35,36]. The resultant transmission electron microscopy (TEM) images showed that the cristae morphology did not significantly change upon the DAPIT silencing (Figure 9a–g).

However, the previously described [17] cristae narrowing upon transition from a low to high glucose proceeded also in DAPIT-silenced cells, albeit in a lower extent, since cristae width was rather smaller within the estimated ensemble (275, 275 and 450 estimates in 20, 11 and 3-mM glucose, respectively), when compared to INS-1E cells transfected with scrambled siRNA. Further studies are required to investigate what stands behind the literally cell memory regarding glucose levels. Indeed, the *in vivo* glucose-dependent changes persist during the isolation procedure of mitochondria. The fact that the *in vivo* situation is reflected by certain persisting structural (e.g., of cristae) and/or conformational pattern suggests that this is due to a specific persisting assembly of the ATP synthase or other cristae-shaping proteins. Note also, that at 3-mM glucose ATP synthase tetramers largely disappeared and hexamers vanished (Figure 10a,b), as reported elsewhere for hypoxic HepG2 cells [18,44].

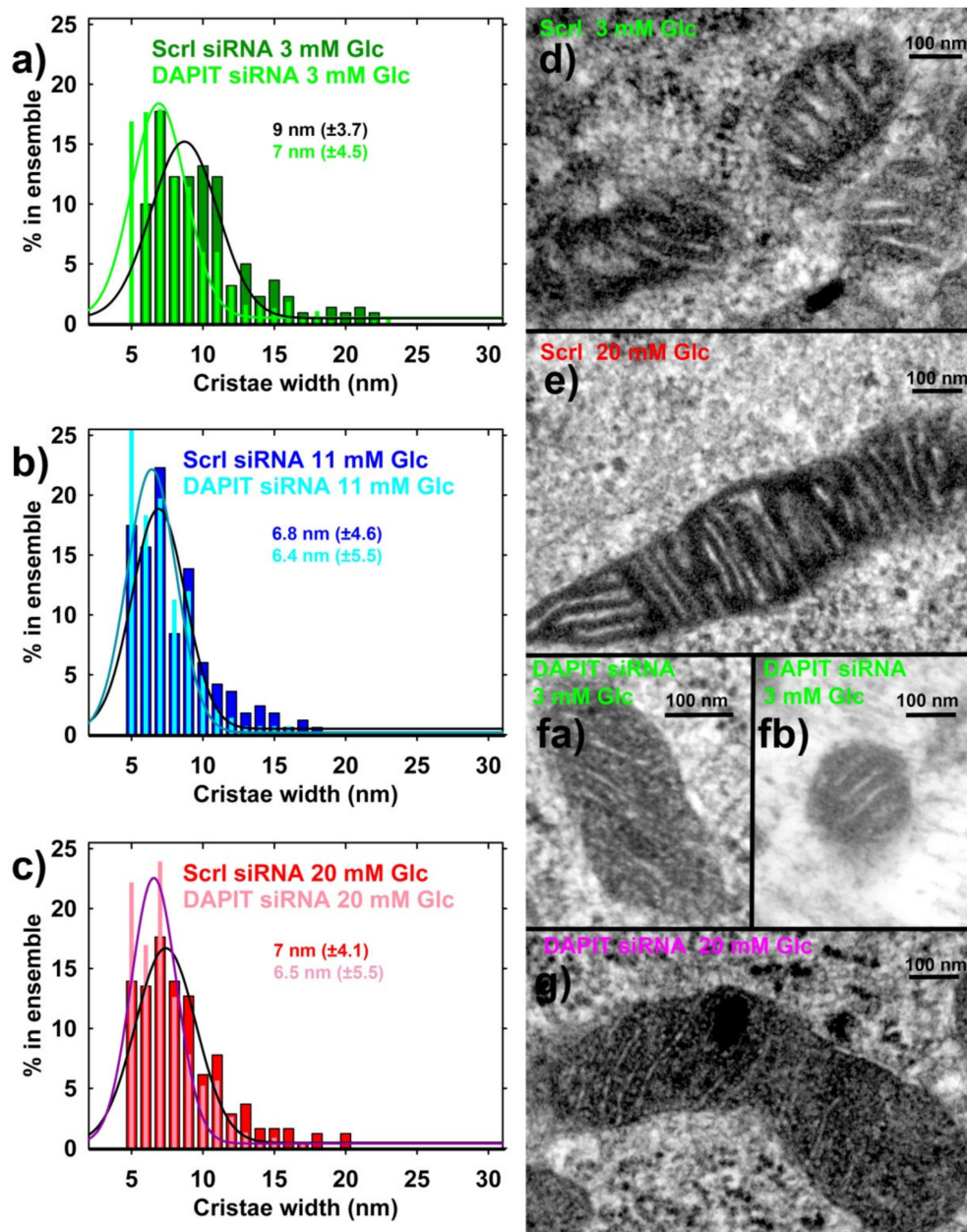


Figure 9. Mitochondrial cristae in DAPIT-deficient INS-1E cells—i.e., silenced for DAPIT, when compared to INS-1E cells transfected with scrambled siRNA ($N = 2$). (a–c) SDS–polyacrylamide of cristae width; (d–g) exemplar TEM images of sections of mitochondrial tubules (i.e., “mitochondria”). Independent incubations with the designated glucose concentrations were performed twice, while $n = 275$ crista width estimations were made from 15 TEM images for each condition ($n = 450$ for DAPIT siRNA at 3-mM glucose). Values of most frequent crista width are listed with SDs taken as 0.5 of half-width, as derived from Gaussian fits of the data (displayed on histograms).

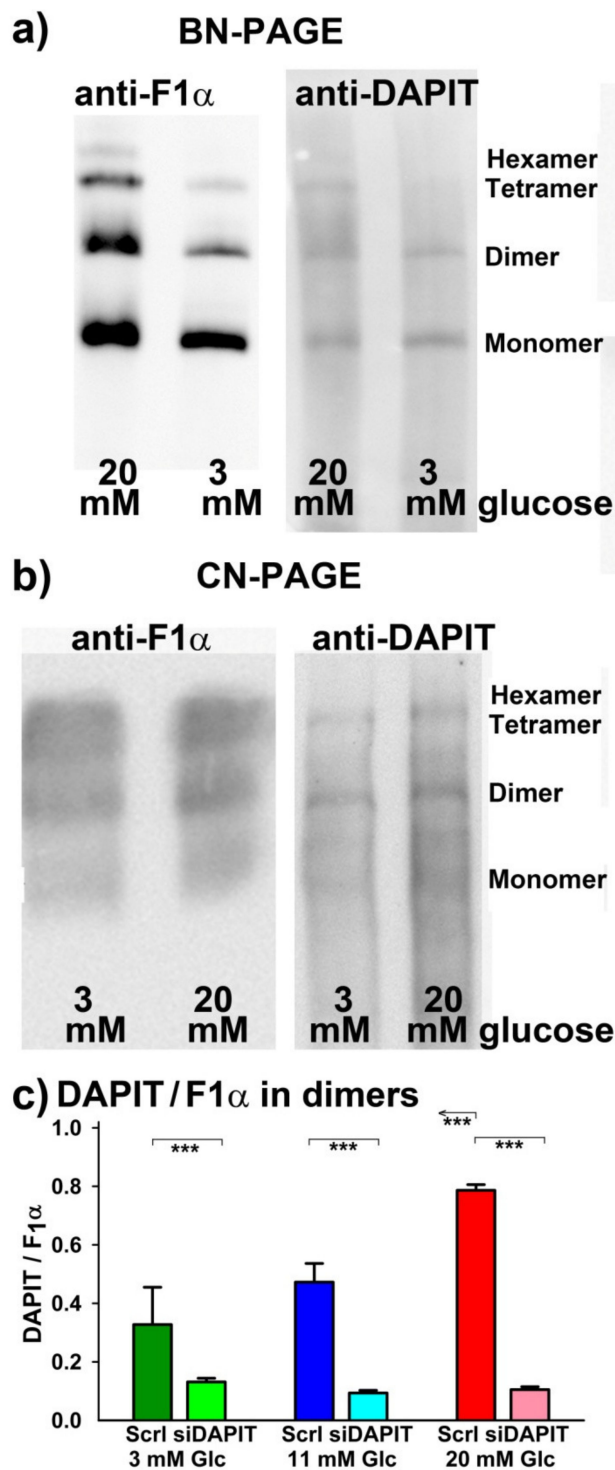


Figure 10. Rough estimations of DAPIT to F₁α stoichiometry in ATP synthase dimers. (a) Exemplar BN-PAGE shows missing hexamers and majority of tetramers at 3-mM glucose; (b) CN-PAGE immunostained with anti-F₁α or anti-DAPIT antibody as indicated; (c) DAPIT/F₁α stoichiometry was estimated from N = 3 CN-PAGEs separating ATP synthase monomers/oligomers after dual western blotting. *** p < 0.001 (n = 3), for significant differences of DAPIT-silenced vs. INS-1E^{Scrl} cells.

3.8. Rough Estimation of Stoichiometry for the DAPIT Relatively to the ATP synthase F₁α

Finally, we attempted to derive how the DAPIT to F₁α stoichiometry may change with the increasing glucose. Moreover, we verified whether such stoichiometry approaches to zero upon

DAPIT silencing. Thus, parallel BN-PAGEs (Figure 10a) and parallel CN-PAGEs (Figure 10b) were run, followed by western blotting, and were immunostained either against $F_1\alpha$, to distinguish monomeric, dimeric and tetrameric ATP synthase; or against DAPIT (Supplementary File 1; Figure S6), to identify roughly its bound amount to either monomeric, dimeric and tetrameric ATP synthase. Acid stripping of PVDF membranes allowed to cross-correlate antigen amounts.

Typical results of semiquantification from CN-PAGE are shown in Figure 10c, estimating only situation in dimers, i.e., anti-DAPIT antibody staining density ratios relatively to the immunostaining of ATP synthase dimers by anti- $F_1\alpha$ antibodies. Our attempts to evaluate these ratios relatively to tetramers failed due to a rather highly variable fraction of tetramers occurring in CN-PAGEs. Thus, we repeatedly found that the apparent staining ratio of DAPIT to $F_1\alpha$ exclusively among the fraction of dimers was increasing at 20-mM glucose (and slightly at 11 mM) relatively to 3-mM glucose (Figure 10c). The expected theoretical maximum saturated stoichiometry should be 2:6 within a single dimer of the ATP synthase. Different antibody efficiency prevents to get absolute stoichiometry values. Note also, that at 3-mM glucose ATP synthase tetramers largely disappeared and hexamers vanished (Figure 10a,b), as reported elsewhere for hypoxic HepG2 cells [18,44].

4. Discussion

In this work, we demonstrated that when a fraction predominates of vestigial ATP synthase molecules deficient of USMG5/DAPIT, rat pancreatic β -cells (INS-1E cells) almost do not elevate ATP levels as responding to high glucose. Despite these levels were merely elevated only by 6%, such DAPIT deficiency surprisingly did not inhibit glucose-stimulated insulin secretion (GSIS). The latter result represents a remarkable paradox, specific for pancreatic β -cells. The glucose-stimulated insulin secretion (GSIS) was not substantially hampered in DAPIT-deficient cells. This paradox can be explained on the basis of the recently revisited mechanism for the induction of insulin exocytosis. We demonstrated that H_2O_2 , originating from NADPH oxidase-4 (NOX4), is essentially required together with ATP, as a logical sum for insulin secretion stimulated with glucose [8]. Candidate NADPH oxidases, i.e., unidentified isoforms, were implied in GSIS previously [45–48]. Therefore, at virtually no ATP increase, the existing basal ATP levels are sufficient for GSIS, together with NOX4-ensured redox signaling.

Indeed, the basal total ATP in DAPIT-deficient INS-1E cells is sufficient together with elevated H_2O_2 (NOX4 was not hampered) to close the ATP-sensitive K^+ channel and so to trigger insulin granule exocytosis. Apparently, the only negligibly increasing ATP at 11 and 20-mM glucose in DAPIT-deficient INS-1E cells and still existing GSIS provide another independent yet indirect support for the existence of the NOX4-dependent mechanism [8]. Note, that constitutively expressed NOX4 does not need to be assembled [49]; on the contrary the deletion of NOX2, an inducible NOX isoform, enhanced GSIS in pancreatic islets via decrease in superoxide production and elevated cAMP concentrations [48]. Actually, the observation, that despite a very little elevation of ATP in DAPIT-deficient cells, there is still virtually unaffected secretion of insulin responding to glucose, is very similar to the effect of oligomycin described in Ref. [7] (Figure 6D therein).

Our demonstrations that the increased DAPIT expression correlates with the elevated incremental ATP levels is similar to the correlation with elevated ATP previously described in He–La cells [29], which were rather of a weak character. In our case, with a prevailing population of vestigial ATP synthase molecules set by DAPIT silencing [26], we recognized almost no elevation in incremental ATP as a response on higher glucose concentration. This finding supports the requirement of completely assembled ATP synthase for efficient and maximum synthesis of ATP.

It is necessary to further study whether any assembly intermediates of the ATP synthase [50] (or vestigial ATP synthase molecules in deletion experiments, [26]) contribute to the synthesis of ATP at all. Note that our silencing left a substantial amount of DAPIT mRNA expressed. Despite this fact, the surplus accumulation of ATP was decreased by 94%, likewise the extent of increase in phosphorylating/non-phosphorylating respiration ratio, calculated as $V_3/V_4 - 1$, which decreased by

40%. We also observed similar ATP and respiratory decreases upon silencing of the ATP synthase F_0 sector subunit *e* (Leguina Ruzzi, unpublished).

As we demonstrated in INS-1E cells, expression of the DAPIT and other F_0 subunits determined the intensity of ATP synthesis. The latter is indicated by the V_3/V_4 ratio, increases with the increasing glucose from insulin non-stimulating (3 mM) to insulin stimulating concentration (>8 mM) [11,12,14–16]. However, as we now show, this does not proceed in DAPIT-deficient cells. Hence, a special attention should be paid to the relationships of respiration vs. oxidative phosphorylation in DAPIT-deficient cells. With 20-mM glucose, the V_3/V_4 respiration rate ratio diminished only to ~70% upon DAPIT silencing, whereas the net GSIS rate accounted for 80%. The fraction of respiration employed for the synthesis of ATP was only 5% at 3-mM glucose and was constant at ~40% with 11 and 20-mM glucose. This phenomenon should be independent of the DAPIT-deficiency, since DAPIT does not interact with the respiratory chain supercomplexes.

We also revealed that the two-week delivery of glucose from hyaluronic acid implants elevates transcription of USMG5/DAPIT and other subunits of the membrane F_0 sector of the ATP synthase; and, as exemplified by the subunit $F_1\alpha$, one can expect also elevations of other subunits of the F_1 moiety. Currently, we cannot distinguish whether there was a direct glucose-induction of the selected ATP synthase subunits, whether faster metabolism due to permanently higher glucose presence increased transcription rate; or whether the elevated transcription was evoked by the induced mild hypoinsulinemia in mice. Note that in this way, we simulated chronic states, imposing a rather mild hyperglycemia (7.5 and 9-mM blood glucose) by the constant glucose systemic delivery to mice, using hyaluronic acid implants. One may consider that even if the turnover of DAPIT was faster than the turnover of the other F_0 or F_1 subunits, glucose- or metabolism-induced DAPIT expression would ensure the maintenance of complete ATP synthase. Indeed, ubiquitin degradation exists for certain mitochondrial matrix proteins [51] and this may principally differentiate between subunits. In contrast, if autophagy is involved, all subunits would be degraded simultaneously.

In vivo, postprandial and fasting states are alternating [2,5]. For pancreatic β -cells, this means insulin secreting period and basal period. Various secretagogues coming from metabolized meals induce insulin release by different mechanisms during secreting period, while a rather low insulin secretion exists in the basal state [1–6]. Traditionally emphasized prominent role of glucose stems not only from the complex mechanisms of GSIS, but is also supported by demonstrations that glucose also serves in the maintenance of expression of *Ins* gene and other β -cell specific genes [4,6,39,52]; or may act in identity self-checking of β -cells [52]. The revealed upregulation of subunits of the ATP synthase membrane F_0 sector, including USMG5/DAPIT, and upregulation of the subunit $F_1\alpha$, by two-week glucose delivery is thus only one among numerous other complex processes induced by glucose.

One can also speculate that the glucose/metabolism-induced DAPIT expression may be part of physiological regulations in pancreatic β -cells. This would be enabled, if a fraction of vestigial ATP synthase molecules exists within the ensemble of ATP synthase dimers located in rows along the cristae rims, i.e., the sharp cristae edges. In this case, the newly expressed DAPIT molecules may gradually saturate the vacant sites. These vacant sites may hypothetically arise from a preferable DAPIT degradation. Using DAPIT silencing, we demonstrated that if such degradation existed, it would inhibit ATP synthesis. According this hypothetical view, the preferential rapid expression of DAPIT and its binding into the vacant sites would then switch on ATP synthesis. DAPIT would then act reciprocally to the physiological inhibitor of the ATP synthase, the ATPase inhibitory factor IF1 [11,13].

Speculatively, the DAPIT deficiency (a lower stoichiometry relatively to the F_0 -sector of the ATP synthase) may exist at low glucose (insulin release nonstimulating), such as given by a higher degradation; and this would cause a substantial ATP synthase inhibition. At high glucose (insulin release stimulating), the resulting glucose/metabolism-induced expression of DAPIT could overcome such loss, restoring ATP synthesis. Alternatively, an excessive DAPIT stoichiometry may be established at high glucose, if such an excessive stoichiometry is required to the optimum ATP synthase operation, hence optimum ATP synthesis at its maximum efficiency. We supported these speculations by our

results with rough estimations of possible stoichiometry of DAPIT relatively to the rest of the ATP synthase in dimers. One should take these results with caution, since the provided anti-DAPIT antibody may partly cross-react with some other ATP synthase subunits (Supplementary File 1; Figure S6) and thus distort these estimations. However, since DAPIT silencing substantially reduced immunostaining with these anti-DAPIT antibodies, certain specificity for DAPIT is evident. Our findings of a possible variable DAPIT-ATP synthase stoichiometry thus require further testing.

The above speculations may be plausible if degradation of DAPIT or its glucose- or metabolic induction would be independent of the degradation or expression for the remaining subunits of the ATP synthase. The existence of the vestigial ATP synthase molecules *in vivo* which lack the USMG5/DAPIT protein would be possible at least for a small fraction, since DAPIT is one of the outmost subunits (Figure 1) that is also lastly added among the F_0 -sector subunits of the ATP synthase during biogenesis [26].

A complex assembly of the entire human ATP synthase was described recently to consist of separate steps assembling independently the F_1 -moiety with the *c*-ring and complex of subunits *b*, *e*, *g* [50]. Since DAPIT binds the mtDNA-encoded subunit *a* [20,26], synchronous processes of translation on ribosomes proximal to mitochondria, adjacent protein import into the mitochondrial matrix and translation by mt ribosomes participate in final steps of the ATP synthase assembly. One may emphasize here that a parallel mtDNA transcription must take place, concerning the mtDNA-encoded subunits *a*/ATP6 and ATP8/A6 L. When this is impaired, DAPIT cannot bind to the ATP synthase and the resulting vestigial macromolecules should contain even less subunits.

In this respect, we observed that the mtDNA replication is largely independent of glucose- or metabolic induced upregulations. However, the optimum mtDNA replication again requires the completely assembled ATP synthase. This represents a feedback loop. Similar results were obtained for induction of PGC-1 α , as one of the factors of mitochondrial biogenesis.

In addition, unlike the published reports for fibroblasts [35,36], we showed the absence of major effects of DAPIT deficiency on morphology of mitochondrial cristae in INS-1E cells. The reason of this discrepancy may stem from more stable mitochondrial network and its rich cristae in INS-1E cells relatively to fibroblasts. That is why we can interpret the above discussed respirometry analyses without a major contribution of cristae morphology changes. As we also demonstrated, DAPIT-deficient vestigial ATP synthase dimers may form thinner cristae. This is supported by our evaluated distribution histograms of cristae width (Figure 9a–c). Nevertheless, unlike in reported observations with mutant DAPIT [35,36], general cristae morphology was not disrupted in DAPIT-deficient INS-1E cells and the previously observed cristae narrowing [17] also took place at high glucose, albeit in a smaller extent. Again, we can explain this by the existing rich cristae in INS-1E cells, when compared to fibroblasts. Hypothetically, DAPIT interactions with the subunit *g* may control both ATP synthesis as well as the inner mitochondrial membrane morphology, particularly at the crista rims. This prediction is based on the recently revealed structure of the ATP synthase tetramer, in which interactions contributing to the tetramer formation involve subunits *g* from the neighbor dimers with the DAPIT in proximity to each of them [20].

In this way, the release of DAPIT from the dimeric/tetrameric ATP synthase would destabilize rows of ATP synthase dimers since it would disconnect the two neighbor dimers within tetramers. In an opposite, binding of DAPIT into yet vacant sites in the dimeric/tetrameric ATP synthase would strengthen rows of ATP synthase dimers/tetramers. Thus, longitudinal interactions within the rim hypothetically govern the extent or strength of the rim stabilization [18]. A stabilized rim (row of the ATP synthase dimers) may lead to cristae narrowing; and, in contrast, the destabilized rim may enable wide cristae [18,35]. In addition, prolonged INS-1E cell exposure to 3-mM glucose may fragment mitochondrial network [53].

5. Conclusions

In conclusion, our results with the DAPIT-deficient rat β -cell line (INS-1E cells) indicate that the vestigial ATP synthase lacking DAPIT exhibits much lower efficiency of ATP synthesis. However, despite the fact that the glucose-induced ATP increment was only around 6% in DAPIT-deficient INS-1E cells, this was still sufficient to initiate GSIS by the mechanism(s) independent of ATP elevation, i.e., independent of the oxidative phosphorylation. The result is compatible with the existence of the recently revealed NOX4-dependent redox signaling essential for GSIS [8]. In general, we demonstrated that the optimum expression of DAPIT is elementary required to reach the maximum ATP synthesis. The elevated expression of DAPIT at high glucose further increases the ATP synthesis efficiency. Moreover, we described rather a compensating response of pancreatic islets cells, i.e., including β -cells, lying in the elevated transcription of the ATP synthase F_0 subunits *e*, *f*, *g* and DAPIT, as induced by the enhanced metabolism upon higher glucose intake.

Supplementary Materials: The following are available online at <http://www.mdpi.com/2218-273X/10/7/1026/s1>, Figure S1: Typical changes in DAPIT mRNA levels in INS-1E cells; Figure S2: Downregulation/recovery of transcripts for F_0 subunits *e*, *f* and *g*; Figure S3: Typical results of DAPIT silencing; Figure S4: western blots of $F_1\alpha$; Figure S5: Surplus ATP accumulation; Figure S6: Anti-DAPIT/USMG5 antibodies recognize a complex above ~75 kDa.

Author Contributions: Conceptualization, A.L.-R. and P.J.; methodology A.L.-R., A.V., B.H., H.E., V.P., J.T. and A.D.; validation, A.L.-R., B.H., H.E., V.P., J.T.; formal analysis, A.L.-R. and P.J.; investigation, A.L.-R., A.V., B.H., H.E., V.P., J.T. and A.D.; resources, P.J.; data curation, P.J.; writing—original draft preparation, P.J.; writing—review and editing, P.J.; visualization, P.J.; supervision, P.J.; project administration, P.J.; funding acquisition, P.J. All authors have read and agreed to the published version of the manuscript.

Funding: This research was funded by the Grant Agency of the Czech Republic (Grantová Agentura České republiky, GAČR), Grant Number 20–00408S.

Acknowledgments: We gratefully acknowledge receiving of a Juvederm Ultra 4 hyaluronic acid filler for performing hyaluronic acid implants from Semira Kwabi (Skin Clinic, London, UK) and the excellent technical assistance of Jana Vaicová with insulin release assays and Jitka Smiková with cell culture media preparation and cell cultivation; and Katarína Smolková and Lydie Plecítá-Hlavatá for their advice and fruitful discussion.

Conflicts of Interest: The authors declare no conflicts of interest. The funders had no role in the design of the study; in the collection, analyses or interpretation of data; in the writing of the manuscript or in the decision to publish the results.

References

1. Ashcroft, F.M.; Rorsman, P. Diabetes Mellitus and the β Cell: The Last Ten Years. *Cell* **2012**, *148*, 1160–1171. [CrossRef] [PubMed]
2. Prentki, M.; Matschinsky, F.M.; Madiraju, S.R.M. Metabolic Signaling in Fuel-Induced Insulin Secretion. *Cell Metab.* **2013**, *18*, 162–185. [CrossRef] [PubMed]
3. Maechler, P. Mitochondrial function and insulin secretion. *Mol. Cell. Endocrinol.* **2013**. [CrossRef] [PubMed]
4. Rutter, G.A.; Pullen, T.J.; Hodson, D.J.; Martinez-Sanchez, A. Pancreatic β -cell identity, glucose sensing and the control of insulin secretion. *Biochem. J.* **2015**, *466*, 203–218. [CrossRef]
5. Ježek, P.; Jabůrek, M.; Holendová, B.; Plecítá-Hlavatá, L. Fatty Acid-Stimulated Insulin Secretion vs. Lipotoxicity. *Molecules* **2018**, *23*, 1483. [CrossRef]
6. Ježek, P.; Jabůrek, M.; Plecítá-Hlavatá, L. Contribution of Oxidative Stress and Impaired Biogenesis of Pancreatic β -Cells to Type 2 Diabetes. *Antioxid. Redox Signal.* **2019**. [CrossRef]
7. Fex, M.; Nicholas, L.M.; Vishnu, N.; Medina, A.; Sharoyko, V.V.; Nicholls, D.G.; Spégel, P.; Mulder, H. The pathogenetic role of β -cell mitochondria in type 2 diabetes. *J. Endocrinol.* **2018**, *236*, R145–r159. [CrossRef]
8. Plecítá-Hlavatá, L.; Jabůrek, M.; Holendová, B.; Tauber, J.; Pavluch, V.; Berková, Z.; Cahová, M.; Schroeder, K.; Brandes, R.P.; Siemen, D.; et al. Glucose-Stimulated Insulin Secretion Fundamentally Requires H₂O₂ Signaling by NADPH Oxidase 4. *Diabetes* **2020**. [CrossRef]
9. Leturque, A.; Brot-Laroche, E.; Le Gall, M. GLUT2 mutations, translocation, and receptor function in diet sugar managing. *Am. J. Physiology. Endocrinol. Metab.* **2009**, *296*, E985–E992. [CrossRef]

10. Park, J.H.; Kim, S.J.; Park, S.H.; Son, D.G.; Bae, J.H.; Kim, H.K.; Han, J.; Song, D.K. Glucagon-like peptide-1 enhances glucokinase activity in pancreatic beta-cells through the association of Epac2 with Rim2 and Rab3A. *Endocrinology* **2012**, *153*, 574–582. [CrossRef]
11. Kahancová, A.; Sklenář, F.; Ježek, P.; Dlasková, A. Regulation of glucose-stimulated insulin secretion by ATPase Inhibitory Factor 1 (IF1). *FEBS Lett.* **2018**, *592*, 999–1009. [CrossRef] [PubMed]
12. Špaček, T.; Šantorová, J.; Zacharovová, K.; Berková, Z.; Hlavatá, L.; Saudek, F.; Ježek, P. Glucose-stimulated insulin secretion of insulinoma INS-1E cells is associated with elevation of both respiration and mitochondrial membrane potential. *Int. J. Biochem. Cell Biol.* **2008**, *40*, 1522–1535. [CrossRef] [PubMed]
13. Kahancová, A.; Sklenář, F.; Ježek, P.; Dlasková, A. Overexpression of native IF1 downregulates glucose-stimulated insulin secretion by pancreatic INS-1E cells. *Sci. Rep.* **2020**, *10*, 1551. [CrossRef] [PubMed]
14. Affourtit, C.; Alberts, B.; Barlow, J.; Carré, J.E.; Wynne, A.G. Control of pancreatic β -cell bioenergetics. *Biochem. Soc. Trans.* **2018**, *46*, 555–564. [CrossRef] [PubMed]
15. Bartley, C.; Brun, T.; Oberhauser, L.; Grimaldi, M.; Molica, F.; Kwak, B.R.; Bosco, D.; Chanson, M.; Maechler, P. Chronic fructose renders pancreatic β -cells hyper-responsive to glucose-stimulated insulin secretion through extracellular ATP signaling. *Am. J. Physiol. Endocrinol. Metab.* **2019**, *317*, E25–e41. [CrossRef]
16. Gerencser, A.A. Metabolic activation-driven mitochondrial hyperpolarization predicts insulin secretion in human pancreatic beta-cells. *Biochim. Et Biophys. Acta (Bba) - Bioenerg.* **2018**, *1859*, 817–828. [CrossRef]
17. Dlasková, A.; Engstová, H.; Špaček, T.; Kahancová, A.; Pavluch, V.; Smolková, K.; Špačková, J.; Bartoš, M.; Hlavatá, L.P.; Ježek, P. 3D super-resolution microscopy reflects mitochondrial cristae alternations and mtDNA nucleoid size and distribution. *Biochim. Et Biophys. Acta. Bioenerg.* **2018**, *1859*, 829–844. [CrossRef]
18. Dlaskova, A.; Spacek, T.; Engstova, H.; Spackova, J.; Schrofel, A.; Holendova, B.; Smolkova, K.; Plecita-Hlavata, L.; Jezek, P. Mitochondrial cristae narrowing upon higher 2-oxoglutarate load. *Biochim. Et Biophys. Acta. Bioenerg.* **2019**, *1860*, 659–678. [CrossRef]
19. Klusch, N.; Murphy, B.J.; Mills, D.J.; Yildiz, O.; Kuhlbrandt, W. Structural basis of proton translocation and force generation in mitochondrial ATP synthase. *eLife* **2017**, *6*. [CrossRef]
20. Gu, J.; Zhang, L.; Zong, S.; Guo, R.; Liu, T.; Yi, J.; Wang, P.; Zhuo, W.; Yang, M. Cryo-EM structure of the mammalian ATP synthase tetramer bound with inhibitory protein IF1. *Science* **2019**, *364*, 1068–1075. [CrossRef]
21. Davies, K.M.; Anselmi, C.; Wittig, I.; Faraldo-Gomez, J.D.; Kuhlbrandt, W. Structure of the yeast F1Fo-ATP synthase dimer and its role in shaping the mitochondrial cristae. *Proc. Natl. Acad. Sci. USA* **2012**, *109*, 13602–13607. [CrossRef] [PubMed]
22. Daum, B.; Walter, A.; Horst, A.; Osiewacz, H.D.; Kuhlbrandt, W. Age-dependent dissociation of ATP synthase dimers and loss of inner-membrane cristae in mitochondria. *Proc. Natl. Acad. Sci. USA* **2013**, *110*, 15301–15306. [CrossRef] [PubMed]
23. Davies, K.M.; Strauss, M.; Daum, B.; Kief, J.H.; Osiewacz, H.D.; Rycovska, A.; Zickermann, V.; Kuhlbrandt, W. Macromolecular organization of ATP synthase and complex I in whole mitochondria. *Proc. Natl. Acad. Sci. USA* **2011**, *108*, 14121–14126. [CrossRef]
24. Strauss, M.; Hofhaus, G.; Schroder, R.R.; Kuhlbrandt, W. Dimer ribbons of ATP synthase shape the inner mitochondrial membrane. *EMBO J.* **2008**, *27*, 1154–1160. [CrossRef] [PubMed]
25. Jiko, C.; Davies, K.M.; Shinzawa-Itoh, K.; Tani, K.; Maeda, S.; Mills, D.J.; Tsukihara, T.; Fujiyoshi, Y.; Kuhlbrandt, W.; Gerle, C. Bovine F1Fo ATP synthase monomers bend the lipid bilayer in 2D membrane crystals. *eLife* **2015**, *4*, e06119. [CrossRef] [PubMed]
26. He, J.; Ford, H.C.; Carroll, J.; Douglas, C.; Gonzales, E.; Ding, S.; Fearnley, I.M.; Walker, J.E. Assembly of the membrane domain of ATP synthase in human mitochondria. *Proc. Natl. Acad. Sci. USA* **2018**, *115*, 2988–2993. [CrossRef] [PubMed]
27. Kontro, H.; Hulmi, J.J.; Rahkila, P.; Kainulainen, H. Cellular and tissue expression of DAPIT, a phylogenetically conserved peptide. *Eur. J. Histochem. EJH* **2012**, *56*, e18. [CrossRef]
28. Kontro, H.; Cannino, G.; Rustin, P.; Dufour, E.; Kainulainen, H. DAPIT Over-Expression Modulates Glucose Metabolism and Cell Behaviour in HEK293T Cells. *PLoS ONE* **2015**, *10*, e0131990. [CrossRef]
29. Ohsakaya, S.; Fujikawa, M.; Hisabori, T.; Yoshida, M. Knockdown of DAPIT (diabetes-associated protein in insulin-sensitive tissue) results in loss of ATP synthase in mitochondria. *J. Biol. Chem.* **2011**, *286*, 20292–20296. [CrossRef]

30. Paivarinne, H.; Kainulainen, H. DAPIT, a novel protein down-regulated in insulin-sensitive tissues in streptozotocin-induced diabetes. *Acta Diabetol.* **2001**, *38*, 83–86. [CrossRef]
31. Nagata, Y.; Yamagishi, M.; Konno, T.; Nakanishi, C.; Asano, Y.; Ito, S.; Nakajima, Y.; Seguchi, O.; Fujino, N.; Kawashiri, M.A.; et al. Heat Failure Phenotypes Induced by Knockdown of DAPIT in Zebrafish: A New Insight into Mechanism of Dilated Cardiomyopathy. *Sci. Rep.* **2017**, *7*, 17417. [CrossRef] [PubMed]
32. Eydt, K.; Davies, K.M.; Behrendt, C.; Wittig, I.; Reichert, A.S. Cristae architecture is determined by an interplay of the MICOS complex and the F1FO ATP synthase via Mic27 and Mic10. *Microb. Cell (Graz Austria)* **2017**, *4*, 259–272. [CrossRef] [PubMed]
33. Rampelt, H.; Bohnert, M.; Zerbes, R.M.; Horvath, S.E.; Warscheid, B.; Pfanner, N.; van der Laan, M. Mic10, a Core Subunit of the Mitochondrial Contact Site and Cristae Organizing System, Interacts with the Dimeric F1Fo-ATP Synthase. *J. Mol. Biol.* **2017**, *429*, 1162–1170. [CrossRef] [PubMed]
34. Barca, E.; Ganetzky, R.D.; Potluri, P.; Juanola-Falgarona, M.; Gai, X.; Li, D.; Jalas, C.; Hirsch, Y.; Emmanuele, V.; Tadesse, S.; et al. USMG5 Ashkenazi Jewish founder mutation impairs mitochondrial complex V dimerization and ATP synthesis. *Hum. Mol. Genet.* **2018**, *27*, 3305–3312. [CrossRef]
35. Siegmund, S.E.; Grassucci, R.; Carter, S.D.; Barca, E.; Farino, Z.J.; Juanola-Falgarona, M.; Zhang, P.; Tanji, K.; Hirano, M.; Schon, E.A.; et al. Three-Dimensional Analysis of Mitochondrial Crista Ultrastructure in a Patient with Leigh Syndrome by In Situ Cryoelectron Tomography. *iScience* **2018**, *6*, 83–91. [CrossRef] [PubMed]
36. Liu, W.; Zhang, Z.; Zhang, Z.M.; Hao, P.; Ding, K.; Li, Z. Integrated phenotypic screening and activity-based protein profiling to reveal potential therapy targets of pancreatic cancer. *Chem. Commun. (Camb. Engl.)* **2019**, *55*, 1596–1599. [CrossRef] [PubMed]
37. Guo, H.; Bueler, S.A.; Rubinstein, J.L. Atomic model for the dimeric F(O) region of mitochondrial ATP synthase. *Science* **2017**, *358*, 936–940. [CrossRef] [PubMed]
38. Ježek, J.; Dlasková, A.; Zelenka, J.; Jabůrek, M.; Ježek, P. H₂O₂-Activated Mitochondrial Phospholipase iPLA₂ γ Prevents Lipotoxic Oxidative Stress in Synergy with UCP2, Amplifies Signaling via G-Protein-Coupled Receptor GPR40, and Regulates Insulin Secretion in Pancreatic β -Cells. *Antioxid. Redox Signal.* **2015**, *23*, 958–972. [CrossRef] [PubMed]
39. Merglen, A.; Theander, S.; Rubi, B.; Chaffard, G.; Wollheim, C.B.; Maechler, P. Glucose sensitivity and metabolism-secretion coupling studied during two-year continuous culture in INS-1E insulinoma cells. *Endocrinology* **2004**, *145*, 667–678. [CrossRef]
40. Alán, L.; Olejár, T.; Cahová, M.; Zelenka, J.; Berková, Z.; Smětáková, M.; Saudek, F.; Matěj, R.; Ježek, P. Delta Cell Hyperplasia in Adult Goto-Kakizaki (GK/MolTac) Diabetic Rats. *J. Diabetes Res.* **2015**, *2015*, 1–16. [CrossRef]
41. Vaghy, P.L.; Matlib, M.A.; Schwartz, A. Phosphate induced swelling, inhibition and partial uncoupling of oxidative phosphorylation in heart mitochondria in the absence of external calcium and the presence of EGTA. *Biochem. Biophys. Res. Commun.* **1981**, *100*, 37–44. [CrossRef]
42. Praveen, S.S.; Hanumantha, R.; Belovich, J.M.; Davis, B.L. Novel hyaluronic acid coating for potential use in glucose sensor design. *Diabetes Technol. Ther.* **2003**, *5*, 393–399. [CrossRef] [PubMed]
43. Hadler, N.M. Enhanced diffusivity of glucose in a matrix of hyaluronic acid. *J. Biol. Chem.* **1980**, *255*, 3532–3535. [PubMed]
44. Plecítá-Hlavatá, L.; Engstová, H.; Alán, L.; Špaček, T.; Dlasková, A.; Smolková, K.; Špačková, J.; Tauber, J.; Strádalová, V.; Malínský, J.; et al. Hypoxic HepG2 cell adaptation decreases ATP synthase dimers and ATP production in inflated cristae by mitofilin down-regulation concomitant to MICOS clustering. *FASEB J.* **2016**, *30*, 1941–1957. [CrossRef]
45. Morgan, D.; Rebelato, E.; Abdulkader, F.; Graciano, M.F.R.; Oliveira-Emilio, H.R.; Hirata, A.E.; Rocha, M.S.; Bordin, S.; Curi, R.; Carpinelli, A.R. Association of NAD(P)H Oxidase with Glucose-Induced Insulin Secretion by Pancreatic β -Cells. *Endocrinology* **2009**, *150*, 2197–2201. [CrossRef]
46. Newsholme, P.; Morgan, D.; Rebelato, E.; Oliveira-Emilio, H.C.; Procopio, J.; Curi, R.; Carpinelli, A. Insights into the critical role of NADPH oxidase(s) in the normal and dysregulated pancreatic beta cell. *Diabetologia* **2009**, *52*, 2489–2498. [CrossRef]
47. Bedard, K.; Krause, K.-H. The NOX Family of ROS-Generating NADPH Oxidases: Physiology and Pathophysiology. *Physiol. Rev.* **2007**, *87*, 245–313. [CrossRef]

48. Li, N.; Li, B.; Brun, T.; Deffert-Delbouille, C.; Mahiout, Z.; Daali, Y.; Ma, X.-J.; Krause, K.-H.; Maechler, P. NADPH Oxidase NOX2 Defines a New Antagonistic Role for Reactive Oxygen Species and cAMP/PKA in the Regulation of Insulin Secretion. *Diabetes* **2012**, *61*, 2842–2850. [CrossRef]
49. Serrander, L.; Cartier, L.; Bedard, K.; Banfi, B.; Lardy, B.; Plastre, O.; Sienkiewicz, A.; Fórró, L.; Schlegel, W.; Krause, K.-H. NOX4 activity is determined by mRNA levels and reveals a unique pattern of ROS generation. *Biochem. J.* **2007**, *406*, 105–114. [CrossRef]
50. Fujikawa, M.; Sugawara, K.; Tanabe, T.; Yoshida, M. Assembly of human mitochondrial ATP synthase through two separate intermediates, F1-c-ring and b-e-g complex. *Febs Lett.* **2015**, *589*, 2707–2712. [CrossRef]
51. Lavie, J.; De Belvalet, H.; Sonon, S.; Ion, A.M.; Dumon, E.; Melsers, S.; Lacombe, D.; Dupuy, J.W.; Lalou, C.; Bénard, G. Ubiquitin-Dependent Degradation of Mitochondrial Proteins Regulates Energy Metabolism. *Cell Rep.* **2018**, *23*, 2852–2863. [CrossRef] [PubMed]
52. Swisa, A.; Glaser, B.; Dor, Y. Metabolic Stress and Compromised Identity of Pancreatic Beta Cells. *Front. Genet.* **2017**, *08*, 21. [CrossRef] [PubMed]
53. Plecítá-Hlavatá, L.; Lessard, M.; Santorová, J.; Bewersdorf, J.; Jezek, P. Mitochondrial oxidative phosphorylation and energetic status are reflected by morphology of mitochondrial network in INS-1E and HEP-G2 cells viewed by 4Pi microscopy. *Biochim. Et Biophys. Acta* **2008**, *1777*, 834–846. [CrossRef] [PubMed]



© 2020 by the authors. Licensee MDPI, Basel, Switzerland. This article is an open access article distributed under the terms and conditions of the Creative Commons Attribution (CC BY) license (<http://creativecommons.org/licenses/by/4.0/>).

Article

Transport of Ca^{2+} and Ca^{2+} -Dependent Permeability Transition in the Liver and Heart Mitochondria of Rats with Different Tolerance to Acute Hypoxia

Konstantin N. Belosludtsev ^{1,2,*}, Mikhail V. Dubinin ², Eugeny Yu. Talanov ¹,
Vlada S. Starinets ², Kirill S. Tenkov ², Nadezhda M. Zakharova ³ and Natalia V. Belosludtseva ¹

¹ Institute of Theoretical and Experimental Biophysics, Russian Academy of Sciences, Institutskaya 3, Pushchino, 142290 Moscow Region, Russia; evg-talanov@yandex.ru (E.Y.T.); natago_imagination@rambler.ru (N.V.B.)

² Department of Biochemistry, Cell Biology and Microbiology, Mari State University, pl. Lenina 1, Yoshkar-Ola, 424001 Mari El, Russia; dubinin1989@gmail.com (M.V.D.); vlastar@list.ru (V.S.S.); kirill.tenkove@gmail.com (K.S.T.)

³ Institute of Cell Biophysics, Russian Academy of Sciences, PSCBR RAS, Institutskaya 3, Pushchino, 142290 Moscow Region, Russia; n.m.zakharova@gmail.com

* Correspondence: bekonik@gmail.com; Tel.: +7-929-913-8910

Received: 4 December 2019; Accepted: 7 January 2020; Published: 9 January 2020

Abstract: The work examines the kinetic parameters of Ca^{2+} uptake via the mitochondrial calcium uniporter complex (MCUC) and the opening of the Ca^{2+} -dependent permeability transition pore (MPT pore) in the liver and heart mitochondria of rats with high resistance (HR) and low resistance (LR) to acute hypoxia. We found that the rate of Ca^{2+} uptake by mitochondria of the liver and heart in HR rats is higher than that in LR rats, which is associated with a higher level of the channel-forming subunit MCU in liver mitochondria of HR rats and a lower content of the dominant-negative channel subunit MCUB in heart mitochondria of HR rats. It was shown that the liver mitochondria of HR rats are more resistant to the induction of the MPT pore than those of LR rats (the calcium retention capacity of liver mitochondria of HR rats was found to be 1.3 times greater than that of LR rats). These data correlate with the fact that the level of F_0F_1 -ATP synthase, a possible structural element of the MPT pore, in the liver mitochondria of HR rats is lower than in LR rats. In heart mitochondria of rats of the two phenotypes, no statistically significant difference in the formation of the MPT pore was revealed. The paper discusses how changes in the expression of the MCUC subunits and the putative components of the MPT pore can affect Ca^{2+} homeostasis of mitochondria in animals with originally different tolerance to hypoxia and in hypoxia-induced tissue injury.

Keywords: hypoxia; resistance to hypoxia; mitochondria; mitochondrial calcium transport; mitochondrial calcium uniporter complex; mitochondrial Ca^{2+} -induced permeability transition pore; cyclophilin D; ATP synthase

1. Introduction

Hypoxia/ischemia is a widespread phenomenon that occurs both in conditions of oxygen deficiency in the environment and in various pathologies as a result of a decrease in oxygen delivery to the cell to a level insufficient to maintain its functions and structure. Hypoxic conditions in the body are observed in ischemic and reperfusion injuries of organs, hemodynamic disorders, coronary insufficiency, blood loss, hemorrhagic shock, arterial hypertension, pulmonary insufficiency, systemic inflammatory response syndrome, traumatic shock, exposure to adverse environmental factors, extreme conditions, and other stressful effects.

The main intracellular targets of hypoxia of various etiologies are mitochondria and aerobic energy metabolism [1,2]. Hypoxia alters mitochondrial dynamics and morphology and provokes mitochondrial dysfunction, which can lead to a drop in the ATP synthesis, an increase in the production of reactive oxygen species, and other adverse events, including the disturbance of ionic, mainly Ca^{2+} , homeostasis. Excessive accumulation of Ca^{2+} in cytoplasm and mitochondria in hypoxia and subsequent reoxygenation can finally initiate cell injury and death via the opening of the Ca^{2+} -dependent mitochondrial permeability transition pore (MPT pore) and the subsequent release of proapoptotic proteins from organelles [3].

As a major large-capacity buffer system of Ca^{2+} ions, mitochondria are involved in the regulation of intracellular Ca^{2+} homeostasis. Changes in mitochondrial $[\text{Ca}^{2+}]$ modulate key cellular processes, ranging from aerobic metabolism (through Ca^{2+} -sensitive dehydrogenases, and enzymes of the Krebs cycle [4]) to the release of proapoptotic factors [5–8], as well as local modulation of the activity of channels and enzymes [9,10].

In recent studies, it has been found that mitochondria contain several proteins involved in mitochondrial Ca^{2+} uptake: mitochondrial Ca^{2+} uniporter complex (MCUC), RaM (the rapid mode of Ca^{2+} uptake), Letm1 (leucine zipper and EF-hand-containing transmembrane protein 1), mitochondrial ryanodine receptor type 1, and uncoupling proteins [5,11]. Among them, the MCUC is believed to be the main calcium transport system, which mediates the electrophoretic influx of the ion into mitochondria. This multiprotein complex is composed of the pore-forming and calcium-conducting subunit MCU (mitochondrial calcium uniporter subunit), its paralogue MCUB (mitochondrial calcium uniporter dominant negative beta subunit), and regulatory subunits: the small membrane-spanning protein EMRE (essential MCU regulatory subunit), the peripheral membrane proteins acting as gatekeepers MICU1 and MICU2 (mitochondrial calcium uptake proteins 1 and 2), and MCUR1 (MCU regulator protein 1) [5,6]. Variations in the ratio of the subunits of MCUC determine the dynamics of mitochondrial Ca^{2+} uptake in different tissues and pathophysiological states. For example, a decrease in the expression of MICU1 in the heart tissue correlates with the lowered activation threshold of Ca^{2+} influx and the decreased calcium capacity of heart mitochondria in comparison with those of liver mitochondria [12]. MCUB mRNA is highly expressed in the heart and minimally expressed in skeletal muscle, which can be the cause of variations in the tissue-dependent mitochondrial Ca^{2+} uptake: the Ca^{2+} influx into skeletal muscle mitochondria is significantly greater than that into cardiac ones [13].

Excessive accumulation of Ca^{2+} in mitochondria leads to the opening of the Ca^{2+} -dependent mitochondrial permeability transition pore (MPT pore), which can be a key step in the mechanism of the activation of programmed cell death or, under certain conditions, can serve as an additional nonspecific calcium release pathway. The molecular structure of the MPT pore is as yet not clearly established. The MPT pore complex is considered to be a multiprotein mega-channel, which includes proteins of the inner and outer mitochondrial membranes. Among possible candidates for the role of the channel-forming subunit of the MPT pore are considered a number of proteins of the inner mitochondrial membrane, including ATP synthase, adenine nucleotide translocator, and phosphate carrier. At the same time, the only protein that is currently claimed to be an integral part of the MPT pore is the regulatory protein cyclophilin D, which is able to interact with the above-mentioned proteins. Cyclophilin D is the target of the cyclic undecapeptide cyclosporin A (CsA), which desensitizes the MPT pore complex to calcium ions at nanomolar concentrations [5,14].

Studies on the role of mitochondrial Ca^{2+} transport systems in the pathogenesis of hypoxia have been ongoing for a long time. It was found that the pharmacological or genetic modulation of cyclophilin D leads to the inhibition of pore opening in mitochondria and increases the resistance of cell cultures and tissues to the hypoxic state. At the same time, the question of how the structure and operation of the mitochondrial Ca^{2+} transport system and the MPT pore can be regulated in hypoxia and hypoxic adaptation remains unclear. The answer to this question should be found when conducting studies on animals with different individual resistance to acute hypoxia [15–17]. It is known that the onset and severity of the acute hypoxia response of rats drastically differ within the

population, and two opposite, extreme phenotypes of animals, with high resistance (HR) and low resistance (LR) to hypoxia, have significantly different “functional-metabolic profiles” [18]. Thus, we have shown earlier that the liver mitochondria of HR and LR rats have different resistance to the formation of Ca^{2+} -dependent mitochondrial pores of two types, the MPT pore and the lipid pore induced by saturated long-chain fatty acids [19].

In the present work, we attempted to determine the structural and functional features of the mitochondrial Ca^{2+} transport multiprotein systems, the MCUC and the MPT pore, in liver and heart tissues of animals with different tolerance to oxygen shortage. The study demonstrates that: (1) the rate of accumulation of Ca^{2+} ions by mitochondria isolated from the liver and heart of HR rats is considerably higher than that of LR rats, which highly correlates changes observed in the content, the ratio, and mRNA level of the subunits of the MCUC. In HR rats, the levels of the pore-forming uniporter subunit, MCU, and the key regulatory uniporter subunit, MICU1, in liver mitochondria are significantly higher than in LR rats. The level of the dominant-negative channel subunit, MCUB, is lower in heart mitochondria of HR rats compared to those of LR rats; (2) the liver mitochondria of HR animals are more resistant to the induction of the MPT pore than those of LR animals. This difference can be associated with the lower level of ATP synthase, a protein considered to be the channel-forming component of the MPT pore, in liver tissue of HR animals. In heart mitochondria of rats of the two phenotypes, no difference in the formation of MPT pore was revealed.

2. Materials and Methods

2.1. Testing the Tolerance of Rats to Extreme Hypoxia Conditions

Experiments were conducted on Wistar male rats (220–250 g) with different baseline resistance to hypoxia, low-resistance (LR) and high-resistance (HR) rats. The resistance of rats was tested one month prior to the experiments using a special procedure [19]. Animals were placed into a hypoxic chamber and then tested for the ability to endure a critical life-incompatible O_2 concentration. For this test, the concentration of oxygen in the chamber was reduced to 3.1% by its displacement with nitrogen gas, and the time of the onset of pathological breathing (apnea) (T_a) was determined. This parameter characterizes the viability of animals under extreme hypoxic conditions and reflects the ability to fully mobilize the nonspecific protective functions responsible for the survival of the organism in the sublethal period. After registering T_a , the hypoxic chamber was opened, and the normal posture and locomotor activity of the animals restored within 5–10 min. The T_a value was 1–2 min for LR rats and more than 10 min for HR rats. Each group of rats amounted to approximately 20% of the total number of animals tested ($n = 30$). An interval of one month after the procedure of testing the tolerance of rats to hypoxia conditions was chosen on the basis of earlier studies to eliminate the effect of hypoxic exposure and to identify the basal differences between two rat phenotypes [15,16,18]. After this interval, two extreme types of animals with different tolerance to acute oxygen deficiency exhibit characteristic features of the ultrastructure and functional activity of mitochondria of different organs [16,19].

The laboratory animals were treated in accordance with the European Convention for the Protection of Vertebrates used for experimental and other purposes (Strasbourg, 1986) and the principles of the Helsinki Declaration (2000). All the protocols were approved by the Institute of Theoretical and Experimental Biophysics RAS Ethics Committee (Order No. 173/k of 03.10.2011, Protocol No. 03/2019 of 05.03.2019).

2.2. Isolation of Rat Liver and Heart Mitochondria

Mitochondria were isolated from the liver and heart of Wistar rats by differential centrifugation as described earlier [19]. The homogenization buffer contained 210 mM mannitol, 70 mM sucrose, 1 mM EDTA, and 10 mM HEPES/KOH buffer, pH 7.4. Subsequent centrifugations were performed in the same buffer, except that, instead of EDTA, 100 μM EGTA was used. Final suspensions contained 70–80 mg of

mitochondrial protein/mL and 25–35 mg of mitochondrial protein/mL (liver and heart mitochondria, respectively), as determined by the Lowry method [20].

2.3. Ca^{2+} Uptake by Mitochondria

The Ca^{2+} concentration in the incubation medium was monitored spectrophotometrically with an arsenazo III indicator at 675–685 nm using a plate reader Tecan Spark 10M (Tecan, Männedorf, Switzerland) at 25 °C under constant stirring. At a neutral pH, Ca^{2+} forms a complex with arsenazo III, which has a blue color. The color intensity is proportional to the concentration of Ca^{2+} in a buffer and can be measured spectrophotometrically. Mitochondria (0.4–0.5 mg of mitochondrial protein/mL) were suspended in an incubation medium containing 210 mM mannitol, 70 mM sucrose, 1 mM KH_2PO_4 , 50 μ M arsenazo III, 10 μ M EGTA, and 10 mM HEPES-KOH (pH 7.4) and energized with 2.5 mM glutamate + 2.5 mM malate. After the addition of 50 μ M $CaCl_2$, the rate of Ca^{2+} uptake by mitochondria ($nmol\ Ca^{2+} \times min^{-1} \times mg^{-1}$ of mitochondrial protein) was determined in the presence of 1 μ M CsA. To determine the ability of mitochondria to retain Ca^{2+} , 10 μ M $CaCl_2$ was added into the reaction medium successively, with an interval of ~90 s. After several additions, external $[Ca^{2+}]$ increased, indicating a massive release of the ion from the organelles due to the opening of the MPT pore. The amount of Ca^{2+} released upon permeability transition (defined as Ca^{2+} retention capacity) was used as a measure of the MPT pore opening probability.

2.4. Electrophoresis and Immunoblotting of Mitochondrial Proteins

To prepare samples for quantifying the levels of mitochondrial proteins, aliquots of native mitochondria (2 mg/mL) were solubilized in Laemmli buffer in Eppendorf tubes and heated for 3 min at 95 °C. Sample aliquots normalized by the protein concentration (10 μ g of mitochondrial protein) were applied to the lanes and subjected to electrophoresis followed by Western blot analysis. Mitochondrial samples were separated by 12.5% SDS-PAGE and transferred to a 0.45 μ m nitrocellulose membrane (Amersham, Munich, Germany). The proteins of PageRuler Prestained Protein Ladder (Thermo Scientific, Waltham, MA USA) were used as markers. After overnight blocking, the membrane was incubated with the appropriate primary antibody. The monoclonal rabbit anti-MCU (#14997), anti-CBARA/MICU1 (#12524), and anti-ANT2/SLC25A5 (#14671) antibodies were from Cell Signaling Technology Inc. (Danvers, MA, USA). The total OXPHOS Rodent WB Antibody Cocktail (#ab110413) containing the α -subunit of complex V (CV-ATP5A-55 kDa), anti-VDAC1 (#ab154856), and the polyclonal rabbit antibodies Anti-CCDC109B (#ab170715), anti-cyclophilin F (CypD) (#ab64935), and anti-ANT1 (#ab102032) were from Abcam (Cambridge, United Kingdom). The immunoreactivity was detected using the appropriate secondary antibody conjugated to horseradish peroxidase (#7074, Cell Signaling Technology Inc., Danvers, MA, USA). Peroxidase activity was detected with ECL chemiluminescence reagents (Pierce, Rockford, IL, USA). The relative levels of the detected proteins were visualized using an LI-COR system (LI-COR, Lincoln, NE, USA). Optical density measurements were performed using the LI-COR Image Studio software.

2.5. RNA Extraction, Reverse Transcription, and Quantitative Real-Time PCR

Total RNA was isolated from 100 mg of deep-frozen tissue samples (the liver or the heart) using an ExtractRNA kit (Eurogen, Moscow, Russia) in accordance with the protocol of the manufacturer. The resulting RNA preparation was treated with RNase-free DNase I (Thermo Scientific, Waltham, MA USA). The concentration of total RNA was measured spectrophotometrically using a Nanodrop ND-1000 spectrophotometer (ND Technologies, Fremont, CA, USA). Two micrograms of total RNA was taken for cDNA synthesis; reverse transcription was performed using an oligo(dT)15 primer and MMLV reverse transcriptase (Eurogen, Moscow, Russia) according to the manufacturer's instructions. Real-time PCR was performed using a DTLite5 amplifier (DNA-Technology LLC, Moscow, Russia) using the qPCRmix-HS SYBR reaction mixture (Eurogen, Moscow, Russia). The selection and analysis of gene-specific primers were performed using Primer-BLAST [21] (the oligonucleotide sequences are

presented below; see Table 1). The relative level of the expression of each gene was normalized by the level of mRNA of the cytoskeletal protein beta-actin (Actb), and a comparative C_T method was used to quantify the results [22].

Table 1. List of gene-specific primers for RT-PCR analysis.

Gene	GenBank #	Sequence 5'-3'	Product Size (bp)
<i>MCU</i>	NM_001106398.1	F: GCCACCAAAGAGAGACCTCC R: GCTCAATGCACAGTGTGGTG	98
<i>MCUb</i>	XM_006224254.3	F: CGCCCCAGGTTTCAGGTATG R: GGCAGGGTGAGGGTTACAAA	136
<i>MICU1</i>	NM_199412.1	F: AGGACTTTGTGCGCTCCATA R: GTTCCTGGGCAATTTTCTTCCA	105
<i>Slc25a4 (Ant1)</i>	NM_053515.1	F: TGCCAGACCCCAAGAATGTG R: GTACATAATATCAGCCCTTCCG	149
<i>Ppif</i>	NM_172243.1	F: GGTGCTGGAGTTAAAGGCAGATG R: TGATTGGTGAAGTCGCCAGC	150
<i>Atp5f1a</i>	NM_023093.1	F: GACAGACCGGAAAACCTCG R: GGTGGACCGTTTCTGACCAA	125
<i>Vdac1</i>	NM_031353.1	F: AGGGCTACGGCTTTGGCTTA R: AAACGTCAGCCCATACTCGG	155

2.6. Statistical Analysis

The data were analyzed using the GraphPad Prism 7 and Excel software and presented as mean (median) \pm SEM of 3–5 experiments. Statistical differences between the means were determined by Mann–Whitney U test; $p < 0.05$ was considered to be statistically significant.

3. Results

3.1. Mitochondrial Ca^{2+} Uptake and the Features of Subunit Composition of the Mitochondrial Ca^{2+} Uniporter Complex in the Liver and Heart of Rats with Different Tolerance to Acute Hypoxia

In this work, we first analyzed the functional and structural features of the system of mitochondrial Ca^{2+} transport in the liver and the heart of animals with different tolerance to oxygen shortage, LR and HR rats. Figure 1A shows the kinetics of uptake of Ca^{2+} (50 μ M) by the liver mitochondria of LR (dotted line) and HR rats (solid line) in the presence of CsA, which was necessary to block the possible opening of the MPT pore. One can see that the rate of Ca^{2+} influx into the liver mitochondria of HR rats is 1.3 times higher compared with that of LR rats (Figure 1B). The heart mitochondria of HR rats were found to accumulate Ca^{2+} ions also significantly faster than those of LR rats, although the difference is less pronounced than for liver mitochondria (about 10–15%) (Figure 1C).

Mitochondrial Ca^{2+} uptake is mediated by an electrogenic uniport, referred to as “ Ca^{2+} uniporter”, a complex of proteins of the inner mitochondrial membrane, including the pore-forming subunit MCU and its dominant-negative form MCUB, and the regulatory subunits MICU1, MICU2, EMRE, and MCUR1. It is considered that the contents of MCU, MCUB, and MICU1 and their stoichiometry can predominantly regulate the mitochondrial Ca^{2+} transport in accordance with physiological needs [5,6,23]. Since the mitochondria of HR animals accumulate Ca^{2+} faster as compared to the organelles of LR rats, one can assume that the adaptation to hypoxic stress is associated with changes in the relative content of these subunits in the mitochondrial membrane. Therefore, we quantified the uniporter protein constituents and their mRNA level in the liver and cardiac muscle of rats depending on the baseline resistance of animals to hypoxia.

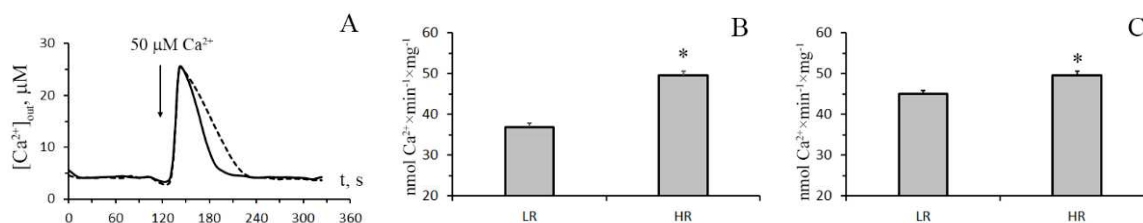


Figure 1. Ca²⁺ ion uptake by mitochondria of the liver and heart of hypoxia low-resistance (LR) and high-resistance (HR) rats. **(A)** The changes in the external concentration of Ca²⁺ ions in the incubation medium during their accumulation by the liver mitochondria of HR (the solid line) and LR (the dotted line) rats. The incubation medium contained 210 mM mannitol, 70 mM sucrose, 2.5 mM malate, 2.5 mM glutamate, 1 mM KH₂PO₄, 10 µM EGTA, 1 µM cyclosporin A, and 10 mM Hepes/KOH buffer (pH 7.4). Additions: rat liver mitochondria (0.4 mg/mL), 50 µM CaCl₂. The typical traces of five independent experiments are presented. **(B)** The rates of Ca²⁺ uptake by liver mitochondria (shaded columns) of HR and LR rats. **(C)** The rates of Ca²⁺ uptake by heart mitochondria of HR and LR rats. Values are given as means ± SEM (n = 5). * The difference between HR and LR animals is statistically significant (p < 0.05).

The immunoblotting of the members of the MCUC protein family of the mitochondria isolated from the liver of rats of two phenotypes reveals that in HR rats, the levels of MCU and MICU1 were higher than in LR rats by 1.3 and 1.35 times, respectively (Figure 2A,B), whereas no significant difference in the level of the dominant-negative uniporter subunit MCUb was observed. As for heart tissue, a comparative analysis of the protein level of the components of the MCUC showed that there was a significant decrease in the content of MCUb and a slight tendency to an increase in the content of MCU in the cardiac mitochondria of HR rats relative to those of LR animals (Figure 2C,D). VDAC1 participates in the formation of MAM (mitochondria-associated membranes) contacts, which are the main pathway of Ca²⁺ transfer from the endoplasmic reticulum to mitochondria [5,14]. One can see that the amount of VDAC1 in liver mitochondria did not differ. At the same time, the level of VDAC1 in heart mitochondria of HR rats was higher than that of LR rats.

The results of the real-time PCR analysis confirm the data obtained and also indicate that the changes occur at the level of transcription. The mRNA content of MCU in the liver of HR rats is significantly increased in comparison with that of LR rats. At the same time, the expression profile of MICU1 and MCUb in the liver of rats of two phenotypes does not differ (Figure 3A). So, the MCU/MCUB expression ratio grew from 4.6 in the liver of LR animals to 7.0 in the liver of HR rats ($2^{-\Delta Ct} MCU = 0.014 \pm 0.001$ and 0.025 ± 0.001 in the liver tissue of LR and HR rats, respectively; $2^{-\Delta Ct} MCUb = 0.003 \pm 0.0005$ and 0.0035 ± 0.00038 in LR and HR rats, respectively). Figure 3B demonstrates that the expression level of MCUb is significantly lower in the heart tissue of HR animals in comparison with that of LR animals. The MCU/MCUB expression ratio grew from 3.5 in the heart of LR animals to 8.8 in the heart of HR rats ($2^{-\Delta Ct} MCU = 0.024 \pm 0.005$ and 0.034 ± 0.008 in the heart tissue of LR and HR rats, respectively; $2^{-\Delta Ct} MCUb = 0.007 \pm 0.0007$ and 0.0038 ± 0.0005 in LR and HR rats, respectively).

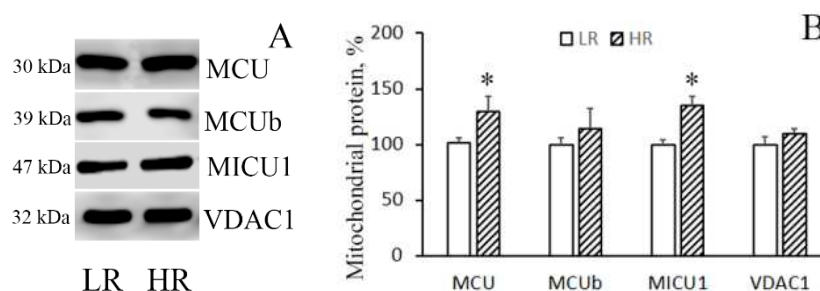


Figure 2. Cont.

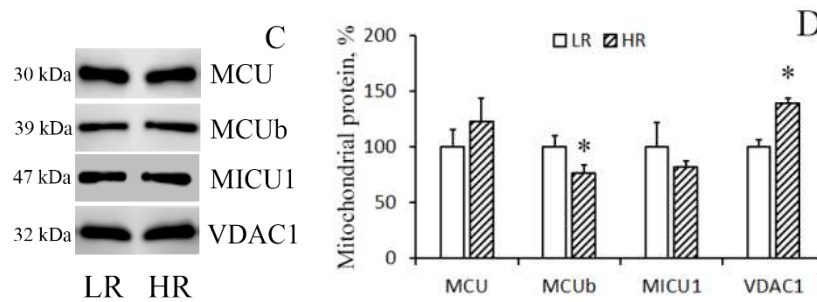


Figure 2. Levels of the subunits of MCUC and VDAC1 in liver (A,B) and heart (C,D) mitochondria of LR and HR rats. Western blot analysis of the members of the MCU protein family (MCU, MCUB, and MICU1) and VDAC1 in the liver (A) and heart (C) mitochondria of LR and HR rats. Summarized data of densitometric band analysis of these proteins in the liver (B) and heart (D) mitochondria of LR and HR rats. Values are given as means \pm SEM (n = 3). * The difference between HR and LR animals is statistically significant ($p < 0.05$).

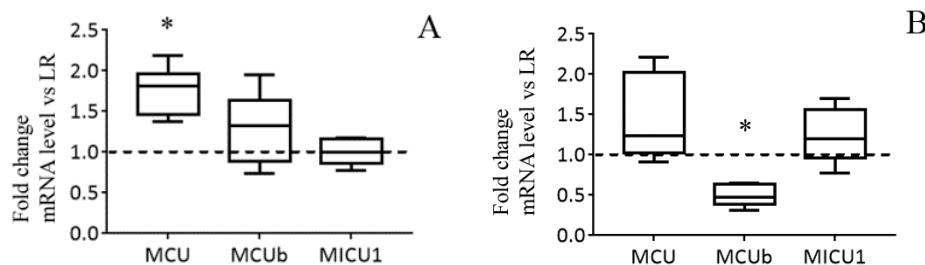


Figure 3. The mRNA levels of the subunits of MCUC in liver (A) and heart (B) of HR rats normalized to those of LR rats. The median and extreme values are presented (n = 8). The horizontal line is the mean value of the mRNA levels in LR rats. * The difference between HR and LR animals is statistically significant ($p < 0.05$).

On the basis of the results obtained, one can conclude that an increase in the relative amount of the pore-forming subunit of MCUC, MCU, in liver mitochondria and a decrease in the dominant-negative subunit, MCUB, in heart mitochondria underlie the increased rate of mitochondrial Ca^{2+} uptake in HR rats relative to that in LR rats.

3.2. A Comparison of the Resistance of Mitochondria to the Opening of MPT Pore and of the Levels of Its Probable Molecular Components in the Liver and Heart of HR and LR Rats

The pathophysiological phenomenon of the Ca^{2+} -induced MPT pore opening is well known to be central to mitochondrial vital functions and can play a lethal role in many pathophysiological conditions including hypoxia cell injury. So, the next objective of our work was to examine whether the resistance of mitochondria to the opening of the MPT pore changes depending on the baseline tolerance of an animal to hypoxic condition. The mitochondrial Ca^{2+} retention capacity (CRC) is related to the threshold concentration of Ca^{2+} necessary for the pore to open. One of the ways to assess this parameter is to introduce Ca^{2+} into the suspension of mitochondria in small successive doses, and the number of such additions until the MPT pore is triggered will reflect the CRC of the organelles. Figure 4A shows the results of such experiments. It can be seen that the number of successive Ca^{2+} additions (and, therefore, the threshold pore-opening Ca^{2+} concentration) in the case of the liver mitochondria of HR rats was greater compared to the organelles of the liver of LR rats. The parameter of CRC of HR rat liver mitochondria increased 1.3-fold (Figure 4B). This implies that their resistance to the opening of the MPT pore would also be higher.

By now, the structure of the MPT pore, which is believed to be a mega-channel penetrating both the inner and outer mitochondrial membranes, has yet to be determined. Three proteins of the inner mitochondrial membrane, namely, adenylate translocator (ANT), ATP synthase, and cyclophilin D, are

considered to be essential components of the pore complex [14,24]. To elucidate a possible molecular mechanism of the resistance of HR rat liver mitochondria to the induction of MPT pore opening, we have compared the levels of these proteins in the organelles of the liver of rats of two phenotypes.

Figure 4C,D show immunoblots of cyclophilin D, ANT1, and α -subunit of ATP synthase of mitochondria from the liver of HR and LR rats. One can see that the amount of cyclophilin D and ANT1 in the mitochondria did not differ. The levels of mitochondrial ATP synthase in the liver of HR rats, on the other hand, were reduced, with the reduction being statistically significant. The results of the real-time PCR analysis confirm the data obtained and also indicate that the changes occur at the level of transcription. So, the mRNA content of *Atp5f1a* in the liver of HR rats is significantly decreased in comparison with that of LR rats. At the same time, the expression profile of ANT1 and cyclophilin D in the liver of rats of two phenotypes does not differ (Figure 5A). We suppose that the decrease in the content of ATP synthase can be the cause of the increased resistance of liver mitochondria of HR rats to the MPT pore opening.

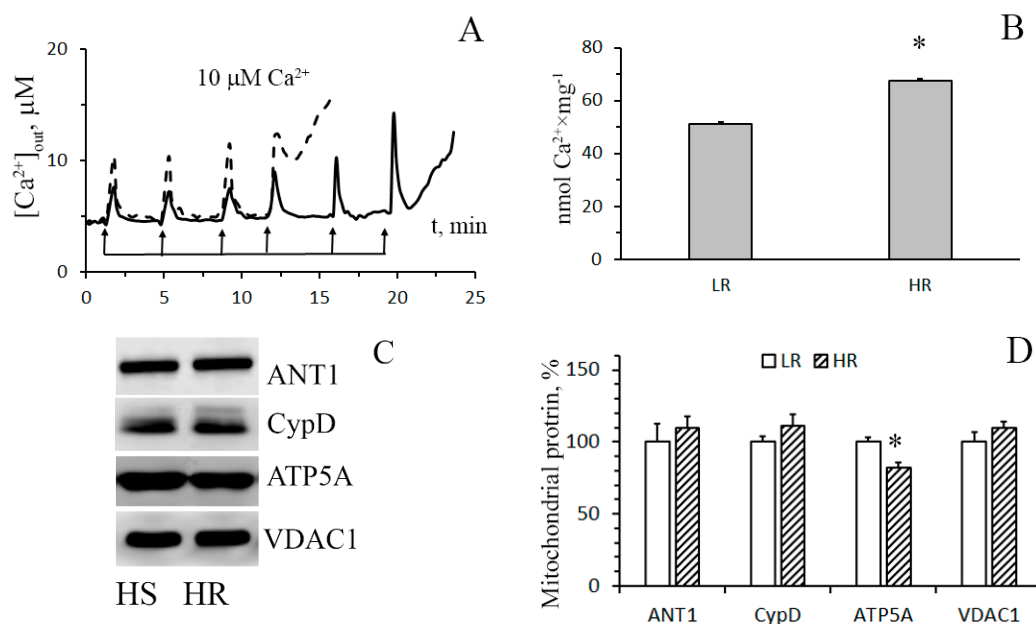


Figure 4. The parameters of formation and levels of putative protein components of the Ca²⁺-induced MPT pore in the liver mitochondria of HR and LR rats. **(A)** Changes in the external concentration of Ca²⁺ in a suspension of liver mitochondria of HR (the solid line) and LR (the dotted line) rats after sequential additions of 10 μ M Ca²⁺. The incubation medium was the same as in Figure 1, with the exception of cyclosporin A. Additions: rat liver mitochondria (0.4 mg/mL). The figure shows traces of a typical experiment conducted at the same time on the same mitochondrial preparation. Similar results were obtained in five independent experiments. **(B)** Calcium retention capacity of liver mitochondria of LR and HR rats. The values are given as means \pm SEM (n = 5). **(C)** Western blot analysis of MPT-related proteins: CypD, ANT1, ATP5A, and VDAC1 in liver mitochondria of LR and HR rats. **(D)** Summarized data on the relative contents of the MPT-related proteins. Values are given as means \pm SEM (n = 3). * The difference between HR and LR animals is statistically significant ($p < 0.05$).

Figure 6 shows the data of the estimation of maximal calcium capacity and Western blot analysis of the MPT-related proteins in mitochondria from the heart of HR and LR animals. In contrast to mitochondria from the liver tissue, cardiac mitochondria from rats of both groups display no statistically significant difference in the CRC and the content of ATP synthase and ANT1. At the same time, the levels of the regulatory protein, cyclophilin D, and VDAC1, which is assumed to form the channel of the MPT pore in the outer mitochondrial membrane, in heart mitochondria of HR rats were higher than those of LR rats. The results of real-time PCR analysis are consistent with the data of immunoblotting (Figure 5B).

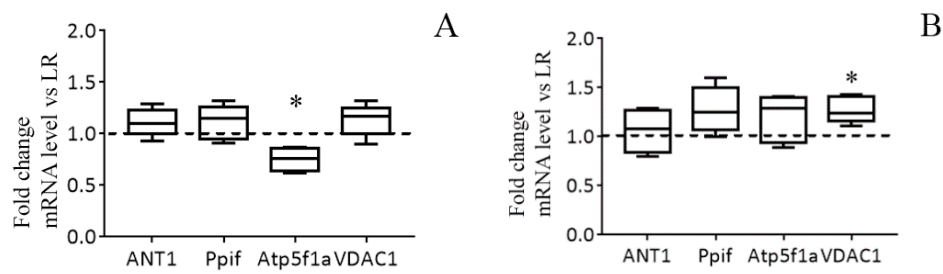


Figure 5. The mRNA levels of the MPT in liver (A) and heart (B) of HR rats normalized to those of LR rats. The median and extreme values are presented (n = 8). The horizontal line is the mean value of the mRNA levels in LR rats. * The difference between HR and LR animals is statistically significant (p < 0.05).

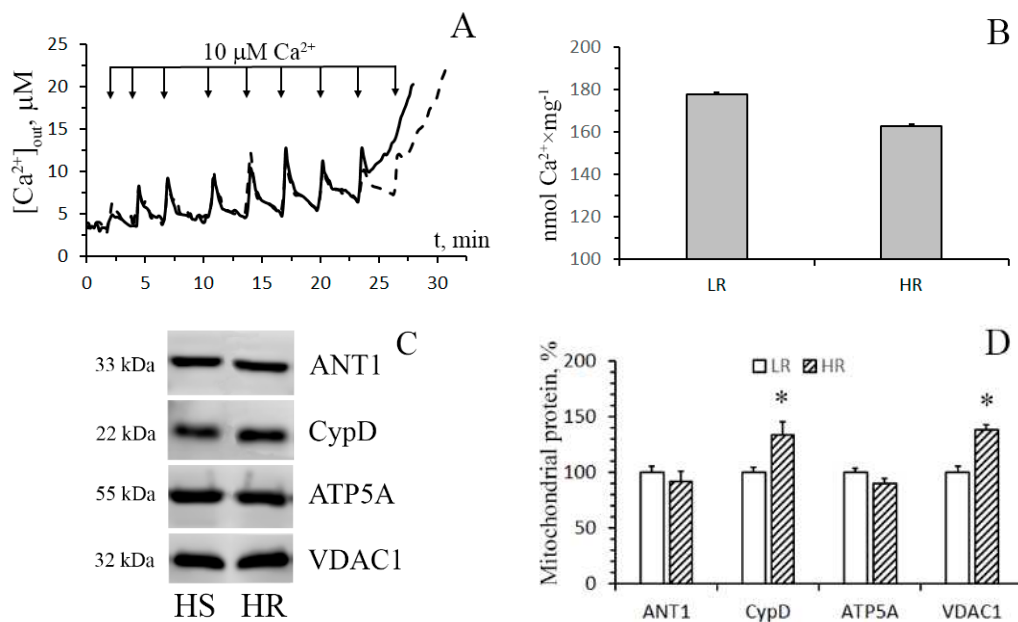


Figure 6. Induction of the Ca²⁺-induced MPT pore in the heart mitochondria of HR and LR rats. (A) Changes in the external concentration of Ca²⁺ in a suspension of heart mitochondria of HR (the solid line) and LR (the dotted line) rats after sequential additions of 10 µM Ca²⁺. The incubation medium was the same as in Figure 1, with the exception of cyclosporin A. Additions: heart mitochondria (0.4 mg/mL); 10 µM CaCl₂. The figure shows traces of a typical experiment conducted at the same time on the same mitochondrial preparation. Similar results were obtained in five independent experiments. (B) Calcium retention capacity of heart mitochondria of LR and HR rats. The values are given as means ± SEM (n = 5). The medium composition and experimental conditions were as indicated in Figure 4A. (C) Western blot analysis of MPT-related proteins: CypD, ANT1, ATP5A, and VDAC1, in heart mitochondria of LR and HR rats. (D) Summarized data on the relative contents of the MPT-related proteins. Values are given as means ± SEM (n = 3). * The difference between HR and LR animals is statistically significant (p < 0.05).

4. Discussion

It is generally accepted that mitochondria are one of the main intracellular targets of hypoxia. Structural, biochemical, and functional abnormalities of mitochondria are widely believed to be important pathogenetic factors that underlie hypoxic or ischemic cell injury [1,18]. Apart from disordering mitochondrial ATP synthesis, network dynamics, and redox state, hypoxia also dysregulates the Ca²⁺ homeostasis of these organelles and the cell as a whole. The hypoxia-induced dramatic alterations in Ca²⁺ transport in mitochondria may not only be related to the decreased oxidative phosphorylation (OXPHOS), a metabolic shift toward glycolysis, and the development of oxidative

stress, but also induce cell death pathways via mitochondrial Ca^{2+} overload and the formation of Ca^{2+} -dependent MPT pore in the inner mitochondrial membrane, leading to the release of proapoptotic proteins into the cytosol [3]. Consequently, it has been proposed that mitochondrial Ca^{2+} transport pathways might be targets for protective intervention, as well as involved in the formation of the molecular mechanism of cell resistance to hypoxia and ischemia. The purpose of our work was to study in more detail the features of structure and operation of the Ca^{2+} transport systems in the mitochondria of the liver and heart of rats with originally different tolerance to acute hypoxia.

The results obtained in this work indicate that mitochondria of HR and LR rats are characterized by fundamentally different genetically programmed rearrangements of the systems regulating Ca^{2+} homeostasis. In the case of HR rats, the rearrangements of the Ca^{2+} uniporter can increase the efficiency of Ca^{2+} accumulation by liver and heart mitochondria. At the same time, the organelles of the liver of HR rats become more resistant to the opening of the Ca^{2+} -dependent MPT pore in comparison with those of LR rats. Along with the well-characterized distinction in the intensity of OXPHOS in mitochondria of the vital organs of LR and HR rats [18,25], these effects might contribute to the development of individual systemic resistance of animals to acute hypoxia.

It is well known that individuals of an animal population differ in their tolerance to oxygen deficiency [15–17,25]. As shown earlier, animals that belong to two opposite, in regard to hypoxia tolerance, types (LR and HR) have essentially different “functional-metabolic” profiles, including the effectiveness of energy support of the organism, the regulation of central nervous cardiovascular systems, neurohumoral regulation, stress-activating and stress-limiting systems, the oxygen-transporting function of blood, and the state of membranes and receptors. LR animals are considered to have a weak type of the nervous system, increased excitability, and emotional reactivity. LR animals respond to hypoxia with agitation and high locomotor activity. In contrast, HR animals have reduced excitability and anxiety, milder aggressiveness, more pronounced internal inhibition, low sensitivity to any provocative factors, and a tendency to social domination [18].

It was previously shown that mitochondria of the vital organs of LR and HR rats differ in both structural and basic functional parameters. Thus, the mitochondria of the cerebral cortex of HR rats are characterized by a denser packing of cristae and a more electron-dense matrix, smaller sizes, and higher concentrations of the respiratory chain complexes and the respiration substrate, succinate (i.e., they are functionally more active compared to mitochondria of LR rats) [16,25]. In contrast, in brain mitochondria of LR rats, the number of mitochondrial cristae is decreased, and this is consistent with the lower content of their respiratory electron carriers compared to mitochondria of HR rats. It was also found that in liver mitochondria of HR animals, the rate of the ATP-dependent potassium transport, which reflects the activity of the mitochondrial ATP-sensitive potassium channel, was increased [17].

Here, we have demonstrated that, in addition to the above structural–functional features, the mitochondria of the liver and heart of rats with originally different tolerance to hypoxia are distinguished in respect to the rate of influx of Ca^{2+} ions via MCUC. The liver and heart mitochondria of HR rats are characterized by a significant increase in the efficiency of Ca^{2+} uniport compared to the organelles of LR rats, with the difference being especially pronounced for the liver tissue. To elucidate the causes of these functional effects, we have examined structural changes in the Ca^{2+} transport system of mitochondria of LR and HR rats and revealed that these changes do occur in the macromolecular complex of the mitochondrial Ca^{2+} uniporter in the heart and liver tissues.

The MCUC is considered to consist of two transmembrane channel subunits: MCU and MCUB. MCU forms a highly selective Ca^{2+} channel, which transfers the ion across the inner mitochondrial membrane. MCUB is a dominant-negative MCU paralogue, and its overexpression impairs the ion-transporting function of the complex [13]. MCU and MCUB are associated with other subunits: MICU1-2, EMRE, and MCUR1, which act as regulators of the uniporter.

As follows from the data obtained, in HR animals, the contents of the pore-forming subunit MCU and the gate subunit MICU1 are substantially increased in liver mitochondria, whereas the level of the dominant-negative subunit, MCUB, is decreased in heart mitochondria. The data are confirmed by the

results of real-time PCR analysis and indicate that these changes occur at the level of transcription. At the same time, there is almost no difference between liver and heart mitochondria of LR and HR animals in the content of the regulatory uniporter subunit EMRE and the expression of its gene.

It is known that the activity of MCUC is regulated by changes in the ratio of the Ca^{2+} -conducting pore subunits MCU and MCUB [5,26,27]. Therefore, both an increase in the level of MCU and a decrease in the content of its paralogue MCUB, which we recorded in mitochondria of the liver and heart of HR animals, can be the cause of the increased rate of Ca^{2+} influx into the organelles. Based on the data obtained, we can conclude that the structural changes in the pore-forming subunits of MCUC in HR rats increase the efficiency of Ca^{2+} accumulation in the mitochondrial matrix and, as a result, might underlie the fine control of cytoplasmic free Ca^{2+} at low levels.

On the other hand, excessive accumulation of Ca^{2+} into mitochondria can result in the opening of MPT in the inner mitochondrial membrane. As a result, all transmembrane ionic gradients and the membrane potential collapse, and mitochondria swell, which leads to the rupture of their outer membrane and the release of proapoptotic proteins (cytochrome *c*, apoptosis-inducing factor, and others) from the organelles. This can facilitate the activation of the caspase cascade, DNA damage, and eventually cell death. The opening of the MPT pore is believed to be triggered by hypoxia and subsequent reoxygenation [3,14]. The data obtained in this work show that liver (but not heart) mitochondria of HR rats have a significantly higher Ca^{2+} capacity (i.e., are more resistant to the induction of the MPT pore than the organelles of LR rats). Similar results were partially obtained by us earlier [19]. In order to gain insight into the molecular mechanism of tolerance of liver mitochondria of HR rats to MPT, we assayed for levels of MPT-associated mitochondrial proteins: cyclophilin D, ATP synthase (α -subunit), and adenylate translocator ANT1 (Figure 4). Our results indicate that the levels of cyclophilin D and ANT1 in mitochondria of the liver of HR and LR rats are not distinguished. There is, however, a significant decrease in the content of the α -subunit of ATP synthase (a protein that supposedly forms the channel of the MPT pore) in liver mitochondria of HR rats. Thus, the increased tolerance of liver mitochondria of HR rats to MPT, as compared with mitochondria of LR rats, can be related to a lowered expression of the MPT pore-forming protein. This is in agreement with the earlier report that the changes in expression of ATP synthase had significant effects on the probability of MPT induction [28].

However, the question as to which subunit of this multisubunit complex is the central structural component of the MPT pore, or whether it is formed by MPT-specific conformation of dimers of ATP synthase, remains the province of further investigations.

It should be noted that the CRC index of mitochondria isolated from the heart of HR rats was slightly lower compared to that of LR rats, although this difference was not statistically significant. This trend toward a decline in the Ca^{2+} buffering capacity is likely explained by the fact that the content of cyclophilin D, a major regulatory protein of the MPT pore [14,29,30], in heart mitochondria of HR rats is increased (Figure 6). It is believed that VDAC1 is also involved in the formation of the MPT pore complex in mitochondria. In addition, this protein participates in the formation of MAM contacts, which are the main pathway of Ca^{2+} transfer from the endoplasmic reticulum to mitochondria [5,14]. So, the changes observed in the level of VDAC1 can also contribute to the tissue-specific modulation of mitochondrial Ca^{2+} handling and the MTP opening.

Based on the results obtained, one can assume that the increase in the rate of Ca^{2+} transport in mitochondria is not accompanied by a higher susceptibility of mitochondria to calcium overload and the induction of the MPT pore. As follows from our data, changes in the levels of the MPT-related proteins can play a crucial role in the regulation of pore formation in mitochondria. At the same time, the high rate of mitochondrial Ca^{2+} uptake may provide a more effective removal of excess Ca^{2+} ions from the cytosol under physiological conditions and hypoxia.

5. Conclusions

The results obtained point out that liver and heart mitochondria of HR animals exhibit functional and structural features in Ca^{2+} ion transport, which may be essential for proper mitochondrial function in hypoxia and contribute to the formation of adaptive signs to provide the development of cellular response to oxygen shortage. So, apart from the increased activity of the ATP-sensitive potassium channel and respiratory chain complexes, mitochondria of HR animals are characterized by the increased rate of uptake of Ca^{2+} ions. At the same time, compared to liver mitochondria of LR animals, the organelles of HR rats are more resistant to the opening of the Ca^{2+} -dependent MPT pore. Taking into account the fact that the MPT pore opening is one of the key pathogenic events in oxygen deficiency, it can be supposed that these changes contribute to the molecular basis underlying cellular sensitivity to hypoxic injury.

Author Contributions: Conceptualization, K.N.B.; investigation, K.N.B., N.V.B., E.Y.T., V.S.S., N.M.Z., K.S.T., and M.V.D.; writing—original draft preparation, K.N.B.; writing—review and editing, K.N.B., N.V.B., and M.V.D.; project administration, K.N.B.; funding acquisition, K.N.B. All authors have read and agreed to the published version of the manuscript.

Funding: This study was funded by grants from the Russian Foundation for Basic Research (18-315-20011 to Konstantin N. Belosludtsev).

Acknowledgments: We thank Ivan V. Semenov from the ICB RAS for technical support in carrying out the experiments.

Conflicts of Interest: The authors declare no conflict of interest.

References

1. Bargiela, D.; Burr, S.P.; Chinnery, P.F. Mitochondria and Hypoxia: Metabolic Crosstalk in Cell-Fate Decisions. *Trends Endocrinol. Metab.* **2018**, *29*, 249–259. [CrossRef] [PubMed]
2. Lukyanova, L.D. Mitochondrial signaling in hypoxia. *OJEMD* **2013**, *3*, 20–32. [CrossRef]
3. Halestrap, A.P.; Richardson, A.P. The mitochondrial permeability transition: A current perspective on its identity and role in ischaemia/reperfusion injury. *J. Mol. Cell. Cardiol.* **2015**, *78*, 129–141. [CrossRef] [PubMed]
4. Denton, R.M. Regulation of mitochondrial dehydrogenases by calcium ions. *Biochim. Biophys. Acta* **2009**, *1787*, 1309–1316. [CrossRef]
5. Belosludtsev, K.N.; Dubinin, M.V.; Belosludtseva, N.V.; Mironova, G.D. Mitochondrial Ca^{2+} transport: Mechanisms, molecular structures, and role in cells. *Biochemistry (Moscow)* **2019**, *84*, 593–607. [CrossRef]
6. Giorgi, C.; Marchi, S.; Pinton, P. The machineries, regulation and cellular functions of mitochondrial calcium. *Nat. Rev. Mol. Cell Biol.* **2018**, *19*, 713–730. [CrossRef]
7. Scorrano, L. Divide et impera: Ca^{2+} signals, mitochondrial fission and sensitization to apoptosis. *Cell Death Differ.* **2003**, *10*, 1287–1289. [CrossRef] [PubMed]
8. Tinel, H.; Cancela, J.M.; Mogami, H.; Gerasimenko, J.V.; Gerasimenko, O.V.; Tepikin, A.V.; Petersen, O.H. Active mitochondria surrounding the pancreatic acinar granule region prevent spreading of inositol trisphosphate-evoked local cytosolic Ca^{2+} signals. *EMBO J.* **1999**, *18*, 4999–5008. [CrossRef] [PubMed]
9. Gilibert, J.A.; Parekh, A.B. Respiring mitochondria determine the pattern of activation and inactivation of the store-operated Ca^{2+} current I (CRAC). *EMBO J.* **2000**, *19*, 6401–6407. [CrossRef] [PubMed]
10. Hoth, M.; Button, D.C.; Lewis, R.S. Mitochondrial control of calcium-channel gating: A mechanism for sustained signaling and transcriptional activation in T lymphocytes. *Proc. Natl. Acad. Sci. USA* **2000**, *97*, 10607–10612. [CrossRef]
11. Elustondo, P.A.; Nichols, M.; Robertson, G.S.; Pavlov, E.V. Mitochondrial Ca^{2+} uptake pathways. *J. Bioenerg. Biomembr.* **2017**, *49*, 113–119. [CrossRef] [PubMed]
12. Paillard, M.; Csordas, G.; Szanda, G.; Golenar, T.; Debattisti, V.; Bartok, A.; Wang, N.; Moffat, C.; Seifert, E.L.; Spat, A.; et al. Tissue-specific mitochondrial decoding of cytoplasmic Ca^{2+} signals is controlled by the stoichiometry of MICU1/2 and MCU. *Cell Rep.* **2017**, *18*, 2291–2300. [CrossRef]
13. Raffaello, A.; De Stefani, D.; Sabbadin, D.; Teardo, E.; Merli, G.; Picard, A.; Checchetto, V.; Moro, S.; Szabo, I.; Rizzuto, R. The mitochondrial calcium uniporter is a multimer that can include a dominant-negative pore-forming subunit. *EMBO J.* **2013**, *32*, 2362–2376. [CrossRef] [PubMed]

14. Briston, T.; Selwood, D.L.; Szabadkai, G.; Duchon, M.R. Mitochondrial permeability transition: A molecular lesion with multiple drug targets. *Trends Pharmacol. Sci.* **2019**, *40*, 50–70. [CrossRef] [PubMed]
15. Berezovsky, V.A. *Hypoxia and Individual Features of Reactivity*; Naukova Dumka: Kiev, Ukraine, 1978; p. 213.
16. Lukyanova, L.D.; Germanova, E.L.; Kopaladze, R.A. Development of resistance of an organism under various conditions of hypoxic preconditioning: Role of the hypoxic period and reoxygenation. *Bull. Exp. Biol. Med.* **2009**, *147*, 400–404. [CrossRef]
17. Mironova, G.D.; Shigaeva, M.I.; Gritsenko, E.N.; Murzaeva, S.V.; Gorbacheva, O.S.; Germanova, E.L.; Lukyanova, L.D. Functioning of the mitochondrial ATP-dependent potassium channel in rats varying in their resistance to hypoxia. Involvement of the channel in the process of animal's adaptation to hypoxia. *J. Bioenerg. Biomembr.* **2010**, *42*, 473–481. [CrossRef]
18. Lukyanova, L.D.; Kirova, Y.I. Mitochondria-controlled signaling mechanisms of brain protection in hypoxia. *Front. Neurosci.* **2015**, *9*, 1–15. [CrossRef]
19. Belosludtsev, K.N.; Saris, N.E.; Belosludtseva, N.V.; Trudovishnikov, A.S.; Lukyanova, L.D.; Mironova, G.D. Physiological aspects of the mitochondrial cyclosporin A-insensitive palmitate/Ca²⁺-induced pore: Tissue specificity, age profile and dependence on the animal's adaptation to hypoxia. *J. Bioenerg. Biomembr.* **2009**, *41*, 395–401. [CrossRef]
20. Lowry, O.H.; Rosebrough, N.J.; Farr, A.L.; Randall, R.J. Protein measurement with the Folin phenol reagent. *J. Biol. Chem.* **1951**, *193*, 265–275.
21. Ye, J.; Coulouris, G.; Zaretskaya, I.; Cutcutache, I.; Rozen, S.; Madden, T. Primer-BLAST: A tool to design target-specific primers for polymerase chain reaction. *BMC Bioinform.* **2012**, *13*, 134. [CrossRef]
22. Schmittgen, T.D.; Livak, K.J. Analyzing real-time PCR data by the comparative C(T) method. *Nat. Protoc.* **2008**, *3*, 1101–1108. [CrossRef] [PubMed]
23. De Stefani, D.; Rizzuto, R.; Pozzan, T. Enjoy the Trip: Calcium in Mitochondria Back and Forth. *Annu. Rev. Biochem.* **2016**, *85*, 161–192. [CrossRef]
24. Bonora, M.; Pinton, P. A New Current for the Mitochondrial Permeability Transition. *Trends Biochem. Sci.* **2019**, *44*, 559–561. [CrossRef] [PubMed]
25. Mironova, G.D.; Pavlik, L.L.; Kirova, Y.I.; Belosludtseva, N.V.; Mosentsov, A.M.; Khmil, N.V.; Germanova, E.L.; Lukyanova, L.D. Effect of hypoxia on mitochondrial enzymes and ultrastructure in the brain cortex of rats with different tolerance to oxygen shortage. *J. Bioenerg. Biomembr.* **2019**, *51*, 329–340. [CrossRef] [PubMed]
26. Belosludtsev, K.N.; Talanov, E.Y.; Starinets, V.S.; Agafonov, A.V.; Dubinin, M.V.; Belosludtseva, N.V. Transport of Ca²⁺ and Ca²⁺-Dependent Permeability Transition in Rat Liver Mitochondria under the Streptozotocin-Induced Type I Diabetes. *Cells* **2019**, *8*, 1014. [CrossRef]
27. Suarez, J.; Cividini, F.; Scott, B.T.; Lehmann, K.; Diaz-Juarez, J.; Diemer, T.; Dai, A.; Suarez, J.A.; Jain, M.; Dillmann, W.H. Restoring mitochondrial calcium uniporter expression in diabetic mouse heart improves mitochondrial calcium handling and cardiac function. *J. Biol. Chem.* **2018**, *293*, 8182–8195. [CrossRef]
28. Neginskaya, M.A.; Solesio, M.E.; Berezhnaya, E.V.; Amodeo, G.F.; Mnatsakanyan, N.; Jonas, E.A.; Pavlov, E.V. ATP Synthase C-Subunit-Deficient Mitochondria Have a Small Cyclosporine A-Sensitive Channel, but Lack the Permeability Transition Pore. *Cell Rep.* **2019**, *26*, 11–17. [CrossRef]
29. Laker, R.C.; Taddeo, E.P.; Akhtar, Y.N.; Zhang, M.; Hoehn, K.L.; Yan, Z. The mitochondrial permeability transition pore regulator cyclophilin D exhibits tissue-specific control of metabolic homeostasis. *PLoS ONE* **2016**, *11*, e0167910. [CrossRef]
30. Schneider, M.D. Cyclophilin D: Knocking on death's door. *Sci. STKE* **2005**, *5*, pe26. [CrossRef]



© 2020 by the authors. Licensee MDPI, Basel, Switzerland. This article is an open access article distributed under the terms and conditions of the Creative Commons Attribution (CC BY) license (<http://creativecommons.org/licenses/by/4.0/>).

Review

Routes for Potassium Ions across Mitochondrial Membranes: A Biophysical Point of View with Special Focus on the ATP-Sensitive K⁺ Channel

Yevheniia Kravenska , Vanessa Checchetto and Ildiko Szabo *

Department of Biology, University of Padova, 35131 Padova, Italy; k.evgeniya.v@gmail.com (Y.K.); vanessa.checchetto@unipd.it (V.C.)

* Correspondence: ildiko.szabo@unipd.it

Abstract: Potassium ions can cross both the outer and inner mitochondrial membranes by means of multiple routes. A few potassium-permeable ion channels exist in the outer membrane, while in the inner membrane, a multitude of different potassium-selective and potassium-permeable channels mediate K⁺ uptake into energized mitochondria. In contrast, potassium is exported from the matrix thanks to an H⁺/K⁺ exchanger whose molecular identity is still debated. Among the K⁺ channels of the inner mitochondrial membrane, the most widely studied is the ATP-dependent potassium channel, whose pharmacological activation protects cells against ischemic damage and neuronal injury. In this review, we briefly summarize and compare the different hypotheses regarding the molecular identity of this patho-physiologically relevant channel, taking into account the electrophysiological characteristics of the proposed components. In addition, we discuss the characteristics of the other channels sharing localization to both the plasma membrane and mitochondria.

Keywords: mitochondria; ion channels; electrophysiology; ATP-dependent potassium channel

Citation: Kravenska, Y.; Checchetto, V.; Szabo, I. Routes for Potassium Ions across Mitochondrial Membranes: A Biophysical Point of View with Special Focus on the ATP-Sensitive K⁺ Channel. *Biomolecules* **2021**, *11*, 1172. <https://doi.org/10.3390/biom11081172>

Academic Editor: Ferdinando Palmieri

Received: 22 June 2021

Accepted: 2 August 2021

Published: 8 August 2021

Publisher's Note: MDPI stays neutral with regard to jurisdictional claims in published maps and institutional affiliations.



Copyright: © 2021 by the authors. Licensee MDPI, Basel, Switzerland. This article is an open access article distributed under the terms and conditions of the Creative Commons Attribution (CC BY) license (<https://creativecommons.org/licenses/by/4.0/>).

1. Introduction

In 1961, Peter Mitchell formulated the chemiosmotic theory [1], according to which (i) electron transport through the respiratory chain of mitochondria promotes the flow of protons from the matrix into the intermembrane space, allowing the formation of a H⁺ gradient (protonmotive force), (ii) this process is directly related to the activity of F₁F₀-ATP synthase and to the production/hydrolysis of ATP, (iii) the inner mitochondrial membrane (IMM) is impermeable to ions, including H⁺. Despite this assumption, the author predicted the necessity for ions to be transported through the IMM. Indeed, extensive research over the last few decades has highlighted an important role for potassium transporters/channels in the regulation of the IMM potential ($\Delta\psi$), redox state and mitochondrial volume, as summarized by recent, detailed reviews, e.g., [2–7]. By modulating these important factors, K⁺ channels impact not only on bioenergetic efficiency and ATP production by mitochondria, but also on cellular signaling events such as, for example, apoptotic signaling [8,9], Wnt signaling [10], and cGMP-related pathways [11]. As a consequence, IMM K⁺ channels emerged as important players in the context of cancer [12], cardioprotection [13], and neuronal protection [9], and may even play a role in the inflammatory response [14]. Thanks to intensive research carried out by several excellent groups in the field, mitochondrial potassium channels are currently in the spotlight of the scientific community working on different pathologies.

2. Multiple Routes for Potassium across the Outer and Inner Mitochondrial Membranes

The passage of this ion, which is normally present at a concentration greater than 100 mM in the cytosol, follows the electrochemical gradient largely dictated by the very negative resting membrane potential across the IMM (around –180 mV). Mitochondria

maintain the matrix K^+ concentration at 150–180 mM [15]. The influx of K^+ can occur through the mitochondrial channels, while the excess K^+ matrix is expelled by the antiporter K^+/H^+ . The consensus view is that the voltage-dependent anion channel isoforms (VDACs) of the outer mitochondrial membrane (OMM) [16,17] are sufficiently large to allow the flux of different metabolites and ions, including K^+ . Indeed, VDACs (VDAC1–3) show a slight cation selectivity in the partially closed state [18] and, although tightly regulated [19], they may ensure a continuous flux of potassium into and out of the mitochondrial intermembrane space, allowing an equilibrium between this compartment and the cytosol. It was surprising, therefore, that an inwardly rectifying K^+ channel that was responsive to voltage, osmotic pressure and cAMP has been identified directly by patch clamping mitochondria isolated from the spinal cord [20]. The physiological importance of this channel is not clear, but importantly, this work confirmed the idea that VDAC may adopt a completely closed state across the OMM [21], since no VDAC-like current was observed by electrophysiology. It is of note that even though VDACs were shown to mediate calcium flux across the OMM [22,23], a small channel, namely a functional $\alpha 7$ nicotinic acetylcholine receptor, was able to regulate calcium flux across the OMM [24], suggesting that the OMM might indeed be not freely permeable to ions such as calcium and potassium.

In contrast to the OMM, the IMM harbors a number of potassium channels, and a K^+/H^+ exchanger. Given that several recent reviews dealt with the former topic (see also [5] in this Special Issue), here we only mention the main classes of K^+ channels, that can allow the passage of only K^+ (K^+ -selective channels) or of other cations as well (K^+ -permeable channels). In the former category, the following channels have been identified directly by patch clamping of mitochondria: (1) ATP-dependent potassium channel [25]; (2) voltage-gated shaker type K^+ channel Kv1.3 [26,27]; (3) calcium-activated intermediate-conductance K^+ channel (IK(Ca)) [28]; (4) calcium-activated big conductance potassium channel (BK(Ca)) [29,30]; (5) small-conductance calcium-activated K^+ channel (SK(Ca)) [31]; (6) renal medullary channel ROMK [32]; and (7) two-pore potassium channel TASK-3 [33]. The hyperpolarization-activated, cyclic-nucleotide-gated channel isoforms HCNs belong to the latter category of potassium-permeable channels [34,35].

In most of the above studies, the mitochondrial channels recorded in the IMM highly resembled those of the plasma membrane (PM), at least regarding their conductance, which is a basic biophysical feature of all ion channels. In fact, our current understanding is that, for example in the cases of TASK-3, IK(Ca), SK(Ca), Kv1.3, and HCN, the same proteins residing in the PM locate to the IMM as well, giving rise to comparable channel activities. Although mitoplasts are well distinguishable from other organelles when performing patch-clamp experiments, more sophisticated methodologies that exclude the possibility of contamination are also available [36,37]. In most studies, multiple techniques were exploited to confirm dual localization of a given protein, such as Western blot to assess contaminations by other membranes, immunogold electron microscopy and modulation of mitochondrial activity and/or K^+ uptake into mitochondria by pharmacological or genetic tools. Kv7.4 [38] and Kv1.5 [39] have been identified in the IMM of cardiomyocytes and macrophages, respectively, using biochemical/pharmacological tools only.

The mechanism of dual targeting is not known for most IMM K^+ channels. With the exception of HCNs and ROMK2 (see below), bioinformatic tools do not predict mitochondrial localization due to the lack of a typical N-terminal mitochondria-targeting sequence. Our recent data indicate that, for example, in the case of Kv1.3, association of the channel with caveolin-1 promotes PM targeting, while the lack of such functional coupling causes accumulation of the channel in mitochondria, with severe consequences on mitochondrial function and cell survival [40]. Whether association with caveolin may play a role in channel trafficking and subcellular targeting also in the case of other K^+ channels is an interesting point for future investigation. Another interesting candidate worth consideration is SKD3 (suppressor of potassium transport defect 3), also known as caseinolytic peptidase B protein homolog (CLPB), a broadly expressed member of the

family of ATPases associated with diverse cellular activities (AAA+). A recent study highlighted that ATP controls the ability of SKD3 to self-associate or form complexes with other proteins in the intermembrane space of mitochondria [41]. Human CLPB contains an ankyrin-repeat domain, and, for example, channels of the Kv7 family harbor an ankyrin-binding domain [42]. Whether and how this IMS-located protein might regulate IMM K⁺ channel import/assembly/function or exert a quality control remains an open question.

Since patch clamping of mitoplasts (i.e., of mitochondria devoid of the OMM) is technically demanding, unfortunately a complete biophysical and pharmacological characterization has not been carried out in all cases, thus hampering a strict comparison of the PM-located channels with those of their IMM counterparts. Nevertheless, as illustrated in Table 1, a relatively good match has been found in many cases, at least regarding the conductance values. It is of note that for some of the mentioned channels, the range of described conductance values is quite wide, which can be due to several factors. First of all, the composition of the working solutions (in particular, by the concentration of Ca²⁺ and K⁺) and the type of cells/tissues/organisms are not the same in each work. Depending on the cell type, the general composition and characteristics of the channels may differ, for example, due to lack of interaction with specific receptors/regulatory subunits. Within the same family of channels, differences in conductance can be explained by alternative splicing, post-translational modifications, as well as by the homo- and heteromerization of the channel [6]. The protocol applied to elicit channel activity is also important, since a wider range of voltages makes it possible to determine the conductance with greater accuracy.

Important questions are still unanswered, in particular regarding Kv channels that are normally active in the PM at depolarizing voltages. Thus, the factors allowing these channels to operate at the very negative IMM potential ($\Delta\psi$, around -160 to -180 mV) remain to be determined. Although the fact that, e.g., Kv1.3 is active in the IMM is indicated by changes in $\Delta\psi$ upon its inhibition using specific blockers [26], recent studies pointed to its involvement in the apoptotic cascade via its interaction with complex I [43] and to its role in linking respiration to proliferation, not necessarily relying on Kv1.3 ability to mediate K⁺ flux [44]. It is interesting to note that other mitochondrial potassium channels are also physically and/or functionally coupled to respiratory chain complexes: mitoBK (Ca) functionally and physically interacts with complex IV [45], mitoKATP function has been linked to complex II [46,47], ROMK2 is associated with complex V [48], while TASK-3 [49] and HCN [34] also seem to interact with complex V. It is tempting to speculate that the specific association of different K⁺ channels with distinct OXPHOS complexes may allow a reciprocal fine-tuning of their activities.

Table 1. Comparison of single-channel conductance values of the plasma membrane- and the inner mitochondrial membrane-located K⁺ channels obtained by the patch-clamp technique (in excised inside-out or mitoplast-attached configurations). Open probabilities are also reported, where available.

Channel	Conductance of PM Channel	Conductance of Mitochondrial Channel
<i>ATP-dependent K⁺ channel</i>	13–68 pS in 140 mM KCl [50,51] 20–80 pS in 140 (bath)/5.4–100 (pipette) mM KCl [52] ~80 pS in 145 mM K ⁺ [53,54] 135 pS in 120 (bath)/60 (pipette) mM K ⁺ [55]	From 10 to 100 pS in 150 mM KCl (see Table 2).
	<i>Open probability:</i> <i>N</i> Po ~0.32 at -100 mV [51] ≈0.9 between -100 and 60 mV [54]	<i>Open probability:</i> 0.74 at 40 mV [56] 0.57 at -50 mV [32] 0.24 at -60 mV [57]

Table 1. Cont.

Channel	Conductance of PM Channel	Conductance of Mitochondrial Channel
Kv1.3	24 pS in 140 mM KCl [58]	~25 pS in 134 mM K ⁺ [26] 109 pS in 150 mM KCl [27]
	<i>Open probability:</i> ~0.013 at 50 mV [58]	<i>Open probability:</i> 0.5 at –60 mV to 0.75 at 60 mV [27]
BK(Ca)	~180 pS in 143 KCl [59] 187 pS in 144 KCl [60] 260–293 pS in 150 KCl [61] 250 to 300 pS in 150 mM K ⁺ (e.g., [62])	190 pS in 130 (bath)/10 (pipette) mM K ⁺ [63] 145 to 307 pS in 150 mM K ⁺ [11,29,64–68]
	<i>Open probability:</i> ~0.27 at –40 mV [61]	<i>Open probability:</i> 0.79 at 80 mV [63] 0.5 at –33 mV [29] ~0.16 at –60 mV to ~0.94 at 60 mV [65] ~0.54–0.9 at 60 mV [11,66] ~0.25–0.76 at –40 mV [67,68]
IK(Ca)	~25 pS in 150 (bath)/140 (pipette) mM KCl [69] 31 pS in 160 mM K ⁺ [70] 33–34 pS in 130 (bath)/145 (pipette) mM KCl [71] 39 pS in 120 mM K ⁺ [72]	10 to 90 pS in 150 mM KCl [28]
	<i>Open probability:</i> 0.6 and 0.4 at –50 and 50 mV, respectively [69] <0.5 between –120 and 60 mV [70] 0.021 at –60 mV, 0.013 at –20 mV [71]	
SK(Ca)	8 pS in 200 (bath)/4 (pipette) mM KCl [73] 15 pS in 140 mM KCl [74] 40–50 pS in 140 mM KCl (pipette) [75]	Not determined at single channel level (for whole-mitoplast recording, see [31])
	~30 pS in 5 (bath)/140 (pipette) mM KCl [76] 39 pS in 145 K ⁺ mM [77]	94 pS in 150 mM KCl [32]
ROMK	<i>Open probability:</i> 0.88 between –40 and –80 mV [76] 0.82 at –60 mV and 0.92 at –30 mV [77]	<i>Open probability:</i> 0.21 at 50 mV to 0.57 at –50 mV [32]
	18 pS in 140 mM KCl (pipette) [78] 17–27 pS in 140 mM KCl [79]	12–83 pS in 150 mM KCl [33]
TASK-3	18 pS in 140 mM KCl (pipette) [78] 17–27 pS in 140 mM KCl [79]	12–83 pS in 150 mM KCl [33]
HCN	~1 pS for I _f in 5.4 (bath)/70 (pipette) mM KCl [80] 0.46 and 1.71 pS for HCN1 and HCN2, respectively (in 110 mM KCl) [81]	Not determined at single channel level (for whole-mitoplast recording, see [34])

As mentioned above, all these channel activities mediate influx of K⁺ into the matrix. This K⁺ flux in the presence of permeable anions (e.g., inorganic phosphate) takes place along with osmosis of single-channel conductance values of osmotically obligated water and therefore results in mitochondrial swelling. Therefore, to control K⁺ concentration, a K⁺/H⁺ exchanger ensures exit of K⁺ in the so-called K⁺ cycle [82]. The molecular identity of this exchanger remains debated, even though convincing evidence has been accumulated in favor of the hypothesis that envisions LETM1 as the K⁺/H⁺ exchanger (for a recent review see [83]). LETM1 has originally been identified as a protein linked to mitochondrial K⁺ homeostasis [84], but was later proposed to be the long-sought electroneutral calcium/proton antiporter (2H⁺/Ca²⁺) of the IMM [85,86]. However, a more recent work provided compelling evidence, using a novel potassium probe mitoPOP able to monitor the mitochondrial K⁺ concentration, that (i) LETM1 deletion caused K⁺ accumulation in the mitochondrial matrix; (ii) LETM1, able to transport both K⁺ and Na⁺, regulated mitochondrial calcium fluxes in a sodium-dependent manner [87]. Thus, in the so-called calcium cycle, LETM1 would exert a regulatory effect on calcium exit through the Na⁺/Ca²⁺ antiporter, whose function would be linked to the extrusion of matrix Na⁺ via LETM1. Unfortunately, more recent works [88,89] did not consider this possibility when interpreting experimental

results. Independently of the nature of the transported ions, LETM1 remains an important player in mitochondrial biology, as it has recently been shown to cause cristae-like invaginations even in artificial liposomes, raising the possibility that this transporter contributes to cristae shaping [90]. A previous work linked LETM1 function to mitochondrial fragmentation, but observed no changes in mitochondrial morphology in fibroblasts from Wolf–Hirschhorn syndrome patients, in which monoallelic LETM1 deletion occurs [91].

3. The Mitochondrial ATP-Dependent Potassium Channel(s)

In addition to uncertainties regarding LETM1, the field of mitochondrial potassium-transporting proteins has to deal with the molecular identification of one of the most important and most well-known activities, the elusive mitochondrial ATP-dependent potassium channel (KATP). KATP exerts crucial function in the PM, for example by regulating insulin secretion [92]. The PM channel comprises four channels forming subunits Kir6.1 or Kir6.2 (encoded by *KCNJ8* and *KCNJ11*, respectively) and of four regulatory SUR subunits (SUR1, SUR2A/SUR2B, encoded by *ABCC8* and *ABCC9*, respectively), which act as sulphonylurea receptors. The association of a particular SUR with a specific Kir6.x subunit constitutes the ATP-dependent K⁺ current (KATP) in each tissue (for reviews, see e.g., [92,93]). Soon after the first report that applied the patch clamp technique to mitoplasts obtained by osmotic swelling and rupture of the OMM [94], Inoue and colleagues identified, using the same technique, a channel in the IMM that was inhibited by ATP, and was therefore named as mitoKATP [25].

The conductance of KATP of the PM ranges from 33–35 pS for the channels composed of Kir6.1 to 67–80 pS for those constituted by Kir6.2, in symmetrical 140 mM KCl (for review see e.g., [18]). However, conductance as low as 13 pS (in 140 mM symmetrical KCl solution) was recorded in rat mesenteric artery vascular smooth muscle cells (VSMC) [51]. In this latter cell type, the diversity of molecular entities of KATP channels is illustrated by their single-channel conductance ranging from 13 to 135 pS, with distinct conductance values of 13, 20, 50, 111 and 135 pS, recorded under similar ionic conditions in various studies [51,95].

Attribution of these channel activities with different conductance values to KATP in most experiments is based on the pharmacological profiling of channel activities. The hallmarks of PM KATP comprise inhibition by ATP/Mg²⁺ or glibenclamide and activation by P-1075, BMS 191095, cromakalim, pinacidil and nicorandil [96–102]. Therefore, these drugs have been tested on mitochondrial K⁺ channel activities by different groups. In addition, diazoxide was identified as an agent that activates mitoKATP more efficiently than PM KATP, and HMR 1098 was proposed as a specific inhibitor of PM KATP but not of mitoKATP [103,104].

The above pharmacological drugs were then exploited in different cell types to measure mitoKATP activity in mitoplasts directly by patch clamp. As mentioned above, in the first study, a ~10 pS channel was identified as mitoKATP [25], but in subsequent studies, different conductance values were observed. Table 2 summarizes all data published to date, in which the main biophysical and pharmacological properties of mitoKATP activity in the native IMM were determined using the patch clamp technique. Although in two studies (in Jurkat [56] and in rat liver mitochondria [25]) an ATP-sensitive channel with low conductance was observed (15 and 9.7 pS in 100/33 mM KCl or symmetrical 150 mM KCl, respectively), in other works, the conductance reached ~100 pS (in 150 mM KCl) [32,57,105]. Thus, the conductance values around 100 pS recorded in native mitochondrial membranes are compatible with the ones observed for PM KATP formed by Kir6.2-SUR2A complexes [53,54]. This finding, along with the pharmacological profile mentioned above, prompted the researchers to propose the Kir6.2 inward rectifying channel as the main pore-forming constituent of mitoKATP.

Table 2. Biophysical characteristics of mitoKATP channel activities recorded by patch clamping of the inner mitochondrial membrane (excised inside-out configuration). “+” and “−” denote activation or inhibition of mitoKATP, respectively.

Tissue/Cell Origin	of	Method of Mitoplast Preparation	Recording Medium	Single-Channel Conductance	Modulation	Reference
Rat liver		Giant mitoplasts obtained by digitonin–swelling fusion	<ul style="list-style-type: none"> Pipette: 100 mM KCl, 7.5 mM sodium-MOPS, pH 7.2, 1 mM EGTA, 0.55 mM CaCl₂ Bath: 33.3 mM KCl, 66.7 mM NaCl, 7.7 mM Na-MOPS, pH 7.2, 2 mM EGTA 	9.7 pS at negative membrane potentials	<ul style="list-style-type: none"> ATP 2 mM (−) 4-aminopyridine −5 mM (−) glybenclamide 5 μM (−) 	[25]
Jurkat lymphocyte	T	Swelling	Pipette/bath: 150 mM KCl, 10 mM HEPES and 100 (or 200) μM CaCl ₂ (pH = 7.2)	15 and 82 pS at negative and positive potentials, respectively	<ul style="list-style-type: none"> 5-hydroxydecanoic acid 1 mM (−) nitric oxide 2 μM (−) ATP 0.5–25 mM (−) 	[56]
Human dermal fibroblast		Swelling	Pipette/bath: 150 mM KCl, 10 mM HEPES, and 200 μM CaCl ₂ at pH 7.2.	100 pS	<ul style="list-style-type: none"> 1 mM Mg²⁺ plus 500 μM ATP (−) diazoxide 30 μM (+) BMS 191,095 10 μM (+) glibenclamide 30 μM (−) 5-hydroxydecanoic acid 150 μM (−) 	[105]
Heart-derived H9c2 cells and H9c2 ROMK2		Swelling	Pipette/bath: 150 mM of KCl, 10 mM of HEPES, and 200 μM of CaCl ₂ at pH = 7.2	94–97 pS	<ul style="list-style-type: none"> 5-hydroxydecanoic acid 100 μM (−) tertiapin Q 100 nM (−) 	[32]

Table 2. Cont.

Tissue/Cell Origin	of	Method of Mitoplast Preparation	Recording Medium	Single-Channel Conductance	Modulation	Reference
Overexpressing cells					<ul style="list-style-type: none"> • 1 mM Mg²⁺ plus 500 μM ATP (–) • diazoxide (+) • glibenclamide 50 μM (–, partial inhibition) 	
Primary Human dermal fibroblasts		Swelling	Pipette/bath: 150 mM of KCl, 10 mM of HEPES, and 200 μM of CaCl ₂ at pH = 7.2	100 pS	<ul style="list-style-type: none"> • naringenin (Nar) 10 μM (+) • diazoxide 30 μM (+) • 5-hydroxydecanoic acid 500 μM (plus Nar) (–) • glibenclamide 10 μM (plus Nar) (–) 	[57]

Despite the fact that the molecular composition of mitoKATP was not elucidated, the field of mitoKATP channel underwent a rapid evolution when pharmacological studies highlighted an important role of this channel in cardioprotection, in particular in attenuating the damage caused by ischemia-reperfusion (for recent reviews see, e.g., [6,7,13]). Moreover, mitoKATP activation has been proposed to exert neuroprotective effects [106] and to modulate mitochondrial dynamics, biogenesis and neurodegenerative disorders such as Parkinson [107]. Interestingly, diazoxide, the activator of mitoKATP, was shown to improve memory in a mouse model of Alzheimer's disease and ameliorate amyloid- β and tau pathologies [108]. Neuronal injury was also attenuated in models of the metabolic disease methyl-malonic acidemia by mitoKATP openers [109].

Most of the above studies underlining the patho-physiological role of mitoKATP were carried out with diazoxide as a channel activator. However, this drug also exerts K^+ channel-independent effects, such as inhibition of complex II of the respiratory chain (succinate dehydrogenase) and uncoupling action, leading researchers to question the role of mitoKATP in ischemic preconditioning [110]. Moreover, diazoxide seems to also have an impact on the expression of some proteins, as it upregulates the two components of the calcium-release-activated calcium channel (I_{CRAC} , also called the SOCE channel), STIM1 and Orai1 in cardiomyocytes [111]. The antioxidant *N*-acetyl cysteine (NAC), 5-hydroxydecanoate (5-HD), and the MAPK pathway inhibitor UO126 were able to attenuate diazoxide-induced upregulation of STIM1 and Orai1 expression, suggesting that an ROS- and MAPK-dependent pathway is activated by this mitoKATP opener. The authors hypothesized that alteration of the distribution pattern of STIM1, causing decreased Ca^{2+} influx into the cells, may contribute to cardioprotection against ischemic insults. However, direct electrophysiological evidence that I_{CRAC} activity is decreased in cells incubated with diazoxide has not been reported.

Thus, while the protective effect of diazoxide against ischemic damage has been confirmed in several studies, the specificity of action via mitoKATP channels could not be proven in the absence of the molecular identity of this channel. As mentioned above, based on the conductance values observed in native IMM and by analogy with the PM KATP channel, Kir6.2 was first proposed as the pore-forming component, while SUR subunits were proposed as regulatory components of this complex (Figure 1). However, mitoKATP channel activity, determined using the thallium (Tl^+) flux assay in mitochondria isolated from WT or Kir6.2^{-/-} littermate hearts was identical, even though the channel was required for the action of diazoxide to promote ischemic preconditioning. The authors therefore concluded that Kir6.2 is not a component of mitoKATP [112]. Direct electrophysiological recordings on mitoplasts from Kir6.2^{-/-} animals would be useful to further strengthen such a conclusion.

As an alternative to the Kir6.2 hypothesis, a multi-protein complex comprising complex II (succinate dehydrogenase), complex V (ATP synthase), an ATP-binding cassette protein 1 (mABC1), the phosphate carrier and the adenine nucleotide translocator (ANT) [46] was put forward. This multi-protein complex was incorporated into proteoliposomes and was characterized using the planar lipid bilayer electrophysiological technique, revealing a passage of K^+ , giving rise to a conductance of 200 pS in 500 mM K^+ (Hepes was used as a counterion). Interestingly, the observed activity showed low selectivity towards potassium but was inhibited by ATP, glybenclamide, or 5-HD, even in the presence of the activator diazoxide, as one would expect for mitoKATP. Unfortunately, mass spectrometry analysis was not provided on the complex isolated from the IMM, thus it cannot be excluded that other protein(s) present in the preparation are responsible for the observed channel activity. It is of note that ANT and the phosphate carrier can form ion channels on their own (for detailed review see e.g., [18]) and ANT was shown to also mediate proton leak [113]. In addition, highly purified complex V also forms channels under certain conditions (in a Ca^{2+} -dependent way) with characteristics resembling the permeability transition pore (PTP) [114]. However, the described conductance values of ANT, complex V and the

phosphate carrier measured in K^+ -based medium are different from those observed in the study of Ardehali and colleagues.

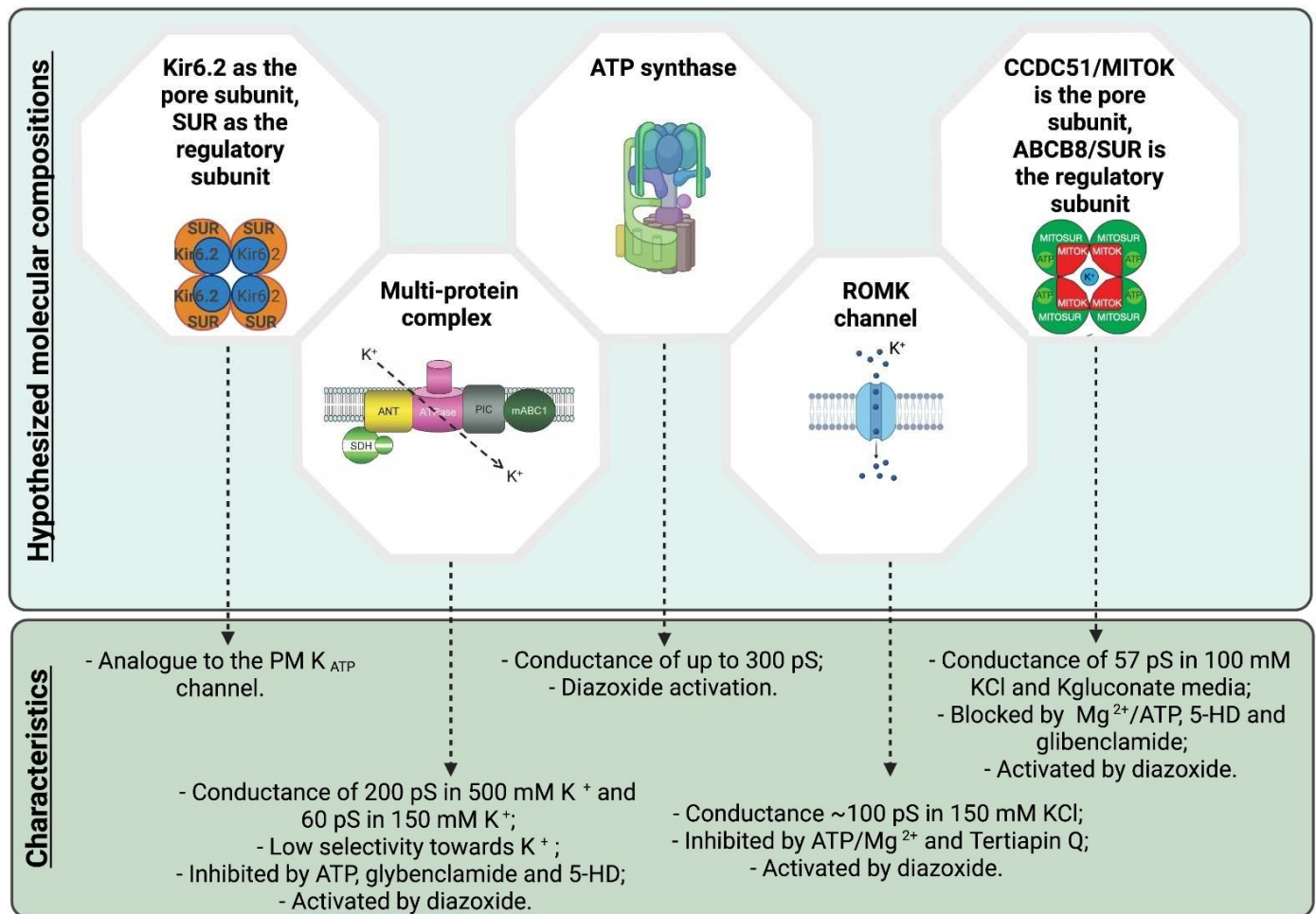


Figure 1. Schematic summary of the various hypotheses for the molecular composition of mitoKATP (see text for details). Created with BioRender.com (accessed on 22 June 2021).

Interestingly, a recent study re-proposed the participation of complex V in mitoKATP formation [115]. In particular, isolated ATP synthase (purity was, however, not assessed using mass spectrometry) was studied under ionic conditions that are physiologically relevant (with a ratio of $10^6:1$ between K^+ and H^+), and so in the presence of both protons and potassium ions. Based on electrophysiological experiments, the authors concluded that the ATP synthase allows the passage of K^+ in addition to protons (a unitary conductance of up to ~ 300 pS was observed) and underlies the so-called K^+ uniporter (mitoKATP). Interestingly, diazoxide in this context would act as an activator of mitoKATP by directly binding to the inhibitory protein of complex V, IF1 [116]. The proposal that complex V is responsible also for the formation of the PTP makes it all quite intriguing. Altogether, the authors proposed that the increase in ATP synthesis guided by K^+ and H^+ would allow complex V to operate as a primary mitochondrial uniporter of K^+ that regulates the match between energy supply and demand, and as the recruitable mitochondrial KATP channel that can limit ischemia-reperfusion injury. While genetic deletion or point mutants of certain subunits of the ATP synthase were shown to alter PTP properties in classical biochemical and electrophysiological assays [117–120], efforts to specifically study (diazoxide-dependent) K^+ transport across genetically modified ATP synthase complexes have not been taken into consideration up to date.

In parallel with the above studies, research also focused on the renal outer medullary kidney channel (ROMK2) as a possible mitoKATP channel forming protein. ROMK2 is a short, mitochondria-targeted isoform of ROMK (also called Kir1.1, encoded by *KCNJ1*) which was shown to co-localize with mitochondrial ATP synthase in cardiomyocytes [48]. ROMK itself is ATP-sensitive and can associate with SUR2B. The single-channel conductance of PM ROMK at negative voltages is 32–43 pS (with 110 mM KCl in the pipette). In the work of Foster and colleagues [48], short hairpin RNA-mediated knockdown of ROMK inhibited the ATP-sensitive, diazoxide-activated component of mitochondrial thallium uptake, used as a proxy for potassium uptake into the matrix. Importantly, tertiapin Q, a venom toxin-derived inhibitor of ROMK channels, almost completely abolished thallium uptake. Moreover, the expression level of ROMK2 in the heart-derived cell line H9C2 correlated well with sensitivity to cell death triggered by oxidative stress (via application of tertbutyl hydroperoxide (tBHP)). Thus, these results strongly suggest that ROMK2 might correspond, at least in some tissues, to mitoKATP. Electrophysiological evidence in favor of this hypothesis was provided more recently by the group of Adam Szewczyk, where patch clamp on dermal fibroblast mitochondria revealed a 100 pS (in symmetric 150 mM KCl) channel activity that was ascribed to ROMK and was activated by diazoxide while suppressed by ATP/Mg²⁺, glibenclamide and 5-hydroxydecanoic acid [105]. Moreover, genetic overexpression of ROMK2 in heart-derived H9c2 cells enhanced mitoKATP activity directly recorded in the IMM by patch clamp. This channel displayed the typical biophysical and pharmacological characteristics of mitoKATP (~100 pS in 150 mM KCl, inhibition by ATP/Mg²⁺, activation by diazoxide) and was inhibited by Tertiapin Q [32]. On the other hand, the observation that recombinant ROMK2 incorporated into nanodiscs shows a chord conductance of only 10 pS in 50/150 mM KCl, is intriguing [121]. Further work is required to find the reason for this difference in the biophysical properties of the recombinant versus native ROMK2 channels. While the electrophysiological and pharmacological properties of ROMK2 altogether are compatible with this protein being mitoKATP, a recent study using genetic, global or cardiomyocyte-specific knockout mice for ROMK2 discovered that isolated mitochondria from the latter mice still showed swelling upon addition of the mitoKATP opener BMS-191095 and were characterized by unchanged matrix volume responses during oxidative phosphorylation [122].

ROMK-less heart mitochondria exhibited a decreased threshold for calcium-triggered PTP opening but molecular details of how the presence of ROMK can de-sensitize PTP towards a calcium increase are missing: the association of ROMK2 with the ATP synthase (see above) might contribute to this effect. Alternatively, mitoKATP opening may slightly depolarize the IMM and reduce the driving force for Ca²⁺ entry, thereby counteracting mitochondrial Ca²⁺ overload and subsequent mPTP opening [123]. Altogether, the authors of this seminal work concluded that cardiomyocyte ROMK is not a major component of the cardioprotective mitoKATP channel, although to our knowledge the possibility that other Kir channel-forming subunits undertook the function of ROMK in the KO heart has not been ruled out.

As a last chapter in the “saga” of mitoKATP identification, a mitochondria-specific, ubiquitously expressed coiled-coil domain containing protein, CCDC51, was proposed to form a K⁺-permeable monovalent cationic pore [124]. The channel formed by recombinant CCDC51 was inhibited by ATP, glibenclamide and 5-hydroxydecanoate and was activated by diazoxide, only when co-assembled with a mitochondrial ABC protein (ABCB8). The conductance of the CCDC51–ABCB8 complex, reconstituted in proteoliposomes and studied by electrophysiology (planar lipid bilayer), was 57 pS in 100 mM K-gluconate medium. Importantly, using cells where CCDC51 was genetically deleted, it has been demonstrated that this protein controls mitochondrial volume and efficiency of oxidative phosphorylation, as expected for mitoKATP. Moreover, diazoxide-triggered ⁸⁶Rb⁺ (used as surrogate of K⁺) influx into isolated energized liver mitochondria was completely abolished in CCDC51-less organelles, suggesting that at least in the liver, diazoxide does not trigger K⁺ uptake by acting on ATP synthase or on the complex comprising complexes II and V, ANT, mABC1 and the phosphate carrier or on Kir6.2/Kir6.1 channels. Most importantly, the whole-body

deletion of CCDC51 almost completely suppressed the cardioprotection that was elicited by the pharmacological preconditioning induced by diazoxide, suggesting again a crucial role for CCDC51 (in complex with ABCB8) in the protective action of diazoxide. In order to correlate these results with mitoKATP channel activities described so far in the IMM from different tissues, it will be very important to characterize by patch clamp the ATP- and diazoxide-dependent activities in the IMM of mitochondria from different CCDC51-KO mouse tissues (a work that is under way in our laboratory).

As a future perspective, one may envision a collaborative effort among chemists, cell biologists, electrophysiologists and cardiologists, to understand if mitoKATP composition can vary depending on the tissue type. A recent study described the synthesis of a mitochondriotropic, triphenylphosphonium-linked [125] variant of the mitoKATP activator spirocyclic benzopyrane F81 and showed that mito-F81 exerted cardioprotective effects at a 10-fold lower dose with respect to the parent compound [126]. Unfortunately, this study did not directly test the inhibitory effect of the modified compound on mitoKATP in electrophysiological experiments nor compared EC_{50} values of the two compounds for inhibition of TI^+ uptake. Nonetheless, this compound has the advantage of most probably acting prevalently on mitoKATP (and not on PM KATP) and could be used in various cell lines knocked-out for Kir6.2, ROMK, CCDC51, and ANT, as well as in various ATP synthase subunit-knocked down cells. In addition, this compound could also be used for affinity chromatography followed by mass spectrometry to identify the proteins interacting with high affinity. On the other hand, caution should be taken, as TPP^+ -targeting may modify the original properties of chemicals, decrease their affinity for the target (e.g., [127]) and trigger additional and/or off-target effects as well (e.g., [43,128]).

4. Future Outlook

In summary, while huge progress has been made in mitochondrial potassium channels in the last few decades, many questions remain open. A cross-disciplinary effort will likely resolve the mysteries regarding possible plasticity in channel formation, dual (or even multiple) targeting to intracellular membranes, and pharmacological regulation. In addition, recent studies highlighted a differential role for some PM and mitochondrial channels, exploiting mitochondria-targeted drugs. While a thorough characterization of these drugs is mandatory, they may represent a handy pharmacological tool against various diseases (see, e.g., [126,127,129]).

Administration of organelle-specific drugs is the modern trend to achieve significant therapeutic effects (e.g., [130]). However, the problem of possible off-target effects is certainly the barrier that must be overcome in molecular pharmacology to achieve selective targeting and accumulation in mitochondria [5,131]. In the past few decades, various strategies have been developed to target drugs into the mitochondria. Such strategies involve direct conjugation of a targeting ligand to drugs and/or attachment of the targeting ligand to a nanocarrier [132]. The direct conjugation of the ligand is certainly a valid approach through which drugs can easily reach the mitochondria—it is the simplest and easiest method; however, the conjugation procedure can decrease the biochemical effects within the mitochondria. In the nanocarrier system, on the other hand, the therapeutic effect is not lost because the problem of physical interaction and solubility is solved, but optimization is still a challenge due to the use of many different possible compositions to identify the best nanocarrier. Finally, the administration of thermoresponsive drugs to the mitochondria for cancer therapy has recently been described [133].

Mitochondria-targeted drugs have been extensively studied in clinical applications, and several formulations have been approved by the US Food and Drug Administration and European Medicines Agency for clinical applications in patients with cancer. A brief overview of some major approaches aiming to modulate the Krebs cycle, electron transport chain, anaplerosis, mitoROS release and mitochondria-driven apoptosis in cancer is given in e.g., [134].

In terms of future perspectives, hopefully mitochondrial ion channels will become preferred targets not only in the context of cancer but also of other human diseases. To our knowledge, to date, no drugs specifically targeting these channels are in clinical use.

Author Contributions: All authors contributed to the writing of the manuscript. All authors have read and agreed to the published version of the manuscript.

Funding: The work in the laboratory of the authors is financed by the Italian Association for Cancer Research (IG AIRC (IG 2017, Id.20286), FISM/AISM (Prot. 284/18/F14), Telethon (GGP19118) and Italian Ministry of University and Education (PRIN 20174TB8KW_004) and Marie-Curie Seal of Excellence postdoctoral fellowship (to Y.K.).

Acknowledgments: The authors are grateful to all colleagues who participated in the works discussed in this review. We also thank for the support the Italian Association for Cancer Research (IG AIRC (IG 2017, Id.20286), FISM/AISM (Prot. 284/18/F14), Telethon (GGP19118) and Italian Ministry of University and Education (PRIN 20174TB8KW_004) and the Marie-Curie Seal of Excellence project.

Conflicts of Interest: The authors declare that they have no conflict of interest.

References

- Mitchell, P. Coupling of Phosphorylation to Electron and Hydrogen Transfer by a Chemi-Osmotic type of Mechanism. *Nature* **1961**, *191*, 144–148. [CrossRef] [PubMed]
- Laskowski, M.; Augustynek, B.; Kulawiak, B.; Koprowski, P.; Bednarczyk, P.; Jarmuszkiewicz, W.; Szewczyk, A. What do we not know about mitochondrial potassium channels? *Biochim. Biophys. Acta* **2016**, *1857*, 1247–1257. [CrossRef]
- Szewczyk, A.; Bednarczyk, P.; Jedraszko, J.; Kampa, R.P.; Koprowski, P.; Krajewska, M.; Kucman, S.; Kulawiak, B.; Laskowski, M.; Rotko, D.; et al. Mitochondrial potassium channels—An overview. *Postepy Biochem.* **2018**, *64*, 196–212. [CrossRef]
- Szteyn, K.; Singh, H. BK(Ca) Channels as Targets for Cardioprotection. *Antioxidants* **2020**, *9*, 760. [CrossRef]
- Wrzosek, A.; Augustynek, B.; Żochowska, M.; Szewczyk, A. Mitochondrial Potassium Channels as Druggable Targets. *Biomolecules* **2020**, *10*, 1200. [CrossRef]
- Checchetto, V.; Leanza, L.; De Stefani, D.; Rizzuto, R.; Gulbins, E.; Szabo, I. Mitochondrial K(+) channels and their implications for disease mechanisms. *Pharmacol. Ther.* **2021**, *227*, 107874. [CrossRef] [PubMed]
- Pereira, O., Jr.; Kowaltowski, A.J. Mitochondrial K(+) Transport: Modulation and Functional Consequences. *Molecules* **2021**, *26*, 2935. [CrossRef]
- Checchetto, V.; Azzolini, M.; Peruzzo, R.; Capitano, P.; Leanza, L. Mitochondrial potassium channels in cell death. *Biochem. Biophys. Res. Commun.* **2018**, *500*, 51–58. [CrossRef]
- Krabbendam, I.E.; Honrath, B.; Culmsee, C.; Dolga, A.M. Mitochondrial Ca(2+)-activated K(+) channels and their role in cell life and death pathways. *Cell Calcium*. **2018**, *69*, 101–111. [CrossRef] [PubMed]
- Costa, R.; Peruzzo, R.; Bachmann, M.; Monta, G.D.; Vicario, M.; Santinon, G.; Mattarei, A.; Moro, E.; Quintana-Cabrera, R.; Scorrano, L.; et al. Impaired Mitochondrial ATP Production Downregulates Wnt Signaling via ER Stress Induction. *Cell Rep.* **2019**, *28*, 1949–1960. [CrossRef] [PubMed]
- Frankenreiter, S.; Bednarczyk, P.; Kniess, A.; Bork, N.I.; Straubinger, J.; Koprowski, P.; Wrzosek, A.; Mohr, E.; Logan, A.; Murphy, M.P.; et al. cGMP-Elevating Compounds and Ischemic Conditioning Provide Cardioprotection Against Ischemia and Reperfusion Injury via Cardiomyocyte-Specific BK Channels. *Circulation* **2017**, *136*, 2337–2355. [CrossRef]
- Bachmann, M.; Pontarin, G.; Szabo, I. The Contribution of Mitochondrial Ion Channels to Cancer Development and Progression. *Cell. Physiol. Biochem. Int. J. Exp. Cell. Physiol. Biochem. Pharmacol.* **2019**, *53*, 63–78. [CrossRef]
- Hausenloy, D.J.; Schulz, R.; Girao, H.; Kwak, B.R.; De Stefani, D.; Rizzuto, R.; Bernardi, P.; Di Lisa, F. Mitochondrial ion channels as targets for cardioprotection. *J. Cell. Mol. Med.* **2020**, *24*, 7102–7114. [CrossRef]
- Ponnalagu, D.; Singh, H. Insights into the Role of Mitochondrial Ion Channels in Inflammatory Response. *Front. Physiol.* **2020**, *11*, 258. [CrossRef]
- Garlid, K.D. Cation transport in mitochondria—The potassium cycle. *Biochim. Biophys. Acta (BBA)-Bioenerg.* **1996**, *1275*, 123–126. [CrossRef]
- Shoshan-Barmatz, V.; Shteinfer-Kuzmine, A.; Verma, A. VDAC1 at the Intersection of Cell Metabolism, Apoptosis, and Diseases. *Biomolecules* **2020**, *10*, 1485. [CrossRef]
- De Pinto, V. Renaissance of VDAC: New Insights on a Protein Family at the Interface between Mitochondria and Cytosol. *Biomolecules* **2021**, *11*, 107. [CrossRef] [PubMed]
- Szabo, I.; Zoratti, M. Mitochondrial channels: Ion fluxes and more. *Physiol. Rev.* **2014**, *94*, 519–608. [CrossRef] [PubMed]
- De Pinto, V.; Reina, S.; Gupta, A.; Messina, A.; Mahalakshmi, R. Role of cysteines in mammalian VDAC isoforms' function. *Biochim. Biophys. Acta (BBA)-Bioenerg.* **2016**, *1857*, 1219–1227. [CrossRef]

20. Fieni, F.; Parkar, A.; Misgeld, T.; Kerschensteiner, M.; Lichtman, J.W.; Pasinelli, P.; Trotti, D. Voltage-dependent inwardly rectifying potassium conductance in the outer membrane of neuronal mitochondria. *J. Biol. Chem.* **2010**, *285*, 27411–27417. [CrossRef] [PubMed]
21. Báthori, G.; Szabó, I.; Schmehl, I.; Tombola, F.; Messina, A.; De Pinto, V.; Zoratti, M. Novel aspects of the electrophysiology of mitochondrial porin. *Biochem. Biophys. Res. Commun.* **1998**, *243*, 258–263. [CrossRef] [PubMed]
22. De Stefani, D.; Bononi, A.; Romagnoli, A.; Messina, A.; De Pinto, V.; Pinton, P.; Rizzuto, R. VDAC1 selectively transfers apoptotic Ca²⁺ signals to mitochondria. *Cell Death Differ.* **2012**, *19*, 267–273. [CrossRef]
23. Shimizu, H.; Schredelseker, J.; Huang, J.; Lu, K.; Naghdi, S.; Lu, F.; Franklin, S.; Fiji, H.D.; Wang, K.; Zhu, H.; et al. Mitochondrial Ca(2+) uptake by the voltage-dependent anion channel 2 regulates cardiac rhythmicity. *eLife* **2015**, *4*, e04801. [CrossRef]
24. Gergalova, G.; Lykhmus, O.; Kalashnyk, O.; Koval, L.; Chernyshov, V.; Kryukova, E.; Tsetlin, V.; Komisarenko, S.; Skok, M. Mitochondria express alpha7 nicotinic acetylcholine receptors to regulate Ca²⁺ accumulation and cytochrome c release: Study on isolated mitochondria. *PLoS ONE* **2012**, *7*, e31361. [CrossRef]
25. Inoue, I.; Nagase, H.; Kishi, K.; Higuti, T. ATP-sensitive K⁺ channel in the mitochondrial inner membrane. *Nature* **1991**, *352*, 244–247. [CrossRef]
26. Szabo, I.; Bock, J.; Jekle, A.; Soddemann, M.; Adams, C.; Lang, F.; Zoratti, M.; Gulbins, E. A novel potassium channel in lymphocyte mitochondria. *J. Biol. Chem.* **2005**, *280*, 12790–12798. [CrossRef]
27. Bednarczyk, P.; Kowalczyk, J.E.; Beresewicz, M.; Dołowy, K.; Szewczyk, A.; Zabłocka, B. Identification of a voltage-gated potassium channel in gerbil hippocampal mitochondria. *Biochem. Biophys. Res. Commun.* **2010**, *397*, 614–620. [CrossRef]
28. De Marchi, U.; Sassi, N.; Fioretti, B.; Catacuzzeno, L.; Cereghetti, G.M.; Szabo, I.; Zoratti, M. Intermediate conductance Ca²⁺-activated potassium channel (KCa3.1) in the inner mitochondrial membrane of human colon cancer cells. *Cell Calcium*. **2009**, *45*, 509–516. [CrossRef] [PubMed]
29. Siemen, D.; Loupatatzis, C.; Borecky, J.; Gulbins, E.; Lang, F. Ca²⁺-Activated K Channel of the BK-Type in the Inner Mitochondrial Membrane of a Human Glioma Cell Line. *Biochem. Biophys. Res. Commun.* **1999**, *257*, 549–554. [CrossRef]
30. Singh, H.; Stefani, E.; Toro, L. Intracellular BK(Ca) (iBK(Ca)) channels. *J. Physiol.* **2012**, *590*, 5937–5947. [CrossRef] [PubMed]
31. Dolga, A.M.; Netter, M.F.; Perocchi, F.; Doti, N.; Meissner, L.; Tobaben, S.; Grohm, J.; Zischka, H.; Plesnila, N.; Decher, N.; et al. Mitochondrial small conductance SK2 channels prevent glutamate-induced oxytosis and mitochondrial dysfunction. *J. Biol. Chem.* **2013**, *288*, 10792–10804. [CrossRef]
32. Laskowski, M.; Augustynek, B.; Bednarczyk, P.; Żochowska, M.; Kalisz, J.; O'Rourke, B.; Szewczyk, A.; Kulawiak, B. Single-Channel Properties of the ROMK-Pore-Forming Subunit of the Mitochondrial ATP-Sensitive Potassium Channel. *Int. J. Mol. Sci.* **2019**, *20*, 5323. [CrossRef] [PubMed]
33. Toczyłowska-Mamińska, R.; Olszewska, A.; Laskowski, M.; Bednarczyk, P.; Skowronek, K.; Szewczyk, A. Potassium channel in the mitochondria of human keratinocytes. *J. Invest. Dermatol.* **2014**, *134*, 764–772. [CrossRef] [PubMed]
34. León-Aparicio, D.; Salvador, C.; Aparicio-Trejo, O.E.; Briones-Herrera, A.; Pedraza-Chaverri, J.; Vaca, L.; Sampieri, A.; Padilla-Flores, T.; López-González, Z.; León-Contreras, J.C.; et al. Novel Potassium Channels in Kidney Mitochondria: The Hyperpolarization-Activated and Cyclic Nucleotide-Gated HCN Channels. *Int. J. Mol. Sci.* **2019**, *20*, 4995. [CrossRef] [PubMed]
35. Padilla-Flores, T.; López-González, Z.; Vaca, L.; Aparicio-Trejo, O.E.; Briones-Herrera, A.; Riveros-Rosas, H.; Pedraza-Chaverri, J.; León-Aparicio, D.; Salvador, C.; Sampieri, A.; et al. “Funny” channels in cardiac mitochondria modulate membrane potential and oxygen consumption. *Biochem. Biophys. Res. Commun.* **2020**, *524*, 1030–1036. [CrossRef]
36. Bednarczyk, P.; Kampa, R.P.; Gałęcka, S.; Sęk, A.; Walewska, A.; Koprowski, P. Patch-Clamp Recording of the Activity of Ion Channels in the Inner Mitochondrial Membrane. *Methods Mol. Biol.* **2021**, *2276*, 235–248. [CrossRef]
37. Kirichok, Y.; Krapivinsky, G.; Clapham, D.E. The mitochondrial calcium uniporter is a highly selective ion channel. *Nature* **2004**, *427*, 360–364. [CrossRef]
38. Testai, L.; Barrese, V.; Soldovieri, M.V.; Ambrosino, P.; Martelli, A.; Vinciguerra, I.; Miceli, F.; Greenwood, I.A.; Curtis, M.J.; Breschi, M.C.; et al. Expression and function of Kv7.4 channels in rat cardiac mitochondria: Possible targets for cardioprotection. *Cardiovasc. Res.* **2016**, *110*, 40–50. [CrossRef]
39. Leanza, L.; Zoratti, M.; Gulbins, E.; Szabo, I. Induction of apoptosis in macrophages via Kv1.3 and Kv1.5 potassium channels. *Curr. Med. Chem.* **2012**, *19*, 5394–5404. [CrossRef]
40. Capera, J.; Pérez-Verdaguer, M.; Peruzzo, R.; Navarro-Pérez, M.; Martínez-Pinna, J.; Alberola-Die, A.; Morales, A.; Leanza, L.; Szabó, I.; Felipe, A. A novel mitochondrial Kv1.3-caveolin axis controls cell survival and apoptosis. *eLife* **2021**, *10*, e69099. [CrossRef]
41. Thevarajan, I.; Zolkiewski, M.; Zolkiewska, A. Human CLPB forms ATP-dependent complexes in the mitochondrial intermembrane space. *Int. J. Biochem. Cell Biol.* **2020**, *127*, 105841. [CrossRef]
42. Capera, J.; Serrano-Novillo, C.; Navarro-Pérez, M.; Cassinelli, S.; Felipe, A. The Potassium Channel Odyssey: Mechanisms of Traffic and Membrane Arrangement. *Int. J. Mol. Sci.* **2019**, *20*, 734. [CrossRef]
43. Peruzzo, R.; Mattarei, A.; Azzolini, M.; Becker-Flegler, K.A.; Romio, M.; Rigoni, G.; Carrer, A.; Biasutto, L.; Parrasia, S.; Kadow, S.; et al. Insight into the mechanism of cytotoxicity of membrane-permeant psoralenic Kv1.3 channel inhibitors by chemical dissection of a novel member of the family. *Redox Biol.* **2020**, *37*, 101705. [CrossRef]

44. Styles, F.L.; Al-Owais, M.M.; Scragg, J.L.; Chuntharpursat-Bon, E.; Hettiarachchi, N.T.; Lippiat, J.D.; Minard, A.; Bon, R.S.; Porter, K.; Sukumar, P.; et al. Kv1.3 voltage-gated potassium channels link cellular respiration to proliferation through a non-conducting mechanism. *Cell Death Dis.* **2021**, *12*, 372. [CrossRef]
45. Bednarczyk, P.; Wieckowski, M.R.; Broszkiewicz, M.; Skowronek, K.; Siemen, D.; Szewczyk, A. Putative Structural and Functional Coupling of the Mitochondrial BK Channel to the Respiratory Chain. *PLoS ONE* **2013**, *8*, e68125. [CrossRef]
46. Ardehali, H.; Chen, Z.; Ko, Y.; Mejía-Alvarez, R.; Marbán, E. Multiprotein complex containing succinate dehydrogenase confers mitochondrial ATP-sensitive K⁺ channel activity. *Proc. Natl. Acad. Sci. USA* **2004**, *101*, 11880–11885. [CrossRef]
47. Wojtovich, A.P.; Brookes, P.S. The endogenous mitochondrial complex II inhibitor malonate regulates mitochondrial ATP-sensitive potassium channels: Implications for ischemic preconditioning. *Biochim. Biophys. Acta (BBA)-Bioenerg.* **2008**, *1777*, 882–889. [CrossRef] [PubMed]
48. Foster, D.B.; Ho, A.S.; Rucker, J.; Garlid, A.O.; Chen, L.; Sidor, A.; Garlid, K.D.; O'Rourke, B. Mitochondrial ROMK channel is a molecular component of mitoK(ATP). *Circ. Res.* **2012**, *111*, 446–454. [CrossRef] [PubMed]
49. Yao, J.; McHedlishvili, D.; McIntire, W.E.; Guagliardo, N.A.; Erisir, A.; Coburn, C.A.; Santarelli, V.P.; Bayliss, D.A.; Barrett, P.Q. Functional TASK-3-Like Channels in Mitochondria of Aldosterone-Producing Zona Glomerulosa Cells. *Hypertension* **2017**, *70*, 347–356. [CrossRef] [PubMed]
50. Kono, Y.; Horie, M.; Takano, M.; Otani, H.; Xie, L.H.; Akao, M.; Tsuji, K.; Sasayama, S. The properties of the Kir6.1–6.2 tandem channel co-expressed with SUR2A. *Pflug. Arch. Eur. J. Physiol.* **2000**, *440*, 692–698. [CrossRef]
51. Tang, G.; Wu, L.; Liang, W.; Wang, R. Direct stimulation of K(ATP) channels by exogenous and endogenous hydrogen sulfide in vascular smooth muscle cells. *Mol. Pharmacol.* **2005**, *68*, 1757–1764. [CrossRef] [PubMed]
52. Noma, A. ATP-regulated K⁺ channels in cardiac muscle. *Nature* **1983**, *305*, 147–148. [CrossRef] [PubMed]
53. Isomoto, S.; Kondo, C.; Yamada, M.; Matsumoto, S.; Higashiguchi, O.; Horio, Y.; Matsuzawa, Y.; Kurachi, Y. A Novel Sulfonylurea Receptor Forms with BIR (Kir6.2) a Smooth Muscle Type ATP-sensitive K⁺ Channel. *J. Biol. Chem.* **1996**, *271*, 24321–24324. [CrossRef] [PubMed]
54. Okuyama, Y.; Yamada, M.; Kondo, C.; Satoh, E.; Isomoto, S.; Shindo, T.; Horio, Y.; Kitakaze, M.; Hori, M.; Kurachi, Y. The effects of nucleotides and potassium channel openers on the SUR2A/Kir6.2 complex K⁺ channel expressed in a mammalian cell line, HEK293T cells. *Pflügers Arch.* **1998**, *435*, 595–603. [CrossRef] [PubMed]
55. Standen, N.B.; Quayle, J.M.; Davies, N.W.; Brayden, J.E.; Huang, Y.; Nelson, M.T. Hyperpolarizing vasodilators activate ATP-sensitive K⁺ channels in arterial smooth muscle. *Science* **1989**, *245*, 177. [CrossRef] [PubMed]
56. Dahlem, Y.A.; Horn, T.F.; Buntinas, L.; Gono, T.; Wolf, G.; Siemen, D. The human mitochondrial KATP channel is modulated by calcium and nitric oxide: A patch-clamp approach. *Biochim. Biophys. Acta (BBA)-Bioenerg.* **2004**, *1656*, 46–56. [CrossRef] [PubMed]
57. Kampa, R.P.; Kicinska, A.; Jarmuszkiewicz, W.; Pasikowska-Piwko, M.; Dolegowska, B.; Debowska, R.; Szewczyk, A.; Bednarczyk, P. Naringenin as an opener of mitochondrial potassium channels in dermal fibroblasts. *Exp. Dermatol.* **2019**, *28*, 543–550. [CrossRef]
58. Pahapill, P.A.; Schlichter, L.C. Modulation of potassium channels in intact human T lymphocytes. *J. Physiol.* **1992**, *445*, 407–430. [CrossRef]
59. Marty, A. Ca-dependent K channels with large unitary conductance in chromaffin cell membranes. *Nature* **1981**, *291*, 497–500. [CrossRef]
60. Pallotta, B.S.; Magleby, K.L.; Barrett, J.N. Single channel recordings of Ca²⁺-activated K⁺ currents in rat muscle cell culture. *Nature* **1981**, *293*, 471–474. [CrossRef]
61. Kravenska, Y.; Nieznanska, H.; Nieznanski, K. Prion protein protects the large-conductance calcium-activated potassium channel from the inhibitory effect of Tau protein. 2021. submitted.
62. Latorre, R.; Morera, F.J.; Zaelzer, C. SYMPOSIUM REVIEW: Allosteric interactions and the modular nature of the voltage- and Ca²⁺-activated (BK) channel. *J. Physiol.* **2010**, *588*, 3141–3148. [CrossRef] [PubMed]
63. Soltysinska, E.; Bentzen, B.H.; Barthmes, M.; Hattel, H.; Thrush, A.B.; Harper, M.-E.; Qvortrup, K.; Larsen, F.J.; Schiffer, T.A.; Losa-Reyna, J.; et al. KCNMA1 encoded cardiac BK channels afford protection against ischemia-reperfusion injury. *PLoS ONE* **2014**, *9*, e103402. [CrossRef] [PubMed]
64. Xu, W.; Liu, Y.; Wang, S.; McDonald, T.; Van Eyk, J.E.; Sidor, A.; Rourke, B. Cytoprotective Role of Ca²⁺-Activated K⁺ Channels in the Cardiac Inner Mitochondrial Membrane. *Science* **2002**, *298*, 1029. [CrossRef] [PubMed]
65. Kicinska, A.; Augustynek, B.; Kulawiak, B.; Jarmuszkiewicz, W.; Szewczyk, A.; Bednarczyk, P. A large-conductance calcium-regulated K⁺ channel in human dermal fibroblast mitochondria. *Biochem. J.* **2016**, *473*, 4457–4471. [CrossRef]
66. Balderas, E.; Torres, N.S.; Rosa-Garrido, M.; Chaudhuri, D.; Toro, L.; Stefani, E.; Olcese, R. MitoBKCa channel is functionally associated with its regulatory β 1 subunit in cardiac mitochondria. *J. Physiol.* **2019**, *597*, 3817–3832. [CrossRef]
67. Kicinska, A.; Kampa, R.P.; Daniluk, J.; Sek, A.; Jarmuszkiewicz, W.; Szewczyk, A.; Bednarczyk, P. Regulation of the Mitochondrial BK(Ca) Channel by the Citrus Flavonoid Naringenin as a Potential Means of Preventing Cell Damage. *Molecules* **2020**, *25*, 3010. [CrossRef]
68. Kravenska, Y.; Nieznanska, H.; Nieznanski, K.; Lukyanetz, E.; Szewczyk, A.; Koprowski, P. The monomers, oligomers, and fibrils of amyloid- β inhibit the activity of mitoBKCa channels by a membrane-mediated mechanism. *Biochim. Biophys. Acta (BBA)-Biomembr.* **2020**, *1862*, 183337. [CrossRef]

69. Grygorczyk, R.; Schwarz, W.; Passow, H. Ca^{2+} -activated K^+ channels in human red cells. Comparison of single-channel currents with ion fluxes. *Biophys. J.* **1984**, *45*, 693–698. [CrossRef]
70. Logsdon, N.J.; Kang, J.; Togo, J.A.; Christian, E.P.; Aiyar, J. A novel gene, hKCa4, encodes the calcium-activated potassium channel in human T lymphocytes. *J. Biol. Chem.* **1997**, *272*, 32723–32726. [CrossRef] [PubMed]
71. Chen, P.C.; Ruan, J.S.; Wu, S.N. Evidence of Decreased Activity in Intermediate-Conductance Calcium-Activated Potassium Channels During Retinoic Acid-Induced Differentiation in Motor Neuron-Like NSC-34 Cells. *Cell. Physiol. Biochem.* **2018**, *48*, 2374–2388. [CrossRef]
72. Ishii, T.M.; Silvia, C.; Hirschberg, B.; Bond, C.T.; Adelman, J.P.; Maylie, J. A human intermediate conductance calcium-activated potassium channel. *Proc. Natl. Acad. Sci. USA* **1997**, *94*, 11651–11656. [CrossRef]
73. Koselski, M.; Olszewska, A.; Hordyjewska, A.; Malecka-Massalska, T.; Trebacz, K. Three types of ion channels in the cell membrane of mouse fibroblasts. *Physiol. Res.* **2017**, *66*, 63–73. [CrossRef]
74. Light, D.B.; Van Eenenaam, D.P.; Sorenson, R.L.; Levitt, D.G. Potassium-selective ion channels in a transformed insulin-secreting cell line. *J. Membr. Biol.* **1987**, *95*, 63–72. [CrossRef] [PubMed]
75. Palmer, L.G.; Frindt, G. Regulation of apical K channels in rat cortical collecting tubule during changes in dietary K intake. *Am. J. Physiol.* **1999**, *277*, F805–F812. [CrossRef] [PubMed]
76. Lu, M.; Leng, Q.; Egan, M.E.; Caplan, M.J.; Boulpaep, E.L.; Giebisch, G.H.; Hebert, S.C. CFTR is required for PKA-regulated ATP sensitivity of Kir1.1 potassium channels in mouse kidney. *J. Clin. Investig.* **2006**, *116*, 797–807. [CrossRef] [PubMed]
77. Ho, K.; Nichols, C.G.; Lederer, W.J.; Lytton, J.; Vassilev, P.M.; Kanazirska, M.V.; Hebert, S.C. Cloning and expression of an inwardly rectifying ATP-regulated potassium channel. *Nature* **1993**, *362*, 31–38. [CrossRef]
78. Ashmole, I.; Vavoulis, D.V.; Stansfeld, P.J.; Mehta, P.R.; Feng, J.F.; Sutcliffe, M.J.; Stanfield, P.R. The response of the tandem pore potassium channel TASK-3 (K2P9.1) to voltage: Gating at the cytoplasmic mouth. *J. Physiol.* **2009**, *587*, 4769–4783. [CrossRef]
79. Kim, Y.; Bang, H.; Kim, D. TASK-3, a new member of the tandem pore K^+ channel family. *J. Biol. Chem.* **2000**, *275*, 9340–9347. [CrossRef]
80. DiFrancesco, D. Characterization of single pacemaker channels in cardiac sino-atrial node cells. *Nature* **1986**, *324*, 470–473. [CrossRef]
81. Liu, C.; Xie, C.; Grant, K.; Su, Z.; Gao, W.; Liu, Q.; Zhou, L. Patch-clamp fluorometry-based channel counting to determine HCN channel conductance. *J. Gen. Physiol.* **2016**, *148*, 65–76. [CrossRef]
82. Garlid, K.D.; Pucek, P. The mitochondrial potassium cycle. *IUBMB Life* **2001**, *52*, 153–158. [CrossRef]
83. Austin, S.; Nowikovsky, K. LETM1: Essential for Mitochondrial Biology and Cation Homeostasis? *Trends Biochem. Sci.* **2019**, *44*, 648–658. [CrossRef]
84. Nowikovsky, K.; Froschauer, E.M.; Zsurka, G.; Samaj, J.; Reipert, S.; Kolisek, M.; Wiesenberger, G.; Schweyen, R.J. The LETM1/YOL027 gene family encodes a factor of the mitochondrial K^+ homeostasis with a potential role in the Wolf-Hirschhorn syndrome. *J. Biol. Chem.* **2004**, *279*, 30307–30315. [CrossRef]
85. Jiang, D.; Zhao, L.; Clish, C.B.; Clapham, D.E. Letm1, the mitochondrial $\text{Ca}^{2+}/\text{H}^+$ antiporter, is essential for normal glucose metabolism and alters brain function in Wolf-Hirschhorn syndrome. *Proc. Natl. Acad. Sci. USA* **2013**, *110*, E2249–E2254. [CrossRef]
86. Tsai, M.F.; Jiang, D.; Zhao, L.; Clapham, D.; Miller, C. Functional reconstitution of the mitochondrial $\text{Ca}^{2+}/\text{H}^+$ antiporter Letm1. *J. Gen. Physiol.* **2014**, *143*, 67–73. [CrossRef] [PubMed]
87. Austin, S.; Tavakoli, M.; Pfeiffer, C.; Seifert, J.; Mattarei, A.; De Stefani, D.; Zoratti, M.; Nowikovsky, K. LETM1-Mediated K^+ and Na^+ Homeostasis Regulates Mitochondrial Ca^{2+} Efflux. *Front. Physiol.* **2017**, *8*, 839. [CrossRef]
88. Natarajan, G.K.; Glait, L.; Mishra, J.; Stowe, D.F.; Camara, A.K.S.; Kwok, W.M. Total Matrix Ca^{2+} Modulates Ca^{2+} Efflux via the $\text{Ca}^{2+}/\text{H}^+$ Exchanger in Cardiac Mitochondria. *Front. Physiol.* **2020**, *11*, 510600. [CrossRef] [PubMed]
89. Dos Santos, G.R.R.; Rezende Leite, A.C.; Lander, N.; Chiurillo, M.A.; Vercesi, A.E.; Docampo, R. Trypanosoma cruzi Letm1 is involved in mitochondrial Ca^{2+} transport, and is essential for replication, differentiation, and host cell invasion. *FASEB J. Off. Publ. Fed. Am. Soc. Exp. Biol.* **2021**, *35*, e21685. [CrossRef]
90. Nakamura, S.; Matsui, A.; Akabane, S.; Tamura, Y.; Hatano, A.; Miyano, Y.; Omote, H.; Kajikawa, M.; Maenaka, K.; Moriyama, Y.; et al. The mitochondrial inner membrane protein LETM1 modulates cristae organization through its LETM domain. *Commun. Biol.* **2020**, *3*, 99. [CrossRef] [PubMed]
91. Dimmer, K.S.; Navoni, F.; Casarin, A.; Trevisson, E.; Endeles, S.; Winterpacht, A.; Salviati, L.; Scorrano, L. LETM1, deleted in Wolf-Hirschhorn syndrome is required for normal mitochondrial morphology and cellular viability. *Hum. Mol. Genet.* **2008**, *17*, 201–214. [CrossRef]
92. Pipatpolkai, T.; Usher, S.; Stansfeld, P.J.; Ashcroft, F.M. New insights into K^+ (ATP) channel gene mutations and neonatal diabetes mellitus. *Nat. Rev. Endocrinol.* **2020**, *16*, 378–393. [CrossRef] [PubMed]
93. Tinker, A.; Aziz, Q.; Li, Y.; Specterman, M. ATP-Sensitive Potassium Channels and Their Physiological and Pathophysiological Roles. *Compr. Physiol.* **2018**, *8*, 1463–1511. [CrossRef] [PubMed]
94. Sorgato, M.C.; Keller, B.U.; Stühmer, W. Patch-clamping of the inner mitochondrial membrane reveals a voltage-dependent ion channel. *Nature* **1987**, *330*, 498–500. [CrossRef]
95. Zhang, H.; Bolton, T.B. Activation by intracellular GDP, metabolic inhibition and pinacidil of a glibenclamide-sensitive K^+ -channel in smooth muscle cells of rat mesenteric artery. *Br. J. Pharmacol.* **1995**, *114*, 662–672. [CrossRef]

96. Grover, G.J.; McCullough, J.R.; Henry, D.E.; Conder, M.L.; Sleph, P.G. Anti-ischemic effects of the potassium channel activators pinacidil and cromakalim and the reversal of these effects with the potassium channel blocker glyburide. *J. Pharmacol. Exp. Ther.* **1989**, *251*, 98.
97. Xu, X.; Tsai, T.D.; Lee, K.S. A specific activator of the ATP-inhibited K⁺ channels in guinea pig ventricular cells. *J. Pharmacol. Exp. Ther.* **1993**, *266*, 978.
98. Ashcroft, F.M.; Gribble, F.M. New windows on the mechanism of action of KATP channel openers. *Trends Pharmacol. Sci.* **2000**, *21*, 439–445. [CrossRef]
99. Baukrowitz, T.; Fakler, B. KATP channels gated by intracellular nucleotides and phospholipids. *Eur. J. Biochem.* **2000**, *267*, 5842–5848. [CrossRef]
100. Moreau, C.; Jacquet, H.; Prost, A.-L.; D'Hahan, N.; Vivaudou, M. The molecular basis of the specificity of action of KATP channel openers. *EMBO J.* **2000**, *19*, 6644–6651. [CrossRef]
101. Sato, T.; Sasaki, N.; Seharaseyon, J.; O'Rourke, B.; Marbán, E. Selective Pharmacological Agents Implicate Mitochondrial but Not Sarcolemmal KATP Channels in Ischemic Cardioprotection. *Circulation* **2000**, *101*, 2418–2423. [CrossRef] [PubMed]
102. Moreau, C.; Prost, A.-L.; Dérand, R.; Vivaudou, M. SUR, ABC proteins targeted by KATP channel openers. *J. Mol. Cell. Cardiol.* **2005**, *38*, 951–963. [CrossRef]
103. Gögelein, H.; Hartung, J.; Englert, H.C.; Schölkens, B.A. HMR 1883, a novel cardioselective inhibitor of the ATP-sensitive potassium channel. Part I: Effects on cardiomyocytes, coronary flow and pancreatic beta-cells. *J. Pharmacol. Exp. Ther.* **1998**, *286*, 1453–1464.
104. Russ, U.; Lange, U.; Löffler-Walz, C.; Hambrock, A.; Quast, U. Interaction of the sulfonylthiourea HMR 1833 with sulfonylurea receptors and recombinant ATP-sensitive K(+) channels: Comparison with glibenclamide. *J. Pharmacol. Exp. Ther.* **2001**, *299*, 1049. [PubMed]
105. Bednarczyk, P.; Kicinska, A.; Laskowski, M.; Kulawiak, B.; Kampa, R.; Walewska, A.; Krajewska, M.; Jarmuszkiewicz, W.; Szewczyk, A. Evidence for a mitochondrial ATP-regulated potassium channel in human dermal fibroblasts. *Biochim. Biophys. Acta Bioenerg.* **2018**, *1859*, 309–318. [CrossRef] [PubMed]
106. Liu, D.; Lu, C.; Wan, R.; Auyeung, W.W.; Mattson, M.P. Activation of mitochondrial ATP-dependent potassium channels protects neurons against ischemia-induced death by a mechanism involving suppression of Bax translocation and cytochrome c release. *J. Cereb. Blood Flow Metab. Off. J. Int. Soc. Cereb. Blood Flow Metab.* **2002**, *22*, 431–443. [CrossRef] [PubMed]
107. Peng, K.; Hu, J.; Xiao, J.; Dan, G.; Yang, L.; Ye, F.; Zou, Z.; Cao, J.; Sai, Y. Mitochondrial ATP-sensitive potassium channel regulates mitochondrial dynamics to participate in neurodegeneration of Parkinson's disease. *Biochim. Biophys. Acta Mol. Basis Dis.* **2018**, *1864*, 1086–1103. [CrossRef]
108. Liu, D.; Pitta, M.; Lee, J.H.; Ray, B.; Lahiri, D.K.; Furukawa, K.; Mughal, M.; Jiang, H.; Villarreal, J.; Cutler, R.G.; et al. The KATP channel activator diazoxide ameliorates amyloid- β and tau pathologies and improves memory in the 3xTgAD mouse model of Alzheimer's disease. *J. Alzheimer's Dis. JAD* **2010**, *22*, 443–457. [CrossRef]
109. Kowaltowski, A.J.; Maciel, E.N.; Fornazari, M.; Castilho, R.F. Diazoxide protects against methylmalonate-induced neuronal toxicity. *Exp. Neurol.* **2006**, *201*, 165–171. [CrossRef]
110. Dröse, S.; Brandt, U.; Hanley, P.J. K⁺-independent actions of diazoxide question the role of inner membrane KATP channels in mitochondrial cytoprotective signaling. *J. Biol. Chem.* **2006**, *281*, 23733–23739. [CrossRef]
111. Gavali, J.T.; Carrillo, E.D.; García, M.C.; Sánchez, J.A. The mitochondrial K-ATP channel opener diazoxide upregulates STIM1 and Orai1 via ROS and the MAPK pathway in adult rat cardiomyocytes. *Cell Biosci.* **2020**, *10*, 96. [CrossRef]
112. Wojtovich, A.P.; Urciuoli, W.R.; Chatterjee, S.; Fisher, A.B.; Nehrke, K.; Brookes, P.S. Kir6.2 is not the mitochondrial KATP channel but is required for cardioprotection by ischemic preconditioning. *Am. J. Physiol. Heart Circ. Physiol.* **2013**, *304*, H1439–H1445. [CrossRef]
113. Bertholet, A.M.; Chouchani, E.T.; Kazak, L.; Angelin, A.; Fedorenko, A.; Long, J.Z.; Vidoni, S.; Garrity, R.; Cho, J.; Terada, N.; et al. H(+) transport is an integral function of the mitochondrial ADP/ATP carrier. *Nature* **2019**, *571*, 515–520. [CrossRef]
114. Urbani, A.; Giorgio, V.; Carrer, A.; Franchin, C.; Arrigoni, G.; Jiko, C.; Abe, K.; Maeda, S.; Shinzawa-Itoh, K.; Bogers, J.F.M.; et al. Purified F-ATP synthase forms a Ca(2+)-dependent high-conductance channel matching the mitochondrial permeability transition pore. *Nat. Commun.* **2019**, *10*, 4341. [CrossRef] [PubMed]
115. Juhaszova, M.; Kobrinsky, E.; Zorov, D.B.; Nuss, H.B.; Yaniv, Y.; Fishbein, K.W.; de Cabo, R.; Montoliu, L.; Gabelli, S.B.; Aon, M.A.; et al. ATP synthase K⁺- and H⁺-flux drive ATP synthesis and enable mitochondrial K⁺-uniporter function. *bioRxiv* **2019**, 355776, preprint. [CrossRef]
116. Contessi, S.; Metelli, G.; Mavelli, I.; Lippe, G. Diazoxide affects the IF1 inhibitor protein binding to F1 sector of beef heart F0F1ATP synthase. *Biochem. Pharmacol.* **2004**, *67*, 1843–1851. [CrossRef] [PubMed]
117. Antoniel, M.; Jones, K.; Antonucci, S.; Spolaore, B.; Fogolari, F.; Petronilli, V.; Giorgio, V.; Carraro, M.; Di Lisa, F.; Forte, M.; et al. The unique histidine in OSCP subunit of F-ATP synthase mediates inhibition of the permeability transition pore by acidic pH. *EMBO Rep.* **2018**, *19*, 257–268. [CrossRef]
118. Carraro, M.; Checchetto, V.; Sartori, G.; Kucharczyk, R.; di Rago, J.P.; Minervini, G.; Franchin, C.; Arrigoni, G.; Giorgio, V.; Petronilli, V.; et al. High-Conductance Channel Formation in Yeast Mitochondria is Mediated by F-ATP Synthase e and g Subunits. *Cell. Physiol. Biochem. Int. J. Exp. Cell. Physiol. Biochem. Pharmacol.* **2018**, *50*, 1840–1855. [CrossRef]

119. Mnatsakanyan, N.; Llaguno, M.C.; Yang, Y.; Yan, Y.; Weber, J.; Sigworth, F.J.; Jonas, E.A. A mitochondrial megachannel resides in monomeric F(1)F(O) ATP synthase. *Nat. Commun.* **2019**, *10*, 5823. [CrossRef] [PubMed]
120. Neginskaya, M.A.; Solesio, M.E.; Berezhnaya, E.V.; Amodeo, G.F.; Mnatsakanyan, N.; Jonas, E.A.; Pavlov, E.V. ATP Synthase C-Subunit-Deficient Mitochondria Have a Small Cyclosporine A-Sensitive Channel, but Lack the Permeability Transition Pore. *Cell Rep.* **2019**, *26*, 11–17. [CrossRef]
121. Krajewska, M.; Koprowski, P. Solubilization, purification, and functional reconstitution of human ROMK potassium channel in copolymer styrene-maleic acid (SMA) nanodiscs. *Biochim. Biophys. Acta Biomembr.* **2021**, *1863*, 183555. [CrossRef]
122. Papanicolaou, K.N.; Ashok, D.; Liu, T.; Bauer, T.M.; Sun, J.; Li, Z.; da Costa, E.; D’Orleans, C.C.; Nathan, S.; Lefer, D.J.; et al. Global knockout of ROMK potassium channel worsens cardiac ischemia-reperfusion injury but cardiomyocyte-specific knockout does not: Implications for the identity of mitoKATP. *J. Mol. Cell. Cardiol.* **2020**, *139*, 176–189. [CrossRef]
123. Holmuhamedov, E.L.; Wang, L.; Terzic, A. ATP-sensitive K⁺ channel openers prevent Ca²⁺ overload in rat cardiac mitochondria. *J. Physiol.* **1999**, *519 Pt 2*, 347–360. [CrossRef]
124. Paggio, A.; Checchetto, V.; Campo, A.; Menabo, R.; Di Marco, G.; Di Lisa, F.; Szabo, I.; Rizzuto, R.; De Stefani, D. Identification of an ATP-sensitive potassium channel in mitochondria. *Nature* **2019**, *572*, 609–613. [CrossRef] [PubMed]
125. Smith, R.A.; Hartley, R.C.; Murphy, M.P. Mitochondria-targeted small molecule therapeutics and probes. *Antioxid. Redox Signal.* **2011**, *15*, 3021–3038. [CrossRef]
126. Testai, L.; Sestito, S.; Martelli, A.; Gorica, E.; Flori, L.; Calderone, V.; Rapposelli, S. Synthesis and pharmacological characterization of mitochondrial K(ATP) channel openers with enhanced mitochondriotropic effects. *Bioorganic Chem.* **2021**, *107*, 104572. [CrossRef]
127. Leanza, L.; Romio, M.; Becker, K.A.; Azzolini, M.; Trentin, L.; Manago, A.; Venturini, E.; Zaccagnino, A.; Mattarei, A.; Carraretto, L.; et al. Direct Pharmacological Targeting of a Mitochondrial Ion Channel Selectively Kills Tumor Cells In Vivo. *Cancer Cell* **2017**, *31*, 516–531. [CrossRef] [PubMed]
128. Szabo, I.; Zoratti, M.; Biasutto, L. Targeting mitochondrial ion channels for cancer therapy. *Redox Biol.* **2020**, *42*, 101846. [CrossRef]
129. Bachmann, M.; Rossa, A.; Antoniazzi, G.; Biasutto, L.; Carrer, A.; Campagnaro, M.; Leanza, L.; Gonczi, M.; Csernoch, L.; Paradisi, C.; et al. Synthesis and cellular effects of a mitochondria-targeted inhibitor of the two-pore potassium channel TASK-3. *Pharmacol. Res.* **2021**, *164*, 105326. [CrossRef]
130. Biasutto, L.; Mattarei, A.; La Spina, M.; Azzolini, M.; Parrasia, S.; Szabò, I.; Zoratti, M. Strategies to target bioactive molecules to subcellular compartments. Focus on natural compounds. *Eur. J. Med. Chem.* **2019**, *181*, 111557. [CrossRef]
131. Peixoto, P.M.; Ryu, S.Y.; Kinnally, K.W. Mitochondrial ion channels as therapeutic targets. *FEBS Lett.* **2010**, *584*, 2142–2152. [CrossRef]
132. Heller, A.; Brockhoff, G.; Goepferich, A. Targeting drugs to mitochondria. *Eur. J. Pharm. Biopharm.* **2012**, *82*, 1–18. [CrossRef] [PubMed]
133. Ruan, L.; Zhou, M.; Chen, J.; Huang, H.; Zhang, J.; Sun, H.; Chai, Z.; Hu, Y. Thermoresponsive drug delivery to mitochondria in vivo. *Chem. Commun.* **2019**, *55*, 14645–14648. [CrossRef] [PubMed]
134. Hare, J.I.; Lammers, T.; Ashford, M.B.; Puri, S.; Storm, G.; Barry, S.T. Challenges and strategies in anti-cancer nanomedicine development: An industry perspective. *Adv. Drug Deliv. Rev.* **2017**, *108*, 25–38. [CrossRef] [PubMed]

Review

Welcome to the Family: Identification of the NAD⁺ Transporter of Animal Mitochondria as Member of the Solute Carrier Family SLC25

Mathias Ziegler ^{1,*}, Magnus Monné ^{2,3,*}, Andrey Nikiforov ⁴, Gennaro Agrimi ^{2,5}, Ines Heiland ^{6,7} and Ferdinando Palmieri ^{2,5}

¹ Department of Biomedicine, University of Bergen, 5009 Bergen, Norway

² Department of Biosciences, Biotechnologies and Biopharmaceutics, University of Bari, Via E. Orabona 4, 70125 Bari, Italy; gennaro.agrimi@uniba.it (G.A.); ferdpalmieri@gmail.com (F.P.)

³ Department of Sciences, University of Basilicata, Via Ateneo Lucano 10, 85100 Potenza, Italy

⁴ Institute of Cytology, Russian Academy of Sciences, 194064 St. Petersburg, Russia; andrey.nikiforov@gmail.com

⁵ Center of Excellence in Comparative Genomics, University of Bari, Via E. Orabona 4, 70125 Bari, Italy

⁶ Department of Arctic and Marine Biology, UiT The Arctic University of Norway, 9037 Tromsø, Norway; ines.heiland@uit.no

⁷ Department of Clinical Medicine, University of Bergen, 5009 Bergen, Norway

* Correspondence: mathias.ziegler@uib.no (M.Z.); magnus.monne@unibas.it (M.M.)

Abstract: Subcellular compartmentation is a fundamental property of eukaryotic cells. Communication and metabolic and regulatory interconnectivity between organelles require that solutes can be transported across their surrounding membranes. Indeed, in mammals, there are hundreds of genes encoding solute carriers (SLCs) which mediate the selective transport of molecules such as nucleotides, amino acids, and sugars across biological membranes. Research over many years has identified the localization and preferred substrates of a large variety of SLCs. Of particular interest has been the SLC25 family, which includes carriers embedded in the inner membrane of mitochondria to secure the supply of these organelles with major metabolic intermediates and coenzymes. The substrate specificity of many of these carriers has been established in the past. However, the route by which animal mitochondria are supplied with NAD⁺ had long remained obscure. Only just recently, the existence of a human mitochondrial NAD⁺ carrier was firmly established. With the realization that SLC25A51 (or MCART1) represents the major mitochondrial NAD⁺ carrier in mammals, a long-standing mystery in NAD⁺ biology has been resolved. Here, we summarize the functional importance and structural features of this carrier as well as the key observations leading to its discovery.

Keywords: mitochondrial carrier; mitochondrial transporter; membrane transport; mitochondria; solute carrier family 25; SLC25; SLC25A51; NAD⁺ transporters; NAD

Citation: Ziegler, M.; Monné, M.; Nikiforov, A.; Agrimi, G.; Heiland, I.; Palmieri, F. Welcome to the Family: Identification of the NAD⁺ Transporter of Animal Mitochondria as Member of the Solute Carrier Family SLC25. *Biomolecules* **2021**, *11*, 880. <https://doi.org/10.3390/biom11060880>

Academic Editor: Jeffrey Stuart

Received: 6 May 2021

Accepted: 8 June 2021

Published: 14 June 2021

Publisher's Note: MDPI stays neutral with regard to jurisdictional claims in published maps and institutional affiliations.



Copyright: © 2021 by the authors. Licensee MDPI, Basel, Switzerland. This article is an open access article distributed under the terms and conditions of the Creative Commons Attribution (CC BY) license (<https://creativecommons.org/licenses/by/4.0/>).

1. Introduction

Transmembrane transport proteins (transporters or carriers) catalyse the translocation of specific ions, nutrients, metabolites, cofactors, and proteins across biological membranes, which otherwise would be impermeable to these molecules. It has been estimated that 10% of all human genes encode polypeptides involved in solute transport across the plasma and intracellular membranes [1]. Based on sequence homology, more than 400 human transporters have been classified into 66 solute carrier (SLC) protein families, excluding active transporters (ABC transporters and ATPase pumps) and ion channels [1,2]. For example, members of the major facilitator superfamily, which have twelve transmembrane helices, are subdivided into various SLC families, and mitochondrial carriers, which have six transmembrane helices, belong to the SLC25 family. About 30% of the SLCs are orphans,

i.e., what they transport is unknown. There is also a long list of molecules that are probable substrates of yet unidentified transporters based on the knowledge about the cellular compartmentalization of enzymes and biochemical compounds. It is a great challenge to find the missing pieces in this metabolic puzzle, trying to identify the physiological substrate for a transporter or vice versa.

Nicotinamide adenine dinucleotide (NAD^+) is the most widely used cofactor of enzymatic redox reactions in the cell. It has the capacity to be an electron donor in its reduced form (NADH) and electron acceptor in its oxidized form (NAD^+). It is also an important signalling molecule involved in a multitude of signalling processes in different cellular compartments. NAD^+ appears to be present in all cellular organelles, with mitochondria containing up to 70% of the total cellular NAD^+ [3]. There are several routes of NAD^+ biosynthesis. With regard to the pyridine base, NAD^+ can be synthesized from several different precursors in animals: nicotinamide (Nam) and nicotinic acid (together known as vitamin B3), tryptophan, and nicotinamide riboside (NR). They are obtained from diet and imported into cells by various SLC transporters (SLC5A8, SLC22A13, and members of the SLC29 family for vitamin B3; e.g., SLC7A5 and SLC36A4 for tryptophan) [4,5]. The majority of NAD^+ is synthesized from nicotinamide, which is also released by NAD^+ consuming signalling reactions (Figure 1). The first enzyme of the so-called NAD^+ salvage pathway is nicotinamide phosphoribosyl transferase (NAMPT) and is predominantly localized to the cytosol and the nucleus [6,7]. To maintain mitochondrial NAD^+ concentrations, cytoplasmic NAD^+ or an NAD^+ intermediate, such as nicotinamide mononucleotide (NMN), need to be imported into mitochondria. It has been known for a long time that NADH cannot be transported directly into mitochondria. Various systems have evolved to shuttle the reducing equivalents of cytosolic NADH into the mitochondrial matrix, e.g., the malate-aspartate and glycerol-3-phosphate shuttles [8,9]. Proteins, which all belong to the mitochondrial carrier family, have been identified that transport NAD^+ , and to a lesser extent, NMN and nicotinic acid adenine dinucleotide (NAAD), in yeast and plant mitochondria [10,11] or NAD^+ into human and plant peroxisomes [12–14]. However, until very recently, no NAD^+ transporter had been found in animal mitochondria.

In 2020, SLC25A51 (along with SLC25A52, which is 96% identical) was concluded to be a human mitochondrial NAD^+ transporter by three independent research teams [15–17]. Although SLC25A51 is a member of the mitochondrial carrier family, it is not a close homologue of previously identified NAD^+ carriers. Using functional assays, yeast complementation, and genetic engineering, the role of SLC25A51 as a human mitochondrial NAD^+ transporter was established. These approaches are different from the EPRA method (where the protein is recombinantly expressed, purified, and reconstituted into liposomes for transport assays *in vitro*) that has been applied for the identification of the NAD^+ carriers in plants and yeast and the majority of the other SLC25 members. The SLC25 carrier family transports a wide range of substrates from protons, inorganic ions, and small metabolites to nucleotides and large cofactors [18]. In this review, human NAD^+ metabolism and its compartmentalisation as well as the discovery and characteristics of SLC25A51 and the other NAD^+ carriers are discussed.

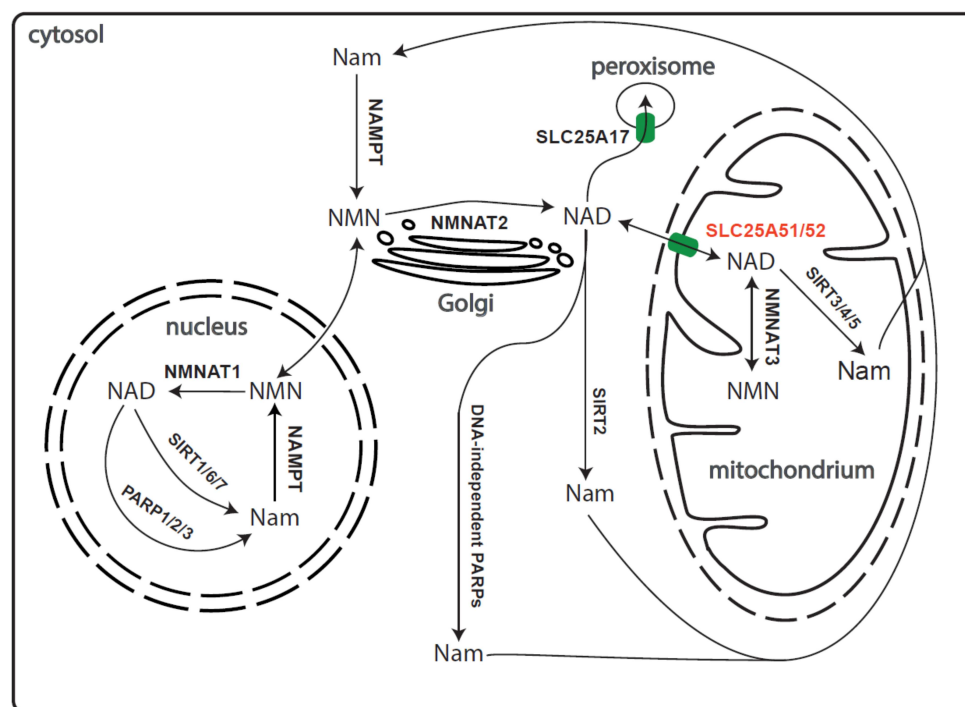


Figure 1. Compartmentalisation of NAD⁺ biosynthesis and salvage pathway in human cells. The figure shows the compartmentalisation of NAD⁺ synthesis, consumption, and salvage. The three different isoforms of NMNAT show distinct subcellular localisations with NMNAT1 primarily localized to the nucleus, NMNAT2 localized to the Golgi apparatus, and NMNAT3 in the mitochondria. The peroxisomal and mitochondrial SLC transporters are highlighted in green. (Abbrev.: Nam: nicotinamide; NMN: nicotinamide mononucleotide; NMNAT1/2/3: NMN adenylyltransferase 1/2/3; SIRT: sirtuin; PARP: poly-ADP-ribosyl polymerase; NAMPT: Nam phosphoribosyltransferase).

2. Human NAD⁺ Biosynthesis and Its Compartmentation

In human cells, the majority of NAD⁺ is produced from Nam in a two-step pathway. The first step is catalysed by NAMPT in which NMN is formed from Nam and phosphoribosylpyrophosphate (PRPP). The affinity of NAMPT towards its substrates is enhanced by autophosphorylation of the enzyme, ATP being the phosphoryl donor [19]. Under these conditions, the affinity of NAMPT towards Nam is in the low nanomolar range, thereby assuring efficient recycling of Nam produced from NAD⁺ in signalling reactions (Figure 1) [20]. Formation of the dinucleotide, NAD⁺, is accomplished by NMN adenylyltransferases, NMNATs. Mammalian cells have three NMNAT genes encoding isoforms that are present in the nucleus (NMNAT1), the Golgi complex, facing the cytosol (NMNAT2) and the mitochondria (NMNAT3) (Figure 1).

In addition to the NAMPT-dependent NAD⁺ synthesizing pathway, alternative precursors can also maintain cellular NAD⁺ homeostasis. Quinolinic acid, a product of tryptophan degradation in the kynurenine pathway, is converted to NAMN, the acidic form of NMN, and thereby enters NAD⁺ synthesis [21]. This route appears to be important for liver NAD⁺ homeostasis, at least in mice [22]. Likewise, nicotinic acid is also converted to NAMN by nicotinic acid phosphoribosyltransferase. NMNATs form the dinucleotide, NAAD, from NAMN and ATP, in the same manner as NAD⁺ from NMN and ATP [21]. Thus, all NAD⁺ biosynthetic pathways require NMNAT activity [23]. In mammals, NAAD is amidated to NAD⁺ by NAD⁺ synthetase using glutamine as an amide donor and the energy of ATP to accomplish the reaction [21]. Thereby, the conversion of Nam to NAD⁺ through NAMPT activity is not only the shortest, but also the energetically least-demanding pathway. This pathway is also known as Nam salvage pathway as it is required to resynthesize NAD⁺ from Nam, generated by NAD-consuming signalling reactions. NAD-dependent signalling reactions such as the de-acetylation of proteins by

sirtuins or the mono- and poly-ADP-ribosylation through ADP-ribosyl transferases (ART) or poly-ADP-ribosyltransferases (PARPs) [4,24,25], have been shown to lead to a constant turnover of cellular NAD⁺ pools, resulting in half-lives of only a few hours in human cells [22].

In recent years, the use of the nucleoside of Nam, NR, has gained tremendous interest. Having the ribose already attached, it can be readily converted to NMN by phosphorylation, thereby providing an efficient, PRPP-independent route to NAD⁺ [25,26]. Since NAMPT represents the rate-limiting reaction in human NAD⁺ biosynthesis, bypassing it using NR can potentially boost cellular NAD⁺ levels with a wide range of beneficial physiological effects. Likewise, dietary supplementation with NMN has also been proposed as a strategy to improve NAD⁺ availability [25,27]. Physiological improvements have been largely ascribed to the activation of NAD-dependent signalling pathways, in particular, SIRT-dependent protein deacetylation. Furthermore, some beneficial effects of NAD⁺ supplementation have been associated with enhanced mitochondrial functions, mediated, at least in part, by the activation of nuclear SIRT1, resulting in transcriptional activation of genes promoting mitochondrial proliferation. However, there also appear to be direct mitochondrial effects that might be explained by increased availability of NAD⁺ within these organelles. It should be noted that, so far, effects of NR supplementation on mitochondrial function have largely been observed in preclinical animal models, not humans.

NAD-dependent metabolic and signalling processes are strictly compartmentalized. This raises the question how various NAD⁺ pools are formed and maintained, and how they interact. To date, the cytosolic, nuclear, and mitochondrial NAD⁺ pools have been best described. Using the PARAPLAY assay, which is based on expression of the catalytic domain of poly-ADP-ribosyltransferase 1 (PARP1) in various subcellular compartments [28], pools of NAD⁺ in peroxisomes, ER, and Golgi complex [29,30] were demonstrated. It was shown that NAD⁺ is transported into peroxisomes using the mitochondrial type carrier SLC25A17 [13]. How NAD⁺ enters the ER or the Golgi complex is currently unknown.

For a long time, nuclear and cytosolic NAD⁺ were thought to form a single pool as it was believed that the free dinucleotide can diffuse through nuclear pores whose diameters are much larger than the size of NAD⁺. The analysis is complicated by the fact that both NAMPT and NMNAT activities are present in both compartments and recent work has demonstrated that the interactions between the nuclear and cytosolic NAD⁺ pools are complex. Using genetically encoded biosensors for NAD⁺ targeted to various cellular compartments, it was suggested that the depletion of NMNAT2 in HEK293T cells decreased cytoplasmic but not nuclear NAD⁺ concentrations [31]. Ryu et al. [32] found that stimulation of NAD⁺ synthesis in the cytosol, through the induction of NMNAT2, leads to a decrease in the level of NAD⁺ in the nucleus and suppression of PARP1 activity, regulating the expression of genes involved in adipogenic differentiation. Moreover, a model was proposed according to which the NAD⁺ nuclear pool is regulated by competition between NMNAT1 and NMNAT2 for their common substrate, namely NMN. Thus, despite the fact that we cannot exclude the direct exchange of NAD⁺ between the cytosol and the nucleus, depletion of the dinucleotide in one compartment cannot be fully offset by another pool. This may result in the nonviability of embryos observed in mice knocked out for NMNAT1 [33] or NMNAT2 [34].

3. The Mitochondrial NAD⁺ Pool

Despite the important role of the mitochondrial NAD⁺ pool for cellular metabolism and regulation, there are still many open questions related to its formation and maintenance. As most available evidence suggests NMNAT3 to be a mitochondrial isoform [6,35], it has been thought that NMNAT3 is essential to establish and maintain the mitochondrial NAD⁺ pool. It has been shown that an increase in the level of cytosolic NMN leads to an increase in the level of mitochondrial NAD⁺ in cultured human cells [6]. Based on these data, it was suggested that the cytosolic precursor of mitochondrial NAD⁺ is the mononucleotide NMN, which, after being imported into the mitochondrial matrix, is adenylated

to the dinucleotide NAD⁺ by NMNAT3. This hypothesis was also supported by in vitro data, according to which mitochondria isolated from rat liver can synthesize NAD⁺ from NMN and ATP [36]. Using mitochondria isolated from murine skeletal muscle or C2C12 myoblasts, Davila et al. [37] confirmed this observation. However, they demonstrated that the NMNAT activity was not located in the mitochondrial matrix but depended on the nuclear enzyme NMNAT1 [37]. Consequently, the detected mitochondria-associated NMNAT activity may have been the result of a contamination with the nuclear protein. Increased expression of NMNAT3 in transgenic mice and in cultured cells, however, efficiently increases mitochondrial NAD⁺ levels in various tissues [38,39]. Suppressed expression of this protein in some cells leads to a significant decrease in mitochondrial NAD⁺ concentrations, while in others, it has no effect on the mitochondrial NAD⁺ pool [31]. Mice lacking *Nmnat3* have, nevertheless, normal mitochondrial dinucleotide levels in most tissues [40]. Moreover, NMNAT3 was found to play a key role in maintaining the NAD⁺ pool in mature erythrocytes in which mitochondria are absent [41].

Thus, data on the role of NMNAT3 in maintaining the mitochondrial NAD⁺ pool have remained controversial. NMNAT3 may be an important regulator of mitochondrial NAD⁺ content, but there need to be alternative mechanisms that mediate the generation of the mitochondrial NAD⁺ pool.

In recent years, the focus of studies on the mechanisms of maintenance of mitochondrial NAD⁺ in mammals has shifted to reconsider the possibility of a transporter carrying the dinucleotide into the organelles. It was found that NMNAT2 depletion in HEK293T and HeLa cells decreased cytoplasmic and mitochondrial NAD⁺ levels, whereas NR did not restore mitochondrial NAD⁺ concentrations in NMNAT2 knockdowns in HeLa cells. These data suggested that NAD⁺ produced in the cytoplasm can influence mitochondrial stores [31]. Moreover, using C2C12 cells and NAR labelled with two different isotopes for ribose and Nam (¹³C on the pyridine carboxyl group and a deuterium on the ribose moiety), Davila et al. [37] demonstrated the incorporation of both labels into mitochondrial NAD⁺. Furthermore, given that NAR is converted to NAD⁺ in the cytosol via NAMN and NAAD, the cytosolic NMN pool was not labelled. This led to the suggestion that the mitochondrial NAD⁺ pool can be established through direct import of NAD⁺ [37]. These observations prompted intensive research efforts in various laboratories to address the possibility of the existence of a mitochondrial NAD⁺ carrier in mammalian cells.

4. Identification of Mitochondrial NAD⁺ Transporters in Yeast, Plants, and Bacteria

The mitochondrial NAD⁺ carriers in *Saccharomyces cerevisiae*, Ndt1p, and Ndt2p, which have 70% sequence identity, belong to the mitochondrial carrier family having the typical signature motif sequences (conserved consensus sequences initiating with PX[DE]XX[KR]) in three tandemly repeated domains [10]. These two proteins were addressed because they cluster with mitochondrial nucleotide carriers in phylogenetic trees and especially close to the FAD transporter Flx1p and pyrimidine nucleotide transporter Rim2p, which both have a rare tryptophan instead of the first negatively charged residue of the second signature motif just like Ndt1p and Ndt2p [10]. The substrates of Ndt1p were identified by the EPRA method, i.e., by expression in *Escherichia coli*, purification, reconstituted into liposomes and transport assays [10,18,42]. Ndt1p, which was found to be localized to mitochondria as well as Ndt2p, mainly transports NAD⁺ (K_m of 0.38 mM), and to a lesser extent, (d)AMP, (d)GMP, and NAAD. In addition, the nucleotides of uridine, thymine, and cytosine were transported by Ndt1p less efficiently than those of adenine and guanine with the following order of potency: monophosphates > diphosphates > triphosphates. By contrast, α-NAD⁺, NADH, NMN, NAMN, as well as FAD and FMN are very poor substrates of Ndt1p; and NADP, NADPH, Nam, and nicotinic acid are not transported at all by Ndt1p [10]. Furthermore, this carrier functions as a slower uniporter and a faster antiporter of substrates. In addition, yeast cells lacking Ndt1p or Ndt2p have growth defects on non-fermentable carbon sources and reduced mitochondrial levels of NAD⁺, a phenotype that becomes more pronounced in double knockout cells [10,43].

It should be emphasized that in *S. cerevisiae*, there is good evidence that there are no NAD⁺ biosynthetic enzymes within mitochondria [10]. Based on the biochemical characterization of Ndt1p, the high sequence identity between Ndt1p and Ndt2p, and the properties of the deleted strains, it was concluded that the main physiological role of both Ndt1p and Ndt2p is to import NAD⁺ from the cytosol into the mitochondrial matrix in exchange for (d)AMP and (d)GMP [10].

Two of the 58 mitochondrial carriers of *Arabidopsis thaliana*, AtNDT1 and AtNDT2 (with 61% sequence identity in their carrier domains), display considerable similarity to yeast Ndt1p and Ndt2p with percentages of identity ranging from 26 to 34% [11]. The transport properties of these two plant carriers were characterized by the EPRA method, demonstrating that NAD⁺ is transported by both of them (K_m values in submillimolar range) as well as NAAD, NMN, ADP, and AMP, and to a lesser extent NAMN, FAD, FMN, and several other nucleotides with the bases A, G, C, U, and T, whereas pyrophosphate is only transported by AtNDT1 [11]. The specific activity of AtNDT2 is about three times higher than that of AtNDT1 and both carriers exhibit antiport transport rates much higher than those of uniport. Furthermore, the expression of AtNDT1 and AtNDT2 in yeast lacking Ndt1p and Ndt2p restores mitochondrial NAD⁺ transport. Initially, subcellular localization studies of AtNDT1 and AtNDT2 suggested that they are found in chloroplasts and mitochondria, respectively [11]. However, later, AtNDT1 was reported to localize to mitochondria [44], in agreement with previous unpublished results (E. Blanco and F. Palmieri, personal communication). Both proteins are expressed in developing and metabolically active tissues: AtNDT1 in leaf mesophyll cells and root tips; AtNDT2 in meristematic shoots, vascular bundles of leaves, siliques, petal veins, pollen, and roots [11]. Diminished expression of AtNDT1 in *Arabidopsis* leads to impairments in the reproduction system, such as reduction in pollen, silique length, and seeds, whereas the vegetative growth is increased due to enhanced photosynthesis, leaf number, starch, and sucrose levels [44]. Reduced expression of AtNDT2 also affects the plant reproductive phase, in this case by decreasing seed quantity and quality [45]. Moreover, reduced AtNDT2 levels in flowers and seedlings trigger increased expression of several enzymes involved in NAD⁺ biosynthesis. In conclusion, AtNDT1 and AtNDT2 catalyse the import of NAD⁺ into mitochondria, probably in exchange for intramitochondrial ADP or AMP.

Two other members of the mitochondrial carrier family have been found to transport NAD⁺, the human SLC25A17 and the *Arabidopsis* PXN. Notably, at variance to all the other NAD⁺-transporting proteins mentioned above, these two carriers are localized to peroxisomes. Both of them have been characterized biochemically by the EPRA method. Although SLC25A17 transports NAD⁺ along with PAP (adenosine 3',5'-diphosphate) and ADP to a lesser extent than the main substrates of this carrier (CoA, FAD, FMN, and AMP), it is most likely that SLC25A17 also plays a role in peroxisomal NAD⁺ import in humans [13]. PXN transports NAD⁺ (K_m values in submillimolar range), NADH, AMP, and ADP at low rates, in addition to CoA, dephospho-CoA, PAP, and acetyl-CoA that are transported at higher rates [12,14], and is therefore also involved in peroxisomal NAD⁺ import in plants.

It should be mentioned that membrane transporters not belonging to the mitochondrial carrier family have also been identified to transport NAD⁺: the plasma membrane nucleotide transporter NTT4 and Npt1_{Ct} of *Protochlamydia amoebophila* UWE25 and *Chlamydia trachomatis*, respectively. Both are obligate intracellular symbionts in protozoa [46,47]. These two transporters are of the NTT family, whose members are found in intracellular bacteria and plant plastids and are predicted to have 10–12 transmembrane helices.

5. Discovery of a Mammalian Mitochondrial NAD⁺ Carrier

It has long been believed that in human and animal cells, there is no transport of NAD⁺ between mitochondria and the cytosol. This idea was supported in *in vitro* experiments with mitochondria isolated from rat liver, in which it was shown that NAD⁺ does not pass through the inner membrane of the organelle [36]. The absence of NAD⁺ transport

between the cytosol and mitochondria was also supported by data on the maintenance of mitochondrial NAD^+ within physiological concentrations with significant depletion of other pools (cytosolic and nuclear) evoked by genotoxic stress during treatment of cells with the DNA alkylating agent MMS [48] or after suppression of the activity of the NAMPT by the inhibitor FK866 [49]. The only alternative to the import of NAD^+ from the cytosol seemed to be intramitochondrial synthesis.

On the other hand, mitochondrial NAD^+ carriers have been identified in yeast and plants [10,18]. Previous attempts to detect a mitochondrial NAD^+ transporter in human cells based on homology with the characterized transporters in yeast (Ndt1p and Ndt2p) and plants (AtNDT1 and AtNDT2) were unsuccessful. It was shown that the mitochondrial folate and FAD carrier SLC25A32, which is the closest homologue in mammals of the above-mentioned characterized NAD^+ transporters, does not influence mitochondrial NAD^+ [35,48]. Other potential candidates from the SLC25 family—the pyrimidine nucleotide transporters SLC25A33 and SLC25A36—did not exhibit NAD^+ transporter activity either [35,50]. Consequently, alternative mechanisms of mitochondrial NAD^+ generation have been forwarded; in particular, those including mitochondrial NMNAT3 [6,35]. However, more recent research showed, albeit indirectly, that mitochondrial NAD^+ originates from the cytosol [37]. Eventually, at the end of 2020, three research groups independently characterized the mitochondrial NAD^+ transporter in human cells—SLC25A51 (also called MCART1) [15–17].

Genetic coessentiality analyses showed strong negative interactions of SLC25A51 with mitochondrial transporters essential for one-carbon and glutathione metabolism as well as a strong negative interaction with the glucose transporter at the plasma membrane *SLC2A1/GLUT1*. Since SLC25A51, furthermore, showed negative interactions with mitochondrial transporters for other cofactors, it was a likely candidate for the mitochondrial NAD^+ transporter. Targeted metabolomics in SLC25A51-deficient cells showed a depletion of riboflavin as well as purine nucleotides and an increased level of glutathione metabolism-related metabolites [15,16]. The role of SLC25A51 as a NAD^+ transporter was further confirmed through knockouts in various cell lines, which led to dramatic impairment of mitochondrial respiration [15–17].

In a variety of cells, knockout or knockdown of the gene encoding the SLC25A51 protein resulted in a decreased oxygen consumption rate because of impaired respiratory complex I activity [15–17]. LC-MS-based metabolomics analyses of SLC25A51 KO cells revealed extensive alterations in major mitochondrial metabolic pathways such as the TCA cycle, one-carbon flux, fatty acid oxidation, and ETC function [15,16]. Moreover, cells lacking SLC25A51, cultivated in a medium containing galactose instead of glucose as a carbon source, were unable to generate ATP in mitochondria [16]. Thus, SLC25A51 deficiency led to dramatic impairment of mitochondrial respiration. Using targeted metabolomics, a genetically encoded cpVenus NAD^+ sensor or the PARAPLAY system, it was shown that SLC25A51 deficiency selectively depleted mitochondrial (but not whole cell) NAD^+ , whereas overexpression of SLC25A51 significantly increased mitochondrial NAD^+ levels [15–17]. It was also found that NAD^+ uptake into mitochondria isolated from SLC25A51 KD or KO cells was substantially decreased compared to control mitochondria. On the contrary, mitochondria from cells overexpressing SLC25A51 demonstrated increased NAD^+ uptake capacity [16,17]. It is noteworthy that in *in vitro* experiments using $^{13}\text{C}_5\text{-NAD}^+$, unlabelled NAD^+ or NADH, but not NMN, competed for isotope-labelled NAD^+ uptake into mitochondria [16]. Moreover, to validate the function of SLC25A51 as NAD^+ transporter, it was tested whether the human SLC25A51 and yeast mitochondrial NAD^+ transporters Ndt1p and Ndt2p functionally substitute each other. Overexpression of the SLC25A51 protein rescued slow growth and normalized mitochondrial NAD^+ levels of the yeast strain in which both *NDT1* and *NDT2* were deleted [15,16]. Ectopically expressed SLC25A51 also fully rescued impaired uptake of $^3\text{H-NAD}^+$ into mitochondria isolated from *NDT1* and *NDT2* double knockout yeast [17]. Using this experimental system, the authors also determined kinetic parameters of SLC25A51-mediated NAD^+ transport ($K_m = 200 \mu\text{M}$

$\pm 60 \mu\text{M}$; $V_{\text{max}} = 1200 \text{ pmol sec}^{-1} \text{ mg}^{-1}$) On the other hand, overexpression of the yeast protein Ndt1p rescued mitochondrial NAD^+ levels and mitochondrial respiration in human SLC25A51 knock out cells [15,16]. Thus, it was convincingly demonstrated that the proteins SLC25A51 and Ndt1p (as well as Ndt2p) are functional homologues.

Despite the fact that the mitochondrial NAD^+ uptake was not confirmed by a direct transport method upon reconstitution of the protein into liposomes, it is highly probable that SLC25A51 is indeed a mitochondrial NAD^+ carrier in human cells. Further validation and investigation will provide more insights into the transport characteristics and the physiological effects of alterations in SLC25A51 expression.

Available data show that SLC25A51 expression is relatively constant across human tissues, with highest expression in testis, breast, bone marrow, parathyroid gland, and adipose tissues. Notably, expression of the close homologue SLC25A52 is mainly detectable in testis with some low-level expression in other tissues [51].

6. Molecular Characterisation of the Mitochondrial Carrier SLC25A51

SLC25A51 has been included into the solute carrier family 25 (SLC25), also named mitochondrial carrier family (MCF), due to the presence of three signature motif sequences in three tandemly repeated 100-residue domains, which are characteristic for the members of this protein family (Figure 2) [52–55]. In fact, SLC25A51 was initially called Mitochondrial Carrier Triple Repeat Protein 1 (MCART1). Typically, each 100-residue domain of a mitochondrial carrier (MC) contains two transmembrane helices and the conserved residues of the signature motif (PX[DE]XX[KR]X[KR]_{20–30}[DE]GXXXX[WYF][KR]G; PROSITE PS50920, PFAM PF00153, and IPR00193). The first part of the signature motif (PX[DE]XX[KR]X[KR]) marks the end of the odd-numbered transmembrane helices, whereas the last residues are located just before the beginning of the even-numbered transmembrane helices. In humans, the SLC25 family consists of 53 members annotated from SLC25A1 to SLC25A53 and many of them have been found to transport nucleotides, amino acids, carboxylates, inorganic anions, and cofactors across the inner mitochondrial membrane [18,56–58], and mutations in 18 of these MCs cause human diseases [59]. The six transmembrane helices (H1–H6) of MCs are structured in a barrel around a central substrate translocation pore [60–62] and the N- and C-termini of the proteins are in the mitochondrial intermembrane space [63–65].

SLC25A51 is quite different from the other members of the SLC25 family, displaying distinct variations as shown by sequence comparison with typical SLC25 representatives (see Figure 2). Most noteworthy, the signature motif lacks the first negatively charged residue in the first and third repeat (exhibiting a glutamine and an asparagine, respectively), the first positively charged residue in the first and second repeats (showing a leucine and a glutamine, respectively), as well as the first glycine in the third repeat (having a lysine) (Figure 2). In the conformational changes of MCs occurring during the translocation of the substrates, the first two charged residues of each signature motif form an interconnected charged network of salt bridges between H1, H3, and H5 that take part in the closing of the substrate translocation pore towards the mitochondrial matrix (i.e., of the matrix gate) [60]. Given that SLC25A51 lacks many of the aforementioned charged residues in the signature motif, it is left with only one salt bridge (between H3 and H5) out of the three characteristic ones of the matrix gate. Other differences of SLC25A51 with respect to the sequence features of a typical MC are: the possibility of only one salt bridge (between H4 and H6) out of the usual three of the cytoplasmic gate (which closes the substrate translocation pore towards the intermembrane space) and the lack of cardiolipin-binding motif 1 (Figure 2) [62]. By contrast, other MC motifs are quite conserved in SLC25A51: the GXXG motif and other small residues taking part in helical packing, the cardiolipin-binding motif 2 (corresponding to the last three residues of the signature motif), and the glutamine and tyrosine braces participating in the matrix and cytoplasmic gates, respectively (Figure 2) [66].

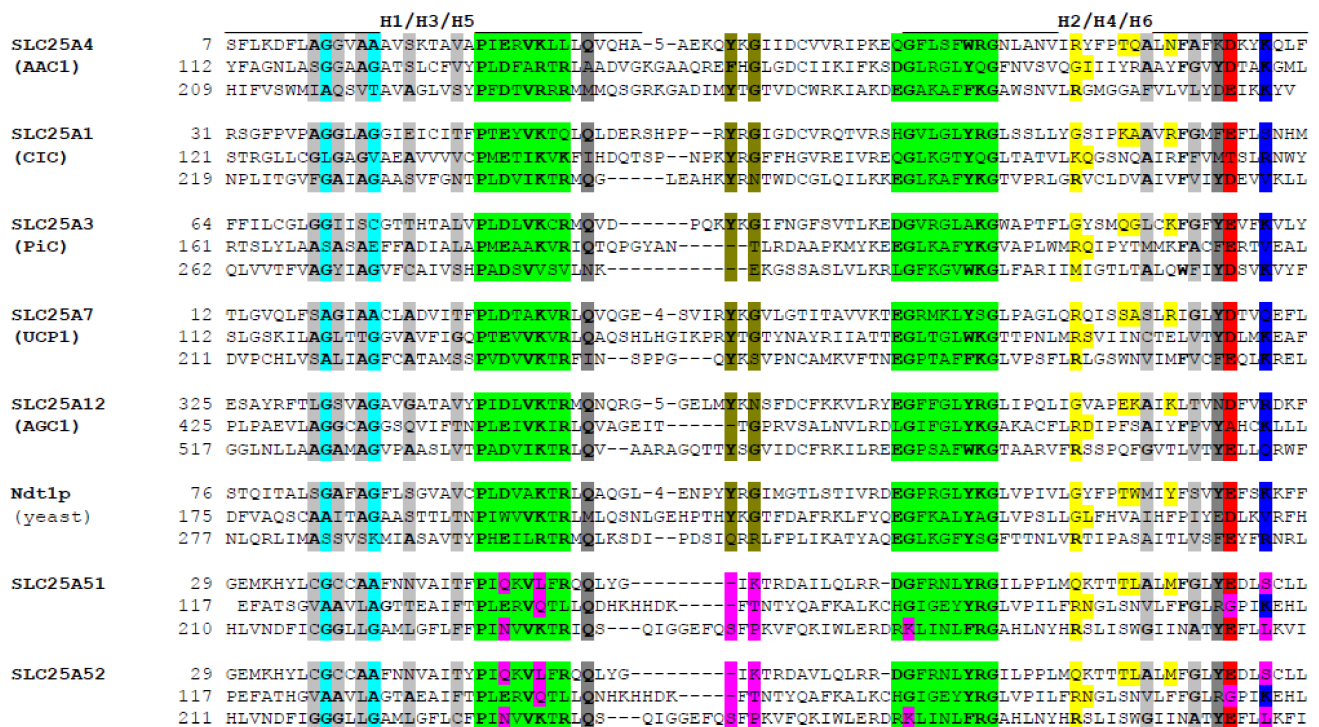


Figure 2. Sequence comparison of the three mitochondrial carrier domain repeats in nucleotide transporter SLC25A4 (ADP/ATP carrier 1, AAC1), carboxylate transporter SLC25A1 (citrate carrier, CIC), phosphate transporter SLC25A3 (PiC), proton transporter SLC25A7 (uncoupling protein 1, UCP1), amino acid transporter SLC25A12 (aspartate-glutamate carrier 1, AGC1), NAD⁺ transporter Ndt1p (*S. cerevisiae*), SLC25A51, and SLC25A52. The following sequence features are indicated: position of the transmembrane helices H1–6 (a line above the sequences), the conserved residues (bold), the helical packing GXXXG motif (cyan), other helical packing small amino acids (light grey), the signature motif sequences (green), the glutamine and tyrosine braces (dark grey), the cardiolipin-binding motif 1 (olive), the contact point residues of the proposed substrate binding site (yellow), and the negatively (red) and positively (blue) charged residues of the cytosolic gate. The distinct sequence variations in SLC25A51 (and SLC25A52) discussed in the text are indicated in magenta.

Based on available structures of the ADP/ATP carrier [60,61], which have been used to understand substrate binding and the translocation mechanism of MCs, a 3D-model of SLC25A51 was generated in a conformation with the matrix gate closed and the cytoplasmic gate open (Figure 3). The substrate binding site of MCs is mainly formed by the so-called “contact point” residues (indicated in yellow in Figure 2), which are located in the even-numbered transmembrane helices and protrude in the substrate translocation pore approximately at the midpoint of the membrane between the matrix and cytoplasmic gates (four, two, and one residues on H2, H4, and H6, respectively, Figure 3) [67]. NAD⁺ was docked into the SLC25A51 homology model to get structural insight into protein-substrate interactions (Figure 3). In the highest-rated docking solution, NAD⁺ is bound in the central cavity of the SLC25A51 structural model at the midpoint between the intermembrane space and the matrix sides of the membrane, and between the cytoplasmic and matrix gate areas (Figure 3A). It is noteworthy that the substrate interacts with residues of all six transmembrane helices (Figure 3B) and forms a total of nine hydrogen bonds with the carrier. In particular, NAD⁺ is bound through hydrogen bonds with each of the three contact points interacting with six out of the seven contact point residues. Of course, the hypothetical substrate binding site of SLC25A51, suggested by this docking solution, awaits experimental validation. However, it is worth mentioning that in most of the other lower-ranking docking solutions, NAD⁺, although having different conformations and interacting with different residues, was bound at the midpoint of the membrane through multiple hydrogen bonds with contact point residues and other residues of all the transmembrane helices. Most likely, this is a consequence of NAD⁺ being one of the largest

substrates known for mitochondrial carriers and having many potential hydrogen bond donors and acceptors.

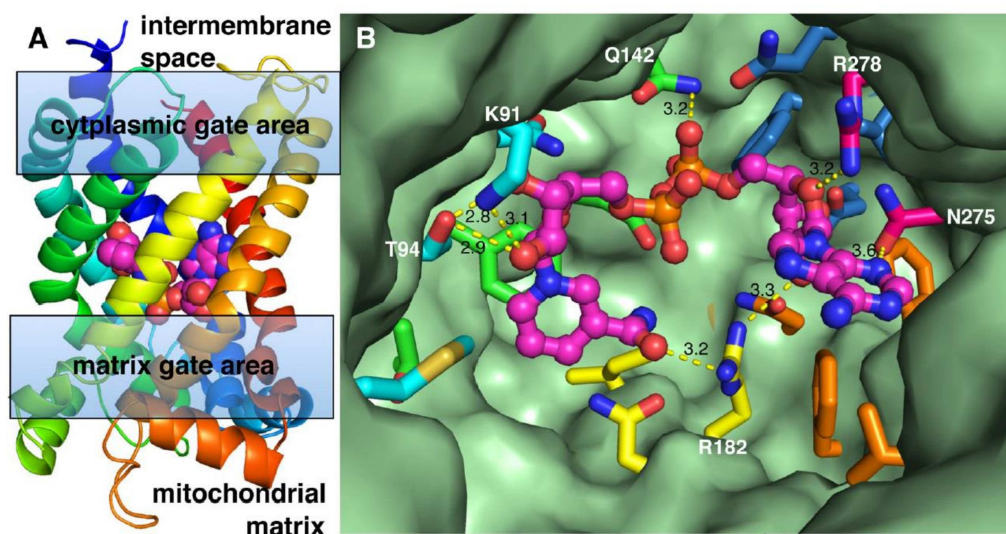


Figure 3. Docking of NAD⁺ into the structural homology model of SLC25A51. A structural homology model of SLC25A51 was generated based on the bovine and yeast ADP/ATP carrier structures (PDB ID: 1OKC, 4C9Q, and 4C9G) by Modeller [68]. Conformationally flexible NAD⁺ was docked into the active site of the SLC25A51 structural model with flexible side chains by Autodock Vina [69]. (A) The highest-ranked docking solution (binding energy = -9.9 kcal/mol; interface area = 532 Å²) is displayed with the protein in cartoon with rainbow colours from N-terminus (blue) to C-terminus (red) and NAD⁺ in spheres (carbons in magenta) viewed from the mitochondrial inner membrane plane. (B) The residues of the substrate binding site of the same docking solution are viewed from the intermembrane space side: NAD⁺ and the residues interacting with it are shown in ball-and-stick and sticks, respectively, with carbons in the same colour as in (A).

7. Hypotheses about the Evolution of SLC25A51

The *SLC25A51* gene is conserved with at least 45% sequence identity on protein level in mammals, birds, fish, amphibians, insects, and nematodes (Figure 4). Notably, it is not found in plants or fungi, where other MCs have been found to transport NAD⁺ [10–14]. Human SLC25A51 is a close paralog of SLC25A52 (Figure 2, sharing 96% identical amino acid sequence, also called MCART2) and, to a lesser extent, to SLC25A53 (30% sequence identity, MCART6) [15–17]. These three MCs are found on the same branch in phylogenetic trees and are distinct from all other human SLC25 members [18,70,71]. They are also distant from all other MCs known to transport NAD⁺ (less than 18% overall sequence identity): the human peroxisomal SLC25A17 [13]; yeast mitochondrial Ndt1p and Ndt2p [10]; *Arabidopsis thaliana* AtNDT1 and AtNDT2 [11] and peroxisomal PXN [12,14]. Differently from these NAD⁺-transporting carriers, SLC25A51, SLC25A52, and SLC25A53 do not have a tryptophan, instead of the first negatively charged residue in the second signature motif (Figure 2). SLC25A33 and SLC25A36 have this tryptophan too, although they transport pyrimidine nucleotides and not NAD⁺ [50]. Furthermore, the residues of the contact points and the conserved three-fold-symmetry-related positions typical for NAD⁺-transporting MCs are different from those of SLC25A51, which are almost identical to those of SLC25A52 and SLC25A53. Moreover, it is noteworthy that the genes of human SLC25A51, SLC25A52, and SLC25A53 do not have introns, although homologues in lower species do. SLC25A51 first appeared in Protostomia and is related to oxaloacetate-type SLC25 transporters [72]. SLC25A53 appears to have evolved from SLC25A51 in vertebrates, whereas SLC25A52 can only be found in primates (schematic overview Figure 5). Plant and fungal Ndt1/2, on the other hand, appear to have evolved independently and are more closely related to the mitochondrial folate and FAD transporters [73,74]. In addition, our analyses indicate that

SLC25A51 binds NAD⁺ in a different way than the yeast and plant MCs transporting NAD⁺ given that their sequences and the residues of their substrate binding sites are so different.

human	1	MMDSEAH...EKRP...ILTSKQDISPHITNVGEMKHLYCGCCAAFNVAITFFIQVLFVFRQQLYGIKTRDAILQLRRDGFNRLYRGILPPLMQ
bovine	1	MMDSEAH...EKRP...ILTSKQDIAPHIATVSEMKHLYCGCCAAFNVAITFFIQVLFVFRQQLYGIKTRDAILQLRRDGFNRLYRGILPPLMQ
mouse	1	MMDSEAH...EKRP...MLTSNQDLSPHIAGVGMKHLYCGYCAAFNVAITFFIQVLFVFRQQLYGIKTRDAVLQRKDGFRNLYRGILPPLMQ
bird	1	MLLPSEWCSELEKRTTEVFSKRNMMGSGGFSSEEDPSSDVTATSSKHLYCGYCAAFNVAITFFIQVLFVFRQQLYGIKTRDAIHLQKDGFRNLYRGILPPLMQ
fish	1	MGVVTMDSDSA...RQFQ...GKLSGHALIGANLARG.KHYVGSGLAAFTNIIITFFIQVLFVFRQQLYGIKTRDAIHLQKDGFRNLYRGILPPLMQ
insect	1	MKDDGAPNVAKTDPFPKRFPSGRAHSPHGDEAG...KLLHGSVFSKRFFGFSQWEEFA.GCCAAFNVAITFFIQVLFVFRQQLYGIKTRDAIHLQKDGFRNLYRGILPPLMQ
nematode	1	
frog	1	MMDSEAH...EKRS...VLTAKHDYKPYAVTVGSGKHLYCGYFAAFNVAITFFIQVLFVFRQQLYGIKTRDAVRLQTDGIRNLYRGILPPLMQ

human	91	KTTTLALMFGLYEDLSCLLHKHVS...APEFATRSVAALVAGTTEAIFTPLEAVQITLLQDHRKHDKFTNTYQAFK.ALKCHGIREYRGLVPIILFRNGLSNVLFVFRQQLYGIKTRDAIHLQKDGFRNLYRGILPPLMQ
bovine	91	KTTTLALMFGLYEDLSCLLHKHVS...TPEFATRSMAAVLAGTTEAIFTPLEAVQITLLQDHRKHDKFTNTYQAFK.ALKCHGIREYRGLVPIILFRNGLSNVLFVFRQQLYGIKTRDAIHLQKDGFRNLYRGILPPLMQ
mouse	91	KTTTLALMFGLYEDLSRLLHKHVS...APEFATRSVAALVAGTTEAIFTPLEAVQITLLQDHRKHDKFTNTYQAFK.ALKCHGIREYRGLVPIILFRNGLSNVLFVFRQQLYGIKTRDAIHLQKDGFRNLYRGILPPLMQ
bird	109	KTTTLALMFGLYEDFSLLHSHHT...APELLTRSMVAALVAGTTEAIFTPLEAVQITLLQDHRKHDKFTNTYQAFK.VLRVYGMREYRGLVPIILFRNGLSNVLFVFRQQLYGIKTRDAIHLQKDGFRNLYRGILPPLMQ
fish	93	KTTTVAIMFGLYEDFSRLLRHARSSGAPVLTTRSAALVAGTTEAIFTPLEAVQITLLQDHRKHDKFTNTYQAFK.VLRVYGMREYRGLVPIILFRNGLSNVLFVFRQQLYGIKTRDAIHLQKDGFRNLYRGILPPLMQ
insect	114	KTISLSIMFVFDGTRRYLVEDYR...LNDYGAQVLAADVAGSARISILLPPEAVQITLLQDHRKHDKFTNTYQAFK.VLRVYGMREYRGLVPIILFRNGLSNVLFVFRQQLYGIKTRDAIHLQKDGFRNLYRGILPPLMQ
nematode	2	RTTSRALMFGLYEDFQISLKCPRSPNSFSICHAAFLSGVCEAMLCPLERVQITLLQDHRKHDKFTNTYQAFK.VLRVYGMREYRGLVPIILFRNGLSNVLFVFRQQLYGIKTRDAIHLQKDGFRNLYRGILPPLMQ
frog	93	KTTTLALMFGLYEDFSLLRHHT...SPEVVTTRSMVAALVAGTTEAIFTPLEAVQITLLQDHRKHDKFTNTYQAFK.VLRVYGMREYRGLVPIILFRNGLSNVLFVFRQQLYGIKTRDAIHLQKDGFRNLYRGILPPLMQ

human	202	P.....TATTHSAHLVNDPFCGGLLGAMLGFLFPFNNVVKTRIQSQIGGEFQSPFKVQKIWLERDRKLIINLFRGALHNYHRSLSISWGIINATYEFLLKVI
bovine	202	P.....TATTHSAHLVNDPFCGGLLGAMLGFLFPFNNVVKTRIQSQIGGEFQSPFKVQKIWLERDRKLIINLFRGALHNYHRSLSISWGIINATYEFLLKVI
mouse	203	P.....TATTYS AHLVNDPFCGGLLGAVLGLFSPFNNVVKTRIQSQIGGEFQSPFKVQKIWLERDRKLIINLFRGALHNYHRSLSISWGIINATYEFLLKVI
bird	220	P.....EATSYSTHLVNDPFCGGLLGAMLGFLFPFNNVVKTRIQSQIGGEFQSPFSTVEVKIWERDRKLIINLFRGALHNYHRSLSISWGIINATYEFLLKVI
fish	208	P.....DARSRMGNMNDPFCGGLLGALGIMFYPLNVKTRIQSQIGGEFQSPFSTVEVKIWERDRKLIINLFRGALHNYHRSLSISWGIINATYEFLLKVI
insect	226	P.....KRKSVSTRIVQEFIRAGAVIGASISTIFYPLNVKTRIQSQIGGEFQSPFSTVEVKIWERDRKLIINLFRGALHNYHRSLSISWGIINATYEFLLKVI
nematode	116	VGIPQAGRLPESLQQLIGDFVAGSLLGATISTAFFPLGVINKHMQAKVGVKYEYSGFKVFRDWWQLRNRSLRGLYLGVHNLNFTRSVWAGIINSMYGIILRRALAPPE
frog	204	P.....EARTYSANLINDPFCGGLLGAMLGFLFPFNNVVKTRIQSQIGGEFQSPFKVQKIWLERDRKLIINLFRGALHNYHRSLSISWGIINATYEFLLKVI

Figure 4. Multiple sequence alignment of representative SLC25A51 homologs from various species: human (*Homo sapiens*, NP_219480), bovine (*Bos taurus*, NP_001092864), mouse (*Mus musculus*, NP_001009949), bird (*Gallus gallus*, XP_003643156), fish (*Danio rerio*, XP_002664343), insect (*Drosophila melanogaster*, NP_651766), nematode (*Caenorhabditis elegans*, NP_501642), and frog (*Xenopus tropicalis*, NP_001107506). The conserved residues are coloured based on the property of the side chain: hydroxyl group S and T (magenta); amide group N and Q (green); positively charged R, K, and H (cyan); negatively charged D and E (red); aromatic F, W, and Y (brown); sulfur-containing C and M (light yellow); hydrophobic A, G, L, I, and V (black and bold); P (dark yellow).

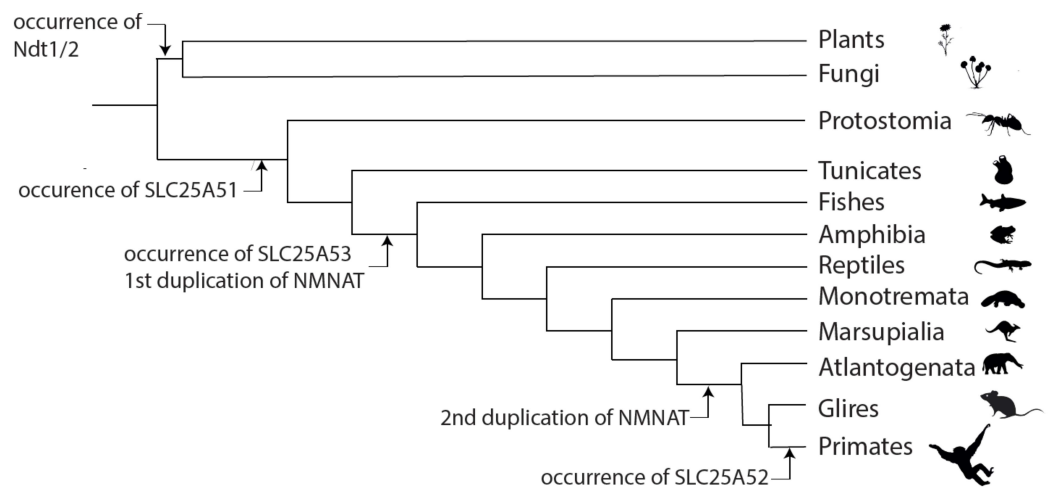


Figure 5. Evolutionary events related to compartmentation of NAD⁺ biosynthesis. The scheme illustrates major evolutionary events related to mitochondrial NAD⁺ metabolism. Ndt1/2 can only be found in plants and fungi, whereas SLC25A51 homologues can be detected in all Metazoan starting from Protostomia. The functionally uncharacterized paralogue SLC25A53 is first found in vertebrates, whereas SLC25A52 can only be found in primates. In parallel, the different isoforms of NMNATs developed. The first duplication of NMNATs in the last common ancestor of vertebrates gave rise to NMNAT2, whereas the later gene duplication in mammals lead to the development of the mitochondrial isoform NMNAT3 [75]. The tree is a schematic representation of selected taxa and is based on information from Tree of Life Web Project [76].

8. Conclusions and Perspectives

The identification of SLC25A51 as a human mitochondrial NAD⁺ carrier is a leap forward in understanding cellular NAD⁺ metabolism and how NAD⁺ pools are distributed between the cytoplasm and mitochondria. It strengthens the hypothesis that NAD⁺ biosynthesis does not necessarily occur in mitochondria. Just as its counterparts in yeast and plants, as well as the peroxisomal NAD⁺ carriers, the mitochondrial NAD⁺ transporter of animals—SLC25A51—is a member of the mitochondrial carrier SLC25 family. However, it seems to have a distant evolutionary origin and a different substrate binding site with respect to the other NAD⁺ carriers. The appearance of SLC25A51 in Protostomia may reflect changes or differences in cellular NAD⁺ utilization, metabolism, and regulation compared to lower organisms or to yeast and plants.

On the other hand, the discovery of a human mitochondrial NAD⁺ carrier SLC25A51 raises a number of important questions, which need to be addressed in future research. What is the role of NMNAT3 in mitochondria? Is NMNAT3 involved in regulation of the mitochondrial NAD⁺ pool, in the synthesis or degradation of NAD⁺ from or to NMN in certain cells or conditions? Does SLC25A51 play a role in the concentration gradient of NAD⁺ between mitochondria and cytoplasm (higher in mitochondria) of various tissues and cell types? The transport properties of SLC25A51 have not been defined yet. What is the substrate specificity of SLC25A51? What is its ability to transport putative substrates such as NAD⁺, NMN, NAAD, α -NAD⁺, NADH, NAMN, NADP, NADPH, Nam, NA, FAD, FMN, and (deoxy-) nucleotides? Does SLC25A51 catalyse unidirectional transport and/or antiport of substrates, and what are its kinetic parameters? A biochemical characterization of SLC25A51 to answer the last two questions would help to understand what the physiological substrates of this carrier protein are and the preferred direction. An additional area of interest for future studies is in elucidating how this transporter is regulated in vivo, for example, by post-translational modifications. Regulation could be critical, because high expression of the carrier or a functional homolog affects mitochondrial function. A further issue is that SLC25A51 does not appear to be essential, suggesting that there may be other mitochondrial transporters capable of transporting NAD. The very close paralog SLC25A52 is likely to have similar transport properties as SLC25A51, but there could be differences.

Funding: We acknowledge support from the Research Council of Norway (302314 to M.Z. and 309,567 to M.Z. and I.H.) as well as the PoLiMeR Innovative Training Network (Marie Skłodowska-Curie grant agreement 812,616 to M.Z.) and the MESI-STRAT project (grant agreement 754,688 to M.Z. and I.H.), which received funding from the European Union Horizon 2020 Research and Innovation Program. A.N. was supported by the Russian Science Foundation (grant № 21-14-00319). Research in the Italian laboratories was supported by grants from Ministero dell'Università e della Ricerca (PRIN 2017PAB8EM) and Center of Excellence in Genomics (CEGBA).

Institutional Review Board Statement: Not applicable.

Informed Consent Statement: Not applicable.

Conflicts of Interest: The authors declare no conflict of interest.

References

- Hediger, M.A.; Clemençon, B.; Burrier, R.E.; Bruford, E.A. The ABCs of membrane transporters in health and disease (SLC series): Introduction. *Mol. Aspects Med.* **2013**, *34*, 95–107. [CrossRef] [PubMed]
- Perland, E.; Fredriksson, R. Classification Systems of Secondary Active Transporters. *Trends Pharmacol. Sci.* **2017**, *38*, 305–315. [CrossRef] [PubMed]
- Stein, L.R.; Imai, S. The dynamic regulation of NAD metabolism in mitochondria. *Trends Endocrinol. Metab.* **2012**, *23*, 420–428. [CrossRef]
- Nikiforov, A.; Kulikova, V.; Ziegler, M. The human NAD metabolome: Functions, metabolism and compartmentalization. *Crit. Rev. Biochem. Mol. Biol.* **2015**, *50*, 284–297. [CrossRef] [PubMed]
- Kropotov, A.; Kulikova, V.; Nerinovski, K.; Yakimov, A.; Svetlova, M.; Solovjeva, L.; Sudnitsyna, J.; Migaud, M.E.; Khodorkovskiy, M.; Ziegler, M.; et al. Equilibrative Nucleoside Transporters Mediate the Import of Nicotinamide Riboside and Nicotinic Acid Riboside into Human Cells. *Int. J. Mol. Sci.* **2021**, *22*, 1391. [CrossRef] [PubMed]

6. Nikiforov, A.; Dolle, C.; Niere, M.; Ziegler, M. Pathways and subcellular compartmentation of NAD biosynthesis in human cells: From entry of extracellular precursors to mitochondrial NAD generation. *J. Biol. Chem.* **2011**, *286*, 21767–21778. [CrossRef] [PubMed]
7. Stromland, O.; Niere, M.; Nikiforov, A.A.; VanLinden, M.R.; Heiland, I.; Ziegler, M. Keeping the balance in NAD metabolism. *Biochem. Soc. Trans.* **2019**, *47*, 119–130. [CrossRef] [PubMed]
8. Indiveri, C.; Kramer, R.; Palmieri, F. Reconstitution of the malate/aspartate shuttle from mitochondria. *J. Biol. Chem.* **1987**, *262*, 15979–15983. [CrossRef]
9. Bücher, T.; Klingenberg, M. Wege des Wasserstoffs in der lebendigen Organisation. *Angew. Chem.* **1958**, *70*, 552–570. [CrossRef]
10. Todisco, S.; Agrimi, G.; Castegna, A.; Palmieri, F. Identification of the mitochondrial NAD⁺ transporter in *Saccharomyces cerevisiae*. *J. Biol. Chem.* **2006**, *281*, 1524–1531. [CrossRef]
11. Palmieri, F.; Rieder, B.; Ventrella, A.; Blanco, E.; Do, P.T.; Nunes-Nesi, A.; Trauth, A.U.; Fiermonte, G.; Tjaden, J.; Agrimi, G.; et al. Molecular identification and functional characterization of *Arabidopsis thaliana* mitochondrial and chloroplastic NAD⁺ carrier proteins. *J. Biol. Chem.* **2009**, *284*, 31249–31259. [CrossRef]
12. Agrimi, G.; Russo, A.; Pierri, C.L.; Palmieri, F. The peroxisomal NAD⁺ carrier of *Arabidopsis thaliana* transports coenzyme A and its derivatives. *J. Bioenerg. Biomembr.* **2012**, *44*, 333–340. [CrossRef]
13. Agrimi, G.; Russo, A.; Scarcia, P.; Palmieri, F. The human gene SLC25A17 encodes a peroxisomal transporter of coenzyme A, FAD and NAD⁺. *Biochem. J.* **2012**, *443*, 241–247. [CrossRef]
14. Bernhardt, K.; Wilkinson, S.; Weber, A.P.; Linka, N. A peroxisomal carrier delivers NAD(+) and contributes to optimal fatty acid degradation during storage oil mobilization. *Plant J.* **2012**, *69*, 1–13. [CrossRef]
15. Girardi, E.; Agrimi, G.; Goldmann, U.; Fiume, G.; Lindinger, S.; Sedlyarov, V.; Srndic, I.; Gurtl, B.; Agerer, B.; Kartnig, F.; et al. Epistasis-driven identification of SLC25A51 as a regulator of human mitochondrial NAD import. *Nat. Commun.* **2020**, *11*, 6145. [CrossRef]
16. Kory, N.; Uit de Bos, J.; van der Rijt, S.; Jankovic, N.; Gura, M.; Arp, N.; Pena, I.A.; Prakash, G.; Chan, S.H.; Kunchok, T.; et al. MCART1/SLC25A51 is required for mitochondrial NAD transport. *Sci. Adv.* **2020**, *6*. [CrossRef]
17. Luongo, T.S.; Eller, J.M.; Lu, M.J.; Niere, M.; Raith, F.; Perry, C.; Bornstein, M.R.; Oliphint, P.; Wang, L.; McReynolds, M.R.; et al. SLC25A51 is a mammalian mitochondrial NAD(+) transporter. *Nature* **2020**, *588*, 174–179. [CrossRef]
18. Palmieri, F.; Monne, M. Discoveries, metabolic roles and diseases of mitochondrial carriers: A review. *Biochim. Biophys. Acta* **2016**, *1863*, 2362–2378. [CrossRef]
19. Burgos, E.S.; Schramm, V.L. Weak coupling of ATP hydrolysis to the chemical equilibrium of human nicotinamide phosphoribosyltransferase. *Biochemistry* **2008**, *47*, 11086–11096. [CrossRef]
20. Bockwoldt, M.; Houry, D.; Niere, M.; Gossmann, T.I.; Reinartz, I.; Schug, A.; Ziegler, M.; Heiland, I. Identification of evolutionary and kinetic drivers of NAD-dependent signaling. *Proc. Natl. Acad. Sci. USA* **2019**, *116*, 15957–15966. [CrossRef]
21. Dolle, C.; Skoge, R.H.; Vanlinden, M.R.; Ziegler, M. NAD biosynthesis in humans—enzymes, metabolites and therapeutic aspects. *Curr. Top. Med. Chem.* **2013**, *13*, 2907–2917. [CrossRef] [PubMed]
22. Liu, L.; Su, X.; Quinn, W.J., 3rd; Hui, S.; Krukenberg, K.; Frederick, D.W.; Redpath, P.; Zhan, L.; Chellappa, K.; White, E.; et al. Quantitative Analysis of NAD Synthesis-Breakdown Fluxes. *Cell Metab.* **2018**, *27*, 1067–1080.e5. [CrossRef] [PubMed]
23. de Figueiredo, L.F.; Gossmann, T.I.; Ziegler, M.; Schuster, S. Pathway analysis of NAD⁺ metabolism. *Biochem. J.* **2011**, *439*, 341–348. [CrossRef]
24. Yang, Y.; Sauve, A.A. NAD(+) metabolism: Bioenergetics, signaling and manipulation for therapy. *Biochim. Biophys. Acta* **2016**, *1864*, 1787–1800. [CrossRef] [PubMed]
25. Katsyuba, E.; Romani, M.; Hofer, D.; Auwerx, J. NAD(+) homeostasis in health and disease. *Nat. Metab.* **2020**, *2*, 9–31. [CrossRef] [PubMed]
26. Bieganowski, P.; Brenner, C. Discoveries of nicotinamide riboside as a nutrient and conserved NRK genes establish a Preiss-Handler independent route to NAD⁺ in fungi and humans. *Cell* **2004**, *117*, 495–502. [CrossRef]
27. Yoshino, J.; Baur, J.A.; Imai, S.I. NAD(+) Intermediates: The Biology and Therapeutic Potential of NMN and NR. *Cell Metab.* **2018**, *27*, 513–528. [CrossRef] [PubMed]
28. VanLinden, M.R.; Niere, M.; Nikiforov, A.A.; Ziegler, M.; Dolle, C. Compartment-Specific Poly-ADP-Ribose Formation as a Biosensor for Subcellular NAD Pools. *Methods Mol. Biol.* **2017**, *1608*, 45–56. [CrossRef]
29. Dolle, C.; Niere, M.; Lohndal, E.; Ziegler, M. Visualization of subcellular NAD pools and intra-organellar protein localization by poly-ADP-ribose formation. *Cell. Mol. Life Sci.* **2010**, *67*, 433–443. [CrossRef]
30. VanLinden, M.; Høyland, L.; Dietze, J.; Tolås, I.; Sverke, L.; Niere, M.; Cimadamore-Werthein, C.; Hoeven, B.v.d.; Strömland, Ø.; Sauter, R.; et al. Chronic depletion of subcellular NAD pools reveals their interconnectivity and a buffering function of mitochondria. *Nat. Portf.* **2020**. [CrossRef]
31. Cambronne, X.A.; Stewart, M.L.; Kim, D.; Jones-Brunette, A.M.; Morgan, R.K.; Farrens, D.L.; Cohen, M.S.; Goodman, R.H. Biosensor reveals multiple sources for mitochondrial NAD(+). *Science* **2016**, *352*, 1474–1477. [CrossRef]
32. Ryu, K.W.; Nandu, T.; Kim, J.; Challa, S.; DeBerardinis, R.J.; Kraus, W.L. Metabolic regulation of transcription through compartmentalized NAD(+) biosynthesis. *Science* **2018**, *360*. [CrossRef]

33. Conforti, L.; Janeckova, L.; Wagner, D.; Mazzola, F.; Cialabrini, L.; Di Stefano, M.; Orsomando, G.; Magni, G.; Bendotti, C.; Smyth, N.; et al. Reducing expression of NAD⁺ synthesizing enzyme NMNAT1 does not affect the rate of Wallerian degeneration. *FEBS J.* **2011**, *278*, 2666–2679. [CrossRef]
34. Gilley, J.; Adalbert, R.; Yu, G.; Coleman, M.P. Rescue of peripheral and CNS axon defects in mice lacking NMNAT2. *J. Neurosci.* **2013**, *33*, 13410–13424. [CrossRef]
35. VanLinden, M.R.; Dolle, C.; Pettersen, I.K.; Kulikova, V.A.; Niere, M.; Agrimi, G.; Dyrstad, S.E.; Palmieri, F.; Nikiforov, A.A.; Tronstad, K.J.; et al. Subcellular Distribution of NAD⁺ between Cytosol and Mitochondria Determines the Metabolic Profile of Human Cells. *J. Biol. Chem.* **2015**, *290*, 27644–27659. [CrossRef]
36. Barile, M.; Passarella, S.; Danese, G.; Quagliariello, E. Rat liver mitochondria can synthesize nicotinamide adenine dinucleotide from nicotinamide mononucleotide and ATP via a putative matrix nicotinamide mononucleotide adenylyltransferase. *Biochem. Mol. Biol. Int.* **1996**, *38*, 297–306.
37. Davila, A.; Liu, L.; Chellappa, K.; Redpath, P.; Nakamaru-Ogiso, E.; Paoletta, L.M.; Zhang, Z.; Migaud, M.E.; Rabinowitz, J.D.; Baur, J.A. Nicotinamide adenine dinucleotide is transported into mammalian mitochondria. *elife* **2018**, *7*. [CrossRef]
38. Gulshan, M.; Yaku, K.; Okabe, K.; Mahmood, A.; Sasaki, T.; Yamamoto, M.; Hikosaka, K.; Usui, I.; Kitamura, T.; Tobe, K.; et al. Overexpression of Nmnat3 efficiently increases NAD and NGD levels and ameliorates age-associated insulin resistance. *Aging Cell* **2018**, *17*, e12798. [CrossRef]
39. Son, M.J.; Kwon, Y.; Son, T.; Cho, Y.S. Restoration of Mitochondrial NAD(+) Levels Delays Stem Cell Senescence and Facilitates Reprogramming of Aged Somatic Cells. *Stem Cells* **2016**, *34*, 2840–2851. [CrossRef]
40. Yamamoto, M.; Hikosaka, K.; Mahmood, A.; Tobe, K.; Shojaku, H.; Inohara, H.; Nakagawa, T. Nmnat3 Is Dispensable in Mitochondrial NAD Level Maintenance In Vivo. *PLoS ONE* **2016**, *11*, e0147037. [CrossRef]
41. Hikosaka, K.; Ikutani, M.; Shito, M.; Kazuma, K.; Gulshan, M.; Nagai, Y.; Takatsu, K.; Konno, K.; Tobe, K.; Kanno, H.; et al. Deficiency of nicotinamide mononucleotide adenylyltransferase 3 (nmnat3) causes hemolytic anemia by altering the glycolytic flow in mature erythrocytes. *J. Biol. Chem.* **2014**, *289*, 14796–14811. [CrossRef] [PubMed]
42. Palmieri, F.; Agrimi, G.; Blanco, E.; Castegna, A.; Di Noia, M.A.; Iacobazzi, V.; Lasorsa, F.M.; Marobbio, C.M.; Palmieri, L.; Scarcia, P.; et al. Identification of mitochondrial carriers in *Saccharomyces cerevisiae* by transport assay of reconstituted recombinant proteins. *Biochim. Biophys. Acta* **2006**, *1757*, 1249–1262. [CrossRef] [PubMed]
43. Agrimi, G.; Brambilla, L.; Frascotti, G.; Pisano, I.; Porro, D.; Vai, M.; Palmieri, L. Deletion or overexpression of mitochondrial NAD⁺ carriers in *Saccharomyces cerevisiae* alters cellular NAD and ATP contents and affects mitochondrial metabolism and the rate of glycolysis. *Appl. Environ. Microbiol.* **2011**, *77*, 2239–2246. [CrossRef] [PubMed]
44. de Souza Chaves, I.; Feitosa-Araujo, E.; Florian, A.; Medeiros, D.B.; da Fonseca-Pereira, P.; Charton, L.; Heyneke, E.; Apfata, J.A.C.; Pires, M.V.; Mettler-Altmann, T.; et al. The mitochondrial NAD(+) transporter (NDT1) plays important roles in cellular NAD(+) homeostasis in *Arabidopsis thaliana*. *Plant J.* **2019**, *100*, 487–504. [CrossRef]
45. Feitosa-Araujo, E.; de Souza Chaves, I.; Florian, A.; da Fonseca-Pereira, P.; Condori Apfata, J.A.; Heyneke, E.; Medeiros, D.B.; Pires, M.V.; Mettler-Altmann, T.; Neuhaus, H.E.; et al. Downregulation of a Mitochondrial NAD⁺ Transporter (NDT2) Alters Seed Production and Germination in *Arabidopsis*. *Plant Cell Physiol.* **2020**, *61*, 897–908. [CrossRef]
46. Haferkamp, I.; Schmitz-Esser, S.; Linka, N.; Urbany, C.; Collingro, A.; Wagner, M.; Horn, M.; Neuhaus, H.E. A candidate NAD⁺ transporter in an intracellular bacterial symbiont related to Chlamydiae. *Nature* **2004**, *432*, 622–625. [CrossRef]
47. Fisher, D.J.; Fernandez, R.E.; Maurelli, A.T. Chlamydia trachomatis transports NAD via the Npt1 ATP/ADP translocase. *J. Bacteriol.* **2013**, *195*, 3381–3386. [CrossRef]
48. Yang, H.; Yang, T.; Baur, J.A.; Perez, E.; Matsui, T.; Carmona, J.J.; Lamming, D.W.; Souza-Pinto, N.C.; Bohr, V.A.; Rosenzweig, A.; et al. Nutrient-sensitive mitochondrial NAD⁺ levels dictate cell survival. *Cell* **2007**, *130*, 1095–1107. [CrossRef]
49. Pittelli, M.; Formentini, L.; Faraco, G.; Lapucci, A.; Rapizzi, E.; Cialdai, F.; Romano, G.; Moneti, G.; Moroni, F.; Chiarugi, A. Inhibition of nicotinamide phosphoribosyltransferase: Cellular bioenergetics reveals a mitochondrial insensitive NAD pool. *J. Biol. Chem.* **2010**, *285*, 34106–34114. [CrossRef]
50. Di Noia, M.A.; Todisco, S.; Cirigliano, A.; Rinaldi, T.; Agrimi, G.; Iacobazzi, V.; Palmieri, F. The human SLC25A33 and SLC25A36 genes of solute carrier family 25 encode two mitochondrial pyrimidine nucleotide transporters. *J. Biol. Chem.* **2014**, *289*, 33137–33148. [CrossRef]
51. Uhlen, M.; Fagerberg, L.; Hallstrom, B.M.; Lindskog, C.; Oksvold, P.; Mardinoglu, A.; Sivertsson, A.; Kampf, C.; Sjostedt, E.; Asplund, A.; et al. Proteomics. Tissue-based map of the human proteome. *Science* **2015**, *347*, 1260419. [CrossRef]
52. Saraste, M.; Walker, J.E. Internal sequence repeats and the path of polypeptide in mitochondrial ADP/ATP translocase. *FEBS Lett.* **1982**, *144*, 250–254. [CrossRef]
53. Palmieri, F. Mitochondrial carrier proteins. *FEBS Lett.* **1994**, *346*, 48–54. [CrossRef]
54. Palmieri, F. The mitochondrial transporter family SLC25: Identification, properties and physiopathology. *Mol. Aspects Med.* **2013**, *34*, 465–484. [CrossRef]
55. Monne, M.; Palmieri, F. Antiporters of the mitochondrial carrier family. *Curr. Top. Membr.* **2014**, *73*, 289–320. [CrossRef]
56. Palmieri, F.; Pierri, C.L. Structure and function of mitochondrial carriers—Role of the transmembrane helix P and G residues in the gating and transport mechanism. *FEBS Lett.* **2010**, *584*, 1931–1939. [CrossRef]

57. Monne, M.; Daddabbo, L.; Gagneul, D.; Obata, T.; Hielscher, B.; Palmieri, L.; Miniero, D.V.; Fernie, A.R.; Weber, A.P.M.; Palmieri, F. Uncoupling proteins 1 and 2 (UCP1 and UCP2) from *Arabidopsis thaliana* are mitochondrial transporters of aspartate, glutamate, and dicarboxylates. *J. Biol. Chem.* **2018**, *293*, 4213–4227. [CrossRef]
58. Monne, M.; Vozza, A.; Lasorsa, F.M.; Porcelli, V.; Palmieri, F. Mitochondrial Carriers for Aspartate, Glutamate and Other Amino Acids: A Review. *Int. J. Mol. Sci.* **2019**, *20*, 4456. [CrossRef]
59. Palmieri, F.; Scarcia, P.; Monne, M. Diseases Caused by Mutations in Mitochondrial Carrier Genes SLC25: A Review. *Biomolecules* **2020**, *10*, 655. [CrossRef]
60. Pebay-Peyroula, E.; Dahout-Gonzalez, C.; Kahn, R.; Trezeguet, V.; Lauquin, G.J.; Brandolin, G. Structure of mitochondrial ADP/ATP carrier in complex with carboxyatractyloside. *Nature* **2003**, *426*, 39–44. [CrossRef]
61. Ruprecht, J.J.; Hellawell, A.M.; Harding, M.; Crichton, P.G.; McCoy, A.J.; Kunji, E.R. Structures of yeast mitochondrial ADP/ATP carriers support a domain-based alternating-access transport mechanism. *Proc. Natl. Acad. Sci. USA* **2014**, *111*, E426–434. [CrossRef]
62. Ruprecht, J.J.; King, M.S.; Zogg, T.; Aleksandrova, A.A.; Pardon, E.; Crichton, P.G.; Steyaert, J.; Kunji, E.R.S. The Molecular Mechanism of Transport by the Mitochondrial ADP/ATP Carrier. *Cell* **2019**, *176*, 435–447.e15. [CrossRef] [PubMed]
63. Capobianco, L.; Brandolin, G.; Palmieri, F. Transmembrane topography of the mitochondrial phosphate carrier explored by peptide-specific antibodies and enzymatic digestion. *Biochemistry* **1991**, *30*, 4963–4969. [CrossRef]
64. Palmieri, F.; Bisaccia, F.; Capobianco, L.; Dolce, V.; Fiermonte, G.; Iacobazzi, V.; Zara, V. Transmembrane topology, genes, and biogenesis of the mitochondrial phosphate and oxoglutarate carriers. *J. Bioenerg. Biomembr.* **1993**, *25*, 493–501. [CrossRef]
65. Bisaccia, F.; Capobianco, L.; Brandolin, G.; Palmieri, F. Transmembrane topography of the mitochondrial oxoglutarate carrier assessed by peptide-specific antibodies and enzymatic cleavage. *Biochemistry* **1994**, *33*, 3705–3713. [CrossRef]
66. Kunji, E.R.S.; King, M.S.; Ruprecht, J.J.; Thangaratnarah, C. The SLC25 Carrier Family: Important Transport Proteins in Mitochondrial Physiology and Pathology. *Physiology Bethesda* **2020**, *35*, 302–327. [CrossRef]
67. Robinson, A.J.; Kunji, E.R. Mitochondrial carriers in the cytoplasmic state have a common substrate binding site. *Proc. Natl. Acad. Sci. USA* **2006**, *103*, 2617–2622. [CrossRef]
68. Fiser, A.; Sali, A. Modeller: Generation and refinement of homology-based protein structure models. *Methods Enzymol.* **2003**, *374*, 461–491. [CrossRef]
69. Trott, O.; Olson, A.J. AutoDock Vina: Improving the speed and accuracy of docking with a new scoring function, efficient optimization, and multithreading. *J. Comput. Chem.* **2010**, *31*, 455–461. [CrossRef]
70. Palmieri, F.; Pierri, C.L.; De Grassi, A.; Nunes-Nesi, A.; Fernie, A.R. Evolution, structure and function of mitochondrial carriers: A review with new insights. *Plant J.* **2011**, *66*, 161–181. [CrossRef]
71. Palmieri, F.; Pierri, C.L. Mitochondrial metabolite transport. *Essays Biochem.* **2010**, *47*, 37–52. [CrossRef] [PubMed]
72. Palmieri, L.; Vozza, A.; Agrimi, G.; De Marco, V.; Runswick, M.J.; Palmieri, F.; Walker, J.E. Identification of the yeast mitochondrial transporter for oxaloacetate and sulfate. *J. Biol. Chem.* **1999**, *274*, 22184–22190. [CrossRef]
73. Titus, S.A.; Moran, R.G. Retrovirally mediated complementation of the glyB phenotype. Cloning of a human gene encoding the carrier for entry of folates into mitochondria. *J. Biol. Chem.* **2000**, *275*, 36811–36817. [CrossRef] [PubMed]
74. Spaan, A.N.; Ijlst, L.; van Roermund, C.W.; Wijburg, F.A.; Wanders, R.J.; Waterham, H.R. Identification of the human mitochondrial FAD transporter and its potential role in multiple acyl-CoA dehydrogenase deficiency. *Mol. Genet. Metab.* **2005**, *86*, 441–447. [CrossRef] [PubMed]
75. Lau, C.; Dolle, C.; Gossmann, T.I.; Agledal, L.; Niere, M.; Ziegler, M. Isoform-specific targeting and interaction domains in human nicotinamide mononucleotide adenylyltransferases. *J. Biol. Chem.* **2010**, *285*, 18868–18876. [CrossRef] [PubMed]
76. Maddison, D.R.; Schulz, K.-S.; Maddison, W.P. The Tree of Life Web Project. *Zootaxa* **2007**, 19–40. [CrossRef]

Review

From the Identification to the Dissection of the Physiological Role of the Mitochondrial Calcium Uniporter: An Ongoing Story

Giorgia Pallafacchina ^{1,2,*}, Sofia Zanin ^{3,†} and Rosario Rizzuto ^{2,*}

¹ Department of Biomedical Sciences, University of Padua, 35131 Padua, Italy

² Neuroscience Institute, Italian National Research Council (CNR), 35131 Padua, Italy

³ Department of Immunology, Infectiology and Haematology, Institut Necker-Enfants Malades (INEM), INSERM U1151-CNRS UMR 8253, 75015 Paris, France; sofia.zanin@inserm.fr

* Correspondence: giorgia.pallafacchina@unipd.it (G.P.); rosario.rizzuto@unipd.it (R.R.); Tel.: +39-049-827-6029 (G.P.); +39-049-827-3001 (R.R.)

† These authors equally contributed to the work.

Abstract: The notion of mitochondria being involved in the decoding and shaping of intracellular Ca^{2+} signals has been circulating since the end of the 19th century. Despite that, the molecular identity of the channel that mediates Ca^{2+} ion transport into mitochondria remained elusive for several years. Only in the last decade, the genes and pathways responsible for the mitochondrial uptake of Ca^{2+} began to be cloned and characterized. The gene coding for the pore-forming unit of the mitochondrial channel was discovered exactly 10 years ago, and its product was called mitochondrial Ca^{2+} uniporter or MCU. Before that, only one of its regulators, the mitochondria Ca^{2+} uptake regulator 1, MICU1, has been described in 2010. However, in the following years, the scientific interest in mitochondrial Ca^{2+} signaling regulation and physiological role has increased. This shortly led to the identification of many of its components, to the description of their 3D structure, and the characterization of the uniporter contribution to tissue physiology and pathology. In this review, we will summarize the most relevant achievements in the history of mitochondrial Ca^{2+} studies, presenting a chronological overview of the most relevant and landmarking discoveries. Finally, we will explore the impact of mitochondrial Ca^{2+} signaling in the context of muscle physiology, highlighting the recent advances in understanding the role of the MCU complex in the control of muscle trophism and metabolism.

Keywords: MCU; mitochondrial Ca^{2+} uniporter; Ca^{2+} signaling; mitochondrial metabolism; skeletal muscle mitochondria

Citation: Pallafacchina, G.; Zanin, S.; Rizzuto, R. From the Identification to the Dissection of the Physiological Role of the Mitochondrial Calcium Uniporter: An Ongoing Story. *Biomolecules* **2021**, *11*, 786. <https://doi.org/10.3390/biom11060786>

Academic Editor:
Ferdinando Palmieri

Received: 18 April 2021
Accepted: 20 May 2021
Published: 23 May 2021

Publisher's Note: MDPI stays neutral with regard to jurisdictional claims in published maps and institutional affiliations.



Copyright: © 2021 by the authors. Licensee MDPI, Basel, Switzerland. This article is an open access article distributed under the terms and conditions of the Creative Commons Attribution (CC BY) license (<https://creativecommons.org/licenses/by/4.0/>).

1. Introduction

Every cell type, in every tissue and at any evolutionary level, can communicate with the surrounding environment and with neighboring cells. Both intercellular and extracellular communication play fundamental roles in shaping cell behavior and driving cell fate decisions. Cell-to-cell and environmental signals are normally conveyed by distinct extracellular mediators (hydrophilic or hydrophobic compounds, mechanical, ionic, cell-cell interactions, etc.) that are normally perceived by cells through surface receptors. These receptors convey them into a limited number of intracellular molecules, which are referred to as 'second messengers', which, in turn, forward the message to intracellular effectors finally activating the ultimate cellular responses. Despite the plethora of different signals and stimuli that cells may receive, only a few molecules to date have been described as second messengers of intracellular communication. Among them, the most common and, definitively, the most extensively studied is Ca^{2+} .

Ca^{2+} ions participate in the decoding of a vast range of stimuli and the variety of cellular components involved in the Ca^{2+} signal transduction is extremely wide, including basically all kinds of components, organelles, and molecules [1–3]. The research studies

on Ca^{2+} second messenger started more than one hundred years ago, with the initial recognition of the role of Ca^{2+} in muscle cell contraction [4]. Since then, the understanding of Ca^{2+} signaling regulation and dynamics has progressively increased leading to the definition of the concept of Ca^{2+} compartmentalization and to the demonstration of the existence of microdomains of local high Ca^{2+} concentration [5], which are crucial for the fine-tuning and correct triggering of the Ca^{2+} -dependent cellular effects [1].

Mitochondria play a fundamental and multifaceted role in the orchestration of cellular Ca^{2+} signals. Indeed, mitochondria are not a store of rapidly releasable Ca^{2+} (such as the ER), but rather they efficiently accumulate Ca^{2+} upon Ca^{2+} entry from the extracellular space or upon release from ER Ca^{2+} stores [6]. Upon cytosolic Ca^{2+} elevation, the entry of Ca^{2+} into mitochondria exerts a central function in the modulation of cell metabolism. Mitochondria host the enzymes and complexes of the TCA cycle, fatty acid oxidation (FAO), and oxidative phosphorylation (OXPHOS) thus representing the site of the major metabolic pathways and enzymes for cell energy supply, which deserved them the name of 'cellular powerhouses'. Interestingly, Ca^{2+} entry and oxidative activity are two strictly intertwined aspects of mitochondrial physiology. The increase of the mitochondrial matrix Ca^{2+} level stimulates both Ca^{2+} -sensitive dehydrogenases [7–9] and respiratory chain complexes [10,11] resident in the organelles, fueling the TCA cycle activity as well as aerobic respiration and thus boosting the overall oxidative metabolism. This makes mitochondria the central hubs for the rapid and effective adaptation of cell metabolism to the changes in energy requirements that are typically decoded as variations of intracellular Ca^{2+} concentration.

In addition, mitochondria also actively participate in the tuning of global Ca^{2+} signals thanks to their ability to take up Ca^{2+} during intracellular Ca^{2+} elevation with a net result of buffering the cytosolic cation concentration thus modulating the overall cellular Ca^{2+} response. This buffering capacity is due to two crucial characteristics of the mitochondria: (i) their strategic position in close contacts to the Ca^{2+} release channels of the ER store [6] and the plasma membrane in immune cells [12] (ii) the presence on their inner membrane of highly selective and efficient machinery for taking up Ca^{2+} , the MCU complex.

Finally, the large buffering capacity of mitochondria can protect cells from Ca^{2+} overload. Indeed, an excessive accumulation of the cation in the mitochondrial matrix triggers the permeability transition pore (PTP) opening, the release of pro-apoptotic factors, and finally, induction of programmed cell death [13]. Given the strong association between mitochondrial Ca^{2+} overload and apoptosis induction, the maintenance of mitochondrial Ca^{2+} homeostasis is thus a crucial aspect for ensuring cell survival [14,15].

Given the extreme relevance of mitochondria Ca^{2+} signaling for cell physiology, the unveiling of the molecular factors mediating mitochondrial Ca^{2+} entry and the mechanism(s) of their regulation has been one of the scientific challenges of recent years. In this review, we aim to summarize some of the milestone achievements in the history of mitochondrial Ca^{2+} research with a particular focus on the recent findings of the mitochondrial Ca^{2+} uniporter and its role in organ physiology. We will briefly describe the early studies leading to the demonstration of the Ca^{2+} accumulation capacity of mitochondria, then we will go through the historical chronicle of the discoveries of the mitochondrial Ca^{2+} uniporter genes and multiple regulators (Figure 1) and we will conclude with an excursus on the physiological relevance of mitochondrial Ca^{2+} uptake in the context of skeletal muscle tissue.

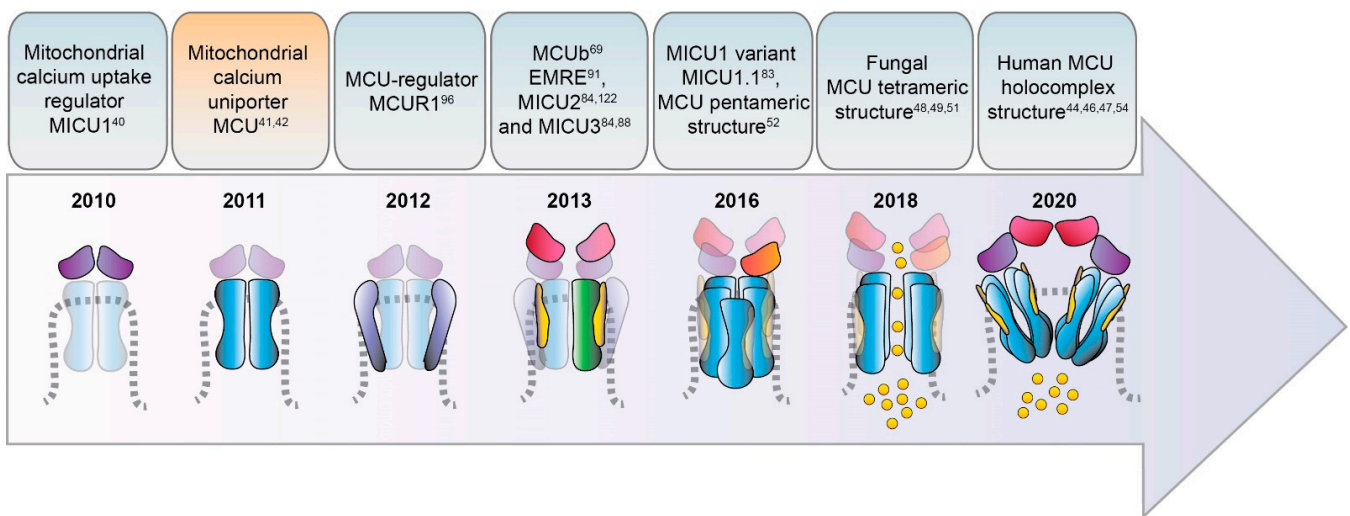


Figure 1. Timeline of the identification of MCU complex components. The most relevant findings on the structure and composition of the MCU complex discovery are summarized and chronologically presented along a timeline covering the last 10 years. Schematic cartoons show the different components of the MCU complex according to the date of their discovery along the timeline.

2. Timeline of MCU Identification

It is suggestive to recall that the notion of Ca^{2+} ions being relevant to organ physiology dates back to more than one century ago when the first report on the physiological action of Ca^{2+} ions appeared in 1883 [4]. At that time, Ringer described the effects of Ca^{2+} addition to isolated frog hearts and demonstrated that the supplementation of Ca^{2+} in the perfusion solution actively induces and sustains the contraction of the organ *ex vivo* [4]. This seminal observation revealed that Ca^{2+} is a fundamental messenger within cells, a concept that then extended to virtually every cell type and physiological and pathological process, giving rise to a broad field of study commonly referred to as the field of intracellular Ca^{2+} signaling. The intrinsic ability of contracting myocytes to operate *ex vivo* and to rapidly and effectively respond to environmental condition changes made them the ideal experimental system for the investigation of the role of Ca^{2+} in organ and cell physiology and was extensively exploited by researchers in the following years.

The original concept of the existence of intracellular compartments acting as Ca^{2+} stores to accumulate the cation required to sustain muscle contraction has been later postulated and demonstrated in 1947 by Heilbrunn [16]. However, although surprising, the identification of the sarco/endoplasmic reticulum (SR/ER) as the principal cellular Ca^{2+} store came only 20 years later. It was in the 1960's, with the identification of Ca^{2+} pumping machinery on intracellular membranes (in particular the calcium pump of the sarcoplasmic reticulum, better known as SERCA) by three independent scientists [17–20] and the advent of new methodologies for the measurement of intracellular Ca^{2+} concentration [21] that the ER and its specialized counterpart in muscle cells (the SR) were recognized the main cellular reservoir of Ca^{2+} .

Before that, the pioneering work of Slater & Cleland on cardiac myocyte preparations from rat hearts firstly described some subcellular compartments, called "sarcosomes" at that time, as the entities actively accumulating Ca^{2+} [22]. Interestingly, these "sarcosomes" did not consist of ER but, instead, they corresponded to isolated mitochondria, to which the addition of Ca^{2+} caused the block of their oxidative phosphorylation activity. Thus, Ca^{2+} ions behaved as mitochondria uncouplers. Despite that, Ca^{2+} appeared to exert a peculiar inhibitory action on mitochondrial OXPHOS activity, which differed from the other irreversible uncouplers known at that period (dinitrophenol, dicoumarol, rotenone, antimycin A, azide, or cyanide), due to the reversibility of its action [23]. This assigned to Ca^{2+} ions a functional role in mitochondria activity.

After that, a series of land-marking works in the early 60's experimentally revealed that energized mitochondria can actively take up Ca^{2+} [24–26]. Interestingly, these results anticipated the clear demonstration of a driving force for Ca^{2+} accumulation in mitochondria, i.e., the chemiosmotic theory, postulated and validated by Peter Mitchell [27]. This theory is based on the following concepts: (i) the activity of the respiratory chain complexes is linked to the extrusion of protons from the matrix to the intermembrane space (IMS) across the inner membrane of mitochondria (IMM). (ii) The accumulation of protons in the IMS generates a difference in the charges across the IMM of around $-150 \div -180$ mV (negative inside) establishing the so-called mitochondrial membrane potential ($\Delta\Psi_m$). (iii) This steep $\Delta\Psi_m$ represents the main driving force for the proton gradient-sustained synthesis of ATP and Ca^{2+} cation entry into the matrix.

Shortly after, at the University of Bristol, Denton and his group made important discoveries on the Ca^{2+} -dependent modulation of three critical oxidative enzymes resident in mitochondria [7–9]: pyruvate dehydrogenase phosphatase (the enzyme that dephosphorylates and relieves pyruvate dehydrogenase (PDH) activity allowing the conversion of NAD^+ , coenzyme A (CoA) and pyruvate into NADH, CO_2 , and acetyl-CoA, providing substrates to the citric acid (TCA) cycle and cellular respiration), NAD-isocitrate dehydrogenase and oxoglutarate dehydrogenase. The fact that these mitochondrial rate-limiting enzymes are under the control of Ca^{2+} definitively sets the cation at the center of the cell oxidative metabolism. Moreover, the evidence that mitochondria can take up Ca^{2+} in response to elevation of cytosolic Ca^{2+} levels, as shown in insulin-treated epididymal adipose tissue [28], established an active role of mitochondrial Ca^{2+} entry in shaping cell oxidative metabolism to match the increased cellular energy demands thus tailoring the metabolic outcomes according to the different environmental cues.

Despite all these conceptual advancements, two major issues were destined to puzzle the scientific community for decades. On one end, there is the apparent paradox between the physiological concentration of cytosolic Ca^{2+} , which was estimated in the submicromolar range [29–31], and the low affinity of the mitochondrial Ca^{2+} uptake, whose half-maximal rate (K_m) was measured in the order of several μM (reviewed in [32]). On the other end, the fundamental question about the molecular identity of the IMM apparatus responsible for the entry of Ca^{2+} into mitochondria was still without an answer.

It took around 30 and 50 years, respectively, to find solutions to those two enigmas. The answer to the former came with the advent of innovative and sophisticated technologies allowing the assessment of Ca^{2+} distribution at the sub-cellular and sub-organellar levels, including mitochondria. Indeed, thanks to the development of Ca^{2+} -sensitive genetic probes and recombinant fluorescent proteins targeted to specific intracellular microdomains [33,34], it was possible to measure variations of Ca^{2+} concentration in defined and limited areas of the cell (such as the cytosolic face of plasmalemma [35] or the surface of outer mitochondrial membrane [36], or the Golgi cisternae [37]) as well as the relative positioning of the intracellular organelles. These studies were pivotal in the field of cell biology for two main reasons: i) they allowed the observation of the intrinsic heterogeneity of cellular Ca^{2+} distribution, definitively demonstrating that large variations in Ca^{2+} concentration are highly regionalized within the cell cytoplasm and allowing the direct measure of Ca^{2+} levels in the mitochondria matrix as well as in the ER lumen; ii) they pinpointed the fact that organelles, including ER and mitochondria, are in close contact with each other through macromolecular structures involving proteins from both the compartments. In the case of ER-mitochondrial contacts, these structures are biochemically isolated as mitochondria-associated membranes (MAMs) and are formed by membrane channels, as the IP_3R and VDAC, respectively, and adaptor proteins of both organelles, such as Grp75, mitofusins, PACS [38]. Upon cell stimulation, the massive release of Ca^{2+} through the ER membrane clusters of IP_3Rs generates microdomains of high Ca^{2+} concentration right at the mouth of the channel pores, exactly where mitochondria are located. This allows mitochondria to perceive a local cation concentration sufficient to meet the low affinity of the mitochondrial Ca^{2+} uptake machinery [36,39]. Thus, their strategic position in proxim-

ity of ER Ca^{2+} release channels and their ability to take up Ca^{2+} with high conductance make mitochondria the ideal operator for cushioning the sudden Ca^{2+} rise in the cytosol of stimulated cells, thus behaving as an instrumental Ca^{2+} buffer [6]. The fact that Ca^{2+} entry into mitochondria stimulates the TCA cycle, respiration, and ATP production then places mitochondrial Ca^{2+} uptake as a key element for the prompt modulation of cell metabolism to rapidly and efficiently adapt to a variety of environmental cues and energy demands.

Another fundamental advancement in mitochondrial signaling occurred when scientists found the answer to the second big question, i.e., the molecular identity of the mitochondrial Ca^{2+} uniporter (MCU) machinery. The chronicle of MCU discoveries actually started in 2010, with the identification of the first gene required for the uptake of Ca^{2+} by mitochondria, *CBARA1*, coding for the mitochondrial Ca^{2+} uptake 1 protein (MICU1) [40], then followed by the identification of the mitochondrial channel and the elucidation of its interactors, as described below. The search of the other mitochondrial Ca^{2+} channel components has been proceeding expansively in the last decade (see next paragraph for a detailed timeline) and it is presently still actively ongoing. The discoveries of many different groups worldwide have been indeed instrumental to provide cell biologists with new knowledge on the functional role of mitochondrial Ca^{2+} and with new tools for the genetic and molecular intervention on global Ca^{2+} signaling and cell energetics.

3. Discovery and Characterization of the MCU Complex Components

3.1. MCU

The chronicle of MCU discovery starts with two pioneering studies published in 2011 [41,42] (Figure 1) that finally identified and cloned the long-sought MCU pore-forming unit gene, *CCDC109A*. MCU is a highly conserved 40 kDa protein ubiquitously expressed in plants, metazoans, protozoans, and fungi but not present in yeast [43]. This pore-forming unit oligomerizes to form the active channel within the inner mitochondrial membrane (IMM) and it directly interacts with the channel regulator MICU1, which was identified one year earlier [40]. These reports clearly demonstrated that the transient downregulation of MCU inhibits the mitochondrial accumulation of Ca^{2+} that follows the IP_3 -generating agonist in stimulated cells. Of note, the blunted mitochondrial Ca^{2+} uptake response occurs without changes in the mitochondria morphology or membrane potential of the MCU-silenced cells [41]. On the contrary, MCU overexpression enhances agonist-induced mitochondrial Ca^{2+} uptake in mammalian cells. In addition, *in vitro* experiments, in which recombinant MCU proteins were inserted in a planar lipid bilayer, showed that this pore-subunit alone is sufficient to form the channel. Indeed, in this setting, the MCU electrophysiological activity is completely abolished by the addition of the known inhibitor Ruthenium Red, firmly pointing at MCU as the genuine core component of the mitochondrial Ca^{2+} machinery.

Sequence and topology analyses revealed that both the *N*- and *C*-termini of MCU are located in the mitochondrial matrix and that MCU is endowed with two transmembrane domains, linked by a short highly conserved acidic loop exposed in the intermembrane space (IMS) which contains the so-called acidic “DIME” motif. The acidic residues present in this stretch (in particular E257, D261, E264) are critical for the Ca^{2+} transport since, if substituted with uncharged residues, MCU mutants failed to rescue the mitochondrial Ca^{2+} uptake in MCU-silenced cells [41,42]. However, the definitive description of MCU 3D structure had to wait till the very last years, when cryo-EM and X-ray diffraction analyses finally allowed the resolution of full-length MCU structure [44–51]. These studies coherently confirmed that purified MCU from different sources (fungi and metazoan) arranges in a tetramer, confuting previous assumptions on a putative pentameric MCU architecture [52]. Notably, the cryo-EM data also unveiled the exact position of the MCU channel selectivity filter, in which the DIME motif is fundamental for the coordination of Ca^{2+} ions and which was definitively shown to reside at the beginning of the second transmembrane α -helix [50] and not in the linker region between the two transmembrane helices, as previously suggested [52].

More recently, the structure of the human MCU together with its auxiliary component EMRE was obtained [53]. Each human MCU arranges in tetramers and each subunit complexes with one EMRE peptide. Differently from the three described for fungal MCU, human MCU appears organized in four domains, which are: (i) the *N*-terminal domain (NTD), (ii) the linker helix domain (LHD) —absent in fungi—, (iii) the coiled-coil domain (CCD), and iv) the transmembrane domain (TMD) (Figure 2).

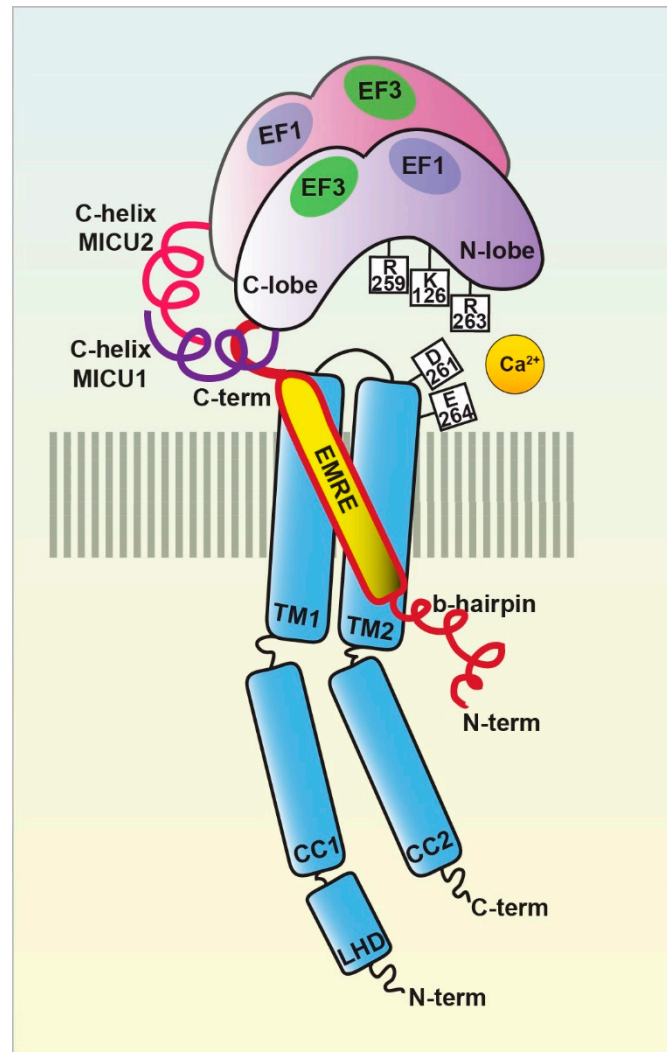


Figure 2. The MCU holocomplex structure. Schematic representation of the MCU holocomplex (uniplex) components and their relevant domains: the pore-forming subunit MCU (light blue) with the two transmembrane (TM) and coiled-coil (CC) domains and the linker helix domain (LHD); the essential mitochondrial Ca^{2+} uniporter regulator EMRE (yellow); the mitochondrial Ca^{2+} uptake proteins MICU1 (violet) and MICU2 (purple), with the EF-hands relevant for the MICU dimer interaction highlighted. The critical residues of the MCU DIME motif forming the Ca^{2+} selectivity filter are indicated, together with the MICU1 residues of the K-R ring coordinating the MCU acidic region.

Moreover, in the very last year, further insight into MCU channel modulation and function has been gained thanks to the achievement of the human MCU-MICUs holocomplex structure in both the Ca^{2+} -free and Ca^{2+} -bound state by several independent reports. The gating mechanism by which MICU1 regulates the uniporter activity via the conformational change triggered by Ca^{2+} was finally unveiled [44]. Furthermore, the precise description of the molecular interactions between MCU-EMRE-MICU1-MICU2 in the human MCU supercomplex (MEMMS) has been also obtained [54] (Figure 2). Indeed, MEMMS appears as a 480 kDa integral unit where EMRE coordinates the matrix gate of

the MCU channel and MICU proteins interact with the C-terminus of EMRE in the IMS thus enhancing Ca^{2+} influx through the MCU pore in high $[\text{Ca}^{2+}]_i$ conditions [54] (Figure 3). Finally, the distinct Ca^{2+} -dependent assembly conformations of the beetle and human MCU holocomplexes with human MICUs have also been detailed [46,47]. In the presence of Ca^{2+} , the multiprotein complex shows a two-fold symmetry and consists of two V-shaped MCU-EMRE tetrameric subcomplexes and two MICU1-MICU2 heterodimers that bridge the tops of the subcomplexes (Figure 1). In this setting, the assembly of the MICU1-MICU2 heterodimers to the MCU-EMRE subcomplexes is ensured by the interaction between MICU1 and EMRE [47] (Figure 2). Differently, in the absence of Ca^{2+} , the holocomplex adopts alternative less stable conformations with both monomeric and dimeric forms of the MCU-EMRE tetramers, where the MICU1-MICU2 heterodimer block the channel entrance formed by MCU transmembrane domains [47] (Figures 2 and 3).

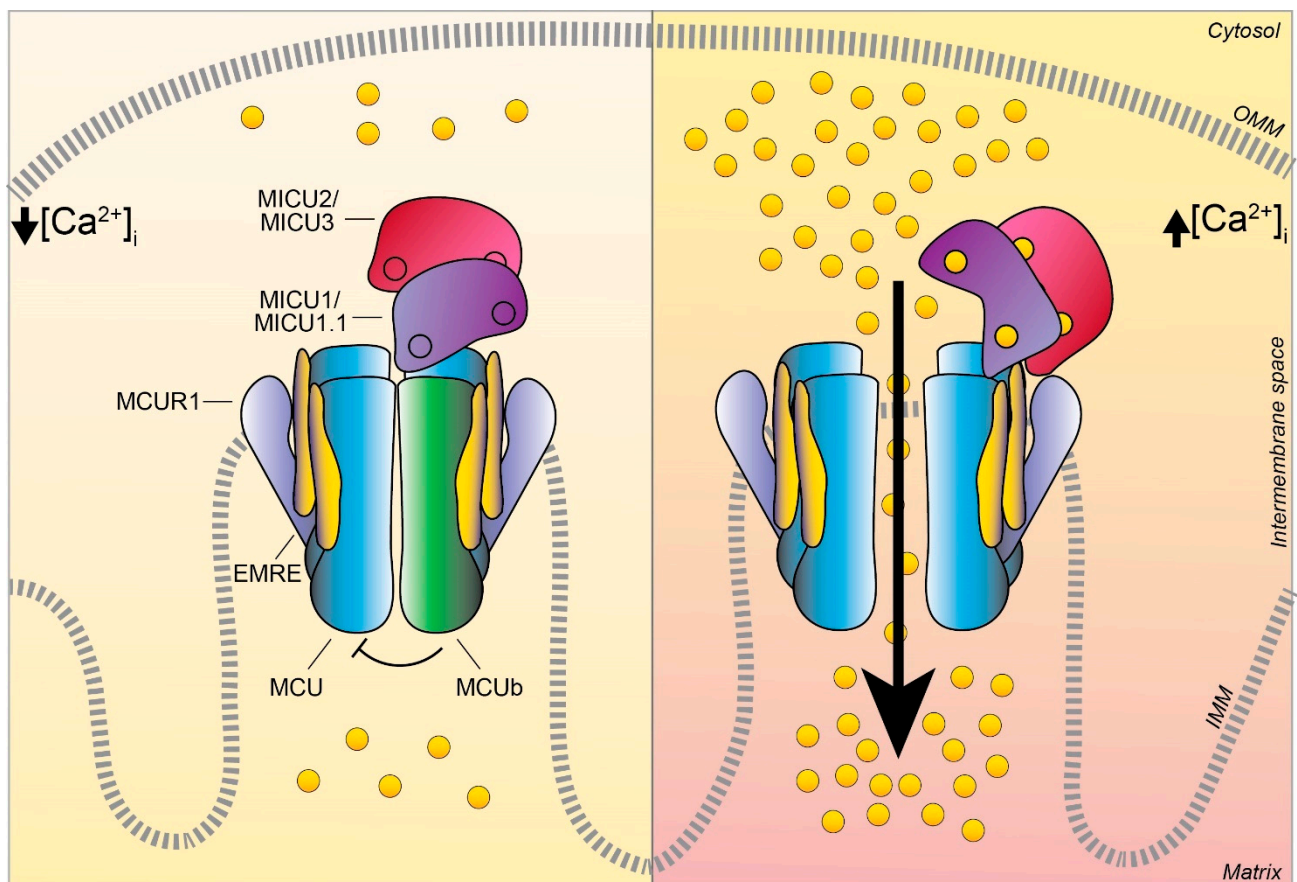


Figure 3. The MCU complex activity at low and high intracellular Ca^{2+} concentration. Schematic representation of the proteins involved in the MCU complex-mediated mitochondrial Ca^{2+} uptake: the pore-forming subunits MCU (light blue) and MCUb (green), the essential mitochondrial Ca^{2+} uniporter regulator EMRE (yellow), the mitochondrial Ca^{2+} uptake proteins MICU1 / MICU1.1 (violet), MICU2/ MICU3 (purple), and the MCU regulator 1 MCUR1 (light violet). The EF-hand Ca^{2+} binding domains of MICU proteins are indicated as little circles. At low intracellular Ca^{2+} concentration, the cation does not permeate through the MCU channel since the heterodimers formed by MICU1/MICU1.1–MICU2/MICU3 block the channel pore, thus preventing Ca^{2+} flux in resting conditions. Differently, at high intracellular Ca^{2+} concentration, MICU proteins undergo conformational changes relieving the inhibition on MCU and positively regulating channel activity, leading to an efficient mitochondrial Ca^{2+} uptake. OMM, outer mitochondrial membrane; IMM, inner mitochondrial membrane.

A large body of experimental evidence on the MCU complex functional role has accumulated since the discovery of the MCU. The genetic manipulation of the MCU led to the generation of germline and tissue-specific transgenic models [55–62], which provided

pivotal tools for understanding the pathophysiological implications of the mitochondrial Ca^{2+} signaling in vivo that would have otherwise remained unexplored.

In 2013, three independent groups showed that the MCU silencing/knockout or its overexpression affect survival in different in vivo models [55,63,64]. In *Trypanosoma brucei*, for instance, the downregulation or the conditional knockout of the uniporter augments the AMP/ATP ratio, thus affecting the parasite growth in vitro. On the contrary, when MCU is overexpressed, mitochondrial Ca^{2+} accumulation produces a high concentration of ROS and sensitizes trypanosomes to apoptotic stimuli [63]. In zebrafish (*Danio rerio*), instead, the knockdown of MCU has shown crucial alterations not only during the early step of gastrulation, where the blastomere convergence and extension are altered, but also at later stages of development as the maturation of the notochord and anteroposterior axis formation were strongly impaired in morphant fish [64]. A series of recently published works and our unpublished observation in the zebrafish knockout model obtained with CRISPR/Cas9 gene ablation gave further insight into the role of MCU during development. For example, the ablation of the MCU gene in *Danio rerio* inhibits mitochondrial Ca^{2+} influx, reduces oxidative phosphorylation, and induces lipid accumulation, a phenotype that was also observed in the hepatic tissue of liver-specific KO mouse [65]. Notably, the inactivation of MCU has shown to be protective in neurons of Parkinson Disease zebrafish genetic model (namely in *pink*^{-/-} fish), suggesting the crucial role of the MCU-dependent mitochondrial Ca^{2+} load on neuronal fitness [66].

As for mammals, the MCU^{-/-} mouse [55] develops normally and displays minor defects without signs of impaired cell survival. Under stress conditions, relatively mild metabolic alterations were observed, such as increased plasma lactate levels in line with impaired exercise performance. However, the same group soon after those findings, showed that embryos from MCU^{-/-} mice in a pure C57BL/6 background were not viable, displaying embryonic lethality at around E 11.5–E 13.5, thus suggesting a major involvement of mitochondrial Ca^{2+} uptake in organ metabolism and organism development that was compensated in a mixed genetic background [67].

Of note, some years later, it has been reported that the block of MCU-dependent Ca^{2+} uptake affects *Drosophila melanogaster* development. In particular, the inhibition of the uniporter activity has been shown to be detrimental for memory establishment during the pupation stage. Indeed, during the development of adult flies, alterations in the structural and functional neuronal substrates, crucial for memory formation, occur in the MCU deficient fly [58].

The genetic manipulation of MCU in *C. elegans* model also provided additional interesting notions on its role in organism physiology. Indeed, MCU^{-/-} *C. elegans* is viable and grossly normal, mirroring what was found in the first MCU^{-/-} mouse model described [55], even though it presents some defects in the epidermal wound repair mechanisms. More recently, the characterization of *C. elegans* deficient of a functional MCU [68] suggested that uniporter activity is essential for mitochondrial Ca^{2+} transfer during high-intensity stimulation of the worm pharynx muscle. However, a lot still remains to be explored on the role of MCU in this model and most of the knowledge on mitochondrial Ca^{2+} regulation of muscle physiology has been achieved using the mammalian mouse model where MCU expression was genetically targeted, which we will briefly review in the following paragraphs.

3.2. MCUB

In 2013, Raffaello and co-authors discovered that MCU is not the only pore-forming subunit of the mitochondrial Ca^{2+} uniporter, since an alternative MCU isoform exists, named MCUB, which crosses the IMM and associates to MCU to form the calcium channel [69] (Figures 1 and 3). The MCUB protein is encoded by the MCU *CCDC109a* paralog gene *CCDC109b*. Interestingly, this gene is found in vertebrates, but it is not present in other organisms in which MCU is expressed, such as plants, Nematoda, and Arthropoda. Despite the high structural similarity with MCU, MCUB sequence presents two critical aminoacidic

substitutions in the loop region and in the TM1 domain, which explains its inability to transport Ca^{2+} . Indeed, MCUB acts as a negative regulator of MCU activity, drastically reducing mitochondrial Ca^{2+} currents in vitro in planar lipid bilayer experiments and also when overexpressed in mammalian cells [69]. On the contrary, in other organisms, such as trypanosomatid species, the ortholog of MCUB is capable to conduct the cation and its overexpression facilitates mitochondrial Ca^{2+} uptake [70].

Interestingly, MCUB displays different expression levels in the different mammalian tissues, and the MCUB:MCU proportion appears also the distinctive feature ensuring the appropriate mitochondrial Ca^{2+} current to each cell type [69,71]. For instance, a high MCUB/MCU ratio (3:1) is typical of cells with low mitochondrial Ca^{2+} transients, such as adult cardiomyocytes (Figure 4). In fact, MCUB can be described as a protective gene in cardiac myocytes since i) its expression is transiently induced after ischemia-reperfusion injury and ii) transgenic mice overexpressing MCUB have a reduced mitochondrial Ca^{2+} uptake ability, thus preventing Ca^{2+} overload, which is sufficient to protect myocytes from ischemia-reperfusion injury and to decelerate their ongoing necrosis [72,73]. A low MCUB/MCU ratio (1:40) is instead a characteristic of tissues with an extremely high capacity of mitochondrial Ca^{2+} accumulation, such as skeletal muscle [69,74] (Figure 4).

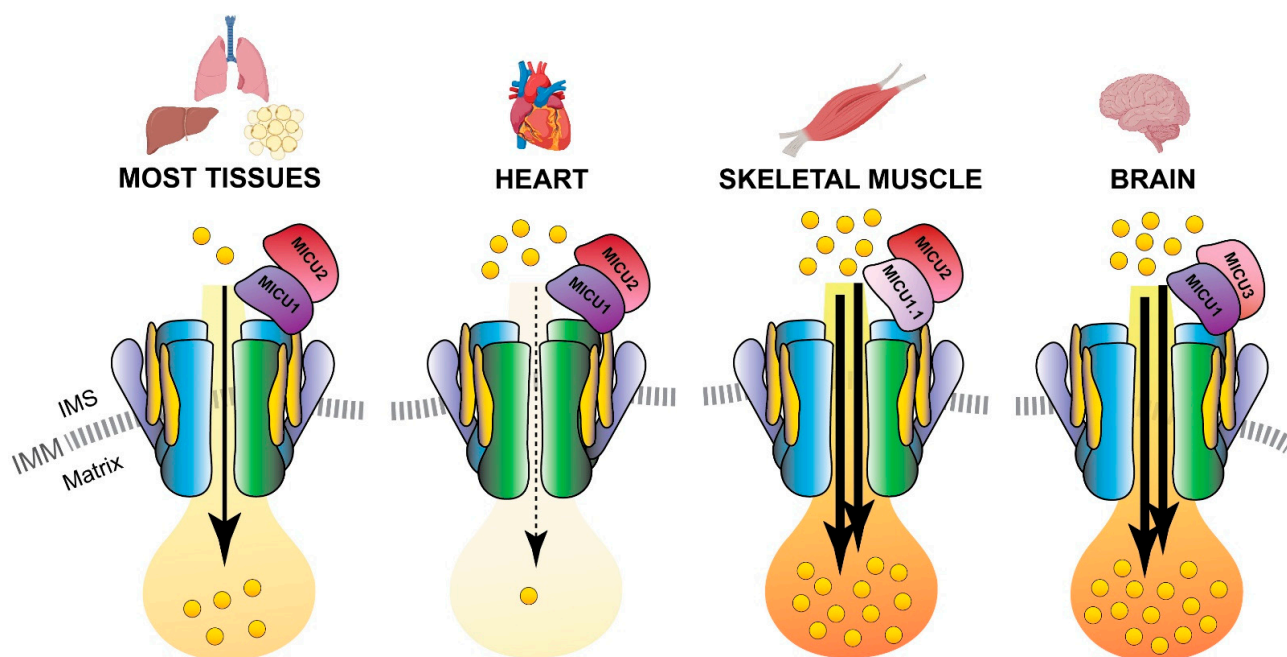


Figure 4. MCU holo-complex composition in different tissues. Schematic representation of the tissue-specific components of the MCU holo-complex. The presence of a relatively high MCUB:MCU ratio in the heart ensures a reduced Ca^{2+} load in cardiomyocyte mitochondria. On the contrary, the expression of the MICU1.1 variant and MICU3 determines an elevated Ca^{2+} flux in the mitochondria of skeletal muscle fibers and neurons, respectively. IMS, inter-membrane space; IMM, inner mitochondrial membrane.

These lines of evidence highlight the importance of MCU:MCUB proportion in the control of mitochondrial Ca^{2+} uniporter activity and further investigation will be of fundamental relevance for the understanding of its role in the pathophysiology of different tissues.

3.3. MICU1

MICU1 was actually the first component to be described as the regulator of the long-sought MCU channel and its identification even anticipated that of the pore-forming subunit MCU (Figure 1). Indeed, in 2010, an integrative strategy combining comparative physiology, evolutionary genomics, and organelle proteomics revealed the 54 kDa protein, encoded by the *CBARA* gene and residing in the IMS, to be the mitochondrial calcium

uptake 1 (MICU1), which does not take part to the pore-forming domain of the channel, but it strongly regulates its activity in a Ca^{2+} -dependent way [40,75]. Indeed, after the N-terminal mitochondrial targeting sequence, MICU1 shows two canonical EF-hand Ca^{2+} binding domains that confers the Ca^{2+} -sensitivity (Figures 2 and 3). In the last decade, several lines of evidence confirmed the initial hypothesis about the role of MICU1 as both MCU gatekeeper at low Ca^{2+} concentration and MCU positive regulator at high Ca^{2+} concentration, thus explaining the sigmoid cooperative effect of the MCU activation curve [75].

The downregulation of MICU1 was initially shown to abolish mitochondrial Ca^{2+} influx in intact and permeabilized HeLa cells [40]. Later studies also demonstrated that the absence of MICU1 also leads to an adaptive Ca^{2+} accumulation inside the mitochondria matrix, triggering excessive ROS production and the consequent higher sensitivity to apoptotic stress. In addition, the ability of MICU1 to sense cytosolic Ca^{2+} levels confers to MICU1 the capacity to set the threshold for the activation of mitochondrial Ca^{2+} uptake. Nevertheless, this occurs without altering the overall kinetics of the channel [75,76].

Two in vivo studies, performed in MICU1^{-/-} mouse models have strengthened this concept and gave additional insight into the physiological role of this MCU regulator. In more detail, the characterization of MICU1^{-/-} transgenic mice reveals that, despite partial postnatal mortality, the viable animals show marked ataxia and muscle weakness [77], a phenotype which is reminiscent of that of human patients bearing MICU1 genomic mutation [78]. Moreover, the MICU1^{-/-} mice display several biochemical defects, including an increase in resting mitochondrial Ca^{2+} levels, altered mitochondrial morphology, and a decreased ATP production [77]. Interestingly, the loss of MICU1 triggers a sustained pro-inflammatory response after partial hepatectomy and failure of liver regeneration in MICU1-deficient mice. In this scenario, the lack of MICU1 enhances mitochondrial permeability transition pore (PTP) opening in hepatocytes, thus leading to massive necrosis [79].

Interestingly, more recently, evidence of a new role of MICU1 in the regulation of crucial metabolic steps of cell metabolism has emerged. Indeed, MICU1 was shown to inhibit the mitochondrial transport of pyruvate and fatty acids and, interestingly, this MICU1 function appears independent of Ca^{2+} and MCU core-complex composition [80]. This study reveals a mechanism that controls the MCU-mediated Ca^{2+} flux machinery and that relies on TCA cycle substrate availability. According to this view, the MICU1 regulatory axis acts as a metabolic homeostatic circuit to protect cells from the risk of bioenergetic crisis and mitochondrial Ca^{2+} overload during periods of nutrient stress. Altogether these findings [77,79,80] highlight once more the crucial importance of the fine-tuning of mitochondrial Ca^{2+} uptake by Ca^{2+} and MICUs, especially in the context of promotion of cell survival under stress conditions.

In addition to that, new important functions of MICU1 in the control of mitochondrial cristae junctions have been revealed by the recent super-resolution structured illumination microscopy (SIM) and electron microscopy studies of Gottschalk and collaborators [81]. According to the authors, MICU1 appears to act as a Ca^{2+} -dependent regulator of cristae junctions' integrity and cytochrome c localization. Another intriguing feature of MICU1 regulatory function on the determination of uniporter cation selectivity has recently emerged [82]. MICU1 was revealed as the primary responsible for conferring and ensuring the stringent MCU selectivity for Ca^{2+} over Mn^{2+} since. Indeed, when present, MICU1 impedes Mn^{2+} ions to cross the MCU channel pore; on the contrary, in the absence of MICU1, both Ca^{2+} and Mn^{2+} cations can enter the mitochondrial matrix. This additional MICU1 checkpoint is of fundamental importance to guarantee cell survival of cells sensitive to Mn^{2+} such as neurons, thus setting MICU1 as a crucial safeguard against cellular toxicity due to manganese in neurodegenerative diseases [82].

3.4. MICU1.1

A variant of MICU1, named MICU1.1, has been discovered by our group as an alternative splicing product of the *MICU1* mRNA [83] (Figure 1). MICU1.1 is well-conserved

among species and expressed almost exclusively in skeletal muscle tissue, where it is by far the most abundant MICU moiety (Figure 4), although limited but still appreciable levels are found also in the brain [83]. Similar to MICU1, MICU1.1 behaves as a positive regulator of MCU. Indeed, MICU1.1 expression increases mitochondrial Ca^{2+} uptake upon stimulation in HeLa cells and skeletal muscle in vivo, and this increase is even higher than that observed after expression of the conventional MICU1 isoform [83]. This behavior is explained by the fact that the muscular MICU1.1-MICU2 heterodimer (see next paragraph for a detailed description of MICU2), binds Ca^{2+} more efficiently than the canonical MICU1-MICU2 pair, thus activating the uniporter at lower Ca^{2+} concentrations [83]. This peculiar feature is of critical importance for the physiology of skeletal muscle tissue, and the presence of MICU1.1 is functional to ensure the Ca^{2+} uptake required for the matching of ATP production to the energy expenditure of muscle contractile activity [83]. These findings shed light on a novel modality by which MCU machinery can be modulated in skeletal muscle mitochondria and widen the scenario of the possible endogenous regulators of mitochondrial Ca^{2+} uptake, opening the path for future investigations on other tissue-specific isoforms and mechanisms controlling mitochondrial Ca^{2+} uptake.

3.5. MICU2

The first information about the existence of other genuine MCU regulators, in addition to MICU1, was provided by human genome sequencing studies a few years later [84] (Figure 1). Initially known as EF-hand domain-containing family member A1 (EFHA1), the mitochondrial calcium uptake protein 2 or MICU2, was found to be a paralog of MICU1 [84]. MICU2 resides in the IMS, contains two EF-hand Ca^{2+} -binding domains, and interacts with both MICU1 and MCU [84] (Figure 2). The analysis of *MICU2* transcript expression shown that this regulator has a peculiar cell-type distribution: it is present at high levels in the intestine, prostate, and cardiac tissues [84]. Biochemical data evidenced that MICU2 stability is strictly dependent on the presence of MICU1: indeed, silencing of MICU1 leads to loss of also MICU2 protein, while MICU1 (or MCU) overexpression stabilizes both MICUs in mammalian cells [84]. Moreover, the recently reported human MICU1-MICU2 crystal structure [45,85] revealed interesting details on the architecture of the heterodimer and of MICU2 in both the Ca^{2+} -bound and Ca^{2+} -free condition. The MICU1-MICU2 interaction sites have been identified and correspond to Glu242 in MICU1 and Arg352 in MICU2 in the Ca^{2+} -free state, while Phe383 in MICU1 and Glu196 in MICU2 contribute to the interaction of the two proteins in the Ca^{2+} -bound state.

Although the functional role of MICU2 is still controversial, recent findings clarify some key aspects of uniporter modulation by this regulator. In mammalian cells, for example, it has been shown that MICU2 positively regulates MCU activation by controlling the cytosolic $[\text{Ca}^{2+}]$ threshold for the relief of MICU1-mediated inhibition of MCU. This function allows MICU2 to restrict the spatial Ca^{2+} crosstalk between inositol 1,4,5-trisphosphate receptor (InsP3R) and MCU channels [86].

Subsequently, the generation and characterization of the *MICU2*^{-/-} mouse model highlighted other important properties of this regulator [87]. *MICU2* genetic ablation produces a decrease in the threshold for mitochondrial Ca^{2+} uptake due to loss of the gate-keeping activity and overall loss of MCU-dependent Ca^{2+} influx due to the destabilization of the entire uniporter complex. These findings lead to the conclusion that the amount of MCU and MICUs proteins is crucial to maintain the stability of the whole complex. Moreover, some phenotypic features of the *MICU2*^{-/-} mice are in common with models of cardiac pathologies, suggesting that MICU2 may act as a possible cardioprotective factor.

3.6. MICU3

MICU3, previously known as EFHA2, is another MICU1 paralog, originally identified by the same genetic sequence analysis that described MICU2 [84] (Figure 1). This finding added another level of complexity to the regulation of the MCU machinery. *MICU3* is an evolutionarily conserved gene since it is present in plants and in vertebrates, with a

peculiar tissue-specific distribution: indeed, it is mainly expressed in the brain, much less expressed in skeletal muscle, and virtually absent in other tissues [88,89]. The *MICU3* gene encodes a 55 kDa protein that shares 34% and 47% protein sequence similarity with *MICU1* and *MICU2*, respectively [84]. Like the other *MICUs*, also *MICU3* has an *N*-terminal mitochondrial targeting sequence and binds Ca^{2+} thanks to the presence of EF-hand domains. The crystal structure of human *MICU3* has been recently characterized in both Ca^{2+} -free and Ca^{2+} -bound conditions [90]. This crystallographic analysis revealed a *MICU3* 3D structure very similar to that of *MICU2*, in line with the role of these factors as MCU channel gatekeepers at low intracellular Ca^{2+} levels. Upon cytosolic Ca^{2+} increase, *MICU* heterodimers, including those containing *MICU3*, undergo a conformational change that releases the latch formed upon the uniporter mouth, thus allowing Ca^{2+} flux through the MCU pore [90] (Figures 3 and 4).

Regarding its functional role, our group showed that *MICU3* acts as a positive regulator of mitochondrial Ca^{2+} uptake through *MICU1* [88]. Indeed, *MICU3* forms heterodimers exclusively with *MICU1*, but not with *MICU2*, and the *MICU1*-*MICU3* interaction leads to a significant increase of mitochondrial Ca^{2+} uptake, demonstrating the stimulatory action of *MICU3* on uniporter activity [88]. Moreover, *MICU3* downregulation blocks Ca^{2+} influx elicited by synaptic activity in primary cortical neurons, suggesting a specific role of this MCU regulator on neuronal function [88]. This line of evidence lets to hypothesize that the primary role of *MICU3* is to enhance MCU opening to ensure mitochondrial Ca^{2+} uptake in response to both small and fast cytosolic Ca^{2+} rises, typical of synaptic neuronal stimulation (Figure 4).

3.7. EMRE

The Essential MCU REgulator (EMRE) is an additional constituent of the uniporter, discovered by quantitative mass spectrometry analysis of affinity-purified MCU complex components [91] (Figure 1). EMRE is a metazoan-specific protein of 10 kDa, ubiquitously expressed in all mammalian tissue, with one transmembrane domain, a mitochondrial targeting sequence, and a highly conserved C-terminus [91]. Moreover, it is required for the binding of *MICU1* to MCU (Figure 2). Initial biochemical and cellular studies revealed that it is required for MCU function [91,92]. Indeed, in yeast cells, reconstituted with human MCU protein, the expression of MCU alone is not sufficient for uniporter activity, because the MCU channel is active only when also EMRE is co-expressed with the MCU pore-forming unit [92]. Interestingly, the knockdown of EMRE led to the loss of mitochondrial Ca^{2+} uptake to a similar extent to what was observed in *MCU*-silenced HEK-293T and HeLa cells [91]. The following studies tried to give a more detailed explanation of the EMRE function within the MCU complex [93]. EMRE was shown to control MCU activity by sensing Ca^{2+} elevation inside the matrix via its C-terminal domain and coordinating the other MCU regulators. Indeed, when EMRE acidic C-terminus was either deleted or substituted with neutral residues, mitochondrial Ca^{2+} permeation through the uniporter increased and the Ca^{2+} concentration inside the matrix consistently augmented [93]. After that, a dual-mode of action for the small MCU regulator has been proposed, in contrast with the previously described model [94]. According to this view, EMRE stimulates MCU channel activity via the interaction of transmembrane helices from both proteins, proposing a different EMRE orientation in which the *N*-terminus is present inside the matrix, while its C-terminal portion faces the IMS. In addition, EMRE was proposed to exert its MCU-regulation activity by binding *MICU1* via its conserved C-terminal poly-aspartate tail (Figure 2). In the same year, another interesting aspect of EMRE-dependent MCU regulation has been revealed: the m-AAA protease-mediated degradation of EMRE is an essential event to guarantee the correct MCU-*MICU* proteins' assembly [95]. Indeed, the deficiency of m-AAA leads to EMRE accumulation, which prevents the MCU-*MICUs* association by competing for MCU binding. This generates a constitutively active MCU-EMRE channel that finally induces mitochondrial Ca^{2+} overload and eventually death of neuronal cells.

Very recently, the cryo-EM structure of the human MCU complex added new insights into the interaction of EMRE within the complex and defined the structural elements by which EMRE exerts its action on the channel [53]. In particular, it confirmed that EMRE crosses the IMM with its *N*-terminus facing the mitochondrial matrix. Secondly, it proposed that EMRE interaction with MCU occurs along with three major contact points of EMRE *N*-terminus, thus allowing Ca^{2+} ions to exit the channel vestibule. Finally, EMRE seems also to be crucial for MCU dimerization since, in its absence, the MCU channel is found as a monomer [53].

These new findings added important notions on the mechanisms of action and regulation of the MCU complex and highlighted the need for a precise orchestration of the holocomplex assembly to ensure its fundamental role in regulating cellular Ca^{2+} signals, cell metabolism, and cell survival.

3.8. MCUR1

The mitochondrial calcium uniporter regulator 1 or MCUR1 has been firstly described as an IMM-resident protein of 35 kDa, encoded by the *CCDC90A* gene, resulted from an RNAi screening searching for mitochondrial membrane components involved in mitochondrial Ca^{2+} uptake regulation [96] (Figure 1).

Only recently, crystallographic analysis of human MCUR1 revealed the sites of its interaction with MCU. Human MCUR1 structure shows that this coiled-coil-containing protein contains different domains called head, neck, stalk, and a membrane anchor. The head segment is presented as the responsible portion of the direct binding to the *N*-terminus of MCU, while the length of the stalk portion seems to be of crucial importance for the interaction with the uniporter, even though it is not directly involved in MCU-MCUR1 connection [97]. Moreover, it has been shown that the MCUR1-dependent regulation of MCU depends on MCUR1 protein level and stability, similarly to what is reported for EMRE during MCU complex assembly [97].

Despite the precise function of MCUR1 remains to be clarified, several lines of evidence suggest that it regulates the mitochondrial Ca^{2+} entry through MCU [96,98]. This hypothesis has been strengthened by the fact that MCUR1 expression controls the Ca^{2+} threshold required for permeability transition via PTP, thus proposing a possible mechanism in which MCUR1 could bridge the MCU and PTP complexes [99]. In contrast to this view, Paupe and collaborators showed that MCUR1 is not a direct regulator of MCU, but rather a cytochrome c oxidase (COX) assembly factor [100]. This concept originated from the observation that mammalian and yeast cells (note that the latter lack MCU expression), in which the *CCDC90A* gene was silenced, showed an incorrect COX assembly leading to a decrease of the mitochondrial membrane potential and, consequently, to the collapse of the driving force for mitochondrial Ca^{2+} uptake [100].

The latest findings assigned back to MCUR1 a relevant role in the control of cell metabolism [101] and autophagy [96,99,102] through modulation of mitochondrial Ca^{2+} . Intriguingly, the putative *Saccharomyces cerevisiae* MCUR1 homologs, Put6 and Put7, act as regulators of mitochondrial proline metabolism. Indeed, their loss results in a massive defect in yeast proline utilization, which is rescued by the heterologous expression of human MCUR1 [101]. In mammalian cells, MCUR1 downregulation has been also linked to AMPK phosphorylation and LC3 processing [96], which directly links MCUR1 levels to the activation of the autophagy pro-survival pathway, in particular under stress conditions, as reported in vascular endothelial cells during oxygen and glucose deprivation [102].

Interestingly, recent evidence of a possible implication of MCUR1 in human pathology has been provided in the hepatocellular carcinoma cell (HCC) model. In this context, MCUR1-dependent mitochondrial Ca^{2+} uptake has been reported to stimulate *in vitro* invasion and *in vivo* metastasis by promoting EMT via the ROS/Nrf2/Notch pathway and Snail transcription, pointing to MCUR1 as a potential therapeutic target for hepatocellular carcinoma treatment [103].

4. Mitochondrial Ca²⁺ Uptake in Physiology: Skeletal Muscle as a Paradigm

The fact that skeletal muscle comprises around 40% of human body mass [104], is primarily responsible for everyday locomotor activity and plays a pivotal role in the maintenance of whole-body health, temperature, and energy homeostasis, makes it a key model system for biomedical and life science investigations. Skeletal muscle is indeed composed of excitable cells, namely the myofibers, which react to the nerve electrical stimulation by contracting, thus generating muscle force. Myofibers are giant, multinucleated syncytial cells with paradigmatic morphology, from which they derived their name, and that contain a highly organized cytoplasmic architecture. The muscle fiber cytoplasm is filled with a repetitive and regularly aligned array of contracting units, the "sarcomeres", consisting of fibrillar and structural proteins, of which the myosin and actin filaments are the best known [105]. Myofibers are terminally differentiated cells that definitively exited the cell cycle, so the muscle is a post-mitotic tissue. Despite that, skeletal muscles can regenerate after damage and restore, in a relatively short time, both the size and the properties they had before the injury [106], thanks to the proliferation and differentiation of a population of resident muscle progenitor cells called satellite cells [107,108].

Of most relevance, muscles can contract to generate force, and, importantly, relax afterward to return to their resting length and condition. Obviously, contraction activity is a highly demanding process that massively consumes the cellular energy stored in the form of ATP molecules. Myosin, the major sarcomeric filament and the effective motor core of the myofiber, is the most abundant protein in muscle, comprising 25% of the total tissue protein [109] and it possesses the catalytic activity to hydrolyze ATP. The energy of ATP hydrolysis serves to promote actin filament sliding, thus producing sarcomere shortening and fiber contraction [110,111]. However, a consistent amount of ATP is also necessary for the activity of muscle fiber ion pumps (Na⁺/K⁺ ATPase and Ca²⁺ ATPase in the sarcolemma, sarcoplasmic reticulum Ca²⁺ ATPase in the ER). In addition, muscle is an extremely plastic tissue; muscle fibers can adapt and promptly respond to different workload demands shaping both their metabolic output and gene expression profile to match with changes in energy requirements of different types of exercise as well as during different phases of a single bout of exercise. For this reason, muscle metabolism needs to be highly efficient but flexible and rapidly adaptable. The main sources of ATP in muscles are the catabolism of glucose (primarily aerobic during the peak of exercise activity, but also anaerobic at the initial step of the exercise sprint) and the oxidation of fatty acids (especially in the recovery phase after exercise). Other metabolic routes participate in the overall tissue energetics to a much-reduced extent [112].

Finally, we will briefly describe the key molecular events leading to muscle contraction and muscle metabolic adaptation, with particular emphasis on the role played by Ca²⁺ signaling on these two processes. The start of muscle contraction occurs at the membrane of myofibers, where the motor neuron-released neurotransmitter triggers sarcolemma depolarization and the consequent opening of voltage-gated ion channels (the DHPR). DHPR are structurally and functionally coupled to the Ca²⁺ release channels of the endo-sarcoplasmic reticulum (SR), the Ryanodine receptor (RyR), so that RyR also opens [113]. This induces a rapid and massive release of Ca²⁺ from the SR with the subsequent intracellular Ca²⁺ elevation and activation of troponins which, in turn, allow the actomyosin sliding and promote sarcomere contraction. This process is commonly defined as excitation-contraction coupling or ECC [114]. Despite the role of Ca²⁺ in skeletal muscle is, in the first place, associated with actomyosin contraction and ECC, the cation exerts at least two other crucial functions in muscle physiology. On the one hand, the elevation of intracellular Ca²⁺ regulates a plethora of Ca²⁺-sensitive effectors, such as nuclear transcription factors, calmodulins, and kinases which sequentially activate gene expression and downstream signaling cascades [115]. Secondly, intracellular Ca²⁺ increase leads to mitochondrial Ca²⁺ uptake and the consequent stimulation of muscle aerobic metabolism and oxidative respiration [116–118]. Indeed, the cytosolic Ca²⁺ rise induced in the myofiber by nerve activity leads to Ca²⁺ binding to calmodulin and consequent activation of the Ca²⁺-calmodulin-

dependent phosphatase Calcineurin. Calcineurin dephosphorylates its target, the Nuclear Factor of Activated T-cells or NFAT [119] that, once dephosphorylated, is allowed to translocate to the nucleus and modulate the transcription of target genes, such as those of myosin heavy chains [120,121]. This Ca^{2+} -dependent, Calcineurin-NFAT-mediated regulation of gene transcription was shown to be crucial for the expression of muscle-specific structural genes that characterize the different fiber-type populations [120,121].

On the other hand, the activity-dependent intracellular Ca^{2+} mobilization induces Ca^{2+} uptake by myofiber mitochondria and enhances mitochondrial metabolism through the TCA cycle and respiratory chain [116–118], as discussed before (Figure 5). Thus, the dynamics of intracellular Ca^{2+} and in particular of mitochondrial Ca^{2+} are necessarily associated with the regulation of skeletal muscle metabolism. This concept has been recently explored and we will report here some of the latest advances in the study of mitochondrial Ca^{2+} signaling and its influence on muscle metabolism and adaptation to both physiologic workload demands and pathologic conditions.

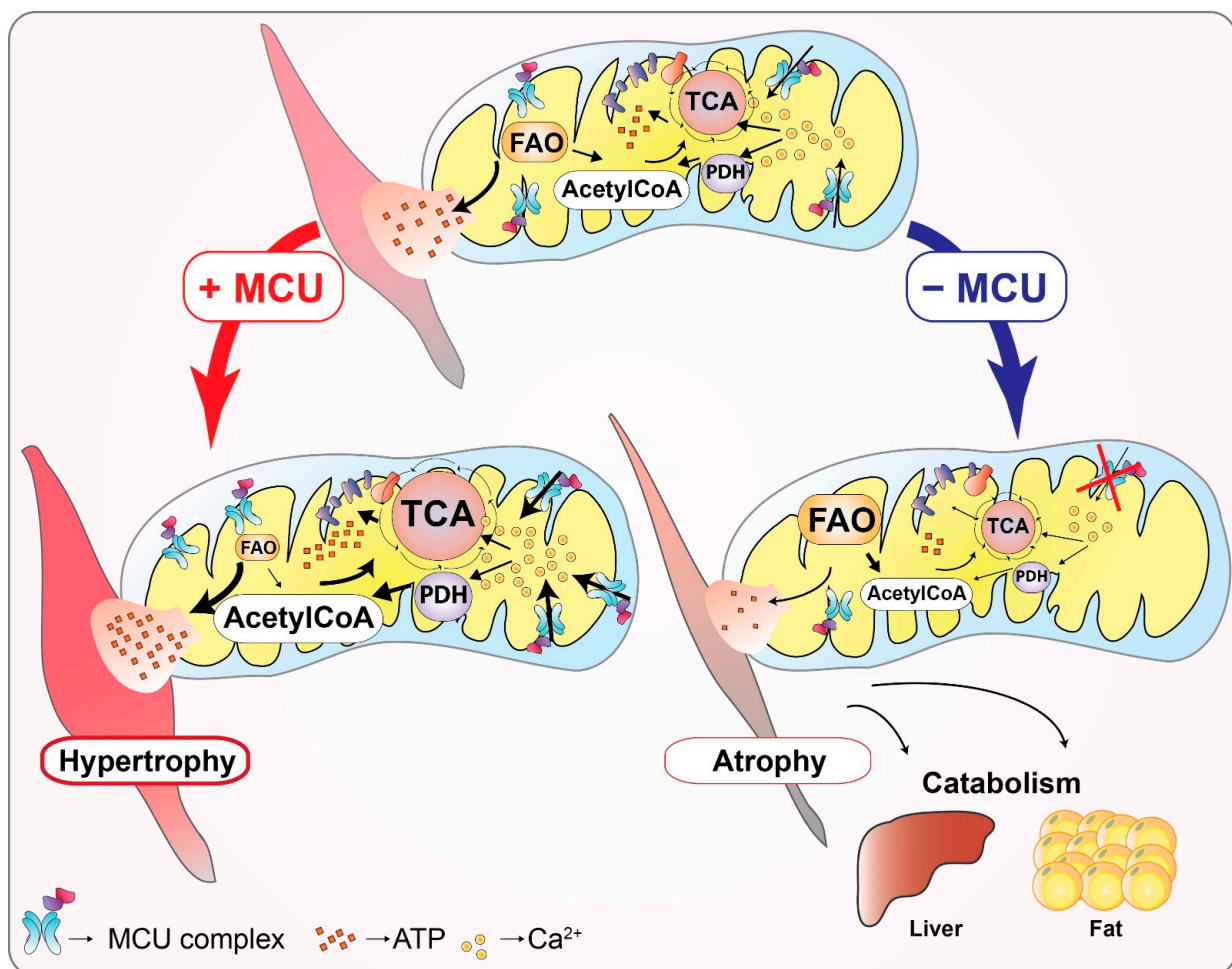


Figure 5. The role of MCU in the control of skeletal muscle trophism and metabolism. Schematic representation of the effects of manipulation of MCU activity on mitochondrial metabolism and trophism of the skeletal muscle tissue. In physiological conditions, Ca^{2+} entry into mitochondria stimulates glucose and fatty acids utilization to produce energy through the TCA cycle, via the activity of pyruvate dehydrogenase (PDH) and fatty acid oxidation (FAO), respectively. The enhanced mitochondrial Ca^{2+} uptake by MCU overexpression promotes muscle fiber oxidative metabolism leading to muscle hypertrophy via Akt pathway activation and upregulation of PGC1 α 4. On the contrary, the reduction of Ca^{2+} entry in the mitochondria by MCU deletion induces muscle metabolism rewiring towards an increased FAO, provokes muscle atrophy, impairs exercise performance, and causes global metabolic alterations, leading to an enhanced liver and adipose tissue catabolism.

The molecular identification of the mitochondrial Ca^{2+} channel components [40–42,84,88,91,96,122] (see the previous paragraph for details) definitively boosted this field of research, allowing the genetic manipulation of mitochondrial Ca^{2+} uptake in vivo, including in skeletal muscle. Despite the first report of *MCU* gene deletion in the total knock out mouse model showed an unexpectedly mild phenotype, the *MCU*^{-/-} mice display a reduction of both resting mitochondrial Ca^{2+} concentration and mitochondrial Ca^{2+} uptake after stimulation at the cellular level, and increased serum lactate at the systemic level [55]. These data suggested the presence of impaired regulation of mitochondrial oxidative metabolism although the initial measurement of O_2 consumption in *MCU*^{-/-} and wt MEF cells did not reveal significant differences [55]. Nevertheless, the presence of a defective mitochondrial energetic control was clearly demonstrated in the muscle tissue of *MCU*^{-/-} mice, by the presence of an elevated amount of the phosphorylated inactive form of PDH, which reduces TCA cycle activity, and by a reduced exercise performance and muscle force of the KO animals [55] (Figure 5).

In addition, the fact that the *MCU*^{-/-} mouse model presents a highly variable phenotypic severity that is dependent on the genetic background, i.e., relatively mild in the mixed background mice [55] but embryonic lethal in the pure C57BL/6 mice [67], brought back up the concern about the possibility that long-term genetic manipulation of *MCU* may induce unpredictable developmental compensatory mechanisms that might mask the physiologic effects of the targeted gene deletion.

A few years later, the modulation of mitochondrial Ca^{2+} uptake in a skeletal muscle-specific manner has been made possible by the selective manipulation of *MCU* expression in muscle fibers. The in vivo application of this approach was instrumental to decipher the complex role of mitochondrial Ca^{2+} signaling in controlling muscle tissue homeostasis as well as in rewiring the systemic metabolism of the whole organism [61,62] and proved that variations in mitochondrial Ca^{2+} dynamics directly control muscle trophism [117]. Indeed, the transient downregulation of mitochondrial Ca^{2+} uptake by AAV-mediated *MCU* silencing in mouse muscle induced remarkable fiber atrophy and impaired activation of the pyruvate dehydrogenase complex [117], in agreement with what was reported for the *MCU*^{-/-} mice [55]. On the contrary, AAV-induced *MCU* overexpression produced significant muscle hypertrophy, which was shown to be mediated by the IGF1-Akt pathway and by the transcriptional activation of one of the key regulators of exercise-induced muscle hypertrophy [123], the peroxisome proliferator-activated receptor- γ coactivator 1 alpha 4 gene (*PGC1 α 4*) [117] (Figure 5).

In line with the high relevance of the *MCU* complex activity in the maintenance of muscle function demonstrated in animal and in vitro experimental models, *MICU1* was identified as the disease-causing gene of a human disease phenotype characterized by proximal myopathy, learning difficulties, and a progressive extrapyramidal movement disorder [78]. From a clinical point of view, the pathology has an early onset, characterized by proximal muscle weakness, elevated serum creatine kinases, and intellectual impairment, progressing with extrapyramidal motor involvement and involuntary movements causing severe disability [78]. The whole exome-sequencing of affected patients revealed different loss-of-function mutations in the *MICU1* gene. Myopathic features such as the presence of centrally nucleated fibers, areas devoid of mitochondria (cores), and significant variability in myofiber size are found in the muscles of the analyzed patients. Despite that, the overall fiber-type distribution is maintained. However, the characterization of dermal fibroblast cells from *MICU1*-deficient patients together with that of muscle fibers from skeletal muscle-specific *MICU1* KO mouse model (*skmMicu1*^{-/-}) revealed a complex cellular mechanism underlying skeletal muscle dysfunction in the absence of this crucial regulator of mitochondrial Ca^{2+} entry [124]. The analysis of the mitochondrial Ca^{2+} dynamics of patient fibroblasts and *skmMicu1*^{-/-} mouse myofibers showed the loss of both *MCU* gatekeeper activity and cooperative *MCU* activation [124]. Indeed, *MICU1*-deficient cells showed an increased mitochondrial Ca^{2+} resting level and an enhanced rate of mitochondrial Ca^{2+} uptake [78]. Nevertheless, the values of mitochondrial Ca^{2+} peak in

stimulated MICU1 KO cells are not different from those of wt cells [78]. In addition, the cytosolic Ca^{2+} transients after cell stimulation are reduced in *MICU1*-deficient cells as a consequence of the enhanced mitochondrial buffering capacity [78]. The cellular and global metabolism seem not to be affected by *MICU1* deletion, as shown by an O_2 consumption rate of patient cells [78] and a blood lactate level of *skmMicu1*^{-/-} mice [124] similar to controls. Despite that, the *skmMicu1*^{-/-} mice showed enhanced lactate and creatine kinase levels, accompanied by reduced running time and overall decreased performance when assessed after treadmill running until exhaustion. The mechanism underlying muscle failure was unveiled by Evan's blue dye analysis of muscle fiber integrity, which revealed clear signs of sarcolemma damage in *skmMicu1*^{-/-} fibers, not found in wt fibers [124]. MICU1 appears then as a crucial mediator of the role of mitochondrial Ca^{2+} in myofiber plasma membrane recovery after exercise-induced damage in *in vivo* mouse skeletal muscle, but also in human fibroblasts of patients with MICU1 mutation after laser-induced injury [124]. These findings are in line with the notion that impaired mitochondrial Ca^{2+} signaling causes defects in the plasma membrane repair machinery in the C2C12 muscle cell model. Interestingly, the mitochondrial Ca^{2+} -mediated healing of membrane damage has been shown to rely mainly on the activity of the small GTPase RhoA and the dynamics of actin filaments, while it appears substantially independent from the mitochondrial ATP and energy production [125]. The contribution of mitochondrial Ca^{2+} signaling to the repair of fiber sarcolemma brings an additional level of complexity to the regulation of muscle fiber homeostasis by mitochondrial Ca^{2+} providing new opportunities for future investigations and, possibly, offering new targetable pathways for therapeutic interventions against neuromuscular disorders.

5. Conclusions and Future Perspectives

In this review, we provided a historical overview of the achievements in the study of mitochondrial Ca^{2+} signaling. We presented a synopsis of the discoveries that, in the last decade, led to the identification of most of the components that constitute the mitochondrial Ca^{2+} uptake machinery (see Figure 1), highlighting the regulatory factors that govern the fine-tuning of Ca^{2+} entry in the organelle (see Figures 2–4) and, finally, focusing on the relevance of mitochondrial Ca^{2+} in the context of skeletal muscle. We described the recent advances in the comprehension of Ca^{2+} signaling the control of muscle metabolism at the level of myofiber, tissue, and whole organism (see Figure 5).

Despite the increasing knowledge on mitochondrial Ca^{2+} signaling in cell and organ physiology, several questions on the function and regulation of mitochondrial Ca^{2+} are still unanswered.

One of the key unsolved issues still puzzling the scientific community concerns the variability of the germline MCU KO mouse model phenotype, which depends on the genetic background of the animals. Although a definitive explanation could not be provided so far, we might speculate on the compensatory mechanisms responsible for the relatively mild phenotype of the outbred MCU-deficient mice. One of those envisages the possibility that, in the absence of MCU, its alternative MCUB isoform may exert a limited Ca^{2+} channel activity. Indeed, although MCUB has been demonstrated to act as a dominant-negative subunit of the uniporter both in cellular and *in vitro* systems [69], it remains to experimentally validate whether the protein retains some Ca^{2+} permeability, which might result in a low Ca^{2+} flux rate, below the detection of the electrophysiological measures used to assess MCUB channel activity, but sufficient to allow some Ca^{2+} entry into the matrix in the absence of the canonical MCU.

A second, more general possible compensatory mechanism consists in the adaptation of embryonic cells to the lack of MCU activating alternative strategies and molecular routes to maintain the homeostatic matrix Ca^{2+} level, such as the modulation of IMM ion transporters and exchangers expression (as was shown for the $\text{Na}^+/\text{Ca}^{2+}$ exchanger NCLX [56]).

However, the observed lethality of inbred MCU KO mice leaves the question about MCU function during development still open. This is an issue that definitively deserves to be more deeply investigated.

Another aspect of the biology of mitochondrial Ca^{2+} that remains to be clarified despite being relevant for many developmental processes concerns its specific role in cell death. The fact that intracellular Ca^{2+} signaling plays a key role in all types of cell death (apoptosis, necrosis, necroptosis, and autophagy-mediated) [15] is a widely accepted concept. However, whether and to what extent mitochondria Ca^{2+} uptake dictates the cell decision either to survive or to perish is still debated. Studies characterizing the heart of MCU-constitutive KO mice [55] and cardiac-specific MCU-deleted animals [56,57] showed contrasting results about the role of MCU in cardiomyocyte cell death following in vivo cardiac ischemia-reperfusion injury. Indeed, the hearts of germline MCU KO mice resulted not protected from the ischemia-reperfusion damage despite they display resistance to elevated Ca^{2+} -mediated activation of the mitochondrial Permeability Transition Pore (mtPTP) [55]. On the contrary, the targeted ablation of MCU in adult cardiomyocytes showed the inhibition of Ca^{2+} -induced mtPTP opening together with a reduced cardiomyocyte death after ischemia-reperfusion [56,57].

The different results obtained from constitutive versus inducible tissue-specific MCU KO mouse models suggest the possibility that the MCU deletion may lead to long-term changes in the gene expression program. The characterization of these changes and the mechanisms by which they take place are yet to be defined.

Finally, although the quantitative proteomic data provided by the group of Mootha clearly indicate that all the components of the MCU holocomplex (uniporter) and associated regulators have been already identified [91], the possibility that additional still unknown modulators and tissue-specific factors may control the uniporter channel activity still exists. In addition to that, the eventuality of cell-type-specific alternative splicing isoforms of known uniporter proteins (as in the case of MICU1-MICU1.1 in skeletal muscle fibers [83]) should be considered in the plethora of the MCU regulatory mechanisms still to be characterized.

These considerations support the concept that the mitochondria of different cell types might have different Ca^{2+} levels and Ca^{2+} responses to match their metabolic requirement and physiological function. Indeed, timely and tissue-specific regulation of the mitochondrial Ca^{2+} uniporter activity is ensured by the different proportions of the MCU holocomplex components, as depicted in Figure 4, thus warranting the appropriate metabolic activation for each cell type.

Concluding, our understanding of mitochondrial Ca^{2+} role and regulation has grown massively in the last ten days; however, additional investigations are still needed to unravel the unresolved issues. Hopefully, scientists will take up this challenge and their work will provide further knowledge on the signaling and regulation of mitochondrial Ca^{2+} to better understand its role in cells and organs in physiology as well as to possibly develop new routes of intervention in pathological conditions.

Author Contributions: G.P. and R.R. designed the manuscript; G.P. and S.Z. drafted the text; S.Z. prepared the figures; G.P. and R.R. critically discussed the content and G.P., S.Z. and R.R. revised the manuscript; R.R. is the funding recipient. All authors have read and agreed to the published version of the manuscript.

Funding: This research was funded by TELETHON, grant number GGP16029; AIRC 5x1000, grant number 22759; Italian Ministry of Health “Ricerca Finalizzata”, grant number RF2016-02363566; CARIPARO (Fondazione Cassa di Risparmio di Padova e Rovigo), Excellence Scientific Research grant call 2017 and 2018, to R.R.

Institutional Review Board Statement: Not applicable.

Informed Consent Statement: Not applicable.

Data Availability Statement: Not applicable.

Acknowledgments: We thank Valentina Menegazzi for her administrative and technical support. Part of Figure 4 was created with BioRender, which we acknowledge.

Conflicts of Interest: The authors declare no conflict of interest.

References

- Raffaello, A.; Mammucari, C.; Gherardi, G.; Rizzuto, R. Calcium at the Center of Cell Signaling: Interplay between Endoplasmic Reticulum, Mitochondria, and Lysosomes. *Trends Biochem. Sci.* **2016**, *41*, 1035–1049. [CrossRef] [PubMed]
- Clapham, D.E. Calcium Signaling. *Cell* **2007**, *131*, 1047–1058. [CrossRef]
- Berridge, M.J.; Lipp, P.; Bootman, M.D. The versatility and universality of calcium signalling. *Nat. Rev. Mol. Cell Biol.* **2000**, *1*, 11–21. [CrossRef]
- Ringer, S. A third contribution regarding the Influence of the Inorganic Constituents of the Blood on the Ventricular Contraction. *J. Physiol.* **1883**, *4*, 222–225. [CrossRef]
- Rizzuto, R.; Pozzan, T. Microdomains of Intracellular Ca²⁺: Molecular Determinants and Functional Consequences. *Physiol. Rev.* **2006**, *86*, 369–408. [CrossRef] [PubMed]
- Rizzuto, R.; De Stefani, D.; Raffaello, A.; Mammucari, C. Mitochondria as sensors and regulators of calcium signalling. *Nat. Rev. Mol. Cell Biol.* **2012**, *13*, 566–578. [CrossRef]
- Denton, R.M.; Randle, P.J.; Martin, B.R. Stimulation by calcium ions of pyruvate dehydrogenase phosphate phosphatase. *Biochem. J.* **1972**, *128*, 161–163. [CrossRef] [PubMed]
- Denton, R.M.; A Richards, D.; Chin, J.G. Calcium ions and the regulation of NAD⁺-linked isocitrate dehydrogenase from the mitochondria of rat heart and other tissues. *Biochem. J.* **1978**, *176*, 899–906. [CrossRef]
- McCormack, J.G.; Denton, R.M. The effects of calcium ions and adenine nucleotides on the activity of pig heart 2-oxoglutarate dehydrogenase complex. *Biochem. J.* **1979**, *180*, 533–544. [CrossRef]
- Territo, P.R.; Mootha, V.K.; French, S.A.; Balaban, R.S. Ca²⁺ activation of heart mitochondrial oxidative phosphorylation: role of the F₀/F₁-ATPase. *Am. J. Physiol. Physiol.* **2000**, *278*, C423–C435. [CrossRef]
- Glancy, B.; Willis, W.T.; Chess, D.J.; Balaban, R.S. Effect of Calcium on the Oxidative Phosphorylation Cascade in Skeletal Muscle Mitochondria. *Biochem.* **2013**, *52*, 2793–2809. [CrossRef] [PubMed]
- Quintana, A.; Pasche, M.; Junker, C.; Alansary, D.; Rieger, H.; Kummerow, C.; Nuñez, L.; Villalobos, C.; Meraner, P.; Becherer, U.; et al. Calcium microdomains at the immunological synapse: how ORAI channels, mitochondria and calcium pumps generate local calcium signals for efficient T-cell activation. *EMBO J.* **2011**, *30*, 3895–3912. [CrossRef] [PubMed]
- Rasola, A.; Bernardi, P. The mitochondrial permeability transition pore and its involvement in cell death and in disease pathogenesis. *Apoptosis* **2007**, *12*, 815–833. [CrossRef] [PubMed]
- Penna, E.; Espino, J.; De Stefani, D.; Rizzuto, R. The MCU complex in cell death. *Cell Calcium* **2018**, *69*, 73–80. [CrossRef] [PubMed]
- Pinton, P.; Romagnoli, A.; Rizzuto, R.; Giorgi, C. Ca²⁺ signaling, mitochondria and cell death. *Curr. Mol. Med.* **2008**, *8*, 119–130. [CrossRef]
- Heilbrunn, L.V.; Wiercinski, F.J. The action of various cations on muscle protoplasm. *J. Cell. Comp. Physiol.* **1947**, *29*, 15–32. [CrossRef]
- Hasselbach, W.; Makinose, M. [The calcium pump of the “relaxing granules” of muscle and its dependence on ATP-splitting]. *Biochem Z* **1961**, *333*, 518–528.
- Hasselbach, W. Structural and enzymatic properties of the calcium transporting membranes of the sarcoplasmic reticulum. *Ann. N. Y. Acad. Sci.* **1966**, *137*, 1041–1048. [CrossRef]
- Ebashi, S.; Lipmann, F. Adenosine triphosphate-linked concentration of calcium ions in a particulate fraction of rabbit muscle. *J. Cell Biol.* **1962**, *14*, 389–400. [CrossRef]
- Weber, A.; Herz, R.; Reiss, I. On the Mechanism of the Relaxing Effect of Fragmented Sarcoplasmic Reticulum. *J. Gen. Physiol.* **1963**, *46*, 679–702. [CrossRef]
- Jöbsis, F.; O’Connor, M. Calcium release and reabsorption in the sartorius muscle of the toad. *Biochem. Biophys. Res. Commun.* **1966**, *25*, 246–252. [CrossRef]
- Slater, E.C.; Cleland, K.W. The effect of calcium on the respiratory and phosphorylative activities of heart-muscle sarcosomes. *Biochem. J.* **1953**, *55*, 566–580. [CrossRef]
- Chance, B. On possible mechanisms for the control of electron transport in the respiratory chain. In Proceedings of the 3rd International Congress of Biochemistry, Brussels, Belgium, 1956.
- Stathopoulos, P.B.; Zheng, L.; Li, G.-Y.; Plevin, M.J.; Ikura, M. Structural and Mechanistic Insights into STIM1-Mediated Initiation of Store-Operated Calcium Entry. *Cell* **2008**, *135*, 110–122. [CrossRef] [PubMed]
- DeLuca, H.F.; Engstrom, G.W. CALCIUM UPTAKE BY RAT KIDNEY MITOCHONDRIA. *Proc. Natl. Acad. Sci. USA* **1961**, *47*, 1744–1750. [CrossRef]
- Lehninger, A.L.; Rossi, C.S.; Greenawalt, J.W. Respiration-dependent accumulation of inorganic phosphate and Ca⁺⁺ by rat liver mitochondria. *Biochem. Biophys. Res. Commun.* **1963**, *10*, 444–448. [CrossRef]
- Mitchell, P.J. Coupling of Phosphorylation to Electron and Hydrogen Transfer by a Chemi-Osmotic type of Mechanism. *Nat. Cell Biol.* **1961**, *191*, 144–148. [CrossRef] [PubMed]

28. Denton, R.M.; Coore, H.G.; Martin, B.R.; Randle, P.J. Insulin activates Pyruvate Dehydrogenase in Rat Epididymal Adipose Tissue. *Nat. New Biol.* **1971**, *231*, 115–116. [CrossRef]
29. Ridgway, E.; Ashley, C. Calcium transients in single muscle fibers. *Biochem. Biophys. Res. Commun.* **1967**, *29*, 229–234. [CrossRef]
30. Rudolf, R.; Mongillo, M.; Rizzuto, R.; Pozzan, T. Looking forward to seeing calcium. *Nat. Rev. Mol. Cell Biol.* **2003**, *4*, 579–586. [CrossRef]
31. Takahashi, A.; Camacho, P.; Lechleiter, J.D.; Herman, B. Measurement of Intracellular Calcium. *Physiol. Rev.* **1999**, *79*, 1089–1125. [CrossRef]
32. Carafoli, E. The interplay of mitochondria with calcium: An historical appraisal. *Cell Calcium* **2012**, *52*, 1–8. [CrossRef] [PubMed]
33. Rizzuto, R.; Brini, M.; Pozzan, T. Targeting Recombinant Aequorin to Specific Intracellular Organelles. In *Methods in Cell Biology*; Elsevier B.V.: Amsterdam, The Netherlands, 1994; Volume 40, pp. 339–358.
34. De Giorgi, F.; Brini, M.; Bastianutto, C.; Marsault, R.; Montero, M.; Pizzo, P.; Rossi, R.; Rizzuto, R. Targeting aequorin and green fluorescent protein to intracellular organelles. *Gene* **1996**, *173*, 113–117. [CrossRef]
35. Marsault, R.; Murgia, M.; Pozzan, T.; Rizzuto, R. Domains of high Ca²⁺ beneath the plasma membrane of living A7r5 cells. *EMBO J.* **1997**, *16*, 1575–1581. [CrossRef]
36. Rizzuto, R.; Pinton, P.; Carrington, W.; Fay, F.S.; Fogarty, K.E.; Lifshitz, L.M.; Tuft, R.A.; Pozzan, T. Close Contacts with the Endoplasmic Reticulum as Determinants of Mitochondrial Ca²⁺ Responses. *Science* **1998**, *280*, 1763–1766. [CrossRef]
37. Pinton, P.; Pozzan, T.; Rizzuto, R. The Golgi apparatus is an inositol 1,4,5-trisphosphate-sensitive Ca²⁺ store, with functional properties distinct from those of the endoplasmic reticulum. *EMBO J.* **1998**, *17*, 5298–5308. [CrossRef] [PubMed]
38. Hayashi, T.; Rizzuto, R.; Hajnoczky, G.; Su, T.-P. MAM: more than just a housekeeper. *Trends Cell Biol.* **2009**, *19*, 81–88. [CrossRef] [PubMed]
39. Rizzuto, R.; Brini, M.; Murgia, M.; Pozzan, T. Microdomains with high Ca²⁺ close to IP₃-sensitive channels that are sensed by neighboring mitochondria. *Science* **1993**, *262*, 744–747. [CrossRef] [PubMed]
40. Perocchi, F.; Gohil, V.M.; Girgis, H.S.; Bao, X.R.; McCombs, J.E.; Palmer, A.E.; Mootha, V.K. MICU1 encodes a mitochondrial EF hand protein required for Ca²⁺ uptake. *Nat. Cell Biol.* **2010**, *467*, 291–296. [CrossRef] [PubMed]
41. De Stefani, D.; Raffaello, A.; Teardo, E.; Szabò, I.; Rizzuto, R. A forty-kilodalton protein of the inner membrane is the mitochondrial calcium uniporter. *Nature* **2011**, *476*, 336–340. [CrossRef]
42. Baughman, J.M.; Perocchi, F.; Girgis, H.S.; Plovanich, M.; Belcher-Timme, C.A.; Sancak, Y.; Bao, X.R.; Strittmatter, L.; Goldberger, O.; Bogorad, R.L.; et al. Integrative genomics identifies MCU as an essential component of the mitochondrial calcium uniporter. *Nat. Cell Biol.* **2011**, *476*, 341–345. [CrossRef]
43. Kovács-Bogdán, E.; Sancak, Y.; Kamer, K.J.; Plovanich, M.; Jambhekar, A.; Huber, R.J.; Myre, M.A.; Blower, M.D.; Mootha, V.K. Reconstitution of the mitochondrial calcium uniporter in yeast. *Proc. Natl. Acad. Sci. USA* **2014**, *111*, 8985–8990. [CrossRef]
44. Fan, M.; Zhang, J.; Tsai, C.-W.; Orlando, B.J.; Rodriguez, M.; Xu, Y.; Liao, M.; Tsai, M.-F.; Feng, L. Structure and mechanism of the mitochondrial Ca²⁺ uniporter holocomplex. *Nat. Cell Biol.* **2020**, *582*, 129–133. [CrossRef]
45. Wu, W.; Shen, Q.; Zhang, R.; Qiu, Z.; Wang, Y.; Zheng, J.; Jia, Z. The structure of the MICU1- MICU2 complex unveils the regulation of the mitochondrial calcium uniporter. *EMBO J.* **2020**, *39*. [CrossRef] [PubMed]
46. Wang, Y.; Han, Y.; She, J.; Nguyen, N.X.; Mootha, V.K.; Bai, X.-C.; Jiang, Y. Structural insights into the Ca²⁺-dependent gating of the human mitochondrial calcium uniporter. *eLife* **2020**, *9*, 1–19. [CrossRef] [PubMed]
47. Wang, C.; Jacewicz, A.; Delgado, B.D.; Baradaran, R.; Long, S.B. Structures reveal gatekeeping of the mitochondrial Ca²⁺ uniporter by MICU1-MICU2. *eLife* **2020**, *9*, 1–30. [CrossRef] [PubMed]
48. Nguyen, N.X.; Armache, J.-P.; Lee, C.; Yang, Y.; Zeng, W.; Mootha, V.K.; Cheng, Y.; Bai, X.-C.; Jiang, Y. Cryo-EM structure of a fungal mitochondrial calcium uniporter. *Nat. Cell Biol.* **2018**, *559*, 570–574. [CrossRef]
49. Yoo, J.; Wu, M.; Yin, Y.; Herzik, M.A., Jr.; Lander, G.C.; Lee, S.-Y. Cryo-EM structure of a mitochondrial calcium uniporter. *Science* **2018**, *361*, 506–511. [CrossRef]
50. Fan, C.; Fan, M.; Orlando, B.J.; Fastman, N.M.; Zhang, J.; Xu, Y.; Chambers, M.G.; Xu, X.; Perry, K.; Liao, M.; et al. X-ray and cryo-EM structures of the mitochondrial calcium uniporter. *Nat. Cell Biol.* **2018**, *559*, 575–579. [CrossRef]
51. Baradaran, R.; Wang, C.; Siliciano, A.F.; Long, S.B. Cryo-EM structures of fungal and metazoan mitochondrial calcium uniporters. *Nat. Cell Biol.* **2018**, *559*, 580–584. [CrossRef]
52. Oxenoid, K.; Dong, Y.; Cao, C.; Cui, T.; Sancak, Y.; Markhard, A.L.; Grabarek, Z.; Kong, L.; Liu, Z.; Ouyang, B.; et al. Architecture of the mitochondrial calcium uniporter. *Nat. Cell Biol.* **2016**, *533*, 269–273. [CrossRef]
53. Wang, Y.; Nguyen, N.X.; She, J.; Zeng, W.; Yang, Y.; Bai, X.-C.; Jiang, Y. Structural Mechanism of EMRE-Dependent Gating of the Human Mitochondrial Calcium Uniporter. *Cell* **2019**, *177*, 1252–1261. [CrossRef]
54. Zhuo, W.; Zhou, H.; Guo, R.; Yi, J.; Zhang, L.; Yu, L.; Sui, Y.; Zeng, W.; Wang, P.; Yang, M. Structure of intact human MCU supercomplex with the auxiliary MICU subunits. *Protein Cell* **2021**, *12*, 220–229. [CrossRef]
55. Pan, X.; Liu, J.; Nguyen, T.; Liu, C.; Sun, J.; Teng, Y.; Fergusson, M.M.; Rovira, I.I.; Allen, M.; Springer, D.A.; et al. The physiological role of mitochondrial calcium revealed by mice lacking the mitochondrial calcium uniporter. *Nat. Cell Biol.* **2013**, *15*, 1464–1472. [CrossRef] [PubMed]
56. Kwong, J.Q.; Lu, X.; Correll, R.N.; Schwanekamp, J.A.; Vagnozzi, R.J.; Sargent, M.A.; York, A.J.; Zhang, J.; Bers, D.M.; Molkenin, J.D. The Mitochondrial Calcium Uniporter Selectively Matches Metabolic Output to Acute Contractile Stress in the Heart. *Cell Rep.* **2015**, *12*, 15–22. [CrossRef] [PubMed]

57. Luongo, T.S.; Lambert, J.P.; Yuan, A.; Zhang, X.; Gross, P.; Song, J.; Shanmughapriya, S.; Gao, E.; Jain, M.; Houser, S.R.; et al. The Mitochondrial Calcium Uniporter Matches Energetic Supply with Cardiac Workload during Stress and Modulates Permeability Transition. *Cell Rep.* **2015**, *12*, 23–34. [CrossRef] [PubMed]
58. Drago, I.; Davis, R.L. Inhibiting the Mitochondrial Calcium Uniporter during Development Impairs Memory in Adult *Drosophila*. *Cell Rep.* **2016**, *16*, 2763–2776. [CrossRef]
59. Choi, S.; Quan, X.; Bang, S.; Yoo, H.; Kim, J.; Park, J.; Park, K.-S.; Chung, J. Mitochondrial calcium uniporter in *Drosophila* transfers calcium between the endoplasmic reticulum and mitochondria in oxidative stress-induced cell death. *J. Biol. Chem.* **2017**, *292*, 14473–14485. [CrossRef]
60. Hamilton, J.; Brustovetsky, T.; Rysted, J.E.; Lin, Z.; Usachev, Y.M.; Brustovetsky, N. Deletion of mitochondrial calcium uniporter incompletely inhibits calcium uptake and induction of the permeability transition pore in brain mitochondria. *J. Biol. Chem.* **2018**, *293*, 15652–15663. [CrossRef]
61. Gherardi, G.; Nogara, L.; Ciciliot, S.; Fadini, G.P.; Blaauw, B.; Braghetta, P.; Bonaldo, P.; De Stefani, D.; Rizzuto, R.; Mammucari, C. Loss of mitochondrial calcium uniporter rewires skeletal muscle metabolism and substrate preference. *Cell Death Differ.* **2019**, *26*, 362–381. [CrossRef]
62. Kwong, J.Q.; Huo, J.; Bround, M.J.; Boyer, J.G.; Schwaneckamp, J.A.; Ghazal, N.; Maxwell, J.T.; Jang, Y.C.; Khuchua, Z.; Shi, K.; et al. The mitochondrial calcium uniporter underlies metabolic fuel preference in skeletal muscle. *JCI Insight* **2018**, *3*. [CrossRef] [PubMed]
63. Huang, G.; Vercesi, A.E.; Docampo, R. Essential regulation of cell bioenergetics in *Trypanosoma brucei* by the mitochondrial calcium uniporter. *Nat. Commun.* **2013**, *4*, 1–14. [CrossRef] [PubMed]
64. Prudent, J.; Popgeorgiev, N.; Bonneau, B.; Thibaut, J.; Gadet, R.; Lopez, J.; Gonzalo, P.; Rimokh, R.; Manon, S.; Houart, C.; et al. Bcl-wav and the mitochondrial calcium uniporter drive gastrula morphogenesis in zebrafish. *Nat. Commun.* **2013**, *4*, 2330. [CrossRef]
65. Tomar, D.; Jaña, F.; Dong, Z.; Quinn, W.J.; Jadiya, P.; Breves, S.L.; Daw, C.C.; Srikantan, S.; Shanmughapriya, S.; Nemani, N.; et al. Blockade of MCU-Mediated Ca²⁺ Uptake Perturbs Lipid Metabolism via PP4-Dependent AMPK Dephosphorylation. *Cell Rep.* **2019**, *26*, 3709–3725. [CrossRef] [PubMed]
66. Soman, S.; Keatinge, M.; Moein, M.; Da Costa, M.; Mortiboys, H.; Skupin, A.; Sugunan, S.; Bazala, M.; Kuznicki, J.; Bandmann, O. Inhibition of the mitochondrial calcium uniporter rescues dopaminergic neurons in pink1^{-/-} zebrafish. *Eur. J. Neurosci.* **2017**, *45*, 528–535. [CrossRef]
67. Murphy, E.; Pan, X.; Nguyen, T.; Liu, J.; Holmström, K.M.; Finkel, T. Unresolved questions from the analysis of mice lacking MCU expression. *Biochem. Biophys. Res. Commun.* **2014**, *449*, 384–385. [CrossRef]
68. Álvarez-Illera, P.; García-Casas, P.; Fonteriz, R.I.; Montero, M.; Alvarez, J. Mitochondrial Ca²⁺ Dynamics in MCU Knockout *C. elegans* Worms. *Int. J. Mol. Sci.* **2020**, *21*, 8622. [CrossRef] [PubMed]
69. Raffaello, A.; De Stefani, D.; Sabbadin, D.; Teardo, E.; Merli, G.; Picard, A.; Checchetto, V.; Moro, S.; Szabò, I.; Rizzuto, R. The mitochondrial calcium uniporter is a multimer that can include a dominant-negative pore-forming subunit. *EMBO J.* **2013**, *32*, 2362–2376. [CrossRef]
70. Chiurillo, M.A.; Lander, N.; Bertolini, M.S.; Storey, M.; Vercesi, A.E.; Docampo, R. Different Roles of Mitochondrial Calcium Uniporter Complex Subunits in Growth and Infectivity of *Trypanosoma cruzi*. *mBio* **2017**, *8*, e00574-17. [CrossRef]
71. Fieni, F.; Lee, S.B.; Jan, Y.N.; Kirichok, Y. Activity of the mitochondrial calcium uniporter varies greatly between tissues. *Nat. Commun.* **2012**, *3*, 1–12. [CrossRef]
72. Huo, J.; Lu, S.; Kwong, J.Q.; Bround, M.J.; Grimes, K.M.; Sargent, M.A.; Brown, M.E.; Davis, M.E.; Bers, D.M.; Molkenstin, J.D. MCUb Induction Protects the Heart From Postischemic Remodeling. *Circ. Res.* **2020**, *127*, 379–390. [CrossRef]
73. Lambert, J.P.; Luongo, T.S.; Tomar, D.; Jadiya, P.; Gao, E.; Zhang, X.; Lucchese, A.M.; Kolmetzky, D.W.; Shah, N.S.; Elrod, J.W. MCUB Regulates the Molecular Composition of the Mitochondrial Calcium Uniporter Channel to Limit Mitochondrial Calcium Overload During Stress. *Circulation* **2019**, *140*, 1720–1733. [CrossRef]
74. Mammucari, C.; Raffaello, A.; Reane, D.V.; Gherardi, G.; De Mario, A.; Rizzuto, R. Mitochondrial calcium uptake in organ physiology: from molecular mechanism to animal models. *Pflügers Arch. Eur. J. Physiol.* **2018**, *470*, 1165–1179. [CrossRef] [PubMed]
75. Csordás, G.; Golenár, T.; Seifert, E.L.; Kamer, K.J.; Sancak, Y.; Perocchi, F.; Moffat, C.; Weaver, D.; Perez, S.D.L.F.; Bogorad, R.; et al. MICU1 Controls Both the Threshold and Cooperative Activation of the Mitochondrial Ca²⁺ Uniporter. *Cell Metab.* **2013**, *17*, 976–987. [CrossRef] [PubMed]
76. Mallilankaraman, K.; Doonan, P.; Cárdenas, C.; Chandramoorthy, H.C.; Müller, M.; Miller, R.; Hoffman, N.E.; Gandhirajan, R.K.; Molgó, J.; Birnbaum, M.J.; et al. MICU1 Is an Essential Gatekeeper for MCU-Mediated Mitochondrial Ca²⁺ Uptake that Regulates Cell Survival. *Cell* **2012**, *151*, 630–644. [CrossRef]
77. Liu, J.C.; Liu, J.; Holmström, K.M.; Menazza, S.; Parks, R.J.; Fergusson, M.M.; Yu, Z.-X.; Springer, D.A.; Halsey, C.; Liu, C.; et al. MICU1 Serves as a Molecular Gatekeeper to Prevent In Vivo Mitochondrial Calcium Overload. *Cell Rep.* **2016**, *16*, 1561–1573. [CrossRef]
78. Logan, C.V.; Szabadkai, G.; A Sharpe, J.; A Parry, D.; Torelli, S.; Childs, A.-M.; Kriek, M.; Phadke, R.; A Johnson, C.; Roberts, N.Y.; et al. Loss-of-function mutations in MICU1 cause a brain and muscle disorder linked to primary alterations in mitochondrial calcium signaling. *Nat. Genet.* **2013**, *46*, 188–193. [CrossRef] [PubMed]

79. Antony, A.N.; Paillard, M.; Moffat, C.; Juskeviciute, E.; Correnti, J.; Bolon, B.; Rubin, E.; Csordás, G.; Seifert, E.L.; Hoek, J.B.; et al. MICU1 regulation of mitochondrial Ca²⁺ uptake dictates survival and tissue regeneration. *Nat. Commun.* **2016**, *7*, 10955. [CrossRef] [PubMed]
80. Nemani, N.; Dong, Z.; Daw, C.C.; Madaris, T.R.; Ramachandran, K.; Enslow, B.T.; Rubannelsonkumar, C.S.; Shanmughapriya, S.; Mallireddigari, V.; Maity, S.; et al. Mitochondrial pyruvate and fatty acid flux modulate MICU1-dependent control of MCU activity. *Sci. Signal.* **2020**, *13*, eaaz6206. [CrossRef] [PubMed]
81. Gottschalk, B.; Klec, C.; Leitinger, G.; Bernhart, E.; Rost, R.; Bischof, H.; Madreiter-Sokolowski, C.T.; Radulović, S.; Eroglu, E.; Sattler, W.; et al. MICU1 controls cristae junction and spatially anchors mitochondrial Ca²⁺ uniporter complex. *Nat. Commun.* **2019**, *10*, 1–17. [CrossRef]
82. Kamer, K.J.; Sancak, Y.; Fomina, Y.; Meisel, J.D.; Chaudhuri, D.; Grabarek, Z.; Mootha, V.K. MICU1 imparts the mitochondrial uniporter with the ability to discriminate between Ca²⁺ and Mn²⁺. *Proc. Natl. Acad. Sci. USA* **2018**, *115*, E7960–E7969. [CrossRef]
83. Reane, D.V.; Vallese, F.; Checchetto, V.; Acquasaliente, L.; Butera, G.; De Filippis, V.; Szabò, I.; Zanotti, G.; Rizzuto, R.; Raffaello, A. A MICU1 Splice Variant Confers High Sensitivity to the Mitochondrial Ca²⁺ Uptake Machinery of Skeletal Muscle. *Mol. Cell* **2016**, *64*, 760–773. [CrossRef] [PubMed]
84. Plovanich, M.; Bogorad, R.L.; Sancak, Y.; Kamer, K.J.; Strittmatter, L.; Li, A.A.; Girgis, H.S.; Kuchimanchi, S.; De Groot, J.; Speciner, L.; et al. MICU2, a Paralog of MICU1, Resides within the Mitochondrial Uniporter Complex to Regulate Calcium Handling. *PLoS ONE* **2013**, *8*, e55785. [CrossRef]
85. Wu, W.; Shen, Q.; Lei, Z.; Qiu, Z.; Li, D.; Pei, H.; Zheng, J.; Jia, Z. The crystal structure of MICU 2 provides insight into Ca²⁺ binding and MICU 1- MICU 2 heterodimer formation. *EMBO Rep.* **2019**, *20*, e47488. [CrossRef]
86. Payne, R.; Hoff, H.; Roskowski, A.; Foskett, J.K. MICU2 Restricts Spatial Crosstalk between InsP₃ R and MCU Channels by Regulating Threshold and Gain of MICU1-Mediated Inhibition and Activation of MCU. *Cell Rep.* **2017**, *21*, 3141–3154. [CrossRef] [PubMed]
87. Bick, A.G.; Wakimoto, H.; Kamer, K.J.; Sancak, Y.; Goldberger, O.; Axelsson, A.; DeLaughter, D.M.; Gorham, J.M.; Mootha, V.K.; Seidman, J.G.; et al. Cardiovascular homeostasis dependence on MICU2, a regulatory subunit of the mitochondrial calcium uniporter. *Proc. Natl. Acad. Sci. USA* **2017**, *114*, E9096–E9104. [CrossRef] [PubMed]
88. Patron, M.; Granatiero, V.; Espino, J.; Rizzuto, R.; De Stefani, D. MICU3 is a tissue-specific enhancer of mitochondrial calcium uptake. *Cell Death Differ.* **2018**, *26*, 179–195. [CrossRef]
89. Márkus, N.M.; Hasel, P.; Qiu, J.; Bell, K.F.S.; Heron, S.; Kind, P.C.; Dando, O.; Simpson, T.I.; Hardingham, G.E. Expression of mRNA Encoding Mcu and Other Mitochondrial Calcium Regulatory Genes Depends on Cell Type, Neuronal Subtype, and Ca²⁺ Signaling. *PLoS ONE* **2016**, *11*, e0148164. [CrossRef]
90. Xing, Y.; Wang, M.; Wang, J.; Nie, Z.; Wu, G.; Yang, X.; Shen, Y. Dimerization of MICU Proteins Controls Ca²⁺ Influx through the Mitochondrial Ca²⁺ Uniporter. *Cell Rep.* **2019**, *26*, 1203–1212. [CrossRef] [PubMed]
91. Sancak, Y.; Markhard, A.L.; Kitami, T.; Kovács-Bogdán, E.; Kamer, K.J.; Udeshi, N.D.; Carr, S.A.; Chaudhuri, D.; Clapham, D.E.; Li, A.; et al. EMRE Is an Essential Component of the Mitochondrial Calcium Uniporter Complex. *Science* **2013**, *342*, 1379–1382. [CrossRef]
92. Yamamoto, T.; Yamagoshi, R.; Harada, K.; Kawano, M.; Minami, N.; Ido, Y.; Kuwahara, K.; Fujita, A.; Ozono, M.; Watanabe, A.; et al. Analysis of the structure and function of EMRE in a yeast expression system. *Biochim. Biophys. Acta (BBA) Bioenerg.* **2016**, *1857*, 831–839. [CrossRef] [PubMed]
93. Vais, H.; Mallilankaraman, K.; Mak, D.-O.D.; Hoff, H.; Payne, R.; Tanis, J.E.; Foskett, J.K. EMRE Is a Matrix Ca²⁺ Sensor that Governs Gatekeeping of the Mitochondrial Ca²⁺ Uniporter. *Cell Rep.* **2016**, *14*, 403–410. [CrossRef] [PubMed]
94. Tsai, M.-F.; Phillips, C.B.; Ranaghan, M.; Tsai, C.-W.; Wu, Y.; Williams, C.; Miller, C. Dual functions of a small regulatory subunit in the mitochondrial calcium uniporter complex. *eLife* **2016**, *5*. [CrossRef] [PubMed]
95. König, T.; Tröder, S.E.; Bakka, K.; Korwitz, A.; Richter-Dennerlein, R.; Lampe, P.A.; Patron, M.; Mühlmeister, M.; Guerrero-Castillo, S.; Brandt, U.; et al. The m-AAA Protease Associated with Neurodegeneration Limits MCU Activity in Mitochondria. *Mol. Cell* **2016**, *64*, 148–162. [CrossRef]
96. Mallilankaraman, K.; Cárdenas, C.; Doonan, P.J.; Chandramoorthy, H.C.; Irrinki, K.M.; Golenár, T.; Csordás, G.; Madireddi, P.; Yang, J.; Müller, M.; et al. MCUR1 is an essential component of mitochondrial Ca²⁺ uptake that regulates cellular metabolism. *Nat. Cell Biol.* **2012**, *14*, 1336–1343. [CrossRef] [PubMed]
97. Adlakha, J.; Karamichali, I.; Sangwallek, J.; Deiss, S.; Bär, K.; Coles, M.; Hartmann, M.D.; Lupas, A.N.; Alvarez, B.H. Characterization of MCU-Binding Proteins MCUR1 and CCDC90B—Representatives of a Protein Family Conserved in Prokaryotes and Eukaryotic Organelles. *Structure* **2019**, *27*, 464–475. [CrossRef]
98. Vais, H.; Tanis, J.E.; Müller, M.; Payne, R.; Mallilankaraman, K.; Foskett, J.K. MCUR1, CCDC90A, Is a Regulator of the Mitochondrial Calcium Uniporter. *Cell Metab.* **2015**, *22*, 533–535. [CrossRef] [PubMed]
99. Chaudhuri, D.; Artiga, D.J.; Abiria, S.A.; Clapham, D.E. Mitochondrial calcium uniporter regulator 1 (MCUR1) regulates the calcium threshold for the mitochondrial permeability transition. *Proc. Natl. Acad. Sci. USA* **2016**, *113*, E1872–E1880. [CrossRef]
100. Paupe, V.; Prudent, J.; Dassa, E.P.; Rendon, O.Z.; Shoubridge, E.A. CCDC90A (MCUR1) Is a Cytochrome c Oxidase Assembly Factor and Not a Regulator of the Mitochondrial Calcium Uniporter. *Cell Metab.* **2015**, *21*, 109–116. [CrossRef]
101. Zulkifli, M.; Neff, J.K.; Timbalia, S.A.; Garza, N.M.; Chen, Y.; Watrous, J.D.; Murgia, M.; Trivedi, P.P.; Anderson, S.K.; Tomar, D.; et al. Yeast homologs of human MCUR1 regulate mitochondrial proline metabolism. *Nat. Commun.* **2020**, *11*, 1–15. [CrossRef]

102. Natarajan, V.; Mah, T.; Peishi, C.; Tan, S.Y.; Chawla, R.; Arumugam, T.V.; Ramasamy, A.; Mallilankaraman, K. Oxygen Glucose Deprivation Induced Prosurvival Autophagy Is Insufficient to Rescue Endothelial Function. *Front. Physiol.* **2020**, *11*. [CrossRef]
103. Jin, M.; Wang, J.; Ji, X.; Cao, H.; Zhu, J.; Chen, Y.; Yang, J.; Zhao, Z.; Ren, T.; Xing, J. MCUR1 facilitates epithelial-mesenchymal transition and metastasis via the mitochondrial calcium dependent ROS/Nrf2/Notch pathway in hepatocellular carcinoma. *J. Exp. Clin. Cancer Res.* **2019**, *38*, 1–13. [CrossRef]
104. Janssen, I.; Heymsfield, S.B.; Wang, Z.; Ross, R. Skeletal muscle mass and distribution in 468 men and women aged 18–88 yr. *J. Appl. Physiol.* **2000**, *89*, 81–88. [CrossRef] [PubMed]
105. Schiaffino, S.; Reggiani, C. Fiber Types in Mammalian Skeletal Muscles. *Physiol. Rev.* **2011**, *91*, 1447–1531. [CrossRef]
106. Ciciliot, S. Regeneration of Mammalian Skeletal Muscle: Basic Mechanisms and Clinical Implications. *Curr. Pharm. Des.* **2010**, *16*, 906–914. [CrossRef] [PubMed]
107. Mauro, A. Satellite cell of skeletal muscle fibers. *J. Cell Biol.* **1961**, *9*, 493–495. [CrossRef]
108. Montarras, D.; L'Honoré, A.; Buckingham, M. Lying low but ready for action: the quiescent muscle satellite cell. *FEBS J.* **2013**, *280*, 4036–4050. [CrossRef]
109. Wilborn, C.D.; Willoughby, D.S. The Role of Dietary Protein Intake and Resistance Training on Myosin Heavy Chain Expression. *J. Int. Soc. Sports Nutr.* **2004**, *1*, 27–34. [CrossRef]
110. Lynn, R.W.; Taylor, E.W. Mechanism of adenosine triphosphate hydrolysis by actomyosin. *Biochemistry* **1971**, *10*, 4617–4624. [CrossRef] [PubMed]
111. Huxley, H. Electron microscope studies of the organisation of the filaments in striated muscle. *Biochim. Biophys. Acta (BBA) Bioenerg.* **1953**, *12*, 387–394. [CrossRef]
112. Hargreaves, M.; Spriet, L.L. Skeletal muscle energy metabolism during exercise. *Nat. Metab.* **2020**, *2*, 817–828. [CrossRef] [PubMed]
113. Dirksen, R.T. Bi-directional coupling between dihydropyridine receptors and ryanodine receptors. *Front. Biosci.* **2002**, *7*, d659–670. [CrossRef]
114. Franzini-Armstrong, C.; O Jorgensen, A. Structure and Development of E-C Coupling Units in Skeletal Muscle. *Annu. Rev. Physiol.* **1994**, *56*, 509–534. [CrossRef] [PubMed]
115. Bravo-Sagua, R.; Parra, V.; Muñoz-Cordova, F.; Sanchez-Aguilera, P.; Garrido, V.; Contreras-Ferrat, A.; Chiong, M.; Lavandero, S. Sarcoplasmic reticulum and calcium signaling in muscle cells: Homeostasis and disease. *International Review of Cell and Molecular Biology* **2020**, *350*, 197–264. [CrossRef] [PubMed]
116. Das, A.M.; A Harris, D. Control of mitochondrial ATP synthase in heart cells: inactive to active transitions caused by beating or positive inotropic agents. *Cardiovasc. Res.* **1990**, *24*, 411–417. [CrossRef] [PubMed]
117. Mammucari, C.; Gherardi, G.; Zamparo, I.; Raffaello, A.; Boncompagni, S.; Chemello, F.; Cagnin, S.; Braga, A.; Zanin, S.; Pallafacchina, G.; et al. The Mitochondrial Calcium Uniporter Controls Skeletal Muscle Trophism In Vivo. *Cell Rep.* **2015**, *10*, 1269–1279. [CrossRef]
118. Díaz-Vegas, A.R.; Cordova, A.; Valladares, D.; Llanos, P.; Hidalgo, C.; Gherardi, G.; De Stefani, D.; Mammucari, C.; Rizzuto, R.; Contreras-Ferrat, A.; et al. Mitochondrial Calcium Increase Induced by RyR1 and IP3R Channel Activation After Membrane Depolarization Regulates Skeletal Muscle Metabolism. *Front. Physiol.* **2018**, *9*, 791. [CrossRef] [PubMed]
119. Rao, A.; Luo, C.; Hogan, P.G. Transcription factors of the nfat family: Regulation and Function. *Annu. Rev. Immunol.* **1997**, *15*, 707–747. [CrossRef]
120. McCullagh, K.J.A.; Calabria, E.; Pallafacchina, G.; Ciciliot, S.; Serrano, A.L.; Argentini, C.; Kalkhovde, J.M.; Lømo, T.; Schiaffino, S. NFAT is a nerve activity sensor in skeletal muscle and controls activity-dependent myosin switching. *Proc. Natl. Acad. Sci. USA* **2004**, *101*, 10590–10595. [CrossRef]
121. Calabria, E.; Ciciliot, S.; Moretti, I.; Garcia, M.; Picard, A.; Dyar, K.A.; Pallafacchina, G.; Tothova, J.; Schiaffino, S.; Murgia, M. NFAT isoforms control activity-dependent muscle fiber type specification. *Proc. Natl. Acad. Sci. USA* **2009**, *106*, 13335–13340. [CrossRef] [PubMed]
122. Patron, M.; Checchetto, V.; Raffaello, A.; Teardo, E.; Reane, D.V.; Mantoan, M.; Granatiero, V.; Szabò, I.; De Stefani, D.; Rizzuto, R. MICU1 and MICU2 Finely Tune the Mitochondrial Ca²⁺ Uniporter by Exerting Opposite Effects on MCU Activity. *Mol. Cell* **2014**, *53*, 726–737. [CrossRef]
123. Ruas, J.L.; White, J.P.; Rao, R.R.; Kleiner, S.; Brannan, K.T.; Harrison, B.C.; Greene, N.P.; Wu, J.; Estall, J.L.; Irving, B.A.; et al. A PGC-1 α Isoform Induced by Resistance Training Regulates Skeletal Muscle Hypertrophy. *Cell* **2012**, *151*, 1319–1331. [CrossRef] [PubMed]
124. Debattisti, V.; Horn, A.; Singh, R.; Seifert, E.L.; Hogarth, M.W.; Mazala, D.A.; Huang, K.T.; Horvath, R.; Jaiswal, J.K.; Hajnóczky, G. Dysregulation of Mitochondrial Ca²⁺ Uptake and Sarcolemma Repair Underlie Muscle Weakness and Wasting in Patients and Mice Lacking MICU1. *Cell Rep.* **2019**, *29*, 1274–1286. [CrossRef] [PubMed]
125. Horn, A.; Van Der Meulen, J.H.; Defour, A.; Hogarth, M.; Sreetama, S.C.; Reed, A.; Scheffer, L.; Chandel, N.S.; Jaiswal, J.K. Mitochondrial redox signaling enables repair of injured skeletal muscle cells. *Sci. Signal.* **2017**, *10*, eaaj1978. [CrossRef] [PubMed]

Review

The Mitochondrial Carnitine Acyl-carnitine Carrier (SLC25A20): Molecular Mechanisms of Transport, Role in Redox Sensing and Interaction with Drugs

Annamaria Tonazzi ^{1,†}, Nicola Giangregorio ^{1,†}, Lara Console ², Ferdinando Palmieri ^{1,3,*} and Cesare Indiveri ^{1,2,*}

- ¹ Institute of Biomembranes, Bioenergetics and Molecular Biotechnologies (IBIOM), National Research Council, Via Orabona 4, 70126 Bari, Italy; a.tonazzi@ibiom.cnr.it (A.T.); n.giangregorio@ibiom.cnr.it (N.G.)
- ² Unit of Biochemistry and Molecular Biotechnology, Department DiBEST (Biologia, Ecologia, Scienze della Terra), University of Calabria, Via P. Bucci 4C, 87036 Arcavacata di Rende, Italy; lara.console@unical.it
- ³ Department of Biosciences, Biotechnologies and Biopharmaceutics, University of Bari, 70125 Bari, Italy
- * Correspondence: ferdinando.palmieri@uniba.it (F.P.); cesare.indiveri@unical.it (C.I.); Tel.: +39-080-544-3323 (F.P.); +39-0984-492939 (C.I.)
- † These authors contributed equally to this work.

Abstract: The SLC25A20 transporter, also known as carnitine acyl-carnitine carrier (CAC), catalyzes the transport of short, medium and long carbon chain acyl-carnitines across the mitochondrial inner membrane in exchange for carnitine. The 30-year story of the protein responsible for this function started with its purification from rat liver mitochondria. Even though its 3D structure is not yet available, CAC is one of the most deeply characterized transport proteins of the inner mitochondrial membrane. Other than functional, kinetic and mechanistic data, post-translational modifications regulating the transport activity of CAC have been revealed. CAC interactions with drugs or xenobiotics relevant to human health and toxicology and the response of the carrier function to dietary compounds have been discovered. Exploiting combined approaches of site-directed mutagenesis with chemical targeting and bioinformatics, a large set of data on structure/function relationships have been obtained, giving novel information on the molecular mechanism of the transport catalyzed by this protein.

Keywords: carnitine; carnitine acyl-carnitine carrier; carnitine acyl-carnitine translocase; membrane transport; mitochondria; mitochondrial carrier; mitochondrial transporter; post-translational modification; solute carrier family 25; SLC25A20

Citation: Tonazzi, A.; Giangregorio, N.; Console, L.; Palmieri, F.; Indiveri, C. The Mitochondrial Carnitine Acyl-carnitine Carrier (SLC25A20): Molecular Mechanisms of Transport, Role in Redox Sensing and Interaction with Drugs. *Biomolecules* **2021**, *11*, 521. <https://doi.org/10.3390/biom11040521>

Academic Editor: Vladimír N. Uversky

Received: 8 March 2021

Accepted: 26 March 2021

Published: 31 March 2021

Publisher's Note: MDPI stays neutral with regard to jurisdictional claims in published maps and institutional affiliations.



Copyright: © 2021 by the authors. Licensee MDPI, Basel, Switzerland. This article is an open access article distributed under the terms and conditions of the Creative Commons Attribution (CC BY) license (<https://creativecommons.org/licenses/by/4.0/>).

1. Introduction

The mitochondrial carnitine acyl-carnitine carrier (CAC) is the member A20 of the SLC25 protein family, including 53 solute transporters in humans [1–3], the majority of which are localized in the inner mitochondrial membrane. Until now, only one family member has been found in the peroxisomal membrane [4]. Furthermore, approximately one-third of them are still orphans, i.e., their transported substrates are unknown. This family members share a peculiar structural fold of six transmembrane segments characterized by 3-fold repeated couples of hydrophobic α -helices. Each couple is connected by a hydrophilic loop and contains the SLC25 sequence motif PX[D/E]XX[K/R] at about the boundary of the odd α -helix and the loop. The structural information on the SLC25 proteins derives mainly from the ADP/ATP carrier, which has been crystallized in both the outwards and inward open conformations [5,6]. All the other carrier structures have been predicted by homology modeling, including CAC, whose structure has been corroborated by site-directed mutagenesis and chemical targeting approaches. CAC is a key component of the carnitine shuttle [7], which is crucial for the mitochondrial β -oxidation pathway.

In this shuttle (Figure 1), fatty acids are activated by the cytosolic acyl-CoA synthetase (ACSL) to fatty acyl-CoAs thioesters [8,9]. Since the mitochondrial inner membrane is not permeable to acyl-CoAs, acyl groups are transferred from CoA to carnitine by the action of “carnitine palmitoyltransferase-1a and b” (CPT-1a; CPT-1b), an integral outer membrane enzyme [10]. The acyl-carnitines cross the outer mitochondrial membrane through an almost unspecific pore constituted by the voltage-dependent anion channel (VDAC) [11] and, then, are specifically translocated across the inner mitochondrial membrane by the action of CAC. In the mitochondrial matrix, the enzyme carnitine palmitoyltransferase 2 (CPT-2) catalyzes the trans-esterification of the acyl groups from carnitine to mitochondrial CoA with the release of free carnitine, thereby providing acyl-CoA substrates for fatty acid β -oxidation. CAC and CPT-2 form a supramolecular complex in the inner mitochondrial membrane, devoted to acyl-carnitine channeling from the carrier to the enzyme (Figure 1) [12]. The carnitine released in this reaction is translocated backward to the cytosol by the same carrier via an acyl-carnitine/carnitine antiport reaction. The β -oxidation pathway is active in many tissues, especially those characterized by higher metabolic expenditure. It provides a large portion of the energy required by heart muscle, kidneys and also skeletal muscle, when glycogen has been consumed [13,14]. This pathway is also active in hepatocytes where fatty acid oxidation provides acetyl-CoA for ketone body synthesis during prolonged fasting conditions, in which glycogen stores have been depleted [15]. Neurons also perform fatty acid oxidation even though at a very low rate. Indeed, CAC also has been described in brain [16–18]. The crucial role of CAC in energy metabolism was demonstrated by the discovery of inherited defects of its gene *SLC25A20* causing secondary carnitine deficiency [19–24], a syndrome that arises in the very first stage of life as a life-threatening pathology. In this altered metabolic condition, acyl-carnitines fail to reach the mitochondrial matrix with consequent strong impairment of the β -oxidation. This syndrome is more severe than the primary carnitine deficiency caused by defects of the plasma membrane transporter OCTN2 (*SLC22A5*) [25–27]. Recent findings have correlated alterations of CAC expression or regulation with diabetes [28,29].

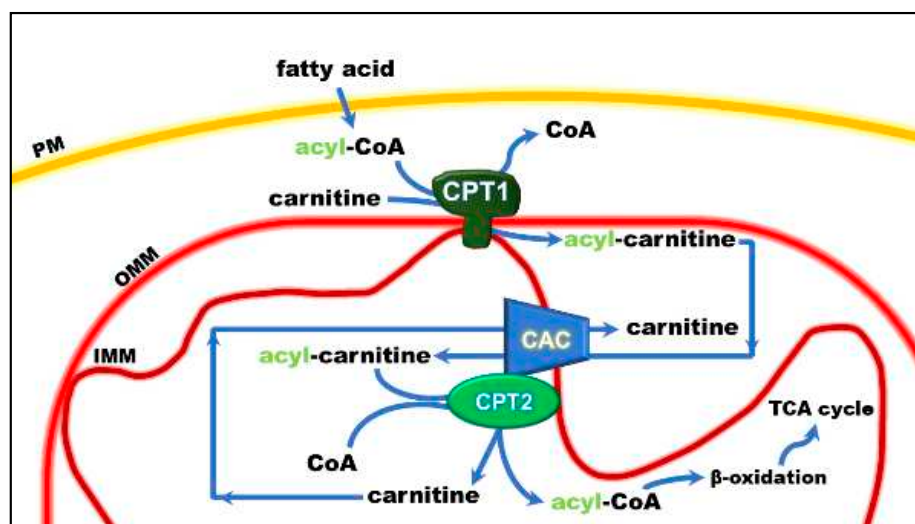


Figure 1. Role of the carnitine shuttle in the mitochondrial β -oxidation pathway. The shuttle is constituted by carnitine palmitoyltransferase 1 (CPT1) that converts acyl-CoAs into acyl-carnitines; carnitine/acyl-carnitine carrier (CAC) that allows the uptake of acyl-carnitines in the mitochondrial matrix in exchange with free carnitine, and carnitine palmitoyltransferase 2 (CPT2) that converts acyl-carnitines back to acyl-CoAs and releases free carnitine, which is ready to be translocated back to the cytosol by CAC. Once in the matrix, acyl-CoA undergoes β -oxidation with the production of acetyl-CoA that enters the tricarboxylic acid cycle (TCA). Other abbreviations: IMM, inner mitochondrial membrane; OMM, outer mitochondrial membrane; PM, plasma membrane.

Unlike most mitochondrial carriers, which are obligatory antiporters [30], CAC can catalyze, besides the antiport reaction, also a unidirectional transport of substrates even though at a rate about one order of magnitude lower than the antiport [31,32]. Interestingly CAC is not only operating in animals but also yeast and plants. The *Saccharomyces cerevisiae* and the *Aspergillus nidulans* CACs share 29% and 42% identity with the human CAC, respectively [33–36]. The main function of these transporters, in contrast to that of mammalian CACs, is to transport acetylcarnitine rather than medium- and long-chain acyl-carnitines into mitochondria [33,37]. The plant CAC ortholog, identified based on the 37% sequence identity with the human counterpart, most probably plays a different role, that is, the transport of glutamate [38,39]. It is still not clear if CAC also operates in peroxisomes, where very long, branched-chain, and medium-chain fatty acids are imported [40,41].

The history of CAC started with the detection of an acyl-carnitine uptake into mitochondria, which was saturable, stereospecific, inhibitable, and temperature-dependent [42–44]. Then, the availability of methodologies capable of handling hydrophobic membrane proteins allowed us to purify the protein responsible for the observed transport phenomena. In 1990, a classical approach based on chromatography fractionation of a rat liver mitochondrial extract and on transport assay of the fractions by proteoliposome technology was adopted [45]. The purified protein was used for the first functional characterization [31,32,46–48]. Later, CAC was identified at a molecular level [19,49] and obtained on a large-scale by overexpression in *Escherichia coli* [50] by a procedure introduced in our laboratory for the bacterial overexpression of the oxoglutarate carrier [51] and recently named the expression, purification, reconstitution assay (EPRA) method [52]. The recombinant purified CAC was employed in studies of structure/function relationships, interaction with drugs and xenobiotics, and post-translational modifications that modulate its transport function [53–64].

This article, starting from some basic information on CAC, provides an up-to-date comprehensive overview of the most recent discoveries about its molecular mechanism of transport and the modulation/regulation of its transport function.

2. The Functional Role of CAC

Studies performed with intact mitochondria concurred to propose that the function of CAC in cells is that of catalyzing an antiport of acyl-carnitines with free carnitine according to the core activity of the carnitine shuttle [7] (Figure 1). Physiologically, the acyl-carnitines are transported from the cytosol to the mitochondrial matrix and the free carnitine in the opposite direction to sustain the intramitochondrial reactions of the β -oxidation pathway [42,65]. Later on, the studies in proteoliposomes confirmed this function. In the *in vitro* system, CAC purified from rat liver or recombinant CAC was inserted into the liposomal membrane with the same orientation as in the native membrane, thus representing a mitochondrion mimic single-protein model [32,50] (Figure 2).

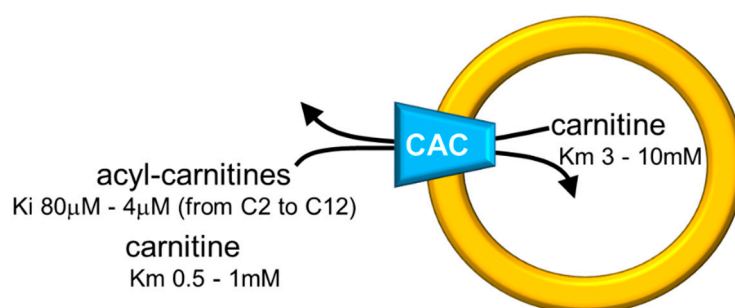


Figure 2. Sketch of the proteoliposome model with reconstituted CAC. Proteoliposomes contained 4% cardiolipin. Range of inhibition constants (K_i) for acyl-carnitines of various chain lengths on the external side and ranges of carnitine K_m on both sides of CAC are reported.

The *in vitro* system allowed measurements of substrate affinity (Figure 2), giving further support to the preferential direction of transport of acyl-carnitines towards the

internal space of proteoliposomes corresponding to the mitochondrial matrix and carnitine in the counter-direction. In vivo, this transport mode is driven by the higher acyl-carnitine concentration (see Figure 1) in the cytosol than in the matrix space, where acyl-carnitines are rapidly removed by the action of CPT2 that strictly interacts with the carrier [46,66]. Interestingly, the affinity profile of the carrier follows the specificity for acyl-carnitines of the CPT1 [67,68]. The possibility to manage the single-protein experimental system led to establishing that CAC catalyzes the transport of acetyl-carnitine too [54], suggesting that shorter carbon chain esters of carnitine cross the inner mitochondrial membrane via CAC as the longer chain derivatives, in contrast to what previously hypothesized [69]. This indicates the role of CAC in participating in the scavenger action of acetyl-CoA from mitochondria [50,70,71]. In this frame, the matrix enzyme carnitine acetyltransferase converts acetyl-CoA to acetyl-carnitine, which can be exported from mitochondria in antiport with extramitochondrial carnitine. In this pathway, CAC works in a reverse mode mediating the efflux of carnitine derivatives from mitochondria [72]. However, a definitive demonstration of the reverse mode of action in vivo is still missing. The affinity of CAC for acetyl-carnitine is much lower than that for long-chain acyl-carnitines, at least on the external face of the carrier (Figure 2). Using the in vitro experimental system, a bisubstrate kinetic study carried out by varying both the internal and the external substrate concentrations demonstrated that CAC catalyzes the antiport of substrates according to a “ping-pong mechanism” [1,32,73]. This mechanism of transport involves only binary carrier substrate complexes and implies that CAC possesses a single “reorienting” binding site and two conformations, one with the substrate-binding site accessible from the cytosol and the other with the substrate-binding site accessible from the matrix. Therefore, the ping-pong mechanism, so named for the analogy with that of certain enzymes, is basically the same mechanism as the early hypothesized “single binding center-gating pore mechanism” [74,75] and as the recently described “alternating access mechanism” [5], which is based on numerous molecular details. It is worth mentioning that, according to the ping-pong mechanism, the K_m for carnitine on the external or the internal side of CAC is influenced by the counter-substrate concentration, thus being variable within a certain range (Figure 2).

CAC also catalyzes a uniport reaction with a lower rate compared to the antiport. This almost unique feature among mitochondrial carriers was known since the 80s from studies in intact mitochondria [76] and later was confirmed by studies performed with proteoliposomes [31,32]. The rate of the unidirectional transport of carnitine is regulated by the counter-substrate; the uniport progressively decreases by increasing the concentration of the counter-substrate until the antiport mode is triggered. Physiologically, the net flux of carnitine allows for providing the matrix with carnitine newly synthesized in the cytosol or absorbed from the diet [31]. It must be stressed that (i) the last step of the carnitine biosynthesis occurs in the cytosol where the enzyme γ -butyrobetaine dioxygenase is located [77,78], (ii) the endogenous synthesis is not sufficient for the body’s needs, and (iii) more than 50% of carnitine is absorbed from the diet [79–82]. Therefore, the entire mitochondrial carnitine pool derives from extramitochondrial sources. As said before, CAC provides the matrix with carnitine through the uniport function. This role is crucial during mitochondrial biogenesis; however, no information is available on this issue. The uniport function should also be important for net export of carnitine to allow carnitine excretion and renewal. Very little information is available on the carnitine recycling. Indeed, even though it is known that an aliquot of carnitine is excreted through the urine, the flux of the molecule from the mitochondrial matrix to be excreted has never been dealt with.

Early studies showed the high sensitivity of CAC to sulfhydryl reagents [65,83]. Subsequent studies in proteoliposomes led to discrimination between two functional alterations caused by the reaction of SH reagents with two different cysteine populations: class-I cysteines are responsible for the induction of an “unphysiological” unspecific uniport; class-II cysteines are responsible for the inactivation of the carrier (both antiport and uniport function). On the one hand, the reaction of class-I cysteines with $HgCl_2$ or mercurial derivatives, at relatively high concentration, converts the carrier to a “pore-like” trans-

porter with reduced substrate specificity and uncoupling of the antiport function. This unphysiological activity reveals an intrinsic property of the mitochondrial carrier protein family members, i.e., a built-in channel normally hidden by appropriate gates [47,48] (and see Section 3). Indeed, this phenomenon also has been observed with other mitochondrial carrier proteins [84–86]. On the other hand, the reaction of class-II cysteines with HgCl_2 and other mercurials at a low (nanomolar) concentration or with NEM and MTS leads to the inactivation of the transporter. Later, class-II Cys residues and the molecular basis of their inhibition were identified. This aspect will be dealt with in the following sections. In contrast, class-I Cys residues responsible for pore-like activity have not yet been identified.

Overexpression of recombinant CAC in *E. coli* [50] boosted the characterization of this transporter. Indeed, the recombinant protein showed the same properties as the native one indicating that it is suitable for functional studies. This breakthrough opened the perspective of studying the human CAC as well [34,87]. Novel functional information was achieved in a rather short time. The absolute need for cardiolipin, suggested by studies with the protein purified from rat liver, was clearly demonstrated with the recombinant CAC that is cardiolipin free and is inactive if not supplemented with the phospholipid [50,88,89]. Therefore, CAC belongs to the mitochondrial molecular systems, which require cardiolipin for an activity like many other mitochondrial carriers [4,90–93] or are modulated by cardiolipin as the NADH dehydrogenase [94,95]. Other important achievements following the involvement of recombinant CAC and site-directed mutagenesis strategy will be dealt with in the next section.

3. Structure-Function Relationships

The molecular basis of CAC substrate-binding and transport, as well as its regulation by post-translational modifications, have been explored using the site-directed mutagenesis approach complemented with bioinformatics and chemical targeting, together with parallel investigations in intact mitochondria to explore the physiological roles of these modifications. Together with those regarding the oxoglutarate carrier [96–98], the structure/function relationship studies concerning CAC are the most advanced within the mitochondrial carrier family members. These studies started with the construction of the homology model of CAC in its cytosolic open conformation based on the ADP/ATP carrier (AAC, *SLC25A4*) structure [99]. Later, the structural fold and dynamics have been updated with the homology model of the matrix open conformation of CAC obtained by using the recently solved AAC structure in its matrix open conformation as a template [5]. The molecular map of the amino acids involved in the catalytic process of CAC has been defined together with the role of specific residues in the molecular mechanism of transport and the regulation of the carrier function.

3.1. Substrate Binding Site and Translocation Events

The residues responsible for substrate-binding were first hypothesized by bioinformatics in some yeast carriers, including the homolog of the human CAC [100,101]. Then, the identification of the amino acid residues of the mammalian CAC involved in substrate-binding and translocation has been conducted, exploiting site-directed mutagenesis, on the rat and human CACs that are virtually coincident, being 92% identical. The impairment or loss of function observed in conservative or non-conservative mutants, respectively, clearly demonstrated the role of each crucial residue in terms of the importance of the chemical features of the amino acid side-chains. As reported below, the amino acids involved in carnitine binding/translocation have been mapped. Asp-179, Arg-275, and Arg-178 (Figure 3a) undergo ionic and/or hydrogen bond interactions with carnitine, being involved in binding the trimethylammonium and the carboxyl groups, respectively. These charged residues that line the central water-filled cavity of the transport protein are conserved along with the CAC orthologs [87] according to their important role. The electric charges of the residues at positions 179 and 275 are more important than the side-chain length since the V_{max} and/or the K_m values show the greatest changes upon substituting

the charged residues with neutral ones. In line with the crucial role of Arg-275, the point mutation Arg275Gln in the CAC of three patients was associated with severe carnitine deficiency [102]. His-29 is also conserved throughout the CAC sub-family members. The mutation of His-29 with Ala, Asp, Lys, Phe, Asn, or Tyr severely impairs the function. Only if His-29 is substituted by Gln, the activity of the transporter is comparable to that of the wild-type CAC. Indeed, the N amide of Gln structurally corresponds to the τ -N (distal) of the His-29 imidazole, indicating that the main role of His-29 in the formation of an H-bond with the substrate. This bond is established with the β -OH of carnitine or with the β -O- of acyl-carnitines. Therefore, His-29 plays a role in facilitating the correct positioning of the substrate preceding the translocation event towards the opposite side of the membrane (Figure 3b) [103].

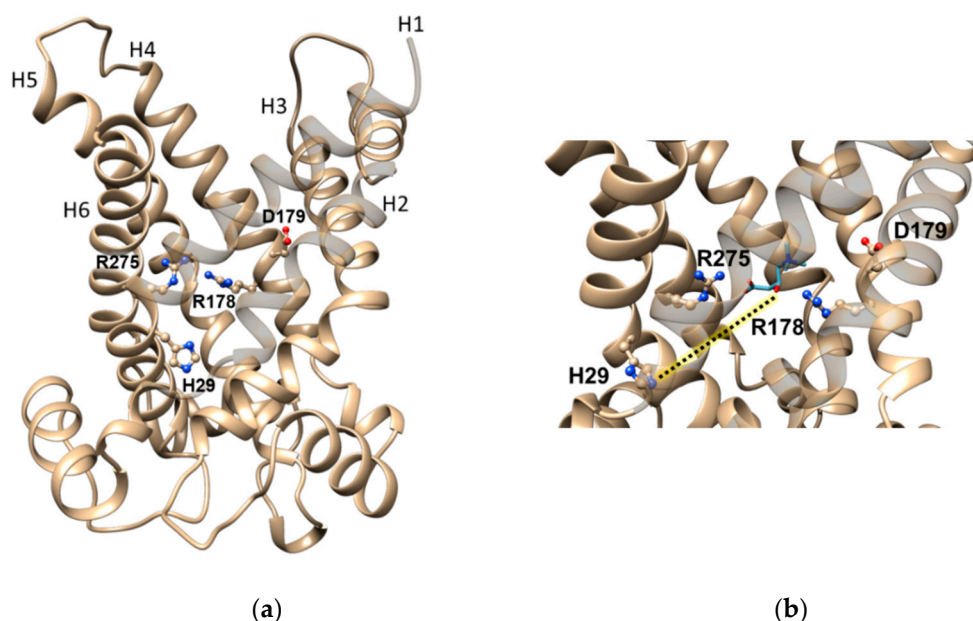


Figure 3. Ribbon diagrams of CAC showing the amino acids involved in carnitine binding. (a) Lateral view of the CAC structural model. The residues Arg-178, Asp-179, Arg-275, and His-29 are highlighted with a ball and stick representation. The transmembrane spanning α -helices are numbered. (b) Enlarged view of the residues interacting with carnitine. The dotted line indicates the following step in the translocation process in which carnitine will interact with His-29 before the matrix gate opens (see also Figure 5). Amino acid residues are displayed with ball and stick representation in which oxygen and nitrogen atoms are depicted in red and blue respectively. CAC model and carnitine position have been obtained as [87].

Besides carnitine, acyl-carnitines are transported by CAC. These carnitine derivatives contain hydrophobic chains, esterified to the hydroxyl group of carnitine, with a length ranging from 2 (acetyl) to 16 (palmitoyl) or more carbon atoms. Val-25, Pro-78, Val-82, Met-84, and Cys-89, all belonging to the first and second transmembrane α -helices of the protein (H1-H2), constitute the “hydrophobic pocket” of CAC that binds the carbon chain of the acyl-carnitines (Figure 4). The ability of this “hydrophobic pocket” to interact with hydrophobic molecules correlates well with the higher average hydrophobicity of transmembrane α -helices H1 and H2 of CAC concerning that of the corresponding α -helices of the other members of the SLC25 family [66,100].

Once the carnitine or the acyl-carnitine has interacted with the proper residues in the c-state, a charged gate constituted by the amino acid side chains of Asp-32, Lys-35, Glu-132, Lys-135, Asp-231, and Lys-234 (Figure 5a) located below the binding site, needs to be unlocked for the translocation to occur [99,104–107]. The six residues form three ion pairs resulting from the interactions between the couples: Asp-32 with Lys-135, Glu-132 with Lys-234, and Asp-231 with Lys-35. The role of these residues and their interactions

have been validated using the mutagenesis approach [87]. Once the gate is opened by the fast interaction of the substrate with at least one of the charged residues, i.e., Lys-35, the carrier changes its conformation from the cytosolic state opened to the matrix opened state. The protein is stabilized in the matrix opened conformation by a gate, similar to the matrix one that is formed towards the cytosolic face and is composed of four charged residues, namely, Lys-97, Glu-191, Lys-194, and Glu-288 (Figure 5b). The other two residues of the cytosolic gate of CAC are uncharged in contrast to the corresponding residues of other carriers [96,106]. The free energy of the cytosolic gate of CAC is, therefore, lower than that of the matrix gate. This probably determines an imperfect coupling of the flux of substrates in the outward and inward directions, conferring to CAC the capacity to mediate a uniport reaction besides the antiport reaction [31,106].

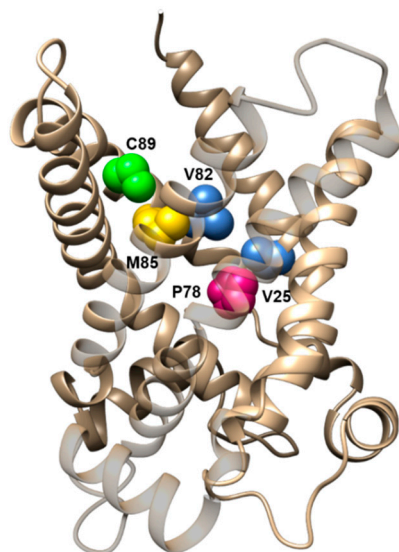


Figure 4. Lateral view of the CAC structural model highlighting the residues involved in binding the acyl moieties of acyl-carnitines. CAC residues are displayed with sphere representation.

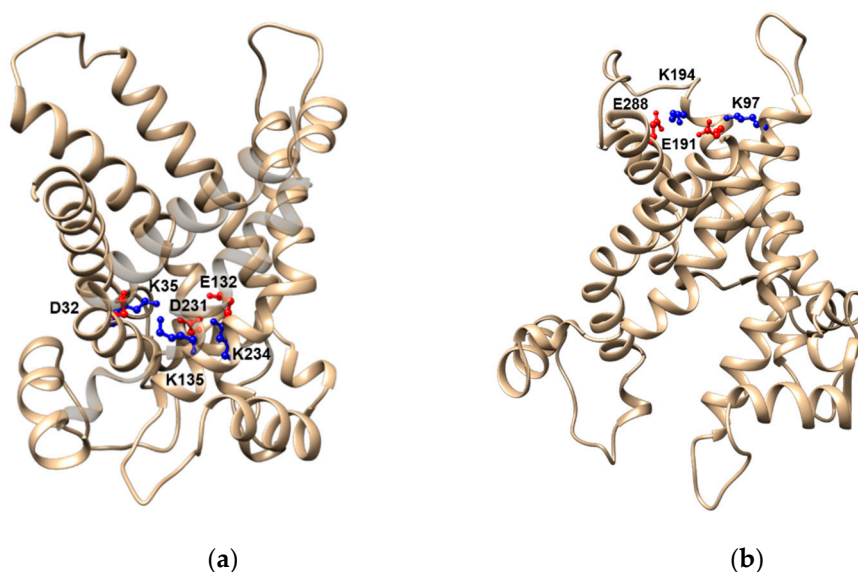


Figure 5. Lateral views of CAC highlighting the residues of the matrix and cytosolic gates. (a) The residues Asp-32, Lys-35, Glu-132, Lys-135, Asp-231, and Lys-234 forming the matrix gate are depicted in red (negatively charged residues) or in blue (positively charged residues); (b) the residues Lys-97, Glu-191, Lys-194, and Glu-288 forming the cytosolic gate are depicted in red (negatively charged residues) or in blue (positively charged residues).

3.2. The Molecular Basis of the Antiport Mode

CAC shares with the other mitochondrial carriers the peculiar structure constituted by six transmembrane segments arranged in three intramembrane domains, which rotate to allow the conformational changes required for the transport reaction [5]. The antiport mode of transport is determined by the coupling of substrate-binding with gate opening on one side and gate closing on the other side. Indeed, given that the substrate considerably decreases the activation free-energy barrier of the carrier transition, the rate of transition of the unbound carrier from an outward open conformation (c-state) to the inward open one (m-state) or vice versa (Figure 6) is much lower than that of the substrate-bound carrier [108].

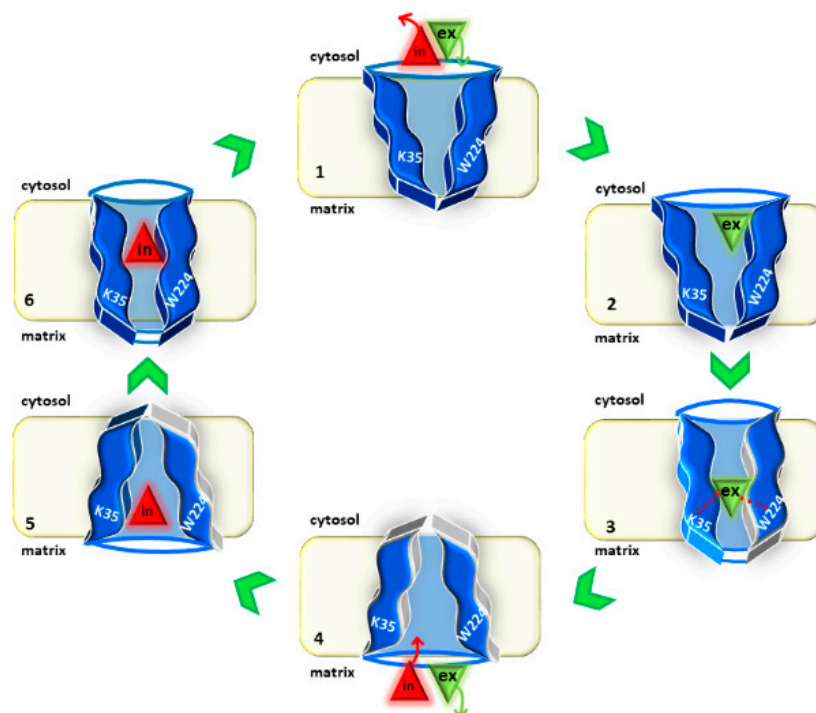


Figure 6. Sketch of the transport cycle of CAC. The states of the transporter during the antiport reaction are displayed: (1) c-state in the absence of substrate, (2) c-state with the external substrate entering the carrier, (3) occluded state or transition state with the external substrate bound to the substrate-binding site, (4) m-state in the absence of substrate, (5) m-state with the internal substrate entering the carrier, (6) occluded state or transition state with the internal substrate bound to the substrate-binding site. The role of K35 and W224 during the transport cycle is highlighted with dotted lines.

In the case of CAC, the identification of the residues, which are crucial for the coupling of substrate-binding with gate opening, was achieved by mutations that specifically abolish the antiport function without interfering with the uniport function. One of these residues is Lys-35, whose substitution with an uncharged residue impairs the antiport reaction, suggesting that Lys-35 interacts with the carboxyl group of carnitine favoring the gate opening [109]. The companion amino acid residue involved in binding the ammonium group of carnitine is Trp-224, whose substitution completely abolishes the antiport function and converts the protein into a uniporter with a specific activity and substrate specificity equal to those of the unidirectional transport activity of the wild-type CAC. The distance between Lys-35 and Trp-224 in the cytosolic open conformation (Figure 7a) corresponds to the distance between the ammonium and the carboxyl groups of carnitine, in line with the interaction of carnitine with these residues, which triggers the gate opening and closing. The distance between these residues increases in the matrix open conformation preceding the substrate release (Figure 7b). In the absence of the interaction of carnitine with Lys-35 and Trp-224, the CAC gate could open as well, but at a much lower rate constant leading to

the uniport function. Trp-224 is conserved in all CAC sub-family members. Indeed, the substitution of this residue in the CAC of *A. nidulans* leads to the same alterations as in the mammalian transporter, indicating that the molecular determinant of the antiport function has been conserved during evolution [110]. Interestingly, a corresponding Trp residue is not present in the other proteins of the SLC25 family except in the ornithine/citrulline carrier, whose substrate, ornithine, harbors a positively charged amino group. In this carrier, the substitution of the Trp unveils a low rate of uniport activity [110,111].

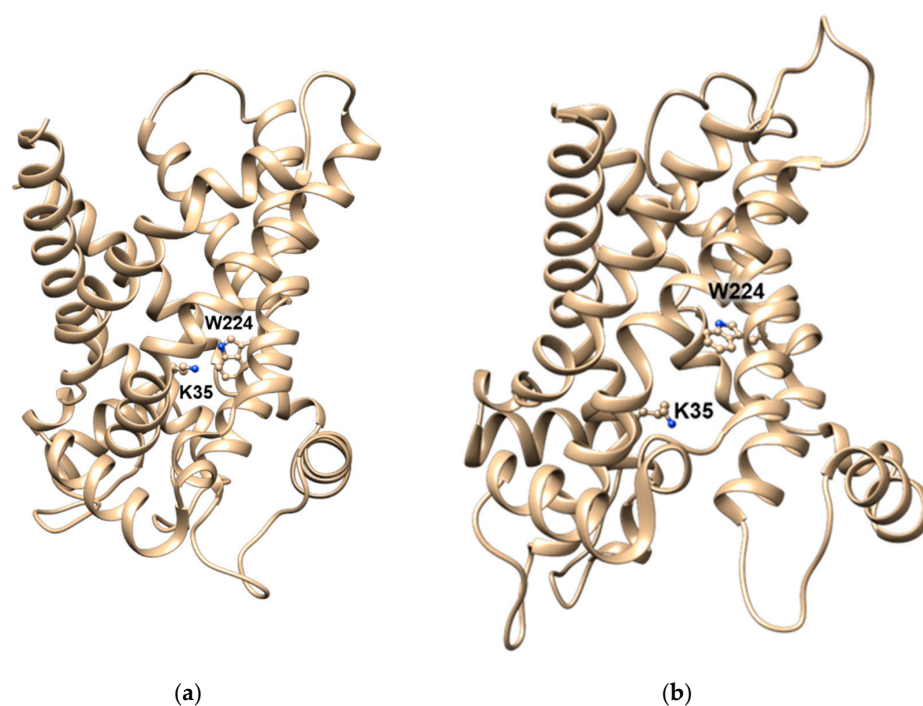


Figure 7. Lateral views of the CAC structural model showing the residues involved in the coupling of substrate-binding with gate opening and gate closing. (a) Ribbon diagram of the carrier in c-state in which the residues Trp 224 and K35 are at a distance of 4 Å and are depicted with a ball and stick; (b) ribbon diagram of the carrier in m-state in which the residues Trp 224 and K35 are at a distance of 12 Å and are depicted in ball and stick.

4. CAC as a Redox Sensor

The capacity of CAC of interacting with thiol-reactive compounds was demonstrated initially in intact mitochondria [83], then confirmed and deepened in studies with the native protein by transport assays in proteoliposomes (see Section 3). However, the molecular determinants of the CAC redox sensitivity were identified only after the production of the recombinant CAC that gave the possibility to perform site-directed mutagenesis. Out of the six Cys residues of the protein, the sole Cys-136 and Cys-155 (Figure 8) are able to sense thiol-reagents at sub-micromolar concentrations as well as physiological effectors involved in cell redox sensing and control. Indeed, mutants in which one of the two Cys residues was substituted with Ser or Ala were less sensitive to thiol-reagents, and the mutant harboring the substitution of both Cys-136 and Cys-155 were mostly insensitive to reagents. Moreover, the mutant containing only Cys-136 and Cys-155, but lacking the other four Cys residues, exhibited the same reactivity as the wild-type protein. [88,112] The high sensitivity of the two residues is linked to their location in the core of the transport pathway, or in its vicinity, and to the local amino acid environment that confers peculiar properties to the cysteine thiol groups in terms of reactivity (pKa of the thiol groups) and propensity to undergo disulfide cross-linking. Indeed, some physiological or chemical reactants act on the “molecular sensor” constituted by Cys-136 and Cys-155. This cysteine couple, according to the oxidation state, behaves as an on-off switch of the protein. Indeed,

if these two cysteines are oxidized to a disulfide, CAC is inactive due to a block of the conformational changes needed for the transition from the outward to the inward open conformation and vice versa. On the other way round, if the disulfide is converted to the thiol form of the Cys residues by a chemical or a physiological reactant, the CAC function is rescued [89]. Most likely, in vivo, the transporter exists as a mixture of the two states. Therefore, the actual transport capacity (specific activity) in vivo depends on the fraction of the protein, which is in the active (reduced) state. This is in line with the observation that the protein after extraction and isolation from the native membrane is not fully active. The maximal activity can only be observed after treating CAC with a strong reducing agent, such as DTE. The fraction of reduced (or oxidized) protein is variable and depends on incubation conditions of the mitochondria or on other factors, which cannot be precisely controlled in experiments. The redox sensing property of CAC allows its modulation by physiological effectors and, in turn, modulation of the β -oxidation pathway flux. The studies that will be resumed below uncover the molecular basis of the redox sensing feature of CAC.

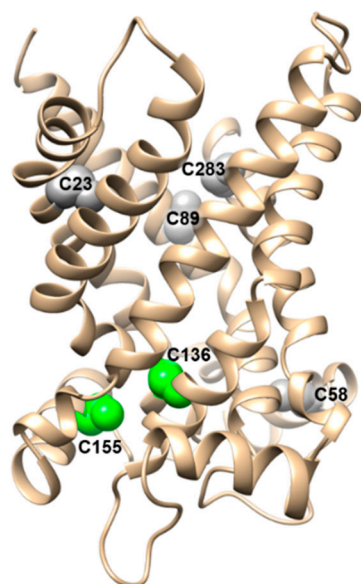


Figure 8. CAC structural model showing the two redox-sensitive cysteines. Lateral view of a ribbon diagram of the carrier in which the cysteine residues are displayed by a sphere representation. Cys-136 and Cys-155 are highlighted in green.

4.1. Regulation of CAC by H_2O_2

CAC senses strong redox cellular changes through H_2O_2 , an endogenous compound whose concentration can increase under oxidizing conditions, reaching millimolar levels locally, especially in mitochondria [113–116]. H_2O_2 inhibits CAC transport activity to an extent depending on both its concentration and time of reaction. H_2O_2 interacts with the thiol groups of Cys136 and Cys155, inducing the formation of a disulfide leading to inhibition. After shorter interaction times (0–2 min) with H_2O_2 , sulfenic acid derivatives are formed, which evolve to disulfide (S-S) or to sulfinic (SO_2^-) and sulphonic (SO_3^-) species after longer reaction times (30 min). The reactions leading to sulfenic acid and disulfides can be reverted by reducing agents (glutathione), while those generating sulfinic and sulphonic acid are irreversible, thus abolishing the ability of the carrier to be switched-on by reducing agents [63]. Translating these data to cellular metabolism, it appears that low H_2O_2 levels regulate the activity of CAC, thus tuning the mitochondrial oxidation of fatty acids. At higher H_2O_2 concentrations, maintained for a longer time, which may occur under pathological conditions, the transporter is blocked, and fatty acid oxidation is arrested. Therefore, under conditions of strong oxidative stress, H_2O_2 , acting on CAC as a signal molecule, may contribute to switching energy production from aerobic lipid metabolism

to anaerobic glycolytic metabolism [117], causing a reduced oxygen consumption and a reduced formation of ROS. These effects can be interpreted as a protective mechanism against oxidative stress.

4.2. Regulation of CAC by Glutathione

Differently from oxidant species, such as H_2O_2 that “switch off” the CAC, reduced glutathione “switch on” the transporter acting on the disulfide between Cys-136 and Cys-155 [118]. Indeed, the physiological GSH/GSSG couple is, normally, present at a ratio of over 100/1, thus prevailing the reducing power. However, the ratio GSH/GSSG can change depending on the redox state of the cell. Thus, the CAC activity can also be modulated by the GSH/GSSG couple. Experimental data obtained by the EPRA method using the Cys mutants of CAC demonstrate that (i) GSH and GSSG cause activation or inhibition, respectively, acting on the SH/S-S exchange between Cys136 and Cys155 and (ii) the thiol group of Cys136 is the residue reacting first with GSSG. The action mechanism of these effectors implies the reversible glutathionylation of the transporter. In cells, the degree and the rate of conversion between the two forms may, in turn, depend on the activity of the enzyme Glutaredoxin-1 (Grx1) located in the intermembrane space of mitochondria [119,120] even though no direct evidence is provided so far of the contribution of this enzyme to the regulation of CAC by GSH/GSSG. CAC is the first mitochondrial carrier known to be responsive to the redox state of mitochondria and undergoes a full redox cycle from a reduced/activated state to an oxidized/inactivated state and vice versa. This responsiveness, again, relapses on the rate of fatty acid oxidation and hence on the production of ATP [118]

4.3. Modulation of CAC by NO

Nitrosylation processes modulate a huge number of cell pathways [121,122]. Row proteomic data indicated that CAC is targeted by NO among many other proteins [123]. When treating the native or the recombinant CAC with NO inhibitory effects can be observed [62]. The effects strictly depend on the presence of Cys-136, and the inhibition of transport is based on the steric hindrance caused by the NO-Cys bond close to the active site of CAC, where Cys-136 is located. CAC S-nitrosylation may occur under specific conditions in which mitochondrial oxidation of fatty acids must be slowed down, for example, to avoid CoA trapping by acetyl-CoA. Such conditions may intervene during impairment of the respiratory chain activity, which can be caused, among other motives, by increased intramitochondrial NO level and inhibition of complex I [124]. This phenomenon may control/regulate the fatty acyl flux into β -oxidation during altered mitochondrial metabolism, such as in ischemia and reperfusion. The NO-mediated inhibition of CAC may act in preventing the accumulation of reducing equivalents and decreasing ROS formation following re-oxygenation. Furthermore, the inhibition of CAC and the consequent impairment of β -oxidation may also contribute to the metabolic switch towards glycolytic metabolism [48,49] that has an important role in ischemic conditions [50].

4.4. Modulation of CAC by H_2S

Beyond the previously described signals acting on CAC, it has been demonstrated that CAC is an H_2S sensor. H_2S is one of the endogenous gas transmitters (NO, CO and H_2S), which is produced by several enzymatic pathways, two of them being mitochondrial [125–129]. H_2S exerts its action on CAC interacting with the “crucial” Cys-136 and Cys-155 couple. Actually, it shows a higher affinity for Cys-155 compared to Cys-136, in contrast with H_2O_2 , NO, and GSSG, which “prefer” Cys-136. This difference is related to the solubility, reactivity, and size of H_2S (or HS^-). H_2S first reacts with Cys-155 forming $-SSH$; then the free $-SH$ of Cys136 reacts with the $-SSH$ producing the disulfide Cys136-S-S-Cys155, which inactivates CAC [89]. Furthermore, H_2S in the solution can form polysulfides [130] which can reduce protein disulfides and, hence, convert the Cys-136/Cys-155 disulfide to free thiol groups. Such a reaction well explains the reactivation

of the inhibited transporter observed after long time incubations. Thanks to its gaseous nature and its affinity for CAC, H₂S manages the rate/flow of fatty acid mitochondrial β -oxidation, exerting a prompt and fine-tuned modulation of this pathway. Therefore, under certain conditions, e.g., those of oxidative stress, the H₂S-mediated regulation of CAC activity can cause a switch of aerobic metabolism to glycolysis with consequent cardio-protection upon ischemia/reperfusion [61].

5. Other Regulatory Mechanisms

CAC is also a target of non-enzymatic acetylation processes, which lead to inhibition of its transport activity [60]. This mechanism, too, contributes to the regulation of the mitochondrial β -oxidation pathway. The effect of acetylation on CAC is opposite to that described for the citrate carrier (CIC, *SLC25A1*), which is activated by acetylation [131]. The different behavior of CAC and CIC versus acetylation correlates well with the roles of the two transporters in the β -oxidation and biosynthesis of fatty acids, respectively, because CAC is necessary for their β -oxidation and CIC is necessary for their biosynthesis. The acetylation of CAC exerts a dynamic control on the protein as the non-enzymatic process of acetylation can be followed by enzymatic deacetylation by the action of NAD⁺ dependent SIRT3. Notably, this process links the activity of CAC to the acetyl-CoA level in the mitochondria [60,132].

CAC is also subjected to transcriptional control. Its gene is located on chromosome 3p21.31, spans about 42 kb, and is split into nine exons with the translation start site in exon 1 [133,134]. This gene is differentially expressed in human tissues. High levels of transcripts are found in the liver, heart, and skeletal muscle, where β -oxidation is greatly exploited for energy production; much lower levels are observed in other tissues, such as the brain, placenta, pancreas, and lung [135]. Research on the proximal promoter has revealed the presence of binding sites for different transcription factors. For example, it has been demonstrated that an active binding site for PPAR α is present in the CAC gene promoter at position $-99/-80$ bp and that PPAR α is a strong activator of CAC gene expression [136]. CAC expression is also regulated by other transcription factors, such as PGC-1 α and 1 β , the estrogen-related receptor (ERR), the general factor Sp1, the specific factors FOXA2 and SRC-3, and possibly other factors not yet identified [137]. In addition, CAC gene expression is upregulated by drugs, such as statins, fibrates, and 9-cis-retinoic acid [138].

Another regulatory mechanism of CAC is exerted by the Micro-RNAs (miRNAs) 132 and 212, which lead to CAC suppression, causing inhibition of β -oxidation and accumulation of cellular long-chain fatty acyl-carnitine esters in pancreatic β -cells, ultimately leading to stimulation of insulin secretion. Interestingly, miRNAs 132 and 212 are upregulated in pancreatic β -cells in response to obesity in two mouse strains with different susceptibility to obesity-induced diabetes. Therefore, the downregulation of CAC may be a mechanism to enhance the insulin secretory response [28].

6. Interaction of CAC with Xenobiotics

An important aspect concerning the involvement of CAC in human health is its capacity to interact with xenobiotics. In addition, this ability is mostly related to the high reactivity of the Cys residues of the transporter. In some cases, the interaction occurs via the substrate-binding site or with a mixed mechanism. In the following sections, the activation or inhibition effects exerted by different xenobiotics are described and explained based on the chemical properties of each compound. Most of the interacting compounds are largely used or newly proposed drugs.

6.1. Polyphenols

The polyphenolic fraction extracted from several cherry cultivars is known for its antioxidant properties. Polyphenols can prevent CAC oxidation by atmospheric O₂ or partially reverse protein oxidation by intracellularly-produced cell H₂O₂. The data obtained with the EPRA method highlighted that the antioxidant effect on CAC is mainly

exerted by the compound 8 trans-3-O-feruloyl-quinic acid (3FQA), which is the most hydrosoluble/bioavailable and abundant in the cherry extracts. The last feature of this compound favors its approach to the substrate-binding site for reducing the disulfide between Cys136 and Cys155, which characterizes CAC under its oxidized state [139]. Therefore, the polyphenol action can improve mitochondrial functionality by acting on the fatty acid β -oxidation pathway. This, in turn, improves several defects correlated to elevated oxidative stress occurring in several diseases, such as Alzheimer's disease, Down's syndrome, and heart diseases.

6.2. Dantrolene

Dantrolene, a drug that possesses antioxidant properties [28] and is specifically used in the management of malignant hyperthermia, activates the oxidized (disulfide) fraction of CAC with a half-maximal effective concentration (EC₅₀) of 9.3 μ M. The effect of dantrolene on CAC activity also has been characterized with the EPRA method [58].

6.3. β -Lactam Antibiotics

The first report concerning the action of drugs on mitochondrial transport of carnitine dates back to 1994 [140]. The authors of this paper hypothesized that the toxicity of some β -lactam antibiotics was due to the inhibition of mitochondrial carnitine transport. However, it was only in 2008 when the molecular interaction of β -lactams with CAC was demonstrated [57] in liposomes reconstituted with the rat liver CAC. β -lactam antibiotics, which are among the most commonly used antibiotics in human therapy, are competitive inhibitors of CAC, probably due to their structural similarity with carnitine. In addition, they irreversibly bind CAC after longer incubation times and knock off carnitine transport [57]. In vivo, inactivation of CAC could impair fatty acid β -oxidation at a variable extent depending on the type of antibiotic and the therapy duration, leading to metabolic consequences of tissues, such as the liver or muscles, that greatly rely on fatty acid oxidation for energy production. Finally, the molecular interaction between β -lactam antibiotics and CAC, described above, may contribute to determining some mild side-effects of β -lactams [57].

6.4. Proton Pump Inhibitors

Omeprazole, a known K^+/H^+ -ATPase inhibitor that is largely used to treat gastric acid-related disorders, also interacts with CAC. The molecular mechanism of interaction of omeprazole with CAC relies on forming S-S mixed disulfide(s) with Cys-136 or Cys-155, just as it does with the K^+/H^+ -ATPase. Interestingly, omeprazole interacts with Cys-136, as other previously characterized sulfhydryl reagents, but also with Cys-283, which is not targeted by other reagents of the same type. The reaction with both Cys residues leads to the complete inactivation of the transporter. According to computational analysis, two omeprazole molecules are involved in this interaction, one for each Cys residue. In vivo, these implications deserve attention for their impact on the process of fatty acid β -oxidation leading to a mild carnitine deficiency-like syndrome [56,141].

6.5. Mildronate

Mildronate, an anti-ischemic drug also used as performance-enhancing, is a competitive inhibitor of CAC. It not only interacts with the substrate-binding site of CAC, but it is also transported by this carrier due to the high similarity with carnitine. The administered mildronate is taken up by the cells via OCTN2 and then inhibits acyl-carnitine transport into the mitochondrial matrix. Moreover, the matrix taken up mildronate acts on intramitochondrial metabolism enzymes. Therefore, CAC has a crucial role in the molecular mechanisms underlying the effects of mildronate [142].

6.6. Ingenols

Among several protein targets of ingenols, a class of drugs used for actinic keratosis, there is CAC. The carrier is inhibited by ingenol mebutate (IngMeb), which thus blocks acyl-carnitine uptake into the mitochondria and, hence, the mitochondrial fatty acid oxidation. The discovery that IngMeb and its more stable analog ingenol disoxate (IngDsx) inhibit CAC contributes to explain, at the molecular level, some of the mitochondrial defects observed in cells treated with high concentrations of these drugs [55].

6.7. Heavy Metals

CAC plays a major role in mercury toxicology, being one of the most crucial targets of mercury. Indeed, the mercury compounds mercury chloride and methylmercury inactivate CAC *in vitro* and *in vivo* at submicromolar concentrations [59], which are at concentrations lower than those, which inactivate thioredoxin [143]. Using zebrafish as an animal model and HeLa cells as a human cell model, it has been demonstrated that mercury impairs the viability of zebrafish and human cells, respectively, at concentrations corresponding to those present in the environment after pollution. By parallel experiments performed using the EPRA method, the molecular mechanism of action has been disclosed. The compounds act by targeting the transporter via mercury-thiol bonds with Cys-136 and Cys-155. The data correlate well with the previous findings on CAC purified from rat liver [47]. From a physiological point of view, this is relevant since the average concentration of mercury in human tissues (about 0.15 μM) can increase to more than 5 μM upon acute or chronic exposure to pollutants [144]. Overexposure to mercury causes mitochondrial toxicity by the chemical CAC knocking off [59]. As mercury, also copper exerts a strong inhibition on CAC, even though at higher concentrations [64]. The effect and the mechanism of interaction between copper and CAC have been defined by site-directed mutagenesis and computational chemistry approaches. The oxidation state of the cation does not influence its effectiveness as an inhibitor since Cu^{2+} and Cu^+ show the same IC_{50} . The mechanism of interaction with CAC consists of the formation of a cross-link among the copper ion and the two Cys-136 and Cys-155 residues. This cross-link, similarly to the disulfide between the two Cys residues, “switches off” the transporter [64].

7. Conclusions

The carnitine acyl-carnitine carrier (CAC) has a long history being one of those membrane transporters whose study started with its functional characterization in intact mitochondria and continued with its biochemical description and investigation at the molecular level using the native purified protein or the bacterially expressed recombinant purified protein. The more recent studies of CAC, performed by joining up-to-date methodological approaches, such as *in vitro* transport assay, site-directed mutagenesis, and bioinformatics, confirmed and extended previous findings as well as discovered molecular mechanisms of its transport activation and inhibition. Thus, several regulatory properties of CAC, which are based on post-translational modifications of Cys or Lys residues of the transporter, emerged from these studies. In particular, two specific Cys residues behave like an on-off switch of the carrier, responding to signals of physiological effectors, such as GSH, hydrogen sulfide, and nitric oxide. Altogether, the summarized studies highlight the transporter's involvement in fatty acid metabolism, suggesting a central role of CAC in controlling the β -oxidation pathway in response to the redox state of the cell. Therefore, CAC represents an exciting drug target.

Author Contributions: A.T. and C.I. contributed to collecting bibliography, in writing the manuscript, and in conceiving and creating the figures; N.G. contributed in collecting bibliography, writing the manuscript and creating figures; L.C. contributed in creating figures and in the critical revision of the manuscript; C.I. and F.P. supervised the work and wrote and revised the manuscript. All authors contributed to the article. All authors have read and agreed to the published version of the manuscript.

Funding: This research was funded by the University of Calabria “Fondi di Ateneo 2019” to C.I.

Conflicts of Interest: The authors declare no conflict of interest.

Abbreviations

CAC: carnitine acyl-carnitine carrier; EPRA: expression, purification and reconstitution assay; NEM: N-ethylmaleimide; MTS: methanethiosulfonate reagents; IngMeb: ingenol mebutate; IngDsx: ingenol disoxate; SLC25: solute carrier family 25.

References

1. Palmieri, F. The mitochondrial transporter family SLC25: Identification, properties and physiopathology. *Mol. Aspects Med.* **2013**, *34*, 465–484. [CrossRef]
2. Palmieri, F.; Pierri, C.L. Mitochondrial metabolite transport. *Essays Biochem.* **2010**, *47*, 37–52. [CrossRef]
3. Palmieri, F.; Scarcia, P.; Monne, M. Diseases Caused by Mutations in Mitochondrial Carrier Genes SLC25: A Review. *Biomolecules* **2020**, *10*, 655. [CrossRef]
4. Agrimi, G.; Russo, A.; Scarcia, P.; Palmieri, F. The human gene SLC25A17 encodes a peroxisomal transporter of coenzyme A, FAD and NAD⁺. *Biochem. J.* **2012**, *443*, 241–247. [CrossRef]
5. Ruprecht, J.J.; King, M.S.; Zögg, T.; Aleksandrova, A.A.; Pardon, E.; Crichton, P.G.; Steyaert, J.; Kunji, E.R.S. The Molecular Mechanism of Transport by the Mitochondrial ADP/ATP Carrier. *Cell* **2019**, *176*, 435–447.e415. [CrossRef]
6. Ruprecht, J.J.; Hellawell, A.M.; Harding, M.; Crichton, P.G.; McCoy, A.J.; Kunji, E.R. Structures of yeast mitochondrial ADP/ATP carriers support a domain-based alternating-access transport mechanism. *Proc. Natl. Acad. Sci. USA* **2014**, *111*, E426–E434. [CrossRef]
7. Stanley, C.A.; Palmieri, F.; Bennett, M.J. Disorders of the mitochondrial carnitine shuttle. *Online Metab. Mol. Bases Inherit. Dis.* **2013**. [CrossRef]
8. Bhuiyan, J.; Pritchard, P.H.; Pande, S.V.; Secombe, D.W. Effects of high-fat diet and fasting on levels of acyl-coenzyme A binding protein in liver, kidney, and heart of rat. *Metabolism* **1995**, *44*, 1185–1189. [CrossRef]
9. Indiveri, C.; Iacobazzi, V.; Tonazzi, A.; Giangregorio, N.; Infantino, V.; Convertini, P.; Console, L.; Palmieri, F. The mitochondrial carnitine/acylcarnitine carrier: Function, structure and physiopathology. *Mol. Asp. Med.* **2011**, *32*, 223–233. [CrossRef]
10. Casals, N.; Zammit, V.; Herrero, L.; Fadó, R.; Rodríguez-Rodríguez, R.; Serra, D. Carnitine palmitoyltransferase 1C: From cognition to cancer. *Prog. Lipid Res.* **2016**, *61*, 134–148. [CrossRef]
11. De Pinto, V. Renaissance of VDAC: New Insights on a Protein Family at the Interface between Mitochondria and Cytosol. *Biomolecules* **2021**, *11*, 107. [CrossRef] [PubMed]
12. Console, L.; Giangregorio, N.; Indiveri, C.; Tonazzi, A. Carnitine/acylcarnitine translocase and carnitine palmitoyltransferase 2 form a complex in the inner mitochondrial membrane. *Mol. Cell Biochem.* **2014**. [CrossRef] [PubMed]
13. Wang, Z.; Ying, Z.; Bosy-Westphal, A.; Zhang, J.; Schautz, B.; Later, W.; Heymsfield, S.B.; Muller, M.J. Specific metabolic rates of major organs and tissues across adulthood: Evaluation by mechanistic model of resting energy expenditure. *Am. J. Clin Nutr* **2010**, *92*, 1369–1377. [CrossRef] [PubMed]
14. Console, L.; Scalise, M.; Giangregorio, N.; Tonazzi, A.; Barile, M.; Indiveri, C. The Link Between the Mitochondrial Fatty Acid Oxidation Derangement and Kidney Injury. *Front. Physiol.* **2020**, *11*, 794. [CrossRef]
15. Talley, J.T.; Mohiuddin, S.S. *Biochemistry, Fatty Acid Oxidation*; StatPearls: Treasure Island, FL, USA, 2020.
16. Nalecz, K.A.; Miecz, D.; Berezowski, V.; Cecchelli, R. Carnitine: Transport and physiological functions in the brain. *Mol. Aspects Med.* **2004**, *25*, 551–567. [CrossRef]
17. Tonazzi, A.; Mantovani, C.; Colella, M.; Terenghi, G.; Indiveri, C. Localization of mitochondrial carnitine/acylcarnitine translocase in sensory neurons from rat dorsal root Ganglia. *Neurochem. Res.* **2013**, *38*, 2535–2541. [CrossRef]
18. Kaminska, J.; Nalecz, K.A.; Azzi, A.; Nalecz, M.J. Purification of carnitine carrier from rat brain mitochondria. *Biochem. Mol. Biol. Int.* **1993**, *29*, 999–1007.
19. Huizing, M.; Iacobazzi, V.; Ijlst, L.; Savelkoul, P.; Ruitenbeek, W.; van den Heuvel, L.; Indiveri, C.; Smeitink, J.; Trijbels, F.; Wanders, R.; et al. Cloning of the human carnitine-acylcarnitine carrier cDNA and identification of the molecular defect in a patient. *Am. J. Hum. Genet.* **1997**, *61*, 1239–1245. [CrossRef]
20. Ijlst, L.; Ruiter, J.P.; Oostheim, W.; Niezen-Koning, K.E.; Palmieri, F.; Wanders, R.J. Identification of a missense mutation in a patient with lethal carnitine acyl-carnitine carrier deficiency. *Adv. Exp. Med. Biol.* **1999**, *466*, 347–351. [CrossRef]
21. Iacobazzi, V.; Pasquali, M.; Singh, R.; Matern, D.; Rinaldo, P.; Amat di San Filippo, C.; Palmieri, F.; Longo, N. Response to therapy in carnitine/acylcarnitine translocase (CACT) deficiency due to a novel missense mutation. *Am. J. Med. Genet. A* **2004**, *126A*, 150–155. [CrossRef]
22. Iacobazzi, V.; Invernizzi, F.; Baratta, S.; Pons, R.; Chung, W.; Garavaglia, B.; Dionisi-Vici, C.; Ribes, A.; Parini, R.; Huertas, M.D.; et al. Molecular and functional analysis of SLC25A20 mutations causing carnitine-acylcarnitine translocase deficiency. *Hum. Mutat.* **2004**, *24*, 312–320. [CrossRef] [PubMed]

23. Hsu, B.Y.; Iacobazzi, V.; Wang, Z.; Harvie, H.; Chalmers, R.A.; Saudubray, J.M.; Palmieri, F.; Ganguly, A.; Stanley, C.A. Aberrant mRNA splicing associated with coding region mutations in children with carnitine-acylcarnitine translocase deficiency. *Mol. Genet. Metab.* **2001**, *74*, 248–255. [CrossRef]
24. Huizing, M.; Wendel, U.; Ruitenbeek, W.; Iacobazzi, V.; Lglst, L.; Veenhuizen, P.; Savelkoul, P.; van den Heuvel, L.P.; Smeitink, J.A.; Wanders, R.J.; et al. Carnitine-acylcarnitine carrier deficiency: Identification of the molecular defect in a patient. *J. Inher. Metab. Dis.* **1998**, *21*, 262–267. [CrossRef]
25. Console, L.; Scalise, M.; Mazza, T.; Pochini, L.; Galluccio, M.; Giangregorio, N.; Tonazzi, A.; Indiveri, C. Carnitine Traffic in Cells. Link With Cancer. *Front. Cell Dev. Biol.* **2020**, *8*, 583850. [CrossRef]
26. Magoulas, P.L.; El-Hattab, A.W. Systemic primary carnitine deficiency: An overview of clinical manifestations, diagnosis, and management. *Orphanet. J. Rare Dis.* **2012**, *7*, 68. [CrossRef]
27. Rose, E.C.; di San Filippo, C.A.; Ndukwe Erlingsson, U.C.; Ardon, O.; Pasquali, M.; Longo, N. Genotype-phenotype correlation in primary carnitine deficiency. *Hum. Mutat.* **2012**, *33*, 118–123. [CrossRef] [PubMed]
28. Soni, M.S.; Rabaglia, M.E.; Bhatnagar, S.; Shang, J.; Ilkayeva, O.; Mynatt, R.; Zhou, Y.P.; Schadt, E.E.; Thornberry, N.A.; Muoio, D.M.; et al. Downregulation of carnitine acyl-carnitine translocase by miRNAs 132 and 212 amplifies glucose-stimulated insulin secretion. *Diabetes* **2014**, *63*, 3805–3814. [CrossRef]
29. Peluso, G.; Petillo, O.; Margarucci, S.; Mingrone, G.; Greco, A.V.; Indiveri, C.; Palmieri, F.; Melone, M.A.; Reda, E.; Calvani, M. Decreased mitochondrial carnitine translocase in skeletal muscles impairs utilization of fatty acids in insulin-resistant patients. *Front. Biosci. J. Virtual Libr.* **2002**, *7*, a109–a116. [CrossRef]
30. Monne, M.; Palmieri, F. Antiporters of the mitochondrial carrier family. *Curr. Top. Membr.* **2014**, *73*, 289–320. [CrossRef]
31. Indiveri, C.; Tonazzi, A.; Palmieri, F. Characterization of the unidirectional transport of carnitine catalyzed by the reconstituted carnitine carrier from rat liver mitochondria. *Biochim. Biophys. Acta* **1991**, *1069*, 110–116. [CrossRef]
32. Indiveri, C.; Tonazzi, A.; Palmieri, F. The reconstituted carnitine carrier from rat liver mitochondria: Evidence for a transport mechanism different from that of the other mitochondrial translocators. *Biochim. Biophys. Acta* **1994**, *1189*, 65–73. [CrossRef]
33. Palmieri, L.; Lasorsa, F.M.; Iacobazzi, V.; Runswick, M.J.; Palmieri, F.; Walker, J.E. Identification of the mitochondrial carnitine carrier in *Saccharomyces cerevisiae*. *FEBS Lett.* **1999**, *462*, 472–476. [CrossRef]
34. De Lucas, J.R.; Indiveri, C.; Tonazzi, A.; Perez, P.; Giangregorio, N.; Iacobazzi, V.; Palmieri, F. Functional characterization of residues within the carnitine/acylcarnitine translocase RX(2)PANAAXF distinct motif. *Mol. Membr. Biol.* **2008**, *25*, 152–163. [CrossRef]
35. Ramon De Lucas, J.; Martinez, O.; Perez, P.; Isabel Lopez, M.; Valenciano, S.; Laborda, F. The *Aspergillus nidulans* carnitine carrier encoded by the acuH gene is exclusively located in the mitochondria. *FEMS Microbiol. Lett.* **2001**, *201*, 193–198. [CrossRef]
36. Perez, P.; Martinez, O.; Romero, B.; Olivas, I.; Pedregosa, A.M.; Palmieri, F.; Laborda, F.; Ramon De Lucas, J. Functional analysis of mutations in the human carnitine/acylcarnitine translocase in *Aspergillus nidulans*. *Fungal Genet. Biol.* **2003**, *39*, 211–220. [CrossRef]
37. Palmieri, F.; Agrimi, G.; Blanco, E.; Castegna, A.; Di Noia, M.A.; Iacobazzi, V.; Lasorsa, F.M.; Marobbio, C.M.; Palmieri, L.; Scarcia, P.; et al. Identification of mitochondrial carriers in *Saccharomyces cerevisiae* by transport assay of reconstituted recombinant proteins. *Biochim. Biophys. Acta* **2006**, *1757*, 1249–1262. [CrossRef] [PubMed]
38. Jacques, F.; Rippa, S.; Perrin, Y. Physiology of L-carnitine in plants in light of the knowledge in animals and microorganisms. *Plant. Sci.* **2018**, *274*, 432–440. [CrossRef]
39. Porcelli, V.; Voza, A.; Calcagnile, V.; Gorgoglione, R.; Arrigoni, R.; Fontanesi, F.; Marobbio, C.M.T.; Castegna, A.; Palmieri, F.; Palmieri, L. Molecular identification and functional characterization of a novel glutamate transporter in yeast and plant mitochondria. *Biochim. Biophys. Acta Bioenerg.* **2018**, *1859*, 1249–1258. [CrossRef] [PubMed]
40. Houten, S.M.; Wanders, R.J.A.; Ranea-Robles, P. Metabolic interactions between peroxisomes and mitochondria with a special focus on acylcarnitine metabolism. *Biochim. Biophys. Acta Mol. Basis Dis.* **2020**, *1866*, 165720. [CrossRef]
41. Juraszek, B.; Nałęcz, K.A. SLC22A5 (OCTN2) Carnitine Transporter-Indispensable for Cell Metabolism, a Jekyll and Hyde of Human Cancer. *Molecules* **2019**, *25*, 14. [CrossRef]
42. Pande, S.V. A mitochondrial carnitine acylcarnitine translocase system. *Proc. Natl. Acad. Sci. USA* **1975**, *72*, 883–887. [CrossRef] [PubMed]
43. Fritz, I.B.; Yue, K.T. Long-Chain Carnitine Acyltransferase and the Role of Acylcarnitine Derivatives in the Catalytic Increase of Fatty Acid Oxidation Induced by Carnitine. *J. Lipid Res.* **1963**, *4*, 279–288. [CrossRef]
44. Ramsay, R.R.; Tubbs, P.K. The mechanism of fatty acid uptake by heart mitochondria: An acylcarnitine-carnitine exchange. *FEBS Lett.* **1975**, *54*, 21–25. [CrossRef]
45. Indiveri, C.; Tonazzi, A.; Palmieri, F. Identification and purification of the carnitine carrier from rat liver mitochondria. *Biochim. Biophys. Acta* **1990**, *1020*, 81–86. [CrossRef]
46. Indiveri, C.; Tonazzi, A.; Prezioso, G.; Palmieri, F. Kinetic characterization of the reconstituted carnitine carrier from rat liver mitochondria. *Biochim. Biophys. Acta* **1991**, *1065*, 231–238. [CrossRef]
47. Indiveri, C.; Tonazzi, A.; Dierks, T.; Krämer, R.; Palmieri, F. The mitochondrial carnitine carrier: Characterization of SH-groups relevant for its transport function. *Biochim. Biophys. Acta* **1992**, *1140*, 53–58. [CrossRef]

48. Indiveri, C.; Tonazzi, A.; Giangregorio, N.; Palmieri, F. Probing the active site of the reconstituted carnitine carrier from rat liver mitochondria with sulfhydryl reagents. A cysteine residue is localized in or near the substrate binding site. *Eur. J. Biochem.* **1995**, *228*, 271–278. [CrossRef]
49. Indiveri, C.; Iacobazzi, V.; Giangregorio, N.; Palmieri, F. The mitochondrial carnitine carrier protein: cDNA cloning, primary structure and comparison with other mitochondrial transport proteins. *Biochem. J.* **1997**, *321 Pt 3*, 713–719. [CrossRef]
50. Indiveri, C.; Iacobazzi, V.; Giangregorio, N.; Palmieri, F. Bacterial overexpression, purification, and reconstitution of the carnitine/acylcarnitine carrier from rat liver mitochondria. *Biochem. Biophys. Res. Commun.* **1998**, *249*, 589–594. [CrossRef]
51. Fiermonte, G.; Walker, J.E.; Palmieri, F. Abundant bacterial expression and reconstitution of an intrinsic membrane-transport protein from bovine mitochondria. *Biochem. J.* **1993**, *294 Pt 1*, 293–299. [CrossRef]
52. Palmieri, F.; Monne, M. Discoveries, metabolic roles and diseases of mitochondrial carriers: A review. *Biochim. Biophys. Acta* **2016**, *1863*, 2362–2378. [CrossRef]
53. Scalise, M.; Pochini, L.; Giangregorio, N.; Tonazzi, A.; Indiveri, C. Proteoliposomes as tool for assaying membrane transporter functions and interactions with xenobiotics. *Pharmaceutics* **2013**, *5*, 472–497. [CrossRef]
54. Scalise, M.; Galluccio, M.; Pochini, L.; Console, L.; Barile, M.; Giangregorio, N.; Tonazzi, A.; Indiveri, C. Studying Interactions of Drugs with Cell Membrane Nutrient Transporters: New Frontiers of Proteoliposome Nanotechnology. *Curr. Pharm. Des.* **2017**, *23*, 3871–3883. [CrossRef]
55. Parker, C.G.; Kuttruff, C.A.; Galmozzi, A.; Jørgensen, L.; Yeh, C.H.; Hermanson, D.J.; Wang, Y.; Artola, M.; McKerrall, S.J.; Joslyn, C.M.; et al. Chemical Proteomics Identifies SLC25A20 as a Functional Target of the Ingenol Class of Actinic Keratosis Drugs. *ACS Cent. Sci.* **2017**, *3*, 1276–1285. [CrossRef]
56. Tonazzi, A.; Eberini, I.; Indiveri, C. Molecular mechanism of inhibition of the mitochondrial carnitine/acylcarnitine transporter by omeprazole revealed by proteoliposome assay, mutagenesis and bioinformatics. *PLoS ONE* **2013**, *8*, e82286. [CrossRef]
57. Pochini, L.; Galluccio, M.; Scumaci, D.; Giangregorio, N.; Tonazzi, A.; Palmieri, F.; Indiveri, C. Interaction of beta-lactam antibiotics with the mitochondrial carnitine/acylcarnitine transporter. *Chem. Biol. Interact.* **2008**, *173*, 187–194. [CrossRef]
58. Bolognino, I.; Giangregorio, N.; Pisani, L.; de Candia, M.; Purgatorio, R.; Tonazzi, A.; Altomare, C.D.; Cellamare, S.; Catto, M. A Prospective Repurposing of Dantrolene as a Multitarget Agent for Alzheimer’s Disease. *Molecules* **2019**, *24*, 4298. [CrossRef]
59. Tonazzi, A.; Giangregorio, N.; Console, L.; Scalise, M.; La Russa, D.; Notaristefano, C.; Brunelli, E.; Barca, D.; Indiveri, C. Mitochondrial carnitine/acylcarnitine transporter, a novel target of mercury toxicity. *Chem. Res. Toxicol.* **2015**, *28*, 1015–1022. [CrossRef] [PubMed]
60. Giangregorio, N.; Tonazzi, A.; Console, L.; Indiveri, C. Post-translational modification by acetylation regulates the mitochondrial carnitine/acylcarnitine transport protein. *Mol. Cell Biochem.* **2017**, *426*, 65–73. [CrossRef]
61. Giangregorio, N.; Tonazzi, A.; Console, L.; Lorusso, I.; De Palma, A.; Indiveri, C. The mitochondrial carnitine/acylcarnitine carrier is regulated by hydrogen sulfide via interaction with C136 and C155. *Biochim. Biophys. Acta* **2016**, *1860*, 20–27. [CrossRef]
62. Tonazzi, A.; Giangregorio, N.; Console, L.; De Palma, A.; Indiveri, C. Nitric oxide inhibits the mitochondrial carnitine/acylcarnitine carrier through reversible S-nitrosylation of cysteine 136. *Biochim. Biophys. Acta* **2017**, *1858*, 475–482. [CrossRef]
63. Tonazzi, A.; Console, L.; Indiveri, C. Inhibition of mitochondrial carnitine/acylcarnitine transporter by H₂O₂: Molecular mechanism and possible implication in pathophysiology. *Chem. Biol. Interact.* **2013**. [CrossRef]
64. Giangregorio, N.; Tonazzi, A.; Console, L.; Prejanò, M.; Marino, T.; Russo, N.; Indiveri, C. Effect of Copper on the Mitochondrial Carnitine/Acylcarnitine Carrier Via Interaction with Cys136 and Cys155. Possible Implications in Pathophysiology. *Molecules* **2020**, *25*, 820. [CrossRef]
65. Murthy, M.S.; Pande, S.V. Mechanism of carnitine acylcarnitine translocase-catalyzed import of acylcarnitines into mitochondria. *J. Biol. Chem.* **1984**, *259*, 9082–9089. [CrossRef]
66. Tonazzi, A.; Console, L.; Giangregorio, N.; Indiveri, C.; Palmieri, F. Identification by site-directed mutagenesis of a hydrophobic binding site of the mitochondrial carnitine/acylcarnitine carrier involved in the interaction with acyl groups. *Biochim. Biophys. Acta Bioenerg.* **2012**, *1817*, 697–704. [CrossRef]
67. Bartelds, B.; Takens, J.; Smid, G.B.; Zammit, V.A.; Prip-Buus, C.; Kuipers, J.R.; van der Leij, F.R. Myocardial carnitine palmitoyltransferase I expression and long-chain fatty acid oxidation in fetal and newborn lambs. *Am. J. Physiol. Heart Circ. Physiol.* **2004**, *286*, H2243–H2248. [CrossRef]
68. Eaton, S. Control of mitochondrial beta-oxidation flux. *Prog. Lipid Res.* **2002**, *41*, 197–239. [CrossRef]
69. Violante, S.; Ijlst, L.; Te Brinke, H.; Tavares de Almeida, I.; Wanders, R.J.; Ventura, F.V.; Houten, S.M. Carnitine palmitoyltransferase 2 and carnitine/acylcarnitine translocase are involved in the mitochondrial synthesis and export of acylcarnitines. *FASEB J.* **2013**, *27*, 2039–2044. [CrossRef]
70. Arduini, A.; Zammit, V. Acetate transport into mitochondria does not require a carnitine shuttle mechanism. *Magn. Reson. Med.* **2017**, *77*, 11. [CrossRef]
71. Ramsay, R.; Arduini, A. The carnitine acyltransferases and their role in modulating acyl-CoA pools. *Arch. Biochem. Biophys.* **1993**, *302*, 307–314. [CrossRef] [PubMed]
72. Davies, M.N.; Kjalarsdottir, L.; Thompson, J.W.; Dubois, L.G.; Stevens, R.D.; Ilkayeva, O.R.; Brosnan, M.J.; Rolph, T.P.; Grimsrud, P.A.; Muoio, D.M. The Acetyl Group Buffering Action of Carnitine Acetyltransferase Offsets Macronutrient-Induced Lysine Acetylation of Mitochondrial Proteins. *Cell Rep.* **2016**, *14*, 243–254. [CrossRef]

73. Bisaccia, F.; De Palma, A.; Dierks, T.; Krämer, R.; Palmieri, F. Reaction mechanism of the reconstituted tricarboxylate carrier from rat liver mitochondria. *Biochim. Biophys. Acta* **1993**, *1142*, 139–145. [CrossRef]
74. Klingenberg, M. The ADP, ATP shuttle of the mitochondrion. *Trends Biochem. Sci.* **1979**, *4*, 249–252. [CrossRef]
75. Klingenberg, M. The ADP and ATP transport in mitochondria and its carrier. *Biochim. Biophys. Acta* **2008**, *1778*, 1978–2021. [CrossRef] [PubMed]
76. Pande, S.V.; Parvin, R. Carnitine-acylcarnitine translocase catalyzes an equilibrating unidirectional transport as well. *J. Biol. Chem.* **1980**, *255*, 2994–3001. [CrossRef]
77. Longo, N.; Amat di San Filippo, C.; Pasquali, M. Disorders of carnitine transport and the carnitine cycle. *Am. J. Med. Genet. C Semin Med. Genet.* **2006**, *142C*, 77–85. [CrossRef]
78. Vaz, F.M.; Wanders, R.J. Carnitine biosynthesis in mammals. *Biochem. J.* **2002**, *361*, 417–429. [CrossRef] [PubMed]
79. Pochini, L.; Galluccio, M.; Scalise, M.; Console, L.; Indiveri, C. OCTN: A Small Transporter Subfamily with Great Relevance to Human Pathophysiology, Drug Discovery, and Diagnostics. *SLAS Discov.* **2019**, *24*, 89–110. [CrossRef] [PubMed]
80. Noland, R.C.; Koves, T.R.; Seiler, S.E.; Lum, H.; Lust, R.M.; Ilkayeva, O.; Stevens, R.D.; Hegardt, F.G.; Muoio, D.M. Carnitine insufficiency caused by aging and overnutrition compromises mitochondrial performance and metabolic control. *J. Biol. Chem.* **2009**, *284*, 22840–22852. [CrossRef]
81. Almanna, M.; Alfadhel, M.; El-Hattab, A.W. Carnitine Inborn Errors of Metabolism. *Molecules* **2019**, *24*, 3251. [CrossRef]
82. El-Hattab, A.W.; Scaglia, F. Disorders of carnitine biosynthesis and transport. *Mol. Genet. Metab.* **2015**, *116*, 107–112. [CrossRef]
83. Pande, S.V.; Parvin, R. Characterization of carnitine acylcarnitine translocase system of heart mitochondria. *J. Biol. Chem.* **1976**, *251*, 6683–6691. [CrossRef]
84. Tonazzi, A.; Indiveri, C. Chemical modification of the mitochondrial ornithine/citrulline carrier by SH reagents: Effects on the transport activity and transition from carrier to pore-like function. *Biochim. Biophys. Acta Biomembr.* **2003**, *1611*, 123–130. [CrossRef]
85. Krämer, R. Mitochondrial carrier proteins can reversibly change their transport mode: The cases of the aspartate/glutamate and the phosphate carrier. *Exp. Physiol.* **1998**, *83*, 259–265. [CrossRef] [PubMed]
86. Stappen, R.; Kramer, R. Functional properties of the reconstituted phosphate carrier from bovine heart mitochondria: Evidence for asymmetric orientation and characterization of three different transport modes. *Biochim. Biophys. Acta* **1993**, *1149*, 40–48. [CrossRef]
87. Giangregorio, N.; Tonazzi, A.; Console, L.; Indiveri, C.; Palmieri, F. Site-directed mutagenesis of charged amino acids of the human mitochondrial carnitine/acylcarnitine carrier: Insight into the molecular mechanism of transport. *Biochim. Biophys. Acta Biomembr.* **2010**, *1797*, 839–845. [CrossRef]
88. Indiveri, C.; Giangregorio, N.; Iacobazzi, V.; Palmieri, F. Site-directed mutagenesis and chemical modification of the six native cysteine residues of the rat mitochondrial carnitine carrier: Implications for the role of cysteine-136. *Biochemistry* **2002**, *41*, 8649–8656. [CrossRef]
89. Giangregorio, N.; Tonazzi, A.; Indiveri, C.; Palmieri, F. Conformation-dependent accessibility of Cys-136 and Cys-155 of the mitochondrial rat carnitine/acylcarnitine carrier to membrane-impermeable SH reagents. *Biochim. Biophys. Acta Biomembr.* **2007**, *1767*, 1331–1339. [CrossRef]
90. Fiermonte, G.; Dolce, V.; Palmieri, F. Expression in *Escherichia coli*, functional characterization, and tissue distribution of isoforms A and B of the phosphate carrier from bovine mitochondria. *J. Biol. Chem.* **1998**, *273*, 22782–22787. [CrossRef]
91. Fiermonte, G.; Paradies, E.; Todisco, S.; Marobbio, C.M.; Palmieri, F. A novel member of solute carrier family 25 (SLC25A42) is a transporter of coenzyme A and adenosine 3',5'-diphosphate in human mitochondria. *J. Biol. Chem.* **2009**, *284*, 18152–18159. [CrossRef]
92. Porcelli, V.; Fiermonte, G.; Longo, A.; Palmieri, F. The human gene SLC25A29, of solute carrier family 25, encodes a mitochondrial transporter of basic amino acids. *J. Biol. Chem.* **2014**, *289*, 13374–13384. [CrossRef]
93. Di Noia, M.A.; Todisco, S.; Cirigliano, A.; Rinaldi, T.; Agrimi, G.; Iacobazzi, V.; Palmieri, F. The human SLC25A33 and SLC25A36 genes of solute carrier family 25 encode two mitochondrial pyrimidine nucleotide transporters. *J. Biol. Chem.* **2014**, *289*, 33137–33148. [CrossRef] [PubMed]
94. Jussupow, A.; Di Luca, A.; Kaila, V.R.I. How cardiolipin modulates the dynamics of respiratory complex I. *Sci. Adv.* **2019**, *5*, eaav1850. [CrossRef] [PubMed]
95. Klingenberg, M. Cardiolipin and mitochondrial carriers. *Biochim. Biophys. Acta* **2009**, *1788*, 2048–2058. [CrossRef] [PubMed]
96. Miniero, D.V.; Cappello, A.R.; Curcio, R.; Ludovico, A.; Daddabbo, L.; Stipani, I.; Robinson, A.J.; Kunji, E.R.; Palmieri, F. Functional and structural role of amino acid residues in the matrix alpha-helices, termini and cytosolic loops of the bovine mitochondrial oxoglutarate carrier. *Biochim. Biophys. Acta* **2011**, *1807*, 302–310. [CrossRef]
97. Cappello, A.R.; Curcio, R.; Valeria Miniero, D.; Stipani, I.; Robinson, A.J.; Kunji, E.R.; Palmieri, F. Functional and structural role of amino acid residues in the even-numbered transmembrane alpha-helices of the bovine mitochondrial oxoglutarate carrier. *J. Mol. Biol.* **2006**, *363*, 51–62. [CrossRef]
98. Cappello, A.R.; Miniero, D.V.; Curcio, R.; Ludovico, A.; Daddabbo, L.; Stipani, I.; Robinson, A.J.; Kunji, E.R.; Palmieri, F. Functional and structural role of amino acid residues in the odd-numbered transmembrane alpha-helices of the bovine mitochondrial oxoglutarate carrier. *J. Mol. Biol.* **2007**, *369*, 400–412. [CrossRef]

99. Pebay-Peyroula, E.; Dahout-Gonzalez, C.; Kahn, R.; Trézéguet, V.; Lauquin, G.J.; Brandolin, G. Structure of mitochondrial ADP/ATP carrier in complex with carboxyatractyloside. *Nature* **2003**, *426*, 39–44. [CrossRef] [PubMed]
100. Robinson, A.J.; Kunji, E.R. Mitochondrial carriers in the cytoplasmic state have a common substrate binding site. *Proc. Natl. Acad. Sci. USA* **2006**, *103*, 2617–2622. [CrossRef] [PubMed]
101. Kunji, E.R.; Robinson, A.J. The conserved substrate binding site of mitochondrial carriers. *Biochim. Biophys. Acta* **2006**, *1757*, 1237–1248. [CrossRef]
102. Chinen, Y.; Yanagi, K.; Nakamura, S.; Nakayama, N.; Kamiya, M.; Nakayashiro, M.; Kaname, T.; Naritomi, K.; Nakanishi, K. A novel homozygous missense SLC25A20 mutation in three CACT-deficient patients: Clinical and autopsy data. *Human Genome Var.* **2020**, *7*, 11. [CrossRef] [PubMed]
103. Tonazzi, A.; Giangregorio, N.; Indiveri, C.; Palmieri, F. Site-directed mutagenesis of the His residues of the rat mitochondrial carnitine/acylcarnitine carrier: Implications for the role of His-29 in the transport pathway. *Biochim. Biophys. Acta Biomembr.* **2009**, *1787*, 1009–1015. [CrossRef]
104. Ruprecht, J.J.; Kunji, E.R.S. The SLC25 Mitochondrial Carrier Family: Structure and Mechanism. *Trends Biochem. Sci.* **2020**, *45*, 244–258. [CrossRef] [PubMed]
105. Ruprecht, J.J.; Kunji, E.R. Structural changes in the transport cycle of the mitochondrial ADP/ATP carrier. *Curr. Opin. Struct. Biol.* **2019**, *57*, 135–144. [CrossRef]
106. Robinson, A.J.; Overy, C.; Kunji, E.R. The mechanism of transport by mitochondrial carriers based on analysis of symmetry. *Proc. Natl. Acad. Sci. USA* **2008**, *105*, 17766–17771. [CrossRef]
107. Palmieri, F.; Pierri, C.L. Structure and function of mitochondrial carriers-role of the transmembrane helix P and G residues in the gating and transport mechanism. *FEBS Lett.* **2010**, *584*, 1931–1939. [CrossRef]
108. Pietropaolo, A.; Pierri, C.L.; Palmieri, F.; Klingenberg, M. The switching mechanism of the mitochondrial ADP/ATP carrier explored by free-energy landscapes. *Biochim. Biophys. Acta* **2016**, *1857*, 772–781. [CrossRef] [PubMed]
109. Giangregorio, N.; Console, L.; Tonazzi, A.; Palmieri, F.; Indiveri, C. Identification of amino acid residues underlying the antiport mechanism of the mitochondrial carnitine/acylcarnitine carrier by site-directed mutagenesis and chemical labeling. *Biochemistry* **2014**, *53*, 6924–6933. [CrossRef] [PubMed]
110. Giangregorio, N.; Tonazzi, A.; Console, L.; Pistillo, M.; Scalera, V.; Indiveri, C. Tryptophan 224 of the rat mitochondrial carnitine/acylcarnitine carrier is crucial for the antiport mechanism. *Biochim. Biophys. Acta Bioenerg.* **2019**, *1860*, 708–716. [CrossRef] [PubMed]
111. Monné, M.; Miniero, D.V.; Daddabbo, L.; Robinson, A.J.; Kunji, E.R.; Palmieri, F. Substrate specificity of the two mitochondrial ornithine carriers can be swapped by single mutation in substrate binding site. *J. Biol. Chem.* **2012**, *287*, 7925–7934. [CrossRef]
112. Tonazzi, A.; Giangregorio, N.; Indiveri, C.; Palmieri, F. Identification by site-directed mutagenesis and chemical modification of three vicinal cysteine residues in rat mitochondrial carnitine/acylcarnitine transporter. *J. Biol. Chem.* **2005**, *280*, 19607–19612. [CrossRef]
113. Bae, Y.S.; Oh, H.; Rhee, S.G.; Yoo, Y.D. Regulation of reactive oxygen species generation in cell signaling. *Mol. Cells* **2011**, *32*, 491–509. [CrossRef]
114. Stone, J.R.; Yang, S. Hydrogen peroxide: A signaling messenger. *Antioxid. Redox Signal.* **2006**, *8*, 243–270. [CrossRef]
115. Veal, E.A.; Day, A.M.; Morgan, B.A. Hydrogen peroxide sensing and signaling. *Mol. Cell* **2007**, *26*, 1–14. [CrossRef]
116. Schroder, E.; Eaton, P. Hydrogen peroxide as an endogenous mediator and exogenous tool in cardiovascular research: Issues and considerations. *Curr. Opin. Pharmacol.* **2008**, *8*, 153–159. [CrossRef] [PubMed]
117. Scalise, M.; Galluccio, M.; Accardi, R.; Cornet, I.; Tommasino, M.; Indiveri, C. Human OCTN2 (SLC22A5) is down-regulated in virus- and nonvirus-mediated cancer. *Cell Biochem. Funct.* **2012**, *30*, 419–425. [CrossRef] [PubMed]
118. Giangregorio, N.; Palmieri, F.; Indiveri, C. Glutathione controls the redox state of the mitochondrial carnitine/acylcarnitine carrier Cys residues by glutathionylation. *Biochim. Biophys. Acta* **2013**, *1830*, 5299–5304. [CrossRef] [PubMed]
119. Pai, H.V.; Starke, D.W.; Lesnefsky, E.J.; Hoppel, C.L.; Mieyal, J.J. What is the functional significance of the unique location of glutaredoxin 1 (GRx1) in the intermembrane space of mitochondria? *Antioxid. Redox Signal.* **2007**, *9*, 2027–2033. [CrossRef]
120. Stroher, E.; Millar, A.H. The biological roles of glutaredoxins. *Biochem. J.* **2012**, *446*, 333–348. [CrossRef]
121. Fernando, V.; Zheng, X.; Walia, Y.; Sharma, V.; Letson, J.; Furuta, S. S-Nitrosylation: An Emerging Paradigm of Redox Signaling. *Antioxidants* **2019**, *8*, 404. [CrossRef]
122. Piantadosi, C.A. Regulation of mitochondrial processes by protein S-nitrosylation. *Biochim. Biophys. Acta* **2012**, *1820*, 712–721. [CrossRef] [PubMed]
123. Doulias, P.T.; Tenopoulou, M.; Greene, J.L.; Raju, K.; Ischiropoulos, H. Nitric oxide regulates mitochondrial fatty acid metabolism through reversible protein S-nitrosylation. *Sci. Signal.* **2013**, *6*, rs1. [CrossRef]
124. Clementi, E.; Brown, G.C.; Feilisch, M.; Moncada, S. Persistent inhibition of cell respiration by nitric oxide: Crucial role of S-nitrosylation of mitochondrial complex I and protective action of glutathione. *Proc. Natl. Acad. Sci. USA* **1998**, *95*, 7631–7636. [CrossRef]
125. Zhong, H.; Yu, H.; Chen, J.; Sun, J.; Guo, L.; Huang, P.; Zhong, Y. Hydrogen Sulfide and Endoplasmic Reticulum Stress: A Potential Therapeutic Target for Central Nervous System Degeneration Diseases. *Front. Pharmacol.* **2020**, *11*, 702. [CrossRef] [PubMed]

126. Kimura, H. Physiological role of hydrogen sulfide and polysulfide in the central nervous system. *Neurochem. Int.* **2013**, *63*, 492–497. [CrossRef]
127. Olas, B. Hydrogen sulfide in signaling pathways. *Clin. Chim. Acta* **2015**, *439*, 212–218. [CrossRef]
128. Wallace, J.L.; Wang, R. Hydrogen sulfide-based therapeutics: Exploiting a unique but ubiquitous gasotransmitter. *Nat. Rev. Drug Discov.* **2015**, *14*, 329–345. [CrossRef] [PubMed]
129. Giuffrè, A.; Vicente, J.B. Hydrogen Sulfide Biochemistry and Interplay with Other Gaseous Mediators in Mammalian Physiology. *Oxid. Med. Cell Longev.* **2018**, *2018*, 6290931. [CrossRef] [PubMed]
130. Ida, T.; Sawa, T.; Ihara, H.; Tsuchiya, Y.; Watanabe, Y.; Kumagai, Y.; Suematsu, M.; Motohashi, H.; Fujii, S.; Matsunaga, T.; et al. Reactive cysteine persulfides and S-polythiolation regulate oxidative stress and redox signaling. *Proc. Natl. Acad. Sci. USA* **2014**, *111*, 7606–7611. [CrossRef] [PubMed]
131. Palmieri, E.M.; Spera, I.; Menga, A.; Infantino, V.; Porcelli, V.; Iacobazzi, V.; Pierri, C.L.; Hooper, D.C.; Palmieri, F.; Castegna, A. Acetylation of human mitochondrial citrate carrier modulates mitochondrial citrate/malate exchange activity to sustain NADPH production during macrophage activation. *Biochim. Biophys. Acta* **2015**, *1847*, 729–738. [CrossRef] [PubMed]
132. Pietrocola, F.; Galluzzi, L.; Bravo-San Pedro, J.M.; Madeo, F.; Kroemer, G. Acetyl coenzyme A: A central metabolite and second messenger. *Cell Metab.* **2015**, *21*, 805–821. [CrossRef]
133. Iacobazzi, V.; Naglieri, M.A.; Stanley, C.A.; Wanders, R.J.; Palmieri, F. The structure and organization of the human carnitine/acylcarnitine translocase (CACT1) gene. *Biochem. Biophys. Res. Commun.* **1998**, *252*, 770–774. [CrossRef]
134. Viggiano, L.; Iacobazzi, V.; Marzella, R.; Cassano, C.; Rocchi, M.; Palmieri, F. Assignment of the carnitine/acylcarnitine translocase gene (CACT) to human chromosome band 3p21.31 by in situ hybridization. *Cytogenet. Cell Genet.* **1997**, *79*, 62–63. [CrossRef] [PubMed]
135. Huizing, M.; Ruitenbeek, W.; van den Heuvel, L.P.; Dolce, V.; Iacobazzi, V.; Smeitink, J.A.; Palmieri, F.; Trijbels, J.M. Human mitochondrial transmembrane metabolite carriers: Tissue distribution and its implication for mitochondrial disorders. *J. Bioenerg. Biomembr.* **1998**, *30*, 277–284. [CrossRef]
136. Tachibana, K.; Takeuchi, K.; Inada, H.; Yamasaki, D.; Ishimoto, K.; Tanaka, T.; Hamakubo, T.; Sakai, J.; Kodama, T.; Doi, T. Regulation of the human SLC25A20 expression by peroxisome proliferator-activated receptor alpha in human hepatoblastoma cells. *Biochem. Biophys. Res. Commun.* **2009**, *389*, 501–505. [CrossRef]
137. Iacobazzi, V.; Infantino, V.; Palmieri, F. Transcriptional Regulation of the Mitochondrial Citrate and Carnitine/ Acylcarnitine Transporters: Two Genes Involved in Fatty Acid Biosynthesis and β -oxidation. *Biology* **2013**, *2*, 284–303. [CrossRef] [PubMed]
138. Iacobazzi, V.; Convertini, P.; Infantino, V.; Scarcia, P.; Todisco, S.; Palmieri, F. Statins, fibrates and retinoic acid upregulate mitochondrial acylcarnitine carrier gene expression. *Biochem. Biophys. Res. Commun.* **2009**, *388*, 643–647. [CrossRef] [PubMed]
139. Console, L.; Giangregorio, N.; Cellamare, S.; Bolognino, I.; Palasciano, M.; Indiveri, C.; Incampo, G.; Campana, S.; Tonazzi, A. Human mitochondrial carnitine acylcarnitine carrier: Molecular target of dietary bioactive polyphenols from sweet cherry (*Prunus avium* L.). *Chem. Biol. Interact.* **2019**, *307*, 179–185. [CrossRef] [PubMed]
140. Tune, B.M.; Hsu, C.Y. Toxicity of cephaloridine to carnitine transport and fatty acid metabolism in rabbit renal cortical mitochondria: Structure-activity relationships. *J. Pharmacol. Exp. Ther.* **1994**, *270*, 873–880.
141. Tonazzi, A.; Giangregorio, N.; Console, L.; Indiveri, C. Mitochondrial carnitine/acylcarnitine translocase: Insights in structure/function relationships. Basis for drug therapy and side effects prediction. *Mini Rev. Med. Chem.* **2015**, *15*, 396–405. [CrossRef]
142. Oppedisano, F.; Fanello, D.; Calvani, M.; Indiveri, C. Interaction of mildronate with the mitochondrial carnitine/acylcarnitine transport protein. *J. Biochem. Mol. Toxicol.* **2008**, *22*, 8–14. [CrossRef] [PubMed]
143. Branco, V.; Godinho-Santos, A.; Goncalves, J.; Lu, J.; Holmgren, A.; Carvalho, C. Mitochondrial thioredoxin reductase inhibition, selenium status, and Nrf-2 activation are determinant factors modulating the toxicity of mercury compounds. *Free Radic. Biol. Med.* **2014**, *73*, 95–105. [CrossRef] [PubMed]
144. McKelvey, W.; Gwynn, R.C.; Jeffery, N.; Kass, D.; Thorpe, L.E.; Garg, R.K.; Palmer, C.D.; Parsons, P.J. A biomonitoring study of lead, cadmium, and mercury in the blood of New York city adults. *Environ. Health Perspect.* **2007**, *115*, 1435–1441. [CrossRef] [PubMed]

Review

The Mitochondrial Citrate Carrier SLC25A1/CIC and the Fundamental Role of Citrate in Cancer, Inflammation and Beyond

Rami Mosaoa ^{1,2}, Anna Kasprzyk-Pawelec ¹, Harvey R. Fernandez ³ and Maria Laura Avantiaggiati ^{1,*}

¹ Department of Oncology, Georgetown University Medical Center, Washington, DC 20057, USA; rmm84@georgetown.edu (R.M.); ak1801@georgetown.edu (A.K.-P.)

² Department of Biochemistry, Faculty of Science, King Abdulaziz University, Jeddah 21589, Saudi Arabia

³ Department of Neuroscience, Georgetown University Medical Center, Washington, DC 20057, USA; Harvey.Fernandez@georgetown.edu

* Correspondence: ma364@georgetown.edu

Abstract: The mitochondrial citrate/isocitrate carrier, CIC, has been shown to play an important role in a growing list of human diseases. CIC belongs to a large family of nuclear-encoded mitochondrial transporters that serve the fundamental function of allowing the transit of ions and metabolites through the impermeable mitochondrial membrane. Citrate is central to mitochondrial metabolism and respiration and plays fundamental activities in the cytosol, serving as a metabolic substrate, an allosteric enzymatic regulator and, as the source of Acetyl-Coenzyme A, also as an epigenetic modifier. In this review, we highlight the complexity of the mechanisms of action of this transporter, describing its involvement in human diseases and the therapeutic opportunities for targeting its activity in several pathological conditions.

Keywords: SLC25A1; CIC; CTP; citrate; mitochondria; cancer; metabolism; inflammation; diabetes; 22.q11.2; NAFLD/NASH

Citation: Mosaoa, R.; Kasprzyk-Pawelec, A.; Fernandez, H.R.; Avantiaggiati, M.L. The Mitochondrial Citrate Carrier SLC25A1/CIC and the Fundamental Role of Citrate in Cancer, Inflammation and Beyond. *Biomolecules* **2021**, *11*, 141. <https://doi.org/10.3390/biom11020141>

Academic Editor:
Ferdinando Palmieri
Received: 29 December 2020
Accepted: 20 January 2021
Published: 22 January 2021

Publisher's Note: MDPI stays neutral with regard to jurisdictional claims in published maps and institutional affiliations.



Copyright: © 2021 by the authors. Licensee MDPI, Basel, Switzerland. This article is an open access article distributed under the terms and conditions of the Creative Commons Attribution (CC BY) license (<https://creativecommons.org/licenses/by/4.0/>).

1. Introduction

The mitochondrial citrate carrier SLC25A1, also known as citrate transporter protein (CTP) or citrate/isocitrate carrier (CIC), is a mitochondrial membrane transporter encoded in the nucleus by the *SLC25A1* gene located on chromosome 22q11.2. Historically, CIC was first purified and reconstituted by Palmieri [1–3] and subsequently by Kaplan [4], and as of today, it is the only known human mitochondrial transporter for citrate, which renders its activity of paramount importance. The known function of CIC consists of promoting the export of citrate or isocitrate from the mitochondria into the cytosol in exchange for malate (Figure 1). Cytosolic citrate has several fundamental functions, on one side providing the source of Acetyl-Coenzyme A (Ac-CoA) for fatty acids and sterol biosynthesis, and on the other, serving as an allosteric regulator of enzymes that control glycolysis, lipogenesis and gluconeogenesis [5,6]. The activity of phosphofructokinase (PFK), a glycolytic enzyme, is inhibited by citrate binding, while 1,6-bisphosphatase (Fbp1) and Acetyl-CoA Carboxylase Alpha (ACACA), necessary for gluconeogenesis and lipid synthesis, respectively, are activated by citrate [7–9]. We and others have shown that through reverse import activity, CIC can also promote the entry of cytosolic citrate into the mitochondria, stimulating the tricarboxylic acid (TCA) cycle and oxidative phosphorylation (OXPHOS) and maintaining redox balance through the generation of NADPH, all activities that are important for the expansion of cancer stem/initiating cells and for the anchorage-independent growth of tumor cells [10,11]. In addition, CIC is likely a mediator of the “mitochondrial-to-nucleus-cross-talk” through which metabolic adjustments originating in the mitochondria are transmitted to the nucleus and reshape the transcription program via epigenetic regulation [12]. This activity of CIC, albeit still understudied, stems from its

ability to provide Ac-CoA for acetylation reactions, to enhance the availability of TCA cycle intermediates that act as epigenetic regulators, particularly succinate, fumarate and alpha-ketoglutarate (α -KG), and to prevent the accumulation of L- and D-2-hydroxyglutaric acids, two oncometabolites that inhibit histone demethylases and are abnormally elevated when CIC activity is impaired [5].

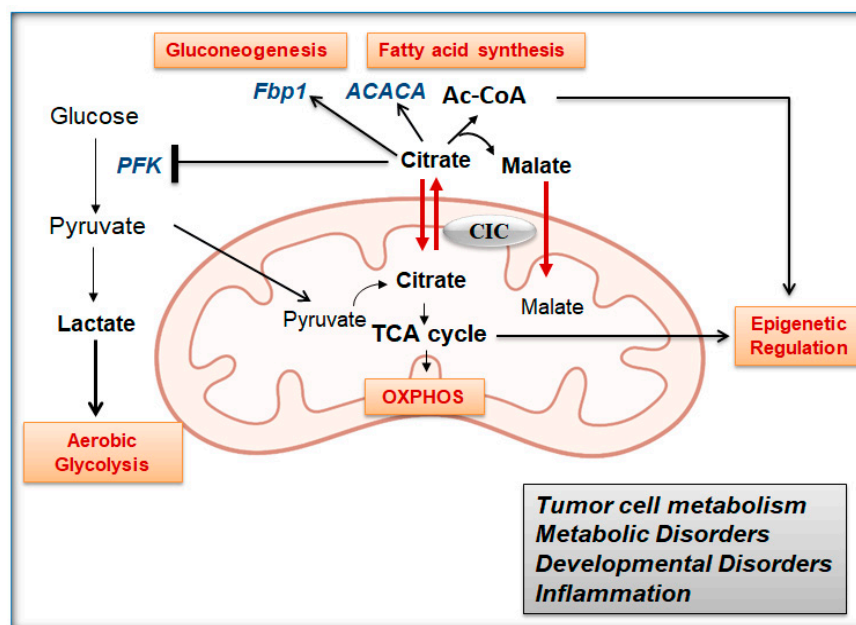


Figure 1. Preview of the activities of citrate/isocitrate carrier (CIC) (also see text for explanation).

Through all these complex functions, CIC sits at the center of the metabolic landscape of cells, serving a key role for the generation and optimal utilization of resources needed to meet the energetic demand of tissues under physiological conditions. It is, therefore, not surprising that loss of CIC is pathogenic, and in fact, mutations or mono-allelic deletions of the *SLC25A1* gene have been linked to a complex and heterogeneous spectrum of developmental diseases. Alterations of CIC activity also occur in autoimmune disorders such as rheumatoid arthritis and Bechet's disease and in Down syndrome [13,14]. Furthermore, amplifications of the *SLC25A1* gene or enhanced transcription rates are a hallmark of several cancer types as well as of metabolic disorders [15,16]. Here, we will dissect the complexity of the mechanisms of action of CIC in human diseases and rationalize the advantages of therapeutic targeting of its activities.

2. A Brief History of CIC Inhibitor Compounds

Given the involvement of CIC and of the lipogenic pathway in cancer, the development of CIC inhibitors has been at the cornerstone of the field, but not without challenges (Figure 2). The first-generation inhibitor benzenetricarboxylate (BTA) is a false and non-cleavable analog of citrate that had been widely employed in *in vitro* assays on reconstituted liposomes to block CIC transport activity [1–4].

In vivo, BTA requires very high concentrations (5 mM) and is also potentially able to interfere with the activity of other citrate-binding proteins. A second inhibitor, CTPI-1, or 4-Chloro-3-[[[3-nitrophenyl]amino]sulfonyl]-benzoic acid (CNASB), was discovered by Kaplan's group based on a homology model of *Caenorhabditis elegans* CIC. CTPI-1 is the first competitive inhibitor and was shown to interact with key residues involved in citrate binding [17]. Among these, Arg181 in yeast protein is replaced by Lys190 in human protein. Given that this residue is in the citrate binding pocket, the affinity of CTPI-1 for the human protein is not ideal, with an experimental K_D of 60 μ M, as determined with surface plasmon resonance (SPR) [10]. Accordingly, CTPI-1 also requires very high

concentrations for in vivo activity (1–2 mM). Based on this, our group undertook several approaches to optimize compounds specific for the human CIC protein, employing an in silico homology model, docking experiments and searching similar compounds in available databases, followed by SPR to characterize the interaction of purified CIC with identified candidates [10]. By exchanging the position of the chlorine atom, we identified a compound (CTPI-2, or 2-(4-Chloro-3-nitro-benzenesulfonylamino)-benzoic acid) that now exhibits an experimental K_D between 1 and 3.5 μM , a 20-fold improvement in binding activity relative to CTPI-1, and inhibits citrate transport and tumor proliferation at significantly lower doses (10–50 μM).

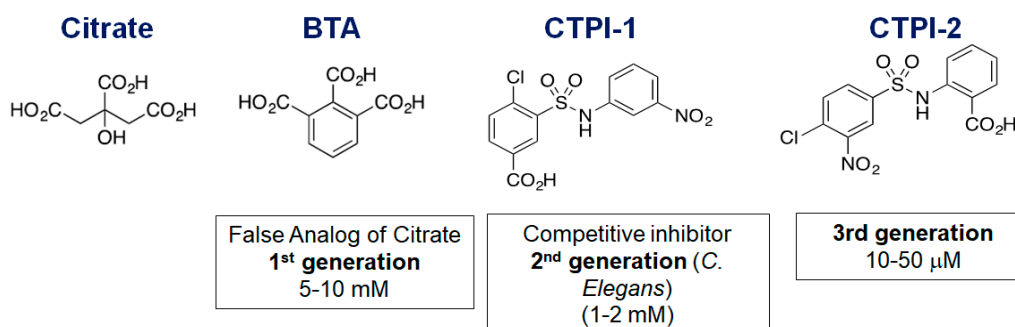


Figure 2. Comparison of the structure of CIC inhibitors. The in vivo IC_{50} is indicated for each of the compounds.

Interestingly, all of the CIC inhibitors are relatively insoluble (unpublished observations). We believe that the relative insolubility of these drugs is important for their interaction with—and transport through—the cytoplasmic and mitochondrial membranes and, thus, may be an intrinsic characteristic of this class of agents. As discussed in this review, CTPI-2 and other CIC inhibitors belong to a novel class of promising therapeutics.

3. Regulation of CIC Expression Levels: Hints on Its Biological Functions

There are several ways through which CIC activity can be engaged in cells under physiological and pathological conditions, and these often involve transcriptional regulation. Early work performed by the Palmieri group showed that the transcription rate of the CIC promoter is under the control of the master regulator of lipid anabolic pathways, sterol regulatory element-binding factor 1 (SREBP1) [18] (Figure 3), and of Forkhead Box A1 (FOXA1), which, via CIC, induces glucose-stimulated insulin secretion [19].

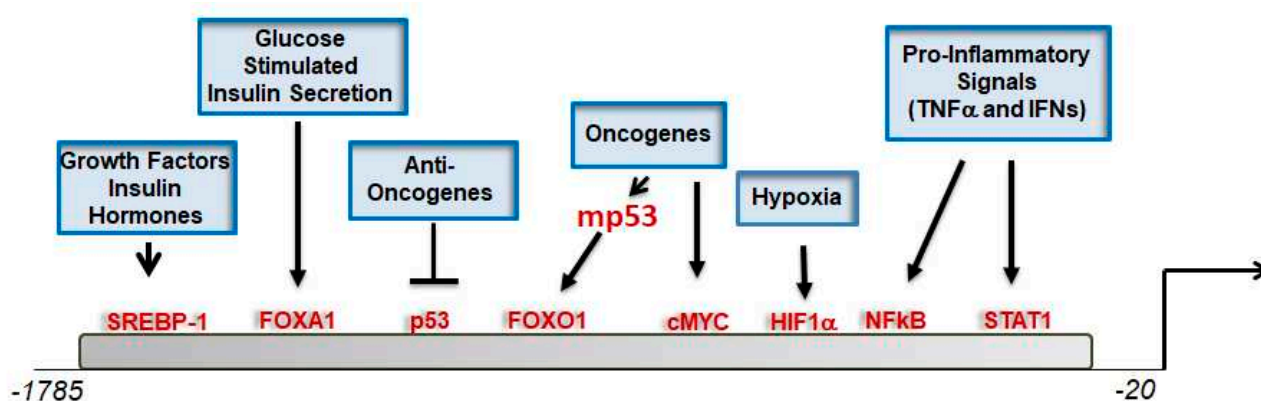


Figure 3. Schematic representation of the CIC promoter and transcription factors' binding sites (TFBSs) identified in various studies. The positions of these TFBSs are representative and do not reflect the actual position in the promoter.

The tumor suppressor p53 also interacts with the CIC promoter [20]. However, while wild-type p53 suppresses transcription, tumor-associated mutant(s) forms of p53 do not

bind to the promoter directly but are recruited therein through interaction with the transcription factor Forkhead Box O1 (FOXO1), which has very important activities in the regulation of insulin signaling, gluconeogenesis and glycogenolysis. Binding sites for the p65 subunit of nuclear factor kappa B (NF κ B) and for signal transducer and activator of transcription 1 (STAT1) promote CIC transcription in response to tumor necrosis factor alpha (TNF α) and interferon gamma (IFN γ), two important mediators of inflammation [21]. Further, the transcription factors Myc, hypoxia-inducible factor 1 alpha (HIF1 α) and peroxisome proliferator-activated receptor gamma (PPAR γ) also interact with the CIC promoter [22]. These mechanisms of activation anticipated fundamental activities of CIC in the metabolism and inflammation and suggested that this protein might provide a link between oncogenic pathways and the glucose and lipid tumor cell metabolism, as discussed below.

4. CIC Activity in Glucose and Lipid Metabolism: Implications for Metabolic Diseases

Citrate is at the cross-roads of multiple metabolic pathways (depicted in Figure 4) and it is an indispensable carbon source in both the mitochondria and the cytosol. When glucose is abundant, the majority of mitochondrial and cytosolic citrate comes from the oxidative decarboxylation of pyruvate to form Ac-CoA via the pyruvate dehydrogenase complex (PDC) and subsequent condensation of Ac-CoA with oxaloacetate to form citrate and Co-A. These reactions, coupled with the activity of pyruvate carboxylase (PC) that provides mitochondrial oxaloacetate, promote the TCA cycle and the generation of NAD⁺, NADH and FADH₂ for the electron transport chain (ETC), also allowing for CIC-mediated transport of citrate. Through the export activity, CIC is proposed to be essential for lipid and cholesterol synthesis.

In agreement with this idea, the activity of CTPI-2 and of a liver-targeted CIC knockout was recently studied in a well-established murine model of diet-induced Non-alcoholic fatty liver disease (NAFLD) and non-alcoholic steatohepatitis (NASH), the diet-induced obesity (DIO) mouse model [16]. When these mice are fed a diet enriched in starch and lard, they develop severe obesity, accompanied by hypercholesterolemia, hypertriglyceridemia, glucose intolerance, hyperglycemia and fatty liver disease, which, with time, can progress to steatohepatitis and eventually to hepatocellular carcinoma. CTPI-2 not only reverts or prevents steatosis and markedly reduces obesity, depending upon the administration schedule, but also normalizes cholesterol and triglyceride levels as well as hyperglycemia and glucose intolerance (Figure 5). Indeed, normalization of glucose metabolism is the most significant outcome of CTPI-2 treatment. A global metabolomic analysis provided strong evidence that gluconeogenesis, a key contributor to the levels of circulating glucose, is a major target pathway inhibited by CTPI-2, together with the expected inhibition of fatty acid synthesis sustained by a reduction in the Ac-CoA pool.

Another important clue derived from studying the effects of CTPI-2 *in vivo* is that the expression levels of CIC are regulated systemically by the levels of circulating glucose, being repressed by a low-glucose diet and strongly induced by a calorie equivalent, high-glucose regimen that leads to hyperglycemia. Together with the finding that CTPI-2 reverts glucose intolerance and insulin resistance, these results raise the fascinating possibility that CTPI-2 and, in general, CIC inhibitors may act as glucose-mimetic agents. These results expand the potential applicability of this class of drugs to metabolic syndrome and diabetes, which have reached epidemic proportions worldwide and are a major cause of morbidity and mortality. Studies in this direction should be very exciting.

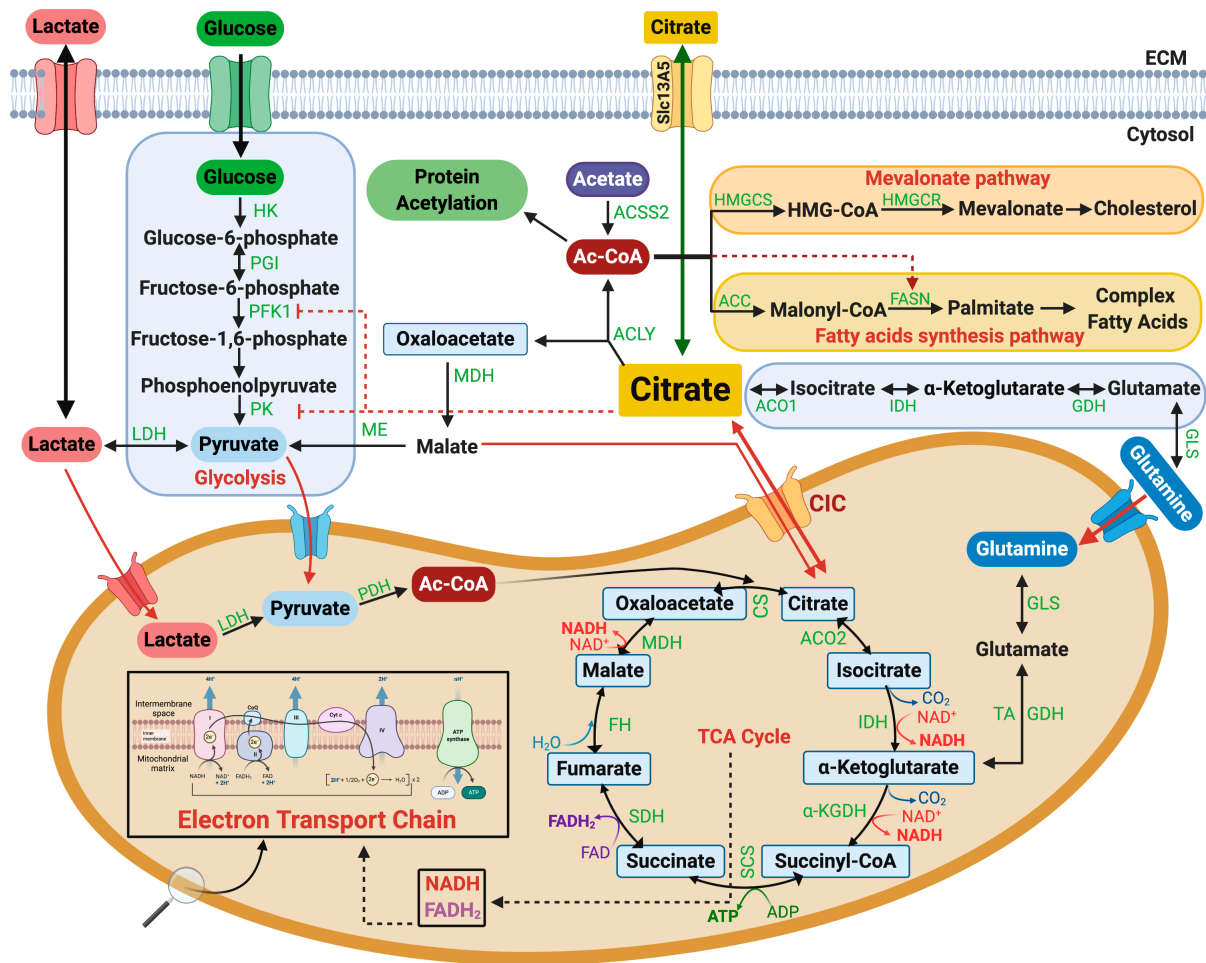


Figure 4. Pathways to the generation of cytosolic and mitochondrial citrate and its utilization. Glucose-derived citrate is obtained through the conversion of glucose to glucose-6-phosphate, which, with a series of enzymatic reactions, is then converted to pyruvate. Pyruvate is reduced to lactate via lactate dehydrogenase (LDH) or, alternatively, transported into mitochondria to produce Acetyl-Coenzyme A (Ac-CoA) via pyruvate dehydrogenase (PDH). Citrate synthase then catalyzes the condensation of acetyl-CoA with oxaloacetate to yield citrate that is exported in the cytosol by CIC. Lactate can also enter the mitochondria and be converted to pyruvate by a mitochondrial lactate dehydrogenase (mtLDH) regenerating citrate. Mitochondrial citrate and, to a lesser extent, lactate fuel the tricarboxylic acid (TCA) cycle and the electron transport chain (ETC). Citrate can also be uptaken from the extracellular space and transported to the cytosol via SLC13A5. In the cytosol, citrate provides Ac-CoA via ATP citrate lyase (ACLY) for protein acetylation and can enter the mevalonate pathway for cholesterol biosynthesis mediated by hydroxymethylglutaryl-CoA synthase (HMGCS) and hydroxy-3-methylglutaryl-CoA reductase (HMGCR) and the fatty acid synthetic pathway via acetyl-CoA carboxylase (ACC) and fatty acid synthase (FASN). Cytosolic Ac-CoA can be also generated by acetyl-CoA synthetase 2 (ACSS2) which converts acetate derived from deacetylation reactions to acetyl-CoA. Cytosolic citrate inhibits phosphofructokinase 1 (PFK1) and pyruvate kinase (PK), thus playing an active role in controlling glycolytic flux. An alternative source of mitochondrial or cytosolic citrate is supplied by reductive carboxylation of alpha-ketoglutarate to isocitrate, mediated in the cytosol by isocitrate dehydrogenase 1 (IDH1) and in the mitochondria by IDH2. Additional abbreviations: HK—hexokinase; G6PD—glucose-6-phosphate dehydrogenase; 6PGL—6-phosphogluconolactonase; 6PGD—6-phosphogluconate dehydrogenase; Rpi—ribose-5-phosphate isomerase; PGI—phosphoglucose isomerase; ME—malic enzyme; MDH—malate dehydrogenase; CS—citrate synthase; ACO2—aconitase 2; IDH—iso-citrate dehydrogenase; α -KGDH— α -Ketoglutarate dehydrogenase; SCS—succinyl coenzyme A synthetase; SDH—succinate dehydrogenase; FH—fumarase; ACO1—aconitase 1; GHD—glutamate dehydrogenase; GLS—glutaminase.

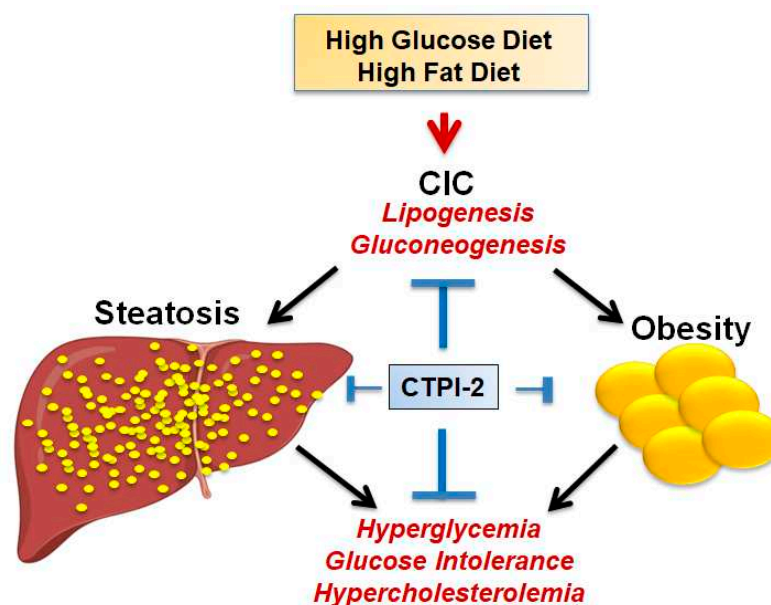


Figure 5. Schematic representation of some of the salient effects of CTPI-2 in the non-alcoholic fatty liver disease/non-alcoholic steatohepatitis (NAFLD/NASH) model.

Interestingly however, the knockout of the *SLC25A1* gene targeted to the liver through an Albumin/Cre-regulated promoter (L-CIC-KO) only partially recapitulates the effects of CTPI-2. While CTPI-2 completely normalizes the biochemical and histological characteristics of DIO mice in the liver, adipose tissue and systemically, in the liver of the CIC-KO mice, steatosis is reduced but not completely blunted. There are two non-mutually exclusive possible explanations for this result. The first is that the beneficial effects of CTPI-2 rely upon inhibition of CIC systemically and not only in the liver but, at the very least, also in the adipose tissue, which is a key contributor to the metabolic alterations observed in NAFLD/NASH. These beneficial effects might also rely upon induction of weight loss by CTPI-2. Testing of this hypothesis will require the generation of additional mouse models harboring the *Slc25a1* gene knockout also in the adipose tissue. An alternative possibility is that when the knockout of CIC is imposed during embryogenesis and development, as in the case of the Albumin/Cre-regulated promoter for the induction of the L-CIC-KO, there is a strong selective pressure for compensation to loss of CIC.

5. Is CIC Rate Limiting for De Novo Lipid Synthesis?

As shown in Figure 4, there are at least three CIC-independent pathways for providing cytosolic citrate or the universal precursor for de novo fatty acid synthesis, Ac-CoA. Acyl-CoA synthetase short-chain family member 2, *ACSS2*, converts acetate derived from deacetylation reactions to acetyl-CoA. There is evidence that *ACSS2* enriches the Ac-CoA pool, directing it to fatty acid and phospholipid synthesis in conditions of metabolic stress [23,24].

Several groups have also reported on the importance of plasma membrane citrate transporters (PMCTs), which uptake citrate from the extracellular space to enrich the cytosolic pool and display a tissue-specific pattern of expression. These transporters differ from CIC not only structurally, but also because they operate in a Na⁺- or K⁺-dependent manner. Interestingly, an alternatively spliced product of CIC itself, membrane CIC (mCIC), can serve this function, especially in the prostate [25,26]. The *SLC13A5* transporter, the human counterpart of the *fly* gene *I'm not dead yet* (*INDY*), is the most relevant PMCT as it is widely expressed in many tissues [27,28]. Extracellular citrate is derived from the liver and renal catabolism, and also through nutritional intake and bone remodeling, and is present in the plasma at very high—but homeostatically regulated—concentrations. It is possible that the activity of this transporter contributes to the cytosolic pool of citrate. Consistent with

this idea, similarly to CIC, SLC13A5 is upregulated in diet-induced NAFLD/NASH and its inhibition prevents some of the pathological hallmarks of this disease [28]. Moreover, SLC13A5 is induced in DIO livers treated with CTPI-2, coinciding with a reduction in the concentration of serum citrate, thus suggesting that this protein can provide a mechanism of compensation when CIC is inhibited [16]. With this in mind, combinatorial therapy with CTPI-2 and SLC13A5 inhibitors (e.g., gluconate [29]) is likely to be more effective than treatment with either agent alone in NAFLD/NASH.

Last but not least, an important mode of replenishing the cytosolic citrate pool has been described by DeBerardinis' group and occurs in tumor cells with defective mitochondria that cannot derive citrate from glucose via mitochondrial oxidative metabolism [30]. In cells with defective respiratory complex activities, glucose is diverted towards lactic acid production and glutamine provides the source of citrate. This pathway involves the reductive carboxylation of glutamine-derived α -KG to citrate via the action of isocitrate dehydrogenase 1 (IDH1) in the cytosol or of IDH2 in the mitochondria (Figure 4). This alternative source of citrate comes into play not only as an adjustment to defective mitochondrial oxidative capacity but also during hypoxia and in response to stress signals that generally alter the ratio between α -KG and citrate [31,32]. Recent work, also from DeBerardinis' group, demonstrates that reductive carboxylation provides a source for lipid synthesis in cancer cells when CIC is inactivated via RNA interference, pointing to reductive carboxylation as a potential mechanism of compensation for CIC deficiency as well [33]. Furthermore, in children affected by DiGeorge syndrome sustained by hemizygous loss of the 22q11.2 chromosome, a CIC loss-of-function metabolic/mitochondrial signature was identified but was hallmarked by an increase in reductive carboxylation and enhanced α -KG levels associated with increased concentrations of 2-hydroxyglutaric acid, cholesterol and fatty acids—highly indicative of compensation through this pathway [34].

Based on these lines of evidence, it seems unlikely that CIC is rate-limiting for lipid and sterol biosynthesis or for other cytosolic functions related to citrate in all situations. It is possible that the opportunities for compensation of CIC activity through the above-mentioned pathways are tissue-specific, are dictated by the impending selective pressure for compensation (embryogenesis/development vs. post-natal life) and differ depending upon the nutritional/metabolic environment and the duration of such inhibition (chronic vs. acute). Whether the lipid synthetic pathway is altered in children harboring loss-of-function mutations of the *SLC25A1* gene and correlates with the severity of the clinical manifestations is a very important question that is still unanswered.

6. Pro-Oncogenic Activities of CIC, the Reversal of the Warburg Effect and the Phenomenon of Metabolic Addiction

For many years, the field of tumor cell metabolism has been pervaded by the assumption that mitochondria are dysfunctional in cancer cells and that tumors depend upon glycolysis for growth. The Warburg effect, described by Otto Warburg in 1920, is based upon the observation that cancer cells avidly uptake glucose and direct it towards fermentation to lactate in the cytosol, even at high oxygen concentration, rather than to complete oxidation in the mitochondria, a much more efficient pathway for ATP generation. This is, of course, the basis for positron emission tomography, or PET scans. However, two important concepts have emerged in recent years. First, the lactate generated through glycolysis can fuel the TCA cycle and mitochondrial oxidative phosphorylation [35], and therefore, glycolysis is not mutually exclusive with OXPHOS as these pathways can operate simultaneously in tumor cells. Second, and equally importantly, tumors contain metabolically heterogeneous populations of cells that utilize different branches of the metabolism depending upon proliferation rates as well as upon the “geographical” location of cells within tumors which, due to the irregularity of the tumor vasculature, are exposed to hypoxia and have less access to nutrients. This heterogeneity has not only been shown *in vitro* but also in patients affected by lung cancer and glioblastoma [36,37].

Several lines of evidence have demonstrated that CIC supports the outgrowth of cancer cells, yet the pro-proliferative activity of CIC relies upon promotion of OXPHOS

and blunting of glycolysis, presumably due to the negative feedback loop that cytosolic citrate provided by CIC imposes on PFK [10,15,33]. Indeed, a consequence of CIC inhibition, genetically or pharmacologically, is impairment of mitochondrial oxidative capacity, reduction in mitochondrial-derived ATP output, accumulation of reactive oxygen species (ROS) and reduced abundance of TCA cycle intermediates. How CIC influences OXPHOS is still not entirely clear, but such regulation might occur at least in part due to promotion of malate entry into the mitochondria, in turn leading to increased TCA cycle flux and generation of adequate ratios of reducing equivalents, including NADH/NAD⁺, for the electron transport chain. In addition, the reverse import activity of cytosolic citrate via CIC can also promote mitochondrial oxidative metabolism through similar mechanisms.

Oxidative phosphorylation also provides a mechanism of resistance and adaptation to various stress conditions, as well as to chemotherapeutic agents and radiotherapy (Figure 6). In lung, prostate and glioblastoma cancer cells, CIC inhibition results in compromised mitochondrial oxidative capacity and oxidative stress and leads to increased sensitivity to radiation therapy [38,39]. Similarly, cancer cells resistant to platinum-derived agents or to Epidermal Growth Factor Receptor (EGFR), inhibitors develop an addiction to CIC-mediated promotion of mitochondrial respiration, and inhibition of CIC leads to synthetic lethality [10]. These therapy-resistant populations have characteristics of cancer stem cells and acquire markers of dormancy in a mitochondrial respiration-dependent manner. CIC allows these cells to survive therapeutic attacks in a paradoxically high energetic state. These results are in agreement with the idea that the cancer stem cell population provides a reservoir of cells left behind by conventional therapies and suggest that inhibition of CIC can be exploited as a therapeutic strategy to specifically target and eradicate therapy-resistant cells. Furthermore, CIC-dependent mitochondrial oxidative metabolism and redox balance provide a mechanism of adaptation and survival when tumor cells are challenged by limiting concentrations of glucose or must overcome addiction to the extracellular matrix and adapt to anchorage-independent growth [11,15], which is fundamental for the invasive and metastatic behavior of tumor cells.

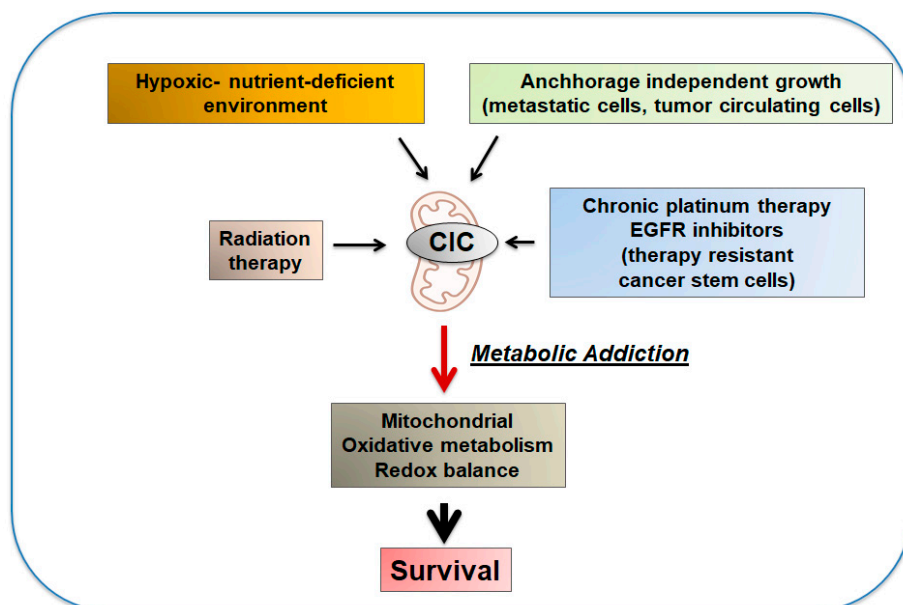


Figure 6. Involvement of CIC-dependent mitochondrial oxidative metabolism in adaptation to stress (see text for explanation).

In essence, these observations indicate that there is a therapeutic opportunity for targeting CIC activity, particularly in stress growth conditions and in cancer cell populations (e.g., cancer stem cells, therapy-resistant cells and metastatic, circulating tumor cells) that develop a strong dependency upon this protein and mitochondrial oxidative metabolism for

survival. Although, as discussed above, there are many mechanisms that could compensate for CIC inhibition, especially because the metabolism of tumors is endowed with a high degree of heterogeneity and plasticity, cancer cells that have evolved to employ CIC for survival might develop a “metabolic addiction” to CIC and, thus, will not so quickly or easily surrender its activity. This phenomenon parallels the well-known oncogene addiction whereby tumor cells that have acquired oncogenic potential through the action of one driver oncogene remain dependent upon that oncogene to maintain their proliferative capacity, in spite of the accumulation of other complex genetic alterations. This is an attractive possibility that deserves further scrutiny.

7. CIC Inhibition Inhibits the Growth of Different Tumor Types

Given the large body of literature demonstrating a role of CIC in various malignancies, here, we summarize the results of these studies and we group them by tissue/tumor type.

CIC activity has been studied by several groups in breast cancer. CIC mRNA levels are generally elevated in breast cancer cells, particularly in triple-negative breast cancer cell lines (TNBC) [15]. Furthermore, CIC overexpression is associated with metastatic disease and poor patient prognosis [40]. In the MBA-231 TNBC cell line, which has high levels of CIC, the introduction of a CIC dominant negative mutant protein that competes with endogenous CIC or treatment with BTA or CTPI-1, leads to reduction in tumor size in vivo and in proliferation in vitro [15,41]. The effects of CIC inhibition were shown to be dependent upon changes in histone acetylation, mitochondrial dysfunction and ROS production. Targeting ACLY also effectively inhibits breast tumorigenesis [41].

In colorectal cancer (CRC), the expression levels of CIC were found to be upregulated by PPAR γ coactivator 1 α (PGC1 α) and correlated with enhanced OXPHOS, TCA cycle flux and with de novo lipogenesis [42]. In this context, PGC1 α promotes tumor growth and loss of PGC1 α leads to a reduction in CIC and ACLY expression and to blunting of tumor growth, an effect recapitulated by inhibition of fatty acid synthesis. These studies reveal a strong connection between CIC and PGC1 α and lead to the proposal that the activity of PGC1 α on mitochondrial and lipid metabolism is mediated, at least in part, via CIC. Intriguingly, independent experiments in vivo where rats were injected with CRC cell lines revealed that a combination chemotherapy frequently used for the treatment of CRC (Irinotecan combined with 5-fluorouracil) has a prominent impact on adipose tissue, causing adipocytes to decrease in size [43]. This effect was correlated to reduced expression of proteins involved in fatty acid synthesis, including CIC, and in the esterification of fatty acids. This observation implies that CIC is also relevant to the loss of adipose tissue mass that occurs during chemotherapy.

CIC upregulation via PGC1 α was also found in liver cancer cell lines (HCC) [44,45]. Higher citrate flux from mitochondria into the cytosol was reported in the hepatoma cell lines MH-3924A and Hepa-6 compared to normal liver cells, as well as in HEPG2 cells. Poolsri and colleagues showed that treatment of HepG2 or of another HCC cell line, HuH-7, with the CIC inhibitor CTPI-1 and with the SLC13A5 inhibitor (PMCTi) leads to significant reduction in cell viability [46]. However, this combination is non-toxic to primary normal human hepatocytes but, nevertheless, acts synergistically in promoting apoptosis, paralleled by inhibition of fatty acid biosynthesis compared to each inhibitor alone. This result is in agreement with the possibility that in the liver, combined inhibition of CIC and SLC13A5 provides a therapeutic benefit.

Recent studies have shown that in patients affected by papillary thyroid carcinoma (PTC), the long non-coding RNA for association with Brahma, (lncBRM), is significantly upregulated, correlating with poor overall survival [47]. lncBRM targets CIC activity via the microRNA miR-331-3p and promotes PTC cell proliferation, migration and invasion, an effect that is rescued by inhibiting CIC. These results suggest that also non-coding RNAs can regulate CIC expression or activity.

Reprogramming towards the citrate-mediated lipogenic pathway is a hallmark of prostate cancer. Recent studies have shown that prostate cancer cells exhibit elevated

levels of citrate and display enhanced uptake of fatty acids, particularly at a metastatic stage [48–50]. Inhibition of cluster of differentiation 36 (CD36), which promotes fatty acid uptake, or of CIC, leads to suppression of cancer progression. As mentioned previously, CIC expression was also found to be increased in prostate cancer cells under conditions of cycling hypoxia/re-oxygenation stress, and its inhibition results in increased sensitivity to radiation therapy. These effects were connected to reduced mitochondrial oxidative capacity, generation of ROS and impaired DNA repair capacity [38].

Viewed together with the evidence discussed before (Section 6), these multiple studies highlight that CIC is essential for the growth and proliferation of different cancer types and underscore the potential importance of advancing CIC inhibitors to the clinical setting, where they are likely to be most effective in combinatorial therapies.

8. CIC and Citrate Are Important Mediators of Inflammation

Since the 19th century, inflammation has been considered a key promoter of many human diseases, including cancer, playing a role in as many as 20% of all tumors in humans [51,52]. As of today, there are several lines of evidence suggesting that CIC may fuel inflammation [53].

CIC was shown to be induced in monocytes/macrophages by lipopolysaccharides (LPS) and in the U937 monocytic cell line by $\text{TNF}\alpha$ and $\text{IFN}\gamma$ [21] (Figure 7). This activation occurs via $\text{NF-}\kappa\text{B}$ and STAT1 and leads to an increase in the cytosolic pool of citrate used for de novo fatty acid synthesis. Inhibition of CIC with CTPI-1 or with interfering RNAs leads to reduction in citrate export and depletion of pro-inflammatory prostaglandin E2 (PGE2), which is derived through Ac-CoA metabolism, and also of nitric oxide (NO), an important mediator of the inflammatory response. Subsequent studies showed that ACLY also promotes pro-inflammatory changes in macrophages through mechanisms similar to those shown for CIC [54]. Given that ACLY consumes citrate to provide Ac-CoA, the involvement of this protein underscores the importance of the lipid synthetic pathway in this reprogramming and, likely, also of epigenetic modifications induced via acetylation. The expression levels of CIC and ACLY were subsequently found to be increased in cytokine-stimulated natural killer (NK) cells [55], suggesting that similar activities of CIC may take place in other immune cell populations.

Based on the above mentioned studies, important targets of CIC pro-inflammatory activities are macrophages. This was later corroborated in murine models of NAFLD/NASH [16]. Inflammation is a major driver of pathology in this disease, eventually responsible for the evolution to irreversible fibrosis driven by remodeling of the extracellular matrix under the constant insults propelled by pro-inflammatory signals [56]. Macrophages and, particularly, the M1 population are at least in part responsible for these alterations [57]. M1 macrophages produce both pro-inflammatory and immuno-stimulatory cytokines, particularly interleukin (IL)-12, IL-6, IL-1 α , $\text{TNF-}\alpha$ and IL-1 β , and create an environment that is microbicidal in the context of the innate immune response and leads to cell death. The alternative M2 pathway of activation plays an important role in tissue repair and homeostasis. M2 macrophages produce IL-10, mitogens and fibronectin and deplete the environment of L-arginine via induction of Arginase-I, which is required for T cell functions. In patients with NASH, resident and recruited macrophages in the liver as well as recruited macrophages in the adipose tissue contribute to the production of local and systemic $\text{TNF-}\alpha$ and IL-6, two important mediators of inflammation. In the murine model of this disease, inhibition of CIC with CTPI-2 results in lower serum levels of IL-6, $\text{TNF}\alpha$ and monocyte chemoattractant protein 1 (MCP1), concomitant with an increase in cytoprotective IL-10 and IL-4 [16]. Moreover, CTPI-2 leads to reduced macrophage recruitment in the liver, but more prominently so in the adipose tissue, as well as suppression of markers of the M1 phenotype and attenuation of the levels of tissue-damaging cytokines, particularly iNOS and $\text{TNF}\alpha$, while not affecting or moderately increasing markers of M2 activation [16]. These lines of evidence argue—but do not prove, yet—that CIC contributes to the polarization of macrophages towards a pro-inflammatory M1 phenotype and raise the important question as to whether such reprogramming occurs via CIC-induced

epigenetic modifications. Given that inflammation is an important driver of oncogenesis, it is further possible that this activity of CIC also contributes to tumor proliferation.

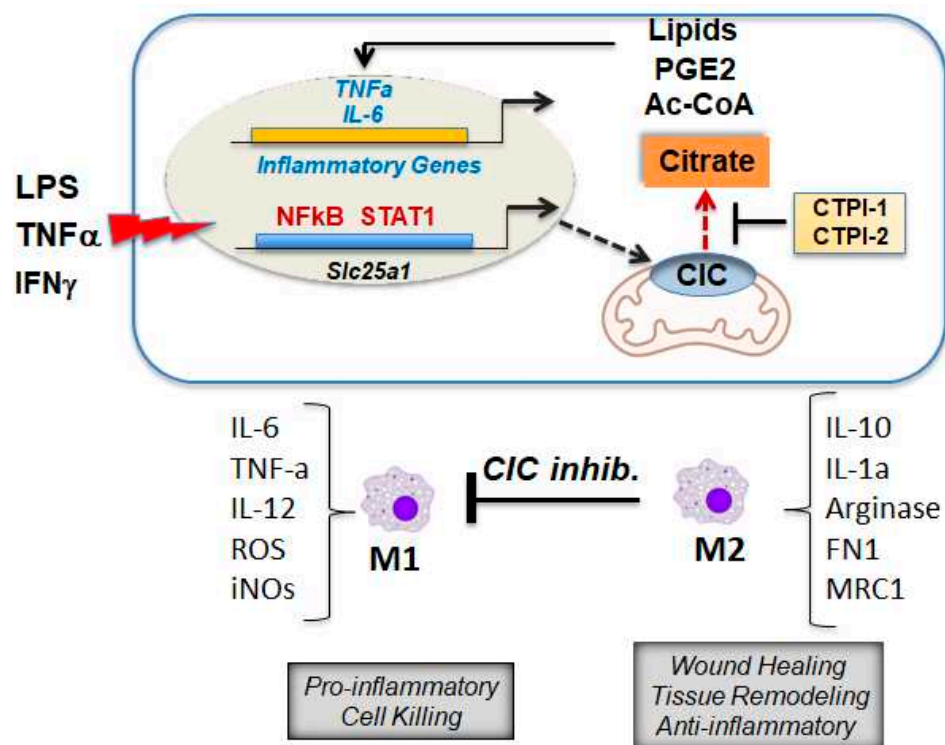


Figure 7. CIC induces a pro-inflammatory program in macrophages (see text for explanation). The transcription rate of the *SLC25A1* gene is induced in monocytes by lipopolysaccharides (LPS), tumor necrosis factor alpha (TNF α) and interferon gamma (IFN γ) via recruitment to the promoter of nuclear factor kappa B (NF κ B) and signal transducer and activator of transcription 1 (STAT1). CIC induction in these situations leads not only to the expected increase in Ac-CoA but also to enhanced synthesis of prostaglandin E2 (PGE2) and inducible nitric oxide synthetase (iNOS). At the bottom of the figure, there is a simplistic representation of the macrophage populations depicted in the two opposite phenotypes, M1 and M2. In the NAFLD/NASH liver, CIC inhibition represses markers of the pro-inflammatory macrophage phenotype. Abbreviations that are not in the main text: reactive oxygen species, ROS; iNOS, inducible nitric oxide synthase; FN1, fibronectin 1; MRC1, Mannose Receptor C-Type 1.

On the more speculative side, while the finding that CIC is under the control of NF κ B and STAT1 highlights its involvement as a mediator of inflammation, it also suggests that CIC might be connected to the innate anti-viral immune response, especially considering the prominent role of STAT1 in the regulation of this pathway. Interestingly, various citrate derivatives were shown to elicit anti-pathogen defenses providing protection not only from microbial but also from viral infections [58]. We posit that even though CIC has thus far been linked to cancer, developmental diseases and metabolic disorders, it is unlikely that the pro-inflammatory activities of CIC have been selected during evolution to sustain pathological conditions that often result in death. From an evolutionary point of view, this would make no sense. It is possible, instead, that there is a physiological role of CIC in the pro-inflammatory arm of the innate immune response and that such activity is aberrantly co-opted in disease states sustained by this protein.

9. Loss of CIC during Embryogenesis and Development: The L-and D-2HGA “Affair”

Alterations in the *SLC25A1* gene play a role in the pathogenesis of various developmental disorders, as recently reviewed by Palmieri and colleagues [5]. Heterozygous

SLC25A1 gene deletions are associated with congenital 22q11.2 microdeletion syndromes, namely Velo-Cardio-Facial and DiGeorge syndromes [59,60]. This is a group of disorders characterized by cleft palate, heart abnormalities, recurrent infections and autoimmunity, craniofacial and palate abnormalities and developmental and intellectual delay. Although only one copy of the *SLC25A1* gene is lost in 22q11.2 deletion syndrome, together with 30–40 other genes, a reduction in CIC levels in zebrafish (*Danio Rerio*) leads to abnormal morphant development in a dose-dependent manner, thus suggesting that reduced *SLC25A1* allele dosage is indeed pathogenic [15,61,62]. However, importantly, 22q11.2 microdeletion syndrome is survivable and affected individuals can have long life expectancy when severe heart abnormalities do not complicate the disease.

Various *SLC25A1* missense or truncating mutations spanning throughout the coding region have been reported as either homozygous or compound heterozygous in a heterogeneous group of developmental disorders and in D-2-/L-2-hydroxyglutaric aciduria [5,63–68]. Some of these compound mutations lead to a more complete and severe loss of CIC activity relative to 22.q11.2 deletion syndromes and are accompanied by a broader clinical spectrum of manifestations, which includes various craniofacial abnormalities (facial dysmorphism and macro/microcephaly), brain abnormalities, epilepsy, respiratory insufficiency and encephalopathy. A variable degree of metabolic dysfunction is seen in the affected individuals, represented by lactic acidosis, urinary excretion of TCA cycle intermediates (fumarate, succinate and α -KG) as well as of two metabolites, D2-L2 hydroxyglutaric acids (D-L-2HG). In addition, defects in respiratory complex subunits have been occasionally described in patients harboring *SLC25A1* gene mutations [67]. This clinical spectrum of manifestations together with lactic acidosis and the alterations of the TCA cycle are hallmarks of mitochondrial dysfunction and point to the possibility that diseases sustained by CIC deficiency should be re-classified as mitochondrial disorders.

Whilst the accumulation of TCA cycle intermediates downstream of citrate/isocitrate can be explained by the lack of the only mechanism of export of citrate away from the mitochondria, namely CIC (Figure 8), an important question in the context of these disorders regards both the origin and the significance of the D-2-/L-2-hydroxyglutaric aciduria (D-L-2HGA).

Individual L- or D-2HGAs are severe developmental disorders caused by mutations in L2-hydroxyglutarate dehydrogenase (*L2HGDH*) or D-2-hydroxyglutarate dehydrogenase (*D2HGDH*) that eliminate L2- or D2-HG, respectively. Neomorphic mutations of *IDH2* that convert α -KG to D-2HG can also cause 2HGA [69,70]. However, combined D-L-2-HGA is only sustained by *SLC25A1* gene mutations, with an apparent preference for D-2HG accumulation in all body fluids. Combined L-D-2HGA was already suspected as a distinct clinical entity by the Jakobs group before alterations of the *SLC25A1* gene were discovered as the cause of the disease [71].

The first attempt to classify these disorders came from the seminal work of the Salomons group that retrospectively examined a number of patients presenting with various degrees of pathological manifestations [72], reviewed in [5]. The most important outcome of this analysis is that there is a clear correlation between the extent of loss of the citrate export activity of CIC—which differs depending upon the affected amino acid—and the severity of the clinical course, as well as life expectancy. Noticeably, the most severe phenotype is seen with the compound heterozygous mutations p.A9Profs*82 and p.P45L, which have been described in several affected patients. p.A9Profs*82 results in a truncated protein, while P45 maps to the region involved in mitochondrial translocation, likely displacing CIC from the mitochondria and resulting in more severe complete loss of mitochondrial activities compared to other mutations. This allele combination is likely to recapitulate a nearly complete null phenotype. Children carrying these mutations display the most severe and earliest onset spectrum of clinical manifestations, culminating in early death [65,66]. These comprise craniofacial abnormalities and facial dysmorphism, microcephaly as well as hallmarks of mitochondrial dysfunction including encephalopathy, myopathy, respiratory insufficiency, lactic acidosis and accumulation of TCA cycle intermediates. However,

whether these clinical manifestations are actually connected to accumulation of L-D-2HGs is still not entirely clear. For example, in two siblings harboring the p.A9Profs*82 and p.P45L alleles, only one displayed very high levels of 2-HGs, while in serial measurements performed in the second sibling, 2-HGs levels were near-normal or moderately elevated, yet the clinical course was similarly devastating in both patients [65]. In other instances of *SLC25A1* gene mutations, the levels of L-D-2HGs have been reported either as very high or only moderately or inconsistently increased. Therefore, an important question is whether in some situations, accumulation of 2-HGs is an innocent bystander alteration of CIC inactivation, while in others, the contribution of additional factors exacerbates the extent of 2-HGA and the associated pathology. Development of molecular biomarkers for 2HG activities (e.g., alterations in methylation patterns) is also needed to overcome the shortcomings of snapshot measurements of these metabolites in hardly accessible biological fluids (e.g., cerebrospinal fluid or intracellular space).

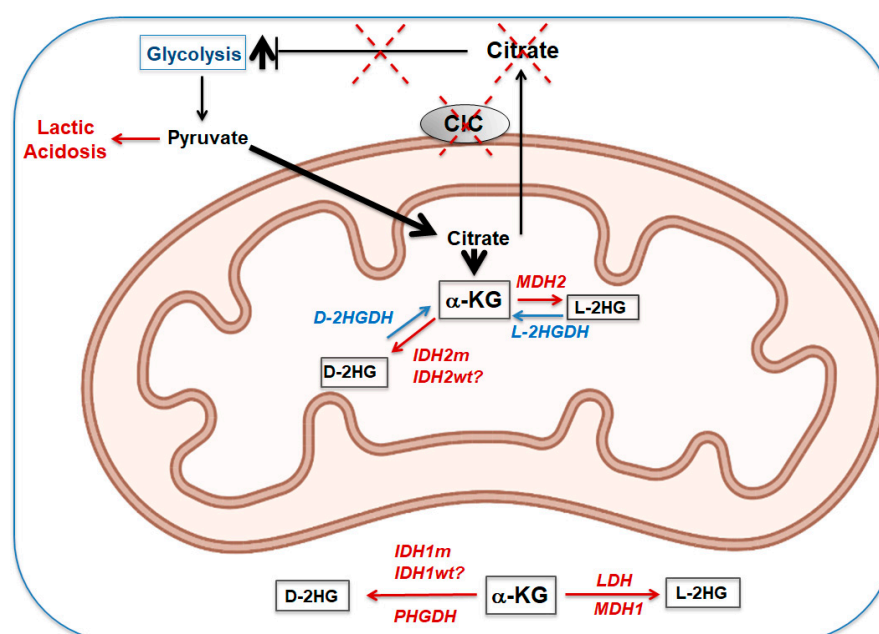


Figure 8. Mitochondrial and cytosolic pathways leading to D2-L2 hydroxyglutaric acid (D-L-2HG) accumulation (see text for explanation). The proposed model envisions that as a consequence of disruption of CIC-mediated citrate export activity, cytosolic citrate is reduced, leading to loss of the feedback loop on PFK. This leads to enhanced glycolysis and production of pyruvate, which, on one side, is converted to lactate, resulting in lactic acidosis. Excess pyruvate also enters mitochondria, where it is converted to citrate/isocitrate. Due to a lack of the export activity of CIC, this excess citrate is converted to TCA cycle intermediates downstream of citrate, leading to accumulation of α -KG and also of succinate, fumarate and malate (not shown in the figure), which are then secreted in urine. In red are the potential steps for conversion of α -KG to L-2HG or D-2HG, by either IDH1 or IDH2; in blue are the enzymes involved in the degradation pathway. IDH1/IDH2m or wt: mutant or wild-type forms of these enzymes. See text for additional abbreviations.

The reason why cells where CIC is inactive accumulate 2HGs is also not entirely clear (see Figure 6). Wild-type IDH1 and IDH2 have been reported to produce low levels of 2-HGs under reductive carboxylation conditions [73], raising the possibility that this mechanism comes into play in these disorders. Alternative sources of 2-HGs are the promiscuous activities of malate or lactate dehydrogenase (MDH1/2 and LDH, respectively), impaired activity of L2- or D2-HGDHs due to excess substrate(s) or altered redox balance [69,74,75]. Reduced concentrations of malate and increased levels of NADH, hypoxia or metabolic acidosis due to enhanced lactic acid concentrations can all favor the promiscuous activity

of MDH2 or LDH [73]. Furthermore, 3-phosphoglycerate dehydrogenase (PHGDH) can also catalyze the NADH-dependent reduction of α -KG to D-2HG [76].

It is noticeable that all these routes for the accumulation of 2-HGs involve α -KG, and therefore, understanding and targeting the pathways leading to α -KG accumulation or the enzymes involved in its conversion to 2-HGs should provide important strategies to ameliorate L-D-2HGA. Based on these considerations, here, we pose several questions, the answer to which, we believe, should advance this field forward:

1. What levels of L-D-2HG in the context of *SLC25A1* gene deficiency are to be considered pathogenic?
2. Given that L- or D-HGs interfere with α -KG-dependent dioxygenases and affect methylation of histones and DNA, are alterations in L-D-2HG levels reflected in changes in the epigenetic landscape of CIC-deficient cells?
3. What is the origin of L-D-2HG accumulation in CIC-deficient cells?
4. Can correction of α -KG levels normalize any of the pathological manifestations seen in children with CIC deficiency?
5. Are there differences in the lipid synthetic pathway in diseases sustained by CIC deficiency that aggravate the clinical manifestations?
6. Is the multi-organ involvement seen in severe CIC deficiency syndromes due to systemic alterations (e.g., changes in circulating levels of TCA cycle intermediates, accumulation of toxic byproducts of the metabolism and elevated levels of 2-HGs) or to loss of tissue-specific activities of CIC?

Though many of the pathological manifestations due to CIC deficiency are acquired during embryogenesis and development and, therefore, are likely irreversible, the answers to these questions could lead to the development of therapeutic strategies able to ameliorate at least some aspects of these devastating disorders.

Funding: Research in the Avantaggiati lab on *SLC25A1* was funded by R01CA193698, R21DE028670 and R21CA256546.

Institutional Review Board Statement: Not applicable.

Informed Consent Statement: Not applicable.

Acknowledgments: Some of the figures in this article were created with BioRender (Biorender.com). M.L.A. acknowledges all the past and present members of the laboratory that contributed to the discovery of CIC as a target of mutant p53 and to its subsequent characterization, as well as the collaborators who have contributed to the work. These include Vamsi Kolukula, Anju Preet, Mingjun Tan, Shreyas Gadre, Olga Catalina-Rodriguez, Christopher Albanese, Amrita Cheema and Al Fornace.

Conflicts of Interest: The authors declare no conflict of interest.

References

1. Stipani, I.; Kramer, R.; Palmieri, F.; Klingenberg, M. Citrate transport in liposomes reconstituted with Triton extracts from mitochondria. *Biochem. Biophys. Res. Commun.* **1980**, *97*, 1206–1214. [CrossRef]
2. Stipani, I.; Palmieri, F. Purification of the active mitochondrial tricarboxylate carrier by hydroxylapatite chromatography. *FEBS Lett.* **1983**, *161*, 269–274. [CrossRef]
3. Bisaccia, F.; de Palma, A.; Palmieri, F. Identification and purification of the tricarboxylate carrier from rat liver mitochondria. *Biochim. Biophys. Acta Gen. Subj.* **1989**, *977*, 171–176. [CrossRef]
4. Kaplan, R.; Mayor, J.; Wood, D. The mitochondrial tricarboxylate transport protein. cDNA cloning, primary structure, and comparison with other mitochondrial transport proteins. *J. Biol. Chem.* **1993**, *268*, 13682–13690. [CrossRef]
5. Palmieri, F.; Scarcia, P.; Monné, M. Diseases Caused by Mutations in Mitochondrial Carrier Genes *SLC25*: A Review. *Biomolecules* **2020**, *10*, 655. [CrossRef] [PubMed]
6. Kunji, E.R.S.; King, M.S.; Ruprecht, J.J.; Thangaratnarajah, C. The *SLC25* Carrier Family: Important Transport Proteins in Mitochondrial Physiology and Pathology. *Physiology* **2020**, *35*, 302–327. [CrossRef]
7. van Schaftingen, E.; Hers, H.G. Inhibition of fructose-1,6-bisphosphatase by fructose 2,6-bisphosphate. *Proc. Natl. Acad. Sci. USA* **1981**, *78*, 2861–2863. [CrossRef] [PubMed]
8. Icard, P.; Fournel, L.; Coquerel, A.; Gligorov, J.; Alifano, M.; Lincet, H. Citrate targets FBPase and constitutes an emerging novel approach for cancer therapy. *Cancer Cell Int.* **2018**, *18*, 175. [CrossRef]

9. Munday, M.R. Regulation of Mammalian Acetyl-CoA Carboxylase. *Biochem. Soc. Trans.* **2002**, *30*, 1059–1064. [CrossRef]
10. Fernandez, H.R.; Gadre, S.M.; Tan, M.; Graham, G.T.; Mosaoa, R.; Ongkeko, M.S.; Kim, K.A.; Riggins, R.B.; Parasido, E.; Petrini, I.; et al. The mitochondrial citrate carrier, SLC25A1, drives stemness and therapy resistance in non-small cell lung cancer. *Cell Death Differ.* **2018**, *25*, 1239–1258. [CrossRef]
11. Jiang, L.; Shestov, A.A.; Swain, P.; Yang, C.; Parker, S.J.; Wang, Q.A.; Terada, L.S.; Adams, N.D.; McCabe, M.T.; Pietrak, B.; et al. Reductive carboxylation supports redox homeostasis during anchorage-independent growth. *Nat. Cell Biol.* **2016**, *532*, 255–258. [CrossRef] [PubMed]
12. Morciano, P.; Carrisi, C.; Capobianco, L.; Mannini, L.; Burgio, G.; Cestra, G.; de Benedetto, G.E.; Corona, D.F.; Musio, A.; Cenci, G. A conserved role for the mitochondrial citrate transporter Sea/SLC25A1 in the maintenance of chromosome integrity. *Hum. Mol. Genet.* **2009**, *18*, 4180–4188. [CrossRef] [PubMed]
13. Santarsiero, A.; Leccese, P.; Convertini, P.; Padula, A.; Abriola, P.; D’Angelo, S.; Bisaccia, F.; Infantino, V. New Insights into Behçet’s Syndrome Metabolic Reprogramming: Citrate Pathway Dysregulation. *Mediat. Inflamm.* **2018**, *2018*, 1419352. [CrossRef] [PubMed]
14. Convertini, P.; Menga, A.; Andria, G.; Scala, I.; Santarsiero, A.; Morelli, M.A.C.; Iacobazzi, V.; Infantino, V. The contribution of the citrate pathway to oxidative stress in Down syndrome. *Immunology* **2016**, *149*, 423–431. [CrossRef] [PubMed]
15. Catalina-Rodriguez, O.; Kolukula, V.K.; Tomita, Y.; Preet, A.; Palmieri, F.; Wellstein, A.; Byers, S.; Giaccia, A.J.; Glasgow, E.; Albanese, C.; et al. The mitochondrial citrate transporter, CIC, is essential for mitochondrial homeostasis. *Oncotarget* **2012**, *3*, 1220–1235. [CrossRef] [PubMed]
16. Tan, M.; Mosaoa, R.; Graham, G.T.; Kasprzyk-Pawelec, A.; Gadre, S.; Parasido, E.; Catalina-Rodriguez, O.; Foley, P.; Giaccone, G.; Cheema, A.; et al. Inhibition of the mitochondrial citrate carrier, Slc25a1, reverts steatosis, glucose intolerance, and inflammation in preclinical models of NAFLD/NASH. *Cell Death Differ.* **2020**, *27*, 2143–2157. [CrossRef]
17. Sun, J.; Aluvila, S.; Kotaria, R.; Mayor, J.A.; Walters, D.E.; Kaplan, R.S. Mitochondrial and Plasma Membrane Citrate Transporters: Discovery of Selective Inhibitors and Application to Structure/Function Analysis. *Mol. Cell. Pharmacol.* **2010**, *2*, 101–110.
18. Infantino, V.; Iacobazzi, V.; de Santis, F.; Mastrapasqua, M.; Palmieri, F. Transcription of the mitochondrial citrate carrier gene: Role of SREBP-1, upregulation by insulin and downregulation by PUFA. *Biochem. Biophys. Res. Commun.* **2007**, *356*, 249–254. [CrossRef]
19. Iacobazzi, V.; Infantino, V.; Bisaccia, F.; Castegna, A.; Palmieri, F. Role of FOXA in mitochondrial citrate carrier gene expression and insulin secretion. *Biochem. Biophys. Res. Commun.* **2009**, *385*, 220–224. [CrossRef]
20. Kolukula, V.K.; Sahu, G.; Wellstein, A.; Rodriguez, O.C.; Preet, A.; Iacobazzi, V.; D’Orazi, G.; Albanese, C.; Palmieri, F.; Avantaggiati, M.L. SLC25A1, or CIC, is a novel transcriptional target of mutant p53 and a negative tumor prognostic marker. *Oncotarget* **2014**, *5*, 1212–1225. [CrossRef]
21. Infantino, V.; Iacobazzi, V.; Menga, A.; Avantaggiati, M.L.; Palmieri, F. A key role of the mitochondrial citrate carrier (SLC25A1) in TNF α - and IFN γ -triggered inflammation. *Biochim. Biophys. Acta Bioenerg.* **2014**, *1839*, 1217–1225. [CrossRef]
22. Damiano, F.; Gnoni, G.V.; Siculella, L. Citrate carrier promoter is target of peroxisome proliferator-activated receptor alpha and gamma in hepatocytes and adipocytes. *Int. J. Biochem. Cell Biol.* **2012**, *44*, 659–668. [CrossRef]
23. Huang, Z.; Zhang, M.; Plec, A.A.; Estill, S.J.; Cai, L.; Repa, J.J.; McKnight, S.L.; Tu, B.P. ACS2 promotes systemic fat storage and utilization through selective regulation of genes involved in lipid metabolism. *Proc. Natl. Acad. Sci. USA* **2018**, *115*, E9499–E9506. [CrossRef]
24. Schug, Z.T.; Peck, B.; Jones, D.T.; Zhang, Q.; Grosskurth, S.; Alam, I.S.; Goodwin, L.M.; Smethurst, E.; Mason, S.; Blyth, K.; et al. Acetyl-CoA Synthetase 2 Promotes Acetate Utilization and Maintains Cancer Cell Growth under Metabolic Stress. *Cancer Cell* **2015**, *27*, 57–71. [CrossRef]
25. Mazurek, M.P.; Prasad, P.D.; Gopal, E.; Fraser, S.P.; Bolt, L.; Rizaner, N.; Palmer, C.P.; Foster, C.S.; Palmieri, F.; Ganapathy, V.; et al. Molecular origin of plasma membrane citrate transporter in human prostate epithelial cells. *EMBO Rep.* **2010**, *11*, 431–437. [CrossRef]
26. Mycielska, M.E.; Dettmer, K.; Rümmele, P.; Schmidt, K.M.; Prehn, C.; Milenkovic, V.M.; Jagla, W.; Madej, G.M.; Lantow, M.; Schladt, M.T.; et al. Extracellular Citrate Affects Critical Elements of Cancer Cell Metabolism and Supports Cancer Development In Vivo. *Cancer Res.* **2018**, *78*, 2513–2523. [CrossRef]
27. Rogina, B. INDY—A New Link to Metabolic Regulation in Animals and Humans. *Front. Genet.* **2017**, *8*, 66. [CrossRef]
28. Brachs, S.; Winkel, A.F.; Tang, H.; Birkenfeld, A.L.; Brunner, B.; Jahn-Hofmann, K.; Margerie, D.; Ruetten, H.; Schmoll, D.; Spranger, J. Inhibition of citrate cotransporter Slc13a5/mINDY by RNAi improves hepatic insulin sensitivity and prevents diet-induced non-alcoholic fatty liver disease in mice. *Mol. Metab.* **2016**, *5*, 1072–1082. [CrossRef]
29. Mycielska, M.E.; Mohr, M.T.J.; Schmidt, K.; Drexler, K.; Rümmele, P.; Haferkamp, S.; Schlitt, H.J.; Gaumann, A.; Adamski, J.; Geissler, E.K. Potential Use of Gluconate in Cancer Therapy. *Front. Oncol.* **2019**, *9*, 522. [CrossRef]
30. Mullen, A.R.; Wheaton, W.W.; Jin, E.S.; Chen, P.-H.; Sullivan, L.B.; Cheng, T.; Yang, Y.; Linehan, W.M.; Chandel, N.S.; de Berardinis, R.J. Reductive carboxylation supports growth in tumour cells with defective mitochondria. *Nat. Cell Biol.* **2011**, *481*, 385–388. [CrossRef]
31. Sun, R.C.; Denko, N.C. Hypoxic Regulation of Glutamine Metabolism through HIF1 and SIAH2 Supports Lipid Synthesis that Is Necessary for Tumor Growth. *Cell Metab.* **2014**, *19*, 285–292. [CrossRef]

32. Fendt, S.-M.; Bell, E.L.; Keibler, M.A.; Olenchock, B.A.; Mayers, J.R.; Wasylenko, T.M.; Vokes, N.I.; Guarente, L.; Heiden, M.G.V.; Stephanopoulos, G. Reductive glutamine metabolism is a function of the α -ketoglutarate to citrate ratio in cells. *Nat. Commun.* **2013**, *4*, 1–11. [CrossRef]
33. Jiang, L.; Boufersaoui, A.; Yang, C.; Ko, B.; Rakheja, D.; Guevara, G.; Hu, Z.; de Berardinis, R.J. Quantitative metabolic flux analysis reveals an unconventional pathway of fatty acid synthesis in cancer cells deficient for the mitochondrial citrate transport protein. *Metab. Eng.* **2017**, *43*, 198–207. [CrossRef]
34. Napoli, E.; Tassone, F.; Wong, S.; Angkustsiri, K.; Simon, T.J.; Song, G.; Giulivi, C. Mitochondrial Citrate Transporter-dependent Metabolic Signature in the 22q11.2 Deletion Syndrome. *J. Biol. Chem.* **2015**, *290*, 23240–23253. [CrossRef]
35. Faubert, B.; Li, K.Y.; Cai, L.; Hensley, C.T.; Kim, J.; Zacharias, L.G.; Yang, C.; Brandon, F.; Doucette, S.; Burguete, D.; et al. Lactate Metabolism in Human Lung Tumors. *Cell* **2017**, *171*, 358–371.e9. [CrossRef]
36. Chen, P.-H.; Cai, L.; Huffman, K.; Yang, C.; Kim, J.; Faubert, B.; Boroughs, L.; Ko, B.; Sudderth, J.; McMillan, E.A.; et al. Metabolic Diversity in Human Non-Small Cell Lung Cancer Cells. *Mol. Cell* **2019**, *76*, 838–851.e5. [CrossRef]
37. Sellers, K.; Fox, M.P.; Bousamra, M.; Slone, S.P.; Higashi, R.M.; Miller, D.M.; Wang, Y.; Yan, J.; Yuneva, M.O.; Deshpande, R.; et al. Pyruvate carboxylase is critical for non-small-cell lung cancer proliferation. *J. Clin. Investig.* **2015**, *125*, 687–698. [CrossRef]
38. Vasan, K.; Werner, M.; Chandel, N.S. Mitochondrial Metabolism as a Target for Cancer Therapy. *Cell Metab.* **2020**, *32*, 341–352. [CrossRef]
39. Hlouschek, J.; Hansel, C.; Jendrossek, V.; Matschke, J. The Mitochondrial Citrate Carrier (SLC25A1) Sustains Redox Homeostasis and Mitochondrial Metabolism Supporting Radioresistance of Cancer Cells with Tolerance to Cycling Severe Hypoxia. *Front. Oncol.* **2018**, *8*, 170. [CrossRef]
40. Gandhi, N.; Das, G.M. Metabolic Reprogramming in Breast Cancer and Its Therapeutic Implications. *Cells* **2019**, *8*, 89. [CrossRef]
41. Özkaya, A.B.; Ak, H.; Atay, S.; Aydin, H.H. Targeting Mitochondrial Citrate Transport in Breast Cancer Cell Lines. *Anti-Cancer Agents Med. Chem.* **2015**, *15*, 374–381. [CrossRef] [PubMed]
42. Bhalla, K.; Hwang, B.J.; Dewi, R.E.; Ou, L.; Twaddel, W.; Fang, H.-B.; Vafai, S.B.; Vazquez, F.; Puigserver, P.; Boros, L.; et al. PGC1 Promotes Tumor Growth by Inducing Gene Expression Programs Supporting Lipogenesis. *Cancer Res.* **2011**, *71*, 6888–6898. [CrossRef] [PubMed]
43. Ebadi, M.; Field, C.J.; Lehner, R.; Mazurak, V. Chemotherapy diminishes lipid storage capacity of adipose tissue in a preclinical model of colon cancer. *Lipids Health Dis.* **2017**, *16*, 1–12. [CrossRef]
44. Kaplan, R.S.; Morris, H.P.; Coleman, P.S. Kinetic characteristics of citrate influx and efflux with mitochondria from Morris hepatomas 3924A and 16. *Cancer Res.* **1982**, *42*, 4399–4407.
45. Zhu, P.; Wang, Y.; Wu, J.; Huang, G.; Liu, B.; Ye, B.; Du, Y.; Gao, G.; Tian, Y.; He, L.; et al. LncBRM initiates YAP1 signalling activation to drive self-renewal of liver cancer stem cells. *Nat. Commun.* **2016**, *7*, 13608. [CrossRef]
46. Poolsri, W.-A.; Phokrai, P.; Suwankulan, S.; Phakdeeto, N.; Phunsomboon, P.; Pekkthong, D.; Richert, L.; Pongcharoen, S.; Srisawang, P. Combination of Mitochondrial and Plasma Membrane Citrate Transporter Inhibitors Inhibits De Novo Lipogenesis Pathway and Triggers Apoptosis in Hepatocellular Carcinoma Cells. *BioMed Res. Int.* **2018**, *2018*, 1–15. [CrossRef]
47. Liu, S.; Zhang, D.; Chen, L.; Gao, S.; Huang, X. Long Non-coding RNA BRM Promotes Proliferation and Invasion of Papillary Thyroid Carcinoma by Regulating the MicroRNA-331-3p/SLC25A1 Axis. *Oncol. Lett.* **2020**, *19*, 3071–3078. [CrossRef]
48. Liu, Y.; Zuckier, L.S.; Ghesani, N.V. Dominant uptake of fatty acid over glucose by prostate cells: A potential new diagnostic and therapeutic approach. *Anticancer Res.* **2010**, *30*, 369–374.
49. Mitra, R.; Le, T.T. Enhanced detection of metastatic prostate cancer cells in human plasma with lipid bodies staining. *BMC Cancer* **2014**, *14*, 91. [CrossRef]
50. Wang, Y.; Ma, S.; Ruzzo, W.L. Spatial modeling of prostate cancer metabolic gene expression reveals extensive heterogeneity and selective vulnerabilities. *Sci. Rep.* **2020**, *10*, 1–14. [CrossRef]
51. Grivennikov, S.I.; Greten, F.R.; Karin, M. Immunity, Inflammation, and Cancer. *Cell* **2010**, *140*, 883–899. [CrossRef]
52. Furman, D.; Campisi, J.; Verdin, E.; Carrera-Bastos, P.; Targ, S.; Franceschi, C.; Ferrucci, L.; Gilroy, D.W.; Fasano, A.; Miller, G.W.; et al. Chronic inflammation in the etiology of disease across the life span. *Nat. Med.* **2019**, *25*, 1822–1832. [CrossRef]
53. Infantino, V.; Convertini, P.; Cucci, L.; Panaro, M.A.; di Noia, M.A.; Calvello, R.; Palmieri, F.; Iacobazzi, V. The mitochondrial citrate carrier: A new player in inflammation. *Biochem. J.* **2011**, *438*, 433–436. [CrossRef]
54. Infantino, V.; Iacobazzi, V.; Palmieri, F.; Menga, A. ATP-citrate lyase is essential for macrophage inflammatory response. *Biochem. Biophys. Res. Commun.* **2013**, *440*, 105–111. [CrossRef]
55. Assmann, N.; O'Brien, K.L.; Donnelly, R.P.; Dyck, L.; Zaiatz-Bittencourt, V.; Loftus, R.M.; Heinrich, P.; Oefner, P.J.; Lynch, L.; Gardiner, C.M.; et al. Srebp-controlled glucose metabolism is essential for NK cell functional responses. *Nat. Immunol.* **2017**, *18*, 1197–1206. [CrossRef]
56. Mendez-Sanchez, N.; Valencia-Rodríguez, A.; Coronel-Castillo, C.; Vera-Barajas, A.; Contreras-Carmona, J.; Ponciano-Rodríguez, G.; Zamora-Valdés, D. The cellular pathways of liver fibrosis in non-alcoholic steatohepatitis. *Ann. Transl. Med.* **2020**, *8*, 400. [CrossRef]
57. Li, H.; Zhou, Y.; Wang, H.; Zhang, M.; Qiu, P.; Zhang, R.; Zhao, Q.; Liu, J. Crosstalk Between Liver Macrophages and Surrounding Cells in Nonalcoholic Steatohepatitis. *Front. Immunol.* **2020**, *11*, 1169. [CrossRef]
58. Wang, H.; Li, Z.; Niu, J.; Xu, Y.; Ma, L.; Lu, A.; Wang, X.; Qian, Z.; Huang, Z.; Jin, X.; et al. Antiviral effects of ferric ammonium citrate. *Cell Discov.* **2018**, *4*, 1–11. [CrossRef]

59. Stoffel, M.; Karayiorgou, M.; Espinosa, R.; Beau, M.M.L. The Human Mitochondrial Citrate Transporter Gene (SLC20A3) Maps to Chromosome Band 22q11 within a Region Implicated in DiGeorge Syndrome, Velo-Cardio-Facial Syndrome and Schizophrenia. *Hum. Genet.* **1996**, *98*, 113–115. [CrossRef]
60. Maynard, T.M.; Meechan, D.W.; Dudevoir, M.L.; Gopalakrishna, D.; Peters, A.Z.; Heindel, C.C.; Sugimoto, T.J.; Wu, Y.; Lieberman, J.A.; la Mantia, A.-S. Mitochondrial localization and function of a subset of 22q11 deletion syndrome candidate genes. *Mol. Cell. Neurosci.* **2008**, *39*, 439–451. [CrossRef]
61. Chaouch, A.; Porcelli, V.; Cox, D.J.; Edvardson, S.; Scarcia, P.; de Grassi, A.; Pierri, C.L.; Cossins, J.; Laval, S.H.; Griffin, H.; et al. Mutations in the Mitochondrial Citrate Carrier SLC25A1 are Associated with Impaired Neuromuscular Transmission. *J. Neuromuscul. Dis.* **2014**, *1*, 75–90. [CrossRef] [PubMed]
62. Al-Futaisi, A.; Ahmad, F.; Al-Kasbi, G.; Al-Thihli, K.; Koul, R.; Al-Maawali, A. Missense mutations in SLC25A1 are associated with congenital myasthenic syndrome type 23. *Clin. Genet.* **2019**, *97*, 666–667. [CrossRef]
63. Edvardson, S.; Porcelli, V.; Jalas, C.; Soiferman, D.; Kellner, Y.; Shaag, A.; Korman, S.H.; Pierri, C.L.; Scarcia, P.; Fraenkel, N.D.; et al. Agenesis of corpus callosum and optic nerve hypoplasia due to mutations in SLC25A1 encoding the mitochondrial citrate transporter. *J. Med. Genet.* **2013**, *50*, 240–245. [CrossRef] [PubMed]
64. Nota, B.; Struys, E.A.; Pop, A.; Jansen, E.E.; Ojeda, M.R.F.; Kanhai, W.A.; Kranendijk, M.; van Dooren, S.J.; Bevova, M.R.; Sistermans, E.A.; et al. Deficiency in SLC25A1, Encoding the Mitochondrial Citrate Carrier, Causes Combined D-2- and L-2-Hydroxyglutaric Aciduria. *Am. J. Hum. Genet.* **2013**, *92*, 627–631. [CrossRef] [PubMed]
65. Prasun, P.; Young, S.; Salomons, G.; Werneke, A.; Jiang, Y.-H.; Struys, E.; Paige, M.; Avantaggiati, M.L.; McDonald, M. Expanding the Clinical Spectrum of Mitochondrial Citrate Carrier (SLC25A1) Deficiency: Facial Dysmorphism in Siblings with Epileptic Encephalopathy and Combined D,L-2-Hydroxyglutaric Aciduria. *JIMD Rep.* **2014**, *19*, 111–115. [CrossRef]
66. Smith, A.; McBride, S.; Marcadier, J.L.; Michaud, J.; Al-Dirbashi, O.Y.; Schwartzentruber, J.; Beaulieu, C.L.; Katz, S.L.; Majewski, J. Severe Neonatal Presentation of Mitochondrial Citrate Carrier (SLC25A1) Deficiency. *JIMD Rep.* **2016**, *30*, 73–79. [CrossRef]
67. Cohen, I.; Staretz-Chacham, O.; Wormser, O.; Perez, Y.; Golubitzky, A.; Kadir, R.; Birk, O.S. A novel homozygous SLC25A1 mutation with impaired mitochondrial complex V: Possible phenotypic expansion. *Am. J. Med. Genet. Part A* **2017**, *176*, 330–336. [CrossRef]
68. Eguchi, M.; Ozaki, E.; Yamauchi, T.; Ohta, M.; Higaki, T.; Masuda, K.; Imoto, I.; Ishii, E.; Eguchi-Ishimae, M. Manifestation of Recessive Combined D-2-, L-2-Hydroxyglutaric Aciduria in Combination with 22q11.2 Deletion Syndrome. *Am. J. Med. Genet. A* **2018**, *176*, 351–358. [CrossRef]
69. Ye, D.; Guan, K.-L.; Xiong, Y. Metabolism, Activity, and Targeting of D- and L-2-Hydroxyglutarates. *Trends Cancer* **2018**, *4*, 151–165. [CrossRef]
70. Rzem, R.; Vincent, M.-F.; van Schaftingen, E.; da Cunha, M.V. L-2-Hydroxyglutaric aciduria, a defect of metabolite repair. *J. Inherit. Metab. Dis.* **2007**, *30*, 681–689. [CrossRef]
71. Kranendijk, M.; Struys, E.A.; Salomons, G.S.; van der Knaap, M.S.; Jakobs, C. Progress in understanding 2-hydroxyglutaric acidurias. *J. Inherit. Metab. Dis.* **2012**, *35*, 571–587. [CrossRef]
72. Pop, A.; Williams, M.; Struys, E.A.; Monné, M.; Jansen, E.E.W.; de Grassi, A.; Kanhai, W.A.; Scarcia, P.; Ojeda, M.R.F.; Porcelli, V.; et al. An overview of combined D-2- and L-2-hydroxyglutaric aciduria: Functional analysis of CIC variants. *J. Inherit. Metab. Dis.* **2018**, *41*, 169–180. [CrossRef]
73. Matsunaga, H.; Futakuchi-Tsuchida, A.; Takahashi, M.; Ishikawa, T.; Tsuji, M.; Ando, O. IDH1 and IDH2 Have Critical Roles in 2-Hydroxyglutarate Production in D-2-Hydroxyglutarate Dehydrogenase Depleted Cells. *Biochem. Biophys. Res. Commun.* **2012**, *423*, 553–556. [CrossRef]
74. Ježek, P. 2-Hydroxyglutarate in Cancer Cells. *Antioxid. Redox Signal.* **2020**, *33*, 903–926. [CrossRef]
75. Intlekofer, A.M.; Wang, B.; Liu, H.; Shah, H.; Carmona-Fontaine, C.; Rustenburg, A.S.; Salah, S.; Gunner, S.S.M.R.; Chodera, C.C. L-2-Hydroxyglutarate production arises from noncanonical enzyme function at acidic pH. *Nat. Chem. Biol.* **2017**, *13*, 494–500. [CrossRef]
76. Fan, J.; Teng, X.; Liu, L.; Mattaini, K.R.; Looper, R.E.; Heiden, M.G.V.; Rabinowitz, J.D. Human Phosphoglycerate Dehydrogenase Produces the Oncometabolite d-2-Hydroxyglutarate. *ACS Chem. Biol.* **2014**, *10*, 510–516. [CrossRef]

Review

Renaissance of VDAC: New Insights on a Protein Family at the Interface between Mitochondria and Cytosol

Vito De Pinto ^{1,2,3} 

¹ Department of Biomedicine and Biotechnology Sciences, University of Catania, Via S. Sofia 64, 95123 Catania, Italy; vdpbiofa@unicat.it; Tel.: +39-095-73842444

² we.MitoBiotech.srl, c.so Italia 172, 95129 Catania, Italy

³ National Institute of Biostructures and Biosystems, Section of Catania, 00136 Rome, Italy

Abstract: It has become impossible to review all the existing literature on Voltage-Dependent Anion selective Channel (VDAC) in a single article. A real Renaissance of studies brings this protein to the center of decisive knowledge both for cell physiology and therapeutic application. This review, after highlighting the similarities between the cellular context and the study methods of the solute carriers present in the inner membrane and VDAC in the outer membrane of the mitochondria, will focus on the isoforms of VDAC and their biochemical characteristics. In particular, the possible reasons for their evolutionary onset will be discussed. The variations in their post-translational modifications and the differences between the regulatory regions of their genes, probably the key to understanding the current presence of these genes, will be described. Finally, the situation in the higher eukaryotes will be compared to that of yeast, a unicellular eukaryote, where there is only one active isoform and the role of VDAC in energy metabolism is better understood.

Keywords: Voltage-Dependent Anion selective Channel; isoforms; oxidative post-translational modification; gene promoter; yeast; bioenergetics; metabolism

Citation: De Pinto, V. Renaissance of VDAC: New Insights on a Protein Family at the Interface between Mitochondria and Cytosol. *Biomolecules* **2021**, *11*, 107. <https://doi.org/10.3390/biom11010107>

Received: 30 November 2020

Accepted: 12 January 2021

Published: 15 January 2021

Publisher's Note: MDPI stays neutral with regard to jurisdictional claims in published maps and institutional affiliations.



Copyright: © 2021 by the author. Licensee MDPI, Basel, Switzerland. This article is an open access article distributed under the terms and conditions of the Creative Commons Attribution (CC BY) license (<https://creativecommons.org/licenses/by/4.0/>).

1. Introduction

The study of Voltage-Dependent Anion selective Channel (VDAC), at that time more commonly called mitochondrial porin, broke by chance in the laboratory of Prof. Palmieri, at the University of Bari, where I was an internal student and then researcher. The goal of the laboratory was to isolate and characterize the mitochondrial carriers, today grouped in the family of solute carriers (SLC25) to which Prof. Palmieri has given a decisive contribution [1]. As it was later understood, the mitochondrial porin has physical-chemical characteristics very similar to those of the SLC25 family, since it is a protein deeply immersed in the phospholipid membrane with very few portions exposed to the aqueous solvent. For this reason, VDAC was initially thought to be another contaminant solute carrier obtained during the purification procedures of the phosphate transporter which was the primary target of the laboratory [2]. VDAC, although found in the outer membrane, shared with the SLC25 family present in the inner membrane, a very similar molecular weight (around 30 kDa) and a similar affinity for the stationary chromatographic phase of hydroxyapatite in purification procedures [3,4]. This made it very difficult to distinguish VDAC from other integral membrane proteins. A big step forward was the use of radioactive dicyclohexylcarbodiimide (DCCD). This ATP-synthase inhibitor, at very low concentrations, was able to mark only three proteins in mitochondria: an 8 kDa protein, the c subunit of ATPase, a band of about 16 kDa and one of about 35 kDa. Excluding the c subunit band, so hydrophobic to be soluble in apolar solvents, the 35 kDa DCCD-binding protein was observed in our laboratory as one of the bands in the crowded Mr 30–35 kDa area in SDS-PAGE. The DCCD binding was used as a specific indication for the purification of what was considered one of the putative carriers [2]. It was named DCCD-binding protein, pending the discovery of a functional activity [5]. After numerous

attempts to identify any specific substrate exchange activity with the techniques used by us, an intuition by Prof. Palmieri led me to the laboratory of Prof. Roland Benz, then at the University of Konstanz, where the purified protein (personally carried by hand in a large Dewar jar) showed a powerful and immediate pore-forming activity in planar artificial membranes [5,6]. The presence of a mitochondrial pore-forming protein in *Paramecium* extracts was first claimed in 1976 [7] and then the functional identification of this protein as a component of the mitochondrial outer membrane was first reported by Colombini in 1979 [8]. The study of this pore-forming protein distinguished this research from the more established one of the laboratory, which was related to transport proteins of the inner mitochondrial membrane. Nevertheless, the technologies, then in full development, for the study of integral membrane proteins could be applied to both types of proteins. For example, a modification of the chromatography with hydroxyapatite and celite allowed the production of large amounts of VDAC, with a very simple methodology that eventually became standard in all laboratories in the world [9]. With this methodology various structural approaches were attempted but resulted as only partially successful. Following a course of crystallization of membrane proteins held in Martinsried (DE) with teachers as Hartmut Michel and Johann Deisenhofer (who were awarded the Nobel Prize for photosynthetic reaction center the following year), a large preparation of VDAC in Triton X-100 was thrown away, as the detergent prevented the formation of crystals. It was in that context that more modern and dialyzable detergents were tested for the first time on VDAC purification, such as LDAO [10]. The use of this detergent, which was later adopted by all laboratories, led to the crystallization of VDAC, which was obtained a good twenty years later [11–13]. Another structural aspect that, in retrospect, can be considered one of the most important was the identification of the VDAC DCCD-binding amino acid residue. DCCD binds negatively charged residues exposed to a hydrophobic environment: a physical-chemical apparent incongruity that made the binding of DCCD to mitochondrial membrane proteins so rare. The identification procedure advanced with a direct but artisanal experimental strategy, given the instrumental means available at the time. In the end, however, VDAC1 bovine heart glutamate 73 was identified as the binding site of DCCD [14]. The transmembrane arrangement of the protein and its secondary structure was not yet known, although there were predictions based not only on bioinformatics [15,16] but mostly on the electrophysiology data obtained by Colombini's and Forte's groups [17,18]. VDAC is the hexokinase-binding protein on the outer membrane surface [19] and binding of hexokinase to VDAC was found to be inhibited by DCCD [20]. In [20] it was proposed that the C-terminal end of VDAC contained the DCCD binding site. The identification of E73 as the DCCD-binding residue did not fit with the contemporary models, since the residue was initially located in an outside loop of the current folding pattern [17,18]. The crystal structure of the pore definitely solved the dispute, locating the E73 in the middle of a transmembrane β -strand, facing the hydrophobic phospholipid layer [11–13]. The hexokinase-VDAC binding has intriguing functional implication that continues to be highly relevant and whose mechanism has not yet been clarified.

2. The Next Twenty Years of Achievements

Studies focused on the biochemical-structural aspects of the protein underwent a strong acceleration following the use of molecular biology technologies that became within the reach of all laboratories. In the case of VDAC, this led to a great expansion of knowledge of the protein's genetic and cellular activities.

The milestones in a twenty years path of achievements, in my opinion, were: (I) the identification of three isoforms of VDAC in the superior metazoa [21,22]. (II) The definition of the structure of VDAC1, obtained in the same year by three different groups with different techniques (crystallization and NMR) [11–13], and of VDAC2 [23]. Surprisingly, the structure proposed a new type of domain: a mixed β -barrel with odd number of β -strands (19 β -strands), i.e., with the presence of parallel β -strands (the first and the last) in addition to the antiparallel strands. (III) The topological arrangement of VDAC in the outer

membrane [24]. (IV) The functional discovery of the oligomerization of VDAC and its role in hexokinase binding and apoptosis triggering [25–28]. (V) The involvement of VDAC in many pathologies, from tumors [29] to neurodegenerative diseases like ALS [30], Parkinson's disease [31], Alzheimer's disease [32], type 2 diabetes [33], and the identification of it as a potential therapeutic target [34–37].

The discovery of more isoforms of VDAC suggests that evolution developed variants with slight amino acidic differences in its protein armory for precise but still undefined purposes. The production of stem cells and mice knockout for the individual isoforms has allowed us to start providing clues about their function [38–41]. A major part of our current research endeavor resides in this question, i.e., in identification of the function of individual isoforms.

3. VDAC Isoforms: A Puzzle to Unveil

Most of the literature about VDAC1 was covered in the excellent and extensive review by Shoshan-Barmatz in this special issue [42]. We will thus focus on two aspects that, in our opinion, deserve further attention: the presence in the genome of more VDAC isoforms and their utilization.

In higher metazoa three VDAC genes with the same exon-intron structure [43] evolved: while the nucleotide changes among the three VDAC isoforms modified the encoding sequences so that they have peculiar differences (such as the cysteine content, which will be discussed later), they have not affected the structure of the splicing sequences nor have they modified the gene organization. The only exceptions are for the VDAC2 gene, which appears identical to the other two but with the addition of an extra exon upstream of the first one, which gives VDAC2 a short additional sequence to the N-terminal; and for VDAC3, where the presence of an internal starting codon (ATG), resulting in the insertion of a single methionine residue at amino acid position 39 of the mature VDAC3 protein, was reported but whose relevance was not established [44,45]. Notably, the function of VDAC2 is still unknown. Descending the evolutionary scale, for example, the additional exon of VDAC2 is no longer present in fish [23]. The relevance of the individual isoforms of VDAC has been addressed by the development of knockout cells for the individual isoforms [39,40]. Surprisingly, the overall proclaimed result was that each VDAC isoform, individually, is not needed for cell survival [38]. This notion was especially obtained to exclude the presence of VDAC in the permeability transition pore structure (PTP) in which it was previously involved [41]. On the other hand, the non-essentiality of the existence of VDAC strongly clashes with the abundance with which nature has provided the mitochondrion with this protein.

4. The Most Abundant Post-Translational Modifications of Mammalian VDACs Occur on Cysteines

We have been studying post-translational modifications of VDAC isoforms for some years now. The initial starting point was the consideration of the different number of cysteines present in VDAC isoforms and the suspicion that this difference was not a mere coincidence but was likely linked to a specific function or structural involvement of these residues in protein folding (Figure 1). In particular, since the VDAC3 isoform was the least studied, a set of mutagenesis of the individual cysteines and/or of small clusters, and even all cysteines in the sequence, was undertaken. These mutants were tested for their electrophysiological activity after *in vitro* expression, purification and reconstitution in a planar lipid bilayer, and in yeast devoided of VDAC pore-forming activity following endogenous gene inactivation [44]. The results clearly showed an inverse correlation between the number of cysteines present in the VDAC3 sequence and the reconstituted pore-forming activity. Additionally, the recovery of the fermentation activity of the mutant yeast progressed when it was transformed with VDAC3 in which the cysteines were progressively eliminated [46,47]. At the same time, work by another group [48] proposed that the cause of the reduced activity of VDAC3 when cysteines were present in its sequence was due to the formation of intra-chain disulfide bridges [49].

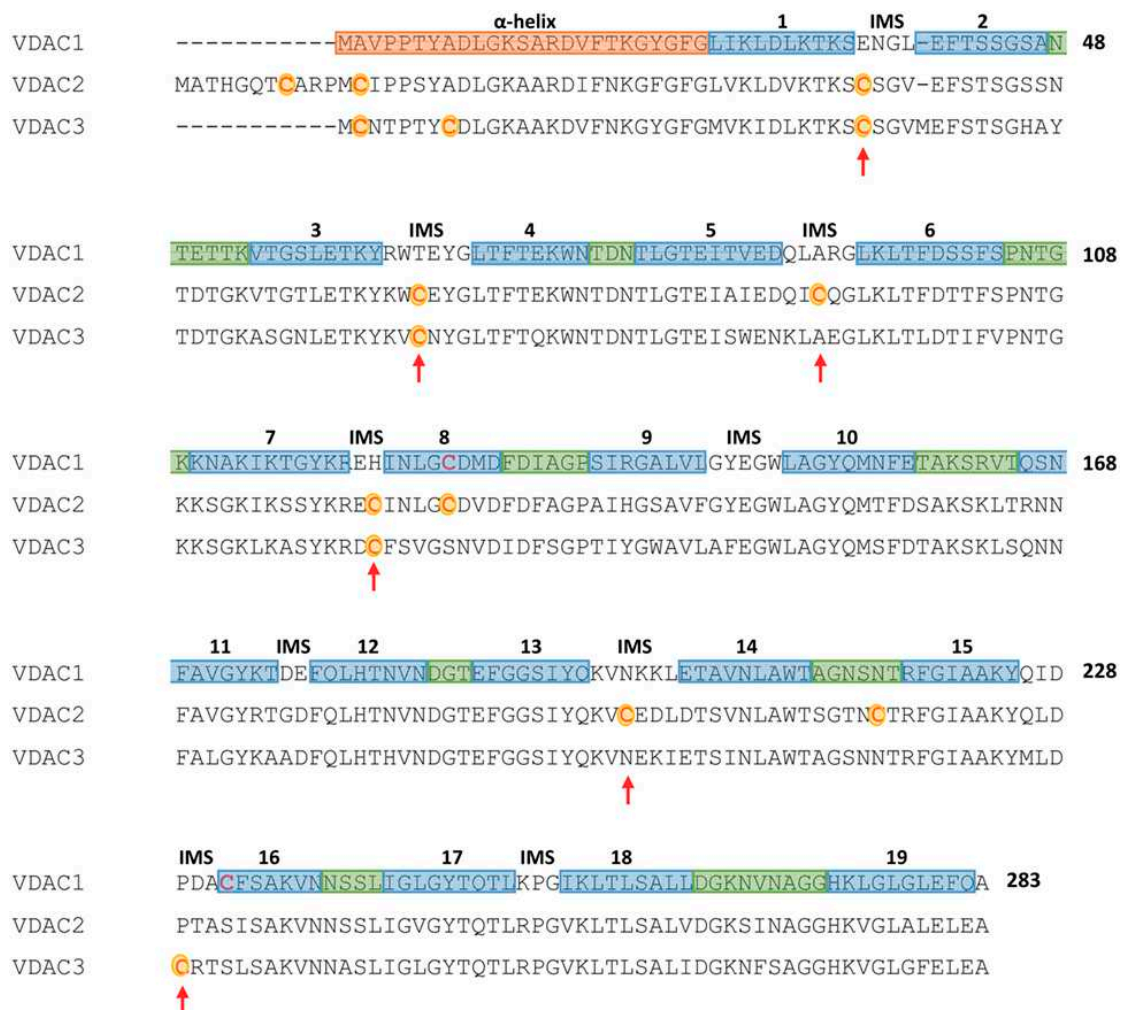


Figure 1. Secondary structure elements and cysteines localization in a multi-alignment of human Voltage-Dependent Anion selective Channel (VDAC) isoforms. Color code: light blue: β -strands; green: loops exposed to cytosol; orange: the N-terminal sequence containing α -helical portions; no color: loops exposed to inter-membrane space. Cysteine residues of VDAC2 and VDAC3 are in red and highlighted in yellow; red arrows point cysteine residues exposed to inter-membrane space (Figure obtained with the support of F. Zinghirino).

The need to investigate this functional result more thoroughly led us to collaborate with the mass spectrometry unit to unequivocally highlight, at a molecular level, the oxidation state of cysteines, in particular, and of other residues in the VDAC3 isoform, first [50], and in other isoforms later [51,52]. While some of these experiments are still ongoing, especially the part regarding the presence of intra-chain disulfide bridges, the results of our studies are summarized in the following sections.

4.1. Methods: Avoiding Unreliable Results

The technique of protein isolation from animal cells and/or tissues has been modified and adapted to eliminate any risk of oxidation or accidental modification due to isolation protocols or electrophoretic techniques. We used enriched extracts rather than purifying proteins after SDS-PAGE or 2D electrophoresis. To this end, reduction and alkylation of sulfur were performed on purified mitochondria, and only later the chromatographic separation was run. The eluted proteins were cleaned by PlusOne 2-D Clean-Up kit (GE Healthcare Life Sciences, Milan, Italy), then RapiGest SF (Waters, Milan, Italy), to eliminate non-protein contaminating molecules. The sample was then subjected to proteolytic cleavage and the peptide mixture loaded on UP-nanoLC and then analysed by a highly sensitive Orbitrap Fusion Tribrid (Q-OT-qIT) mass spectrometer. This modified procedure

is all the more delicate and important to develop when considering that the main PTM studied was the oxidation of -SH [53,54].

4.2. Cysteine Oxidations in VDAC Isoforms

We initially focused on oxidative post-translational modifications of VDAC3 cysteines [46,50] and later on other isoforms [51,52]. In addition, starting materials from different organisms such as rat tissues and human cell cultures were compared. The first novel finding was that VDAC cysteines can undergo progressive oxidation of sulphur. Some oxidations are reversible, others are difficult to reverse or are practically non-reversible under physiological conditions. The oxidation state of sulphur can go from the redox-reactive thiol (-SH) to sulfhydration (SSH), disulfide bonds (RS-SR), sulfenylation (SOH), sulfinic acid (SO₂H), and sulfonic acid (SO₃H) [55]. Except for sulfonic acid, all the reported oxidative post-translational modifications are readily reversible. The variable oxidation of cysteines could be due to the presence of ROS, particularly abundant in the intermembrane space, where there is also an acidic pH favourable to oxidation. The question we asked was whether these modifications were random or precisely targeted. In fact, VDAC, despite being an integral membrane protein, has the inner side of the pore and the loops exposed to the water environment: the walls of the hydrophilic channel and the connection loops between the β -strands are exposed to the inside and outside of the outer mitochondrial membrane. Moreover, the location of the N-terminal segment (amino acids 1–19), which contains portions of α -helix, is not unequivocally defined and even less is known about the structure and location of the further distal segment at the N-terminal (11 additional amino acids) found in the VDAC2 sequence. Most of the cysteines of VDAC2 and VDAC3 indeed are exposed to the aqueous environment and in certain situations are close enough to each other to suggest that they may engage in the formation of disulphide bridges. Taken together, the finding of cysteine oxidative post-translational modifications [52–55] indicate that each VDAC sulphur amino acid has a preferential sensitivity to oxidation. Indeed, some cysteines oscillate between different oxidative states (from reduced to sulfinic acid), others are always irreversibly oxidized (sulfonic acid), while many others are always reduced (for a detailed review see [55]). Therefore, the latter cysteines have the potential to form disulfide bonds. The propensity to oxidation is a preserved characteristic of single cysteines depending on their location within the sequence and therefore in the 3D structure of the pore: those in the same position, in different organisms, have the same type of oxidation [55]. Moreover, this propensity to oxidation of cysteines is peculiar to VDAC because no other mitochondrial proteins isolated with the same chromatography technique show the presence of oxidized cysteines [51]. The significance of the oxidative modifications peculiar to VDAC could modulate an unknown function of the proteins, and/or the buffering of the oxidative potential of the ROS produced in the mitochondrion [52].

4.3. Other Post-Translational Modifications in VDACS

In VDACS other more common post-translational modifications were detected. For example, phosphorylation is very common and dynamic [56]. In our hands, in particular, Ser 104 was usually found phosphorylated, but, in general, in low amounts [55].

Acetylation was always detected at the N-terminal amino acid of the three isoforms [50,51], together with the loss of the starting methionine. Furthermore, succinated cysteines were not found in human VDAC1 isoform but were exclusively found in VDAC2 and 3 [51]. No selenocysteine was found, as well as no evidence of ubiquitin and ubiquitination was detected. A very rare and unique post-translational modification, the deamidation of specific asparagine and glutamine was found in cultured NSC34 cells transformed to express the SOD1G93A variant: this cell line is the most used cell model of ALS. It is tempting to speculate that this modification might be associated with the pathology [54].

5. VDAC Isoforms Genes Expression Regulation: The Key to Understanding Isoforms Functions?

The studies of the structure, activity, and regulation of VDAC genes aim at obtaining a reliable picture of their differences in tissue expression or sensitivity to specific stimuli [57]. In humans, for each VDAC gene, several different transcript splice variants were identified: they did not vary in the coding region but mainly in the length of their 5'-UTR and 3'-UTR. This finding led us to the hypothesis that there might be different mechanisms of transcript regulation and expression in various cellular contexts. Other splice variants were detected, including processed transcripts that do not contain open reading frame (ORF), retained intron, and transcripts involved in the nonsense-mediated decay mechanism. It is not known whether the identified VDACs splice variants have any functional biological role. However, gene expression data collected from NIH Genotype-Tissue Expression project (GTEx) [58], report their transcription, including the generation of non-protein coding transcripts.

5.1. VDAC Genes Expression Profile

All three VDAC isoforms are ubiquitously expressed, with the highest levels found in skeletal and heart muscles as determined by RNA-seq GTEx. The level of the VDAC1 and VDAC2 transcripts is comparable, while VDAC3 is lower than the other two isoforms, confirming previous experimental conclusions drawn by RT-PCR [59]. While confirming that VDAC isoforms are ubiquitously expressed, the comparison with the data present in a second repository (RNA-seq CAGE RIKEN FANTOM 5' project) [60] of Expression Atlas repository of EMBL-EBI [61] revealed that the VDAC3 expression levels were higher than VDAC2 and VDAC1, whose transcripts are scarcely represented in all tissues [57]. The data emerging from this analysis highlight for the first time the prevalence of VDAC3 gene transcription as compared to other isoforms reflecting a higher promoter activity. The special version of RNA-seq methodology based on cap analysis of gene expression adopted by the FANTOM5 consortium explains the difference in the results obtained in the former database.

5.2. VDACs Genes Promoter Structures and Activity

The promoters of the human VDACs genes were also characterized. The organization of the core promoter is similar to that of most TATA-less human promoters of ubiquitously expressed genes, where the presence of abundant GC regions, alternative binding sites Inr, DPE, and BRE assure a basal levels of transcription. Interestingly, a non-canonical initiation site termed the TCT motif (polypyrimidine initiator), which is a target for translation regulation by the mTOR pathway, oxidative, and metabolic stress [62], was also identified in VDAC2 and VDAC3 promoters [57]. Gene reporter assays revealed that VDAC3 promoter had the highest transcriptional activity and VDAC1 promoter was, on the contrary, the least active [57]. We proposed that a quantitative regulation of the transcript levels due to their different stability, or to maintain a high level of transcripts to promptly respond to a particular stimulation, is necessary for the cell.

5.3. Specific Functions of Transcription Factors Binding Sites in VDAC Genes Promoters

The basal expression level of VDAC genes seems to be subject to quantitative regulation of expression. Using a bioinformatics approach, the main transcription factors regulating the activity of VDAC promoter regions were identified, and a quest for the corresponding binding sites located in the promoters was performed. In all three VDACs promoters, the majority of identified TFs classes belong to the E2FF, NRF1, SP1, KLFS, EBOX families which are prevalently involved in cell proliferation and differentiation, apoptosis, and metabolism regulation [63–69]. This result suggests that VDAC expression may have a central role in regulating mitochondrial function. VDAC promoters are also equipped with unique transcription factor binding sites. These transcription factors may

be the key to understanding the difference among the VDAC isoforms in terms of binding sites specific to the promoters of each VDAC gene.

The unique transcription regulators in VDAC1 promoter suggest a prevalent role of this protein in the mitochondrial outer membrane in physiological context and in altered environmental conditions in which cells have to restore the mitochondria energy balance [70–72]. VDAC2 promoter showed the presence of different factors specially active during the development of specialized tissues and organogenesis processes mainly related to nervous system genesis and growth [73,74]. VDAC3 promoter analyzed in [57] shows a particular abundance of transcription factors binding sites involved in the development of germinal tissues, organogenesis, and sex determination [39,75]. Converging evidence reported in the literature confirms the crucial role of VDAC isoforms in the specific context where the transcription factors that bind to their promoters exert a function.

In conclusion, the study of the features of the promoters of each VDAC isoform indicates that they evolved different control sequences, requiring transcription factors that link these genes to specific functions. Interestingly, the accumulated evidence points to the same biological area that was involved in the functions of the proteins.

The families of transcription regulators identified as unique in VDAC1 promoter suggest that this isoform has the main role of mitochondrial channel protein in a physiological cell context and is the main tool used to maintain mitochondria energy balance [40]. Several observations, obtained by experimental work, showed the involvement of VDAC1 in regulating cellular and mitochondrial pathways in physiology and pathology [76]. VDAC2 was indicated as the isoform indispensable for apoptosis [41,77,78] and autophagy in various cellular contexts [79]. VDAC2 promoter contains TF binding sites related to factors specially involved in developing specialized tissues, in particular of the nervous system, and the organogenesis and development processes. VDAC3 promoter is rich in GC repeats, which are typically found in epigenetic control systems of the expression of the transcript. Results from VDAC3 knockout mice show that the gene deletion affects the sperm organization and mobility [39]: the abundant presence of TF binding sites involved in germinal tissue development and sex determination might confirm its role in spermatogenesis.

6. The Role of VDAC Isoforms in Yeast

Unlike vertebrates, unicellular eukaryotic organisms such as *Neurospora crassa* and *Saccharomyces cerevisiae* do not have the same gene multiplicity for VDAC isoforms. The case of yeast has been studied and definitively clarified by us. After the discovery and characterization of yeast VDAC [80,81], Forte's group, using genetic ablation of the gene coding the former VDAC protein, discovered a second isoform, named yVDAC2, with a partially conserved sequence, which was predicted to form channels [82]. Our group expressed the yeast VDAC2 isoform and characterized its activity after reconstitution in planar membranes. We found that recombinant yVDAC2 is also able to fold forming a pore and that its electrophysiological characteristics are very similar to those of yVDAC1 [83,84]. While the expression pattern and the physiological role of yVDAC2 remain unknown, knockout out of yVDAC1 forces cells to adopt a fermentative energy metabolism, highlighting the failure of yVDAC2 to compensate for the lack of yVDAC1 [82].

Proteomic analysis of the yeast mitochondrion, recently carried out at such high resolution as to allow a realistic estimate of the number of individual proteins present per mitochondrion [85], showed that yVDAC2 is present in an almost infinitesimal amount, even under conditions of stimulation of its presence [85]. The lack of support of a physiological role of yVDAC2 in a yVDAC1-free mitochondrion was also highlighted at the transcription level: a microarray experiment analyzing the transcriptomic profile of a yeast strain without VDAC1 ($\Delta por1$ mutant) grown on glucose showed that there is no increase in the expression levels of yVDAC2. Together, these results indicate that there is no coordination between the expression of the two genes; the fact that there is a second VDAC gene could be the result of a gene duplication that has led to the presence of some sort of inactive pseudogene in the yeast genome [86].

Even the analysis of the global permeability of the outer mitochondrial membrane of yeast, while highlighting the possible existence of other minor (quantitatively) proteins capable of forming pores, found no evidence of a γ VDAC2 contribution to it [87]. We calculated that at least 90% of the permeability of the mitochondrial outer membrane is due to γ VDAC1 and that the only proteins that can realistically support the permeability of small metabolites in the absence of γ VDAC1 are the Tom40 and Sam50 channels (for a complete discussion see [86]).

The main unresolved questions are: how can the yeast mitochondria not be degraded and inactivated in the absence of VDAC1? How can the yeast mitochondria survive when VDAC1 is absent?

The transcriptomic profile of the $\Delta por1$ strain compared to the wild type (WT) strain provided interesting information. There is a marked aliquot of genes whose expression is completely modified in $\Delta por1$: particularly impressive is the full inactivation of the mitochondrial genome. This drastic change can be attributed to the reduced transport capacity of nucleotides in the absence of VDAC1, also due to the impossibility to import carriers, a function recently linked to VDAC1 [88]. In these conditions, the mass of the organelle is reduced by more than 65% [86]. This result indicates a truly essential role of γ VDAC1 in mitochondrial physiology. In fact, deletion of γ VDAC1 causes a general reorganization of energy metabolism, as evidenced by a large number of up- and down-regulated genes associated with glycolysis, alcoholic fermentation, oxidative phosphorylation, TCA cycle, and lipid synthesis [86]. Our results showed that, in the absence of γ VDAC1, cells survive by shifting the pyruvate metabolism from mitochondrion to cytosolic acetyl-CoA production by PDH bypass. This change leads to an increase in fatty acids and phospholipids that go into intracellular deposits or contribute to extending the size of the plasma membrane, as indicated by detailed microscopy experiments. Overall, these results indicate that VDAC1 in yeast contributes to the global regulation of energy metabolism.

7. Today's Big Challenges—Conclusions

I hope that this quick review of the biological functions related to the onset of VDAC isoforms during evolution supports the hypothesis that they are involved in specific functions, as well as having, all of them, the ability to form large, porous aqueous channels. It is difficult to identify functional specificities based on small structural differences, such as the disposition and reactivity of some residues, the presence of small amino acid traits whose 3D organization and mobility have not yet been precisely defined, as it is the case of N-terminal extensions. These clues will have to be explored and revealed, together with the other major unsolved issue of this protein: the mechanism of voltage dependence. The road is open in this direction, and the end of the knowledge of the functions of VDAC isoforms will make it possible to steer the path of discovery of therapeutic molecules targeting this intriguing pore.

Funding: This research was funded by Università di Catania—linea PIACERI, grant VDAC, and linea CHANCE.

Acknowledgments: I wish to thank all the members of my research group that contributed to the production of many results outlined in this article and are hardly working to develop further experiments: Angela Messina, Francesca Guarino, Simona Reina, Andrea Magrì, Marianna Flora Tomasello, Maria Carmela Di Rosa, Maria Gaetana Pittalà, Federica Zinghirino, Stefano Conti Nibali, Pierpaolo Risiglione, Xena Giada Pappalardo, Salvatore Cubisino. I also acknowledge the staff of the proteomic unit at the University of Catania, Salvatore Foti and Rosaria Saletti, for their indispensable support. Salvatore Oddo is acknowledged for the friendly revision of the English text.

Conflicts of Interest: The author declares no conflict of interest.

References

- Palmieri, F.; Pierri, C.L. Mitochondrial metabolite transport. *Essays Biochem.* **2010**, *47*, 37–52. [CrossRef]
- De Pinto, V.; Tommasino, M.; Palmieri, F.; Kadenbach, B. Purification of the active mitochondrial phosphate carrier by affinity chromatography with an organomercurial agarose column. *FEBS Lett.* **1982**, *148*, 103–106. [CrossRef]
- Bisaccia, F.; Palmieri, F. Specific elution from hydroxylapatite of the mitochondrial phosphate carrier by cardiolipin. *Biochim. Biophys. Acta Bioenerg.* **1984**, *766*, 386–394. [CrossRef]
- Palmieri, F.; Indiveri, C.; Bisaccia, F.; Iacobazzi, V. Mitochondrial metabolite carrier proteins: Purification, reconstitution, and transport studies. *Methods Enzymol.* **1995**, *260*, 349–369. [CrossRef]
- De Pinto, V.; Tommasino, M.; Benz, R.; Palmieri, F. The 35 kDa DCCD-binding protein from pig heart mitochondria is the mitochondrial porin. *Biochim. Biophys. Acta Biomembr.* **1985**, *813*, 230–242. [CrossRef]
- De Pinto, V.; Benz, R.; Caggese, C.; Palmieri, F. Characterization of the mitochondrial porin from *Drosophila melanogaster*. *Biochim. Biophys. Acta Biomembr.* **1989**, *987*, 1–7. [CrossRef]
- Schein, S.J.; Colombini, M.; Finkelstein, A. Reconstitution in planar lipid bilayers of a voltage-dependent anion-selective channel obtained from paramecium mitochondria. *J. Membr. Biol.* **1976**, *30*, 99–120. [CrossRef]
- Colombini, M. A candidate for the permeability pathway of the outer mitochondrial membrane. *Nature* **1979**, *279*, 643–645. [CrossRef]
- De Pinto, V.; Prezioso, G.; Palmieri, F. A simple and rapid method for the purification of the mitochondrial porin from mammalian tissues. *Biochim. Biophys. Acta Biomembr.* **1987**, *905*, 499–502. [CrossRef]
- De Pinto, V.; Benz, R.; Palmieri, F. Interaction of non-classical detergents with the mitochondrial porin: A new purification procedure and characterization of the pore-forming unit. *Eur. J. Biochem.* **1989**, *183*, 179–187. [CrossRef]
- Hiller, S.; Garces, R.G.; Malia, T.J.; Orekhov, V.Y.; Colombini, M.; Wagner, G. Solution structure of the integral human membrane protein VDAC-1 in detergent micelles. *Science* **2008**, *321*, 1206–1210. [CrossRef]
- Ujwal, R.; Cascio, D.; Colletier, J.P.; Faham, S.; Zhang, J.; Toro, L.; Ping, P.; Abramson, J. The crystal structure of mouse VDAC1 at 2.3 Å resolution reveals mechanistic insights into metabolite gating. *Proc. Natl. Acad. Sci. USA* **2008**, *105*, 17742–17747. [CrossRef]
- Bayrhuber, M.; Meins, T.; Habeck, M.; Becker, S.; Giller, K.; Villinger, S.; Vonnrhein, C.; Griesinger, C.; Zweckstetter, M.; Zeth, K. Structure of the human voltage-dependent anion channel. *Proc. Natl. Acad. Sci. USA* **2008**, *105*, 15370–15375. [CrossRef]
- De Pinto, V.; Al Jamal, J.A.; Palmieri, F. Location of the dicyclohexylcarbodiimide-reactive glutamate residue in the bovine heart mitochondrial porin. *J. Biol. Chem.* **1993**, *268*, 12977–12982. [CrossRef]
- Forte, M.; Guy, H.R.; Mannella, C.A. Molecular genetics of the VDAC ion channel: Structural model and sequence analysis. *J. Bioenerg. Biomembr.* **1987**, *19*, 341–350. [CrossRef]
- De Pinto, V.; Prezioso, G.; Palmieri, F.; Thinnes, F.; Link, T.A. Peptide-Specific Antibodies and Proteases as Probes of the Transmembrane Topology of the Bovine Heart Mitochondrial Porin. *Biochemistry* **1991**, *30*, 10191–10200. [CrossRef]
- Blachly-Dyson, E.; Peng, S.; Colombini, M.; Forte, M. Selectivity changes in site-directed mutants of the VDAC ion channel: Structural implications. *Science* **1990**, *247*, 1233–1236. [CrossRef]
- Thomas, L.; Blachly-Dyson, E.; Colombini, M.; Forte, M. Mapping of residues forming the voltage sensor of the voltage-dependent anion-selective channel. *Proc. Natl. Acad. Sci. USA* **1993**, *90*, 5446–5449. [CrossRef]
- Lindén, M.; Gellerfors, P.; Dean Nelson, B. Pore protein and the hexokinase-binding protein from the outer membrane of rat liver mitochondria are identical. *FEBS Lett.* **1982**, *141*, 189–192. [CrossRef]
- Nakashima, R.A. Hexokinase-binding properties of the mitochondrial VDAC protein: Inhibition by DCCD and location of putative DCCD-binding sites. *J. Bioenerg. Biomembr.* **1989**, *21*, 461–470. [CrossRef]
- Blachly-Dyson, E.; Zambronicz, E.B.; Wei, H.Y.; Adams, V.; McCabe, E.R.B.; Adelman, J.; Colombini, M.; Forte, M. Cloning and functional expression in yeast of two human isoforms of the outer mitochondrial membrane channel, the voltage-dependent anion channel. *J. Biol. Chem.* **1993**, *268*, 1835–1841. [CrossRef]
- Sampson, M.J.; Lovell, R.S.; Craigen, W.J. The murine voltage-dependent anion channel gene family. Conserved structure and function. *J. Biol. Chem.* **1997**, *272*, 18966–18973. [CrossRef] [PubMed]
- Schredelseker, J.; Paz, A.; López, C.J.; Altenbach, C.; Leung, C.S.; Drexler, M.K.; Chen, J.N.; Hubbell, W.L.; Abramson, J. High resolution structure and double electron-electron resonance of the zebrafish voltage-dependent anion channel 2 reveal an oligomeric population. *J. Biol. Chem.* **2014**, *289*, 12566–12577. [CrossRef]
- Tomasello, M.F.; Guarino, F.; Reina, S.; Messina, A.; De Pinto, V. The Voltage-Dependent Anion selective Channel 1 (VDAC1) topography in the mitochondrial outer membrane as detected in intact cell. *PLoS ONE* **2013**, *8*, e81522. [CrossRef] [PubMed]
- Guo, X.W.; Smith, P.R.; Cognon, B.; D’Arcangelis, D.; Dolginova, E.; Mannella, C.A. Molecular design of the voltage-dependent, anion-selective channel in the mitochondrial outer membrane. *J. Struct. Biol.* **1995**, *114*, 41–59. [CrossRef]
- Zalk, R.; Israelson, A.; Garty, E.S.; Azoulay-Zohar, H.; Shoshan-Barmatz, V. Oligomeric states of the voltage-dependent anion channel and cytochrome c release from mitochondria. *Biochem. J.* **2005**, *386*, 73–83. [CrossRef] [PubMed]
- Gonçalves, R.P.; Buzhynskyy, N.; Prima, V.; Sturgis, J.N.; Scheuring, S. Supramolecular assembly of VDAC in native mitochondrial outer membranes. *J. Mol. Biol.* **2007**, *369*, 413–418. [CrossRef] [PubMed]
- Keinan, N.; Tyomkin, D.; Shoshan-Barmatz, V. Oligomerization of the Mitochondrial Protein Voltage-Dependent Anion Channel Is Coupled to the Induction of Apoptosis. *Mol. Cell. Biol.* **2010**, *30*, 698–709. [CrossRef]
- Mazure, N.M. VDAC in cancer. *Biochim. Biophys. Acta Bioenerg.* **2017**, *1858*, 665–673. [CrossRef]



30. Israelson, A.; Arbel, N.; Da Cruz, S.; Ilieva, H.; Yamanaka, K.; Shoshan-Barmatz, V.; Cleveland, D.W. Misfolded mutant SOD1 directly inhibits VDAC1 conductance in a mouse model of inherited ALS. *Neuron* **2010**, *67*, 575–587. [CrossRef]
31. Rostovtseva, T.K.; Gurnev, P.A.; Protchenko, O.; Hoogerheide, D.P.; Yap, T.L.; Philpott, C.C.; Lee, J.C.; Bezrukov, S.M. α -synuclein shows high affinity interaction with voltage-dependent anion channel, suggesting mechanisms of mitochondrial regulation and toxicity in Parkinson disease. *J. Biol. Chem.* **2015**, *290*, 18467–18477. [CrossRef] [PubMed]
32. Reddy, P.H. Is the mitochondrial outer membrane protein VDAC1 therapeutic target for Alzheimer's disease? *Biochim. Biophys. Acta Mol. Basis Dis.* **2013**, *1832*, 67–75. [CrossRef]
33. Zhang, E.; Mohammed Al-Amily, I.; Mohammed, S.; Luan, C.; Asplund, O.; Ahmed, M.; Ye, Y.; Ben-Hail, D.; Soni, A.; Vishnu, N.; et al. Preserving Insulin Secretion in Diabetes by Inhibiting VDAC1 Overexpression and Surface Translocation in β Cells. *Cell Metab.* **2019**, *29*, 64–77. [CrossRef]
34. Camara, A.K.S.; Zhou, Y.F.; Wen, P.C.; Tajkhorshid, E.; Kwok, W.M. Mitochondrial VDAC1: A key gatekeeper as potential therapeutic target. *Front. Physiol.* **2017**, *8*, 460. [CrossRef] [PubMed]
35. Reina, S.; De Pinto, V. Anti-Cancer Compounds Targeted to VDAC: Potential and Perspectives. *Curr. Med. Chem.* **2017**, *24*, 4447–4469. [CrossRef] [PubMed]
36. Ben-Hail, D.; Begas-Shvartz, R.; Shalev, M.; Shteinfer-Kuzmine, A.; Gruzman, A.; Reina, S.; De Pinto, V.; Shoshan-Barmatz, V. Novel compounds targeting the mitochondrial protein VDAC1 inhibit apoptosis and protect against mitochondrial dysfunction. *J. Biol. Chem.* **2016**, *291*, 24986–25003. [CrossRef]
37. Arif, T.; Krelin, Y.; Nakdimon, I.; Benharroch, D.; Paul, A.; Dadon-Klein, D.; Shoshan-Barmatz, V. VDAC1 is a molecular target in glioblastoma, with its depletion leading to reprogrammed metabolism and reversed oncogenic properties. *Neuro. Oncol.* **2017**, *19*, 951–964. [CrossRef]
38. Wu, S.; Sampson, M.J.; Decker, W.K.; Craigen, W.J. Each mammalian mitochondrial outer membrane porin protein is dispensable: Effects on cellular respiration. *Biochim. Biophys. Acta Mol. Cell Res.* **1999**, *1452*, 68–78. [CrossRef]
39. Sampson, M.J.; Decker, W.K.; Beaudet, A.L.; Ruitenbeek, W.; Armstrong, D.; Hicks, M.J.; Craigen, W.J. Immobile Sperm and Infertility in Mice Lacking Mitochondrial Voltage-dependent Anion Channel Type 3. *J. Biol. Chem.* **2001**, *276*, 1954–1960. [CrossRef]
40. Anfous, K.; Armstrong, D.D.; Craigen, W.J. Altered mitochondrial sensitivity for ADP and maintenance of creatine-stimulated respiration in oxidative striated muscles from VDAC1-deficient mice. *J. Biol. Chem.* **2001**, *276*, 39206–39212. [CrossRef]
41. Baines, C.P.; Kaiser, R.A.; Sheiko, T.; Craigen, W.J.; Molkentin, J.D. Voltage-dependent anion channels are dispensable for mitochondrial-dependent cell death. *Nat. Cell Biol.* **2007**, *9*, 550–555. [CrossRef] [PubMed]
42. Shoshan-Barmatz, V.; Shteinfer-Kuzmine, A.; Verma, A. VDAC1 at the intersection of cell metabolism, apoptosis, and diseases. *Biomolecules* **2020**, *10*, 1485. [CrossRef] [PubMed]
43. Young, M.J.; Bay, D.C.; Hausner, G.; Court, D.A. The evolutionary history of mitochondrial porins. *BMC Evol. Biol.* **2007**, *7*, 31. [CrossRef] [PubMed]
44. Sampson, M.J.; Ross, L.; Decker, W.K.; Craigen, W.J. A novel isoform of the mitochondrial outer membrane protein VDAC3 via alternative splicing of a 3-base exon. Functional characteristics and subcellular localization. *J. Biol. Chem.* **1998**, *273*, 30482–30486. [CrossRef]
45. Decker, W.K.; Craigen, W.J. The tissue-specific, alternatively spliced single ATG exon of the type 3 voltage-dependent anion channel gene does not create a truncated protein isoform in vivo. *Mol. Genet. Metab.* **2000**, *70*, 69–74. [CrossRef]
46. Reina, S.; Checchetto, V.; Saletti, R.; Gupta, A.; Chaturvedi, D.; Guardiani, C.; Guarino, F.; Scorciapino, M.A.; Magri, A.; Foti, S.; et al. VDAC3 as a sensor of oxidative state of the intermembrane space of mitochondria: The putative role of cysteine residue modifications. *Oncotarget* **2016**, *7*, 2249–2268. [CrossRef]
47. Queralt-Martín, M.; Bergdoll, L.; Tejjido, O.; Munshi, N.; Jacobs, D.; Kuszak, A.J.; Protchenko, O.; Reina, S.; Magri, A.; De Pinto, V.; et al. A lower affinity to cytosolic proteins reveals VDAC3 isoform-specific role in mitochondrial biology. *J. Gen. Physiol.* **2020**, *152*, e201912501. [CrossRef]
48. Okazaki, M.; Kurabayashi, K.; Asanuma, M.; Saito, Y.; Dodo, K.; Sodeoka, M. VDAC3 gating is activated by suppression of disulfide-bond formation between the N-terminal region and the bottom of the pore. *Biochim. Biophys. Acta Biomembr.* **2015**, *1848*, 3188–3196. [CrossRef]
49. Checchetto, V.; Reina, S.; Magri, A.; Szabo, I.; De Pinto, V. Recombinant human voltage dependent anion selective channel isoform 3 (hVDAC3) forms pores with a very small conductance. *Cell. Physiol. Biochem.* **2014**, *34*, 842–853. [CrossRef]
50. Saletti, R.; Reina, S.; Pittalà, M.G.G.; Belfiore, R.; Cunsolo, V.; Messina, A.; De Pinto, V.; Foti, S. High resolution mass spectrometry characterization of the oxidation pattern of methionine and cysteine residues in rat liver mitochondria voltage-dependent anion selective channel 3 (VDAC3). *Biochim. Biophys. Acta Biomembr.* **2017**, *1859*, 301–311. [CrossRef]
51. Saletti, R.; Reina, S.; Pittalà, M.G.G.; Magri, A.; Cunsolo, V.; Foti, S.; De Pinto, V. Post-translational modifications of VDAC1 and VDAC2 cysteines from rat liver mitochondria. *Biochim. Biophys. Acta Bioenerg.* **2018**, *1859*, 806–816. [CrossRef] [PubMed]
52. De Pinto, V.; Reina, S.; Gupta, A.; Messina, A.; Mahalakshmi, R. Role of cysteines in mammalian VDAC isoforms' function. *Biochim. Biophys. Acta Bioenerg.* **2016**, *1857*, 789–798. [CrossRef] [PubMed]
53. Pittalà, M.G.G.; Saletti, R.; Reina, S.; Cunsolo, V.; De Pinto, V.; Foti, S. A high resolution mass spectrometry study reveals the potential of disulfide formation in human mitochondrial voltage-dependent anion selective channel isoforms (HVDACs). *Int. J. Mol. Sci.* **2020**, *21*, 1468. [CrossRef] [PubMed]

54. Pittalà, M.G.G.; Reina, S.; Cubisino, S.A.M.; Cucina, A.; Formicola, B.; Cunsolo, V.; Foti, S.; Saletti, R.; Messina, A. Post-translational modification analysis of VDAC1 in ALS-SOD1 model cells reveals specific asparagine and glutamine deamidation. *Antioxidants* **2020**, *9*, 1218. [CrossRef]
55. Reina, S.; Pittalà, M.G.G.; Guarino, F.; Messina, A.; De Pinto, V.; Foti, S.; Saletti, R. Cysteine Oxidations in Mitochondrial Membrane Proteins: The Case of VDAC Isoforms in Mammals. *Front. Cell Dev. Biol.* **2020**, *8*, 397. [CrossRef]
56. Kerner, J.; Lee, K.; Tandler, B.; Hoppel, C.L. VDAC proteomics: Post-translation modifications. *Biochim. Biophys. Acta Biomembr.* **2012**, *1818*, 1520–1525. [CrossRef]
57. Zinghirino, F.; Pappalardo, X.G.; Messina, A.; Guarino, F.; De Pinto, V. Is the secret of VDAC isoforms in their gene regulation? Characterization of human vDAC genes expression profile, promoter activity, and transcriptional regulators. *Int. J. Mol. Sci.* **2020**, *21*, 7388. [CrossRef]
58. Ardlie, K.G.; DeLuca, D.S.; Segrè, A.V.; Sullivan, T.J.; Young, T.R.; Gelfand, E.T.; Trowbridge, C.A.; Maller, J.B.; Tukiainen, T.; Lek, M.; et al. The Genotype-Tissue Expression (GTEx) pilot analysis: Multitissue gene regulation in humans. *Science* **2015**, *348*, 648–660. [CrossRef]
59. De Pinto, V.; Guarino, F.; Guarnera, A.; Messina, A.; Reina, S.; Tomasello, F.M.; Palermo, V.; Mazzoni, C. Characterization of human VDAC isoforms: A peculiar function for VDAC3? *Biochim. Biophys. Acta Bioenerg.* **2010**, *1797*, 1268–1275. [CrossRef]
60. Noguchi, S.; Arakawa, T.; Fukuda, S.; Furuno, M.; Hasegawa, A.; Hori, F.; Ishikawa-Kato, S.; Kaida, K.; Kaiho, A.; Kanamori-Katayama, M.; et al. FANTOM5 CAGE profiles of human and mouse samples. *Sci. Data* **2017**, *4*, 170112. [CrossRef]
61. Papatheodorou, I.; Moreno, P.; Manning, J.; Fuentes, A.M.P.; George, N.; Fexova, S.; Fonseca, N.A.; Füllgrabe, A.; Green, M.; Huang, N.; et al. Expression Atlas update: From tissues to single cells. *Nucleic Acids Res.* **2020**, *48*, D77–D83. [CrossRef]
62. Nepal, C.; Hadzhiev, Y.; Balwierz, P.; Tarifeño-Saldivia, E.; Cardenas, R.; Wragg, J.W.; Suzuki, A.M.; Carninci, P.; Peers, B.; Lenhard, B.; et al. Dual-initiation promoters with intertwined canonical and TCT/TOP transcription start sites diversify transcript processing. *Nat. Commun.* **2020**, *11*, 1–7. [CrossRef] [PubMed]
63. Grandori, C.; Cowley, S.M.; James, L.P.; Eisenman, R.N. The Myc/Max/Mad network and the transcriptional control of cell behavior. *Annu. Rev. Cell Dev. Biol.* **2000**, *16*, 653–699. [CrossRef] [PubMed]
64. Thiel, G.; Cibelli, G. Regulation of life and death by the zinc finger transcription factor Egr-1. *J. Cell. Physiol.* **2002**, *193*, 287–292. [CrossRef] [PubMed]
65. Liu, Z.H.; Dai, X.M.; Du, B. Hes1: A key role in stemness, metastasis and multidrug resistance. *Cancer Biol. Ther.* **2015**, *16*, 353–359. [CrossRef] [PubMed]
66. Triner, D.; Castillo, C.; Hakim, J.B.; Xue, X.; Greenson, J.K.; Nuñez, G.; Chen, G.Y.; Colacino, J.A.; Shah, Y.M. Myc-Associated Zinc Finger Protein Regulates the Proinflammatory Response in Colitis and Colon Cancer via STAT3 Signaling. *Mol. Cell. Biol.* **2018**, *38*, 22. [CrossRef]
67. Woo, A.J.; Kim, J.; Xu, J.; Huang, H.; Cantor, A.B. Role of ZBP-89 in human globin gene regulation and erythroid differentiation. *Blood* **2011**, *118*, 3684–3693. [CrossRef]
68. Qu, H.; Qu, D.; Chen, F.; Zhang, Z.; Liu, B.; Liu, H. ZBTB7 overexpression contributes to malignancy in breast cancer. *Cancer Invest.* **2010**, *28*, 672–678. [CrossRef]
69. Niederreither, K.; Dollé, P. Retinoic acid in development: Towards an integrated view. *Nat. Rev. Genet.* **2008**, *9*, 541–553. [CrossRef]
70. Labrecque, M.; Prefontaine, G.; Beischlag, T. The Aryl Hydrocarbon Receptor Nuclear Translocator (ARNT) Family of Proteins: Transcriptional Modifiers with Multi-Functional Protein Interfaces. *Curr. Mol. Med.* **2013**, *13*, 1047–1065. [CrossRef]
71. Hayes, J.D.; Dinkova-Kostova, A.T. The Nrf2 regulatory network provides an interface between redox and intermediary metabolism. *Trends Biochem. Sci.* **2014**, *39*, 199–218. [CrossRef]
72. Anckar, J.; Sistonen, L. Regulation of HSF1 function in the heat stress response: Implications in aging and disease. *Annu. Rev. Biochem.* **2011**, *80*, 1089–1115. [CrossRef] [PubMed]
73. Li, N.; Zhao, C.T.; Wang, Y.; Yuan, X.B. The transcription factor Cux1 regulates dendritic morphology of cortical pyramidal neurons. *PLoS ONE* **2010**, *5*, e10596. [CrossRef] [PubMed]
74. Kageyama, R.; Shimojo, H.; Ohtsuka, T. Dynamic control of neural stem cells by bHLH factors. *Neurosci. Res.* **2019**, *138*, 12–18. [CrossRef] [PubMed]
75. Pan, L.; Liu, Q.; Li, J.; Wu, W.; Wang, X.; Zhao, D.; Ma, J. Association of the VDAC3 gene polymorphism with sperm count in Han-Chinese population with idiopathic male infertility. *Oncotarget* **2017**, *8*, 45242–45248. [CrossRef] [PubMed]
76. Guarino, F.; Zinghirino, F.; Mela, L.; Pappalardo, X.G.; Ichas, F.; De Pinto, V.; Messina, A. NRF-1 and HIF-1 α contribute to modulation of human VDAC1 gene promoter during starvation and hypoxia in HeLa cells. *Biochim. Biophys. Acta Bioenerg.* **2020**, *1861*, 148289. [CrossRef]
77. Cheng, E.H.Y.; Sheiko, T.V.; Fisher, J.K.; Craigen, W.J.; Korsmeyer, S.J. VDAC2 inhibits BAK activation and mitochondrial apoptosis. *Science* **2003**, *301*, 513–517. [CrossRef]
78. Chin, H.S.; Li, M.X.; Tan, I.K.L.; Ninnis, R.L.; Reljic, B.; Scicluna, K.; Dagley, L.F.; Stephens, A.N.; Kelly, G.L.; Samson, A.; et al. VDAC2 enables BAX to mediate apoptosis and limit tumor development. *Nat. Commun.* **2018**, *9*, 4976. [CrossRef]
79. Naghdi, S.; Hajnóczky, G. VDAC2-specific cellular functions and the underlying structure. *Biochim. Biophys. Acta Mol. Cell Res.* **2016**, *1863*, 2503–2514. [CrossRef]
80. Mihara, K.; Sato, R. Molecular cloning and sequencing of cDNA for yeast porin, an outer mitochondrial membrane protein: A search for targeting signal in the primary structure. *EMBO J.* **1985**, *4*, 769–774. [CrossRef]

81. Ludwig, O.; Krause, J.; Hay, R.; Benz, R. Purification and characterization of the pore forming protein of yeast mitochondrial outer membrane. *Eur. Biophys. J.* **1988**, *15*, 269–276. [CrossRef]
82. Blachly-Dyson, E.; Song, J.; Wolfgang, W.J.; Colombini, M.; Forte, M. Multicopy suppressors of phenotypes resulting from the absence of yeast VDAC encode a VDAC-like protein. *Mol. Cell. Biol.* **1997**, *17*, 5727–5738. [CrossRef] [PubMed]
83. Guardiani, C.; Magri, A.; Karachitos, A.; Di Rosa, M.C.; Reina, S.; Bodrenko, I.; Messina, A.; Kmita, H.; Ceccarelli, M.; De Pinto, V. yVDAC2, the second mitochondrial porin isoform of *Saccharomyces cerevisiae*. *Biochim. Biophys. Acta Bioenerg.* **2018**, *1859*, 270–279. [CrossRef] [PubMed]
84. Magri, A.; Karachitos, A.; Di Rosa, M.C.; Reina, S.; Conti Nibali, S.; Messina, A.; Kmita, H.; De Pinto, V. Recombinant yeast VDAC2: A comparison of electrophysiological features with the native form. *FEBS Open Bio* **2019**, *9*. [CrossRef] [PubMed]
85. Morgenstern, M.; Stiller, S.B.; Lübbert, P.; Peikert, C.D.; Dannenmaier, S.; Drepper, F.; Weill, U.; Höß, P.; Feuerstein, R.; Gebert, M.; et al. Definition of a High-Confidence Mitochondrial Proteome at Quantitative Scale. *Cell Rep.* **2017**, *19*, 2836–2852. [CrossRef] [PubMed]
86. Magri, A.; Di Rosa, M.C.; Orlandi, I.; Guarino, F.; Reina, S.; Guarnaccia, M.; Morello, G.; Spampinato, A.; Cavallaro, S.; Messina, A.; et al. Deletion of Voltage-Dependent Anion Channel 1 knocks mitochondria down triggering metabolic rewiring in yeast. *Cell. Mol. Life Sci.* **2020**, *77*, 3195–3213. [CrossRef]
87. Krüger, V.; Becker, T.; Becker, L.; Montilla-Martinez, M.; Ellenrieder, L.; Vögtle, F.N.; Meyer, H.E.; Ryan, M.T.; Wiedemann, N.; Warscheid, B.; et al. Identification of new channels by systematic analysis of the mitochondrial outer membrane. *J. Cell Biol.* **2017**, *216*, 3485–3495. [CrossRef]
88. Ellenrieder, L.; Dieterle, M.P.; Doan, K.N.; Mårtensson, C.U.; Floerchinger, A.; Campo, M.L.; Pfanner, N.; Becker, T. Dual Role of Mitochondrial Porin in Metabolite Transport across the Outer Membrane and Protein Transfer to the Inner Membrane. *Mol. Cell* **2019**, *73*, 1056–1065. [CrossRef]

Review

Sequence Features of Mitochondrial Transporter Protein Families

Gergely Gyimesi *  and Matthias A. Hediger 

Membrane Transport Discovery Lab, Department of Nephrology and Hypertension, and Department of Biomedical Research, Inselspital, University of Bern, Kinderklinik, Freiburgstrasse 15, CH-3010 Bern, Switzerland; matthias.hediger@ibmm.unibe.ch

* Correspondence: gergely.gyimesi@dbmr.unibe.ch; Tel.: +41-31-632-2293

Received: 20 October 2020; Accepted: 22 November 2020; Published: 28 November 2020

Abstract: Mitochondrial carriers facilitate the transfer of small molecules across the inner mitochondrial membrane (IMM) to support mitochondrial function and core cellular processes. In addition to the classical SLC25 (solute carrier family 25) mitochondrial carriers, the past decade has led to the discovery of additional protein families with numerous members that exhibit IMM localization and transporter-like properties. These include mitochondrial pyruvate carriers, sideroflexins, and mitochondrial cation/H⁺ exchangers. These transport proteins were linked to vital physiological functions and disease. Their structures and transport mechanisms are, however, still largely unknown and understudied. Protein sequence analysis per se can often pinpoint hotspots that are of functional or structural importance. In this review, we summarize current knowledge about the sequence features of mitochondrial transporters with a special focus on the newly included SLC54, SLC55 and SLC56 families of the SLC solute carrier superfamily. Taking a step further, we combine sequence conservation analysis with transmembrane segment and secondary structure prediction methods to extract residue positions and sequence motifs that likely play a role in substrate binding, binding site gating or structural stability. We hope that our review will help guide future experimental efforts by the scientific community to unravel the transport mechanisms and structures of these novel mitochondrial carriers.

Keywords: mitochondrial carriers; SLC transporters; SLC25; MCF; SLC54; MPC; SLC55; LETM; SLC56; sideroflexin; ABC transporter; sequence analysis; protein targeting

1. Introduction

Mitochondria are believed to have evolved through an endosymbiotic event, where an α -proteobacteria has been engulfed by a host cell, possibly an archaeon [1,2]. This event is thought to have arisen only once, and in the last 2 billion years, mitochondria have evolved together and in close concordance with their host cells [1,3,4]. During this time, significant changes in the genome of the endosymbiont have taken place, which involved the transfer of most mitochondrial proteins to the nucleus, as well as the emergence of novel protein families in the nuclear genome that are targeted to mitochondria [4,5]. The vestigial mitochondrial genomes of vertebrates in general code for 13 internal membrane proteins that are involved in electron transport and coupled oxidative phosphorylation [6,7], while the part of the mitochondrial proteome related to transmembrane transport, i.e., the exchange of metabolites and ions with the host cell, is almost exclusively of eukaryotic origin [4,5].

Proteins in the human inner mitochondrial membrane (IMM) are quite distinct from one another in terms of their structure and sequence features as well as their trafficking and import mechanisms into mitochondria. Based on this diversity, they are likely polyphyletic in origin and presumably arose independently of each other. Membrane proteins that take part in transmembrane solute transport across the IMM include members of the following families: SLC25 (mitochondrial carriers),

SLC8 (SLC8B1/NCLX Na⁺/Ca²⁺/Li⁺ exchanger), SLC54 (MPC, mitochondrial pyruvate carriers), SLC55 (LETM, leucine zipper-EF-hand-containing transmembrane proteins), SLC56 (sideroflexins), ATP-binding cassette (ABC) transporters (ABCB7, ABCB8, ABCB10) and various ion channels [8]. The discovery, biological function, physiological role and disease involvement of many of these transport proteins and channels are comprehensively presented in excellent articles of the present review series. In particular, ion channels are covered in detail in the review by Szabo et al. and will not be discussed here. Metabolite and ion transport between the cytoplasm and the mitochondria also require the broad-specificity channels of the outer mitochondrial membrane (OMM). The most prominent class of such channels, the voltage-dependent anion channels (VDACs), is discussed in detail by Shoshan-Barmatz et al. in this review series [9], but other OMM transporters with unknown substrate specificity may also be present [10]. In this review, we focus on the discussion of specific structure and sequence features that shape trafficking and functional properties of transporter-like proteins in the IMM.

Trafficking of Membrane Transporters into Mitochondria

Transporters of the mitochondrial inner membrane are synthesized in the cytoplasm and imported into the mitochondria through specialized import machinery [11]. In contrast to most mitochondrial proteins, most mitochondrial carriers typically do not contain an N-terminal mitochondrial targeting sequence (MTS). Instead, the nascent precursor transporter proteins bind to the ATP-hydrolyzing Hsp70 and Hsp90 chaperones in the cytoplasm, which deliver them to the translocase of the outer membrane (TOM) complex. Here, the Tom70 receptor, part of TOM, binds both the precursor protein and the chaperones, and transfers the precursor protein to Tom22, where it then gets translocated in a loop-wise fashion through Tom40, the channel component of TOM [12,13]. Once in the intermembrane space, the hydrophobic regions of the precursor transporter proteins are shielded by the heterohexameric chaperone complex Tim9-Tim10-Tim12. This complex of the precursor protein and the chaperones then binds to the receptor-like protein Tim54, which is part of the translocase of the inner membrane (TIM22) complex in the IMM. Here, another member of TIM22, the channel-forming Tim22 protein, then inserts the precursor protein into the inner mitochondrial membrane [11] (Figure 1).

As an alternative import mechanism, certain precursor transporter proteins do carry the MTS on their N-termini, which typically forms a short (15–50 residues) amphipathic helix with a net positive charge [14,15]. Transporters containing an N-terminal MTS, such as SLC55/LETM and mitochondrial ABCB transporters, are delivered from the cytoplasm by the Tom20 receptor of the TOM complex, recognizing the hydrophobic side of the amphipathic helix formed by the MTS [16]. Upon transfer to the intermembrane space through Tom40, the targeting sequence binds to the Tim50 receptor component of another inner membrane complex, TIM23 [17]. This activates the Tim23 channel subunit of the TIM23 complex to allow the translocation of the bound precursor protein through the IMM [11]. Precursor proteins that are destined to the lipid bilayer contain a hydrophobic stop-transfer signal sequence, which is recognized within the IMM by the small transmembrane protein Mgr2, initiating the lateral release of the imported precursor protein into the membrane [11,18,19] (Figure 1). Interestingly, an alternative mechanism exists, where Oxa1, the main component of the oxidase assembly (OXA) translocase complex, inserts the hydrophobic segment into the inner membrane bilayer after they pass through the Tim23 pore [11] (Figure 1). It has been shown that even a single protein with multiple membrane-spanning segments can use different mechanisms to import individual transmembrane segments into the membrane, such as the yeast protein Mdl1, a mitochondrial ABCB family homolog [20]. Further details about the molecular machinery for importing metabolite transporters into mitochondria are discussed by Rampelt et al. as part of the present special review series.

Hydrogenosomes and mitosomes are cellular organelles that share a common evolutionary origin with mitochondria [21], and the comparison of their protein import machineries has shed light on important events shaping the early evolution of the mitochondrial import machinery [22].

Protein precursors destined to the hydrogenosomes and mitosomes may contain N-terminal presequences that are typically shorter than MTSs and also lack a marked positive charge [22]. Nevertheless, various hydrogenosomal proteins from the primitive eukaryote *Trichomonas vaginalis* readily target into mitochondria when expressed in yeast, and vice versa [22]. Furthermore, the Tom20 receptor and the acidic N-terminal extension of the Tom22 receptor, both playing fundamental roles in the recognition of the positively charged amphipathic presequence, seem to have evolved independently after the last common eukaryotic ancestor [23], indicating that the primitive TOM import complex did not have these features. All these arguments suggest that the MTS and the corresponding recognition and import machinery evolved in a convergent way in various eukaryotic lineages on top of a pre-existing ancestral protein import machinery, which was most likely independent of the MTS [22]. Based on this reasoning, proteins utilizing the conserved MTS-independent import pathway, such as most SLC25 carriers, might have been one of the earliest groups of proteins that developed mitochondrial localization.

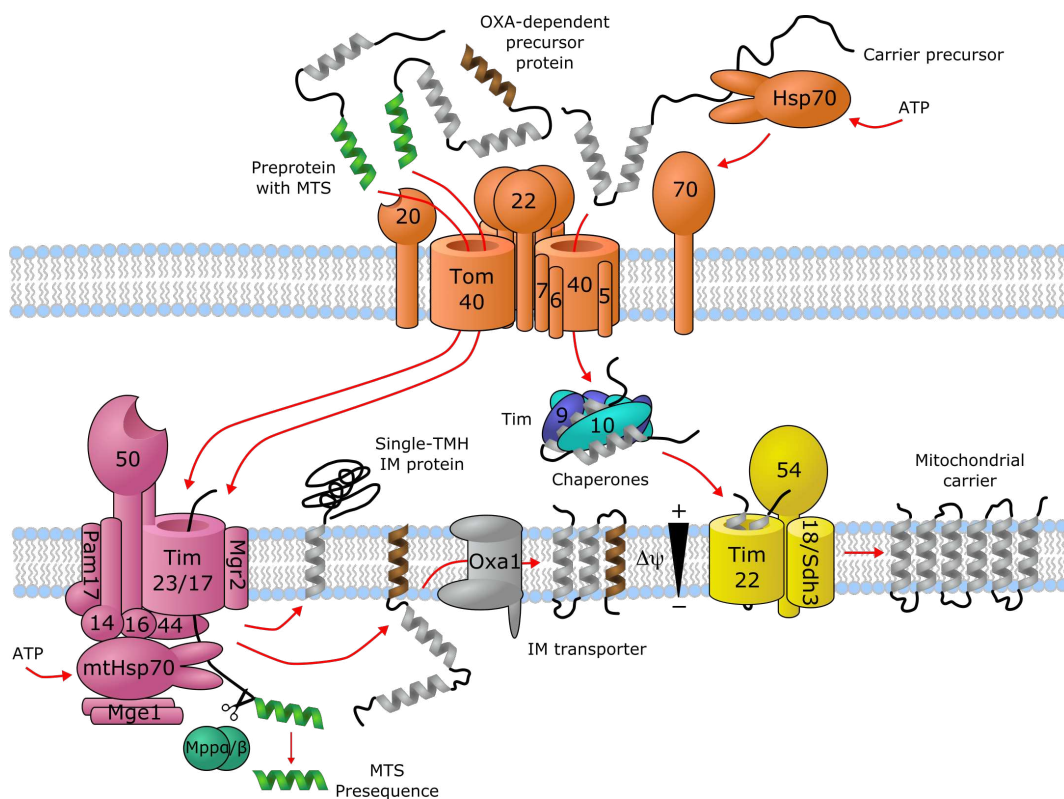


Figure 1. Import machinery for mitochondrial transporters. The TOM (orange), TIM23 (purple) and TIM22 (yellow) complexes are depicted, with numbers representing the corresponding Tom/Tim protein names. Proteins with a single transmembrane helix (TMH) and OXA-dependent transporters employ the TIM23 import pathway, while carriers with no mitochondrial targeting sequence (MTS) are imported through TIM22. For details, see text. Figure is based on [11–13,17–19].

The development of a positively charged MTS has been linked to the appearance of the electron transport chain, which resulted in a markedly negative membrane potential across the IMM [22]. In this scenario, a positively charged presequence would confer an evolutionary advantage during the membrane translocation of the precursor protein due to the electrophoretic effect [22]. In addition, a functional MTS can arise de novo fairly easily through random mutations or DNA rearrangements [24–27]. The development of an MTS-dependent import machinery with an easily generatable MTS could thus have promoted the evolvability of the host organism [27].

2. SLC25—Mitochondrial Carrier Family (MCF)

The largest protein family of mitochondrial solute transporters is the SLC25 (mitochondrial carrier) family. In human there are a total of 53 members that fulfil the vital roles of uniport or exchange of ions, metabolites and other solutes across the IMM [28]. It has been recognized early on that the sequence of the ADP/ATP translocase (SLC25A4) has a repeating sequence element that contains two hydrophobic segments and repeats 3 times in the sequence [29]. Such an internal repeat symmetry is commonly found in membrane transporters [30]. Indeed, such features were later found in several other members of the protein family [31–34], along with conserved proline, glycine and acidic amino acid residues [35]. The conserved residues were later compiled into a consensus characteristic or “signature motif” for mitochondrial carriers, P_x(D/E)_{xx}(K/R) [36], and the conserved charged residues were indeed found to take part in specific conserved salt-bridge contacts, termed the matrix network [37–42], in the 3D structure of the proteins [43,44]. The signature motif can be extended in the C-terminal direction to include a proximal glutamine (Q) residue, which helps stabilize the salt-bridge contacts on the matrix side of the carrier, forming the “Q brace” [44,45]. There is a similar cluster of charged residues on the intermembrane side of the even-numbered TM helices, forming the cytoplasmic salt-bridge network, where the charged residues of a (Y/F)(D/E)_{xx}(K/R) motif engage in salt-bridge contacts [42,44]. This network is stabilized by the so-called tyrosine (Y) brace, formed by the hydrogen bonding of the tyrosine residues of the motif to these salt bridges [45]. A further sequence motif, (Y/W/L/F)(K/R)G_{xx}P, present in the connecting loop between each short matrix helix and the following transmembrane helix, has been described, replacement of which disrupts the function of the transporter [46]. In addition, close helix-helix contacts in the matrix-facing state are formed by two conserved sequence motifs, π G π x π G on the odd-numbered, and π xxx π on the even-numbered helices, where π stands for a residue with a small side-chain [45,47,48]. Further details of these sequence motifs, including their roles in the transport mechanism and a functional interpretation of individual amino acid residues is covered in detail by Kunji et al. in this special issue. In particular, disease-causing mutations in context of the 3D structure of SLC25 carriers and their sequence motifs are extensively reviewed by Palmieri et al. in the present review series [49].

Interestingly, the sequence motif (QYKG_{xx}DC_xRK) in the short matrix helices has also been described, which is only conserved in a subset of mitochondrial carriers, such as ADP/ATP (SLC25A4–6, SLC25A31), aspartate/glutamate (SLC25A12–13), ornithine (SLC25A2, SLC25A15), glutamate (SLC25A18, SLC25A22), and carnitine (SLC25A20) carriers, one ATP/P_i carrier (SLC25A24) and three carriers with unknown function (SLC25A9, SLC25A34, SLC25A45) [50]. This motif was proposed to harbor residues that go through post-translational modification thereby locally altering the protein structure and thus modulating function. One example for this is acetylation at K163 of SLC25A5 (AAC2), corresponding to the last residue of the motif, while the cysteine residue of the motif might interact with oxidizing/reducing agents [50]. Further investigation is required to reveal the precise functional role of this sequence motif.

Most SLC25 family proteins do not contain an MTS at their N-termini. Instead, they seem to hold mitochondrial targeting information in all three segments of their three-fold repeat sequence [51,52]. SLC25 proteins are embedded into the IMM by the TIM22 machinery, as described in the previous chapter. It was suggested that the three repeating segments of SLC25 proteins act in a cooperative manner to facilitate receptor binding and translocation into mitochondria [53], nevertheless, a single unit consisting of a matrix loop and the following transmembrane helix is enough for mitochondrial localization [52]. The net positive charge of the short matrix loop helices have been shown to be essential for import into mitochondria, and these regions are thought to interact with the Tom40 channel component of the TOM complex, which effectively functions as a selectivity filter [52].

Interestingly, certain SLC25 proteins, such as the mitochondrial phosphate carrier (SLC25A3) and citrate/tricarboxylate carrier (SLC25A1) have been proposed to harbor an N-terminal MTS, based on physicochemical composition of their N-terminal sequences and observation of mature protein forms truncated at the anticipated cleavage site [31,54]. This is also partially supported by

TargetP-2.0 predictions, which report an MTS of 49 amino acids with likelihood 0.5749 for SLC25A3, exactly as anticipated from experiments where a protein fragment N-terminally truncated at the same position was identified [31]. For SLC25A1, the presence of an MTS was predicted with likelihood 0.3753. Whether a functional N-terminal MTS is present in these proteins has not been investigated experimentally. For all other human SLC25 proteins, the likelihood of an MTS at the N-terminus was less than 0.17 according to TargetP-2.0 predictions.

3. SLC54—Mitochondrial Pyruvate Carriers (MPC)

The mitochondrial pyruvate carriers have been identified as IMM transporters responsible for pyruvate uptake into the mitochondria [55,56]. MPC1 (SLC54A1) and MPC2 (SLC54A2) function as heterodimers [56,57], while humans as well as other placental mammals also contain a paralog of MPC1 called MPC1L (SLC54A3), the two sharing 48.2% sequence identity in human [58]. A detailed discussion of the biological role and function of MPCs and their links to disease can be found in a comprehensive review by Martinou et al. and Taylor et al. in this special issue.

MPCs have been predicted to harbor 2–3 transmembrane helices (TMHs) [55,56,59]. Interestingly, they are unrelated to SLC25 carriers and instead have been shown to be homologous to the 3-TMH repeating element in SWEET (“Sugars will eventually be exported transporters”) transporters [60,61], which show a 3 + 1 + 3 TMH architecture [62,63]. Proteins from the SWEET family also exist as homodimers of half-transporters encompassing the 3-TMH repeat, called SemiSWEET [62,64]. While there are relatively few studies on the structure and transport mechanism of MPCs, the structure and mechanism of SWEET and SemiSWEET transporters are quite well described [62,65–69]. Based on the suggested similarity, it can be speculated that the structure of a functional MPC transporter is similar to those of the homodimers of SemiSWEET proteins, or a single protomer of a SWEET-fold transporter. Based on this proposed similarity and the available structures for SWEET and SemiSWEET transporters, it should be possible to interpret disease-causing mutations in a structural context in the future, such as L79H and R97W in human SLC54A1/MPC1 [55,70,71].

Nevertheless, even without a structural context, one can analyze residue conservation in MPC proteins based on sequence alignment and the help of the “MPC” (PF03650) domain from the Pfam database [72]. The information of residue conservation encoded by profile hidden Markov models (HMM) of Pfam domains can be visualized as a HMM logo by a suitable software, such as Skyline [73] (Figure 2). We submitted the amino acid sequences of human SLC54A1–3 to three different methods to predict the location of transmembrane regions (HMMTOP [74], SPOCTOPUS [75], MEMSAT-SVM [76]) and secondary structural elements (PSIPRED [77]). Combining information on conservation with transmembrane region prediction pinpoints possible conserved charged/polar residues in transmembrane regions, which would imply that they might have a functional or structural role. Such residues may be S52/S54/S68, R68/R70/R84, H84/H86/N100 in MPC1/MPC1L/MPC2, respectively (Figure 2). Interestingly, residues N33/S35/K49 in MPC1/MPC1L/MPC2, respectively, represent a position which shows slight preference for polar/charged residues, but is asymmetric between MPC1/SLC54A1 and MPC2/SLC54A2 proteins, which could hint at a possible substrate-binding role [42]. We can also observe based on Figure 2 that the disease-associated mutation R97W [55] modifies an amino acid at a location that is considerably conserved in the family with a preference for basic sidechains, explaining the deleterious effects of the mutation. Intriguingly, the other currently known point mutation, L79H, is located at a poorly conserved position, and so is not expected to have a direct impact on the structure or function of the mature protein monomer. Several positions might contain structurally important residues with a clear preference for aromatic sidechains, such as F27/F29/F43, W28/W30/W44, W34/W36/W50, F66/F68/W82, F69/F71/Y85 in MPC1/MPC1L/MPC2, respectively. The detailed investigation of these residues in future studies might reveal more about their role in transporter function.

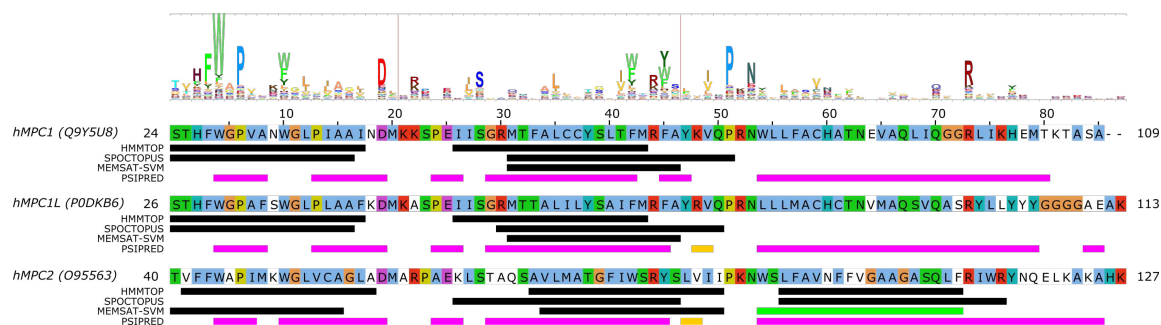


Figure 2. Sequence analysis of human MPC (SLC54) proteins. The diagram above the alignment shows the part of the HMM logo corresponding to the sequence (see text). At each position in the HMM logo, higher columns correspond to higher sequence conservation, and letters are drawn proportional to their frequency of occurrence at that position. Vertical lines in the HMM logo show positions with non-zero insertion frequency. Transmembrane regions predicted by three different methods (HMMTOP, SPOCTOPUS, MEMSAT-SVM) are marked by black lines. Green lines mark transmembrane regions predicted to by pore-lining by MEMSAT-SVM. Secondary structure as predicted by PSIPRED is shown as magenta lines (α -helix) and golden lines (β -strand). Uniprot sequence identifiers are shown next to protein names for each sequence.

4. SLC56—Sideroflexins

Sideroflexin 1 (SLC56A1/SFXN1) has been described as the gene whose defects are responsible for the flexed-tail mouse phenotype with sideroblastic anemia [78]. Later, it was found that SLC56A1/SFXN1 plays a role in serine transport into the mitochondria, which in turn fuels one-carbon metabolism [79]. SLC56A3/SFXN3 and SLC56A2/SFXN2 can compensate for this function, as well as yeast and *Drosophila* homologues, indicating an ancestral function, while SLC56A4/SFXN4 and SLC56A5/SFXN5 were unable to do so, indicating a possible altered transport rate or substrate selectivity [79]. Regarding their mitochondrial targeting, sideroflexins do not show any canonical MTS [78], and instead are targeted to the mitochondria via the TIM22 import complex [80–82], similarly to SLC25 proteins.

Very little is currently known about the structure and function of sideroflexin transporters. No structural homologs exist and, interestingly, no internal repeat symmetry has been described for SLC56 proteins. Five transmembrane helices were proposed to be conserved among family members and a few consensus motifs have been described [78]. Nevertheless, sequence analysis can potentially hint at functionally important regions in SLC56 proteins. Since the 3D structure and thus the membrane-spanning regions of SLC56 proteins are not known, we submitted the amino acid sequences of human SLC56A1–5 to various methods to predict the location of transmembrane regions and secondary structural elements as for MPC/SLC54 proteins. Interestingly, while four regions are more-less robustly predicted as transmembrane by various methods (Figure 3, alignment positions 140–160, 175–195, 225–250, 260–285, marked as Region 3–6, respectively), there appears to be significant inconsistency in predicting the first TM helical region (alignment region 75–125). The predictions by HMMTOP suggest two distinct regions (alignment positions 75–100 and 105–125, marked Region 1 and 2), and a third region overlapping with the first two (alignment position 90–110). However, the third region seems less likely due to the lack of sequence conservation as reported by the HMM logo, and the probability of residue insertions in alignment region 100–105 (Figure 3). SPOCTOPUS consistently does not report a TM segment in alignment region 75–125, while MEMSAT-SVM consistently reports the presence of a TM segment in Region 1 (Figure 3). Interestingly, MEMSAT-SVM also reports a sixth TM segment in Region 2 in SLC56A4, which is also predicted to be transmembrane by HMMTOP. This region is predicted to be helical by PSIPRED, and marked as pore-lining by SPOCTOPUS, likely hinting at its amphipathic nature. Region 2 also contains a sequence motif that is seemingly conserved in the protein family, and that has been described as “asparagine rich” already after the identification of SLC56A1/SFXN1 [78]. This motif could be described by the consensus

WQWxNQSxNxxxN motif, where polar residues N, S and Q are in conserved positions. According to PSIPRED predictions, occasional coil and strand content can occur near the second Q and second N residues (Figure 3). Such local distortions of helical geometry typically signal the location of substrate-binding sites in transmembrane transporter proteins [42,43,83,84], which, combined with the conservation pattern of residues, suggests that this region could have a functional role. Given that this putative functional region is often missed by transmembrane segment prediction software, while region 75–100 is consistently predicted by MEMSAT-SVM as transmembrane, combined with the presence of a non-conserved, insertion-prone region at 100–105, it is tempting to speculate that in fact regions 75–100 and 105–125 constitute two independent transmembrane helices, leading to an overall topology with six transmembrane helices in all SLC56 proteins.

Analysis of the other regions proposed as transmembrane also show remarkably conserved polar or charged residues that might play a role in shaping transport function. In Region 1, a conserved Arg residue is apparent from the HMM logo (Figure 3), corresponding to R92/R91/R91/R109/R108 in SLC56A1–5, respectively. Region 3 contains a conserved aromatic/hydrophobic residue (Y151/Y150/Y150/L166/Y167 in SLC56A1–5, respectively). Region 4 shows the consensus sequence pattern RxVPFxxVxxAxxxNxxxMR, of which P181/P180/P180/P201/P204 (SLC56A1–5, resp.) are conserved, indicating a possible structural role, while the N192/N191/N191/N212/N215 residues in the second half of the proposed transmembrane helix might play a functional role, and the highly conserved basic residue R197/R196/R196/R217/R220, proposed to be at the edge of the TM helix, might play a role in gating. Region 5 contains a conserved Ser-Arg (SR) motif with R233/R232/R232/R253/R256 highly preferred to be basic. In Region 6, the sequence pattern PxAxAFPQ is apparent, with the first proline residue (P281/P280/P280/P301/P304, SLC56A1–5, resp.) being highly conserved, suggesting the presence of a functionally or structurally relevant kink in the transmembrane helix in this region. Interestingly, regions outside the predicted transmembrane segments also contain seemingly conserved sequence motifs. The region just N-terminal to the first predicted transmembrane segment (Region 1) harbors the HPDT motif that is well conserved in human sideroflexin proteins and has been recognized early on [78]. The proposed loop between Regions 4 and 5 also contains some remarkably conserved amino acid residues, such as E200/E199/E199/E220/E223, S218/S217/S217/S238/S241, (in SLC56A1–5, resp.), which might play a functional role; and G204/G203/G203/G224/G227, which could be important in maintaining structure, such as close helix-helix contacts. Finally, the last five C-terminal residues of human sideroflexin proteins contain the consensus sequence FNKGL of unknown function, with a highly conserved glycine residue. Notably, no disease-linked genetic defects that modify a single amino acid position have been described for SLC56 proteins so far, instead, only mutations causing frameshift and/or premature termination have been reported [85].

Since the above descriptions are only based on computer predictions, they are speculative at this point. However, given the current scarcity of structure-function studies on sideroflexin proteins, these amino acid positions can be helpful to identify functionally relevant hot spots. These hypotheses, however, await validation by future experimental studies.

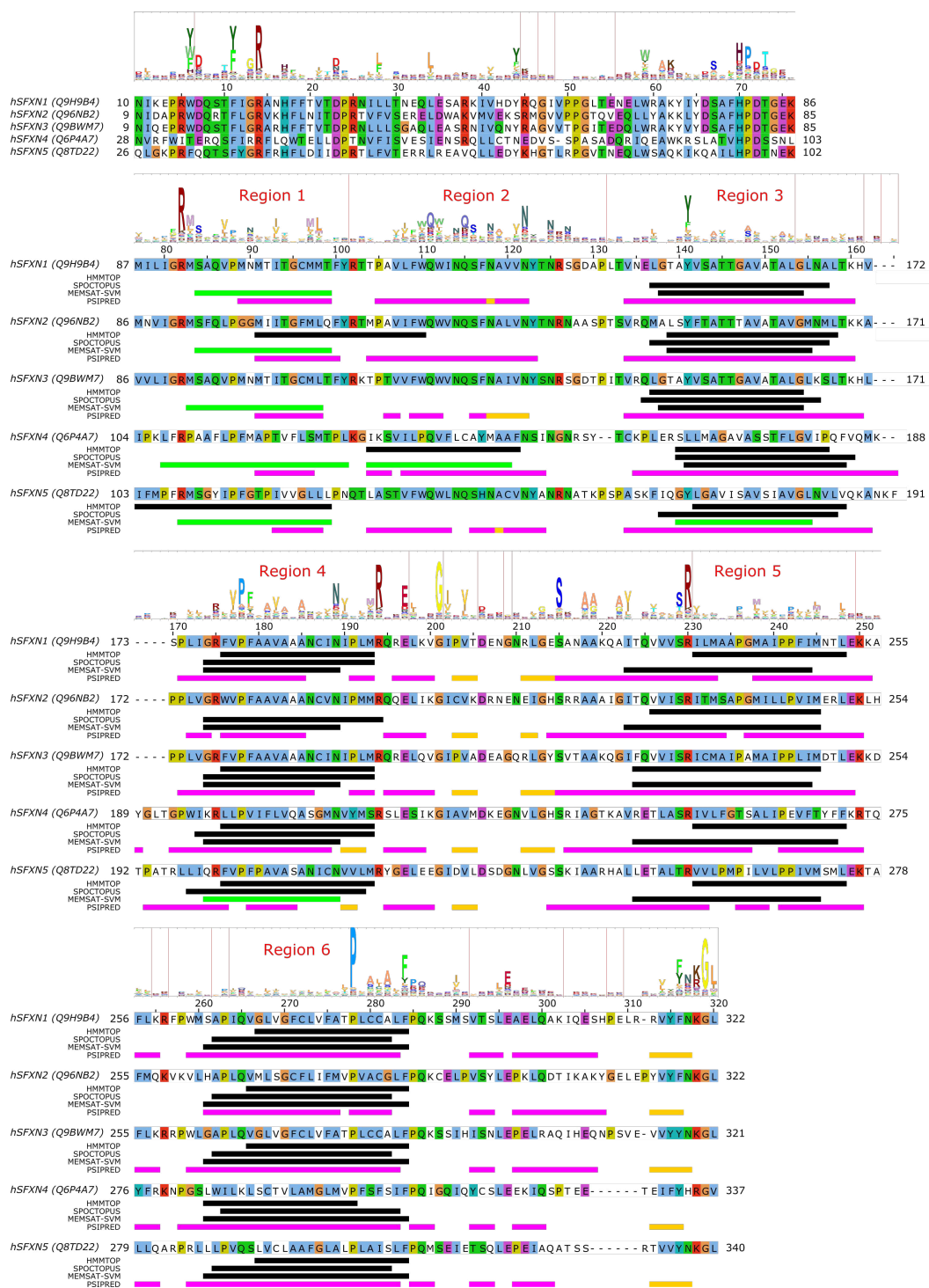


Figure 3. Sequence analysis of human sideroflexin proteins (SLC56 family). The HMM logo is shown above the sequence alignment (see text). Vertical lines in the HMM logo show positions with non-zero insertion frequency. Transmembrane regions predicted by three different methods (HMMTOP, SPOCTOPUS, MEMSAT-SVM) are marked by black lines. Green lines mark transmembrane regions predicted to by pore-lining by MEMSAT-SVM. Secondary structure as predicted by PSIPRED is shown as magenta lines (α -helix) and golden lines (β -strand). Uniprot sequence identifiers are shown next to protein names for each sequence.

5. The SLC55/LETM Mitochondrial Cation/Proton Exchanger Family

LETM1 (SLC55A1) has had a controversial role, as it was first proposed to be a part of the mitochondrial K^+/H^+ exchanger (KHE) pathway [86,87]. However, later, through a genome-wide genetic screen, it was found to be responsible for altered Ca^{2+} levels in mitochondria [88], and subsequently the purified LETM1 protein in liposomes was shown to mediate Ca^{2+}/H^+ exchange [88–90]. However, later it was argued that K^+/H^+ and unspecific and electroneutral cation/ H^+ exchange better explain the effect seen upon knockout of LETM1 in model cells and the effects seen in the mitochondria of model animals and patients with LETM1 deletion [91]. For a more detailed review of mitochondrial K^+ homeostasis, see the comprehensive reviews by Szabo et al. and Szewczyk et al. in this special issue. Nevertheless, the structure of LETM1 was proposed to be a hexamer and the predicted single TMH (alignment region 60–80 in Figure 4 [86]) contains a conserved acidic residue (E221), the mutation of which causes loss of the ability for the protein to take up Ca^{2+} into liposomes [90], which can be interpreted as E221 being part of the substrate-binding site. Interestingly, this residue is not conserved in LETMD1/SLC55A3 (N151, Figure 4), while other polar residues are present in the transmembrane region, such as S145, hinting at a substrate spectrum or a function that is likely different from LETM1/SLC55A1 and LETM2/SLC55A2. Nevertheless, the transport mechanism of the protein remains unknown, even though it has been shown that a change in external pH causes conformational changes in LETM1 [90]. In the proposed transmembrane region of SLC55 proteins, two proline residues seem to be conserved based on our sequence alignment and the HMM logo (Figure 4, P211/P180/F140 and P219/P188/P148 in SLC55A1–3, respectively). Conserved proline residues often signal positions with structurally important kinks in helices [92,93]. LETM1 contains the mitochondrial signal peptide [90], similarly to LETM2 (likelihood 0.3338) and LETMD1 (likelihood 0.9889) according to TargetP-2.0 [94] predictions, indicating that SLC55 proteins likely get translocated into the mitochondria via the TIM23 translocation complex. Currently, no single-point mutations linked to disease have been reported for SLC55 proteins.

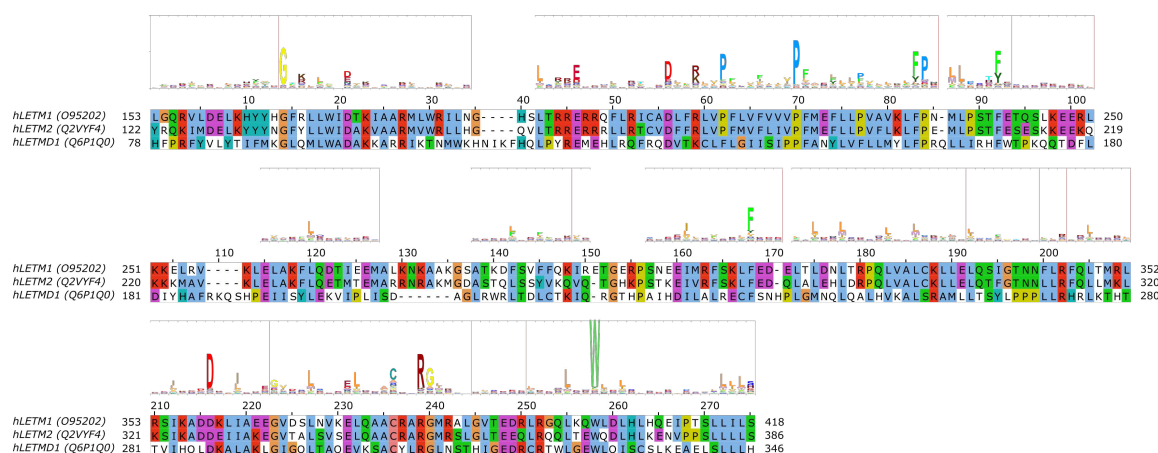


Figure 4. Sequence analysis of human LETM proteins (SLC55 family). HMM logo is shown over the alignment, based on the “LETM1” HMM model from Pfam (see text). Only the alignment region covered by the HMM model is shown. Certain non-conserved residue positions with ambiguous matches with the protein sequences have been removed from the HMM logo.

6. ATP-Binding Cassette (ABC) Transporters in Mitochondria

Currently, 3 of the 48 human ATP-binding cassette (ABC) transporters have been shown to be present in mitochondria, which are ABCB7, ABCB8 and ABCB10 (also known as ABC7 [95], M-ABC1 [96], and M-ABC2 [97], respectively). ABCB6 has also been suggested to be a mitochondrial transporter [98], but this has later been challenged [99,100]. The three mitochondrial ABC transporter proteins, in contrast to solute carriers, contain a mitochondrial targeting sequence at their N-termini [95–97,101], indicating that they are most likely translocated into the mitochondrial

inner membrane via the TIM23 machinery. The presence of an N-terminal cleavable targeting signal is also supported by TargetP-2.0 predictions (likelihoods 0.9634, 0.7184, and 0.207 for human ABCB7, ABCB8, and ABCB10, respectively), while human ABCB6 was not predicted to contain a signal peptide (likelihood 0.0001).

A yeast ABC transporter protein (Mdl1) showing considerable sequence similarity to human ABCB proteins [102], was shown to use both the conservative Oxa1-mediated import machinery and lateral release from the TIM23 complex to translocate to the IMM [20]. Based on this, it is likely that human ABCB proteins also use the same pathway for mitochondrial targeting. In addition, the homologous yeast Mdl2 protein and Atm1 (human ABCB7 ortholog) have also been suggested to employ OXA-mediated membrane insertion into the IMM [103]. Nevertheless, while it is plausible that human mitochondrial ABCB proteins also employ a similar mechanism, this has not yet been experimentally studied.

ABCB transporters in the mitochondria are so-called “half transporters”, consisting of one nucleotide-binding domain (NBD) and one transmembrane domain (TMD), with homodimeric complexes forming the functional transporter unit. Recent structural studies of human ABCB10 [104] and yeast Atm1 [105] have highlighted conserved sequence motifs that are located along cavities forming the putative substrate-binding site in the TMD. Interestingly, they are not lying in overlapping locations in the two different proteins. For human ABCB7, residues R315, R319, N378, N425, T429, R432 and E433 (corresponding to R280, R284, N343, N390, S394, R397, D398 in yeast Atm1, respectively) in TMH4, TMH5 and TMH6 near the cytoplasmic membrane interface have been proposed to take part in substrate binding based on the yeast Atm1 structure with bound glutathione [105]. While one of these positions, E433 have been found to be mutated to lysine in patients with X-linked sideroblastic anemia (XLSA) [106], biochemical validation of these binding site residues is still missing [105]. For human ABCB10, a conserved signature sequence of (N/I)xxR (containing N229 and R232) and NxxDGxR (containing N289, D292, R295) in TMH2 and TMH3, respectively, were found and have been proposed to take part in substrate binding [104]. In the case of ABCB10, the missing identity of the transported substrate hampers biochemical studies on the functional role of individual residues. It has been proposed that ABCB10 transports an intermediate in the heme biosynthesis pathway [107]. Structure-function studies elucidating functionally relevant residues or sequence motifs of human ABCB8 are still missing. In neither ABCB8 nor in ABCB10 have disease-linked single-point mutations been described yet.

7. Mitochondrial Calcium Transport via SLC8 Family

SLC8B1 (NCLX, Na⁺/Ca²⁺/Li⁺ exchanger) was identified as the ion exchanger protein responsible for the exit of Ca²⁺ from the mitochondria [108]. SLC8B1 is thought to exchange 3 Na⁺ ions for 1 Ca²⁺ ion based on similarity to other Na⁺/Ca²⁺ exchangers [109–111], and is unique in the property that Li⁺ ions can replace Na⁺ ions in transport [112]. Recently, it has been reported that Na⁺ taken up into the mitochondrial matrix by SLC8B1 in exchange for Ca²⁺ derived from calcium precipitates upon matrix acidification controls hypoxic signaling via the mitochondrial respiratory chain [113]. Specifically, it was reported that the Na⁺ imported into the matrix reduces membrane fluidity through interaction with phospholipids. This in turn was shown to lead to the generation of reactive oxygen species (ROS) by altering certain elements of the electron transport chain, thereby promoting an adaptive short-time elevation of mitochondrial complex III-dependent ROS production during acute hypoxia. Indeed, inhibition of Na⁺ import via SLC8B1 was sufficient to prevent this pathway leading to adaptation to acute hypoxia [113].

While the mechanism of mitochondrial targeting of SLC8B1 has not yet been studied, the sequence of human SLC8B1 does not seem to contain a mitochondrial targeting sequence according to TargetP-2.0 predictions (likelihood 0.0016). This suggests that other internal targeting signals are present that direct the protein into the mitochondria, possibly similarly to SLC25, MPC and sideroflexin proteins.

Disease-related mutations have not been reported for SLC8B1 thus far. However, residues responsible for the unique Li⁺-exchange capacity of SLC8B1 have been investigated in detail. Based on the determined structure of an archaeal NCX homologue, NCX_Mj, it was found that only 3 of the 12 ion-coordinating residues were shared with human SLC8B1 [114]. By mutating the 9 different residues to their human counterparts, it was possible to engineer a mutant of NCX_Mj that can also mediate Li⁺-dependent Ca²⁺ exchange [114]. In a later study, it was found that mutation of residue D471 to alanine can shift the selectivity toward Na⁺, while mutations at several positions can render SLC8B1 a Li⁺-selective exchanger [115]. All these positions cluster close to the Na⁺-binding sites shown by the X-ray structures of NCX_Mj [116,117] and the homologous H⁺/Ca²⁺ exchanger CAX_Af from the euryarchaeota *A. fulgidus* [118].

8. Additional Families with Members Proposed to be Localized in the IMM

8.1. The SLC9 Na⁺/H⁺ Exchanger Family

SLC9B2 (NHA2, Na⁺/H⁺ antiporter 2) might localize to the mitochondria [119,120], but this has been disputed [121]. Otherwise, SLC9B2 is more similar to prokaryotic Na⁺/H⁺ exchangers (NHEs) than to eukaryotic ones [121], and is the only human member of the Cation/Proton Antiporter 2 (CPA2) subfamily [122]. SLC9B2 does not seem to contain a MTS according to TargetP-2.0 predictions (likelihood 0).

8.2. The SLC1 Glutamate/Neutral Amino Acid Transporter Family

A splice variant of SLC1A5 (SLC1A5_var) was recently reported to have a mitochondrial localization and to function as the “long sought-after mitochondrial glutamine transporter” [123]. However, several inconsistencies urge us to treat this conclusion with caution. Firstly, the software the authors used for signal peptide detection (PrediSi) is designed to detect the signal peptides of proteins secreted through the Sec pathway [124], and is therefore unsuitable to detect a MTS. In contrast, methods that were specifically developed to detect MTS, such as TargetP-2.0, do not detect the presence of an MTS in SLC1A5_var (likelihood 0). Furthermore, the antibodies used by the authors to detect SLC1A5_var are claimed to “recognize the SLC1A5_var after peptide-N-glycosidase F (PNGase F) treatment” [123]. However, the only N-linked glycosylation sites on SLC1A5 are N163 and N212 [125], which are present in exon 1 that is in fact not present in the splice variant SLC1A5_var. Therefore, PNGase F treatment should not affect SLC1A5_var recognition. Due to the missing N-glycosylation sites, it is also likely, contrary to what the authors claim, that SLC1A5_var is not glycosylated. Finally, SLC1A5_var, in line with what is reported by the authors in their Figure 1A, is missing residues 2–203 of, but is otherwise identical to, canonical SLC1A5. According to sequence alignment of human SLC1 family members and the structure of a thermostable variant of the paralogous human SLC1A3 [126], this would mean that SLC1A5_var is missing the first 4 TMHs of the transporter protein, constituting most of the scaffold subdomain of the transporter. The importance of this region in transport is underlined by the fact that TMH3 forms part of the binding site for the allosteric SLC1A3 inhibitor UCPH₁₀₁, and TMH1 has been proposed to interact extensively with the lipid bilayer, harboring a possible lipid-binding site [126]. Thus, these regions are likely to be important in SLC1A5 as well, and it is questionable whether SLC1A5_var could function as a transporter with such an N-terminal truncation. Therefore, given the above-mentioned issues with the antibody used and the detection of an MTS, it is somewhat doubtful whether SLC1A5_var is truly a mitochondrial glutamine transporter. As an alternative, glutamine may be converted to glutamate in the mitochondrial intermembrane space via the phosphate-dependent glutaminase GLS [127] that is thought to be attached to the outer surface of the inner mitochondrial membrane [128]. Glutamate that is generated may then cross the IMM by the mitochondrial glutamate carriers SLC25A22 or SLC25A12. On the other hand, should GLS face the intra-mitochondrial matrix, a mitochondrial glutamine carrier is required. The need for such a carrier has been reviewed in detail in [129]. However, to clarify this subject matter, a conclusive

subcellular localization study of GLS in the mitochondrial inner membrane is still required, in order to reveal whether the enzyme is active on the intermembrane space or within the mitochondrial matrix.

9. Conclusions and Open Questions

The spectrum of primary and secondary active transporters in the mitochondrial inner membrane has greatly broadened in the past decade through the functional identification of mitochondrial pyruvate carriers, sideroflexins, and other mitochondrial transporters such as SLC8B1. This plurality of IMM transporters that show marked dissimilarity to SLC25 carriers, with no apparent common evolutionary history to the SLC25 family, hints that many other, as of yet unidentified secondary transporter families could exist in mitochondria. For the classical SLC25 mitochondrial carriers, their structure, targeting mechanism and transport properties are quite well-studied, but for the more recently identified proteins, structural information, and a general understanding of their transport mechanisms are still lacking. Interestingly, the sideroflexin (SLC56) protein family seems to share no significant sequence similarity to any protein with a known structure, and is therefore likely to possess a yet undescribed and novel structural fold. Further studies would be needed to clarify residues involved in substrate binding for sideroflexins. Another structurally enigmatic family of proteins are the LETM/SLC55 transporters, which likely function in a hexameric unit that can change conformation upon changes in pH, which can be a basis for an alternating-access mechanism [90]. Nevertheless, the transport mechanism of any single-helix membrane-spanning ion exchanger such as LETM1 has not been described yet. Despite the lack of information on many of these proteins, we aimed to summarize sequence elements involved in targeting and function of mitochondrial transporters, and have also suggested residues that could have a functional relevance based on sequence analysis of less well-characterized transporter families. The subsequent verification of the resulting hypotheses could greatly contribute to our understanding of their transport mechanisms. In this review, we have omitted the discussion of disease-causing mutations of SLC25 carriers, as these have been reported in detail in other articles of the present review series [49]. However, for non-SLC25 proteins, we have discussed the limited number of point mutations that are known to be linked to disease and involve single-residue changes. For these proteins, on the one hand, more information about their biological role and disease involvement would be desirable. On the other hand, for some transporters, e.g., pyruvate carriers of the SLC54 family, structural model building could help understand their transport mechanism and interpret certain disease-associated mutations. These endeavors can also potentially aid the generation of therapeutic modulators for future clinical applications.

Funding: This work has been supported by the Schweizerischer Nationalfonds (Swiss National Science Foundation) Grant Sinergia #CRSII5_180326, entitled “The role of mitochondrial carriers in metabolic tuning and reprogramming by calcium flow across membrane contact sites”.

Conflicts of Interest: The authors declare no conflict of interest.

References

1. Koonin, E.V. The Origin and Early Evolution of Eukaryotes in the Light of Phylogenomics. *Genome Biol.* **2010**, *11*, 209. [CrossRef] [PubMed]
2. Gray, M.W. Mitochondrial Evolution. *Cold Spring Harb. Perspect. Biol.* **2012**, *4*, a011403. [CrossRef] [PubMed]
3. Sicheritz-Pontén, T.; Kurland, C.G.; Andersson, S.G. A Phylogenetic Analysis of the Cytochrome b and Cytochrome c Oxidase I Genes Supports an Origin of Mitochondria from within the Rickettsiaceae. *Biochim. Biophys. Acta* **1998**, *1365*, 545–551. [CrossRef]
4. Kurland, C.G.; Andersson, S.G. Origin and Evolution of the Mitochondrial Proteome. *Microbiol. Mol. Biol. Rev.* **2000**, *64*, 786–820. [CrossRef]
5. Karlberg, O.; Canbäck, B.; Kurland, C.G.; Andersson, S.G. The Dual Origin of the Yeast Mitochondrial Proteome. *Yeast* **2000**, *17*, 170–187. [CrossRef]

6. Gray, M.W.; Lang, B.F.; Cedergren, R.; Golding, G.B.; Lemieux, C.; Sankoff, D.; Turmel, M.; Brossard, N.; Delage, E.; Littlejohn, T.G.; et al. Genome Structure and Gene Content in Protist Mitochondrial DNAs. *Nucleic Acids Res.* **1998**, *26*, 865–878. [CrossRef]
7. Wolstenholme, D.R. Animal Mitochondrial DNA: Structure and Evolution. *Int. Rev. Cytol.* **1992**, *141*, 173–216. [CrossRef]
8. Vothknecht, U.C.; Szabo, I. Mitochondrial Ion Channels and Transporters in Plants: Prediction and Facts. *Mitochondrion* **2020**, *53*, 224–233. [CrossRef]
9. Shoshan-Barmatz, V.; Shteinifer-Kuzmine, A.; Verma, A. VDAC1 at the Intersection of Cell Metabolism, Apoptosis, and Diseases. *Biomolecules* **2020**, *10*, 1485. [CrossRef]
10. Becker, T.; Wagner, R. Mitochondrial Outer Membrane Channels: Emerging Diversity in Transport Processes. *Bioessays News Rev. Mol. Cell. Dev. Biol.* **2018**, *40*, e1800013. [CrossRef]
11. Wiedemann, N.; Pfanner, N. Mitochondrial Machineries for Protein Import and Assembly. *Annu. Rev. Biochem.* **2017**, *86*, 685–714. [CrossRef] [PubMed]
12. Mokranjac, D.; Neupert, W. Cell Biology: Architecture of a Protein Entry Gate. *Nature* **2015**, *528*, 201–202. [CrossRef] [PubMed]
13. Shiota, T.; Imai, K.; Qiu, J.; Hewitt, V.L.; Tan, K.; Shen, H.H.; Sakiyama, N.; Fukasawa, Y.; Hayat, S.; Kamiya, M.; et al. Molecular Architecture of the Active Mitochondrial Protein Gate. *Science* **2015**, *349*, 1544–1548. [CrossRef]
14. von Heijne, G.; Steppuhn, J.; Herrmann, R.G. Domain Structure of Mitochondrial and Chloroplast Targeting Peptides. *Eur. J. Biochem.* **1989**, *180*, 535–545. [CrossRef] [PubMed]
15. Garg, S.G.; Gould, S.B. The Role of Charge in Protein Targeting Evolution. *Trends Cell Biol.* **2016**, *26*, 894–905. [CrossRef] [PubMed]
16. Abe, Y.; Shodai, T.; Muto, T.; Mihara, K.; Torii, H.; Nishikawa, S.; Endo, T.; Kohda, D. Structural Basis of Presequence Recognition by the Mitochondrial Protein Import Receptor Tom20. *Cell* **2000**, *100*, 551–560. [CrossRef]
17. Mokranjac, D.; Neupert, W. The Many Faces of the Mitochondrial TIM23 Complex. *Biochim. Biophys. Acta* **2010**, *1797*, 1045–1054. [CrossRef]
18. Ieva, R.; Schrempp, S.G.; Opaliński, L.; Wollweber, F.; Höß, P.; Heißwolf, A.K.; Gebert, M.; Zhang, Y.; Guiard, B.; Rospert, S.; et al. Mgr2 Functions as Lateral Gatekeeper for Preprotein Sorting in the Mitochondrial Inner Membrane. *Mol. Cell* **2014**, *56*, 641–652. [CrossRef]
19. Steffen, J.; Koehler, C.M. The Great Escape: Mgr2 of the Mitochondrial TIM23 Translocon Is a Gatekeeper Tasked with Releasing Membrane Proteins. *Mol. Cell* **2014**, *56*, 613–614. [CrossRef]
20. Bohnert, M.; Rehling, P.; Guiard, B.; Herrmann, J.M.; Pfanner, N.; van der Laan, M. Cooperation of Stop-Transfer and Conservative Sorting Mechanisms in Mitochondrial Protein Transport. *Curr. Biol.* **2010**, *20*, 1227–1232. [CrossRef]
21. van der Giezen, M.; Slotboom, D.J.; Horner, D.S.; Dyal, P.L.; Harding, M.; Xue, G.P.; Embley, T.M.; Kunji, E.R.S. Conserved Properties of Hydrogenosomal and Mitochondrial ADP/ATP Carriers: A Common Origin for Both Organelles. *EMBO J.* **2002**, *21*, 572–579. [CrossRef] [PubMed]
22. Garg, S.; Stölting, J.; Zimorski, V.; Rada, P.; Tachezy, J.; Martin, W.F.; Gould, S.B. Conservation of Transit Peptide-Independent Protein Import into the Mitochondrial and Hydrogenosomal Matrix. *Genome Biol. Evol.* **2015**, *7*, 2716–2726. [CrossRef] [PubMed]
23. Fukasawa, Y.; Oda, T.; Tomii, K.; Imai, K. Origin and Evolutionary Alteration of the Mitochondrial Import System in Eukaryotic Lineages. *Mol. Biol. Evol.* **2017**, *34*, 1574–1586. [CrossRef] [PubMed]
24. Baker, A.; Schatz, G. Sequences from a Prokaryotic Genome or the Mouse Dihydrofolate Reductase Gene Can Restore the Import of a Truncated Precursor Protein into Yeast Mitochondria. *Proc. Natl. Acad. Sci. USA* **1987**, *84*, 3117–3121. [CrossRef] [PubMed]
25. Kaiser, C.A.; Preuss, D.; Grisafi, P.; Botstein, D. Many Random Sequences Functionally Replace the Secretion Signal Sequence of Yeast Invertase. *Science* **1987**, *235*, 312–317. [CrossRef]
26. Lemire, B.D.; Fankhauser, C.; Baker, A.; Schatz, G. The Mitochondrial Targeting Function of Randomly Generated Peptide Sequences Correlates with Predicted Helical Amphiphilicity. *J. Biol. Chem.* **1989**, *264*, 20206–20215.
27. Dunn, C.D.; Paavilainen, V.O. Wherever I May Roam: Organellar Protein Targeting and Evolvability. *Curr. Opin. Genet. Dev.* **2019**, *58*, 9–16. [CrossRef]

28. Palmieri, F. The Mitochondrial Transporter Family SLC25: Identification, Properties and Physiopathology. *Mol. Asp. Med.* **2013**, *34*, 465–484. [CrossRef]
29. Saraste, M.; Walker, J.E. Internal Sequence Repeats and the Path of Polypeptide in Mitochondrial ADP/ATP Translocase. *FEBS Lett.* **1982**, *144*, 250–254. [CrossRef]
30. Forrest, L.R. Structural Symmetry in Membrane Proteins. *Annu. Rev. Biophys.* **2015**, *44*, 311–337. [CrossRef]
31. Runswick, M.J.; Powell, S.J.; Nyren, P.; Walker, J.E. Sequence of the Bovine Mitochondrial Phosphate Carrier Protein: Structural Relationship to ADP/ATP Translocase and the Brown Fat Mitochondria Uncoupling Protein. *EMBO J.* **1987**, *6*, 1367–1373. [CrossRef] [PubMed]
32. Runswick, M.J.; Walker, J.E.; Bisaccia, F.; Iacobazzi, V.; Palmieri, F. Sequence of the Bovine 2-Oxoglutarate/Malate Carrier Protein: Structural Relationship to Other Mitochondrial Transport Proteins. *Biochemistry* **1990**, *29*, 11033–11040. [CrossRef] [PubMed]
33. Indiveri, C.; Iacobazzi, V.; Giangregorio, N.; Palmieri, F. The Mitochondrial Carnitine Carrier Protein: cDNA Cloning, Primary Structure and Comparison with Other Mitochondrial Transport Proteins. *Biochem. J.* **1997**, *321* (Pt 3), 713–719. [CrossRef]
34. Palmieri, F. Mitochondrial Carrier Proteins. *FEBS Lett.* **1994**, *346*, 48–54. [CrossRef]
35. Walker, J.E. The Mitochondrial Transporter Family. *Curr. Opin. Struct. Biol.* **1992**, *2*, 519–526. [CrossRef]
36. Nelson, D.R.; Felix, C.M.; Swanson, J.M. Highly Conserved Charge-Pair Networks in the Mitochondrial Carrier Family. *J. Mol. Biol.* **1998**, *277*, 285–308. [CrossRef]
37. Falconi, M.; Chillemi, G.; Di Marino, D.; D’Annessa, I.; Morozzo della Rocca, B.; Palmieri, L.; Desideri, A. Structural Dynamics of the Mitochondrial ADP/ATP Carrier Revealed by Molecular Dynamics Simulation Studies. *Proteins* **2006**, *65*, 681–691. [CrossRef]
38. Giangregorio, N.; Tonazzi, A.; Indiveri, C.; Palmieri, F. Conformation-Dependent Accessibility of Cys-136 and Cys-155 of the Mitochondrial Rat Carnitine/Acylcarnitine Carrier to Membrane-Impermeable SH Reagents. *Biochim. Biophys. Acta* **2007**, *1767*, 1331–1339. [CrossRef]
39. Cappello, A.R.; Miniero, D.V.; Curcio, R.; Ludovico, A.; Daddabbo, L.; Stipani, I.; Robinson, A.J.; Kunji, E.R.S.; Palmieri, F. Functional and Structural Role of Amino Acid Residues in the Odd-Numbered Transmembrane Alpha-Helices of the Bovine Mitochondrial Oxoglutarate Carrier. *J. Mol. Biol.* **2007**, *369*, 400–412. [CrossRef]
40. Palmieri, F. Diseases Caused by Defects of Mitochondrial Carriers: A Review. *Biochim. Biophys. Acta* **2008**, *1777*, 564–578. [CrossRef]
41. Lauria, G.; Sanchez, P.; Della Rocca, B.M.; Pierri, C.L.; Polizio, F.; Stipani, I.; Desideri, A. Structural-Dynamical Properties of the Transmembrane Segment VI of the Mitochondrial Oxoglutarate Carrier Studied by Site Directed Spin-Labeling. *Mol. Membr. Biol.* **2008**, *25*, 236–244. [CrossRef] [PubMed]
42. Robinson, A.J.; Overy, C.; Kunji, E.R.S. The Mechanism of Transport by Mitochondrial Carriers Based on Analysis of Symmetry. *Proc. Natl. Acad. Sci. USA* **2008**, *105*, 17766–17771. [CrossRef] [PubMed]
43. Pebay-Peyroula, E.; Dahout-Gonzalez, C.; Kahn, R.; Trézéguet, V.; Lauquin, G.J.M.; Brandolin, G. Structure of Mitochondrial ADP/ATP Carrier in Complex with Carboxyatractyloside. *Nature* **2003**, *426*, 39–44. [CrossRef] [PubMed]
44. Ruprecht, J.J.; Hellowell, A.M.; Harding, M.; Crichton, P.G.; McCoy, A.J.; Kunji, E.R.S. Structures of Yeast Mitochondrial ADP/ATP Carriers Support a Domain-Based Alternating-Access Transport Mechanism. *Proc. Natl. Acad. Sci. USA* **2014**, *111*, E426–E434. [CrossRef] [PubMed]
45. Ruprecht, J.J.; Kunji, E.R.S. The SLC25 Mitochondrial Carrier Family: Structure and Mechanism. *Trends Biochem. Sci.* **2020**, *45*, 244–258. [CrossRef]
46. Cappello, A.R.; Curcio, R.; Valeria Miniero, D.; Stipani, I.; Robinson, A.J.; Kunji, E.R.S.; Palmieri, F. Functional and Structural Role of Amino Acid Residues in the Even-Numbered Transmembrane Alpha-Helices of the Bovine Mitochondrial Oxoglutarate Carrier. *J. Mol. Biol.* **2006**, *363*, 51–62. [CrossRef]
47. Ruprecht, J.J.; Kunji, E.R. Structural Changes in the Transport Cycle of the Mitochondrial ADP/ATP Carrier. *Curr. Opin. Struct. Biol.* **2019**, *57*, 135–144. [CrossRef]
48. Ruprecht, J.J.; King, M.S.; Zögg, T.; Aleksandrova, A.A.; Pardon, E.; Crichton, P.G.; Steyaert, J.; Kunji, E.R.S. The Molecular Mechanism of Transport by the Mitochondrial ADP/ATP Carrier. *Cell* **2019**, *176*, 435.e15–447.e15. [CrossRef]
49. Palmieri, F.; Scarcia, P.; Monné, M. Diseases Caused by Mutations in Mitochondrial Carrier Genes SLC25: A Review. *Biomolecules* **2020**, *10*, 655. [CrossRef]

50. Pierri, C.L.; Palmieri, F.; De Grassi, A. Single-Nucleotide Evolution Quantifies the Importance of Each Site along the Structure of Mitochondrial Carriers. *Cell. Mol. Life Sci.* **2014**, *71*, 349–364. [CrossRef]
51. Brix, J.; Rüdiger, S.; Bukau, B.; Schneider-Mergener, J.; Pfanner, N. Distribution of Binding Sequences for the Mitochondrial Import Receptors Tom20, Tom22, and Tom70 in a Presequence-Carrying Preprotein and a Non-Cleavable Preprotein. *J. Biol. Chem.* **1999**, *274*, 16522–16530. [CrossRef] [PubMed]
52. Kreimendahl, S.; Schwichtenberg, J.; Günnewig, K.; Brandherm, L.; Rassow, J. The Selectivity Filter of the Mitochondrial Protein Import Machinery. *BMC Biol.* **2020**, *18*, 156. [CrossRef] [PubMed]
53. Wiedemann, N.; Pfanner, N.; Ryan, M.T. The Three Modules of ADP/ATP Carrier Cooperate in Receptor Recruitment and Translocation into Mitochondria. *EMBO J.* **2001**, *20*, 951–960. [CrossRef] [PubMed]
54. Kaplan, R.S.; Mayor, J.A.; Wood, D.O. The Mitochondrial Tricarboxylate Transport Protein. cDNA Cloning, Primary Structure, and Comparison with Other Mitochondrial Transport Proteins. *J. Biol. Chem.* **1993**, *268*, 13682–13690.
55. Bricker, D.K.; Taylor, E.B.; Schell, J.C.; Orsak, T.; Boutron, A.; Chen, Y.C.; Cox, J.E.; Cardon, C.M.; Van Vranken, J.G.; Dephoure, N.; et al. A Mitochondrial Pyruvate Carrier Required for Pyruvate Uptake in Yeast, *Drosophila*, and Humans. *Science* **2012**, *337*, 96–100. [CrossRef]
56. Herzig, S.; Raemy, E.; Montessuit, S.; Veuthey, J.L.; Zamboni, N.; Westermann, B.; Kunji, E.R.S.; Martinou, J.C. Identification and Functional Expression of the Mitochondrial Pyruvate Carrier. *Science* **2012**, *337*, 93–96. [CrossRef]
57. Tavoulari, S.; Thangaratnarajah, C.; Mavridou, V.; Harbour, M.E.; Martinou, J.C.; Kunji, E.R. The Yeast Mitochondrial Pyruvate Carrier Is a Hetero-Dimer in Its Functional State. *EMBO J.* **2019**, *38*. [CrossRef]
58. Vanderperre, B.; Cermakova, K.; Escoffier, J.; Kaba, M.; Bender, T.; Nef, S.; Martinou, J.C. MPC1-like Is a Placental Mammal-Specific Mitochondrial Pyruvate Carrier Subunit Expressed in Postmeiotic Male Germ Cells. *J. Biol. Chem.* **2016**, *291*, 16448–16461. [CrossRef]
59. Bender, T.; Pena, G.; Martinou, J.C. Regulation of Mitochondrial Pyruvate Uptake by Alternative Pyruvate Carrier Complexes. *EMBO J.* **2015**, *34*, 911–924. [CrossRef]
60. Chen, L.Q.; Hou, B.H.; Lalonde, S.; Takanaga, H.; Hartung, M.L.; Qu, X.Q.; Guo, W.J.; Kim, J.G.; Underwood, W.; Chaudhuri, B.; et al. Sugar Transporters for Intercellular Exchange and Nutrition of Pathogens. *Nature* **2010**, *468*, 527–532. [CrossRef]
61. Chen, L.Q. SWEET Sugar Transporters for Phloem Transport and Pathogen Nutrition. *New Phytol.* **2014**, *201*, 1150–1155. [CrossRef] [PubMed]
62. Xu, Y.; Tao, Y.; Cheung, L.S.; Fan, C.; Chen, L.Q.; Xu, S.; Perry, K.; Frommer, W.B.; Feng, L. Structures of Bacterial Homologues of SWEET Transporters in Two Distinct Conformations. *Nature* **2014**, *515*, 448–452. [CrossRef]
63. Medrano-Soto, A.; Ghazi, F.; Hendargo, K.J.; Moreno-Hagelsieb, G.; Myers, S.; Saier, M.H. Expansion of the Transporter-Opsin-G Protein-Coupled Receptor Superfamily with Five New Protein Families. *PLoS ONE* **2020**, *15*, e0231085. [CrossRef]
64. Xuan, Y.H.; Hu, Y.B.; Chen, L.Q.; Sosso, D.; Ducat, D.C.; Hou, B.H.; Frommer, W.B. Functional Role of Oligomerization for Bacterial and Plant SWEET Sugar Transporter Family. *Proc. Natl. Acad. Sci. USA* **2013**, *110*, E3685–E3694. [CrossRef] [PubMed]
65. Wang, J.; Yan, C.; Li, Y.; Hirata, K.; Yamamoto, M.; Yan, N.; Hu, Q. Crystal Structure of a Bacterial Homologue of SWEET Transporters. *Cell Res.* **2014**, *24*, 1486–1489. [CrossRef] [PubMed]
66. Jaehme, M.; Guskov, A.; Slotboom, D.J. Crystal Structure of the Vitamin B3 Transporter PnuC, a Full-Length SWEET Homolog. *Nat. Struct. Mol. Biol.* **2014**, *21*, 1013–1015. [CrossRef]
67. Lee, Y.; Nishizawa, T.; Yamashita, K.; Ishitani, R.; Nureki, O. Structural Basis for the Facilitative Diffusion Mechanism by SemiSWEET Transporter. *Nat. Commun.* **2015**, *6*, 6112. [CrossRef]
68. Han, L.; Zhu, Y.; Liu, M.; Zhou, Y.; Lu, G.; Lan, L.; Wang, X.; Zhao, Y.; Zhang, X.C. Molecular Mechanism of Substrate Recognition and Transport by the AtSWEET13 Sugar Transporter. *Proc. Natl. Acad. Sci. USA* **2017**, *114*, 10089–10094. [CrossRef]
69. Latorraca, N.R.; Fastman, N.M.; Venkatakrishnan, A.J.; Frommer, W.B.; Dror, R.O.; Feng, L. Mechanism of Substrate Translocation in an Alternating Access Transporter. *Cell* **2017**, *169*, 96.e12–107.e12. [CrossRef]
70. Brivet, M.; Garcia-Cazorla, A.; Lyonnet, S.; Dumez, Y.; Nassogne, M.C.; Slama, A.; Boutron, A.; Touati, G.; Legrand, A.; Saudubray, J.M. Impaired Mitochondrial Pyruvate Importation in a Patient and a Fetus at Risk. *Mol. Genet. Metab.* **2003**, *78*, 186–192. [CrossRef]

71. Oonthonpan, L.; Rauckhorst, A.J.; Gray, L.R.; Boutron, A.C.; Taylor, E.B. Two Human Patient Mitochondrial Pyruvate Carrier Mutations Reveal Distinct Molecular Mechanisms of Dysfunction. *JCI Insight* **2019**, *5*. [CrossRef] [PubMed]
72. El-Gebali, S.; Mistry, J.; Bateman, A.; Eddy, S.R.; Luciani, A.; Potter, S.C.; Qureshi, M.; Richardson, L.J.; Salazar, G.A.; Smart, A.; et al. The Pfam Protein Families Database in 2019. *Nucleic Acids Res.* **2019**, *47*, D427–D432. [CrossRef] [PubMed]
73. Wheeler, T.J.; Clements, J.; Finn, R.D. Skylign: A Tool for Creating Informative, Interactive Logos Representing Sequence Alignments and Profile Hidden Markov Models. *BMC Bioinform.* **2014**, *15*, 7. [CrossRef]
74. Tusnády, G.E.; Simon, I. The HMMTOP Transmembrane Topology Prediction Server. *Bioinformatics* **2001**, *17*, 849–850. [CrossRef]
75. Viklund, H.; Bernsel, A.; Skwark, M.; Elofsson, A. SPOCTOPUS: A Combined Predictor of Signal Peptides and Membrane Protein Topology. *Bioinformatics* **2008**, *24*, 2928–2929. [CrossRef] [PubMed]
76. Nugent, T.; Jones, D.T. Detecting Pore-Lining Regions in Transmembrane Protein Sequences. *BMC Bioinform.* **2012**, *13*, 169. [CrossRef]
77. Jones, D.T. Protein Secondary Structure Prediction Based on Position-Specific Scoring Matrices. *J. Mol. Biol.* **1999**, *292*, 195–202. [CrossRef] [PubMed]
78. Fleming, M.D.; Campagna, D.R.; Haslett, J.N.; Trenor, C.C.; Andrews, N.C. A Mutation in a Mitochondrial Transmembrane Protein Is Responsible for the Pleiotropic Hematological and Skeletal Phenotype of Flexed-Tail (*f/f*) Mice. *Genes Dev.* **2001**, *15*, 652–657. [CrossRef] [PubMed]
79. Kory, N.; Wyant, G.A.; Prakash, G.; Uit de Bos, J.; Bottanelli, F.; Pacold, M.E.; Chan, S.H.; Lewis, C.A.; Wang, T.; Keys, H.R.; et al. SFXN1 Is a Mitochondrial Serine Transporter Required for One-Carbon Metabolism. *Science* **2018**, *362*. [CrossRef]
80. Acoba, M.G.; Alpergin, E.S.S.; Renuse, S.; Fernández-del-Río, L.; Lu, Y.W.; Clarke, C.F.; Pandey, A.; Wolfgang, M.J.; Claypool, S.M. The Mitochondrial Carrier SFXN1 Is Critical for Complex III Integrity and Cellular Metabolism. *bioRxiv* **2020**. [CrossRef]
81. Jackson, T.D.; Hock, D.; Palmer, C.S.; Kang, Y.; Fujihara, K.M.; Clemons, N.J.; Thorburn, D.R.; Stroud, D.A.; Stojanovski, D. The TIM22 Complex Regulates Mitochondrial One-Carbon Metabolism by Mediating the Import of Sideroflexins. *bioRxiv* **2020**. [CrossRef]
82. Horten, P.; Colina-Tenorio, L.; Rampelt, H. Biogenesis of Mitochondrial Metabolite Carriers. *Biomolecules* **2020**, *10*, 1008. [CrossRef] [PubMed]
83. Yamashita, A.; Singh, S.K.; Kawate, T.; Jin, Y.; Gouaux, E. Crystal Structure of a Bacterial Homologue of Na⁺/Cl⁻-Dependent Neurotransmitter Transporters. *Nature* **2005**, *437*, 215–223. [CrossRef] [PubMed]
84. Boudker, O.; Ryan, R.M.; Yernool, D.; Shimamoto, K.; Gouaux, E. Coupling Substrate and Ion Binding to Extracellular Gate of a Sodium-Dependent Aspartate Transporter. *Nature* **2007**, *445*, 387–393. [CrossRef]
85. Hildick-Smith, G.J.; Cooney, J.D.; Garone, C.; Kremer, L.S.; Haack, T.B.; Thon, J.N.; Miyata, N.; Lieber, D.S.; Calvo, S.E.; Akman, H.O.; et al. Macrocytic Anemia and Mitochondriopathy Resulting from a Defect in Sideroflexin 4. *Am. J. Hum. Genet.* **2013**, *93*, 906–914. [CrossRef]
86. Nowikovsky, K.; Froschauer, E.M.; Zsurka, G.; Samaj, J.; Reipert, S.; Kolisek, M.; Wiesenberger, G.; Schweyen, R.J. The LETM1/YOL027 Gene Family Encodes a Factor of the Mitochondrial K⁺ Homeostasis with a Potential Role in the Wolf-Hirschhorn Syndrome. *J. Biol. Chem.* **2004**, *279*, 30307–30315. [CrossRef]
87. Froschauer, E.; Nowikovsky, K.; Schweyen, R.J. Electroneutral K⁺/H⁺ Exchange in Mitochondrial Membrane Vesicles Involves Yol027/Letm1 Proteins. *Biochim. Biophys. Acta* **2005**, *1711*, 41–48. [CrossRef]
88. Jiang, D.; Zhao, L.; Clapham, D.E. Genome-Wide RNAi Screen Identifies Letm1 as a Mitochondrial Ca²⁺/H⁺ Antiporter. *Science* **2009**, *326*, 144–147. [CrossRef]
89. Tsai, M.F.; Jiang, D.; Zhao, L.; Clapham, D.; Miller, C. Functional Reconstitution of the Mitochondrial Ca²⁺/H⁺ Antiporter Letm1. *J. Gen. Physiol.* **2014**, *143*, 67–73. [CrossRef]
90. Shao, J.; Fu, Z.; Ji, Y.; Guan, X.; Guo, S.; Ding, Z.; Yang, X.; Cong, Y.; Shen, Y. Leucine Zipper-EF-Hand Containing Transmembrane Protein 1 (LETM1) Forms a Ca²⁺/H⁺ Antiporter. *Sci. Rep.* **2016**, *6*, 34174. [CrossRef]
91. Nowikovsky, K.; Bernardi, P. LETM1 in Mitochondrial Cation Transport. *Front. Physiol.* **2014**, *5*, 83. [CrossRef] [PubMed]

92. Cordes, F.S.; Bright, J.N.; Sansom, M.S.P. Proline-Induced Distortions of Transmembrane Helices. *J. Mol. Biol.* **2002**, *323*, 951–960. [CrossRef]
93. Law, E.C.; Wilman, H.R.; Kelm, S.; Shi, J.; Deane, C.M. Examining the Conservation of Kinks in Alpha Helices. *PLoS ONE* **2016**, *11*, e0157553. [CrossRef] [PubMed]
94. Almagro Armenteros, J.J.; Salvatore, M.; Emanuelsson, O.; Winther, O.; von Heijne, G.; Elofsson, A.; Nielsen, H. Detecting Sequence Signals in Targeting Peptides Using Deep Learning. *Life Sci. Alliance* **2019**, *2*. [CrossRef] [PubMed]
95. Csere, P.; Lill, R.; Kispal, G. Identification of a Human Mitochondrial ABC Transporter, the Functional Orthologue of Yeast Atm1p. *FEBS Lett.* **1998**, *441*, 266–270. [CrossRef]
96. Hogue, D.L.; Liu, L.; Ling, V. Identification and Characterization of a Mammalian Mitochondrial ATP-Binding Cassette Membrane Protein. *J. Mol. Biol.* **1999**, *285*, 379–389. [CrossRef]
97. Zhang, F.; Hogue, D.L.; Liu, L.; Fisher, C.L.; Hui, D.; Childs, S.; Ling, V. M-ABC2, a New Human Mitochondrial ATP-Binding Cassette Membrane Protein. *FEBS Lett.* **2000**, *478*, 89–94. [CrossRef]
98. Krishnamurthy, P.C.; Du, G.; Fukuda, Y.; Sun, D.; Sampath, J.; Mercer, K.E.; Wang, J.; Sosa-Pineda, B.; Murti, K.G.; Schuetz, J.D. Identification of a Mammalian Mitochondrial Porphyrin Transporter. *Nature* **2006**, *443*, 586–589. [CrossRef]
99. Kiss, K.; Brozik, A.; Kucsma, N.; Toth, A.; Gera, M.; Berry, L.; Vallentin, A.; Vial, H.; Vidal, M.; Szakacs, G. Shifting the Paradigm: The Putative Mitochondrial Protein ABCB6 Resides in the Lysosomes of Cells and in the Plasma Membrane of Erythrocytes. *PLoS ONE* **2012**, *7*, e37378. [CrossRef]
100. Kiss, K.; Kucsma, N.; Brozik, A.; Tusnady, G.E.; Bergam, P.; van Niel, G.; Szakacs, G. Role of the N-Terminal Transmembrane Domain in the Endo-Lysosomal Targeting and Function of the Human ABCB6 Protein. *Biochem. J.* **2015**, *467*, 127–139. [CrossRef]
101. Graf, S.A.; Haigh, S.E.; Corson, E.D.; Shirihai, O.S. Targeting, Import, and Dimerization of a Mammalian Mitochondrial ATP Binding Cassette (ABC) Transporter, ABCB10 (ABC-Me). *J. Biol. Chem.* **2004**, *279*, 42954–42963. [CrossRef] [PubMed]
102. Dean, M.; Allikmets, R.; Gerrard, B.; Stewart, C.; Kistler, A.; Shafer, B.; Michaelis, S.; Strathern, J. Mapping and Sequencing of Two Yeast Genes Belonging to the ATP-Binding Cassette Superfamily. *Yeast* **1994**, *10*, 377–383. [CrossRef] [PubMed]
103. Stiller, S.B.; Höpker, J.; Oeljeklaus, S.; Schütze, C.; Schrempp, S.G.; Vent-Schmidt, J.; Horvath, S.E.; Frazier, A.E.; Gebert, N.; van der Laan, M.; et al. Mitochondrial OXA Translocase Plays a Major Role in Biogenesis of Inner-Membrane Proteins. *Cell Metab.* **2016**, *23*, 901–908. [CrossRef] [PubMed]
104. Shintre, C.A.; Pike, A.C.W.; Li, Q.; Kim, J.I.; Barr, A.J.; Goubin, S.; Shrestha, L.; Yang, J.; Berridge, G.; Ross, J.; et al. Structures of ABCB10, a Human ATP-Binding Cassette Transporter in Apo- and Nucleotide-Bound States. *Proc. Natl. Acad. Sci. USA* **2013**, *110*, 9710–9715. [CrossRef] [PubMed]
105. Srinivasan, V.; Pierik, A.J.; Lill, R. Crystal Structures of Nucleotide-Free and Glutathione-Bound Mitochondrial ABC Transporter Atm1. *Science* **2014**, *343*, 1137–1140. [CrossRef] [PubMed]
106. Bekri, S.; Kispal, G.; Lange, H.; Fitzsimons, E.; Tolmie, J.; Lill, R.; Bishop, D.F. Human ABC7 Transporter: Gene Structure and Mutation Causing X-Linked Sideroblastic Anemia with Ataxia with Disruption of Cytosolic Iron-Sulfur Protein Maturation. *Blood* **2000**, *96*, 3256–3264. [CrossRef]
107. Seguin, A.; Takahashi-Makise, N.; Yien, Y.Y.; Huston, N.C.; Whitman, J.C.; Musso, G.; Wallace, J.A.; Bradley, T.; Bergonia, H.A.; Kafina, M.D.; et al. Reductions in the Mitochondrial ABC Transporter Abcb10 Affect the Transcriptional Profile of Heme Biosynthesis Genes. *J. Biol. Chem.* **2017**, *292*, 16284–16299. [CrossRef]
108. Palty, R.; Silverman, W.F.; Hershinkel, M.; Caporale, T.; Sensi, S.L.; Parnis, J.; Nolte, C.; Fishman, D.; Shoshan-Barmatz, V.; Herrmann, S.; et al. NCLX Is an Essential Component of Mitochondrial Na⁺/Ca²⁺ Exchange. *Proc. Natl. Acad. Sci. USA* **2010**, *107*, 436–441. [CrossRef]
109. Khananshvili, D. Distinction between the Two Basic Mechanisms of Cation Transport in the Cardiac Na⁺-Ca²⁺ Exchange System. *Biochemistry* **1990**, *29*, 2437–2442. [CrossRef]
110. Pitts, B.J. Stoichiometry of Sodium-Calcium Exchange in Cardiac Sarcolemmal Vesicles. Coupling to the Sodium Pump. *J. Biol. Chem.* **1979**, *254*, 6232–6235.
111. Reeves, J.P.; Hale, C.C. The Stoichiometry of the Cardiac Sodium-Calcium Exchange System. *J. Biol. Chem.* **1984**, *259*, 7733–7739. [PubMed]

112. Palty, R.; Ohana, E.; Hershinkel, M.; Volokita, M.; Elgazar, V.; Beharier, O.; Silverman, W.F.; Argaman, M.; Sekler, I. Lithium-Calcium Exchange Is Mediated by a Distinct Potassium-Independent Sodium-Calcium Exchanger. *J. Biol. Chem.* **2004**, *279*, 25234–25240. [CrossRef] [PubMed]
113. Hernansanz-Agustín, P.; Choya-Foces, C.; Carregal-Romero, S.; Ramos, E.; Oliva, T.; Villa-Piña, T.; Moreno, L.; Izquierdo-Álvarez, A.; Cabrera-García, J.D.; Cortés, A.; et al. Na⁺ Controls Hypoxic Signalling by the Mitochondrial Respiratory Chain. *Nature* **2020**, *586*, 287–291. [CrossRef] [PubMed]
114. Refaeli, B.; Giladi, M.; Hiller, R.; Khananshvili, D. Structure-Based Engineering of Lithium-Transport Capacity in an Archaeal Sodium-Calcium Exchanger. *Biochemistry* **2016**, *55*, 1673–1676. [CrossRef]
115. Roy, S.; Dey, K.; Hershinkel, M.; Ohana, E.; Sekler, I. Identification of Residues That Control Li⁺ versus Na⁺ Dependent Ca²⁺ Exchange at the Transport Site of the Mitochondrial NCLX. *Biochim. Biophys. Acta. Mol. Cell Res.* **2017**, *1864*, 997–1008. [CrossRef]
116. Liao, J.; Li, H.; Zeng, W.; Sauer, D.B.; Belmares, R.; Jiang, Y. Structural Insight into the Ion-Exchange Mechanism of the Sodium/Calcium Exchanger. *Science* **2012**, *335*, 686–690. [CrossRef]
117. Liao, J.; Marinelli, F.; Lee, C.; Huang, Y.; Faraldo-Gómez, J.D.; Jiang, Y. Mechanism of Extracellular Ion Exchange and Binding-Site Occlusion in a Sodium/Calcium Exchanger. *Nat. Struct. Mol. Biol.* **2016**, *23*, 590–599. [CrossRef]
118. Nishizawa, T.; Kita, S.; Maturana, A.D.; Furuya, N.; Hirata, K.; Kasuya, G.; Ogasawara, S.; Dohmae, N.; Iwamoto, T.; Ishitani, R.; et al. Structural Basis for the Counter-Transport Mechanism of a H²⁺/Ca²⁺ Exchanger. *Science* **2013**, *341*, 168–172. [CrossRef]
119. Battaglino, R.A.; Pham, L.; Morse, L.R.; Vokes, M.; Sharma, A.; Odgren, P.R.; Yang, M.; Sasaki, H.; Stashenko, P. NHA-Oc/NHA2: A Mitochondrial Cation-Proton Antiporter Selectively Expressed in Osteoclasts. *Bone* **2008**, *42*, 180–192. [CrossRef]
120. Fuster, D.G.; Zhang, J.; Shi, M.; Bobulescu, I.A.; Andersson, S.; Moe, O.W. Characterization of the Sodium/Hydrogen Exchanger NHA2. *J. Am. Soc. Nephrol.* **2008**, *19*, 1547–1556. [CrossRef]
121. Donowitz, M.; Ming Tse, C.; Fuster, D. SLC9/NHE Gene Family, a Plasma Membrane and Organellar Family of Na⁺/H⁺ Exchangers. *Mol. Asp. Med.* **2013**, *34*, 236–251. [CrossRef]
122. Masrati, G.; Dwivedi, M.; Rimon, A.; Gluck-Margolin, Y.; Kessel, A.; Ashkenazy, H.; Mayrose, I.; Padan, E.; Ben-Tal, N. Broad Phylogenetic Analysis of Cation/Proton Antiporters Reveals Transport Determinants. *Nat. Commun.* **2018**, *9*, 4205. [CrossRef]
123. Yoo, H.C.; Park, S.J.; Nam, M.; Kang, J.; Kim, K.; Yeo, J.H.; Kim, J.K.; Heo, Y.; Lee, H.S.; Lee, M.Y.; et al. A Variant of SLC1A5 Is a Mitochondrial Glutamine Transporter for Metabolic Reprogramming in Cancer Cells. *Cell Metab.* **2020**, *31*, 267–283.e12. [CrossRef]
124. Hiller, K.; Grote, A.; Scheer, M.; Münch, R.; Jahn, D. PrediSi: Prediction of Signal Peptides and Their Cleavage Positions. *Nucleic Acids Res.* **2004**, *32*, W375–W379. [CrossRef]
125. Console, L.; Scalise, M.; Tarmakova, Z.; Coe, I.R.; Indiveri, C. N-Linked Glycosylation of Human SLC1A5 (ASCT2) Transporter Is Critical for Trafficking to Membrane. *Biochim. Biophys. Acta* **2015**, *1853*, 1636–1645. [CrossRef]
126. Canul-Tec, J.C.; Assal, R.; Cirri, E.; Legrand, P.; Brier, S.; Chamot-Rooke, J.; Reyes, N. Structure and Allosteric Inhibition of Excitatory Amino Acid Transporter 1. *Nature* **2017**, *544*, 446–451. [CrossRef]
127. Kandasamy, P.; Gyimesi, G.; Kanai, Y.; Hediger, M.A. Amino Acid Transporters Revisited: New Views in Health and Disease. *Trends Biochem. Sci.* **2018**, *43*, 752–789. [CrossRef]
128. Welbourne, T.; Routh, R.; Yudkoff, M.; Nissim, I. The Glutamine/Glutamate Couplet and Cellular Function. *News Physiol. Sci.* **2001**, *16*, 157–160. [CrossRef]
129. Scalise, M.; Pochini, L.; Galluccio, M.; Console, L.; Indiveri, C. Glutamine Transport and Mitochondrial Metabolism in Cancer Cell Growth. *Front. Oncol.* **2017**, *7*, 306. [CrossRef]

Publisher’s Note: MDPI stays neutral with regard to jurisdictional claims in published maps and institutional affiliations.



© 2020 by the authors. Licensee MDPI, Basel, Switzerland. This article is an open access article distributed under the terms and conditions of the Creative Commons Attribution (CC BY) license (<http://creativecommons.org/licenses/by/4.0/>).

Review

VDAC1 at the Intersection of Cell Metabolism, Apoptosis, and Diseases

Varda Shoshan-Barmatz *, Anna Shteinfer-Kuzmine and Ankit Verma

Department of Life Sciences and the National Institute for Biotechnology in the Negev, Ben-Gurion University of the Negev, Beer-Sheva 84105, Israel; shteinfe@post.bgu.ac.il (A.S.-K.); verma@post.bgu.ac.il (A.V.)

* Correspondence: vardasb@bgu.ac.il

Received: 10 September 2020; Accepted: 22 October 2020; Published: 26 October 2020

Abstract: The voltage-dependent anion channel 1 (VDAC1) protein, is an important regulator of mitochondrial function, and serves as a mitochondrial gatekeeper, with responsibility for cellular fate. In addition to control over energy sources and metabolism, the protein also regulates epigenomic elements and apoptosis via mediating the release of apoptotic proteins from the mitochondria. Apoptotic and pathological conditions, as well as certain viruses, induce cell death by inducing VDAC1 overexpression leading to oligomerization, and the formation of a large channel within the VDAC1 homo-oligomer. This then permits the release of pro-apoptotic proteins from the mitochondria and subsequent apoptosis. Mitochondrial DNA can also be released through this channel, which triggers type-I interferon responses. VDAC1 also participates in endoplasmic reticulum (ER)-mitochondria cross-talk, and in the regulation of autophagy, and inflammation. Its location in the outer mitochondrial membrane, makes VDAC1 ideally placed to interact with over 100 proteins, and to orchestrate the interaction of mitochondrial and cellular activities through a number of signaling pathways. Here, we provide insights into the multiple functions of VDAC1 and describe its involvement in several diseases, which demonstrate the potential of this protein as a druggable target in a wide variety of pathologies, including cancer.

Keywords: apoptosis; cancer; diseases; metabolism; mitochondria; VDAC1; virus

1. Mitochondria as Signaling Hubs

Mitochondria as cellular energy powerhouses provide a central location for the multiple metabolic reactions required to satisfy the energy and biomolecule demands of cells, and serve to integrate the diverse metabolic pathways and provide cells with metabolic flexibility. The appreciation of mitochondria as sites of biosynthesis and bioenergy production has dramatically expanded in recent years, and they are now known to play a crucial role in almost all aspects of cell biology and to regulate cellular homeostasis, metabolism, innate immunity, apoptosis, epigenetics, cellular fate, and more [1,2]. Mitochondrial dysfunction induces stress responses, which link the fitness of this organelle to the condition of the whole organism. These functions typically center around the metabolic traffic in and out of the mitochondria, and they are likely to contribute to the exceptional variability of mitochondrial disease manifestations. The voltage-dependent anion channel 1 (VDAC1) protein, which is located in the outer mitochondrial membrane (OMM), serves as a gatekeeper that can regulate the metabolic and energetic cross-talk between mitochondria and the rest of the cell, and plays a role in mitochondria-mediated apoptosis [3–5].

Other different aspects of VDAC1 structures [6] and functions, such as in cell stress [5], Ca^{2+} regulation [7,8], metabolism [5], and apoptosis [7,9], and as a therapeutic target [10–15], were presented in ours and others' recent reviews.

2. VDAC1 Structural Elements: The N-Terminal Domain and Its Oligomeric State

Three mammalian isoforms of VDAC (VDAC1, VDAC2, and VDAC3) that share a number of functional and structural attributes have been identified [16–18]. Information about VDAC isoform function and structure was obtained from channel activity of purified and reconstituted protein and, using cell-based assays for survival, metabolism, reactive oxygen species (ROS), and cellular Ca^{2+} regulation, and by gene knockout mouse models [17]. VDAC1 is the most abundant isoform and the focus of this review. VDAC2 knock out is lethal and is considered to be an anti-apoptotic protein. VDAC3 is the least known, active as channel. While VDAC 1 contains two cysteines, VDAC2 and VDAC3, with nine and six cysteines, respectively, are proposed to function as oxidative stress sensors [17]. The crystalline structure of the most prevalent and studied isoform, VDAC1, was solved at atomic resolution, revealing a β -barrel composed of 19 transmembrane β -strands connected by flexible loops. The β 1 and β 19 strands, together, are arranged in parallel, where the N-terminal region (26-residues) lies inside the pore [19–21], but can flick out of it [22,23] and interact with hexokinase (HK) [4,5,24–30], A β [31,32], and other proteins, such as the anti-apoptotic proteins, Bcl-2 and Bcl-xL [4,27,33–37]. Thus, this region of the protein is well positioned to regulate the traffic of materials through the VDAC1 channel [19,21].

The diameter of the channel pore has been estimated as 2.6–3.0 nm [19], but this can decrease to about 1.5 nm when the N-terminal flexible region is located inside the pore [19–21]. The sequence of rich with glycine residues (21GlyTyrGlyPheGly25) [19–21] connecting the N-terminal region to β 1 strand is thought to confer the flexibility needed for this region to move in and out of the VDAC1 channel [23]. This mobility has been reported to be important for channel gating, dimerization of VDAC1 [23], and interaction with HK and members of the apoptosis regulating Bcl-2 family (i.e., Bax, Bcl-2, and Bcl-xL) [23,27,33,34,38,39].

Membranal and purified VDAC1, can form dimers, trimers, tetramers, hexamers, and higher-order oligomeric forms [4,30,40–47] through contact sites that have been identified [48]. We have demonstrated this oligomerization to be a dynamic process that occurs in response to a variety of apoptotic stimuli, acting through a range of signaling processes [28,40,42,44,45,47,49–54], as presented below (Section 5.1).

3. VDAC1 Extra-Mitochondrial Localization, Function, and Association with Pathological Conditions

In addition to the mitochondrial membrane, VDAC has also been detected in other cell compartments [16,55–65], including the plasma membrane [16,57], the sarcoplasmic reticulum (SR) of skeletal muscles [66], and the endoplasmic reticulum (ER) of the rat cerebellum [64,67].

Antibodies raised against the N-terminus of VDAC1 interacted with the plasma membrane of bovine astrocytes and blocked a high conductance anion channel [61]. Interestingly, when detected in the plasma membrane (pl-VDAC1), the amino acid residues that were exposed to the cytosol in the mitochondrial protein were found to face the extracellular space [55,60,68–71]. This was demonstrated in epithelial cells, astrocytes, and neurons [56,57] and in differentiated hippocampal neurons [55]. VDAC1 has also been identified in the brain post-synaptic membrane fraction [60] and in the caveolae or caveolae-related domains of established T lymphoid-like cell lines [58]. The protein has also been found to participate in the multi-protein complexes found in lipid rafts, together with the estrogen receptor α (mER α) and insulin-growth factor-1 receptor (IGF-1R) [58,62–64]. In red blood cells that do not possess mitochondria, VDAC1 has been found in the endoplasmic reticulum, and Golgi apparatus [59].

The plasma membrane form of VDAC1 may have an extended N-terminal signal peptide which is responsible for its targeting to the cell membrane [71,72]. Alternatively, the human plasminogen kringle 5 (K5) may induce translocation of VDAC1 to the cell surface, where the protein was recently identified as the receptor for K5 on HUVEC membrane [73,74]. Additional mechanisms, such as the presence of alternative mRNA untranslated regions, have also been suggested [57,64].

The levels of pl-VDAC1 were reported to be increased under pathological conditions such as Alzheimer's disease (AD) [75–77], where it has been suggested that pl-VDAC1 serves as an

“amyloid-regulated” apoptosis related channel [62,63,65]. We recently described a direct interaction between A β and the N-terminal region of VDAC1, and demonstrated that VDAC1 is required for A β entry into the cells [78,79] and apoptosis induction [31,32]. We have also recently demonstrated that VDAC is overexpressed in type 2 diabetes (T2D) [80–83] and mistargeted to the β -cell plasma membrane [84]. This overexpression under pathological conditions is also seen in cancer [3,15,85,86], autoimmune diseases such as lupus [87], non-alcoholic steatohepatitis (NASH) [88], inflammatory bowel disease (IBD) (unpublished data), and cardiac diseases [89,90], as presented below (Section 8).

The exact functions of extra-mitochondrial VDAC are unknown, although several possible roles have been proposed (reviewed in [64,91,92]), and include regulation of tissue volume in the brain [61], and other cell types [70,93,94], or release of ATP in β -cells [84] and in human erythrocytes [95].

4. VDAC1, a Multi-Functional Channel Controlling Cell Energy, Metabolism, and Oxidative Stress

To reach the mitochondrion matrix or to be released to the cytosol, all metabolites and ions must traverse the OMM via VDAC1, the sole channel mediating the flux of ions, nucleotides, and other metabolites up to ~5000 Da. In this way, VDAC maintains control of the metabolic and ion cross-talk between the mitochondria and the rest of the cell (Figure 1). Nucleotides and metabolites transported include pyruvate, malate, succinate, and NADH/NAD⁺, as well as lipids, heme, cholesterol, and ions such as Ca²⁺ [3–5,96]. In contrast, there are over 50 mitochondrial substrate-specific carrier proteins of the family solute carrier family 25 (SLC25) in the inner mitochondrial membrane (IMM), such as the (ADP/ATP) antiporter, the adenine nucleotide translocator (ANT), the transporter of Pi (PiC), as well as transporters of aspartate/glutamate, pyruvate, acyl carnitine, and citrate, among others [97].

Closure [98] or down-regulation of VDAC1 channel expression reduced the exchange of metabolites between the mitochondria and the rest of the cell and inhibited cell growth [86,99], indicating the importance of the protein to the maintenance of physiological cellular function.

As already described, the mitochondria are the energy source of the cell. They are responsible for the ATP generated during glycolysis and oxidative phosphorylation (OXPHOS). This is then exported to the cytosol and exchanged for ADP, which is recycled again in the mitochondria to generate ATP. This shuttling process that also involves ANT and creatinine kinase (CrK), located between the IMM and OMM [100], and may be regulated by tubulin $\alpha\beta$ heterodimers [101], but it is ultimately facilitated by VDAC1, which thereby controls the electron transport chain [4] (Figure 1) and the energy state of the cell [98].

In addition to ATP, VDAC1 is also involved in the transfer of a number of other essential molecules across the OMM. These include Ca²⁺, cholesterol, fatty acids, and reactive oxygen species (ROS). Controlling the flow of Ca²⁺ allows VDAC1 to regulate mitochondrial Ca²⁺ homeostasis, oxidative phosphorylation, and Ca²⁺ cross-talk between the VDAC1 in the OMM and the IP3 receptor in the ER. This takes place through the mitochondria associated membranes (MAM) and involves the chaperone GRP75 [67,102,103].

VDAC1 [104] is a necessary component of the cholesterol transport multi-protein complex, the transduceosome, composed of the translocator protein (TSPO), and the steroidogenic acute regulatory protein (STAR) [88,105] (Figure 1).

VDAC1 is also part of a complex mediating the transport of fatty acids through the OMM [88,105,106] composed of carnitine palmitoyltransferase 1a (CPT1a), which faces the intermembrane space (IMS), and the long chain acetyl coenzyme-A (acyl-CoA) synthetase (ACSL) protein. Once activated by ACSL, VDAC1 transfers acyl-CoAs across the OMM to the IMS, where they are converted into acylcarnitines by CPT1a (Figure 1). They are then transferred across the IMM by carnitine/acylcarnitine translocase, and converted back into acyl-CoA by CPT2 in the IMM, and, subsequently, undergo β -oxidation in the matrix [105,107]. In this respect, VDAC1 has recently been reported to serve as a lipid sensor [108]. Finally, VDAC is also involved in regulating oxidative stress [5]. ROS formed by reaction with O₂•⁻ at complex III are released through VDAC1 where they activates

c-Jun N-terminal kinase (JNK), the extracellular signal-regulated kinase (ERK 1/2), and p38, members of the mitogen-activated protein kinase (MAPK) family of serine/threonine kinases whose signaling may be detrimental to mitochondrial function [109,110]. Importantly, ROS release and consequent cytotoxicity are decreased when HK-I and HK-II bind to VDAC1 [111–114].

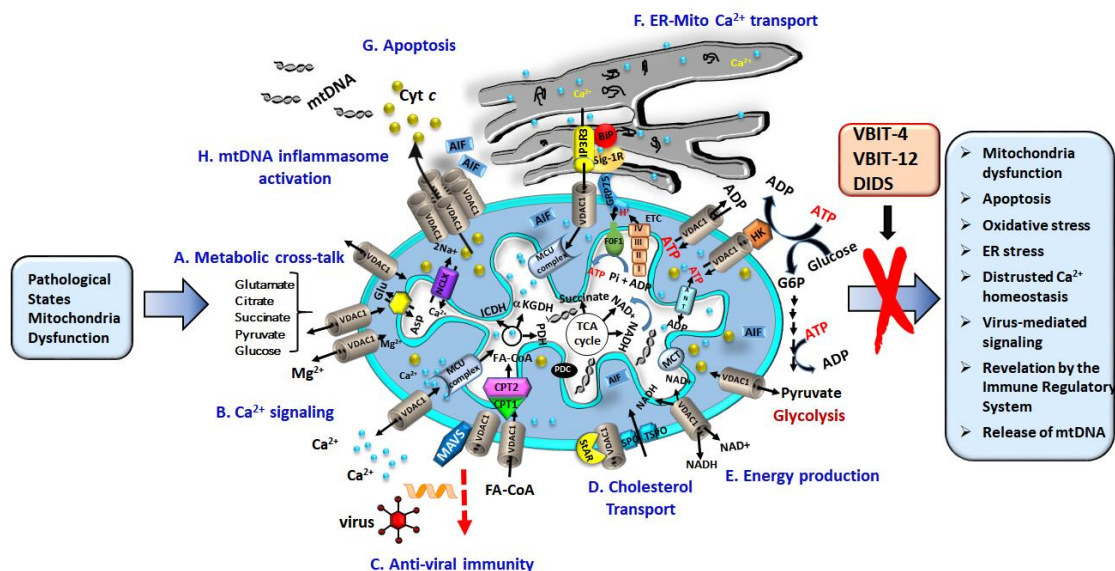


Figure 1. Voltage-dependent anion channel 1 (VDAC1) as a multi-functional channel mediates metabolites, nucleotides, and Ca^{2+} transport, controlling energy production, endoplasmic reticulum (ER)-mitochondria cross-talk, and apoptosis. VDAC1 is responsible for a number of functions in the cell and mitochondria including: (A) transfer of metabolites between the mitochondria and cytosol; (B) passage of Ca^{2+} to and from the intermembrane space (IMS) to facilitate Ca^{2+} signaling; (C) Mitochondrial antiviral-signaling protein (MAVS) associated with VDAC1 enable anti-viral signaling. (D) Transfer of acetyl coenzyme-A (acyl-CoAs) across the outer mitochondrial membrane (OMM) to the IMS, for conversion into acylcarnitine by CPT1a for further processing by β -oxidation. Together with Star and translocator protein (TSPO), VDAC1 forms the multi-protein transduceosome, which transports cholesterol. (E) Recycling ATP/ADP, NAD^+/NADH , and acyl-CoA between the cytosol and the IMS, and regulating glycolysis via association with HK; (F) contributing to ER-mitochondria contacts, where Ca^{2+} released by IP_3 activation of inositol 1,4,5-trisphosphate receptors (IP_3R) in the ER is directly transferred to IMS via VDAC1, and then is transported to the matrix by the Ca^{2+} uniporter (MCU complex). In the matrix Ca^{2+} regulates energy production via activation of the tricarboxylic acid cycle (TCA) cycle enzymes: pyruvate dehydrogenase (PDH), isocitrate dehydrogenase (ICDH), and α -ketoglutarate dehydrogenase (α -KGDH). The electron transport chain (ETC) and the ATP synthase (FoF1) are also presented. (G) VDAC1 oligomers forming a hydrophilic protein-conducting channel capable of mediating the release of apoptogenic proteins (e.g., Cyto c and apoptosis-inducing factor (AIF)) from the mitochondrial IMS to the cytosol, leading to apoptosis. (H). VDAC1 oligomers allow mtDNA release triggering inflammasome activation. Pathological conations lead to dysfunction of the mitochondria as reflected in the activities presented in the box on the right. These altered activities can be prevented by VDAC1-interacting molecules, such as DIDS, VBIT-4 and VBIT-12.

VDAC1 is also affected by hypoxic conditions. The C-terminal end of VDAC1 is cleaved (VDAC1- ΔC), with silencing of hypoxia inducible factor 1A (HIF-1 α) prevents such cleavage [115,116]. This formation of VDAC1- ΔC , is thought to prevent apoptosis and permit the maintenance of ATP and cell survival in hypoxia [117].

As described, the location of VDAC1 in the OMM provides the perfect opportunity to preside over the traffic of metabolites between the mitochondria and the cytosol, where it interacts with

other proteins in order to orchestrate and integrate mitochondrial functions with other cellular activities [3,4,30,41,42,118,119] (Figure 1).

VDAC1 activities are modulated by Ca^{2+} , ATP, glutamate, and NADH, as well as by a variety of proteins (see Section 7) [120–123]. Using a photo-reactive ATP analog, we identified three potential nucleotide binding sites [122]. Subsequent NMR spectroscopy and site-directed mutagenesis revealed that hVDAC1 possesses one major binding region for ATP, UTP, and GTP that is formed by the N-terminal α -helix, the linker connecting the helix to the first β -strand, and adjacent barrel residues [124]. The crystal structure of mouse VDAC1 in the presence of ATP, revealed an additional low-affinity binding site [125]. With respect to a high and low affinity ATP binding site, it should be noted that the cellular concentration of ATP is 1–2 mM.

In addition, Ca^{2+} binds to VDAC1 although the physiological function of this connection is not clear. Binding of Ca^{2+} to purified and bilayer reconstituted VDAC1 maintained the channel in an open configuration, which could be useful in upregulating the exchange of metabolites [126]. The divalent cation-binding sites bind the lanthanides, La^{3+} and Tb^{3+} , as well as ruthenium red (RuR), and its analogue Ru360 [127–129], the photo-reactive analogue azido ruthenium (AzRu) [130]. All reduce the conductance of native, but not mutant, VDAC1.

VDAC1 undergoes all known types of post-translational modifications (PTMs), including nitrosylation, acetylation, carbonylation, and phosphorylation [124]. TVDAC1 contains two cysteines; Cys²³² is found in the carboxyamidomethylated form, while Cys¹²⁷ is in the oxidized form of sulfonic acid [131]. VDAC1 possesses several potentially phosphorylatable serine and threonine residues, many of which have indeed been shown to undergo phosphorylation [132–134] by protein kinase A (PKA) [133], protein kinase C (PKC) ϵ [132], and GSK3b [135]. Both VDAC1 and VDAC2 are phosphorylated at a specific Tyr residue under hypoxic conditions [134].

Under pathological conditions, such as oxidation, aging, or after ischemic reperfusion injury, VDAC was shown to undergo nitration [136–138], while the protein undergoes carbonylation in the Alzheimer's disease-affected brain or after exposure to acrolein, produced by lipid peroxidation [139].

5. VDAC1, at the Nexus of Mitochondria-Mediated Apoptosis, and mtDNA Release

Mitochondria play a crucial role in the induction of apoptosis [140]. Changes in the permeability of the mitochondrial membrane in response to an apoptotic signal facilitate the release of apoptogenic proteins, including apoptosis-inducing factor (AIF), cytochrome *c* (Cyto *c*), and second mitochondria-derived activator of caspase and Direct Inhibitor of apoptosis-binding protein with low pI (SMAC/Diablo) crossing the OMM into the cytoplasm [3,140]. Once in the cytosol, Cyto *c* and SMAC/Diablo stimulate a caspase activating cascade, and AIF translocates to the nucleus where it activates nucleases and initiates a sequence of events leading to the degradation of proteins and DNA, and cell death. The release of the apoptogenic proteins is thought to be through a channel in the mitochondrial membrane, which may be composed of Bax and/or Bak oligomers [141,142], hetero-oligomers of VDAC1 and Bax [143,144], or VDAC1 oligomers [28,30,33,40–42,47,50,51] (Figure 1) (for reviews, see [4,28,30]). In this context, reconstituted liposomes containing purified VDAC1 have been shown to release encapsulated Cyto *c* to the external medium [37,47,145].

VDAC1 promotes apoptosis by mediating the release of apoptosis-causing proteins through an oligomeric channel. However, VDAC1, can also regulate the process by interacting with anti-apoptotic proteins [3–5,42] providing an additional measure of apoptosis control.

The crucial role of VDAC1 in apoptosis induction is demonstrated by the effects of VDAC1 silencing or over-expression [4,24,29,33,44,146–148]. Over-expression of VDAC1 was shown to induce apoptosis in all cell types [24,29,51,146–148], and cell death could be prevented by reagents such as RuR [29,149], 4,4 diisothiocyanostilbene-2,2-disulfonic acid (DIDS), 4-acetamido-4-isothiocyanato-stilbene-2,2-disulfonic acid (SITS), 4,4' diisothiocyanatodihydrostilbene-2,2'-disulfonic acid (H_2DIDS), 4,4'-dinitrostilbene-2,2'-disulfonic acid (DNDS), or diphenylamine-2-carboxylate (DPC) [54] that interact with VDAC1 [24,29,33,44,51,146–148], or by the overexpression of anti-apoptotic proteins such as Bcl2 and

HK-I [24,26,29]. As a corollary, reducing VDAC1 expression with siRNA negated cisplatin-induced apoptosis and Bax activation in non-small cell lung cancer (NSCLC) cells [150], reduced apoptosis induced by endostatin [151], and inhibited selenite-induced permeability transition pore (PTP) opening in HeLa cells [152].

5.1. Oligomerized VDAC1 Releases Cyto c, AIF, and SMAC/Diablo

Nucleotides and small molecules up to 5 kDa can pass through the VDAC1 pore, but not a folded protein like Cyto c (12 kDa). Therefore, we proposed that VDAC1 oligomerization can form a large channel, able to export pro-apoptotic proteins IMS to the cytoplasm to initiate apoptosis [24,28,30,33,40–42,44,47,50,51,145]. This change in VDAC1's structural state occurs in response to pro-apoptotic stimuli such as curcumin, As₂O₃, etoposide, cisplatin, selenite, H₂O₂, or UV light. Even in the absence of stimuli, overexpression of VDAC1 shifts the equilibrium towards oligomerization and, this led to apoptosis in several tested cell types [24,29,33,44,51,146–148].

The oligomerization process is significantly affected by the lipid composition of the OMM [153], and is enhanced by p53 [154].

As already described, a number of materials that interact with VDAC1 can interfere with oligomerization and attenuate the resultant apoptosis. Two new compounds we have developed, AKOS-022 and VBIT-4, similarly interact with VDAC1 to reduce its oligomerization and subsequent apoptosis induced by a variety of stimuli in various cell lines [53]. Importantly these new molecules protect against mitochondrial dysfunction, specifically restoring the membrane potential of the mitochondria, which is altered by apoptotic stimuli, thereby reversing energy and metabolic changes, decreasing the production of ROS, and maintaining physiological levels of intracellular Ca²⁺. Inhibiting the initiation of apoptosis at an early stage by inhibiting VDAC1 oligomerization may represent an effective approach to prevent or slow the enhanced apoptosis seen in neurodegenerative disorders [155,156] and various cardiovascular diseases [157–159].

All of these observations suggest the presence of a dynamic equilibrium in which VDAC1 shifts from a monomeric form towards oligomerization in response to pro-apoptotic stimuli or VDAC1 overexpression. In this way, the levels of VDAC1 expression and oligomerization are possible targets for intervention in mitochondrial-mediated apoptosis.

5.2. Release of Mitochondrial DNA (mtDNA) through the VDAC1 Channel

Human mitochondrial DNA (mtDNA) is a circular molecule of 16,569 bp, that encodes 13 polypeptides, as well as the 22 tRNAs and two rRNAs that are required for their translation [160]. The noncoding region (NCR) regulates transcription and translation of the mtDNA.

Many mtDNA genomes possess a third, linear strand region in the major NCR, which forms a triple-stranded structure known as the mitochondrial displacement loop, or D-loop. Although the precise function of the mitochondrial D-loop is unclear, a number of proposed options include DNA topology, replication, recombination, membrane association and dNTP metabolism [161]. The region is known to include promoter for adjacent transcripts possessing a high level of sequence variability, and has been associated with certain cancers, as well as aging in skeletal muscles, and skin fibroblasts [161].

Alteration in mtDNA content can impair cell metabolism and the innate immune system, including elevating the expression of interferon-stimulated genes [162].

Recently, we demonstrated that short mtDNA fragments, corresponding to a region within the D-loop, crossed the OMM and were released into the cytosol via the oligomerized VDAC1 channel and then triggered type-I interferon signaling and increased disease severity in a systemic lupus erythematosus (SLE) mouse model [87]. We also showed that our novel molecule VBIT-4 could inhibit this process [87]. Thus, inhibiting VDAC1 oligomerization and preventing mtDNA from passing through the OMM may represent a novel strategy for treating not only autoimmune diseases, such as SLE, but also other diseases.

A number of studies have now reported that viruses damage the host cell mtDNA to control the cell. For example, the Zta protein encoded by the Ebola virus translocates into the mitochondria and affects mtDNA replication [163]. Similarly, hepatitis C virus (HCV) infection leads to mtDNA damage [164], and the herpes simplex virus produces UL12.5 protein leading to mtDNA degradation [165], while HIV and hepatitis C virus infections cause mtDNA depletion in co-infected patients [166].

These observations are interpreted to indicate the importance of the mtDNA and the integrity of mitochondria and their metabolism for a variety of human pathologies.

5.3. VDAC1 Overexpression and Induction of Apoptosis

As already described, overexpression of VDAC1 is associated with apoptosis [3]. Levels of VDAC1 expression may be increased by a variety of agents, for example, in A375 human malignant melanoma cells by the tyrosinase inhibitor arbutin (hydroquinone-O-beta-D-glucopyranoside) [167], but increases in expression were also seen in acute lymphoblastic leukemia (ALL) cell lines following prednisolone treatment [168]. Other examples are listed in Table 1. Interestingly, cisplatin upregulated VDAC1 expression in a cisplatin-sensitive cervix squamous cell carcinoma cell line (A431), but down-regulated VDAC1 in a cisplatin-resistant cell line (A431/Pt) [169]. Pyrroloquinoline quinone (PQQ), an essential micronutrient [170] found in fruits and vegetables and cocoa powder has also been demonstrated to increase VDAC1 expression, but this was attributed to the induction of mitochondrial biogenesis [171].

Table 1. Compounds and conditions inducing VDAC1 overexpression and cell death.

No.	Compound	Ref.	No.	Compound	Ref.
1	Prednisolone1	[168]	11	Etoposide	[51]
2	Cisplatin	[51,169]	12	Selenite	[51]
3	Arsenic trioxide (As ₂ O ₃)	[51]	13	A23187	[51]
4	Arbutin (hydroquinone-O-β-D glucopyranoside)	[167,172]	14	Somatostatin	[65,173]
5	Hepatitis E virus ORF3 protein	[174]	15	H ₂ O ₂	[51]
6	UV irradiation	[175]	16	Thapsigargin	[51]
7	Mechlorethamine and its derivative, melphalan	[176]	17	Ionomycin	[51]
8	Vacuolating cytotoxin	[177]	18	Vorinostat	[51,178]
9	Quinocetone	[179]	19	DSS	(unpublished data)
10	Endostatin	[151]	20	Pyrroloquinoline quinone (PQQ)	[171]
			21	Plasminogen kringle 5 (PK5)	[74]

VDAC1 has been identified as a receptor of plasminogen kringle 5 (K5) known to display a potent anti-angiogenesis effect through inducing endothelial cell (EC) apoptosis. It is proposed that K5 induces apoptosis by up-regulating VDAC1 expression level via inhibiting the ubiquitin-dependent degradation of VDAC1 by promoting its phosphorylation through AKT-GSK3 pathway. In addition, K5 promoted translocation of VDAC1 to the plasma membrane where it binds to K5 [74].

The mechanism for up-regulation of the expression of VDAC1 is thought to involve an increase in the intracellular concentration of ionized calcium ([Ca²⁺]_i), [7,8,50,51]. Increasing the [Ca²⁺]_i directly by the addition of A23187, ionomycin, or thapsigargin also upregulated VDAC1 expression, and promoted oligomerization, and apoptosis [50,51,109]. As a corollary, chelating Ca²⁺ with BAPTA-AM and thereby reducing [Ca²⁺]_i, inhibited the overexpression and oligomerization of VDAC1, and subsequent apoptosis. This process of overexpression of VDAC1 induced by apoptosis stimuli, stress conditions, and pathological conditions leading to oligomerization and triggering apoptosis [40,41] is presented in Figure 2.



Figure 2. Sequence of events leading to VDAC1 overexpression, oligomerization, and apoptosis. Apoptosis stimuli or pathological conditions enhance VDAC1 expression via Ca^{2+} or transcription factors (TFs) activating promoter, leading to VDAC1 transcription.

The increase in VDAC1 transcription is a result of modulation of the interaction between transcription factors (TFs) and the VDAC1 promoter, or possibly by alterations in the expression of specific microRNA. We therefore propose that the expression of VDAC1 may represent a new possibly general mechanism of action by which inducers of apoptosis and pathological conditions upregulate the expression of VDAC1 (Figure 3).

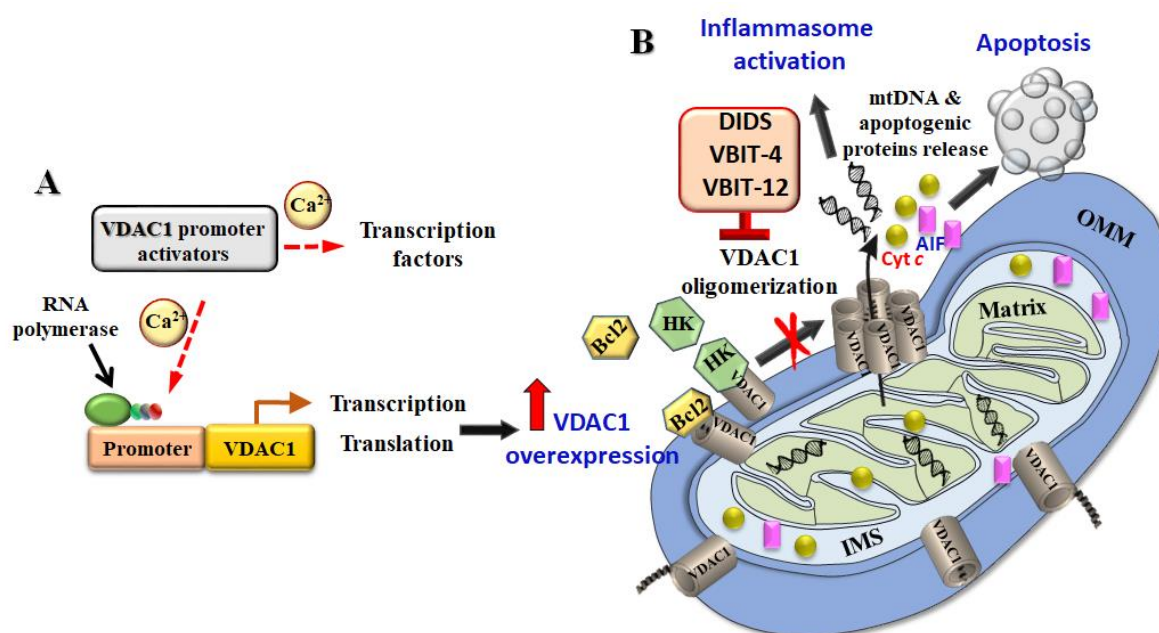


Figure 3. Proposed model for the mechanism of action for activators of the VDAC1 promoter leading oligomerization, and apoptosis. (A) Apoptotic stimuli act either by directly activating the VDAC1 promoter or by stimulating the activity of TFs, thereby inducing VDAC1. Ca^{2+} directly or via a TF leads to promoter activation. (B) Overexpressed VDAC1 shifts the equilibrium to the VDAC1 oligomeric state, mediating the release of apoptogenic proteins, and leading to apoptosis. VDAC1-interacting molecules such as VBIT-4, inhibit VDAC1 oligomerization and apoptosis.

6. VDAC1, Metabolism, and a Link to Epigenetics

Epigenetic changes involving methylation of DNA and/or modification to histones by acetylation, ubiquitination, methylation, phosphorylation, SUMOylation, glycosylation, or biotinylation represent an innate mechanism that links nutritional status to gene expression, and play a critical role in many cellular processes [180–186]. The enzymes responsible for these modifications include histone acetyltransferases (HATs), histone deacetylases (HDACs), methyltransferases (KMTs), and demethylases (KDMs) [187–189].

Most chromatin-modifying enzymes utilize metabolites as co-factors or substrates, and, thus, are directly dependent on metabolites such as acetyl-CoA, citrate, ketoglutarate, and NAD^+ , among others. Therefore, by supplying these metabolites, mitochondria can regulate the expression of different genes to facilitate diverse cellular functions [190]. Metabolites of the TCA cycle are also involved in controlling chromatin modifications, DNA methylation, hypoxic response, immunity, and post-translational modifications of proteins, and can thereby influence the function [191]. Since such

metabolites require VDAC1 for their transport to the cytosol in order to reach the nucleus, VDAC1 is thus a critical regulator of gene expression [192] (Figure 4).

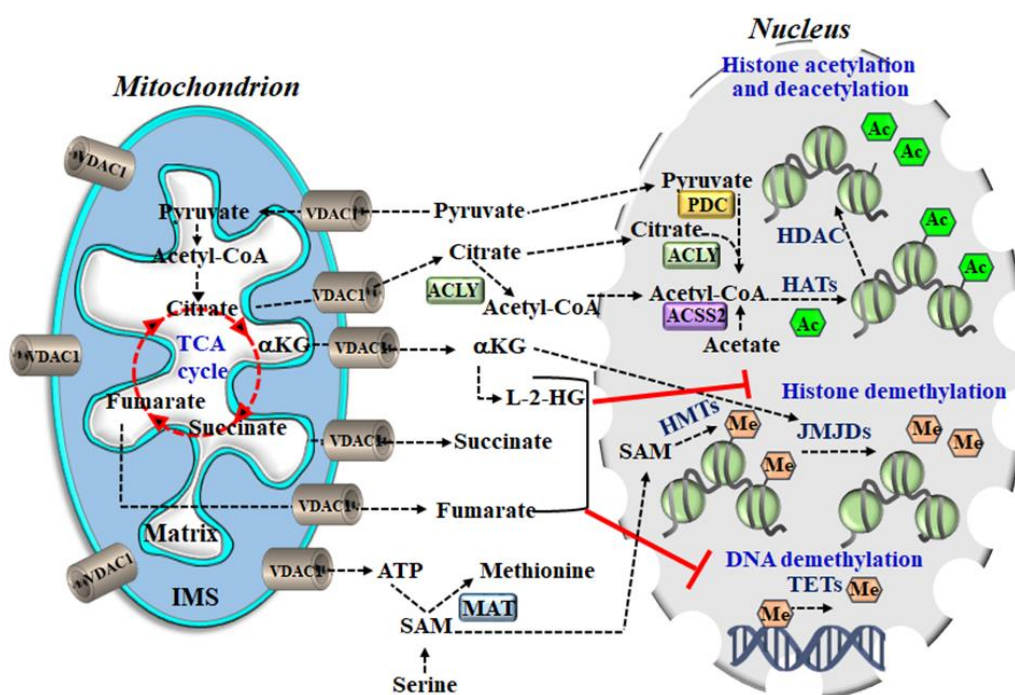


Figure 4. Mitochondrial metabolites are transported by VDAC1 to the cytosol and are then transported to the nucleus where they serve as substrates for enzymes that modify chromatin. Mitochondrial metabolic pathways including the TCA cycle generate substrates required for the methylation, acetylation, or demethylation reactions that modify chromatin. Specifically, histone acetylation by histone acetyltransferases (HATs) is dependent on the availability of acetyl groups provided by acetyl-CoA, which is produced in the cytosol by ACLY using citrate exported from the TCA cycle in mitochondria. α -ketoglutarate (α -KG) is an essential co-factor of 2-oxoglutarate-dependent dioxygenases (2-OGDD), including the histone demethylases Jumonji domains (JMJDs) and ten-eleven translocations (TETs), which are DNA demethylases. Succinate is the product of 2-OGDD enzyme reaction; thus, when it accumulates, it works as an antagonist of the reaction. Moreover, 2-Hydroxyglutarate (2-HG) and fumarate can also rewire the epigenetic landscape of the cells through inhibition of histone and DNA demethylation. The metabolites cross the IMM via specific transporters, and cross the OMM via a single protein VDAC1. The metabolites directly relevant to chromatin regulation reach the nucleus where several metabolic enzymes are localized including: methionine adenosyl-transferase (MAT); ATP-citrate lyase (ACLY), which catalyzes the ATP-dependent cleavage of mitochondrial-derived citrate into oxaloacetate; acetyl-CoA; pyruvate dehydrogenase complex (PDC); and acetyl-CoA synthetase 2 (ACSS2).

Relevant metabolites include:

1. Acetyl-CoA is a required co-factor for enzymes such as histone acetyltransferases (HATs) that catalyze the transfer of an acetyl group, to form ϵ -N-acetyl-lysine and acetylate histones in a process that is known to alter chromatin dynamics and to drive the epigenetic control of gene expression by activating transcriptional programs [193]. Practically, histone acetylation is dynamically regulated by the opposing actions of HATs and histone deacetylases (HDACs) that catalyze the addition and removal of the acetyl group, respectively. Intracellular concentrations of acetyl-CoA can vary roughly ~10-fold under normal physiological conditions, but they fall within the K_m range of HATs. Histone acetylation activity is, thus, essentially regulated by the availability of acetyl CoA.

2. NAD⁺ is essential for the deacetylation activity of sirtuins, a subgroup of HDAC, and changes in the NAD⁺/NADH ratio are thought to positively regulate sirtuin activity.
3. Citrate in the cytosol can be converted to acetyl-CoA by the enzyme ATP-citrate lyase (ACLY), which catalyzes the ATP-dependent cleavage of mitochondrial-derived citrate into oxaloacetate and acetyl-CoA [194]. The acetyl-CoA can then serve as a donor for HAT-mediated histone acetylation. However, citrate can also be converted to acetyl-CoA in the nucleus by ACLY [194].
4. α -ketoglutarate (α -KG) is an essential co-factor for 2-oxoglutarate-dependent dioxygenases (2-OGDD), including the histone demethylases with a Jumonji domain (JMJDs) and ten-eleven translocation (TET) DNA demethylases. α -KG has a direct impact on gene expression and, thus, can influence cellular fate by regulating histones and DNA demethylases. Succinate is the product of 2-oxoglutarate dependent dioxygenase (2-OGDD) enzyme reactions and, thus, when it accumulates, it works as an antagonist to the reaction.
5. The 2-Hydroxyglutarate (2-HG) is not part of the TCA cycle, but it can be derived from α -KG by enzymes in the mitochondrial matrix and cytosol. The 2-HG competitively inhibits 2-OGDDs and together with fumarate, can rewire the epigenetic landscape of the cells through inhibition of histone and DNA demethylases.

The 2-HG inhibits the activity of α -KG dependent dioxygenases such as TETs and JMJDs, which has broad implications for the regulation of epigenome.

6. Succinate and fumarate both behave as α -KG competitive antagonists and inhibit TETs and JMJDs. Both of these metabolites inhibit TET-catalyzed hydroxylation of 5 mC and the activity of histone demethylases KDM2A and KDM4A [195].
7. S-adenosylmethionine (SAM) serves as the methyl donor in reactions catalyzed by methionine adenosyl-transferase (MAT). DNA methylation at CpG sites represses gene expression by impeding access to transcription factors and inhibition of RNA polymerase II.

Methylation markers on lysine residues in histone proteins also have a key role in regulating chromatin structure and gene transcription. Multiple lysine residues (H3K4, H3K9, H3K27, H3K36, H3K79, etc.) may be mono-, di- or tri-methylated, giving rise to a very complex histone methylation profile.

The dynamics of DNA and histone methylation are also regulated by the activity of DNA and histone demethylases, respectively. Demethylation of histone lysine marks are mediated by flavin-dependent histone lysine demethylases that consist of lysine-specific protein demethylases (KDM1) and JMJD enzymes, and the ten-eleven translocation hydroxylases (TET1-3).

We recently [192] demonstrated that depleting VDAC1 in glioblastoma cells U87-MG-derived tumors affects the metabolism–epigenetics axis of the tumor. Analysis with DNA microarrays, q-PCR, and specific antibodies revealed epigenetic alterations in the methylation and acetylation of histones and the levels of epigenetic-related enzyme levels following depletion of VDAC1 in these cells. These findings support the importance of VDAC1, as a transporter of epigenetic associated metabolites. Depletion of VDAC1 down-regulates mitochondrial metabolism [43,51,99,196] because of the decrease in substrates transported into the mitochondria and the inability of the produced metabolites to exit the mitochondria. This restricts the availability of substrates for chromatin modifications and affects the interplay between metabolism and epigenetics.

7. Proteins Interacting with VDAC1 Modulate VDAC1 Activity and They Are Regulated by VDAC1

As already discussed, VDAC1 may be considered a hub protein that interacts with more than 100 proteins associated, on one hand, with cell survival and, on the other, with apoptotic cell death [4,30,41,42]. Together, they integrate mitochondrial activities with other cellular processes [197]. The interacting proteins may be located in the OMM, IMM, IMS, cytosol, ER, plasma membrane,

or/and nucleus [60,66]. Thus, VDAC1 in the OMM is a convergence locus for signals concerning the fate of the cell [4,41–43,198].

Importantly, we have been able to develop VDAC1-based peptides, which can interfere with these interactions, leading to impaired cell metabolism and apoptosis [27,34,39,199,200].

7.1. VDAC1 Interacting Metabolism-Related Proteins

VDAC1 interacts with a large number of metabolism-related proteins. Mitochondrial-bound HK (HK-I and HK-II) is overexpressed in cancer [4,201,202]. As a rate-limiting enzyme of glycolysis, HK association with VDAC1 offers several advantages to cancer cells [4,43]. HK binding to VDAC1 [24–29] allows direct coupling of mitochondrially generated ATP to glucose phosphorylation. Thus, the formation of a VDAC1-HK complex coordinates glycolytic flux with the actions of the TCA cycle and ATP synthase [4,44,201].

The formation of the HK-VDAC1 complex is regulated by Akt [203] and glycogen synthase kinase 3 beta (GSK3 β), while the HK-VDAC complex is disrupted by VDAC phosphorylation [204]. The physical interaction of ANT and VDAC is thought to be essential for the regulation of PTP formation, [205,206]. This structure was suggested to include VDAC1 in the OMM, ANT in the IMM, and cyclophilin D (CyD) in the matrix [123,207,208]. However, mitochondria lacking all three VDAC isoforms retained an unaltered ability to undergo permeability transition [209], and an ANT knock-out study showed that it is not essential for PTP activity [210]. Recently, however, it was proposed that dimers of the ATP synthase complex can form the PTP [206].

VDAC1 also interacts with glycerol kinase (GK), c-Raf kinase, and the glycolytic enzyme glyceraldehyde 3-phosphate dehydrogenase, (GAPDH) [4,30,41,42,211]. Mitochondrial creatine kinase (MtCK) interacts with octameric VDAC1 [46] and lowers the affinity of VDAC1 for HK and Bax [212].

VDAC-tubulin interaction was proposed to serve as a metabolic switch to increase or decrease mitochondrial metabolism, ATP generation, and cytosolic ATP/ADP ratios [213].

Finally, other energy metabolism proteins that interact with VDAC1 include the OMM protein CPT1a that catalyzes the primary step of fatty acid oxidation [88,105], TSPO, which is involved in the transport of cholesterol into mitochondria [214], and the gluconeogenesis/glycolysis enzyme aldolase [91].

7.2. VDAC1 Interacting Apoptosis-Related Proteins

The Bcl-2 family of proteins comprises both pro-apoptotic members (e.g. Bid, Bax, Bim, and Bak), and pro-survival agents (e.g., Bcl-2, Bcl-xL, and Mcl-1) [215,216]. These proteins were shown to interact with VDAC1 to inhibit apoptosis [27,33–35,217–221]. Interaction of Bcl-2 and Bcl-xL with VDAC1 in a reconstituted membrane bilayer reduced the channel conductance of native, but not mutated VDAC1, and protected cells expressing native, but not mutated VDAC1 from apoptosis [27,34]. Site-directed mutagenesis was used to identify the VDAC1 domains that interact with Bcl-2 and Bcl-xL to purvey the anti-apoptotic effect [27]. The results indicated that the N-terminal region of VDAC1 was important for this interaction [4,23,27,33,38], and also for association with HK [33,39]. Another member of the family, Mcl-1 has been shown to directly interact with VDAC to increase mitochondrial Ca²⁺ uptake and ROS generation [217].

As a result of their ability to regulate the activity of both VDAC1 and IP₃R, it is likely that the anti-apoptotic ability of Bcl-2, Bcl-XL, and Mcl-1 is mediated by the control of Ca²⁺ fluxes across the ER and mitochondrial membranes [28,222–224]. In this respect, we demonstrated that the BH4 domain of Bcl-XL, but not that of Bcl-2, selectively targets VDAC1 and inhibits apoptosis by decreasing VDAC1-mediated Ca²⁺ uptake into the mitochondria [225].

It has been shown that activating transcription factor 2 (ATF2), associated with cell death or cellular stress states in several melanoma and tumor cell lines, involves Bim and VDAC1, where VDAC1

depletion significantly prevented ATF2-related apoptosis [225]. In addition, ATF2 prevented HK interaction with VDAC1, sensitizing cells to apoptosis.

The inhibition of As₂O₃-, ethanol-, endostatin-, and cisplatin-induced apoptosis by siRNA has been interpreted by a number of studies to suggest that VDAC1 interacts with pro-apoptotic proteins Bax and Bak to allow Cyto *c* release [37,150,151,226,227].

The HK-VDAC1 interaction prevents release of pro-apoptotic factors such as Cyto *c*, and subsequent apoptosis. Thus, HK plays a role in tumor cell survival via inhibition of apoptosis [24].

The recently reported interaction between TSPO and VDAC1 [228] is thought to play a role in the activation of the mitochondrial apoptosis pathway through TSPO involvement in the generation of ROS [229–231]. The grouping of TSPO molecules around VDAC1 is thought to increase ROS generation in the proximity of VDAC, leading to apoptosis induction [231,232]. In addition, by interaction with VDAC1, TSPO inhibits mitochondrial autophagy and contributes to the efficiency of mitochondrial quality control machinery [5,8,9,233], regulating mitochondrial structure and function [233,234].

Yet another observation of the pro and anti-apoptotic effects associated with VDAC1 is the inhibition of apoptosis by the phosphorylation of serine 193 of VDAC1 by NIMA-related protein kinase 1 (Nek1) [235,236] while the pro-apoptotic protein BNIP3 was shown to interact with VDAC1 to induce mitochondrial release of endonuclease G [237].

7.3. Interacting Cytoskeletal Proteins

The cytoskeleton is involved in the regulation of bioenergetic functions in the cell with VDAC1 considered as the main regulator by interacting with several cytoskeletal proteins. Direct Ca²⁺-dependent binding of gelsolin (Gsn) to the C terminal of VDAC1 inhibits the activity of the VDAC1 channel and reduces the release of Cyto *c* from liposomes [238–241]. Binding to another member of the gelsolin family (adseverin) has a similarly anti-apoptotic effect [241].

The tubulin βII isoform in oxidative skeletal muscles and brain synaptosomes has been shown to act as a regulator of mitochondrial function by modifying the permeability of the VDAC channel for adenine nucleotides [242]. Tubulin was shown to associate with VDAC1 [242–244] and, at nanomolar concentrations, α and β tubulin heterodimers induce voltage-sensitive reversible closure of VDAC, reconstituted into planar phospholipid membranes [242]. This is proposed to sustain the Warburg effect [245]. The interaction between βII-tubulin and VDAC is thought to form a super-complex termed the mitochondrial interactome, composed of the ATP synthasome (ATP synthase, the respiratory system, and inorganic phosphate transporter), tubulin, VDAC1, and MtCK [246]. This construct can regulate mitochondrial respiration in adult cardiomyocytes and other metabolically active cells. The VDAC1-tubulin interaction, therefore, represents a new pharmacological target for the development of novel anti-cancer agents [213].

Other cytoskeleton-associated proteins that bind VDAC1 include the microtubule-associated protein 2 (MAP2) [247] and the dynein light chain (Tctex-1/DYNLT1) that is responsible for microtubule-based motile processes [248]. The function of the VDAC1–DYNLT1 interaction is not yet clear.

Actin was also shown to interact directly with VDACS, and also with another ten membrane channel proteins [249].

7.4. VDAC1 Interacting Signaling Proteins

Association of endothelial NO synthase (eNOS) with VDAC1 upregulated eNOS activity. This increase was dependent on [Ca²⁺]_i [250].

Superoxide dismutase 1 (SOD1) is a predominantly cytosolic protein, with a mutant SOD1, associated with amyotrophic lateral sclerosis (ALS), found in mitochondria-rich fractions of cells [251–253]. This mutant SOD1 was found to bind VDAC1 reconstituted in a lipid bilayer and to inhibit the conductance of the VDAC1 channel [254]. Mutant SOD1 could also interact with Bcl2 and alter the interaction between Bcl-2 and VDAC1, thus, reducing OMM permeability [255,256].

The mitochondrial anti-viral signaling protein MAVS, also known as IFN-beta promoter stimulator-1 (IPS-1), virus induced signaling adaptor (VISA), or caspase activation recruitment domain adaptor inducing I FN- β (Cardif) [257] localized in the OMM, interacts with VDAC1 and modulates its stability via the ubiquitin–proteasome pathway [258].

Several additional proteins were also proposed to interact with VDAC1. These include PBP74, also known as mtHSP70/GRP75/mortalin [248], and CRYAB (α -crystallin B) [259]. The pre-synaptic protein α -synuclein interacts with the mitochondria via VDAC1 [260–262]. The nAChRs were identified in the mitochondria and proposed to regulate Cyto c release via interaction with VDAC [263,264].

α -synuclein is a neuron-specific protein localized in the presynaptic nerve terminals and nucleus. Although its exact function is still unknown, it is well established that α -synuclein is involved in synaptic activity through regulation of vesicle docking, fusion, and neurotransmitter release [265,266]. A number of studies have shown that the pre-synaptic protein α -synuclein interacts with the mitochondria via VDAC1 [260,261] and can pass through the VDAC1 channel to target complexes of the mitochondrial respiratory chain in the inner mitochondrial membrane [267].

7.5. Viral Proteins Interact with VDAC1 to Modulate Expression Level and Function

A number of studies have reported that certain viruses induce VDAC overexpression, or that some of their proteins interact with VDAC. Furthermore, silencing VDAC expression dramatically reduces the expression of viral proteins as summarized in Table 2 and in the following:

1. Influenza A Virus: the virus attacks the respiratory system including the nose, throat, and lungs. One of the virus proteins interacting with VDAC1 [268] is influenza A virus protein (PB1-F2). The protein is localized to both mitochondrial membranes, OMM and IMM, and is a 90-amino-acid protein expressed from the +1 open reading frame in the PB1 gene of influenza A viruses. PB1-F2 contributes to the pathogenesis of the virus by binding to the mitochondria, altering their morphology, and inducing apoptosis via direct interaction with VDAC1 [268].
2. Hepatitis B Virus (HBV): one of five known human hepatitis viruses: hepatitis A, B, C, D, and E. This virus causes hepatitis B in which the virus attacks the liver and can cause acute and chronic liver disease such as cirrhosis and hepatocellular carcinoma. Hepatitis B viral protein (HBx) is a multifunctional protein encoded by the HBV genome that stimulates HBV replication. HBx binds to the mitochondria and co-localizes with VDAC-1, where it alters the mitochondrial transmembrane potential by creating together a hexamer that affects mitochondrial physiology [269].
3. Hepatitis E Virus (HEV): HEV infections are often asymptomatic, although they can be severe and cause fulminant hepatitis and extra-hepatic manifestations including neurological and kidney injuries. Chronic HEV infections may also occur in immunocompromised patients causing inflammation of the liver. The open reading frame 3 (ORF3) protein is a small phosphoprotein of 113 or 114 aa proposed to act as an adaptor to link the intracellular transduction pathways, reduce the host inflammatory response, and protect virus-infected cells [270]. ORF3 protein interacts with several of the host's cellular proteins, including VDAC1, where in a cross-linking study, ORF3-expressing cells were shown to produce higher levels of oligomeric VDAC1 [174,271].
4. Human Immunodeficiency Virus type 1 (HIV-1): the virus causes acquired immunodeficiency syndrome, with progressive breakdown of the immune system, and promotes life-threatening opportunistic infections. A viral protein R (Vpr) is a 96-amino-acid (14-kDa) protein. This protein stimulates virus transcription and interacts with the host's proteins, playing an active role in viral pathogenic factors. Vpr protein induces cell cycle arrest in proliferating cells, as well as regulating activation and apoptosis of infected T-lymphocytes via interaction with VDAC1 [239].
5. Dengue Virus (DENV): the virus causes dengue fever characterized by headache, severe muscle and joint pain, and upper respiratory symptoms. The protein, DENV E, is an envelope protein (E protein) which is the key component of the dengue virion. The ENV E protein plays a vital role

in the viral lifecycle by mediating interaction with host cells and facilitating invasion. It has been reported that this protein interacts with various proteins in host cells, including with the cellular chaperone GRP78 along with mitochondrial VDAC1. Furthermore, down-regulation of VDAC by siRNA reduced the expression of several DENV proteins: NS1, NS3, NS5, and DENV E [272]. Thus, VDAC plays a significant role in DENV infection.

6. The Infectious Bursal Disease Virus (IBDV): the virus causes immunosuppressive disease in young chickens. The VP5 protein, a non-structural protein of IBDV, is associated within the plasma membrane of the host-infected cells and plays an essential part in pathogenesis of IBDV. VP5 induces apoptosis in host cells via interaction with VDAC [273], with the VDAC inhibitor DIDS [53] decreasing VP5 expression and apoptosis [274]. On the other hand, silencing VDAC1 expression decreases the expression of VP1, VP2, and VP5 [275]. VP1 and VP2 are essential structural proteins that participate in IBDV capsid assembly and penetration into the host cell, as well as replication of virus. The VP2 carries neutralizing epitopes which control antibody-mediated neutralization of IBDV infection. VP2 acts as an apoptotic inducer in infected cells.
7. Japanese Encephalitis Virus infection (JEV): the virus causes Japanese encephalitis. The JEV invades the CNS, resulting in neuroinflammation, which negates the neuroprotective role of microglia, as characterized by increased microglial activation and neuronal death. The JEV envelope protein (JEV-E) is the major structural protein that facilitates the viral infection by recognizing host cellular receptors and mediating membrane fusion. The primary target of this protein is to neutralize antibodies; therefore, it is a key virulence factor involved in pathogenesis. The JEV-E protein interacts with VDAC, and in response to JEV infection, VDAC1 is overexpressed and co-localized with the ER protein GRP78, a multifunctional chaperone protein (HSP70) increasing MAM [276].
8. Ostreid herpes virus-1 (OsHV-1): OsHV-1 is a variant of herpes virus, and it has been a major threat to Pacific cupped oysters. It contributes to the pathogenesis of mass mortality disease in the early life-stage of oysters. Infected oysters exhibit an increase in glycolysis and increased VDAC1 expression, as revealed in both mRNA and protein levels, while this increase in VDAC1 levels correlates with susceptibility of oysters to OsHV-1 [277].

Table 2. Different viruses target VDAC to modulate mitochondrial activities-VDAC1 is a key protein in the viruses’ effects on the host cells.

Virus	Virus Type	Viral Protein	Action on VDAC1	Reference
HIV-1 Human Immunodeficiency Virus type 1	Single-stranded positive RNA	Vpr	Interacts with VDAC1 and induces apoptosis	[239,278]
DENV Dengue Virus	Single-stranded positive RNA	DENV-E	Interacts with GRP78, a chaperone interacting with VDAC1. Down-regulation of VDAC reduced DENV protein expression	[272]
Influenza A Virus	Single-stranded negative-sense RNA	PB1-F2	Induces apoptosis via interaction with VDAC1	[268]
IBDV Infectious Bursal Disease Virus	Double-stranded RNA	VP5	Induces apoptosis in DF-1 cells via interaction with VDAC1	[53,273,274,279]
HBV Hepatitis B Virus	DNA	HBx	HBx interaction with VDAC1 to form a hexamer, causing mitochondria dysfunction	[269,280]
HEV Hepatitis E Virus	Single-stranded positive sense RNA	ORF3	Expression of ORF3 increases VDAC1 levels, siRNA against ORF3 reduces VDAC1 levels	[174,271]
Japanese Encephalitis Virus	Single-stranded, positive-sense RNA	JEV E	JEV E protein interacts with VDAC. Upon JEV infection, VDAC1 was co-localized with the ER protein GRP78 (HSP-70)	[276]
OsHV-1 Ostreid Herpes Virus-1	DNA		Increases VDAC1 expression at the mRNA and protein levels	[277]

Thus, VDAC1-interacting protein complexes are formed under physiological and pathological conditions, mediating, and/or regulating metabolic, apoptotic, and other processes that may be impaired in disease.

8. VDAC1 Overexpression in Disease States and Association with Apoptosis

Mitochondrial dysfunction has been implicated in many diseases including cancer, Alzheimer's disease (AD), Parkinson's disease (PD), amyotrophic lateral sclerosis (ALS), type 2 diabetes (T2D), and cardiovascular diseases (CVDs). VDAC1 is essential for proper mitochondrial function and, consequently, for normal cell physiology. Thus, an association of VDAC1 with various pathologies is only to be expected. In this context, VDAC1 has been shown to be over expressed in cancer [3,86], in the affected regions of AD brains [75–77], in β -cells in T2D [80,81,84], and in autoimmune diseases such as lupus [87], NASH [88], IBD (unpublished data), and in CVDs [89] (Figure 4). Since as already described, overexpression of VDAC1 induces apoptosis and cell death [29,51,99,146,147], this may represent a common mechanism in CVDs, AD, and T2D although it is currently a matter of debate whether the over expression is a cause or result of the pathology.

Importantly, reducing the levels of VDAC1 with a specific siRNA, or our newly developed small molecules, e.g., VBIT-4 and VBIT-12, could inhibit VDAC1 oligomerization, correct the misdirection of the protein to the plasma membrane (PM) [84], and prevent mitochondria dysfunction and apoptosis [53] in both T2D [84] and models of lupus [87]. The following is a summary of VDAC1 overexpression in certain diseases.

8.1. Cancer and VDAC1

Our understanding of cancer has recently seen a major paradigm shift towards the concept of cancer being a metabolic disorder. This notion was first introduced by Otto Warburg, who suggested that a hallmark of cancer cells is deregulation of cellular energy, and metabolism. Indeed, there are extensive reviews of the evidence supporting the general hypothesis that the main characteristics of cancer, including genomic instability and aerobic glycolysis, can be linked to impaired mitochondrial function and energy metabolism [281,282]. By regulating the metabolic and energetic functions of mitochondria, VDAC1 can, therefore, control the fate of cancer cells. VDAC1 is highly expressed in various tumors obtained from patients, and in tumors established in mouse models, as well as in cancer cell lines [3,15,85,86,283], providing supporting evidence for its significance in high energy-demanding cancer cells. Indeed, its pivotal role in regulating cancer cellular energy, metabolism, and viability is also underscored by the findings that abrogation of VDAC1 expression reduced cellular ATP levels, cell proliferation, and tumor growth [85,86,99,196]. The overexpressed VDAC1 contributes to cancer cell metabolism by facilitating the passage of essential metabolites, and delivering mitochondrial ATP directly to HK, which is also overexpressed in cancer (HK-I, HK-II) [5,284]. This fuels the high level of glycolytic flux seen in tumors, which have a high demand for metabolites or metabolite precursors. As a corollary, down-regulation of VDAC1 in tumor cells, with subsequent reduction in metabolite exchange between the mitochondria and cytosol, inhibited the growth of cells and tumors [43,85,86,99,196].

Interactions between VDAC1 and the anti-apoptotic proteins Bcl-2, Bcl-xL [27,33,34,285], and HK [33,39] protect tumor cells from apoptosis [33,39]. Reduction of VDAC1 expression by a specific miRNA, miR320a, promoted mitophagy in serum starved cervical cancer cells [286] and blocked tumor cell proliferation and invasion in NSCLC, both in vitro and in vivo [287]. Another miRNA species, miR-7, was shown to inhibit VDAC1 expression, proliferation and metastasis in hepatocellular carcinoma [288], possibly by affecting the PTP [289].

These results all suggest that VDAC1 could be a useful druggable target for anti-cancer therapy.

8.2. Over-Expression of VDAC1 in Neurodegenerative Diseases

There is now emerging evidence connecting mitochondrial dysfunction to neurodegenerative disorders [290] with caspase-mediated apoptosis implicated in the premature neuronal cell death seen in neurological disorders (Table 3) [291–296].

A number of studies have linked VDAC dysfunction to AD [63,297–299], Down’s syndrome [299], and familial amyotrophic lateral sclerosis (ALS) [254,300]. High levels of VDAC1 were demonstrated in the dystrophic neurites of A β deposits in AD post-mortem patient brains and in brains of amyloid precursor protein (APP) transgenic mice [75–77]. Moreover, increases in VDAC levels in the thalamus of mice were shown to be associated with neurodegeneration in the Batten disease model [301]. Similarly spatial cognitive deficits in an animal model of Wernicke–Korsakoff syndrome were reported to be associated with changes in thalamic VDAC levels [302]. The involvement of plasmalemmal VDAC in AD was also proposed [62,63].

AD brains exhibit a significant loss of neurons, mainly due to apoptosis, with neurons in AD brains [31,64,303,304] displaying the hallmarks of apoptosis [305]. As VDAC1 overexpression was shown to trigger apoptotic cell death [29,51,99,146–148], we propose that overexpressed VDAC1 in the AD brain may be responsible for the observed neuronal cell death.

Table 3. VDAC1 association with diseases.

Disease	VDAC1 State	Function	Reference
Cancer	Overexpressed	Increased cancer cell metabolic activity	[3,15,85,86,99,196,283]
Alzheimer’s disease	Overexpressed	Neuronal cell death	[75–77]
ALS—Amyotrophic lateral sclerosis	Interacted with mutated SOD	Enhanced cell survival	[254,255,306]
Type 2 diabetes	Overexpressed	Impaired generation of cellular ATP	[80,81,84,307]
Systemic lupus erythematosus	Overexpressed	Mediated release of mtDNA and triggered type-I interferon responses	[87]
Cardiovascular diseases	Overexpressed	Cardiomyocyte cell death	[90,308–314]
Non-alcoholic fatty liver disease (NAFLD)	Overexpressed	Mediated transport of fatty acids across the OMM	[88,105,107]
Rheumatoid arthritis	Overexpressed	Cardiac cell death and functional impairment	[315], Figure 5
Acute kidney injury	Deletion of VDAC1 hinders recovery of mitochondrial and renal functions	Required for the recovery of renal mitochondrial function	[315]
Spinal cord injury	Overexpressed	Oligomerization and apoptosis	[316]

Proteomics studies have identified nitration and carbonylation of VDAC1 in the brains of AD patients, suggesting that VDAC1 channel activity contributes to the pathogenesis and progression of AD [317]. In addition, VDAC1-deficient transgenic mice exhibit deficits in long-term potentiation and learning behavior, suggesting that VDAC1 is an absolute requirement for normal brain activity [318].

Mutations in superoxide dismutase (SOD1) are the second most common cause of familial ALS, a progressive neurodegenerative disease characterized by the loss of motor neurons in the brain and spinal cord [319]. SOD1 mutants interfere with various aspects of mitochondrial function including mitochondrial energy metabolism, transport, fission, and fusion [320–323]. An inverse correlation between mutant SOD1 mitochondrial association in motor neuron-like NSC-34 cells and disease duration was reported in patients carrying mutations in SOD1 [324]. In addition, the misfolded SOD1 could also directly bind VDAC1, resulting in destabilization of VDAC1 conductance and channel instability, and inhibiting VDAC1 transport of adenine nucleotides across the OMM [254,306].

Recently [255], we demonstrated that mutant SOD1^{G93A} and SOD1^{G85R}, but not wild-type SOD1, directly interact with VDAC1 and reduce its channel conductance, but no such interaction was obtained with N-terminal-truncated VDAC1. Moreover, a VDAC1-derived N-terminal peptide inhibited mutant SOD1-induced toxicity, suggesting that its specific interaction with the N-terminal domain of the VDAC1 is associated with mutant SOD1 toxicity.

In addition, proteins including SOD1, α -synuclein, and apoE, which all bind VDAC1 have been implicated in affecting intraneuronal Ca²⁺ in several neurodegenerative diseases, [7]. These findings

suggest that VDAC1 could represent a potential target for novel therapeutic strategies also for neurodegenerative diseases.

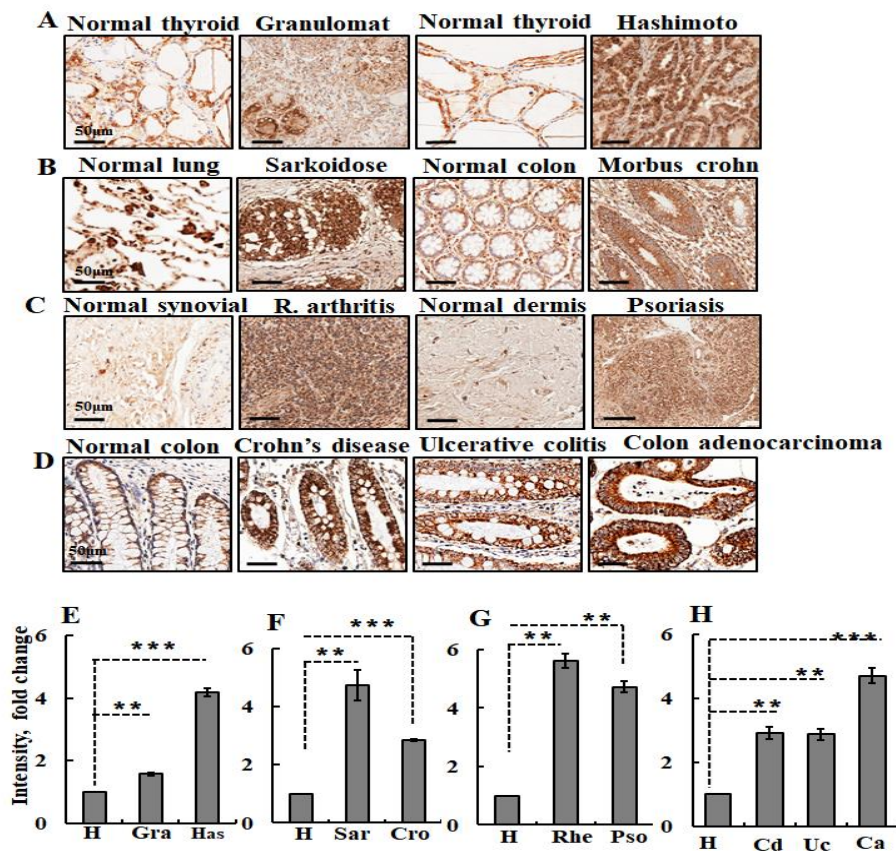


Figure 5. VDAC1 is overexpressed in tissue samples from autoimmune disease patients. (A–D) immunohistochemistry staining (IHC) of VDAC1 was performed on tissue microarray slides obtained from Provitro AG (Charité Campus Mitte 10,117 Berlin, Germany) (A–C) and US Biomax, Inc. (MD USA) (D). The array contains tissue sections from healthy (normal thyroid, lung, colon, synovial, dermis samples), (A) granulomat (Gra), Hashimoto thyroiditis (Thyroid, Has), (B) sarcoidosis (lung, Sar), Morbus Crohn (Sigma), (C) rheumatoid arthritis (Synovial, Rhe), psoriasis (Pso), (D) Crohn’s disease (Cd), ulcerative colitis (Uc), colon adenocarcinoma (Ca). (E–H) Quantitative analysis of VDAC1 expression levels are also presented. Representative sections of the indicated tissues were incubated overnight at 4 °C with anti-VDAC1 antibodies diluted in 1% BSA in phosphate buffered saline (PBS) and then with secondary antibodies diluted in 1% BSA in PBS. The slides were subsequently treated with 3’3-diaminobenzidine tetra-hydrochloride (DAB) and counter-stained with hematoxylin. Negative controls were incubated without primary antibody. Sections of tissue were observed under an Olympus microscope, and images were taken at 200× magnification with the same light intensity and exposure time. Quantitation of VDAC1 expression levels in the whole area of the provided sections, as reflected in the staining intensity, was performed using a panoramic microscope and HistoQuant software (Quant Center 2.0 software, 3DHISTECH Ltd). The results are the mean values ± SEM, ** $p < 0.01$, *** $p < 0.001$.

8.3. Type 2 Diabetes (T2D) and VDAC1

VDAC is also overexpressed in T2D, which is the most common metabolic disease [325]. Elevated levels of VDAC were found in mouse coronary vascular endothelial cells isolated from diabetic mice [307] and in the β cells of T2D patients [80]. Interestingly, hyperglycemia increases VDAC1 expression in both pancreatic β -cells [80] and in the kidney [81]. Recently [84], we demonstrated up-regulation of VDAC1 in islets from T2D donors and in NS1 cells under glucotoxic conditions,

with the result that VDAC1 is mislocalized to the plasma membrane of the insulin-secreting β cells, with loss of ATP. Specific anti-VDAC1 antibodies, and our VDAC1 inhibitor, VBIT-4, could restore generation of cellular ATP and normalize glucose-stimulated insulin secretion in T2D islets [84]. Similarly, treatment of db/db mice with VBIT-4 prevented hyperglycemia, and maintained normal glucose tolerance and physiological regulation of insulin secretion [84]. Thus, β -cell function was preserved by targeting the overexpressed VDAC1. Interestingly, lncRNA-H19/miR-675 was reported to regulate high glucose-induced apoptosis by targeting VDAC1, thus, providing a novel therapeutic strategy for the treatment of diabetic cardiomyopathy [326]. These findings point to the connection between VDAC, mitochondrial function, and the pathogenesis of T2D. The involvement of VDAC1 in T2D was also demonstrated in mice subjected to combination of a high-fat diet (HFD) and low-dose of streptozotocin (STZ), representing a model for type 2. These STZ/HFD-32 treated mice showed symptoms of T2D-like disease reflected in increased blood glucose [82].

8.4. Autoimmune and Inflammatory Diseases and Increased VDAC1 Expression Levels

Autoimmune diseases often are characterized by T-cell hyperactivity and β -cell overstimulation leading to overproduction of autoantibodies [327]. Inflammation is an important host defense response to injury, tissue ischemia, auto immune responses, and infectious agents [328]. This is now viewed as one of the major causes for the development of diseases, such as cancer, cardiovascular disease, diabetes, obesity, osteoporosis, rheumatoid arthritis, inflammatory bowel disease, asthma, and CNS-related diseases, such as depression and Parkinson's disease.

Recently [87], we demonstrated that VDAC1, but not VDAC2, are over-expressed in diseases (such as SLE) that are associated with type-1 interferon signaling. SLE is a non-organ-specific autoimmune disease characterized by β cell hyperactivity, abnormally activated T cells, defects in the clearance of apoptotic cells, and immune complexes. We found that VDAC1 oligomers in the OMM promoted mtDNA release and our small molecule, VBIT-4, which inhibits VDAC1 oligomerization, decreased mtDNA release, type-I interferon signaling, neutrophil extracellular traps, and disease severity in a mouse model of systemic lupus erythematosus.

Additionally, we found that VDAC1 expression is upregulated in several autoimmune diseases, including Hashimoto thyroiditis, also known as chronic lymphocytic thyroiditis, an autoimmune disease in which the thyroid gland is gradually destroyed; rheumatoid arthritis (synovial), a persistent auto-immune disease primarily characterized by cytokine-mediated inflammation of the synovial inside layer of the joints and obliteration of cartilage and bone; psoriasis, an immune-mediated skin disease characterized by abnormal keratinocyte differentiation and proliferation; and Crohn's disease, a chronic intestinal inflammatory condition caused by multiple factors. In addition to the non-immune contributing factors, the breach of the intestinal epithelial barrier and dysfunction of both innate and adaptive immunity that predominates during the inflammatory process is considered to be one of the earliest etiological factors involved in IBD. Still more diseases with VDAC1 overexpression are sarcoidosis, a disease involving abnormal collections of inflammatory cells that form lumps, with the disease usually beginning in the lungs, skin, or lymph nodes; and chronic granulomatous disease (CGD), an inherited primary immunodeficiency disease presenting with accumulation of immune cells at sites of infection or inflammation.

Representative images from healthy and diseased tissues and quantitative analysis of VDAC1 expression levels in the various pathological tissues are presented in Figure 5. These findings suggest that VDAC1 is a potential therapeutic target for lupus and other autoimmune diseases.

8.5. Cardiovascular Diseases, Apoptosis, and VDAC

The involvement of VDAC1 in the pathogenesis of cardiac abnormalities has been proposed. In the context of cardiac I/R, upregulation of VDAC1 expression and phosphorylation have been shown to augment cardiomyocyte damage, and inhibition of these processes was mechanistically linked to the nutritional preconditioning function of resveratrol [309,311–313]. Oxidative stress damage in

H9c2 myoblasts was reported to increase VDAC1 expression levels and its oligomerization [308,314]. Recently, it has been demonstrated that silencing VDAC1 promotes tBHP-induced apoptosis in H9C2 cells via decreasing mitochondrial HK-II binding and enhancing glycolytic stress [329]. In addition, VDAC1 was found to be involved in detrimental Ca^{2+} transfer from the ER to the mitochondria [106]. Upregulated transcriptional levels of a diverse array of genes including VDAC1 were found in the septal tissue of human patients with hypertrophic cardiomyopathy [310]. In addition, prominent upregulation of VDAC1 expressional levels in a rat model of cardiac hypertrophy induced by renal artery ligation and treatment with siRNA against VDAC1 partially inhibited the observed apoptotic cell death [259]. It was also reported that the expressional levels of VDAC1 were down-regulated in a cellular model of cardiomyocyte hypertrophy induced by the α 1-adrenergic agonist phenylephrine that was prevented by peroxisome proliferator-activated receptor α (PPAR α) [330]. Recently, we demonstrated an increase in the expressed levels of VDAC1 in the setting of common cardiac pathologies including in the post-MI setup, chronic left ventricular (LV) dilatation and dysfunction, and hyperaldosteronism [90].

It is still unclear how the expression of VDAC1 is affected by common cardiac pathologies including pathological hypertrophy and ischemic cardiomyopathy. It is possible, however, that increased cardiomyocyte susceptibility to mitochondrial-mediated cell death is related to an increase in VDAC1 levels.

8.6. Non-Alcoholic Fatty Liver Disease (NAFLD)

Chronic liver disease represents a significant public health problem world-wide, with viral hepatitis and non-alcoholic fatty liver disease (NAFLD) affecting about 20% of the general population [331]. NAFLD is characterized by excessive abnormal accumulation of fatty acids and triglycerides within the hepatocytes of non-alcohol users. NAFLD and the progressive state, non-alcoholic steatohepatitis (NASH) manifest as liver pathologies characterized by severe metabolic alterations due to fat accumulation that leads to liver damage, inflammation, and fibrosis [331]. Mitochondria play a prominent role in hepatosteatosis disease pathogenesis [332]. The involvement of VDAC in steatosis and NASH is suggested by several studies [83,88,333]. Mitochondria lacking VDAC1 do not oxidize fatty acids, and a VDAC1 inhibitor inhibited the oxidation of palmitate [334]. In addition, closure of the VDAC channel produces steatosis both in alcoholic steatohepatitis and NASH [83,333] because VDAC1 participates in the complex responsible for transporting fatty acids across the OMM [105,107].

Recently, we demonstrated that a cell-penetrating VDAC1-based peptide, R-Tf-D-LP4, arrested steatosis and the NASH produced by feeding mice a high-fat diet (HFD-32), and reversed liver pathology to a normal-like state [88]. R-Tf-D-LP4 treatment eliminated inflammation, liver fibrosis, and restored normal levels of glucose and liver enzymes. Peptide treatment also affected carbohydrate and lipid metabolism, increasing the expression of enzymes and factors associated with fatty acid transport to the mitochondria, enhancing β -oxidation and thermogenic processes, but decreasing the expression of enzymes and regulators of fatty acid synthesis [88] as well as HCC [283]. Thus, we suggest that R-Tf-D-LP4 peptide inhibits steatosis and NASH by increasing fatty acid oxidation via alterations in the liver transcriptional program; thus, it offers a promising therapeutic approach for steatosis and NASH.

8.7. Rheumatoid Arthritis, Acute Kidney and Spinal Cord Injury, and VDAC1 Expression

Rheumatoid arthritis (RA) is a chronic inflammatory disorder characterized by destructive polyarthritis, which destroys the joint synovial membrane, cartilage, and bone, resulting in disability [335]. Systemic inflammation mediated by cytokines is central to the pathogenesis of RA [336]. In a monkey model of RA [315], the heart receptor-interacting protein kinase 1 (RIPK1), a key pro-apoptotic signaling molecule, was shown to be upregulated, to bind VDAC1, and to promote oligomerization and subsequent cardiac cell death and functional impairment.

Acute kidney injury (AKI) is a clinical syndrome characterized by a rapid decline in kidney function and failure to regulate fluids, electrolytes, and the acid–base balance [337]. Mitochondrial dysfunction

and ATP deficits are the most pronounced in tubular cells of the renal cortex and precede the clinical manifestations of AKI [338,339]. Ischemic insults could damage kidney function which then recovered in wild-type, but not in VDAC1-deficient mice. This suggests that VDAC1 regulates the recovery of renal mitochondrial function and dynamics and ATP levels, and increases survival after AKI [340]. VDAC oligomerization with subsequent release of Cyto *c* to the cytoplasm has also been implicated in cisplatin-induced apoptosis and nephrotoxicity [341].

In spinal cord injury (SCI), damage to the spinal cord can cause temporary or permanent changes in its function. Symptoms may include loss of muscle function, sensation, or autonomic function in the parts of the body served by the spinal cord. The primary injury immediately after trauma, may cause neuronal/oligodendrocyte cell death and axonal shear that is then followed by a secondary injury characterized by progressive pathology, including microvascular perfusion changes, inflammation, free radical generation, and apoptosis/necrosis [342]. This secondary injury often alters the metabolism of intact axonal tracts, as a result of extensive oligodendrocyte cell death. VDAC1 levels were shown to be significantly increased after spinal cord injury. Inhibition of VDAC1 oligomerization by DIDS, protects the spinal cord from demyelination and promotes locomotor function recovery after spinal cord injury [316]. Prevention of VDAC1 oligomerization might therefore be beneficial for clinical treatment of SCI.

In conclusion, considering that VDAC1 overexpression is associated with a variety of pathological conditions including cancer [3,86], AD [75–77], T2D [80,81], and the autoimmune disease lupus [87], understanding the regulatory mechanisms of VDAC1 overexpression and mislocalization to the PM may be clinically relevant to these diseases.

9. VDAC1-Based Strategies to Treat Diseases Such as Cancer, Neurodegenerative, Autoimmune, NASH, and T2D

Targeting VDAC1 is likely to be effective for conditions associated with altered cell metabolism and/or apoptosis and by VDAC1 overexpression [29,51,99,146,147], which we suggest may be a common mechanism in the pathology of CVDs, AD, and T2D. Alternatively, modulating VDAC1 to activate apoptosis could be a possible therapeutic strategy for cancer. Thus, a new generation of VDAC1-based therapeutics may impact the treatment of a wide variety of diseases.

VDAC1-silencing strategy—we recently demonstrated that using specific si-RNA to silence human VDAC1 (si-hVDAC1) in cultured cells and in mouse models reduced cell energy homeostasis and inhibited the growth of various cancer cell types including glioblastoma multiforme (GBM), lung cancer, and triple negative breast cancer [85,86,343]. “Tumor” cells remaining after the treatment appeared to have undergone re-programmed metabolism and cell differentiation into normal-like cells with inhibited angiogenesis, epithelial mesenchymal transition (EMT), invasiveness, and stemness. Depletion of VDAC1 altered the expression of hundreds of genes including transcription factors (TFs) that regulate signaling pathways associated with cancer [85]. Interestingly, this re-programming was related to the time during which the tumor cell was depleted of hVDAC1, suggesting that a chain of events is involved [344].

Silencing VDAC1 expression by specific siRNA in PC12 cells and SH-SY5Y cells prevented A β entry into the cytosol, and reduced A β -induced toxicity [31]. These results suggest the involvement of VDAC1 in A β -cell toxicity, raising the possibility that A β enters the cell via pVDAC1 [31].

VDAC1-based peptides—A hallmark of cancer cells is their ability to avoid apoptosis [345,346] by overexpressing anti-apoptotic proteins such as HK-I, HK-II, Bcl2, and Bcl-xL [201,284,347–352], which interact with VDAC1 to prevent apoptosis [4,23,24,26,27,29,33–39,201,202,204,353]. We have designed a number of cell-penetrating VDAC1 peptides that target amino acids important for the interactions with HK, Bcl-2 and Bcl-xL as identified by point mutations and consideration of the VDAC1 domains [24,27,29,33,34,39,199]. Two of these VDAC1-based peptides, Tf-D-LP4 and the VDAC1-N-terminus, could induce cell death in a variety of cancer cell lines, regardless of cancer type or mutation status, but with a definite specificity for cancerous cells [33,39,199].

Tf-D-LP4 in treating cancer—The peptides were used in several disease mouse models. Tf-D-LP4 crossed the blood-brain barrier in a GBM mouse model to inhibit tumor growth by decreasing the energy metabolism while inducing apoptosis and also upregulating pro apoptotic proteins [200]. Similar effects were seen in lung and breast cancer [354]. Thus, the peptide has the potential to serve as the basis for new anti-cancer therapies.

Tf-D-LP4 in treating steatosis and NASH—the peptide was also found to be effective in treating non-alcoholic fatty liver disease (NAFLD), as induced by treating mice with streptozotocin (STZ) and a high-fat diet (STZ/HFD-32). R-Tf-D-LP4 treatment eliminated inflammation, liver fibrosis, and normalized the liver enzymes [88]. In addition, the peptide increased the expression of proteins associated with fatty acid transport to the mitochondria, and enhanced β -oxidation and thermogenic processes, while decreasing the expression of enzymes and regulators of fatty acid synthesis [88]. The VDAC1-based peptide, thus, offers a promising therapeutic approach for steatosis and NASH.

The bold letters indicate the cell-penetrating peptide sequence (Antp, Tf), the italic letters indicate amino acids involved in the tryptophan zipper (hairpin formation), and the underlined sequences represent amino acids in D conformation.

Tf-D-LP4 in treating type 2 diabetes (T2D)—STZ/HFD-32 mice also displayed symptoms of a T2D-like disease. R-Tf-D-LP4 peptide treatment restored the elevated blood glucose to close to normal levels, and increased the number and average size of islets and their insulin content, as compared to untreated controls [82]. Moreover, peptide treatment of STZ/HFD-32 fed mice increased the expression of β -cell maturation and differentiation, PDX1 transcription factor, which enhanced the expression of the insulin-encoding gene, and is essential for islet development, function, proliferation, and maintenance of glucose homeostasis in the pancreas. These results suggest that the VDAC1-based R-Tf-D-LP4 peptide has potential as a treatment for diabetes.

VDAC1-N-terminal-Antp peptide in treating cancer—The VDAC1 N-terminal domain (26 amino acids) is required for interaction with VDAC1-associated proteins and apoptosis [33,39]. A number of VDAC1 N-terminal peptides fused to Antp (Penetrating), a 16-residue-long sequence from the *Drosophila antennapedia* homeodomain were prepared (Table 4). One of these, the D- Δ (1-14)N-Ter-Antp peptide, composed of the VDAC1 N-terminal region (15–26 amino acids), and Antp was shown to induce apoptosis in a variety of cancer cell lines [354].

Table 4. Amino acid sequences and analytical data for the VDAC1-based peptides.

Peptide	Sequence	No. of AA	Molecular Mass, Da
Tf-D-LP4	HAIYPRHSWTWE-199-KKLETAVNLA WTA GNSN-216-KWTWK	34	4111
R-Tf-D-LP4	KWTWK-216-NSNGATWALNVATELKK-199-EWTWSHRPYIAH	34	4111
N-Ter	1-MAVPPTYADLGKSARDVFTKGYGFGL-26-	26	2762
N-Ter-Antp	1-MAVPPTYADLGKSARDVFTKGYGFGL-26-RQIKIWFQNR RMK WKK	42	4990
D- Δ (1-14)N-Ter-Antp	15-RDVFTKGYGFGL-26-RQIKIWFQNR RMK WKK	28	3588
Δ N-Ter Δ (21-26)-Antp	1-MAVPPTYADLGKSARDVFTK-20-RQIKIWFQNR RMK WKK	36	4396
Δ (1-4)N-Ter Δ (21-26)-Antp	5-PTYADLGKSARDVFTK-20-RQIKIWFQNR RMK WKK	32	3997
Δ (1-9)N-Ter Δ (21-26)-Antp	10-LGKSARDVFTK-20-RQIKIWFQNR RMK WKK	27	3450

VDAC1-N-terminal peptide (N-Ter)—the peptide without the cell penetrating sequence ANTP directly interacted with A β , and prevented A β cellular entry and A β -induced mitochondria-mediated apoptosis [31].

VDAC1 N-terminal peptides prevent mutant SOD1 toxicity—A VDAC1-derived N-terminal peptide version that did not induce cell death, inhibited mutant SOD1-induced toxicity. The peptide enhanced survival of motor neuron-like NSC-34 cells expressing mutant SOD1 [255]. VDAC1 N-terminal peptides targeting mutant SOD1 may represent potential new therapeutic strategies for ALS.

VDAC1-interacting small molecules, VBIT-4 and VBIT-12, treating diseases with overexpressed VDAC1—our newly developed small molecules, VBIT-4 and VBIT-12, were used to prevent mitochondria dysfunction and apoptosis in conditions thought to be caused by VDAC1 over expression

and oligomerization [53]. The effect of VBIT-4 was validated in T2D [84] in lupus models [87] and on fibrosis induced by hyperaldosteronism in the heart [90], and the efficacy of VBIT-12 in DSS-induced colitis (unpublished data).

VDAC inhibitor DIDS inhibits the effects of IBDV [53]—as described in Section 7.5, DIDS decreased the expression of VP5 and apoptosis [274] induced by IBDV, causing immunosuppressive disease in young chickens and up-regulated VDAC1 expression in cells.

In addition, although not a specific inhibitor of VDAC1 oligomerization, DIDS could protect rats from the secondary response to spinal cord injury [54]. In this model, DIDS reduced oligodendrocyte cell death, and improved axonal density, to promote motor function recovery.

10. Conclusions

Mitochondria represent the energy hub of the cell, and their dysfunction plays a critical role in tumorigenesis and a broad range of other pathologies including AD, CVDs, T2D, and a wide variety of autoimmune diseases, which are characterized by over-expression of the VDAC1 protein. The ability of VDAC1 to control transport through the mitochondrial membrane gives the protein the ideal opportunity to serve as a gatekeeper, orchestrate the traffic of metabolites, and regulate apoptosis, and other cell stress-associated processes. The strategic location in the OMM also makes VDAC1 well positioned to interact with over 100 proteins, allowing it to mediate and regulate the integration of mitochondrial and cellular functions, significantly by modulating Ca^{2+} homeostasis. One of the most important protein interactions is with itself since the dynamic oligomerization of VDAC1 is seen to be a pivotal regulation point in apoptosis regulation and the decision of cell fate. These, together with its overexpression in cancer and other diseases, including Alzheimer's disease, some cardiovascular diseases and type 2 diabetes, suggest that VDAC1 overexpression is associated with cell response to stress conditions. As treatments that affect the degree of expression and/or oligomer formation of VDAC1 have been efficacious in a wide variety of models, targeting VDAC1 has vast therapeutic potential to modulate the biology of cancer and other diseases.

Author Contributions: A.S.-K. and A.V. performed the experiments and data analysis. V.S.-B. wrote the manuscript. All authors have read and agreed to the published version of the manuscript.

Funding: This research was supported by grants from the Israel Science Foundation (974/19).

Conflicts of Interest: The authors declare no conflict of interest

Abbreviations

AIF, apoptosis-inducing factor; ANT, adenine nucleotide translocase; Bcl-2, B-cell lymphoma 2; caspase, cysteinyl/aspartate-specific protease; Cyto *c*, Cytochrome *c*; DIDS, 4,4'-diisothiocyanostilbene-2,2'-disulfonic acid; ER, endoplasmic reticulum; G-6-P, glucose-6-phosphate; HK, hexokinase; IMM, inner mitochondrial membrane; mtDNA, mitochondrial DNA, OMM, outer mitochondrial membrane; RNAi, interference RNA; ROS, reactive oxygen species; RuR, ruthenium red; SR, sarcoplasmic reticulum; TSPO, translocator protein; VDAC, voltage-dependent anion channel.

References

1. Zeth, K.; Zachariae, U. Ten Years of High Resolution Structural Research on the Voltage Dependent Anion Channel (VDAC)—Recent Developments and Future Directions. *Front. Physiol.* **2018**, *9*, 108. [CrossRef] [PubMed]
2. Shoshan-Barmatz, V.; Maldonado, E.N.; Krelin, Y. VDAC1 at the crossroads of cell metabolism, apoptosis and cell stress. *Cell Stress* **2017**, *1*, 11–36. [CrossRef] [PubMed]
3. Shoshan-Barmatz, V.; De, S.; Meir, A. The Mitochondrial Voltage-Dependent Anion Channel 1, Ca^{2+} Transport, Apoptosis, and Their Regulation. *Front. Oncol.* **2017**, *7*, 60. [CrossRef] [PubMed]
4. Shoshan-Barmatz, V.; Krelin, Y.; Shteinifer-Kuzmine, A. VDAC1 functions in Ca^{2+} homeostasis and cell life and death in health and disease. *Cell Calcium.* **2018**, *69*, 81–100. [CrossRef]
5. Shoshan-Barmatz, V.; Krelin, Y.; Chen, Q. VDAC1 as a Player in Mitochondria-Mediated Apoptosis and Target for Modulating Apoptosis. *Curr. Med. Chem.* **2017**, *24*, 4435–4446. [CrossRef] [PubMed]

6. Camara, A.K.S.; Zhou, Y.; Wen, P.C.; Tajkhorshid, E.; Kwok, W.M. Mitochondrial VDAC1: A Key Gatekeeper as Potential Therapeutic Target. *Front. Physiol.* **2017**, *8*, 460. [CrossRef]
7. Fang, D.; Maldonado, E.N. VDAC Regulation: A Mitochondrial Target to Stop Cell Proliferation. *Adv. Cancer Res.* **2018**, *138*, 41–69. [CrossRef] [PubMed]
8. Karachitos, A.; Jordan, J.; Kmita, H. VDAC-Targeted Drugs Affecting Cytoprotection and Mitochondrial Physiology in Cerebrovascular and Cardiovascular Diseases. *Curr. Med. Chem.* **2017**, *24*, 4419–4434. [CrossRef]
9. Mazure, N.M. VDAC in cancer. *Biochim. Biophys. Acta Bioenerg.* **2017**, *1858*, 665–673. [CrossRef]
10. Reina, S.; De Pinto, V. Anti-Cancer Compounds Targeted to VDAC: Potential and Perspectives. *Curr. Med. Chem.* **2017**, *24*, 4447–4469. [CrossRef]
11. Shoshan-Barmatz, V.; Krelm, Y.; Shteinfein-Kuzmine, A.; Arif, T. Voltage-Dependent Anion Channel 1 as an Emerging Drug Target for Novel Anti-Cancer Therapeutics. *Front. Oncol.* **2017**, *7*, 154. [CrossRef] [PubMed]
12. Wallace, D.C. A mitochondrial paradigm of metabolic and degenerative diseases, aging, and cancer: A dawn for evolutionary medicine. *Annu. Rev. Genet.* **2005**, *39*, 359–407. [CrossRef]
13. McBride, H.M.; Neuspiel, M.; Wasiak, S. Mitochondria: More than just a powerhouse. *Curr. Biol.* **2006**, *16*, R551–R560. [CrossRef] [PubMed]
14. Shoshan-Barmatz, V.; Ben-Hail, D.; Admoni, L.; Krelm, Y.; Tripathi, S.S. The mitochondrial voltage-dependent anion channel 1 in tumor cells. *Biochim. Biophys. Acta* **2015**, *1848 Pt B*, 2547–2575. [CrossRef]
15. Shoshan-Barmatz, V.; De Pinto, V.; Zweckstetter, M.; Raviv, Z.; Keinan, N.; Arbel, N. VDAC, a multi-functional mitochondrial protein regulating cell life and death. *Mol. Asp. Med.* **2010**, *31*, 227–285. [CrossRef]
16. De Pinto, V.; Guarino, F.; Guarnera, A.A.; Messina, S.; Reina, F.M.; Palermo, T.V.; Mazzoni, C. Characterization of human VDAC isoforms: A peculiar function for VDAC3? *Biochim. Biophys. Acta* **2010**, *1797*, 1268–1275. [CrossRef]
17. Messina, A.; Reina, S.; Guarino, F.; De Pinto, V. VDAC isoforms in mammals. *Biochim. Biophys. Acta* **2012**, *1818*, 1466–1476. [CrossRef] [PubMed]
18. Raghavan, A.; Sheiko, T.; Graham, B.H.; Craigen, W.J. Voltage-dependant anion channels: Novel insights into isoform function through genetic models. *Biochim. Biophys. Acta* **2012**, *1818*, 1477–1485. [CrossRef] [PubMed]
19. Bayrhuber, M.; Meins, T.; Habeck, M.; Becker, S.; Giller, K.; Villinger, S.; Vonrhein, C.; Griesinger, C.; Zweckstetter, M.; Zeth, K. Structure of the human voltage-dependent anion channel. *Proc. Natl. Acad. Sci. USA* **2008**, *105*, 15370–15375. [CrossRef] [PubMed]
20. Hiller, S.; Garces, R.G.; Malia, T.J.; Orekhov, V.Y.; Colombini, M.; Wagner, G. Solution structure of the integral human membrane protein VDAC-1 in detergent micelles. *Science* **2008**, *321*, 1206–1210. [CrossRef]
21. Ujwal, R.; Cascio, D.; Colletier, J.P.; Faham, S.; Zhang, J.; Toro, L.; Ping, P.; Abramson, J. The crystal structure of mouse VDAC1 at 2.3 Å resolution reveals mechanistic insights into metabolite gating. *Proc. Natl. Acad. Sci. USA* **2008**, *105*, 17742–17747. [CrossRef] [PubMed]
22. Hiller, S.; Wagner, G. The role of solution NMR in the structure determinations of VDAC-1 and other membrane proteins. *Curr. Opin. Struct. Biol.* **2009**, *19*, 396–401. [CrossRef]
23. Geula, S.; Ben-Hail, D.; Shoshan-Barmatz, V. Structure-based analysis of VDAC1: N-terminus location, translocation, channel gating and association with anti-apoptotic proteins. *Biochem. J.* **2012**, *444*, 475–485. [CrossRef] [PubMed]
24. Abu-Hamad, S.; Zaid, H.; Israelson, A.; Nahon, E.; Shoshan-Barmatz, V. Hexokinase-I protection against apoptotic cell death is mediated via interaction with the voltage-dependent anion channel-1: Mapping the site of binding. *J. Biol. Chem.* **2008**, *283*, 13482–13490. [CrossRef] [PubMed]
25. Neumann, D.; Buckers, J.; Kastrup, L.; Hell, S.W.; Jakobs, S. Two-color STED microscopy reveals different degrees of colocalization between hexokinase-I and the three human VDAC isoforms. *PMC Biophys.* **2010**, *3*, 4. [CrossRef]
26. Azoulay-Zohar, H.; Israelson, A.; Abu-Hamad, S.; Shoshan-Barmatz, V. In self-defence: Hexokinase promotes voltage-dependent anion channel closure and prevents mitochondria-mediated apoptotic cell death. *Biochem. J.* **2004**, *377 Pt 2*, 347–355. [CrossRef]
27. Arbel, N.; Ben-Hail, D.; Shoshan-Barmatz, V. Mediation of the antiapoptotic activity of Bcl-xL protein upon interaction with VDAC1 protein. *J. Biol. Chem.* **2012**, *287*, 23152–23161. [CrossRef]
28. Shoshan-Barmatz, V.; Arbel, N.; Arzoine, L. VDAC, the voltage-dependent anion channel: Function, regulation & mitochondrial signaling in cell life and death. *Cell Sci.* **2008**, *4*, 74–118.

29. Zaid, H.; Abu-Hamad, S.; Israelson, A.; Nathan, I.; Shoshan-Barmatz, V. The voltage-dependent anion channel-1 modulates apoptotic cell death. *Cell Death Differ.* **2005**, *12*, 751–760. [CrossRef]
30. Shoshan-Barmatz, V.; Mizrachi, D. VDAC1: From structure to cancer therapy. *Front. Oncol.* **2012**, *2*, 164. [CrossRef]
31. Smilansky, A.; Dangoor, L.; Nakdimon, I.; Ben-Hail, D.; Mizrachi, D.; Shoshan-Barmatz, V. The Voltage-dependent Anion Channel 1 Mediates Amyloid beta Toxicity and Represents a Potential Target for Alzheimer Disease Therapy. *J. Biol. Chem.* **2015**, *290*, 30670–30683. [CrossRef]
32. Thinnies, F.P. Apoptogenic interactions of plasmalemmal type-1 VDAC and Aβ peptides via GxxxG motifs induce Alzheimer’s disease—A basic model of apoptosis? *Wien. Med. Wochenschr.* **2011**, *161*, 274–276. [CrossRef]
33. Abu-Hamad, S.; Arbel, N.; Calo, D.; Arzoine, L.; Israelson, A.; Keinan, N.; Ben-Romano, R.; Friedman, O.; Shoshan-Barmatz, V. The VDAC1 N-terminus is essential both for apoptosis and the protective effect of anti-apoptotic proteins. *J. Cell Sci.* **2009**, *122 Pt 11*, 1906–1916. [CrossRef]
34. Arbel, N.; Shoshan-Barmatz, V. Voltage-dependent anion channel 1-based peptides interact with Bcl-2 to prevent antiapoptotic activity. *J. Biol. Chem.* **2010**, *285*, 6053–6062. [CrossRef]
35. Malia, T.J.; Wagner, G. NMR structural investigation of the mitochondrial outer membrane protein VDAC and its interaction with antiapoptotic Bcl-xL. *Biochemistry* **2007**, *46*, 514–525. [CrossRef]
36. Shimizu, S.; Ide, T.; Yanagida, T.; Tsujimoto, Y. Electrophysiological study of a novel large pore formed by Bax and the voltage-dependent anion channel that is permeable to cytochrome c. *J. Biol. Chem.* **2000**, *275*, 12321–12325. [CrossRef] [PubMed]
37. Shimizu, S.; Narita, M.; Tsujimoto, Y. Bcl-2 family proteins regulate the release of apoptogenic cytochrome c by the mitochondrial channel VDAC. *Nature* **1999**, *399*, 483–487. [CrossRef]
38. Shi, Y.; Chen, J.; Weng, C.; Chen, R.; Zheng, Y.; Chen, Q.; Tang, H. Identification of the protein-protein contact site and interaction mode of human VDAC1 with Bcl-2 family proteins. *Biochem. Biophys. Res. Commun.* **2003**, *305*, 989–996. [CrossRef]
39. Arzoine, L.; Zilberberg, N.; Ben-Romano, R.; Shoshan-Barmatz, V. Voltage-dependent anion channel 1-based peptides interact with hexokinase to prevent its anti-apoptotic activity. *J. Biol. Chem.* **2009**, *284*, 3946–3955. [CrossRef] [PubMed]
40. Keinan, N.; Tyomkin, D.; Shoshan-Barmatz, V. Oligomerization of the mitochondrial protein voltage-dependent anion channel is coupled to the induction of apoptosis. *Mol. Cell Biol.* **2010**, *30*, 5698–5709. [CrossRef] [PubMed]
41. Shoshan-Barmatz, V.; Israelson, A.; Brdiczka, D.; Sheu, S.S. The voltage-dependent anion channel (VDAC): Function in intracellular signalling, cell life and cell death. *Curr. Pharm. Des.* **2006**, *12*, 2249–2270. [CrossRef] [PubMed]
42. Shoshan-Barmatz, V.; Mizrachi, D.; Keinan, N. Oligomerization of the mitochondrial protein VDAC1: From structure to function and cancer therapy. *Prog. Mol. Biol. Transl. Sci.* **2013**, *117*, 303–334. [CrossRef] [PubMed]
43. Shoshan-Barmatz, V.; Golan, M. Mitochondrial VDAC1: Function in cell life and death and a target for cancer therapy. *Curr. Med. Chem.* **2012**, *19*, 714–735. [CrossRef] [PubMed]
44. Shoshan-Barmatz, V.; Keinan, N.; Zaid, H. Uncovering the role of VDAC in the regulation of cell life and death. *J. Bioenerg. Biomembr.* **2008**, *40*, 183–191. [CrossRef]
45. Zeth, K.; Meins, T.; Vonrhein, C. Approaching the structure of human VDAC1, a key molecule in mitochondrial cross-talk. *J. Bioenerg. Biomembr.* **2008**, *40*, 127–132. [CrossRef]
46. Schlattner, U.; Tokarska-Schlattner, M.; Wallimann, T. Mitochondrial creatine kinase in human health and disease. *Biochim. Biophys. Acta* **2006**, *1762*, 164–180. [CrossRef]
47. Zalk, R.; Israelson, A.; Garty, E.S.; Azoulay-Zohar, H.; Shoshan-Barmatz, V. Oligomeric states of the voltage-dependent anion channel and cytochrome c release from mitochondria. *Biochem. J.* **2005**, *386 Pt 1*, 73–83. [CrossRef]
48. Geula, S.; Naveed, H.; Liang, J.; Shoshan-Barmatz, V. Structure-based analysis of VDAC1 protein: Defining oligomer contact sites. *J. Biol. Chem.* **2012**, *287*, 2179–2190. [CrossRef]
49. Ujwal, R.; Cascio, D.; Chaptal, V.; Ping, P.; Abramson, J. Crystal packing analysis of murine VDAC1 crystals in a lipidic environment reveals novel insights on oligomerization and orientation. *Channels (Austin)* **2009**, *3*, 167–170. [CrossRef]

50. Keinan, N.; Pahima, H.; Ben-Hail, D.; Shoshan-Barmatz, V. The role of calcium in VDAC1 oligomerization and mitochondria-mediated apoptosis. *Biochim. Biophys. Acta* **2013**, *1833*, 1745–1754. [CrossRef]
51. Weisthal, S.; Keinan, N.; Ben-Hail, D.; Arif, T.; Shoshan-Barmatz, V. Ca²⁺-mediated regulation of VDAC1 expression levels is associated with cell death induction. *Biochim. Biophys. Acta* **2014**, *1843*, 2270–2281. [CrossRef] [PubMed]
52. Huang, L.; Han, J.; Ben-Hail, D.; He, L.; Li, B.; Chen, Z.; Wang, Y.; Yang, Y.; Liu, L.; Zhu, Y.; et al. A new fungal diterpene induces VDAC1-dependent apoptosis in Bax/Bak-deficient cells. *J. Biol. Chem.* **2015**, *290*, 23563–23578. [CrossRef] [PubMed]
53. Ben-Hail, D.; Begas-Shvartz, R.; Shalev, M.; Shteinfefer-Kuzmine, A.; Gruzman, A.; Reina, S.; De Pinto, V.; Shoshan-Barmatz, V. Novel Compounds Targeting the Mitochondrial Protein VDAC1 Inhibit Apoptosis and Protect against Mitochondrial Dysfunction. *J. Biol. Chem.* **2016**, *291*, 24986–25003. [CrossRef] [PubMed]
54. Ben-Hail, D.; Shoshan-Barmatz, V. VDAC1-interacting anion transport inhibitors inhibit VDAC1 oligomerization and apoptosis. *Biochim. Biophys. Acta* **2016**, *1863 Pt A*, 1612–1623. [CrossRef]
55. Akanda, N.; Tofighi, R.; Brask, J.; Tamm, C.; Elinder, F.; Ceccatelli, S. Voltage-dependent anion channels (VDAC) in the plasma membrane play a critical role in apoptosis in differentiated hippocampal neurons but not in neural stem cells. *Cell Cycle* **2008**, *7*, 3225–3234. [CrossRef]
56. Bahamonde, M.I.; Valverde, M.A. Voltage-dependent anion channel localises to the plasma membrane and peripheral but not perinuclear mitochondria. *Pflugers Arch.* **2003**, *446*, 309–313. [CrossRef]
57. Bathori, G.; Parolini, I.; Szabo, I.; Tombola, F.; Messina, A.; Oliva, M.; Sargiacomo, M.; De Pinto, V.; Zoratti, M. Extramitochondrial porin: Facts and hypotheses. *J. Bioenerg. Biomembr.* **2000**, *32*, 79–89. [CrossRef]
58. Bathori, G.; Parolini, I.; Tombola, F.; Szabo, I.; Messina, A.; Oliva, M.; De Pinto, V.; Lisanti, M.; Sargiacomo, M.; Zoratti, M. Porin is present in the plasma membrane where it is concentrated in caveolae and caveolae-related domains. *J. Biol. Chem.* **1999**, *274*, 29607–29612. [CrossRef]
59. Bouyer, G.; Cueff, A.; Egee, S.; Kmiecik, J.; Maksimova, Y.; Glogowska, E.; Gallagher, P.G.; Thomas, S.L. Erythrocyte peripheral type benzodiazepine receptor/voltage-dependent anion channels are upregulated by Plasmodium falciparum. *Blood* **2011**, *118*, 2305–2312. [CrossRef]
60. De Pinto, V.; Messina, A.; Lane, D.J.; Lawen, A. Voltage-dependent anion-selective channel (VDAC) in the plasma membrane. *FEBS Lett.* **2010**, *584*, 1793–1799. [CrossRef]
61. Dermietzel, R.; Hwang, T.K.; Buettner, R.; Hofer, A.; Dotzler, E.; Kremer, M.; Deutzmann, R.; Thinner, F.P.; Fishman, G.I.; Spray, D.C.; et al. Cloning and in situ localization of a brain-derived porin that constitutes a large-conductance anion channel in astrocytic plasma membranes. *Proc. Natl. Acad. Sci. USA* **1994**, *91*, 499–503. [CrossRef]
62. Marin, R.; Ramirez, C.M.; Gonzalez, M.; Gonzalez-Munoz, E.; Zorzano, A.; Camps, M.; Alonso, R.; Diaz, M. Voltage-dependent anion channel (VDAC) participates in amyloid beta-induced toxicity and interacts with plasma membrane estrogen receptor alpha in septal and hippocampal neurons. *Mol. Membr. Biol.* **2007**, *24*, 148–160. [CrossRef] [PubMed]
63. Ramirez, C.M.; Gonzalez, M.; D'iaz, M.; Alonso, R.; Marin, R. VDAC and ERalpha interaction in caveolae from human cortex is altered in Alzheimer's disease. *Mol. Cell Neurosci.* **2009**, *42*, 172–183. [CrossRef] [PubMed]
64. Sabirov, R.Z.; Merzlyak, P. Plasmalemmal VDAC controversies and maxi-anion channel puzzle. *Biochim. Biophys. Acta* **2012**, *1818*, 1570–1580. [CrossRef]
65. Thinner, F.P. Neuroendocrine differentiation of LNCaP cells suggests: VDAC in the cell membrane is involved in the extrinsic apoptotic pathway. *Mol. Genet. Metabol.* **2009**, *97*, 241–243. [CrossRef]
66. Shoshan-Barmatz, V.N.; Hadad, F.I.; Shafir, I.; Orr, M.V.; Heilmeyer, L.M. VDAC/porin is present in sarcoplasmic reticulum from skeletal muscle. *FEBS Lett.* **1996**, *386*, 205–210. [CrossRef]
67. Shoshan-Barmatz, V.N.; Zalk, R.; Gincel, D.; Vardi, N. Subcellular localization of VDAC in mitochondria and ER in the cerebellum. *Biochim. Biophys. Acta* **2004**, *1657*, 105–114. [CrossRef] [PubMed]
68. Thinner, F.P. After all, plasmalemmal expression of type-1 VDAC can be understood. Phosphorylation, nitrosylation, and channel modulators work together in vertebrate cell volume regulation and either apoptotic pathway. *Front. Physiol.* **2015**, *6*, 126. [CrossRef] [PubMed]
69. Stadtmuller, U.; Eben-Brunnen, J.; Schmid, A.; Hesse, D.; Klebert, S.; Kratzin, H.D.; Hesse, J.; Zimmermann, B.; Reymann, S.; Thinner, F.P.; et al. Mitochondria-derived and extra-mitochondrial human type-1 porin are

- identical as revealed by amino acid sequencing and electrophysiological characterisation. *Biol. Chem.* **1999**, *380*, 1461–1466. [CrossRef] [PubMed]
70. Okada, S.F.; O’Neal, W.K.; Huang, P.; Nicholas, R.A.; Ostrowski, L.E.; Craigen, W.J.; Lazarowski, E.R.; Boucher, R.C. Voltage-dependent anion channel-1 (VDAC-1) contributes to ATP release and cell volume regulation in murine cells. *J. Gen. Physiol.* **2004**, *124*, 513–526. [CrossRef]
71. Buettner, R.; Papoutsoglou, G.; Scemes, E.; Spray, D.C.; Dermietzel, R. Evidence for secretory pathway localization of a voltage-dependent anion channel isoform. *Proc. Natl. Acad. Sci. USA* **2000**, *97*, 3201–3206. [CrossRef]
72. Thinnies, F.P.; Gotz, H.; Kayser, H.; Benz, R.; Schmidt, W.E.; Kratzin, H.D.; Hilschmann, N. Identification of human porins. I. Purification of a porin from human B-lymphocytes (Porin 31HL) and the topochemical proof of its expression on the plasmalemma of the progenitor cell. *Biol. Chem. Hoppe. Seyler.* **1989**, *370*, 1253–1264. [CrossRef]
73. Gonzalez-Gronow, M.; Kalfa, T.; Johnson, C.E.; Gawdi, G.; Pizzo, S.V. The voltage-dependent anion channel is a receptor for plasminogen kringle 5 on human endothelial cells. *J. Biol. Chem.* **2003**, *278*, 27312–27318. [CrossRef]
74. Li, L.; Yao, Y.C.; Gu, X.Q.; Che, D.; Ma, C.Q.; Dai, Z.Y.; Li, C.; Zhou, T.; Cai, W.B.; Yang, Z.H.; et al. Plasminogen kringle 5 induces endothelial cell apoptosis by triggering a voltage-dependent anion channel 1 (VDAC1) positive feedback loop. *J. Biol. Chem.* **2014**, *289*, 32628–32638. [CrossRef] [PubMed]
75. Manczak, M.; Reddy, P.H. Abnormal interaction of VDAC1 with amyloid beta and phosphorylated tau causes mitochondrial dysfunction in Alzheimer’s disease. *Hum. Mol. Genet.* **2012**, *21*, 5131–5146. [CrossRef] [PubMed]
76. Cuadrado-Tejedor, M.; Vilarino, M.; Cabodevilla, F.; Del Rio, J.; Frechilla, D.; Perez-Mediavilla, A. Enhanced expression of the voltage-dependent anion channel 1 (VDAC1) in Alzheimer’s disease transgenic mice: An insight into the pathogenic effects of amyloid-beta. *J. Alzheimers Dis.* **2011**, *23*, 195–206. [CrossRef]
77. Perez-Gracia, E.; Torreon-Escribano, B.; Ferrer, I. Dystrophic neurites of senile plaques in Alzheimer’s disease are deficient in cytochrome c oxidase. *Acta Neuropathol.* **2008**, *116*, 261–268. [CrossRef]
78. Hur, J.Y.; Teranishi, Y.; Kihara, T.; Yamamoto, N.G.; Inoue, M.; Hosia, W.; Hashimoto, M.; Winblad, B.; Frykman, S.; Tjernberg, L.O. Identification of novel gamma-secretase-associated proteins in detergent-resistant membranes from brain. *J. Biol. Chem.* **2012**, *287*, 11991–12005. [CrossRef] [PubMed]
79. Inoue, M.; Hur, J.Y.; Kihara, T.; Teranishi, Y.; Yamamoto, N.G.; Ishikawa, T.; Wiehager, B.; Winblad, B.; Tjernberg, L.O.; Schedin-Weiss, S. Human brain proteins showing neuron-specific interactions with gamma-secretase. *FEBS J.* **2015**, *282*, 2587–2599. [CrossRef] [PubMed]
80. Ahmed, M.; Muhammed, S.; Kessler, B.; Salehi, A. Mitochondrial proteome analysis reveals altered expression of voltage dependent anion channels in pancreatic beta-cells exposed to high glucose. *Islets* **2010**, *2*, 283–292. [CrossRef] [PubMed]
81. Gong, D.; Chen, X.; Middleditch, M.; Huang, L.; Vazhoor Amarsingh, G.; Reddy, S.; Lu, J.; Zhang, S.; Phillips, R.; Phillips, A.R.J.; et al. Quantitative proteomic profiling identifies new renal targets of copper(II)-selective chelation in the reversal of diabetic nephropathy in rats. *Proteomics* **2009**, *9*, 4309–4320. [CrossRef]
82. Pittala, S.; Levy, I.; De, S.; Kumar Pandey, S.; Melnikov, N.; Shoshan-Barmatz, V. The VDAC1-based R-Tf-D-LP4 Peptide as a Potential Treatment for Diabetes Mellitus. *Cells* **2020**, *9*, 481. [CrossRef]
83. Zhong, Z.; Lemasters, J.J. A Unifying Hypothesis Linking Hepatic Adaptations for Ethanol Metabolism to the Proinflammatory and Profibrotic Events of Alcoholic Liver Disease. *Alcohol. Clin. Exp. Res.* **2018**, *42*, 2072–2089. [CrossRef]
84. Zhang, E.; Al-Amily, I.; Mohammed, S.; Luan, C.; Asplund, O.; Ahmed, M.; Ben-Hail, D.; Ye, Y.; Soni, A.; Groop, L.; et al. Preserving Insulin Secretion in Diabetes by Inhibiting VDAC1 Overexpression and Surface Translocation in β Cells. *Cell Metabol.* **2019**, *29*, 64–77. [CrossRef]
85. Arif, T.; Krelin, Y.; Nakdimon, I.; Benharroch, D.; Paul, A.; Dadon-Klein, D.; Shoshan-Barmatz, V. VDAC1 is a molecular target in glioblastoma, with its depletion leading to reprogrammed metabolism and reversed oncogenic properties. *Neuro Oncol.* **2017**, *19*, 951–964. [CrossRef]
86. Arif, T.; Vasilkovsky, L.; Refaely, K.A.; Shoshan-Barmatz, V. Silencing VDAC1 Expression by siRNA Inhibits Cancer Cell Proliferation and Tumor Growth In Vivo. *Mol. Ther. Nucleic Acids* **2014**, *3*, e159. [CrossRef]

87. Kim, J.R.; Gupta, L.P.; Blanco, S.; Yang, A.; Shteinfer-Kuzmine, W.; Kang, Z.; Zhu, X.; Park, S.-J.; Chung, J.H.; Shoshan-Barmatz, V.; et al. VDAC oligomers form mitochondrial pores to release mtDNA fragments and promote lupus-like disease. *Science* **2019**, *366*, 1531–1536. [CrossRef]
88. Pittala, S.; Krelin, Y.; Kuperman, Y.; Shoshan-Barmatz, V. A Mitochondrial VDAC1-Based Peptide Greatly Suppresses Steatosis and NASH-Associated Pathologies in a Mouse Model. *Mol. Ther.* **2019**, *27*, 1848–1862. [CrossRef] [PubMed]
89. Branco, A.F.; Pereira, S.L.; Moreira, A.C.; Holy, J.; Sardao, V.A.; Oliveira, P.J. Isoproterenol cytotoxicity is dependent on the differentiation state of the cardiomyoblast H9c2 cell line. *Cardiovasc. Toxicol.* **2011**, *11*, 191–203. [CrossRef]
90. Klapper-Goldstein, H.; Verma, A.; Elyagon, S.; Gillis, R.; Murninkas, M.; Pittala, S.; Paul, A.; Shoshan-Barmatz, V. VDAC1 overexpression in the diseased myocardium of humans and rats and the effect of VDAC1-interacting compound on atrial fibrosis induced by hyperaldosteronism. **2020**. under revision.
91. Shoshan-Barmatz, V.; Israelson, A. The voltage-dependent anion channel in endoplasmic/sarcoplasmic reticulum: Characterization, modulation and possible function. *J. Membr. Biol.* **2005**, *204*, 57–66. [CrossRef]
92. Shoshan-Barmatz, V.; Nahon-Crystal, E.; Shteinfer-Kuzmine, A.; Gupta, R. VDAC1, mitochondrial dysfunction, and Alzheimer's disease. *Pharmacol. Res.* **2018**, *131*, 87–101. [CrossRef]
93. Leal Denis, M.F.; Alvarez, H.A.; Lauri, N.; Alvarez, C.L.; Chara, O.; Schwarzbaum, P.J. Dynamic Regulation of Cell Volume and Extracellular ATP of Human Erythrocytes. *PLoS ONE* **2016**, *11*, e0158305. [CrossRef]
94. Sridharan, M.; Bowles, E.A.; Richards, J.P.; Krantic, M.; Davis, K.L.; Dietrich, K.A.; Stephenson, A.H.; Ellsworth, M.L.; Sprague, R.S. Prostacyclin receptor-mediated ATP release from erythrocytes requires the voltage-dependent anion channel. *Am. J. Physiol. Heart Circ. Physiol.* **2012**, *302*, H553–H559. [CrossRef] [PubMed]
95. Marginedas-Freixa, I.; Alvarez, C.L.; Moras, M.; Leal Denis, M.F.; Hattab, C.; Halle, F.; Bihel, F.; Mouro-Chanteloup, I.; Lefevre, S.D.; Le Van Kim, C.; et al. Human erythrocytes release ATP by a novel pathway involving VDAC oligomerization independent of pannexin-1. *Sci. Rep.* **2018**, *8*, 11384. [CrossRef] [PubMed]
96. Shoshan-Barmatz, V.; Ben-Hail, D. VDAC, a multi-functional mitochondrial protein as a pharmacological target. *Mitochondrion* **2012**, *12*, 24–34. [CrossRef] [PubMed]
97. Palmieri, F.; Pierri, C.L. Mitochondrial metabolite transport. *Essays Biochem.* **2010**, *47*, 37–52. [CrossRef]
98. Vander Heiden, M.G.; Chandel, N.S.; Li, X.X.; Schumacker, P.T.; Colombini, M.; Thompson, C.B. Outer mitochondrial membrane permeability can regulate coupled respiration and cell survival. *Proc. Natl. Acad. Sci. USA* **2000**, *97*, 4666–4671. [CrossRef]
99. Abu-Hamad, S.; Sivan, S.; Shoshan-Barmatz, V. The expression level of the voltage-dependent anion channel controls life and death of the cell. *Proc. Natl. Acad. Sci. USA* **2006**, *103*, 5787–5792. [CrossRef]
100. Dolder, M.; Wendt, S.; Wallimann, T. Mitochondrial creatine kinase in contact sites: Interaction with porin and adenine nucleotide translocase, role in permeability transition and sensitivity to oxidative damage. *Biol. Signals Recept.* **2001**, *10*, 93–111. [CrossRef]
101. Gurnev, P.A.; Rostovtseva, T.K.; Bezrukov, S.M. Tubulin-blocked state of VDAC studied by polymer and ATP partitioning. *FEBS Lett.* **2011**, *585*, 2363–2366. [CrossRef]
102. Csordás, G.; Renken, C.; Várnai, P.; Walter, L.; Weaver, D.; Buttle, K.F.; Balla, T.; Mannella, C.A.; Hajnóczky, G. Structural and functional features and significance of the physical linkage between ER and mitochondria. *J. Cell Biol.* **2006**, *174*, 915–921. [CrossRef] [PubMed]
103. Marchi, S.; Patergnani, S.; Pinton, P. The endoplasmic reticulum-mitochondria connection: One touch, multiple functions. *Biochim. Biophys. Acta* **2014**, *1837*, 461–469. [CrossRef]
104. Rone, M.B.; Fan, J.; Papadopoulos, V. Cholesterol transport in steroid biosynthesis: Role of protein-protein interactions and implications in disease states. *Biochim. Biophys. Acta* **2009**, *1791*, 646–658. [CrossRef] [PubMed]
105. Lee, K.; Kerner, J.; Hoppel, C.L. Mitochondrial carnitine palmitoyltransferase 1a (CPT1a) is part of an outer membrane fatty acid transfer complex. *J. Biol. Chem.* **2011**, *286*, 25655–25662. [CrossRef] [PubMed]
106. Paillard, M.; Tubbs, E.; Thiebaut, P.A.; Gomez, L.; Fauconnier, J.; Da Silva, C.C.; Teixeira, G.; Mewton, N.; Belaidi, E.; Durand, A.; et al. Depressing mitochondria-reticulum interactions protects cardiomyocytes from lethal hypoxia-reoxygenation injury. *Circulation* **2013**, *128*, 1555–1565. [CrossRef]

107. Tonazzi, A.; Giangregorio, N.; Console, L.; Indiveri, C. Mitochondrial carnitine/acylcarnitine translocase: Insights in structure/function relationships. Basis for drug therapy and side effects prediction. *Mini Rev. Med. Chem.* **2015**, *15*, 396–405. [CrossRef]
108. Qiu, J.; Tan, Y.-W.; Hagenston, A.M.; Martel, M.-A.; Kneisel, N.; Skehel, P.A.; Wyllie, D.J.A.; Bading, H.; Hardingham, G.E. Mitochondrial calcium uniporter Mcu controls excitotoxicity and is transcriptionally repressed by neuroprotective nuclear calcium signals. *Nat. Commun.* **2013**, *4*, 2034. [CrossRef]
109. Kamata, H.; Honda, S.; Maeda, S.; Chang, L.; Hirata, H.; Karin, M. Reactive oxygen species promote TNF α -induced death and sustained JNK activation by inhibiting MAP kinase phosphatases. *Cell* **2005**, *120*, 649–661. [CrossRef]
110. Son, Y.; Cheong, Y.K.; Kim, N.H.; Chung, H.T.; Kang, D.G.; Pae, H.O. Mitogen-Activated Protein Kinases and Reactive Oxygen Species: How Can ROS Activate MAPK Pathways? *J. Signal. Transduct.* **2011**, *2011*, 792639. [CrossRef]
111. Ahmad, A.; Ahmad, S.; Schneider, B.K.; Allen, C.B.; Chang, L.Y.; White, C.W. Elevated expression of hexokinase II protects human lung epithelial-like A549 cells against oxidative injury. *Am. J. Physiol. Lung. Cell Mol. Physiol.* **2002**, *283*, L573–L584. [CrossRef] [PubMed]
112. Da-Silva, W.S.; Gomez-Puyou, A.; de Gomez-Puyou, M.T.; Moreno-Sanchez, R.; De Felice, F.G.; de Meis, L.; Oliveira, M.F.; Galina, A. Mitochondrial bound hexokinase activity as a preventive antioxidant defense: Steady-state ADP formation as a regulatory mechanism of membrane potential and reactive oxygen species generation in mitochondria. *J. Biol. Chem.* **2004**, *279*, 39846–39855. [CrossRef] [PubMed]
113. Sun, L.; Shukair, S.; Naik, T.J.; Moazed, F.; Ardehali, H. Glucose phosphorylation and mitochondrial binding are required for the protective effects of hexokinases I and II. *Mol. Cell Biol.* **2008**, *28*, 1007–1017. [CrossRef]
114. Bryson, J.M.; Coy, P.E.; Gottlob, K.; Hay, N.; Robey, R.B. Increased hexokinase activity, of either ectopic or endogenous origin, protects renal epithelial cells against acute oxidant-induced cell death. *J. Biol. Chem.* **2002**, *277*, 11392–11400. [CrossRef]
115. Brahimi-Horn, M.C.; Lacas-Gervais, S.; Adaixo, R.; Ilc, K.; Rouleau, M.; Notte, A.; Dieu, M.; Michiels, C.; Voeltzel, T.; Maguer-Satta, V.; et al. Local mitochondrial-endolysosomal microfusion cleaves voltage-dependent anion channel 1 to promote survival in hypoxia. *Mol. Cell Biol.* **2015**, *35*, 1491–1505. [CrossRef] [PubMed]
116. Mazure, N.M. News about VDAC1 in Hypoxia. *Front. Oncol.* **2016**, *6*, 193. [CrossRef] [PubMed]
117. Brahimi-Horn, M.C.; Ben-Hail, D.; Ilie, M.; Gounon, P.; Rouleau, M.; Hofman, V.; Doyen, J.; Mari, B.; Shoshan-Barmatz, V.; Hofman, P.; et al. Expression of a truncated active form of VDAC1 in lung cancer associates with hypoxic cell survival and correlates with progression to chemotherapy resistance. *Cancer Res.* **2012**, *72*, 2140–2150. [CrossRef]
118. Aram, L.; Geula, S.; Arbel, N.; Shoshan-Barmatz, V. VDAC1 cysteine residues: Topology and function in channel activity and apoptosis. *Biochem. J.* **2010**, *427*, 445–454. [CrossRef]
119. Colombini, M. VDAC structure, selectivity, and dynamics. *Biochim. Biophys. Acta* **2012**, *1818*, 1457–1465. [CrossRef]
120. Gincel, D.; Shoshan-Barmatz, V. Glutamate interacts with VDAC and modulates opening of the mitochondrial permeability transition pore. *J. Bioenerg. Biomembr.* **2004**, *36*, 179–186. [CrossRef]
121. Rostovtseva, T.K.; Komarov, A.; Bezrukov, S.M.; Colombini, M. VDAC channels differentiate between natural metabolites and synthetic molecules. *J. Membr. Biol.* **2002**, *187*, 147–156. [CrossRef]
122. Yehezkel, G.; Hadad, N.; Zaid, H.; Sivan, S.; Shoshan-Barmatz, V. Nucleotide-binding sites in the voltage-dependent anion channel: Characterization and localization. *J. Biol. Chem.* **2006**, *281*, 5938–5946. [CrossRef]
123. Shoshan-Barmatz, V.; Gincel, D. The voltage-dependent anion channel: Characterization, modulation, and role in mitochondrial function in cell life and death. *Cell Biochem. Biophys.* **2003**, *39*, 279–292. [CrossRef]
124. Villinger, S.; Giller, K.; Bayrhuber, M.; Lange, A.; Griesinger, C.; Becker, S.; Zweckstetter, M. Nucleotide interactions of the human voltage-dependent anion channel. *J. Biol. Chem.* **2014**, *289*, 13397–13406. [CrossRef] [PubMed]
125. Choudhary, O.P.; Paz, A.; Adelman, J.L.; Colletier, J.P.; Abramson, J.; Grabe, M. Structure-guided simulations illuminate the mechanism of ATP transport through VDAC1. *Nat. Struct. Mol. Biol.* **2014**, *21*, 626–632. [CrossRef] [PubMed]

126. Bathori, G.; Csordas, G.; Garcia-Perez, C.; Davies, E.; Hajnoczky, G. Ca^{2+} -dependent control of the permeability properties of the mitochondrial outer membrane and voltage-dependent anion-selective channel (VDAC). *J. Biol. Chem.* **2006**, *281*, 17347–17358. [CrossRef] [PubMed]
127. Gincel, D.; Zaid, H.; Shoshan-Barmatz, V. Calcium binding and translocation by the voltage-dependent anion channel: A possible regulatory mechanism in mitochondrial function. *Biochem. J.* **2001**, *358 Pt 1*, 147–155. [CrossRef]
128. Israelson, A.; Abu-Hamad, S.; Zaid, H.; Nahon, E.; Shoshan-Barmatz, V. Localization of the voltage-dependent anion channel-1 Ca^{2+} -binding sites. *Cell Calcium.* **2007**, *41*, 235–544. [CrossRef]
129. Gincel, D.; Vardi, N.; Shoshan-Barmatz, V. Retinal voltage-dependent anion channel: Characterization and cellular localization. *Investig. Ophthalmol. Vis. Sci.* **2002**, *43*, 2097–2104.
130. Israelson, A.; Arzoine, L.; Abu-hamad, S.; Khodorkovsky, V.; Shoshan-Barmatz, V. A photoactivable probe for calcium binding proteins. *Chem. Biol.* **2005**, *12*, 1169–1178. [CrossRef]
131. Pittala, M.G.G.; Saletti, R.; Reina, S.; Cunsolo, V.; De Pinto, V.; Foti, S. A High Resolution Mass Spectrometry Study Reveals the Potential of Disulfide Formation in Human Mitochondrial Voltage-Dependent Anion Selective Channel Isoforms (hVDACs). *Int. J. Mol. Sci.* **2020**, *21*, 1468. [CrossRef]
132. Baines, C.P.; Song, C.X.; Zheng, Y.T.; Wang, G.W.; Wang, Z.O.; Guo, Y.; Bolli, R.; Cardwell, E.M. Protein kinase Cepsilon interacts with and inhibits the permeability transition pore in cardiac mitochondria. *Circ. Res.* **2003**, *92*, 873–880. [CrossRef] [PubMed]
133. Bera, A.K.; Ghosh, S.; Das, S. Mitochondrial VDAC can be phosphorylated by cyclic AMP-dependent protein kinase. *Biochem. Biophys. Res. Commun.* **1995**, *209*, 213–217. [CrossRef]
134. Liberatori, S.; Canas, B.; Tani, C.; Bini, L.; Buonocore, G.; Godovac-Zimmermann, J.; Mishra, O.P.; Delivoria-Papadopoulos, M.; Bracci, R.; Pallini, V. Proteomic approach to the identification of voltage-dependent anion channel protein isoforms in guinea pig brain synaptosomes. *Proteomics* **2004**, *4*, 1335–1340. [CrossRef] [PubMed]
135. Kerner, J.; Lee, K.; Tandler, B.; Hoppel, C.L. VDAC proteomics: Post-translation modifications. *Biochim. Biophys. Acta* **2012**, *1818*, 1520–1525. [CrossRef]
136. Aulak, K.S.; Koeck, T.; Crabb, J.W.; Stuehr, D.J. Dynamics of protein nitration in cells and mitochondria. *Am. J. Physiol. Heart Circul. Physiol.* **2004**, *286*, H30–H38. [CrossRef] [PubMed]
137. Kanski, J.; Behring, A.; Pelling, J.; Schoneich, C. Proteomic identification of 3-nitrotyrosine-containing rat cardiac proteins. *Effects Biol. Aging* **2005**, *288*, H371–H381. [CrossRef]
138. Turko, I.V.; Li, L.; Aulak, K.S.; Stuehr, D.J.; Chang, J.Y.; Murad, F. Protein tyrosine nitration in the mitochondria from diabetic mouse heart. Implications to dysfunctional mitochondria in diabetes. *J. Biol. Chem.* **2003**, *278*, 33972–33977. [CrossRef]
139. Mello, C.F.; Sultana, R.; Piroddi, M.; Cai, J.; Pierce, W.M.; Klein, J.B.; Butterfield, D.A. Acrolein induces selective protein carbonylation in synaptosomes. *Neuroscience* **2007**, *147*, 674–967. [CrossRef]
140. Kroemer, G.; Galluzzi, L.; Brenner, C. Mitochondrial membrane permeabilization in cell death. *Physiol. Rev.* **2007**, *87*, 99–163. [CrossRef]
141. Antignani, A.; Youle, R.J. How do Bax and Bak lead to permeabilization of the outer mitochondrial membrane? *Curr. Opin. Cell Biol.* **2006**, *18*, 685–689. [CrossRef]
142. Lovell, J.F.; Billen, L.P.; Bindner, S.; Shamas-Din, A.; Fradin, C.; Leber, B.; Andrews, D.W. Membrane binding by tBid initiates an ordered series of events culminating in membrane permeabilization by Bax. *Cell* **2008**, *135*, 1074–1084. [CrossRef]
143. Banerjee, J.; Ghosh, S. Bax increases the pore size of rat brain mitochondrial voltage-dependent anion channel in the presence of tBid. *Biochem. Biophys. Res. Commun.* **2004**, *323*, 310–314. [CrossRef] [PubMed]
144. Shimizu, S.; Tsujimoto, Y. Proapoptotic BH3-only Bcl-2 family members induce cytochrome c release, but not mitochondrial membrane potential loss, and do not directly modulate voltage-dependent anion channel activity. *Proc. Natl. Acad. Sci. USA* **2000**, *97*, 577–582. [CrossRef] [PubMed]
145. Madesh, M.; Hajnoczky, G. VDAC-dependent permeabilization of the outer mitochondrial membrane by superoxide induces rapid and massive cytochrome c release. *J. Cell Biol.* **2001**, *155*, 1003–1015. [CrossRef]
146. Ghosh, T.; Pandey, N.; Maitra, A.; Brahmachari, S.K.; Pillai, B. A role for voltage-dependent anion channel Vdac1 in polyglutamine-mediated neuronal cell death. *PLoS ONE* **2007**, *2*, e1170. [CrossRef]
147. Godbole, A.; Varghese, J.; Sarin, A.; Mathew, M.K. VDAC is a conserved element of death pathways in plant and animal systems. *Biochim. Biophys. Acta* **2003**, *1642*, 87–96. [CrossRef]

148. Lu, A.J.; Dong, C.W.; Du, C.S.; Zhang, Q.Y. Characterization and expression analysis of *Paralichthys olivaceus* voltage-dependent anion channel (VDAC) gene in response to virus infection. *Fish. Shellfish Immunol.* **2007**, *23*, 601–613. [CrossRef] [PubMed]
149. Israelson, A.; Zaid, H.; Abu-Hamad, S.; Nahon, E.; Shoshan-Barmatz, V. Mapping the ruthenium red-binding site of the voltage-dependent anion channel-1. *Cell Calcium.* **2008**, *43*, 196–204. [CrossRef] [PubMed]
150. Tajeddine, N.; Galluzzi, L.; Kepp, O.; Hangen, E.; Morselli, E.; Senovilla, L.; Araujo, N.; Pinna, G.; Larochette, N.; Zamzami, N.; et al. Hierarchical involvement of Bak, VDAC1 and Bax in cisplatin-induced cell death. *Oncogene* **2008**, *27*, 4221–4232. [CrossRef] [PubMed]
151. Yuan, S.; Fu, Y.; Wang, X.; Shi, H.; Huang, Y.; Song, X.; Li, L.; Song, N.; Luo, Y. Voltage-dependent anion channel 1 is involved in endostatin-induced endothelial cell apoptosis. *FASEB J.* **2008**, *22*, 2809–2820. [CrossRef] [PubMed]
152. Tomasello, F.; Messina, A.; Lartigue, L.; Schembri, L.; Medina, C.; Reina, S.; Thoraval, D.; Crouzet, M.; Ichas, F.; De Pinto, V.; et al. Outer membrane VDAC1 controls permeability transition of the inner mitochondrial membrane in cellulo during stress-induced apoptosis. *Cell Res.* **2009**, *19*, 1363–1376. [CrossRef] [PubMed]
153. Betaneli, V.; Petrov, E.P.; Schwillle, P. The role of lipids in VDAC oligomerization. *Biophys. J.* **2012**, *102*, 523–531. [CrossRef] [PubMed]
154. Vaseva, A.V.; Marchenko, N.D.; Ji, K.; Tsirka, S.E.; Holzmann, S.; Moll, U.M. P53 opens the mitochondrial permeability transition pore to trigger necrosis. *Cell* **2012**, *149*, 1536–1548. [CrossRef]
155. Obulesu, M.; Lakshmi, M.J. Apoptosis in Alzheimer’s disease: An understanding of the physiology, pathology and therapeutic avenues. *Neurochem. Res.* **2014**, *39*, 2301–2312. [CrossRef]
156. Sureda, F.X.; Junyent, F.; Verdaguer, E.; Auladell, C.; Pelegri, C.; Vilaplana, J.; Folch, J.; Canudas, A.M.; Zarate, C.B.; Palles, M.; et al. Antiapoptotic drugs: A therapeutic strategy for the prevention of neurodegenerative diseases. *Curr. Pharm. Des.* **2011**, *17*, 230–245. [CrossRef]
157. Kostin, S.; Pool, L.; Elsasser, A.; Hein, S.; Drexler, H.C.; Arnon, E.; Hayakawa, Y.; Zimmermann, R.; Bauer, E.; Klovekorn, W.P.; et al. Myocytes die by multiple mechanisms in failing human hearts. *Circ. Res.* **2003**, *92*, 715–724. [CrossRef]
158. Kroemer, G.; El-Deiry, W.S.; Golstein, P.; Peter, M.E.; Vaux, D.; Vandenabeele, P.; Zhivotovsky, B.; Blagosklonny, M.V.; Malorni, W.; Knight, R.A.; et al. Classification of cell death: Recommendations of the Nomenclature Committee on Cell Death. *Cell Death Differ.* **2005**, *12* (Suppl. S2), 1463–1467. [CrossRef]
159. Marunouchi, T.; Tanonaka, K. Cell Death in the Cardiac Myocyte. *Biol. Pharm. Bull.* **2015**, *38*, 1094–1097. [CrossRef]
160. Sharma, P.; Sampath, H. Mitochondrial DNA Integrity: Role in Health and Disease. *Cells* **2019**, *8*, 100. [CrossRef]
161. Nicholls, T.J.; Minczuk, M. In D-loop: 40 years of mitochondrial 7S DNA. *Exp. Gerontol.* **2014**, *56*, 175–181. [CrossRef] [PubMed]
162. West, A.P.; Khoury-Hanold, W.; Staron, M.; Tal, M.C.; Pineda, C.M.; Lang, S.M.; Bestwick, M.; Duguay, B.A.; Raimundo, N.; MacDuff, D.A.; et al. Mitochondrial DNA stress primes the antiviral innate immune response. *Nature* **2015**, *520*, 553–557. [CrossRef]
163. Wiedmer, A.; Wang, P.; Zhou, J.; Rennekamp, A.J.; Tiranti, V.; Zeviani, M.; Lieberman, P.M. Epstein-Barr virus immediate-early protein Zta co-opts mitochondrial single-stranded DNA binding protein to promote viral and inhibit mitochondrial DNA replication. *J. Virol.* **2008**, *82*, 4647–4655. [CrossRef] [PubMed]
164. Machida, K.; Cheng, K.T.; Lai, C.K.; Jeng, K.S.; Sung, V.M.; Lai, M.M. Hepatitis C virus triggers mitochondrial permeability transition with production of reactive oxygen species, leading to DNA damage and STAT3 activation. *J. Virol.* **2006**, *80*, 7199–7207. [CrossRef] [PubMed]
165. Martinez, R.; Shao, L.; Bronstein, J.C.; Weber, P.C.; Weller, S.K. The product of a 1.9-kb mRNA which overlaps the HSV-1 alkaline nuclease gene (UL12) cannot relieve the growth defects of a null mutant. *Virology* **1996**, *215*, 152–164. [CrossRef]
166. De Mendoza, C.; Martin-Carbonero, L.; Barreiro, P.; de Baar, M.; Zahonero, N.; Rodriguez-Novoa, S.; Benito, J.M.; Gonzalez-Lahoz, J.; Soriano, V. Mitochondrial DNA depletion in HIV-infected patients with chronic hepatitis C and effect of pegylated interferon plus ribavirin therapy. *AIDS* **2007**, *21*, 583–588. [CrossRef]

167. Nawarak, J.; Huang-Liu, R.; Kao, S.H.; Liao, H.H.; Sinchaikul, S.; Chen, S.T.; Cheng, S.L. Proteomics analysis of A375 human malignant melanoma cells in response to arbutin treatment. *Biochim. Biophys. Acta* **2009**, *1794*, 159–167. [CrossRef]
168. Jiang, N.; Kham, S.K.; Koh, G.S.; Suang Lim, J.Y.; Ariffin, H.; Chew, F.T.; Yeoh, A.E. Identification of prognostic protein biomarkers in childhood acute lymphoblastic leukemia (ALL). *J. Proteomics* **2011**, *74*, 843–857. [CrossRef]
169. Castagna, A.; Antonioli, P.; Astner, H.; Hamdan, M.; Righetti, S.C.; Perego, P.; Zunino, F.; Righetti, P.G. A proteomic approach to cisplatin resistance in the cervix squamous cell carcinoma cell line A431. *Proteomics* **2004**, *4*, 3246–3267. [CrossRef]
170. Zhang, Y.; Rosenberg, P.A. The essential nutrient pyrroloquinoline quinone may act as a neuroprotectant by suppressing peroxynitrite formation. *Eur. J. Neurosci.* **2002**, *16*, 1015–1024. [CrossRef]
171. Ebeling, M.C.; Polanco, J.R.; Qu, J.; Tu, C.; Montezuma, S.R.; Ferrington, D.A. Improving retinal mitochondrial function as a treatment for age-related macular degeneration. *Redox Biol.* **2020**, *34*, 101552. [CrossRef] [PubMed]
172. Cheng, S.L.; Liu, R.H.; Sheu, J.N.; Chen, S.T.; Sinchaikul, S.; Tsay, G.J. Toxicogenomics of A375 human malignant melanoma cells treated with arbutin. *J. Biomed. Sci.* **2007**, *14*, 87–105. [CrossRef] [PubMed]
173. Liu, Z.; Bengtsson, S.; Krogh, M.; Marquez, M.; Nilsson, S.; James, P.; Aliaya, A.; Holmberg, A.R. Somatostatin effects on the proteome of the LNCaP cell-line. *Int. J. Oncol.* **2007**, *30*, 1173–1179. [CrossRef]
174. Moin, S.M.; Panteva, M.; Jameel, S. The hepatitis E virus Orf3 protein protects cells from mitochondrial depolarization and death. *J. Biol. Chem.* **2007**, *282*, 21124–21133. [CrossRef]
175. Voehringer, D.W.; Hirschberg, D.L.; Xiao, J.; Lu, Q.; Roederer, M.; Lock, C.B.; Herzenberg, L.A.; Steinman, L. Gene microarray identification of redox and mitochondrial elements that control resistance or sensitivity to apoptosis. *Proc. Natl. Acad. Sci. USA* **2000**, *97*, 2680–2685. [CrossRef] [PubMed]
176. Sharaf El Dein, O.; Gallerne, C.; Brenner, C.; Lemaire, C. Increased expression of VDAC1 sensitizes carcinoma cells to apoptosis induced by DNA cross-linking agents. *Biochem. Pharmacol.* **2012**, *83*, 1172–1182. [CrossRef]
177. Lan, C.H.; Sheng, J.Q.; Fang, D.C.; Meng, Q.Z.; Fan, L.L.; Huang, Z.R. Involvement of VDAC1 and Bcl-2 family of proteins in VacA-induced cytochrome c release and apoptosis of gastric epithelial carcinoma cells. *J. Dig. Dis.* **2010**, *11*, 43–49. [CrossRef]
178. Leone, A.; Roca, M.S.; Ciardiello, C.; Terranova-Barberio, M.; Vitagliano, C.; Ciliberto, G.; Mancini, R.; Di Gennaro, E.; Bruzzese, F.; Budillon, A. Vorinostat synergizes with EGFR inhibitors in NSCLC cells by increasing ROS via up-regulation of the major mitochondrial porin VDAC1 and modulation of the c-Myc-NRF2-KEAP1 pathway. *Free Radic. Biol. Med.* **2015**, *89*, 287–299. [CrossRef]
179. Yang, X.; Tang, S.; Dai, C.; Li, D.; Zhang, S.; Deng, S.; Zhou, Y.; Xiao, X. Quinocetone induces mitochondrial apoptosis in HepG2 cells through ROS-dependent promotion of VDAC1 oligomerization and suppression of Wnt1/beta-catenin signaling pathway. *Food Chem. Toxicol.* **2017**, *105*, 161–176. [CrossRef]
180. Dehan, P.; Kustermans, G.; Guenin, S.; Horion, J.; Boniver, J.; Delvenne, P. DNA methylation and cancer diagnosis: New methods and applications. *Expert. Rev. Mol. Diagn.* **2009**, *9*, 651–657. [CrossRef]
181. Hirst, M.; Marra, M.A. Epigenetics and human disease. *Int. J. Biochem. Cell Biol.* **2009**, *41*, 136–146. [CrossRef]
182. Jaenisch, R.; Bird, A. Epigenetic regulation of gene expression: How the genome integrates intrinsic and environmental signals. *Nat. Genet.* **2003**, *33*, 245–254. [CrossRef]
183. Kouzarides, T. Chromatin modifications and their function. *Cell* **2007**, *128*, 693–705. [CrossRef]
184. Lawrence, M.; Daujat, S.; Schneider, R. Lateral Thinking: How Histone Modifications Regulate Gene Expression. *Trends Genet.* **2016**, *32*, 42–56. [CrossRef]
185. Stefanska, B.; Karlic, H.; Varga, F.; Fabianowska-Majewska, K.; Haslberger, A. Epigenetic mechanisms in anti-cancer actions of bioactive food components—the implications in cancer prevention. *Br. J. Pharmacol.* **2012**, *167*, 279–297. [CrossRef]
186. Zhao, Z.; Wang, L.; Di, L. Compartmentation of metabolites in regulating epigenome of cancer. *Mol. Med.* **2016**, *22*, 349–360. [CrossRef]
187. Gronbaek, K.; Treppendahl, M.; Asmar, F.; Guldborg, P. Epigenetic Changes in Cancer as Potential Targets for Prophylaxis and Maintenance Therapy. *Basic Clin. Pharmacol. Toxicol.* **2008**, *103*, 389–396. [CrossRef]
188. Urvalek, A.; Laursen, K.B.; Gudas, L.J. The roles of retinoic acid and retinoic acid receptors in inducing epigenetic changes. *Subcell. Biochem.* **2014**, *70*, 129–149. [CrossRef]

189. Chen, Z.X.; Riggs, A.D. DNA methylation and demethylation in mammals. *J. Biol. Chem.* **2011**, *286*, 18347–18353. [CrossRef]
190. Chandel, N.S. Evolution of Mitochondria as Signaling Organelles. *Cell Metab.* **2015**, *22*, 204–206. [CrossRef]
191. Martinez-Reyes, I.; Chandel, N.S. Mitochondrial TCA cycle metabolites control physiology and disease. *Nat. Commun.* **2020**, *11*, 102. [CrossRef]
192. Amsalem, Z.; Arif, T.; Shteinfer-Kuzmine, A.; Chalifa-Caspi, V.; Shoshan-Barmatz, V. The Mitochondrial Protein VDAC1 at the Crossroads of Cancer Cell Metabolism: The Epigenetic Link. *Cancers (Basel)* **2020**, *12*, 1031. [CrossRef]
193. Sivanand, S.; Viney, I.; Wellen, K.E. Spatiotemporal Control of Acetyl-CoA Metabolism in Chromatin Regulation. *Trends Biochem. Sci.* **2018**, *43*, 61–74. [CrossRef]
194. Wellen, K.E.; Hatzivassiliou, G.; Sachdeva, U.M.; Bui, T.V.; Cross, J.R.; Thompson, C.B. ATP-citrate lyase links cellular metabolism to histone acetylation. *Science* **2009**, *324*, 1076–1080. [CrossRef]
195. Xiao, M.; Yang, H.; Xu, W.; Ma, S.; Lin, H.; Zhu, H.; Liu, L.; Liu, Y.; Yang, C.; Xu, Y.; et al. Inhibition of alpha-KG-dependent histone and DNA demethylases by fumarate and succinate that are accumulated in mutations of FH and SDH tumor suppressors. *Genes Dev.* **2012**, *26*, 1326–1338. [CrossRef]
196. Koren, I.; Raviv, Z.; Shoshan-Barmatz, V. Downregulation of voltage-dependent anion channel-1 expression by RNA interference prevents cancer cell growth in vivo. *Cancer Biol. Ther.* **2010**, *9*, 1046–1052. [CrossRef]
197. Ko, J.H.; Gu, W.; Lim, I.; Zhou, T.; Bang, H. Expression profiling of mitochondrial voltage-dependent anion channel-1 associated genes predicts recurrence-free survival in human carcinomas. *PLoS ONE* **2014**, *9*, e110094. [CrossRef]
198. Caterino, M.; Ruoppolo, M.; Mandola, A.; Costanzo, M.; Orru, S.; Imperlini, E. Protein-protein interaction networks as a new perspective to evaluate distinct functional roles of voltage-dependent anion channel isoforms. *Mol. Biosyst.* **2017**, *13*, 2466–2476. [CrossRef]
199. Prezma, T.; Shteinfer, A.; Admoni, L.; Raviv, Z.; Sela, I.; Levi, I.; Shoshan-Barmatz, V. VDAC1-based peptides: Novel pro-apoptotic agents and potential therapeutics for B-cell chronic lymphocytic leukemia. *Cell Death Dis.* **2013**, *4*, e809. [CrossRef]
200. Shteinfer-Kuzmine, A.; Arif, T.; Krelin, Y.; Tripathi, S.S.; Paul, A.; Shoshan-Barmatz, V. Mitochondrial VDAC1-based peptides: Attacking oncogenic properties in glioblastoma. *Oncotarget* **2017**, *8*, 31329–31346. [CrossRef]
201. Mathupala, S.P.; Ko, Y.H.; Pedersen, P.L. Hexokinase II: Cancer's double-edged sword acting as both facilitator and gatekeeper of malignancy when bound to mitochondria. *Oncogene* **2006**, *25*, 4777–4786. [CrossRef] [PubMed]
202. Pedersen, P.L.; Mathupala, S.; Rempel, A.; Geschwind, J.F.; Ko, Y.H. Mitochondrial bound type II hexokinase: A key player in the growth and survival of many cancers and an ideal prospect for therapeutic intervention. *Biochim. Biophys. Acta* **2002**, *1555*, 14–20. [CrossRef]
203. Majewski, N.; Nogueira, V.; Robey, R.B.; Hay, N. Akt inhibits apoptosis downstream of BID cleavage via a glucose-dependent mechanism involving mitochondrial hexokinases. *Mol. Cell Biol.* **2004**, *24*, 730–740. [CrossRef]
204. Pastorino, J.G.; Hoek, J.B.; Shulga, N. Activation of glycogen synthase kinase 3beta disrupts the binding of hexokinase II to mitochondria by phosphorylating voltage-dependent anion channel and potentiates chemotherapy-induced cytotoxicity. *Cancer Res.* **2005**, *65*, 10545–10554. [CrossRef]
205. Allouche, M.; Pertuiset, C.; Robert, J.L.; Martel, C.; Veneziano, R.; Henry, C.; Dein, O.S.; Saint, N.; Brenner, C.; Chopineau, J. ANT-VDAC1 interaction is direct and depends on ANT isoform conformation in vitro. *Biochem. Biophys. Res. Commun.* **2012**, *429*, 12–17. [CrossRef]
206. Bernardi, P.; Di Lisa, F.; Fogolari, F.; Lippe, G. From ATP to PTP and Back: A Dual Function for the Mitochondrial ATP Synthase. *Circ. Res.* **2015**, *116*, 1850–1862. [CrossRef]
207. Tsujimoto, Y.; Shimizu, S. Role of the mitochondrial membrane permeability transition in cell death. *Apoptosis* **2007**, *12*, 835–840. [CrossRef]
208. Kinnally, K.W.; Peixoto, P.M.; Ryu, S.Y.; Dejean, L.M. Is mPTP the gatekeeper for necrosis, apoptosis, or both? *Biochim. Biophys. Acta* **2011**, *1813*, 616–622. [CrossRef]
209. Baines, C.P.; Kaiser, R.A.; Sheiko, T.; Craigen, W.J.; Molkentin, J.D. Voltage-dependent anion channels are dispensable for mitochondrial-dependent cell death. *Nat. Cell. Biol.* **2007**, *9*, 550–555. [CrossRef]

210. Kokoszka, J.E.; Waymire, K.G.; Levy, S.E.; Sligh, J.E.; Cai, J.; Jones, D.P.; MacGregor, G.R.; Wallace, D.C. The ADP/ATP translocator is not essential for the mitochondrial permeability transition pore. *Nature* **2004**, *427*, 461–465. [CrossRef]
211. Patterson, R.L.; van Rossum, D.B.; Kaplin, A.I.; Barrow, R.K.; Snyder, S.H. Inositol 1,4,5-trisphosphate receptor/GAPDH complex augments Ca²⁺ release via locally derived NADH. *Proc. Natl. Acad. Sci. USA* **2005**, *102*, 1357–1359. [CrossRef] [PubMed]
212. Vyssokikh, M.; Zorova, L.; Zorov, D.; Heimlich, G.; Jurgensmeier, J.; Schreiner, D.; Brdiczka, D. The intra-mitochondrial cytochrome c distribution varies correlated to the formation of a complex between VDAC and the adenine nucleotide translocase: This affects Bax-dependent cytochrome c release. *Biochim. Biophys. Acta* **2004**, *1644*, 27–36. [CrossRef] [PubMed]
213. Maldonado, E.N. VDAC-Tubulin, an Anti-Warburg Pro-Oxidant Switch. *Front. Oncol.* **2017**, *7*, 4. [CrossRef] [PubMed]
214. Azarashvili, T.; Krestinina, O.; Baburina, Y.; Odinkova, I.; Grachev, D.; Papadopoulos, V.; Akatov, V.; Lemasters, J.J.; Reiser, G. Combined effect of G3139 and TSPO ligands on Ca²⁺-induced permeability transition in rat brain mitochondria. *Arch. Biochem. Biophys.* **2015**, *587*, 70–77. [CrossRef] [PubMed]
215. Youle, R.J.; Strasser, A. The BCL-2 protein family: Opposing activities that mediate cell death. *Nat. Rev. Mol. Cell Biol.* **2008**, *9*, 47–59. [CrossRef]
216. Danial, N.N. BCL-2 family proteins: Critical checkpoints of apoptotic cell death. *Clin. Cancer Res.* **2007**, *13*, 7254–7263. [CrossRef]
217. Huang, H.; Shah, K.; Bradbury, N.A.; Li, C.; White, C. Mcl-1 promotes lung cancer cell migration by directly interacting with VDAC to increase mitochondrial Ca²⁺ uptake and reactive oxygen species generation. *Cell Death Dis.* **2014**, *5*, e1482. [CrossRef]
218. Shimizu, S.; Konishi, A.; Kodama, T.; Tsujimoto, Y. BH4 domain of antiapoptotic Bcl-2 family members closes voltage-dependent anion channel and inhibits apoptotic mitochondrial changes and cell death. *Proc. Natl. Acad. Sci. USA* **2000**, *97*, 3100–3105. [CrossRef]
219. Sugiyama, T.; Shimizu, S.; Matsuoka, Y.; Yoneda, Y.; Tsujimoto, Y. Activation of mitochondrial voltage-dependent anion channel by pro-apoptotic BH3-only protein Bim. *Oncogene* **2002**, *21*, 4944–4956. [CrossRef]
220. Tsujimoto, Y.; Shimizu, S. The voltage-dependent anion channel: An essential player in apoptosis. *Biochimie* **2002**, *84*, 187–193. [CrossRef]
221. Yamagata, H.; Shimizu, S.; Nishida, Y.; Watanabe, Y.; Craigen, W.J.; Tsujimoto, Y. Requirement of voltage-dependent anion channel 2 for pro-apoptotic activity of Bax. *Oncogene* **2009**, *28*, 3563–3572. [CrossRef] [PubMed]
222. Monaco, G.; Vervliet, T.; Akl, H.; Bultynck, G. The selective BH4-domain biology of Bcl-2-family members: IP3Rs and beyond. *Cell Mol. Life Sci.* **2013**, *70*, 1171–1183. [CrossRef]
223. Eckenrode, E.F.; Yang, J.; Velmurugan, G.V.; Foskett, J.K.; White, C. Apoptosis protection by Mcl-1 and Bcl-2 modulation of inositol 1,4,5-trisphosphate receptor-dependent Ca²⁺ signaling. *J. Biol. Chem.* **2010**, *285*, 13678–13684. [CrossRef] [PubMed]
224. Distelhorst, C.W.; Bootman, M.D. Bcl-2 interaction with the inositol 1,4,5-trisphosphate receptor: Role in Ca²⁺ signaling and disease. *Cell Calcium.* **2011**, *50*, 234–241. [CrossRef]
225. Monaco, G.; Decrock, E.; Arbel, N.; van Vliet, A.R.; La Rovere, R.M.; De Smedt, H.; Parys, J.B.; Agostinis, P.; Leybaert, L.; Shoshan-Barmatz, V.; et al. The BH4 domain of anti-apoptotic Bcl-XL, but not that of the related Bcl-2, limits the voltage-dependent anion channel 1 (VDAC1)-mediated transfer of pro-apoptotic Ca²⁺ signals to mitochondria. *J. Biol. Chem.* **2015**, *290*, 9150–9161. [CrossRef] [PubMed]
226. Adachi, M.; Higuchi, H.; Miura, S.; Azuma, T.; Inokuchi, S.; Saito, H.; Kato, S.; Ishii, H. Bax interacts with the voltage-dependent anion channel and mediates ethanol-induced apoptosis in rat hepatocytes. *Am. J. Physiol. Gastrointest Liver. Physiol.* **2004**, *287*, G695–G705. [CrossRef] [PubMed]
227. Zheng, Y.; Shi, Y.; Tian, C.; Jiang, C.; Jin, H.; Chen, J.; Almasan, A.; Tang, H.; Chen, Q. Essential role of the voltage-dependent anion channel (VDAC) in mitochondrial permeability transition pore opening and cytochrome c release induced by arsenic trioxide. *Oncogene* **2004**, *23*, 1239–1247. [CrossRef]
228. Shoshan-Barmatz, V.; Pittala, S.; Mizrachi, D. VDAC1 and the TSPO: Expression, Interactions, and Associated Functions in Health and Disease States. *Int. J. Mol. Sci.* **2019**, *20*, 3348. [CrossRef]

229. Levin, E.; Premkumar, A.; Veenman, L.; Kugler, W.; Leschiner, S.; Spanier, I.; Weisinger, G.; Lakomek, M.; Weizman, A.; Snyder, S.H.; et al. The peripheral-type benzodiazepine receptor and tumorigenicity: Isoquinoline binding protein (IBP) antisense knockdown in the C6 glioma cell line. *Biochemistry* **2005**, *44*, 9924–9935. [CrossRef]
230. Veenman, L.; Levin, E.; Weisinger, G.; Leschiner, S.; Spanier, I.; Snyder, S.H.; Weizman, A.; Gavish, M. Peripheral-type benzodiazepine receptor density and in vitro tumorigenicity of glioma cell lines. *Biochem. Pharmacol.* **2004**, *68*, 689–698. [CrossRef]
231. Veenman, L.; Papadopoulos, V.; Gavish, M. Channel-like functions of the 18-kDa translocator protein (TSPO): Regulation of apoptosis and steroidogenesis as part of the host-defense response. *Curr. Pharm. Des.* **2007**, *13*, 2385–2405. [CrossRef] [PubMed]
232. Veenman, L.; Shandalov, Y.; Gavish, M. VDAC activation by the 18 kDa translocator protein (TSPO), implications for apoptosis. *J. Bioenerg. Biomembr.* **2008**, *40*, 199–205. [CrossRef] [PubMed]
233. Gatliff, J.; Campanella, M. TSPO is a REDOX regulator of cell mitophagy. *Biochem. Society Transact.* **2015**, *43*, 543–552. [CrossRef]
234. Gatliff, J.; East, D.; Crosby, J.; Abeti, R.; Harvey, R.; Craigen, W.; Parker, P.; Campanella, M. TSPO interacts with VDAC1 and triggers a ROS-mediated inhibition of mitochondrial quality control. *Autophagy* **2014**, *10*, 2279–2296. [CrossRef] [PubMed]
235. Chen, Y.; Craigen, W.J.; Riley, D.J. Nek1 regulates cell death and mitochondrial membrane permeability through phosphorylation of VDAC1. *Cell Cycle* **2009**, *8*, 257–267. [CrossRef]
236. Chen, Y.; Gaczynska, M.; Osmulski, P.; Polci, R.; Riley, D.J. Phosphorylation by Nek1 regulates opening and closing of voltage dependent anion channel 1. *Biochem. Biophys. Res. Commun.* **2010**, *394*, 798–803. [CrossRef]
237. Zhang, X.; Bian, X.; Kong, J. The proapoptotic protein BNIP3 interacts with VDAC to induce mitochondrial release of endonuclease G. *PLoS ONE* **2014**, *9*, e113642. [CrossRef]
238. Kusano, H.; Shimizu, S.; Koya, R.C.; Fujita, H.; Kamada, S.; Kuzumaki, N.; Tsujimoto, Y. Human gelsolin prevents apoptosis by inhibiting apoptotic mitochondrial changes via closing VDAC. *Oncogene* **2000**, *19*, 4807–4814. [CrossRef]
239. Qiao, H.; McMillan, J.R. Gelsolin segment 5 inhibits HIV-induced T-cell apoptosis via Vpr-binding to VDAC. *FEBS Lett.* **2007**, *581*, 535–540. [CrossRef]
240. Li, G.H.; Arora, P.D.; Chen, Y.; McCulloch, C.A.; Liu, P. Multifunctional roles of gelsolin in health and diseases. *Med. Res. Rev.* **2012**, *32*, 999–1025. [CrossRef]
241. Miura, N.; Takemori, N.; Kikugawa, T.; Tanji, N.; Higashiyama, S.; Yokoyama, M. Adseverin: A novel cisplatin-resistant marker in the human bladder cancer cell line HT1376 identified by quantitative proteomic analysis. *Mol. Oncol.* **2012**, *6*, 311–322. [CrossRef] [PubMed]
242. Rostovtseva, T.K.; Sheldon, K.L.; Hassanzadeh, E.; Monge, C.; Saks, V.; Bezrukov, S.M.; Sackett, D.L. Tubulin binding blocks mitochondrial voltage-dependent anion channel and regulates respiration. *Proc. Natl. Acad. Sci. USA* **2008**, *105*, 18746–18751. [CrossRef] [PubMed]
243. Carre, M.; Andre, N.; Carles, G.; Borghi, H.; Bricchese, L.; Briand, C.; Braguer, D. Tubulin is an inherent component of mitochondrial membranes that interacts with the voltage-dependent anion channel. *J. Biol. Chem.* **2002**, *277*, 33664–33669. [CrossRef] [PubMed]
244. Puurand, M.; Tepp, K.; Timohhina, N.; Aid, J.; Shevchuk, I.; Chekulayev, V.; Kaambre, T. Tubulin betaII and betaIII Isoforms as the Regulators of VDAC Channel Permeability in Health and Disease. *Cells* **2019**, *8*, 239. [CrossRef]
245. Rostovtseva, T.K.; Bezrukov, S.M. VDAC inhibition by tubulin and its physiological implications. *Biochim. Biophys. Acta* **2012**, *1818*, 1526–1535. [CrossRef]
246. Saks, V.; Guzun, R.; Timohhina, N.; Tepp, K.; Varikmaa, M.; Monge, C.; Beraud, N.; Kaambre, T.; Kuznetsov, A.; Kadaja, L.; et al. Structure-function relationships in feedback regulation of energy fluxes in vivo in health and disease: Mitochondrial interactosome. *Biochim. Biophys. Acta* **2010**, *1797*, 678–697. [CrossRef]
247. Linden, M.; Karlsson, G. Identification of porin as a binding site for MAP2. *Biochem. Biophys. Res. Commun.* **1996**, *218*, 833–836. [CrossRef]
248. Schwarzer, C.; Barnikol-Watanabe, S.; Thinner, F.P.; Hilschmann, N. Voltage-dependent anion-selective channel (VDAC) interacts with the dynein light chain Tctex1 and the heat-shock protein PBP74. *Int. J. Biochem. Cell Biol.* **2002**, *34*, 1059–1070. [CrossRef]

249. Sasaki, S.; Yui, N.; Noda, Y. Actin directly interacts with different membrane channel proteins and influences channel activities: AQP2 as a model. *Biochim. Biophys. Acta* **2014**, *1838*, 514–520. [CrossRef]
250. Sun, J.; Liao, J.K. Functional interaction of endothelial nitric oxide synthase with a voltage-dependent anion channel. *Proc. Natl. Acad. Sci. USA* **2002**, *99*, 13108–13113. [CrossRef]
251. Bergemalm, D.; Jonsson, P.A.; Graffmo, K.S.; Andersen, P.M.; Brannstrom, T.; Rehnmark, A.; Marklund, S.L. Overloading of stable and exclusion of unstable human superoxide dismutase-1 variants in mitochondria of murine amyotrophic lateral sclerosis models. *J. Neurosci.* **2006**, *26*, 4147–4154. [CrossRef] [PubMed]
252. Deng, H.X.; Shi, Y.; Furukawa, Y.; Zhai, H.; Fu, R.; Liu, E.; Gorrie, G.H.; Khan, M.S.; Hung, W.Y.; Bigio, E.H.; et al. Conversion to the amyotrophic lateral sclerosis phenotype is associated with intermolecular linked insoluble aggregates of SOD1 in mitochondria. *Proc. Natl. Acad. Sci. USA* **2006**, *103*, 7142–7147. [CrossRef] [PubMed]
253. Liu, J.; Lillo, C.; Jonsson, P.A.; Vande Velde, C.; Ward, C.M.; Miller, T.M.; Subramaniam, J.R.; Rothstein, J.D.; Marklund, S.; Andersen, P.M.; et al. Toxicity of familial ALS-linked SOD1 mutants from selective recruitment to spinal mitochondria. *Neuron* **2004**, *43*, 5–17. [CrossRef] [PubMed]
254. Israelson, A.; Arbel, N.; Da Cruz, S.; Ilieva, H.; Yamanaka, K.; Shoshan-Barmatz, V.; Cleveland, D.W. Misfolded mutant SOD1 directly inhibits VDAC1 conductance in a mouse model of inherited ALS. *Neuron* **2010**, *67*, 575–587. [CrossRef] [PubMed]
255. Shteinfer-Kuzmine, A.; Argueti, S.; Gupta, R.; Shvil, N.; Abu-Hamad, S.; Gropper, Y.; Hoerber, J.; Magri, A.; Messina, A.; Kozlova, E.N.; et al. A VDAC1-Derived N-Terminal Peptide Inhibits Mutant SOD1-VDAC1 Interactions and Toxicity in the SOD1 Model of ALS. *Front. Cell Neurosci.* **2019**, *13*, 346. [CrossRef]
256. Tan, W.; Nanche, N.; Bogush, A.; Pedrini, S.; Trotti, D.; Pasinelli, P. Small peptides against the mutant SOD1/Bcl-2 toxic mitochondrial complex restore mitochondrial function and cell viability in mutant SOD1-mediated ALS. *J. Neurosci.* **2013**, *33*, 11588–11598. [CrossRef]
257. Xu, L.G.; Wang, Y.Y.; Han, K.J.; Li, L.Y.; Zhai, Z.; Shu, H.B. VISA is an adapter protein required for virus-triggered IFN-beta signaling. *Mol. Cell.* **2005**, *19*, 727–740. [CrossRef]
258. Guan, K.; Zheng, Z.; Song, T.; He, X.; Xu, C.; Zhang, Y.; Ma, S.; Wang, Y.; Xu, Q.; Cao, Y.; et al. MAVS regulates apoptotic cell death by decreasing K48-linked ubiquitination of voltage-dependent anion channel 1. *Mol. Cell Biol.* **2013**, *33*, 3137–3149. [CrossRef]
259. Mitra, A.; Basak, T.; Datta, K.; Naskar, S.; Sengupta, S.; Sarkar, S. Role of alpha-crystallin B as a regulatory switch in modulating cardiomyocyte apoptosis by mitochondria or endoplasmic reticulum during cardiac hypertrophy and myocardial infarction. *Cell Death Dis.* **2013**, *4*, e582. [CrossRef]
260. Shen, J.; Du, T.; Wang, X.; Duan, C.; Gao, G.; Zhang, J.; Lu, L.; Yang, H. Alpha-Synuclein amino terminus regulates mitochondrial membrane permeability. *Brain. Res.* **2014**, *1591*, 14–26. [CrossRef]
261. Jacobs, D.; Hoogerheide, D.P.; Rovini, A.; Jiang, Z.; Lee, J.C.; Rostovtseva, T.K.; Bezrukov, S.M. Probing Membrane Association of alpha-Synuclein Domains with VDAC Nanopore Reveals Unexpected Binding Pattern. *Sci. Rep.* **2019**, *9*, 4580. [CrossRef] [PubMed]
262. Lu, L.; Zhang, C.; Cai, Q.; Lu, Q.; Duan, C.; Zhu, Y.; Yang, H. Voltage-dependent anion channel involved in the alpha-synuclein-induced dopaminergic neuron toxicity in rats. *Acta Biochim. Biophys. Sin (Shanghai)* **2013**, *45*, 170–178. [CrossRef] [PubMed]
263. Gergalova, G.; Lykhmus, O.; Kalashnyk, O.; Koval, L.; Chernyshov, V.; Kryukova, E.; Tsetlin, V.; Komisarenko, S.; Skok, M. Mitochondria express alpha7 nicotinic acetylcholine receptors to regulate Ca²⁺ accumulation and cytochrome c release: Study on isolated mitochondria. *PLoS ONE* **2012**, *7*, e31361. [CrossRef]
264. Skok, M.; Gergalova, G.; Lykhmus, O.; Kalashnyk, O.; Koval, L.; Uspenska, K. Nicotinic acetylcholine receptors in mitochondria: Subunit composition, function and signaling. *Neurotransmitter* **2016**, *3*, e1290. [CrossRef]
265. Breydo, L.; Wu, J.W.; Uversky, V.N. Alpha-Synuclein misfolding and Parkinson's disease. *Biochim. Biophys. Acta Mol. Basis Dis.* **2012**, *1822*, 261–285. [CrossRef]
266. Fields, C.R.; Bengoa-Vergniory, N.; Wade-Martins, R. Targeting Alpha-Synuclein as a Therapy for Parkinson's Disease. *Front. Mol. Neurosci.* **2019**, *12*, 299. [CrossRef] [PubMed]
267. Rostovtseva, T.K.; Gurnev, P.A.; Protchenko, O.; Hoogerheide, D.P.; Yap, T.L.; Philpott, C.C.; Lee, J.C.; Bezrukov, S.M. Alpha-Synuclein Shows High Affinity Interaction with Voltage-dependent Anion Channel, Suggesting Mechanisms of Mitochondrial Regulation and Toxicity in Parkinson Disease. *J. Biol. Chem.* **2015**, *290*, 18467–18477. [CrossRef]

268. Zamarin, D.; Garcia-Sastre, A.; Xiao, X.; Wang, R.; Palese, P. Influenza virus PB1-F2 protein induces cell death through mitochondrial ANT3 and VDAC1. *PLoS Pathog.* **2005**, *1*, e4. [CrossRef]
269. Rahmani, Z.; Huh, K.W.; Lasher, R.; Siddiqui, A. Hepatitis B virus X protein colocalizes to mitochondria with a human voltage-dependent anion channel, HVDAC3, and alters its transmembrane potential. *J. Virol.* **2000**, *74*, 2840–2846. [CrossRef]
270. Holla, R.P.; Ahmad, I.; Ahmad, Z.; Jameel, S. Molecular virology of hepatitis E virus. *Semin. Liver. Dis.* **2013**, *33*, 3–14. [CrossRef]
271. Deniaud, A.; Brenner, C.; Kroemer, G. Mitochondrial membrane permeabilization by HIV-1 Vpr. *Mitochondrion* **2004**, *4*, 223–233. [CrossRef]
272. Jitobaom, K.; Tongluan, N.; Smith, D.R. Involvement of voltage-dependent anion channel (VDAC) in dengue infection. *Sci. Rep.* **2016**, *6*, 35753. [CrossRef]
273. Lin, W.; Zhang, Z.; Xu, Z.; Wang, B.; Li, X.; Cao, H.; Wang, Y.; Zheng, S.J. The association of receptor of activated protein kinase C 1 (RACK1) with infectious bursal disease virus viral protein VP5 and voltage-dependent anion channel 2 (VDAC2) inhibits apoptosis and enhances viral replication. *J. Biol. Chem.* **2015**, *290*, 8500–8510. [CrossRef]
274. Li, Z.; Wang, Y.; Xue, Y.; Li, X.; Cao, H.; Zheng, S.J. Critical role for voltage-dependent anion channel 2 in infectious bursal disease virus-induced apoptosis in host cells via interaction with VP5. *J. Virol.* **2012**, *86*, 1328–1338. [CrossRef]
275. Han, C.; Zeng, X.; Yao, S.; Gao, L.; Zhang, L.; Qi, X.; Duan, Y.; Yang, B.; Gao, Y.; Liu, C.; et al. Voltage-Dependent Anion Channel 1 Interacts with Ribonucleoprotein Complexes To Enhance Infectious Bursal Disease Virus Polymerase Activity. *J. Virol.* **2017**, *91*, e00584-17. [CrossRef]
276. Fongsaran, C.; Phaonakrop, N.; Roytrakul, S.; Thepparit, C.; Kuadkitkan, A.; Smith, D.R. Voltage dependent anion channel is redistributed during Japanese encephalitis virus infection of insect cells. *Sci. World J.* **2014**, *2014*, 976015. [CrossRef]
277. Delisle, L.; Fuhrmann, M.; Quere, C.; Pauletto, M.; Pichereau, V.; Pernet, F.; Corporeau, C. The Voltage-Dependent Anion Channel (VDAC) of Pacific Oysters *Crassostrea gigas* Is Upaccumulated During Infection by the Ostreid Herpesvirus-1 (OsHV-1): An Indicator of the Warburg Effect. *Mar. Biotechnol. (NY)* **2018**, *20*, 87–97. [CrossRef]
278. Borgne-Sanchez, A.; Dupont, S.; Langonne, A.; Baux, L.; Lecoeur, H.; Chauvier, D.; Lassalle, M.; Deas, O.; Briere, J.J.; Brabant, M.; et al. Targeted Vpr-derived peptides reach mitochondria to induce apoptosis of alphaVbeta3-expressing endothelial cells. *Cell Death Differ.* **2007**, *14*, 422–435. [CrossRef]
279. Han, D.; Antunes, F.; Canali, R.; Rettori, D.; Cadenas, E. Voltage-dependent anion channels control the release of the superoxide anion from mitochondria to cytosol. *J. Biol. Chem.* **2003**, *278*, 5557–5563. [CrossRef]
280. Shirakata, Y.; Koike, K. Hepatitis B virus X protein induces cell death by causing loss of mitochondrial membrane potential. *J. Biol. Chem.* **2003**, *278*, 22071–22078. [CrossRef]
281. Seyfried, T.N.; Shelton, L.M. Cancer as a metabolic disease. *Nutr. Metab. (Lond.)* **2010**, *7*, 7. [CrossRef]
282. Seyfried, T.N. Cancer as a mitochondrial metabolic disease. *Front. Cell Dev. Biol.* **2015**, *3*, 43. [CrossRef]
283. Pittala, S.; Krelm, Y.; Shoshan-Barmatz, V. Targeting Liver Cancer and Associated Pathologies in Mice with a Mitochondrial VDAC1-Based Peptide. *Neoplasia* **2018**, *20*, 594–609. [CrossRef]
284. Pedersen, P.L. Voltage dependent anion channels (VDACs): A brief introduction with a focus on the outer mitochondrial compartment's roles together with hexokinase-2 in the “Warburg effect” in cancer. *J. Bioenerg. Biomembr.* **2008**, *40*, 123–126. [CrossRef]
285. Shi, Y.; Jiang, C.; Chen, Q.; Tang, H. One-step on-column affinity refolding purification and functional analysis of recombinant human VDAC1. *Biochem. Biophys. Res. Commun.* **2003**, *303*, 475–482. [CrossRef]
286. Li, Q.Q.; Zhang, L.; Wan, H.Y.; Liu, M.; Li, X.; Tang, H. CREB1-driven expression of miR-320a promotes mitophagy by down-regulating VDAC1 expression during serum starvation in cervical cancer cells. *Oncotarget* **2015**, *6*, 34924–34940. [CrossRef]
287. Zhang, G.; Jiang, G.; Wang, C.; Zhong, K.; Zhang, J.; Xue, Q.; Li, X.; Jin, H.; Li, B. Decreased expression of microRNA-320a promotes proliferation and invasion of non-small cell lung cancer cells by increasing VDAC1 expression. *Oncotarget* **2016**, *7*, 49470–49480. [CrossRef]
288. Wang, F.; Qiang, Y.; Zhu, L.; Jiang, Y.; Wang, Y.; Shao, X.; Yin, L.; Chen, J.; Chen, Z. MicroRNA-7 downregulates the oncogene VDAC1 to influence hepatocellular carcinoma proliferation and metastasis. *Tumour. Biol.* **2016**, *37*, 10235–10246. [CrossRef]

289. Chaudhuri, A.D.; Choi, D.C.; Kabaria, S.; Tran, A.; Junn, E. MicroRNA-7 Regulates the Function of Mitochondrial Permeability Transition Pore by Targeting VDAC1 Expression. *J. Biol. Chem.* **2016**, *291*, 6483–6493. [CrossRef]
290. Yuan, J.; Yankner, B.A. Apoptosis in the nervous system. *Nature* **2000**, *407*, 802–809. [CrossRef]
291. Friedlander, R.M. Apoptosis and caspases in neurodegenerative diseases. *N. Eng. J. Med.* **2003**, *348*, 1365–1375. [CrossRef]
292. Gervais, F.G.; Xu, D.; Robertson, G.S.; Vaillancourt, J.P.; Zhu, Y.; Huang, J.; LeBlanc, A.; Rigby, S.M.; Shearman, M.S.; Clarke, E.E.; et al. Involvement of caspases in proteolytic cleavage of Alzheimer's amyloid-beta precursor protein and amyloidogenic A beta peptide formation. *Cell* **1999**, *97*, 395–406. [CrossRef]
293. Li, M.; Ona, V.O.; Guegan, C.; Chen, M.; Jackson-Lewis, V.; Andrews, L.J.; Olszewski, A.J.; Stieg, P.E.; Lee, J.P.; Przedborski, S.; et al. Functional role of caspase-1 and caspase-3 in an ALS transgenic mouse model. *Science* **2000**, *288*, 335–339. [CrossRef]
294. Mattson, M.P.; Gleichmann, M.; Cheng, A. Mitochondria in neuroplasticity and neurological disorders. *Neuron* **2008**, *60*, 748–766. [CrossRef]
295. Petrozzi, L.; Ricci, G.; Giglioli, N.J.; Siciliano, G.; Mancuso, M. Mitochondria and neurodegeneration. *Biosci. Rep.* **2007**, *27*, 87–104. [CrossRef] [PubMed]
296. Radi, E.; Formichi, P.; Battisti, C.; Federico, A. Apoptosis and oxidative stress in neurodegenerative diseases. *J. Alzheimers Dis.* **2014**, *42* (Suppl. S3), S125–S152. [CrossRef]
297. Ferrer, I. Altered mitochondria, energy metabolism, voltage-dependent anion channel, and lipid rafts converge to exhaust neurons in Alzheimer's disease. *J. Bioenerg. Biomembr.* **2009**, *41*, 425–431. [CrossRef] [PubMed]
298. Reddy, P.H. Is the mitochondrial outer membrane protein VDAC1 therapeutic target for Alzheimer's disease? *Biochim. Biophys. Acta* **2013**, *1832*, 67–75. [CrossRef]
299. Yoo, B.C.; Fountoulakis, M.; Cairns, N.; Lubec, G. Changes of voltage-dependent anion-selective channel proteins VDAC1 and VDAC2 brain levels in patients with Alzheimer's disease and Down syndrome. *Electrophoresis* **2001**, *22*, 172–179. [CrossRef]
300. Fukada, K.; Zhang, F.; Vien, A.; Cashman, N.R.; Zhu, H. Mitochondrial proteomic analysis of a cell line model of familial amyotrophic lateral sclerosis. *Mol. Cell Proteom.* **2004**, *3*, 1211–1223. [CrossRef]
301. Kielar, C.; Wishart, T.M.; Palmer, A.; Dihanich, S.; Wong, A.M.; Macauley, S.L.; Chan, C.H.; Sands, M.S.; Pearce, D.A.; Cooper, J.D.; et al. Molecular correlates of axonal and synaptic pathology in mouse models of Batten disease. *Hum. Mol. Genet.* **2009**, *18*, 4066–4080. [CrossRef] [PubMed]
302. Bueno, K.O.; de Souza Resende, L.; Ribeiro, A.F.; Dos Santos, D.M.; Goncalves, E.C.; Vigil, F.A.; de Oliveira Silva, I.F.; Ferreira, L.F.; de Castro Pimenta, A.M.; Ribeiro, A.M. Spatial cognitive deficits in an animal model of Wernicke-Korsakoff syndrome are related to changes in thalamic VDAC protein concentrations. *Neuroscience* **2015**, *294*, 29–37. [CrossRef]
303. Lezi, E.; Swerdlow, R.H. Mitochondria in neurodegeneration. *Adv. Exp. Med. Biol.* **2012**, *942*, 269–286. [CrossRef] [PubMed]
304. Silva, D.F.; Selfridge, J.E.; Lu, J.; Cardoso, S.M.; Swerdlow, R.H. Mitochondrial abnormalities in Alzheimer's disease: Possible targets for therapeutic intervention. *Adv. Pharmacol.* **2012**, *64*, 83–126. [CrossRef]
305. Colurso, G.J.; Nilson, J.E.; Vervoort, L.G. Quantitative assessment of DNA fragmentation and beta-amyloid deposition in insular cortex and midfrontal gyrus from patients with Alzheimer's disease. *Life Sci.* **2003**, *73*, 1795–1803. [CrossRef]
306. Magri, A.; Belfiore, S.; Reina, M.F.; Tomasello, M.C.; Di Rosa, F.; Guarino, L.; Leggio, V.; De Pinto, V.; Messina, A.; Hexokinase, I. N-terminal based peptide prevents the VDAC1-SOD1 G93A interaction and re-establishes ALS cell viability. *Sci. Rep.* **2016**, *6*, 34802. [CrossRef]
307. Sasaki, K.; Donthamsetty, R.; Heldak, M.; Cho, Y.E.; Scott, B.T.; Makino, A. VDAC: Old protein with new roles in diabetes. *Am. J. Physiol. Cell Physiol.* **2012**, *303*, C1055–C1060. [CrossRef]
308. Jiang, L.; Wang, H.; Chen, G.; Feng, Y.; Zou, J.; Liu, M.; Liu, K.; Wang, N.; Zhang, H.; Wang, K.; et al. WDR26/MIP2 interacts with VDAC1 and regulates VDAC1 expression levels in H9c2 cells. *Free Radic. Biol. Med.* **2018**, *117*, 58–65. [CrossRef]

309. Liao, Z.; Liu, D.; Tang, L.; Yin, D.; Yin, S.; Lai, S.; Yao, J.; He, M. Long-term oral resveratrol intake provides nutritional preconditioning against myocardial ischemia/reperfusion injury: Involvement of VDAC1 downregulation. *Mol. Nutr. Food Res.* **2015**, *59*, 454–464. [CrossRef]
310. Lim, D.S.; Roberts, R.; Marian, A.J. Expression profiling of cardiac genes in human hypertrophic cardiomyopathy: Insight into the pathogenesis of phenotypes. *J. Am. Coll. Cardiol.* **2001**, *38*, 1175–1180. [CrossRef]
311. Schwertz, H.; Carter, J.M.; Abdudurehman, M.; Russ, M.; Buerke, U.; Schlitt, A.; Muller-Werdan, U.; Prondzinsky, R.; Werdan, K.; Buerke, M. Myocardial ischemia/reperfusion causes VDAC phosphorylation which is reduced by cardioprotection with a p38 MAP kinase inhibitor. *Proteomics* **2007**, *7*, 4579–4588. [CrossRef] [PubMed]
312. Tian, M.; Xie, Y.; Meng, Y.; Ma, W.; Tong, Z.; Yang, X.; Lai, S.; Zhou, Y.; He, M.; Liao, Z. Resveratrol protects cardiomyocytes against anoxia/reoxygenation via dephosphorylation of VDAC1 by Akt-GSK3 beta pathway. *Eur. J. Pharmacol.* **2019**, *843*, 80–87. [CrossRef] [PubMed]
313. Tong, Z.; Xie, Y.; He, M.; Ma, W.; Zhou, Y.; Lai, S.; Meng, Y.; Liao, Z. VDAC1 deacetylation is involved in the protective effects of resveratrol against mitochondria-mediated apoptosis in cardiomyocytes subjected to anoxia/reoxygenation injury. *Biomed Pharmacother.* **2017**, *95*, 77–83. [CrossRef] [PubMed]
314. Yang, M.; Xu, Y.; Heisner, J.S.; Sun, J.; Stowe, D.F.; Kwok, W.M.; Camara, A.K.S. Peroxynitrite nitrates adenine nucleotide translocase and voltage-dependent anion channel 1 and alters their interactions and association with hexokinase II in mitochondria. *Mitochondrion* **2019**, *46*, 380–392. [CrossRef]
315. Zeng, F.; Wen, W.; Cui, W.; Zheng, W.; Liu, Y.; Sun, X.; Hou, N.; Ma, D.; Yuan, Y.; Shi, H.; et al. Central role of RIPK1-VDAC1 pathway on cardiac impairment in a non-human primate model of rheumatoid arthritis. *J. Mol. Cell Cardiol.* **2018**, *125*, 50–60. [CrossRef]
316. Paschon, V.; Morena, B.C.; Correia, F.F.; Beltrame, G.R.; Dos Santos, G.B.; Cristante, A.F.; Kihara, A.H. VDAC1 is essential for neurite maintenance and the inhibition of its oligomerization protects spinal cord from demyelination and facilitates locomotor function recovery after spinal cord injury. *Sci. Rep.* **2019**, *9*, 14063. [CrossRef]
317. Lovell, M.A.; Xie, C.; Markesbery, W.R. Acrolein is increased in Alzheimer’s disease brain and is toxic to primary hippocampal cultures. *Neurobiol. Aging.* **2001**, *22*, 187–194. [CrossRef]
318. Weeber, E.J.; Levy, M.; Sampson, M.J.; Anflous, K.; Armstrong, D.L.; Brown, S.E.; Sweatt, J.D.; Craig, W.J. The role of mitochondrial porins and the permeability transition pore in learning and synaptic plasticity. *J. Biol. Chem.* **2002**, *277*, 18891–18897. [CrossRef]
319. Cleveland, D.W.; Rothstein, J.D. From Charcot to Lou Gehrig: Deciphering selective motor neuron death in ALS. *Nat. Rev. Neurosci.* **2001**, *2*, 806–819. [CrossRef]
320. Carri, M.T.; Cozzolino, M. SOD1 and mitochondria in ALS: A dangerous liaison. *J. Bioenerg. Biomembr.* **2011**, *43*, 593–599. [CrossRef]
321. Ferri, A.; Cozzolino, M.; Crosio, C.; Nencini, M.; Casciati, A.; Gralla, E.B.; Rotilio, G.; Valentine, J.S.; Carri, M.T. Familial ALS-superoxide dismutases associate with mitochondria and shift their redox potentials. *Proc. Natl. Acad. Sci. USA* **2006**, *103*, 13860–13865. [CrossRef] [PubMed]
322. Magrane, J.; Sahawneh, M.A.; Przedborski, S.; Estevez, A.G.; Manfredi, G. Mitochondrial dynamics and bioenergetic dysfunction is associated with synaptic alterations in mutant SOD1 motor neurons. *J. Neurosci.* **2012**, *32*, 229–242. [CrossRef] [PubMed]
323. Shi, P.; Wei, Y.M.; Zhang, J.Y.; Gal, J.; Zhu, H.N. Mitochondrial Dysfunction is a Converging Point of Multiple Pathological Pathways in Amyotrophic Lateral Sclerosis. *J. Alzheimers Dis.* **2010**, *20*, S311–S324. [CrossRef]
324. Abu-Hamad, S.; Kahn, J.; Leyton-Jaimes, M.F.; Rosenblatt, J.; Israelson, A. Misfolded SOD1 Accumulation and Mitochondrial Association Contribute to the Selective Vulnerability of Motor Neurons in Familial ALS: Correlation to Human Disease. *ACS Chem. Neurosci.* **2017**, *8*, 2225–2234. [CrossRef] [PubMed]
325. Zimmet, P.; Alberti, K.G.; Shaw, J. Global and societal implications of the diabetes epidemic. *Nature* **2001**, *414*, 782–787. [CrossRef]
326. Li, X.; Wang, H.; Yao, B.; Xu, W.; Chen, J.; Zhou, X. lncRNA H19/miR-675 axis regulates cardiomyocyte apoptosis by targeting VDAC1 in diabetic cardiomyopathy. *Sci. Rep.* **2016**, *6*, 36340. [CrossRef]
327. Liu, Y.; Yin, H.; Zhao, M.; Lu, Q. TLR2 and TLR4 in autoimmune diseases: A comprehensive review. *Clin. Rev. Allergy Immunol.* **2014**, *47*, 136–147. [CrossRef]

328. Libby, P. Inflammatory mechanisms: The molecular basis of inflammation and disease. *Nutr. Rev.* **2007**, *65 Pt 2*, S140–S146. [CrossRef]
329. Yang, M.; Li, K.; Sun, J.; Stowe, D.; Tajkhorshid, E.; Kwok, W.; Camara, A.K.S. Knockout of VDAC1 in H9c2 Cells Promotes tBHP-induced Cell Apoptosis Through Decreased Mitochondrial HK II Binding and Enhanced Glycolytic Stress. *FASEB J.* **2020**, *34*, 1. [CrossRef]
330. Kar, D.; Bandyopadhyay, A. Targeting Peroxisome Proliferator Activated Receptor alpha (PPAR alpha) for the Prevention of Mitochondrial Impairment and Hypertrophy in Cardiomyocytes. *Cell Physiol. Biochem.* **2018**, *49*, 245–259. [CrossRef]
331. Law, K.; Brunt, E.M. Nonalcoholic fatty liver disease. *Clin. Liver. Dis.* **2010**, *14*, 591–604. [CrossRef]
332. Pessayre, D. Role of mitochondria in non-alcoholic fatty liver disease. *J. Gastroenterol. Hepatol.* **2007**, *22* (Suppl. S1), S20–S27. [CrossRef] [PubMed]
333. Holmuhamedov, E.L.; Czerny, C.; Beeson, C.C.; Lemasters, J.J. Ethanol suppresses ureagenesis in rat hepatocytes: Role of acetaldehyde. *J. Biol. Chem.* **2012**, *287*, 7692–7700. [CrossRef] [PubMed]
334. Turkaly, P.; Kerner, J.; Hoppel, C. A 22 kDa polyanion inhibits carnitine-dependent fatty acid oxidation in rat liver mitochondria. *FEBS Lett.* **1999**, *460*, 241–245. [CrossRef]
335. Smolen, J.S.; Aletaha, D.; McInnes, I.B. Rheumatoid arthritis. *Lancet* **2016**, *388*, 2023–2038. [CrossRef]
336. McInnes, I.B.; Schett, G. The pathogenesis of rheumatoid arthritis. *N. Engl. J. Med.* **2011**, *365*, 2205–2219. [CrossRef]
337. Bonventre, J.V.; Weinberg, J.M. Recent advances in the pathophysiology of ischemic acute renal failure. *J. Am. Soc. Nephrol.* **2003**, *14*, 2199–2210. [CrossRef]
338. Che, R.; Yuan, Y.; Huang, S.; Zhang, A. Mitochondrial dysfunction in the pathophysiology of renal diseases. *Am. J. Physiol. Renal. Physiol.* **2014**, *306*, F367–F378. [CrossRef]
339. Ralto, K.M.; Parikh, S.M. Mitochondria in Acute Kidney Injury. *Semin Nephrol.* **2016**, *36*, 8–16. [CrossRef]
340. Nowak, G.; Megyesi, J.; Craigen, W.J. Deletion of VDAC1 Hinders Recovery of Mitochondrial and Renal Functions After Acute Kidney Injury. *Biomolecules* **2020**, *10*, 585. [CrossRef]
341. Jeong, J.J.; Park, N.; Kwon, Y.J.; Ye, D.J.; Moon, A.; Chun, Y.J. Role of annexin A5 in cisplatin-induced toxicity in renal cells: Molecular mechanism of apoptosis. *J. Biol. Chem.* **2014**, *289*, 2469–2481. [CrossRef]
342. Sekhon, L.H.; Fehlings, M.G. Epidemiology, demographics, and pathophysiology of acute spinal cord injury. *Spine (Phila Pa 1976)* **2001**, *26* (Suppl. S24), S2–S12. [CrossRef] [PubMed]
343. Arif, T.; Paul, A.; Krelin, Y.; Shteinfer-Kuzmine, A.; Shoshan-Barmatz, V. Mitochondrial VDAC1 Silencing Leads to Metabolic Rewiring and the Reprogramming of Tumour Cells into Advanced Differentiated States. *Cancers (Basel)* **2018**, *10*, 499. [CrossRef] [PubMed]
344. Arif, T.; Stern, O.; Pittala, S.; Chalifa-Caspi, V.; Shoshan-Barmatz, V. Rewiring of Cancer Cell Metabolism by Mitochondrial VDAC1 Depletion Results in Time-Dependent Tumor Reprogramming: Glioblastoma as a Proof of Concept. *Cells* **2019**, *8*, 1330. [CrossRef] [PubMed]
345. Hanahan, D.; Weinberg, R.A. Hallmarks of cancer: The next generation. *Cell* **2011**, *144*, 646–674. [CrossRef] [PubMed]
346. Fulda, S. Tumor resistance to apoptosis. *Int. J. Cancer* **2009**, *124*, 511–515. [CrossRef] [PubMed]
347. Takehara, T.; Liu, X.; Fujimoto, J.; Friedman, S.L.; Takahashi, H. Expression and role of Bcl-xL in human hepatocellular carcinomas. *Hepatology* **2001**, *34*, 55–61. [CrossRef] [PubMed]
348. Ding, Z.; Yang, X.; Pater, A.; Tang, S.C. Resistance to apoptosis is correlated with the reduced caspase-3 activation and enhanced expression of antiapoptotic proteins in human cervical multidrug-resistant cells. *Biochem. Biophys. Res. Commun.* **2000**, *270*, 415–420. [CrossRef] [PubMed]
349. Grobholz, R.; Zentgraf, H.; Kohrmann, K.U.; Bleyl, U. Bax, Bcl-2, fas and Fas-L antigen expression in human seminoma: Correlation with the apoptotic index. *Apmis* **2002**, *110*, 724–732. [CrossRef]
350. Krajewska, M.; Moss, S.F.; Krajewski, S.; Song, K.; Holt, P.R.; Reed, J.C. Elevated expression of Bcl-X and reduced Bak in primary colorectal adenocarcinomas. *Cancer Res.* **1996**, *56*, 2422–2427. [PubMed]
351. Pedersen, P.L. Warburg, me and Hexokinase 2: Multiple discoveries of key molecular events underlying one of cancers' most common phenotypes, the "Warburg Effect", i.e., elevated glycolysis in the presence of oxygen. *J. Bioenerg. Biomembr.* **2007**, *39*, 211–222. [CrossRef] [PubMed]
352. Mathupala, S.P.; Ko, Y.H.; Pedersen, P.L. Hexokinase-2 bound to mitochondria: Cancer's stygian link to the "Warburg Effect" and a pivotal target for effective therapy. *Semin. Cancer Biol.* **2009**, *19*, 17–24. [CrossRef] [PubMed]

353. Pastorino, J.G.; Shulga, N.; Hoek, J.B. Mitochondrial binding of hexokinase II inhibits Bax-induced cytochrome c release and apoptosis. *J. Biol. Chem.* **2002**, *277*, 7610–7618. [CrossRef]
354. Shteinifer-Kuzmine, A.; Amsalem, Z.; Arif, T.; Zooravlov, A.; Shoshan-Barmatz, V. Selective induction of cancer cell death by VDAC1-based peptides and their potential use in cancer therapy. *Mol. Oncol.* **2018**, *12*, 1077–1103. [CrossRef]

Publisher’s Note: MDPI stays neutral with regard to jurisdictional claims in published maps and institutional affiliations.



© 2020 by the authors. Licensee MDPI, Basel, Switzerland. This article is an open access article distributed under the terms and conditions of the Creative Commons Attribution (CC BY) license (<http://creativecommons.org/licenses/by/4.0/>).

Review

Characterization of In Vivo Function(s) of Members of the Plant Mitochondrial Carrier Family

Adriano Nunes-Nesi ^{1,*}, João Henrique F. Cavalcanti ²  and Alisdair R. Fernie ^{3,*}

¹ Departamento de Biologia Vegetal, Universidade Federal de Viçosa, Viçosa 36570-900, Minas Gerais, Brazil

² Instituto de Educação, Agricultura e Ambiente, Universidade Federal do Amazonas, Humaitá 69800-000, Amazonas, Brazil; jcavalcanti@ufam.edu.br

³ Max-Planck-Institute of Molecular Plant Physiology, 14476 Postdam-Golm, Germany

* Correspondence: nunesnesi@ufv.br (A.N.-N.); fernie@mpimp-golm.mpg.de (A.R.F.); Tel.: +55-(31)-3612-5357 (A.N.-N.); +49-(0)331-567-8211 (A.R.F.)

Received: 24 May 2020; Accepted: 13 August 2020; Published: 24 August 2020

Abstract: Although structurally related, mitochondrial carrier family (MCF) proteins catalyze the specific transport of a range of diverse substrates including nucleotides, amino acids, dicarboxylates, tricarboxylates, cofactors, vitamins, phosphate and H⁺. Despite their name, they do not, however, always localize to the mitochondria, with plasma membrane, peroxisomal, chloroplast and thylakoid and endoplasmic reticulum localizations also being reported. The existence of plastid-specific MCF proteins is suggestive that the evolution of these proteins occurred after the separation of the green lineage. That said, plant-specific MCF proteins are not all plastid-localized, with members also situated at the endoplasmic reticulum and plasma membrane. While by no means yet comprehensive, the in vivo function of a wide range of these transporters is carried out here, and we discuss the employment of genetic variants of the MCF as a means to provide insight into their in vivo function complementary to that obtained from studies following their reconstitution into liposomes.

Keywords: mitochondrial carrier family; MCF; function; mitochondria; plant metabolism; plant development

1. Introduction

The characterization of heterologously expressed, liposome-reconstituted proteins has provided considerable insight into the transport capacities of human, yeast and plant MCF members [1–13]. Moreover, inference from phylogenetic analysis has been demonstrated, at least in some cases, to provide good hints as to the function of plant MCF proteins on the basis of the experimentally characterized functions of, for example, yeast proteins with which they share high homology [14]. While these studies have provided a wealth of information concerning the potential substrates that can be transported by a relatively large number of the transporters [15], the biological relevance of these properties remains dependent on the context of where and when they are expressed. The advent of next-generation technologies, and before that of microarrays, has led to the establishment of considerable data regarding the expression of MCF members in *Arabidopsis* [16–19] and several other species ([20,21]). Bioinformatic analysis has revealed that, as for the previous identification of an *Arabidopsis* monolignol transporter [22], co-expression analysis provides clues as to the in vivo function of a range of MCF transporters [23]. In addition, comparative studies are naturally confined to the subfamilies which are conserved across the eukaryotic lineage [14]. Succinate/fumarate carriers are apparently absent in animals while yeasts appear to lack uncoupling proteins (UCPs). The presence of a subfamily in two of the three lineages suggests that it is likely to have been lost—perhaps due to compensation by other transporters rendering it redundant [24]. By contrast, the presence of a

subfamily in a single lineage, for example the mitochondrial GTP/GDP transporter of yeast or the plastidial adenine nucleotide carriers and Brittle1 protein, is likely indicative of an innovation that occurred after the separation of the eukaryotes. In certain functional clades, plants exhibit a higher number of paralogs (although many of these remain to be experimentally proven), which may indicate that gene duplication and/ or retention occurred more often for these transporters in plants. Indeed, this is highly likely, given the documented fact that gene duplication is generally considerably more prominent in plants [25]. While it is tempting to suggest that the increased number of transporters gives flexibility to immobile plants [24], this is unlikely to be the reason, since mobile algae also possess, at least for some clades, more MCFs than human or yeast [14]. A more attractive proposition is thus that plants contain more MCF proteins due to the presence of the plastid organelle [24]. While arguments for this were initially made on comparison of the NAD transporters NDT1 and NDT2 [24], with the former thought to be a plastidial and the latter a mitochondrial localized transporter [26]; this needs revision now that, as detailed below, both have been reclassified as mitochondrial [27,28]. That said, there are several proteins that exhibit dual targeting and thus may fulfill different functions at the different locations. Examples include the dual mitochondrial and plastidial localized SAM [29–31] and Brittle1 transporters [32–34]. Moreover, it is important to note that plant specific MCF proteins including the adenine nucleotide carriers ER-ANT1 and PM-ANT1 do not only comprise plastidial carriers [35,36]. In this article, we will summarize functional insights obtained from evaluating spatio-temporal differences in expression, subcellular localization and finally from the study of transgenic plants exhibiting altered expression of the transporter(s) of interest.

2. Expression of MCF Members

2.1. Environmental Specific Gene Expression

To have a broad view of the expression profile exhibited by MCF genes we used information available in The Bio-Analytical Resource for Plant Biology database [37,38] and prepared a heatmap documenting the relative expression levels of 58 MCs in *A. thaliana* within a wide range of tissues and environmental conditions (Figure 1). We first turned our attention to the MCF gene expression levels under a range of stresses concerning exposure to cold, osmotic, salt, drought, oxidative, UV-B, wounding and heat stress in shoots and roots (Figure 1a,b). Interestingly, out of 58 MCFs, eight transporters (BAC2, DIC2, MTM1, DIC1, PNC2, APC1, PHT3;2 and AAC2) display expression profiles that are highly upregulated in shoots under conditions of cold, osmotic and salt stress whereas the other 50 genes were generally characterized as displaying lower and more specific changes (Figure 1a). In general, in root tissues the expression profile of plants under different stress conditions appears to be independent of the alterations verified in shoots suggesting a molecular plasticity between the tissues in response to environmental stress (Figure 1a,b). However, seven transporters (BAC2, DIC1, DIC2, MTM1, PHT3;2, AT3G55640 and PNC2) are highly upregulated under cold, osmotic and salt stress (Figure 1b). Of the seven genes highly expressed in roots, six were also upregulated in shoots, but the importance of these genes seems to be different during the stress in the two organs. For example, BAC2, an amino acid transporter, exhibits a moderate expression in roots of plants submitted to few hours of osmotic and salt stress (Figure 1b); however in shoots BAC2 is highly upregulated shortly after the beginning of stress application, remaining highly expressed during the whole period of stress exposure (Figure 1a). In this context, it is noteworthy that compelling evidence suggests that BAC2 plays a role in mechanisms of nitrogen recycling during stress establishment and recovery [39,40]. Furthermore, genes encoding UCP subfamily members are highlighted as stress-response genes [41,42]. Even though their role in plant metabolism is currently unclear, evidence suggests that UCP activity acts to dissipating the proton gradient generated on ATP synthesis while preventing the accumulation of reactive oxygen species under stress [43]. However, UCP isoforms are specifically induced and/or repressed in diverse conditions, despite being generally downregulated (Figure 1a). The transcript levels of UCP1 and UCP2 were not induced under the different stress conditions. This finding is in

agreement with a study by Van Aken et al. [44], which suggests that the UCP proteins are not among the most stress responsive mitochondrial proteins. Other interesting patterns are also apparent from our in silico expression analysis; for example, when the expression profile of PiC2 (a phosphate transporter also known as PHT3:2) is studied, distinct patterns are apparent in roots and shoots (Figure 1a,b). In roots only, a moderate increase in expression was observed after 6-h exposure to salt stress, while in shoots, gene expression was highly upregulated by cold, osmotic, salt, oxidative, UV-B and wounding stresses. Differential root and shoot expression patterns are also apparent for DIC1, DIC2 and PNC2 displaying differences in expression under cold and salt stress in roots and cold, osmotic, salt, oxidative, UV-B and wounding stress in shoots, respectively.

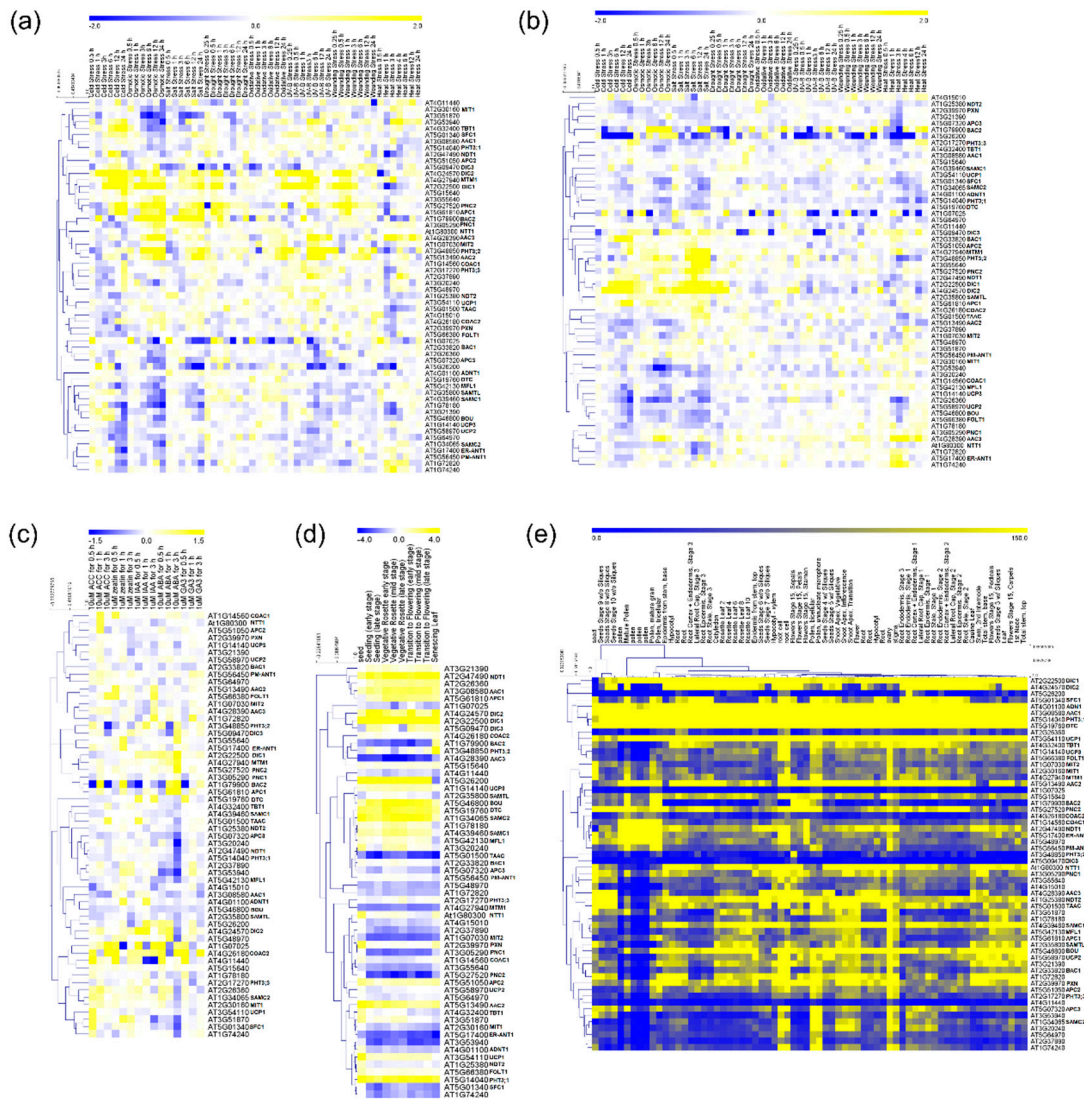


Figure 1. Hierarchical cluster of gene expression analysis of mitochondrial carrier family (MCF) genes of *Arabidopsis thaliana*. Heat map of MCF genes in shoots (a) and roots (b) of plants under a range of stress situations. Heat map of MCF genes expression in plants submitted to hormone treatment (c), throughout plant development (d) and in several tissues (e). The values are stated as log₂ ratio (a–d) and relative value (e). The complete data set is presented in the supplemental information online (Supplementary File S1). For definitions of gene names, please see the main text.

2.2. Hormone Treatment Gene Expression

Differential gene expression profiling following hormone treatment provides interesting clues as to the putative roles of MCF members within plant metabolism. Compelling evidence suggests

a close association between hormones with energy metabolism [45,46]. However, to date, there is a lack of studies into the role of MCF members in this vein. Our meta-analysis of the Arabidopsis expression profiling database [37,38] reveals that hormone application MCF members are most responsive to abscisic acid (ABA), with seven genes affected negatively by application of ABA (APC3, AT2G37890, AT3G53940, MFL1, AAC1, AT3G51870, SFC1). By contrast, BAC2, APC1 and COAC2 are highly upregulated following ABA treatment (Figure 1c). Interestingly, APC family members exhibit differential dynamics influenced by ABA, with APC1 being upregulated while APC3 decreases following application of ABA. While these observations suggest that shed MCFs may be associated with hormone effects in vivo investigations are required in order to confirm this.

2.3. Developmental-Specific Gene Expression

Since transporters are an essential component linking the entirety of cellular metabolism and integrating branched biochemical pathways among subcellular compartmentalization their importance throughout the plant lifespan can be anticipated (Figure 1d). MCF gene expression profiling across development shows two distinct patterns, with one set of genes being upregulated while others are downregulated. Some insight into MCF function may be retrieved from Figure 1d. The expression of adenylate carriers at specific stages of development (Figure 1d) indicates a strong induction of AAC1 and APC1 in senescent leaves. Interestingly, a moderate induction of expression of AAC2 and APC2 is observed in the same tissues, concomitantly with a reduction of AAC3, ADNT1, ER-ANT1 and PM-ANT1 expression. Thus, it appears that natural senescence causes remarkable changes in the expression of different adenylate carriers in plants [23]. Furthermore, BAC2 displays low transcript levels in most development stages, even lower levels during shoot senescence and higher expression in senescing leaves (Figure 1d). Nevertheless, it has been suggested that BAC2 plays a role during senescence being involved in nitrogen remobilization [39,40]. Considering that adenylate carriers might also act during natural senescence [23], it appears that BAC2 shows a synergy with energy generation beyond nitrogen recycling per se. Since natural senescence is characterized by carbohydrate starvation, amino acid degradation (e.g., lysine and arginine; both amino acids transported by BAC2) by mitochondria can most likely sustain energy demand by the cell [47–49]. Despite the association between adenylate carriers and BAC2 transporter being interesting, further experimental validation is required to ensure that the observed coexpression is biologically relevant and to test the above-mentioned hypothesis.

2.4. Tissue-Specific Gene Expression

We next evaluated the expression profiles of MCF genes across plant tissues (Figure 1e). Several MCF transporters (for example AT4G11440, SFC1) are expressed constitutively in different tissues, suggesting that they are involved in essential housekeeping functions. By contrast, the majority of the biochemically characterized MCFs are differentially expressed among different cell types. Particularly, the NAD transporter NDT1 [27], AAC1, AAC2, and SAMC1 [29,31] are highly expressed in mature pollen and also developing seeds, which is in agreement with the reported import of NAD, ADP and methionine [31,50] into mitochondria of these tissues. Other transporters, including CAC, DIC1, DIC2, NDT1, AAC1, AAC2, BAC2 and a few, as yet, uncharacterized proteins, were predominantly expressed in pollen, seeds and vegetative rosettes, while many genes of unknown function were predominantly expressed in embryo and seedling stages or in heterotrophic root and stem tissues. As for the other transcript data described above, it is important to note that conclusions related to function await validation.

3. Subcellular Localization of MCF Members and Characterization of Lines Deficient in the Expression of the Transporters

Of the 58 MCF members in Arabidopsis, only 28 have thus far been reported to localize to the mitochondria by organellar proteomics and localization by fluorescent protein tagging, while a

total of 12 MCF members have been reported (sometimes erroneously) to localize elsewhere [51,52]. As mentioned above, these lists are reliant either on the specific expression of fluorescent fusion proteins or are based on proteomics on highly purified organelles the results of which have been used to generate databases such as SUBA [53] and ARAMEMNON [54]. These studies reveal the presence of MCF members at several other locations including the peroxisome, plastid and endoplasmic reticulum (Figure 2) [29,35,55–61]. Here, we detail the localization experiments alongside characterization of mutants/transgenic lines of the transports focusing on the underlying mechanisms by which the in vivo function of these proteins are realized. Given that the function of those transporters whose function is intimately related to plant respiration have been reviewed very recently [52], we will only cover these in brief here and spend greater time discussing transporters with different functions.

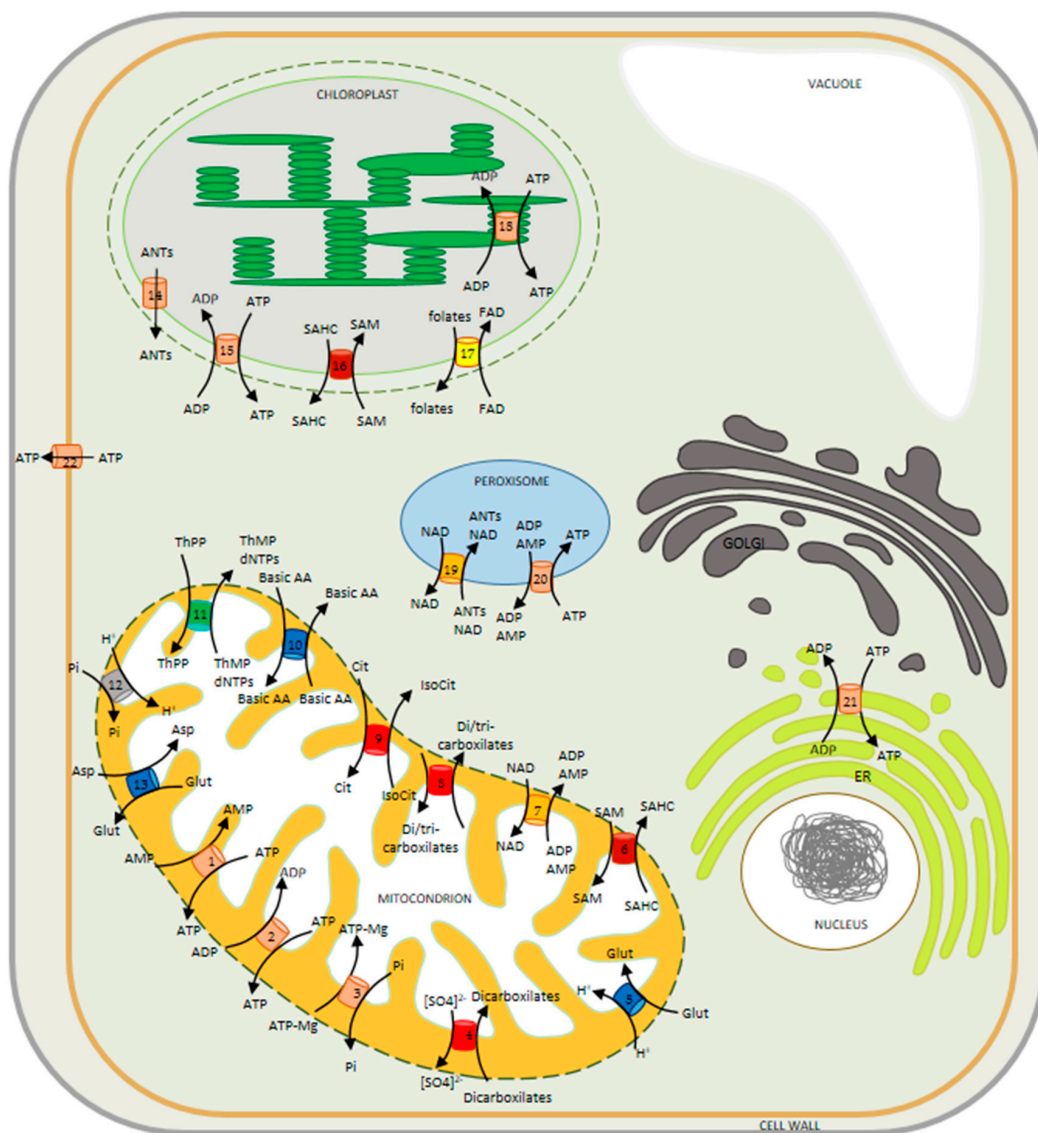


Figure 2. Model illustrating the mitochondrial carriers described and characterized in plant cells. All carriers belong to the mitochondrial carrier family (MCF). Carriers localized in the inner mitochondrial membrane: (1) ATP/AMP carrier, ADNT1; (2) ATP/ADP carriers, AACs; (3) AMP-ADP-ATP/Pi carriers, APCs; (4) dicarboxylate carriers, DIC1-3; (5) glutamate-H⁺ carrier, BOU;

(6) *S*-adenosylmethionine carrier, SAMC1; (7) NAD carriers, NDT1-2; (8) dicarboxylate/tricarboxylate carrier, DTC; (9) Citrate/isocitrate carrier, SFC1; (10) basic amino acids carries BAC1-2; (11) thiamine pyrophosphate carrier; TPC; (12) phosphate (Pi) carriers, PiC1-3; (13) uncoupling protein, UCP1-2. Carriers localized in the inner membrane of chloroplast: (14) ATP/ADP/AMP exporter, ATBT1; (15) ATP/ADP carrier, NTT1; (16) *S*-adenosylmethionine carrier, SAMC1; (17) folates transporter, FOLT1. Carrier localized in the membrane of thylakoid: (18) ATP/ADP transporter, TAAC. Carriers localized in the membranes of peroxisome [NAD transporter (19); adenine nucleotide carriers, PNC1/2 (20)], endoplasmic reticulum [ATP/ADP exchanger, ER-ANT1 (21)] and plasma membrane [ATP exporter, PM-ANT1, (22)]. The colors on transporters indicate the subfamilies of mitochondrial carriers, defined by substrate specificity; being red-orange for adenylates transporters; red for di-/tri-carboxylates transporters; dark-red for *S*-adenosylmethionine transporters; yellow for folate/FAD transporter; blue for amino acids transporters; orange for NAD transporters; gray for phosphate transporter; and green for thiamine pyrophosphate transporter. Abbreviations: Asp, aspartate; ANTs, adenine nucleotides; Basic AA, Basic amino acids; Cit, citrate; dNTPs, deoxynucleoside triphosphates; ER, endoplasmic reticulum; Glu, glutamate; IsoCit, isocitrate; SAM, *S*-adenosylmethionine; SAHC, *S*-adenosylhomocysteine; ThPP, thiamine pyrophosphate; ThMP, thiamine monophosphate.

3.1. Non-Mitochondrial MCFs

We include here all MCFs that have been reported as non-mitochondrial, although we stress that for at least one of these, highly convincing evidence exists that it is indeed mitochondrial. Three MCFs contain no N-terminal presequence and are localized at the endoplasmic reticulum (ER-ANT; [35]), Golgi apparatus (UCP2; [62]) or plasma membrane (PM-ANT; [36]). Current thinking suggests that these localizations are due to the specific transmembrane domain lengths in these proteins which resemble the average for their respective locations [63]. However, UCP2 has alternatively been reported to reside in the mitochondria [64] and as such its localization should currently be regarded as unclear. Six further MCF members have been reported to be found in plastids—with four of these proteins having cleavable N-terminal presequences and in the case of Brittle 1, the removal of this presequence targeted the protein to the mitochondrion [34]. One of the two transporters lacking a cleavable N-terminal presequence NDT1 was subsequently convincingly demonstrated not to be plastidic but rather mitochondrial by a wide range of evidence (see [27] for details). This casts doubt on localization results based purely on fluorescent marker proteins and acts as a cautionary note that it is better to adopt multiple strategies for assignment. As such, we will discuss the function of NDT1 in detail, below; however, given that some ambiguity exists concerning the location of UCP2 we will treat this as a non-mitochondrial member for now. The final members of this list (PNC1/2 and PXN) all reside in the peroxisome despite the fact that none of them contained either classical PTSI C-terminal sequence or the N-terminal presequences observed for plastid targeted MCF proteins [57,65].

Assigning the location of these proteins, as well as assessing their patterns of transcription, provides some contextualization for their *in vivo* function. However, far more insight can be achieved by evaluating the biological roles of the transporters by assessing plants deficient in the expression of the transporters in question and when possible comparative physiology between these mutants and their counterparts in yeast. Of the 11 family members (at least putatively) assigned a non-mitochondrial location; however, this is often not possible. That said the peroxisomal nucleotide carriers PNC1 and PNC2 are functionally highly similar to their yeast counterparts [57,66]. Investigation of transgenic *Arabidopsis* lines has revealed that PNC1 and PNC2 play an essential role in energy provision via their catalysis of the counter exchanges of ATP with ADP or AMP to plant peroxisomes, and that lack of these proteins impairs fatty acid breakdown and other peroxisomal reactions, including auxin metabolism [57]. The third reported MCF that localizes to the peroxisome is PXN, which was confirmed to catalyze NAD⁺ uptake in exchange mainly with AMP but also with NADH, ADP and nicotinate adenine dinucleotide. The absence of this carrier in *Arabidopsis* led to an accumulation of oil bodies in seedlings and an impaired peroxisome localized β -oxidation [65]. The ER-ANT1 *Arabidopsis* knockout mutant exhibits stunted growth but survives and produces fertile seeds [67],

this work thus suggested the presence of a further carrier(s) capable of energy provision to the ER. The presence of such a transporter was recently supported by the characterization of the mammalian AXER protein—for which an Arabidopsis homolog has been identified [68]. By contrast, the PM-ANT1 is highly expressed in developing pollen and plants exhibiting a mutation in this carrier are impaired in flower development particularly during anther dehiscence. These phenotypes were interpreted to suggest that the transporter mediates ATP export specifically from pollen cells and that enhanced eATP acts as a signal that is received by the stromium cells of the anther [36]. As for the ER-ANT, it can be supposed that Arabidopsis contains other proteins that mediate ATP export at the plasma membrane since the effects of downregulating PM-ANT were confined to the flower [24], while the role of extracellular ATP is far more widespread [69]. Before turning to the plastid localized members of the MCF—one final other member needs to be discussed, UCP2. As we mentioned above, it is currently ambiguous where this is localized with it variously being reported to localize to the Golgi apparatus and the mitochondria, as detailed in our accompanying article [15]. UCP2 displays similar substrate specificities to UCP1 [64] and knockout of either transporter in Arabidopsis resulted in similar metabolic phenotypes consistent with both transporting organic acids. However, notably, the metabolic phenotype of *ucp1ucp2* double mutants under salt stress is more reminiscent of the *ucp1* than the *ucp2* single mutant, suggesting that UCP1 plays the dominant role under these conditions [64]. This fact notwithstanding, proteomics analyses have suggested, in contrast to the GFP fluorescence studies of Monne et al. [64], that UCP2 actually resides at the Golgi apparatus [62]. As such, further research is imperative to establish both the location and function of this isoform.

Having described those few transporters (potentially) localized to the peroxisome, endoplasmic reticulum, Golgi apparatus and plasma membrane we next turn to the five MCF members believed to localize to the plastid. It is perhaps unsurprising that the most similar organelle to the mitochondria harbors so many MCF members or the breadth of substrates that they cover being reported to transport adenylates, folates, FAD, *S*-adenosine methione (SAM) and iron. Taking these one by one, two transporters have been implicated in adenylate transport pANT1 and the thylakoid lumen transporter TAAC [70]. pANT1 has been demonstrated to locate either to the plastid [61] in the presence of its N-terminal extension, or to the mitochondria in its absence [34]. However, as yet, unlike its paralog Brittle1 in maize [71,72], mutants of the Arabidopsis gene remain to be characterized. This is not the case for the TAAC transporter, however, with loss of function mutants leading to the assumption that this transporter mediated ATP provision to the thylakoid lumen. As such, it was suggested to play a role in photoinhibition and photoprotection of photosystem II, as well as regulating the electrochemical proton gradient across the thylakoid membrane [73]. However, although these roles are not obviated by the later finding that the TAAC is also located at the plastid envelope [70], they do probably need critical reassessment particularly given that its transcript and protein abundances also suggest it to play a role in developing plastids that are essentially free of thylakoids [24]. Next in the list is FOLT1, which catalyzes the transfer of folate and its derivatives [60,74]. The absence of major phenotypical differences in the loss of function mutant was taken to suggest the presence of an additional plastidial folate transport system with the fact that the major facilitator family transporter has been demonstrated to transport FAD [75], perhaps being part of such a system. A highly similar member of the MCF, namely NDT1, was additionally proposed to have a plastidial localization on the basis of GFP fluorescence analysis alone [26]; however, more comprehensive evaluation including that of Arabidopsis knockout mutant revealed that NDT1, like NDT2, actually resides at the inner mitochondrial membrane (IMM) [27,28]. We discuss this in detail below. Suffice it to say the fact that plastids lack the enzymatic machinery to make NAD^+ means that a transporter capable of importing it into the plastid remains to be found. More clear is the localization of the SAM and *S*-adenosylhomocysteine (SAHC) transporter. SAM, like NAD^+ , is synthesized exclusively in the cytosol and has to be exported to the organelles where it is needed as substrate [76]. For this purpose Arabidopsis harbors two homologs to the transporters from yeast and mammalia [30,77], the N-terminal sequence of SAMC1 targets it to the plastid whereas SAMC2 resides at both plastid and mitochondrial membranes [29,31]. Moreover, loss of SAMC1

function resulted in a dwarf phenotype and a compromised prenyl lipid metabolism [29]. Finally, the mitoferrin-like transporter Mfl1 is a component of the inner plastid envelope and investigations into the corresponding mutant plants suggest its involvement in iron uptake by the chloroplast and revealed that it displayed reduced vegetative growth [78].

3.2. Mitochondrial MCFs

Counterintuitively, the mitochondrially localized MCFs are arguably less well characterized than those that localize to other membrane systems—largely due to the complexities that arise as a result of overlap or even redundancy of function. That said, several of the 28 proteins which have been identified to be present at the IMM have been well characterized, and many more have been at least partially characterized. While we grouped the transporters described in the previous section on the basis of their location here it makes more sense to group according to substrate specificity.

3.2.1. Coenzyme A Transporters

Plants produce coenzyme A (CoA) in the cytosol which is then imported into the organelles where it is used in essential pathways such as the tricarboxylic acid (TCA) cycle in the mitochondria, fatty acid synthesis in the chloroplast, and β -oxidation in peroxisomes. A plant peroxisomal CoA transporter also able to transport NAD was identified and named peroxisomal NAD⁺ carrier (PXN; [79]) and also discussed in the previous section. In addition to CoA, PXN was shown to be able to accept as substrates NAD⁺, NADH, AMP, ADP, and adenosine 3',5'-phosphate [65,79]. The lack of PXN in Arabidopsis seedlings delays the breakdown of fatty acids released from storage oil and thereby leads to the retention of oil bodies. This phenotype indicates that a defective PXN function leads to defects in β -oxidation during seedling establishment suggesting that PXN delivers NAD⁺ for optimal fatty acid degradation during storage oil mobilization [65]. Regarding specifically the mitochondrial CoA transporters, MCFs members putative CoA transporters were first identified in *Saccharomyces cerevisiae* [80] and mammals [81]. Next, comparative genomic analysis showed that nonflowering plants have one homolog of these mitochondrial CoA transporters, whereas in angiosperms plants have two distinct homologs [82]. The homolog proteins from maize (GRMZM2G161299 and GRMZM2G420119) and Arabidopsis (At1g14560 and At4g26180) are able to complement the growth defect exhibited by yeast mitochondrial CoA carrier mutant and also restore its mitochondrial CoA level, suggesting that these proteins have CoA transport activity in mitochondrial membrane [82]. Despite current knowledge related to the identity of CoA transporter candidates and the important function of CoA for mitochondrial reactions in plants, functional characterization of mutant plants, as well as biochemical properties, such as substrate specificities, still remain to be investigated.

3.2.2. Phosphate Transporters

The orthophosphate (Pi) uptake by the mitochondrial matrix is essential for the oxidative phosphorylation of ADP to ATP. In Arabidopsis, three genes were identified as encoding mitochondrial Pi carriers (*AtMPTs*), all members of MCF [83]. Expression analysis demonstrated that *AtMPTs* are upregulated by high-salinity stress in *A. thaliana* seedlings [84]. Overexpressing *AtMPTs* in Arabidopsis resulted in plants with a higher sensitivity to salt stress during seed germination and seedling establishment stages, as well as higher ATP content and energy charge in comparison with wild-type plants under salt stress. Further analyses revealed that activity *AtMPTs* might be involved with gibberellin metabolism in *A. thaliana* during salt stress. Recently, it was shown that *AtMPT3* overexpression displays multiple developmental defects in Arabidopsis plants including dwarfed stature and reduced fertility [85]. In addition to changes in transcription of genes involved in plant metabolism and leaf and flower development, *AtMPT3* overexpressing plants exhibited higher ATP content, faster respiration rate, and increased reactive oxygen species (ROS) production. Taken together, these studies demonstrated the importance of *MPTs* activity for plant growth and development under

optimal and adverse conditions, through complex regulatory mechanisms related not only with ATP production but also with development and signaling processes.

3.2.3. NAD Transporters

In addition to the peroxisome NAD transporter (PXN) described above, two other MCF members, namely *AtNDT1* and *AtNDT2*, are able to catalyze the import of NAD in organelles [26]. These proteins were able to complement the phenotype exhibited by yeast mutant lacking NAD⁺ transport [26]. In the same study, it was demonstrated that *AtNDT1* and *AtNDT2* are capable of importing NAD⁺ against ADP or AMP, and do not accept NADH, NADP⁺, NADPH, nicotinamide or nicotinic acid as transport substrates. Despite the similarities in terms of biochemical properties of these transporters, initial GFP-protein localization analysis indicated that *AtNDT1* was located in the plastid membrane and *AtNDT2* in the mitochondrial membrane [26]. However, as discussed in the previous section, the plastid localization of *AtNDT1* was, for a long time, not well accepted, since GFP-tagging and immunolocalization analyses were not able to find *AtNDT1* targeted to chloroplast membranes [60] and a recent proteome study identified *AtNDT1* in mitochondrial membranes [86]. Recently, both *AtNDT1*- and *AtNDT2*-GFP fusion proteins were found exclusively located in the mitochondria, clearly indicating their mitochondrial localization [27]. Despite the similar biochemical properties and the same subcellular localization, the biological characterization of *AtNDT1* and *AtNDT2* proteins revealed that both proteins play important and non-redundant functions in Arabidopsis plants [27,28]. Physiological and metabolic analyses of plants with reduced *AtNDT1* expression, revealed increased leaf number and leaf area which was concomitant with increased photosynthetic activity and starch accumulation [27]. In addition to other analyses, these results suggested that downregulation of *AtNDT1* alters NAD⁺ metabolism and transport, leading to metabolic shifts which increased photosynthesis, activation state of the stromal NADP dependent malate dehydrogenase (NADP-MDH) and starch accumulation. Moreover, it was verified that plants with impaired *AtNDT1* transport exhibited reduced pollen grain viability, tube growth, short siliques and higher rate of seed abortion, demonstrating the important role of *AtNDT1* in reproductive tissues. Similarly, plants with reduced expression of *AtNDT2* were affected in reproductive phase [28]. The plants with impaired NDT2 transport exhibited a reduced seed yield, followed by reduced seed germination and retardation in seedling establishment. Remarkably, NDT2 mutants exhibited changes on primary metabolism in dry and germinated seeds and an increase in fatty acid levels observed during seedling establishment. Interestingly, flowers and seedlings of NDT2 mutants displayed upregulation of *de novo* and salvage pathway genes encoding for NAD biosynthesis enzymes, suggesting that these genes have a transcriptional control mediated by NDT2 activity. Recently, it was suggested that *AtNDT2* protein might be a key regulator of the mitochondrial NAD⁺ and NADH pools and compromised NAD⁺ import activity in *ndt2* mutants cannot be fully compensated for by other transporters [87], highlighting the importance role of NDT2 for NAD⁺ import by plant mitochondria. Taken together, these results suggest that correct NDT1 and NDT2 expression is necessary for maintaining NAD⁺ balance among organelles that modulate metabolism, physiology and developmental processes in plant tissues.

3.2.4. Uncoupling Proteins

Uncoupling proteins (UCPs) have been described as being involved in the dissipation of proton gradients across the IMM that is normally used for ATP synthesis [64,88]. Based on homology with UCP from humans, former studies identified six genes in Arabidopsis genome (*AtUCP1*–6) encoding putative UCPs [89]. Formerly, it was shown that the isoform *AtUCP1* (At3g54110) is localized to IMM and exhibits the activity of uncoupling protein similar to the human UCP1 [88–90]. The function of the other isoform *AtUCP2* (At5g58970) was less understood because it was detected in the Golgi apparatus [62] and also in the plasma membrane [63]. Recently it was shown that, exactly like *AtUCP1*, *AtUCP2* is also a mitochondrial localized protein [64]. Astonishingly, both *AtUCP1* and *AtUCP2* were shown to be able to transport amino acids (glutamate, aspartate, cysteine sulfinate, and cysteate), dicarboxylates (malate,

oxaloacetate, and 2-oxoglutarate), phosphate, sulfate, and thiosulfate [64]. In addition, it was verified that both proteins catalyze an electroneutral aspartate/glutamate heteroexchange activity, in contrast to that mediated by the mammalian mitochondrial aspartate glutamate carrier. Three other former members of the *AtUCP* subfamily of Arabidopsis MCF (*AtUCP4-6*) were renamed as dicarboxylate carriers (*AtDIC1-3*), because these proteins transport oxaloacetate, malate, succinate, phosphate, sulfate, thiosulfate, and sulfite [91].

Regarding the physiological role of UCP proteins in plants, several studies have been performed. In Arabidopsis plants, the silencing of *AtUCP1* resulted in lower photosynthetic rates, specifically caused by restricted photorespiration, with reduced oxidation of photorespiratory glycine in the mitochondrion [88]. This study indicated that the function of *AtUCP1* is related to maintaining the redox poise of the mitochondrial electron transport chain and thus facilitating the photosynthetic metabolism in the chloroplast [88]. Uncoupled mitochondrial respiration might be important in plants undergoing stress situations, during which both respiration and photosynthesis may be impaired. In agreement, overexpressing *AtUCP1* in the IMM increases uncoupling respiration, reducing the cellular ATP content, and also decreasing the accumulation of reactive oxygen species (ROS) under abiotic stresses [92]. Transcriptome and metabolite analyses demonstrated that UCP1 overexpression in tobacco plants induces a hypoxic stress that disrupts cellular energy homeostasis and triggers a reconfiguration of metabolism [93]. Under stress conditions, the UCP activity would maintain the redox poise inside the mitochondria and in the chloroplasts allowing photosynthesis and mitochondrial activity. To verify the role of UCP1 in plant responses to drought stress, it was hypothesized that UCP1 overexpression would help tobacco plants cope with drought stress [94]. As expected, the UCP1 overexpressing plants maintained higher rates of respiration and photosynthesis and reduced the levels of H₂O₂ in leaves during the drought stress period. Together, these results demonstrated the importance of UCP1 under both optimal conditions and drought stress [94]. These results clearly demonstrate the importance of UCP1 in plant stress responses.

As mentioned above, in addition to the uncoupling function of UCPs, it was recently demonstrated that *AtUCP1* and *AtUCP2* are able to transport of amino acids and dicarboxylic acids through the IMM [64]. It is also suggested that *AtUCP1* and *AtUCP2* also catalyze an aspartate_{out}/glutamate_{in} exchange across the mitochondrial membrane and, thereby, contribute to the export of reducing equivalents from the mitochondria in photorespiration [64]. Notably, *AtUCP1* and *AtUCP2* have broad substrate specificities, especially the dicarboxylates intermediates of TCA cycle. Thus, in agreement with previously proposed role of *AtUCP1* in photorespiration and photosynthesis [88], the role of *AtUCP1* and *AtUCP2* might be related with glycolate pathway for the shuttling of redox equivalents across the mitochondria as part of the malate/aspartate shuttle [52,64].

3.2.5. Organic Acid Transporters

Several metabolites associated with the activity of TCA cycle should be exchanged across the IMM to link several mitochondrial enzymes to those in other cellular compartments [51,95]. In plants, three sub classes of MCF members are involved in the transport of organic acids, which are likely relevant for the activity of TCA cycle and reactions occurring in other organelles: dicarboxylic acid carriers (DICs), dicarboxylic/tricarboxylic acid carriers (DTCs), and succinate/fumarate carrier (SFC). These transporters are discussed in the following subsections.

Dicarboxylic Acid Transporters

As indicated above, in the Arabidopsis genome, three potential homologues of yeast and mammalian mitochondrial dicarboxylate carriers (DICs), previously reported as *AtUCP4-6*, were described and designated as *AtDIC1-3* (*AtDIC1*, At2g22500; *AtDIC2*, At4g24570; and *AtDIC3*, At5g09470) [91]. *AtDIC3* shares only 55–60% identical amino acids with *AtDIC1* and *AtDIC2*, whereas *AtDIC1* and *AtDIC2* share 70% identical amino acids, suggesting that *AtDIC1* and *AtDIC2* are more closely related [91]. In a recent mitochondrial proteomic study it was verified that *AtDIC3* is not as

highly expressed as *AtDIC1-2*, with *AtDIC1* being more abundant than *AtDIC2* (59 and 21 protein copies per mitochondria respectively) [96]. The Arabidopsis DICs transport several dicarboxylates including malate, oxaloacetate and succinate as well as phosphate, sulfate and thiosulfate at high rates, whereas 2-oxoglutarate was revealed to be less preferred substrate. The kinetic properties of recombinant *AtDIC1-3* proteins were also evaluated [91]. Despite the identification and characterization of the biochemical properties of DICs proteins in Arabidopsis, the physiological functions of these transporters have still not been elucidated. Surprisingly, according to our current knowledge, the isolation and characterization of mutant plants for each *AtDIC* isoforms still need to be performed. This fact led us to different questions regarding the physiological roles of these carriers in plants under distinct physiological conditions.

Dicarboxylic/Tricarboxylic Acid Transporters

Dicarboxylate/Tricarboxylate carriers (DTCs) are proteins that catalyze the transport of dicarboxylic acids (such as malate, maleate, oxaloacetate and 2-oxoglutarate) and tricarboxylic acids (such as citrate, isocitrate, *cis*-aconitate and *trans*-aconitate) across the IMM [97]. These transporters are the most abundant MC proteins in the IMM of Arabidopsis, comprising about 0.8% of the total IMM area (6836 protein copies per mitochondria) [96]. Unlike the other three more abundant carrier proteins in the IMM (ADP/ATP carriers (*AtAAC1-3*) and mitochondrial phosphate carriers (*AtMPT2-3*) and uncoupling proteins (*AtUCP1-3*), only one DTC homolog was identified in Arabidopsis (*At5g19760*). DTC proteins have also been reported in different plant species [97–101]. Interestingly, the number of DTC homologs in different plant species varies without a pattern; in the Brassica genus, the number of DTC homologs varies from one in *A. thaliana* and *Arabidopsis lyrata*, two in *Brassica oleracea*, and three in *Brassica rapa* [52], and four in tobacco (*NtDTC1-4*) [97]. Biochemical characterization of *AtDTC* and *NtDTCs* revealed that the transport activity of these proteins involves an obligatory electroneutral exchange of dicarboxylates such as malate and 2-oxoglutarate and tricarboxylates such as citrate [97]. Furthermore, it was demonstrated that DTCs are able to catalyze homoexchange transport activities, such as dicarboxylate/dicarboxylate and tricarboxylate/tricarboxylate [97]. This biochemical characterization of DTCs also demonstrated that these proteins are able to transport several intermediates of the TCA cycle, with the exception of succinyl-CoA and fumarate, for which there is no available information.

Succinate/Fumarate Transporter

Considering that degradation of storage compounds at early stages of seedling development is essential to plant development, providing energy and intermediates required for construction of the photosynthetic apparatus and thus allowing autotrophic growth, the transport of metabolites from and into mitochondria is essential. In this regard, a homologue of the mitochondrial succinate/fumarate carrier from yeast (*Sfc1p*) was identified in the Arabidopsis genome and named as *AtSFC1* [102]. Recently, biochemical characterization of the *AtSFC1* encoded protein demonstrated that this carrier transports citrate, isocitrate and aconitate and, to a lesser extent, succinate and fumarate [103]. Further gene expression analysis in Arabidopsis indicated that *AtSFC1* is highly expressed in heterotrophic tissues. In agreement, lower expression of *AtSFC1* reduced seed germination and impaired radicle growth, a phenotype that was related with reduced root respiration rate. Together, these results suggested that *AtSFC1* is involved in storage oil mobilization at early stages of seedling growth and might be important for nitrogen assimilation in root tissues by catalyzing citrate/isocitrate or citrate/succinate exchanges [103]. Notwithstanding that *SFC1* was previously supposed to be a succinate/fumarate carrier [102], the fact that mitochondria lack the transport machinery capable of importing succinate into the mitochondria from lipid mobilization during seed germination remains to be understood.

3.2.6. Amino Acid Transporters

In plants, as well as in other organisms, mitochondria play an important role in amino acid metabolism. Several intermediates needed for amino acid biosynthesis are intermediates of the TCA cycle, and, conversely, amino acids may be converted into TCA cycle intermediates [104]. In addition, reactions involved in the catabolism of amino acids take place in mitochondria [48,105]. Thus, amino acid transporters must play important roles in the import of amino acids and the export of precursors for biosynthetic pathways.

Research efforts have been devoted to understanding the roles of a putative amino acid transporter named A BOUT DE SOUFFLE (BOU), which was identified in *Arabidopsis* (At5g46800) for a long time [106]. Physiological characterization of BOU transporter in plants indicated that this protein plays important roles in fatty acid β -oxidation [106], photorespiration and growth of meristem cells [107]. Seedlings from the *bou* mutant stopped developing after germination and degradation of storage lipids but were not able to proceed towards autotrophic growth. Further analyses revealed that the *bou* mutant's post germination phenotype is similar to that displayed by mutants impaired in fatty acid β -oxidation indicating that BOU might be a mitochondrial acyl-carnitine carrier [106]. Further studies demonstrated that BOU gene is co-expressed with photorespiratory genes in leaf tissues, suggesting that this transporter might be involved with photorespiration [107]. Physiological characterization of the knockout mutant *bou-2* showed that the mutant plants exhibit the typical photorespiratory growth phenotype, together with elevated CO₂ compensation point and glycine accumulation. Furthermore, it was observed that the shoot apical meristem organization is compromised in seedlings from the *bou-2* line. These results demonstrated that BOU transporter might be involved in photorespiratory metabolism and is necessary for meristem growth at ambient CO₂ [107]. Despite the studies indicating the important function of BOU transporter in plants, the specific substrate for the BOU transporter protein was revealed only recently [108]. Detailed biochemical characterization of *Arabidopsis* BOU and YMC2P from *S. cerevisiae* revealed the transport properties and kinetic parameters of these proteins. Both YMC2P and BOU proteins are able to transport glutamate, but not other amino acids or many other tested metabolites [108]. Together these studies demonstrated that BOU protein, by importing glutamate into mitochondria, plays an important role in carbon and nitrogen metabolism and potentially also mitochondrial protein synthesis.

In *Arabidopsis*, another two MCF members, *AtBAC1* (At2g33820) and *AtBAC2* (At1g79900), catalyze the transport of basic amino acids through the IMM [9,109–111]. Sequence analysis indicated that *AtBAC1* shares 36% of identity with BOU, whereas *AtBAC2* is 40% similar to the human SLC25A29 transporter, although it is also related to BOU (36% identity) and aspartate/glutamate carriers (AGCs; 30–33% identity) [9]. Experiments with recombinant proteins from *AtBAC1* and *AtBAC2* reconstituted in liposomes indicated that both proteins transport lysine, arginine, ornithine and histidine [109,110]. These transporters exhibit differences in terms of substrate specificity; in comparison with *AtBAC1*, the isoform *AtBAC2* is less specific for L-amino acids and also the only *AtBAC* able to transport the neutral amino acid citrulline [109,110].

Regarding the physiological roles of these proteins, the two *AtBACs* seem to play different functions in plants. It has been demonstrated that *AtBAC1* is likely involved in remobilization of storage compounds after seed germination in *Arabidopsis* and rice plants [109,111,112]. Meanwhile, *AtBAC2* seems to play an important role during stress recovery, since it seems to be more expressed in responses to hyperosmotic stress and also during dark induced senescence [39,40]. It was demonstrated that overexpression of *AtBAC2* in transgenic plants allows plants to use arginine as a source of nitrogen [39] and that this isoform of BAC is necessary for the complete recovery of leaf growth after hyperosmotic stress [40]. These results are in agreement with studies demonstrating that some amino acids accumulate in plant tissues during stress establishment and are degraded during the period of stress recovery [48,113]. Thus, the arginine transport, mediated by *AtBAC2*, and degradation inside the mitochondria might be important in reducing the excess of arginine, recycling the nitrogen and urea and thus providing intermediates for the synthesis of primary molecules necessary for plant

growth during stress recovery [40]. Furthermore, in the same study, transcription analysis revealed that under stress conditions *AtBAC2* expression affects the transcript levels of several genes such as those encoding stress-related transcription factors, arginine metabolism enzymes, and transporters. Taken together, these studies indicate the clear importance of basic amino acid mitochondrial transport in responses to hyperosmotic stress.

3.2.7. Iron Transporters

Mitochondrial iron (Fe) transporters, also named Mitoferrins (mIT), were first identified and characterized in drosophila, zebrafish and humans [114–116]. In plants, a mIT homolog was first identified in rice [117]. In this species, a silenced mutant line for mIT resulted in a lethal phenotype. The mIT protein from rice was able to complement the growth of yeast mutant which was defective in mitochondrial Fe transport. Interestingly, the growth of mIT-knockdown rice mutant plants was impaired despite abundant Fe accumulation [117]. Further analyses of the rice mIT mutants revealed that Fe-s cluster synthesis is affected in the knockdown plants. These results clearly suggested that mIT plays an essential role for rice growth and development [117]. In Arabidopsis, two genes encode for mIT (*AtmIT1* and *AtmIT2*) [118]. Both mITs from Arabidopsis belong to the MCF and exhibit homology with mITs from other organisms. Single *AtmITs* mutant plants do not exhibit clear phenotypes, but in the double mutant plants, silenced for both genes showed embryo lethal phenotype were shown to be essential for Fe homeostasis and embryogenesis in Arabidopsis. Additional analyses demonstrated that both transporters are necessary for mitochondrial Fe uptake and also for the correct mitochondrial function. Together, these studies indicate that mITs are necessary for the maintenance of both mitochondrial and whole plant Fe homeostasis, and consequently essential for the proper growth and development of the plant.

4. Conclusions

Research into the in vivo functions of the plant mitochondrial carrier family has made impressive advances since the last comprehensive reviews were published some eight to nine years ago [14,23]. Indeed, despite the fact that lesser technological advances have been made than those described for the metabolic role of the transporters in the accompanying article [15], arguably greater progress has been made here. As we describe above, next-generation sequencing-based transcript profiling has greatly expanded the species and conditions for which expression analysis information is available for the plant MCF. Moreover, since 2012 a total of 21 MCF proteins have been characterized at the genetic level—largely by accession mutants of the various Arabidopsis T-DNA insertional mutant collections. Thus, we now have information on the effect of mutation in all of the major clades. That said a considerable number of gaps still need filling and even such well-studied proteins as the ATP/ADP transporters have not been properly characterized in vivo. It seems likely that, due to functional redundancies, a range of double and triple mutants may be required in order to provide clearer clues in this direction. An additional area of interest for future work will be in elucidating the means by which these transporters are regulated in vivo. A wide range of post-translational modifications have been reported for plants [119], and many of these also occur within the MCF family; however, their physiological relevance is currently unclear. Despite these open questions immense advances have made within the last eight years and our understanding of plant organellar transport has been particularly enriched within this period.

Supplementary Materials: The following are available online at <http://www.mdpi.com/2218-273X/10/9/1226/s1>, File S1.

Author Contributions: J.H.F.C. performed the genomic analysis. A.N.-N. and A.R.F. wrote the manuscript. All authors agreed to the published version of the manuscript.

Funding: This research was funded by Collaborative Research Centers, SFB (Sonderforschungsbereich, Grant TRR 175/1) to A.R.F. and Conselho Nacional de Desenvolvimento Científico e Tecnológico (CNPq) (Grant 306818/2016-7) to A.N.-N.

Conflicts of Interest: The authors declare no conflict of interest.

References

1. Kunji, E.R.S.; Robinson, A.J. Coupling of proton and substrate translocation in the transport cycle of mitochondrial carriers. *Curr. Opin. Struct. Biol.* **2010**, *20*, 440–447. [CrossRef] [PubMed]
2. Palmieri, F. The mitochondrial transporter family (slc25): Physiological and pathological implications. *Pflug. Arch. Eur. J. Physiol.* **2004**, *447*, 689–709. [CrossRef] [PubMed]
3. Palmieri, F. New functions for novel mitochondrial transporters. *Biochim. Biophys. Acta Bioenerg.* **2008**, *1777*, S3. [CrossRef]
4. Klingenberg, M. The ADP and ATP transport in mitochondria and its carrier. *Biochim. Biophys. Acta Biomembr.* **2008**, *1778*, 1978–2021. [CrossRef]
5. Palmieri, F.; Pierri, C.L. Mitochondrial metabolite transport. *Essays Biochem.* **2010**, *47*, 37–52.
6. Palmieri, F.; Pierri, C.L. Structure and function of mitochondrial carriers - role of the transmembrane helix p and g residues in the gating and transport mechanism. *Febs Lett.* **2010**, *584*, 1931–1939. [CrossRef]
7. Satrustegui, J.; Pardo, B.; Del Arco, A. Mitochondrial transporters as novel targets for intracellular calcium signaling. *Physiol. Rev.* **2007**, *87*, 29–67. [CrossRef]
8. Monne, M.; Miniero, D.V.; Daddabbo, L.; Palmieri, L.; Porcelli, V.; Palmieri, F. Mitochondrial transporters for ornithine and related amino acids: A review. *Amino Acids* **2015**, *47*, 1763–1777. [CrossRef]
9. Monne, M.; Voza, A.; Lasorsa, F.M.; Porcelli, V.; Palmieri, F. Mitochondrial carriers for aspartate, glutamate and other amino acids: A review. *Int. J. Mol. Sci.* **2019**, *20*, 4456. [CrossRef]
10. Palmieri, F. Mitochondrial transporters of the SLC25 family and associated diseases: A review. *J. Inherit. Metab. Dis.* **2014**, *37*, 565–575. [CrossRef]
11. Robinson, A.J.; Kunji, E.R.S.; Gross, A. Mitochondrial carrier homolog 2 (MTCH2): The recruitment and evolution of a mitochondrial carrier protein to a critical player in apoptosis. *Exp. Cell Res.* **2012**, *318*, 1316–1323. [CrossRef] [PubMed]
12. Ruprecht, J.J.; Kunji, E.R.S. The SLC25 mitochondrial carrier family: Structure and mechanism. *Trends Biochem. Sci.* **2020**, *45*, 244–258. [CrossRef] [PubMed]
13. Taylor, E.B. Functional properties of the mitochondrial carrier system. *Trends Cell Biol.* **2017**, *27*, 633–644. [CrossRef] [PubMed]
14. Palmieri, F.; Pierri, C.L.; De Grassi, A.; Nunes-Nesi, A.; Fernie, A.R. Evolution, structure and function of mitochondrial carriers: A review with new insights. *Plant J.* **2011**, *66*, 161–181. [CrossRef] [PubMed]
15. Fernie, A.R.; Cavalcanti, J.H.F.; Nunes-Nesi, A. Metabolic roles of plant mitochondrial carriers. *Biomolecules* **2020**, *10*, 1013. [CrossRef]
16. Genevestigator. Available online: <https://genevestigator.com/gv/> (accessed on 24 May 2020).
17. Ferrari, C.; Shivhare, D.; Hansen, B.O.; Pasha, A.; Esteban, E.; Provart, N.J.; Kragler, F.; Fernie, A.R.; Tohge, T.; Mutwil, M. Expression atlas of *Selaginella moellendorffii* provides insights into the evolution of vasculature, secondary metabolism, and roots. *Plant Cell* **2020**, *32*, 853–870. [CrossRef]
18. Sibout, R.; Proost, S.; Hansen, B.O.; Vaid, N.; Giorgi, F.M.; Ho-Yue-Kuang, S.; Legee, F.; Cezart, L.; Bouchabke-Coussa, O.; Soulhat, C.; et al. Expression atlas and comparative coexpression network analyses reveal important genes involved in the formation of lignified cell wall in brachypodium distachyon. *New Phytol.* **2017**, *215*, 1009–1025. [CrossRef]
19. Schwacke, R.; Ponce-Soto, G.Y.; Krause, K.; Bolger, A.M.; Arsova, B.; Hallab, A.; Gruden, K.; Stitt, M.; Bolger, M.E.; Usadel, B. Mapman4: A refined protein classification and annotation framework applicable to multi-omics data analysis. *Mol. Plant* **2019**, *12*, 879–892. [CrossRef]
20. Mutwil, M.; Klie, S.; Tohge, T.; Giorgi, F.M.; Wilkins, O.; Campbell, M.M.; Fernie, A.R.; Usadel, B.; Nikoloski, Z.; Persson, S. Planet: Combined sequence and expression comparisons across plant networks derived from seven species. *Plant Cell* **2011**, *23*, 895–910. [CrossRef]
21. Ruprecht, C.; Mendrinna, A.; Tohge, T.; Sampathkumar, A.; Klie, S.; Fernie, A.R.; Nikoloski, Z.; Persson, S.; Mutwil, M. Famnet: A framework to identify multiplied modules driving pathway expansion in plants. *Plant Physiol.* **2016**, *170*, 1878–1894. [CrossRef]

22. Alejandro, S.; Lee, Y.; Tohge, T.; Sudre, D.; Osorio, S.; Park, J.; Bovet, L.; Lee, Y.; Geldner, N.; Fernie, A.R.; et al. AtABCG29 is a monolignol transporter involved in lignin biosynthesis. *Curr. Biol.* **2012**, *22*, 1207–1212. [CrossRef] [PubMed]
23. Da Fonseca-Pereira, P.; Neri-Silva, R.; Cavalcanti, J.H.F.; Brito, D.S.; Weber, A.P.M.; Araujo, W.L.; Nunes-Nesi, A. Data-mining bioinformatics: Connecting adenylate transport and metabolic responses to stress. *Trends Plant Sci.* **2018**, *23*, 961–974. [CrossRef] [PubMed]
24. Haferkamp, I.; Schmitz-Esser, S. The plant mitochondrial carrier family: Functional and evolutionary aspects. *Front. Plant Sci.* **2012**, *3*, 2. [CrossRef] [PubMed]
25. Zhang, J.Z. Evolution by gene duplication: An update. *Trends Ecol. Evol.* **2003**, *18*, 292–298. [CrossRef]
26. Palmieri, F.; Rieder, B.; Ventrella, A.; Blanco, E.; Do, P.T.; Nunes-Nesi, A.; Trauth, A.U.; Fiermonte, G.; Tjaden, J.; Agrimi, G.; et al. Molecular identification and functional characterization of *Arabidopsis thaliana* mitochondrial and chloroplastic NAD⁺ carrier proteins. *J. Biol. Chem.* **2009**, *284*, 31249–31259. [CrossRef]
27. de Souza Chaves, I.; Feitosa-Araujo, E.; Florian, A.; Medeiros, D.B.; da Fonseca-Pereira, P.; Charton, L.; Heyneke, E.; Apfata, J.A.C.; Pires, M.V.; Mettler-Altmann, T.; et al. The mitochondrial NAD⁺ transporter (NDT1) plays important roles in cellular NAD⁺ homeostasis in *Arabidopsis thaliana*. *Plant J. Cell Mol. Biol.* **2019**, *100*, 487–504. [CrossRef]
28. Feitosa-Araujo, E.; Chaves, I.S.; Florian, A.; da Fonseca-Pereira, P.; Apfata, J.A.C.; Heyneke, E.; Medeiros, D.B.; Pires, M.V.; Mettler-Altmann, T.; Neuhaus, H.E.; et al. Down-regulation of a mitochondrial NAD⁺ transporter (NDT2) alters seed production and germination in *Arabidopsis*. *Plant Cell Physiol.* **2020**, *61*, 897–908. [CrossRef]
29. Bouvier, F.; Linka, N.; Isner, J.-C.; Mutterer, J.; Weber, A.P.M.; Camara, B. *Arabidopsis* SAMT1 defines a plastid transporter regulating plastid biogenesis and plant development. *Plant Cell* **2006**, *18*, 3088–3105. [CrossRef]
30. Agrimi, G.; Di Noia, M.A.; Marobbio, C.M.T.; Fiermonte, G.; Lasorsa, F.M.; Palmieri, F. Identification of the human mitochondrial s-adenosylmethionine transporter: Bacterial expression, reconstitution, functional characterization and tissue distribution. *Biochem. J.* **2004**, *379*, 183–190. [CrossRef]
31. Palmieri, L.; Arrigoni, R.; Blanco, E.; Carrari, F.; Zanor, M.I.; Studart-Guimaraes, C.; Fernie, A.R.; Palmieri, F. Molecular identification of an *Arabidopsis* s-adenosylmethionine transporter. Analysis of organ distribution, bacterial expression, reconstitution into liposomes, and functional characterization. *Plant Physiol.* **2006**, *142*, 855–865. [CrossRef]
32. Bahaji, A.; Jose Munoz, F.; Ovecka, M.; Baroja-Fernandez, E.; Montero, M.; Li, J.; Hidalgo, M.; Almagro, G.; Teresa Sesma, M.; Ezquer, I.; et al. Specific delivery of AtBT1 to mitochondria complements the aberrant growth and sterility phenotype of homozygous *Atbt1* *Arabidopsis* mutants. *Plant J.* **2011**, *68*, 1115–1121. [CrossRef] [PubMed]
33. Bahaji, A.; Munoz, F.J.; Segui-Simarro, J.M.; Camacho-Fernandez, C.; Rivas-Sendra, A.; Parra-Vega, V.; Ovecka, M.; Li, J.; Sanchez-Lopez, A.M.; Almagro, G.; et al. Mitochondrial *Zea mays* Brittle1-1 is a major determinant of the metabolic fate of incoming sucrose and mitochondrial function in developing maize endosperms. *Front. Plant Sci.* **2019**, *10*, 242. [CrossRef] [PubMed]
34. Bahaji, A.; Ovecka, M.; Barany, I.; Carmen Risueno, M.; Jose Munoz, F.; Baroja-Fernandez, E.; Montero, M.; Li, J.; Hidalgo, M.; Teresa Sesma, M.; et al. Dual targeting to mitochondria and plastids of AtBT1 and ZmBT1, two members of the mitochondrial carrier family. *Plant Cell Physiol.* **2011**, *52*, 597–609. [CrossRef] [PubMed]
35. Leroch, M.; Neuhaus, H.E.; Kirchberger, S.; Zimmermann, S.; Melzer, M.; Gerhold, J.; Tjaden, J. Identification of a novel adenine nucleotide transporter in the endoplasmic reticulum of *Arabidopsis*. *Plant Cell* **2008**, *20*, 438–451. [CrossRef]
36. Rieder, B.; Neuhaus, H.E. Identification of an *Arabidopsis* plasma membrane-located ATP transporter important for anther development. *Plant Cell* **2011**, *23*, 1932–1944. [CrossRef]
37. The Bio-Analytic Resource for Plant Biology. Available online: <http://www.bar.utoronto.ca/#> (accessed on 24 May 2020).
38. Klepikova, A.V.; Kasianov, A.S.; Gerasimov, E.S.; Logacheva, M.D.; Penin, A.A. A high resolution map of the *Arabidopsis thaliana* developmental transcriptome based on RNA-seq profiling. *Plant J. Cell Mol. Biol.* **2016**, *88*, 1058–1070. [CrossRef]

39. Toka, I.; Planchais, S.; Cabassa, C.; Justin, A.-M.; De Vos, D.; Richard, L.; Savoure, A.; Carol, P. Mutations in the hyperosmotic stress-responsive mitochondrial basic amino acid carrier2 enhance proline accumulation in *Arabidopsis*. *Plant Physiol.* **2010**, *152*, 1851–1862. [CrossRef]
40. Planchais, S.; Cabassa, C.; Toka, I.; Justin, A.M.; Renou, J.P.; Savoure, A.; Carol, P. Basic amino acid carrier 2 gene expression modulates arginine and urea content and stress recovery in *Arabidopsis* leaves. *Front. Plant Sci.* **2014**, *5*, 330. [CrossRef]
41. Figueira, T.R.; Arruda, P. Differential expression of uncoupling mitochondrial protein and alternative oxidase in the plant response to stress. *J. Bioenerg. Biomembr.* **2011**, *43*, 67–70. [CrossRef]
42. Smith, A.M.; Ratcliffe, R.G.; Sweetlove, L.J. Activation and function of mitochondrial uncoupling protein in plants. *J. Biol. Chem.* **2004**, *279*, 51944–51952. [CrossRef]
43. Borecky, J.; Nogueira, F.T.; de Oliveira, K.A.; Maia, I.G.; Vercesi, A.E.; Arruda, P. The plant energy-dissipating mitochondrial systems: Depicting the genomic structure and the expression profiles of the gene families of uncoupling protein and alternative oxidase in monocots and dicots. *J. Exp. Bot.* **2006**, *57*, 849–864. [CrossRef] [PubMed]
44. Van Aken, O.; Zhang, B.; Carrie, C.; Uggalla, V.; Paynter, E.; Giraud, E.; Whelan, J. Defining the mitochondrial stress response in *Arabidopsis thaliana*. *Mol. Plant* **2009**, *2*, 1310–1324. [CrossRef] [PubMed]
45. Ribeiro, D.M.; Araújo, W.L.; Fernie, A.R.; Schippers, J.H.; Mueller-Roeber, B. Translatome and metabolome effects triggered by gibberellins during rosette growth in *Arabidopsis*. *J. Exp. Bot.* **2012**, *63*, 2769–2786. [CrossRef] [PubMed]
46. Racca, S.; Welchen, E.; Gras, D.E.; Tarkowská, D.; Turečková, V.; Maurino, V.G.; Gonzalez, D.H. Interplay between cytochrome c and gibberellins during *Arabidopsis* vegetative development. *Plant J. Cell Mol. Biol.* **2018**, *94*, 105–121. [CrossRef]
47. Keech, O.; Pesquet, E.; Ahad, A.; Askne, A.; Nordvall, D.; Vodnala, S.M.; Tuominen, H.; Hurry, V.; Dizengremel, P.; Gardeström, P. The different fates of mitochondria and chloroplasts during dark-induced senescence in *Arabidopsis* leaves. *Plant Cell Environ.* **2007**, *30*, 1523–1534. [CrossRef]
48. Hildebrandt, T.M.; Nunes Nesi, A.; Araújo, W.L.; Braun, H.P. Amino acid catabolism in plants. *Mol. Plant* **2015**, *8*, 1563–1579. [CrossRef]
49. Chrobok, D.; Law, S.R.; Brouwer, B.; Lindén, P.; Ziolkowska, A.; Liebsch, D.; Narsai, R.; Szal, B.; Moritz, T.; Rouhier, N.; et al. Dissecting the metabolic role of mitochondria during developmental leaf senescence. *Plant Physiol.* **2016**, *172*, 2132–2153. [CrossRef]
50. Gallardo, K.; Job, C.; Groot, S.P.C.; Puype, M.; Demol, H.; Vandekerckhove, J.; Job, D. Importance of methionine biosynthesis for *Arabidopsis* seed germination and seedling growth. *Physiol. Plant* **2002**, *116*, 238–247. [CrossRef]
51. Lee, C.P.; Millar, A.H. The plant mitochondrial transportome: Balancing metabolic demands with energetic constraints. *Trends Plant Sci.* **2016**, *21*, 662–676. [CrossRef]
52. Toleco, M.R.; Naake, T.; Zhang, Y.; Heazlewood, J.L.; Fernie, A.R. Plant mitochondrial carriers: Molecular gatekeepers that help to regulate plant central carbon metabolism. *Plants* **2020**, *9*, 117. [CrossRef]
53. Subcellular Localization Database for *Arabidopsis* Proteins. Available online: <https://suba.live/> (accessed on 24 May 2020).
54. ARAMEMNON, Plant Membrane Protein Database. Available online: <http://aramemnon.uni-koeln.de> (accessed on 24 May 2020).
55. Eubel, H.; Meyer, E.H.; Taylor, N.L.; Bussell, J.D.; O’Toole, N.; Heazlewood, J.L.; Castleden, I.; Small, I.D.; Smith, S.M.; Millar, A.H. Novel proteins, putative membrane transporters, and an integrated metabolic network are revealed by quantitative proteomic analysis of *Arabidopsis* cell culture peroxisomes. *Plant Physiol.* **2008**, *148*, 1809–1829. [CrossRef] [PubMed]
56. Millar, A.H.; Heazlewood, J.L. Genomic and proteomic analysis of mitochondrial carrier proteins in *Arabidopsis*. *Plant Physiol.* **2003**, *131*, 443–453. [CrossRef] [PubMed]
57. Linka, N.; Theodoulou, F.L.; Haslam, R.P.; Linka, M.; Napier, J.A.; Neuhaus, H.E.; Weber, A.P.M. Peroxisomal ATP import is essential for seedling development in *Arabidopsis thaliana*. *Plant Cell* **2008**, *20*, 3241–3257. [CrossRef] [PubMed]
58. Fukao, Y.; Hayashi, Y.; Mano, S.; Hayashi, M.; Nishimura, M. Developmental analysis of a putative ATP/ADP carrier protein localized on glyoxysomal membranes during the peroxisome transition in pumpkin cotyledons. *Plant Cell Physiol.* **2001**, *42*, 835–841. [CrossRef] [PubMed]

59. Arai, Y.; Hayashi, M.; Nishimura, M. Proteomic identification and characterization of a novel peroxisomal adenine nucleotide transporter supplying ATP for fatty acid beta-oxidation in soybean and Arabidopsis. *Plant Cell* **2008**, *20*, 3227–3240. [CrossRef]
60. Bedhomme, M.; Hoffmann, M.; McCarthy, E.A.; Gambonnet, B.; Moran, R.G.; Rebeille, F.; Ravel, S. Folate metabolism in plants—An Arabidopsis homolog of the mammalian mitochondrial folate transporter mediates folate import into chloroplasts. *J. Biol. Chem.* **2005**, *280*, 34823–34831. [CrossRef]
61. Kirchberger, S.; Tjaden, J.; Neuhaus, H.E. Characterization of the Arabidopsis Brittle1 transport protein and impact of reduced activity on plant metabolism. *Plant J.* **2008**, *56*, 51–63. [CrossRef]
62. Parsons, H.T.; Christiansen, K.; Knierim, B.; Carroll, A.; Ito, J.; Batth, T.S.; Smith-Moritz, A.M.; Morrison, S.; McInerney, P.; Hadi, M.Z.; et al. Isolation and proteomic characterization of the Arabidopsis golgi defines functional and novel components involved in plant cell wall biosynthesis. *Plant Physiol.* **2012**, *159*, 12–26. [CrossRef]
63. Nikolovski, N.; Rubtsov, D.; Segura, M.P.; Miles, G.P.; Stevens, T.J.; Dunkley, T.P.; Munro, S.; Lilley, K.S.; Dupree, P. Putative glycosyltransferases and other plant golgi apparatus proteins are revealed by lopit proteomics. *Plant Physiol.* **2012**, *160*, 1037–1051. [CrossRef]
64. Monne, M.; Daddabbo, L.; Gagneul, D.; Obata, T.; Hielscher, B.; Palmieri, L.; Miniero, D.V.; Fernie, A.R.; Weber, A.P.M.; Palmieri, F. Uncoupling proteins 1 and 2 (UCP1 and UCP2) from *Arabidopsis thaliana* are mitochondrial transporters of aspartate, glutamate, and dicarboxylates. *J. Biol. Chem.* **2018**, *293*, 4213–4227. [CrossRef]
65. Bernhardt, K.; Wilkinson, S.; Weber, A.P.; Linka, N. A peroxisomal carrier delivers NAD⁺ and contributes to optimal fatty acid degradation during storage oil mobilization. *Plant J. Cell Mol. Biol.* **2012**, *69*, 1–13. [CrossRef] [PubMed]
66. Palmieri, L.; Rottensteiner, H.; Girzalsky, W.; Scarcia, P.; Palmieri, F.; Erdmann, R. Identification and functional reconstitution of the yeast peroxisomal adenine nucleotide transporter. *Embo J.* **2001**, *20*, 5049–5059. [CrossRef] [PubMed]
67. Hoffmann, C.; Plochanski, B.; Haferkamp, I.; Leroch, M.; Ewald, R.; Bauwe, H.; Riemer, J.; Herrmann, J.M.; Neuhaus, H.E. From endoplasmic reticulum to mitochondria: Absence of the Arabidopsis ATP antiporter endoplasmic reticulum adenylate transporter1 perturbs photorespiration. *Plant Cell* **2013**, *25*, 2647–2660. [CrossRef] [PubMed]
68. Klein, M.C.; Zimmermann, K.; Schorr, S.; Landini, M.; Klemens, P.A.W.; Altensell, J.; Jung, M.; Krause, E.; Nguyen, D.; Helms, V.; et al. Axer is an ATP/ADP exchanger in the membrane of the endoplasmic reticulum. *Nat. Commun.* **2018**, *9*, 3489. [CrossRef]
69. Geigenberger, P.; Riewe, D.; Fernie, A.R. The central regulation of plant physiology by adenylates. *Trends Plant Sci.* **2010**, *15*, 98–105. [CrossRef]
70. Thuswaldner, S.; Lagerstedt, J.O.; Rojas-Stuetz, M.; Bouhidel, K.; Der, C.; Leborgne-Castel, N.; Mishra, A.; Marty, F.; Schoefs, B.; Adamska, I.; et al. Identification, expression, and functional analyses of a thylakoid ATP/ADP carrier from Arabidopsis. *J. Biol. Chem.* **2007**, *282*, 8848–8859. [CrossRef]
71. Comparot-Moss, S.; Denyer, K. The evolution of the starch biosynthetic pathway in cereals and other grasses. *J. Exp. Bot.* **2009**, *60*, 2481–2492. [CrossRef]
72. Beckles, D.M.; Smith, A.M.; ap Rees, T. A cytosolic ADP-glucose pyrophosphorylase is a feature of graminaceous endosperms, but not of other starch-storing organs. *Plant Physiol.* **2001**, *125*, 818–827. [CrossRef]
73. Yin, L.; Lundin, B.; Bertrand, M.; Nurmi, M.; Solymosi, K.; Kangasjarvi, S.; Aro, E.-M.; Schoefs, B.; Spetea, C. Role of thylakoid ATP/ADP carrier in photoinhibition and photoprotection of photosystem II in Arabidopsis. *Plant Physiol.* **2010**, *153*, 666–677. [CrossRef]
74. Tzagoloff, A.; Jang, J.; Glerum, D.M.; Wu, M. Flx1 codes for a carrier protein involved in maintaining a proper balance of flavin nucleotides in yeast mitochondria. *J. Biol. Chem.* **1996**, *271*, 7392–7397. [CrossRef]
75. Klaus, S.M.J.; Kunji, E.R.S.; Bozzo, G.G.; Noiri, A.; de la Garza, R.D.; Basset, G.J.C.; Ravel, S.; Rebeille, F.; Gregory, J.F.; Hanson, A.D. Higher plant plastids and cyanobacteria have folate carriers related to those of trypanosomatids. *J. Biol. Chem.* **2005**, *280*, 38457–38463. [CrossRef] [PubMed]
76. Hanson, A.D.; Roje, S. One-carbon metabolism in higher plants. *Annu. Rev. Plant Physiol. Plant Mol. Biol.* **2001**, *52*, 119–137. [CrossRef] [PubMed]

77. Marobbio, C.M.T.; Agrimi, G.; Lasorsa, F.M.; Palmieri, F. Identification and functional reconstitution of yeast mitochondrial carrier for s-adenosylmethionine. *Embo J.* **2003**, *22*, 5975–5982. [CrossRef] [PubMed]
78. Tarantino, D.; Morandini, P.; Ramirez, L.; Soave, C.; Murgia, I. Identification of an Arabidopsis mitoferrinlike carrier protein involved in Fe metabolism. *Plant Physiol. Biochem.* **2011**, *49*, 520–529. [CrossRef]
79. Agrimi, G.; Russo, A.; Pierri, C.L.; Palmieri, F. The peroxisomal NAD⁺ carrier of *Arabidopsis thaliana* transports coenzyme A and its derivatives. *J. Bioenerg. Biomembr.* **2012**, *44*, 333–340. [CrossRef]
80. Prohl, C.; Pelzer, W.; Diekert, K.; Kmita, H.; Bedekovics, T.; Kispal, G.; Lill, R. The yeast mitochondrial carrier leu5p and its human homologue graves' disease protein are required for accumulation of coenzyme a in the matrix. *Mol. Cell. Biol.* **2001**, *21*, 1089–1097. [CrossRef]
81. Fiermonte, G.; Paradies, E.; Todisco, S.; Marobbio, C.M.T.; Palmieri, F. A novel member of solute carrier family 25 (slc25a42) is a transporter of coenzyme a and adenosine 3',5'-diphosphate in human mitochondria. *J. Biol. Chem.* **2009**, *284*, 18152–18159. [CrossRef]
82. Zallot, R.; Agrimi, G.; Lerma-Ortiz, C.; Teresinski, H.J.; Frelin, O.; Ellens, K.W.; Castegna, A.; Russo, A.; de Crecy-Lagard, V.; Mullen, R.T.; et al. Identification of mitochondrial coenzyme a transporters from maize and Arabidopsis. *Plant Physiol.* **2013**, *162*, 581–588. [CrossRef]
83. Hamel, P.; Saint-Georges, Y.; de Pinto, B.; Lachacinski, N.; Altamura, N.; Dujardin, G. Redundancy in the function of mitochondrial phosphate transport in *Saccharomyces cerevisiae* and *Arabidopsis thaliana*. *Mol. Microbiol.* **2004**, *51*, 307–317. [CrossRef]
84. Zhu, W.; Miao, Q.; Sun, D.; Yang, G.; Wu, C.; Huang, J.; Zheng, C. The mitochondrial phosphate transporters modulate plant responses to salt stress via affecting ATP and gibberellin metabolism in *Arabidopsis thaliana*. *PLoS ONE* **2012**, *7*, e43530. [CrossRef]
85. Jia, F.; Wan, X.; Zhu, W.; Sun, D.; Zheng, C.; Liu, P.; Huang, J. Overexpression of mitochondrial phosphate transporter 3 severely hampers plant development through regulating mitochondrial function in Arabidopsis. *PLoS ONE* **2015**, *10*, e0129717. [CrossRef] [PubMed]
86. Senkler, J.; Senkler, M.; Eubel, H.; Hildebrandt, T.; Lengwenus, C.; Schertl, P.; Schwarzlander, M.; Wagner, S.; Wittig, I.; Braun, H.P. The mitochondrial complexome of *Arabidopsis thaliana*. *Plant J. Cell Mol. Biol.* **2017**, *89*, 1079–1092. [CrossRef] [PubMed]
87. Luo, L.; He, Y.; Zhao, Y.; Xu, Q.; Wu, J.; Ma, H.; Guo, H.; Bai, L.; Zuo, J.; Zhou, J.M.; et al. Regulation of mitochondrial NAD pool via NAD⁺ transporter 2 is essential for matrix NADH homeostasis and ROS production in Arabidopsis. *Sci. China Life Sci.* **2019**, *62*, 991–1002. [CrossRef] [PubMed]
88. Sweetlove, L.J.; Lytovchenko, A.; Morgan, M.; Nunes-Nesi, A.; Taylor, N.L.; Baxter, C.J.; Eickmeier, I.; Fernie, A.R. Mitochondrial uncoupling protein is required for efficient photosynthesis. *Proc. Natl. Acad. Sci. USA* **2006**, *103*, 19587–19592. [CrossRef]
89. Vercesi, A.E.; Borecky, J.; Maia Ide, G.; Arruda, P.; Cuccovia, I.M.; Chaimovich, H. Plant uncoupling mitochondrial proteins. *Annu. Rev. Plant Biol.* **2006**, *57*, 383–404. [CrossRef]
90. Borecky, J.; Maia, I.G.; Costa, A.D.T.; Jezek, P.; Chaimovich, H.; de Andrade, P.B.M.; Vercesi, A.E.; Arruda, P. Functional reconstitution of *Arabidopsis thaliana* plant uncoupling mitochondrial protein (*AtPUMP1*) expressed in *Escherichia coli*. *Febs Lett.* **2001**, *505*, 240–244. [CrossRef]
91. Palmieri, L.; Picault, N.; Arrigoni, R.; Besin, E.; Palmieri, F.; Hodges, M. Molecular identification of three *Arabidopsis thaliana* mitochondrial dicarboxylate carrier isoforms: Organ distribution, bacterial expression, reconstitution into liposomes and functional characterization. *Biochem. J.* **2008**, *410*, 621–629. [CrossRef]
92. Barreto, P.; Okura, V.K.; Neshich, I.A.; Maia Ide, G.; Arruda, P. Overexpression of UCP1 in tobacco induces mitochondrial biogenesis and amplifies a broad stress response. *BMC Plant Biol.* **2014**, *14*, 144. [CrossRef]
93. Barreto, P.; Okura, V.; Pena, I.A.; Maia, R.; Maia, I.G.; Arruda, P. Overexpression of mitochondrial uncoupling protein 1 (UCP1) induces a hypoxic response in *Nicotiana tabacum* leaves. *J. Exp. Bot.* **2016**, *67*, 301–313. [CrossRef]
94. Barreto, P.; Yassitepe, J.; Wilson, Z.A.; Arruda, P. Mitochondrial uncoupling protein 1 overexpression increases yield in *Nicotiana tabacum* under drought stress by improving source and sink metabolism. *Front. Plant Sci.* **2017**, *8*, 1836. [CrossRef]
95. Sweetlove, L.J.; Beard, K.F.; Nunes-Nesi, A.; Fernie, A.R.; Ratcliffe, R.G. Not just a circle: Flux modes in the plant TCA cycle. *Trends Plant Sci.* **2010**, *15*, 462–470. [CrossRef] [PubMed]

96. Fuchs, P.; Rugen, N.; Carrie, C.; Elsässer, M.; Finkemeier, I.; Giese, J.; Hildebrandt, T.M.; Kühn, K.; Maurino, V.G.; Ruberti, C.; et al. Single organelle function and organization as estimated from Arabidopsis mitochondrial proteomics. *Plant J. Cell Mol. Biol.* **2020**, *101*, 420–441. [CrossRef] [PubMed]
97. Picault, N.; Palmieri, L.; Pisano, I.; Hodges, M.; Palmieri, F. Identification of a novel transporter for dicarboxylates and tricarboxylates in plant mitochondria—bacterial expression, reconstitution, functional characterization, and tissue distribution. *J. Biol. Chem.* **2002**, *277*, 24204–24211. [CrossRef] [PubMed]
98. Regalado, A.; Pierri, C.L.; Bitetto, M.; Laera, V.L.; Pimentel, C.; Francisco, R.; Passarinho, J.; Chaves, M.M.; Agrimi, G. Characterization of mitochondrial dicarboxylate/tricarboxylate transporters from grape berries. *Planta* **2013**, *237*, 693–703. [CrossRef]
99. Deng, W.; Luo, K.; Li, Z.; Yang, Y. Molecular cloning and characterization of a mitochondrial dicarboxylate/tricarboxylate transporter gene in citrus junos response to aluminum stress. *Mitochondrial DNA* **2008**, *19*, 376–384.
100. Spagnoletta, A.; De Santis, A.; Tampieri, E.; Baraldi, E.; Bachi, A.; Genchi, G. Identification and kinetic characterization of HtDTC, the mitochondrial dicarboxylate-tricarboxylate carrier of jerusalem artichoke tubers. *J. Bioenerg. Biomembr.* **2006**, *38*, 57–65. [CrossRef]
101. Genchi, G.; Spagnoletta, A.; De Santis, A.; Stefanizzi, L.; Palmieri, F. Purification and characterization of the reconstitutively active citrate carrier from maize mitochondria. *Plant Physiol.* **1999**, *120*, 841–848. [CrossRef]
102. Catoni, E.; Schwab, R.; Hilpert, M.; Desimone, M.; Schwacke, R.; Flugge, U.I.; Schumacher, K.; Frommer, W.B. Identification of an Arabidopsis mitochondrial succinate-fumarate translocator. *Febs Lett.* **2003**, *534*, 87–92. [CrossRef]
103. Brito, D.S.; Agrimi, G.; Charton, L.; Brilhaus, D.; Bitetto, M.G.; Lana-Costa, J.; Messina, E.; Nascimento, C.P.; Araujo, E.F.; Viana Pires, M.; et al. Biochemical and functional characterization of a mitochondrial citrate carrier in *Arabidopsis thaliana*. *Biochem. J.* **2020**, *447*, 1759–1777. [CrossRef]
104. Nunes-Nesi, A.; Fernie, A.R.; Stitt, M. Metabolic and signaling aspects underpinning the regulation of plant carbon nitrogen interactions. *Mol. Plant* **2010**, *3*, 973–996. [CrossRef]
105. Galili, G.; Amir, R.; Fernie, A.R. The regulation of essential amino acid synthesis and accumulation in plants. *Annu. Rev. Plant Biol.* **2016**, *67*, 153–178. [CrossRef] [PubMed]
106. Lawand, S.; Dorne, A.J.; Long, D.; Coupland, G.; Mache, R.; Carol, P. Arabidopsis a bout de souffle, which is homologous with mammalian carnitine acyl carrier, is required for postembryonic growth in the light. *Plant Cell* **2002**, *14*, 2161–2173. [CrossRef] [PubMed]
107. Eisenhut, M.; Planchais, S.; Cabassa, C.; Guivarc’h, A.; Justin, A.M.; Taconnat, L.; Renou, J.P.; Linka, M.; Gagneul, D.; Timm, S.; et al. Arabidopsis a bout de souffle is a putative mitochondrial transporter involved in photorespiratory metabolism and is required for meristem growth at ambient CO₂ levels. *Plant J. Cell Mol. Biol.* **2013**, *73*, 836–849. [CrossRef] [PubMed]
108. Porcelli, V.; Vozza, A.; Calcagnile, V.; Gorgoglione, R.; Arrigoni, R.; Fontanesi, F.; Marobbio, C.M.T.; Castegna, A.; Palmieri, F.; Palmieri, L. Molecular identification and functional characterization of a novel glutamate transporter in yeast and plant mitochondria. *Biochim. Biophys. Acta Bioenerg.* **2018**, *1859*, 1249–1258. [CrossRef]
109. Hoyos, M.E.; Palmieri, L.; Wertin, T.; Arrigoni, R.; Polacco, J.C.; Palmieri, F. Identification of a mitochondrial transporter for basic amino acids in *Arabidopsis thaliana* by functional reconstitution into liposomes and complementation in yeast. *Plant J.* **2003**, *33*, 1027–1035. [CrossRef]
110. Palmieri, L.; Todd, C.D.; Arrigoni, R.; Hoyos, M.E.; Santoro, A.; Polacco, J.C.; Palmieri, F. Arabidopsis mitochondria have two basic amino acid transporters with partially overlapping specificities and differential expression in seedling development. *Biochim. Biophys. Acta Bioenerg.* **2006**, *1757*, 1277–1283. [CrossRef]
111. Catoni, E.; Desimone, M.; Hilpert, M.; Wipf, D.; Kunze, R.; Schneider, A.; Fluegge, U.-I.; Schumacher, K.; Frommer, W.B. Expression pattern of a nuclear encoded mitochondrial arginine-ornithine translocator gene from Arabidopsis. *BMC Plant Biol.* **2003**, *3*, 1. [CrossRef]
112. Taylor, N.L.; Howell, K.A.; Heazlewood, J.L.; Tan, T.Y.; Narsai, R.; Huang, S.; Whelan, J.; Millar, A.H. Analysis of the rice mitochondrial carrier family reveals anaerobic accumulation of a basic amino acid carrier involved in arginine metabolism during seed germination. *Plant Physiol.* **2010**, *154*, 691–704. [CrossRef]
113. Batista-Silva, W.; Heinemann, B.; Rugen, N.; Nunes-Nesi, A.; Araújo, W.L.; Braun, H.P.; Hildebrandt, T.M. The role of amino acid metabolism during abiotic stress release. *Plant Cell Environ.* **2019**, *42*, 1630–1644. [CrossRef]

114. Shaw, G.C.; Cope, J.J.; Li, L.T.; Corson, K.; Hersey, C.; Ackermann, G.E.; Gwynn, B.; Lambert, A.J.; Wingert, R.A.; Traver, D.; et al. Mitoferrin is essential for erythroid iron assimilation. *Nature* **2006**, *440*, 96–100. [CrossRef]
115. Paradkar, P.N.; Zumbrennen, K.B.; Paw, B.H.; Ward, D.M.; Kaplan, J. Regulation of mitochondrial iron import through differential turnover of mitoferrin 1 and mitoferrin 2. *Mol. Cell Biol.* **2009**, *29*, 1007–1016. [CrossRef] [PubMed]
116. Metzendorf, C.; Wu, W.; Lind, M.I. Overexpression of drosophila mitoferrin in l(2)mbn cells results in dysregulation of fer1hch expression. *Biochem. J.* **2009**, *421*, 463–471. [CrossRef] [PubMed]
117. Bashir, K.; Ishimaru, Y.; Nishizawa, N.K. Identification and characterization of the major mitochondrial Fe transporter in rice. *Plant Signal. Behav.* **2011**, *6*, 1591–1593. [CrossRef] [PubMed]
118. Jain, A.; Dashner, Z.S.; Connolly, E.L. Mitochondrial iron transporters (MIT1 and MIT2) are essential for iron homeostasis and embryogenesis in *Arabidopsis thaliana*. *Front. Plant Sci.* **2019**, *10*, 1449. [CrossRef]
119. Millar, A.H.; Heazlewood, J.L.; Giglione, C.; Holdsworth, M.J.; Bachmair, A.; Schulze, W.X. The scope, functions, and dynamics of posttranslational protein modifications. *Annu. Rev. Plant Biol.* **2019**, *70*, 119–151. [CrossRef]



© 2020 by the authors. Licensee MDPI, Basel, Switzerland. This article is an open access article distributed under the terms and conditions of the Creative Commons Attribution (CC BY) license (<http://creativecommons.org/licenses/by/4.0/>).

Review

Mitochondrial Potassium Channels as Druggable Targets

Antoni Wrzosek, Bartłomiej Augustynek [†], Monika Żochowska and Adam Szewczyk * 

Laboratory of Intracellular Ion Channels, Nencki Institute of Experimental Biology, Polish Academy of Sciences, 02-093 Warsaw, Poland; A.Wrzosek@nencki.edu.pl (A.W.); bartlomiej.augustynek@dbmr.unibe.ch (B.A.); M.Zochowska@nencki.edu.pl (M.Ż.)

* Correspondence: A.Szewczyk@nencki.edu.pl; Tel.: +48-225-892-269

[†] Present address: Department of BioMedical Research, University of Bern, Inselspital Bern, Bülhstrasse 28, CH-3010 Bern, Switzerland.

Received: 24 June 2020; Accepted: 13 August 2020; Published: 18 August 2020

Abstract: Mitochondrial potassium channels have been described as important factors in cell pro-life and death phenomena. The activation of mitochondrial potassium channels, such as ATP-regulated or calcium-activated large conductance potassium channels, may have cytoprotective effects in cardiac or neuronal tissue. It has also been shown that inhibition of the mitochondrial Kv1.3 channel may lead to cancer cell death. Hence, in this paper, we examine the concept of the druggability of mitochondrial potassium channels. To what extent are mitochondrial potassium channels an important, novel, and promising drug target in various organs and tissues? The druggability of mitochondrial potassium channels will be discussed within the context of channel molecular identity, the specificity of potassium channel openers and inhibitors, and the unique regulatory properties of mitochondrial potassium channels. Future prospects of the druggability concept of mitochondrial potassium channels will be evaluated in this paper.

Keywords: mitochondria; potassium channels; ATP; calcium; ROS; potassium channel openers

1. Introduction

The mitochondrial potassium channels field started in the beginning of the 1990s when the first paper describing potassium channel sensitive to ATP and antidiabetic sulphonylurea–glibenclamide (mitoK_{ATP} channel) was described [1]. It was a strong indication that mitochondria may contain potassium channels similar to those present in the plasma membrane. For almost a decade after, it was not clear what the role of mitochondrial potassium channels was. This was because channels would not support, due to membrane potential dissipation, a canonical function of mitochondria i.e., ATP synthesis. The finding of calcium-activated large conductance channel in inner mitochondrial membrane (mitoBK_{Ca}) would not help position potassium channel in mitochondrial function [2]. The discovery that activation of the mitochondrial potassium channel by potassium channel openers induces protective mechanisms in cardiac myocytes positioned these proteins as an important player in ischemic preconditioning [3]. This was a starting point for trials to target various mitochondrial potassium channels with drugs to affect cell life.

Potassium channels, which are present in the plasma membrane, are the targets of many substances employed in medicine. This is because K⁺ trafficking through the plasmalemma plays an important role in a variety of processes, including the regulation of heart function, muscle contraction, neurotransmitter release, neuronal excitability, insulin secretion, epithelial electrolyte transport, and cell proliferation [4–6]. Hence, plasma membrane potassium channels have been recognized as potential therapeutic drug targets for many years. For example, voltage-regulated

potassium channels offer opportunities for the development of new drugs for cancer, autoimmune diseases; and metabolic, neurological, and cardiovascular disorders [4–7]. Clinically used potassium channel modulators comprise of hypoglycemic sulfonylureas (potassium channel blockers, such as glibenclamide), antiarrhythmic agents (nonselective potassium channel blockers, such as dexsotalol or nifekalant), antianginal and cardioprotective agents (potassium channel openers, such as nicorandil or levosimendan), and anticonvulsants (potassium channel openers, such as retigabine) [8].

The mitochondria, due to their crucial functions within all mammalian cells, are increasingly considered to be targets in drug development [9–12]. Targeting mitochondrial potassium channels in various cell types is an important aim of future studies in this context. The discovery and characterization of mitochondrial K^+ channels in the liver, heart, brain, endothelium, or fibroblast cells clarified the mitochondrial K^+ flux phenomenon [13–16].

First, the phenomenon of potassium uniport, which has been described previously in mitochondria, is attributed to potassium selective channels [17]. Second, potassium channels in the mitochondrial membrane are similar, due not only to biophysical properties but also pharmacological ones of potassium channels present in the plasma membrane. For example, mitochondrial ATP-regulated potassium (mitoK_{ATP}) channels were sensitive not only to ATP but also to antidiabetic sulfonylureas, such as glibenclamide and 5-hydroxydecanoic acid (5-HD), and to potassium channel openers, such as diazoxide [1,18–20]. Recently, the molecular identities of mitochondrial (mitoBK_{Ca}) and plasma membrane large conductance Ca^{2+} -activated potassium (BK_{Ca}) channels were determined to have a common genetic origin [21].

To date, potassium ions' influx into the mitochondria was considered a consequence of high membrane potential (negative in the matrix). Due to K^+/H^+ exchanger activity in the inner mitochondrial membrane, no harmful accumulation of K^+ in the matrix was observed [17]. This kind of description would limit potassium channel action only as part of mitochondrial osmotic controllers. Currently, K^+ flux is considered to be a regulator of mitochondrial membrane potential and respiration, reactive oxygen species (ROS) synthesis, and mitochondrial plasticity, i.e., morphological changes [6,14,16].

The presence of mitoK_{ATP} channels in the inner mitochondrial membrane suggests that mitochondria may be a target of potassium channel openers known to interact with plasma membrane K_{ATP} channels [22]. Furthermore, linking cytoprotective phenomena with mitochondrial potassium channels (and not with the potassium channel in plasma membrane) gave rise to a new area of research investigating cytoprotective mechanisms via activation of or mitochondrial potassium channels [23]. This finding raised the question of the extent to which mitochondrial potassium channels could be applicable targets for cardiac or neuronal protection in various physiological insults. Interestingly, mitochondrial voltage regulated (mitoKv1.3) channel inhibition was recently described as an early event of cancer cell death [24]. Summarizing, mitochondrial potassium channels' activation or inhibition by specific drugs could be used in cytoprotective or cell death regulation.

The druggability of mitochondrial potassium channels will be discussed in this paper within the context of channel molecular identity and the specificity of potassium channel openers and inhibitors towards mitochondrial channels (see Figure 1).

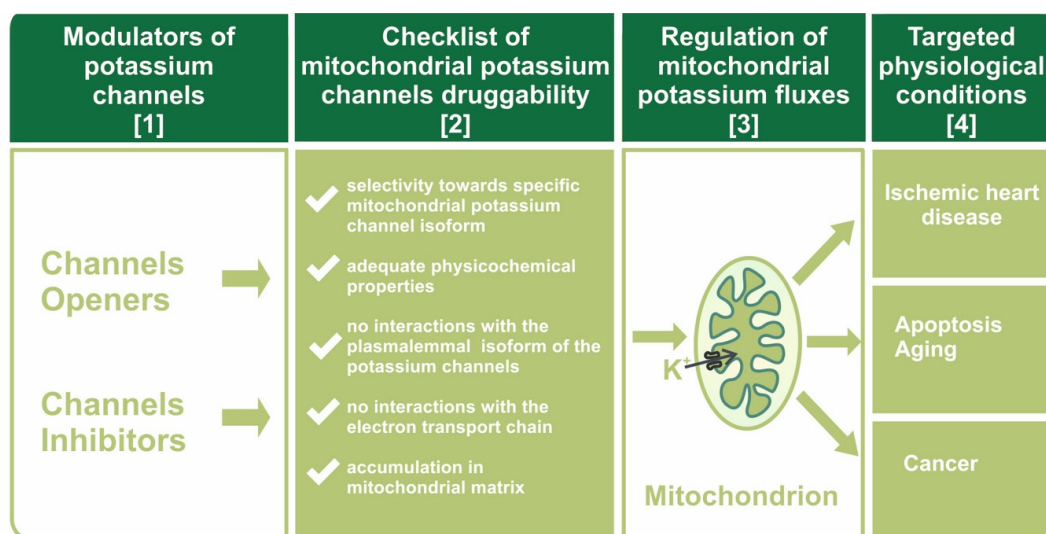


Figure 1. Scheme of the druggability concept towards mitochondrial potassium channels. Modulators of potassium channels (column [1]) must possess unique properties (column [2]) to affect K^+ flux into the mitochondrial matrix (column [3]) in a specific way, thereby causing beneficial physiological effects (column [4]).

The concept of the druggability of mitochondrial potassium channels is also based on drug properties, such as lipophilicity and positive charge, leading to their accumulation in mitochondria. This effect may promote specific drug actions on mitochondrial potassium channels. Moreover, the unique environment for potassium channels in the inner mitochondrial membrane merits critical analysis. Additionally, some pitfalls of using mitochondrial potassium channels as drug targets will be discussed in this paper.

2. Three-Dimensional Mitochondrial Potassium Channel Mapping

To consider mitochondrial potassium channels as important targets for drugs, one should first define three parameters. We call this concept three-dimensional mitochondrial potassium channel mapping: “3D mitoK channel mapping”.

The first dimension of “3D mitoK channel mapping” concerns the molecular identity of mitochondrial potassium channels. There are various potassium channels in the inner mitochondrial membrane [16]. Before the era of mitochondrial potassium channels [1], the universal description as “potassium uniport” was used to describe the phenomenon of K^+ electrogenic influx into the mitochondrial matrix [17]. The current (June 2020) list of identified mitochondrial potassium channels is as follows:

- **mitoK_{ATP} channel:** mitochondrial ATP-regulated potassium channel, the first potassium channel described in the inner mitochondrial membrane [1]. Most likely, these channels might be formed by two proteins: ROMK-type channels (encoded by *KCNJ1* gene) [25–28] or the recently described CCDC51 protein (encoded by *CCDC51* gene) [29]. Additionally, ABCB8 protein (mitochondrial sulfonylurea receptor) is part of the mitoK_{ATP} channel [29].
- **mitoBK_{Ca} channel** (encoded by *KCNMA1* gene): mitochondrial large conductance calcium-activated potassium channel. This channel is a VEDEC isoform of the BK_{Ca} channel, which is known to be present in the plasma membrane of various cell types [21]
- **mitoIK_{Ca} channel** (encoded by *KCNN4* gene): mitochondrial intermediate conductance calcium-activated potassium channel [30]
- **mitoSK_{Ca} channel** (encoded by *KCNN1*, *KCNN2*, and *KCNN3* genes): mitochondrial small conductance calcium-activated potassium channel [31]

- **mitoKv1.3 channel** (encoded by *KCNA3* gene): mitochondrial 1.3 voltage-gated potassium channel (the first number denotes subfamily, and the second denotes the order of discovery) [32]
- **mitoKv1.5 channel** (encoded by *KCNA5* gene): mitochondrial 1.5 voltage-gated potassium channel [33]
- **mitoKv7.4 channel** (encoded by *KCNQ4* gene): mitochondrial 7.4 voltage-gated potassium channel [34]
- **mitoTASK3 channel** (encoded by *KCNK9* gene): tandem pore-domain acid-sensitive potassium channel type 3 [35]
- **mitoSLO2** (in *C. elegans* encoded by gene *SLO2*, in mammals encoded by gene *KCNT2*): mitochondrial sodium-activated potassium channel [36,37]
- **mitoHCN** (encoded by *HCN1*, *HCN2*, *HCN3*, and *HCN4* genes): mitochondrial hypopolarization-activated cyclic nucleotide-gated channel [38,39]

The second dimension of “3D mitoK channel mapping” concerns the tissue profile of mitochondrial potassium channels. There is a different set of mitochondrial potassium channels in various tissues [18]. One should not expect that all of the above mentioned channel proteins exist in all types of mitochondria. For example, in cardiomyocyte mitochondria, five different potassium channels were described, but in skin fibroblast mitochondria, only two types of potassium channels were observed [25,40], and in keratinocyte mitochondria, only mitoTASK3 channel was observed [35]. The mitoK_{ATP}, mitoBK_{Ca}, and mitoKv1.3 channels are the most abundant channels in mammalian mitochondria [15].

The third dimension of “3D mitoK channel mapping” concerns the level (amount) of specific mitochondrial potassium channels in specific tissues. For example, it is believed that the number of mitoK_{ATP} channels is higher in the brain than in cardiac mitochondria [41]. Interestingly, the mitoBK_{Ca} channel in the brain is distributed in various amounts in various brain regions [42].

To summarize, before targeting with drugs specific K⁺ channels in mitochondria, one should consider the following: (1) Type of mitochondrial potassium channel, (2) presence of mitochondrial potassium channels in specific tissues, and (3) the abundance of the mitochondrial potassium channel in targeted tissue versus other tissue.

Additional aspects of this problem concern the presence of mitochondrial channels within various cell compartments. The BK_{Ca} channels, which are highly abundant in the cell membrane of various cells, are present in only the inner mitochondrial membrane (mitoBK_{Ca} channels) but not in plasma membrane of cardiomyocytes [14]. This observation is notably unique for mitochondrial potassium channels and may support that mitochondrial potassium channels and cardiac tissue are druggable targets. The BK_{Ca} channel was also observed in the nucleus membrane [43].

Finally, within the same cell, there are mitochondria both having and not having the potassium channel. It was shown that mitoBK_{Ca} channels are probably not present in all mitochondria within one neuron cell [42]. This uneven distribution of mitoBK_{Ca} channels and the functional consequences of the intracellular heterogeneity of mitochondrial potassium channels still need to be elucidated.

3. Plasma Membrane Versus Mitochondrial Potassium Channels: Molecular Identity

Identifying the molecular identity of the mitochondrial potassium channel is a key element for the rational design and application of these proteins as precise drug targets. This step is important because highly similar proteins are both present in the plasma membrane and inner mitochondrial membrane. In recent years, there has been considerable progress in this area, but there are still many open questions [13].

The plasmalemmal ATP-regulated potassium channel (K_{ATP}) was first described in cardiomyocytes [44]. This K_{ATP} channel is also present in skeletal muscles, and in pancreas, where it plays a crucial role in the regulation of insulin secretion from β cells. It seems that plasmalemmal K_{ATP} channels have different structures and molecular compositions depending on their localization [45]. The plasmalemmal K_{ATP} channel consists of four Kir6.X pore forming subunits (either Kir6.1 or Kir6.2)

and four SUR subunits (SUR1, SUR2, or SUR2B) [46]. K_{ATP} channels are sensitive to changes in ATP concentrations, and by sensing the ATP/ADP ratio in the cytoplasm, these channels possess the unique ability to couple cellular metabolism with plasma membrane potential. As mentioned, K_{ATP} potassium channels of similar electrophysiological and pharmacological properties were also found in the mitochondrial inner membrane: mito K_{ATP} channels. These channels might be formed by two proteins: ROMK-type channels [26] or CCDC61/ABCB8 protein complex [29].

In fact, the mito K_{ATP} channel was the first potassium channel ever identified in the mitochondrial inner membrane [1]. This channel was detected in the mitochondria of several tissues, such as the liver, heart, skeletal muscles, and brain [15]. Although the channel's electrophysiological properties are relatively well described, there is no consensus regarding its molecular topology in the inner mitochondrial membrane. Several groups have investigated this issue, proving that the molecular identity of mito K_{ATP} is most likely different from its plasmalemmal counterpart. Recent discoveries indicate that the ROMK2 (renal outer medullary potassium channel 2; Kir1.1b) protein is a candidate for the molecular constituent of the mito K_{ATP} channel [26]. It appears that when overexpressed, the ROMK2 protein tends to localize in the mitochondrial inner membrane. Moreover, shRNA-mediated knockdown of ROMK inhibited ATP-sensitive, diazoxide-activated components of mitochondrial thallium uptake. The ROMK (Kir1.1a) protein was first described in the plasma membrane of renal cells. However, this protein was later found to be widely expressed within different tissues. ROMK proteins are encoded by distinct splice variants of the *Kcnj1* gene. The expression of ROMK in mitochondria and patch-clamp measurements confirmed its functional properties as a mito K_{ATP} channel [27]. Recently, it was proposed that the CCDC61 and ABCB8 proteins constitute a mito K_{ATP} channel composed of pore-forming and ATP-binding subunits (mitochondrial sulfonylurea receptor) [29]. Planar lipid bilayer reconstitution of the pore subunit together with the mitochondrial sulfonylurea receptor showed the canonical properties of the mito K_{ATP} channel. Overexpression of the mito K_{ATP} channel triggers mitochondrial swelling, whereas genetic ablation of this subunit causes instability in mitochondrial membrane potential and decreases oxidative phosphorylation [29].

The BK_{Ca} ($K_{Ca1.1}$) is ubiquitously expressed within different tissues. The BK_{Ca} channel was first discovered in the plasmalemma of chromaffin cells [47]. However, the activity of the BK_{Ca} channel has also been described in other cellular structures, such as nuclei, ER, or mitochondria (named mito BK_{Ca} channel) [2]. Expression of the mito BK_{Ca} channel has been reported in several mammalian cell types, including heart [48], brain [42,49–51], skeletal muscle [52], endothelium [53], and fibroblasts [40]. The channel was also found in the mitochondria of certain plants [54] and members of the Protista kingdom [55].

A functional BK_{Ca} channel is composed of four α -subunits. Each α -subunit spanned the membrane seven times. The BK_{Ca} channel represents a unique class of ion channels not only because of its high single channel conductance but also because it can be activated by Ca^{2+} alone, membrane depolarization alone, or by both factors synergistically [56]. This dual regulation allows BK_{Ca} channels to couple intracellular signaling to membrane potential and significantly modulate physiological responses, such as neuronal signaling and muscle contraction [57].

Unlike K_{ATP} channels, all BK_{Ca} channels found in distinct locations within the cell seem to be the products of alternative splicing of a single *Kcnma1* gene [58,59]. Unfortunately, the exact molecular identity of each isoform has not been determined. However, one of the mitochondrial splice variants of the BK_{Ca} channel is believed to have an extended C-terminal domain ending with the amino acid residue VEDEC [60].

It was shown that increased expression of the Kv1.3 potassium (mitoKv1.3) channel in the mitochondria of many types of cancer cells and participation in the process of apoptosis have made it a potential target in cancer therapy [61]. The mitoKv1.3 channel is located on the inner mitochondrial membrane in the same orientation as on the plasma membrane [32]. Similar Kv1.3 channel is also detected in the Golgi apparatus and in the membrane of endoplasmic reticulum. Activation of the Kv1.3 channel located in plasmalemma leads to increased cell proliferation and

differentiation. In contrast, the mitoKv1.3 channel plays a key role in activating the apoptotic pathway. CTLL-2 cells overexpressing mitoKv1.3 channels were sensitive to pro-apoptotic factors, such as TNF α , staurosporine, sphingomyelinase, and C6-ceramide. CTLL-2 cells deficient in mitoKv1.3 channels showed no signs of apoptosis, while cells of the same CTLL-2 line with Kv1.3 channels expressed from a mitochondria-targeted vector showed induction of apoptosis in response to TNF α . Induction of apoptosis in mitochondria occurs by blocking the mitoKv1.3 channel through interacting with lysine 128 pro-apoptotic Bax protein, and as a result, the channel pore is impermeable to K⁺ ions. Hyperpolarization of the mitochondrial membrane leads to increased synthesis of reactive oxygen species (ROS) and the release of cytochrome c followed by membrane depolarization and initiation of apoptosis [62].

Molecular definition of mitochondrial potassium channels is important for designing drugs specifically targeting these proteins. This approach probably will help to describe differences between mitochondrial and plasma membrane potassium channels, which is a crucial step in the activity regulation of only mitochondrial potassium channels.

4. Unique Regulation of Mitochondrial Potassium Channels: Destination Context?

Mitochondrial potassium channels are regulated by similar factors (as plasma membrane potassium channels) such as ATP, Ca²⁺, ROS, heme, gasotransmitters, or free fatty acids. Additionally, such parameters as membrane potential and/or pH regulate in principle potassium channels in the same way in both the plasma membrane and the mitochondrial inner membrane [15,16,19,63–65].

Recently, unique (specific for mitochondria) regulation of mitochondrial potassium channels was reported. The single-channel activity of the mitoBK_{Ca} channel was measured by patch-clamping mitoplasts isolated from the human astrocytoma (glioblastoma) U-87 MG cell line [66]. The channel was activated by Ca²⁺ at micromolar concentrations and by the potassium channel opener NS1619. The channel was inhibited by paxilline and iberiotoxin, which are well characterized inhibitors of BK_{Ca} channels localized in plasmalemma and inner mitochondrial membrane. It was shown that substrates of the respiratory chain, such as NADH, succinate, and glutamate/malate, decrease the activity of the channel at positive voltages. This effect was abolished by rotenone, antimycin, and cyanide, which are inhibitors of the mitochondrial respiratory chain. The putative interaction of the β 4 subunit of mitoBK_{Ca} with cytochrome c oxidase (COX) was demonstrated using blue native electrophoresis technique. These results indicated possible structural and functional coupling of the mitoBK_{Ca} channel with the mitochondrial respiratory chain in human astrocytoma U-87 MG cells [66]. Direct regulation of mitoBK_{Ca} channels by mitochondrial respiratory chain redox status may play an important role in the ischemia-reperfusion phenomenon.

The interaction of the mitoBK_{Ca} channel with COX has an additional consequence. It was suggested that mitochondria interact with near-infrared light (wavelengths between 700 and 1400 nm) are absorbed by complexes of the respiratory chain. In the near-infrared region, the 820 nm absorption band belongs mainly to the relatively oxidized Cu_A and the 760 nm absorption band to the relatively reduced Cu_B chromophore of COX. The absorption of photons (at 760 and 820 nm) by COX is hypothesized to enhance respiratory chain function and increase the synthesis of ATP by mitochondria. The mitoBK_{Ca} channels of the astrocytoma (glioblastoma) U-87 MG cell line were investigated using a patch clamp technique with an illumination system [67]. It was found that the mitoBK_{Ca} channel activity was modulated by illumination by infrared light. Activation of the mitoBK_{Ca} channel (depending on respiratory chain redox state) was observed after illumination using specific light wavelengths: 760 nm or 820 nm. These findings confirmed the functional coupling of the respiratory chain via COX to the mitoBK_{Ca} channel and regulation of its transporting activity by infrared light [67].

Mitochondria are highly dynamic intracellular structures in which, depending on metabolic activity, the inner mitochondrial membrane could be dramatically remodeled. It was shown for the first time that mechanical stimulation of the mitoBK_{Ca} channel resulted in an increased probability of

channel opening as was measured by the patch-clamp technique in mitochondria isolated from human astrocytoma U-87 MG cells [68]. These results indicated the possible involvement of the mitoBK_{Ca} channels in mitochondrial activities in which changes in membrane shape and tension play a crucial role, such as fusion/fission and cristae remodeling [68].

These examples illustrate that localization of potassium channels in mitochondrial inner membrane may form a new context of channel regulation. These newly described regulatory mechanisms, as a consequence of mitochondrial localization, may facilitate the design of drugs specifically acting on mitochondrial potassium channels.

5. Searching for Specific Drugs Targeting mitoKv1.3 Channels

Because many cancer cells are deficient in pro-apoptotic proteins, such as Bax or Bak, which causes apoptosis resistance and inhibits the action of chemotherapeutics, it is important to develop a therapy that would cause cancer cells to undergo apoptosis in spite of these deficiencies. The mitochondrial Kv1.3 potassium channel, which is blocked by the Bax protein, has become such a therapeutic target [69]. Inhibitors of this channel have also been shown to be able to activate the internal apoptotic pathway in Bax/Bak deficiency. Three inhibitors were tested: Psora-4, PAP-1, and clofazimine on CTLL-2 cells that do not express Kv1.3 and other potassium channels and on the Kv1.3 transfected line. The three inhibitors blocked the mitochondrial Kv1.3 channel and induced apoptosis only in cells expressing Kv1.3 (Figure 2).

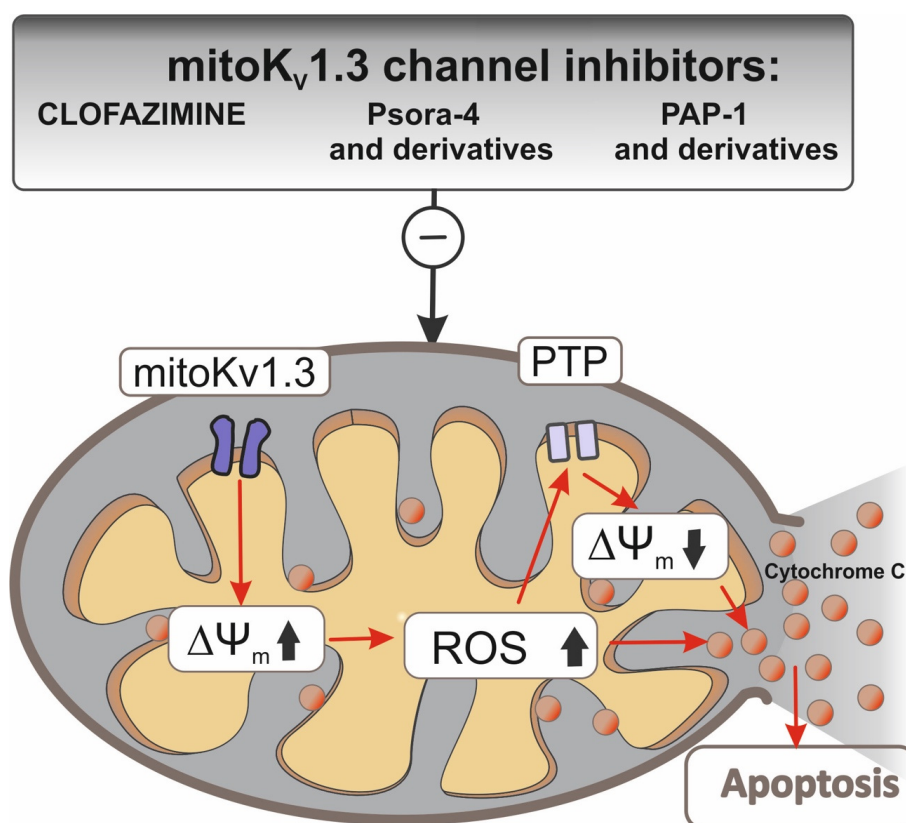


Figure 2. Interactions of Kv1.3 channel inhibitors in mitochondria. Inhibition of the Kv1.3 channel in the inner mitochondrial membrane (IMM) by clofazimin and Psora-4 and PAP-1 and their mitochondrial-directed derivatives (PCTP, PCARBTP, PAPTP) causes hyperpolarization. Hyperpolarization induces an increase in ROS synthesis. If basal ROS production is relatively high as for cancer cells, a further increase in ROS synthesis may lead to a critical level that leads to PTP opening, swelling, and loss of membrane potential, depolarization, and consequent release of cytochrome c from IMM. This chain of events leads to an apoptotic cascade and, as a consequence, to cell death.

In the case of clofazimine, its pro-apoptotic effect was also tested *in vivo* in a mouse model of the orthotopic melanoma B16F10 line. A 90% tumor mass reduction after intraperitoneal administration relative to the untreated control was observed with no side effects on healthy tissue [70].

B-cells (B-lymphocytes) from patients suffering from chronic lymphocytic leukemia have been shown to show an increased level of functional mitoKv1.3 channels compared to cells from healthy donors [71]. This finding paved the way for testing the effects of mitoKv1.3 inhibitors, such as Psora-4, PAP-1, and clofazimine, in the treatment of leukemia. These molecules were highly effective in inducing cell death, especially in combination with inhibitors of multidrug resistance (MDR) pumps. Kv1.3 channel-expressing B-cells undergo apoptosis after treatment with Kv1.3 inhibitors, while healthy T cells from the same patient with reduced Kv1.3 channel expression were resistant to the inhibitors used. The selective action of Kv1.3 channel inhibitors depends not only on the level of Kv1.3 channel expression but also on the presence of mild oxidative stress, which sensitizes even a healthy cell to Kv1.3 channel inhibitors, while the pretreatment of B-cell ROS scavengers makes them resistant to the effects of inhibitors [71].

The different functions of the plasmalemma and mitochondrial Kv1.3 channel necessitated the development of selective inhibitors for mitoKv1.3. Two psoralen derivatives (PAP-1) were developed that accumulate in negatively charged mitochondria due to the lipophilic, positively charged triphenylphosphate (TPP⁺) group [72,73]. In PAPTP, the TPP⁺ group is connected by a stable C-C bond. In PCARBTP, it is linked by an ester bond to the PAP-1 core via carbamate. Under physiological conditions, PCARBTP is hydrolyzed to PAPOH. Mitochondriotropic PAP-1 derivatives have been shown to effectively block mitoKv1.3. Many pancreatic ductal adenocarcinoma (PDAC) lines have been shown to overexpress the mitoKv1.3 channel. The MTT test on five PDAC lines showed 90% mortality after using PAPTP and PCARBTP (Table 1). *In vivo* tests resulted in a 60% reduction in tumor weight and no effect on healthy tissues after using PCARBTP. In addition, it has been shown that the selective apoptotic effect of PAP-1 derivatives on cancer cells, as opposed to effects on healthy cells, is associated not only with increased expression of the mitoKv1.3 channel but also with altered redox status in cancer cells. Increased synthesis of ROS in cancer cells after blocking the mitoKv1.3 channel with a high baseline ROS causes the critical level to be exceeded and the apoptotic path to be initiated [72].

Table 1. Compound modulating activity of mitoKv1.3 potassium channels.

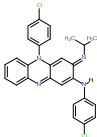
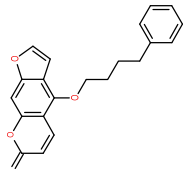
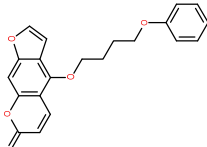
Chemical IUPAC Name	Abbreviation	Chemical Structure
(3E)-N,5-bis(4-chlorophenyl)-3-isopropylimino-phenazin-2-amine	Clofazimine	
4-(4-phenylbutoxy)furo[3,2-g]chromen-7-one	Psora-4	
4-(4-phenoxybutoxy)furo[3,2-g]chromen-7-one	PAP-1	

Table 1. Cont.

Chemical IUPAC Name	Abbreviation	Chemical Structure
(3-(4-(4-((7-oxo-7H-furo[3,2-g]benzopyran-4-yl)oxy)butoxy)phenyl)propyl)triphenyl phosphonium iodide	PAPTP	
4-[4-(4-hydroxyphenoxy)butoxy]furo[3,2-g]chromen-7-one	PAPOH *	
3-[[4-[4-(7-oxofuro[3,2-g]chromen-4-yl)oxybutoxy]phenoxy]carbonylamino]propyl-triphenoxy-phosphonium iodide	PCARBTP	
(3-(((4-(4-((7-oxo-7H-furo[3,2-g]chromen-4-yl)oxy)butoxy)phenoxy)carbonyl)oxy)propyl) triphenyl phosphonium iodide	PCTP	
(4-((7-oxo-7H-furo[3,2-g]chromen-4-yl)oxy)butyl) triphenyl phosphonium iodide	P5TP	

* The compound PAPOH is a product of hydrolysis of PCARBTP and PCTP.

A mitochondrial-targeted Psora-4 derivative called P5TP was obtained in which the distal phenyl ring was replaced by the TPP⁺ group [74]. A new derivative of PAP-1 in which the TPP⁺ group was attached by means of an unstable connection with the carbonate group was named PCTP.

Both derivatives were tested for their effect on viability in Kv1.3-transfected CTLL-2 cells. The use of P5TP did not improve significantly compared to Psora-4 or PAP-1, but PCTP was already effective and selective, and cell viability was dependent on the dose used and was not dependent on the presence of MDR (Multi Drug Resistance) inhibitors. As with previous derivatives, PCTP promoted apoptosis on four PDAC lines in murine melanoma B16-F10 cells by inhibiting the Kv1.3 channel, causing mitochondrial network fragmentation, depolarization, and ROS synthesis, and is a promising drug for in vivo testing [74].

The treatment of brain tumors, particularly glioblastoma (GBM) with Kv 1.3 channel inhibitors, is complex. Although in vitro, experiments on mouse and human GBM lines showed nearly 90% cell mortality after using PAPTP, PCARBTP, and clofazimine; in vivo tests on GBM-implanted mice did not yield any results. The blood-brain barrier (BBB) hinders the achievement of an effective dose in the tumor. It is therefore necessary to find a way to increase the bioavailability of drugs and enable them to pass through the BBB [75].

In summary, mitochondrial Kv1.3 potassium channels appear to be an effective and safe therapeutic target in the treatment of various types of cancer, including those resistant to chemotherapy. Certain difficulties with the bioavailability of mitoKv1.3 inhibitors found in *in vivo* studies, especially in the case of brain or pancreatic tumors, may be overcome by appropriate structural modifications. These drugs' efficiency and specificity in relation to cancer cells should be explored in the future.

6. Off-Target Action and Drug Repositioning of Potassium Channel Modulators

Since the discovery of potassium channels in eukaryotic cells, a large number of endogenous and synthesized substances have been discovered that modulate potassium channel activity. Due to the similar structure of potassium channels, some of these compounds interact with the channels found in the inner mitochondrial membrane. As mentioned above, a number of plasma membrane modulators, potassium channel openers, and inhibitors have been tested, and some have also been shown to regulate potassium channels located in the inner mitochondrial membrane [18].

Unfortunately, the accumulation of drugs in mitochondria will increase the probability of side effects (off-target effects) on mitochondrial enzymes, especially interactions with the respiratory chain or ATP synthase, which may be harmful due to multiple negative consequences on cellular function [76] (see Table 2). The potassium channel opener diazoxide is still used as the primary treatment to control hypoglycemia in insulinoma [77]. Diazoxide-sensitive K_{ATP} channels were discovered in mitochondria; moreover, it was shown that the mito K_{ATP} channel is more sensitive to diazoxide than its counterpart in the plasma membrane [20]. It was also observed that diazoxide is responsible for protecting heart cells in the processes of ischemia and reperfusion heart injury [14]. Additionally, diazoxide besides stimulation of the mito K_{ATP} channel activity has been shown to have protonophoretic properties [78]. It has also been shown that diazoxide is an inhibitor of succinate dehydrogenase (SDH, Complex II) [79,80]. Determining whether the cytoprotective effect of diazoxide is closely related to its effects on mito K_{ATP} or whether it has a synergistic effect with other targets requires further study. It is possible that diazoxide may exert its cytoprotective effect by inhibiting respiratory chain complex II and producing ROS reactive oxygen species [80,81], or mito K_{ATP} channels may be involved as an independent factor [82]. Researchers have speculated that targeting nucleotide-requiring enzymes, particularly SDH and cellular ATPases, diazoxide reduces ROS generation and nucleotide degradation, resulting in preservation of tissue ATP levels during ischemia [83].

A similar relationship, as in the case of diazoxide, occurs in the case of the mitoBK $_{Ca}$ channel, for which small molecules NS1619, CGS7184, NS11021, and paxilline, in addition to modulating the activity of channel, affect the activity of a number of proteins associated with the regulation of Ca^{2+} ions and respiratory chain proteins [84–87].

Table 2. Off-target action of selected mitochondrial potassium channel modulators.

Mitochondrial Potassium Channels	Potassium Channel Modulators	Off-Target Action
mito K_{ATP} Channel opener	diazoxide	- SDH inhibitor [79,80] - protonophoric properties [78] - induce translocation of PKC- ξ [88] - increase the expression of p-AKT and p-Foxo1 [89]
Channel blocker	Glibenclamide	- inhibits cardiac cAMP-activated Cl^- channels [90] - inhibitors of guinea-pig atrial chloride current [91]
mitoBK $_{Ca}$ Channel openers	NS1619	- SERCA inhibition [85] - inhibition L-type calcium channels [92] - stimulate Ca^{2+} -gated chloride currents [93]
	CGS7184	- RyR channel inhibition by CGS7184 [86,87]

Table 2. Cont.

Mitochondrial Potassium Channels	Potassium Channel Modulators	Off-Target Action
Channel blocker	paxilline	-modulation of the ATP-dependent Ca ²⁺ -ATPase at the phosphoenzyme level [94]
mitoK _v 1.3 Channel blocker	Clofazimine	- inhibitor of acid sphingomyelinase [95]
mitoK _v 7.4 Channel opener	Retigabine	- interaction with GABAergic and glutamatergic neurotransmission [96]
mitoTASK3 Channel openers	Halothane	-inhibition of synthesis of 5-hydroxytryptamine [97]
	Terbinafine	- CYP2D6 inhibition [98]
Channel blocker	Lidocaine	-interaction with Ca-ATPase in cardiac sarcoplasmic reticulum [99]
mitoHCN Channel blocker	ZD7288	- reduce T-type calcium channel currents [100]
		- inhibitor Na ⁺ current [101]

Notably, CGS7184, BMS191095, and NS1619, which show strong activating properties of the mitoBK_{Ca} potassium channel as measured in the patch-clamp technique administered to the cells and tissue, have the opposite effect [102–104]. Thus, despite similar interactions with mitoBK_{Ca}, the effect on cell survival is definitely different. In addition to the activation of mitoBK_{Ca}, CGS7184 and NS1619 cause an increase of cytosolic calcium ions concentration. The effect is the same for both compounds, whereas the mechanism of Ca²⁺ increase seems to be totally different [85,86]. The potassium channel opener CGS7184 releases Ca²⁺ by interacting with the RyR channel located in the endoplasmic reticulum, while NS1619 releases Ca²⁺ by inhibiting SERCA activity, a Ca²⁺-ATPase, and Ca²⁺ accumulation by endoplasmic reticulum. This difference seems to be important: in the case of CGS7184, the depletion of Ca²⁺ from the ER leads to activation of Ca²⁺-ATPase and ATP hydrolyses, while NS1619 inhibiting SERCA leads to inhibition of ATP depletion by this enzyme [85]. A similar effect targeting cellular ATPases occurs in the presence of the potassium channel opener diazoxide [83]. The mitoBK_{Ca} channel opener NS1619 significantly inhibits the electron transport chain and ATP hydrolysis [105]. An important effect of SERCA inhibition by the potassium channel opener NS1619 is its regulation by pH. At a low pH, SERCA is strongly inhibited by NS1619, and inhibition decreases with increasing pH [85]. Acidification of the cellular environment occurs in ischemia, which changes notably rapidly in the reperfusion and releases an inhibition of SERCA caused by NS1619. SERCA is less sensitive to lower pH and can efficiently hydrolyze ATP during ischemia [105]. Another mitoBK_{Ca} channel opener, NS11021, is highly specific to the mitoBK_{Ca} channel in isolated mitoplast membranes but used in cellular systems accelerate oxygen consumption by cells. It is greatly interesting that besides the activation of mitoBK_{Ca} channels, NS11021 also has strong mitochondrial uncoupling properties [106,107]. NS13558, which is a derivative of NS11021, and to which BK_{Ca} channels are insensitive, has the same property to uncouple the inner mitochondrial membrane and activate the respiratory chain. It is also interesting that NS11021 has a protective effect, despite its uncoupling properties on renal proximal tubular cells from cold storage [108]. It seems that some synergistic effects, in addition to the activation of mitochondrial potassium channels, also play a significant role.

We should also mention that the typical mitoBK_{Ca} channel blocker paxilline has protective effects, independent of channel inhibition, on cellular damage [109]. Paxilline has also been shown to inhibit SERCA at low concentrations, similar to NS1619 [94]. Paxilline has also been shown to reverse the protective effect of NS11021 at low concentrations on cells. This effect, in turn, can be closely related to inhibition of the mitoBK_{Ca} channel [110].

Drug repositioning involves the investigation of existing drugs for new therapeutic applications. Recently, a new set of mitochondrial potassium channels was discovered in skin-derived cells:

keratinocytes, dermal fibroblasts, and endothelial cells [25,35,40,53,111]. Naringenin, a plant-derived flavonoid, has been known for many years to have the potential to improve many health problems, such as cardiovascular, metabolic, neurological, and pulmonary disorders; and cancer [112,113]. Recently, the cardioprotective function of naringenin due to activation of the cardiac mitoBK_{Ca} channel was shown [114]. Additionally, with the use of patch-clamp single channel measurements, it was shown in skin fibroblasts that both the mitoK_{ATP} and mitoBK_{Ca} channels were activated by naringenin [111]. These studies suggest that naringenin may function as a potassium channel opener towards mitochondrial potassium channels in skin-derived cells.

7. Targeting Drugs into Mitochondria: A Unique Environment for Potassium Channels?

The organelle-specific delivery of drugs is a general problem and modern trend to achieve significant therapeutic effects and minimal off-target effects in molecular pharmacology.

Mitochondria constitute a unique biophysical environment for potassium channels compared to plasma membrane location. These differences may facilitate the search for drugs specific to mitochondrial potassium channels. Mitochondria are the only intracellular organelles with such a high membrane potential (approximately 180–200 mV with a negatively charged matrix). This property promotes accumulation in mitochondrial matrix lipophilic substances being positively charged.

Tetraphenylphosphonium cation (TPP⁺) is a clear example of such a substance. This property was used to measure mitochondrial membrane potential with the use of a TPP⁺ selective electrode. Although several methods can be used to measure the membrane potential in mitochondria, the use of the TPP⁺ selective electrode is still used in many studies with isolated mitochondria due to its sensitivity [115]. Hence, mitochondrial potassium channel openers or inhibitors with properties mentioned above (lipophilic cations or with TPP⁺ moiety) may reflect preference towards mitochondrial potassium channels.

The second unique property of mitochondria concerns matrix pH. Slight alkalization of the mitochondrial matrix (due to respiratory chain activity) will support the accumulation of weak acids in the mitochondrial matrix. Mitochondrial potassium channel openers or inhibitors with weak acid properties may accumulate in the mitochondrial matrix.

These properties constitute a particular attribute of mitochondria as an “antenna” for collecting substances with specific properties and attracting and accumulating them within mitochondria. To what extent these properties may be applied to increase the druggability of mitochondrial potassium channels is a matter of further investigation. Because of the presence of potassium channels in various cellular destinations, it is important to devise new approaches to target drugs into the mitochondria. Targeting mitochondrial potassium channel openers or inhibitors could regulate mitochondrial potassium channels in a more specific and efficient way.

There are various strategies to target drugs into mitochondria [116]. Some of these strategies are based, as previously mentioned, on the use of lipophilic cations, such as TPP⁺, attached to specific molecules (for review see [117]). This kind of mitochondrial targeting was initiated in 1995 with a tri-phenylphosphonium-thiobutyl conjugate as an antioxidant agent. Other lipophilic cations, such as dequalinium and rhodamine 123, were also mitochondria-targeting [118–122]. These cations play the role of “carrier” towards negatively charged mitochondrial matrix.

There are two well-known approaches for mitochondrial drug delivery: direct conjugation of the targeting ligand to drugs and attachment of the targeting ligand to a nanocarrier [116]. Direct drug-targeting ligand conjugation is simple and easy to control, and the drugs can readily reach the mitochondria; however, the conjugation procedure can diminish the biochemical effects within mitochondria. In the case of the nanocarrier system, there is no concern for a loss of therapeutic effect because the physical interaction and solubility issue would be solved, but optimization has remained a challenge due to the use of many different compositions to prepare the nanocarrier. For mitochondrial targeting, some peptides have been prepared and successfully applied based on the cell-penetrating peptide sequence [123]. The mitochondria-targeting peptides (mitochondria-penetrating peptide,

mitochondria-targeting sequence, SS peptide, and other peptides) were conjugated with various drugs to improve their therapeutic efficacy. The SS (Szeto-Schiller) peptide antioxidants represent a novel approach with targeted delivery of antioxidants to the inner mitochondrial membrane. The structural motif of these SS peptides centers on alternating aromatic residues and basic amino acids (aromatic-cationic peptides). Mitochondrial targeting sequences (MTSs) can be utilized as vehicles to deliver metalloporphyrin superoxide dismutase (SOD) mimics into the matrix. Recently, thermo responsive drug delivery to mitochondria was described and may represent an interesting and promising technique for cancer therapy [124].

8. Concluding Remarks

In this paper, we have described our current understanding of the interactions of numerous drugs with mitochondrial potassium channels. Mitochondria are a unique target for pharmacological intervention due to their high membrane potential and alkaline pH in the matrix. Regulation of the mitochondrial potassium channels by drugs is a complex issue. Increased understanding of the regulation of mitochondrial potassium channels by drugs will not only lead to increased knowledge of mitochondrial channels but may also contribute to the future application of these substances i.e., its druggability. We have also described the secondary effects of the drugs (off-target) in addition to their interaction with their primary target i.e., mitochondrial potassium channels.

The rational pharmacology of mitochondrial potassium channels should be preceded by the molecular identification of these proteins. Identification of the molecular identity of mitochondrial potassium channels will increase insight into the interactions of drugs with mitochondrial potassium channels. This outcome should be possible due to the recent molecular identification of pore-forming and regulatory subunits of mitoK_{ATP} or mitoBK_{Ca} channels. More detailed knowledge would provide more possibilities for the development of therapeutic strategies based on the selective modulation of mitochondrial potassium channels in various tissues. Therapies targeting mitochondrial potassium channels may play an important role in curing a variety of diseases.

In summary, more specific modulators of potassium channels are required for the advanced concept of druggability of mitochondrial potassium channels.

Author Contributions: Conceptualization, A.S., A.W., B.A. and M.Ż.; writing—review and editing, A.S., A.W., B.A. and M.Ż.; supervision, A.S.; funding acquisition, A.S. All authors have read and agreed to the published version of the manuscript.

Funding: This research was funded by National Science Center of Poland, grants number 2016/21/B/NZ1/02769 and 2019/34/A/NZ1/00352 (to A.S.).

Acknowledgments: This study was supported by the Nencki Institute of Experimental Biology and grants 2016/21/B/NZ1/02769 and 2019/34/A/NZ1/00352 from the Polish National Science Center, Poland. The authors wish to thank Bogusz Kulawiak for his insightful discussions.

Conflicts of Interest: The authors declare no conflict of interest. The funders had no role in the design of the study; in the collection, analyses, or interpretation of data; in the writing of the manuscript, or in the decision to publish the results.

References

1. Inoue, I.; Nagase, H.; Kishi, K.; Higuti, T. ATP-sensitive K⁺ channel in the mitochondrial inner membrane. *Nature* **1991**, *352*, 244–247. [CrossRef] [PubMed]
2. Siemen, D.; Loupatatzis, C.; Borecky, J.; Gulbins, E.; Lang, F. Ca²⁺-activated K channel of the BK-type in the inner mitochondrial membrane of a human glioma cell line. *Biochem. Biophys. Res. Commun.* **1999**, *257*, 549–554. [CrossRef] [PubMed]
3. Liu, Y.; Sato, T.; O'Rourke, B.; Marban, E. Mitochondrial ATP-dependent potassium channels: Novel effectors of cardioprotection? *Circulation* **1998**, *97*, 2463–2469. [CrossRef] [PubMed]
4. Crotti, L.; Odening, K.E.; Sanguinetti, M.C. Heritable arrhythmias associated with abnormal function of cardiac potassium channels. *Cardiovasc. Res.* **2020**. [CrossRef] [PubMed]

5. D'Adamo, M.C.; Liantonio, A.; Rolland, J.F.; Pessia, M.; Imbrici, P. Kv1.1 Channelopathies: Pathophysiological Mechanisms and Therapeutic Approaches. *Int. J. Mol. Sci.* **2020**, *21*, 2935. [CrossRef] [PubMed]
6. Trombetta-Lima, M.; Krabbendam, I.E.; Dolga, A.M. Calcium-activated potassium channels: Implications for aging and age-related neurodegeneration. *Int. J. Biochem. Cell Biol.* **2020**, *123*, 105748. [CrossRef]
7. Zhang, L.; Zheng, Y.; Xie, J.; Shi, L. Potassium channels and their emerging role in parkinson's disease. *Brain Res. Bull.* **2020**, *160*, 1–7. [CrossRef]
8. Walsh, K.B. Screening Technologies for Inward Rectifier Potassium Channels: Discovery of New Blockers and Activators. *SLAS Discov.* **2020**, *25*, 420–433. [CrossRef]
9. Moos, W.H.; Dykens, J.A. Mitochondrial drugs come of age. *Drug Dev. Res.* **2015**, *76*, 57–60. [CrossRef]
10. Olszewska, A.; Szewczyk, A. Mitochondria as a pharmacological target: Magnum overview. *IUBMB Life* **2013**, *65*, 273–281. [CrossRef]
11. Stoker, M.L.; Newport, E.; Hult, J.C.; West, A.P.; Morten, K.J. Impact of pharmacological agents on mitochondrial function: A growing opportunity? *Biochem. Soc. Trans.* **2019**, *47*, 1757–1772. [CrossRef] [PubMed]
12. Szewczyk, A.; Wojtczak, L. Mitochondria as a Pharmacological Target. *Pharmacol. Rev.* **2002**, *54*, 101–127. [CrossRef] [PubMed]
13. Laskowski, M.; Augustynek, B.; Kulawiak, B.; Koprowski, P.; Bednarczyk, P.; Jarmuszkiewicz, W.; Szewczyk, A. What do we not know about mitochondrial potassium channels? *Biochim. Biophys. Acta (BBA)-Bioenerg.* **2016**, *1857*, 1247–1257. [CrossRef] [PubMed]
14. O'Rourke, B. Evidence for mitochondrial K⁺ channels and their role in cardioprotection. *Circ. Res.* **2004**, *94*, 420–432. [CrossRef]
15. Szabo, I.; Zoratti, M. Mitochondrial channels: Ion fluxes and more. *Physiol. Rev.* **2014**, *94*, 519–608. [CrossRef]
16. Szewczyk, A.; Jarmuszkiewicz, W.; Kunz, W.S. Mitochondrial potassium channels. *IUBMB Life* **2009**, *61*, 134–143. [CrossRef]
17. Garlid, K.D.; Paucek, P. Mitochondrial potassium transport: The K⁺ cycle. *Biochim. Biophys. Acta* **2003**, *1606*, 23–41. [CrossRef]
18. Augustynek, B.; Kunz, W.S.; Szewczyk, A. Guide to the Pharmacology of Mitochondrial Potassium Channels. *Handb. Exp. Pharmacol.* **2017**, *240*, 103–127.
19. Leanza, L.; Checchetto, V.; Biasutto, L.; Rossa, A.; Costa, R.; Bachmann, M.; Zoratti, M.; Szabo, I. Pharmacological modulation of mitochondrial ion channels. *Br. J. Pharmacol.* **2019**, *176*, 4258–4283. [CrossRef]
20. Paucek, P.; Mironova, G.; Mahdi, F.; Beavis, A.D.; Woldegiorgis, G.; Garlid, K.D. Reconstitution and partial purification of the glibenclamide-sensitive, ATP-dependent K⁺ channel from rat liver and beef heart mitochondria. *J. Biol. Chem.* **1992**, *267*, 26062–26069.
21. Singh, H.; Lu, R.; Bopassa, J.C.; Meredith, A.L.; Stefani, E.; Toro, L. mitoBK_{Ca} is encoded by the *Kcnma1* gene, and a splicing sequence defines its mitochondrial location. *Proc. Natl. Acad. Sci. USA* **2013**, *110*, 10836–10841. [CrossRef] [PubMed]
22. Szewczyk, A.; Marban, E. Mitochondria: A new target for K channel openers? *Trends Pharmacol. Sci.* **1999**, *20*, 157–161. [CrossRef]
23. Hausenloy, D.J.; Schulz, R.; Girao, H.; Kwak, B.R.; De Stefani, D.; Rizzuto, R.; Bernardi, P.; Di Lisa, F. Mitochondrial ion channels as targets for cardioprotection. *J. Cell Mol. Med.* **2020**. [CrossRef]
24. Peruzzo, R.; Mattarei, A.; Romio, M.; Paradisi, C.; Zoratti, M.; Szabo, I.; Leanza, L. Regulation of Proliferation by a Mitochondrial Potassium Channel in Pancreatic Ductal Adenocarcinoma Cells. *Front. Oncol.* **2017**, *7*, 239. [CrossRef]
25. Bednarczyk, P.; Kicinska, A.; Laskowski, M.; Kulawiak, B.; Kampa, R.; Walewska, A.; Krajewska, M.; Jarmuszkiewicz, W.; Szewczyk, A. Evidence for a mitochondrial ATP-regulated potassium channel in human dermal fibroblasts. *Biochim. Biophys. Acta Bioenerg.* **2018**, *1859*, 309–318. [CrossRef] [PubMed]
26. Foster, D.B.; Ho, A.S.; Rucker, J.; Garlid, A.O.; Chen, L.; Sidor, A.; Garlid, K.D.; O'Rourke, B. Mitochondrial ROMK channel is a molecular component of mitoK(ATP). *Circ. Res.* **2012**, *111*, 446–454. [CrossRef]
27. Laskowski, M.; Augustynek, B.; Bednarczyk, P.; Zochowska, M.; Kalisz, J.; O'Rourke, B.; Szewczyk, A.; Kulawiak, B. Single-Channel Properties of the ROMK-Pore-Forming Subunit of the Mitochondrial ATP-Sensitive Potassium Channel. *Int. J. Mol. Sci.* **2019**, *20*, 5323. [CrossRef]

28. Papanicolaou, K.N.; Ashok, D.; Liu, T.; Bauer, T.M.; Sun, J.; Li, Z.; da Costa, E.; D’Orleans, C.C.; Nathan, S.; Lefer, D.J.; et al. Global knockout of ROMK potassium channel worsens cardiac ischemia-reperfusion injury but cardiomyocyte-specific knockout does not: Implications for the identity of mitoK_{ATP}. *J. Mol. Cell Cardiol.* **2020**, *139*, 176–189. [CrossRef]
29. Paggio, A.; Checchetto, V.; Campo, A.; Menabò, R.; Di Marco, G.; Di Lisa, F.; Szabo, I.; Rizzuto, R.; De Stefani, D. Identification of an ATP-sensitive potassium channel in mitochondria. *Nature* **2019**, *572*, 609–613. [CrossRef]
30. De Marchi, U.; Sassi, N.; Fioretti, B.; Catacuzzeno, L.; Cereghetti, G.M.; Szabo, I.; Zoratti, M. Intermediate conductance Ca²⁺-activated potassium channel (K_{Ca}3.1) in the inner mitochondrial membrane of human colon cancer cells. *Cell Calcium.* **2009**, *45*, 509–516. [CrossRef]
31. Dolga, A.M.; Netter, M.F.; Perocchi, F.; Doti, N.; Meissner, L.; Tobaben, S.; Grohm, J.; Zischka, H.; Plesnila, N.; Decher, N.; et al. Mitochondrial small conductance SK2 channels prevent glutamate-induced oxytosis and mitochondrial dysfunction. *J. Biol. Chem.* **2013**, *288*, 10792–10804. [CrossRef] [PubMed]
32. Szabo, I.; Bock, J.; Jekle, A.; Soddemann, M.; Adams, C.; Lang, F.; Zoratti, M.; Gulbins, E. A novel potassium channel in lymphocyte mitochondria. *J. Biol. Chem.* **2005**, *280*, 12790–12798. [CrossRef] [PubMed]
33. Leanza, L.; Zoratti, M.; Gulbins, E.; Szabo, I. Induction of apoptosis in macrophages via Kv1.3 and Kv1.5 potassium channels. *Curr. Med. Chem.* **2012**, *19*, 5394–5404. [CrossRef] [PubMed]
34. Testai, L.; Barrese, V.; Soldovieri, M.V.; Ambrosino, P.; Martelli, A.; Vinciguerra, I.; Miceli, F.; Greenwood, I.A.; Curtis, M.J.; Breschi, M.C.; et al. Expression and function of Kv7.4 channels in rat cardiac mitochondria: Possible targets for cardioprotection. *Cardiovasc. Res.* **2016**, *110*, 40–50. [CrossRef] [PubMed]
35. Toczyłowska-Maminska, R.; Olszewska, A.; Laskowski, M.; Bednarczyk, P.; Skowronek, K.; Szewczyk, A. Potassium channel in the mitochondria of human keratinocytes. *J. Invest. Dermatol.* **2014**, *134*, 764–772. [CrossRef]
36. Wojtovich, A.P.; Smith, C.O.; Urciuoli, W.R.; Wang, Y.T.; Xia, X.M.; Brookes, P.S.; Nehrke, K. Cardiac Slo2.1 Is Required for Volatile Anesthetic Stimulation of K⁺ Transport and Anesthetic Preconditioning. *Anesthesiology* **2016**, *124*, 1065–1076. [CrossRef]
37. Wojtovich, A.P.; Sherman, T.A.; Nadtochiy, S.M.; Urciuoli, W.R.; Brookes, P.S.; Nehrke, K. SLO-2 is cytoprotective and contributes to mitochondrial potassium transport. *PLoS ONE* **2011**, *6*, e28287. [CrossRef]
38. León-Aparicio, D.; Salvador, C.; Aparicio-Trejo, O.E.; Briones-Herrera, A.; Pedraza-Chaverri, J.; Vaca, L.; Sampieri, A.; Padilla-Flores, T.; López-González, Z.; León-Contreras, J.C.; et al. Novel Potassium Channels in Kidney Mitochondria: The Hyperpolarization-Activated and Cyclic Nucleotide-Gated HCN Channels. *Int. J. Mol. Sci.* **2019**, *20*, 4995.
39. Padilla-Flores, T.; López-González, Z.; Vaca, L.; Aparicio-Trejo, O.E.; Briones-Herrera, A.; Riveros-Rosas, H.; Pedraza-Chaverri, J.; León-Aparicio, D.; Salvador, C.; Sampieri, A.; et al. “Funny” channels in cardiac mitochondria modulate membrane potential and oxygen consumption. *Biochem. Biophys. Res. Commun.* **2020**, *524*, 1030–1036. [CrossRef]
40. Kicinska, A.; Augustynek, B.; Kulawiak, B.; Jarmuszkiewicz, W.; Szewczyk, A.; Bednarczyk, P. A large-conductance calcium-regulated K⁺ channel in human dermal fibroblast mitochondria. *Biochem. J.* **2016**, *473*, 4457–4471. [CrossRef]
41. Garlid, K.D.; Halestrap, A.P. The mitochondrial K_{ATP} channel—Fact or fiction? *J. Mol. Cell Cardiol.* **2012**, *52*, 578–583. [CrossRef] [PubMed]
42. Piwonska, M.; Wilczek, E.; Szewczyk, A.; Wilczynski, G.M. Differential distribution of Ca²⁺-activated potassium channel beta4 subunit in rat brain: Immunolocalization in neuronal mitochondria. *Neuroscience* **2008**, *153*, 446–460. [CrossRef] [PubMed]
43. Li, B.; Jie, W.; Huang, L.; Wei, P.; Li, S.; Luo, Z.; Friedman, A.K.; Meredith, A.L.; Han, M.-H.; Zhu, X.-H.; et al. Nuclear BK channels regulate gene expression via the control of nuclear calcium signaling. *Nat. Neurosci.* **2014**, *17*, 1055–1063. [CrossRef] [PubMed]
44. Noma, A. ATP-regulated K⁺ channels in cardiac muscle. *Nature* **1983**, *305*, 147–148. [CrossRef] [PubMed]
45. Tinker, A.; Aziz, Q.; Li, Y.; Specterman, M. ATP-Sensitive Potassium Channels and Their Physiological and Pathophysiological Roles. *Compr. Physiol.* **2018**, *8*, 1463–1511.
46. Inagaki, N.; Gonoi, T.; Clement, J.P.T.; Namba, N.; Inazawa, J.; Gonzalez, G.; Aguilar-Bryan, L.; Seino, S.; Bryan, J. Reconstitution of I_{K_{ATP}}: AN inward rectifier subunit plus the sulfonylurea receptor. *Science* **1995**, *270*, 1166–1170. [CrossRef]

47. Marty, A. Ca-dependent K channels with large unitary conductance in chromaffin cell membranes. *Nature* **1981**, *291*, 497–500. [CrossRef]
48. Xu, W.; Liu, Y.; Wang, S.; McDonald, T.; Van Eyk, J.E.; Sidor, A.; O'Rourke, B. Cytoprotective role of Ca²⁺-activated K⁺ channels in the cardiac inner mitochondrial membrane. *Science* **2002**, *298*, 1029–1033. [CrossRef]
49. Kulawiak, B.; Bednarczyk, P. Reconstitution of brain mitochondria inner membrane into planar lipid bilayer. *Acta Neurobiol. Exp.* **2005**, *65*, 271–276.
50. Singh, H.; Li, M.; Hall, L.; Chen, S.; Sukur, S.; Lu, R.; Caputo, A.; Meredith, A.L.; Stefani, E.; Toro, L. MaxiK channel interactome reveals its interaction with GABA transporter 3 and heat shock protein 60 in the mammalian brain. *Neuroscience* **2016**, *317*, 76–107. [CrossRef]
51. Skalska, J.; Bednarczyk, P.; Piwonska, M.; Kulawiak, B.; Wilczynski, G.; Dolowy, K.; Kudin, A.P.; Kunz, W.S.; Szewczyk, A. Calcium ions regulate K⁺ uptake into brain mitochondria: The evidence for a novel potassium channel. *Int. J. Mol. Sci.* **2009**, *10*, 1104–1120. [CrossRef] [PubMed]
52. Skalska, J.; Piwonska, M.; Wyroba, E.; Surmacz, L.; Wieczorek, R.; Koszela-Piotrowska, I.; Zielinska, J.; Bednarczyk, P.; Dolowy, K.; Wilczynski, G.M.; et al. A novel potassium channel in skeletal muscle mitochondria. *Biochim. Biophys. Acta* **2008**, *1777*, 651–659. [CrossRef] [PubMed]
53. Bednarczyk, P.; Koziel, A.; Jarmuszkiewicz, W.; Szewczyk, A. Large-conductance Ca²⁺-activated potassium channel in mitochondria of endothelial EA.hy926 cells. *Am. J. Physiol. Heart Circ. Physiol.* **2013**, *304*, H1415–H1427. [CrossRef] [PubMed]
54. Koszela-Piotrowska, I.; Matkovic, K.; Szewczyk, A.; Jarmuszkiewicz, W. A large-conductance calcium-activated potassium channel in potato (*Solanum tuberosum*) tuber mitochondria. *Biochem. J.* **2009**, *424*, 307–316. [CrossRef]
55. Laskowski, M.; Kicinska, A.; Szewczyk, A.; Jarmuszkiewicz, W. Mitochondrial large-conductance potassium channel from *Dictyostelium discoideum*. *Int. J. Biochem. Cell Biol.* **2015**, *60*, 167–175. [CrossRef]
56. Magleby, K.L. Gating mechanism of BK (Sl α 1) channels: So near, yet so far. *J. Gen. Physiol.* **2003**, *121*, 81–96. [CrossRef]
57. Nardi, A.; Olesen, S.P. BK channel modulators: A comprehensive overview. *Curr. Med. Chem.* **2008**, *15*, 1126–1146. [CrossRef]
58. Latorre, R.; Brauchi, S. Large conductance Ca²⁺-activated K⁺ (BK) channel: Activation by Ca²⁺ and voltage. *Biol. Res.* **2006**, *39*, 385–401. [CrossRef]
59. Sakai, Y.; Harvey, M.; Sokolowski, B. Identification and quantification of full-length BK channel variants in the developing mouse cochlea. *J. Neurosci. Res.* **2011**, *89*, 1747–1760. [CrossRef]
60. Ahmad, T.; Mukherjee, S.; Pattnaik, B.; Kumar, M.; Singh, S.; Kumar, M.; Rehman, R.; Tiwari, B.K.; Jha, K.A.; Barhanpurkar, A.P.; et al. Miro1 regulates intercellular mitochondrial transport & enhances mesenchymal stem cell rescue efficacy. *EMBO J.* **2014**, *33*, 994–1010.
61. Gulbins, E.; Sassi, N.; Grassme, H.; Zoratti, M.; Szabo, I. Role of Kv1.3 mitochondrial potassium channel in apoptotic signalling in lymphocytes. *Biochim. Biophys. Acta* **2010**, *1797*, 1251–1259. [CrossRef] [PubMed]
62. Szabo, I.; Bock, J.; Grassme, H.; Soddemann, M.; Wilker, B.; Lang, F.; Zoratti, M.; Gulbins, E. Mitochondrial potassium channel Kv1.3 mediates Bax-induced apoptosis in lymphocytes. *Proc. Natl. Acad. Sci. USA* **2008**, *105*, 14861–14866. [CrossRef]
63. Rotko, D.; Bednarczyk, P.; Koprowski, P.; Kunz, W.S.; Szewczyk, A.; Kulawiak, B. Heme is required for carbon monoxide activation of mitochondrial BKCa channel. *Eur. J. Pharmacol.* **2020**, *881*, 173191. [CrossRef] [PubMed]
64. Rotko, D.; Kunz, W.S.; Szewczyk, A.; Kulawiak, B. Signaling pathways targeting mitochondrial potassium channels. *Int. J. Biochem. Cell Biol.* **2020**, *125*, 105792. [CrossRef] [PubMed]
65. Walewska, A.; Szewczyk, A.; Koprowski, P. Gas Signaling Molecules and Mitochondrial Potassium Channels. *Int. J. Mol. Sci.* **2018**, *19*, 3227. [CrossRef]
66. Bednarczyk, P.; Wieckowski, M.R.; Broszkiewicz, M.; Skowronek, K.; Siemen, D.; Szewczyk, A. Putative Structural and Functional Coupling of the Mitochondrial BK Channel to the Respiratory Chain. *PLoS ONE* **2013**, *8*, e68125. [CrossRef]
67. Szewczyk, A.; Bednarczyk, P. Modulation of the Mitochondrial Potassium Channel Activity by Infrared Light. *Biophys. J.* **2018**, *114*, 43A. [CrossRef]

68. Walewska, A.; Kulawiak, B.; Szewczyk, A.; Koprowski, P. Mechanosensitivity of mitochondrial large-conductance calcium-activated potassium channels. *Biochim. Biophys. Acta Bioenerg.* **2018**, *1859*, 797–805. [CrossRef]
69. Checchetto, V.; Prosdocimi, E.; Leanza, L. Mitochondrial Kv1.3: A New Target in Cancer Biology? *Cell Physiol. Biochem.* **2019**, *53*, 52–62.
70. Leanza, L.; Henry, B.; Sassi, N.; Zoratti, M.; Chandy, K.G.; Gulbins, E.; Szabo, I. Inhibitors of mitochondrial Kv1.3 channels induce Bax/Bak-independent death of cancer cells. *EMBO Mol. Med.* **2012**, *4*, 577–593. [CrossRef]
71. Leanza, L.; Trentin, L.; Becker, K.A.; Frezzato, F.; Zoratti, M.; Semenzato, G.; Gulbins, E.; Szabo, I. Clofazimine, Psora-4 and PAP-1, inhibitors of the potassium channel Kv1.3, as a new and selective therapeutic strategy in chronic lymphocytic leukemia. *Leukemia* **2013**, *27*, 1782–1785. [CrossRef] [PubMed]
72. Leanza, L.; Romio, M.; Becker, K.A.; Azzolini, M.; Trentin, L.; Manago, A.; Venturini, E.; Zaccagnino, A.; Mattarei, A.; Carraretto, L.; et al. Direct Pharmacological Targeting of a Mitochondrial Ion Channel Selectively Kills Tumor Cells In Vivo. *Cancer Cell* **2017**, *31*, 516–531. [CrossRef] [PubMed]
73. Teisseyre, A.; Palko-Labuz, A.; Sroda-Pomianek, K.; Michalak, K. Voltage-Gated Potassium Channel Kv1.3 as a Target in Therapy of Cancer. *Front. Oncol.* **2019**, *9*, 933. [CrossRef] [PubMed]
74. Mattarei, A.; Romio, M.; Manago, A.; Zoratti, M.; Paradisi, C.; Szabo, I.; Leanza, L.; Biasutto, L. Novel Mitochondria-Targeted Furocoumarin Derivatives as Possible Anti-Cancer Agents. *Front. Oncol.* **2018**, *8*, 122. [CrossRef]
75. Venturini, E.; Leanza, L.; Azzolini, M.; Kadow, S.; Mattarei, A.; Weller, M.; Tabatabai, G.; Edwards, M.J.; Zoratti, M.; Paradisi, C.; et al. Targeting the Potassium Channel Kv1.3 Kills Glioblastoma Cells. *Neurosignals* **2017**, *25*, 26–38. [CrossRef]
76. Szewczyk, A.; Kajma, A.; Malinska, D.; Wrzosek, A.; Bednarczyk, P.; Zablocka, B.; Dolowy, K. Pharmacology of mitochondrial potassium channels: Dark side of the field. *FEBS Lett.* **2010**, *584*, 2063–2069. [CrossRef]
77. Gilliaux, Q.; Bertrand, C.; Hanon, F.; Donckier, J.E. Preoperative treatment of benign insulinoma: Diazoxide or somatostatin analogues? *Acta Chir. Belg.* **2020**. [CrossRef]
78. Kowaltowski, A.J.; Seetharaman, S.; Paucek, P.; Garlid, K.D. Bioenergetic consequences of opening the ATP-sensitive K⁺ channel of heart mitochondria. *Am. J. Physiol. Heart Circ. Physiol.* **2001**, *280*, H649–H657. [CrossRef]
79. Akopova, O.; Kolchinskaya, L.; Nosar, V.; Mankovska, I.; Sagach, V. Diazoxide affects mitochondrial bioenergetics by the opening of mKATP channel on submicromolar scale. *BMC Mol. Cell Biol.* **2020**, *21*, 31. [CrossRef]
80. Drose, S.; Brandt, U.; Hanley, P.J. K⁺-independent actions of diazoxide question the role of inner membrane K_{ATP} channels in mitochondrial cytoprotective signaling. *J. Biol. Chem.* **2006**, *281*, 23733–23739. [CrossRef]
81. Hanley, P.J.; Mickel, M.; Loffler, M.; Brandt, U.; Daut, J. K_{ATP} channel-independent targets of diazoxide and 5-hydroxydecanoate in the heart. *J. Physiol.* **2002**, *542*, 735–741. [CrossRef]
82. Dröse, S.; Bleier, L.; Brandt, U. A Common Mechanism Links Differently Acting Complex II Inhibitors to Cardioprotection: Modulation of Mitochondrial Reactive Oxygen Species Production. *Mol. Pharmacol.* **2011**, *79*, 814–822. [CrossRef]
83. Dzeja, P.P.; Bast, P.; Ozcan, C.; Valverde, A.; Holmuhamedov, E.L.; Van Wylen, D.G.; Terzic, A. Targeting nucleotide-requiring enzymes: Implications for diazoxide-induced cardioprotection. *Am. J. Physiol. Heart Circ. Physiol.* **2003**, *284*, H1048–H1056. [CrossRef] [PubMed]
84. Debska, G.; Kicinska, A.; Dobrucki, J.; Dworakowska, B.; Nurowska, E.; Skalska, J.; Dolowy, K.; Szewczyk, A. Large-conductance K⁺ channel openers NS1619 and NS004 as inhibitors of mitochondrial function in glioma cells. *Biochem. Pharmacol.* **2003**, *65*, 1827–1834. [CrossRef]
85. Wrzosek, A. The potassium channel opener NS1619 modulates calcium homeostasis in muscle cells by inhibiting SERCA. *Cell Calcium.* **2014**, *56*, 14–24. [CrossRef]
86. Wrzosek, A.; Tomaskova, Z.; Ondrias, K.; Łukasiak, A.; Szewczyk, A. The potassium channel opener CGS7184 activates Ca²⁺ release from the endoplasmic reticulum. *Eur. J. Pharmacol.* **2012**, *690*, 60–67. [CrossRef] [PubMed]
87. Wrzosek, A.; Tomaskova, Z.; Ondrias, K.; Łukasiak, A.; Szewczyk, A. CGS7184 a potassium channel opener modulates activity of mitochondria and Ca²⁺ homeostasis. *Biochim. Biophys. Acta (BBA)–Bioenerg.* **2012**, *1817*, S88–S89. [CrossRef]

88. Kim, M.Y.; Kim, M.J.; Yoon, I.S.; Ahn, J.H.; Lee, S.H.; Baik, E.J.; Moon, C.H.; Jung, Y.S. Diazoxide acts more as a PKC-Epsilon activator, and indirectly activates the mitochondrial K(ATP) channel conferring cardioprotection against hypoxic injury. *Br. J. Pharmacol.* **2006**, *149*, 1059–1070. [CrossRef] [PubMed]
89. Duan, P.; Wang, J.; Li, Y.; Wei, S.; Su, F.; Zhang, S.; Duan, Y.; Wang, L.; Zhu, Q. Opening of mitoKATP improves cardiac function and inhibits apoptosis via the AKT-Foxo1 signaling pathway in diabetic cardiomyopathy. *Int. J. Mol. Med.* **2018**, *42*, 2709–2719. [CrossRef]
90. Tominaga, M.; Horie, M.; Sasayama, S.; Okada, Y. Glibenclamide, an ATP-sensitive K⁺ channel blocker, inhibits cardiac cAMP-activated Cl⁻ conductance. *Circ. Res.* **1995**, *77*, 417–423. [CrossRef]
91. Sakaguchi, M.; Matsuura, H.; Ehara, T. Swelling-induced Cl⁻ current in guinea-pig atrial myocytes: Inhibition by glibenclamide. *J. Physiol.* **1997**, *505*, 41–52. [CrossRef] [PubMed]
92. Park, W.S.; Kang, S.H.; Son, Y.K.; Kim, N.; Ko, J.-H.; Kim, H.K.; Ko, E.A.; Kim, C.D.; Han, J. The mitochondrial Ca²⁺-activated K⁺ channel activator, NS 1619 inhibits L-type Ca²⁺ channels in rat ventricular myocytes. *Biochem. Biophys. Res. Commun.* **2007**, *362*, 31–36. [CrossRef] [PubMed]
93. Saleh, S.N.; Angermann, J.E.; Sones, W.R.; Leblanc, N.; Greenwood, I.A. Stimulation of Ca²⁺-gated Cl⁻ currents by the calcium-dependent K⁺ channel modulators NS1619 [1,3-dihydro-1-[2-hydroxy-5-(trifluoromethyl)phenyl]-5-(trifluoromethyl)-2 H-benzimidazol-2-one] and isopimaric acid. *J. Pharmacol. Exp. Ther.* **2007**, *321*, 1075–1084. [CrossRef]
94. Bilmen, J.G.; Wootton, L.L.; Michelangeli, F. The mechanism of inhibition of the sarco/endoplasmic reticulum Ca²⁺ ATPase by paxilline. *Arch. Biochem. Biophys.* **2002**, *406*, 55–64. [CrossRef]
95. Kornhuber, J.; Muehlbacher, M.; Trapp, S.; Pechmann, S.; Friedl, A.; Reichel, M.; Mühle, C.; Terfloth, L.; Groemer, T.W.; Spitzer, G.M.; et al. Identification of novel functional inhibitors of acid sphingomyelinase. *PLoS ONE* **2011**, *6*, e23852. [CrossRef] [PubMed]
96. Rundfeldt, C.; Netzer, R. Investigations into the mechanism of action of the new anticonvulsant retigabine—Interaction with GABAergic and glutamatergic neurotransmission and with voltage gated ion channels. *Arzneimittelforschung* **2000**, *50*, 1063–1070. [CrossRef] [PubMed]
97. De Crescenzo, V.; Dubuis, E.; Constantin, S.; Rebocho, M.; Girardin, C.; Bonnet, P.; Vandier, C. Halothane differentially decreases 5-hydroxytryptamine-induced contractions in normal and chronic hypoxic rat pulmonary arteries. *Acta Physiol. Scand.* **2001**, *173*, 247–255. [CrossRef]
98. Madani, S.; Barilla, D.; Cramer, J.; Wang, Y.; Paul, C. Effect of terbinafine on the pharmacokinetics and pharmacodynamics of desipramine in healthy volunteers identified as cytochrome P450 2D6 (CYP2D6) extensive metabolizers. *J. Clin. Pharmacol.* **2002**, *42*, 1211–1218. [CrossRef]
99. Karon, B.S.; Geddis, L.M.; Kutchai, H.; Thomas, D.D. Anesthetics alter the physical and functional properties of the Ca-ATPase in cardiac sarcoplasmic reticulum. *Biophys. J.* **1995**, *68*, 936–945. [CrossRef]
100. Sánchez-Alonso, J.L.; Halliwell, J.V.; Colino, A. ZD 7288 inhibits T-type calcium current in rat hippocampal pyramidal cells. *Neurosci. Lett.* **2008**, *439*, 275–280. [CrossRef]
101. Wu, X.; Liao, L.; Liu, X.; Luo, F.; Yang, T.; Li, C. Is ZD7288 a selective blocker of hyperpolarization-activated cyclic nucleotide-gated channel currents? *Channels* **2012**, *6*, 438–442. [CrossRef] [PubMed]
102. Augustynek, B.; Koprowski, P.; Rotko, D.; Kunz, W.S.; Szewczyk, A.; Kulawiak, B. Mitochondrial BK Channel Openers CGS7181 and CGS7184 Exhibit Cytotoxic Properties. *Int. J. Mol. Sci.* **2018**, *19*, 253. [CrossRef] [PubMed]
103. Chmielewska, L.; Malinska, D. Cytoprotective action of the potassium channel opener NS1619 under conditions of disrupted calcium homeostasis. *Pharmacol. Rep.* **2011**, *63*, 176–183. [CrossRef]
104. Malinska, D.; Kulawiak, B.; Wrzosek, A.; Kunz, W.S.; Szewczyk, A. The cytoprotective action of the potassium channel opener BMS-191095 in C2C12 myoblasts is related to the modulation of calcium homeostasis. *Cell Physiol. Biochem.* **2010**, *26*, 235–246. [CrossRef] [PubMed]
105. Łukasiak, A.; Skup, A.; Chlopicki, S.; Łomnicka, M.; Kaczara, P.; Proniewski, B.; Szewczyk, A.; Wrzosek, A. SERCA, complex I of the respiratory chain and ATP-synthase inhibition are involved in pleiotropic effects of NS1619 on endothelial cells. *Eur. J. Pharmacol.* **2016**, *786*, 137–147. [CrossRef] [PubMed]
106. Bentzen, B.H.; Andersen, R.W.; Olesen, S.P.; Grunnet, M.; Nardi, A. Synthesis and characterisation of NS13558: A new important tool for addressing KCa1.1 channel function ex vivo. *Naunyn Schmiedebergs Arch. Pharmacol.* **2010**, *381*, 271–283. [CrossRef]

107. Bentzen, B.H.; Nardi, A.; Calloe, K.; Madsen, L.S.; Olesen, S.r.-P.; Grunnet, M. The Small Molecule NS11021 Is a Potent and Specific Activator of Ca²⁺-Activated Big-Conductance K⁺ Channels. *Mol. Pharmacol.* **2007**, *72*, 1033–1044. [CrossRef]
108. Shrum, S.; Rusch, N.J.; MacMillan-Crow, L.A. Specific BK Channel Activator NS11021 Protects Rat Renal Proximal Tubular Cells from Cold Storage-Induced Mitochondrial Injury In Vitro. *Biomolecules* **2019**, *9*, 825. [CrossRef]
109. Kulawiak, B.; Szewczyk, A. Glutamate-induced cell death in HT22 mouse hippocampal cells is attenuated by paxilline, a BK channel inhibitor. *Mitochondrion* **2012**, *12*, 169–172. [CrossRef]
110. Bentzen, B.H.; Osadchii, O.; Jespersen, T.; Hansen, R.S.; Olesen, S.P.; Grunnet, M. Activation of big conductance Ca²⁺-activated K⁺ channels (BK) protects the heart against ischemia-reperfusion injury. *Pflug. Arch.* **2009**, *457*, 979–988. [CrossRef]
111. Kampa, R.P.; Kicinska, A.; Jarmuszkiewicz, W.; Pasikowska-Piwko, M.; Dolegowska, B.; Debowska, R.; Szewczyk, A.; Bednarczyk, P. Naringenin as an opener of mitochondrial potassium channels in dermal fibroblasts. *Exp. Dermatol.* **2019**, *28*, 543–550. [CrossRef] [PubMed]
112. Fuster, M.G.; Carissimi, G.; Montalban, M.G.; Villora, G. Improving Anticancer Therapy with Naringenin-Loaded Silk Fibroin Nanoparticles. *Nanomaterials* **2020**, *10*, 718. [CrossRef] [PubMed]
113. Rivoira, M.A.; Rodriguez, V.; Talamoni, G.; de Talamoni, N.T. New perspectives in the pharmacological potential of naringin in medicine. *Curr. Med. Chem.* **2020**. [CrossRef] [PubMed]
114. Testai, L.; Da Pozzo, E.; Piano, I.; Pistelli, L.; Gargini, C.; Breschi, M.C.; Braca, A.; Martini, C.; Martelli, A.; Calderone, V. The Citrus Flavanone Naringenin Produces Cardioprotective Effects in Hearts from 1 Year Old Rat, through Activation of mitoBK Channels. *Front. Pharmacol.* **2017**, *8*, 71. [CrossRef]
115. Teodoro, J.S.; Palmeira, C.M.; Rolo, A.P. Mitochondrial Membrane Potential (DeltaPsi) Fluctuations Associated with the Metabolic States of Mitochondria. *Methods Mol. Biol.* **2018**, *1782*, 109–119.
116. Heller, A.; Brockhoff, G.; Goepferich, A. Targeting drugs to mitochondria. *Eur. J. Pharm. Biopharm.* **2012**, *82*, 1–18. [CrossRef]
117. Battogtokh, G.; Cho, Y.Y.; Lee, J.Y.; Lee, H.S.; Kang, H.C. Mitochondrial-Targeting Anticancer Agent Conjugates and Nanocarrier Systems for Cancer Treatment. *Front. Pharmacol.* **2018**, *9*, 922. [CrossRef]
118. Christman, J.E.; Miller, D.S.; Coward, P.; Smith, L.H.; Teng, N.N. Study of the selective cytotoxic properties of cationic, lipophilic mitochondrial-specific compounds in gynecologic malignancies. *Gynecol. Oncol.* **1990**, *39*, 72–79. [CrossRef]
119. Dairkee, S.H.; Hackett, A.J. Differential retention of rhodamine 123 by breast carcinoma and normal human mammary tissue. *Breast Cancer Res. Treat.* **1991**, *18*, 57–61. [CrossRef]
120. Ernster, L.; Schatz, G. Mitochondria: A historical review. *J. Cell Biol.* **1981**, *91*, 227s–255s. [CrossRef]
121. Lampidis, T.J.; Munck, J.N.; Krishan, A.; Tapiero, H. Reversal of resistance to rhodamine 123 in adriamycin-resistant Friend leukemia cells. *Cancer Res.* **1985**, *45*, 2626–2631. [PubMed]
122. Weiss, M.J.; Wong, J.R.; Ha, C.S.; Bleday, R.; Salem, R.R.; Steele, G.D., Jr.; Chen, L.B. Dequalinium, a topical antimicrobial agent, displays anticarcinoma activity based on selective mitochondrial accumulation. *Proc. Natl. Acad. Sci. USA* **1987**, *84*, 5444–5448. [CrossRef] [PubMed]
123. Szeto, H.H. Cell-permeable, mitochondrial-targeted, peptide antioxidants. *AAPS J.* **2006**, *8*, E277–E283. [CrossRef] [PubMed]
124. Ruan, L.; Zhou, M.; Chen, J.; Huang, H.; Zhang, J.; Sun, H.; Chai, Z.; Hu, Y. Thermoresponsive drug delivery to mitochondria in vivo. *Chem. Commun.* **2019**, *55*, 14645–14648. [CrossRef]



© 2020 by the authors. Licensee MDPI, Basel, Switzerland. This article is an open access article distributed under the terms and conditions of the Creative Commons Attribution (CC BY) license (<http://creativecommons.org/licenses/by/4.0/>).

Review

Proteomic and Bioinformatic Profiling of Transporters in Higher Plant Mitochondria

Ian Max Møller ^{1,*} , R. Shyama Prasad Rao ² , Yuexu Jiang ³, Jay J. Thelen ⁴ and Dong Xu ³ 

¹ Department of Molecular Biology and Genetics, Aarhus University, Forsøgsvej 1, DK-4200 Slagelse, Denmark

² Biostatistics and Bioinformatics Division, Yenepoya Research Center, Yenepoya University, Mangaluru 575018, Karnataka, India; drrsprao@gmail.com

³ Department of Electrical Engineering and Computer Science, Bond Life Sciences Center, University of Missouri, Columbia, MO 65211, USA; yjm85@mail.missouri.edu (Y.J.); xudong@missouri.edu (D.X.)

⁴ Department of Biochemistry, University of Missouri, Bond Life Sciences Center, University of Missouri, Columbia, MO 65211, USA; thelenj@missouri.edu

* Correspondence: ian.max.moller@mbg.au.dk

Received: 9 July 2020; Accepted: 13 August 2020; Published: 16 August 2020

Abstract: To function as a metabolic hub, plant mitochondria have to exchange a wide variety of metabolic intermediates as well as inorganic ions with the cytosol. As identified by proteomic profiling or as predicted by MU-LOC, a newly developed bioinformatics tool, *Arabidopsis thaliana* mitochondria contain 128 or 143 different transporters, respectively. The largest group is the mitochondrial carrier family, which consists of symporters and antiporters catalyzing secondary active transport of organic acids, amino acids, and nucleotides across the inner mitochondrial membrane. An impressive 97% (58 out of 60) of all the known mitochondrial carrier family members in *Arabidopsis* have been experimentally identified in isolated mitochondria. In addition to many other secondary transporters, *Arabidopsis* mitochondria contain the ATP synthase transporters, the mitochondria protein translocase complexes (responsible for protein uptake across the outer and inner membrane), ATP-binding cassette (ABC) transporters, and a number of transporters and channels responsible for allowing water and inorganic ions to move across the inner membrane driven by their transmembrane electrochemical gradient. A few mitochondrial transporters are tissue-specific, development-specific, or stress-response specific, but this is a relatively unexplored area in proteomics that merits much more attention.

Keywords: ABC transporter; aquaporin; ATP synthase; ion channels; mitochondrial carrier family

1. Introduction

Eukaryotic multicellular organisms need to exchange energy, matter, and information between the environment and their cells, between their cells, and within their cells. To perform these tasks, they need a diverse array of specialized proteins to move ions and molecules across the biological membranes, which delimit the cells and the subcellular compartmentation. These proteins are collectively known as transporters, which include carriers, channels, and pumps [1].

The mitochondrion is a metabolic hub, not only for energy metabolism—the tricarboxylic acid (TCA) cycle and oxidative phosphorylation—but also for the biosynthesis of coenzymes, amino acids, some fatty acids, and lipids [2,3]. In photosynthetic cells in the light, there is a massive flow of fixed carbon from the chloroplasts to the rest of the cell, especially to the mitochondria via the cytosol, but metabolic cooperation between plastids and mitochondria also takes place in darkness [4,5]. Retrograde signaling from the mitochondria to the nucleus probably involves export of peptides [6,7]. In addition to this, to grow and divide the mitochondria one needs to import the vast majority of its proteins as well as some tRNAs and rRNA [8–10].

All of these processes require the presence of many different transporters in the mitochondria. The outer membrane contains only two types: (i) Porin also called voltage-dependent anion channel (VDAC) or voltage-dependent gated ion channel (VIC), which makes the outer mitochondrial membrane (OMM) permeable to all molecules smaller than 5 kDa, obviating the need for other transporters of small ions and molecules [11,12]. (ii) Translocase Outer Membrane (TOM), the subcomplex of the Mitochondrial Protein Translocase (MPT) responsible for importing proteins across the OMM. In addition to Translocase Inner Membrane (TIM), the MPT subcomplex responsible for importing proteins across the inner mitochondrial membrane (IMM), the IMM contains many other transporters of several different classes. The mitochondrial transportome was comprehensively reviewed by Lee and Millar [13].

It is the purpose of this review first to compile a list of the transporters identified by proteomic profiling of isolated plant mitochondria. This list will then be compared to a list of transporters predicted by MU-LOC [14], a newly developed program, to predict mitochondrial proteins based on their amino acid sequences and their gene expression patterns. Finally, for each transporter class or family, we will briefly discuss the properties of the transporters present in plant mitochondria.

2. The Experimental Proteome and Transportome in Plant Mitochondria

2.1. The Experimental Mitochondrial Proteome

The mitochondrial proteome has been characterized in some depth in *Arabidopsis thaliana* cell cultures and in potato (*Solanum tuberosum* L.) tubers. In both, almost 1100 proteins were identified as summarized by Rao et al. [8]. Since then, Senkler et al. [15] published what they called the “mitochondrial complexome of *Arabidopsis thaliana*”, in which they identified 1359 proteins involved in various complexes both in the membranes and in the soluble fraction. Altogether, the mitochondrial proteome in a plant probably contains 2000–2500 proteins [8] or about 10% of the total *Arabidopsis* proteome (Table 1). Plant mitochondrial DNA encodes at most 40 proteins [16], which are synthesized inside the mitochondria on mitochondrial ribosomes, while the remaining 2000+ proteins are encoded in the nuclear DNA, synthesized on cytosolic ribosomes, or on polysomes associated with the mitochondrial surface, and imported across the OMM and IMM [17].

The largest protein groups in the identified proteome of both *Arabidopsis* and potato mitochondria are related to energy and metabolism, with around 150 and 200 proteins, respectively; protein fate, protein synthesis, and RNA processing are each represented by approximately 100 proteins, while transport has around 50 proteins [8]. In this Gene Ontology (GO) nomenclature, many transporters are listed under different GO terms, e.g., ATP synthase subunits are found under energy. The actual number of identified transporters is therefore much larger, as discussed below. However, it is not just the number of unique proteins that is important. The abundance of each protein is also important, and Salvato et al. [18] used spectral counting to estimate the abundance of the identified proteins. The 52 proteins under the GO term Transporter showed an overall average abundance, but with significant variation among the transporters. Fuch et al. [19] went one step further by estimating the copy number of the individual proteins and protein complexes present in a single mitochondrion. Based on that, they could then calculate the surface area occupied by the various membrane proteins. They found that VDAC and TOM cover 34% and 12% of the surface area of the OMM, respectively. The five respiratory complexes cover 18% of the IMM, while the most abundant of the other carriers—ADP/ATP carrier, phosphate carrier, the uncoupling protein, and the tricarboxylate/dicarboxylate carrier—cover a total of about 11% of the IMM [19].

Table 1. Number of proteins in different transporter classes and families, and their experimental (proteomic) identification in isolated mitochondria of Arabidopsis and rice and mitochondrial localization prediction status (using MU-LOC) in Arabidopsis, rice, human, and mouse.

	<i>A. thaliana</i>			<i>O. sativa</i>			<i>H. sapiens</i>			<i>M. musculus</i>						
	Transport DB #	Experimental *	%	Predicted #	%	Transport DB #	Experimental *	%	Predicted #	%	Transport DB #	Predicted #	%	Transport DB #	Predicted #	%
Whole proteome	26,091	-	-	-	-	55,890	-	-	-	-	37,742	-	-	34,966	-	-
ATP-dependent																
ABC transporters	124	6	5	13	11	129	0	0	11	9	77	10	13	65	5	8
F-ATPase	44	16	36	17	39	50	7	14	13	26	60	25	42	58	19	33
MPT family	25	19	76	10	40	30	2	7	10	33	29	6	21	40	6	15
P-type ATPases	50	2	4	4	8	45	0	0	3	7	68	6	9	50	0	0
Other ATP-dependent	50	4	8	14	28	30	0	0	10	33	19	4	21	34	4	12
Secondary transporters																
MC family	60	58	97	30	50	61	50	82	33	54	63	25	40	64	21	33
Other families	722	13	2	34	5	799	0	0	50	6	511	39	8	473	28	6
Ion channels	151	11	7	15	10	137	0	0	10	7	588	9	2	470	8	2
Unclassified	53	0	0	6	11	4	0	0	0	0	52	5	10	36	2	6
Total (Transporters)	1279	129	10	143	11	1285	59	5	140	11	1467	129	9	1290	93	7

See Table S1 for a full list of transporters from TransportDB (<http://www.membranetransport.org/transportDB2/index.html>) and their mitochondrial prediction status (using MU-LOC).

* See Table S2 for a list of experimentally identified mitochondrial transporters.

2.2. The Experimental Mitochondrial Transportome

Membrane transporters, and other transmembrane, integral-membrane proteins, are generally more difficult to identify than soluble proteins using “bottom-up” proteomics due to the paucity of charged and polar amino acids, which most sequencing-grade proteases recognize as cleavage sites. Moreover, these proteins with their hydrophobic transmembrane helices are more difficult to solubilize, and the large hydrophobic peptides formed do not ionize well for the mass spectrometry detection [20–23].

In-depth proteome profiling has only been done on mitochondria isolated from a very limited number of plant species and cell types, notably *Arabidopsis* cell cultures and potato tubers. Furthermore, the plants/cell cultures have mostly been grown under standard environmental conditions (no stress), and none of the tissues or cells have been photosynthetic. The only major exceptions to this are two developmental studies in germinating rice seeds under normoxia and hypoxia [24] and in maize embryos during seed development [25]. For that reason, the experimentally characterized mitochondrial proteome, although quite comprehensive, can be expected to lack cell-specific, tissue-specific, and environmental-specific mitochondrial proteins and protein isoforms.

In spite of these limitations, 128 transporters have been experimentally identified in *Arabidopsis* mitochondria (Table 1). The most numerous are the secondary transporters with 71 proteins, including 58 belonging to the Mitochondrial Carrier (MC) family. There are also many F-ATPases (ATP synthase subunits), and MPT proteins (subunits in the TOM and TIM complexes). Finally, 11 channels or pores have been found and most of them water channels (aquaporins) or OMM porin, as well as ion channels (Table S1). We will discuss the different transporter classes and families in more detail after looking at the predicted mitochondrial transportome.

3. Mitochondrial Transporters—Predictions

We accessed the database TransportDB 2.0 [26] and extracted the membrane transport proteins in *Arabidopsis* and rice and, for comparison, in *Homo sapiens* and *Mus musculus*, similar to what was done by Hwang et al. [27]. The results are shown in Table 1. For most of the protein groups, the numbers are similar to those of Hwang et al. [27]. For plants, the only major difference is found for the group “Other ATP-dependent transporters”, where Hwang et al. [27] found 78 and 63 transporters in *Arabidopsis* and rice, respectively. We have divided this group into three groups—F-ATPases, MPT family, and Other ATP-dependent—but their sum in Table 1 is markedly higher for both *Arabidopsis* and rice (119 and 110 transporters, respectively). The grand total number of transporters (about 1280 proteins) makes up 5% of the total proteome in *Arabidopsis*, but only 2% in rice due to its enormous proteome (Table 1). The total number of transporters is about the same in plants as in human and mouse, but the distribution between transporter classes is quite different. Plants have twice as many ATP-binding cassette (ABC) transporters and about 200 more secondary transporters than mammals, while the humans and mice have a staggering 588 and 470 ion channels, respectively, or more than three times as many as plants. For comparison, the unicellular eukaryote *Saccharomyces cerevisiae* has only 341 transporters (~5.4% of the proteome), while *Escherichia coli* has 661 transporters (~12.3% of proteome) [26, 27, TransportDB 2.0]. The distribution of different classes of transporters in yeast and *Arabidopsis* is similar. On the other hand, *E. coli* has almost twice as many ABC transporters (246 or 37.2% of total transporters versus 9.7% in *Arabidopsis*), but far fewer other ATP-dependent class of transporters. *E. coli* also has a relatively lower proportion of secondary active transporters (281 or 42.7%) and ion channels (3.2%) compared to *Arabidopsis* (61.1% and 11.8%, respectively).

In the process of investigating and compiling the mitochondrial proteomes [8,18], it became clear that the existing prediction programs could at most recognize about 50% of the experimentally identified proteins as mitochondrial in spite of the fact that more than 90% of these proteins were probably bona fide mitochondrial. Transporters were particularly poorly predicted, with the best program identifying only 13 out of 59 proteins [8,18]. We, therefore, developed a new prediction program, MU-LOC, which was significantly better at predicting mitochondrial proteins over six

state-of-the-art tools for plant mitochondrial targeting prediction as benchmarked on two independent datasets [14]. It was trained based on amino acid composition, protein position weight matrix, and gene co-expression information using a deep neural network, and has the advantage of predicting plant mitochondrial proteins either possessing or lacking N-terminal pre-sequences.

When all the transporters from *Arabidopsis* and rice (Table S1) were processed by the MU-LOC program, 143 and 140 of the proteins, respectively, were predicted to localize to the mitochondria (Table 1, Table S1), which is about 11% of the total number of transporters in *Arabidopsis*. Thus, the mitochondrial proteome, which makes up about 10% of the total proteome (see above), contains a proportional number of transporters at least in *Arabidopsis*. It is encouraging to see that the subgroups, F-ATPases, MPT family, and MC family, which are known to be predominantly mitochondrial [28,29], are heavily predicted to belong in the mitochondria (Table 1, Table S1). The overlap between the experimental and the predicted proteins will be discussed separately below under each transporter class and family.

MU-LOC was developed to predict mitochondrial proteins in plant cells, where one of the challenges is that hundreds of proteins are dually targeted to mitochondria and plastids [30,31]. The protein features used to discriminate (see above) are actually species/kingdom neutral, so MU-LOC should also be able to predict mitochondrial localization in animal cells. We, therefore, applied MU-LOC to the total transportome in human and mouse cells (Table 1, Table S1). The numbers of transporters of different classes predicted by MU-LOC to be mitochondrial in mammals do not differ markedly from the values for plants and certainly do not reflect the large differences in the total transportome. The high diversity in ion channels probably developed in animals in parallel with muscles and nerves. Here, rapid changes in plasma membrane potential are required and only ion channels can provide that with their short response times and large capacities [27]. It therefore makes perfect sense if there is no evolutionary increase in the number of ion channels in animal mitochondria, where the membrane potential is harnessed to produce ATP and/or transport metabolites across the IMM and where a sudden membrane potential collapse would have very negative consequences for cellular metabolism.

The ability of MU-LOC to predict mitochondrial localization of membrane transporters appears to be equally good for mammalian cells, although experimental verification is lacking. We consider this to be outside the scope of this review.

4. The Different Transporter Classes and Families

The *Arabidopsis* mitochondrial transportome contains 128 experimentally identified proteins and 143 predicted proteins, or 211 proteins in all, which is 17% of the total number of proteins in the *Arabidopsis* transportome. Out of the 211 proteins, 61 proteins (29%) were both predicted and experimentally identified (Figure 1).

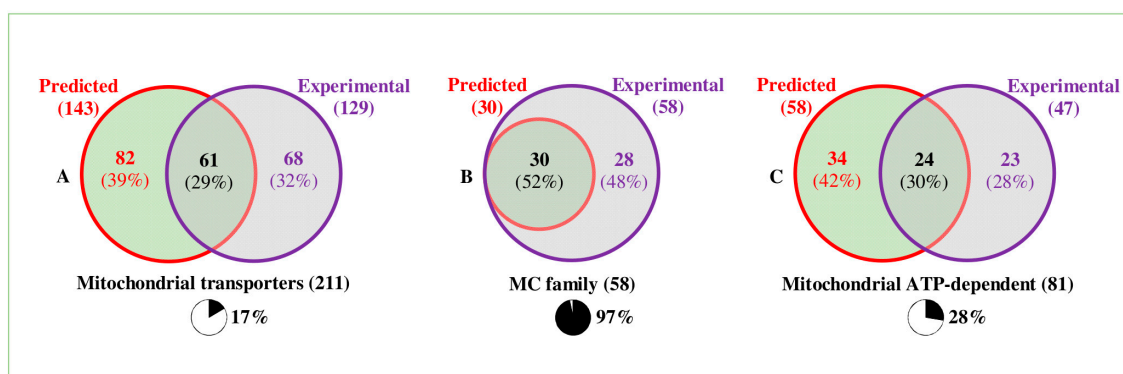


Figure 1. *Arabidopsis* mitochondrial transporters in Venn diagrams. (A) A total of 211 transporters (17% of all the transporters in *Arabidopsis*) are either predicted to be or experimentally known to be mitochondrial. Out of these, 61 are both predicted and experimental. (B) Nearly all (97%) Mitochondrial Carrier (MC) family members have been experimentally identified in mitochondria, while only 50% are predicted to be mitochondrial. (C) A total of 81 ATP-dependent transporters (28% of all ATP-dependent transporters in *Arabidopsis*) are predicted to be or experimentally known to be mitochondrial. Out of these, 24 (30%) are both predicted and experimental.

4.1. ATP-Dependent Transporters

4.1.1. ABC Transporters

A total of 13 ABC transporters are predicted by MU-LOC to be mitochondrial in *Arabidopsis*, while only six ABC transporters have been experimentally found to date (Table 1, Table S1). Three proteins were both predicted and found: iron-sulfur clusters transporter ATM1 (At4g28630), ATM2 (At4g28620), and ATM3 (At5g58270). They all take part in the export of iron-sulfur clusters synthesized in the matrix to the intermembrane space from where the clusters are distributed to the rest of the cell [32,33].

In fact, iron-storing ferritin and the entire iron-sulfur biosynthesis pathway were found in potato mitochondria: frataxin, iron-sulfur cluster assembly proteins, iron-sulfur cluster scaffold protein, iron-sulfur cluster co-chaperone protein, Cys desulfurase, and ferredoxin [18,34].

4.1.2. The Mitochondrial Protein Translocator (MPT) Family

The MPT family consists of subunits in the TOM and TIM complexes, where the majority of the subunits have been identified and about half predicted (Table 1, Table S1) [35]. This transporter family is the subject of another review in this Special Issue and will not be treated any further here.

4.1.3. F-ATPases

The *Arabidopsis* genome encodes 44 F-ATPase transporters belonging to the ATP synthase in mitochondria and plastids as well as to the P-type ATPase in the vacuole. Of these, MU-LOC predicted 17 to be mitochondrial and 16 were found experimentally, while the overlap was about 50% (9 proteins).

4.1.4. P-ATPases

The *Arabidopsis* genome encodes 50 P-ATPase transporters belonging mainly to ATPases in the plasma membrane. Of these, MU-LOC predicted four to be mitochondrial, and two were found experimentally with no overlap. The experimentally found were At1g54280, a phospholipid transporting ATPase annotated to be located in the plasma membrane, and At4g33520, a copper-transporting ATPase annotated to be located in the plastid envelope (as annotated in UniProt). Both would be very useful to have in the IMM.

4.2. Secondary Transporters

This is by far the largest group of transporters in plants and in plant mitochondria (Table 1, Table S1), where they are located in the IMM. These transporters are either symporters or antiporters, and use the electrochemical gradient established across the IMM to move ions into or out of the mitochondrial matrix. The size and diversity of transporters in this family reflect the metabolic complexity of mitochondria and its importance as an energetic conduit for the cell [13,28,29].

4.2.1. The Mitochondrial Carrier (MC) Family

The MC family (MCF) is predicted to contain 58–60 members in *Arabidopsis* [28, TransportDB 2.0] and 50–61 members in rice [24, TransportDB 2.0]. The majority of the MCF members are localized in the IMM, although at least 10 are found in plastids, peroxisomes, endoplasmic reticulum, and plasma membrane [29].

About half of all the MCF members are predicted to be found in the mitochondria of both *Arabidopsis* (30 out of 60) and rice (33 out of 61) (Table S1). In *Arabidopsis*, 58 members have been experimentally identified (including all the predicted), in other words, a very satisfying 97%, while in rice 49 have been identified (including 29 of the predicted), producing an 80% “recovery” rate (Tables S1 and S2, Figure 1). The almost 100% recovery rate for MCF members in proteomic profiling of isolated mitochondria means that most, if not all, of the MC members localized to other membranes [13,29] have also been found in mitochondria. To what extent this is due to dual localization or to contamination of the mitochondrial preparations is an open question.

The MC members catalyze the transport of numerous metabolic intermediates across the IMM—nucleotides like ADP, ATP, and NAD⁺; coenzymes like coenzyme A, thiamine pyrophosphate, and folate; di- and tri-carboxylic acids like malate, oxoglutarate, succinate, fumarate, and citrate; amino acids like glutamate, aspartate, ornithine, citrulline, and carnitine; as well as phosphate and protons. All these carriers have been admirably reviewed by Palmieri et al. [28] and Toleco et al. [36], so we will not discuss them any further except briefly in connection with one important metabolite, ascorbate.

Ascorbate is very important in mitochondrial metabolism where it participates in the ascorbate-glutathione cycle that removes H₂O₂ produced by the respiratory chain e.g., [37]. The last step in ascorbate biosynthesis takes place on the outer surface of the IMM [38], but to date no ascorbate transporter has been identified in the IMM. Ascorbate transport was measured in plant and rat liver mitochondria by Scalera et al. [39]. The protein responsible was in the size range 28–35 kDa, which is where most of the MC family transporters are found, but the gene was not identified. An ascorbate transporter has been identified in the chloroplast envelope [40], which could in principle be dually targeted to IMM. However, since it is 60 kDa it could not be responsible for the transport activity observed by Scalera et al. [39].

4.2.2. Transport of Inorganic Ions

Ca²⁺—*Arabidopsis* contains a Ca²⁺-cation antiporter family with 13 members out of which one is predicted to be mitochondrial, none has been identified by proteomics. Rice contains a Ca²⁺-cation antiporter family with 16 members, out of which three are predicted to be mitochondrial; none has been identified in proteomics. One of the predicted antiporters may be involved in Ca²⁺/Na⁺ exchange.

K⁺—*Arabidopsis* mitochondria contain three members of the Monovalent Cation: Proton Antiporter-2 (CPA2) Family. Two were found experimentally—At1g01790 K⁺ efflux antiporter 1, chloroplastic and At2g28180 Cation/H⁺ antiporter 8—and one was predicted (At5g41610 cation-H⁺ antiporter (Table S1, UniProt)). *Arabidopsis* mitochondria also contain three members of The Monovalent Cation: Proton Antiporter-2 (CPA2) Family. At5g41610 (Cation/H⁺ antiporter 18) was predicted but not found, while At1g01790 (K⁺ efflux antiporter 1, chloroplastic) was found but not predicted. All of these transporters could help the mitochondria regulate the K⁺ concentration in the matrix.

Metal ions—two members of the Cation Diffusion Facilitator (CDF) Family in *Arabidopsis* have been either found and predicted (At1g51610—Metal tolerance protein C4, tonoplast) or just predicted (At2g47830—predicted Metal tolerance protein C1, tonoplast) (Table S1). Unless these are merely contaminants in the isolated mitochondria, they could provide the mitochondria with the means of transporting metal ions, like Pb^{2+} , Ni^{2+} , and Fe^{3+} , across the IMM.

Sulfate—there are 14 members of the sulfate permease family in *Arabidopsis*, but only one (At1g80310) is predicted to be mitochondrial by MU-LOC, and none was found by proteomics (Table S1). The predicted mitochondrial transporter turns out to be a molybdenum transporter located in the tonoplast (as annotated in UniProt).

Nitrite—nitrite is known to reach the mitochondrial matrix, where it can act as an alternative electron acceptor under hypoxia/anoxia [41]. No nitrite carriers are listed in Table S1, but the nitrite carrier found in the inner envelope in chloroplasts (At1g68570) is a member of the proton-dependent oligopeptide transporter family [42]. This family has 18 members in *Arabidopsis*, and several of them transport nitrate. However, none of them is predicted to be mitochondrial by MU-LOC, and none has been found in proteomic studies (Table S1).

4.3. (Ion) Channels

4.3.1. Porin (VDAC or VIC)

The VDAC/VIC family has 36 members in *Arabidopsis* (as listed in TransportDB), and only one has been predicted to be mitochondrial (Table S1). However, six VICs have been found in *Arabidopsis* mitochondria experimentally (Table S2), and they are all bona fide VDACs according to UniProt, but they are not listed in TransportDB (Table S1). The OMM in isolated mitochondria behaves as if it is freely permeable to small molecules, so the VDACs do not appear to be actively gated, but it is possible that porin is involved in tRNA transport [11,12,42].

4.3.2. Aquaporin

Aquaporins allow water, but also other small neutral molecules like hydrogen peroxide and ammonia, to pass membranes in both directions going from higher to lower osmotic potential [43,44]. Contrary to the conclusion by Maurel et al. [44] that “plant mitochondria seem to be deprived of aquaporins”, MU-LOC predicted that 7 out of 39 *Arabidopsis* aquaporins localized to the mitochondria, and proteomic profiling of *Arabidopsis* and potato mitochondria found six aquaporins (only one overlaps between prediction and experimental) (Table S1). It has long been known that (plant) mitochondria can swell and shrink. For instance, the mitochondria swell rapidly when the osmotic potential decreases in the matrix due to a rapid influx of osmolytes e.g., [45], which would only be possible if aquaporins are present in the IMM.

The final steps in substrate oxidation take place in the TCA cycle in the mitochondrial matrix where glycolytic end products are oxidized to CO₂. One still unsolved question is how the CO₂ leaves the mitochondria and in what form? Animal cells have Na⁺/bicarbonate symporters and chloride/bicarbonate antiporters, but none of them are predicted to be mitochondrial by MU-LOC (Table S1). So how does CO₂ get out of the mitochondria? One intriguing possibility is through aquaporins just like other small uncharged molecules [44].

4.3.3. Ion Channels

The Small Conductance Mechanosensitive Ion Channel (MscS) Family contains 11 members in *Arabidopsis*, out of which At4g00290 (mechanosensitive ion channel protein 1, mitochondrial) was both predicted and found, whereas At1g49260 was only predicted. It is possible that the mechanosensitive ion channel protein 1 can catalyze ATP-dependent K⁺ channel activity by teaming up with one of the ABC transporters [46].

Two subunits of the calcium uniporter protein [47,48]—MCU1 (At4g36820) and MCU2 (At2g23790)—have been identified in plant mitochondria (Table S2), but they do not appear in the TransportDB list (Table S1).

The list of *Arabidopsis* ion channels contains eight so-called chloride intracellular channel (CLIC) homologs, out of which three are predicted to be mitochondrial (At1g19570, At5g16710, and At5g36270), and one is both predicted and experimental (At1g75270). They are all annotated as glutathione S-transferases with glutathione-dependent dehydroascorbate reductase activity and appear to be able to transfer Cl⁻ across membranes [49], possibly by a mechanism involving a redox reaction (as annotated in UniProt).

5. Posttranslational Modifications of Transporters

Posttranslational modifications (PTMs) of proteins are a way of regulating cellular and mitochondrial metabolism [37]. In shotgun proteomics, many mitochondrial transporters have been observed to have PTMs of various types: (i) oxidations to give carbonylated side chains on primarily Lys and Pro or sulfoxide on Met [18], although the latter is probably an analytical artefact in some cases; (ii) phosphorylation of Ser, Thr, and Tyr [50–52]; (iii) acetylation of Lys [53]; and (iv) conjugation of Lys side chains with oxidative degradation products of polyunsaturated fatty acids, for instance, 4-hydroxynonenal (HNE) [54,55]. Many of these modifications are no doubt regulatory, while others are damaging and lead to proteolytic degradation [37,56,57].

The modified transporters include the ATP, ADP-translocase, the phosphate transporter, and the dicarboxylate carrier; the former two are both oxidized and acetylated on multiple sites [18,53]. The effect of the modifications is so far unknown. Plasma membrane aquaporins are known to be gated by phosphorylation [44], but aquaporin phosphorylation has never been reported for plant mitochondria.

6. Physiological Changes in the Mitochondrial Transporters

There has been a number of studies of individual mitochondrial transporters during development or during the stress response, e.g., the Ca²⁺ uniporter [48], but very few where the whole mitochondrial transportome has been considered.

6.1. Changes in Rice during Development

Taylor et al. [24] studied members of the MC family in rice. The expression of 44 of the 50 MC genes in rice was quantified in different tissues during the time course of aerobic and anaerobic seed germination, during seedling growth and in response to fungal infection. Several tissue-specific carriers were identified in the shoots and flowers, and the expression of specific ATP/ADP transporters, succinate/fumarate carriers, and a dicarboxylate/tricarboxylate carrier (DTC) increased during fungal infection.

Taylor et al. [24] also used a targeted proteomic approach especially suited for identifying integral-membrane proteins [20], and succeeded in identifying and quantifying five different MC proteins in dry seeds and in seeds incubated under normoxia and anoxia. Significant differences in protein abundance between the treatments were observed for the phosphate carrier and the basic amino acid carrier.

6.2. Changes in Maize during Development

Wang et al. [25] studied mitochondrial development in developing maize seed embryos. They purified mitochondria from 300–600 excised embryos (2–15 g fresh weight) at five time points during the period 14–70 days after pollination (DAP) and did proteome profiling by a shot-gun method. Altogether, they identified and quantified 931 mitochondrial proteins (including 31 transporters—Table S2) and observed that the abundance of 286 proteins changed more than two-fold during embryo development. The abundance of most of these peaked early during development either on day 14 (the

first day investigated) or on day 21 after pollination. Out of the differentially abundant proteins, 11 were transporters, and 7 of these, including two DTCs, showed a pattern where the abundance peaked on day 21, i.e., quite early in development.

7. Conclusions

Plant mitochondria contain more than 100 transporters of all classes and families, both as determined by proteomics of isolated mitochondria and by prediction using the MU-LOC bioinformatics tool with a good overlap between the two methods. By far the largest group is the secondary transporter family Mitochondrial Carriers, which includes many of the well-known inner mitochondrial membrane carriers of organic acids, amino acids, etc. Other well-represented families are the F-ATPases and the Mitochondrial Protein Translocators, but plant mitochondria also contain ABC transporters, water channels, and ion channels. There is a real need for targeted proteomic profiling of mitochondria from a broader tissue spectrum, especially green tissues, but targeted profiling of roots and flowers would also help to obtain a more complete picture of the mitochondrial transportome in plants. It would also be useful to study the transportome under a variety of environmental conditions to identify stress-responsive transporters.

Supplementary Materials: The following are available online at <http://www.mdpi.com/2218-273X/10/8/1190/s1>, Table S1: List of Arabidopsis, rice, human and mouse transporters (from TransportDB - Elbourne et al. 2016), and their MU-LOC prediction and mitochondrial proteomics, Table S2: List of proteomically/experimentally identified Arabidopsis/rice/plant mitochondrial transporters.

Funding: This work was partially supported by the US National Institutes of Health grant R21-LM012790.

Conflicts of Interest: The authors declare no conflict of interest.

Abbreviations

ABC	ATP-binding cassette
DAP	days after pollination
DTC	dicarboxylate/tricarboxylate carrier
GO	gene ontology
IMM	inner mitochondrial membrane
MC	mitochondrial carrier
MCF	MC family
MPT	mitochondrial protein translocase
OMM	outer mitochondrial membrane
PTM	posttranslational modification
TCA	tricarboxylic acid
TIM	translocase inner membrane
TOM	translocase outer membrane
UCP	uncoupling protein
VDAC	voltage-dependent anion channel
VIC	voltage-gated ion channel

References

1. Stein, W.D.; Litman, T. *Channels, Carriers, and Pumps—An Introduction to Membrane Transport*, 2nd ed.; Academic Press: San Diego, CA, USA, 2015.
2. Møller, I.M.; Rasmusson, A.G.; Browse, J.J. Chapter 12 Plant Respiration and Lipid Metabolism. In *Plant Physiology*, 6th Ed.; Taiz, L., Zeiger, E., Murphy, A., Møller, I.M., Eds.; Sinauer Associates: Sunderland, MA, USA, 2014; pp. 317–352.
3. Li-Beisson, Y.; Thelen, J.J.; Fedosejevs, E.; Harwood, J.L. The lipid biochemistry of eukaryotic algae. *Progr. Lipid Res.* **2019**, *74*, 31–68. [CrossRef] [PubMed]
4. Igamberdiev, A.U. Citrate valve integrates mitochondria into photosynthetic metabolism. *Mitochondrion.* **2020**, *52*, 218–230. [CrossRef] [PubMed]

5. Vanlerberghe, G.C.; Dahal, K.; Alber, N.A.; Chadee, A. Photosynthesis, respiration and growth: A carbon and energy balancing act for alternative oxidase. *Mitochondrion* **2020**, *52*, 197–211. [CrossRef] [PubMed]
6. Møller, I.M.; Sweetlove, L.J. ROS signaling—Specificity is required. *Trends Plant Sci.* **2010**, *15*, 370–374. [CrossRef] [PubMed]
7. Tran, H.C.; Van Aken, O. Mitochondrial unfolded protein-related responses across kingdoms: Similar problems, different regulators. *Mitochondrion* **2020**, *53*, 166–177. [CrossRef] [PubMed]
8. Rao, R.S.P.; Salvato, F.; Thal, B.; Eubel, H.; Thelen, J.J.; Møller, I.M. The proteome of higher plant mitochondria. *Mitochondrion*. **2017**, *33*, 22–37. [CrossRef] [PubMed]
9. Jeandard, D.; Smirnova, A.; Tarassov, I.; Barrey, E.; Smirnov, A.; Entelis, N. Import of non-coding RNAs into human mitochondria: A critical review and emerging approaches. *Cells* **2019**, *8*, 286. [CrossRef] [PubMed]
10. Warren, J.M.; Sloan, D.B. Interchangeable parts: The evolutionarily dynamic tRNA population in plant mitochondria. *Mitochondrion* **2020**, *52*, 144–156. [CrossRef]
11. Homblé, F.; Krammer, E.-M.; Prévost, M. Plant VDAC: Facts and speculations. *Biochim. Biophys. Acta (BBA)—Biomembr.* **2012**, *1818*, 1486–1501. [CrossRef]
12. Hemono, M.; Ubrig, E.; Azeredo, K.; Salinas-Giegé, T.; Drouard, L.; Duchêne, A.-M. Arabidopsis voltage-dependent anion channels (VDACs): Overlapping and specific functions in mitochondria. *Cells* **2020**, *9*, 1023. [CrossRef]
13. Lee, C.P.; Millar, A.H. The plant mitochondrial transportome: Balancing metabolic demands with energetic constraints. *Trends Plant Sci.* **2016**, *21*, 662–676. [CrossRef]
14. Zhang, N.; Rao, R.S.P.; Salvato, F.; Havelund, J.F.; Møller, I.M.; Thelen, J.J.; Xu, D. MU-LOC: A machine-learning method for predicting mitochondrially localized proteins in plants. *Front. Plant Sci.* **2018**, *9*, 634. [CrossRef] [PubMed]
15. Senkler, J.; Senkler, M.; Eubel, H.; Hildebrandt, T.; Lengwenus, C.; Schertl, P.; Schwarzländer, M.; Wagner, S.; Wittig, I.; Braun, H.P. The mitochondrial complexome of *Arabidopsis thaliana*. *Plant J.* **2017**, *89*, 1079–1092. [CrossRef] [PubMed]
16. Mower, J.P. Variation in protein gene and intron content among land plant mitogenomes. *Mitochondrion* **2020**, *52*, 203–213. [CrossRef] [PubMed]
17. George, R.; Walsh, P.; Beddoe, T.; Lithgow, T. The nascent polypeptide-associated complex (NAC) promotes interaction of ribosomes with the mitochondrial surface in vivo. *FEBS Lett.* **2002**, *516*, 213–216. [CrossRef]
18. Salvato, F.; Havelund, J.F.; Chen, M.; Rao, R.S.P.; Rogowska-Wrzesinska, A.; Jensen, O.N.; Gang, D.R.; Thelen, J.J.; Møller, I.M. The potato tuber mitochondrial proteome. *Plant Physiol.* **2014**, *164*, 637–653. [CrossRef]
19. Fuchs, P.; Rugen, N.; Carrie, C.; Elsässer, M.; Finkemeier, I.; Giese, J.; Hildebrandt, T.M.; Kühn, K.; Maurino, V.G.; Ruberti, C.; et al. Single organelle function and organization as estimated from *Arabidopsis* mitochondrial proteomics. *Plant J.* **2020**, *101*, 420–441. [CrossRef]
20. Millar, A.H.; Heazlewood, J.L. Genomic and proteomic analysis of mitochondrial carrier proteins in *Arabidopsis*. *Plant Physiol.* **2003**, *131*, 443–453. [CrossRef]
21. Barrera, N.P.; Robinson, C.V. Advances in the mass spectrometry of membrane proteins: From individual proteins to intact complexes. *Annu. Rev. Biochem.* **2011**, *80*, 247–271. [CrossRef]
22. Calabrese, A.N.; Radford, S.E. Mass spectrometry-enabled structural biology of membrane proteins. *Methods* **2018**, *147*, 187–205. [CrossRef]
23. Schey, K.L.; Grey, A.C.; Nicklay, J.J. Mass spectrometry of membrane proteins: A focus on aquaporins. *Biochemistry* **2013**, *52*, 3807–3817. [CrossRef] [PubMed]
24. Taylor, N.L.; Howell, K.A.; Heazlewood, J.L.; Tan, T.Y.; Narsai, R.; Huang, S.; Whelan, J.; Millar, A.H. Analysis of the rice mitochondrial carrier family reveals anaerobic accumulation of a basic amino acid carrier involved in arginine metabolism during seed germination. *Plant Physiol.* **2010**, *154*, 691–704. [CrossRef] [PubMed]
25. Wang, W.Q.; Wang, Y.; Zhang, Q.; Møller, I.M.; Song, S.Q. Changes in the maize embryo mitochondrial proteome during seed development. *Physiol. Plant.* **2018**, *163*, 552–572. [CrossRef] [PubMed]
26. Elbourne, L.D.H.; Tetu, S.G.; Hassan, K.A.; Paulsen, I.T. TransportDB 2.0: A database for exploring membrane transporters in sequenced genomes from all domains of life. *Nucleic Acids Res.* **2016**, *45*, D320–D324. [CrossRef] [PubMed]

27. Hwang, J.U.; Song, W.Y.; Hong, D.; Ko, D.; Yamaoka, Y.; Jang, S.; Yim, S.; Lee, E.; Khare, D.; Kim, K.; et al. Plant ABC transporters enable many unique aspects of a terrestrial plant's lifestyle. *Mol. Plant*. **2016**, *9*, 338–355. [CrossRef]
28. Palmieri, F.; Pierri, C.L.; De Grassi, A.; Nunes-Nesi, A.; Fernie, A.R. Evolution, structure and function of mitochondrial carriers: A review with new insights. *Plant J*. **2011**, *66*, 161–181. [CrossRef]
29. Haferkamp, I.; Schmitz-Esser, S. The plant mitochondrial carrier family: Functional and evolutionary aspects. *Front. Plant Sci*. **2012**, *3*, 2. [CrossRef]
30. Carrie, C.; Small, I. A reevaluation of dual-targeting of proteins to mitochondria and chloroplasts. *Biochim. Biophys. Acta*. **2013**, *1833*, 253–259. [CrossRef]
31. Langner, U.; Baudisch, U.; Klösigen, R.B. Organelle import of proteins with dual targeting properties into mitochondria and chloroplasts takes place by the general import pathways. *Plant Signal. Behav.* **2014**, *9*, e29301. [CrossRef] [PubMed]
32. Chen, S.; Sanchez-Fernandez, R.; Lyver, E.R.; Dancis, A.; Rea, P.A. Functional characterization of AtATM1, AtATM2, and AtATM3, a subfamily of Arabidopsis half-molecule ATP-binding cassette implicated in iron homeostasis. *J. Biol. Chem.* **2007**, *282*, 21561–21571. [CrossRef]
33. Balk, J.; Schaedler, T.A. Iron cofactor assembly in plants. *Annu. Rev. Plant Biol.* **2014**, *65*, 125–153. [CrossRef] [PubMed]
34. Ye, H.; Rouault, T.A. Human iron-sulfur cluster assembly, cellular iron homeostasis, and disease. *Biochemistry* **2010**, *49*, 4945–4956. [CrossRef] [PubMed]
35. Ghifari, A.S.; Gill-Hille, M.; Murcha, M.W. Plant mitochondrial protein import: The ins and outs. *Biochemical J*. **2018**, *475*, 2191–2208. [CrossRef]
36. Toleco, M.R.; Naake, T.; Zhang, Y.; Heazlewood, J.L.; Fernie, A.R. Plant mitochondrial carriers: Molecular gatekeepers that help to regulate plant central carbon metabolism. *Plants*. **2020**, *9*, 117. [CrossRef] [PubMed]
37. Møller, I.M.; Igamberdiev, A.U.; Bykova, N.V.; Finkemeier, I.; Rasmusson, A.G.; Schwarzländer, M. Matrix redox physiology governs the regulation of plant mitochondrial metabolism through post-translational protein modifications. *Plant Cell*. **2020**, *32*, 573–594. [CrossRef]
38. Bartoli, C.G.; Pastori, G.M.; Foyer, C.H. Ascorbate biosynthesis in mitochondria is linked to the electron transport chain between complexes III and IV. *Plant Physiol.* **2000**, *123*, 335–344. [CrossRef]
39. Scalera, V.; Giangregorio, N.; De Leonardis, S.; Console, L.; Carulli, E.S.; Tonazzi, A. Characterization of a novel mitochondrial ascorbate transporter from rat liver and potato mitochondria. *Front. Mol. Biosci.* **2018**, *5*, 58. [CrossRef]
40. Miyaji, T.; Kuromori, T.; Takeuchi, Y.; Yamaji, N.; Yokosho, K.; Shimazawa, A.; Sugimoto, E.; Omote, H.; Ma, J.F.; Shinozaki, K.; et al. MAtpHT4;4 is a chloroplast-localized ascorbate transporter in Arabidopsis. *Nat. Commun.* **2015**, *6*, 5928. [CrossRef]
41. Hebelstrup, K.H.; Møller, I.M. Mitochondrial signaling in plants under hypoxia: Use of Reactive Oxygen Species (ROS) and Reactive Nitrogen Species (RNS). In *Reactive Oxygen and Nitrogen Species Signaling and Communication in Plants*; Taiz, L., Zeiger, E., Murphy, A., Møller, I.M., Eds.; Springer: Berlin, Germany, 2015; pp. 63–77.
42. Sugiura, M.; Georgescu, M.N.; Takahashi, M. A nitrite transporter associated with nitrite uptake by higher plant chloroplasts. *Plant Cell Physiol.* **2007**, *48*, 1022–1035. [CrossRef]
43. Bienert, G.P.; Møller, A.L.B.; Kristiansen, K.A.; Schulz, A.; Møller, I.M.; Schjoerring, J.K.; Jahn, J.P. Specific aquaporins facilitate the diffusion of hydrogen peroxide across membranes. *J. Biol. Chem.* **2007**, *282*, 1183–1192. [CrossRef]
44. Maurel, C.; Boursiac, Y.; Luu, D.T.; Santoni, V.; Shahzad, Z.; Verdoucq, L. Aquaporins in plants. *Physiol Rev.* **2015**, *95*, 1321–1358. [CrossRef] [PubMed]
45. Day, D.A.; Hanson, J.B. Pyruvate and malate transport and oxidation in corn mitochondrial. *Plant Physiol.* **1977**, *59*, 630–635. [CrossRef] [PubMed]
46. Vothknecht, U.; Szabò, I. Channels and transporters for inorganic ions in plant mitochondria: Prediction and facts. *Mitochondrion* **2020**, *153*, 224–233. [CrossRef] [PubMed]
47. Carraretto, L.; Teardo, E.; Checchetto, V.; Finazzi, G.; Uozumi, N.; Szabo, I. Ion channels in plant bioenergetic organelles, chloroplasts and mitochondria: From molecular identification to function. *Mol. Plant* **2016**, *9*, 371–395. [CrossRef]

48. Teardo, E.; Carraretto, L.; Wagner, S.; Formentin, E.; Behera, S.; De Bortoli, S.; Larosa, V.; Fuchs, P.; Schiavo, F.L.; Raffaello, A.; et al. Physiological characterization of a plant mitochondrial calcium uniporter in vitro and in vivo. *Plant Physiol.* **2017**, *173*, 1355–1370. [CrossRef]
49. Elter, A.; Hartel, A.; Sieben, C.; Hertel, B.; Fischer-Schliebs, E.; Lüttge, U.; Moroni, A.; Thiel, G. A plant homolog of animal chloride intracellular channels (CLICs) generates an ion conductance in heterologous systems. *J. Biol. Chem.* **2007**, *282*, 8786–8792. [CrossRef]
50. Nakagami, H.; Sugiyama, N.; Mochida, K.; Daudi, A.; Yoshida, Y.; Toyoda, T.; Tomita, M.; Ishihama, Y.; Shirasu, K. Large-scale comparative phosphoproteomics identifies conserved phosphorylation sites in plants. *Plant Physiol.* **2010**, *153*, 1161–1174. [CrossRef]
51. Meyer, L.J.; Gao, J.; Xu, D.; Thelen, J.J. Phosphoproteomic analysis of seed maturation in Arabidopsis, rapeseed, and soybean. *Plant Physiol.* **2012**, *159*, 517–528. [CrossRef]
52. Havelund, J.F.; Thelen, J.J.; Møller, I.M. Biochemistry, proteomics, and phosphoproteomics of plant mitochondria from non-photosynthetic cells. *Front. Plant Sci.* **2013**, *4*, 51. [CrossRef]
53. König, A.C.; Hartl, M.; Boersema, P.J.; Mann, M.; Finkemeier, I. The mitochondrial lysine acetylome of Arabidopsis. *Mitochondrion.* **2014**, *19*, 252–260. [CrossRef]
54. Winger, A.M.; Taylor, N.L.; Heazlewood, J.L.; Day, D.A.; Millar, A.H. The cytotoxic lipid peroxidation product 4-hydroxy-2-nonenal covalently modifies a selective range of proteins linked to respiratory function in plant mitochondria. *J. Biol. Chem.* **2007**, *282*, 37436. [CrossRef]
55. Møller, I.M.; Rogowska-Wrzesinska, A.; Rao, R.S.P. Protein carbonylation and metal-catalyzed protein oxidation in a cellular perspective. *J. Proteomics.* **2011**, *74*, 2228–2242. [CrossRef] [PubMed]
56. Møller, I.M.; Jensen, P.E.; Hansson, A. Oxidative modifications to cellular components in plants. *Annu. Rev. Plant Biol.* **2007**, *58*, 459–481. [CrossRef]
57. Smakowska, E.; Skibior-Blaszczyk, R.; Czarna, M.; Kolodziejczak, M.; Kwasniak-Owczarek, M.; Parys, K.; Funk, C.; Janska, H. Lack of FTSH4 protease affects protein carbonylation, mitochondrial morphology, and phospholipid content in mitochondria of Arabidopsis: New insights into a complex interplay. *Plant Physiol.* **2016**, *171*, 2516–2535. [CrossRef] [PubMed]



© 2020 by the authors. Licensee MDPI, Basel, Switzerland. This article is an open access article distributed under the terms and conditions of the Creative Commons Attribution (CC BY) license (<http://creativecommons.org/licenses/by/4.0/>).

Review

Peroxisomal Cofactor Transport

Anastasija Plett, Lennart Charton and Nicole Linka *

Institute of Plant Biochemistry and Cluster of Excellence on Plant Sciences (CEPLAS), Heinrich Heine University, Universitätsstrasse 1, 40,225 Düsseldorf, Germany; Anastasija.Plett@hhu.de (A.P.); Lennart.Charton@hhu.de (L.C.)

* Correspondence: Nicole.Linka@hhu.de; Tel.: +49-(0)211-81-10412; Fax: +49-(0)211-81-13706

Received: 2 July 2020; Accepted: 7 August 2020; Published: 12 August 2020

Abstract: Peroxisomes are eukaryotic organelles that are essential for growth and development. They are highly metabolically active and house many biochemical reactions, including lipid metabolism and synthesis of signaling molecules. Most of these metabolic pathways are shared with other compartments, such as Endoplasmic reticulum (ER), mitochondria, and plastids. Peroxisomes, in common with all other cellular organelles are dependent on a wide range of cofactors, such as adenosine 5'-triphosphate (ATP), Coenzyme A (CoA), and nicotinamide adenine dinucleotide (NAD). The availability of the peroxisomal cofactor pool controls peroxisome function. The levels of these cofactors available for peroxisomal metabolism is determined by the balance between synthesis, import, export, binding, and degradation. Since the final steps of cofactor synthesis are thought to be located in the cytosol, cofactors must be imported into peroxisomes. This review gives an overview about our current knowledge of the permeability of the peroxisomal membrane with the focus on ATP, CoA, and NAD. Several members of the mitochondrial carrier family are located in peroxisomes, catalyzing the transfer of these organic cofactors across the peroxisomal membrane. Most of the functions of these peroxisomal cofactor transporters are known from studies in yeast, humans, and plants. Parallels and differences between the transporters in the different organisms are discussed here.

Keywords: peroxisomes; metabolism; carrier; cofactor

1. Introduction

Peroxisomes are eukaryotic organelles that are surrounded by a single lipid bilayer membrane [1,2]. They fulfil a range of metabolic functions, which are essential for development and cellular signaling. Depending on the organism, cell type, growth, and environmental conditions, peroxisomes participate in the detoxification of reactive oxygen/nitrogen species, β -oxidation of fatty acids, synthesis of plasminogen, isoprenoids, penicillin, phylloquinone, glycine betaine, biotin and hormonal signal molecules, catabolism of purines, polyamines, amino acids, and methanol, as well as in the glyoxylate cycle, pentose phosphate pathway, and photorespiration [1,2]. Currently, the list of peroxisomal tasks appears to be far from exhaustive.

The multiple roles of peroxisomes depend on the functional interplay with other organelles. A large number of chemically diverse metabolites consumed and released by the peroxisomes have to be exchanged between subcellular compartments [3–6]. The transfer of metabolites across the peroxisomal membrane has been a controversial scientific debate for several decades. Initial studies on isolated peroxisomes suggested that the peroxisomes are freely permeable. However, this *in vitro* permeability was later withdrawn and explained by disruptions of protein/membrane structures during peroxisome isolation procedure. The current consensus is that transport proteins are responsible for the transfer of solutes into and out of peroxisomes [3–6]. Electrophysiological experiments using purified peroxisomal

membranes revealed the existence of nonspecific porin-like channels that allow the free diffusion of low-molecular weight compounds (<300 Da) with a broad substrate specificity [7,8]. In addition, genetic mutant analyses discovered genes encoding for specific carrier proteins that catalyze the flux of larger hydrophilic solutes, like cofactor molecules, such as ATP, Coenzyme A (CoA), and NAD [9–13].

The transport of these cofactors has a crucial impact on peroxisome function. For example, ATP, CoA, and NAD are required for peroxisomal fatty-acid activation and oxidation via β -oxidation, which is a conserved metabolic pathway in yeast, mammals, humans, and plants [3,14,15]. These cofactor molecules are synthesized outside peroxisomes. Due to their size and charge, they cannot pass the lipid bilayer by free diffusion. Thus, peroxisomal transport proteins are mandatory to replenish the cofactor demand of the peroxisomal enzymes [3,14,15]. Notably, peroxisomes offer an alternative route for cofactor transport. In contrast to mitochondria and chloroplasts, peroxisomes lack a protein synthesis machinery and have the capacity to import folded and even oligomeric proteins [16–18]. It was assumed that the import of tightly bound cofactors, such as flavin adenine dinucleotide (FAD) and thiamine pyrophosphate (TPP), could be coupled to protein transport, as is the case for the Tat system of bacteria and chloroplasts, which export folded proteins to the periplasm or the thylakoid lumen, respectively [19]. For instance, the FAD-dependent alcohol oxidase and acyl-CoA oxidase bind their cofactor FAD in the cytosol and are then imported as fully folded holo-enzymes into yeast peroxisomes [20,21]. Such a cofactor-coupled protein import mechanism was also reported for the mammalian 2-hydroxyacyl-CoA lyase, a TPP-dependent enzyme [22]. However, specific cofactor carrier proteins for ATP, CoA, and NAD are essential to generate and maintain a physiologically relevant peroxisomal pool of free cofactor molecules, which are essential for an efficient and functional metabolism.

Members of the mitochondrial carrier family (MCF) that mediate the transport of a wide range of organic cofactors into peroxisomes have been discovered in diverse eukaryotes [23–27]. This eukaryotic group of membrane transport proteins corresponds to the 2.A.29 family according to the Transporter Classification Database (TCDB) and is named in mammals solute carrier family 25 (SLC25) [28]. MCF is a large family of proteins with about 30 members in yeast and more than 50 in humans and plants. Although the name of this family suggests that they are exclusively located to mitochondria, several members are present in other organelles, such as peroxisomes, endoplasmic reticulum, chloroplasts, and plasma membrane [23,24,26,27,29]. Despite their conserved basic structure composed of three repetitive modules, MCF proteins are highly diverse in terms of substrate specificity and transport mode. They mediate the transport of a large variety of solutes that differ in size and nature, such as protons, inorganic ions, inorganic form of “phosphate”, carboxylic acids, amino acids, and nucleotides. In most cases, MCF members mediate a strict counter-exchange but also operate as a uniporter or symporter [26,27,29,30]. These features suggest that this protein family was most likely exploited as a valuable basis for a fast establishment of a subset of carriers with a broad range of different transport functions in the cell during eukaryotic evolution.

This review deals with MCF proteins that are known to be peroxisomal cofactor carriers in budding yeast *Saccharomyces cerevisiae*, humans, and the model plant *Arabidopsis thaliana* and highlights the recent progress on their biochemical and physiological function for the peroxisomal metabolism.

2. Cofactor Transport for Yeast Peroxisomes

The main metabolic function of peroxisomes in *S. cerevisiae* is the degradation of fatty acids via β -oxidation to use these compounds as carbon and energy source [31]. The pathway depends on the availability of ATP, CoA, and NAD in the peroxisomal matrix (Figure 1). The uptake of fatty acids into peroxisomes occurs via two routes depending on the fatty-acid chain length [32]. Small- and medium-chain fatty acids (C4–12) are transported as free fatty acids through passive diffusion, while long-chain fatty acids (C14–20) are delivered as acyl-CoA esters by a peroxisomal ATP-binding cassette (ABC) transporter Pxa1p-Pxa2p [33,34]. However, during this transport process the CoA moiety is cleaved off. Thus, both entry pathways for fatty acids lead to the delivery of nonesterified fatty acids [35]. However, prior to peroxisomal β -oxidation, these free fatty acids must

be activated to acyl-CoA esters. This intraperoxisomal esterification is catalyzed by a peroxisomal acyl-CoA synthetase Faa2p and/or a bifunctional fatty-acid transporter Fat1p at the peroxisomal membrane and requires ATP and CoA [35]. Once the acyl-CoA esters are fed into the peroxisomal β -oxidation cycle, their oxidative degradation requires NAD as an electron acceptor [31].

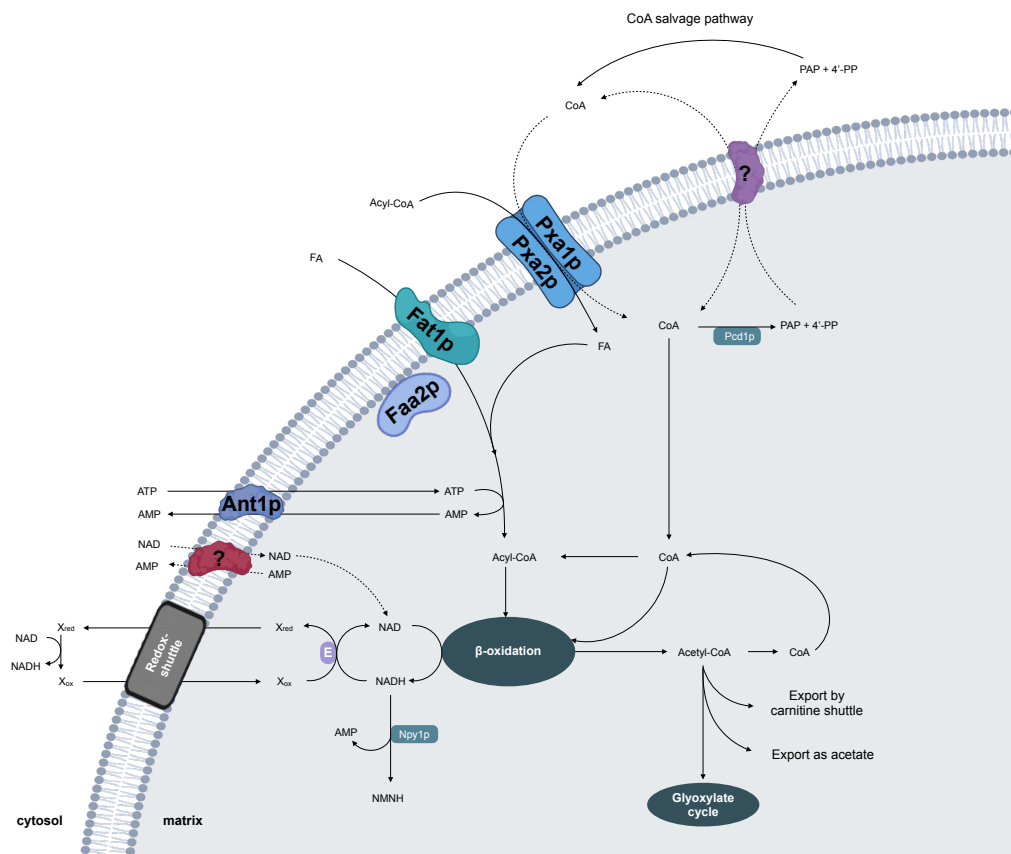


Figure 1. Model for the peroxisomal cofactor transport in yeast. Ant1p: peroxisomal ATP carrier 1; FA, fatty acid; Faa2p: peroxisomal acyl-CoA synthetase 2 (associated at the matrix side of the peroxisomal membrane); Fat1p: peroxisomal acyl-CoA synthetase, also known as peroxisomal fatty-acid transporter 1 (integral membrane protein); NMN(H): nicotinamide mononucleotide (reduced); Npy1p: peroxisomal NAD(H) diphosphatase 1, catalyzing the hydrolysis of NADH to AMP and NMN(H); PAP: adenosine 3',5'-diphosphate; 4'-PP: 4'-phospho-pantetheine; Pcd1p: peroxisomal CoA diphosphatase 1, catalyzing the hydrolysis of CoA to PAP and 4'-PP; Pxa1p/Pxa2p: peroxisomal ATP-binding cassette (ABC) transporter, mediating the import of fatty acids as acyl-CoA esters; (?): proposed cofactor carrier proteins.

In 2001, two groups independently identified one MCF member from *S. cerevisiae* as a peroxisomal ATP carrier, which was named Ant1p for Adenine nucleotide transporter 1 [9,10]. Disruption of Ant1p results in yeast cells that exhibit an impaired growth in the presence of medium-chain fatty acids, such as lauric acid, as the sole carbon source. In vivo activity of the ATP-consuming firefly luciferase, targeted to *ant1* Δ peroxisomes, was strongly reduced, implying a depleted peroxisomal ATP content in the intact mutant cells [36]. Gene expression analysis revealed the presence of oleate response elements in the promoters of ANT1 and other β -oxidation genes, which are responsible for an induced gene expression via the Pip2p-Oaf1p transcription factor when grown in the presence of the long-chain fatty acid, oleic acid [36]. These observations led to the hypothesis that Ant1p is necessary for metabolizing fatty acids via peroxisomal β -oxidation as a carbon and energy source [9,10].

Direct transport studies with purified Ant1p protein provided conclusive evidence for the role of Ant1p as an ATP transporter [9]. *Escherichia coli* has been a suitable system for expression, purification,

and subsequent functional reconstitution into liposomes. In vitro uptake studies using diverse nucleotides as substrates demonstrated that Ant1p specifically catalyzes the transport of ATP, ADP, and AMP [9]. However, the protein does not accept other ATP-related molecules, such as CoA or NAD, as transport substrates [37]. Another unique characteristic of Ant1p is that it exhibits two transport modes. It mediates not only the exchange but also catalyzes the uniport of adenine nucleotides [9].

Based on its transport features, two physiological functions for Ant1p can be concluded: (1) It facilitates the uptake of cytosolic ATP in a unidirectional mode for loading peroxisomes with ATP early in their genesis. (2) During high rates of β -oxidation, ATP is directly consumed by the ATP-dependent fatty-acid activation, releasing high amounts of AMP. Ant1p ensures the counter-exchange of ATP into peroxisomes against AMP to avoid accumulation of the latter molecule in the peroxisome, which would, on the other hand, deplete the nucleotide pool in the cytosol [9,10]. However, the loss of the Ant1p in *S. cerevisiae* did not fully abolish fatty-acid oxidation activity [10]. The *ant1* Δ mutant was still able to degrade lauric acid and oleic acid. Moreover, 20% of the peroxisomal luciferase activity was still detectable, indicating the presence of low ATP levels in *ant1* Δ peroxisomes [10]. In contrast, a complete block of β -oxidation rates for medium- and long-chain fatty acids was observed in yeast cells lacking the two ATP-dependent acyl-CoA synthetases Faa2p and Fat1p [35]. Since no other ATP-generating systems have been discovered so far, future research will address how an alternative bypass route provides peroxisomes with ATP particularly for fatty-acid metabolism.

Very little is known about the uptake of CoA and NAD by yeast peroxisomes. In yeast, cytosolic CoA probably enters the peroxisomal matrix via the Pxa1p–Pxa2p transporter, which cleaves off the CoA moiety from the imported acyl-CoA ester. Alternatively, a specific transport protein might facilitate the CoA uptake. Inside peroxisomes CoA is not only essential for the fatty-acid activation but also for the thiolytic cleavage within the β -oxidation cycle via the action of acyl-CoA thiolases [31]. The CoA bound to the acyl chain is released when acetyl-CoA, the product of β -oxidation, is exported via the carnitine shuttle or enters the glyoxylate cycle. In order to regulate the CoA homeostasis, the peroxisomal CoA diphosphatase Pcd1p hydrolyzes CoA to adenosine 3',5'-diphosphate and 4'-phospho-pantetheine [38]. The resulting products need to exit the peroxisomes to enter the cytosolic CoA salvage pathway. Both CoA derivatives might function as potential counter-exchange substrates for the peroxisomal CoA importer. However, it is currently unclear whether yeast peroxisomes harbor such a CoA transport protein.

An additional cofactor uptake system must exist in yeast for loading the peroxisomal lumen with NAD. During the β -oxidation cycle, NAD is reduced to NADH, which is directly re-oxidized by the peroxisomal malate dehydrogenase Mdh3p, an important component of the malate–oxaloacetate shuttle [39]. By action of this shuttle, peroxisomal NADH is indirectly transported to mitochondria, where it is re-oxidized to NAD, and then returned back to peroxisomes. Genetic in vivo studies with *mdh3* Δ mutants, which were unable to metabolize fatty acids, demonstrated that the peroxisomal membrane of *S. cerevisiae* is impermeable to NAD(H) [39]. This indicated that a direct exchange of NAD against NADH across the peroxisomal membrane does not occur in yeast, and thus the transfer of reducing equivalents is mediated by NAD-linked redox shuttles [40]. In addition, yeast possess additional redox shuttles to maintain the intraperoxisomal redox balance, such as the glycerol-3-phosphate/dihydroxyacetone phosphate NAD-linked shuttle and the 2-oxoglutarate/isocitrate NADP-linked shuttle [40,41]. A prerequisite for redox metabolism is a constant concentration of NAD(H) inside peroxisomal lumen. The NAD(H) homeostasis is achieved by the peroxisomal NADH diphosphatase Npy1p [42], converting NAD(H) to AMP and nicotinamide mononucleotide. In order to recycle these products of NAD hydrolysis in the cytosol, they have to be exported by a specific carrier, which might be coupled to the import of NAD. However, the mechanism to initially generate an NAD pool inside peroxisomes is still unknown.

Members of the MCF have been identified to mediate an efficient subcellular distribution of ATP, CoA, and NAD within the eukaryotic cell. *S. cerevisiae* contains 35 MCF-type proteins, including the mitochondrial CoA carrier Leu5p [43] and the mitochondrial NAD carriers Ndt1p and Ndt2p [44].

Two scenarios are possible: (1) One of the so far uncharacterized MCF or even non-MCF proteins in yeast might catalyze the peroxisomal cofactor uptake. (2) The mitochondrial CoA and/or NAD transporter might be dually localized to mitochondria and peroxisomes to adapt to the cellular needs. Future analyses will discover whether and which carrier-type protein might mediate the peroxisomal cofactor transport.

3. Cofactor Transport for Human Peroxisomes

In humans, peroxisomes are present in all cell types, except in erythrocytes [1,45,46]. The pivotal role of these organelles is emphasized by a variety of severe genetic diseases linked to peroxisome dysfunction. Most of these disorders are caused by mutations in genes coding for peroxisomal enzymes involved in metabolic pathways [45]. In humans, the key metabolic function of human peroxisomes is β -oxidation. While mitochondrial β -oxidation handles the bulk of dietary fatty acids, such as palmitic acid and oleic acid, the peroxisomal β -oxidation plays a crucial role in the degradation of a more diverse spectrum of carboxylic acids, including long-chain fatty acids (LCFAs), very long-chain fatty acids (VLCFAs, $>C22$), branched-chain fatty acids (e.g., pristanic and phytanic acids), and long-chain dicarboxylic acids. In addition to its catabolic functions, peroxisomal β -oxidation is involved in the biosynthesis of the bile acid intermediates di- and tri-hydroxycholestanic acid and the essential omega-3-fatty acid docosahexaenoic acid (C22:6 n-3), a primary structural component of the human brain, cerebral cortex, skin, and retina [1,45,46].

To import the diverse carboxylic acids into peroxisomes, three half-size ABC transporters of the subfamily D (ABCD) reside in the peroxisomal membrane [47–49]. They function mainly as homodimers with partially overlapping substrate specificities. ABCD1 (ALDP) has a higher affinity for saturated VLCFAs, whereas ABCD2 (ALDR) transports shorter and (poly)unsaturated VLCFAs [50,51]. In contrast, ABCD3 (PMP70) imports branched-chain fatty acids, long-chain dicarboxylic acids, and bile acid intermediates into human peroxisomes [52,53]. The peroxisomal ABCD proteins transport their substrates as CoA esters, whereas the peroxisomal membrane-bound acyl-CoA binding protein ACBD5 functions as a cytosolic receptor for VLCFA-CoAs and passes them on to the VLCFA transporter ABCD1 [54]. Furthermore, ABCD1–3 share the same transport mode with the yeast fatty-acid transporter described in the previous chapter [55,56]. An intrinsic acyl-CoA thioesterase activity couples the translocation step to the hydrolysis of the CoA ester, leaving a free acid in the peroxisomes that must be re-activated with CoA for β -oxidation [57]. The human genome encodes several different acyl-CoA synthetases, catalyzing the ATP-dependent activation of fatty acids and related compounds to acyl-CoA in the presence of ATP [58,59]. Few isoforms have been reported to be linked to the peroxisomal membrane, but whether these membrane-associated proteins are active inside or outside the peroxisome has been the subject of recent debates [58,59]. Still, the active site of one human acyl-CoA synthetase has been located to the peroxisomal matrix. It is assumed that the enzyme specifically activates peroxisomal pristanic acid produced by α -oxidation of phytanic acid [60]. Reports on the human ABCD1 suggest that the import of VLCFA-CoA esters into peroxisomes is not dependent on peroxisome internal activation [61]. Still, the complementation of the yeast *pxa1/pxa2* Δ double mutant with the human ABCD1 requires the presence of the peroxisomal acyl-CoA synthetase Faa2p for the activation of the β -oxidation substrates [35]. Future research will resolve these partly contradictory hypotheses.

In the case that β -oxidation substrates enter peroxisomes as free fatty acids, a pool of ATP and CoA is needed for the peroxisomal re-esterification (Figure 2). Consequently, human peroxisomes have to be supplied with both cofactor molecules, if CoA is released in the cytosol by ABCD proteins [55,56]. The resulting acyl-CoA esters are then fed into β -oxidation, which depends on peroxisomal NAD as an electron acceptor. The last step of this pathway, catalyzed by the acyl-CoA thiolase, uses free CoA to cleave off one acetyl-CoA molecule from the acyl-chain [46]. The shortened acyl-CoA ester undergoes additional cycles but will not be completely degraded. Thus, the peroxisomal β -oxidation generates several different medium-chain acyl-CoAs, besides propionyl-CoA and acetyl-CoA. These

products are then exported via the peroxisomal carnitine shuttle from peroxisomes to mitochondria for further metabolism [46]. This export mechanism releases CoA in the peroxisomal lumen, which can be recycled for the thiolytic cleavage during β -oxidation. Peroxisomal thioesterase may also function in exporting the products of β -oxidation by releasing them from CoA esters [62].

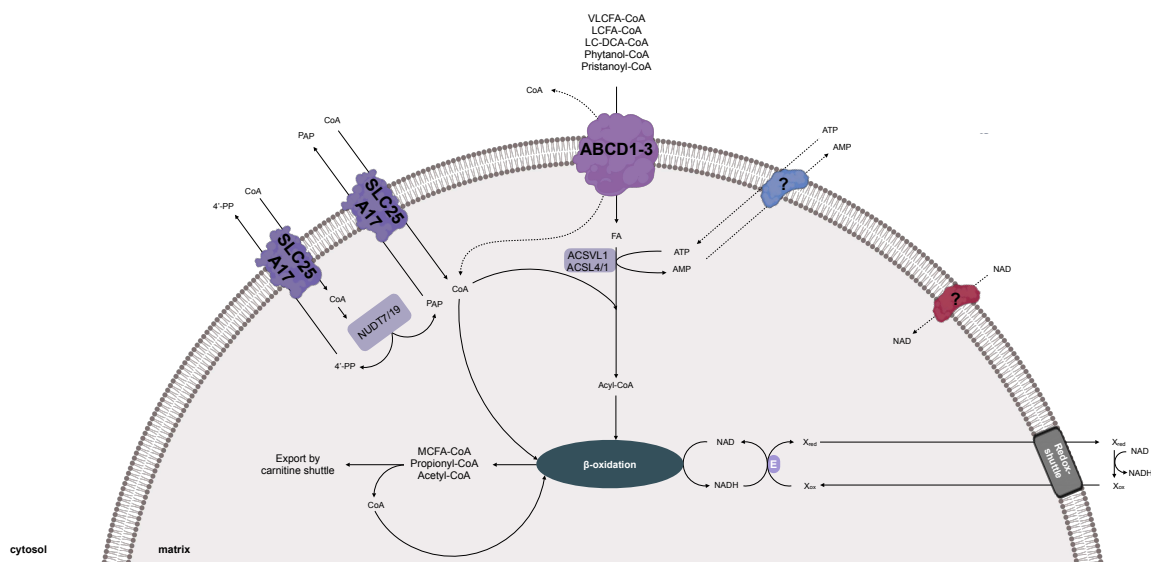


Figure 2. Model for the peroxisomal cofactor transport in human. ABCD1–3: ABC transporters of the subfamily D (ABCD) member 1–3, mediating the import of fatty acids and other β -oxidation-related substrates as CoA esters; ACSVL1: very-long-chain acyl-CoA synthetase 1 (associated at the matrix site of the peroxisomal membrane); ACSL1/4: long-chain acyl-CoA synthetase 1 and 4 (associated at the cytosolic site of the peroxisomal membrane); FA, fatty acid; NUDT7/19: peroxisomal Nudix hydrolase 7 and 19, catalyzing the hydrolysis of CoA to PAP and 4'-PP; LCFA-CoA: long-chain acyl-CoAs; LC-DCA-CoA: long-chain dicarboxyl-CoA; PAP: adenosine 3',5'-diphosphate; 4'-PP: 4'-phospho-pantetheine; VLCFA-CoA: very long-chain acyl-CoAs; SLC25A17: solute carrier family 25 member 17, putative peroxisomal CoA carrier; (?): proposed cofactor carrier proteins.

In humans, one member the MCF has been discovered as peroxisomal membrane protein of 34 kDa (PMP34) [63]. This human MCF protein is classified as member 17 of the solute carrier family 25 (SLC25A17). Due to its high homology to the yeast peroxisomal ATP carrier, it was hypothesized that human SLC25A17 is a functional ortholog of Ant1p [63,64]. To address this, human SLC25A17 was expressed in the *ant1 Δ* yeast mutant [64]. While peroxisomal β -oxidation activity in *ant1 Δ* cells were only 20% of wild type cells, the fatty-acid degradation was restored to approximately 60% of wild type in *ant1 Δ* , expressing the human SLC25A17. This partial rescue of the *ant1 Δ* phenotype with human SLC25A17 suggested a role in providing peroxisomes with ATP for fatty-acid oxidation [64]. Functional reconstitution of yeast expressed and purified SLC25A17 protein in lipid vesicles revealed detectable ATP import activity across the liposomal membrane [64]. Both observations led to the conclusion that the human SLC25A17 functions as an adenine nucleotide transporter, catalyzing an exchange of adenine nucleotides across the peroxisomal membrane [64]. The group of Ferdinando Palmieri repeated the uptake assays with the human SLC25A17 recombinantly expressed in *E.coli* and purified by affinity chromatography [65]. Surprisingly, it exhibited extremely low uptake rates of ATP, which might explain the partial complementation of the *ant1 Δ* mutant with the human SLC25A17 [64]. In contrast, high transport activities of recombinant SLC25A17 were discovered for AMP exchange against CoA, dephospho-CoA, and FAD. It also catalyzes the AMP import against internal FMN, ADP, adenosine 3',5'-diphosphate (PAP), and to a lesser extent, NAD [65]. Considering lower K_M and K_i values suggested a higher affinity of SLC25A17 for CoA, AMP, FAD, and FMN as substrates than for

NAD, ADP, and ATP [65]. The physiological role of such a cofactor carrier with a versatile transport functions remains unclear for human peroxisomes.

The *in vivo* function of SLC25A17 has been further investigated in genetic mutants of orthologs in the model organisms zebrafish (*Danio rerio*) and mice (*Mus musculus*) [66,67]. The zebrafish genome contains two *Slc25a17* proteins, which have been both simultaneously down-regulated by a morpholino-based antisense approach [66]. During the first four days of development, zebrafish embryos rely entirely on its nutrient-rich yolk sac to sustain growth and survival. In this phase, peroxisomal β -oxidation supports the utilization of very long-chain fatty acids, as well as the synthesis of plasmalogens, providing energy and structural cellular components [68]. Silencing of the two *slc25a17* genes at 3–4 days post-fertilization led to an accumulation of very long-chain fatty acids and a reduction of ether-phospholipids in the zebrafish embryos [66]. This altered cellular lipid composition caused a severe failure in the development of multiple organs, including the swim bladder. To test if the loss of peroxisomal CoA or NAD impairs β -oxidation function, these cofactors were co-injected together with the *slc25a17*-specific antisense oligomers into zebrafish embryos. Exogenously supplied CoA efficiently rescued the defective swim bladder, whereas NAD co-injection failed to restore the developmental defects associated with *slc25a17* knockdown [66]. *In vitro* uptake experiments demonstrated that both *Slc25a17* proteins function redundantly with a preference towards CoA, instead of NAD and ATP, similar to the human carrier [66]. These findings suggest that *Slc25a17* and *Slc25a17*-like functions additively as CoA transporters, which are involved in peroxisomal lipid metabolism and are thus essential for normal embryonic growth in zebrafish [66].

Mice lacking the SLC25A17 carrier by insertional mutagenesis did not show any obvious phenotype [67]. In particular, the diverse functions of the peroxisomal β -oxidation were not compromised in the SLC25A17-deficient mice. Only the degradation of phytol-derived branched-chain fatty acids was considerably impaired. Phytol, a constituent of chlorophyll, is converted to phytanic acid [69–71]. This methyl-branched fatty acid first activated by the long-chain acyl-CoA synthetases ACSL1/4 in the cytosol and then imported as acyl-CoA ester via ABCD3 transporter into peroxisomes [58,59], where it enters the peroxisomal α -oxidation. This pathway produces pristanic acid inside peroxisomes. This fatty acid is activated to pristanoyl-CoA catalyzed by the peroxisomal very-long-chain acyl-CoA synthetase ACSVL1 [60] for further conversion by multiple rounds of peroxisomal β -oxidation. The resulting medium-chain fatty acids are then completely oxidized by the mitochondrial β -oxidation [69–71]. Notably, pristanic acid is also present in human diets, and for its degradation via the peroxisomal β -oxidation, it is activated in the cytosol and imported as acyl-CoA ester via the ABCD3 transporter into peroxisomes [69–71].

Upon phytol feeding, the SLC25A17 knockout mice accumulated phytanic and pristanic acid as well as their CoA-esters in the liver, resulting in an enlarged organ and hepatic inflammation [67]. These abnormalities of the phytol-fed knockout mice suggested that the phytol degradation process depends on the peroxisomal cofactor supplied by SLC25A17. Unfortunately, the transport function of mice SLC25A17 has not yet been characterized, and thus we can only hypothesize about its preference for ATP, CoA, or NAD as a substrate [67]. Assuming that mouse SLC25A17 functions as a peroxisomal CoA carrier, as postulated for the zebrafish ortholog, the specific phenotype of the *slc25a17*-deficient mice might be caused by a shortage of peroxisomal CoA. Since the peroxisomal activation of pristanic acid as well as the thiolytic cleavage during β -oxidation of the resulting medium-chain fatty acids demand free CoA in the peroxisomal matrix, the levels of both phytol-derived fatty acids and acyl-CoA esters were elevated in the liver of the KO mice after phytol feeding [67].

In general, the activity of the acyl-CoA thioesterases prevent CoA deficiencies in peroxisomes from humans and mice [62]. These peroxisomal enzymes hydrolyze CoA esters, resulting in CoA formation, and thus can regulate the peroxisomal CoA pool [62]. In order to ensure a net CoA influx, the mice SLC25A17 carrier might catalyze the import of two CoA molecules against one molecule of adenosine 3',5'-diphosphate (PAP) and 4'-phosphopantetheine (4'-PP). Both counter-exchange substrates are products of the hydrolysis of one CoA molecule, provided by peroxisomal Nudix hydrolases [72–74].

For the human SLC25A17, it was shown that it transports PAP, however 4'-PP as a potential substrate has not been tested in this work [65].

Another open question is why the CoA-dependent activation of other β -oxidation substrates is not impaired in the SLC25A17-deficient mice. The mild phenotype of the loss-of-function mutant, which can only be unmasked upon phytol treatments, might point to an alternative way to provide peroxisomes with CoA. For instance, another CoA carrier protein may exist in the peroxisomal membrane or an alternative splicing variant could lead to dual targeting of the human mitochondrial CoA carrier [75,76]. In addition, it cannot be excluded that peroxisomal CoA-dependent enzymes are imported together with their cofactor, as it was described for FAD-dependent enzymes previously [20,21]. Nevertheless, this study may be applicable to the human system, indicating that SLC25A17 deficiency in humans is unlikely to be lethal but could cause an impaired metabolization of branched-chain fatty acids in older adults [67].

Up to now, the SLC25A17 proteins are the only MCF-type cofactor carrier known to be present in peroxisomes of humans, mice, and zebrafish. Orthologs of the peroxisomal ATP carrier Ant1p from yeast or the peroxisomal NAD carrier from *Arabidopsis* are required to provide metabolic pathways with ATP and NAD. Beside β -oxidation, ATP and NAD are also involved in different peroxisome-associated processes in humans and mice. For instance, intraperoxisomal ATP can be used for the post-translational phosphorylation of peroxisomal enzymes by protein kinases [77], proper folding of peroxisomal matrix proteins [78], removal of oxidatively damaged, and misfolded proteins via ATP-stimulated proteases [79,80]. NAD, in particular the phosphorylated, reduced form NADPH, is also needed for the oxidation of unsaturated fatty acids [46,70], as well as for the antioxidants defense systems, such as the ascorbate–glutathione cycle, to detoxify reactive oxygen species, such as the glutathione cycle [81]. Diverse peroxisomal NAD(P)-redox shuttle mechanisms, such as malate/oxaloacetate, lactate/pyruvate, and 2-oxoglutarate/isocitrate-based shuttle systems, regenerate NAD or NADPH and thus participate in regulating the redox homeostasis in human peroxisomes [4]. However, it remains to be investigated whether specific transport proteins are involved in the provision of ATP and NAD for peroxisomes in humans and animals.

4. Cofactor Transport for Plant Peroxisomes

In contrast to humans and animals, peroxisomes are the sole site of β -oxidation in plants. This essential metabolic pathway is involved in diverse developmental and signaling processes, participating in fatty-acid catabolism and the biosynthesis of several major phytohormones, including jasmonic acid, indole-3-acetic acid (auxin), and salicylic acid [2,82,83].

Another important function of β -oxidation is the mobilization of storage oil in oil-seed species, such as the model plant *Arabidopsis thaliana* [84,85]. These plants store energy in form of triacylglycerol in the seeds in order to secure survival of the next generation. During germination the embryos utilize the storage oil to enable the seedling growth and development, until it becomes photoautotrophic. In *Arabidopsis*, the long-chain fatty acids that are hydrolyzed from reserve lipids are imported into peroxisomes for further degradation by β -oxidation [84,85]. The import of fatty acids as CoA esters is mediated by the peroxisomal ABC transporter, which was named COMATOSE (CTS) after its dormancy phenotype in *Arabidopsis* [86–89]. The CTS transport mechanism is the same as described for the peroxisomal ABC transport proteins from yeast and human. The CoA-moiety is cleaved off during the import, which necessitates the re-esterification of fatty acids to CoA prior to entering β -oxidation [90]. This activation reaction is catalyzed by two peroxisomal long-chain acyl-CoA synthetases LACS6 and LCAS7 in an ATP-consuming reaction [91]. In the absence of both enzymes in peroxisomes, *Arabidopsis* seedlings were compromised in storage-oil mobilization, leading to an arrested seedling growth shortly after germination [91]. This phenotype implies that the activation of the fatty acid inside plant peroxisomes is essential for their breakdown. The resulting acyl-CoAs are then degraded by the NAD-dependent β -oxidation cycle [84,85]. The last step of this pathway uses free CoA for the thiolytic cleavage of the acyl-CoA, generating acetyl-CoA and a shortened acyl-CoA. The latter can

re-enter the β -oxidation pathway for further breakdown. The resulting acetyl-CoA is fueled into the peroxisomal glyoxylate cycle, producing four-carbon metabolites that can be converted to sucrose as a carbon and energy source [84,85]. With respect to the cofactor input, the peroxisomal enzymes of fatty-acid degradation have the same demand of ATP, CoA, and NAD in humans, animals and yeast [3,92] (Figure 3).

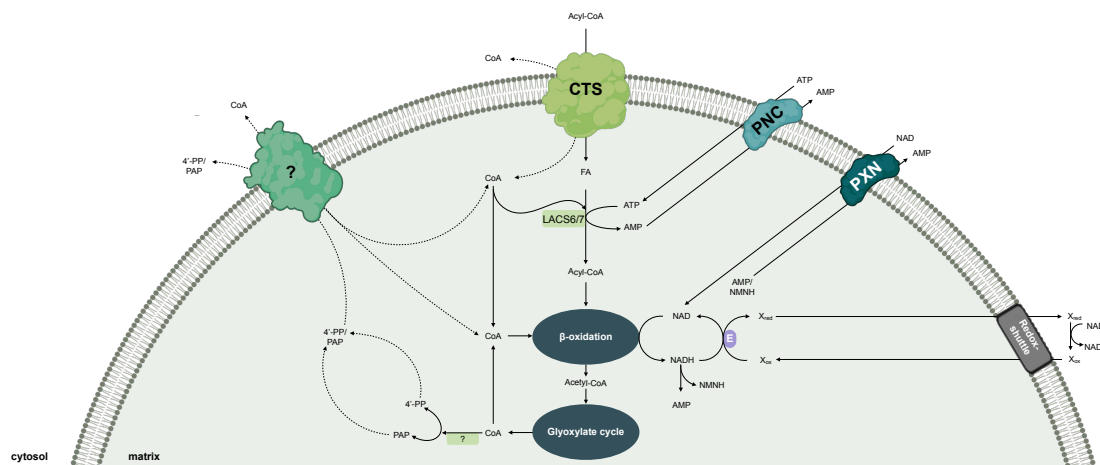


Figure 3. Model for the peroxisomal cofactor transport in plants. CTS: peroxisomal ABC transporter, mediating the import of fatty acids as acyl-CoA esters; FA: fatty acid; LACS6/7: long-chain acyl-CoA synthetase 6 and 7 (associated at the matrix site of the peroxisomal membrane); NMN(H): nicotinamide mononucleotide (reduced); PAP: adenosine 3',5'-diphosphate; 4'-PP: 4'-phospho-pantetheine; PNC, peroxisomal ATP carrier; PXN, peroxisomal NAD carrier; (?): proposed cofactor carrier proteins.

On the basis of amino-acid-sequence similarity to the peroxisomal ATP carrier Ant1p from *S. cerevisiae*, two *Arabidopsis* MCF members have been identified to be localized to the peroxisomal membrane [12,13]. These plant carriers were independently able to suppress the β -oxidation phenotype of the *ant1* Δ yeast mutant [13], indicating that both proteins import ATP into yeast peroxisomes. A biochemical characterization using recombinant PNC proteins revealed that the ATP import was mediated in a strict counter exchange transport mode with ADP or AMP, similar to the yeast ortholog [12,13]. Whereas substrate specificity was similar to the yeast ortholog, none of the PNC proteins showed uniport transport activity. Due to their restricted substrate spectrum, the *Arabidopsis* MCF members were annotated as peroxisomal adenine nucleotide carriers PNC1 and PNC2. *Arabidopsis* mutants were generated in which PNC1 and PNC2 were simultaneously silenced using RNA interference to analyze their *in vivo* role [12,13]. Since the import of cytosolic ATP into peroxisomes is essential for β -oxidation, the seedlings of the RNAi lines were compromised in seedling establishment [12,13]. The arrested seedling phenotype was caused by a block in storage-oil mobilization, resulting in an accumulation of storage-oil-derived fatty acids and acyl-CoA esters. This result suggests that peroxisomal ATP uptake mediated by PNC1/2 is critical for utilizing fatty acids through β -oxidation to fuel seedling growth [12,13]. It is hypothesized that PNC-mediated ATP import occurs in exchange with peroxisomal AMP, which is released during the fatty-acid activation step by LACS6/7 [91]. In addition, other metabolic pathways that are linked to peroxisomal β -oxidation were also affected in these *pnc1/2* RNAi lines, such as biosynthesis of phytohormones, the catabolism of membrane lipids during dark-induced senescence, and the degradation of branched-chain amino acids (unpublished work). Together, these findings emphasize that the peroxisomal ATP carriers are the primary source of peroxisomal ATP, meaning no other major ATP-generating systems, such as substrate-level phosphorylation, exist in *Arabidopsis* peroxisomes.

Our knowledge about other ATP-consuming reactions in plant peroxisomes beside β -oxidation is limited. Recently, it was demonstrated that the ATP-dependent enzymes that catalyze the last steps of the cytosolic mevalonate pathway for the synthesis of isopentenyl diphosphate are located inside plant

peroxisomes [93,94]. Peroxisomal ATP might also be crucial for the regulation of protein function. Phospho-proteomic studies revealed that many enzymes involved in photorespiration are regulated via post-translational phosphorylation [95–97]. Accordingly, several protein kinases have also been identified in plant peroxisomes, but their target proteins still need to be discovered [98,99]. A role of the PNC proteins as ATP/ADP carrier remains to be tested.

In order to support NAD-dependent fatty-acid oxidation during early seedling growth, the import of NAD into Arabidopsis peroxisomes is mediated by the peroxisomal NAD carrier, called PXN [100,101]. PXN belongs to the MCF and represents, regardless of the species, the first, and so far, only discovered peroxisomal carrier for NAD. In vitro uptake experiments of reconstituted recombinant protein discovered that PXN can transport many organic cofactors and related molecules, including NAD, NADH, ADP, AMP, and CoA, in an antiport mode [100,101]. The outcome of the biochemical (in vitro) assays suggest versatile transport functions for PXN, catalyzing the import of NAD or CoA against AMP or the exchange of NAD/NADH. However, complementation studies using different yeast mutants restricted the in vivo function of PXN to provide peroxisomes with cytosolic NAD in exchange with intraperoxisomal AMP [37]. Since the peroxisomal malate/oxaloacetate shuttle is involved in the export of NADH from peroxisomes and the import of re-oxidized NAD [102,103], PXN as an NAD/AMP exchanger might function to build up and/or replenish the peroxisomal NAD pool [14,37,101]. For instance, a net NAD import is facilitated, if the exported AMP is strictly accompanied by a unidirectional AMP import to balance the loss of peroxisomal AMP. Such an adenylate uniporter has only been described for chloroplasts so far [104,105]. In another scenario, PXN might transport two NAD molecules. One NAD is used for the peroxisomal metabolism, the other is hydrolyzed to AMP and reduced nicotinamide mononucleotide by the peroxisomal Nudix hydrolase in Arabidopsis [106,107]. Both hydrolysis products might counter-exchange during the uptake of two NAD molecules [14,101].

The role of PXN in providing the peroxisomal β -oxidation with NAD implies that a deletion of this gene would affect storage-oil mobilization, which is essential for seedling establishment. Surprisingly, Arabidopsis *pxn* knockout mutants did not display any obvious seedling phenotype, as described for the *PNC1/2* RNAi lines [100,101]. The fatty-acid composition in these mutant seedlings revealed that fatty-acid breakdown was delayed during storage-oil turnover, indicating that peroxisomal NAD import mediated by PXN contributes to an optimal operation of storage-oil degradation [100,101]. Recently, PXN was identified to be involved in photorespiration under fluctuating and high-light conditions [108]. The decreased activity of the photosystems in the *pxn* plants could be rescued by elevated CO₂ concentrations, which represses the flux through the photorespiratory pathway. The authors proposed that PXN can supply plant peroxisomes with the increased demand of NADH during photorespiration [108]. Both defined phenotypes point to an alternative mechanism to fuel plant peroxisomes with NAD; most likely by a redundant uptake system, that is either mediated by a specific carrier, protein-coupled NAD import, or by fusion of NAD-preloaded pre-peroxisomes derived from the ER [14].

Plant peroxisomes have to control their peroxisomal CoA pool, since this cofactor is crucial for the proper functioning of β -oxidation. The peroxisomal CoA is again released, for instance, once the acetyl-CoA is fed into the glyoxylate cycle, resulting in CoA recycling. Like in humans and yeast, plant peroxisomes possess several acyl-CoA thioesterases to ensure optimal flux through β -oxidation. They have been proposed to regulate the availability of free CoA in the peroxisomal matrix, by releasing CoA from acyl-CoA esters [109]. In addition, a role in maintaining the peroxisomal CoA has also been reported for the putative Nudix hydrolases of plant peroxisomes [110]. Since the CoA biosynthesis and salvage pathway takes place outside peroxisomes [111], plant peroxisomes depend on the uptake of CoA, which might be mediated by a specific CoA transport protein. A mitochondrial carrier for the distribution of CoA has been identified and characterized in humans, yeast, and plants [43,75], but the knowledge about a peroxisomal CoA carrier is restricted to non-plant organisms. An ortholog of the peroxisomal CoA carrier SLC25A17 in humans and animals is still unknown in Arabidopsis. The peroxisomal NAD carrier PXN, however, showed transport activities for CoA in vitro [100].

However, due to its low affinity to CoA, it is unlikely that PXN is able to transport CoA under physiological conditions [37]. Biochemical and genetic analyses will demonstrate the existence of a peroxisomal CoA carrier in plants in the future.

5. Conclusions

The mitochondrial carrier family (MCF) is a large family of proteins present in all eukaryotic lineages, which are present in several other cellular compartments, including peroxisomes. The peroxisomal MCF-type proteins described so far in yeast, humans, and plants, cluster as a functional branch in phylogenetic analyses [18,110]. These carriers ensure a stable exchange of structurally related cofactor molecules, such as ATP, CoA, and NAD, which are required for the maintenance of peroxisomal reactions, in particular β -oxidation. A detailed characterization of the transport function is indispensable to understand their physiological role in peroxisomes. However, the exciting findings of the knockout mutant displayed that alternative routes with a so far unknown mechanism exist for the cofactor exchange across the peroxisomal membrane.

Beyond cofactors, the diverse anabolic and catabolic reactions in peroxisomes produce a large number of small hydrophilic metabolites, which have to be shuttled across the peroxisomal membrane. Peroxisomes appear to be permeable to small hydrophilic solutes. Experimental evidences suggest a nonselective channel responsible for this exchange, but the proposed protein could not yet be conclusively assigned to the observed channel activity [3,6,8]. This raises the question if other transport proteins might be involved in peroxisomal metabolite transfer. For instance, MCF represents a carrier family with a broad substrate spectrum, catalyzing the transport of small hydrophilic solutes, like amino acids, mono, di- and tricarboxylates, and an inorganic form of phosphate. It could be hypothesized that—beyond the cofactor uptake—MCF-type proteins might play a role in these transport processes. Until now, such an MCF protein has not yet been located in peroxisomes in any eukaryotic organisms.

Author Contributions: Conceptualization, N.L.; writing and editing, A.P., L.C., and N.L. All authors have read and agreed to the published version of the manuscript.

Funding: This research was supported by German Research Foundations (DFG Grant LI1781/2-2).

Acknowledgments: We would like to thank members of the laboratories for stimulating discussions and critical comments on the manuscript. We apologize to those whose scientific work has not been cited. The figures were created with BioRender.com.

Conflicts of Interest: The authors declare no conflicts of interest.

References

1. Islinger, M.; Voelkl, A.; Fahimi, H.D.; Schrader, M. The peroxisome: An update on mysteries 2.0. *Histochem. Cell Biol.* **2018**, *150*, 443–471. [CrossRef]
2. Pan, R.; Liu, J.; Wang, S.; Hu, J. Peroxisomes: Versatile organelles with diverse roles in plants. *New Phytol.* **2020**, *225*, 1410–1427. [CrossRef] [PubMed]
3. Charton, L.; Plett, A.; Linka, N. Plant peroxisomal solute transporter proteins. *J. Integr. Plant Biol.* **2019**, *169*, 1469–1835. [CrossRef]
4. Wanders, R.J.A.; Waterham, H.R.; Ferdinandusse, S. Metabolic interplay between peroxisomes and other subcellular organelles including mitochondria and the endoplasmic reticulum. *Front. Cell Dev. Biol.* **2015**, *3*, 83. [CrossRef] [PubMed]
5. Rottensteiner, H.; Theodoulou, F.L. The ins and outs of peroxisomes: Co-ordination of membrane transport and peroxisomal metabolism. *Biochim. Biophys. Acta* **2006**, *1763*, 1527–1540. [CrossRef] [PubMed]
6. Antonenkov, V.D.; Hiltunen, J.K. Peroxisomal membrane permeability and solute transfer. *Biochim. Biophys. Acta* **2006**, *1763*, 1697–1706. [CrossRef] [PubMed]
7. Van Veldhoven, P.P.; Just, W.W.; Mannaerts, G.P. Permeability of the peroxisomal membrane to cofactors of beta-oxidation. Evidence for the presence of a pore-forming protein. *J. Biol. Chem.* **1987**, *262*, 4310–4318.
8. Antonenkov, V.D.; Hiltunen, J.K. Transfer of metabolites across the peroxisomal membrane. *Biochim. Biophys. Acta* **2011**, *1822*, 1374–1386. [CrossRef]

9. Palmieri, L.; Rottensteiner, H.; Girzalsky, W.; Scarcia, P.; Palmieri, F.; Erdmann, R. Identification and functional reconstitution of the yeast peroxisomal adenine nucleotide transporter. *EMBO J.* **2001**, *20*, 5049–5059. [CrossRef]
10. Van Roermund, C.W.T.; Drissen, R.; van den Berg, M.; Ijlst, L.; Hettema, E.H.; Tabak, H.F.; Waterham, H.R.; Wanders, R.J.A. Identification of a peroxisomal ATP carrier required for medium-chain fatty acid beta-oxidation and normal peroxisome proliferation in *Saccharomyces cerevisiae*. *Mol. Cell. Biol.* **2001**, *21*, 4321–4329. [CrossRef]
11. Bernhardt, K.; Wilkinson, S.; Weber, A.P.M.; Linka, N. A peroxisomal carrier delivers NAD and contributes to optimal fatty acid degradation during storage oil mobilization. *Plant J.* **2012**, *69*, 1–13. [CrossRef] [PubMed]
12. Arai, Y.; Hayashi, M.; Nishimura, M.; Nishimura, M. Proteomic identification and characterization of a novel peroxisomal adenine nucleotide transporter supplying ATP for fatty acid beta-oxidation in soybean and *Arabidopsis*. *Plant Cell* **2008**, *20*, 3227–3240. [CrossRef] [PubMed]
13. Linka, N.; Theodoulou, F.L.; Haslam, R.P.; Linka, M.; Napier, J.A.; Neuhaus, H.E.; Weber, A.P.M. Peroxisomal ATP import is essential for seedling development in *Arabidopsis thaliana*. *Plant Cell* **2008**, *20*, 3241–3257. [CrossRef]
14. Linka, N.; Esser, C. Transport proteins regulate the flux of metabolites and cofactors across the membrane of plant peroxisomes. *Front. Plant Sci.* **2012**, *3*, 3. [CrossRef] [PubMed]
15. Linka, N.; Theodoulou, F.L. Metabolite transporters of the plant peroxisomal membrane: Known and unknown. *Subcell. Biochem.* **2013**, *69*, 169–194. [PubMed]
16. Meinecke, M.; Cizmowski, C.; Schliebs, W.; Kruger, V.; Beck, S.; Wagner, R.; Erdmann, R. The peroxisomal importomer constitutes a large and highly dynamic pore. *Nat. Cell Biol.* **2010**, *12*, 273–277. [CrossRef]
17. Walter, T.; Erdmann, R. Current Advances in Protein Import into Peroxisomes. *Protein J.* **2019**, *38*, 351–362. [CrossRef]
18. Kim, P.K.; Hettema, E.H. Multiple pathways for protein transport to peroxisomes. *J. Mol. Biol.* **2015**, *427*, 1176–1190. [CrossRef]
19. Palmieri, T.; Berks, B.C. The twin-arginine translocation (Tat) protein export pathway. *Nat. Rev. Microbiol.* **2012**, *10*, 483–496. [CrossRef]
20. Titorenko, V.I.; Nicaud, J.M.; Wang, H.; Chan, H.; Rachubinski, R.A. Acyl-CoA oxidase is imported as a heteropentameric, cofactor-containing complex into peroxisomes of *Yarrowia lipolytica*. *J. Cell Biol.* **2002**, *156*, 481–494. [CrossRef]
21. Gunkel, K.; van Dijk, R.; Veenhuis, M.; van der Klei, I.J. Routing of *Hansenula polymorpha* alcohol oxidase: An alternative peroxisomal protein-sorting machinery. *Mol. Biol. Cell* **2004**, *15*, 1347–1355. [CrossRef] [PubMed]
22. Fraccascia, P.; Casteels, M.; De Schryver, E.; Van Veldhoven, P.P. Role of thiamine pyrophosphate in oligomerisation, functioning and import of peroxisomal 2-hydroxyacyl-CoA lyase. *Biochim. Biophys. Acta* **2011**, *1814*, 1226–1233. [CrossRef] [PubMed]
23. Palmieri, F.; Pierri, C.L.; De Grassi, A.; Nunes-Nesi, A.; Fernie, A.R. Evolution, structure and function of mitochondrial carriers: A review with new insights. *Plant J.* **2011**, *66*, 161–181. [CrossRef] [PubMed]
24. Haferkamp, I. The diverse members of the mitochondrial carrier family in plants. *FEBS Lett.* **2007**, *581*, 2375–2379. [CrossRef]
25. Palmieri, F. Mitochondrial transporters of the SLC25 family and associated diseases: A review. *J. Inherit. Metab. Dis.* **2014**, *37*, 565–575. [CrossRef]
26. Toleco, M.; Naake, T.; Zhang, Y.; Heazlewood, J.; Fernie, A.R. Plant mitochondrial carriers: Molecular gatekeepers that help to regulate plant central carbon metabolism. *Plants* **2020**, *9*, 117. [CrossRef]
27. Palmieri, F.; Monné, M. Discoveries, metabolic roles and diseases of mitochondrial carriers: A review. *BBA Mol. Cell Res.* **2016**, *1863*, 2362–2378. [CrossRef]
28. Saier, M.H.; Tran, C.V.; Barabote, R.D. TCDB: The Transporter Classification Database for membrane transport protein analyses and information. *Nucleic Acids Res.* **2006**, *34*, D181–D186. [CrossRef]
29. Palmieri, F. The mitochondrial transporter family SLC25: Identification, properties and physiopathology. *Mol. Asp. Med.* **2013**, *34*, 465–484. [CrossRef]
30. Palmieri, F.; Monné, M. Antiporters of the mitochondrial carrier family. In *Current Topics in Membranes*; Bevenses, M.O., Ed.; Elsevier Inc.: Cambridge, MA, USA, 2014; Volume 73, pp. 289–320.

31. Hiltunen, J.K.; Mursula, A.M.; Rottensteiner, H.; Wierenga, R.K.; Kastaniotis, A.J.; Gurvitz, A. The biochemistry of peroxisomal beta-oxidation in the yeast *Saccharomyces cerevisiae*. *FEMS Microbiol. Rev.* **2003**, *27*, 35–64. [CrossRef]
32. Hetteema, E.H.; van Roermund, C.W.T.; Distel, B.; van den Berg, M.; Vilela, C.; Rodrigues-Pousada, C.; Wanders, R.J.A.; Tabak, H.F. The ABC transporter proteins Pat1 and Pat2 are required for import of long-chain fatty acids into peroxisomes of *Saccharomyces cerevisiae*. *EMBO J.* **1996**, *15*, 3813–3822. [CrossRef] [PubMed]
33. Shani, N.; Valle, D.A. *Saccharomyces cerevisiae* homolog of the human adrenoleukodystrophy transporter is a heterodimer of two half ATP-binding cassette transporters. *Proc. Natl. Acad. Sci. USA* **1996**, *93*, 11901–11906. [CrossRef] [PubMed]
34. Swartzman, E.E.; Viswanathan, M.N.; Thorner, J. The PAL1 gene product is a peroxisomal ATP-binding cassette transporter in the yeast *Saccharomyces cerevisiae*. *J. Cell Biol.* **1996**, *132*, 549–563. [CrossRef] [PubMed]
35. Van Roermund, C.W.T.; Ijlst, L.; Majczak, W.; Waterham, H.R.; Folkerts, H.; Wanders, R.J.A.; Hellingwerf, K.J. Peroxisomal fatty acid uptake mechanism in *Saccharomyces cerevisiae*. *J. Biol. Chem.* **2012**, *287*, 20144–20153. [CrossRef] [PubMed]
36. Rottensteiner, H.; Palmieri, L.; Hartig, A.; Hamilton, B.; Ruis, H.; Erdmann, R.; Gurvitz, A. The peroxisomal transporter gene ANT1 is regulated by a deviant oleate response element (ORE): Characterization of the signal for fatty acid induction. *Biochem. J.* **2002**, *365*, 109–117. [CrossRef]
37. Van Roermund, C.W.T.; Schroers, M.G.; Wiese, J.; Facchinelli, F.; Kurz, S.; Wilkinson, S.; Charton, L.; Wanders, R.J.A.; Waterham, H.R.; Weber, A.P.M.; et al. The peroxisomal NAD carrier from Arabidopsis imports NAD in exchange with AMP. *Plant Physiol.* **2016**, *171*, 2127–2139. [CrossRef]
38. Cartwright, J.L.; Gasmi, L.; Spiller, D.G.; McLennan, A.G. The *Saccharomyces cerevisiae* PCD1 gene encodes a peroxisomal nudix hydrolase active toward coenzyme A and its derivatives. *J. Biol. Chem.* **2000**, *275*, 32925–32930. [CrossRef]
39. Van Roermund, C.W.T.; Elgersma, Y.; Singh, N.; Wanders, R.J.A.; Tabak, H.F. The membrane of peroxisomes in *Saccharomyces cerevisiae* is impermeable to NAD(H) and acetyl-CoA under in vivo conditions. *EMBO J.* **1995**, *14*, 3480–3486. [CrossRef]
40. Al-Saryi, N.A.; Al-Hejjaj, M.Y.; van Roermund, C.W.T.; Hulmes, G.E.; Ekal, L.; Payton, C.; Wanders, R.J.A.; Hetteema, E.H. Two NAD-linked redox shuttles maintain the peroxisomal redox balance in *Saccharomyces cerevisiae*. *Sci. Rep.* **2017**, *7*, 11868–11869. [CrossRef]
41. Van Roermund, C.W.T.; Hetteema, E.H.; Kal, A.J.; van den Berg, M.; Tabak, H.F.; Wanders, R.J.A. Peroxisomal β -oxidation of polyunsaturated fatty acids in *Saccharomyces cerevisiae*: Isocitrate dehydrogenase provides NADPH for reduction of double bonds at even positions. *EMBO J.* **1998**, *17*, 677–687. [CrossRef]
42. Abdelraheim, S.R.; Cartwright, J.L.; Gasmi, L.; McLennan, A.G. The NADH diphosphatase encoded by the *Saccharomyces cerevisiae* NPY1 nudix hydrolase gene is located in peroxisomes. *Arch. Biochem. Biophys.* **2001**, *388*, 18–24. [CrossRef] [PubMed]
43. Prohl, C.; Pelzer, W.; Diekert, K.; Kmita, H.; Bedekovics, T.; Kispal, G.; Lill, R. The yeast mitochondrial carrier Leu5p and its human homologue Graves' disease protein are required for accumulation of coenzyme A in the matrix. *Mol. Cell. Biol.* **2001**, *21*, 1089–1097. [CrossRef] [PubMed]
44. Todisco, S.; Agrimi, G.; Castegna, A.; Palmieri, F. Identification of the mitochondrial NAD transporter in *Saccharomyces cerevisiae*. *J. Biol. Chem.* **2006**, *281*, 1524–1531. [CrossRef] [PubMed]
45. Waterham, H.R.; Ferdinandusse, S.; Wanders, R.J.A. Human disorders of peroxisome metabolism and biogenesis. *Biochim. Biophys. Acta* **2016**, *1863*, 922–933. [CrossRef] [PubMed]
46. Wanders, R.J.A.; Waterham, H.R. Biochemistry of mammalian peroxisomes revisited. *Annu. Rev. Biochem.* **2006**, *75*, 295–332. [CrossRef]
47. Kamijo, K.; Taketani, S.; Yokota, S.; Osumi, T.; Hashimoto, T. The 70-kDa peroxisomal membrane protein is a member of the Mdr (P-glycoprotein)-related ATP-binding protein superfamily. *J. Biol. Chem.* **1990**, *265*, 4534–4540.
48. Mosser, J.; Douar, A.M.; Sarde, C.O.; Kioschis, P.; Feil, R.; Moser, H.; Poustka, A.M.; Mandel, J.L.; Aubourg, P. Putative X-linked adrenoleukodystrophy gene shares unexpected homology with ABC transporters. *Nature* **1993**, *361*, 726–730. [CrossRef]
49. Lombard-Platet, G.; Savary, S.; Sarde, C.O.; Mandel, J.L.; Chimini, G. A close relative of the adrenoleukodystrophy (ALD) gene codes for a peroxisomal protein with a specific expression pattern. *Proc. Natl. Acad. Sci. USA* **1996**, *93*, 1265–1269. [CrossRef]

50. Van Roermund, C.W.T.; Visser, W.F.; Ijlst, L.; van Cruchten, A.; Boek, M.; Kulik, W.; Waterham, H.R.; Wanders, R.J.A. The human peroxisomal ABC half transporter ALDP functions as a homodimer and accepts acyl-CoA esters. *FASEB J.* **2008**, *22*, 4201–4208. [CrossRef]
51. Van Roermund, C.W.T.; Visser, W.F.; Ijlst, L.; Waterham, H.R.; Wanders, R.J.A. Differential substrate specificities of human ABCD1 and ABCD2 in peroxisomal fatty acid β -oxidation. *Biochim. Biophys. Acta* **2011**, *1811*, 148–152. [CrossRef]
52. Van Roermund, C.W.T.; Ijlst, L.; Wagemans, T.; Wanders, R.J.A.; Waterham, H.R. A role for the human peroxisomal half-transporter ABCD3 in the oxidation of dicarboxylic acids. *Biochim. Biophys. Acta* **2013**, *1841*, 563–568. [CrossRef]
53. Ferdinandusse, S.; Jimenez-Sanchez, G.; Koster, J.; Denis, S.; van Roermund, C.W.T.; Silva-Zolezzi, I.; Moser, A.B.; Visser, W.F.; Gulluoglu, M.; Durmaz, O.; et al. A novel bile acid biosynthesis defect due to a deficiency of peroxisomal ABCD3. *Hum. Mol. Genet.* **2015**, *24*, 361–370. [CrossRef] [PubMed]
54. Ferdinandusse, S.; Falkenberg, K.D.; Koster, J.; Mooyer, P.A.; Jones, R.; van Roermund, C.W.T.; Pizzino, A.; Schrader, M.; Wanders, R.J.A.; Vanderver, A.; et al. ACBD5 deficiency causes a defect in peroxisomal very long-chain fatty acid metabolism. *J. Med. Genet.* **2017**, *54*, 330–337. [CrossRef] [PubMed]
55. Imanaka, T. Biogenesis and function of peroxisomes in human disease with a focus on the ABC Transporter. *Biol. Pharm. Bull.* **2019**, *42*, 649–665. [CrossRef] [PubMed]
56. Baker, A.; Carrier, D.J.; Schaedler, T.; Waterham, H.R.; van Roermund, C.W.T.; Theodoulou, F.L. Peroxisomal ABC transporters: Functions and mechanism. *Biochem. Soc. Trans.* **2015**, *43*, 959–965. [CrossRef]
57. Okamoto, T.; Kawaguchi, K.; Watanabe, S.; Agustina, R.; Ikejima, T.; Ikeda, K.; Nakano, M.; Morita, M.; Imanaka, T. Characterization of human ATP-binding cassette protein subfamily D reconstituted into proteoliposomes. *Biochem. Biophys. Res. Commun.* **2018**, *496*, 1122–1127. [CrossRef] [PubMed]
58. Watkins, P.A.; Ellis, J.M. Peroxisomal acyl-CoA synthetases. *Biochim. Biophys. Acta* **2012**, *1822*, 1411–1420. [CrossRef]
59. Grevengoed, T.J.; Klett, E.L.; Coleman, R.A. Acyl-CoA metabolism and partitioning. *Annu. Rev. Nutr.* **2014**, *34*, 1–30. [CrossRef]
60. Steinberg, S.J.; Wang, S.J.; Kim, D.G.; Mihalik, S.J.; Watkins, P.A. Human very-long-chain acyl-CoA synthetase: Cloning, topography, and relevance to branched-chain fatty acid metabolism. *Biochem. Biophys. Res. Commun.* **1999**, *257*, 615–621. [CrossRef]
61. Wiesinger, C.; Kunze, M.; Regelsberger, G.; Forss-Petter, S.; Berger, J. Impaired very long-chain acyl-CoA β -oxidation in human X-linked adrenoleukodystrophy fibroblasts is a direct consequence of ABCD1 transporter dysfunction. *J. Biol. Chem.* **2013**, *288*, 19269–19279. [CrossRef]
62. Hunt, M.C.; Tillander, V.; Alexson, S.E.H. Regulation of peroxisomal lipid metabolism: The role of acyl-CoA and coenzyme A metabolizing enzymes. *Biochimie* **2014**, *98*, 45–55. [CrossRef] [PubMed]
63. Wylin, T.; Baes, M.; Brees, C.; Mannaerts, G.P.; Fransen, M.; Van Veldhoven, P.P. Identification and characterization of human PMP34, a protein closely related to the peroxisomal integral membrane protein PMP47 of *Candida boidinii*. *Eur. J. Biochem.* **1998**, *258*, 332–338. [CrossRef] [PubMed]
64. Visser, W.F.; van Roermund, C.W.T.; Waterham, H.R.; Wanders, R.J.A. Identification of human PMP34 as a peroxisomal ATP transporter. *Biochem. Biophys. Res. Commun.* **2002**, *299*, 494–497. [CrossRef]
65. Agrimi, G.; Russo, A.; Scarcia, P.; Palmieri, F. The human gene SLC25A17 encodes a peroxisomal transporter of coenzyme A, FAD and NAD. *Biochem. J.* **2012**, *443*, 241–247. [CrossRef] [PubMed]
66. Kim, Y.-I.; Nam, I.-K.; Lee, D.-K.; Bhandari, S.; Charton, L.; Kwak, S.; Lim, J.-Y.; Hong, K.; Kim, S.-J.; Lee, J.N.; et al. Slc25a17 acts as a peroxisomal coenzyme A transporter and regulates multiorgan development in zebrafish. *J. Cell. Physiol.* **2020**, *235*, 151–165. [CrossRef]
67. Van Veldhoven, P.P.; De Schryver, E.; Young, S.G.; Zwijssen, A.; Fransen, M.; Espeel, M.; Baes, M.; Van Ael, E. Slc25a17 gene trapped mice: PMP34 plays a role in the peroxisomal degradation of phytanic and pristanic acid. *Front. Cell Dev. Biol.* **2020**, *8*, 144. [CrossRef]
68. Anderson, J.L.; Carten, J.D.; Farber, S.A. Zebrafish lipid metabolism: From mediating early patterning to the metabolism of dietary fat and cholesterol. *Methods Cell Biol.* **2011**, *101*, 111–141.
69. Jansen, G.A.; Wanders, R.J.A. Alpha-oxidation. *Biochim. Biophys. Acta* **2006**, *1763*, 1403–1412. [CrossRef]
70. Van Veldhoven, P.P. Biochemistry and genetics of inherited disorders of peroxisomal fatty acid metabolism. *J. Lipid Res.* **2010**, *51*, 2863–2895. [CrossRef]


71. Wanders, R.J.A. Phytanic acid metabolism in health and disease. *Biochim. Biophys. Acta* **2011**, *1811*, 498–507. [CrossRef]
72. Gasmi, L.; McLennan, A.G. The mouse Nudt7 gene encodes a peroxisomal nudix hydrolase specific for coenzyme A and its derivatives. *Biochem. J.* **2001**, *357*, 33–38. [CrossRef] [PubMed]
73. Ofman, R.; Speijer, D.; Leen, R.; Wanders, R.J.A. Proteomic analysis of mouse kidney peroxisomes: Identification of RP2p as a peroxisomal nudix hydrolase with acyl-CoA diphosphatase activity. *Biochem. J.* **2006**, *393*, 537–543. [CrossRef] [PubMed]
74. Shumar, S.A.; Kerr, E.W.; Geldenhuys, W.J.; Montgomery, G.E.; Fagone, P.; Thirawatananond, P.; Saavedra, H.; Gabelli, S.B.; Leonardi, R. Nudt19 is a renal CoA diphosphohydrolase with biochemical and regulatory properties that are distinct from the hepatic Nudt7 isoform. *J. Biol. Chem.* **2018**, *293*, 4134–4148. [CrossRef] [PubMed]
75. Fiermonte, G.; Paradies, E.; Todisco, S.; Marobbio, C.M.T.; Palmieri, F. A novel member of solute carrier family 25 (SLC25A42) is a transporter of coenzyme A and adenosine 3', 5'-diphosphate in human mitochondria. *J. Biol. Chem.* **2009**, *284*, 18152–18159. [CrossRef] [PubMed]
76. Ast, J.; Stiebler, A.C.; Freitag, J.; Bölker, M. Dual targeting of peroxisomal proteins. *Front. Physiol.* **2013**, *4*, 297. [CrossRef] [PubMed]
77. Oeljeklaus, S.; Schummer, A.; Mastalski, T.; Platta, H.W.; Warscheid, B. Regulation of peroxisome dynamics by phosphorylation. *Biochim. Biophys. Acta* **2016**, *1863*, 1027–1037. [CrossRef]
78. Sakai, Y.; Saiganji, A.; Yurimoto, H.; Takabe, K.; Saiki, H.; Kato, N. The absence of Pmp47, a putative yeast peroxisomal transporter, causes a defect in transport and folding of a specific matrix enzyme. *J. Cell Biol.* **1996**, *134*, 37–51. [CrossRef]
79. Kikuchi, M.; Hatano, N.; Yokota, S.; Shimosawa, N.; Imanaka, T.; Taniguchi, H. Proteomic analysis of rat liver peroxisome: Presence of peroxisome-specific isozyme of Lon protease. *J. Biol. Chem.* **2004**, *279*, 421–428. [CrossRef]
80. Pomatto, L.C.D.; Raynes, R.; Davies, K.J.A. The peroxisomal Lon protease LonP2 in aging and disease: Functions and comparisons with mitochondrial Lon protease LonP1. *Biol. Rev. Camb. Philos. Soc.* **2017**, *92*, 739–753. [CrossRef]
81. Fransen, M.; Nordgren, M.; Wang, B.; Apanasets, O. Role of peroxisomes in ROS/RNS-metabolism: Implications for human disease. *BBA Mol. Basis Dis.* **2012**, *1822*, 1363–1373. [CrossRef]
82. Hu, J.; Baker, A.; Bartel, B.; Linka, N.; Mullen, R.T.; Reumann, S.; Zolman, B.K. Plant peroxisomes: Biogenesis and function. *Plant Cell* **2012**, *24*, 2279–2303. [CrossRef] [PubMed]
83. Reumann, S.; Bartel, B. ScienceDirect Plant peroxisomes: Recent discoveries in functional complexity, organelle homeostasis, and morphological dynamics. *Curr. Opin. Plant Biol.* **2016**, *34*, 17–26. [CrossRef]
84. Graham, I.A. Seed storage oil mobilization. *Annu. Rev. Plant Biol.* **2008**, *59*, 115–142. [CrossRef] [PubMed]
85. Theodoulou, F.L.; Eastmond, P.J. Seed storage oil catabolism: A story of give and take. *Curr. Opin. Plant Biol.* **2012**, *15*, 322–328. [CrossRef] [PubMed]
86. Footitt, S.; Slocombe, S.P.; Larner, V.; Kurup, S.; Wu, Y.; Larson, T.; Graham, I.A.; Baker, A.; Holdsworth, M. Control of germination and lipid mobilization by COMATOSE, the Arabidopsis homologue of human ALDP. *EMBO J.* **2002**, *21*, 2912–2922. [CrossRef] [PubMed]
87. Zolman, B.K.; Silva, I.D.; Bartel, B. The Arabidopsis pxa1 mutant is defective in an ATP-binding cassette transporter-like protein required for peroxisomal fatty acid beta-oxidation. *Plant Physiol.* **2001**, *127*, 1266–1278. [CrossRef]
88. Hayashi, M.; Nito, K.; Takei-Hoshi, R.; Yagi, M.; Kondo, M.; Suenaga, A.; Yamaya, T.; Nishimura, M.; Nishimura, M. Ped3p is a peroxisomal ATP-binding cassette transporter that might supply substrates for fatty acid beta-oxidation. *Plant Cell Physiol.* **2002**, *43*, 1–11. [CrossRef]
89. Hooks, M.A.; Turner, J.E.; Murphy, E.C.; Graham, I.A. Acetate non-utilizing mutants of Arabidopsis: Evidence that organic acids influence carbohydrate perception in germinating seedlings. *Mol. Genet. Genom.* **2004**, *271*, 249–256. [CrossRef]
90. De Marcos Lousa, C.; van Roermund, C.W.T.; Postis, V.L.G.; Dietrich, D.; Kerr, I.D.; Wanders, R.J.A.; Baldwin, S.A.; Baker, A.; Theodoulou, F.L. Intrinsic acyl-CoA thioesterase activity of a peroxisomal ATP binding cassette transporter is required for transport and metabolism of fatty acids. *Proc. Natl. Acad. Sci. USA* **2013**, *110*, 1279–1284. [CrossRef]

91. Fulda, M.; Schnurr, J.; Abbadi, A.; Heinz, E.; Browse, J. Peroxisomal Acyl-CoA synthetase activity is essential for seedling development in *Arabidopsis thaliana*. *Plant Cell* **2004**, *16*, 394–405. [CrossRef]
92. Rinaldi, M.A.; Patel, A.B.; Park, J.; Lee, K.; Strader, L.C.; Bartel, B. The Roles of β -oxidation and cofactor homeostasis in peroxisome distribution and function in *Arabidopsis thaliana*. *Genetics* **2016**, *204*, 1089–1115. [CrossRef]
93. Sapir-Mir, M.; Mett, A.; Belausov, E.; Tal-Meshulam, S.; Frydman, A.; Gidoni, D.; Eyal, Y. Peroxisomal localization of *Arabidopsis* isopentenyl diphosphate isomerases suggests that part of the plant isoprenoid mevalonic acid pathway is compartmentalized to peroxisomes. *Plant Physiol.* **2008**, *148*, 1219–1228. [CrossRef]
94. Simkin, A.J.; Guirimand, G.; Papon, N.; Courdavault, V.; Thabet, I.; Ginis, O.; Bouzid, S.; Giglioli-Guivarc'h, N.; Clastre, M. Peroxisomal localisation of the final steps of the mevalonic acid pathway in planta. *Planta* **2011**, *234*, 903–914. [CrossRef] [PubMed]
95. Hodges, M.; Jossier, M.; Boex-Fontvieille, E.; Tcherkez, G. Protein phosphorylation and photorespiration. *Plant Biol. J.* **2013**, *15*, 694–706. [CrossRef] [PubMed]
96. Kataya, A.R.A.; Muench, D.G.; Moorhead, G.B. A Framework to Investigate peroxisomal protein phosphorylation in *Arabidopsis*. *Trends Plant Sci.* **2019**, *24*, 366–381. [CrossRef] [PubMed]
97. Sandalio, L.M.; Gotor, C.; Romero, L.C.; Romero-Puertas, M.C. Multilevel Regulation of peroxisomal proteome by post-translational modifications. *Int. J. Mol. Sci.* **2019**, *20*, 4881. [CrossRef] [PubMed]
98. Fukao, Y.; Hayashi, M.; Hara-Nishimura, I.; Nishimura, M. Novel glyoxysomal protein kinase, GPK1, identified by proteomic analysis of glyoxysomes in etiolated cotyledons of *Arabidopsis thaliana*. *Plant Cell Physiol.* **2003**, *44*, 1002–1012. [CrossRef]
99. Coca, M.; San Segundo, B. AtCPK1 calcium-dependent protein kinase mediates pathogen resistance in *Arabidopsis*. *Plant J.* **2010**, *2010*, 18. [CrossRef]
100. Agrimi, G.; Russo, A.; Pierri, C.L.; Palmieri, F. The peroxisomal NAD carrier of *Arabidopsis thaliana* transports coenzyme A and its derivatives. *J. Bioenerg. Biomembr.* **2012**, *44*, 333–340. [CrossRef]
101. Pracharoenwattana, I.; Zhou, W.; Smith, S.M. Fatty acid beta-oxidation in germinating *Arabidopsis* seeds is supported by peroxisomal hydroxypyruvate reductase when malate dehydrogenase is absent. *Plant Mol. Biol.* **2010**, *72*, 101–109. [CrossRef]
102. Pracharoenwattana, I.; Cornah, J.E.; Smith, S.M. *Arabidopsis* peroxisomal malate dehydrogenase functions in beta-oxidation but not in the glyoxylate cycle. *Plant J.* **2007**, *50*, 381–390. [CrossRef] [PubMed]
103. Leroch, M.; Kirchberger, S.; Haferkamp, I.; Wahl, M.; Neuhaus, H.E.; Tjaden, J. Identification and characterization of a novel plastidic adenine nucleotide uniporter from *Solanum tuberosum*. *J. Biol. Chem.* **2005**, *280*, 17992–18000. [CrossRef] [PubMed]
104. Kirchberger, S.; Tjaden, J.; Neuhaus, H.E. Characterization of the *Arabidopsis* Brittle1 transport protein and impact of reduced activity on plant metabolism. *Plant J.* **2008**, *56*, 51–63. [CrossRef] [PubMed]
105. Ogawa, T.; Ueda, Y.; Yoshimura, K.; Shigeoka, S. Comprehensive analysis of cytosolic Nudix hydrolases in *Arabidopsis thaliana*. *J. Biol. Chem.* **2005**, *280*, 25277–25283. [CrossRef]
106. Ogawa, T.; Yoshimura, K.; Miyake, H.; Ishikawa, K.; Ito, D.; Tanabe, N.; Shigeoka, S. Molecular characterization of organelle-type Nudix hydrolases in *Arabidopsis*. *Plant Physiol.* **2008**, *148*, 1412–1424. [CrossRef]
107. Li, J.; Tietz, S.; Cruz, J.A.; Strand, D.D.; Xu, Y.; Chen, J.; Kramer, D.M.; Hu, J. Photometric screens identified *Arabidopsis* peroxisome proteins that impact photosynthesis under dynamic light conditions. *Plant J.* **2019**, *97*, 460–474. [CrossRef]
108. Tilton, G.B.; Shockley, J.M.; Browse, J. Biochemical and molecular characterization of ACH2, an acyl-CoA thioesterase from *Arabidopsis thaliana*. *J. Biol. Chem.* **2004**, *279*, 7487–7494. [CrossRef]
109. Ito, D.; Yoshimura, K.; Ishikawa, K.; Ogawa, T.; Maruta, T.; Shigeoka, S. A comparative analysis of the molecular characteristics of the *Arabidopsis* CoA pyrophosphohydrolases AtNUDX11, 15, and 15a. *Biosci. Biotechnol. Biochem.* **2012**, *76*, 139–147. [CrossRef]
110. Webb, M.E.; Smith, A.G. Pantothenate Biosynthesis in Higher Plants. *Adv. Bot. Res.* **2011**, *58*, 203–255.
111. Zallot, R.; Agrimi, G.; Lerma-Ortiz, C.; Teresinski, H.J.; Frelin, O.; Ellens, K.W.; Castegna, A.; Russo, A.; de Crécy-Lagard, V.; Mullen, R.T.; et al. Identification of mitochondrial coenzyme a transporters from maize and *Arabidopsis*. *Plant Physiol.* **2013**, *162*, 581–588. [CrossRef]



Review

Mitochondrial Pyruvate Carrier Function in Health and Disease across the Lifespan

Jane L. Buchanan ¹ and Eric B. Taylor ^{1,2,3,4,5,*} 

¹ Department of Molecular Physiology and Biophysics, University of Iowa Carver College of Medicine, Iowa City, IA 52240, USA; Jane-Buchanan@uiowa.edu

² Holden Comprehensive Cancer Center, University of Iowa Carver College of Medicine, Iowa City, IA 52240, USA

³ Fraternal Order of Eagles Diabetes Research Center (FOEDRC), University of Iowa Carver College of Medicine, Iowa City, IA 52240, USA

⁴ Abboud Cardiovascular Research Center, University of Iowa Carver College of Medicine, Iowa City, IA 52240, USA

⁵ Pappajohn Biomedical Institute, University of Iowa Carver College of Medicine, Iowa City, IA 52240, USA

* Correspondence: Eric-Taylor@uiowa.edu

Received: 18 July 2020; Accepted: 6 August 2020; Published: 8 August 2020

Abstract: As a nodal mediator of pyruvate metabolism, the mitochondrial pyruvate carrier (MPC) plays a pivotal role in many physiological and pathological processes across the human lifespan, from embryonic development to aging-associated neurodegeneration. Emerging research highlights the importance of the MPC in diverse conditions, such as immune cell activation, cancer cell stemness, and dopamine production in Parkinson’s disease models. Whether MPC function ameliorates or contributes to disease is highly specific to tissue and cell type. Cell- and tissue-specific differences in MPC content and activity suggest that MPC function is tightly regulated as a mechanism of metabolic, cellular, and organismal control. Accordingly, recent studies on cancer and diabetes have identified protein–protein interactions, post-translational processes, and transcriptional factors that modulate MPC function. This growing body of literature demonstrates that the MPC and other mitochondrial carriers comprise a versatile and dynamic network undergirding the metabolism of health and disease.

Keywords: mitochondrial pyruvate carrier; MPC; lifespan; pyruvate metabolism; mitochondrial transport

1. Introduction

The mitochondrial pyruvate carrier (MPC) was discovered in 2012 [1,2]. However, as early as 1971, studies predicted that a mitochondrial protein transported pyruvate from the cytoplasm into the mitochondria [3–5]. Since its discovery, the MPC has been the subject of extensive primary literature research articles and reviews detailing key aspects of its structure, function, regulation, and diverse roles in health and disease. To date, most studies examining the MPC’s role in disease using genetically tractable systems have focused on cancer metabolism and diabetes. However, smaller yet important niches for MPC research are becoming evident, highlighting the variety of situations where the MPC controls metabolism and dependent cellular functions. Some of these include embryonic and fetal health, stem cell development, neurogenerative disease, and immune cell function.

A central theme, and the focus of this review, is that the beneficial or harmful role of the MPC in a disease or physiological state is highly specific to tissue and cell type. Cell- and tissue-dependent differences in MPC content and activity suggest that MPC function is tightly regulated as a mechanism

of metabolic, cellular, and organismal control. Several recent studies provide evidence that the MPC is regulated at multiple levels by transcription factors, protein–protein interactions, and post-translational modifications. Here, we examine MPC function across the lifespan, beginning with embryonic and fetal development and ending with aging-associated neurodegeneration.

2. The MPC in the Triumvirate of Mitochondrial Pyruvate Metabolism

Mitochondrial pyruvate metabolism is controlled by a triumvirate of enzymes—the MPC, pyruvate dehydrogenase (PDH), and pyruvate carboxylase (PC) [6–8]—that together modulate many physiological and pathological processes. Pyruvate is the end product of glycolysis, and its metabolism is instrumental in managing carbohydrate loads, producing ATP, and maintaining blood glucose levels. When pyruvate metabolism is dysfunctional, as first recognized in patients with inborn errors in PDH and PC, the effects are wide-ranging. Infants with either PDH or PC genetic mutations often show high blood lactate and ammonia levels, low muscle tone and lethargy, developmental delays, seizures, and even premature death.

MPC mutations are thought to be quite rare but result in the same severe symptoms observed with PDH and PC deficiency [9,10]. The MPC gates pyruvate entry into mitochondria and thus is a pivotal control point for mitochondrial pyruvate metabolism. The mammalian MPC is a complex formed by the MPC1 and MPC2 paralogs that are both necessary to stabilize the other to form a functional MPC [1,2]. Once pyruvate is inside mitochondria, the PDH complex decarboxylates it into acetyl-CoA for forward tricarboxylic acid (TCA)-cycle oxidation and ATP production, or PC carboxylates it into oxaloacetate to support biosynthesis, including nucleotide and amino acid synthesis, de novo lipogenesis, and gluconeogenesis. Not surprisingly, increases or decreases in MPC activity correspond to shifts toward oxidative or glycolytic metabolism, respectively. These metabolic shifts are crucial to support changes in cellular state, and their magnitude may differ depending on cellular state.

3. The MPC in Development

3.1. Embryonic and Fetal Health

Due to the energetic, biosynthetic, and regulatory metabolic demands of rapidly dividing cells, MPC deficiency in utero has severe consequences for the developing fetus. Homozygous *Mpc1* or *Mpc2* deletion in mice results in embryonic lethality within the first three weeks of development [11–13]. In vitro *Mpc1* silencing in mouse oocytes also significantly impairs maturation [14]. Hypomorphic *Mpc1* mice exhibit early perinatal lethality, while a less severe N-terminal *Mpc2* hypomorph allows for normal mouse development [11,13]. In the first study to describe inborn errors of MPC function in humans, an infant patient presented with lactic acidosis, low muscle tone, and brain abnormalities [10]. Biochemical studies of the patient's fibroblasts revealed a defect in pyruvate transport, which contributed to the molecular identification of the MPC several years later [1,2].

In a more recent study, Oonthonpan et al. investigated the biochemical mechanisms by which patient *MPC1* C289T and T236A mutations inactivate the MPC complex [9]. *MPC1* C289T encodes a mis-spliced, truncated protein that is nonfunctional and a full-length R97W point mutant that is less stable but can form pyruvate transport-competent complexes with MPC2. Adding *MPC1* C289T to *Mpc1* knockout mouse C2C12 cells led to no detectable mis-spliced, truncated MPC1 protein and, compared to wild-type MPC1, decreased levels of MPC1 R97W. The other patient mutation investigated, *MPC1* T236A, encodes a full-length L79H point mutant that produces a stable MPC complex with protein levels similar to wild-type MPC complexes. However, MPC complexes with MPC1 L79H are not able to transport pyruvate. The patient with the MPC1 R97W mutation died at 19 months, while three patients with the MPC1 L79H mutation exhibited varying degrees of neurological and cognitive deficits. Notably, mouse studies indicate that alterations in maternal diet may be able to partially compensate for offspring MPC deficiencies in utero. For example, a ketogenic diet [12] or maternal fasting [15], which shifts metabolic substrate use from glucose and thus pyruvate to greater

use of either fatty acids or ketones, attenuates some defects in pyruvate metabolism, such as lactic acidosis, in mice with *Mpc1*-mutated fetuses. A ketogenic diet also rescues many of the developmental defects observed in utero. These studies illustrate the importance of the MPC in embryonic and fetal development and suggest a potential non-pharmacological, diet intervention for MPC insufficiency and other inborn errors in pyruvate metabolism in utero.

3.2. Stem Cells

Proper stem cell function and growth are essential for embryonic, fetal, and postnatal development. In adults, although stem cell activity progressively decreases across the lifespan, stem cells remain important for regeneration and repair of many tissues [16,17]. Whether in embryonic or adult tissues, stem cells exist in an undifferentiated, quiescent state until an activating event (such as implantation in the uterus or stress/injury in the adult) induces a transition to proliferation. Growth is initiated and maintained by increased glycolysis, which supports nucleotide, protein, and lipid synthesis. As stem cells differentiate into specific cell types, their metabolism shifts toward oxidative phosphorylation (OXPHOS) [18]. These metabolic shifts supporting pluripotency or differentiation are controlled by MPC activity and pyruvate utilization. For example, in *Drosophila* intestinal epithelial cells, MPC loss-of-function increases stem cell proliferation, while overexpression of the MPC in epithelial cells suppresses stem cell proliferation [19,20]. Similarly, *MPC1* deletion in intestinal stem cells promotes proliferation [20], while deletion in hair follicle stem cells increases lactate-driven acceleration of the hair cycle [21]. These studies suggest that increased glycolysis due to MPC loss in epithelial or stem cells supports stem cell expansion and prevents differentiation.

Stem cells also play an important role in cancer progression and resistance to drug treatment (see Cancer section). Many cancers exhibit partial to complete loss of MPC expression that is associated with increased cell proliferation, metastasis, and stem cell marker expression [22]. MPC1 is necessary for intestinal stem cell differentiation in zebrafish, and loss of the tumor suppressor Adenomatous Polyposis Coli (APC) downregulates MPC expression to favor stem cell growth over differentiation [23]. Overall, these studies indicate that MPC activity mediates metabolic programming to promote pluripotency or differentiation during embryonic development, adult tissue repair, and tumor growth.

4. The MPC in Post-development Health and Disease

4.1. Cancer

Cancer is a disease that is characterized by abnormal cellular growth and invasion into surrounding tissues. Cancer can occur throughout the human lifespan, but prevalence increases with age and most patients receiving the diagnosis are older than 60. Similar to stem cells, many cancers support growth demands by upregulating glycolysis and channeling glycolytic intermediates into biosynthetic and reducing power-generating pathways [24]. Loss of the MPC initiates or promotes aerobic glycolysis, and in a variety of cancers, MPC disruption correlates with increased growth, metastasis, and poor survival. Nevertheless, some cancers exhibit increased MPC expression and predominantly rely on oxidative phosphorylation to support growth. This difference could be due to the metabolism of surrounding tumor tissue, tissue type, the oxygenation and blood supply of the tumor microenvironment, and the accessibility of immune cells, all of which affect the energy metabolism of a tumor and can determine whether the MPC is a mediator of pro- or anti-cancer effects.

4.1.1. MPC Disruption Promotes Cancer Progression

A wealth of recent studies show that the loss of MPC activity or expression promotes cancer cell progression in diverse tissues (Table 1). In colon cancer cell lines, knockdown of *MPC1* or *MPC2* promotes loss of cell–cell polarity, increases migration capacity, and drives resistance to radiation therapy [25]. In colon cancer cell lines with low MPC protein levels, ectopic expression of the MPC impairs colony formation in soft agar, decreases xenograft growth in mice, and reduces stem cell marker

expression [22]. These studies, although mostly performed in cell culture, suggest that MPC disruption in colon cancer increases growth by inducing aerobic glycolysis. Downregulation of the MPC may also promote colon cancer survival by decreasing production of reactive oxygen species (ROS), making tumor cells less prone to apoptosis by interferon- γ , an important anti-tumor cytokine [26]. Induction of the epithelial–mesenchymal transition (EMT) is associated with MPC loss and increased glutamine metabolism and may mediate increased migration capacity and metastasis. The increase in stemness associated with MPC loss, noted by Schell et al., may explain the increased resistance to radiation therapy, since stem cells are able to self-renew indefinitely [27]. Although the mechanisms by which the MPC controls cancer cell stemness are not fully understood, a noted possibility is by modulating epigenetic programming. The MPC may drive stemness through decreased cytoplasmic acetyl-CoA production dependent on and downstream from mitochondrial pyruvate uptake, resulting in less histone acetylation and preventing differentiation [20].

Another possible explanation for increased stem cell marker expression in colon cancer is that MPC loss in a stem-like cancer cell may drive expansion of the stem-like cell compartment and facilitate a shift in tumor metabolism from an OXPHOS state toward a glycolytic state (Figure 1). Although stem-like cancer cells normally make up approximately 1 to 3% of tumor cells, MPC loss may increase stem-like cell proliferation, resulting in glycolytic, stem-like cells comprising a greater fraction of the tumor. Thus, whether MPC loss occurs in a stem-like cell or differentiated cell may shape the tumor's metabolic status and whether the tumor's growth is enhanced or inhibited in MPC disruption studies. This paradigm illustrates how decreased MPC function in tumors may promote growth and invasion into adjacent tissue. However, a recent study suggests that MPC loss precedes and facilitates tumor formation in colon cancer [28]. In this study, using chemical and genetic colon cancer mouse models, *Mpc1* deletion in intestinal stem cells increased tumor formation and produced higher-grade tumors than *Mpc1*-positive stem cells. Conversely, in a *Drosophila* hyperproliferation model, overexpression of *Mpc1* in intestinal stem cells was sufficient to prevent tumor formation. Taken together, these studies [22,28] suggest that MPC loss in intestinal stem cells supports a glycolytic phenotype that enables tumorigenesis, and MPC loss in stem-like colon cancer cells supports increased glycolysis that drives tumor stemness and growth.

As with colon cancer, in prostate cancer cell lines, *MPC1* knockout or chemical inhibition increases invasiveness, chemotherapy resistance, and stem cell marker expression [29,30]. Increased *MPC1* or *MPC2* expression in prostate cancer patients predicts more favorable outcomes [31]. Conversely, downregulation of *MPC1* expression by chicken ovalbumin upstream promoter-transcription factor II (*COUP-TFII*) leads to increased invasiveness and prostate cancer cell growth in culture [32]. In prostate cancer patients, low *MPC1* and high *COUP-TFII* expression were associated with metastasis [32]. However, in this study, knockdown and overexpression of *MPC1* had no effect on the protein expression of *MPC2*. Given that *MPC1* is needed to form fully stable MPC complexes, this is surprising and may warrant further investigation to determine if the MPC is uniquely regulated in the systems utilized in this study.

In brain cancer, patient data from The Cancer Genome Atlas (TCGA) show that low *MPC1* expression in glioblastoma correlates with worse patient survival and resistance to chemotherapy [33]. Similarly, a TCGA analysis of isocitrate dehydrogenase (IDH)-mutant gliomas associates increased *MPC1* expression with overall survival [34]. Increased *MPC1* expression via *COUP-TFII* inhibition slows growth of human glioblastoma cell lines and decreases tumor volume in xenograft studies with immune-deficient mice [35]. Although these studies suggest that MPC disruption in glioblastoma exacerbates tumor aggressiveness, studies of MPC inhibition or knockout in glioblastoma mouse models would strengthen these findings. Interestingly, in human glioblastoma patients undergoing tumor resection and in an orthotopic mouse model of human glioblastoma, ^{13}C glucose tracing reveals an increase in pyruvate oxidation and glucose-derived glutamine compared to normal adjacent tissue, consistent with enhanced MPC activity [36,37]. There is also clinical evidence that a ketogenic diet may increase progression-free and overall survival for glioblastoma patients by reducing glucose availability for tumors [38]. These clinical studies [36–38] suggest that glioblastoma tumors exhibit increased

pyruvate metabolism *in vivo*, which is difficult to resolve with the low levels of MPC expression observed in TCGA, cell culture, and xenograft studies [33–35]. Overall, more *in vivo* studies testing the direct contribution of the MPC to glioblastoma progression are needed to understand the role of pyruvate oxidation in brain cancer.

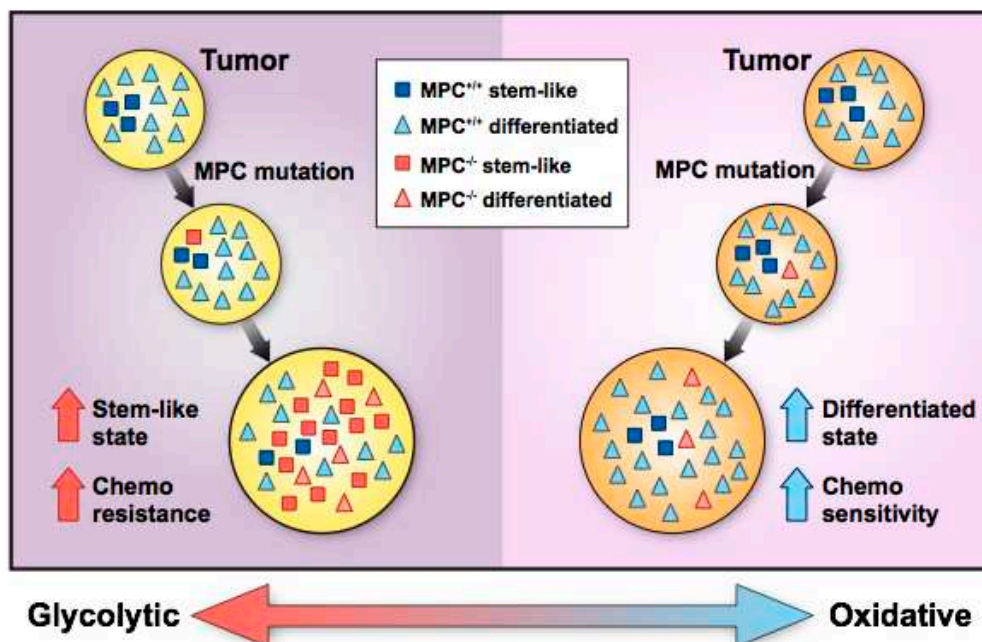


Figure 1. Hypothetical paradigm for the development of mitochondrial pyruvate carrier (MPC)-positive and -negative cancers. Left panel: Lack of MPC expression in stem-like cancer cells increases glycolysis and promotes proliferation, which contributes to tumor initiation and progression. Increased proliferation of MPC-deficient cells leads to a tumor enriched in glycolytic, stem-like cells that convey chemoresistance and invasiveness. Right panel: Sporadic loss of MPC expression in more differentiated, oxidative tumor cells promotes glycolysis but does not accelerate, or even impairs, cell proliferation. The tumor remains mostly oxidative with retained MPC expression, decreased invasiveness, and chemosensitivity.

In kidney cancer, protein and mRNA levels for *MPC1* and *MPC2* are lower in advanced renal cell carcinoma (RCC) tumors compared to normal adjacent tissue [39], and decreased *MPC1* expression in RCC correlates with worse survival outcomes [40]. *MPC1* knockdown and chemical MPC inhibition in RCC cell lines increase migration and invasion, while RCC xenograft tumors with *MPC1* knockdown grow more rapidly than xenograft tumors from RCC cells that were transfected with a scrambled short-hairpin RNA [40]. In esophageal cancer, MPC chemical inhibition increases invasiveness and resistance to chemo/radiotherapy [41]. This same study also found that decreased *MPC1* expression in esophageal squamous cell cancer correlates with worse patient prognosis.

Lastly, in lung cancer, low *MPC1* expression in lung adenocarcinoma patient samples correlates with worse prognosis [42]. Functional experiments from the same study show that *MPC1* knockdown increases the volume of lung adenocarcinoma tumorspheres and stem cell marker expression. Similar to experiments in glioblastoma patients, ^{13}C glucose tracing in non-small cell lung cancer patients (including adenocarcinoma) reveals increased glycolysis and pyruvate oxidation in tumor tissue [43]. Lactate production is also increased, consistent with the idea that circulating lactate may supply tumors with a source of pyruvate for the TCA cycle [44]. Lactate-derived, cytosolic pyruvate requires the MPC to enter the mitochondrial matrix; however, there is evidence that lactate may directly enter the mitochondrial matrix in cultured lung cancer cells, bypassing the MPC [45]. These studies highlight the complexity of elucidating the MPC's role in lung cancer and raise the possibility of other gatekeepers of pyruvate metabolism, such as a potential inner mitochondrial membrane lactate transporter [45–48].

Table 1. The MPC in various disease models.

Disease and Tissue Affected	MPC in Disease Model (MPC Knockout/Knockdown = KO/KD, MPC Re-Expression/Overexpression = O, Xenograft = X, Drug Inhibition of MPC = D, MPC Expression Correlates with Patient Survival = S, MPC Expression/Protein Correlates with Disease = C, MPC Regulation = \$-\$\$\$\$)				MPC Disruption Ameliorates (+) or Exacerbates (-) Disease	Reference
	Cell Culture	Animal	Patient Database	Patient Samples		
Cancer						
Colon	KD				-	[25]
	O, D	X	S		-	[22]
	O				-	[26]
Prostate	KO				-	[29]
	D				-	[30]
				C, S	-	[31]
	KD, O		S		-	[32]
	KO, D	X	S	C	+	[49]
Ovarian	D				-	[29]
Brain			S		-	[33]
			S		-	[34]
	\$				-	[35]
Kidney	D, KO			C	-	[39]
	KD, O, D	X	S	C, S	-	[40]
Esophageal	D			C, S	-	[41]
Lung	O, KD, D	X	S	C	-	[42]
Liver p53 null (?) p53 wild-type	KO, D	KO			+	[50]
	\$\$, D				-	[51]
Breast	D				+	[52]
	\$\$\$, O				+	[53]
Gallbladder	\$\$\$\$\$				+	[54]
Cervical	D	X, D			+	[55]
Pharynx	KD, D				+	[55]
Diabetes-related Diseases						
Skeletal muscle	KD, D				+	[56]
	D*	KO			+	[57]
Liver	KD, O, D	D			+	[58]
	D	KO			+	[59]
	KO, D	KO			+	[60]
	KO, D	KO			+	[61]
	O, D	D			+	[62]
	KO, D	KO			+	[50]
	KO, D	KO, D			+	[63]
	KO, D	KO, D			+	[64]
Whole-body		KO (het)			+	[65]
		KO			-	[66]
		(het)				
Kidney	KD, D				-	[67]
		D		C	-	[68]
				C	-	[69]
Pancreas	KO	KO			-	[70]
		KO			-	[11]
	KD, D	D			-	[71]
Heart		\$\$\$\$			-	[72]

Table 1. Cont.

Disease and Tissue Affected	MPC in Disease Model (MPC Knockout/Knockdown = KO/KD, MPC Re-Expression/Overexpression = O, Xenograft = X, Drug Inhibition of MPC = D, MPC Expression Correlates with Patient Survival = S, MPC Expression/Protein Correlates with Disease = C, MPC Regulation = \$-\$\$\$\$)				MPC Disruption Ameliorates (+) or Exacerbates (-) Disease	Reference
	Cell Culture	Animal	Patient Database	Patient Samples		
Neurodegenerative Diseases						
Alzheimer's	D				+	[73]
	D				-	[74]
	D, O				-	[75]
Parkinson's	D	D			+	[76]
Schizophrenia			S		-	[77]
			S		+	[78]

* Ex vivo permeabilized muscle; \$ MPC expression correlates with chicken ovalbumin upstream promoter-transcription factor II (COUP-TFII); \$\$ MPC proteins interact with PUMA; \$\$\$ MPC expression correlates with estrogen-related receptor alpha (ERR α); \$\$\$\$ MPC activity correlates with hyperacetylation; \$\$\$\$\$ MPC expression correlates with peroxisome proliferator-activated receptor-gamma coactivator 1-alpha (PGC-1 α).

Overall, these studies provide human epidemiological data that associate decreased MPC expression with worse patient prognosis and animal/ cell culture data that suggest MPC loss supports aerobic glycolysis, cancer cell proliferation, and metastasis. In MPC-deficient lung, colon, and prostate cancers, an increase in stem cell markers suggests that MPC loss may increase resistance to chemo/radiation therapy and expand the stem cell compartment to shift tumor metabolism toward a growth-promoting, glycolytic state.

4.1.2. MPC Disruption Inhibits Cancer Progression

Although MPC loss often promotes cancer progression, cancers that rely on mitochondrial pyruvate utilization to maintain growth or spare glutamine for glutathione production are negatively impacted by MPC disruption (Table 1). For example, although MPC inhibition drives cancer progression in most studies of prostate cancer, MPC deletion in models of androgen receptor-driven prostate cancer abolishes cell growth and is rescued by pyruvate supplementation [49]. This is likely because androgens mediate MPC expression and increase pyruvate oxidation and lipogenesis in androgen-receptor-positive prostate cancer. Androgen receptor signaling appears to be a primary driver of prostate cancer progression, with the majority of prostate cancer deaths occurring from androgen-receptor-positive, castrate-resistant prostate cancer, making the MPC an attractive therapeutic target for this prostate cancer subtype.

In liver cancer, the MPC's role may depend on tumor genetics. Tompkins et al. show that liver-specific *Mpc1* knockout in mice impairs chemically induced hepatocellular tumorigenesis by diverting glutamine into the TCA cycle and away from glutathione synthesis [50]. This pro-tumorigenic role for the MPC is consistent with TCGA data showing hepatocellular carcinomas (HCCs) (and prostate cancers) to be the highest MPC-expressing human cancers, with MPC downregulation being a rare event [50]. Conversely, Kim et al. report that protein interactions between PUMA, a p53-controlled mitochondrial protein, and the MPC complex disrupted MPC function in human HCC cell lines and promoted tumorigenesis [51]. The apparent discrepant findings between these two studies might be explained by the p53 mutation status of the HCC models. All HCC studies in the work by Kim et al. contain wild-type p53, since p53 mediates PUMA and therefore MPC function. Conversely, because the chemical model utilized by Tompkins et al. induces random genetic mutations to recapitulate the genetic heterogeneity of human HCC, it may involve mutated p53.

In breast cancer, several studies show that chemical or estrogen-related receptor alpha (ERR α)-mediated disruption of the MPC inhibits proliferation in cell lines [52,53]. In gall bladder cancer, increased *MPC1* expression due to overexpression of peroxisome proliferator-activated receptor-gamma

coactivator 1-alpha (PGC-1 α) promotes metastasis in vitro and in vivo, which may increase OXPHOS and reverse the Warburg effect [54]. Lastly, in cervical cancer, chemical inhibition of the MPC decreases growth of the SiHa cervical cancer cell line [55].

Overall, these studies highlight the importance of tissue type and suggest that metabolic wiring of breast, gallbladder, and cervical cancers differs intrinsically from that of colon, brain, lung, esophageal, and kidney cancer. The requirement for certain hormone and growth factor receptors may also play a role in determining the importance of MPC expression in tumors. Thus far, the idea that MPC disruption downregulates cancer metabolism and impairs tumorigenesis has two limitations: first, only a small number of studies have investigated the role of the MPC in breast, gallbladder, and cervical cancer; second, several studies focused on overexpression or inhibition of transcription factors that likely have effects other than altered MPC expression. Overall, cancers that appear to rely on OXPHOS to maintain growth or spare glutamine for glutathione production are adversely affected by MPC disruption. Other tissue-specific factors that support the MPC's role as a pro-cancer mediator are the presence of androgen receptors in prostate cancer and the potential for mutant p53 in liver cancer.

4.2. Pathology Associated with Immune Cell Function

The role of the MPC in immune cell dysfunction is a new area of research for the MPC field. Similar to many cancer cells, T cells increase aerobic glycolysis during activation and expansion to support the metabolic demands of rapid proliferation and cytokine production [79–81]. Aging-associated inflammation and immune dysfunction are thought to be a consequence of inappropriate T cell expansion. In support of this idea, *Mpc1* deletion in T cells increases the pool of activated T cells in aging mice [82]. *Mpc1* deletion in hematopoiesis also leads to a larger proportion of activated T cells, increasing the probability of autoimmune encephalitis in mice [83]. However, *Mpc2* deletion in long-lived plasma cells increases cell death and loss of vaccine-specific antibodies [84]. The importance of pyruvate-dependent respiration in long-lived plasma cells may be because long-lived plasma cells survive for years after infection or vaccination in the bone marrow, whereas activated T cells and short-lived plasma cells undergo apoptosis after a couple of days [85–88]. Therefore, MPC expression in immune cells may depend on their need to rapidly expand in response to infection or to live in a prolonged, quiescent state across the human lifespan.

4.3. Pathology Associated with Retinal and Visual Function

The retina is an essential component of the human eye, consisting of multiple layers of neuronal and light-sensitive tissue that relay visual images to the brain through electrical signaling. These tissue layers exhibit metabolic synergy in numerous ways. For example, the rods and cones of the photoreceptor layer perform aerobic glycolysis and provide the adjacent retinal pigment epithelium (RPE) with lactate [89,90], and the RPE synthesizes amino acids, such as glutamine and glutamate, to support photoreceptor metabolism and function [91]. Interestingly, although retinal pyruvate oxidation is minimal [89,90], the MPC appears to be essential for photoreceptor integrity and visual function [92]. Retinal-specific *Mpc1* knockout leads to photoreceptor degeneration, potentially by limiting TCA-cycle-derived acetyl-CoA and non-essential amino acids needed for daily biosynthesis of rod outer segments [92]. This study also suggests that high levels of glutamine-derived aspartate may contribute to the progressive decline of visual function in *Mpc1* knockout mice by depleting photoreceptors of glutamate, which is required for synaptic transmission. This finding corroborates a previous study showing that zaprinast, a lead but failed compound in sildenafil (Viagra) development, is a potent MPC inhibitor that induces retinal aspartate accumulation at the expense of glutamate [93]. Overall, the MPC appears to be an integral mediator of retinal structure and visual function. However, given the differential metabolism of retinal layers and the potential confounding effects of constitutive MPC knockout on retinal development, more work remains to understand the MPC's global role in the retina.

4.4. Diabetes

Diabetes mellitus is a metabolic disease that is categorized into type 1 diabetes (T1D) and type 2 diabetes (T2D). T1D onset usually occurs in childhood as a result of autoantibodies that destroy pancreatic beta cells and thus the ability to produce insulin. T2D affects children and adults, although it most commonly manifests during middle age. T2D is characterized by obesity, insulin resistance, and hyperinsulinemia, which result in decreased tissue glucose uptake and increased hepatic gluconeogenesis. Together, these factors drive chronically elevated blood glucose (hyperglycemia). Hyperglycemia is particularly detrimental to nervous tissue and vasculature. T2D patients can exhibit peripheral nerve damage, chronic kidney disease, glaucoma, and vision problems and have increased risk of stroke and hypertension. Whether the MPC ameliorates or contributes to T2D pathology predominantly depends on the tissue in question. Liver and skeletal muscle MPC disruptions improve aspects of T2D pathology, such as hyperglycemia, hepatic inflammation, and obesity. Conversely, in pancreatic beta cells, MPC loss impairs glucose-stimulated insulin secretion and worsens T2D. MPC disruption in the heart and kidney may exacerbate diabetes-mediated damage, although studies are limited in number and the mechanisms are less clear.

4.4.1. MPC Disruption Improves Glycemia and Attenuates Diabetes-Related Pathology

MPC loss or inhibition in skeletal muscle and liver improves T2D pathology. Human myocytes acutely increase glucose uptake after treatment with thiazolidinediones (TZD), a class of drugs that augments peroxisome proliferator-activated receptor gamma (PPAR- γ) activity and acutely inhibits the MPC in biochemical and cell-based assays [56]. Similarly, *Mpc1* knockout in skeletal muscle increases glucose uptake, fat oxidation, and whole-body insulin sensitivity while preserving lean mass during recovery from obesity (Figure 2) [57]. In these studies, MPC disruption causes pyruvate to accumulate in the cytosol, where it is converted to lactate and exported from myocytes [56,57]. It is possible that increased alanine is also excreted; however, this has not been experimentally validated. *In vivo*, lactate is taken up by the liver for gluconeogenesis. Because gluconeogenesis requires more ATP than glycolysis produces, fat oxidation is increased to provide reducing equivalents for net ATP synthesis [57]. Loss of body fat improves insulin sensitivity and promotes glucose uptake by muscle. Consequently, this may explain the whole-body leanness and lower blood glucose levels observed in skeletal muscle *Mpc1*-knockout mouse studies.

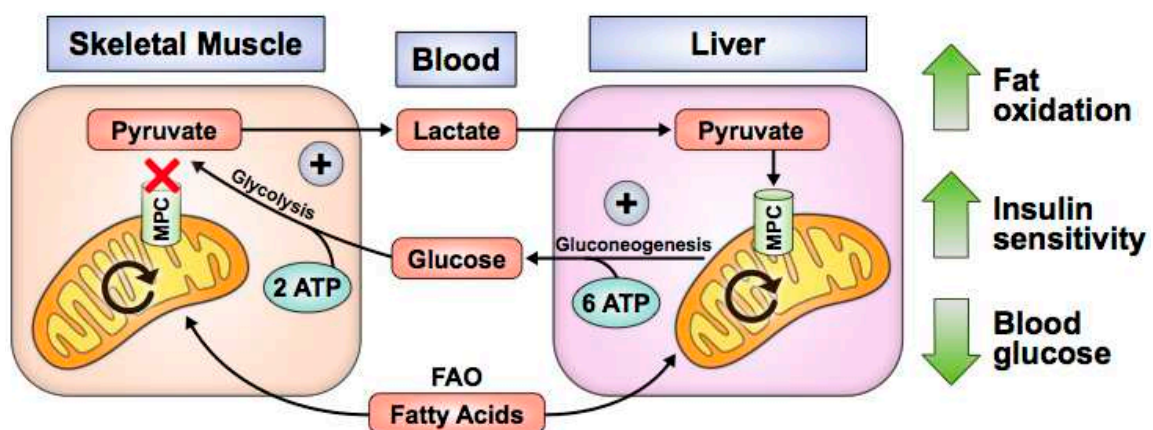


Figure 2. Skeletal muscle MPC disruption increases glucose uptake, fat oxidation, and insulin sensitivity. Fatty acid oxidation (FAO) provides ATP for energetically futile Cori Cycling.

In the liver, *Mpc1* or *Mpc2* knockout decreases hepatic gluconeogenesis and attenuates hyperglycemia in high-fat-diet-induced or leptin-receptor-deficient (*db/db*) mice without causing hypoglycemia in lean, normal chow-fed mice (Figure 3) [58–61]. These studies demonstrate that liver MPC disruption inhibits pyruvate transport into hepatocyte mitochondria and disrupts gluconeogenesis,

likely by impairing pyruvate metabolism to oxaloacetate by pyruvate carboxylase, a key initial step in gluconeogenesis. The drug berberine also decreases hepatic gluconeogenesis in high-fat-diet-induced mice and correlates with decreased MPC protein via sirtuin 3 (SIRT3) deacetylation [62]. Genetic liver MPC disruption in mice also attenuates liver fibrosis and inflammation, which are hallmarks of nonalcoholic fatty liver disease (NAFLD) and nonalcoholic steatohepatitis (NASH) [59,64]. *Mpc1* knockout in hepatocytes improves NAFLD [50], while MPC inhibition with pioglitazone (a TZD), MSCD-0602 (a PPAR- γ -sparing, TZD-like molecule) or liver *Mpc2* deletion correlates with improved NASH [63,64]. MPC disruption may improve NASH/NAFLD phenotypes by decreasing the amount of pyruvate that is metabolized to acetyl-CoA, an essential substrate for de novo lipogenesis, and/or by decreasing mitochondrial ROS production, which is associated with reduced hepatic inflammation [59]. Notably, NAFLD and NASH have been shown to involve excessive TCA cycle flux, which degrades control of mitochondrial oxidative capacity [94]. Blocking pyruvate entry into the mitochondria likely helps to ease this flow of carbon, which has been shown with liver *Mpc1* deletion in NAFLD [59] and with TZD treatment in NASH [95].

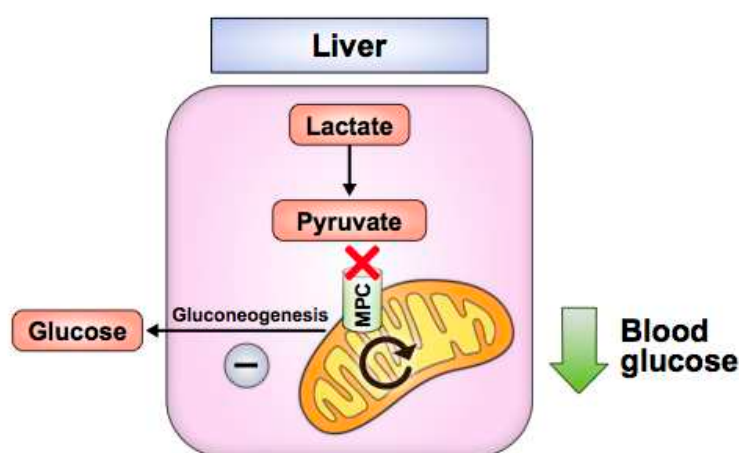


Figure 3. Liver MPC disruption attenuates hyperglycemia by impairing gluconeogenic pyruvate flux.

Pharmacologic inhibition of the MPC may be useful for treating T2D, NAFLD, and NASH. MSDC-0602, a PPAR- γ -sparing, TZD-like molecule that directly inhibits the MPC, may reduce hepatic gluconeogenesis in vivo similar to genetic MPC disruption by obstructing access of pyruvate to pyruvate carboxylase for metabolism to the gluconeogenic precursor, oxaloacetate [60]. In a phase IIb clinical trial, T2D patients receiving another PPAR- γ -sparing, TZD-like molecule with MPC-inhibiting activity, MSDC-0160, showed decreased glycated hemoglobin (HbA1c) compared to placebo after 12 weeks [96]. A more recent phase IIb trial showed that MSDC-0602K decreases blood glucose, glycated hemoglobin, insulin, liver enzymes, and NAFLD activity scores compared to placebo [97]. However, since trace but biologically relevant residual PPAR- γ agonism of these TZD-like molecules is challenging to account for in vivo, improvements in diabetes parameters and NASH cannot yet be fully attributed to MPC inhibition.

Although most of the literature provides evidence that T2D symptoms improve with MPC loss in skeletal muscle and liver, there are a few studies that report opposing changes associated with MPC alterations or studies that have utilized mice heterozygous for either full-body *Mpc1* or *Mpc2* deletion. While the nature of these studies makes results more difficult to interpret, they are mentioned here for the sake of completeness. In striated muscle, inactivation of E4 transcription factor 1 (E4F1), a regulator of several pyruvate oxidation genes, decreases *MPC1* expression and pyruvate dehydrogenase (PDH) activity and correlates with lactic acidemia and endurance defects [98]. However, these effects abated with chemical stimulation of pyruvate dehydrogenase, suggesting that the phenotype was driven predominantly by changes in PDH activity and not the MPC. In another study, after 14 weeks of calorie-restricting middle-aged mice, skeletal muscle MPC content increased and age-related muscle

loss decreased [99]. However, calorie restriction alters metabolic programming other than the MPC, muddying interpretations for the role of the MPC in this study. In heterozygous *Mpc1* knockout models, female mice were reported to exhibit decreased fertility and increased body weight [66], which contrasts with a study by Zou et al. where male mice had decreased body weight [65]. Whether these studies reflect generalizable sex-specific effects of partial MPC disruption or idiosyncrasies of the individual mouse lines used remains to be determined.

4.4.2. MPC Disruption Exacerbates Diabetes-Related Pathology

Decreased pyruvate utilization due to MPC loss may worsen T2D pathology in pancreatic beta cells, kidney, and heart. Islet or beta cell *Mpc2* knockout mice and *Mpc1* knockout in *Drosophila* resulted in impaired glucose-stimulated insulin secretion and elevated glycemia when challenged with a glucose bolus [70]. Similarly, N-terminally truncated, hypomorphic *Mpc2* protein expression due to a global *Mpc2* mutation decreased glucose-stimulated insulin release in mice [11]. *MPC1* and *MPC2* silencing via siRNAs in beta cell lines and rat and human islets also decreased glucose-stimulated insulin secretion [71]. These studies indicate that MPC disruption in pancreatic beta cells impairs glucose-stimulated insulin release. Interestingly, in the absence of a high glucose challenge, these animal models did not display overt diabetes or develop insulin resistance [70]. Overall, these studies fit a straightforward model of how pancreatic beta cells sense glucose, in part through mitochondrial pyruvate oxidation, to determine appropriate levels of insulin secretion (Figure 4).

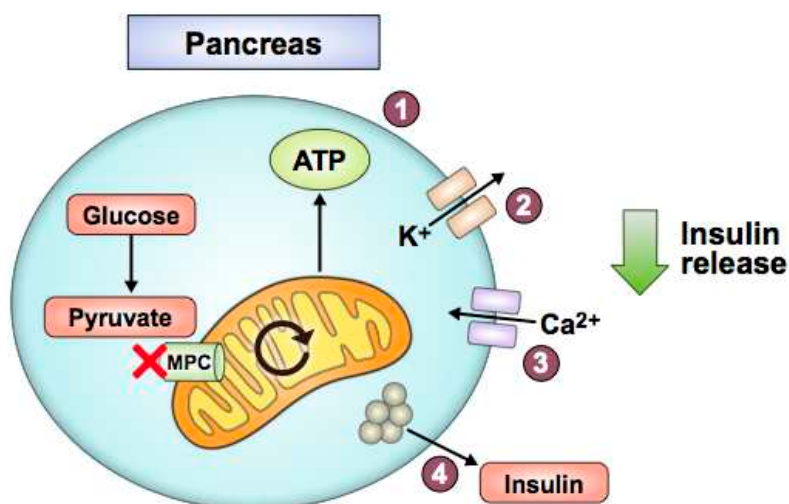


Figure 4. Pancreatic beta cell MPC disruption impairs glucose-stimulated insulin secretion. With decreased pyruvate-fueled mitochondrial ATP production (1), potassium-ATP channels stay open longer (2), and the cell does not depolarize as easily. Consequently, calcium influx is reduced (3), and insulin release does not occur as readily (4).

In a high-glucose cell culture model designed to mimic T2D hyperglycemia, MPC chemical inhibition and siRNA knockdown of *MPC2* in podocytes induced mitochondrial damage and increased apoptosis [67]. Alternatively, the drug artemether protected against diabetic kidney disease in a T2D (*db/db*) mouse model and was associated with increased MPC content [68]. Renal tubule *MPC1* and *MPC2* protein expression were significantly lower in diabetic nephropathy patients compared to patients with non-diabetic kidney disease [69]. These studies raise the possibility that decreased MPC expression contributes to worsened pathology in the diabetic kidney. However, the first study was performed in a cell culture model, potentially limiting its applicability to in vivo processes, the second study uses a drug that has physiological effects other than increased MPC content, and the third study is also correlational. In the heart, decreased MPC activity via acetylation of *Mpc2* lysine 19 and 26 in Akita T1D mice correlates with diabetic cardiomyopathy [72]. However, this is only one associative

study in a T1D model. Further in vivo studies that assess the effects of kidney and heart MPC knockout on diabetes pathology are needed before more definitive conclusions can be made.

4.5. Neurodegenerative Diseases

Neurodegenerative diseases such as Parkinson's disease (PD) and Alzheimer's disease (AD) involve progressive neuronal dysfunction and death and predominantly affect adults near the end of the human lifespan. PD is characterized by the degeneration of dopamine-producing neurons in the substantia nigra region of the brain, resulting in gradual loss of motor function and eventually aspects of cognitive function. AD is characterized by intracellular tau protein aggregation and extracellular beta-amyloid protein aggregation in the cortical regions of the brain, resulting in the decline of executive cognitive functions, social functions, and ultimately death. Early findings suggest the role of the MPC in these diseases can be protective or pathogenic depending on the disease and the model utilized.

4.5.1. MPC Disruption is Protective in Neurodegenerative Disease

Several studies indicate that reduced mitochondrial pyruvate utilization is protective in Parkinson's and Alzheimer's disease. Chemical inhibition of the MPC in a chemically induced PD mouse model increased survival of substantia nigra dopaminergic neurons and augmented striatal dopamine production [76]. This same study also used a genetic PD mouse model and concluded that MPC inhibition with MSDC-0160 decreased neuroinflammation and improved motor function. Although MSDC-0160 is a TZD-like molecule that is thought to have PPAR- γ -sparing effects, it is possible that weak PPAR- γ activity could have contributed to the decreases in neuroinflammation. Chemical inhibition of the MPC in cultured neurons reduced neuronal death from glutamate-induced excitotoxicity, a phenotype that is associated with AD [73]. By decreasing mitochondrial pyruvate utilization, mitochondrial glutamate oxidation is adaptively increased to sustain TCA cycle activity, decreasing the amount of glutamate available for synaptic release.

4.5.2. MPC Disruption Contributes to or does not Affect Neurodegenerative or Psychiatric Disease

There are also studies showing that MPC disruption may worsen pathology in schizophrenia and Alzheimer's disease. An intronic *MPC2* mutation was positively and significantly correlated with schizophrenia in East Asian populations [77]; however, an earlier genome-wide association study (GWAS) study of the same single nucleotide polymorphism (SNP) did not find a significant association [78], possibly due to differences in biostatistical methodology. In an in vitro excitotoxicity model that may inform AD, chemical inhibition of the MPC eliminated the neuroprotective effect of lactate supplementation on glutamate-induced excitotoxicity [74]. These findings differ with the study from Divakaruni et al., in which chemical inhibition of the MPC preserved neuronal viability during glutamate-induced excitotoxicity. Both studies used the same MPC inhibitor, UK5099, and the same concentration of glutamate in culture. However, a key difference is that Jourdain et al. assessed cell viability 2.5 h after treatment with 1 μ M UK5099, whereas Divakaruni et al. assessed viability 24 h after treatment with 10 μ M UK5099. The differences in cell culture models may also explain the opposing study findings. Divakaruni et al.'s model included a complete media with non-glucose substrates, which would enable a metabolic switch to alternative substrates to support OXPHOS after blocking the MPC. Conversely, Jourdain et al. used artificial cerebrospinal fluid supplemented with glucose as the sole carbon fuel, which did not provide cells with alternative mitochondrial fuels when the MPC was inhibited. Lastly, another study showed that decreased *MPC2* protein levels and destabilization of MPC complexes in familial AD cell models are associated with decreased ATP levels, a hallmark of AD pathology [75]. Overall, these studies suggest that MPC disruption can be neuroprotective or neuropathic depending on context. They also raise larger questions about how media composition in ex vivo assays impacts MPC disruption.

5. Regulation of MPC Expression or Activity

Recent studies in cancer and diabetes have elucidated transcription factors, protein interactions, and post-transcriptional modifications that can control MPC expression and function. Several transcription factors have been shown to regulate *MPC1/2* expression in various tissues and diseases. In cancer, upregulation of chicken ovalbumin upstream promoter-transcription factor II (COUP-TFII) transcript expression downregulates *MPC1* expression to drive cell growth and metastasis in prostate cancer and glioblastoma [32,35]. In androgen-receptor-positive prostate cancers, androgen receptor binding to the intron of the *MPC2* locus directly controls transcription of *MPC2* [49]. In renal cell carcinoma, PGC-1 α regulates *MPC1* transcription by recruiting ERR α to the ERR α response element 2 on the *MPC1* promoter [39]. Modulation of MPC expression via PGC-1 α or ERR α also occurs in cholangioma and certain breast cancers [53,54]. To facilitate hepatic gluconeogenesis during fasting, glucagon increases *MPC1* transcription through recruitment of cAMP-responsive element-binding protein (CREB) to the *MPC1* promoter in hepatocytes [58].

Certain protein interactions may also modulate MPC activity. In wild-type p53 hepatocellular carcinoma, p53 disrupts MPC activity by activating transcription of PUMA, a mitochondrial protein that binds to the MPC1 protein and inhibits the oligomerization of MPC1 and MPC2 [51]. This study also found that I κ B kinase beta (IKK β), which promotes a metabolic shift to aerobic glycolysis in many cancers [100], phosphorylates PUMA at serine residues 96 and 106 to enable PUMA binding to the MPC complex and recruits PUMA from the cytoplasm to the mitochondria.

Lastly, post-translational modifications have been identified for the MPC proteins, and several have been suggested to affect MPC activity. In a T1D mouse model, hyperacetylation of Mpc2 at lysine residues 19 and 26 was associated with decreased pyruvate transport in isolated heart mitochondria despite normal expression levels of Mpc1 and Mpc2 [72]. In the same study, a K19Q/K26Q Mpc2 mutant that was designed to structurally and functionally mimic lysine acetylation was expressed in H9C2 cells, leading to decreased pyruvate oxidation. This finding suggests that acetylation at MPC2 lysine residues 19 and 26 may reduce MPC activity in the diabetic heart. Conversely, in the presence of high glucose, sirtuin 3 (SIRT3) binds to and deacetylates MPC1 at lysine residues 45 and 46 and enhances MPC1 activity [101]. Other post-translational modifications have been proposed, but their effect on MPC activity and contribution to physiology or pathology remain unclear. Overall, the current literature suggests that MPC expression can be regulated by various transcription factors and coactivators and that protein interactions or post-translational modifications can modulate MPC activity.

6. Conclusions and Future Directions

Although endocrinology and cancer metabolism have been focal points of early MPC research, future investigations of the MPC will likely further focus on fetal and placental development, immunology, stem cell biology, and neurology as the importance of metabolic function in these processes are realized. A key issue that has yet to be addressed is how MPC regulation is coordinated during transitions from healthy to diseased states across the human lifespan. Future studies will also likely elucidate novel connections between MPC regulation and other mitochondrial transporters, revealing a flexible, dynamic network that modulates human metabolism in health and disease [102,103].

Author Contributions: J.L.B. and E.B.T. conceptualized and wrote this review. All authors have read and agreed to the published version of the manuscript.

Funding: Scholarship to produce this review was supported by National Institutes of Health (NIH) grant R01 DK104998 (E.B.T.) and NIH Medical Scientist Training Program (MSTP) grant T32 GM007337 contributing to the medical and research training of J.L.B.

Acknowledgments: The authors gratefully acknowledge David A. Bader (Duke University), Ajit S. Divakaruni (University of California Los Angeles), Kyle S. McCommis (Saint Louis University), and Peng Wei (University of Utah) for reading and providing critical comments on a draft manuscript.

Conflicts of Interest: E.B.T. has received research grant funding related to the MPC from Cirius Therapeutics and POXEL Pharma administered through the University of Iowa.

References

1. Bricker, D.K.; Taylor, E.B.; Schell, J.C.; Orsak, T.; Boutron, A.; Chen, Y.C.; Cox, J.E.; Cardon, C.M.; Van Vranken, J.G.; Dephoure, N.; et al. A mitochondrial pyruvate carrier required for pyruvate uptake in yeast, *Drosophila*, and humans. *Science* **2012**, *337*, 96–100. [CrossRef] [PubMed]
2. Herzig, S.; Raemy, E.; Montessuit, S.; Veuthey, J.L.; Zamboni, N.; Westermann, B.; Kunji, E.R.; Martinou, J.C. Identification and functional expression of the mitochondrial pyruvate carrier. *Science* **2012**, *337*, 93–96. [CrossRef] [PubMed]
3. Papa, S.; Francavilla, A.; Paradies, G.; Meduri, B. The transport of pyruvate in rat liver mitochondria. *FEBS Lett.* **1971**, *12*, 285–288. [CrossRef]
4. Halestrap, A.P.; Denton, R.M. Specific inhibition of pyruvate transport in rat liver mitochondria and human erythrocytes by alpha-cyano-4-hydroxycinnamate. *Biochem. J.* **1974**, *138*, 313–316. [CrossRef] [PubMed]
5. Halestrap, A.P. The mitochondrial pyruvate carrier. Kinetics and specificity for substrates and inhibitors. *Biochem. J.* **1975**, *148*, 85–96. [CrossRef]
6. Gray, L.R.; Tompkins, S.C.; Taylor, E.B. Regulation of pyruvate metabolism and human disease. *Cell. Mol. Life Sci.* **2014**, *71*, 2577–2604. [CrossRef]
7. Pithukpakorn, M. Disorders of pyruvate metabolism and the tricarboxylic acid cycle. *Mol. Genet. Metab.* **2005**, *85*, 243–246. [CrossRef]
8. Marin-Valencia, I.; Roe, C.R.; Pascual, J.M. Pyruvate carboxylase deficiency: Mechanisms, mimics and anaplerosis. *Mol. Genet. Metab.* **2010**, *101*, 9–17. [CrossRef]
9. Oonthonpan, L.; Rauckhorst, A.J.; Gray, L.R.; Boutron, A.C.; Taylor, E.B. Two human patient mitochondrial pyruvate carrier mutations reveal distinct molecular mechanisms of dysfunction. *JCI Insight* **2019**, *5*. [CrossRef]
10. Brivet, M.; Garcia-Cazorla, A.; Lyonnet, S.; Dumez, Y.; Nassogne, M.C.; Slama, A.; Boutron, A.; Touati, G.; Legrand, A.; Saudubray, J.M. Impaired mitochondrial pyruvate importation in a patient and a fetus at risk. *Mol. Genet. Metab.* **2003**, *78*, 186–192. [CrossRef]
11. Vigueira, P.A.; McCommis, K.S.; Schweitzer, G.G.; Remedi, M.S.; Chambers, K.T.; Fu, X.; McDonald, W.G.; Cole, S.L.; Colca, J.R.; Kletzien, R.F.; et al. Mitochondrial pyruvate carrier 2 hypomorphism in mice leads to defects in glucose-stimulated insulin secretion. *Cell Rep.* **2014**, *7*, 2042–2053. [CrossRef] [PubMed]
12. Vanderperre, B.; Herzig, S.; Krznar, P.; Horl, M.; Ammar, Z.; Montessuit, S.; Pierredon, S.; Zamboni, N.; Martinou, J.C. Embryonic Lethality of Mitochondrial Pyruvate Carrier 1 Deficient Mouse Can Be Rescued by a Ketogenic Diet. *PLoS Genet.* **2016**, *12*, e1006056. [CrossRef] [PubMed]
13. Bowman, C.E.; Zhao, L.; Hartung, T.; Wolfgang, M.J. Requirement for the Mitochondrial Pyruvate Carrier in Mammalian Development Revealed by a Hypomorphic Allelic Series. *Mol. Cell. Biol.* **2016**, *36*, 2089–2104. [CrossRef] [PubMed]
14. Xie, H.L.; Zhu, S.; Zhang, J.; Wen, J.; Yuan, H.J.; Pan, L.Z.; Luo, M.J.; Tan, J.H. Glucose metabolism during in vitro maturation of mouse oocytes: An study using RNA interference. *J. Cell. Physiol.* **2018**, *233*, 6952–6964. [CrossRef] [PubMed]
15. Bowman, C.E.; Selen Alpergin, E.S.; Cavagnini, K.; Smith, D.M.; Scafidi, S.; Wolfgang, M.J. Maternal Lipid Metabolism Directs Fetal Liver Programming following Nutrient Stress. *Cell Rep.* **2019**, *29*, 1299.e1293–1310.e1293. [CrossRef]
16. Signer, R.A.; Morrison, S.J. Mechanisms that regulate stem cell aging and life span. *Cell Stem Cell* **2013**, *12*, 152–165. [CrossRef]
17. Schultz, M.B.; Sinclair, D.A. When stem cells grow old: Phenotypes and mechanisms of stem cell aging. *Development* **2016**, *143*, 3–14. [CrossRef]
18. Tsogtbaatar, E.; Landin, C.; Minter-Dykhous, K.; Folmes, C.D.L. Energy Metabolism Regulates Stem Cell Pluripotency. *Front. Cell Dev. Biol.* **2020**, *8*, 87. [CrossRef]
19. Wisidagama, D.R.; Thummel, C.S. Regulation of *Drosophila* Intestinal Stem Cell Proliferation by Enterocyte Mitochondrial Pyruvate Metabolism. *G3 (Bethesda)* **2019**, *9*, 3623–3630. [CrossRef]
20. Schell, J.C.; Wisidagama, D.R.; Bensard, C.; Zhao, H.; Wei, P.; Tanner, J.; Flores, A.; Mohlman, J.; Sorensen, L.K.; Earl, C.S.; et al. Control of intestinal stem cell function and proliferation by mitochondrial pyruvate metabolism. *Nat. Cell Biol.* **2017**, *19*, 1027–1036. [CrossRef]

21. Flores, A.; Schell, J.; Krall, A.S.; Jelinek, D.; Miranda, M.; Grigorian, M.; Braas, D.; White, A.C.; Zhou, J.L.; Graham, N.A.; et al. Lactate dehydrogenase activity drives hair follicle stem cell activation. *Nat. Cell Biol.* **2017**, *19*, 1017–1026. [CrossRef] [PubMed]
22. Schell, J.C.; Olson, K.A.; Jiang, L.; Hawkins, A.J.; Van Vranken, J.G.; Xie, J.; Egnatchik, R.A.; Earl, E.G.; DeBerardinis, R.J.; Rutter, J. A role for the mitochondrial pyruvate carrier as a repressor of the Warburg effect and colon cancer cell growth. *Mol. Cell* **2014**, *56*, 400–413. [CrossRef] [PubMed]
23. Sandoval, I.T.; Delacruz, R.G.; Miller, B.N.; Hill, S.; Olson, K.A.; Gabriel, A.E.; Boyd, K.; Satterfield, C.; Van Remmen, H.; Rutter, J.; et al. A metabolic switch controls intestinal differentiation downstream of Adenomatous polyposis coli (APC). *Elife* **2017**, *6*. [CrossRef] [PubMed]
24. Vander Heiden, M.G.; Cantley, L.C.; Thompson, C.B. Understanding the Warburg effect: The metabolic requirements of cell proliferation. *Science* **2009**, *324*, 1029–1033. [CrossRef]
25. Takaoka, Y.; Konno, M.; Koseki, J.; Colvin, H.; Asai, A.; Tamari, K.; Satoh, T.; Mori, M.; Doki, Y.; Ogawa, K.; et al. Mitochondrial pyruvate carrier 1 expression controls cancer epithelial-mesenchymal transition and radioresistance. *Cancer Sci.* **2019**, *110*, 1331–1339. [CrossRef]
26. Tai, Y.; Cao, F.; Li, M.; Li, P.; Xu, T.; Wang, X.; Yu, Y.; Gu, B.; Yu, X.; Cai, X.; et al. Enhanced mitochondrial pyruvate transport elicits a robust ROS production to sensitize the antitumor efficacy of interferon-gamma in colon cancer. *Redox Biol.* **2019**, *20*, 451–457. [CrossRef]
27. He, S.; Nakada, D.; Morrison, S.J. Mechanisms of stem cell self-renewal. *Annu. Rev. Cell Dev. Biol.* **2009**, *25*, 377–406. [CrossRef]
28. Bensard, C.L.; Wisidagama, D.R.; Olson, K.A.; Berg, J.A.; Krah, N.M.; Schell, J.C.; Nowinski, S.M.; Fogarty, S.; Bott, A.J.; Wei, P.; et al. Regulation of Tumor Initiation by the Mitochondrial Pyruvate Carrier. *Cell Metab.* **2020**, *31*, 284.e287–300.e287. [CrossRef]
29. Li, X.; Han, G.; Li, X.; Kan, Q.; Fan, Z.; Li, Y.; Ji, Y.; Zhao, J.; Zhang, M.; Grigalavicius, M.; et al. Mitochondrial pyruvate carrier function determines cell stemness and metabolic reprogramming in cancer cells. *Oncotarget* **2017**, *8*, 46363–46380. [CrossRef]
30. Zhong, Y.; Li, X.; Yu, D.; Li, X.; Li, Y.; Long, Y.; Yuan, Y.; Ji, Z.; Zhang, M.; Wen, J.G.; et al. Application of mitochondrial pyruvate carrier blocker UK5099 creates metabolic reprogram and greater stem-like properties in LnCap prostate cancer cells in vitro. *Oncotarget* **2015**, *6*, 37758–37769. [CrossRef]
31. Li, X.; Ji, Y.; Han, G.; Li, X.; Fan, Z.; Li, Y.; Zhong, Y.; Cao, J.; Zhao, J.; Zhang, M.; et al. MPC1 and MPC2 expressions are associated with favorable clinical outcomes in prostate cancer. *BMC Cancer* **2016**, *16*, 894. [CrossRef] [PubMed]
32. Wang, L.; Xu, M.; Qin, J.; Lin, S.C.; Lee, H.J.; Tsai, S.Y.; Tsai, M.J. MPC1, a key gene in cancer metabolism, is regulated by COUPTFII in human prostate cancer. *Oncotarget* **2016**, *7*, 14673–14683. [CrossRef] [PubMed]
33. Chai, Y.; Wang, C.; Liu, W.; Fan, Y.; Zhang, Y. MPC1 deletion is associated with poor prognosis and temozolomide resistance in glioblastoma. *J. Neurooncol.* **2019**, *144*, 293–301. [CrossRef] [PubMed]
34. Karsy, M.; Guan, J.; Huang, L.E. Prognostic role of mitochondrial pyruvate carrier in isocitrate dehydrogenase-mutant glioma. *J. Neurosurg.* **2018**, *130*, 56–66. [CrossRef]
35. Xiao, B.; Fan, Y.; Ye, M.; Lv, S.; Xu, B.; Chai, Y.; Wu, M.; Zhu, X. Downregulation of COUP-TFII inhibits glioblastoma growth via targeting MPC1. *Oncol. Lett.* **2018**, *15*, 9697–9702. [CrossRef]
36. Marin-Valencia, I.; Yang, C.; Mashimo, T.; Cho, S.; Baek, H.; Yang, X.L.; Rajagopalan, K.N.; Maddie, M.; Vemireddy, V.; Zhao, Z.; et al. Analysis of tumor metabolism reveals mitochondrial glucose oxidation in genetically diverse human glioblastomas in the mouse brain in vivo. *Cell Metab.* **2012**, *15*, 827–837. [CrossRef]
37. Maher, E.A.; Marin-Valencia, I.; Bachoo, R.M.; Mashimo, T.; Raisanen, J.; Hatanpaa, K.J.; Jindal, A.; Jeffrey, F.M.; Choi, C.; Madden, C.; et al. Metabolism of [U-13 C]glucose in human brain tumors in vivo. *NMR Biomed.* **2012**, *25*, 1234–1244. [CrossRef]
38. Seyfried, T.N.; Shelton, L.; Arismendi-Morillo, G.; Kalamian, M.; Elsakka, A.; Maroon, J.; Mukherjee, P. Provocative Question: Should Ketogenic Metabolic Therapy Become the Standard of Care for Glioblastoma? *Neurochem. Res.* **2019**, *44*, 2392–2404. [CrossRef]
39. Koh, E.; Kim, Y.K.; Shin, D.; Kim, K.S. MPC1 is essential for PGC-1alpha-induced mitochondrial respiration and biogenesis. *Biochem. J.* **2018**, *475*, 1687–1699. [CrossRef]
40. Tang, X.P.; Chen, Q.; Li, Y.; Wang, Y.; Zou, H.B.; Fu, W.J.; Niu, Q.; Pan, Q.G.; Jiang, P.; Xu, X.S.; et al. Mitochondrial pyruvate carrier 1 functions as a tumor suppressor and predicts the prognosis of human renal cell carcinoma. *Lab. Investig.* **2019**, *99*, 191–199. [CrossRef]

41. Li, Y.; Li, X.; Kan, Q.; Zhang, M.; Li, X.; Xu, R.; Wang, J.; Yu, D.; Goscinski, M.A.; Wen, J.G.; et al. Mitochondrial pyruvate carrier function is negatively linked to Warburg phenotype in vitro and malignant features in esophageal squamous cell carcinomas. *Oncotarget* **2017**, *8*, 1058–1073. [CrossRef] [PubMed]
42. Zou, H.; Chen, Q.; Zhang, A.; Wang, S.; Wu, H.; Yuan, Y.; Wang, S.; Yu, J.; Luo, M.; Wen, X.; et al. MPC1 deficiency accelerates lung adenocarcinoma progression through the STAT3 pathway. *Cell Death Dis.* **2019**, *10*, 148. [CrossRef] [PubMed]
43. Hensley, C.T.; Faubert, B.; Yuan, Q.; Lev-Cohain, N.; Jin, E.; Kim, J.; Jiang, L.; Ko, B.; Skelton, R.; Loudat, L.; et al. Metabolic Heterogeneity in Human Lung Tumors. *Cell* **2016**, *164*, 681–694. [CrossRef] [PubMed]
44. Hui, S.; Ghergurovich, J.M.; Morscher, R.J.; Jang, C.; Teng, X.; Lu, W.; Esparza, L.A.; Reya, T.; Le, Z.; Yanxiang Guo, J.; et al. Glucose feeds the TCA cycle via circulating lactate. *Nature* **2017**, *551*, 115–118. [CrossRef] [PubMed]
45. Chen, Y.J.; Mahieu, N.G.; Huang, X.; Singh, M.; Crawford, P.A.; Johnson, S.L.; Gross, R.W.; Schaefer, J.; Patti, G.J. Lactate metabolism is associated with mammalian mitochondria. *Nat. Chem. Biol.* **2016**, *12*, 937–943. [CrossRef] [PubMed]
46. Valenti, D.; de Bari, L.; Atlante, A.; Passarella, S. L-Lactate transport into rat heart mitochondria and reconstruction of the L-lactate/pyruvate shuttle. *Biochem. J.* **2002**, *364*, 101–104. [CrossRef] [PubMed]
47. Passarella, S.; de Bari, L.; Valenti, D.; Pizzuto, R.; Paventi, G.; Atlante, A. Mitochondria and L-lactate metabolism. *FEBS Lett.* **2008**, *582*, 3569–3576. [CrossRef]
48. Passarella, S.; Schurr, A. L-Lactate Transport and Metabolism in Mitochondria of Hep G2 Cells-The Cori Cycle Revisited. *Front. Oncol.* **2018**, *8*, 120. [CrossRef]
49. Bader, D.A.; Hartig, S.M.; Putluri, V.; Foley, C.; Hamilton, M.P.; Smith, E.A.; Saha, P.K.; Panigrahi, A.; Walker, C.; Zong, L.; et al. Mitochondrial pyruvate import is a metabolic vulnerability in androgen receptor-driven prostate cancer. *Nat. Metab.* **2019**, *1*, 70–85. [CrossRef]
50. Tompkins, S.C.; Sheldon, R.D.; Rauckhorst, A.J.; Noterman, M.F.; Solst, S.R.; Buchanan, J.L.; Mapuskar, K.A.; Pawa, A.D.; Gray, L.R.; Oonthonpan, L.; et al. Disrupting Mitochondrial Pyruvate Uptake Directs Glutamine into the TCA Cycle away from Glutathione Synthesis and Impairs Hepatocellular Tumorigenesis. *Cell Rep.* **2019**, *28*, 2608.e2606–2619.e2606. [CrossRef]
51. Kim, J.; Yu, L.; Chen, W.; Xu, Y.; Wu, M.; Todorova, D.; Tang, Q.; Feng, B.; Jiang, L.; He, J.; et al. Wild-Type p53 Promotes Cancer Metabolic Switch by Inducing PUMA-Dependent Suppression of Oxidative Phosphorylation. *Cancer Cell* **2019**, *35*, 191.e198–203.e198. [CrossRef] [PubMed]
52. Jung, K.H.; Lee, J.H.; Park, J.W.; Moon, S.H.; Cho, Y.S.; Lee, K.H. Troglitazone exerts metabolic and antitumor effects on T47D breast cancer cells by suppressing mitochondrial pyruvate availability. *Oncol. Rep.* **2020**, *43*, 711–717. [CrossRef] [PubMed]
53. Park, S.; Safi, R.; Liu, X.; Baldi, R.; Liu, W.; Liu, J.; Locasale, J.W.; Chang, C.Y.; McDonnell, D.P. Inhibition of ERRA1 Prevents Mitochondrial Pyruvate Uptake Exposing NADPH-Generating Pathways as Targetable Vulnerabilities in Breast Cancer. *Cell Rep.* **2019**, *27*, 3587.e3584–3601.e3584. [CrossRef] [PubMed]
54. Dan, L.; Wang, C.; Ma, P.; Yu, Q.; Gu, M.; Dong, L.; Jiang, W.; Pan, S.; Xie, C.; Han, J.; et al. PGC1alpha promotes cholangiocarcinoma metastasis by upregulating PDHA1 and MPC1 expression to reverse the Warburg effect. *Cell Death Dis.* **2018**, *9*, 466. [CrossRef]
55. Corbet, C.; Bastien, E.; Draoui, N.; Doix, B.; Mignon, L.; Jordan, B.F.; Marchand, A.; Vanherck, J.C.; Chaltin, P.; Schakman, O.; et al. Interruption of lactate uptake by inhibiting mitochondrial pyruvate transport unravels direct antitumor and radiosensitizing effects. *Nat. Commun.* **2018**, *9*, 1208. [CrossRef]
56. Divakaruni, A.S.; Wiley, S.E.; Rogers, G.W.; Andreyev, A.Y.; Petrosyan, S.; Loviscach, M.; Wall, E.A.; Yadava, N.; Heuck, A.P.; Ferrick, D.A.; et al. Thiazolidinediones are acute, specific inhibitors of the mitochondrial pyruvate carrier. *Proc. Natl. Acad. Sci. USA* **2013**, *110*, 5422–5427. [CrossRef]
57. Sharma, A.; Oonthonpan, L.; Sheldon, R.D.; Rauckhorst, A.J.; Zhu, Z.; Tompkins, S.C.; Cho, K.; Grzesik, W.J.; Gray, L.R.; Scerbo, D.A.; et al. Impaired skeletal muscle mitochondrial pyruvate uptake rewires glucose metabolism to drive whole-body leanness. *Elife* **2019**, *8*. [CrossRef]
58. Lou, M.D.; Li, J.; Cheng, Y.; Xiao, N.; Ma, G.; Li, P.; Liu, B.; Liu, Q.; Qi, L.W. Glucagon up-regulates hepatic mitochondrial pyruvate carrier 1 through cAMP-responsive element-binding protein; inhibition of hepatic gluconeogenesis by ginsenoside Rb1. *Br. J. Pharmacol.* **2019**, *176*, 2962–2976. [CrossRef]

59. Rauckhorst, A.J.; Gray, L.R.; Sheldon, R.D.; Fu, X.; Pawa, A.D.; Feddersen, C.R.; Dupuy, A.J.; Gibson-Corley, K.N.; Cox, J.E.; Burgess, S.C.; et al. The mitochondrial pyruvate carrier mediates high fat diet-induced increases in hepatic TCA cycle capacity. *Mol. Metab.* **2017**, *6*, 1468–1479. [CrossRef]
60. McCommis, K.S.; Chen, Z.; Fu, X.; McDonald, W.G.; Colca, J.R.; Kletzien, R.F.; Burgess, S.C.; Finck, B.N. Loss of Mitochondrial Pyruvate Carrier 2 in the Liver Leads to Defects in Gluconeogenesis and Compensation via Pyruvate-Alanine Cycling. *Cell Metab.* **2015**, *22*, 682–694. [CrossRef]
61. Gray, L.R.; Sultana, M.R.; Rauckhorst, A.J.; Oonthonpan, L.; Tompkins, S.C.; Sharma, A.; Fu, X.; Miao, R.; Pawa, A.D.; Brown, K.S.; et al. Hepatic Mitochondrial Pyruvate Carrier 1 Is Required for Efficient Regulation of Gluconeogenesis and Whole-Body Glucose Homeostasis. *Cell Metab.* **2015**, *22*, 669–681. [CrossRef] [PubMed]
62. Li, A.; Liu, Q.; Li, Q.; Liu, B.; Yang, Y.; Zhang, N. Berberine Reduces Pyruvate-driven Hepatic Glucose Production by Limiting Mitochondrial Import of Pyruvate through Mitochondrial Pyruvate Carrier 1. *EBioMedicine* **2018**, *34*, 243–255. [CrossRef] [PubMed]
63. Vigueira, P.A.; McCommis, K.S.; Hodges, W.T.; Schweitzer, G.G.; Cole, S.L.; Oonthonpan, L.; Taylor, E.B.; McDonald, W.G.; Kletzien, R.F.; Colca, J.R.; et al. The beneficial metabolic effects of insulin sensitizers are not attenuated by mitochondrial pyruvate carrier 2 hypomorphism. *Exp. Physiol.* **2017**, *102*, 985–999. [CrossRef] [PubMed]
64. McCommis, K.S.; Hodges, W.T.; Brunt, E.M.; Nalbantoglu, I.; McDonald, W.G.; Holley, C.; Fujiwara, H.; Schaffer, J.E.; Colca, J.R.; Finck, B.N. Targeting the mitochondrial pyruvate carrier attenuates fibrosis in a mouse model of nonalcoholic steatohepatitis. *Hepatology* **2017**, *65*, 1543–1556. [CrossRef]
65. Zou, S.; Lang, T.; Zhang, B.; Huang, K.; Gong, L.; Luo, H.; Xu, W.; He, X. Fatty acid oxidation alleviates the energy deficiency caused by the loss of MPC1 in MPC1(+/-) mice. *Biochem. Biophys. Res. Commun.* **2018**, *495*, 1008–1013. [CrossRef]
66. Li, X.; Li, Y.; Han, G.; Li, X.; Ji, Y.; Fan, Z.; Zhong, Y.; Cao, J.; Zhao, J.; Mariusz, G.; et al. Establishment of mitochondrial pyruvate carrier 1 (MPC1) gene knockout mice with preliminary gene function analyses. *Oncotarget* **2016**, *7*, 79981–79994. [CrossRef]
67. Feng, J.; Ma, Y.; Chen, Z.; Hu, J.; Yang, Q.; Ding, G. Mitochondrial pyruvate carrier 2 mediates mitochondrial dysfunction and apoptosis in high glucose-treated podocytes. *Life Sci.* **2019**, *237*, 116941. [CrossRef]
68. Han, P.; Wang, Y.; Zhan, H.; Weng, W.; Yu, X.; Ge, N.; Wang, W.; Song, G.; Yi, T.; Li, S.; et al. Artemether ameliorates type 2 diabetic kidney disease by increasing mitochondrial pyruvate carrier content in db/db mice. *Am. J. Transl. Res.* **2019**, *11*, 1389–1402.
69. Zhu, H.; Wan, H.; Wu, L.; Li, Q.; Liu, S.; Duan, S.; Huang, Z.; Zhang, C.; Zhang, B.; Xing, C.; et al. Mitochondrial pyruvate carrier: A potential target for diabetic nephropathy. *BMC Nephrol.* **2020**, *21*, 274. [CrossRef]
70. McCommis, K.S.; Hodges, W.T.; Bricker, D.K.; Wisidagama, D.R.; Compan, V.; Remedi, M.S.; Thummel, C.S.; Finck, B.N. An ancestral role for the mitochondrial pyruvate carrier in glucose-stimulated insulin secretion. *Mol. Metab.* **2016**, *5*, 602–614. [CrossRef]
71. Patterson, J.N.; Cousteils, K.; Lou, J.W.; Manning Fox, J.E.; MacDonald, P.E.; Joseph, J.W. Mitochondrial metabolism of pyruvate is essential for regulating glucose-stimulated insulin secretion. *J. Biol. Chem.* **2014**, *289*, 13335–13346. [CrossRef] [PubMed]
72. Vadvalkar, S.S.; Matsuzaki, S.; Eyster, C.A.; Giorgione, J.R.; Bockus, L.B.; Kinter, C.S.; Kinter, M.; Humphries, K.M. Decreased Mitochondrial Pyruvate Transport Activity in the Diabetic Heart: ROLE OF MITOCHONDRIAL PYRUVATE CARRIER 2 (MPC2) ACETYLATION. *J. Biol. Chem.* **2017**, *292*, 4423–4433. [CrossRef] [PubMed]
73. Divakaruni, A.S.; Wallace, M.; Buren, C.; Martyniuk, K.; Andreyev, A.Y.; Li, E.; Fields, J.A.; Cordes, T.; Reynolds, I.J.; Bloodgood, B.L.; et al. Inhibition of the mitochondrial pyruvate carrier protects from excitotoxic neuronal death. *J. Cell Biol.* **2017**, *216*, 1091–1105. [CrossRef] [PubMed]
74. Jourdain, P.; Allaman, I.; Rothenfusser, K.; Fiumelli, H.; Marquet, P.; Magistretti, P.J. L-Lactate protects neurons against excitotoxicity: Implication of an ATP-mediated signaling cascade. *Sci. Rep.* **2016**, *6*, 21250. [CrossRef] [PubMed]
75. Rossi, A.; Rigotto, G.; Valente, G.; Giorgio, V.; Basso, E.; Filadi, R.; Pizzo, P. Defective Mitochondrial Pyruvate Flux Affects Cell Bioenergetics in Alzheimer’s Disease-Related Models. *Cell Rep.* **2020**, *30*, 2332.e2310–2348.e2310. [CrossRef] [PubMed]

76. Ghosh, A.; Tyson, T.; George, S.; Hildebrandt, E.N.; Steiner, J.A.; Madaj, Z.; Schulz, E.; Machiela, E.; McDonald, W.G.; Escobar Galvis, M.L.; et al. Mitochondrial pyruvate carrier regulates autophagy, inflammation, and neurodegeneration in experimental models of Parkinson's disease. *Sci. Transl. Med.* **2016**, *8*, 368ra174. [CrossRef]
77. Yang, Y.; Wang, L.; Li, L.; Li, W.; Zhang, Y.; Chang, H.; Xiao, X.; Li, M.; Lv, L. Genetic association and meta-analysis of a schizophrenia GWAS variant rs10489202 in East Asian populations. *Transl. Psychiatry* **2018**, *8*, 144. [CrossRef]
78. Jin, C.; Zhang, Y.; Wang, J.; Zhou, Z.; Sha, W.; Wang, M.; Zhang, F.; Li, J.; Li, J.; Yu, S.; et al. Lack of association between MPC2 variants and schizophrenia in a replication study of Han Chinese. *Neurosci. Lett.* **2013**, *552*, 120–123. [CrossRef]
79. Krauss, S.; Brand, M.D.; Buttgerit, F. Signaling takes a breath—new quantitative perspectives on bioenergetics and signal transduction. *Immunity* **2001**, *15*, 497–502. [CrossRef]
80. Rathmell, J.C.; Vander Heiden, M.G.; Harris, M.H.; Frauwirth, K.A.; Thompson, C.B. In the absence of extrinsic signals, nutrient utilization by lymphocytes is insufficient to maintain either cell size or viability. *Mol. Cell* **2000**, *6*, 683–692. [CrossRef]
81. Roos, D.; Loos, J.A. Changes in the carbohydrate metabolism of mitogenically stimulated human peripheral lymphocytes. II. Relative importance of glycolysis and oxidative phosphorylation on phytohaemagglutinin stimulation. *Exp. Cell Res.* **1973**, *77*, 127–135. [CrossRef]
82. Ekiz, H.A.; Ramstead, A.G.; Lee, S.H.; Nelson, M.C.; Bauer, K.M.; Wallace, J.A.; Hu, R.; Round, J.L.; Rutter, J.; Drummond, M.J.; et al. T Cell-Expressed microRNA-155 Reduces Lifespan in a Mouse Model of Age-Related Chronic Inflammation. *J. Immunol.* **2020**, *204*, 2064–2075. [CrossRef] [PubMed]
83. Ramstead, A.G.; Wallace, J.A.; Lee, S.H.; Bauer, K.M.; Tang, W.W.; Ekiz, H.A.; Lane, T.E.; Cluntun, A.A.; Bettini, M.L.; Round, J.L.; et al. Mitochondrial Pyruvate Carrier 1 Promotes Peripheral T Cell Homeostasis through Metabolic Regulation of Thymic Development. *Cell Rep.* **2020**, *30*, 2889.e2886–2899.e2886. [CrossRef] [PubMed]
84. Lam, W.Y.; Becker, A.M.; Kennerly, K.M.; Wong, R.; Curtis, J.D.; Llufrío, E.M.; McCommis, K.S.; Fahrman, J.; Pizzato, H.A.; Nunley, R.M.; et al. Mitochondrial Pyruvate Import Promotes Long-Term Survival of Antibody-Secreting Plasma Cells. *Immunity* **2016**, *45*, 60–73. [CrossRef]
85. Sze, D.M.; Toellner, K.M.; Garcia de Vinuesa, C.; Taylor, D.R.; MacLennan, I.C. Intrinsic constraint on plasmablast growth and extrinsic limits of plasma cell survival. *J. Exp. Med.* **2000**, *192*, 813–821. [CrossRef]
86. Jacob, J.; Kassir, R.; Kelsoe, G. In situ studies of the primary immune response to (4-hydroxy-3-nitrophenyl)acetyl. I. The architecture and dynamics of responding cell populations. *J. Exp. Med.* **1991**, *173*, 1165–1175. [CrossRef]
87. Amanna, I.J.; Carlson, N.E.; Slifka, M.K. Duration of humoral immunity to common viral and vaccine antigens. *N. Engl. J. Med.* **2007**, *357*, 1903–1915. [CrossRef]
88. Zhan, Y.; Carrington, E.M.; Zhang, Y.; Heinzl, S.; Lew, A.M. Life and Death of Activated T Cells: How Are They Different from Naive T Cells? *Front. Immunol.* **2017**, *8*, 1809. [CrossRef]
89. Du, J.; Cleghorn, W.; Contreras, L.; Linton, J.D.; Chan, G.C.; Chertov, A.O.; Saheki, T.; Govindaraju, V.; Sadilek, M.; Satrustegui, J.; et al. Cytosolic reducing power preserves glutamate in retina. *Proc. Natl. Acad. Sci. USA* **2013**, *110*, 18501–18506. [CrossRef]
90. Du, J.; Yanagida, A.; Knight, K.; Engel, A.L.; Vo, A.H.; Jankowski, C.; Sadilek, M.; Tran, V.T.; Manson, M.A.; Ramakrishnan, A.; et al. Reductive carboxylation is a major metabolic pathway in the retinal pigment epithelium. *Proc. Natl. Acad. Sci. USA* **2016**, *113*, 14710–14715. [CrossRef]
91. Xu, R.; Ritz, B.K.; Wang, Y.; Huang, J.; Zhao, C.; Gong, K.; Liu, X.; Du, J. The retina and retinal pigment epithelium differ in nitrogen metabolism and are metabolically connected. *J. Biol. Chem.* **2020**, *295*, 2324–2335. [CrossRef] [PubMed]
92. Grenell, A.; Wang, Y.; Yam, M.; Swarup, A.; Dilan, T.L.; Hauer, A.; Linton, J.D.; Philp, N.J.; Gregor, E.; Zhu, S.; et al. Loss of MPC1 reprograms retinal metabolism to impair visual function. *Proc. Natl. Acad. Sci. USA* **2019**, *116*, 3530–3535. [CrossRef] [PubMed]
93. Du, J.; Cleghorn, W.M.; Contreras, L.; Lindsay, K.; Rountree, A.M.; Chertov, A.O.; Turner, S.J.; Sahaboglu, A.; Linton, J.; Sadilek, M.; et al. Inhibition of mitochondrial pyruvate transport by zaprinast causes massive accumulation of aspartate at the expense of glutamate in the retina. *J. Biol. Chem.* **2013**, *288*, 36129–36140. [CrossRef] [PubMed]

94. Sunny, N.E.; Parks, E.J.; Browning, J.D.; Burgess, S.C. Excessive hepatic mitochondrial TCA cycle and gluconeogenesis in humans with nonalcoholic fatty liver disease. *Cell Metab.* **2011**, *14*, 804–810. [CrossRef]
95. Kalavalapalli, S.; Bril, F.; Koelmel, J.P.; Abdo, K.; Guingab, J.; Andrews, P.; Li, W.Y.; Jose, D.; Yost, R.A.; Frye, R.F.; et al. Pioglitazone improves hepatic mitochondrial function in a mouse model of nonalcoholic steatohepatitis. *Am. J. Physiol. Endocrinol. Metab.* **2018**, *315*, E163–E173. [CrossRef]
96. Colca, J.R.; VanderLugt, J.T.; Adams, W.J.; Shashlo, A.; McDonald, W.G.; Liang, J.; Zhou, R.; Orloff, D.G. Clinical proof-of-concept study with MSDC-0160, a prototype mTOT-modulating insulin sensitizer. *Clin. Pharmacol. Ther.* **2013**, *93*, 352–359. [CrossRef]
97. Harrison, S.A.; Alkhoury, N.; Davison, B.A.; Sanyal, A.; Edwards, C.; Colca, J.R.; Lee, B.H.; Loomba, R.; Cusi, K.; Kolterman, O.; et al. Insulin sensitizer MSDC-0602K in non-alcoholic steatohepatitis: A randomized, double-blind, placebo-controlled phase IIIb study. *J. Hepatol.* **2020**, *72*, 613–626. [CrossRef]
98. Lacroix, M.; Rodier, G.; Kirsh, O.; Houles, T.; Delpech, H.; Seyran, B.; Gayte, L.; Casas, F.; Pessemeesse, L.; Heuillet, M.; et al. E4F1 controls a transcriptional program essential for pyruvate dehydrogenase activity. *Proc. Natl. Acad. Sci. USA* **2016**, *113*, 10998–11003. [CrossRef]
99. Chen, C.N.; Lin, S.Y.; Liao, Y.H.; Li, Z.J.; Wong, A.M. Late-onset caloric restriction alters skeletal muscle metabolism by modulating pyruvate metabolism. *Am. J. Physiol. Endocrinol. Metab.* **2015**, *308*, E942–E949. [CrossRef]
100. Tornatore, L.; Thotakura, A.K.; Bennett, J.; Moretti, M.; Franzoso, G. The nuclear factor kappa B signaling pathway: Integrating metabolism with inflammation. *Trends Cell Biol.* **2012**, *22*, 557–566. [CrossRef]
101. Liang, L.; Li, Q.; Huang, L.; Li, D.; Li, X. Sirt3 binds to and deacetylates mitochondrial pyruvate carrier 1 to enhance its activity. *Biochem. Biophys. Res. Commun.* **2015**, *468*, 807–812. [CrossRef] [PubMed]
102. Taylor, E.B. Functional Properties of the Mitochondrial Carrier System. *Trends Cell Biol.* **2017**, *27*, 633–644. [CrossRef] [PubMed]
103. Palmieri, F.; Monne, M. Discoveries, metabolic roles and diseases of mitochondrial carriers: A review. *Biochim. Biophys. Acta* **2016**, *1863*, 2362–2378. [CrossRef] [PubMed]



© 2020 by the authors. Licensee MDPI, Basel, Switzerland. This article is an open access article distributed under the terms and conditions of the Creative Commons Attribution (CC BY) license (<http://creativecommons.org/licenses/by/4.0/>).

Review

On the Detection and Functional Significance of the Protein–Protein Interactions of Mitochondrial Transport Proteins

Youjun Zhang ^{1,2,*}  and Alisdair R. Fernie ^{1,2,*}

¹ Center of Plant Systems Biology and Biotechnology, 4000 Plovdiv, Bulgaria

² Max-Planck-Institut für Molekulare Pflanzenphysiologie, Am Mühlenberg 1, 14476 Potsdam-Golm, Germany

* Correspondence: Yozhang@mpimp-golm.mpg.de (Y.Z.); fernie@mpimp-golm.mpg.de (A.R.F.)

Received: 29 May 2020; Accepted: 23 July 2020; Published: 25 July 2020

Abstract: Protein–protein assemblies are highly prevalent in all living cells. Considerable evidence has recently accumulated suggesting that particularly transient association/dissociation of proteins represent an important means of regulation of metabolism. This is true not only in the cytosol and organelle matrices, but also at membrane surfaces where, for example, receptor complexes, as well as those of key metabolic pathways, are common. Transporters also frequently come up in lists of interacting proteins, for example, binding proteins that catalyze the production of their substrates or that act as relays within signal transduction cascades. In this review, we provide an update of technologies that are used in the study of such interactions with mitochondrial transport proteins, highlighting the difficulties that arise in their use for membrane proteins and discussing our current understanding of the biological function of such interactions.

Keywords: protein–protein interaction; inner mitochondrial membrane; mitochondrial carrier family

1. Introduction

The mitochondrion is an important cellular organelle involved in cellular respiration via the tricarboxylic acid (TCA) cycle and oxidative phosphorylation (OXPHOS), fatty acids biosynthesis [1–4], photorespiration [5], compartmentation of metabolic processes such as amino acids biosynthesis [6,7], and C4 photosynthesis [8]. To perform roles in these many processes, eukaryotic mitochondria exchange metabolites with the cytosol and other organelles through both the outer mitochondrial membrane (OMM) and inner mitochondrial membrane (IMM). The outer membrane has long been believed to allow the diffusion of ions and uncharged small molecules through porous membrane proteins, especially the voltage-dependent anion channel (VDAC) [6,9].

Interestingly, as a convergence point, VDACS interact with diverse partners, including those that are broadly functionally classified as apoptosis-, cell signaling-, and cytoskeleton-related proteins, as well as metabolic enzymes [10]. For larger molecules, including proteins, to be translocated involves three machineries: the sorting and assembly machinery (SAM complex), the translocase of the outer membrane (TOM complex), and the mitochondrial distribution and morphology (MDM) complex [11]. Moreover, recent research has suggested that several outer membrane channels and their transport mechanisms are more diverse than originally thought [12], such as the acyl-dihydroxyacetone phosphate reductase (Ayr1) and two additional anion-selective channels (OMC7 and OMC8), which have been suggested to transport metabolites and ions. However, in all cases, detailed information concerning transported substrates is lacking [12,13]. In addition, several cytoskeleton proteins, such as tubulin, vimentin, plectin, and desmin, have been reported to interact with the mitochondrial outer membrane, where they are suggested to be involved in the ATP/ADP transmission control through VDAC, thereby mediating or influencing mitochondrial function [14].

In sharp contrast, molecules and ions can only pass across the inner mitochondria membrane by the aid of particular membrane transport proteins, each of which is selective for a specific molecule or ion. Around 180 mV of an electrochemical gradient is generated across the inner mitochondrial membrane during the operation of oxidative phosphorylation. Protein translocases of the outer (TOM) and inner (TIM) membrane form a supercomplex spanning the intermembrane space and appear to be held together by the polypeptide in transit [15]. In addition, a wide array of metabolites cross the inner mitochondrial membrane by the nuclear-encoded molecular gatekeepers of the mitochondrial carrier (MC) family [16].

Featuring six conserved transmembrane α -helical regions [17], most mitochondrial carrier family proteins (MCF) are relatively small, around 300 amino acids in length, ranging from 30 to 35 kDa [18]. The primary structure of most MCs is comprised of three homologous regions, each containing around 100 amino acids [19], and with both the N and C terminals exposed to the intermembrane space [20,21]. Every repeat region is suggested to include two transmembrane segments flanking a short helical region that is parallel to the lipid bilayer [22].

In addition, every repeat region is proposed to have two hydrophobic transmembrane segments connected by a long hydrophilic matrix loop [23,24] and the structural motif PX[D/E]XX[K/R]X[K/R] (20–30 residues), [D/E]GXXXX[W/Y/F][K/R]G (IPR00193) [16]. Of the MCFs, the ADP/ATP carriers, which import ADP from the cytosol and export ATP from the mitochondria, are the best investigated and our current understanding of MCFs is largely derived from the crystal structures of different versions and conformations of this carrier [25]. The alternating access mechanism (previously named ping-pong mechanism) of the transport cycle includes substrate binding to the carrier in its c-state (matrix-side closed and cytoplasmic-side open state), undergoing a conformational change to a transition state, and finally relaxation to the m-state (cytoplasmic-side closed and matrix-side open state), followed by the release of the substrate into the mitochondria. In the m-state, the counter-substrate binds to the carrier, undergoes a conformational change and eventually converts to the c-state, and releases the counter-substrate into the cytosol. After release of the counter-substrate, the carrier can start the transport cycle anew. Opened and closed carriers expose the substrate-binding site to one or the other side of the membrane with alternating access ping-pong mechanisms [25–33]. This proposed mechanism was initially based on studies of the high-affinity inhibitor ligands of the ADP/ATP carrier, carboxyatractyloside and bongkreic acid, and their competition with the transported substrates ADP and ATP [29,30].

MCFs mediate the transport of carboxylic acids, fatty acids, amino acids, inorganic ions, cofactors, and nucleotides across the mitochondrial inner membrane across the kingdoms of life [26], and are crucial for many cellular processes [17,34–36]. Given that typical detergent application reveals that MCFs are small in size, the formation of the homomeric and heteromeric complexes may simply help to assemble the transporting complex and avoid random, unfavorable protein–protein interactions in the crowded environment of the inner mitochondrial membrane. These reports, including the tricarboxylate carrier, the dicarboxylate carrier, and the oxoglutarate carrier (Table 1), are, however, as we describe below, erroneous, further highlighting the need for carefully controlled experiments using multiple methods. However, the structural folds of the ADP/ATP carriers were proved to function as monomers [37,38]. MCs are now thought to exist and function as monomers. The only carrier definitely known until now to exist as a homodimer is the human aspartate-glutamate carrier (with 2 isoforms: AGC1 and AGC2). This carrier consists of two domains: an N-terminal soluble regulatory domain (with four calcium-binding sites) and a C-terminal MC catalytic domain [39,40]. Evidence has been provided that two molecules of the aspartate-glutamate carrier are linked together by their N-terminal regulatory domains [41].

Table 1. The interactome of mitochondrial carrier family members and other mitochondrial transporter proteins.

Mitochondria Carrier	Interactor	Reference
VDAC	Tubulin, Desmin, Vimentin, plectin, hexokinase and creatine kinases, MtCK, ANT, cardiolipin	[10,42,43]
Acyl-dihydroxyacetone phosphate reductase	Unclear	[13]
ADP/ATP carrier	Previous suggested as dimer, and now convincingly proved as monomers	[44]
Phosphate carrier	ATP synthase, mitochondrial peptidyl-prolyl cis-trans isomerase, NaStEP, Citrate synthase, isocitrate dehydrogenase and oxoglutarate dehydrogenase	[25,45–47]
Pyruvate carrier	Heterodimer	[48,49]
Tricarboxylate carrier	Homodimer	[50]
Dicarboxylate carrier	Homodimer	[51]
Oxoglutarate carrier	Homodimer, BCL2	[52,53]
Glutamate transporter	Synaptic protein	[54]
Aspartate/glutamate carrier	Homodimer	[36,39,55]

The association of mitochondrial transport proteins plays an important role in the movement of metabolites across the IMM. For example, although not a member of the MCF, the heteromeric complex of the mitochondrial pyruvate carrier (MPC) is strategically positioned at the intersection between glycolysis in the cytosol and OXPHOS in the mitochondria [48]. Similarly, the association of the ATP synthasome, F₀F₁-ATPase, complex of adenine nucleotide translocator (ANT), and the phosphate carrier (PiC), facilitates a mechanism for adenine nucleotide and pyrophosphate release [56–59]. In addition, the interaction between the MCF and mitochondrial proteins may also improve metabolite import; for example, the dicarboxylate carrier (DIC) interacts with malate dehydrogenase, acting as an oxaloacetate shuttle and thereby improving functional coupling of the citric acid cycle with the shuttle [60]. Despite their importance in assisting metabolite transport, MCF protein interactions have been poorly studied in living cells—most likely due to methodological limitations. Indeed, although various protein interaction approaches to investigate membrane–protein interactions have been developed over several decades, such as coimmunoprecipitation and chemical cross-linking, bioluminescence resonance energy transfer (BRET), blue native polyacrylamide gel electrophoresis (BN-PAGE), yeast two-hybrid (Y2H), and fluorescence resonance energy transfer (FRET), only a few have been employed for studying the interactions of mitochondria carriers [48,61–63]. Here, we review such protein–protein interactions of the mitochondrial carrier family and discuss the major challenge of acquiring information about the interactions of integral membrane proteins. Despite the relative paucity of information on such interactions, we argue that they are likely underappreciated across the kingdoms of life and may represent an important constituent of compartmental and regulation of metabolism. In the following review, we detail historical and contemporary observations of protein interactions of MCF, detailing methods by which they are determined, and suggesting possible biological implications of such assemblies.

2. Experimental Evaluation of the Protein–Protein Interactions of Mitochondria Carriers

Protein interactions of the membrane play an important role in several biological systems, such as regulation of metabolic pathways, signal transduction cascades, regulating metabolite import, and the formation of membrane complexes [64]. The cumulative databases of membrane protein

complex structure provide considerable insight into how folding and packing of their transmembrane segments contribute to their diverse functions [65,66]. Single-span transmembrane helices have been suggested to act as anchors for more “interesting” water-soluble domains or merely to constitute models for multipass protein folding, such as leucine zippers, that mediate protein complex association in water-soluble proteins. Transmembrane proteins can additionally direct protein–protein interactions within the membrane and participate in signal transduction across lipid bilayers [64]. Thus, it is of particular importance to prepare the protein components such that the structure, topologies, and functions remain intact prior to their analysis. Given that various diverse types of living cells, such as yeast or tissue culture, are widely used to investigate *in vivo* mitochondria carrier interaction, it is important to choose the correct “horse for the course” in order to maximize the insight that can be achieved. In the following section, we give a brief overview of the available tools.

A major breakthrough methodology was the use of bioluminescence resonance energy transfer (BRET), which can investigate protein–protein interactions in live cells based on the enzymatic activity of luciferase (Figure 1b) [48,67]. For example, regarding signal transduction cascades associated with the outer membrane, interactions between retinoic acid-inducible gene I-like receptors and mitochondrial antiviral signaling (MAVS) are known to trigger the immune signaling pathway [68]. Thus, the interaction between RLR and MAVS results in the multistep structural changes from inactive to active states. However, these signal transduction processes are transient states, and as such, extremely difficult to reconstitute in other membrane systems or *in vitro* experiments [67,68]. For this reason, several studies have rather used the BRET system to provide insight into the structural transition of MAVS between active and inactive conformation *in vivo* [67–69]. In this system, either the N-terminal-fused Rluc- or YFP tags of MAVS could beautifully monitor the interaction between MAVS molecules via a BRET saturation assay. This system is thus strongly recommended to detect the interaction between cytosol proteins and OMM proteins. A further example of the power of this technique came from combining biomolecular fluorescence complementation (BiFC) with the BRET system, which was used to demonstrate that activated MAVS is a highly ordered oligomeric complex and that three proteins associated on the mitochondrial surface [68].

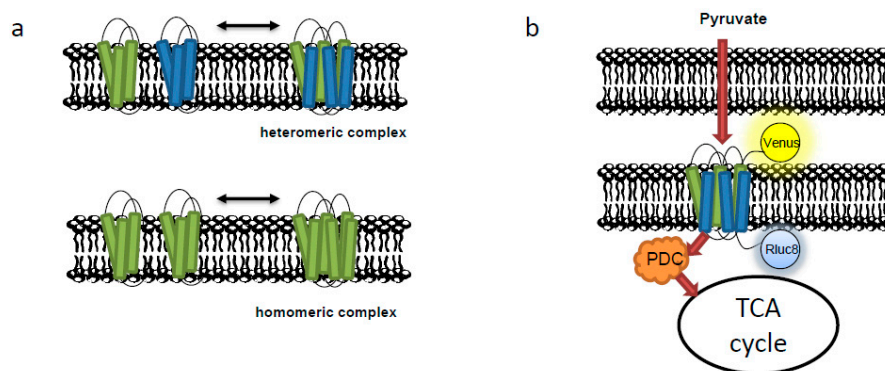


Figure 1. Protein complex of the mitochondrial carriers. (a) The association of both homodimers and heterodimers of the mitochondria carrier may result in the active transporter. (b) Monitoring the heterodimer of the pyruvate carrier by the bioluminescence resonance energy transfer (BRET).

Yet another example is the protein–protein interaction of the mitochondrial pyruvate carrier, which represents a central node of carbon metabolism [48]. The mammal heteromeric complex is composed of two paralogous subunits, MPC1 and MPC2, which regulate pyruvate uptake. In order to monitor the activity and complex formation of the MPC in real time, BRET experiments combining MPC2-RLuc8 and MPC1-Venus were used to detect the assembly of the MPC complex in the presence of various metabolites, including pyruvate lactate, malate, and citrate (Figure 1b) [70]. Using a modified BRET protocol, the authors could monitor the lower MPC activity in cancer cells, which are believed to mainly rely on glycolysis to produce ATP, a characteristic known as the Warburg effect [48].

Intriguingly, this effect was recently shown to be at least partially mediated by the tripartite motif containing-21-dependent ubiquitination and subsequent degradation of phosphofructokinase based regulation of pyruvate kinase turnover in response to cytoskeletal monitoring of cellular tension [71,72]. Returning to the study above, this low activity could intriguingly be turned over by increasing the concentration of cytosolic pyruvate, thus enhancing oxidative phosphorylation. This demonstration shows that the biosensor represents a unique tool for investigating carbon metabolism and bioenergetics under a diverse range of conditions [48,67–69]. Importantly, we present several examples in which the BRET system was used for monitoring the interactions of mitochondrial carriers and which should be adopted in future studies. Moreover, combining BRET with BiFC can monitor three way protein–protein interactions at the cell membrane, whilst combining the BRET and FRET—called SRET—represents an attractive strategy by which to understand heteromerization complex in a physiological environment [73]. The application of such methods to other organelle-bounded molecules are detailed below.

Another widely used method is blue native polyacrylamide gel electrophoresis (BN-PAGE) (Figure 2), which can be employed for one-step purification of protein complexes from total cell and tissue homogenates or from biological membranes, including the mitochondrial membranes. It can also be employed to determine physiological protein–protein interactions and to discover native protein masses and oligomeric states. Native protein complexes are recovered from gels by electroelution or diffusion and are investigated by native electroblotting and immunodetection or by in-gel activity assays or employed for 2D crystallization and electron microscopy. Several studies using this method have reported that mitochondrial carriers are dimeric (composed of two ~32 kDa monomers) and, in some cases, can form physiologically relevant associations with other proteins [74–76]. For example, the conserved mitochondrial inner membrane proteins migrate on BN-PAGE as a large complex of ~150 kDa [75] or the ~30 kDa MPC dimers, due to different amounts of lipids and detergent bound to MPC [77]. Interestingly, two different heterodimers contain either Mpc1 and Mpc2 (MPC_{FERM}) or Mpc1 and Mpc3 (MPC_{OX}) were detected by BN-PAGE and were suggested to depend on the carbon source in yeast cells [70]. MPC_{OX} has higher pyruvate transport activity than MPC_{FERM} owing to differences in the C-terminal region of Mpc2/Mpc3. Moreover, the yeast mitochondrial ADP/ATP carrier (AAC3) was also reported to vary in a detergent- and lipid-dependent manner (from ~60 to ~130 kDa) that is not related to changes in the oligomeric state of the protein, while these also vary due to binding to different amounts of lipids and detergent. However, several studies have consistently shown that yeast ADP/ATP carriers are monomeric in structure and function [44]. As the mitochondrial respiratory chain supercomplexes have been investigated by BN-PAGE under different conditions [78], this method could be used to detect the dynamics of the mitochondrial carrier protein complex. In addition, several mitochondrial carriers were also investigated by BN-PAGE, such as the 2-oxoglutarate carrier [52], the dicarboxylate carrier [51], and the tricarboxylate carrier [50]. We will discuss these below.

Size exclusion chromatography or gel filtration is yet another established technique for the determination of protein interactions relying on the ability, or lack thereof, of particles to pass through a column of porous beads according to their hydrodynamic radius (Figure 2). Given the large amount of bound detergent and lipid, accurate values of the molecular mass and dimensions of the protein need to be carefully accounted for in the case of mitochondrial carriers in solution [37]. For example, the Mpc1/Mpc3 complex eluted as a single peak by size exclusion chromatography, indicating that the complex was monodisperse [49]. Using size exclusion chromatography with mass spectrometry, the conserved protein complexes of 13 plant species were identified, including the mitochondrial membrane protein [79,80]. An important advantage of this method is that it is compatible with physiological conditions and thereby allows the investigation of the dynamics of protein complex formation and disassembly.

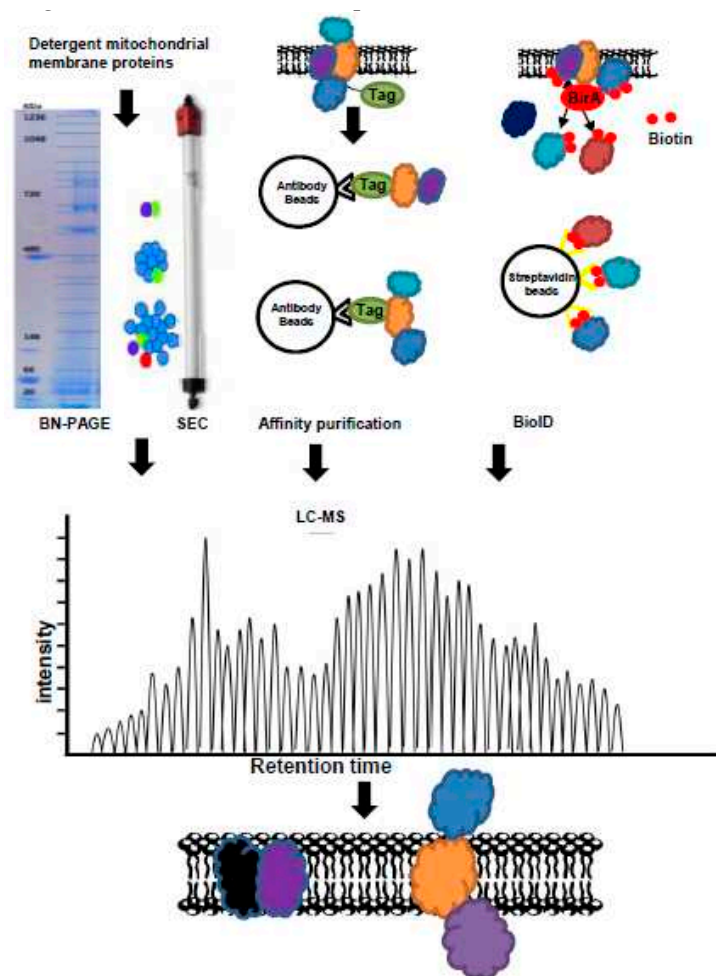


Figure 2. Methods used for protein–protein interaction combined with liquid chromatography–mass spectrometry (LC-MS). BN-PAGE: Blue native polyacrylamide gel electrophoresis, SEC: Size exclusion chromatography, BioID: proximity-dependent biotin identification.

Differential tagging and affinity purification have also been used to investigate the association state of mitochondrial carriers (Figure 2). This method is based on the principle that an associated stable complex in detergent should be copurified by affinity chromatography if one of the components of the complex contains an affinity tag. This approach is higher throughput, faster, and more straightforward than other methods, as the amounts of bound lipid and detergents do not need to be measured. However, the denatured mitochondrial membrane may result in false negative and false positive identifications. To avoid nonspecific aggregation, which can be misinterpreted as native interactions, the misfolding or unfolding of the carriers should be prevented by additional steps. Additional detergents, applied at these steps, also affect the intensity of the LC-MS measurement and necessitate further steps to reduce them. This method was used to obtain a preparation enriched in calcium transporters from Triton X-100 extracts of rat liver mitochondria inner membranes [81]. Similarly, when the yeast phosphate carrier Mir1p was expressed in inclusion bodies as a misfolded form in *E. coli* with a FLAG tag [82], the homo- and heterodimeric forms of phosphate carriers, which were combined by two differently tagged unfunctional monomers by affinity chromatography, were full active after reconstitution suggested the phosphate carrier works as dimer [82]. In addition, affinity purification of the plant TCA cycle enzymes also revealed interaction between the IMM proteins citrate synthase, isocitrate dehydrogenase, oxoglutarate dehydrogenase, and the mitochondrial phosphate carrier proteins [83–86]. Given that affinity purification with mass spectrometry is based on the association of stable complexes, the combination of AP-MS with cross-linking has been suggested to

greatly improve detection of transient and unstable protein–protein interactions of the organelle-bound membrane proteins [87,88].

Chemical cross-linking is a classical method used to freeze protein complexes in their native form, and has proven especially useful for capturing transient protein–protein interactions. Given that such reagents can permeate into the cellular compartment in the case of the membrane-permeable cross-linkers, this can be subsequently combined with mass spectrometry (cross-linking coupled with MS: XL-MS) to give vital insight into the spatial arrangement of protein complexes in organelles at the subunit level [89]. However, the complex fragmentation pattern of cross-linked peptides frequently precludes unambiguous identification of the cross-linked peptides. XL-MS is particularly challenging with respect to data analysis. MS-cleavable cross-linkers, for example, disuccinimidyl dibutyric urea (DSBU; containing cleavable C–N bonds) or disuccinimidyl sulfoxide (DSSO; containing cleavable C–S bonds), are recent innovations. The merits of such MS-cleavable cross-linkers are that their cleavage (in the gas phase during MS) produces distinguishable ion doublets, allowing the cleaved peptides to readily be discovered via a database search [89]. The dynamic interactions of coexisting respiratory supercomplexes have been successfully captured using this technique [90]. It was also used to construct the mitochondrial protein interactome of a large-scale model of stable and transient interactions, and interactions between membrane proteins [91]. That said, one limitation of the XL-MS approach is that cross-links within the target cannot be distinguished as intermolecular or intramolecular, for example, as in mitochondrial prohibitin complexes [92].

The XL-MS method could, however, also provide insight into many protein complexes for the reconstruction of low-resolution three-dimensional structures, but it must be considered that the cross-linking process may result in artefactual protein–protein interactions. In the presence of bongkreikic acid (BKA), the bovine ADP/ATP carrier could be fixed in the matrix state in submitochondrial particles (inside-out membranes) by copper-o-phenanthroline cross-linking, while the presence of CATR locked the carrier in cytoplasmic state and prevented cross-linking. In addition, sodium dodecyl-sulphate (SDS) was reported to inhibit either AAC1 or UCP1 interactions via cross-linking [93,94]. This observation has also been used to support the dimer model with the rationale being that the carriers are unfolded in SDS or solubilized to monomers, and thereby are no longer associated as dimers and cannot be cross-linked to their usual interactors. Both the mitochondrial oxoglutarate and phosphate carriers could be cross-linked in detergent, but not in situ in the membrane [37,53]. Taken together, this suggests that cross-linking occurs in different parts of the mitochondrial carriers, suggesting the presence of many interfaces distinct from dimerization. The combination BN-PAGE and size exclusion chromatography with cross-linking could greatly aid in avoiding protein complex disassembly when the complexes are separated from the mitochondrial membrane by denaturing detergents.

Recently developed proximity-dependent labelling methods have been used to detect the transient protein–protein interactions under native conditions in living cells [95]. The basic principle of the proximity-based biotin labelling method or proximity-dependent biotin identification (BioID) is that a protein of interest (bait) tagged by a promiscuous biotin ligase (BirA R118G mutant, from *E. coli*) could convert the biotinylation of nearby endogenous proteins with lysine side chains (within ~10 nm) after the addition of a biotin supplement to the tissue culture medium as described by Roux et al. (Figure 2) [96]. Due to the covalent biotinylation of the targets, these biotin-labelled proteins are stable following stringent cell lysis treatment with the protein extraction, followed by affinity purification (such as streptavidin beads), and several washing steps. This approach can thereafter be combined with MS measurement to detect biotin-labelled proteins and to screen the protein–protein interaction networks with high spatial resolution in living cells. As such, this approach has been successfully used to evaluate physiologically relevant networks of protein–protein interactions and is especially potent for detecting low-affinity and/or transient associations, such as the interactomes involved in signal transduction [95]. Due to the potential masking of, for example, the mitochondrial targeting sequence,

it is, however, important to consider the effects of the BirA fusion tag at either the N- or C-terminus on the biological activity and/or subcellular localization of the target protein.

In addition, this method was enhanced by targeting of the nearby proteins using a smaller type of biotin ligase (from *Aquifex aeolicus*; BioID2) to link the bait protein, which has the added benefit of decreasing the amount of biotin supplementation that is required. This improved assay has been used to elucidate a mitochondrial macromolecular complex in mammalian cells by fusing the BirA from *A. aeolicus* to the C-terminal of an inner mitochondrial membrane-bound protein prohibitin 2 (PHB2) [97,98]. In this research, the recombinant PHB2 behaved in an almost identical manner to the interacting protein and biotinylated a large number mitochondrial proteins, including its PHB1 isoform, SAM and mitochondrial contact site and cristae organizing system (MICOS) subcomplex [97,98]. Although BioID approaches have been successfully applied to detect the interaction between membrane proteins that exhibit a wide range of subcellular localizations, such as the mitochondria, cell–cell junctions, nuclear lamina, and endoplasmic reticulum, it is still not used for monitoring the interaction of the mitochondrial carriers. Indeed, the BioID approach has an inherent limitation for identifying macromolecular complex in mammalian cells by fusing to prohibitin 2 (PHB2), an IMM-bound protein [97]. Given that both the N and C termini are proposed to be exposed to the intermembrane space [19], the catalytic activity from BirA may not reach the target site of the mitochondrial proteins. Furthermore, if the structural surface of the target protein proximate to the bait lacks lysine residues, this method cannot be used [97]. The combination of proximity-dependent labelling and chemical cross-linking offers great promise to enhance our understanding of multiprotein complexes that are difficult to prepare, such as organelle-bound membrane proteins.

3. Proteins Associated to Mitochondrial Outer Membrane Carrier

Although most of the mitochondrial carriers are enriched in the inner boundary membrane of the mitochondria, recent studies suggest that several outer membrane channels can also transport metabolites and ions without further research of their transported substrate [12,13]. The exchange of hydrophilic compounds, such as metabolites and ions across the OMM of eukaryotes is facilitated by specific voltage-dependent anion channels [6,9] and followed by active transport across the IMM mediated by specific nuclear-encoded membrane transporters. The appearance of Donnan potential, which relates to the distribution of ion species between two ionic solutions across the outer membrane, could render the VDAC formation in either the open or closed state. In the open state, VDAC shows a considerable preference for metabolic anions with weak selectivity. In the closed state, VDACS still conduct small cations, such as K^+ , Na^+ , and Ca^{2+} , and Cl^- by a cation selective pore of 1.8 nm in diameter, while the transition of major anionic metabolites such as ATP, ADP, and respiratory substrates is prevented [99]. Several publications have been reported that the regulation of VDAC conductance contributes to energy metabolism and mitochondrial dysfunction [99,100].

Moreover VDACS have been reported to interact with diverse partners, including proteins of apoptosis, cell signaling, cytoskeleton-related proteins, and metabolic enzymes (Table 1) [10]. For example, glucose-6-phosphate, which is the product of the hexokinase-catalyzed reaction, was suggested to potentiate ATP release from mitochondria with the recovery of normal metabolism and substrate replacement, was even more increased when hexokinase and glucokinase were dissociated following being bound to VDAC [10,42]. Therefore, the effect of hexokinase dissociation from VDAC is the subject of many studies dealing with the development of potent cancer chemotherapies. Similarly, creatine kinase, which also acts as an energy sensor and mediates antiapoptotic effects via VDAC–ANT complexes, exhibits preferential use of mitochondrial ATP. Moreover, interaction of desmin with various contact sites (VDAC, adenine nucleotide translocator (ANT) and mitochondrial contact site complex) affects mitochondrial permeability transition pore (mtPTP) behavior and respiratory function. VDAC forms a barrel comprised of a transmembrane alpha helix and 13-transmembrane beta strands. The resultant beta barrel encloses a large channel (~3 nm in diameter), which in its open configuration is permeable to molecules up to ~5 kDa in size. In vitro studies have revealed that all eukaryotic VDAC

channels adopt multiple conductance states. In the IMS, MtCK binds with high affinity to cardiolipin and other anionic phospholipids cross-linking the two peripheral mitochondrial membranes and the ANT, thus forming a complex of MtCK–VDAC–ANT and cardiolipin [43]. The MtCK–VDAC association is enhanced at physiological calcium concentrations. MtCK associates only with the inner membrane and ANT in the cristae space. MtCK preferentially uses mitochondrial ATP that is exported via ANT to phosphorylate creatine, which has a higher diffusion rate in comparison to ATP, thus providing a spatial energy shuttle. The coupling of these partner proteins thereby links VDAC to other cellular functions such as protein import, apoptosis, control of cellular energy metabolism, and tumorigenesis.

Two clearly distinguishable anion-selective channel activities, OMC7 and OMC8, with pore diameters of roughly 15 Å were detected in vesicles of the OMM. However, as yet, the corresponding channel-forming proteins remain to be identified. In addition, the acyl-dihydroxyacetone phosphate reductase (Ayr1) forms a cation-selective channel. This protein contains a predicted α -helical transmembrane domain and is located in the mitochondrial outer membrane, ER, and lipid particles. However, it is currently unclear whether Ayr1 forms a channel in all these cellular compartments. Several functions in lipid metabolism have been putatively assigned to this protein. Indeed, it is thought to be involved in the biosynthesis of phosphatidic acid, in the mobilization of triacylglycerol, and in the elongation of fatty acids. It contains a predicted Rossmann fold and conserved signature motifs such as a NADPH-binding site that are characteristic for the large protein family of short-chain dehydrogenases [13]. Addition of NADPH induces very fast voltage dependent gating of the channel. This voltage-dependent gating occurs unidirectionally. Moreover, in the presence of NADPH, the Ayr1 channel, even at high voltages $V_m > 100$ mV, remained in the open state. However, whether or not the Ayr1 channel is actively and directly involved in lipid biosynthesis remains to be investigated.

In summary, the old concept that the outer membrane functions as a “molecular size-exclusion filter” for the passage of small hydrophilic molecules through VDAC has been strongly questioned by different observations. First, transport processes can occur in cells deficient of all VDAC isoforms [10]. Secondly, the VDAC channel properties are modulated by a variety of different effectors, suggesting that their specificity is under active control [10]. Thirdly, the outer membrane contains, beside VDAC, additional pore-forming proteins that might mediate metabolite flux [10]. Fourthly, the presence of the NADPH-regulated Ayr1 channel indicates that such transport processes across the outer membrane of mitochondria may be subject to redox regulation. In conclusion, metabolite transport across the OMM is more specific and regulated than originally thought, challenging the view that VDAC allows the unregulated passage of all manner of small molecules.

4. Proteins Associated to the Inner Membrane of Mitochondria

Metabolites, such as amino acids, carboxylic acids, fatty acids, cofactors, inorganic ions, and nucleotides, are specifically transported across the IMM by members of the mitochondrial carrier family (and other mitochondrially localized transporters that do not belong to the family [101]), to join in many cellular processes. Most metabolites transport as strict counter-exchangers of chemically related substrates (antiporters), but some display substrate–proton (symporters) transport activities or unidirectional (uniporters) [16,17,23,32]. It has been debated whether the mitochondrial carriers exist or function as a monomer or dimer. The crystal structures of ADP/ATP carriers exist in the IMM as monomers [26,102,103] and interact with respiratory supercomplexes in the presence of cardiolipin, a unique phospholipid found exclusively in the mitochondrion [104]. The formation of the homomeric and heteromeric complex may simply aid in assembly of the transport complex or act to avoid random, unfavorable protein–protein interactions in the packed environment of the inner mitochondrial membrane, such as the heteromeric complex of the mitochondrial pyruvate carrier [48] and dimeric structure of mitochondrial tricarboxylate carrier [50]. Many mitochondrial carrier proteins do not function as monomers, but have to assemble into oligomeric structures to

become functional [52,53,82]. However, despite the fact that interactions between the mitochondrial carriers and mitochondria proteins are long known, they are not well studied.

Nucleotide transporters include the mitochondrial ADP/ATP carrier, ANT, which we discussed above. Many claims have been made for the association of the ANT carrier with other proteins or protein complexes [34]. For a long time, it was thought that the ANT was a component of the permeability transition pore together with VDAC, BAX, and Bcl2 [25,105]. However, mitochondria lacking the carrier could still be induced to undergo permeability transition, resulting in release of cytochrome c [25,106], suggesting that this may not be the case. It has also been claimed that the ANT carrier, alongside a phosphate carrier, forms a complex with ATP synthase with a 1:1:1 stoichiometry—the so-called ATP synthasome [25,45]. However, the carriers are present in much higher numbers than ATP synthase to account for their relatively slow transport rates compared to the rate of ATP synthesis. Recent studies have revealed that ATP synthase forms rows of dimers on the ridge of cristae [25,107], a formation that is mediated by the Fo subunits of ATP synthase. This molecular arrangement leaves only the rotating c-ring exposed to the lipid bilayer, and thus there is no plausible binding site for carriers [25]. Furthermore, the ATP synthasome is supposedly stable in detergent, but affinity purifications of the carriers or ATP synthase under stabilizing conditions do not lead to detectable cross contaminations [25,108]. Therefore, it appears highly unlikely that the ATP synthasome exists. It has also been claimed that yeast ADP/ATP carriers (Aac2p) exists in physical association with the cytochrome c reductase (cytochrome bc1)–cytochrome c oxidase supercomplex and its associated TIM23 machinery, based on BN-PAGE and tagging experiments [25,109]. However, mitochondrial carriers are extremely unstable under BN-PAGE gel conditions in the absence of inhibitors, leading to aggregation and random association with other proteins [25,74].

In the course of the structural work of yeast ADP/ATP carrier, hundreds of milligrams of tagged Aac2p were purified under stabilizing conditions, but the copurification of other proteins or protein complexes was never observed [25]. Recently, it was claimed that the ANT carrier is associated with the translocase of the inner membrane (TIM) in a 1:1 stoichiometry [25,110]. These claims were based on SILAC experiments, but under the same conditions other mitochondrial carriers are also associated with TIM, but at lower stoichiometric ratios. The latter result indicates that the association is nonspecific, reflecting differences in expression levels or stability between carriers. The mitochondrial ANT carrier is one of the most abundant membrane proteins in the mitochondrion. In addition, the protein is very hydrophobic, leading to its structural instability in detergents. Moreover, as for the Aac2p described above, the protein does not protrude much from the membrane, and the surfaces that are exposed would appear to provide no opportunity for stable interactions [25]. Furthermore, there are no conserved residues on the surface of the carrier or asymmetrical features that are compatible with specific interactions with other proteins [25,37,111] Finally there are no plausible functional roles for these interactions, and the purported protein interaction partners are most likely experimental artefacts [25].

Inorganic ion transporters include the mitochondrial phosphate carrier PIC (SLC25A3) and the uncoupling protein UCP1 (SLC25A7). Whilst strong evidence supports divergent roles for UCP, both in dissipating proton gradients [112,113] and transporting aspartate, glutamate, and cysteinsulfinate [114], PIC has been characterized to transport phosphate in symport with protons for the synthesis of ATP [115,116]. The PIC was suggested in protein complex analysis to interact with mitochondrial peptidyl-prolyl cis-trans isomerase [46]; however, the work has not yet been followed up. Similarly in plants, a novel mitochondrial phosphate carrier interacts with NaStEP (a proteinase inhibitor essential to self-incompatibility) and mediates in the self-incompatibility of the pollen [47], whilst the TCA cycle enzymes citrate synthase, isocitrate dehydrogenase, and oxoglutarate dehydrogenase interact with a putative phosphate transporter in the AP-MS [83] as well as other TCA cycle enzymes to associate as the metabolon. Whilst follow up studies of these interactions were also not carried out, such interactions are not without precedence. Indeed, in the early work of Srere and coworkers looking into enzyme and enzyme protein assemblies, several such interactions were noted, including malate dehydrogenase,

citrate synthase, and aconitase, on the basis of structure modelling studies [117,118]. Furthermore, although not a member of the MCF, the mitochondrial pyruvate carriers transport pyruvate to fuel the tricarboxylic acid cycle and thereby support ATP generation. However, this import also serves as a link to anabolic pathways for lipid and amino acid biosynthesis and gluconeogenesis. Heterocomplexes of MPC have been monitored by BRET [48] and purified following size exclusion chromatography [49]. The heterodimer is the active mitochondrial pyruvate carrier, while individual MPC proteins assemble as nonfunctional homodimers (Table 1) [49].

The situation is similar for other carriers of the MCF. For example, the tricarboxylate carrier catalyzes an electroneutral exchange of the dibasic form of a tricarboxylic acid (citrate, isocitrate, and cis-aconitate) with a proton for another tricarboxylate- H^+ , dicarboxylate (malate and succinate), or phosphoenolpyruvate [50,119–121]. Interestingly, the dimeric form of the tricarboxylate carrier protein was found when eel liver mitochondria were solubilized with the mild detergent digitonin [50]. However, the physiological relevance of this is, as yet, has not been unequivocally resolved. Similarly, the ubiquitously expressed dicarboxylate carrier protein (DIC) was found to exist in the dimeric form after lysis with the mild detergent digitonin using Western blotting, whereas only the monomeric form of DIC was discovered after lysis with SDS [51]. That said, the dimeric structure of the mitochondrial oxoglutarate carrier (OGC) has been demonstrated by the cross-linking and BN-PAGE of digitonin-lysed mitochondria [52,53]. The same is likely true for the dicarboxylate, tricarboxylate, and oxoglutarate carrier proteins, since these will certainly follow the same mechanism of the ADP/ATP carrier that was recently convincingly proven to be a functional monomer [38]. A note of caution in interpreting results from such studies can be provided by the case of UCP. For many years, it was thought that UCP1 formed a homodimer based on analytical ultracentrifugation [122], nucleotide binding [123], and protein cross-linking studies [124]; however, on the basis of size exclusion chromatography [125], UCP is now believed to act as a monomer that binds one purine nucleotide molecule [126]. Arguably more exciting, it has recently been reported that the human glutamate transporter, EAAT5, contains a C-terminal consensus motif that could interact with synaptic proteins that promote ion channel clustering [54]. Moreover, glutamate can also transport into mitochondria through the aspartate/glutamate carrier (AGC), combining the input of glutamate with the release of aspartate [36,39,55]. Size-exclusion chromatography has shown that two molecules of the aspartate/glutamate carrier are linked together by their N-terminal regulatory domains as the dimer (Table 1) [41]. Finally, the transporter activity of the MCFs proteins can perhaps also be modulated by forming complexes with interacting partners, such that the activity of some MPCs may be dependent on the formation of heterocomplexes. An example of this is the fact that an antiapoptotic protein, Bcl-2, was found to be an interacting protein partner of rat OGC, and when coexpressed with OGC in CHO cells, the total mitochondrial glutathione content was significantly increased 24 h post-transfection [127].

5. Conclusions and Perspective

Despite the fact that complex formation of MCFs may play an essential role in metabolite import, MCF protein interactions have been poorly studied in living cells—most likely due to methodological limitations. Although both BN-PAGE and size exclusion chromatography have been used to analyze the heterodimers and homodimer of the MCFs, these dimers were suggested to be functional monomers, especially the ADP/ADP carriers [44]. Moreover, improved BRET has been used to monitor the MPC activity in real time, thus giving the possibility to use it for other MCFs [48]. BRET has been successfully used to monitor the heteromeric complex of the mitochondrial pyruvate carrier [48,49]. Interestingly, the activity of MPC in cancer cells could be monitored in the presence of various metabolites, including lactate, malate, and citrate. This method could be widely used to monitor the assembly of mitochondrial carrier protein as several metabolite transporters may regulate their activity by the complex assembly. However, currently, these methods have not been applied to detecting protein–protein interactions of mitochondrial transport proteins such as MPC and MCFs. Given that physiological studies of the

mitochondrial transport proteins are limited, the identification of interactors will help us to understand the mechanism of the mitochondrial transport proteins *in vivo*.

Moreover, the identification of PPI binding sites will be an important step here. One should note that some, albeit limited, physical evidence exists of MCF protein interactions, but little information is available concerning their biological function, and most examples of this are restricted to signal transduction. Indeed, given the limited exposure of the proteins due to the transmembrane domains, this may prove easier than for the metabolons that are considerably better characterized, such as those of glycolysis [6], the TCA cycle [1,84], and plant specialized metabolism [88]. In addition, the yeast enolase-associated macromolecular complex was identified to contain several mitochondrial carriers, including a phosphate carrier and an ADP/ATP carrier (Figure 3; [128]). As this example illustrates, the possibility of cross subcompartment metabolons exists, potentially suggesting a novel route of metabolic coordination. Given that glycolytic enzymes associated at the OMM of mitochondria form a metabolon [4,62,88,129], the mitochondrial transporters, such as VDAC, may also join the metabolon to improve the metabolite transport efficiency (Figure 3). Since many recent advances have been made in the study of metabolons [88,117], we believe the time is ripe to apply these to study the intriguing prospect that members of the MCF are involved in such structures and other types of protein–protein assemblies

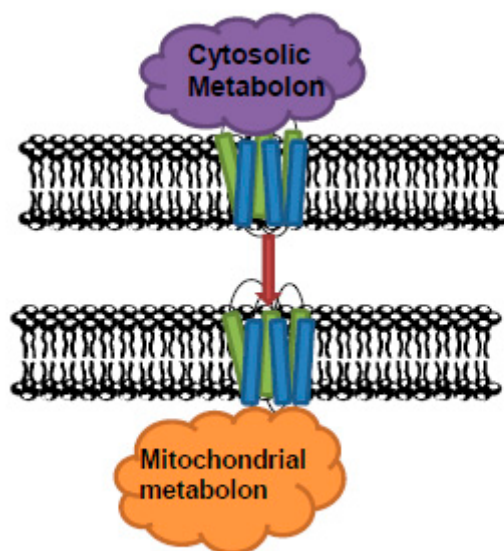


Figure 3. Metabolon associated to the mitochondrial carriers. The mitochondrial transport proteins may also join in the metabolon to improve the metabolite transport efficiency.

Author Contributions: Y.Z. and A.R.F. wrote the manuscript and both agreed to the published version of the manuscript.

Funding: A.R.F. and Y.Z. would like to thank the European Union’s Horizon 2020 research and innovation programme, project PlantaSYST (SGA-CSA No. 739582 under FPA No. 664620) for supporting their research.

Conflicts of Interest: The authors declare no conflict of interest.

References

1. Zhang, Y.; Fernie, A.R. On the role of the tricarboxylic acid cycle in plant productivity. *J. Integr. Plant Biol.* **2018**, *60*, 1199–1216. [CrossRef] [PubMed]
2. Liang, C.; Cheng, S.; Zhang, Y.; Sun, Y.; Fernie, A.R.; Kang, K.; Panagiotou, G.; Lo, C.; Lim, B.L. Transcriptomic, proteomic and metabolic changes in arabidopsis thaliana leaves after the onset of illumination. *BMC Plant Biol.* **2016**, *16*, 43. [CrossRef] [PubMed]

3. Gueguen, V.; Macherel, D.; Jaquinod, M.; Douce, R.; Bourguignon, J. Fatty acid and lipoic acid biosynthesis in higher plant mitochondria. *J. Biol. Chem.* **2000**, *275*, 5016–5025. [CrossRef]
4. Fernie, A.R.; Zhang, Y.; Sweetlove, L.J. Passing the baton: Substrate channelling in respiratory metabolism. *Research* **2018**, *2018*, 1539325. [CrossRef] [PubMed]
5. Linka, M.; Weber, A.P. Shuffling ammonia between mitochondria and plastids during photorespiration. *Trends Plant Sci.* **2005**, *10*, 461–465. [CrossRef] [PubMed]
6. Graham, J.W.; Williams, T.C.; Morgan, M.; Fernie, A.R.; Ratcliffe, R.G.; Sweetlove, L.J. Glycolytic enzymes associate dynamically with mitochondria in response to respiratory demand and support substrate channeling. *Plant Cell* **2007**, *19*, 3723–3738. [CrossRef] [PubMed]
7. Monné, M.; Miniero, D.V.; Obata, T.; Daddabbo, L.; Palmieri, L.; Voza, A.; Nicolardi, M.C.; Fernie, A.R.; Palmieri, F. Functional characterization and organ distribution of three mitochondrial atp-mg/pi carriers in arabidopsis thaliana. *Biochim. Biophys. Acta BBA Bioenerg.* **2015**, *1847*, 1220–1230. [CrossRef] [PubMed]
8. Edwards, G.E.; Franceschi, V.R.; Ku, M.S.B.; Voznesenskaya, E.V.; Pyankov, V.I.; Andreo, C.S. Compartmentation of photosynthesis in cells and tissues of c4 plants. *J. Exp. Bot.* **2001**, *52*, 577–590. [CrossRef]
9. Pastorino, J.G.; Hoek, J.B. Regulation of hexokinase binding to v_oac. *J. Bioenerg. Biomembr.* **2008**, *40*, 171–182. [CrossRef]
10. Kanwar, P.; Samtani, H.; Sanyal, S.K.; Srivastava, A.K.; Suprasanna, P.; Pandey, G.K. V_oac and its interacting partners in plant and animal systems: An overview. *Crit. Rev. Biotechnol.* **2020**, *40*, 715–732. [CrossRef]
11. Becker, T.; Vögtle, F.-N.; Stojanovski, D.; Meisinger, C. Sorting and assembly of mitochondrial outer membrane proteins. *Biochim. Biophys. Acta BBA Bioenerg.* **2008**, *1777*, 557–563. [CrossRef] [PubMed]
12. Becker, T.; Wagner, R. Mitochondrial outer membrane channels: Emerging diversity in transport processes. *BioEssays* **2018**, *40*, 1800013. [CrossRef] [PubMed]
13. Krüger, V.; Becker, T.; Becker, L.; Montilla-Martinez, M.; Ellenrieder, L.; Vögtle, F.-N.; Meyer, H.E.; Ryan, M.T.; Wiedemann, N.; Warscheid, B. Identification of new channels by systematic analysis of the mitochondrial outer membrane. *J. Cell Biol.* **2017**, *216*, 3485–3495. [CrossRef] [PubMed]
14. Vašková, J.; Fírent, J.; Vaško, L. Nuclear Encoded Mitochondrial Proteins in Metabolite Transport and Oxidation Pathway Connecting Metabolism of Nutrients. In *Mitochondrial Diseases*; IntechOpen: London, UK, 2018; pp. 251–289.
15. Neupert, W.; Brunner, M. The protein import motor of mitochondria. *Nat. Rev. Mol. Cell Biol.* **2002**, *3*, 555–565. [CrossRef]
16. Palmieri, F. Mitochondrial carrier proteins. *FEBS Lett.* **1994**, *346*, 48–54. [CrossRef]
17. Palmieri, F. The mitochondrial transporter family slc25: Identification, properties and physiopathology. *Mol. Asp. Med.* **2013**, *34*, 465–484. [CrossRef]
18. Toleco, M.R.; Naake, T.; Zhang, Y.J.; Heazlewood, J.L.; Fernie, A.R. Plant mitochondrial carriers: Molecular gatekeepers that help to regulate plant central carbon metabolism. *Plants* **2020**, *9*, 117. [CrossRef]
19. Saraste, M.; Walker, J.E. Internal sequence repeats and the path of polypeptide in mitochondrial adp/atp translocase. *FEBS Lett.* **1982**, *144*, 250–254. [CrossRef]
20. Palmieri, F.; Bisaccia, F.; Capobianco, L.; Dolce, V.; Fiermonte, G.; Iacobazzi, V.; Zara, V. Transmembrane topology, genes, and biogenesis of the mitochondrial phosphate and oxoglutarate carriers. *J. Bioenerg. Biomembr.* **1993**, *25*, 493–501. [CrossRef]
21. Bisaccia, F.; Capobianco, L.; Brandolin, G.; Palmieri, F. Transmembrane topography of the mitochondrial oxoglutarate carrier assessed by peptide-specific antibodies and enzymic cleavage. *Biochemistry* **1994**, *33*, 3705–3713. [CrossRef]
22. Pebay-Peyroula, E.; Dahout-Gonzalez, C.; Kahn, R.; Trézéguet, V.; Lauquin, G.J.-M.; Brandolin, G. Structure of mitochondrial adp/atp carrier in complex with carboxyatractyloside. *Nature* **2003**, *426*, 39–44. [CrossRef] [PubMed]
23. Palmieri, F.; Monné, M. Discoveries, metabolic roles and diseases of mitochondrial carriers: A review. *Biochim. Biophys. Acta BBA Mol. Cell Res.* **2016**, *1863*, 2362–2378. [CrossRef] [PubMed]
24. Monné, M.; Voza, A.; Lasorsa, F.M.; Porcelli, V.; Palmieri, F. Mitochondrial carriers for aspartate, glutamate and other amino acids: A review. *Int. J. Mol. Sci.* **2019**, *20*, 4456. [CrossRef]

25. Kunji, E.R.; Aleksandrova, A.; King, M.S.; Majd, H.; Ashton, V.L.; Cerson, E.; Springett, R.; Kibalchenko, M.; Tavoulari, S.; Crichton, P.G. The transport mechanism of the mitochondrial adp/atp carrier. *Biochim. Biophys. Acta BBA Mol. Cell Res.* **2016**, *1863*, 2379–2393. [CrossRef]
26. Palmieri, F.; Pierri, C.L.; De Grassi, A.; Nunes-Nesi, A.; Fernie, A.R. Evolution, structure and function of mitochondrial carriers: A review with new insights. *Plant J.* **2011**, *66*, 161–181. [CrossRef] [PubMed]
27. Ruprecht, J.J.; King, M.S.; Zögg, T.; Aleksandrova, A.A.; Pardon, E.; Crichton, P.G.; Steyaert, J.; Kunji, E.R.S. The molecular mechanism of transport by the mitochondrial adp/atp carrier. *Cell* **2019**, *176*, 435–447. [CrossRef]
28. Springett, R.; King, M.S.; Crichton, P.G.; Kunji, E.R.S. Modelling the free energy profile of the mitochondrial adp/atp carrier. *Biochim. Biophys. Acta Bioenerg.* **2017**, *1858*, 906–914. [CrossRef]
29. Klingenberg, M. The adp, atp shuttle of the mitochondrion. *Trends Biochem. Sci.* **1979**, *4*, 249–252. [CrossRef]
30. Klingenberg, M. The adp and atp transport in mitochondria and its carrier. *Biochim. Biophys. Acta BBA Biomembr.* **2008**, *1778*, 1978–2021. [CrossRef]
31. Indiveri, C.; Tonazzi, A.; Palmieri, F. The reconstituted carnitine carrier from rat liver mitochondria: Evidence for a transport mechanism different from that of the other mitochondrial translocators. *Biochim. Biophys. Acta BBA Biomembr.* **1994**, *1189*, 65–73. [CrossRef]
32. Palmieri, F.; Pierri, C.L. Mitochondrial metabolite transport. *Essays Biochem.* **2010**, *47*, 37–52. [PubMed]
33. Pietropaolo, A.; Pierri, C.L.; Palmieri, F.; Klingenberg, M. The switching mechanism of the mitochondrial adp/atp carrier explored by free-energy landscapes. *Biochim. Biophys. Acta BBA Bioenerg.* **2016**, *1857*, 772–781. [CrossRef] [PubMed]
34. Ruprecht, J.J.; Kunji, E.R. The slc25 mitochondrial carrier family: Structure and mechanism. *Trends Biochem. Sci.* **2019**, *45*, 244–258. [CrossRef] [PubMed]
35. Palmieri, F. Mitochondrial transporters of the slc25 family and associated diseases: A review. *J. Inherit. Metab. Dis.* **2014**, *37*, 565–575. [CrossRef]
36. Monne, M.; Palmieri, F. Antiporters of the mitochondrial carrier family. In *Current Topics in Membranes*; Bevensee, M.O., Ed.; Elsevier: Amsterdam, The Netherlands, 2014; Volume 73, pp. 289–320.
37. Kunji, E.R.; Crichton, P.G. Mitochondrial carriers function as monomers. *Biochim. Biophys. Acta BBA Bioenerg.* **2010**, *1797*, 817–831. [CrossRef]
38. Bamber, L.; Harding, M.; Monné, M.; Slotboom, D.-J.; Kunji, E.R. The yeast mitochondrial adp/atp carrier functions as a monomer in mitochondrial membranes. *Proc. Natl. Acad. Sci. USA* **2007**, *104*, 10830–10834. [CrossRef]
39. Palmieri, L.; Pardo, B.; Lasorsa, F.M.; del Arco, A.; Kobayashi, K.; Iijima, M.; Runswick, M.J.; Walker, J.E.; Saheki, T.; Satrustegui, J.; et al. Citrin and aralar1 are ca²⁺-stimulated aspartate/glutamate transporters in mitochondria. *EMBO J.* **2001**, *20*, 5060–5069. [CrossRef]
40. Lasorsa, F.M.; Pinton, P.; Palmieri, L.; Fiermonte, G.; Rizzuto, R.; Palmieri, F. Recombinant expression of the ca²⁺-sensitive aspartate/glutamate carrier increases mitochondrial atp production in agonist-stimulated chinese hamster ovary cells. *J. Biol. Chem.* **2003**, *278*, 38686–38692. [CrossRef]
41. Thangaratnarajah, C.; Ruprecht, J.J.; Kunji, E.R. Calcium-induced conformational changes of the regulatory domain of human mitochondrial aspartate/glutamate carriers. *Nat. Commun.* **2014**, *5*, 1–12. [CrossRef]
42. Compan, V.; Pierredon, S.; Vanderperre, B.; Krznar, P.; Marchiq, I.; Zamboni, N.; Pouyssegur, J.; Martinou, J.-C. Monitoring mitochondrial pyruvate carrier activity in real time using a bret-based biosensor: Investigation of the warburg effect. *Mol. Cell* **2015**, *59*, 491–501. [CrossRef]
43. van der Giezen, M.; Slotboom, D.J.; Horner, D.S.; Dyal, P.L.; Harding, M.; Xue, G.P.; Embley, T.M.; Kunji, E.R.S. Conserved properties of hydrogenosomal and mitochondrial adp/atp carriers: A common origin for both organelles. *EMBO J.* **2002**, *21*, 572–579. [CrossRef] [PubMed]
44. Leroch, M.; Neuhaus, H.E.; Kirchberger, S.; Zimmermann, S.; Melzer, M.; Gerhold, J.; Tjaden, J. Identification of a novel adenine nucleotide transporter in the endoplasmic reticulum of arabidopsis. *Plant Cell* **2008**, *20*, 438–451. [CrossRef] [PubMed]
45. Palmieri, L.; Santoro, A.; Carrari, F.; Blanco, E.; Nunes-Nesi, A.; Arrigoni, R.; Genchi, F.; Fernie, A.R.; Palmieri, F. Identification and characterization of adnt1, a novel mitochondrial adenine nucleotide transporter from arabidopsis. *Plant Physiol.* **2008**, *148*, 1797–1808. [CrossRef] [PubMed]
46. Belzacq, A.-S.; Vieira, H.L.; Kroemer, G.; Brenner, C. The adenine nucleotide translocator in apoptosis. *Biochimie* **2002**, *84*, 167–176. [CrossRef]

47. Lançar-Benba, J.; Foucher, B.; Saint-Macary, M. Purification of the rat-liver mitochondrial dicarboxylate carrier by affinity chromatography on immobilized malate dehydrogenase. *Biochim. Biophys. Acta BBA Biomembr.* **1994**, *1190*, 213–216. [CrossRef]
48. Krause, F. Detection and analysis of protein–protein interactions in organellar and prokaryotic proteomes by native gel electrophoresis:(membrane) protein complexes and supercomplexes. *Electrophoresis* **2006**, *27*, 2759–2781. [CrossRef]
49. Zhang, Y.; Fernie, A.R. Stable and temporary enzyme complexes and metabolons involved in energy and redox metabolism. *Antioxid. Redox Signal.* **2020**. [CrossRef]
50. Kim, D.-H.; Park, S.; Kim, D.-K.; Jeong, M.G.; Noh, J.; Kwon, Y.; Zhou, K.; Lee, N.K.; Ryu, S.H. Direct visualization of single-molecule membrane protein interactions in living cells. *PLoS Biol.* **2018**, *16*, e2006660. [CrossRef]
51. Moore, D.T.; Berger, B.W.; DeGrado, W.F. Protein-protein interactions in the membrane: Sequence, structural, and biological motifs. *Structure* **2008**, *16*, 991–1001. [CrossRef]
52. Stansfeld, P.J. Computational studies of membrane proteins: From sequence to structure to simulation. *Curr. Opin. Struct. Biol.* **2017**, *45*, 133–141. [CrossRef]
53. Shimizu, K.; Cao, W.; Saad, G.; Shoji, M.; Terada, T. Comparative analysis of membrane protein structure databases. *Biochim. Biophys. Acta BBA Biomembr.* **2018**, *1860*, 1077–1091. [CrossRef] [PubMed]
54. Koshiba, T. Protein-protein interactions of mitochondrial-associated protein via bioluminescence resonance energy transfer. *Biophys. Phys.* **2015**, *12*, 31–35. [CrossRef] [PubMed]
55. Sasaki, O.; Yoshizumi, T.; Kuboyama, M.; Ishihara, T.; Suzuki, E.; Kawabata, S.-i.; Koshiba, T. A structural perspective of the mavs-regulatory mechanism on the mitochondrial outer membrane using bioluminescence resonance energy transfer. *Biochim. Biophys. Acta BBA Mol. Cell Res.* **2013**, *1833*, 1017–1027. [CrossRef] [PubMed]
56. Baril, M.; Racine, M.-E.; Penin, F.; Lamarre, D. Mavs dimer is a crucial signaling component of innate immunity and the target of hepatitis c virus ns3/4a protease. *J. Virol.* **2009**, *83*, 1299–1311. [CrossRef]
57. Bender, T.; Pena, G.; Martinou, J.C. Regulation of mitochondrial pyruvate uptake by alternative pyruvate carrier complexes. *EMBO J.* **2015**, *34*, 911–924. [CrossRef]
58. Fernie, A.R.; Zhang, Y.; Sampathkumar, A. Cytoskeleton architecture regulates glycolysis coupling cellular metabolism to mechanical cues. *Trends Biochem. Sci.* **2020**. [CrossRef]
59. Park, J.S.; Burckhardt, C.J.; Lazcano, R.; Solis, L.M.; Isogai, T.; Li, L.; Chen, C.S.; Gao, B.; Minna, J.D.; Bachoo, R. Mechanical regulation of glycolysis via cytoskeleton architecture. *Nature* **2020**, *578*, 621–626. [CrossRef]
60. Carriba, P.; Navarro, G.; Ciruela, F.; Ferré, S.; Casadó, V.; Agnati, L.; Cortés, A.; Mallol, J.; Fuxe, K.; Canela, E. Detection of heteromerization of more than two proteins by sequential bret-fret. *Nat. Methods* **2008**, *5*, 727. [CrossRef]
61. Crichton, P.G.; Harding, M.; Ruprecht, J.J.; Lee, Y.; Kunji, E.R. Lipid, detergent, and coomassie blue g-250 affect the migration of small membrane proteins in blue native gels mitochondrial carriers migrate as monomers not dimers. *J. Biol. Chem.* **2013**, *288*, 22163–22173. [CrossRef]
62. Bricker, D.K.; Taylor, E.B.; Schell, J.C.; Orsak, T.; Boutron, A.; Chen, Y.-C.; Cox, J.E.; Cardon, C.M.; Van Vranken, J.G.; Dephoure, N. A mitochondrial pyruvate carrier required for pyruvate uptake in yeast, drosophila, and humans. *Science* **2012**, *337*, 96–100. [CrossRef]
63. Eubel, H.; Braun, H.-P.; Millar, A. Blue-native page in plants: A tool in analysis of protein-protein interactions. *Plant Methods* **2005**, *1*, 11. [CrossRef] [PubMed]
64. Rampelt, H.; Sucec, I.; Bersch, B.; Horten, P.; Perschil, I.; Martinou, J.-C.; van der Laan, M.; Wiedemann, N.; Schanda, P.; Pfanner, N. The mitochondrial carrier pathway transports non-canonical substrates with an odd number of transmembrane segments. *BMC Biol.* **2020**, *18*, 1–14. [CrossRef] [PubMed]
65. Kunji, E.R.; Harding, M.; Butler, P.J.G.; Akamine, P. Determination of the molecular mass and dimensions of membrane proteins by size exclusion chromatography. *Methods* **2008**, *46*, 62–72. [CrossRef]
66. Jha, P.; Wang, X.; Auwerx, J. Analysis of mitochondrial respiratory chain supercomplexes using blue native polyacrylamide gel electrophoresis (bn-page). *Curr. Protoc. Mouse Biol.* **2016**, *6*, 1–14. [CrossRef]
67. Palmisano, A.; Zara, V.; Honlinger, A.; Voza, A.; Dekker, P.J.; Pfanner, N.; Palmieri, F. Targeting and assembly of the oxoglutarate carrier: General principles for biogenesis of carrier proteins of the mitochondrial inner membrane. *Biochem. J.* **1998**, *333*, 151–158. [CrossRef] [PubMed]

68. Palmieri, L.; Vozza, A.; Hönlinger, A.; Dietmeier, K.; Palmisano, A.; Zara, V.; Palmieri, F. The mitochondrial dicarboxylate carrier is essential for the growth of *saccharomyces cerevisiae* on ethanol or acetate as the sole carbon source. *Mol. Microbiol.* **1999**, *31*, 569–577. [CrossRef] [PubMed]
69. Capobianco, L.; Ferramosca, A.; Zara, V. The mitochondrial tricarboxylate carrier of silver eel: Dimeric structure and cytosolic exposure of both n-and c-termini. *J. Protein Chem.* **2002**, *21*, 515–521. [CrossRef]
70. Tavoulari, S.; Thangaratnarajah, C.; Mavridou, V.; Harbour, M.E.; Martinou, J.C.; Kunji, E.R. The yeast mitochondrial pyruvate carrier is a hetero-dimer in its functional state. *EMBO J.* **2019**, *38*, e100785. [CrossRef]
71. Zhang, Y.; Skirycz, A.; Fernie, A.R. An abundance and interaction encyclopedia of plant protein function. *Trends Plant Sci.* **2020**, *25*, 627–630. [CrossRef]
72. McWhite, C.D.; Papoulas, O.; Drew, K.; Cox, R.M.; June, V.; Dong, O.X.; Kwon, T.; Wan, C.; Salmi, M.L.; Roux, S.J. A pan-plant protein complex map reveals deep conservation and novel assemblies. *Cell* **2020**, *181*, 460–474. [CrossRef]
73. Villa, A.; García-Simón, M.I.; Blanco, P.; Sesé, B.; Bogónez, E.; Satrustegui, J. Affinity chromatography purification of mitochondrial inner membrane proteins with calcium transport activity. *Biochim. Biophys. Acta BBA Biomembr.* **1998**, *1373*, 347–359. [CrossRef]
74. Schroers, A.; Burkovski, A.; Wohlrab, H.; Krämer, R. The phosphate carrier from yeast mitochondria dimerization is a prerequisite for function. *J. Biol. Chem.* **1998**, *273*, 14269–14276. [CrossRef] [PubMed]
75. Zhang, Y.; Swart, C.; Aseeikh, S.; Scossa, F.; Jiang, L.; Obata, T.; Graf, A.; Fernie, A.R. The extra-pathway interactome of the tca cycle: Expected and unexpected metabolic interactions. *Plant Physiol.* **2018**, *177*, 966–979. [CrossRef] [PubMed]
76. Zhang, Y.; Beard, K.F.; Swart, C.; Bergmann, S.; Krahnert, I.; Nikoloski, Z.; Graf, A.; Ratcliffe, R.G.; Sweetlove, L.J.; Fernie, A.R. Protein-protein interactions and metabolite channelling in the plant tricarboxylic acid cycle. *Nat. Commun.* **2017**, *8*, 1–11. [CrossRef] [PubMed]
77. Zhang, Y.; Natale, R.; Domingues, A.P.; Toleco, M.R.; Siemiatkowska, B.; Fàbregas, N.; Fernie, A.R. Rapid identification of protein-protein interactions in plants. *Curr. Protoc. Plant Biol.* **2019**, *4*, e20099. [CrossRef] [PubMed]
78. Zhang, Y.; Chen, M.; Siemiatkowska, B.; Toleco, M.R.; Jing, Y.; Strotmann, V.; Zhang, J.; Stahl, Y.; Fernie, A.R. A highly efficient agrobacterium-mediated method for transient gene expression and functional studies in multiple plant species. *Plant Commun.* **2020**, 100028. [CrossRef]
79. Makowski, M.M.; Willems, E.; Jansen, P.W.; Vermeulen, M. Cross-linking immunoprecipitation-ms (xip-ms): Topological analysis of chromatin-associated protein complexes using single affinity purification. *Mol. Cell. Proteom.* **2016**, *15*, 854–865. [CrossRef]
80. Zhang, Y.; Fernie, A.R. Evidence for metabolons—Enzyme-enzyme assemblies that mediate substrate channeling—And their roles in plants. *Plant Commun.* **2020**, *1*, 100081. [CrossRef]
81. Liu, F.; Rijkers, D.T.; Post, H.; Heck, A.J. Proteome-wide profiling of protein assemblies by cross-linking mass spectrometry. *Nat. Methods* **2015**, *12*, 1179–1184. [CrossRef]
82. Liu, F.; Lössl, P.; Rabbitts, B.M.; Balaban, R.S.; Heck, A.J. The interactome of intact mitochondria by cross-linking mass spectrometry provides evidence for coexisting respiratory supercomplexes. *Mol. Cell. Proteom.* **2018**, *17*, 216–232. [CrossRef]
83. Schweppe, D.K.; Chavez, J.D.; Lee, C.F.; Caudal, A.; Kruse, S.E.; Stuppard, R.; Marcinek, D.J.; Shadel, G.S.; Tian, R.; Bruce, J.E. Mitochondrial protein interactome elucidated by chemical cross-linking mass spectrometry. *Proc. Natl. Acad. Sci. USA* **2017**, *114*, 1732–1737. [CrossRef] [PubMed]
84. Back, J.W.; Sanz, M.A.; de Jong, L.; de Koning, L.J.; Nijtmans, L.G.; de Koster, C.G.; Grivell, L.A.; van der Spek, H.; Muijsers, A.O. A structure for the yeast prohibitin complex: Structure prediction and evidence from chemical crosslinking and mass spectrometry. *Protein Sci.* **2002**, *11*, 2471–2478. [CrossRef] [PubMed]
85. Majima, E.; Takeda, M.; Miki, S.; Shinohara, Y.; Terada, H. Close location of the first loop to the third loop of the mitochondrial adp/atp carrier deduced from cross-linking catalyzed by copper-o-phenanthroline of the solubilized carrier with triton x-100. *J. Biochem.* **2002**, *131*, 461–468. [CrossRef]
86. Klengenber, M.; Appel, M. The uncoupling protein dimer can form a disulfide cross-link between the mobile c-terminal sh groups. *Eur. J. Biochem.* **1989**, *180*, 123–131. [CrossRef]
87. Bisaccia, F.; Zara, V.; Capobianco, L.; Iacobazzi, V.; Mazzeo, M.; Palmieri, F. The formation of a disulfide cross-link between the two subunits demonstrates the dimeric structure of the mitochondrial oxoglutarate carrier. *Biochim. Biophys. Acta BBA Protein Struct. Mol. Enzymol.* **1996**, *1292*, 281–288. [CrossRef]

88. Varnaité, R.; MacNeill, S.A. Meet the neighbors: Mapping local protein interactomes by proximity-dependent labeling with bioid. *Proteomics* **2016**, *16*, 2503–2518. [CrossRef]
89. Roux, K.J.; Kim, D.I.; Raida, M.; Burke, B. A promiscuous biotin ligase fusion protein identifies proximal and interacting proteins in mammalian cells. *J. Cell Biol.* **2012**, *196*, 801–810. [CrossRef]
90. Koshiba, T.; Kosako, H. Mass spectrometry-based methods for analysing the mitochondrial interactome in mammalian cells. *J. Biochem.* **2020**, *167*, 225–231. [CrossRef]
91. Yoshinaka, T.; Kosako, H.; Yoshizumi, T.; Furukawa, R.; Hirano, Y.; Kuge, O.; Tamada, T.; Koshiba, T. Structural basis of mitochondrial scaffolds by prohibitin complexes: Insight into a role of the coiled-coil region. *iScience* **2019**, *19*, 1065–1078. [CrossRef]
92. Lemasters, J.J.; Holmuhamedov, E. Voltage-dependent anion channel (vdac) as mitochondrial governor—Thinking outside the box. *Biochim. Biophys. Acta BBA Mol. Basis Dis.* **2006**, *1762*, 181–190. [CrossRef]
93. Maldonado, E.N.; Lemasters, J.J. Warburg revisited: Regulation of mitochondrial metabolism by voltage-dependent anion channels in cancer cells. *J. Pharmacol. Exp. Ther.* **2012**, *342*, 637–641. [CrossRef]
94. Krasnov, G.S.; Dmitriev, A.A.; Lakunina, V.A.; Kirpiy, A.A.; Kudryavtseva, A.V. Targeting vdac-bound hexokinase ii: A promising approach for concomitant anti-cancer therapy. *Expert Opin. Ther. Targets* **2013**, *17*, 1221–1233. [CrossRef] [PubMed]
95. Dolder, M.; Wendt, S.; Wallimann, T. Mitochondrial creatine kinase in contact sites: Interaction with porin and adenine nucleotide translocase, role in permeability transition and sensitivity to oxidative damage. *Neurosignals* **2001**, *10*, 93–111. [CrossRef]
96. Lee, C.P.; Millar, A.H. The plant mitochondrial transportome: Balancing metabolic demands with energetic constraints. *Trends Plant Sci.* **2016**, *21*, 662–676. [CrossRef]
97. Ruprecht, J.J.; Hellowell, A.M.; Harding, M.; Crichton, P.G.; McCoy, A.J.; Kunji, E.R. Structures of yeast mitochondrial adp/atp carriers support a domain-based alternating-access transport mechanism. *Proc. Natl. Acad. Sci. USA* **2014**, *111*, E426–E434. [CrossRef]
98. Falconi, M.; Chillemi, G.; Di Marino, D.; D’Annessa, I.; Morozzo della Rocca, B.; Palmieri, L.; Desideri, A. Structural dynamics of the mitochondrial adp/atp carrier revealed by molecular dynamics simulation studies. *Proteins Struct. Funct. Bioinform.* **2006**, *65*, 681–691. [CrossRef] [PubMed]
99. Claypool, S.M.; Oktay, Y.; Boontheung, P.; Loo, J.A.; Koehler, C.M. Cardiolipin defines the interactome of the major adp/atp carrier protein of the mitochondrial inner membrane. *J. Cell Biol.* **2008**, *182*, 937–950. [CrossRef]
100. Halestrap, A.P.; McStay, G.P.; Clarke, S.J. The permeability transition pore complex: Another view. *Biochimie* **2002**, *84*, 153–166. [CrossRef]
101. Kokoszka, J.E.; Waymire, K.G.; Levy, S.E.; Sligh, J.E.; Cai, J.; Jones, D.P.; MacGregor, G.R.; Wallace, D.C. The adp/atp translocator is not essential for the mitochondrial permeability transition pore. *Nature* **2004**, *427*, 461–465. [CrossRef]
102. Ko, Y.H.; Delannoy, M.; Hüllihen, J.; Chiu, W.; Pedersen, P.L. Mitochondrial atp synthasome cristae-enriched membranes and a multiwell detergent screening assay yield dispersed single complexes containing the atp synthase and carriers for pi and adp/atp. *J. Biol. Chem.* **2003**, *278*, 12305–12309. [CrossRef]
103. Davies, K.M.; Anselmi, C.; Wittig, I.; Faraldo-Gómez, J.D.; Kühlbrandt, W. Structure of the yeast f1fo-atp synthase dimer and its role in shaping the mitochondrial cristae. *Proc. Natl. Acad. Sci. USA* **2012**, *109*, 13602–13607. [CrossRef] [PubMed]
104. Galber, C.; Valente, G.; von Stockum, S.; Giorgio, V. Purification of Functional f-atp Synthase from Blue Native Page. In *Calcium Signalling*; Springer: Berlin/Heidelberg, Germany, 2019; pp. 233–243.
105. Dienhart, M.K.; Stuart, R.A. The yeast aac2 protein exists in physical association with the cytochrome bc1-cox supercomplex and the tim23 machinery. *Mol. Biol. Cell* **2008**, *19*, 3934–3943. [CrossRef] [PubMed]
106. Mehnert, C.S.; Rampelt, H.; Gebert, M.; Oeljeklaus, S.; Schrempp, S.G.; Kochbeck, L.; Guiard, B.; Warscheid, B.; van der Laan, M. The mitochondrial adp/atp carrier associates with the inner membrane presequence translocase in a stoichiometric manner. *J. Biol. Chem.* **2014**, *289*, 27352–27362. [CrossRef] [PubMed]
107. Miniero, D.V.; Cappello, A.R.; Curcio, R.; Ludovico, A.; Daddabbo, L.; Stipani, I.; Robinson, A.J.; Kunji, E.R.; Palmieri, F. Functional and structural role of amino acid residues in the matrix α -helices, termini and cytosolic loops of the bovine mitochondrial oxoglutarate carrier. *Biochim. Biophys. Acta BBA Bioenerg.* **2011**, *1807*, 302–310. [CrossRef] [PubMed]

108. Sweetlove, L.J.; Lytovchenko, A.; Morgan, M.; Nunes-Nesi, A.; Taylor, N.L.; Baxter, C.J.; Eickmeier, I.; Fernie, A.R. Mitochondrial uncoupling protein is required for efficient photosynthesis. *Proc. Natl. Acad. Sci. USA* **2006**, *103*, 19587–19592. [CrossRef] [PubMed]
109. Smith, A.M.; Ratcliffe, R.G.; Sweetlove, L.J. Activation and function of mitochondrial uncoupling protein in plants. *J. Biol. Chem.* **2004**, *279*, 51944–51952. [CrossRef]
110. Monné, M.; Daddabbo, L.; Gagneul, D.; Obata, T.; Hielscher, B.; Palmieri, L.; Miniero, D.V.; Fernie, A.R.; Weber, A.P.M.; Palmieri, F. Uncoupling proteins 1 and 2 (ucp1 and ucp2) from *Arabidopsis thaliana* are mitochondrial transporters of aspartate, glutamate, and dicarboxylates. *J. Biol. Chem.* **2018**, *293*, 4213–4227. [CrossRef]
111. Palmieri, F.; Quagliariello, E.; Klingenberg, M. Quantitative correlation between the distribution of anions and the pH difference across the mitochondrial membrane. *Eur. J. Biochem.* **1970**, *17*, 230–238. [CrossRef]
112. Fiermonte, G.; Dolce, V.; Palmieri, F. Expression in *Escherichia coli*, functional characterization, and tissue distribution of isoforms a and b of the phosphate carrier from bovine mitochondria. *J. Biol. Chem.* **1998**, *273*, 22782–22787. [CrossRef]
113. Leung, A.W.; Varanyuwatana, P.; Halestrap, A.P. The mitochondrial phosphate carrier interacts with cyclophilin d and may play a key role in the permeability transition. *J. Biol. Chem.* **2008**, *283*, 26312–26323. [CrossRef]
114. García-Valencia, L.E.; Bravo-Alberto, C.E.; Wu, H.-M.; Rodríguez-Sotres, R.; Cheung, A.Y.; Cruz-García, F. Sipp, a novel mitochondrial phosphate carrier, mediates in self-incompatibility. *Plant Physiol.* **2017**, *175*, 1105–1120. [CrossRef]
115. Srere, P.A. The metabolon. *Trends Biochem. Sci.* **1985**, *10*, 109–110. [CrossRef]
116. Vélot, C.; Mixon, M.B.; Teige, M.; Srere, P.A. Model of a quinary structure between krebs tca cycle enzymes: A model for the metabolon. *Biochemistry* **1997**, *36*, 14271–14276. [CrossRef] [PubMed]
117. Palmieri, F.; Stipani, I.; Quagliariello, E.; Klingenberg, M. Kinetic study of the tricarboxylate carrier in rat liver mitochondria. *Eur. J. Biochem.* **1972**, *26*, 587–594. [CrossRef] [PubMed]
118. Bisaccia, F.; De Palma, A.; Palmieri, F. Identification and purification of the tricarboxylate carrier from rat liver mitochondria. *Biochim. Biophys. Acta BBA Bioenerg.* **1989**, *977*, 171–176. [CrossRef]
119. Bisaccia, F.; De Palma, A.; Dierks, T.; Krämer, R.; Palmieri, F. Reaction mechanism of the reconstituted tricarboxylate carrier from rat liver mitochondria. *Biochim. Biophys. Acta BBA Bioenerg.* **1993**, *1142*, 139–145. [CrossRef]
120. Lin, C.; Hackenberg, H.; Klingenberg, E. The uncoupling protein from brown adipose tissue mitochondria is a dimer. A hydrodynamic study. *FEBS Lett.* **1980**, *113*, 304–306. [CrossRef]
121. Jakobs, P.; Braun, A.; Jezek, P.; Trommer, W. Binding of ATP to uncoupling protein of brown fat mitochondria as studied by means of spin-labeled ATP derivatives. *FEBS Lett.* **1991**, *284*, 195–198. [CrossRef]
122. Winkler, E.; Klingenberg, M. Photoaffinity labeling of the nucleotide-binding site of the uncoupling protein from hamster brown adipose tissue. *Eur. J. Biochem.* **1992**, *203*, 295–304. [CrossRef]
123. Lee, Y.; Willers, C.; Kunji, E.R.; Crichton, P.G. Uncoupling protein 1 binds one nucleotide per monomer and is stabilized by tightly bound cardiolipin. *Proc. Natl. Acad. Sci. USA* **2015**, *112*, 6973–6978. [CrossRef]
124. Crichton, P.G.; Lee, Y.; Kunji, E.R. The molecular features of uncoupling protein 1 support a conventional mitochondrial carrier-like mechanism. *Biochimie* **2017**, *134*, 35–50. [CrossRef]
125. Arriza, J.L.; Eliasof, S.; Kavanaugh, M.P.; Amara, S.G. Excitatory amino acid transporter 5, a retinal glutamate transporter coupled to a chloride conductance. *Proc. Natl. Acad. Sci. USA* **1997**, *94*, 4155–4160. [CrossRef] [PubMed]
126. Menga, A.; Iacobazzi, V.; Infantino, V.; Avantaggiati, M.L.; Palmieri, F. The mitochondrial aspartate/glutamate carrier isoform 1 gene expression is regulated by CREB in neuronal cells. *Int. J. Biochem. Cell Biol.* **2015**, *60*, 157–166. [CrossRef] [PubMed]
127. Wilkins, H.M.; Marquardt, K.; Lash, L.H.; Linseman, D.A. Bcl-2 is a novel interacting partner for the 2-oxoglutarate carrier and a key regulator of mitochondrial glutathione. *Free Radic. Biol. Med.* **2012**, *52*, 410–419. [CrossRef] [PubMed]

128. Brandina, I.; Graham, J.; Lemaitre-Guillier, C.; Entelis, N.; Krasheninnikov, I.; Sweetlove, L.; Tarassov, I.; Martin, R.P. Enolase takes part in a macromolecular complex associated to mitochondria in yeast. *Biochim. Biophys. Acta BBA Bioenerg.* **2006**, *1757*, 1217–1228. [CrossRef] [PubMed]
129. Jang, S.; Nelson, J.C.; Bend, E.G.; Rodríguez-Laureano, L.; Tueros, F.G.; Cartagenova, L.; Underwood, K.; Jorgensen, E.M.; Colón-Ramos, D.A. Glycolytic enzymes localize to synapses under energy stress to support synaptic function. *Neuron* **2016**, *90*, 278–291. [CrossRef] [PubMed]



© 2020 by the authors. Licensee MDPI, Basel, Switzerland. This article is an open access article distributed under the terms and conditions of the Creative Commons Attribution (CC BY) license (<http://creativecommons.org/licenses/by/4.0/>).

Review

AGC2 (Citrin) Deficiency—From Recognition of the Disease till Construction of Therapeutic Procedures

Takeyori Saheki ^{1,*}, Mitsuaki Moriyama ², Aki Funahashi ¹ and Eishi Kuroda ¹

¹ Department of Hygiene and Health Promotion Medicine, Kagoshima University Graduate School of Medical and Dental Sciences, 8-35-1 Sakuragaoka, Kagoshima 890-8544, Japan; aki.2784@gmail.com (A.F.); kurodaeishi1029@yahoo.co.jp (E.K.)

² Laboratory of Integrative Physiology in Veterinary Sciences, Osaka Prefecture University, 1-58 Rinku-oraikita, Izumisano, Osaka 598-8531, Japan; moriyama@vet.osakafu-u.ac.jp

* Correspondence: takesah@gmail.com; Tel.: +81-99-275-5291

Academic Editor: Ferdinando Palmieri

Received: 4 June 2020; Accepted: 19 July 2020; Published: 24 July 2020

Abstract: Can you imagine a disease in which intake of an excess amount of sugars or carbohydrates causes hyperammonemia? It is hard to imagine the intake causing hyperammonemia. AGC2 or citrin deficiency shows their symptoms following sugar/carbohydrates intake excess and this disease is now known as a pan-ethnic disease. AGC2 (aspartate glutamate carrier 2) or citrin is a mitochondrial transporter which transports aspartate (Asp) from mitochondria to cytosol in exchange with glutamate (Glu) and H⁺. Asp is originally supplied from mitochondria to cytosol where it is necessary for synthesis of proteins, nucleotides, and urea. In cytosol, Asp can be synthesized from oxaloacetate and Glu by cytosolic Asp aminotransferase, but oxaloacetate formation is limited by the amount of NAD⁺. This means an increase in NADH causes suppression of Asp formation in the cytosol. Metabolism of carbohydrates and other substances which produce cytosolic NADH such as alcohol and glycerol suppress oxaloacetate formation. It is forced under citrin deficiency since citrin is a member of malate/Asp shuttle. In this review, we will describe history of identification of the *SLC25A13* gene as the causative gene for adult-onset type II citrullinemia (CTLN2), a type of citrin deficiency, pathophysiology of citrin deficiency together with animal models and possible treatments for citrin deficiency newly developing.

Keywords: adult-onset type II citrullinemia (CTLN2); aspartate/glutamate carrier (AGC); animal model; argininosuccinate synthetase (ASS); aversion to carbohydrates; citrin; food taste; neonatal intrahepatic cholestasis caused by citrin deficiency (NICCD)

1. Introduction

AGC2 or citrin deficiency is the most prevalent autosomal recessive inherited metabolic disease in East and East-south Asia and it is now known as a pan-ethnic disease [1–9], and is one of the many diseases caused by mutations in the genes encoding members of the SLC25 protein family [10,11]. Its heterozygote frequency in East Asia is up to 1 in 40 [12,13]. There are mainly 2 disease types, CTLN2 (adult-onset type II citrullinemia) and NICCD (neonatal intrahepatic cholestasis caused by citrin deficiency) [14–17]. Citrin deficiency also causes FTTDCD (failure to thrive with dyslipidemia caused by citrin deficiency) [18], pancreatitis [19], NASH [20,21], and hepatoma [22,23]. In this review article, we will describe AGC2 or citrin deficiency starting from the recognition of the disease, discovery of the disease gene for CTLN2 and to pathophysiology of the disease based on the function of AGC2, and therapeutic procedures derived from analysis of food preference.

2. Materials and Methods

Materials and Methods are described in each publication. Human patients and mice are analyzed. Informed consents of all subjects are obtained. Animal experiments were done after getting approval of committee of animal experiment at Kagoshima University, Tokushima Bunri University, and Kumamoto University.

3. Study Started from Enzymology of Argininosuccinate Synthetase (ASS)

Saheki et al. started purification of ASS from rat and human liver in 1973 [24] on the assumption that since ASS activity is the lowest among the urea cycle enzymes, ASS may be tightly regulated by some factors. We purified the enzyme to a homogeneity and crystalized, but they could not find any significant regulatory mechanism in the ASS protein. During the research, we have been asked by many clinicians or clinical researchers whether the hepatic ASS activity of their citrullinemic patients is low or not, since the enzyme catalyzed the synthesis of argininosuccinate from citrulline and Asp in the expense of ATP breakdown. Since ASS deficiency is assumed to cause citrullinemia, Saheki et al. examined Km values for citrulline, Asp, and ATP, and quantified the ASS protein amount by using anti-ASS antiserum together with assaying ASS activity. Luckily enough, we noticed there are two types of enzyme abnormality in the patients' ASS in the liver obtained by biopsy or autopsy almost from the beginning [25]. As you see in Table 1, one group is mainly from neonates, the low ASS activities were from lowered affinities to the substrates, citrulline, Asp, or/and ATP, or enlarged Km values for the substrates. Using autopsied samples, we also examined kidney and brain ASSs, which showed the same abnormalities in the enzyme kinetics. The same abnormalities were found in the cultured skin fibroblast cells [26]. The enzyme amounts are normal (type I) or very minute amounts (type III) are found. These results suggest that the abnormality is in the gene of *ASS1*. Kobayashi et al. [27] found real mutations in the *ASS1* genes. So, this is classical or neonatal citrullinemia (CTLN1). The other group, named as CTLN2 later, consisted from mainly adult patients, showed reduced ASS activities which are explainable with the reduced enzyme amount with normal kinetic properties (type II). ASS activities in the brain, kidney, or cultured fibroblast cells are not different from the control. So that the former should be qualitative abnormality caused by mutations in the *ASS1* gene and the latter is quantitative abnormality. Increased urinary excretion of argininosuccinate [28], the product of ASS reaction, in CTLN2 patients probably suggests normal operation of renal ASS reaction. The number of patients were much larger in the latter group. The symptoms of the latter group are consciousness disturbance and abnormal behavior with hyperammonemia, mild citrullinemia, and mild liver damage. From these enzymological abnormalities and clinical symptoms, we named it adult-onset type II citrullinemia, or CTLN2.

Table 1. Two distinct types of citrullinemia.

Type of Enzyme Abnormality We Named:	Type I	Type III	Type II
ASS activity or enzyme amount:	Abnormal kinetics	Almost null	Decrease of normal ASS
Organ specificity	All cells	All cells	Liver-specific
Type of abnormality	Qualitative		Quantitative
Disease:	CTLN1 (Classical citrullinemia)		CTLN2 (Adult-onset type II citrullinemia)
Gene:	<i>ASS1</i>		<i>SLC25A13</i> (Citrin deficiency)

Before we have genetic information of the disease, we have several important information; for example, the patients showed high serum PSTI (pancreatic secretory trypsin inhibitor) [29], which is secreted not from the pancreas, but from the liver [30]. This is considered an early marker of disease onset [31].

In our group, Dr. Keiko Kobayashi et al. [32–34] performed molecular genetic analysis on these patients after earlier biochemical analysis on the mRNA and protein and found various mutations in the *ASS1* gene in the former group patients, amino acid substitutions in ASS abnormality in its kinetic parameters, splicing site mutations in ASS abnormality with a very minute enzyme amount. They did similar analyses on the samples from patients with type II citrullinemia [35]. Together with our first analysis showing that no abnormalities in the amount and translatable activity of the mRNA [36,37], we finally concluded that there are no abnormalities in the *ASS1* gene in the latter group. Table 1 shows two distinct types of citrullinemia.

4. Pathogenesis of Adult-Onset Type II Citrullinemia

What is the primary defect in CTLN2? The decreased level of ASS protein in the liver of CTLN2 patients is in average 9% of the control level (from almost 0% up to 70%). So far, we have not been able to find out the mechanism of the decrease. We thought that the mechanism is not known but should be caused by genetic abnormality because we have found many patients derived from consanguineous marriage, suggesting that it is an autosomal recessive trait. So, we started genomic analysis using homozygosity mapping with 18 DNA samples from CTLN2 patients derived from consanguineous marriage and DNA samples from control subjects. This homozygosity mapping analysis revealed the disease gene located at chromosome 7q21.3 [38]. The gene mutated in CTLN2 patients were searched for in collaboration with Drs. Steve Scherer and Lap-Che Tui, Toronto, Canada. Finally, Dr. Kobayashi found mutations in *SLC25A13*, which encoded mitochondrial transporter [38], which was published in 1999. The results found showed that among 18 samples from consanguineous marriage contained three heterozygotes, suggesting high prevalence of the disease [38].

A very similar gene, *SLC25A12* [39], encoding aralar reported by del Arco, Spain, was published in 1998. Prof. Ferdinando Palmieri, Italy, proposed collaboration among three groups to elucidate the functions of citrin and aralar. The collaboration was successful to find that the two genes encode mitochondrial membrane aspartate glutamate carrier (AGC) [40]. Both aralar (AGC1) and citrin (AGC2) transports proton and Glu from intermembrane space of mitochondria into mitochondrial matrix and Asp from mitochondria matrix to mitochondrial intermembrane space [40], and both activated by calcium [38,41].

AGC1 (alarar) is expressed mainly in the brain, skeletal muscle, heart, and kidney, while AGC2 (citrin) is located mainly in the liver, kidney and heart. So that AGC1 is the brain/skeletal muscle-type and citrin is the liver-type. More precise distributions of aralar and citrin have been reported by Begum et al. [42] and Amoedo et al. [43].

Citrin deficiency causes CTLN2 (OMIM ID #603471) and NICCD (OMIM ID #605814) [1,14], while aralar deficiency is a rare disease causing global cerebral hypomyelination, developmental arrest, hypotonia, and epilepsy (OMIM ID #612949) [44,45]. Lists of mutations in citrin deficiency and AGC1 deficiency can be found at <http://www.hgmd.cf.ac.uk/ac/gene.php?gene=SLC25A13> and 12.

5. Discovery of NICCD (Neonatal Intrahepatic Cholestasis Caused by Citrin Deficiency) and Citrin Deficiency Disease Types

Since we have discovered the gene for CTLN2, we were very busy creating a diagnostic system for each mutation found in CTLN2 and found many CTLN2 patients not only in Japan, but also in China [3–5]. During this time, three pediatric doctors were interested in neonatal hepatitis or cholestasis during neonates. Prof. Tazawa [15] visited Kagoshima and assayed liver ASS activity of his neonatal patients but without any positive results, but later, we diagnosed with DNA diagnosis that his neonatal transient citrullinemia patients were really suffering from citrin deficiency. At the almost same time, we also diagnosed with DNA diagnosis that the transient citrullinemia patients of Dr. Ohura also had mutations in *SLC25A13* [16]. We also diagnosed the patient of Dr. Tomomasa [17] as a citrin deficiency patient: the patient showed NICCD symptoms at his neonatal period and suffered from CTLN2 later at 16 years old. Thereafter, many NICCD patients have been found in Japan, China, Korea, and other countries [1,6,46–48].

Laboratory findings of the patients were positive signs of several neonatal mass screening tests such as tyrosine, phenylalanine, methionine, and threonine. Some showed galactosemia [49,50] and cholestasis and bleeding diathesis [2]. Extremely high serum levels of α -fetoprotein are impressive [1,51]. However, there was almost no increase in blood ammonia.

About 50% of NICCD patients were found at neonatal screening and about 40% were at about several months with persistent jaundice [1]. Some were found later with failure to thrive and dyslipidemia (FTTDCC) [18]. Among them, a few, one in 100,000 to 200,000 as the incidence developed to CTLN2 at adult age (10 to 80 years old) with symptoms including hyperammonemia, consciousness disturbance, and abnormal behavior. During the period between NICCD and CTLN2, most of the patients showed almost no severe symptoms except tiredness and almost normal laboratory examinations [52]. However, most of citrin deficiency subjects showed peculiar food taste from about 1 year old. Both our nutritional assessment [53] on symptomless citrin deficiency subjects from 1 year old and 36 years old, and Nakamura et al. on CTLN2 patients [54] revealed reduced intake of carbohydrates, which is very important as a pathogenesis of citrin deficiency and for the treatment of citrin deficiency, as stated later. The peculiar food taste of citrin deficiency subjects is shown in Figure 1. The various disease types of citrin deficiency during lifetime are shown in Figure 2.

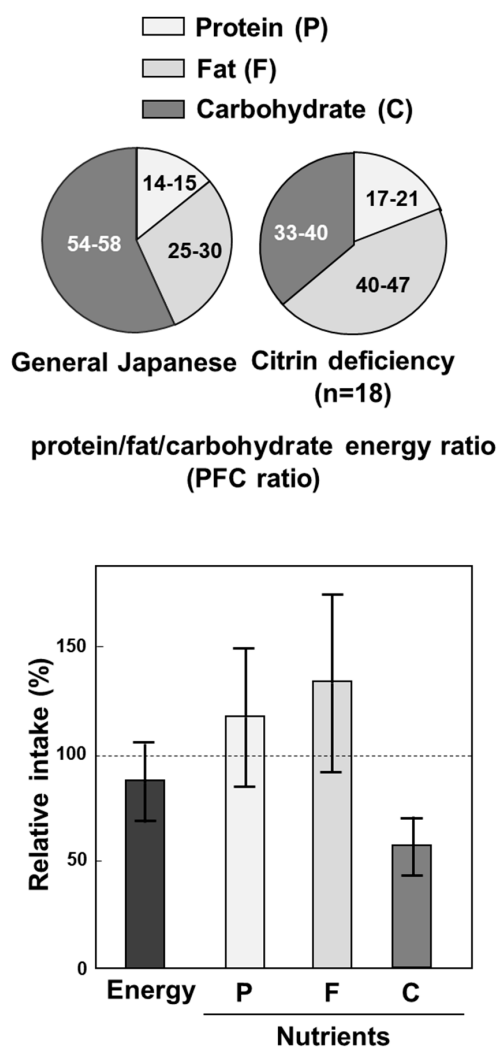


Figure 1. Peculiar food taste of citrin deficiency subjects. Upper panel shows protein, fat, and carbohydrate (PFC) energy ratio, and lower panel shows relative intake of nutrients of general Japanese and citrin deficiency subjects. From [53].

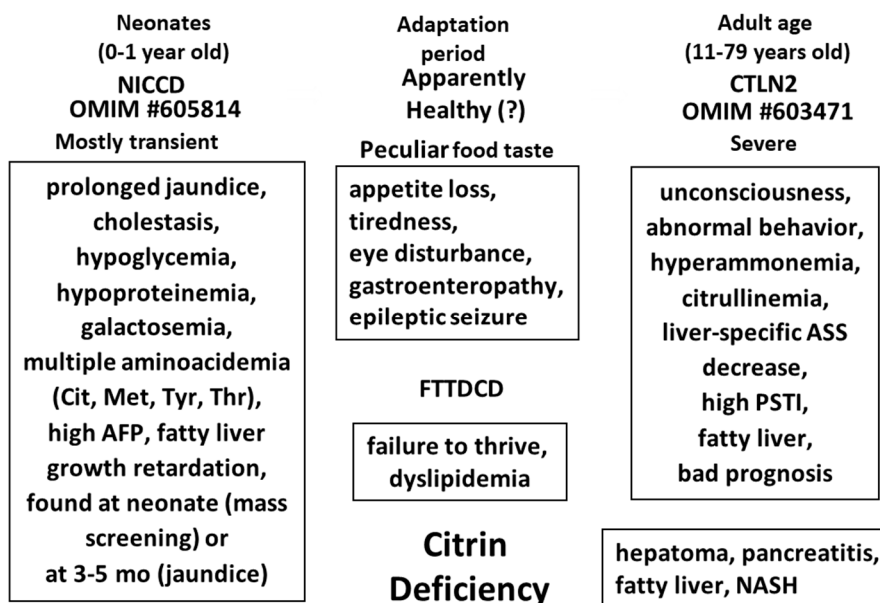


Figure 2. Relation between various disease types during lifetime in citrin deficiency. Modified from [55].

6. The Metabolic Functions of Citrin and Disease Model

The metabolic functions of citrin [56] were shown in Figure 3; (1) as a member of malate/Asp shuttle, it is important for transport of reducing equivalent of NADH into mitochondria which is related to production of ATP in the mitochondria; (2) it plays a role in transport of Asp from mitochondria to cytosol for synthesis of urea, proteins, nucleotides, and urea; (3) it is indispensable for metabolism of lactate to glucose (gluconeogenesis) in order to avoid excess formation of NADH in the cytosol because of stoichiometry of NADH. Mutations of *SLC25A13* gene disturb the metabolic functions listed above.

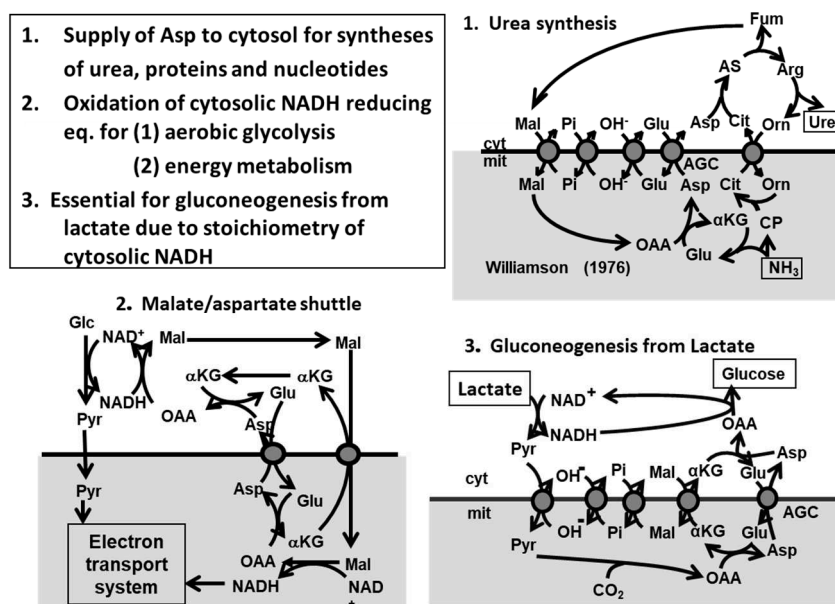


Figure 3. Metabolic functions of citrin. From [57].

We have created, at first, citrin gene knockout mice [58] as a model animal, which showed metabolic defects due to citrin-KO in vitro, but with almost no symptoms in vivo. The reason why the mice showed almost no symptoms, we postulated that the rodent liver contains another NADH shuttle, glycerophosphate shuttle, which compensates the defect of malate/Asp shuttle. So, we created

double gene knockout mice, which lack not only *SLC25A13*, but also *mitochondrial glycerol 3-phosphate dehydrogenase* (*Gpd2*; mGPD), a member of glycerophosphate shuttle. The resultant citrin/mGPD double-KO mice recapitulated human citrin deficiency [59], showing hyperammonemia, citrullinemia, hypoglycemia, and growth retardation.

7. Pathophysiology of the Double-KO Mice

The double-KO mice showed hyperammonemia under fed conditions, but not under starved conditions [59] (Figure 4). Most characteristic is that the double-KO mice showed enhanced severe hyperammonemia when the mice were given sucrose solution forced per os (Figure 4). Furthermore, they did not like to take sucrose solution, as compared with other genotype mice including citrin-KO and mGPD-KO mice. We have shown that not only sucrose, but also, the components, both glucose and fructose [60], had the same effect, as shown in Figure 5. We propose that carbohydrate intake increases cytosolic NADH, which is the reason why citrin deficiency subjects dislike to take carbohydrates. Metabolomic analysis of the double-KO mice liver revealed six major metabolic abnormalities listed as follows [61], (1) a vast increase in glycerol 3-phosphate and ratio of G3P/dihydroxyacetonephosphate, (2) increased concentration of lysine caused by a decreased availability of α -ketoglutarate, resulting in inhibition of breakdown of lysine, (3) increase of citrulline, (4) decreased concentration of Glu, (5) ATP, and (6) citrate. A marked increase in glycerol 3-phosphate (G3P), or G3P/dihydroxyacetone phosphate ratio indicates an increase in the NADH/NAD⁺ ratio in the cytosolic compartment of the liver. This was caused by destruction of two NADH shuttles leading to accumulation of cytosolic NADH, which caused inhibition of glycolytic enzyme, glyceraldehyde 3-phosphate dehydrogenase. The increased NADH also suppressed oxaloacetate formation from malate and malate dehydrogenase, further formation of Asp by cytosolic Asp aminotransferase, together with defect of Asp supply from mitochondria [40], causing inhibition of ASS reaction, resulting in accumulation of citrulline and ammonia, and inhibition of urea synthesis. We postulate that decreased Glu comes from oxidation of NADH in the mitochondria by inactive malate/Asp shuttle and decreased TCA cycle activity, evidenced by low concentration of TCA cycle intermediates [59]. Decreased citrate comes from inhibition of glycolysis and cytosolic increase in NADH/NAD⁺. ATP will decrease by inhibition of glycolysis and inactive malate/Asp shuttle.

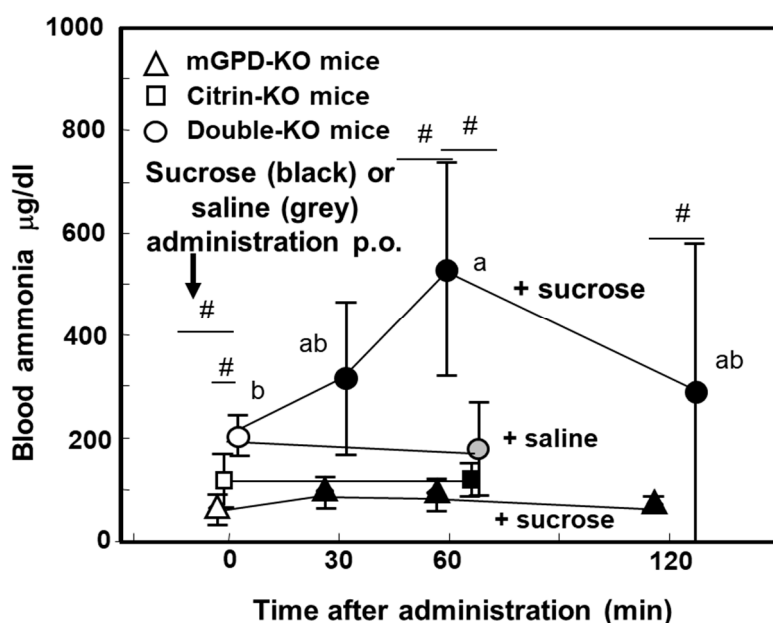


Figure 4. Effect of sucrose or NaCl administration on blood ammonia on fed mGPD-KO, citrin-KO, and double-KO mice. # $p > 0.05$ from value with Saline. Values with same character (a, ab) indicate no statistical difference. From [57].

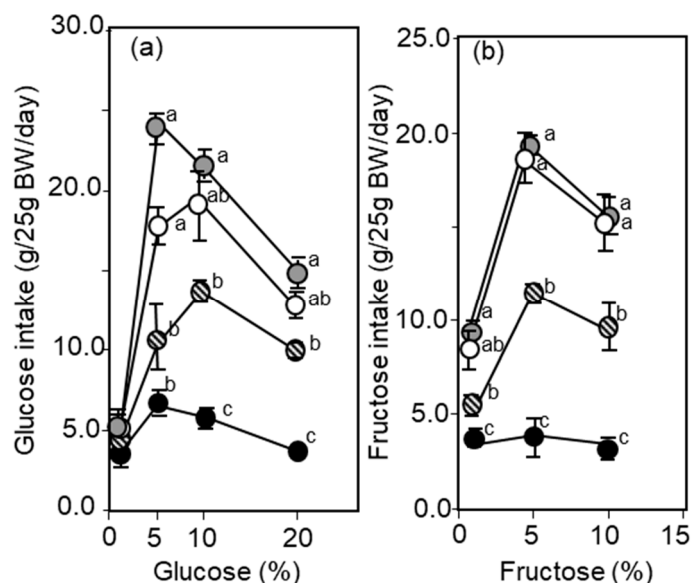


Figure 5. Voluntary intake of various concentrations of glucose (a) or fructose (b) and water (two bottles, water and a test solution) given to four kinds of mice, wild type (white circle), mGPD-KO (circle with stripes), citrin-KO (grey circle), and double-KO (black circle) were monitored. Concentrations are given in the figure. Intakes were compared statistically and differences were expressed with a, b, c. The same character indicates no difference. It is noteworthy that the double-KO mice took only a small amount of glucose and fructose solutions, as compared with other mice. From [59].

Voluntary intake test of sucrose, ethanol, and glycerol [60], of which intakes or administration caused onset or worsening of disease [1,62], revealed that the double-KO mice severely avoided the intakes, citrin-KO and mGPD-KO mice moderately avoided taking the higher concentration solutions of ethanol and glycerol. We found that high correlation between avoidance of intake of the solutions scored from the amounts of intake and comparison between the mice, and simultaneous hepatic increase in G3P and decrease in ATP [60]. We suggest that the two parameters, simultaneous increase in the NADH/NAD⁺ ratio represented by the G3P concentration and decrease in ATP in the liver, send a signal to the brain to induce to suppress the intake of the solution or the foods which increase in hepatic cytosolic NADH and decrease in ATP. This consideration is important from a viewpoint of therapy of citrin deficiency. Namely, correction of either increased G3P or decreased ATP may stop the symptoms of citrin deficiency.

8. Treatment of Citrin Deficiency Based on the Pathophysiology of the Disease

Principle concept of citrin deficiency treatment should be based on the peculiar food intake tendency except that liver transplantation is the most effective in correcting all the metabolic disturbances [63,64], liver transplantation at early stage of the disease, almost all symptoms disappeared, suggesting that it is liver disease. Liver transplantation also normalizes the peculiar food taste (Kobayashi, unpublished data). Liver transplantation itself has some drawback, such as the cost and shortage in liver donors and not all the liver transplantation could help the lives of citrin deficiency patients probably due to immunological complications or other causes. Therefore, nutritional and medicinal therapeutic procedures are important. Basics of the therapy is nutrition. High carbohydrates diet causes anorexia in NICCD patients and hyperammonemia in CTLN2, so that low carbohydrates diet is important. High carbohydrates and low protein diet is the common therapeutic diet for liver diseases, which, however, was reported inappropriate [65]. Rather, carbohydrate-restricted diet or in addition high protein diet were found to be effective [2,66]. Infusion of high glucose solutions [67] or hyperosmotic solutions [62,68] for brain edema, such as Glyceol consisting of 10% glycerol and 5% fructose is contraindication. Infusion of high concentration of glucose caused hyperammonemia and consciousness

disturbance to citrin deficiency patients [67]. You can use lower concentration (less than 10%) of glucose, if the patients needed glucose. You may find many case reports listed in reference [62]; many case-report authors described that patients given Glyceol got irreversible deterioration and mostly died shortly after infusion of Glyceol [62].

On the other hand, we noticed that protein and some kinds of lipid in the diet may be effective for treatment. Nutritional assessment of a young girl with CTLN2 [69] disliked high carbohydrates diet and sweets, and she took her favorite diet which was rich in protein and lipid in spite of that with almost the same amount of carbohydrates as the high carbohydrate diet she took, suggesting an ameliorating effect of the other nutrients [70]. In the double-KO mice with component-defined diet, we showed that the high-carbohydrate diet (AIN-93, a diet for mature rodent recommended by American Institute for Nutrition in 1993) was strongly avoided by the double-KO mice, but addition of 8% protein (casein) by reducing carbohydrates by 8% caused appetite enough to recover the amount intake as usual with high protein laboratory chow (CE2, a diet for rodent breeding supplied from CLEA Japan) [71], as shown in Figure 6. The casein was able to be replaced by single amino acid such as Ala and Glu. Furthermore, addition of 6% MCT (medium-chain triglycerides) alone caused full intake as CE2, but none of triglycerides which consisted from long-chain fatty acids such as soybean oil, fish oil, and lard were effective, as shown in Table 2. It is because MCT is metabolized in the liver but not via tightly-regulated carnitine palmitoyltransferase I pathway.

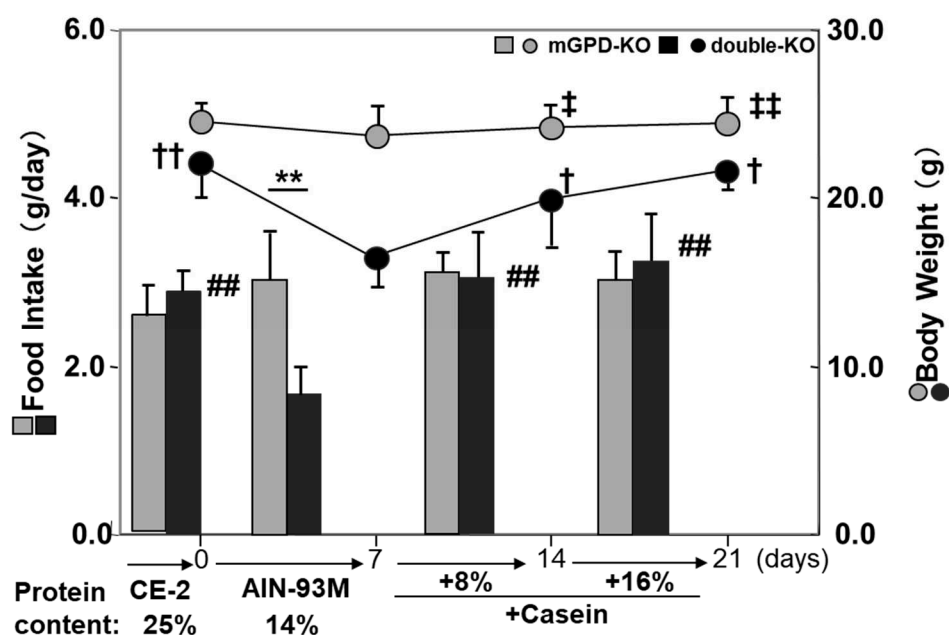


Figure 6. Intake of diet (high carbohydrate diet with defined composition, AIN-93M (recommended for mature rodent by American Institute for Nutrition in 1993) and body weight changes per week of mGPD-KO and double-KO mice and effect of supplementation of casein. The mice were usually given a high protein diet CE-2 (25%) from Clea Japan and changed the diet to AIN-93M (protein content is 14%), the intake is the average of a week and body weight changes in a week were monitored. Supplementation was done with reducing corn starch by the same amount. Differences in body weight for double-KO mice ($\dagger p < 0.05$, $\dagger\dagger p < 0.01$), and for mGPD-KO mice ($\ddagger p < 0.05$; $\ddagger\ddagger p < 0.01$) comparing the AIN-93M diet versus other supplementation were determined using a paired t-tests. Difference in food intake between diets within each genotype were determined using paired t-tests ($\# p < 0.01$; $\#\#\ p < 0.01$) Difference in food intake between genotypes were determined using unpaired t-test ($** p < 0.01$) From [71].

Table 2. Effect of supplementation of protein, amino acids, and lipid on the food intake and body weight changes as shown in Figure 6. From [71].

Change from CE-2 to	Body Weight	Food Intake
AIN93M	Dec	Dec
(Effect of supplements)		
Protein (+8%)	Inc	Inc
Ala (5%)	Inc	Inc
Na-Glu (5%)	Inc	Inc
Na-Pyr (10%)	Inc	Inc
MCT (6%)	Inc	Inc
Soybean oil (6%)	no	no
Lard (6%)	no	no
Olive oil (6%)	no	no
Fish oil (6%)	no	no

Inc, increased; Dec, decreased; No indicates no change.

From the results, we searched for the most effective amino acid(s) [72]. Looking for amino acids which increase hepatic Asp, or decrease hepatic G3P level increased by administration of ethanol to citrin-KO mice [72]. Resultant candidate amino acids were glycine (Gly), Ala, ornithine (Orn), arginine (Arg), serine, Asp, and Glu. During this research, we also looked for amino acids which affect the hepatic citrulline level. Gly and serine were found to increase the hepatic citrulline level and furthermore, blood ammonia levels. According to this finding, we eliminated Gly and serine from the list. Furthermore, we were able to create a severe hyperammonemia model by administration of Gly and sucrose to the double-KO mice [72]. Using this model, we finally decided which amino acid(s) are the most effective. Figure 7a shows you the effect of various amino acids and MCT on decreasing blood ammonia increased by the addition of sucrose and Gly. The most effective were Orn+Asp or Orn+Ala; those decreased blood ammonia as low as wild type mice without Suc + Gly. Figure 7b shows plasma citrulline levels. Orn is well known to stimulate urea synthesis by increasing urea cycle capacity through increasing substrate level of OTC reaction, but increased plasma citrulline level as Arg (Figure 7b). Addition of Ala or Asp to Orn decreased the plasma citrulline level, indicating the action of these two amino acids are different from Orn and Arg. We postulated the acting point of Glu, Asp, and Ala are the same.

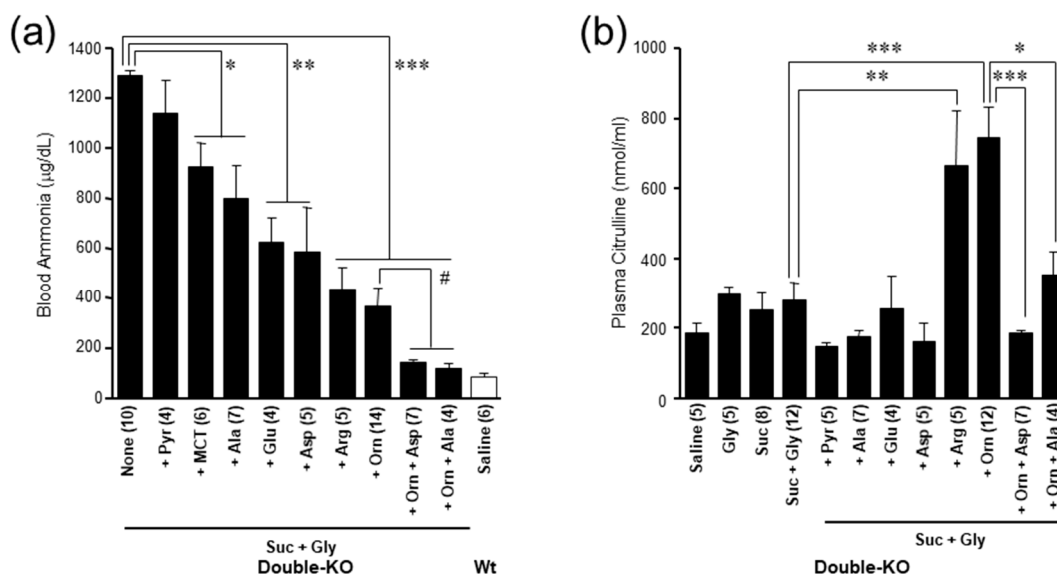


Figure 7. (a) Effects of enteral administration of 0.5 M various amino acids, 0.5 M sodium pyruvate, 5% MCT, or amino acid combination (10 mL/kg bw) on blood ammonia increased by administration of 20%

sucrose +1 M Gly (20 mL/kg bw) in double-KO mice. (b) Effects of administration of amino acid and other substances indicated in the figure on plasma citrulline in the double-KO mice. Asterisks (* $p < 0.05$; ** $p < 0.001$; *** $p < 0.0001$) denote statistical differences between indicated groups by unpaired t-test (Figure 7(a)) Asterisks (* $p < 0.05$; ** $p < 0.001$; *** $p < 0.0001$) denote statistical differences vs saline. Values are shown with mean \pm standard error of mean. From [72].

On the other hand, we also tested Ala and Asp on ureagenesis in the perfused liver [72], as shown in Figure 8. The results show that Ala was effective in ureagenesis in any kinds of genotype mice including the double-KO mice but Asp was not at all effective. We have also reported the similar results with citrin-KO mice showing ineffectiveness of Asp [73]. This is accordant with the report by Stoll et al. [74] that Asp together with Glu and α -ketoglutarate administered are transported into perivenous hepatocytes but not into periportal hepatocytes where the urea cycle enzymes are located. However, it is not consistent with our results showing effectiveness of Asp per os administered, as shown in Figure 7a.

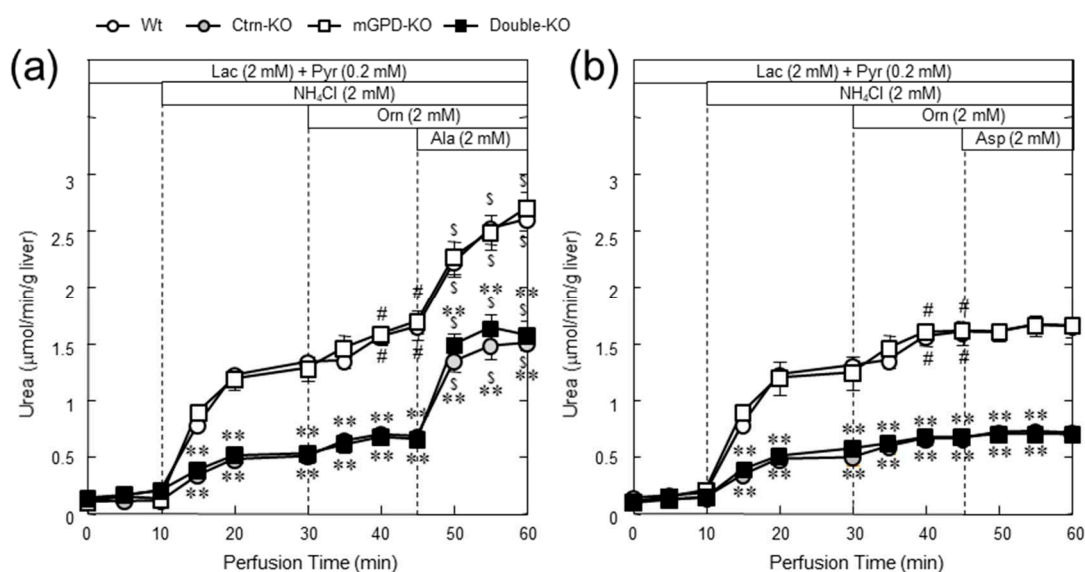


Figure 8. Urea synthesis from ammonium chloride in the perfused liver and effect of Ala (a) and Asp (b). In the upper part of the figures, the addition to the perfusion media is shown. Mice used are, wild type (white circle), citrin-KO (gray circle), mGPD-KO (white square), and double-KO mice (black square). * and ** indicate statistical differences ($p < 0.05$ and $p < 0.01$, respectively) from wild type values and # and \$, $p < 0.05$ from the level at perfusion time 45 and 30 min within the same genotypes. From [72].

9. Importance of Small Intestine on Metabolism of Amino Acids

To solve this discrepancy, we considered the role of the small intestine in metabolism of amino acids. Actually, Neame and Wiseman [75], Parsons and Volman-Mitchell [76], and Windmueller and Spaeth [77] have shown that enterally-administered Asp is converted into Ala in the small intestine and then transported via the portal vein to the liver. In order to examine the role of the small intestine on the function of amino acids in the liver and confirm the results shown by the former researchers, we administered various amino acids enterally and assayed the concentrations of amino acids in the portal vein and abdominal aorta and calculated the difference in the amino acids between the two blood vessels. In our experiment, enteral administration of specific amino acids caused increases in each amino acid within the arterial circulation, and the clear portal-arterial difference, demonstrating an uptake of Gln and output of Ala, citrulline, and Pro (Figure 9). Our findings clearly demonstrate that some part of the Asp, Glu, and Orn were converted to Ala, but no significant conversion of Gly to Ala in the small intestine (Figure 9). It also suggests that the positive effect of Orn on enhancing ureagenesis appears to be more than simply increasing the urea-cycle intermediate levels. The results shown here suggest also that the Ala formed and supplied to the periportal hepatocytes can then be converted

back to Asp by coupling of two cytosolic aminotransferases (Figure 10a,b), and the formed pyruvate can then oxidize malate to oxaloacetate, reinitiating ureagenesis under citrin deficiency (Figure 10b). Actually, the combination of Orn and Asp, L-ornithine L-aspartate (LOLA), which contains no NaCl, was very effective in decreasing blood ammonia [72]. Acting site of Asp, analyzed by using crossover point analysis, clearly is an ASS step, as shown in Figure 11. This will be effective therapeutics for citrin deficiency. We are now examining LOLA as a clinical test.

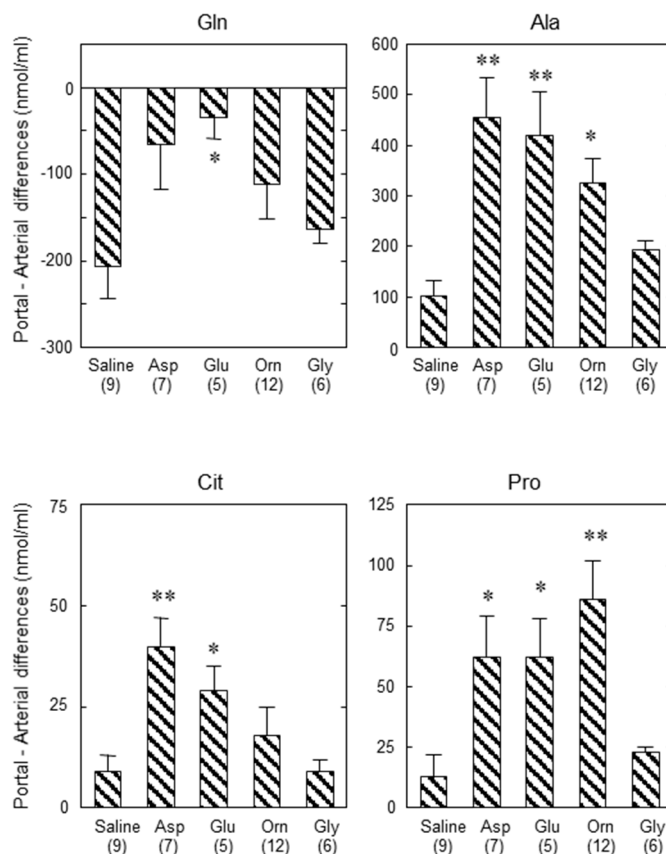


Figure 9. Portal vein-arterial differences in the plasma concentration of Gln, Ala, Cit, and Pro 1 h after administration of saline, Asp, Glu, Orn, or Gly. Plus values indicate output and minus values indicate uptake of the amino acid. Saline, Asp, Glu, Orn, or Gly (20 mL/kg bw; 10 mmol/kg bw) were enterally administered to mGPD-KO mice and 1 h after the administration, blood was collected simultaneously from portal vein and abdominal aorta for portal vein-arterial difference. * $p < 0.05$ and ** $p < 0.001$ vs saline. From [70].

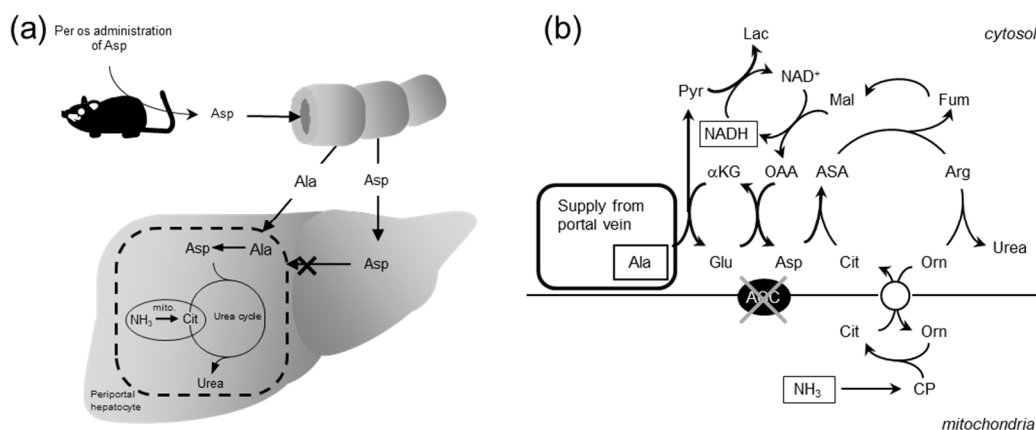


Figure 10. Schematic diagram of Asp metabolism after enteral administration within the small intestine (a) and liver (b) and postulated metabolic pathway of Ala in periportal hepatocytes. From [72].

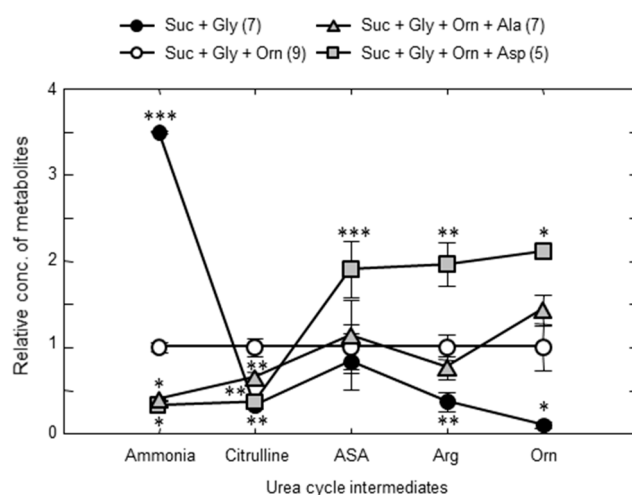


Figure 11. Crossover point analysis of Asp action. Each of hepatic and blood metabolite concentrations under Suc + Gly + Orn was set at 1 and the metabolite concentrations under the other conditions were calculated and plotted. The concentration of blood ammonia was used as ammonia in the figure. The line formed with Asp crossed over the basal line between citrulline and argininosuccinate, indicating that Asp activates ASS step. * $p < 0.05$; ** $p < 0.001$ and *** $p < 0.0001$ from the baseline of Suc + Gly + Orn. From [72].

10. Drugs or Supplements Used as Therapeutics for Citrin Deficiency at Present

L-Arginine: Arg was the first drug found effective in the blood ammonia decreasing drug by Hoshi et al. [78] and Imamura et al. [66]. It was effective at not only decreasing blood ammonia but also effective in decreasing plasma triglyceride [66].

Sodium Pyruvate: Sodium pyruvate was used to consume glycolytic NADH by producing lactate, and then decreasing blood ammonia probably by producing oxaloacetate and aspartate. It was found effective in controlling the pathogenic state of citrin deficiency by Moriyama et al. [73], clinically by Mutoh et al. [69] and Yazaki et al. [79].

MCT: MCT was originally used as an energy supply for various metabolic diseases including NICCD [80]. Hayasaka et al. [81] successfully used MCT for the treatment of CTLN2. They emphasize MCT as the energy source for the liver. But the mechanism of action is not clear yet. Saheki et al. [71] used MCT in the treatment of model mice, and Saheki et al. [82] and Moriyama et al. [83] analyzed the mechanism of action of MCT, the latter using the perfused liver system. Both agreed MCT increased synthesis of Gln. How does Gln, which is not the end product, but an intermediate metabolite of nitrogen metabolism work? Therefore, how Gln works by further metabolism is the next question.

All these clinical tests propose effectiveness of Arg, sodium pyruvate, and MCT in treatment of citrin deficiency. Further extensive clinical trials of these candidates including LOLA are needed.

Funding: This study was supported by KAKENHI, Grants from Ministry of Health, Labor and Welfare of Japan and Grants for Research for Promoting Technological seeds from Japan Science and Technology Agency. Recent several years, this study was greatly supported by Citrin Foundation established by Barbara Yu Fa and Yen How Tai in Singapore.

Acknowledgments: This study was done in collaboration with many collaborators including clinical doctors, patients and their families. The most important researcher in this study is late Keiko Kobayashi who discovered the causative gene for CTLN2 and passed away in 2010. I only list major collaborators who worked with Saheki at Kagoshima University, Tokushima Bunri University and Kumamoto University, Yasushi Imamura, Izumi Yasuda, Yoshiko Setogawa, Qinghua Gao, Miharu Ushikai, Kanako Inoue, and Sumie Furuie. I also thank, Late Nobuhiko Katunuma, Ken-ichi Yamamura, Tatsuhiko Furukawa, and Masahisa Horiuchi, who gave me opportunities to study by providing laboratories and equipments after my retirement at Tokushima Bunri University, Kumamoto University and Kagoshima University, respectively.

Conflicts of Interest: The authors declare no conflict of interest.

References

1. Saheki, T.; Song, Y.Z. *Citrin Deficiency*; Adam, M.P., Ardinger, H.H., Pagon, R.A., Wallace, S.E., Bean, L.J.H., Stephens, K., Amemiya, A., Eds.; University of Washington: Seattle, WA, USA, 1993.
2. Dimmock, D.; Kobayashi, K.; Iijima, M.; Tabata, A.; Wong, L.J.; Saheki, T.; Lee, B.; Scaglia, F. Citrin deficiency: A novel cause of failure to thrive that responds to a high-protein, low-carbohydrate diet. *Pediatrics* **2007**, *119*, e773–e777. [CrossRef] [PubMed]
3. Yasuda, T.; Yamaguchi, N.; Kobayashi, K.; Nishi, I.; Horinouchi, H.; Jalil, M.A.; Li, M.X.; Ushikai, M.; Iijima, M.; Kondo, I.; et al. Identification of two novel mutations in the SLC25A13 gene and detection of seven mutations in 102 patients with adult-onset type II citrullinemia. *Hum. Genet.* **2000**, *107*, 537–545. [CrossRef] [PubMed]
4. Yamaguchi, N.; Kobayashi, K.; Yasuda, T.; Nishi, I.; Iijima, M.; Nakagawa, M.; Osame, M.; Kondo, I.; Saheki, T. Screening of SLC25A13 mutations in early and late onset patients with citrin deficiency and in the Japanese population: Identification of two novel mutations and establishment of multiple DNA diagnosis methods for nine mutations. *Hum. Mutat.* **2002**, *19*, 122–130. [CrossRef] [PubMed]
5. Hwu, W.L.; Kobayashi, K.; Hu, Y.H.; Yamaguchi, N.; Saheki, T.; Chou, S.P.; Wan, J.H. A Chinese adult onset type II citrullinaemia patient with 851del4/1638ins23 mutations in the SLC25A13 Gene. *J. Med. Genet.* **2001**, *38*, E23. [CrossRef] [PubMed]
6. Ko, J.M.; Kim, G.H.; Kim, J.H.; Kim, J.Y.; Choi, J.H.; Ushikai, M.; Saheki, T.; Kobayashi, K.; Yoo, H.W. Six cases of citrin deficiency in Korea. *Int. J. Mol. Med.* **2007**, *20*, 809–815. [CrossRef]
7. Song, Y.Z.; Li, B.X.; Chen, F.P.; Liu, S.R.; Sheng, J.S.; Ushikai, M.; Zhang, C.H.; Zhang, T.; Wang, Z.N.; Kobayashi, K.; et al. Neonatal intrahepatic cholestasis caused by citrin deficiency: Clinical and laboratory investigation of 13 subjects in mainland of China. *Dig. Liver Dis.* **2009**, *41*, 683–689. [CrossRef]
8. Hutchin, T.; Preece, M.A.; Hendriksz, C.; Chakrapani, A.; McClelland, V.; Okumura, F.; Song, Y.Z.; Iijima, M.; Kobayashi, K.; Saheki, T.; et al. Neonatal Intrahepatic Cholestasis Caused by Citrin Deficiency (NICCD) as a Cause of Liver Disease in Infants in the UK. *J. Inherit. Metab. Dis.* **2009**, *32*, S151–S155. [CrossRef]
9. Fiermonte, G.; Parisi, G.; Martinelli, D.; De Leonardis, F.; Torre, G.; Pierri, C.L.; Saccari, A.; Lasorsa, F.M.; Vozza, A.; Palmieri, F.; et al. A new Caucasian case of neonatal intrahepatic cholestasis caused by citrin deficiency (NICCD): A clinical, molecular, and functional study. *Mol. Genet. Metab.* **2011**, *104*, 501–506. [CrossRef]
10. Palmieri, F. The mitochondrial transporter family SLC25; Identification, properties and physiopathology. *Mol. Aspects Med.* **2013**, *34*, 465–484. [CrossRef]
11. Palmieri, F.; Scarcia, P.; Monne, M. Diseases caused by mutations in mitochondrial carrier genes SLC25: A review. *Biomolecules* **2020**, *10*, 655. [CrossRef]
12. Lu, Y.B.; Kobayashi, K.; Ushikai, M.; Tabata, A.; Iijima, M.; Li, M.X.; Lei, L.; Kawabe, K.; Taura, S.; Yang, Y.; et al. Frequency and Distribution in East Asia of 12 Mutations Identified in the SLC25A13 Gene of Japanese Patients With Citrin Deficiency. *J. Hum. Genet.* **2005**, *50*, 338–346. [CrossRef] [PubMed]
13. Kikuchi, A.; Arai-Ichinoi, N.; Sakamoto, O.; Matsubara, Y.; Saheki, T.; Kobayashi, K.; Ohura, T.; Kure, S. Simple and Rapid Genetic Testing for Citrin Deficiency by Screening 11 Prevalent Mutations in SLC25A13. *Mol. Genet. Metab.* **2012**, *105*, 553–558. [CrossRef]
14. Saheki, T.; Kobayashi, K. Mitochondrial aspartate glutamate carrier (citrin) deficiency as the cause of adult-onset type II citrullinemia (CTLN2) and idiopathic neonatal hepatitis (NICCD). *J. Hum. Genet.* **2002**, *47*, 333–341. [CrossRef] [PubMed]
15. Tazawa, Y.; Kobayashi, K.; Ohura, T.; Abukawa, D.; Nishinomiya, F.; Hosoda, Y.; Yamashita, M.; Nagata, I.; Kono, Y.; Yasuda, T.; et al. Infantile cholestatic jaundice associated with adult-onset type II citrullinemia. *J. Pediatr.* **2001**, *138*, 735–740. [CrossRef] [PubMed]
16. Ohura, T.; Kobayashi, K.; Tazawa, Y.; Nishi, I.; Abukawa, D.; Sakamoto, O.; Iinuma, K.; Saheki, T. Neonatal presentation of adult-onset type II citrullinemia. *Hum. Genet.* **2001**, *108*, 87–90. [CrossRef] [PubMed]
17. Tomomasa, T.; Kobayashi, K.; Kaneko, H.; Shimura, H.; Fukusato, T.; Tabata, M.; Inoue, Y.; Ohwada, S.; Kasahara, M.; Morishita, Y.; et al. Possible clinical and histologic manifestations of adult-onset type II citrullinemia in early infancy. *J. Pediatr.* **2001**, *138*, 741–743. [CrossRef]
18. Song, Y.Z.; Guo, L.; Yang, Y.L.; Han, L.S.; Kobayashi, K.; Saheki, T. Failure to thrive and dyslipidemia caused by citrin deficiency: A novel clinical phenotype. *Chin. J. Contemp. Pediatrics* **2009**, *11*, 328–332.

19. Ikeda, S.; Kawa, S.; Takei, Y.; Yamamoto, K.; Shimojo, H.; Tabata, K.; Kobayashi, K.; Saheki, T. Chronic pancreatitis associated with adult-onset type II citrullinemia: Clinical and pathologic findings. *Ann. Intern. Med.* **2004**, *141*, W109–W110. [CrossRef]
20. Komatsu, M.; Yazaki, M.; Tanaka, N.; Sano, K.; Hashimoto, E.; Takei, Y.; Song, Y.Z.; Tanaka, E.; Kiyosawa, K.; Saheki, T.; et al. Citrin deficiency as a cause of chronic liver disorder mimicking non-alcoholic fatty liver disease. *J. Hepatol.* **2008**, *49*, 810–820. [CrossRef]
21. Lee, B.H.; Jin, H.Y.; Kim, G.H.; Choi, J.H.; Yoo, H.W. Nonalcoholic fatty liver disease in 2 siblings with adult-onset type II citrullinemia. *J. Pediatr. Gastroenterol. Nutr.* **2010**, *50*, 682–685. [CrossRef]
22. Soeda, J.; Yazaki, M.; Nakata, T.; Miwa, S.; Ikeda, S.; Hosoda, W.; Iijima, M.; Kobayashi, K.; Saheki, T.; Kojiro, M.; et al. Primary liver carcinoma exhibiting dual hepatocellular-biliary epithelial differentiations associated with citrin deficiency: A case report. *J. Clin. Gastroenterol.* **2008**, *42*, 855–860. [CrossRef] [PubMed]
23. Hagiwara, N.; Sekijima, Y.; Takei, Y.; Ikeda, S.; Kawasaki, S.; Kobayashi, K.; Saheki, T. Hepatocellular carcinoma in a case of adult-onset type II citrullinemia. *Inter. Med.* **2003**, *42*, 978–982. [CrossRef]
24. Saheki, T.; Sase, M.; Nakano, K.; Azuma, F.; Katsunuma, T. Some properties of argininosuccinate synthetase purified from human liver and a comparison with the rat liver enzyme. *J. Biochem.* **1983**, *93*, 1531–1537. [CrossRef] [PubMed]
25. Saheki, T.; Ueda, A.; Hosoya, M.; Kusumi, K.; Takada, S.; Tsuda, M.; Katsunuma, T. Qualitative and quantitative abnormalities of argininosuccinate synthetase in citrullinemia. *Clin. Chim. Acta* **1981**, *109*, 325–335. [CrossRef]
26. Saheki, T.; Ueda, A.; Iizima, K.; Yamada, N.; Kobayashi, K.; Takahashi, K.; Katsunuma, T. Argininosuccinate synthetase activity in cultured skin fibroblasts of citrullinemic patients. *Clin. Chim. Acta* **1982**, *118*, 93–97. [PubMed]
27. Kobayashi, K.; Jackson, M.J.; Tick, D.B.; O'Brien, W.E.; Beaudet, A.L. Heterogeneity of mutations in argininosuccinate synthetase causing human citrullinemia. *J. Biol. Chem.* **1990**, *265*, 11361–11367. [PubMed]
28. Saheki, T.; Kobayashi, K.; Inoue, I.; Matuo, S.; Hagihara, S.; Noda, T. Increased urinary excretion of argininosuccinate in type II citrullinemia. *Clin. Chim. Acta* **1987**, *170*, 297–304. [CrossRef]
29. Kobayashi, K.; Horiuchi, M.; Saheki, T. Pancreatic secretory trypsin inhibitor as a diagnostic marker for adult-onset type II citrullinemia. *Hepatology* **1997**, *25*, 1160–1165. [CrossRef]
30. Kobayashi, K.; Nakata, M.; Terazono, H.; Shinsato, T.; Saheki, T. Pancreatic secretory trypsin inhibitor gene is highly expressed in the liver of adult-onset type II citrullinemia. *FEBS Lett.* **1995**, *372*, 69–73. [CrossRef]
31. Tsuboi, H.; Fijino, Y.; Kobayashi, K.; Saheki, T.; Yamada, T. High serum pancreatic secretory trypsin inhibitor before onset of type II citrullinemia. *Neurology* **2001**, *57*, 933. [CrossRef]
32. Kobayashi, K.; Shaheen, N.; Terazono, H.; Saheki, T. Mutations in argininosuccinate synthetase mRNA of Japanese patients, causing classical citrullinemia. *Am. J. Hum. Genet.* **1994**, *53*, 1103–1112.
33. Kakinoki, H.; Kobayashi, K.; Terazono, H.; Nagata, Y.; Saheki, T. Mutations and DNA diagnoses of classical citrullinemia. *Hum. Mutat.* **1997**, *9*, 250–259. [CrossRef]
34. Kobayashi, K.; Kakinoki, H.; Fukushige, T.; Shaheen, N.; Terazono, H.; Saheki, T. Nature and frequency of mutations in the argininosuccinate synthetase gene that cause classical citrullinemia. *Hum. Genet.* **1995**, *96*, 454–463. [CrossRef] [PubMed]
35. Kobayashi, K.; Shaheen, N.; Kumashiro, R.; Tanikawa, K.; O'Brien, W.E.; Beaudet, A.L.; Saheki, T. A search for the primary abnormality in adult-onset type II citrullinemia. *Am. J. Hum. Genet.* **1993**, *53*, 1024–1030. [PubMed]
36. Sase, M.; Kobayashi, K.; Imamura, Y.; Saheki, T.; Nakano, K.; Miura, S.; Mori, M. Levels of translatable messenger RNA coding for argininosuccinate synthetase in the liver of the patients with quantitative-type citrullinemia. *Hum. Genet.* **1985**, *69*, 130–134. [CrossRef]
37. Kobayashi, K.; Saheki, T.; Imamura, Y.; Noda, T.; Inoue, I.; Matuo, S.; Hagihara, S.; Nomiya, H.; Jinno, Y.; Shimada, K. Messenger RNA coding for argininosuccinate synthetase in citrullinemia. *Am. J. Hum. Genet.* **1986**, *38*, 667–680.
38. Kobayashi, K.; Sinasac, D.S.; Iijima, M.; Boright, A.P.; Begum, L.; Lee, J.R.; Yasuda, T.; Ikeda, S.; Hirano, R.; Terazono, H.; et al. The gene mutated in adult-onset type II citrullinemia encodes a putative mitochondrial carrier protein. *Nat. Genet.* **1999**, *22*, 159–163. [CrossRef]

39. del Arco, A.; Satrústegui, J. Molecular cloning of Aralar, a new member of the mitochondrial carrier superfamily that binds calcium and is present in human muscle and brain. *J. Biol. Chem.* **1998**, *273*, 23327–23334. [CrossRef]
40. Palmieri, L.; Pardo, B.; Lasorsa, F.M.; del Arco, A.; Kobayashi, K.; Iijima, M.; Runswick, M.J.; Walker, J.E.; Saheki, T.; Satrústegui, J.; et al. Citrin and aralar1 are Ca(2+)-stimulated aspartate/glutamate transporters in mitochondria. *EMBO J.* **2001**, *20*, 5060–5069. [CrossRef]
41. Lasorsa, F.M.; Pinton, P.; Palmieri, L.; Fiermonte, G.; Rizzuto, R.; Palmieri, F. Recombinant expression of the Ca(2+)-sensitive aspartate/glutamate carrier increases mitochondrial ATP production in agonist-stimulated Chinese hamster ovary cells. *J. Biol. Chem.* **2003**, *378*, 38685–38692.
42. Begum, L.; Jalil, M.A.; Kobayashi, K.; Iijima, M.; Li, M.X.; Yasuda, T.; Horiuchi, M.; del Arco, A.; Satrústegui, J.; Saheki, T. Expression of three mitochondrial solute carriers, citrin, aralar1 and ornithine transporter, in relation to urea cycle in mice. *Biochim. Biophys. Acta* **2002**, *1574*, 283–292. [CrossRef]
43. Amoedo, N.D.; Punzi, G.; Obre, E.; Lacombe, D.; De Grassi, A.; Pierri, C.L.; Rossignol, R. AGC1/2, the mitochondrial aspartate-glutamate carriers. *Biochim. Biophys. Acta* **2016**, *1863*, 2394–2412. [CrossRef] [PubMed]
44. Wibom, R.; Lasorsa, F.M.; Töhönen, V.; Barbaro, M.; Sterky, F.H.; Kucinski, T.; Naess, K.; Jonsson, M.; Pierri, C.L.; Palmieri, F.; et al. AGC1 deficiency associated with global cerebral hypomyelination. *N. Engl. J. Med.* **2009**, *361*, 489–495. [CrossRef] [PubMed]
45. Falk, M.J.; Li, D.; Gai, X.; McCormick, E.; Place, E.; Lasorsa, F.M.; Otieno, F.G.; Hou, C.; Kim, C.E.; Abdel-Magid, N.; et al. AGC1 deficiency causes infantile epilepsy, abnormal myelination, and reduced N-acetylaspartate. *JIMD Rep.* **2014**, *14*, 77–85. [PubMed]
46. Ohura, T.; Kobayashi, K.; Tazawa, Y.; Abukawa, D.; Sakamoto, O.; Tsuchiya, S.; Saheki, T. Clinical pictures of 75 patients with neonatal intrahepatic cholestasis caused by citrin deficiency (NICCD). *J. Inherit. Metab. Dis.* **2007**, *30*, 139–144. [CrossRef] [PubMed]
47. Kobayashi, K.; Lu, Y.B.; Li, M.X.; Nishi, I.; Hsiao, K.j.; Choeh, K.; Yang, Y.L.; Hwu, W.L.; Reinhardt, J.K.V.; Palmieri, F.; et al. Screening of nine SLC25A13 mutations: Their frequency in patients with citrin deficiency and high carrier rates in Asian populations. *Mol. Genet. Metab.* **2003**, *80*, 356–359. [CrossRef]
48. Ben-Shalom, E.; Kobayashi, K.; Shaag, A.; Yasuda, T.; Gao, H.Z.; Saheki, T.; Bachmann, C.; Elpeleg, O. Infantile citrullinemia caused by citrin deficiency with increased dibasic amino acids. *Mol. Genet. Metab.* **2002**, *77*, 202–208. [CrossRef]
49. Naito, E.; Ito, M.; Matsuura, S.; Yokoto, I.; Saijo, T.; Ogura, Y.; Kitamura, S.; Kobayashi, K.; Saheki, T.; Nishimura, Y.; et al. Type II citrullinemia (citrin deficiency) in a neonate with hypergalactosemia detected by mass screening. *J. Inherit. Metab. Dis.* **2002**, *25*, 71–76. [CrossRef]
50. Ohura, T.; Kobayashi, K.; Abukawa, D.; Tazawa, Y.; Akiyama, J.; Sakamoto, O.; Saheki, T.; Iinuma, K. A novel inborn error of metabolism detected by elevated methionine and/or galactose in newborn screening: Neonatal intrahepatic cholestasis caused by citrin deficiency. *Eur. J. Pediatr.* **2003**, *162*, 317–322. [CrossRef]
51. Tamamori, A.; Okano, Y.; Ozaki, H.; Fujimoto, A.; Kajiwara, M.; Fukuda, K.; Kobayashi, K.; Saheki, T.; Tagami, Y.; Yamano, T. Neonatal intrahepatic cholestasis caused by citrin deficiency: Severe hepatic dysfunction in an infant requiring liver transplantation. *Eur. J. Pediatr.* **2002**, *161*, 609–613. [CrossRef]
52. Okano, Y.; Kobayashi, K.; Ihara, K.; Ito, T.; Yoshino, M.; Watanabe, Y.; Kaji, S.; Ohura, T.; Nagao, M.; Noguchi, A.; et al. Fatigue and quality of life in citrin deficiency during adaptation and compensation stage. *Mol. Genet. Metab.* **2013**, *109*, 9–13. [CrossRef] [PubMed]
53. Saheki, T.; Kobayashi, K.; Terashi, M.; Ohura, T.; Yanagawa, Y.; Okano, Y.; Hattori, T.; Fujimoto, H.; Mutoh, K.; Kizaki, Z.; et al. Reduced carbohydrate intake in citrin-deficient subjects. *J. Inherit. Metab. Dis.* **2008**, *31*, 386–394. [CrossRef] [PubMed]
54. Nakamura, M.; Yazaki, M.; Kobayashi, Y.; Fukushima, K.; Ikeda, S.; Kobayashi, K.; Saheki, T.; Nakaya, Y. The characteristics of food intake in patients with type II citrullinemia. *J. Nutr. Sci. Vitaminol.* **2011**, *57*, 239–245. [CrossRef]
55. Saheki, T.; Kobayashi, K. Physiological role of citrin, a liver-type mitochondrial aspartate-glutamate carrier, and pathophysiology of citrin deficiency. *Recent Res. Devel. Life Sci.* **2005**, *3*, 59–73.
56. Saheki, T.; Kobayashi, K.; Iijima, M.; Horiuchi, M.; Begum, L.; Jalil, M.A.; Li, M.X.; Lu, Y.B.; Ushikai, M.; Tabata, A.; et al. Adult-onset type II citrullinemia and idiopathic neonatal hepatitis caused by citrin

- deficiency: Involvement of the aspartate glutamate carrier for urea synthesis and maintenance of the urea cycle. *Mol. Genet. Metab.* **2004**, *81*, S20–S26. [CrossRef] [PubMed]
57. Saheki, T. What is the function of citrin? In *Citrin Deficiency—A Unique Disease that Many Doctors Don't Know*; Fueisha: Osaka, Japan, 2017; pp. 53–58.
 58. Sinasac, D.S.; Moriyama, M.; Jalil, M.A.; Begum, L.; Li, M.X.; Iijima, M.; Horiuchi, M.; Robinson, B.H.; Kobayashi, K.; Saheki, T.; et al. Slc25a13-knockout mice harbor metabolic deficits but fail to display hallmarks of adult-onset type II citrullinemia. *Mol. Cell. Biol.* **2004**, *24*, 527–536. [CrossRef] [PubMed]
 59. Saheki, T.; Iijima, M.; Li, M.X.; Kobayashi, K.; Horiuchi, M.; Ushikai, M.; Okumura, F.; Meng, X.J.; Inoue, I.; Tajima, A.; et al. Citrin/mitochondrial glycerol-3-phosphate dehydrogenase double-knockout mice recapitulate features of human citrin deficiency. *J. Biol. Chem.* **2007**, *282*, 25041–25052. [CrossRef] [PubMed]
 60. Saheki, T.; Inoue, K.; Ono, H.; Fujimoto, Y.; Furuie, S.; Yamamura, K.; Kuroda, E.; Ushikai, M.; Asakawa, A.; Inui, A.; et al. Oral aversion to dietary sugar, ethanol and glycerol correlates with alterations in specific hepatic metabolites in a mouse model of human citrin deficiency. *Mol. Genet. Metab.* **2017**, *120*, 306–316. [CrossRef]
 61. Saheki, T.; Inoue, K.; Ono, H.; Tushima, A.; Katsura, N.; Yokogawa, M.; Yoshidumi, Y.; Kuhara, T.; Ohse, M.; Eto, K.; et al. Metabolomic analysis reveals hepatic metabolite perturbations in citrin/mitochondrial glycerol-3-phosphate dehydrogenase double-knockout mice, a model of human citrin deficiency. *Mol. Genet. Metab.* **2011**, *104*, 492–500. [CrossRef]
 62. Yazaki, M.; Takei, Y.; Kobayashi, K.; Saheki, T.; Ikeda, S. Risk of worsened encephalopathy after intravenous glycerol therapy in patients with adult-onset type II citrullinemia (CTLN2). *Intern. Med.* **2005**, *44*, 188–195. [CrossRef]
 63. Todo, S.; Starzel, T.E.; Tzakis, A.; Benkov, K.J.; Kalousek, F.; Saheki, T.; Tanikawa, K.; Fenton, W.A. Orthotopic liver transplantation for urea cycle enzyme deficiency. *Hepatology* **1992**, *15*, 419–422. [CrossRef] [PubMed]
 64. Ikeda, S.; Yazaki, M.; Takei, Y.; Ikegami, T.; Hashikura, Y.; Kawasaki, S.; Iwai, M.; Kobayashi, K.; Saheki, T. Type II (adult onset) citrullinaemia: Clinical pictures and the therapeutic effect of liver transplantation. *J. Neurol. Neurosurg. Psychiatry* **2001**, *71*, 663–670. [CrossRef] [PubMed]
 65. Fukushima, K.; Yazaki, M.; Nakamura, M.; Tanaka, N.; Kobayashi, K.; Saheki, T.; Takei, H.; Ikeda, S. Conventional diet therapy for hyperammonemia is risky in the treatment of hepatic encephalopathy associated with citrin deficiency. *Intern. Med.* **2010**, *49*, 243–247. [CrossRef] [PubMed]
 66. Imamura, Y.; Kobayashi, K.; Shibatou, T.; Aburada, S.; Tahara, K.; Kubozono, O.; Saheki, T. Effectiveness of carbohydrate-restricted diet and arginine granules therapy for adult-onset type II citrullinemia: A case report of siblings showing homozygous SLC25A13 mutation with and without the disease. *Hepatol. Res.* **2003**, *26*, 68–72. [CrossRef]
 67. Tamakawa, S.; Nakamura, H.; Katano, T.; Yoshizawa, M.; Ohtake, K.; Kubota, T. Hyperalimentation therapy produces a comatose state in a patient with citrullinemia. *J. Jpn. Soc. Intensive. Care. Med.* **1994**, *1*, 37–41. [CrossRef]
 68. Takahashi, H.; Kagawa, T.; Kobayashi, K.; Hirabayashi, H.; Yui, M.; Begum, L.; Mine, T.; Takagi, S.; Saheki, T.; Shinohara, Y. A Case of adult-onset type ii citrullinemia—Deterioration of clinical course after infusion of hyperosmotic and high sugar solutions. *Med. Sci. Monit.* **2006**, *12*, CS13–CS15. [PubMed]
 69. Mutoh, K.; Kurokawa, K.; Kobayashi, K.; Saheki, T. Treatment of a citrin-deficient patient at the early stage of adult-onset type II citrullinaemia with arginine and sodium pyruvate. *J. Inherit. Metab. Dis.* **2008**, *31*, S343–S347. [CrossRef]
 70. Saheki, T.; Inoue, K.; Tushima, A.; Mutoh, K.; Kobayashi, K. Citrin deficiency and current treatment concepts. *Mol. Genet. Metab.* **2010**, *100*, S59–S64. [CrossRef]
 71. Saheki, T.; Inoue, K.; Ono, H.; Katsura, N.; Yokogawa, M.; Yoshidumi, Y.; Furuie, S.; Kuroda, E.; Ushikai, M.; Asakawa, A.; et al. Effects of supplementation on food intake, body weight and hepatic metabolites in the citrin/mitochondrial glycerol-3-phosphate dehydrogenase double-knockout mouse model of human citrin deficiency. *Mol. Genet. Metab.* **2012**, *107*, 322–329. [CrossRef]
 72. Saheki, T.; Moriyama, M.; Kuroda, E.; Funahashi, A.; Yasuda, I.; Setogawa, Y.; Gao, Q.; Ushikai, M.; Furuie, S.; Yamamura, K.; et al. Pivotal role of inter-organ aspartate metabolism for treatment of mitochondrial aspartate-glutamate carrier 2 (citrin) deficiency, based on the mouse model. *Sci. Rep.* **2019**, *9*, 4179. [CrossRef]

73. Moriyama, M.; Li, M.X.; Kobayashi, K.; Sinasac, D.S.; Kannan, Y.; Iijima, M.; Horiuchi, M.; Tsui, L.C.; Tanaka, M.; Nakamura, Y.; et al. Pyruvate ameliorates the defect in ureogenesis from ammonia in citrin-deficient mice. *J. Hepatol.* **2006**, *44*, 930–938. [CrossRef] [PubMed]
74. Stoll, B.; McNelly, S.; Buscher, H.P.; Häussinger, D. Functional hepatocyte heterogeneity in glutamate, aspartate and alpha-ketoglutarate uptake: A histoautoradiographical study. *Hepatology* **1991**, *13*, 247–253. [CrossRef]
75. Neame, K.D.; Wiseman, G. The transamination of glutamic and aspartic acids during absorption by the small intestine of the dog in vivo. *J. Physiol.* **1957**, *135*, 442–450. [CrossRef] [PubMed]
76. Parsons, D.S.; Volman-Mitchell, H. The transamination of glutamate and aspartate during absorption in vitro by small intestine of chicken, guinea-pig and rat. *J. Physiol.* **1974**, *239*, 677–694. [CrossRef] [PubMed]
77. Windmueller, H.G.; Spaeth, A.E. Metabolism of absorbed aspartate, asparagine, and arginine by rat small intestine in vivo. *Arch. Biochem. Biophys.* **1976**, *175*, 670–676. [CrossRef]
78. Hoshi, M.; Mukai, S.; Shinzawa, J.; Watanabe, S.; Kasukawa, R.; Orikasa, H.; Kobayashi, K.; Saheki, T. A case of adult-onset type II citrullinemia in which oral administration of L-arginine granules improved the patient's encephalopathy and the increased level of ammonia. *Kanzo* **2002**, *43*, 492–497. [CrossRef]
79. Yazaki, M.; Kinoshita, M.; Ogawa, S.; Fujimi, S.; Matsushima, A.; Hineno, A.; Tazawa, K.; Fukushima, K.; Kimura, R.; Yanagida, M.; et al. A 73-year-old patient with adult-onset type II citrullinemia successfully treated by sodium pyruvate and arginine. *Clin. Neurol. Neurosurg.* **2013**, *115*, 1542–1545. [CrossRef]
80. Okano, Y.; Ohura, T.; Sakamoto, O.; Inui, A. Current treatment for citrin deficiency during NICCD and adaptation/compensatin stages: Strategy to prevent CTLN2. *Mol. Genet. Metab.* **2019**, *127*, 175–185. [CrossRef]
81. Hayasaka, K.; Numakura, C.; Toyota, K.; Kakizaki, S.; Watanabe, H.; Haga, H.; Takahashi, H.; Takahashi, Y.; Kaneko, M.; Yamakawa, M.; et al. Medium-chain triglyceride supplementation under a low-carbohydrate formula is a promising therapy for adult-onset type II citrullinemia. *Mol. Genet. Metab. Rep.* **2014**, *1*, 42–50. [CrossRef]
82. Saheki, T.; Funahashi, A.; Kuroda, E.; Yasuda, I.; Gao, Q.; Setogawa, Y.; Ushikai, M.; Horiuchi, M.; Moriyama, M. Effect of MCT on hyperammonemia in citrin deficiency. In *Japanese Journal for Inherited Metabolic Diseases Volume 35, Akita, Japan, 24–26 October 2019*; LETTERPRESS: Hiroshima, Japan, 2019; p. 159.
83. Moriyama, M.; Kuroda, E.; Funahashi, A.; Yasuda, I.; Gao, Q.; Setogawa, Y.; Ushikai, M.; Horiuchi, M.; Saheki, T. Effect of MCT on ureagenesis from ammonia in perfused liver of citrin-deficiency model mouse. *Japanese Journal for Inherited Metabolic Diseases Volume 35, Akita, Japan, 24–26 October 2019*; LETTERPRESS: Hiroshima, Japan, 2019; p. 157.



© 2020 by the authors. Licensee MDPI, Basel, Switzerland. This article is an open access article distributed under the terms and conditions of the Creative Commons Attribution (CC BY) license (<http://creativecommons.org/licenses/by/4.0/>).

Review

The Multifaceted Pyruvate Metabolism: Role of the Mitochondrial Pyruvate Carrier

Joséphine Zangari, Francesco Petrelli, Benoît Maillot and Jean-Claude Martinou *

Department of Cell Biology, Faculty of Sciences, University of Geneva, 30 Quai Ernest Ansermet, 1211 Geneva 4, Switzerland; Josephine.zangari@unige.ch (J.Z.); francesco.petrelli@unige.ch (F.P.); benoit.maillot@unige.ch (B.M.)

* Correspondence: jean-claude.martiou@unige.ch; Tel.: +41-22-3796443

Academic Editor: Ferdinando Palmieri

Received: 18 June 2020; Accepted: 14 July 2020; Published: 17 July 2020

Abstract: Pyruvate, the end product of glycolysis, plays a major role in cell metabolism. Produced in the cytosol, it is oxidized in the mitochondria where it fuels the citric acid cycle and boosts oxidative phosphorylation. Its sole entry point into mitochondria is through the recently identified mitochondrial pyruvate carrier (MPC). In this review, we report the latest findings on the physiology of the MPC and we discuss how a dysfunctional MPC can lead to diverse pathologies, including neurodegenerative diseases, metabolic disorders, and cancer.

Keywords: mitochondria; mitochondrial pyruvate carrier; metabolism; neurodegeneration; metabolic disorders; cancer

1. Introduction

Mitochondria are essential organelles of endosymbiotic origin, which participate in a multitude of cellular functions in eukaryotic cells, including energy metabolism, biosynthetic reactions, signaling, and the execution of programmed cell death. They host the respiratory chain complexes and ATP synthase, all of which participate in the formation of ATP (adenosine triphosphate) through the process known as oxidative phosphorylation (OXPHOS). Electrons released through oxidation of carbohydrates, amino acids, or lipids in the mitochondrial tricarboxylic acid (TCA) cycle are stored in ATP in the form of two energy-rich phosphoanhydride bonds. Of the molecules that can provide electrons to the respiratory chain, pyruvate, the end-product of glycolysis, is the most critical in many cell types including neurons. In mitochondria, oxidation of pyruvate by pyruvate dehydrogenase (PDH) generates acetyl coenzyme A (acetyl-CoA), which can then combine with oxaloacetate (OAA) to form citrate, the first substrate of the TCA cycle (Figure 1).

Furthermore, pyruvate can be carboxylated by the pyruvate carboxylase (PC) to OAA (Figure 1), which represents a major anaplerotic pathway to replenish TCA cycle intermediates, not only for gluconeogenesis but also for other pathways including the urea cycle and lipid synthesis [1].

In addition to glycolysis, there are other, mostly minor sources of pyruvate such as oxidation of lactate by lactate dehydrogenase (LDH), conversion from alanine by alanine transaminase (ALT), or conversion from malate by cytosolic or mitochondrial malic enzyme (ME) (Figure 1). Once formed, pyruvate can be either reduced to lactate by LDH in the cytosol, regenerating NAD^+ to fuel glycolysis, or fully oxidized within mitochondria, through the TCA cycle. The choice between these two pathways has important consequences for the cell, since glycolysis yields two molecules of ATP/molecule of glucose, whereas oxidative phosphorylation yields >30 molecules of ATP/molecule of glucose [2,3].

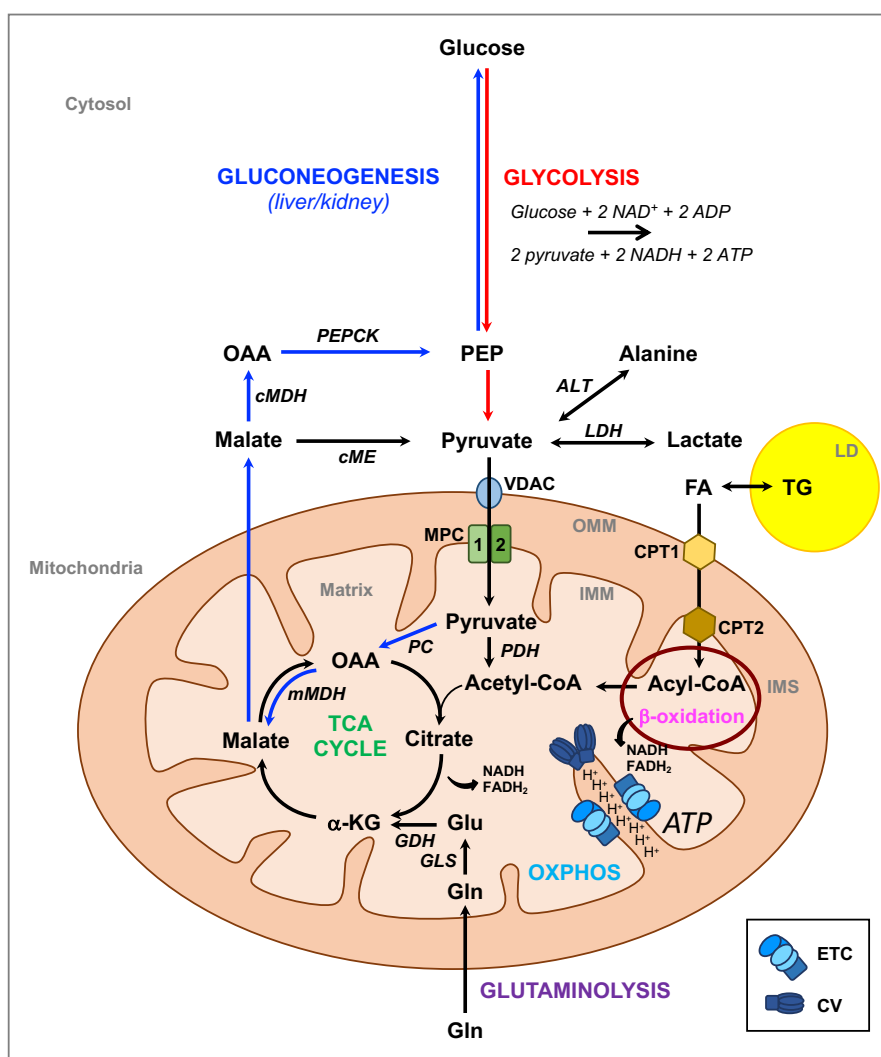


Figure 1. Metabolic pathways involving mitochondria. In the cytosol, pyruvate is produced through glycolysis, which generates two adenosine triphosphate (ATP) and two reduced nicotinamide adenine dinucleotide (NADH) molecules per molecule of glucose. Pyruvate can also be produced from oxidation of lactate by lactate dehydrogenase (LDH), conversion from alanine by alanine transaminase (ALT), or from malate by cytosolic or mitochondrial malic enzyme (ME). Pyruvate can be imported into mitochondria to be oxidized into acetyl coenzyme A (acetyl-CoA) by the pyruvate dehydrogenase (PDH), which then fuels the tricarboxylic acid (TCA) cycle. Import of pyruvate requires the voltage-dependent anion channel (VDAC) to cross the outer mitochondrial membrane (OMM) and the mitochondrial pyruvate carrier (MPC) to cross the inner mitochondrial membrane (IMM). The TCA cycle can also be fueled by glutamine (Gln) through glutaminolysis or by fatty acids (FA) released from lipid droplets (LD) where they are stored in the form of triglycerides (TG). FAs provide acetyl-CoA through FA β -oxidation. The TCA cycle and β -oxidation both generate the reducing equivalents NADH and flavin adenine dinucleotide ($FADH_2$), which transfer electrons to the electron respiratory chain (ETC), generating more than 30 ATP molecules per molecule of glucose. The last reaction is catalyzed by ATP synthase or Complex V (CV). This process requires the presence of oxygen and is known as oxidative phosphorylation (OXPHOS). In the liver and kidney, pyruvate can be converted into oxaloacetate (OAA) by the pyruvate carboxylase (PC), which is then reduced into malate by the malate dehydrogenase (mMDH). Malate is then exported into the cytosol, converted into OAA by malate dehydrogenase (cMDH) and into phosphoenolpyruvate (PEP) by PEP carboxykinase (PEPCK) and from there into glucose through several steps, including the reversible steps of glycolysis. IMS: intermembrane space; CPT1: carnitine palmitoyltransferase 1; CPT2: carnitine palmitoyltransferase 2; GDH: glutamate dehydrogenase; GLS: glutamase; α -KG: α -ketoglutarate.

To enter mitochondria, pyruvate crosses the outer mitochondrial membrane (OMM) to reach the intermembrane space (IMS), probably through the large, relatively non-specific, voltage-dependent anion channel (VDAC), and it is then transported together with a proton across the inner mitochondrial membrane (IMM) by the mitochondrial pyruvate carrier (MPC) [4] (Figure 1). The existence of MPC was proposed on theoretical grounds several decades ago [4], although the molecular identification of the MPC complex was only achieved in 2012 [5,6]. As the sole point of entry for pyruvate into the mitochondrial matrix, the MPC plays a crucial role in coordinating glycolytic and mitochondrial activities, and it provides a key decision point for modulating cellular energy production and metabolism.

In this review, we report the most recent findings on the physiology of the MPC and its participation in various pathologies, including neurodegenerative diseases, metabolic disorders, and cancer.

2. Structure of the MPC

The MPC is encoded by three homologous genes *MPC1*, *MPC2*, and *MPC3* in *Saccharomyces cerevisiae*, by two genes *MPC1* and *MPC2* in flies, and by three genes, *MPC1*, *MPC1-like*, and *MPC2* in mammals [5,6]. In yeast, the active MPC complexes are the MPC1-MPC3 heterodimers, which promote pyruvate transport during respiratory growth, and the MPC1-MPC2 heterodimers, which function during fermentable growth [7,8]. In most mammalian cells, the active carrier is composed of an MPC1 and MPC2 heterodimer, with the exception of spermatocytes, which display MPC1-like and MPC2 heterodimers [9]. Loss of one subunit leads to degradation of the other subunit and disruption of the MPC complex. Functional tests with yeast MPC1 and MPC3 following reconstitution of the carrier in liposomes showed that only heterodimers were able to transport pyruvate [10]. In another report, MPC2 homodimers were also reported to be functional [11], although this was not supported by the results of Tavoulari et al. [10] or by other data reporting that mitochondria from Δ MPC1 mutants were unable to import pyruvate [5,6,12]. The reason for this discrepancy remains unclear.

MPC1 and MPC2 are small integral membrane proteins of, respectively, 12 kDa and 14 kDa. Structure predictions using different algorithms suggest that MPCs belong to the semi-SWEET (Sugar Will Eventually be Exported Transporter) domain family (SLC50 family) [13] or to the SWEET family [14], also known as the PQ-loop family of sugar transporters. The semi-SWEET domain is composed of a simple 1-3-2 triple transmembrane helix bundle (THB), whereas the SWEET domain consists of two semi-SWEET domains linked by a transmembrane helix [15] (Figure 2A). Recently, Medrano-Soto et al. proposed that the MPC belongs to the transporter-opsin-G protein-coupled receptor (TOG) superfamily with seven putative TMSs arranged in a 3+1+3 topology [14]. According to these authors, the MPC1 and MPC2 subunits might have originated from duplication of an MPC precursor, composed of four transmembrane segments, which would have lost its N-terminal transmembrane segment. Although the mechanisms via which the MPC imports pyruvate remain unknown, several hypotheses were postulated using in silico docking analyses, based on structural models of the MPC [16–18].

The heterodimeric composition and homology to the SWEET or semi-SWEET sugar transporters, sets the MPC apart from other families of mitochondrial carriers (named MCF or SLC25). The membrane topology of MPC1 and MPC2 is still not fully resolved and Figure 2 proposes a model based on the semi-SWEET motif. Our earlier biochemical approaches based on the accessibility to proteases or to thiol labeling suggest that MPC1 displays at least two transmembrane segments with the N- and C-termini projecting into the mitochondrial matrix, whereas MPC3 in yeast and MPC2 in mammals probably consist of three transmembrane helices, with the N-term in the matrix and the C-term in the intermembrane space [7]. It was recently reported that, despite this topology, yeast MPC2 and MPC3, both of which display an odd number of transmembrane segments with the N-term in the matrix, are nevertheless imported via the carrier import pathway which includes the receptor Tom70, TIM (Translocase of the Inner Membrane) chaperones, and the TIM22 complex [19,20], and not via the flexible presequence pathway as was previously predicted.

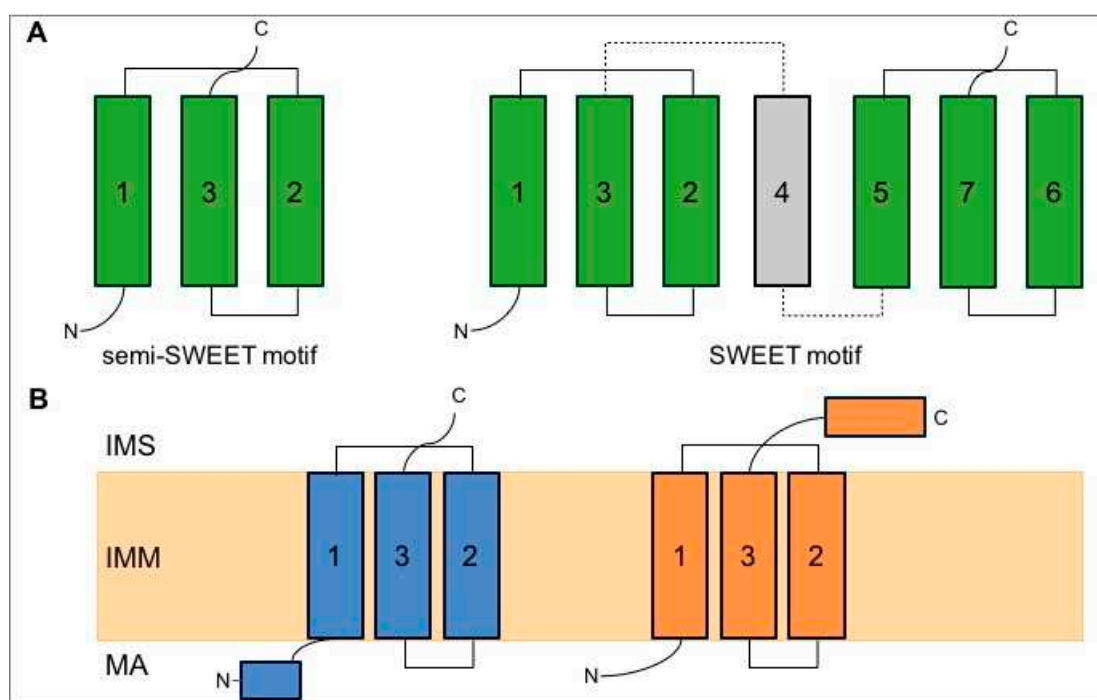


Figure 2. (A) Semi-SWEET and SWEET motifs. Semi-SWEET is composed of a triple helix bundle in this specific order 1-3-2. SWEET contains two semi-SWEET motifs linked together by a helix. All the helices are crossing the membrane. (B) Model for the topology of MPC1 and MPC2 in the inner mitochondrial membrane (IMM). Here, a semi-SWEET structure is proposed for both MPC1 and MPC2. MA: matrix; IMS: intermembrane space.

Several *MPC1* mutations resulting in disruption of the MPC complex or loss of transporter function were reported [21,22]. All of these mutations are accompanied by severe clinical symptoms and premature death.

Solving the three-dimensional structure of the MPC will be key to resolving the remaining uncertainties concerning the structure of the carrier, its membrane topology, and how it transports pyruvate across the IMM.

3. Regulation of MPC Expression

3.1. Transcriptional Regulation of MPC Expression in Yeast and in Mammalian Cells

As mentioned above, in *Saccharomyces cerevisiae*, MPC1 and MPC2 are expressed under fermentative conditions and form the MPC_{FERM} complex, while MPC1 and MPC3 are expressed under respiratory conditions and form the MPC_{OX} complex [7,23]. This switch is orchestrated at the level of transcription by the activity of the high osmolarity glycerol (HOG) mitogen-activated protein (MAP) kinase pathway. Accordingly, the *MPC3* gene promoter is bound directly by the Sko1 transcriptional repressor/activator, which is one of the core transcription factors mediating the transcriptional osmotic stress response downstream of the HOG1 MAP kinase [8].

In mammalian cells, although MPC1 and MPC2 subunits are ubiquitously expressed, their expression is particularly abundant in the heart, kidney, liver, brown adipose tissue, muscles, and brain [24–26]. A number of transcriptional regulatory mechanisms of the MPC genes were reported. Wang and colleagues showed that MPC1 is transcriptionally repressed in human prostate cancer cells by the chicken ovalbumin upstream promoter-transcription factor II (COUP-TFII), a member of the steroid receptor superfamily. MPC1 repression is part of the metabolic switch toward increased glycolysis, which promotes prostate cancer cell growth and invasion [27].

In contrast to COUP-TFII, peroxisome proliferator-activated receptor-gamma co-activator (PGC)-1 alpha (PGC-1 α) was found to increase expression of MPC1 in human renal cell carcinoma [28] and cholangiocarcinoma [29]. Overexpression of PGC-1 α strongly stimulated *MPC1* transcription through binding to the *MPC1* promoter, while depletion of PGC-1 α by small interfering RNA (siRNA) suppressed MPC1 expression. The latter study showed that PGC-1 α reversed the Warburg effect by upregulating expression of both MPC1 and pyruvate dehydrogenase E1 alpha 1 subunit (PDHA1), thus leading to enhanced mitochondrial metabolism. Transcriptional activation of MPC1 by PGC-1 α was shown to be mediated by recruitment of the estrogen-related receptor alpha (ERR α), which bound the ERR α response element located in the proximal *MPC1* promoter region [28,30]. Inhibiting the activity of ERR α decreased expression of MPC1, interfered with pyruvate entry into mitochondria, and increased cellular reliance on glutamine oxidation and the pentose phosphate pathway (PPP) to maintain reduced NAD phosphate (NADPH) homeostasis [30].

More recently, it was shown that colon cancer cells can reprogram cell metabolism to coordinate proper cellular response to interferon- γ (IFN γ), a cytokine that plays a pivotal role in host antitumor immunity. Downregulation of MPC subunit expression via the signal transducer and activator of transcription 3 (STAT3) pathway attenuated IFN γ -mediated apoptosis of the colon cancer cells by preventing production of reactive oxygen species (ROS) [31]. Moreover, inhibition of STAT3-mediated transcription using the inhibitor Stattic partially reversed the inhibition of MPC1 and MPC2 expression and increased the antitumor efficacy of IFN γ .

In prostate adenocarcinoma, the androgen receptor (AR) is a hormone-responsive nuclear receptor transcription factor that coordinates anabolic processes to enable tumor proliferation through transcriptional regulation of metabolic pathways [32]. Massie and colleagues showed that the AR regulated MPC activity via direct transcriptional control of *MPC2*. In AR-driven prostate adenocarcinoma, MPC inhibition led to reduced OXPHOS, activation of the eukaryotic initiation factor 2 α (eIF2 α)/activating transcription factor 4 (ATF4) integrated stress response, and increased glutaminolysis [33]. Importantly, in this experimental model, MPC inhibition by the small-molecule inhibitor MSDC-0160 suppressed tumor growth in vivo, suggesting that the MPC could be a potential therapeutic target for this type of cancer.

Finally, it was found that, in pancreatic cancer, MPC1 is transcriptionally suppressed by the histone lysine demethylase 5A (KDM5A) [34]. Elevated expression of KDM5A and downregulation of MPC1 correlated directly with pancreatic ductal adenocarcinoma progression.

Taken together, these data indicate that a number of different transcription factors can regulate the promoter activity of MPC1 and/or MPC2. How these factors regulate expression of the MPC genes, and how this regulation is integrated into the overall activity of cellular signaling pathways are interesting questions that remain to be further investigated.

3.2. Post-Translational Regulation of MPC Expression

Several studies described the post-translational regulation of MPC activity. Liang and colleagues found that MPC1 is acetylated on lysine residues K₄₅ and K₄₆, and that deacetylation of MPC1 by Sirt3 resulted in increased carrier activity [35].

MPC2 was also reported to be acetylated in a mouse type 1 diabetic heart model. However, in this case, acetylation appeared to stimulate activity of the transporter [36].

An indirect model of post-translational regulation was reported by the group of Kim et al. [37], who showed that, in hepatocarcinoma cells, the BH3 (Bcl-2 homology region 3)-only protein PUMA (p53 upregulated modulator of apoptosis), whose transcription depends on p53, can associate with MPC to disrupt dimer formation and MPC function. High expression levels of PUMA were correlated with decreased mitochondrial pyruvate uptake and increased glycolysis.

4. The MPC and Cell Metabolism

Cell metabolism can be defined as the ensemble of chemical reactions occurring in the cell, including anabolic reactions that convert nutrients into molecular building blocks, and catabolic reactions that convert nutrients into energy. By allowing the import of pyruvate into mitochondria, the MPC participates in both anabolic (synthesis of intermediary metabolites by the TCA cycle) and catabolic (OXPHOS) events.

One of the characteristics of cell metabolism is its plasticity, which results from the interconnectivity between different metabolic pathways. Plasticity ensures that, when one pathway is transiently or permanently interrupted due to lack of an essential metabolite or a key enzyme or transporter, the cell is able to switch to an alternative pathway to compensate for the defect. However, bottlenecks exist, involving certain metabolite carriers, which allows metabolites to cross cellular membranes. Pyruvate metabolism is a good example. As mentioned in the introduction, there are several ways to synthesize this metabolite in the cytosol; however, the MPC is the only route via which pyruvate can cross the IMM. Such molecules provide key regulatory steps for the cell, as well as offer attractive targets for therapeutic intervention.

Nevertheless, because of the metabolic plasticity, cells often find ways to compensate for defective carriers or metabolites. For example, when the MPC is deficient, increased glutaminolysis or oxidation of fatty acids (beta-oxidation) can compensate for the deficit in pyruvate-derived carbon to fuel the TCA cycle [25,38,39].

Different cell types adapt their metabolism differently to changes in their cellular environment and physiology. In cells with high energy demands such as muscle cells and neurons, OXPHOS is the preferred source of ATP. For these cells, either glucose/pyruvate or fatty acids (FAs) provide the main substrates, although neurons preferentially oxidize pyruvate because they do not express many of the enzymes required for beta-oxidation. In contrast, cardiomyocytes in the adult seem to favor FA oxidation over pyruvate [40,41]. Thus, in these cell types, metabolic plasticity is more limited, which may explain the high incidence of degenerative pathologies that affect brain and muscle.

In other cell types, ATP is generated mainly through glycolysis rather than OXPHOS, even when oxygen is available. This is the case for many highly proliferating cells, including antigen-activated lymphocytes [42] and most cancer cells *in vitro*. This type of metabolism is referred to as aerobic glycolysis or the Warburg effect after Otto Warburg who first described this process in cancer cells [43,44].

In highly proliferating cells, an important advantage of glucose fermentation compared to OXPHOS is that carbohydrates are only partially degraded, thus providing intermediary metabolites, particularly nucleotides generated via the pentose pathway [43], as building blocks to maintain rapid growth.

Thus, it is clear from the above that the importance of the MPC in cell metabolism is highly dependent on the cell type and cell context. Below, we review the role of the MPC in different cell types and discuss how a dysfunctional MPC can lead to diverse pathologies.

4.1. The Role of MPC in Neurons and in Neurodegenerative Diseases (NDs)

Neurons rely mainly on glucose as an energy source and to a lesser extent on amino-acid oxidation; however, they lack most enzymes involved in FA oxidation [45]. As a result, the role of the MPC, and of pyruvate metabolism in general, is particularly important in neurons. Pyruvate is generated principally through glycolysis in these cells, but also by conversion from lactate by LDH. Astrocytes provide the major source of lactate which is taken up by neurons by the so-called astrocyte-neuron shuttle [46].

Although most neurons use oxidative phosphorylation to generate the high levels of energy required for neural transmission, some parts of the brain, such as the medial and lateral parietal and prefrontal cortices, were found to rely mainly on aerobic glycolysis [47]. Energy metabolism in the retina is also predominantly through aerobic glycolysis, and only a small fraction of the pyruvate produced by glycolysis is oxidized in mitochondria. Nevertheless, pyruvate oxidation in mitochondria

appears to be essential for retinal function since mice lacking MPC1 in the retina were found to display degeneration of both rod and cone photoreceptors and decline in visual function [48]. MPC-deficient retinas displayed lower ATP and NADH levels although increased glutaminolysis and ketone body oxidation limited degeneration of the photoreceptors.

Neurodegenerative diseases (NDs) are often considered to be metabolic disorders characterized by a decline in the ability to import or metabolize energy sources, resulting either in or from mitochondrial dysfunction [49]. However, even though bioenergetic defects were observed in diverse pathological conditions, both in mice and in patients [50–52], in most cases, it remains unclear whether this is the cause or the consequence of the pathology. Interestingly, it was shown recently that modulation of energy metabolism through MPC inhibition offers a potential pharmacological approach to treatment for NDs, in particular for Parkinson's and Alzheimer's diseases.

Parkinson's disease (PD) is a neurodegenerative disorder resulting in the death of dopaminergic neurons in the substantia nigra pars compacta of the brain. In recent years, epidemiological evidence showed similarities in metabolic dysfunction between type 2 diabetes and PD. Indeed, several clinical trials in PD patients are in progress using anti-diabetic drugs [53–59]. In 2016, Ghosh and colleagues (2016) investigated the activity of the MPC inhibitor MSDC-0160, a derivative of thiazolidinedione, in diverse models of PD [60]. The authors showed that MSDC-0160 protected tyrosine hydroxylase (TH)-positive dopaminergic neurons against the neurotoxicity of MPP⁺ or MPTP *in vitro* and *in vivo*, as well as showed beneficial effects in the *Engrailed* heterozygous mutant mice, which undergo loss of dopaminergic neurons at six weeks of age [60,61]. The mechanisms via which MPC inhibition results in neuronal protection are not well understood. Ghosh and colleagues proposed that inhibition of the MPC may protect neurons through modulation of the mammalian target of rapamycin (mTOR) pathway and autophagy, and indeed MSDS-0160 was shown to reduce neuroinflammation by modulating the NF- κ B (nuclear factor kappa-light-chain-enhancer of activated B cells)/mTOR pathway [60]. This could be especially relevant for PD since neuroinflammation is considered to play an important role in the pathophysiology of the disease [62,63].

MPC inhibition could also be beneficial in the treatment of Alzheimer's disease (AD). A phase IIa clinical study in non-diabetic subjects with mild to moderate AD demonstrated that a three-month treatment with the MPC inhibitor MSDC-0160 resulted in a significant increase of glucose uptake in the regions of the brain normally affected in this pathology [64]. This again argues in favor of a possible neuroprotective effect of this compound. However, these results should be considered in the light of recent findings *in vitro* in which the expression of MPC2 was shown to be decreased in AD-related models [65]. This led to decreased calcium and pyruvate uptake into mitochondria and decreased OXPHOS. The reason for the decrease in calcium import remains unclear. However, another study in hepatocytes and embryonic fibroblasts showed that calcium import into mitochondria through the mitochondrial calcium uniporter (MCU) was decreased following inhibition of MPC activity. This effect was mediated by increased expression of the MCU gatekeeper mitochondrial calcium uptake 1 (MICU1) [66]. It would be interesting to test the expression levels of MICU1 in MPC-deficient neurons.

Another study describing the effects of pharmacological inhibition of the MPC reported that two specific inhibitors, MSDS-0160 and UK5099, protected neurons against glutamate-induced excitotoxicity *in vitro* [67]. This suggests that inhibition of the MPC could be useful in acute pathologies of the brain such as stroke or brain trauma where neurons are frequently exposed to toxic levels of glutamate.

Despite these promising results in PD, AD, and acute neuronal death, the molecular mechanisms underlying these effects remain to be elucidated. Furthermore, most studies showing a beneficial effect of MPC inhibition in these pathologies were based on small-molecule derivatives of thiazolidinediones. Although these compounds were shown to act as MPC inhibitors, off-target effects cannot be excluded. Therefore, it will be important to confirm these results using other chemical classes of MPC inhibitors or using genetic approaches in mouse models in which MPC1 or MPC2 are deleted specifically in neurons and/or glial cells.

4.2. The Role of MPC in Metabolic Disorders

Many studies reported that disruption of the MPC affects gluconeogenesis, a process known to play a role in the pathogenesis of type 2 diabetes (T2D) [68]. T2D can result from the dysfunction of several organs, including pancreas, liver, muscle, and kidney, all of which express the MPC. It will, therefore, be important to analyze the consequences of MPC downregulation in each of these organs.

4.2.1. MPC in Pancreas

Glucose is an important physiological stimulus for insulin secretion by pancreatic β -cells. Elevated blood glucose triggers increased glucose uptake into these cells, synthesis of ATP by OXPHOS, and closure of the plasma membrane ATP-sensitive potassium channels (K_{ATP} channel), which then leads to membrane depolarization, entry of calcium, and insulin secretion. This phenomenon, termed glucose-stimulated insulin secretion (GSIS), requires both pyruvate oxidation and carboxylation in pancreatic β -cells [69–71]. Inhibition of the MPC, either pharmacologically using UK5099 or genetically using siRNAs directed against MPC1 or MPC2, reduced GSIS in the 832/13 cell line derived from INS-1 rat insulinoma cells, as well as in rat and human islets [72]. Oxygen consumption, the ATP/ADP ratio, and the NADPH/NADP⁺ ratio were all reduced upon inhibition of the MPC. Similar results were obtained in mice displaying inactive, truncated MPC2 [26], in mice carrying a targeted deletion of MPC2 in pancreatic cells, as well as in *Drosophila* [73]. All these experiments show that the MPC plays an important and evolutionarily conserved role in insulin-secreting cells through mediating glucose sensing, regulation of insulin secretion, and control of systemic glycemia.

4.2.2. MPC in Liver

Gluconeogenesis

One of the mechanisms via which the liver participates in T2D is through gluconeogenesis [68,74], a major regulatory process in which non-carbohydrate substrates are converted into either free glucose or glycogen (Figure 1). Gluconeogenesis can also take place in the kidney, albeit to a lesser extent.

Hepatic glucose production is a critical physiological process that is required for maintaining normoglycemia during periods of nutrient deprivation. The major non-carbohydrate precursors are lactate, amino acids, and glycerol. Lactate is of particular importance. It is converted into pyruvate by the action of lactate dehydrogenase LDHB, and pyruvate is then imported through the MPC into mitochondria where it is carboxylated into OAA and reduced into malate. Malate is then exported into the cytosol where it can be used to generate glucose through several steps, including the reversible steps of glycolysis (Figure 1).

Lactate for gluconeogenesis is derived mainly from muscle cells undergoing anaerobic glycolysis. Under these conditions, muscle cells release lactate, which is then taken up by the liver to provide a substrate for gluconeogenesis. The glucose produced by the liver can in turn provide an energy source for muscle cells, thereby completing the cycle. This pathway, known as the Cori cycle or the glucose-lactate cycle, can account for up to 40% of plasma glucose turnover.

As expected, liver-specific deletion of MPC1 or MPC2 in mice impairs lactate/pyruvate-triggered hepatic gluconeogenesis [75,76]. However, gluconeogenesis from alanine was increased in MPC-deficient mice, and McCommis et al. [76] suggested that intramitochondrial transamination of alanine to pyruvate may contribute to gluconeogenesis when mitochondrial pyruvate import is inhibited. Thus, pyruvate-alanine cycling may constitute an alternative pathway for gluconeogenesis, which circumvents the MPC. This interesting hypothesis implies the existence of a mitochondrial transporter for alanine, which remains to be identified.

By decreasing gluconeogenesis, MPC inhibition was found to attenuate the development of hyperglycemia induced by a high-fat diet (HFD) leading to improved glucose tolerance [75,77].

MPC in Nonalcoholic Steatohepatitis (NASH)

The rise in the level of obesity in the population dramatically increased the incidence of a variety of related metabolic diseases, including nonalcoholic fatty liver disease (NAFLD). The spectrum of NAFLD ranges from simple hepatic fat accumulation to a more severe disease termed nonalcoholic steatohepatitis (NASH), involving inflammation, hepatocyte death, and fibrosis.

As mentioned above, thiazolidinediones (TZDs) appear to be potent MPC inhibitors [78]. One TZD derivative, MSDC-0602, prevents and reverses stellate cell activation and fibrosis in a mouse model of NASH. Importantly, the effects of this small-molecule inhibitor were duplicated by genetic deletion of MPC2 in hepatocytes and furthermore, the effects of MSDC-0602 were lost when MPC2 was deleted [79]. Thus, the MPC appears to be an attractive target in NASH [80]. Indeed, results from a phase IIb clinical trial on patients with liver biopsy-confirmed NASH [81] showed that MSDC-0602K significantly decreased liver steatosis, although it failed to prevent liver fibrosis.

4.2.3. MPC in Kidney

Diabetic kidney disease (DKD), which is characterized by albuminuria and renal hypertrophy, is the leading cause of kidney failure. It was shown recently that treatment with artemether, a methyl ether derivative of artemisinin used in the treatment of malaria and identified as a possible candidate for treating T2D, prevented kidney hypertrophy and ameliorated the lesions that lead to renal enlargement in T2D db/db mice. Interestingly, the mechanisms underlying this beneficial effect may in part be associated with the ability of artemether to increase MPC1 and MPC2 levels in db/db mice [82]. In particular, podocytes, which play an important role in the development of DKD, undergo increased apoptosis when the MPC is inhibited using UK5099 or RNA interference. These results suggest that enhancing MPC function may reduce injury in high-glucose-treated podocytes and may possibly attenuate DKD.

4.2.4. MPC in Muscle

During T2D, decreased glucose uptake by skeletal muscle significantly drives chronic hyperglycemia [83]. Skeletal muscle-specific MPC knockout in mice (MPC SkmKO) leads to increased glucose uptake in muscle and increased lactate release [84], thus increasing the Cori cycle as explained above. Furthermore, FA oxidation appears to be increased in MPC-deficient cells. Because hepatic gluconeogenesis is energetically supported by FA oxidation and muscle MPC disruption increases muscle FA oxidation, futile Cori cycling is energetically supported by FA oxidation. In conclusion, these findings raise the possibility that selectively decreasing skeletal muscle pyruvate uptake in obese and T2D patients may promote fat loss and restoration of whole-body insulin sensitivity.

In conclusion of this part on metabolism and pathologies, it emerges that, while inhibition of the MPC in complex metabolic diseases, such as T2D, is potentially interesting, it is difficult to predict the outcome in patients for two main reasons: (i) because these pathologies are the result of multiorgan dysfunction, and (ii) because antagonistic effects of MPC inhibition occur in different organs. For example, while MPC inhibition increases glucose uptake in the muscles and decreases gluconeogenesis in the liver, two beneficial effects for T2D, it also decreases insulin secretion, which a priori could be problematic for diabetic patients. Thus, it remains unclear whether the combination of these positive and negative effects will result in an overall benefit for the patient.

Due to embryonic lethality in mice at around E12, it is not possible to generate a constitutive deletion of either MPC1 or MPC2 in all tissues [24–26] and, to date, experiments addressing the role of MPC in the mouse were mainly performed using organ-specific deletion of the carrier. Furthermore, we do not yet know whether a global, conditional knockout of MPC1 or MPC2 in adult mice would be lethal. An alternative approach, therefore, is to address this question pharmacologically by administering small-molecule inhibitors of the MPC, with the caveat that off-target effects cannot be

excluded. Such experiments were performed recently and, as described above, promising results were obtained in mouse models of NASH and T2D.

4.3. The Role of MPC in Cancer

As described above, cancer cells *in vitro* rely mainly on aerobic glycolysis for rapid cell growth (Figure 3), and it is not surprising, therefore, that loss of MPC expression, which favors increased glycolysis, was found to be associated with poor cancer prognosis [85–90].

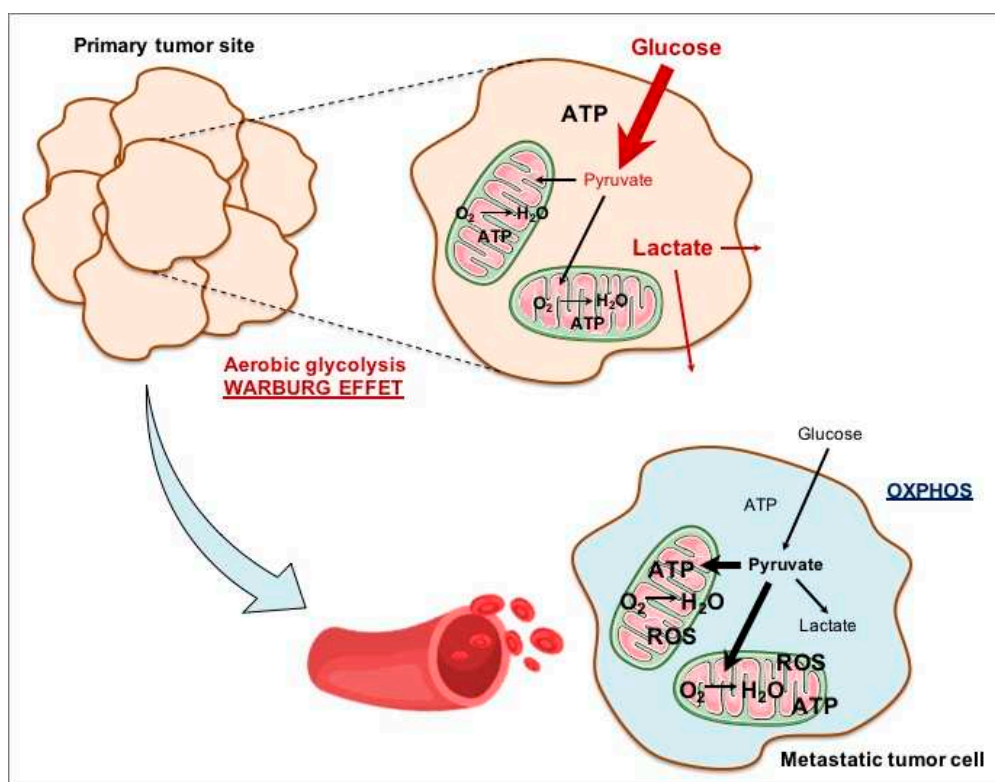


Figure 3. Tumor cell metabolism. In the primary tumor site, cancer cells mainly rely on aerobic glycolysis (Warburg effect) and this metabolism favors cell proliferation and tumor growth. Some cancer cells escape from the primary tumor site through the bloodstream, generating metastasis in other organs. It is thought that, to do this, some cancer cell types switch to a more oxidative metabolism.

One of the main questions in the field is whether loss of functional MPC can initiate tumorigenesis and, conversely, whether increasing MPC activity would result in reduced aerobic glycolysis. Furthermore, if aerobic glycolysis is generally associated with tumor growth, there are a number of reports showing that OXPHOS and ROS production are required for tumor metastasis. In this case, what is the role of the MPC? Does expression of the MPC contribute to poor prognosis, and would inhibition of the MPC be able to reduce cell invasion and metastasis? These are the questions we will address in the next section.

4.3.1. The Role of MPC in Stemness

Re-expression of wild-type (WT) MPC1 and MPC2 in colon cancer cells, which carried mutations or deletions in the MPC1 gene, impaired colony formation in soft agar and spheroid formation *in vitro* and reduced tumor growth *in vivo* [89]. In addition, these antitumoral effects were accompanied by a decrease in stem-cell markers, such as aldehyde dehydrogenase (ALDH) A (ALDHA), lin-28 homolog A (LIN28A), leucine rich repeat containing G protein-coupled receptor 5 (LGR5), and homeobox transcription factor Nanog (NANOG), suggesting that a decrease in MPC expression promotes the

Warburg effect and the maintenance of stemness in colon cancer cells. Consistent with these findings, Zhenhe Suo and colleagues showed that pharmacological or genetic inhibition of the MPC stimulated aerobic glycolysis in prostate, esophageal squamous, and ovarian cancer cells in vitro [87,91–93]. This was associated with higher levels of stem-cell markers including organic cation transporter (OCT) OCT3/4, NANOG, hypoxia inducible factor 1 alpha (HIF1 α), notch receptor 1 (NOTCH1), CD44 antigen, and ALDH [91,93]. Moreover, MPC inhibition conferred on these cells the ability to migrate and an increased resistance to both chemotherapy and radiotherapy [87,91,93]. Similar observations were reported for lung adenocarcinomas [90]. Taken together, these results highlight a role of MPC in determining the stemness status of cancer cells in vitro.

More recently, MPC was shown to be involved in the initiation of intestinal tumor formation in mice and *Drosophila* [94]. Sporadic colon tumors are believed to follow a typical progression pathway in which the initial tumorigenic event triggers intestinal stem-cell hyperplasia, leading to the formation of a benign adenoma. This initial event was associated with hyperactivation of the Wnt/ β -catenin pathway and loss of function of the *APC* tumor suppressor. In this study, expression of both MPC1 and MPC2 was found to be decreased in adenomas in two different mouse models of colon cancer, the azoxymethane and dextran sodium sulfate (AOM-DSS) models, as well as a genetic model of heterozygous loss of *Apc* in intestinal stem cells (*Apc*^{Lrig1KO/+}*Mpc1*^{Lrig1KO} mice) [94]. Targeted deletion of *MPC1* in adult LRIG1⁺ intestinal stem cells (*Mpc1*^{Lrig1KO}) led to an increased tumor burden and a substantial increase in the incidence of macroscopic tumors in the AOM-DSS model. Furthermore, in the heterozygous *Apc* model, the *Apc*^{Lrig1KO/+}*Mpc1*^{Lrig1KO} mice exhibited a higher tumor burden compared to *Apc*^{Lrig1KO/+} mice, and the macroscopic tumor burden was also much higher. These results demonstrate that loss of MPC function is sufficient to promote intestinal tumor initiation in a chemically induced tumor model and in different genetic tumor models. Similarly, in *Drosophila*, loss of the MPC or *Apc* led to hyperproliferation of intestinal stem cells and, importantly, the hyperproliferation following deletion of *Apc* was completely suppressed by ectopic expression of the MPC. Interestingly, the metabolic consequences of MPC loss resulted in all *Mpc1*^{Lrig1KO} adenomas attaining a stem-like phenotype.

In conclusion, decreased mitochondrial pyruvate metabolism through elimination of MPC activity is sufficient to increase the oncogenic susceptibility of both the fly and the mouse intestinal tracts. Thus, constitutive enforcement of the metabolic program found in hyperproliferative colonic lesions predisposes intestinal stem cells to adenoma formation.

4.3.2. The Role of MPC in Epithelial-Mesenchymal Transition (EMT)

During tumorigenesis, cancer cells acquire migratory and invasive properties through induction of the epithelial-mesenchymal transition (EMT). It was proposed that production of ROS can trigger metastasis [95], and some authors proposed that aerobic glycolysis would promote primary tumor formation, while a shift to a more oxidative metabolism would be required for metastasis (Figure 3). In intrahepatic cholangiocarcinoma, known to have a high malignant potential, low *MPC1* expression is correlated with poor prognosis and a significant increase in the percentage of distant metastasis [88]. The most well-known phenomenon associated with metastasis of cancer cells is EMT, which is strongly linked to the function of MPC1. Indeed, MPC1 expression was downregulated in human biliary tract cancer cells undergoing TGF- β (transforming growth factor beta)-induced EMT, and the knockdown of MPC1 expression led to induction of EMT in these cancer cells. These findings support the conclusion that MPC1 functions as a modulator of EMT induction and contributes to the malignant potential of intrahepatic cholangiocarcinoma cells.

Consistent with this conclusion, the study of Takaoka and collaborators found that, in pancreatic and colon cancer cells, EMT was induced following suppression of MPC1 expression [96]. These authors showed that MPC1 and MPC2 knockdown upregulated the glutaminase GLS, inducing EMT. This effect was suppressed in glutamine depletion conditions, revealing glutamine metabolism as an important mechanism inducing EMT. Finally, *MPC1* was found to be downregulated in renal cell carcinoma

tissue when compared with adjacent non-cancerous tissue, and lower MPC1 expression correlated with unfavorable prognosis for renal cell carcinoma patients [97]. Functionally, MPC1 suppressed the invasion of renal carcinoma cells in vitro and reduced their growth in vivo by decreasing the expression of the matrix metalloproteases 7 and 9 (MMP7 and MMP9).

4.3.3. MPC and Lactate in Tumor Growth

The consequence for cancer cells of relying on aerobic glycolysis is, firstly, the need to import high levels of glucose to compensate for the loss of ATP production by OXPHOS and, secondly, high amounts of lactate produced in the cytosol by LDH-mediated reduction of pyruvate are released from the cell. The latter leads to acidification of the extracellular microenvironment, which favors metastasis, angiogenesis, and immunosuppression [98]. Thus, lactate can be seen as an oncometabolite in the metabolic reprogramming of cancer cells. However, the role of lactate in cancer is complex. Recently, two groups reported high levels of lactate in the blood of patients with lung cancers [99,100], as well as in a mouse lung cancer model [100]. Interestingly lactate was found to be imported into tumor cells to at least the same extent as glucose, although the consequences of high levels of lactate in cancer cells remains unclear. In particular, it is unclear whether lactate, after conversion into pyruvate, could fuel the TCA cycle, participate in OXPHOS, and/or lead to the synthesis of intermediary metabolites, including acetyl-CoA, which could influence chromatin remodeling and gene expression.

4.3.4. Inhibition of MPC Activity Delays Tumor Growth

Reduced levels and activity of the MPC are associated with the majority of cancer types. Therefore, in most cases, a therapeutic strategy based on MPC would need to promote MPC expression and/or its activity. However, there are two reports to date of tumors in which inhibition of the MPC was shown to delay tumor growth, as well as a third report showing a promising adjuvant effect of MPC inhibition when coupled with radiotherapy.

In one report (see Section 3.1) the androgen-sensitive prostate tumor was shown to require MPC for growth and it should, therefore, be sensitive to MPC inhibition [33]. In a second report, it was shown that liver-specific disruption of MPC in mice decreased development of a hepatocellular carcinoma induced by a low-dose exposure to *N*-nitrosodiethylamine (DEN) plus carbon tetrachloride (CCl₄) [101]. In the latter case, MPC-disrupted hepatocytes showed increased glutaminolysis to maintain the TCA cycle, and re-synthesis of glutathione was found to occur at a lower rate because less glutamine was available for glutathione synthesis. These findings raise the possibility of a model in which inducing metabolic competition for glutamine by MPC disruption would impair hepatocellular tumorigenesis by limiting glutathione synthesis. In the third report, MPC inhibition led to decreased oxygen consumption by tumor cells, thereby sparing oxygen locally and reducing hypoxia in the vicinity of the tumor. Importantly, this higher oxygen concentration around cells exacerbated the toxic effects of radiotherapy [102].

All together these results suggest that MPC inhibitors could be useful therapeutically to treat some selected cancer types.

5. Conclusions

In conclusion, mitochondrial pyruvate transport is essential for normal embryonic development and plays a key role in the function of many organs in the adult. Being at the heart of cell metabolism, MPC activity is solicited in several processes that require the presence of pyruvate inside mitochondria, to drive either cataplerotic reactions, such as gluconeogenesis or lipid synthesis, or anaplerotic reactions, to drive TCA cycle activity and consequently OXPHOS. Although cells can adapt their metabolism to circumvent impaired metabolic changes, this does not always prevent perturbation of cell homeostasis and pathology. We can see that, if preserving or restoring MPC activity is the objective in several pathologies, including certain cancers, we can also show that inhibition of MPC activity could be

beneficial in some pathologies. These pathologies, which include T2D, NASH, and PD, as well as probably others yet to be discovered, may provide diverse therapeutic applications for MPC inhibitors.

Funding: This research was funded by the Swiss National Science Foundation (31003A_179421) and by Oncosuisse (KFS-4434-02-2018).

Acknowledgments: We would like to thank all current and recently departed members of the JCM lab for their comments. Special acknowledgment goes to Kinsey Maundrell for helping to revise the manuscript.

Conflicts of Interest: The authors declare no conflict of interest.

References

1. Cappel, D.A.; Deja, S.; Duarte, J.A.G.; Kucejova, B.; Inigo, M.; Fletcher, J.A.; Fu, X.; Berglund, E.D.; Liu, T.; Elmquist, J.K.; et al. Pyruvate-Carboxylase-Mediated Anaplerosis Promotes Antioxidant Capacity by Sustaining TCA Cycle and Redox Metabolism in Liver. *Cell Metab.* **2019**, *29*, 1291–1305. [CrossRef] [PubMed]
2. Yetkin-Arik, B.; Vogels, I.M.C.; Nowak-Sliwinska, P.; Weiss, A.; Houtkooper, R.H.; Van Noorden, C.J.F.; Klaassen, I.; Schlingemann, R.O. The role of glycolysis and mitochondrial respiration in the formation and functioning of endothelial tip cells during angiogenesis. *Sci. Rep.* **2019**, *9*, 12608. [CrossRef]
3. Zheng, J. Energy metabolism of cancer: Glycolysis versus oxidative phosphorylation (Review). *Oncol. Lett.* **2012**, *4*, 1151–1157. [CrossRef] [PubMed]
4. Papa, S.; Francavilla, A.; Paradies, G.; Meduri, B. The transport of pyruvate in rat liver mitochondria. *FEBS Lett.* **1971**, *12*, 285–288. [CrossRef]
5. Bricker, D.K.; Taylor, E.B.; Schell, J.C.; Orsak, T.; Boutron, A.; Chen, Y.C.; Cox, J.E.; Cardon, C.M.; Van Vranken, J.G.; Dephoure, N.; et al. A mitochondrial pyruvate carrier required for pyruvate uptake in yeast, *Drosophila*, and humans. *Science* **2012**, *337*, 96–100. [CrossRef]
6. Herzig, S.; Raemy, E.; Montessuit, S.; Veuthey, J.L.; Zamboni, N.; Westermann, B.; Kunji, E.R.; Martinou, J.C. Identification and functional expression of the mitochondrial pyruvate carrier. *Science* **2012**, *337*, 93–96. [CrossRef]
7. Bender, T.; Pena, G.; Martinou, J.C. Regulation of mitochondrial pyruvate uptake by alternative pyruvate carrier complexes. *EMBO J.* **2015**, *34*, 911–924. [CrossRef]
8. Timon-Gomez, A.; Proft, M.; Pascual-Ahuir, A. Differential regulation of mitochondrial pyruvate carrier genes modulates respiratory capacity and stress tolerance in yeast. *PLoS ONE* **2013**, *8*, e79405. [CrossRef]
9. Vanderperre, B.; Cermakova, K.; Escoffier, J.; Kaba, M.; Bender, T.; Nef, S.; Martinou, J.C. MPC1-like Is a Placental Mammal-specific Mitochondrial Pyruvate Carrier Subunit Expressed in Postmeiotic Male Germ Cells. *J. Biol. Chem.* **2016**, *291*, 16448–16461. [CrossRef]
10. Tavoulari, S.; Thangaratnarajah, C.; Mavridou, V.; Harbour, M.E.; Martinou, J.C.; Kunji, E.R. The yeast mitochondrial pyruvate carrier is a hetero-dimer in its functional state. *EMBO J.* **2019**, *38*, e100785. [CrossRef]
11. Nagampalli, R.S.K.; Quesnay, J.E.N.; Adamoski, D.; Islam, Z.; Birch, J.; Sebinelli, H.G.; Girard, R.; Ascencao, C.F.R.; Fala, A.M.; Pauletti, B.A.; et al. Human mitochondrial pyruvate carrier 2 as an autonomous membrane transporter. *Sci. Rep.* **2018**, *8*, 3510. [CrossRef] [PubMed]
12. Lee, J.; Jin, Z.; Lee, D.; Yun, J.H.; Lee, W. Characteristic Analysis of Homo- and Heterodimeric Complexes of Human Mitochondrial Pyruvate Carrier Related to Metabolic Diseases. *Int. J. Mol. Sci.* **2020**, *21*, E3403. [CrossRef]
13. Jezegou, A.; Llinares, E.; Anne, C.; Kieffer-Jaquinod, S.; O'Regan, S.; Aupetit, J.; Chabli, A.; Sagne, C.; Debacker, C.; Chadefaux-Vekemans, B.; et al. Heptahelical protein PQLC2 is a lysosomal cationic amino acid exporter underlying the action of cysteamine in cystinosis therapy. *Proc. Natl. Acad. Sci. USA* **2012**, *109*, E3434–E3443. [CrossRef] [PubMed]
14. Medrano-Soto, A.; Ghazi, F.; Hendaro, K.J.; Moreno-Hagelsieb, G.; Myers, S.; Saier, M.H., Jr. Expansion of the Transporter-Opsin-G protein-coupled receptor superfamily with five new protein families. *PLoS ONE* **2020**, *15*, e0231085. [CrossRef] [PubMed]
15. Feng, L.; Frommer, W.B. Structure and function of SemiSWEET and SWEET sugar transporters. *Trends Biochem. Sci.* **2015**, *40*, 480–486. [CrossRef] [PubMed]
16. Dugan, J.L.; Bourdon, A.K.; Phelix, C.F. Mitochondrial Pyruvate Carrier 1 and 2 Heterodimer, In Silico, Models of Plant and Human Complexes. *Int. J. Knowl. Discov. Bioinform.* **2017**, *7*, 11–42. [CrossRef]

17. Phelix, C.F.; Bourdon, A.K.; Dugan, J.L.; Villareal, G.; Perry, G. MSDC-0160 and MSDC-0602 Binding with Human Mitochondrial Pyruvate Carrier (MPC) 1 and 2 Heterodimer. *Int. J. Knowl. Discov. Bioinform.* **2017**, *7*, 43–67. [CrossRef]
18. Bourdon, A.K.; Villareal, G.; Perry, G.; Phelix, C.F. Alzheimer's and Parkinson's Disease Novel Therapeutic Target. *Int. J. Knowl. Discov. Bioinform.* **2017**, *7*, 68–82. [CrossRef]
19. Rampelt, H.; Sucec, I.; Bersch, B.; Horten, P.; Perschil, I.; Martinou, J.C.; van der Laan, M.; Wiedemann, N.; Schanda, P.; Pfanner, N. The mitochondrial carrier pathway transports non-canonical substrates with an odd number of transmembrane segments. *BMC Biol.* **2020**, *18*, 2. [CrossRef]
20. Gomkale, R.; Cruz-Zaragoza, L.D.; Suppanz, I.; Guiard, B.; Montoya, J.; Callegari, S.; Pacheu-Grau, D.; Warscheid, B.; Rehling, P. Defining the Substrate Spectrum of the TIM22 Complex Identifies Pyruvate Carrier Subunits as Unconventional Cargos. *Curr. Biol.* **2020**, *30*, 1119–1127. [CrossRef]
21. Brivet, M.; Garcia-Cazorla, A.; Lyonnet, S.; Dumez, Y.; Nassogne, M.C.; Slama, A.; Boutron, A.; Touati, G.; Legrand, A.; Saudubray, J.M. Impaired mitochondrial pyruvate importation in a patient and a fetus at risk. *Mol. Genet. Metab.* **2003**, *78*, 186–192. [CrossRef]
22. Oonthonpan, L.; Rauckhorst, A.J.; Gray, L.R.; Boutron, A.C.; Taylor, E.B. Two human patient mitochondrial pyruvate carrier mutations reveal distinct molecular mechanisms of dysfunction. *JCI Insight* **2019**, *5*, 126132. [CrossRef] [PubMed]
23. Compan, V.; Pierredon, S.; Vanderperre, B.; Krznar, P.; Marchiq, I.; Zamboni, N.; Pouyssegur, J.; Martinou, J.C. Monitoring Mitochondrial Pyruvate Carrier Activity in Real Time Using a BRET-Based Biosensor: Investigation of the Warburg Effect. *Mol. Cell* **2015**, *59*, 491–501. [CrossRef] [PubMed]
24. Bowman, C.E.; Zhao, L.; Hartung, T.; Wolfgang, M.J. Requirement for the Mitochondrial Pyruvate Carrier in Mammalian Development Revealed by a Hypomorphic Allelic Series. *Mol. Cell. Biol.* **2016**, *36*, 2089–2104. [CrossRef]
25. Vanderperre, B.; Herzig, S.; Krznar, P.; Horl, M.; Ammar, Z.; Montessuit, S.; Pierredon, S.; Zamboni, N.; Martinou, J.C. Embryonic Lethality of Mitochondrial Pyruvate Carrier 1 Deficient Mouse Can Be Rescued by a Ketogenic Diet. *PLoS Genet.* **2016**, *12*, e1006056. [CrossRef]
26. Vigueira, P.A.; McCommis, K.S.; Schweitzer, G.G.; Remedi, M.S.; Chambers, K.T.; Fu, X.; McDonald, W.G.; Cole, S.L.; Colca, J.R.; Kletzien, R.F.; et al. Mitochondrial pyruvate carrier 2 hypomorphism in mice leads to defects in glucose-stimulated insulin secretion. *Cell Rep.* **2014**, *7*, 2042–2053. [CrossRef]
27. Wang, L.; Xu, M.; Qin, J.; Lin, S.C.; Lee, H.J.; Tsai, S.Y.; Tsai, M.J. MPC1, a key gene in cancer metabolism, is regulated by COUPTFII in human prostate cancer. *Oncotarget* **2016**, *7*, 14673–14683. [CrossRef]
28. Koh, E.; Kim, Y.K.; Shin, D.; Kim, K.S. MPC1 is essential for PGC-1alpha-induced mitochondrial respiration and biogenesis. *Biochem. J.* **2018**, *475*, 1687–1699. [CrossRef]
29. Dan, L.; Wang, C.; Ma, P.; Yu, Q.; Gu, M.; Dong, L.; Jiang, W.; Pan, S.; Xie, C.; Han, J.; et al. PGC1alpha promotes cholangiocarcinoma metastasis by upregulating PDHA1 and MPC1 expression to reverse the Warburg effect. *Cell Death Dis.* **2018**, *9*, 466. [CrossRef]
30. Park, S.; Safi, R.; Liu, X.; Baldi, R.; Liu, W.; Liu, J.; Locasale, J.W.; Chang, C.Y.; McDonnell, D.P. Inhibition of ERRalpha Prevents Mitochondrial Pyruvate Uptake Exposing NADPH-Generating Pathways as Targetable Vulnerabilities in Breast Cancer. *Cell Rep.* **2019**, *27*, 3587–3601. [CrossRef]
31. Tai, Y.; Cao, F.; Li, M.; Li, P.; Xu, T.; Wang, X.; Yu, Y.; Gu, B.; Yu, X.; Cai, X.; et al. Enhanced mitochondrial pyruvate transport elicits a robust ROS production to sensitize the antitumor efficacy of interferon-gamma in colon cancer. *Redox Biol.* **2019**, *20*, 451–457. [CrossRef] [PubMed]
32. Massie, C.E.; Lynch, A.; Ramos-Montoya, A.; Boren, J.; Stark, R.; Fazli, L.; Warren, A.; Scott, H.; Madhu, B.; Sharma, N.; et al. The androgen receptor fuels prostate cancer by regulating central metabolism and biosynthesis. *EMBO J.* **2011**, *30*, 2719–2733. [CrossRef] [PubMed]
33. Bader, D.A.; Hartig, S.M.; Putluri, V.; Foley, C.; Hamilton, M.P.; Smith, E.A.; Saha, P.K.; Panigrahi, A.; Walker, C.; Zong, L.; et al. Mitochondrial pyruvate import is a metabolic vulnerability in androgen receptor-driven prostate cancer. *Nat. Metab.* **2019**, *1*, 70–85. [CrossRef]
34. Cui, J.; Quan, M.; Xie, D.; Gao, Y.; Guha, S.; Fallon, M.B.; Chen, J.; Xie, K. A novel KDM5A/MPC-1 signaling pathway promotes pancreatic cancer progression via redirecting mitochondrial pyruvate metabolism. *Oncogene* **2020**, *39*, 1140–1151. [CrossRef] [PubMed]
35. Liang, L.; Li, Q.; Huang, L.; Li, D.; Li, X. Sirt3 binds to and deacetylates mitochondrial pyruvate carrier 1 to enhance its activity. *Biochem. Biophys. Res. Commun.* **2015**, *468*, 807–812. [CrossRef] [PubMed]

36. Vadvalkar, S.S.; Matsuzaki, S.; Eyster, C.A.; Giorgione, J.R.; Bockus, L.B.; Kinter, C.S.; Kinter, M.; Humphries, K.M. Decreased mitochondrial pyruvate transport activity in the diabetic heart role of mitochondrial pyruvate carrier 2 (MPC2) acetylation. *J. Biol. Chem.* **2017**, *292*, 4423–4433. [CrossRef] [PubMed]
37. Kim, J.; Yu, L.; Chen, W.; Xu, Y.; Wu, M.; Todorova, D.; Tang, Q.; Feng, B.; Jiang, L.; He, J.; et al. Wild-Type p53 Promotes Cancer Metabolic Switch by Inducing PUMA-Dependent Suppression of Oxidative Phosphorylation. *Cancer Cell* **2019**, *35*, 191–203. [CrossRef]
38. Vacanti, N.M.; Divakaruni, A.S.; Green, C.R.; Parker, S.J.; Henry, R.R.; Ciaraldi, T.P.; Murphy, A.N.; Metallo, C.M. Regulation of substrate utilization by the mitochondrial pyruvate carrier. *Mol. Cell* **2014**, *56*, 425–435. [CrossRef]
39. Yang, C.; Ko, B.; Hensley, C.T.; Jiang, L.; Wasti, A.T.; Kim, J.; Sudderth, J.; Calvaruso, M.A.; Lumata, L.; Mitsche, M.; et al. Glutamine oxidation maintains the TCA cycle and cell survival during impaired mitochondrial pyruvate transport. *Mol. Cell* **2014**, *56*, 414–424. [CrossRef]
40. Cao, T.; Liccardo, D.; LaCanna, R.; Zhang, X.; Lu, R.; Finck, B.N.; Leigh, T.; Chen, X.; Drosatos, K.; Tian, Y. Fatty Acid Oxidation Promotes Cardiomyocyte Proliferation Rate but Does Not Change Cardiomyocyte Number in Infant Mice. *Front. Cell Dev. Biol.* **2019**, *7*, 42. [CrossRef]
41. Lopaschuk, G.D.; Jaswal, J.S. Energy metabolic phenotype of the cardiomyocyte during development, differentiation, and postnatal maturation. *J. Cardiovasc. Pharmacol.* **2010**, *56*, 130–140. [CrossRef] [PubMed]
42. Stark, H.; Fichtner, M.; Konig, R.; Lorkowski, S.; Schuster, S. Causes of upregulation of glycolysis in lymphocytes upon stimulation. A comparison with other cell types. *Biochimie* **2015**, *118*, 185–194. [CrossRef]
43. Vander Heiden, M.G.; Cantley, L.C.; Thompson, C.B. Understanding the Warburg effect: The metabolic requirements of cell proliferation. *Science* **2009**, *324*, 1029–1033. [CrossRef] [PubMed]
44. Warburg, O. On respiratory impairment in cancer cells. *Science* **1956**, *124*, 269–270. [PubMed]
45. Ashrafi, G.; Ryan, T.A. Glucose metabolism in nerve terminals. *Curr. Opin. Neurobiol.* **2017**, *45*, 156–161. [CrossRef]
46. Belanger, M.; Allaman, I.; Magistretti, P.J. Brain energy metabolism: Focus on astrocyte-neuron metabolic cooperation. *Cell Metab.* **2011**, *14*, 724–738. [CrossRef]
47. Vaishnavi, S.N.; Vlassenko, A.G.; Rundle, M.M.; Snyder, A.Z.; Mintun, M.A.; Raichle, M.E. Regional aerobic glycolysis in the human brain. *Proc. Natl. Acad. Sci. USA* **2010**, *107*, 17757–17762. [CrossRef] [PubMed]
48. Grenell, A.; Wang, Y.; Yam, M.; Swarup, A.; Dilan, T.L.; Hauer, A.; Linton, J.D.; Philp, N.J.; Gregor, E.; Zhu, S.; et al. Loss of MPC1 reprograms retinal metabolism to impair visual function. *Proc. Natl. Acad. Sci. USA* **2019**, *116*, 3530–3535. [CrossRef]
49. Camandola, S.; Mattson, M.P. Brain metabolism in health, aging, and neurodegeneration. *EMBO J.* **2017**, *36*, 1474–1492. [CrossRef]
50. Ahmed, S.S.; Santosh, W.; Kumar, S.; Christlet, H.T. Metabolic profiling of Parkinson’s disease: Evidence of biomarker from gene expression analysis and rapid neural network detection. *J. Biomed. Sci.* **2009**, *16*, 63. [CrossRef]
51. Butterfield, D.A.; Halliwell, B. Oxidative stress, dysfunctional glucose metabolism and Alzheimer disease. *Nat. Rev. Neurosci.* **2019**, *20*, 148–160. [CrossRef] [PubMed]
52. Saxena, U. Bioenergetics failure in neurodegenerative diseases: Back to the future. *Expert Opin. Ther. Targets* **2012**, *16*, 351–354. [CrossRef] [PubMed]
53. Athauda, D.; Maclagan, K.; Budnik, N.; Zampedri, L.; Hibbert, S.; Skene, S.S.; Chowdhury, K.; Aviles-Olmos, I.; Limousin, P.; Foltynie, T. What Effects Might Exenatide have on Non-Motor Symptoms in Parkinson’s Disease: A Post Hoc Analysis. *J. Parkinsons Dis.* **2018**, *8*, 247–258. [CrossRef] [PubMed]
54. Athauda, D.; Maclagan, K.; Skene, S.S.; Bajwa-Joseph, M.; Letchford, D.; Chowdhury, K.; Hibbert, S.; Budnik, N.; Zampedri, L.; Dickson, J.; et al. Exenatide once weekly versus placebo in Parkinson’s disease: A randomised, double-blind, placebo-controlled trial. *Lancet* **2017**, *390*, 1664–1675. [CrossRef]
55. Aviles-Olmos, I.; Dickson, J.; Kefalopoulou, Z.; Djamshidian, A.; Ell, P.; Soderlund, T.; Whitton, P.; Wyse, R.; Isaacs, T.; Lees, A.; et al. Exenatide and the treatment of patients with Parkinson’s disease. *J. Clin. Investig.* **2013**, *123*, 2730–2736. [CrossRef]
56. Aviles-Olmos, I.; Dickson, J.; Kefalopoulou, Z.; Djamshidian, A.; Kahan, J.; Ell, P.; Whitton, P.; Wyse, R.; Isaacs, T.; Lees, A.; et al. Motor and cognitive advantages persist 12 months after exenatide exposure in Parkinson’s disease. *J. Parkinsons Dis.* **2014**, *4*, 337–344. [CrossRef]

57. Brakedal, B.; Flones, I.; Reiter, S.F.; Torkildsen, O.; Dolle, C.; Assmus, J.; Haugarvoll, K.; Tzoulis, C. Glitazone use associated with reduced risk of Parkinson's disease. *Mov. Disord.* **2017**, *32*, 1594–1599. [CrossRef]
58. Brauer, R.; Bhaskaran, K.; Chaturvedi, N.; Dexter, D.T.; Smeeth, L.; Douglas, I. Glitazone Treatment and Incidence of Parkinson's Disease among People with Diabetes: A Retrospective Cohort Study. *PLoS Med.* **2015**, *12*, e1001854. [CrossRef]
59. Connolly, J.G.; Bykov, K.; Gagne, J.J. Thiazolidinediones and Parkinson Disease: A Cohort Study. *Am. J. Epidemiol.* **2015**, *182*, 936–944. [CrossRef]
60. Ghosh, A.; Tyson, T.; George, S.; Hildebrandt, E.N.; Steiner, J.A.; Madaj, Z.; Schulz, E.; Machiela, E.; McDonald, W.G.; Escobar Galvis, M.L.; et al. Mitochondrial pyruvate carrier regulates autophagy, inflammation, and neurodegeneration in experimental models of Parkinson's disease. *Sci. Transl. Med.* **2016**, *8*, 368ra174. [CrossRef]
61. Blaudin de The, F.X.; Rekaik, H.; Peze-Heidsieck, E.; Massiani-Beaudoin, O.; Joshi, R.L.; Fuchs, J.; Prochiantz, A. Engrailed homeoprotein blocks degeneration in adult dopaminergic neurons through LINE-1 repression. *EMBO J.* **2018**, *37*, e97374. [CrossRef] [PubMed]
62. Johnson, M.E.; Stecher, B.; Labrie, V.; Brundin, L.; Brundin, P. Triggers, Facilitators, and Aggravators: Redefining Parkinson's Disease Pathogenesis. *Trends Neurosci.* **2019**, *42*, 4–13. [CrossRef]
63. Tansey, M.G.; Goldberg, M.S. Neuroinflammation in Parkinson's disease: Its role in neuronal death and implications for therapeutic intervention. *Neurobiol. Dis.* **2010**, *37*, 510–518. [CrossRef] [PubMed]
64. Shah, R.C.; Matthews, D.C.; Andrews, R.D.; Capuano, A.W.; Fleischman, D.A.; VanderLugt, J.T.; Colca, J.R. An evaluation of MSDC-0160, a prototype mTOT modulating insulin sensitizer, in patients with mild Alzheimer's disease. *Curr. Alzheimer Res.* **2014**, *11*, 564–573. [CrossRef] [PubMed]
65. Rossi, A.; Rigotto, G.; Valente, G.; Giorgio, V.; Basso, E.; Filadi, R.; Pizzo, P. Defective Mitochondrial Pyruvate Flux Affects Cell Bioenergetics in Alzheimer's Disease-Related Models. *Cell Rep.* **2020**, *30*, 2332–2348. [CrossRef] [PubMed]
66. Nemani, N.; Dong, Z.; Daw, C.C.; Madaris, T.R.; Ramachandran, K.; Enslow, B.T.; Rubannelsonkumar, C.S.; Shanmughapriya, S.; Mallireddigari, V.; Maity, S.; et al. Mitochondrial pyruvate and fatty acid flux modulate MICU1-dependent control of MCU activity. *Sci. Signal.* **2020**, *13*, eaaz6206. [CrossRef]
67. Divakaruni, A.S.; Wallace, M.; Buren, C.; Martyniuk, K.; Andreyev, A.Y.; Li, E.; Fields, J.A.; Cordes, T.; Reynolds, I.J.; Bloodgood, B.L.; et al. Inhibition of the mitochondrial pyruvate carrier protects from excitotoxic neuronal death. *J. Cell Biol.* **2017**, *216*, 1091–1105. [CrossRef]
68. Hatting, M.; Tavares, C.D.J.; Sharabi, K.; Rines, A.K.; Puigserver, P. Insulin regulation of gluconeogenesis. *Ann. N. Y. Acad. Sci.* **2018**, *1411*, 21–35. [CrossRef]
69. Jensen, M.V.; Joseph, J.W.; Ronnebaum, S.M.; Burgess, S.C.; Sherry, A.D.; Newgard, C.B. Metabolic cycling in control of glucose-stimulated insulin secretion. *Am. J. Physiol. Endocrinol. Metab.* **2008**, *295*, E1287–E1297. [CrossRef]
70. Prentki, M.; Matschinsky, F.M.; Madiraju, S.R. Metabolic signaling in fuel-induced insulin secretion. *Cell Metab.* **2013**, *18*, 162–185. [CrossRef]
71. Sugden, M.C.; Holness, M.J. The pyruvate carboxylase-pyruvate dehydrogenase axis in islet pyruvate metabolism: Going round in circles? *Islets* **2011**, *3*, 302–319. [CrossRef] [PubMed]
72. Patterson, J.N.; Cousteils, K.; Lou, J.W.; Manning Fox, J.E.; MacDonald, P.E.; Joseph, J.W. Mitochondrial metabolism of pyruvate is essential for regulating glucose-stimulated insulin secretion. *J. Biol. Chem.* **2014**, *289*, 13335–13346. [CrossRef] [PubMed]
73. McCommis, K.S.; Hodges, W.T.; Bricker, D.K.; Wisidagama, D.R.; Compan, V.; Remedi, M.S.; Thummel, C.S.; Finck, B.N. An ancestral role for the mitochondrial pyruvate carrier in glucose-stimulated insulin secretion. *Mol. Metab.* **2016**, *5*, 602–614. [CrossRef]
74. Petersen, M.C.; Vatner, D.F.; Shulman, G.I. Regulation of hepatic glucose metabolism in health and disease. *Nat. Rev. Endocrinol.* **2017**, *13*, 572–587. [CrossRef]
75. Gray, L.R.; Sultana, M.R.; Rauckhorst, A.J.; Oonthonpan, L.; Tompkins, S.C.; Sharma, A.; Fu, X.; Miao, R.; Pewa, A.D.; Brown, K.S.; et al. Hepatic Mitochondrial Pyruvate Carrier 1 is Required for Efficient Regulation of Gluconeogenesis and Whole-Body Glucose Homeostasis. *Cell Metab.* **2015**, *22*, 669–681. [CrossRef] [PubMed]

76. McCommis, K.S.; Chen, Z.; Fu, X.; McDonald, W.G.; Colca, J.R.; Kletzien, R.F.; Burgess, S.C.; Finck, B.N. Loss of Mitochondrial Pyruvate Carrier 2 in the Liver Leads to Defects in Gluconeogenesis and Compensation via Pyruvate-Alanine Cycling. *Cell Metab.* **2015**, *22*, 682–694. [CrossRef]
77. Rauckhorst, A.J.; Gray, L.R.; Sheldon, R.D.; Fu, X.; Pawa, A.D.; Feddersen, C.R.; Dupuy, A.J.; Gibson-Corley, K.N.; Cox, J.E.; Burgess, S.C.; et al. The mitochondrial pyruvate carrier mediates high fat diet-induced increases in hepatic TCA cycle capacity. *Mol. Metab.* **2017**, *6*, 1468–1479. [CrossRef] [PubMed]
78. Divakaruni, A.S.; Wiley, S.E.; Rogers, G.W.; Andreyev, A.Y.; Petrosyan, S.; Loviscach, M.; Wall, E.A.; Yadava, N.; Heuck, A.P.; Ferrick, D.A.; et al. Thiazolidinediones are acute, specific inhibitors of the mitochondrial pyruvate carrier. *Proc. Natl. Acad. Sci. USA* **2013**, *110*, 5422–5427. [CrossRef]
79. McCommis, K.S.; Hodges, W.T.; Brunt, E.M.; Nalbantoglu, I.; McDonald, W.G.; Holley, C.; Fujiwara, H.; Schaffer, J.E.; Colca, J.R.; Finck, B.N. Targeting the mitochondrial pyruvate carrier attenuates fibrosis in a mouse model of nonalcoholic steatohepatitis. *Hepatology* **2017**, *65*, 1543–1556. [CrossRef]
80. McCommis, K.S.; Finck, B.N. Treating Hepatic Steatosis and Fibrosis by Modulating Mitochondrial Pyruvate Metabolism. *Cell. Mol. Gastroenterol. Hepatol.* **2019**, *7*, 275–284. [CrossRef]
81. Harrison, S.A.; Alkhoury, N.; Davison, B.A.; Sanyal, A.; Edwards, C.; Colca, J.R.; Lee, B.H.; Looma, R.; Cusi, K.; Kolterman, O.; et al. Insulin sensitizer MSDC-0602K in non-alcoholic steatohepatitis: A randomized, double-blind, placebo-controlled phase IIb study. *J. Hepatol.* **2020**, *72*, 613–626. [CrossRef]
82. Han, P.; Wang, Y.; Zhan, H.; Weng, W.; Yu, X.; Ge, N.; Wang, W.; Song, G.; Yi, T.; Li, S.; et al. Artemether ameliorates type 2 diabetic kidney disease by increasing mitochondrial pyruvate carrier content in db/db mice. *Am. J. Transl. Res.* **2019**, *11*, 1389–1402. [PubMed]
83. DeFronzo, R.A.; Tripathy, D. Skeletal muscle insulin resistance is the primary defect in type 2 diabetes. *Diabetes Care* **2009**, *32* (Suppl. 2), S157–S163. [CrossRef]
84. Sharma, A.; Oonthonpan, L.; Sheldon, R.D.; Rauckhorst, A.J.; Zhu, Z.; Tompkins, S.C.; Cho, K.; Grzesik, W.J.; Gray, L.R.; Scerbo, D.A.; et al. Impaired skeletal muscle mitochondrial pyruvate uptake rewires glucose metabolism to drive whole-body leanness. *Elife* **2019**, *8*, e45873. [CrossRef] [PubMed]
85. Chai, Y.; Wang, C.; Liu, W.; Fan, Y.; Zhang, Y. MPC1 deletion is associated with poor prognosis and temozolomide resistance in glioblastoma. *J. Neurooncol.* **2019**, *144*, 293–301. [CrossRef] [PubMed]
86. Li, X.; Ji, Y.; Han, G.; Li, X.; Fan, Z.; Li, Y.; Zhong, Y.; Cao, J.; Zhao, J.; Zhang, M.; et al. MPC1 and MPC2 expressions are associated with favorable clinical outcomes in prostate cancer. *BMC Cancer* **2016**, *16*, 894. [CrossRef]
87. Li, X.; Li, Y.; Han, G.; Li, X.; Ji, Y.; Fan, Z.; Zhong, Y.; Cao, J.; Zhao, J.; Mariusz, G.; et al. Establishment of mitochondrial pyruvate carrier 1 (MPC1) gene knockout mice with preliminary gene function analyses. *Oncotarget* **2016**, *7*, 79981–79994. [CrossRef]
88. Ohashi, T.; Eguchi, H.; Kawamoto, K.; Konno, M.; Asai, A.; Colvin, H.; Ueda, Y.; Takaoka, H.; Iwagami, Y.; Yamada, D.; et al. Mitochondrial pyruvate carrier modulates the epithelial-mesenchymal transition in cholangiocarcinoma. *Oncol. Rep.* **2018**, *39*, 1276–1282. [CrossRef]
89. Schell, J.C.; Olson, K.A.; Jiang, L.; Hawkins, A.J.; Van Vranken, J.G.; Xie, J.; Egnatchik, R.A.; Earl, E.G.; DeBerardinis, R.J.; Rutter, J. A role for the mitochondrial pyruvate carrier as a repressor of the Warburg effect and colon cancer cell growth. *Mol. Cell* **2014**, *56*, 400–413. [CrossRef]
90. Zou, H.; Chen, Q.; Zhang, A.; Wang, S.; Wu, H.; Yuan, Y.; Wang, S.; Yu, J.; Luo, M.; Wen, X.; et al. MPC1 deficiency accelerates lung adenocarcinoma progression through the STAT3 pathway. *Cell Death Dis.* **2019**, *10*, 148. [CrossRef]
91. Li, X.; Han, G.; Li, X.; Kan, Q.; Fan, Z.; Li, Y.; Ji, Y.; Zhao, J.; Zhang, M.; Grigalavicius, M.; et al. Mitochondrial pyruvate carrier function determines cell stemness and metabolic reprogramming in cancer cells. *Oncotarget* **2017**, *8*, 46363–46380. [CrossRef] [PubMed]
92. Li, Y.; Li, X.; Kan, Q.; Zhang, M.; Li, X.; Xu, R.; Wang, J.; Yu, D.; Goscinski, M.A.; Wen, J.G.; et al. Mitochondrial pyruvate carrier function is negatively linked to Warburg phenotype in vitro and malignant features in esophageal squamous cell carcinomas. *Oncotarget* **2017**, *8*, 1058–1073. [CrossRef]
93. Zhong, Y.; Li, X.; Yu, D.; Li, X.; Li, Y.; Long, Y.; Yuan, Y.; Ji, Z.; Zhang, M.; Wen, J.G.; et al. Application of mitochondrial pyruvate carrier blocker UK5099 creates metabolic reprogram and greater stem-like properties in LnCap prostate cancer cells in vitro. *Oncotarget* **2015**, *6*, 37758–37769. [CrossRef] [PubMed]

94. Bensard, C.L.; Wisidagama, D.R.; Olson, K.A.; Berg, J.A.; Krah, N.M.; Schell, J.C.; Nowinski, S.M.; Fogarty, S.; Bott, A.J.; Wei, P.; et al. Regulation of Tumor Initiation by the Mitochondrial Pyruvate Carrier. *Cell Metab.* **2020**, *31*, 284–300. [CrossRef] [PubMed]
95. Porporato, P.E.; Payen, V.L.; Perez-Escuredo, J.; De Saedeleer, C.J.; Danhier, P.; Copetti, T.; Dhup, S.; Tardy, M.; Vazeille, T.; Bouzin, C.; et al. A mitochondrial switch promotes tumor metastasis. *Cell Rep.* **2014**, *8*, 754–766. [CrossRef]
96. Takaoka, Y.; Konno, M.; Koseki, J.; Colvin, H.; Asai, A.; Tamari, K.; Satoh, T.; Mori, M.; Doki, Y.; Ogawa, K.; et al. Mitochondrial pyruvate carrier 1 expression controls cancer epithelial-mesenchymal transition and radioresistance. *Cancer Sci.* **2019**, *110*, 1331–1339. [CrossRef] [PubMed]
97. Tang, X.P.; Chen, Q.; Li, Y.; Wang, Y.; Zou, H.B.; Fu, W.J.; Niu, Q.; Pan, Q.G.; Jiang, P.; Xu, X.S.; et al. Mitochondrial pyruvate carrier 1 functions as a tumor suppressor and predicts the prognosis of human renal cell carcinoma. *Lab. Investig.* **2019**, *99*, 191–199. [CrossRef]
98. De la Cruz-Lopez, K.G.; Castro-Munoz, L.J.; Reyes-Hernandez, D.O.; Garcia-Carranca, A.; Manzo-Merino, J. Lactate in the Regulation of Tumor Microenvironment and Therapeutic Approaches. *Front. Oncol.* **2019**, *9*, 1143. [CrossRef]
99. Faubert, B.; Li, K.Y.; Cai, L.; Hensley, C.T.; Kim, J.; Zacharias, L.G.; Yang, C.; Do, Q.N.; Doucette, S.; Burguete, D.; et al. Lactate Metabolism in Human Lung Tumors. *Cell* **2017**, *171*, 358–371. [CrossRef]
100. Hui, S.; Ghergurovich, J.M.; Morscher, R.J.; Jang, C.; Teng, X.; Lu, W.; Esparza, L.A.; Reya, T.; Le, Z.; Yanxiang Guo, J.; et al. Glucose feeds the TCA cycle via circulating lactate. *Nature* **2017**, *551*, 115–118. [CrossRef]
101. Tompkins, S.C.; Sheldon, R.D.; Rauckhorst, A.J.; Noterman, M.F.; Solst, S.R.; Buchanan, J.L.; Mapuskar, K.A.; Pawa, A.D.; Gray, L.R.; Oonthonpan, L.; et al. Disrupting Mitochondrial Pyruvate Uptake Directs Glutamine into the TCA Cycle away from Glutathione Synthesis and Impairs Hepatocellular Tumorigenesis. *Cell Rep.* **2019**, *28*, 2608–2619. [CrossRef] [PubMed]
102. Corbet, C.; Bastien, E.; Draoui, N.; Doix, B.; Mignon, L.; Jordan, B.F.; Marchand, A.; Vanherck, J.C.; Chaltin, P.; Schakman, O.; et al. Interruption of lactate uptake by inhibiting mitochondrial pyruvate transport unravels direct antitumor and radiosensitizing effects. *Nat. Commun.* **2018**, *9*, 1208. [CrossRef] [PubMed]



© 2020 by the authors. Licensee MDPI, Basel, Switzerland. This article is an open access article distributed under the terms and conditions of the Creative Commons Attribution (CC BY) license (<http://creativecommons.org/licenses/by/4.0/>).

Review

Metabolic Roles of Plant Mitochondrial Carriers

Alisdair R. Fernie ^{1,*}, João Henrique F. Cavalcanti ²  and Adriano Nunes-Nesi ^{3,*}

¹ Max-Planck-Institute of Molecular Plant Physiology, 14476 Postdam-Golm, Germany

² Instituto de Educação, Agricultura e Ambiente, Universidade Federal do Amazonas, Humaitá 69800-000, Amazonas, Brazil; jcavalcanti@ufam.edu.br

³ Departamento de Biologia Vegetal, Universidade Federal de Viçosa, Viçosa 36570-900, Minas Gerais, Brazil

* Correspondence: fernie@mpimp-golm.mpg.de (A.R.F.); nunesnesi@ufv.br (A.N.-N.);

Tel.: +49-(0)331-567-8211 (A.R.F.); +55-(31)-3612-5357 (A.N.-N.)

Received: 24 May 2020; Accepted: 29 June 2020; Published: 8 July 2020

Abstract: Mitochondrial carriers (MC) are a large family (MCF) of inner membrane transporters displaying diverse, yet often redundant, substrate specificities, as well as differing spatio-temporal patterns of expression; there are even increasing examples of non-mitochondrial subcellular localization. The number of these six trans-membrane domain proteins in sequenced plant genomes ranges from 39 to 141, rendering the size of plant families larger than that found in *Saccharomyces cerevisiae* and comparable with *Homo sapiens*. Indeed, comparison of plant MCs with those from these better characterized species has been highly informative. Here, we review the most recent comprehensive studies of plant MCFs, incorporating the torrent of genomic data emanating from next-generation sequencing techniques. As such we present a more current prediction of the substrate specificities of these carriers as well as review the continuing quest to biochemically characterize this feature of the carriers. Taken together, these data provide an important resource to guide direct genetic studies aimed at addressing the relevance of these vital carrier proteins.

Keywords: amino acid; biological function; ion; inner mitochondrial membrane; mitochondrial carrier family; organic acid; substrate specificity; transport mechanism; vitamin

1. Introduction

The acquisition of the mitochondrial endosymbiont brought a wide range of novel metabolic capabilities to the ancestral eukaryotic lineage [1]. Alongside efficient synthesis of ATP via the process of oxidative phosphorylation, the mitochondria are also the site of numerous other anabolic and catabolic pathways. The host cell has exploited this and depends on the mitochondria as a source of carbon skeletons for several further metabolic pathways including nitrogen assimilation, photorespiration, C₁ metabolism, photosynthesis in C₄ and crassulacean acid metabolism as well as the utilization of storage pools of carbon and nitrogen during seed germination [2,3]. Mitochondria additionally play roles in the biosynthesis of amino acids, tetrapyrroles, fatty acids and vitamin co-factors [4,5]. In order to achieve this, the mitochondrial matrix needs to be supplied by a wide range of solute transporters. Intriguingly, in a model of enzymes allocated to specific cellular compartments of *Arabidopsis*, Mintz-Oron et al. [6] revealed that approximately half of the reactions could be assigned to specific subcellular compartments based on experimental evidence. For the remainder, they predicted the most likely subcellular location based on a parsimony principle of minimizing the number of intracellular transporters required to activate the reactions with a known localization in the corresponding compartments [6]. This method predicted that a metabolic network of some 1200 reactions (compartmented among the cytosol, plastid, mitochondrion, endoplasmic reticulum, peroxisome, vacuole and Golgi apparatus) required a phenomenal 772 intracellular transporters. Similarly, at least 228 metabolites and 89 transport processes are required in the minimal human mitochondrial metabolic network [7], suggesting that the

total number of solute transporters currently catalogued to reside in the plant mitochondria may be insufficient to account for all transport steps required [8]. It is, however, important to note that this list contains not only MCF (mitochondrial carrier family) members but also members of other families [8]. Although the outer mitochondrial membrane is permeable to small solutes (with a molecular mass of less than 4–5 Da) [9–11], the inner membrane is impermeable with only very small uncharged molecules such as O₂ and CO₂ able to readily pass through this membrane. The passage of hydrophilic compounds across the inner mitochondrial membrane is mainly catalyzed by the nuclear encoded mitochondrial carrier family (MCF) [12–15]. MCs (mitochondrial carriers) are small proteins ranging in size from 30–34 kDa and possess common defining structural features. Their primary structure is characterized by three tandemly repeated, approximately 100 amino acid long, homologous domains with each repeat containing two hydrophobic segments, which span the membrane, and a characteristic amino acid sequence motif PX[D/E]XX[K/R]/RX[K/R] (20–30 residues) [D/E]GXXXX[W/Y/F][K/R]G (PROSITE PS50920, PFAM PF00153 and IPR00193). Two sub-families, the aspartate/glutamate and ATPMg-Pi carriers, have additional N-terminal regulatory domains of approximately 150 amino acids that usually contain Ca²⁺-binding motifs [12,16]. The molecules transported by the MCF are highly variable in size and structure, ranging from H⁺ and NAD⁺ and coenzyme A. They also display a range of ionic charges being either positive, negative or zwitterionic at physiological pH. They often act as antiporters, although uniport transport and H⁺-compensated anion symport is also mediated by some MCs. Furthermore, MCs can be subdivided on the basis of their electrical nature with for example the ADP/ATP and aspartate/glutamate transporters drive electrogenic reactions (which result in net charge transfer) whereas the carrier subfamilies for phosphate (Pi), glutamate, and GTP/GDP as well as for 2-oxoglutarate and ornithine are electroneutral.

Considerable research has been conducted on characterizing members of the MCF in both yeast and animals (see [13,14,17–27] for reviews). Regarding other eukaryotes, the MCF members of the early-branching kinetoplastid parasite *Trypanosoma brucei* have been studied by sequence and phylogenetic analyses [27]. This study gave new insights into the evolution and conservation of the 24 identified MCF homologues identified in that organism [27]. In recent years the advent and exploitation of systems biology approaches have provided considerable insight into the putative in vivo function of plant MCFs, whilst the adoption of recombinant enzyme approaches have allowed the biochemical characterization of their functions. In this article, we summarize the structure and transport mechanisms of members of the MCF family, discuss its expansion in plants and finally summarize the biochemical characterization of the transport properties of MCF members that have been reconstituted in liposomes. The reader is referred to our other article in this issue [28] for information concerning the, sometimes unusual, subcellular localization of these proteins and the characterization of transgenic loss-of-function lines.

2. Structure and Transport Mechanisms

Due to its high abundance, the ADP/ATP carrier (AAC) is the member of the family that has been studied the most. It is the first mitochondrial carrier for which a high-resolution X-ray structure was provided [29]. The bovine carrier was crystallized in the presence of a strong inhibitor, the carboxyatractyloside (CATR). The structure gives an insight not only into the overall fold of mitochondrial carriers in general but also into atomic details of the AAC in a conformation that is open toward the intermembrane space (IMS). The three dimensional structure of the ADP/ATP carrier is critical to our understanding in several other ways. First, it exhibits a three-fold pseudo-symmetry in lines with the three-fold sequence repeats mentioned above [30], similar to that observed by electron microscopy [31]. Secondly, it approximately corresponds to the *c* (cytosolic)-state of the ADP/ATP carrier since CATR blocks the carrier in this state [19]. Thirdly, this structure has become a much used template for the building of homology models of various carriers, greatly improving our understanding of MC structure/function relationships [32–38]. The structural fold observed in the bovine transporter was subsequently confirmed by the structures of two yeast isoforms of the

ADP/ATP carrier. Intriguingly, the odd-numbered transmembrane alpha-helices have pronounced kinks at the Pro residue of the highly conserved signature motif Px[DE]xx[KR], with the P kink giving them a pronounced L shape which helps to block access of the central cavity from the mitochondrial matrix in the *c*-state (Figure 1). The charged residues of the signature motifs from inter-domain salt bridges [29,39] are now known as the matrix salt bridge network. Furthermore, residues of the salt bridge interact with a proximal glutamine residue which hydrogen bonds to both salt bridge residues forming a glutamine brace (Q brace [39]). These residues are highly conserved with one to three Q braces typically found in the SLC25 subfamily of the MCF. CATR inhibits the ADP/ATP carrier by binding tightly in the central cavity thus prevent translocation across the membrane. Just last year, the first structure of a mitochondrial carrier in the *m*-state has been solved—the ADP/ATP carrier from the thermotolerant fungus *Thermothelomyces thermophilia* inhibited by bongkreic acid [40]. The *m*-state structure displays the same three-domain architecture, but with the domains rotated compared with the *c*-state, opening the central cavity to the mitochondrial matrix and closing it to the intermembrane space and thereby disrupting the matrix network and Q brace [14]. On the intermembrane side the transmembrane helices are positioned closely together and form the interdomain cytoplasmic salt bridge network (Figure 1). This network is stabilized by hydrogen bonds with the hydroxyl bonds with the hydroxyl groups of the tyrosines of the motif forming a tyrosine brace (Y brace; [39]). Most SLC members have one to three Y braces. Having structural information for both *c*- and *m*-states has significantly advanced our understanding of how these proteins operate at the molecular level. These advances have been excellently covered elsewhere [25], so we will not detail them here except to say that the structural features are likely to be conserved, with few exceptions, throughout the MCF.

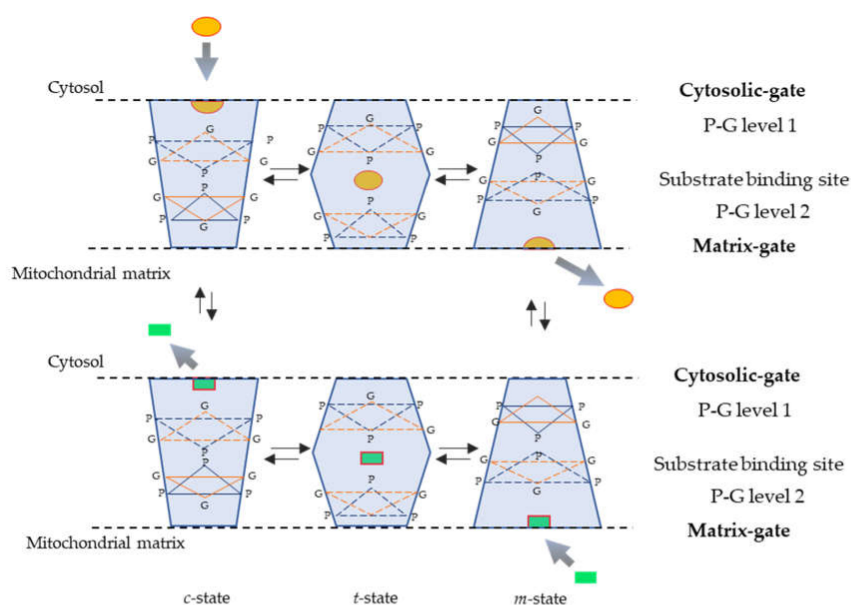


Figure 1. Mechanism of substrate translocation catalyzed by mitochondrial carriers. Simplified scheme depicting the transition of mitochondrial carriers from the *c*-state to the *m*-state and vice versa as previously proposed [14]. The trapezoid shape on the left is used to illustrate the *c*-state after the release of the substrate towards the cytosol and immediately after the entry of the substrate from the cytosolic side; the trapezoid shape on the right illustrates the *m*-state after the release of the substrate into the matrix and immediately after the entry of the substrate from the matrix side; and the two central hexagonal shape solids depict the transition states (*t*-state) of the carrier with the bound substrate entered from the cytosol and from the matrix. The yellow disk and green rectangle shapes represent the substrates entering from the cytosol and from the matrix, respectively; orange triangles represent closed gates, and dotted orange triangles indicate open or partially closed gates. All transport steps are fully reversible. The positions of the salt bridge networks (cytosolic and matrix gates), P-G level 1, substrate binding site and P-G level 2 are indicated on the right.

3. Extension of the MCF

Although only six MC proteins were sequenced following their purification from mitochondria or by DNA sequencing (see [41] and references therein) the genomic era has massively expanded our inventories of the MCFs of various species with *S. cerevisiae* encoding 35 [42], the human genome 50 [18] and *Arabidopsis thaliana* 58 [5]. The first step in identifying MC function is to search for the substrates transported by a specific carrier. In order to do so, the primary tools in our arsenal are phylogenetic clustering, genetic information, knowledge of cellular metabolism and complementation of phenotypes. However, such methods remain inconclusive and overly speculative. To date, the most effective strategy has been heterologous expression in *Escherichia coli* (see for example [43]) or *S. cerevisiae* (see for example [44–46]) and reconstitution of the subsequently purified recombinant carriers into liposomes in which direct transport assays are performed. To date, such gene–function studies have been carried out on 32, 40 and 26 of the MCFs of *S. cerevisiae*, human and *A. thaliana*, respectively. Focusing on the green lineage alone, MCs are highly abundant in the genomes of several species of dicots, monocots and algae with a 2020 update (Table 1 and Table S1) suggesting they range in number from 39 to 141, surpassing the 37 to 125 range when we last reviewed this family in 2011 [12]. In turn, a reasonable understanding of the apparently increasing number of predicted MCF genes in green line in comparison with the report of 2011 [12] is the development of powerful tools concerning both next generation sequencing approaches and/or bioinformatics algorithms for annotation and assembly of new, more accurate *de novo* reference genomes. In this review we demonstrate how the function of *A. thaliana* proteins could be reasonably, yet not completely, accurately predicted via examination of their symmetry-related triplets and subsequent comparison to those of MC subfamilies for which substrate specificities were determined in human, yeast or *Arabidopsis* itself. Those instances in which poor accordance was found between the prediction and experimental results can be split in two: those displaying novel substrate specificity and those residing at different subcellular localization [28]. Table 2 lists the main subfamilies that MCs can be partitioned into on the basis of their substrate specificities. It is, however, important to note that the caveats which we previously mentioned [12] remain valid. In brief: (i) some substrates are transported by more than one subfamily; (ii) the best transported substrate in reconstituted liposomes may not reflect the most important substrate under physiological conditions; (iii) some subfamilies may additionally transport as yet untested substrates (see for example [47]); and (iv) most of the subfamilies presented in this table are present in all eukaryotes. It has been suggested that key amino acids residues important for the transport mechanism are likely symmetrical, and those involved in substrate binding are likely asymmetrical (indicating the asymmetry of the substrates) [32–38]. Hence, scoring the symmetry of residues in the sequence repeats, it is possible to associate the substrate-binding sites and salt bridge networks that are important for the transport mechanism in family members [32–38]. Thus, the substrate specificity defined carrier subfamilies are also characterized by specific amino acid triplets with the number of characterizing triplets ranging from two to eight. Moreover, related subfamilies sharing some triplets, for example the NAD⁺, PyC and FAD families, share triplet 19 as well as some transport substrates [48,49] whereas the OGC and DTC subfamilies also share two triplets (KLK and GTY) as well as some transported substrates [43,50] substrate specificity. Finally, as in our previous study, the uncoupling protein (UCP) and unnamed transporters have been added despite the fact that the substrates are unknown for the latter. However, in contrast to our previous study [12], as detailed below, the substrate specificities of UCP have recently been characterized [51].

Table 1. Mitochondrial carriers (MCs) present in each chromosome of plant genomes recently sequenced.

Dicots	<i>A. thaliana</i>		<i>M. truncatula</i>		<i>G. max</i>		<i>S. lycopersicum</i>		<i>V. vinifera</i>		<i>P. persica</i>		<i>D. carota</i>	
<i>Chr</i>	mbp	MC N°	mbp	MC N°	mbp	MC N°	mbp	MC N°	mbp	MC N°	mbp	MC N°	mbp	MC N°
1	30	10	46	8	57	8	98	9	23	2	48	12	51	13
2	20	10	56	4	49	11	56	5	19	2	30	8	44	14
3	23	9	57	11	46	7	72	7	19	2	27	8	50	4
4	19	10	44	11	52	10	67	7	24	2	26	2	36	10
5	27	20	35	9	42	7	67	5	25	3	19	8	42	8
6	–	–	49	7	51	9	50	6	22	4	31	12	37	4
7	–	–	46	11	45	10	68	1	21	2	22	3	36	14
8	–	–	37	21	48	16	66	6	22	2	23	7	32	5
9	–	–	–	–	50	5	73	6	23	4	–	–	34	2
10	–	–	–	–	52	4	66	4	18	5	–	–	–	–
11	–	–	–	–	35	3	57	4	20	1	–	–	–	–
12	–	–	–	–	40	2	68	5	23	3	–	–	–	–
13	–	–	–	–	46	7	–	–	24	2	–	–	–	–
14	–	–	–	–	49	5	–	–	30	5	–	–	–	–
15	–	–	–	–	52	4	–	–	20	2	–	–	–	–
16	–	–	–	–	38	7	–	–	22	4	–	–	–	–
17	–	–	–	–	42	6	–	–	17	4	–	–	–	–
18	–	–	–	–	58	6	–	–	29	6	–	–	–	–
19	–	–	–	–	51	8	–	–	24	2	–	–	–	–
20	–	–	–	–	48	6	–	–	–	–	–	–	–	–
Unknown	–	–	28	–	29	–	21	–	59	3	1	–	59	7
Total	119	59	397	82	978	141	828	65	485	60	227	60	421	81
Monocots	<i>B. distachyon</i>		<i>S. bicolor</i>		<i>Z. mays</i>		<i>O. sativa</i>		<i>H. vulgare</i>		<i>S. italica</i>		<i>M. acuminata</i>	
<i>Chr</i>	mbp	MC N°	mbp	MC N°	mbp	MC N°	mbp	MC N°	mbp	MC N°	mbp	MC N°	mbp	MC N°
1	75	17	81	15	307	14	43	11	558	5	42	7	28	9
2	59	17	78	6	244	8	36	7	768	3	49	5	22	6
3	60	10	74	9	236	7	36	10	700	10	51	7	30	7
4	49	8	69	9	247	10	36	3	647	9	40	4	30	10
5	29	4	72	2	224	13	30	8	67	10	47	11	29	6
6	–	–	61	5	174	5	31	3	583	5	36	3	35	16
7	–	–	66	3	182	4	30	1	657	4	36	5	29	11
8	–	–	63	2	181	12	28	3	–	–	41	3	35	12
9	–	–	59	7	160	9	23	6	–	–	59	18	34	9
10	–	–	61	4	151	5	23	2	–	–	–	–	34	21
11	–	–	–	–	–	–	29	5	–	–	–	–	26	4
12	–	–	–	–	–	–	28	2	–	–	–	–	–	–
Unknown	0	–	25	–	28	3	1	–	249	4	4	–	140	–
Total	271	56	709	62	2134	90	374	61	4229	50	406	63	472	111

Table 1. Cont.

Chr	Algae		<i>C. reinhardtii</i>		<i>O. tauri</i>		<i>M. commoda</i>	
	mbp	MC N°	mbp	MC N°	mbp	MC N°	mbp	MC N°
1	1	6	1	2	1	5	2	3
2	1	3	1	3	1	3	2	5
3	1	5	1	3	1	5	2	3
4	1	0	0	4	1	0	2	4
5	1	0	0	0	1	0	2	5
6	1	1	1	9	1	1	1	6
7	1	3	1	2	1	3	1	5
8	1	1	1	1	1	1	1	2
9	1	1	1	5	1	1	1	1
10	1	3	1	3	1	3	1	0
11	1	2	0	1	1	3	1	2
12	1	4	1	2	1	3	1	6
13	1	3	1	0	1	2	1	1
14	1	1	0	0	1	1	1	3
15	0	1	0	1	1	1	1	1
16	0	3	1	6	1	2	1	1
17	0	2	1	1	0	3	0	0
18	0	0	–	–	0	2	–	–
19	0	0	–	–	0	0	–	–
20	1	1	–	–	0	0	–	–
21	0	3	–	–	–	–	–	–
Unknown	–	–	10	3	–	–	–	–
Total	13	43	21	46	13	39	21	48

The data were retrieved from comparative genome platform Plaza (<https://bioinformatics.psb.ugent.be/plaza/>), Ensembl-plants (<http://plants.ensembl.org/index.html>) and Phytozome (<http://www.phytozome.net/>). The InterPRO domain used for mitochondrial carrier was 'IPR023395'. All the sequences were validated by protein blast analysis on the non-redundant database (<http://blast.ncbi.nlm.nih.gov/Blast.cgi>). The number of MCs refers to sequences which are longer than 265 amino acids and non-redundant. chr, chromosome; mbp, mega base pairs.

An additional method for analyzing function has been the deduction from phylogenetic trees—an approach that has also been used to address the evolution of the MCFs [12,52]. Intriguingly, either if all MCF members of a single representative of a kingdom [12] or multiple representatives of each kingdom but only a subset of the MCFs are used [52] similar broad conclusions can be made. These are namely that the MCFs are highly divergent, yet that the fact that the vast majority are conserved across plants, animals and yeast lineages suggests that many MC functions existed before the speciation events that have produced the three kingdoms [12]. Interestingly, however, the comparison of intraspecific paralogs suggests that these originated by gene duplication events that occurred independently in those three lineages [12]. At a finer level the comparison of tricarboxylic acid (TCA) cycle relevant MCFs alone revealed that mitochondrial organic acid transporters formed two distinct clades. In the first clade, dicarboxylate carriers (DICs) and dicarboxylate-tricarboxylate carrier (DTC) grouped with 2-OG carriers (OGCs). The succinate-fumarate carrier (SFC) formed the second organic acid clade with other non-plant organic acid transporters including oxodicarboxylate carriers (ODCs), citrate carriers (CiCs), and yeast suppressor of HM (histone-like proteins in yeast mitochondria) mutant 2 (YHM2). Biochemical data would indicate that DTC and CiC must be closely related as they both transport citrate; phylogenetic analysis revealed that SFC, and not DTC, is more similar to CiC [52]. Based on available biochemical data, it thus appears that the transport functions of CiC and DTC have evolved independently but perhaps convergently. As would be expected, the possibility to use phylogeny to detect orthologs between plants is much greater than across kingdoms [12]. The use of tools such as Orthofinder, which provides phylogenetic inference of orthologs [53], and PlaNet and FamNet, which include co-expression data to refine such searches [54,55], render such searches easier and will likely prove highly informative in improving our understanding of plant MCFs beyond Arabidopsis.

Further evolutionary insight into plant MCF members was attained by studying the location of introns in MC genes and examining the synteny between MCF members in the dicot *A. thaliana*, the monocot *Brachipodium distachyon* and the algae *Osterococcus luminarius* [12]. The first of these strategies took its cue from the observation that introns tend to interrupt the coding sequence of the human citrate, carnitine and dicarboxylate carrier genes at positions corresponding to or in the close vicinity of the hydrophilic loops in the MC amino acid sequences [56–58]. Comparison of all 58 members of the *A. thaliana* MCF revealed that hydrophobic loops host a notable excess in intron density compared with transmembrane helices, suggesting that introns are unrepresented in transmembrane helices due to negative selection [12]. In the second analysis, the co-linearity of regions of the *A. thaliana*, *B. distachyon* and *O. luminarius* genomes were exploited. In *O. luminarius* six MCF genes were found in co-linear regions of chromosomes 13 and 21, consistent with the known origin of chromosome 21 in this species [59]. In spite of several whole genome duplication events (see [60,61] for reviews) the same number of gene pairs were found in Arabidopsis, a fact best explained by high rate of gene loss and gene rearrangement in this species [62,63]. By contrast, the genome of *B. distachyon* contains six pairs of MC paralogs in co-linear segments, likely reflecting a lower rate of gene loss and gene rearrangement in this species. Fascinatingly, however, even though approximately 500 million years separate monocots and dicots from the common ancestor of the angiosperm, 15 MCs in Arabidopsis and 13 in Brachipodium are present in conserved synteny blocks with an over-representation for nucleotide carriers being apparent which has been suggested to reflect either that their preferential expansion is tolerated in angiosperms or, more likely, that they functionally contributed to angiosperm evolution [12].

4. Biochemical Characterization of Plant MCF Members

Out of 58 MCF members found in Arabidopsis genome, 17 genes have not been fully characterized and therefore the biochemical role of these proteins remains unknown. In the last 10 years, the biochemical functions of 21 MCs from Arabidopsis have been investigated (Table 2) and studies on the characterization of the physiological importance of these carriers in plants have been reported [28].

4.1. Coenzyme A Carriers

From the subfamily of nucleotides and dinucleotides carriers, two genes encoding for MCF proteins, At1g14560 and At4g26180, based on the presence of sequence motifs (symmetry-related amino acid triplets [12]) were described as potential coenzyme A (CoA) carriers [12]. Comparative genomic analysis allowed the identification of two homologs of these proteins in maize (*Zea mays*; GRMZM2G161299 and GRMZM2G420119) [64]. It was verified that all these proteins from maize and Arabidopsis are targeted to mitochondria and are also able to complement the growth wild type phenotype in the yeast *leu5D* mutant [65] defective for the mitochondrial CoA carrier [64]. These proteins also restored the mitochondrial CoA level in the same yeast mutant. These results clearly demonstrated that these proteins catalyze the transport of CoA through the mitochondrial membrane. It is noteworthy that, to our knowledge, the substrate specificity of this transporter has not yet been fully investigated. This is particularly important, because in addition to CoA, these transporters might also have capacity to transport other substrate or substrates. In this regard, it was reported that the Arabidopsis peroxisomal NAD carrier PXN, in addition to NAD⁺, NADH, AMP, ADP and adenosine 3', 5'-phosphate (PAP), is also able to catalyze CoA transport [66]. PXN is encoded in Arabidopsis by the gene At2g39970 and was investigated regarding its substrate specificity and the transport properties by using a wide range of potential substrates [66]. Detailed biochemical analyses demonstrated that PXN catalyzes fast counter-exchange of substrates and much slower uniport [66]. In the same study, it was shown that the transport catalyzed by PXN is saturable with a submillimolar affinity for NAD⁺, CoA and other substrates. More recently, the physiological function of PXN in plants was further investigated [67]. Interestingly, by using *S. cerevisiae*, uptake analyses indicated that PXN has a low affinity for CoA, which suggests that the PXN function of the CoA transporter might not be possible under physiological conditions. Complementing diverse mutant yeast strains with PXN and investigating the suppression of the mutant phenotypes, the authors provided evidence that PXN is not able to function as a CoA transporter or a redox shuttle by mediating a NAD⁺/NADH exchange, but instead catalyzes the import of NAD into peroxisomes against AMP in intact yeast cells [67]. This work demonstrated that Arabidopsis PXN supplies the peroxisomes with NAD by importing this coenzyme from the cytosol in exchange with AMP.

4.2. Nicotinamide Adenine Dinucleotide (NAD) Carriers

Regarding NAD transport in mitochondria and plastids, in addition to PXN, it has been demonstrated that two MCF members in Arabidopsis, named AtNDT1 and AtNDT2, are able to catalyze the import of NAD in these organelles [68]. Both carriers are able to complement the phenotype of a yeast mutant lacking NAD⁺ transport [68]. Surprisingly, both AtNDT1 and AtNDT2 exhibit similar substrate specificity, being able to import NAD⁺ against ADP or AMP, and not accepting NADH, NADP⁺, NADPH, nicotinamide or nicotinic acid as transport substrates [68]. Intriguingly, despite the similarities in terms of biochemical properties, initial localization analysis indicated that AtNDT1 was located in the plastid membrane while AtNDT2 was in the mitochondrial membrane [68]. Surprisingly, AtNDT1 was found in mitochondrial membranes in proteome studies [69] and previously a GFP-tagging and immunolocalization study was not able to find AtNDT1 targeted to chloroplast membranes [70]. Very recently, both AtNDT1- and AtNDT2-GFP fusion proteins were found exclusively located in the mitochondria, clearly indicating their mitochondrial localization [71].

4.3. Adenylate Carriers

The transport catalyzed by the ADP/ATP carrier plays an important role in sustaining the cellular ATP homeostasis by facilitating the counter exchange of mitochondrial ATP for cytosolic ADP [72]. ADP/ATP carrier proteins have been identified and characterized in different species including organisms of medical and veterinary importance, such as *T. brucei* [27,73,74]. The importance of the efficient adenylate transport systems for intracellular energy partitioning between the cell organelles has

been widely demonstrated in plants (for review see [72]). Adenylate carriers found in different organelles have been previously identified and biochemically characterized in plants. There are three subgroups of MCF responsible for adenylate transport in plants: (1) the well-characterized ADP/ATP carriers, named AAC carriers (*AtAAC1*, At3g08580; *AtAAC2*, At5g13490; and *AtAAC3*, At4g28390), which are required for mitochondrial energy passage (for review see [72]) and represent the most abundant proteins in the inner mitochondrial membrane (*AtAAC1–3*; 53,065 protein copies/mitochondria [75]); (2) the mitochondrial ATP-Mg/phosphate carriers, named as APC carriers (*AtAPC1*, At5g61810; *AtAPC2*, At5g51050; and *AtAPC3*, At5g07320); and (3) the adenine nucleotide transporter ADNT1 (At4g01100), which transport AMP instead of ADP as counter exchange substrate of ATP [76].

In Arabidopsis there are three genes encoding putative APC proteins (*AtAPC1–3*). These proteins belong to the MCF and exhibit high amino acid sequence similarities to their human and yeast counterparts [12,19]. It was demonstrated that all APC proteins from Arabidopsis localize to mitochondria and restore the growth phenotype of APC yeast loss-of-function mutants [77]. Interestingly, these carriers interact with calcium (Ca^{2+}) via their N-terminal EF-hand motifs *in vitro*, suggesting that APC1–3 isoforms represent Ca^{2+} -regulated ATP-Mg/phosphate transporters. Insights into the biochemical characteristics of these APCs were reported based on reconstitution of heterologously expressed proteins into liposomes [16,78]. The obtained results demonstrated that Arabidopsis APCs mediate antiport of ATP, ADP and phosphate and the transport characteristics indicated that the plant APCs preferentially import the Ca^{2+} - and not the Mg^{2+} -complexed form of ATP, at least in an *in vitro* system [78]. It is important to note that recent evidence indicates that not only Mg^{2+} and Ca^{2+} , but also other divalent cations and specifically Mn^{2+} , Fe^{2+} , Zn^{2+} and Cu^{2+} , are transported together with ATP by human and Arabidopsis APCs [79].

Table 2. Subfamilies of mitochondrial carrier defined by substrate specificity.

Subfamilies	Aliases	Main Substrates	Triplets *	References
<i>For nucleotides and dinucleotides</i>				
ADP/ATP	AAC	ADP, ATP	11 (DNS), 19 (AGT), 23 (KL[G/S]), 84 (TYG), 85 (QRX), 88 (NYV)	[19,80]
Coenzyme A/PAP	CoA/PAP	-	23 (K[V/A]Q), 34 (IVR), 88 ([K/Q]SS)	[65,81]
ATP-Mg/Pi	APC	ATP-Mg, ATP-Ca, Pi, AXP	23 (RQ[Q/A]), 30 (DE[A/T/N]), 84 (EYA), 88 (KDS)	[19,76,82–84]
Thiamine pyrophosphate	TPC	Thpp, thmp; (d)NDP, (d)NTP	23 (R[T/S]K), 34 (IT[K/R]), 80 (L[A/T]K), 85 (GAT)	[85–87]
Pyrimidine nucleotides	PNC	Pyrimidine (deoxy)nucleotides	19 (G[G/A]K), 27 (CNY), 30 ([D/E]WE), 37 (QQR), 83 ([PEP], 85 (R[I/V][S/T])	[48,88]
FAD/folate	FAD	Folates, FAD	19 (GGK), 27 (HNY), 30 (DWQ)	[70,89,90]
ANT	ANT	ATP, ADP, AMP	19 (SAK), 30 (DAI), 33 (KAK), 37 (QKR)	[46]
NAD ⁺	NDT/PXN	NAD ⁺ , (d)AMP, (d)GMP	19 (GGK), 27 (CNY), 30 (DWE), 89 (FP[L/F])	[49,68]
GTP/GDP	GGC	GTP, GDP, dgtp, dgdp, ITP, IDP	22 (EGS), 23 (IEL), 84 (QGK), 85 (RSL), 88 (KLS)	[91]
<i>For di-/tri-carboxylates and keto acids</i>				
Dicarboxylates	DIC	Malate, succinate, phosphate, sulfate, thiosulfate	26 (TG[C/S]), 27 (H[N/T][S/Q/N]), 33 (K[N/M]K), 88 (RQ[I/L/T])	[42,92,93]
Di-/tri-carboxylates	DTC	Oxoglutarate, citrate	26 (IGS), 27 (QSL), 33 (KLK), 35 (RRQ), 77 (GTY), 84 (YLH), 88 (RMT), 93 ([K/R]DN)	[50]
Citrate/isocitrate	SFC	Citrate, isocitrate, aconitate	22 (EAG), 84 (KNG), 88 (RNT)	[94–96]
Citrate	CTP	Citrate, malate, isocitrate, cis-aconitate, PEP	22 (E[A/S][S/T]), 84 (KN[S/D]), 88 (RRV)	[97,98]
2-oxoglutarate	OGC	2-Oxoglutarate, malate	26 (VGS), 27 (QTM), 33 (KLK), 35 (RRR), 77 (GTY), 84 (YVH), 88 (RQT), 93 (TSE)	[43,99]
Oxodicarboxylates	ODC	Oxoadipate, oxoglutarate	22 (EE[A/G]), 77 (PTK), 81 (E[H/N]L) 84 (K[F/W]G), 85 (RNG), 88 (KY[M/L])	[100,101]
Oxaloacetate/sulfate	OAC	Oxaloacetate, sulfate, thiosulfate, a-isopropylmalate	23 (VAA), 26 (TGM), 30 (E[F/Y]D), 80 (YRR), 84 ([L/M]GH), 88 (RQ[C/S])	[47,102]

Table 2. Cont.

Subfamilies	Aliases	Main Substrates	Triplets *	References
For amino acids				
Glutamate	GC	Glutamate	22 (GQA), 77 (NTR), 80 (LRV), 84 (EFL), 85 (KSF), 88 (KYA)	[103]
Glutamate	BOU	L-Glutamate	-	[104]
Aspartate/glutamate	AGC	Aspartate, glutamate, cysteinesulfinate	22 (GQA), 77 (QCR), 84 (EFQ), 85 (KSF), 88 (KYT)	[45,105]
Aspartate/glutamate	UCP1–2		23 ([D/E][V/I/S/Q][A/V/T/S]), 88 ([R/K][D/E][F/M])	[12,51]
Ornithine	ORC	Ornithine, (lysine, citrulline, arginine, histidine)	23 ([V/I][A/S]W) but (KSN) in <i>S. cerevisiae</i> , 26 (GL[V/C]) but (ELI) in <i>S. cerevisiae</i> , 84 (EGA), but (QAV) in <i>atbac2</i>	[106–108]
Carnitine	CAC	Carnitine, acylcarnitine	23 (VTW), 85 (FSN)	[44,109]
S-adenosylmethionine	SAMC	S-adenosylmethionine, S-adenosylhomocysteine	19 (G[E/G]G), 23 ([D/E][C/S][A/G]), 26 ([L/F]RT), 80 ([G/A]RW), 85 ([A/S][S/T/D]X), 88 (FQF)	[110–113]
For other substrates				
Phosphate	PiC, mPT	Phosphate	19 (CEG), 23 (HDA), 80 (G[R/K]M), 88 (KKQ)	[114,115]
Iron	MIT, MRS-4, MFRN-2	-	19 (GTG), 22 (E[S/A/H][A/C]), 23 (HDA), 27 ([F/Y][T/N]T)	[12,116]

Abbreviations: AAC, ADP/ATP carrier; AGC, aspartate/glutamate carrier; ANT, peroxisomal adenine nucleotide translocator; APC, ATP-Mg/Pi carrier; CAC, carnitine carrier; CoA/PAP, coenzyme A/adenosine 3',5'-diphosphate carrier; BOU, A bout de soufflé (glutamate transporter); CTP, citrate carrier; DIC, dicarboxylate carrier; DTC, di-/tri-carboxylate carrier; FAD, FAD carrier; GC, glutamate carrier, GGC, GTP/GDP carrier; NDT, NAD⁺ carrier; OAC, oxaloacetate/sulfate carrier; ODC, oxodicarboxylate carrier; OGC, oxoglutarate carrier; ORC, ornithine carrier; PiC, phosphate carrier; mPT, mitochondrial phosphate carrier; PNC, pyrimidine nucleotide carrier; SAMC, S-adenosylmethionine carrier; SFC, succinate/fumarate carrier; TPC, thiamine pyrophosphate carrier; UCP, uncoupling protein. AXP, adenine nucleotides; dNDP, deoxynucleoside diphosphates; dNTP, deoxynucleoside triphosphates; PEP, phosphoenolpyruvate; Pi, phosphate; ThMP, thiamine monophosphate; ThPP, thiamine pyrophosphate. * Symmetry-related amino acid triplets are the triplet sets present in the functionally identified mitochondrial carriers of each family.

4.4. Amino Acid Carriers

Another enigmatic transporter named A BOUT DE SOUFFLE (BOU) was identified in *Arabidopsis At5g46800* a long time ago [117]. Previous studies extensively characterized the physiological function of the BOU transporter in plants and revealed that this protein plays important roles related to fatty acid β -oxidation [117], photorespiration and growth of meristem cells [118]. However, the specific substrate for the BOU transporter protein was unknown until recently [104]. Detailed biochemical characterization of *Arabidopsis* BOU and Ymc2p, the BOU homolog from *S. cerevisiae*, revealed the transport properties and kinetic parameters of these proteins. Both Ymc2p and BOU proteins are able to transport glutamate, and to a lesser extent L-homocysteinesulfinate, but no other amino acids nor many other tested metabolites [104]. This study also revealed that both proteins Ymc2p and BOU catalyze unidirectional transport of glutamate and, as reported for other known MCs, a faster counter exchange mode of transport, and catalyze a transmembrane glutamate⁻ + H⁺ symport. These results led to the conclusion that for both Ymc2p and BOU, the physiological function of these proteins is to catalyze the import uptake of glutamate into the mitochondria.

In *Arabidopsis*, two MCs (*AtBAC1*, At2g33820; and *AtBAC2*, At1g79900) are able to transport basic amino acids [106,119,120]. *AtBAC1* shares a 36% identity with BOU, whereas *AtBAC2* is 40% similar to SLC25A29, although it is also related to BOU (36% identity) and aspartate/glutamate carriers (AGCs, 30–33% identity) [22]. Recombinant proteins from *AtBAC1* and *AtBAC2* were purified and reconstituted in liposomes [106,120]. The results indicated that both proteins transport lysine, arginine, ornithine and histidine [106,120]. Interestingly, it was verified that only *AtBAC2* transports the neutral amino acid citrulline [106,120]. In addition, these studies indicated that *AtBAC1* and *AtBAC2* exhibit differences in terms of substrate specificity, with *AtBAC2* being less specific for L-amino acids. Despite the similar biochemical properties, the physiological roles of *AtBAC1* and *AtBAC2* seem to be different. While *AtBAC1* is likely involved in remobilization of storage compounds after seed germination in

Arabidopsis and rice [106,119,121], *AtBAC2* is more related with stress responses being expressed especially in responses to hyperosmotic stress and also during senescence [106,119,122,123].

4.5. Uncoupling Proteins

Uncoupling proteins (UCPs) have been described as being involved in dissipation of proton gradients across the inner mitochondrial membrane that is normally used for ATP synthesis [92–124]. Homology analysis with UCP from humans revealed that six genes in the Arabidopsis genome (*AtUCP1–6*) encode putative UCPs [124–126]. It was previously demonstrated that the isoform *AtUCP1* (*At3g54110*) is localized to mitochondria and exhibits the activity of an uncoupling protein similar to the human UCP1 [124–126]. The function of the isoform *AtUCP2* (*At5g58970*) was less understood until recently because it was detected in the Golgi apparatus [127] and also in the plasma membrane [128]. Recently, it was shown that *AtUCP2* isoform is also a mitochondrial localized protein [51]. Intriguingly, both isoforms *AtUCP1* and *AtUCP2* were shown to transport amino acids (glutamate, aspartate, cysteine sulfinate, and cysteate), dicarboxylates (malate, oxaloacetate, and 2-oxoglutarate), phosphate, sulfate, and thiosulfate [51]. Further biochemical analyses revealed that both isoforms catalyze an electroneutral aspartate/glutamate heteroexchange activity, in contrast to that mediated by the mammalian mitochondrial aspartate glutamate carrier. Three other former members of the *AtUCP* subfamily of Arabidopsis MCF (*AtUCP4–6*) were renamed as dicarboxylate carriers (DIC) (*AtDIC1*, *At2g22500*, *AtDIC2*, *At4g24570*; and *AtDIC3*, *At5g09470*) since these proteins are able to transport oxaloacetate, malate, succinate, phosphate, sulfate, thiosulfate and sulfite [93].

4.6. Dicarboxylate Carriers

As mentioned above, in the Arabidopsis genome three potential homologues of yeast and mammalian mitochondrial DICs were found and designated as *AtDIC1–3* (*At5G09470*) [93]. *AtDIC3* shares only 55–60% identical amino acids with *AtDIC1* and *AtDIC2*, whereas *AtDIC1* and *AtDIC2* share 70% identical amino acids, suggesting that *AtDIC1* and *AtDIC2* are more closely related [93]. Interestingly, a recent Arabidopsis mitochondrial proteomic study verified that *AtDIC3* is not highly expressed in comparison with *AtDIC1–2*, as *AtDIC1* is more abundant than *AtDIC2* (59 and 21 protein copies per mitochondria respectively) [75]. Transport experiments with recombinant and reconstituted *AtDIC* proteins demonstrated that the substrate specificity of these proteins is unique to plants, indicating the combined characteristics of the DIC and oxaloacetate carrier in yeast [93]. Indeed, the Arabidopsis DICs transport a wide range of dicarboxylates including malate, oxaloacetate and succinate as well as phosphate, sulfate and thiosulfate at high rates, whereas 2-oxoglutarate was revealed to be a very poor substrate. In the same study, the kinetic properties of recombinant *AtDIC1–3* proteins were determined [93]. It was shown that for all *AtDIC* proteins, V_{max} is not significantly different for the three substrates tested (malate, sulfate and phosphate). Nevertheless, the V_{max} for *AtDIC3* was higher than the values observed for *AtDIC1* and *AtDIC2*. Regarding the transport affinity (K_m) of *AtDIC1–3* proteins, for sulfate it was lower than the K_m values for phosphate and malate. For *AtDIC3*, it was verified that the K_m for sulfate was one order of magnitude lower than the K_m values for malate and phosphate; furthermore, the K_m of *AtDIC3* for sulfate was 3–4-fold lower than the K_m values of *AtDIC1* and *AtDIC2* using the same substrate. The identification and characterization of the biochemical properties of DIC proteins in Arabidopsis led to different questions about the physiological roles of these carriers in plants under distinct physiological conditions. Surprisingly, according to our current knowledge, the isolation and characterization of mutant plants for each *AtDIC* isoform still need to be performed.

4.7. Dicarboxylate/Tricarboxylate Carrier

Dicarboxylate/Tricarboxylates carriers (DTCs) are mitochondrial transporters that are able to transport both dicarboxylic acids (such as malate, maleate, oxaloacetate and 2-oxoglutarate) and tricarboxylic acids (such as citrate, isocitrate, *cis*-aconitate and *trans*-aconitate) [50]. In the human

parasite *Trypanosoma brucei*, it was demonstrated that a plant-like mitochondrial carrier family protein, named *TbMCP12*, is able to transport both dicarboxylates and tricarboxylates across the inner mitochondrial membrane (IMM) [129]. Silencing this carrier in *T. brucei* was not lethal, while its overexpression was deleterious. These results indicated that the intracellular abundance of *TbMCP12* is involved in the regulation of NADPH balance and mitochondrial ATP-production. In plants, it was recently demonstrated that DTCs are the most abundant mitochondrial carrier proteins in the IMM of Arabidopsis, comprising 0.8% of the total IMM area (6836 protein copies per mitochondria) [75]. Interestingly, unlike the other three more abundant carrier proteins in the IMM, i.e., ADP/ATP carriers (*AtAAC1–3*; 53,065 protein copies/mitochondria), mitochondrial phosphate carriers (*AtMPT2–3*; 21,325 protein copies/mitochondria) and uncoupling proteins (*AtUCP1–3*; 8595 protein copies/mitochondria), only one DTC homolog is found in Arabidopsis (*At5g19760*). In addition to Arabidopsis, DTCs have been described in several plant species including tobacco (*Nicotiana tabacum*) [50], grapes (*Vitis vinifera*) [130] citrus (*Citrus junos*) [131], Jerusalem artichoke (*Helianthus tuberosus*) [132] (and maize (*Zea mays*)) [133]. Surprisingly, the numbers of DTC homologs found in different plant species vary without a clear pattern, for example, in the Brassica genus, the number of DTC homologs varies from one in *A. thaliana* and *Arabidopsis lyrata*, two in *Brassica oleracea*, and three in *Brassica rapa* [52]. In tobacco, four homologs (*NtDTC1–4*) were identified [50].

For *AtDTC* and *NtDTCs*, the transport activity involves an obligatory electroneutral exchange of dicarboxylates such as malate and 2-oxoglutarate and tricarboxylates such as citrate [50]. In addition to catalyzing the dicarboxylate/tricarboxylate transport activity, it has been demonstrated that DTCs are able to catalyze homoexchange transport activities, such as dicarboxylate/dicarboxylate and tricarboxylate/tricarboxylate [50]. It is unclear so far which of these modalities are relevant in *in vivo* plant systems. From *in vitro* transport assays it is possible to conclude that DTCs are promiscuous in terms of transported substrates [50]. In the same study, it was observed that the highest DTC activities are in the presence of internal 2-oxoglutarate, malate, maleate, oxaloacetate, succinate or malonate. Intriguingly, it was observed also that citrate, isocitrate, *cis*-aconitate, *trans*-aconitate, and sulfate were exchanged for external 2-oxoglutarate, although to a slightly lower extent than the dicarboxylates [50]. Any significant exchange was observed using internal fumarate, phosphoenolpyruvate, phosphate, pyruvate, glutamate, aspartate, glutamine, carnitine, ornithine, or ADP [50]. Together, these results demonstrated that DTCs are able to transport several intermediates of the TCA cycle, with the exception of succinyl-CoA and fumarate for which there is no available information. Another interesting characteristic of DTCs is the pH dependence. It was demonstrated that DTC-mediated oxoglutarate and citrate homoexchanges were dependent on pH, as the oxoglutarate/oxoglutarate and citrate/citrate exchanges increased on decreasing the pH from 8.0 to 5.5 for both *NtDTC1* and *AtDTC*. For *AtDTC*, the homoexchange kinetic constants measured for different substrates in two different pH values indicated that regardless of the substrate, the K_m and V_{max} varies as a function of pH value. Interestingly, the K_m values were increased at pH 7, suggesting that the substrate affinities were reduced; V_{max} values were also decreased at pH 7. Of note, the modulation of transport kinetics by pH is highly important for plant metabolism because it has been demonstrated for Arabidopsis that in the mitochondrial matrix the pH is around 8.1 and that in the cytosol the pH is close to 7.3 [134].

4.8. Succinate/Fumarate Carriers

In Arabidopsis, one of the MCF members (*At5g01340*), named as SFC1 carrier, exhibits 35% similarity with the ACR1 transporter from yeast [96]. The yeast SFC1 is able to transport fumarate, succinate, methylfumarate, 2-OG and OAA against [^{14}C]oxoglutarate [96]. The SFC1 transporter was further shown to prefer succinate and fumarate as substrates since the presence of either substrate almost completely inhibits fumarate/[^{14}C]oxoglutarate exchange [96]. The Arabidopsis SFC1 homolog complemented the *arc1* yeast mutant re-establishing the yeast growth in minimal media with ethanol as the sole carbon source [95]. Despite the predictions and preliminary biochemical information in plants, the biochemical evidence in favor of succinate/fumarate transport is still lacking. Moreover, recently the

SFC1 sequence from Arabidopsis was expressed in *E. coli* and protein was purified and reconstituted in liposomes [94]. Surprisingly, the results of transport properties and kinetic parameters revealed that AtSFC1 transports mainly citrate, isocitrate and aconitate and, to a lesser extent, succinate and fumarate. Furthermore, it was demonstrated that the AtSFC1 carrier catalyzes a fast counter-exchange transport and low uniport of substrates, as well as exhibiting a higher transport affinity for tricarboxylates than dicarboxylates [94]. Intriguingly, there have been both reports and model predictions in Arabidopsis showing net influx of succinate to the mitochondria, which would have been expected as succinate is the preferred substrate of non-plant SFCs. Thus, it is likely that another unidentified transporter is using succinate as a counter-substrate to facilitate fumarate transport.

4.9. Phosphate Carriers

Apart from ADP, the transport of phosphate (Pi) through the IMM is essential for the oxidative phosphorylation of ADP to ATP. In Arabidopsis, three genes encode mitochondrial Pi carriers, namely AtMPT1 (or PiC3; At2g17270), AtMPT3 (or PiC1; At5g14040) and AtMPT2 (or PiC2; At3g48850), and all of them are related to mitochondrial Pi carrier (PiC) from human and yeast [12,105]. Biochemical studies demonstrate that Arabidopsis PiC1 and PiC2 complement yeast mutants deficient in mitochondrial Pi import [106,107], thus confirming that these proteins act as PiCs. Surprisingly, the role of the Arabidopsis PiC3, which is more distantly related to the other PiC1 and 2 plant isoforms [12,135] remains to be elucidated. Interestingly, ADP/ATP carriers (AtAAC1–3; 53,065 protein copies/mitochondria) and PiC1–2 (or AtMPT2–3; 21,325 protein copies/mitochondria) are the most abundant proteins in the IMM [75]. In agreement, it has been proposed that PiCs in the inner mitochondrial membrane are able to physiologically interact with AAC transporters, catalyzing a Pi/H⁺ symport (or Pi/OH[−] antiport) and thus supplying phosphate required for the ATP synthesis [136,137]. Recently, it was shown in Arabidopsis that a putative Pi transporter interacts with TCA cycle enzymes [138,139]. Notwithstanding, the significance of these protein–protein interactions at physiological levels remains to be elucidated.

4.10. Pyruvate Carriers

Pyruvate, the final product of glycolysis in the cytosol, must be transported into mitochondria to supply the carbon skeletons for oxidative metabolism through the TCA cycle reactions. The transport of pyruvate through the IMM must be performed by specific carriers. While candidates for mitochondrial pyruvate carriers (MPCs) have not been identified in the classic MCF yet, the identity and functionality of a series of MPCs, non-MCF members, have been reported in yeast, *T. brucei*, drosophila, mouse and humans [140–142]. The biochemical properties of MPCs have been extensively studied and expertly reviewed [143–146] mainly due to the research efforts to understand the importance of MPCs in metabolism-related human diseases. Furthermore, in *S. cerevisiae* it was demonstrated that MPC is a hetero-dimer in its functional state providing the basis for the structure elucidation of the functional complex [147]. In plants, the biological functions and molecular mechanisms involving MPCs are not well understood. Bioinformatics analysis suggests that a protein named NRG1, a negative regulator of guard cell abscisic acid (ABA) signaling (At4G05590), shares homology with the MPC2 proteins from yeast, drosophila, human and mouse [148]. Besides NRG1 protein, four other MPC candidates are encoded by the Arabidopsis genome [149]. This family of MPCs from Arabidopsis are phylogenetically classified into three categories: MPC1 (At5G20090), MPC2-like proteins (At4G14695, At4G22310 and At4G05590) and At4G26780 [149]; that said, little is known regarding the functions of these proteins. So far it is known that NRG1 is located in the mitochondria and its sequence exhibits transmembrane domains [148]. Furthermore, in Arabidopsis this putative MPC2-like protein seems to be involved in stomata ABA signaling [148]. Interestingly, a recent study demonstrated that AtMPC1 interacts with NRG1 and plays a role in the regulation of stomatal movement and pyruvate cellular content [150]. In addition, it was demonstrated with yeast MPCs that by mimicking the physiological pH gradient between the mitochondria and the cytosol, a quantifiable pyruvate transport

was observed, whilst in the absence of the pH gradient no transport of pyruvate was observed [147]. Recently, it was demonstrated that the formation of *AtMPC* protein complexes is required for cadmium (Cd) tolerance and also prevention of Cd accumulation in *Arabidopsis* [151]. In the same study, it was demonstrated that *AtMPC* complexes are composed of two elements, the *AtMPC1* and *AtMPC2* (*AtNRGA1* or *AtMPC3*). Interrupting the formation of *AtMPCs* by silencing *AtMPC1* element, the synthesis of acetyl-coenzyme A was supplemented by glutamate and thus sustaining the activity of TCA cycle reactions and glutathione synthesis following exposure to Cd stress [151]. Clearly, more molecular, biochemical and physiological research efforts are still needed to understand the transport mechanism, substrate specificities and physiological roles of mitochondrial pyruvate transporters in plants.

4.11. Iron Transporters (Mitoferrins)

Initially, mitochondrial iron (Fe) transporters, namely Mitoferrins (mIT), were identified and characterized in *Drosophila*, zebrafish and humans [152–154]. Plants homologs of mIT were first identified in rice [155] and, recently, two genes encoding for mIT were found in *Arabidopsis*, and named as *AtmIT1* (At2g30160) and *AtmIT2* (At1g07030) [116]. These proteins have an identity of 81% with each other at the amino acid level and share 38% sequence identity with yeast and 32% identity with zebrafish mIT [116]. In addition, both *AtmIT1* and *AtmIT2* proteins exhibit the classical MCF characteristic feature and were predicted to localize to the mitochondria by proteomic study [156] which has been confirmed by subcellular localization experiments with green fluorescent protein (GFP) fusions and Western blot analyses [116]. The rice mIT protein complemented the growth of yeast mutant which was defective in mitochondrial Fe transport [155]. Similarly, the expression of *AtmIT1* or *AtmIT2* can rescue the phenotype of the yeast mutant defective in mitochondrial Fe transport (*mrs3mrs4* mutant; [157]). In mammalian and yeast cells, the redundancy in the roles of mITs has been investigated in terms of biochemical properties and kinetic profiles for Fe²⁺ uptake [154,158]. Moreover, a recent study demonstrated that a purified recombinant mitoferrin⁻¹ (TMfrn1), from *Oreochromis niloticus*, catalyzes the transport free Fe and not a chelated Fe complex. In addition, it was shown that it is selective for alkali divalent ions [159]. In the same study, the results indicated that mITs are high-affinity or high-throughput Fe transporters [159]. Of note, mitochondria are known as organelles where there is utilization of other transition metals than Fe, such as manganese, copper, and zinc; however, despite the importance, the mechanisms by which these metal ions are transported through the IMM are not well understood. In addition, it should be mentioned that the possible substrates used by mITs in exchange for the imported Fe are still unknown. In plant systems the biochemical properties of mITs are much less studied than other organisms. Nevertheless, it has been demonstrated that both *AtmIT1* and *AtmIT2* transporters seem to be important for mitochondrial Fe uptake and also for the correct mitochondrial function, and consequently, they are necessary for the proper growth and development of the plant [116,155].

5. Conclusions

Research into the metabolic roles of plant MCFs has made impressive advances since the last comprehensive reviews were published some eight to nine years ago [12,135]. This was in part due to be expected, given the massive increase in the number of plant species sequenced in the interim as well as the mechanistic insights into MCF function that were facilitated by recent developments in structural biology. Although, as yet, such experiments have not been carried out for plant proteins, their very high homology to their mammalian counterparts renders the findings based on the human ATP/ADP carrier to likely be highly similar to its plant counterpart and indeed to many other plant MCFs. The genome sequencing has additionally expanded the repertoire of MCFs found in any single species thereby reflecting the challenge that remains in their characterization. That said, as we detail above, via use of heterologous expression, the biochemical characterization of a large number of MCF members has been carried out thereby providing the putative metabolic functions of a substantial

number of the family. It is important to state that, as we discuss in the accompanying article [28], experimental proof that these studies do indeed reflect the in vivo role of the proteins remains lacking in some instances. Moreover, a considerable number of MCF proteins remain to be characterized at the biochemical level and such experiments should be a priority for future research. Only once the biochemical potential of each member of the MCF, as well as information concerning their subcellular locations, is acquired alongside that of non-canonical mitochondrial transporters will we be able to accurately model plant mitochondrial function and, for that matter, truly appreciate the importance of this fascinating organelle.

Supplementary Materials: The following are available online at <http://www.mdpi.com/2218-273X/10/7/1013/s1>, Table S1: Orthologous genes of plant mitochondrial carrier family retrieved from Plaza server.

Author Contributions: J.H.F.C. performed the genomic analysis. A.N.-N. and A.R.F. wrote the manuscript. All authors agreed to the published version of the manuscript.

Funding: This research was funded by Collaborative Research Centers, SFB (Sonderforschungsbereich, Grant TRR 175/1) to A.R.F. and Conselho Nacional de Desenvolvimento Científico e Tecnológico (CNPq) (Grant 306818/2016-7) to A.N.-N.

Conflicts of Interest: The authors declare no conflict of interest.

References

1. Roger, A.J.; Muñoz-Gómez, S.A.; Kamikawa, R. The origin and diversification of mitochondria. *Curr. Biol. CB* **2017**, *27*, 1177–1192. [CrossRef]
2. Fernie, A.R.; Carrari, F.; Sweetlove, L.J. Respiratory metabolism: Glycolysis, the TCA cycle and mitochondrial electron transport. *Curr. Opin. Plant Biol.* **2004**, *7*, 254–261. [CrossRef] [PubMed]
3. Eastmond, P.J.; Astley, H.M.; Parsley, K.; Aubry, S.; Williams, B.P.; Menard, G.N.; Craddock, C.P.; Nunes-Nesi, A.; Fernie, A.R.; Hibberd, J.M. Arabidopsis uses two gluconeogenic gateways for organic acids to fuel seedling establishment. *Nat. Commun.* **2015**, *6*, 1–8. [CrossRef] [PubMed]
4. Giege, P.; Heazlewood, J.L.; Roessner-Tunali, U.; Millar, A.H.; Fernie, A.R.; Leaver, C.J.; Sweetlove, L.J. Enzymes of glycolysis are functionally associated with the mitochondrion in arabidopsis cells. *Plant Cell* **2003**, *15*, 2140–2151. [CrossRef] [PubMed]
5. Picault, N.; Hodges, M.; Paimieri, L.; Palmieri, F. The growing family of mitochondrial carriers in arabidopsis. *Trends Plant Sci.* **2004**, *9*, 138–146. [CrossRef] [PubMed]
6. Mintz-Oron, S.; Meir, S.; Malitsky, S.; Ruppin, E.; Aharoni, A.; Shlomi, T. Reconstruction of arabidopsis metabolic network models accounting for subcellular compartmentalization and tissue-specificity. *Proc. Natl. Acad. Sci. USA* **2012**, *109*, 339–344. [CrossRef]
7. Smith, A.C.; Robinson, A.J. A metabolic model of the mitochondrion and its use in modelling diseases of the tricarboxylic acid cycle. *BMC Syst. Biol.* **2011**, *5*, 102–115. [CrossRef] [PubMed]
8. Lee, C.P.; Millar, A.H. The plant mitochondrial transportome: Balancing metabolic demands with energetic constraints. *Trends Plant Sci.* **2016**, *21*, 662–676. [CrossRef]
9. Colombini, M. Candidate for the permeability pathway of the outer mitochondrial-membrane. *Nature* **1979**, *279*, 643–645. [CrossRef]
10. Benz, R.; Kottke, M.; Brdiczka, D. The cationically selective state of the mitochondrial outer-membrane pore—A study with intact mitochondria and reconstituted mitochondrial porin. *Biochim. Biophys. Acta* **1990**, *1022*, 311–318. [CrossRef]
11. Pfaff, E.; Klingenberg, M.; Ritt, E.; Vogell, W. Correlation of unspecific permeable mitochondrial spaces with intermembrane spaces. *Eur. J. Biochem.* **1968**, *5*, 222–232. [CrossRef] [PubMed]
12. Palmieri, F.; Pierri, C.L.; De Grassi, A.; Nunes-Nesi, A.; Fernie, A.R. Evolution, structure and function of mitochondrial carriers: A review with new insights. *Plant J.* **2011**, *66*, 161–181. [CrossRef] [PubMed]
13. Palmieri, F.; Pierri, C.L. Mitochondrial metabolite transport. *Essays in Biochem.* **2010**, *47*, 37–52.
14. Palmieri, F.; Pierri, C.L. Structure and function of mitochondrial carriers—Role of the transmembrane helix p and g residues in the gating and transport mechanism. *Febs Lett.* **2010**, *584*, 1931–1939. [CrossRef] [PubMed]
15. Palmieri, F. The mitochondrial transporter family SLC25: Identification, properties and physiopathology. *Mol. Asp. Med.* **2013**, *34*, 465–484. [CrossRef] [PubMed]

16. Monne, M.; Miniero, D.V.; Obata, T.; Daddabbo, L.; Palmieri, L.; Vozza, A.; Nicolardi, M.C.; Fernie, A.R.; Palmieri, F. Functional characterization and organ distribution of three mitochondrial ATP-Mg/Pi carriers in *Arabidopsis thaliana*. *Biochim. Biophys. Acta-Bioenerg.* **2015**, *1847*, 1220–1230. [CrossRef]
17. Kunji, E.R.S.; Robinson, A.J. Coupling of proton and substrate translocation in the transport cycle of mitochondrial carriers. *Curr. Opin. Struct. Biol.* **2010**, *20*, 440–447. [CrossRef] [PubMed]
18. Palmieri, F. The mitochondrial transporter family (slc25): Physiological and pathological implications. *Pflug. Arch.-Eur. J. Physiol.* **2004**, *447*, 689–709. [CrossRef]
19. Klingenberg, M. The ADP and ATP transport in mitochondria and its carrier. *Biochim. Biophys. Acta-Biomembr.* **2008**, *1778*, 1978–2021. [CrossRef]
20. Satrustegui, J.; Pardo, B.; Del Arco, A. Mitochondrial transporters as novel targets for intracellular calcium signaling. *Physiol. Rev.* **2007**, *87*, 29–67. [CrossRef]
21. Monne, M.; Miniero, D.V.; Daddabbo, L.; Palmieri, L.; Porcelli, V.; Palmieri, F. Mitochondrial transporters for ornithine and related amino acids: A review. *Amino Acids* **2015**, *47*, 1763–1777. [CrossRef]
22. Monne, M.; Vozza, A.; Lasorsa, F.M.; Porcelli, V.; Palmieri, F. Mitochondrial carriers for aspartate, glutamate and other amino acids: A review. *Int. J. Mol. Sci.* **2019**, *20*, 4456. [CrossRef] [PubMed]
23. Palmieri, F. Mitochondrial transporters of the slc25 family and associated diseases: A review. *J. Inherit. Metab. Dis.* **2014**, *37*, 565–575. [CrossRef]
24. Robinson, A.J.; Kunji, E.R.S.; Gross, A. Mitochondrial carrier homolog 2 (MTCH2): The recruitment and evolution of a mitochondrial carrier protein to a critical player in apoptosis. *Exp. Cell Res.* **2012**, *318*, 1316–1323. [CrossRef] [PubMed]
25. Ruprecht, J.J.; Kunji, E.R.S. The SLC25 mitochondrial carrier family: Structure and mechanism. *Trends Biochem. Sci.* **2020**, *45*, 244–258. [CrossRef]
26. Taylor, E.B. Functional properties of the mitochondrial carrier system. *Trends Cell Biol.* **2017**, *27*, 633–644. [CrossRef] [PubMed]
27. Colasante, C.; Peña Diaz, P.; Clayton, C.; Voncken, F. Mitochondrial carrier family inventory of *Trypanosoma brucei brucei*: Identification, expression and subcellular localisation. *Mol. Biochem. Parasitol.* **2009**, *167*, 104–117. [CrossRef] [PubMed]
28. Nunes-Nesi, A.; Cavalcanti, J.H.; Fernie, A.R. Characterization of *in vivo* function(s) of members of the plant mitochondrial carrier family. *Biomolecules* under review.
29. Pebay-Peyroula, E.; Dahout-Gonzalez, C.; Kahn, R.; Trezeguet, V.; Lauquin, G.J.M.; Brandolin, R. Structure of mitochondrial ADP/ATP carrier in complex with carboxyatractyloside. *Nature* **2003**, *426*, 39–44. [CrossRef]
30. Saraste, M.; Walker, J.E. Internal sequence repeats and the path of polypeptide in mitochondrial ADP/ATP translocase. *Febs Lett.* **1982**, *144*, 250–254. [CrossRef]
31. Kunji, E.R.S.; Harding, M. Projection structure of the atractyloside-inhibited mitochondrial ADP/ATP carrier of *Saccharomyces cerevisiae*. *J. Biol. Chem.* **2003**, *278*, 36985–36988. [CrossRef]
32. Walters, D.E.; Kaplan, R.S. Homology-modeled structure of the yeast mitochondrial citrate transport protein. *Biophys. J.* **2004**, *87*, 907–911. [CrossRef] [PubMed]
33. Tonazzi, A.; Giangregorio, N.; Indiveri, C.; Palmieri, F. Identification by site-directed mutagenesis and chemical modification of three vicinal cysteine residues in rat mitochondrial carnitine/acylcarnitine transporter. *J. Biol. Chem.* **2005**, *280*, 19607–19612. [CrossRef]
34. Wohlrab, H. Novel inter- and intrasubunit contacts between transport-relevant residues of the homodimeric mitochondrial phosphate transport protein. *Biochem. Biophys. Res. Commun.* **2004**, *320*, 685–688. [CrossRef]
35. Cappello, A.R.; Curcio, R.; Miniero, D.V.; Stipani, I.; Robinson, A.J.; Kunji, E.R.S.; Palmieri, F. Functional and structural role of amino acid residues in the even-numbered transmembrane alpha-helices of the bovine mitochondrial oxoglutarate carrier. *J. Mol. Biol.* **2006**, *363*, 51–62. [CrossRef] [PubMed]
36. Cappello, A.R.; Miniero, D.V.; Curcio, R.; Ludovico, A.; Daddabbo, L.; Stipani, I.; Robinson, A.J.; Kunji, E.R.S.; Palmieri, F. Functional and structural role of amino acid residues in the odd-numbered transmembrane alpha-helices of the bovine mitochondrial oxoglutarate carrier. *J. Mol. Biol.* **2007**, *369*, 400–412. [CrossRef] [PubMed]
37. Robinson, A.J.; Kunji, E.R.S. Mitochondrial carriers in the cytoplasmic state have a common substrate binding site. *Proc. Natl. Acad. Sci. USA* **2006**, *103*, 2617–2622. [CrossRef]
38. Robinson, A.J.; Overly, C.; Kunji, E.R.S. The mechanism of transport by mitochondrial carriers based on analysis of symmetry. *Proc. Natl. Acad. Sci. USA* **2008**, *105*, 17766–17771. [CrossRef]

39. Ruprecht, J.J.; Hellawell, A.M.; Harding, M.; Crichton, P.G.; McCoy, A.J.; Kunji, E.R. Structures of yeast mitochondrial ADP/ATP carriers support a domain-based alternating-access transport mechanism. *Proc. Natl. Acad. Sci. USA* **2014**, *111*, 426–434. [CrossRef]
40. Ruprecht, J.J.; King, M.S.; Zogg, T.; Aleksandrova, A.A.; Pardon, E.; Crichton, P.G.; Steyaert, J.; Kunji, E.R.S. The molecular mechanism of transport by the mitochondrial ADP/ATP carrier. *Cell* **2019**, *176*, 435–447. [CrossRef]
41. Indiveri, C.; Iacobazzi, V.; Giangregorio, N.; Palmieri, F. The mitochondrial carnitine carrier protein: cDNA cloning, primary structure and comparison with other mitochondrial transport proteins. *Biochem. J.* **1997**, *321*, 713–719. [CrossRef] [PubMed]
42. Palmieri, L.; Palmieri, F.; Runswick, M.J.; Walker, J.E. Identification by bacterial expression and functional reconstitution of the yeast genomic sequence encoding the mitochondrial dicarboxylate carrier protein. *Febs Lett.* **1996**, *399*, 299–302. [CrossRef]
43. Fiermonte, G.; Walker, J.E.; Palmieri, F. Abundant bacterial expression and reconstitution of an intrinsic membrane-transport protein from bovine mitochondria. *Biochem. J.* **1993**, *294*, 293–299. [CrossRef]
44. Palmieri, L.; Lasorsa, F.M.; Iacobazzi, V.; Runswick, M.J.; Palmieri, F.; Walker, J.E. Identification of the mitochondrial carnitine carrier in *Saccharomyces cerevisiae*. *Febs Lett.* **1999**, *462*, 472–476. [CrossRef]
45. Palmieri, L.; Pardo, B.; Lasorsa, F.M.; del Arco, A.; Kobayashi, K.; Iijima, M.; Runswick, M.J.; Walker, J.E.; Saheki, T.; Satrustegui, J.; et al. Citrin and aralar1 are Ca²⁺-stimulated aspartate/glutamate transporters in mitochondria. *Embo J.* **2001**, *20*, 5060–5069. [CrossRef]
46. Palmieri, L.; Rottensteiner, H.; Girzalsky, W.; Scarcia, P.; Palmieri, F.; Erdmann, R. Identification and functional reconstitution of the yeast peroxisomal adenine nucleotide transporter. *Embo J.* **2001**, *20*, 5049–5059. [CrossRef]
47. Marobbio, C.M.T.; Giannuzzi, G.; Paradies, E.; Pierri, C.L.; Palmieri, F. Alpha-isopropylmalate, a leucine biosynthesis intermediate in yeast, is transported by the mitochondrial oxalacetate carrier. *J. Biol. Chem.* **2008**, *283*, 28445–28453. [CrossRef]
48. Marobbio, C.M.T.; Di Noia, M.A.; Palmieri, F. Identification of a mitochondrial transporter for pyrimidine nucleotides in *Saccharomyces cerevisiae*: Bacterial expression, reconstitution and functional characterization. *Biochem. J.* **2006**, *393*, 441–446. [CrossRef]
49. Todisco, S.; Agrimi, G.; Castegna, A.; Palmieri, F. Identification of the mitochondrial NAD(+) transporter in *Saccharomyces cerevisiae*. *J. Biol. Chem.* **2006**, *281*, 1524–1531. [CrossRef]
50. Picault, N.; Palmieri, L.; Pisano, I.; Hodges, M.; Palmieri, F. Identification of a novel transporter for dicarboxylates and tricarboxylates in plant mitochondria—Bacterial expression, reconstitution, functional characterization, and tissue distribution. *J. Biol. Chem.* **2002**, *277*, 24204–24211. [CrossRef]
51. Monne, M.; Daddabbo, L.; Gagneul, D.; Obata, T.; Hielscher, B.; Palmieri, L.; Miniero, D.V.; Fernie, A.R.; Weber, A.P.M.; Palmieri, F. Uncoupling proteins 1 and 2 (UCP1 and UCP2) from *Arabidopsis thaliana* are mitochondrial transporters of aspartate, glutamate, and dicarboxylates. *J. Biol. Chem.* **2018**, *293*, 4213–4227. [CrossRef]
52. Toleco, M.R.; Naake, T.; Zhang, Y.; Heazlewood, J.L.; Fernie, A.R. Plant mitochondrial carriers: Molecular gatekeepers that help to regulate plant central carbon metabolism. *Plants* **2020**, *9*, 117. [CrossRef] [PubMed]
53. Emms, D.M.; Kelly, S. Orthofinder: Phylogenetic orthology inference for comparative genomics. *Genome Biol.* **2019**, *20*, 238–252. [CrossRef] [PubMed]
54. Mutwil, M.; Klie, S.; Tohge, T.; Giorgi, F.M.; Wilkins, O.; Campbell, M.M.; Fernie, A.R.; Usadel, B.; Nikoloski, Z.; Persson, S. Planet: Combined sequence and expression comparisons across plant networks derived from seven species. *Plant Cell* **2011**, *23*, 895–910. [CrossRef]
55. Ruprecht, C.; Mendrinna, A.; Tohge, T.; Sampathkumar, A.; Klie, S.; Fernie, A.R.; Nikoloski, Z.; Persson, S.; Mutwil, M. Famnet: A framework to identify multiplied modules driving pathway expansion in plants. *Plant Physiol.* **2016**, *170*, 1878–1894. [CrossRef] [PubMed]
56. Iacobazzi, V.; Lauria, G.; Palmieri, F. Organization and sequence of the human gene for the mitochondrial citrate transport protein. *DNA Seq.* **1997**, *7*, 127–139. [CrossRef]
57. Iacobazzi, V.; Naglieri, M.A.; Stanley, C.A.; Wanders, R.J.A.; Palmieri, F. The structure and organization of the human carnitine/acylcarnitine translocase (CACT1) gene. *Biochem. Biophys. Res. Commun.* **1998**, *252*, 770–774. [CrossRef] [PubMed]

58. Fiermonte, G.; Dolce, V.; Arrigoni, R.; Runswick, M.J.; Walker, J.E.; Palmieri, F. Organization and sequence of the gene for the human mitochondrial dicarboxylate carrier: Evolution of the carrier family. *Biochem. J.* **1999**, *344*, 953–960. [CrossRef] [PubMed]
59. Palenik, B.; Grimwood, J.; Aerts, A.; Rouze, P.; Salamov, A.; Putnam, N.; Dupont, C.; Jorgensen, R.; Derelle, E.; Rombauts, S.; et al. The tiny eukaryote ostreococcus provides genomic insights into the paradox of plankton speciation. *Proc. Natl. Acad. Sci. USA* **2007**, *104*, 7705–7710. [CrossRef]
60. Soltis, D.E.; Bell, C.D.; Kim, S.; Soltis, P.S. Origin and early evolution of angiosperms. *Ann. N. Y. Acad. Sci.* **2008**, *1133*, 3–25. [CrossRef]
61. Freeling, M. Bias in plant gene content following different sorts of duplication: Tandem, whole-genome, segmental, or by transposition. *Ann. Rev. Plant Biol.* **2009**, *60*, 433–453. [CrossRef] [PubMed]
62. Vandepoele, K.; Simillion, C.; Van de Peer, Y. Detecting the undetectable: Uncovering duplicated segments in arabidopsis by comparison with rice. *Trends Genet.* **2002**, *18*, 606–608. [CrossRef]
63. Thomas, B.C.; Pedersen, B.; Freeling, M. Following tetraploidy in an arabidopsis ancestor, genes were removed preferentially from one homeolog leaving clusters enriched in dose-sensitive genes. *Genome Res.* **2006**, *16*, 934–946. [CrossRef]
64. Zallot, R.; Agrimi, G.; Lerma-Ortiz, C.; Teresinski, H.J.; Frelin, O.; Ellens, K.W.; Castegna, A.; Russo, A.; de Crecy-Lagard, V.; Mullen, R.T.; et al. Identification of mitochondrial coenzyme a transporters from maize and arabidopsis. *Plant Physiol.* **2013**, *162*, 581–588. [CrossRef] [PubMed]
65. Prohl, C.; Pelzer, W.; Diekert, K.; Kmita, H.; Bedekovics, T.; Kispal, G.; Lill, R. The yeast mitochondrial carrier leu5p and its human homologue graves' disease protein are required for accumulation of coenzyme A in the matrix. *Mol. Cell. Biol.* **2001**, *21*, 1089–1097. [CrossRef]
66. Agrimi, G.; Russo, A.; Scarcia, P.; Palmieri, F. The human gene SLC25A17 encodes a peroxisomal transporter of coenzyme a, FAD and NAD⁺. *Biochem. J.* **2012**, *443*, 241–247. [CrossRef] [PubMed]
67. van Roermund, C.W.; Schroers, M.G.; Wiese, J.; Facchinelli, F.; Kurz, S.; Wilkinson, S.; Charton, L.; Wanders, R.J.; Waterham, H.R.; Weber, A.P.; et al. The peroxisomal NAD carrier from arabidopsis imports NAD in exchange with AMP. *Plant Physiol.* **2016**, *171*, 2127–2139. [CrossRef] [PubMed]
68. Palmieri, F.; Rieder, B.; Ventrella, A.; Blanco, E.; Do, P.T.; Nunes-Nesi, A.; Trauth, A.U.; Fiermonte, G.; Tjaden, J.; Agrimi, G.; et al. Molecular identification and functional characterization of *Arabidopsis thaliana* mitochondrial and chloroplastic NAD⁺ carrier proteins. *J. Biol. Chem.* **2009**, *284*, 31249–31259. [CrossRef]
69. Senkler, J.; Senkler, M.; Eubel, H.; Hildebrandt, T.; Lengwenus, C.; Schertl, P.; Schwarzlander, M.; Wagner, S.; Wittig, I.; Braun, H.P. The mitochondrial complexome of *Arabidopsis thaliana*. *Plant J. Cell Mol. Biol.* **2017**, *89*, 1079–1092. [CrossRef]
70. Bedhomme, M.; Hoffmann, M.; McCarthy, E.A.; Gambonnet, B.; Moran, R.G.; Rebeille, F.; Ravel, S. Folate metabolism in plants—An arabidopsis homolog of the mammalian mitochondrial folate transporter mediates folate import into chloroplasts. *J. Biol. Chem.* **2005**, *280*, 34823–34831. [CrossRef]
71. de Souza Chaves, I.; Feitosa-Araujo, E.; Florian, A.; Medeiros, D.B.; da Fonseca-Pereira, P.; Charton, L.; Heyneke, E.; Apfata, J.A.C.; Pires, M.V.; Mettler-Altmann, T.; et al. The mitochondrial nad(+) transporter (ndt1) plays important roles in cellular NAD(+) homeostasis in *Arabidopsis thaliana*. *Plant J. Cell Mol. Biol.* **2019**, *100*, 487–504. [CrossRef] [PubMed]
72. da Fonseca-Pereira, P.; Neri-Silva, R.; Cavalcanti, J.H.F.; Brito, D.S.; Weber, A.P.M.; Araujo, W.L.; Nunes-Nesi, A. Data-mining bioinformatics: Connecting adenylate transport and metabolic responses to stress. *Trends Plant Sci.* **2018**, *23*, 961–974. [CrossRef] [PubMed]
73. Pena-Diaz, P.; Pelosi, L.; Ebikeme, C.; Colasante, C.; Gao, F.; Bringaud, F.; Voncken, F. Functional characterization of tbMCP5, a conserved and essential ADP/ATP carrier present in the mitochondrion of the human pathogen *Trypanosoma brucei*. *J. Biol. Chem.* **2012**, *287*, 41861–41874. [CrossRef]
74. Gnipová, A.; Šubrtová, K.; Panicucci, B.; Horváth, A.; Lukeš, J.; Zíková, A. The ADP/ATP carrier and its relationship to oxidative phosphorylation in ancestral protist *Trypanosoma brucei*. *Eukaryot. Cell* **2015**, *14*, 297–310. [CrossRef] [PubMed]
75. Fuchs, P.; Rugen, N.; Carrie, C.; Elsasser, M.; Finkemeier, I.; Giese, J.; Hildebrandt, T.M.; Kuhn, K.; Maurino, V.G.; Ruberti, C.; et al. Single organelle function and organization as estimated from arabidopsis mitochondrial proteomics. *Plant J. Cell Mol. Biol.* **2020**, *101*, 420–441. [CrossRef] [PubMed]

76. Palmieri, L.; Santoro, A.; Carrari, F.; Blanco, E.; Nunes-Nesi, A.; Arrigoni, R.; Genchi, F.; Fernie, A.R.; Palmieri, F. Identification and characterization of ADNT1, a novel mitochondrial adenine nucleotide transporter from arabidopsis. *Plant Physiol.* **2008**, *148*, 1797–1808. [CrossRef] [PubMed]
77. Stael, S.; Rocha, A.G.; Robinson, A.J.; Kmiecik, P.; Vothknecht, U.C.; Teige, M. Arabidopsis calcium-binding mitochondrial carrier proteins as potential facilitators of mitochondrial ATP-import and plastid SAM-import. *FEBS Lett.* **2011**, *585*, 3935–3940. [CrossRef] [PubMed]
78. Lorenz, A.; Lorenz, M.; Vothknecht, U.C.; Niopek-Witz, S.; Neuhaus, H.E.; Haferkamp, I. In vitro analyses of mitochondrial atp/phosphate carriers from *Arabidopsis thaliana* revealed unexpected Ca²⁺-effects. *BMC Plant Biol.* **2015**, *15*, 238–254. [CrossRef]
79. Monne, M.; Daddabbo, L.; Giannossa, L.C.; Nicolardi, M.C.; Palmieri, L.; Miniero, D.V.; Mangone, A.; Palmieri, F. Mitochondrial ATP-Mg/phosphate carriers transport divalent inorganic cations in complex with ATP. *J. Bioenerg. Biomembr.* **2017**, *49*, 369–380. [CrossRef]
80. Fiore, C.; Trezeguet, V.; Le Saux, A.; Roux, P.; Schwimmer, C.; Dianoux, A.C.; Noel, F.; Lauquin, G.J.-M.; Brandolin, G.; Vignais, P.V. The mitochondrial ADP/ATP carrier: structural, physiological and pathological aspects. *Biochimie.* **1998**, *80*, 137–150. [CrossRef]
81. Fiermonte, G.; Paradies, E.; Todisco, S.; Marobbio, C.M.T.; Palmieri, F. A novel member of solute carrier family 25 (SLC25A42) is a transporter of coenzyme a and adenosine 3',5'-diphosphate in human mitochondria. *J. Biol. Chem.* **2009**, *284*, 18152–18159. [CrossRef] [PubMed]
82. Fiermonte, G.; De Leonardis, F.; Todisco, S.; Palmieri, L.; Lasorsa, F.M.; Palmieri, F. Identification of the mitochondrial ATP-Mg/Pi transporter: bacterial expression, reconstitution, functional characterization and tissue distribution. *J. Biol. Chem.* **2004**, *279*, 30722–30730. [CrossRef] [PubMed]
83. Traba, J.; Froschauer, E.; Wiesenberger, G.; Satrustegui, J.; del Arco, A. Yeast mitochondria import ATP through the calcium-dependent ATP-Mg/Pi carrier Sal1p, and are ATP consumers during aerobic growth in glucose. *Mol. Microbiol.* **2008**, *69*, 570–585. [CrossRef] [PubMed]
84. Traba, J.; Satrustegui, J.; del Arco, A. Characterization of SCaMC-3-like/slc25a41, a novel calcium-independent mitochondrial ATP-Mg/Pi carrier. *Biochem. J.* **2009**, *418*, 125–133. [CrossRef] [PubMed]
85. Dolce, V.; Fiermonte, F.; Runswick, M.J.; Palmieri, F.; Walker, J.E. The human mitochondrial deoxynucleotide carrier and its role in toxicity of nucleoside antivirals. *Proc. Natl Acad. Sci. USA.* **2001**, *98*, 2284–2288. [CrossRef] [PubMed]
86. Marobbio, C.M.T.; Voza, A.; Harding, M.; Bisaccia, F.; Palmieri, F.; Walker, J.E. Identification and reconstitution of the yeast mitochondrial transporter for thiamine pyrophosphate. *EMBO J.* **2002**, *21*, 5653–5661. [CrossRef]
87. Lindhurst, M.J.; Fiermonte, G.; Song, S. Knockout of Slc25a19 causes mitochondrial thiamine pyrophosphate depletion, embryonic lethality, CNS malformations, and anemia. *Proc. Natl Acad. Sci. USA* **2006**, *103*, 15927–15932. [CrossRef]
88. Floyd, S.; Favre, C.; Lasorsa, F.M. The IGF-I-mTOR signaling pathway induces the mitochondrial pyrimidine nucleotide carrier to promote cell growth. *Mol. Biol. Cell.* **2007**, *18*, 3545–3555. [CrossRef]
89. Tzagoloff, A.; Jang, J.; Glerum, D.M.; Wu, M. FLX1 codes for a carrier protein involved in maintaining a proper balance of flavin nucleotides in yeast mitochondria. *J. Biol. Chem.* **1996**, *271*, 7392–7397. [CrossRef]
90. Titus, S.A.; Moran, R.G. Retrovirally mediated complementation of the glyB phenotype: cloning of a human gene encoding the carrier for entry of folates into mitochondria. *J. Biol. Chem.* **2000**, *275*, 36811–36817. [CrossRef]
91. Voza, A.; Blanco, E.; Palmieri, L.; Palmieri, F. Identification of the mitochondrial GTP/GDP transporter in *Saccharomyces cerevisiae*. *J. Biol. Chem.* **2004**, *279*, 20850–20857. [CrossRef]
92. Fiermonte, G.; Palmieri, L.; Dolce, V.; Lasorsa, F.M.; Palmieri, F.; Runswick, M.J.; Walker, J.E. The sequence, bacterial expression and functional reconstitution of the rat mitochondrial dicarboxylate transporter cloned via distant homologs in yeast and *Caenorhabditis elegans*. *J. Biol. Chem.* **1998**, *273*, 24754–24759. [CrossRef] [PubMed]
93. Palmieri, L.; Picault, N.; Arrigoni, R.; Besin, E.; Palmieri, F.; Hodges, M. Molecular identification of three *Arabidopsis thaliana* mitochondrial dicarboxylate carrier isoforms: Organ distribution, bacterial expression, reconstitution into liposomes and functional characterization. *Biochem. J.* **2008**, *410*, 621–629. [CrossRef] [PubMed]

94. Brito, D.S.; Agrimi, G.; Charton, L.; Brilhaus, D.; Bitetto, M.G.; Lana-Costa, J.; Messina, E.; Nascimento, C.P.; Araujo, E.F.; Viana Pires, M.; et al. Biochemical and functional characterization of a mitochondrial citrate carrier in *Arabidopsis thaliana*. *Biochem. J.* **2020**, *477*, 1759–1777. [CrossRef] [PubMed]
95. Catoni, E.; Schwab, R.; Hilpert, M.; Desimone, M.; Schwacke, R.; Flugge, U.I.; Schumacher, K.; Frommer, W.B. Identification of an arabidopsis mitochondrial succinate-fumarate translocator. *Febs Lett.* **2003**, *534*, 87–92. [CrossRef]
96. Palmieri, L.; Lasorsa, F.M.; DePalma, A.; Palmieri, F.; Runswick, M.J.; Walker, J.E. Identification of the yeast ACRI gene product as a succinate-fumarate transporter essential for growth on ethanol or acetate. *Febs Lett.* **1997**, *417*, 114–118. [CrossRef]
97. Kaplan, R.S.; Mayor, J.A.; Wood, D.O. The mitochondrial tricarboxylate transport protein. cDNA cloning, primary structure, and comparison with other mitochondrial transport proteins. *J. Biol. Chem.* **1993**, *268*, 13682–13690. [PubMed]
98. Kaplan, R.S.; Mayor, J.A.; Gremse, D.A.; Wood, D.O. High level expression and characterization of the mitochondrial citrate transport protein from the yeast *Saccharomyces cerevisiae*. *J. Biol. Chem.* **1995**, *270*, 4108–4114. [CrossRef] [PubMed]
99. Indiveri, C.; Palmieri, F.; Bisaccia, F.; Kramer, R. Kinetics of the reconstituted 2-oxoglutarate carrier from bovine heart mitochondria. *Biochim. Biophys. Acta* **1987**, *890*, 310–318. [CrossRef]
100. Palmieri, L.; Agrimi, G.; Runswick, M.J.; Fearnley, I.M.; Palmieri, F.; Walker, J.E. Identification in *Saccharomyces cerevisiae* of two isoforms of a novel mitochondrial transporter for 2-oxoadipate and 2-oxoglutarate. *J. Biol. Chem.* **2001**, *276*, 1916–1922. [CrossRef]
101. Fiermonte, G.; Dolce, V.; Palmieri, L.; Ventura, M.; Runswick, M.J.; Palmieri, F.; Walker, J.E. Identification of the human mitochondrial oxodicarboxylate carrier: bacterial expression, reconstitution, functional characterization, tissue distribution, and chromosomal location. *J. Biol. Chem.* **2001**, *276*, 8225–8230. [CrossRef] [PubMed]
102. Palmieri, L.; Vozza, A.; Agrimi, G.; De Marco, V.; Runswick, M.J.; Palmieri, F.; Walker, J.E. Identification of the yeast mitochondrial transporter for oxaloacetate and sulfate. *J. Biol. Chem.* **1999**, *274*, 22184–22190. [CrossRef]
103. Fiermonte, G.; Palmieri, L.; Todisco, S.; Agrimi, G.; Palmieri, F.; Walker, J.E. Identification of the mitochondrial glutamate transporter: bacterial expression, reconstitution, functional characterization, and tissue distribution of two human isoforms. *J. Biol. Chem.* **2002**, *277*, 19289–19294. [CrossRef] [PubMed]
104. Porcelli, V.; Vozza, A.; Calcagnile, V.; Gorgoglione, R.; Arrigoni, R.; Fontanesi, F.; Marobbio, C.M.T.; Castegna, A.; Palmieri, F.; Palmieri, L. Molecular identification and functional characterization of a novel glutamate transporter in yeast and plant mitochondria. *Biochim. Biophys. Acta-Bioenerg.* **2018**, *1859*, 1249–1258. [CrossRef] [PubMed]
105. Cavero, S.; Vozza, A.; del Arco, A. Identification and metabolic role of the mitochondrial aspartate-glutamate transporter in *Saccharomyces cerevisiae*. *Mol. Microbiol.* **2003**, *50*, 1257–1269. [CrossRef]
106. Hoyos, M.E.; Palmieri, L.; Wertin, T.; Arrigoni, R.; Polacco, J.C.; Palmieri, F. Identification of a mitochondrial transporter for basic amino acids in *Arabidopsis thaliana* by functional reconstitution into liposomes and complementation in yeast. *Plant J.* **2003**, *33*, 1027–1035. [CrossRef]
107. Palmieri, L.; De Marco, V.; Iacobazzi, V.; Palmieri, F.; Runswick, M.J.; Walker, J.E. Identification of the yeast ARG-11 gene as a mitochondrial ornithine carrier involved in arginine biosynthesis. *FEBS Lett.* **1997**, *410*, 447–451. [CrossRef]
108. Fiermonte, G.; Dolce, V.; David, L.; Santorelli, F.M.; Dionisi-Vici, C.; Palmieri, F.; Walker, J.E. The mitochondrial ornithine transporter: bacterial expression, reconstitution, functional characterization, and tissue distribution of two human isoforms. *J. Biol. Chem.* **2003**, *278*, 32778–32783. [CrossRef]
109. Indiveri, C.; Tonazzi, A.; Palmieri, F. Identification and purification of the carnitine carrier from rat liver mitochondria. *Biochim. Biophys. Acta* **1990**, *1020*, 81–86. [CrossRef]
110. Marobbio, C.M.T.; Agrimi, G.; Lasorsa, F.M.; Palmieri, F. Identification and functional reconstitution of yeast mitochondrial carrier for S-adenosylmethionine. *EMBO J.* **2003**, *22*, 5975–5982. [CrossRef]
111. Agrimi, G.; Di Noia, M.A.; Marobbio, C.M.T.; Fiermonte, G.; Lasorsa, F.M.; Palmieri, F. Identification of the human mitochondrial S-adenosylmethionine transporter: bacterial expression, reconstitution, functional characterization and tissue distribution. *Biochem. J.* **2004**, *379*, 183–190. [CrossRef] [PubMed]

112. Palmieri, L.; Arrigoni, R.; Blanco, E.; Carrari, F.; Zanon, M.I.; Studart-Guimarães, C.; Fernie, A.R.; Palmieri, F. Molecular identification of an *Arabidopsis thaliana* S-adenosylmethionine transporter: analysis of organ distribution, bacterial expression, reconstitution into liposomes and functional characterization. *Plant Physiol.* **2006**, *142*, 855–865. [CrossRef]
113. Bouvier, F.; Linka, N.; Isner, J.C.; Mutterer, J.; Weber, A.P.M.; Camara, B. Arabidopsis SAMT1 defines a plastid transporter regulating plastid biogenesis and plant development. *Plant Cell* **2006**, *18*, 3088–3105. [CrossRef] [PubMed]
114. Wohlrab, H.; Briggs, C. Yeast mitochondrial phosphate transport protein expressed in *Escherichia coli*. Site-directed mutations at threonine-43 and at a similar location in the second tandem repeat (isoleucine-141). *Biochemistry* **1994**, *33*, 9371–9375. [CrossRef]
115. Fiermonte, G.; Dolce, V.; Palmieri, F. Expression in *Escherichia coli*, functional characterization, and tissue distribution of isoforms A and B of the phosphate carrier from bovine mitochondria. *J. Biol. Chem.* **1998**, *273*, 22782–22787. [CrossRef] [PubMed]
116. Jain, A.; Dashner, Z.S.; Connolly, E.L. Mitochondrial iron transporters (mit1 and mit2) are essential for iron homeostasis and embryogenesis in *Arabidopsis thaliana*. *Front. Plant Sci.* **2019**, *10*, 1449. [CrossRef] [PubMed]
117. Lawand, S.; Dorne, A.J.; Long, D.; Coupland, G.; Mache, R.; Carol, P. Arabidopsis a bout de souffle, which is homologous with mammalian carnitine acyl carrier, is required for postembryonic growth in the light. *Plant Cell* **2002**, *14*, 2161–2173. [CrossRef] [PubMed]
118. Eisenhut, M.; Planchais, S.; Cabassa, C.; Guivarc’h, A.; Justin, A.M.; Taconnat, L.; Renou, J.P.; Linka, M.; Gagneul, D.; Timm, S.; et al. Arabidopsis a bout de souffle is a putative mitochondrial transporter involved in photorespiratory metabolism and is required for meristem growth at ambient CO₂ levels. *Plant J. Cell Mol. Biol.* **2013**, *73*, 836–849. [CrossRef]
119. Catoni, E.; Desimone, M.; Hilpert, M.; Wipf, D.; Kunze, R.; Schneider, A.; Fluegge, U.-I.; Schumacher, K.; Frommer, W.B. Expression pattern of a nuclear encoded mitochondrial arginine-ornithine translocator gene from arabidopsis. *BMC Plant Biol.* **2003**, *3*, 1–10. [CrossRef]
120. Palmieri, L.; Todd, C.D.; Arrigoni, R.; Hoyos, M.E.; Santoro, A.; Polacco, J.C.; Palmieri, F. Arabidopsis mitochondria have two basic amino acid transporters with partially overlapping specificities and differential expression in seedling development. *Biochim. Biophys. Acta-Bioenerg.* **2006**, *1757*, 1277–1283. [CrossRef]
121. Taylor, N.L.; Howell, K.A.; Heazlewood, J.L.; Tan, T.Y.; Narsai, R.; Huang, S.; Whelan, J.; Millar, A.H. Analysis of the rice mitochondrial carrier family reveals anaerobic accumulation of a basic amino acid carrier involved in arginine metabolism during seed germination. *Plant Physiol.* **2010**, *154*, 691–704. [CrossRef]
122. Toka, I.; Planchais, S.; Cabassa, C.; Justin, A.M.; De Vos, D.; Richard, L.; Savoure, A.; Carol, P. Mutations in the hyperosmotic stress-responsive mitochondrial basic amino acid carrier2 enhance proline accumulation in arabidopsis. *Plant Physiol.* **2010**, *152*, 1851–1862. [CrossRef]
123. Planchais, S.; Cabassa, C.; Toka, I.; Justin, A.M.; Renou, J.P.; Savoure, A.; Carol, P. Basic amino acid carrier 2 gene expression modulates arginine and urea content and stress recovery in arabidopsis leaves. *Front. Plant Sci.* **2014**, *5*, 330–342. [CrossRef] [PubMed]
124. Borecky, J.; Maia, I.G.; Costa, A.D.T.; Jezek, P.; Chaimovich, H.; de Andrade, P.B.M.; Vercesi, A.E.; Arruda, P. Functional reconstitution of *Arabidopsis thaliana* plant uncoupling mitochondrial protein (AtPUMP1) expressed in *Escherichia coli*. *Febs Lett.* **2001**, *505*, 240–244. [CrossRef]
125. Sweetlove, L.J.; Lytovchenko, A.; Morgan, M.; Nunes-Nesi, A.; Taylor, N.L.; Baxter, C.J.; Eickmeier, I.; Fernie, A.R. Mitochondrial uncoupling protein is required for efficient photosynthesis. *Proc. Natl. Acad. Sci. USA.* **2006**, *103*, 19587–19592. [CrossRef] [PubMed]
126. Vercesi, A.E.; Borecky, J.; Maia Ide, G.; Arruda, P.; Cuccovia, I.M.; Chaimovich, H. Plant uncoupling mitochondrial proteins. *Ann. Rev. Plant Biol.* **2006**, *57*, 383–404. [CrossRef]
127. Parsons, H.T.; Christiansen, K.; Knierim, B.; Carroll, A.; Ito, J.; Batth, T.S.; Smith-Moritz, A.M.; Morrison, S.; McInerney, P.; Hadi, M.Z.; et al. Isolation and proteomic characterization of the arabidopsis golgi defines functional and novel components involved in plant cell wall biosynthesis. *Plant Physiol.* **2012**, *159*, 12–26. [CrossRef]
128. Nikolovski, N.; Rubtsov, D.; Segura, M.P.; Miles, G.P.; Stevens, T.J.; Dunkley, T.P.; Munro, S.; Lilley, K.S.; Dupree, P. Putative glycosyltransferases and other plant golgi apparatus proteins are revealed by lopit proteomics. *Plant Physiol.* **2012**, *160*, 1037–1051. [CrossRef]

129. Colasante, C.; Zheng, F.; Kemp, C.; Voncken, F. A plant-like mitochondrial carrier family protein facilitates mitochondrial transport of di- and tricarboxylates in *Trypanosoma brucei*. *Mol. Biochem. Parasitol.* **2018**, *221*, 36–51. [CrossRef]
130. Regalado, A.; Pierri, C.L.; Bitetto, M.; Laera, V.L.; Pimentel, C.; Francisco, R.; Passarinho, J.; Chaves, M.M.; Agrimi, G. Characterization of mitochondrial dicarboxylate/tricarboxylate transporters from grape berries. *Planta* **2013**, *237*, 693–703. [CrossRef]
131. Deng, W.; Luo, K.; Li, Z.; Yang, Y. Molecular cloning and characterization of a mitochondrial dicarboxylate/tricarboxylate transporter gene in *Citrus junos* response to aluminum stress. *Mitochondrial DNA* **2008**, *19*, 376–384. [PubMed]
132. Spagnoletta, A.; De Santis, A.; Tampieri, E.; Baraldi, E.; Bachi, A.; Genchi, G. Identification and kinetic characterization of HtDTC, the mitochondrial dicarboxylate-tricarboxylate carrier of jerusalem artichoke tubers. *J. Bioenerg. Biomembr.* **2006**, *38*, 57–65. [CrossRef] [PubMed]
133. Genchi, G.; Spagnoletta, A.; De Santis, A.; Stefanizzi, L.; Palmieri, F. Purification and characterization of the reconstitutively active citrate carrier from maize mitochondria. *Plant Physiol.* **1999**, *120*, 841–848. [CrossRef]
134. Shen, J.; Zeng, Y.; Zhuang, X.; Sun, L.; Yao, X.; Pimpl, P.; Jiang, L. Organelle pH in the arabidopsis endomembrane system. *Mol. Plant* **2013**, *6*, 1419–1437. [CrossRef] [PubMed]
135. Haferkamp, I.; Schmitz-Esser, S. The plant mitochondrial carrier family: Functional and evolutionary aspects. *Front. Plant Sci.* **2012**, *3*, 2–21. [CrossRef]
136. Pratt, R.D.; Ferreira, G.C.; Pedersen, P.L. Mitochondrial phosphate-transport—Import of the H⁺/Pi symporter and role of the presequence. *J. Biol. Chem.* **1991**, *266*, 1276–1280.
137. Stappen, R.; Kramer, R. Kinetic mechanism of phosphate phosphate and phosphate OH⁻ antiports catalyzed by reconstituted phosphate carrier from beef-heart mitochondria. *J. Biol. Chem.* **1994**, *269*, 11240–11246.
138. Zhang, Y.; Swart, C.; Alseekh, S.; Scossa, F.; Jiang, L.; Obata, T.; Graf, A.; Fernie, A.R. The extra-pathway interactome of the TCA cycle: Expected and unexpected metabolic interactions. *Plant Physiol.* **2018**, *177*, 966–979. [CrossRef]
139. Zhang, Y.; Beard, K.F.M.; Swart, C.; Bergmann, S.; Krahnert, I.; Nikoloski, Z.; Graf, A.; Ratcliffe, R.G.; Sweetlove, L.J.; Fernie, A.R.; et al. Protein-protein interactions and metabolite channelling in the plant tricarboxylic acid cycle. *Nat. Commun.* **2017**, *8*, 15212–15223. [CrossRef] [PubMed]
140. Bricker, D.K.; Taylor, E.B.; Schell, J.C.; Orsak, T.; Boutron, A.; Chen, Y.C.; Cox, J.E.; Cardon, C.M.; Van Vranken, J.G.; Dephoure, N.; et al. A mitochondrial pyruvate carrier required for pyruvate uptake in yeast, drosophila, and humans. *Science* **2012**, *337*, 96–100. [CrossRef]
141. Herzig, S.; Raemy, E.; Montessuit, S.; Veuthey, J.L.; Zamboni, N.; Westermann, B.; Kunji, E.R.; Martinou, J.C. Identification and functional expression of the mitochondrial pyruvate carrier. *Science* **2012**, *337*, 93–96. [CrossRef] [PubMed]
142. Štáfková, J.; Mach, J.; Biran, M.; Verner, Z.; Bringaud, F.; Tachezy, J. Mitochondrial pyruvate carrier in *Trypanosoma brucei*. *Mol. Microbiol.* **2016**, *100*, 442–456. [CrossRef] [PubMed]
143. Vanderperre, B.; Bender, T.; Kunji, E.R.S.; Martinou, J.C. Mitochondrial pyruvate import and its effects on homeostasis. *Curr. Opin. Cell Biol.* **2015**, *33*, 35–41. [CrossRef] [PubMed]
144. Furumoto, T. Pyruvate transport systems in organelles: Future directions in C4 biology research. *Curr. Opin. Plant Biol.* **2016**, *31*, 143–148. [CrossRef]
145. McCommis, K.S.; Finck, B.N. Mitochondrial pyruvate transport: A historical perspective and future research directions. *Biochem. J.* **2015**, *466*, 443–454. [CrossRef]
146. Bender, T.; Martinou, J.C. The mitochondrial pyruvate carrier in health and disease: To carry or not to carry? *Biochim. Biophys. Acta* **2016**, *1863*, 2436–2442. [CrossRef]
147. Tavoulari, S.; Thangaratnarajah, C.; Mavridou, V.; Harbour, M.E.; Martinou, J.C.; Kunji, E.R. The yeast mitochondrial pyruvate carrier is a hetero-dimer in its functional state. *EMBO J.* **2019**, *38*, 1–13. [CrossRef]
148. Li, C.L.; Wang, M.; Ma, X.Y.; Zhang, W. Nrga1, a putative mitochondrial pyruvate carrier, mediates ABA regulation of guard cell ion channels and drought stress responses in arabidopsis. *Mol. Plant* **2014**, *7*, 1508–1521. [CrossRef]
149. Wang, M.; Ma, X.; Shen, J.; Li, C.; Zhang, W. The ongoing story: The mitochondria pyruvate carrier 1 in plant stress response in arabidopsis. *Plant Signal. Behav.* **2014**, *9*, 1–4. [CrossRef]

150. Shen, J.L.; Li, C.L.; Wang, M.; He, L.L.; Lin, M.Y.; Chen, D.H.; Zhang, W. Mitochondrial pyruvate carrier 1 mediates abscisic acid-regulated stomatal closure and the drought response by affecting cellular pyruvate content in *Arabidopsis thaliana*. *BMC Plant Biol.* **2017**, *17*, 217–229. [CrossRef]
151. He, L.; Jing, Y.; Shen, J.; Li, X.; Liu, H.; Geng, Z.; Wang, M.; Li, Y.; Chen, D.; Gao, J.; et al. Mitochondrial pyruvate carriers prevent cadmium toxicity by sustaining the TCA cycle and glutathione synthesis. *Plant Physiol.* **2019**, *180*, 198–211. [CrossRef]
152. Shaw, G.C.; Cope, J.J.; Li, L.; Corson, K.; Hersey, C.; Ackermann, G.E.; Gwynn, B.; Lambert, A.J.; Wingert, R.A.; Traver, D.; et al. Mitoferrin is essential for erythroid iron assimilation. *Nature* **2006**, *440*, 96–100. [CrossRef] [PubMed]
153. Metzendorf, C.; Wu, W.; Lind, M.I. Overexpression of drosophila mitoferrin in l(2)mbn cells results in dysregulation of Fer1HCH expression. *Biochem. J.* **2009**, *421*, 463–471. [CrossRef]
154. Paradkar, P.N.; Zumbrennen, K.B.; Paw, B.H.; Ward, D.M.; Kaplan, J. Regulation of mitochondrial iron import through differential turnover of mitoferrin 1 and mitoferrin 2. *Mol. Cell. Biol.* **2009**, *29*, 1007–1016. [CrossRef]
155. Bashir, K.; Ishimaru, Y.; Nishizawa, N.K. Identification and characterization of the major mitochondrial fe transporter in rice. *Plant Signal. Behav.* **2011**, *6*, 1591–1593. [CrossRef] [PubMed]
156. Millar, A.H.; Heazlewood, J.L. Genomic and proteomic analysis of mitochondrial carrier proteins in arabidopsis. *Plant Physiol.* **2003**, *131*, 443–453. [CrossRef]
157. Moore, M.J.; Wofford, J.D.; Dancis, A.; Lindahl, P.A. Recovery of *mrs3Δmrs4Δ Saccharomyces cerevisiae* cells under iron-sufficient conditions and the role Fe₅₈₀. *Biochemistry* **2018**, *57*, 672–683. [CrossRef]
158. Brazzolotto, X.; Pierrel, F.; Pelosi, L. Three conserved histidine residues contribute to mitochondrial iron transport through mitoferrins. *Biochem. J.* **2014**, *460*, 79–89. [CrossRef] [PubMed]
159. Christenson, E.T.; Gallegos, A.S.; Banerjee, A. In vitro reconstitution, functional dissection, and mutational analysis of metal ion transport by mitoferrin-1. *J. Biol. Chem.* **2018**, *293*, 3819–3828. [CrossRef]



© 2020 by the authors. Licensee MDPI, Basel, Switzerland. This article is an open access article distributed under the terms and conditions of the Creative Commons Attribution (CC BY) license (<http://creativecommons.org/licenses/by/4.0/>).

Review

Biogenesis of Mitochondrial Metabolite Carriers

Patrick Horten ^{1,2}, Lilia Colina-Tenorio ^{1,3} and Heike Rampelt ^{1,3,*} 

¹ Institute of Biochemistry and Molecular Biology, ZBMZ, Faculty of Medicine, University of Freiburg, 79104 Freiburg, Germany; patrick.horten@biochemie.uni-freiburg.de (P.H.);

lilia.colina@biochemie.uni-freiburg.de (L.C.-T.)

² Faculty of Biology, University of Freiburg, 79104 Freiburg, Germany

³ CIBSS Centre for Integrative Biological Signalling Studies, University of Freiburg, 79104 Freiburg, Germany

* Correspondence: heike.rampelt@biochemie.uni-freiburg.de

Academic Editor: Ferdinando Palmieri

Received: 10 June 2020; Accepted: 3 July 2020; Published: 7 July 2020

Abstract: Metabolite carriers of the mitochondrial inner membrane are crucial for cellular physiology since mitochondria contribute essential metabolic reactions and synthesize the majority of the cellular ATP. Like almost all mitochondrial proteins, carriers have to be imported into mitochondria from the cytosol. Carrier precursors utilize a specialized translocation pathway dedicated to the biogenesis of carriers and related proteins, the carrier translocase of the inner membrane (TIM22) pathway. After recognition and import through the mitochondrial outer membrane via the translocase of the outer membrane (TOM) complex, carrier precursors are ushered through the intermembrane space by hexameric TIM chaperones and ultimately integrated into the inner membrane by the TIM22 carrier translocase. Recent advances have shed light on the mechanisms of TOM translocase and TIM chaperone function, uncovered an unexpected versatility of the machineries, and revealed novel components and functional crosstalk of the human TIM22 translocase.

Keywords: mitochondrial carrier; metabolite transport; mitochondrial pyruvate carrier; sideroflexin; TOM; TIM chaperones; TIM22; protein translocation; mitochondrial biogenesis

1. Introduction

The mitochondrial inner membrane separates two aqueous compartments, the matrix and the intermembrane space, that differ in their protein and metabolite composition and host distinct metabolic pathways. The inner membrane is also the site of oxidative phosphorylation, and its integrity is crucial to maintain the electrochemical membrane potential that fuels ATP synthesis as well as mitochondrial biogenesis and function. Therefore, metabolite transport into or out of the matrix relies on carrier proteins that facilitate diffusion of specific substrates across the membrane or use the membrane potential to transport metabolites.

Most mitochondrial metabolite carriers belong to the mitochondrial carrier family (MCF, in humans SLC25 for solute carrier family 25). It comprises more than 50 members in humans and over 30 in yeast, and includes the most abundant inner membrane proteins [1–4]. MCF substrates range from nucleotides and amino acids to cofactors, intermediates of oxidative metabolism, and inorganic ions. Thus, they perform crucial functions in mitochondrial metabolism, and mutations in carrier genes are associated with a variety of human pathologies [5]. The mitochondrial pyruvate carrier (MPC) belongs to an unrelated protein family and functions as a hetero-dimer that requires both subunits for carrier activity [6,7]. The sideroflexin family constitutes a third metabolite carrier family, members of which have recently been discovered to function as serine transporters in one-carbon metabolism [8–10].

Like the vast majority of mitochondrial proteins, carriers are encoded in the nuclear genome and synthesized by cytosolic ribosomes. Therefore, they have to be specifically recognized

and imported into the correct mitochondrial compartment. A multitude of protein translocases cooperates in the biogenesis of proteins destined for the different mitochondrial compartments [11–14]. Most precursors of mitochondrial inner membrane proteins are imported by the presequence translocase of the inner membrane (TIM23). However, carrier precursors generally lack a presequence, although a few contain an N-terminal extension that can improve solubility and translocation across the outer membrane [15–17]. Instead, carriers are targeted to mitochondria by internal signals. The internal targeting signals are not well defined, and carriers apparently contain several such motifs with different properties. For their biogenesis, metabolite carriers utilize a specialized import pathway involving the carrier translocase of the inner membrane (TIM22) [12,13,17–20] (Figure 1). This pathway can be divided into consecutive, biochemically defined stages: Stages I and II take place in the cytosol and on the mitochondrial surface, leading to import of the carrier precursor by the translocase of the outer membrane (TOM). In the intermembrane space (IMS), the precursor is bound by small TIM chaperones (stage III) and handed over to the TIM22 translocase (stage IV) which integrates the carrier into the inner membrane (stage V). The membrane potential across the inner membrane provides the driving force for membrane integration: Positively charged carrier sequences are subject to an electrophoretic force that pulls them into the matrix.

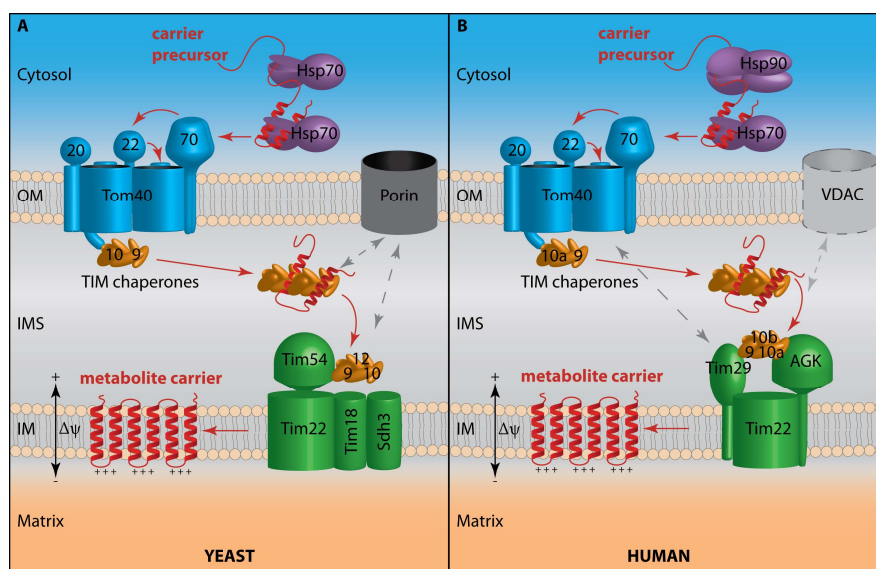


Figure 1. The carrier pathway in the yeast *S. cerevisiae* (A) and in humans (B) handles the recognition, translocation and membrane integration of mitochondrial metabolite carriers into the inner membrane. Carrier precursors are bound by chaperones in the cytosol and recognized at the translocase of the outer membrane (TOM) by the Tom70 receptor. After their transfer through the outer membrane, they are bound in the intermembrane space by the hexameric TIM chaperones, Tim9-Tim10 in yeast (A) or Tim9-Tim10a in humans (B). The TIM chaperones guide the precursor through the aqueous compartment to the membrane-bound TIM chaperone complex consisting of Tim9-Tim10-Tim12 in yeast (A) or Tim9-Tim10a-Tim10b in humans (B). Substrate transfer to the carrier translocase of the inner membrane (TIM22) is aided by interactions with outer membrane proteins (dashed arrows) involving the metabolite channel porin/VDAC in yeast (A), or the TOM complex in humans (B). In humans, VDAC was found in association with TIM22 components (B) and, thus, might participate in carrier biogenesis similarly to porin. The TIM22 carrier translocase integrates the precursors into the inner membrane in a membrane potential-dependent manner. OM, outer membrane; IMS, intermembrane space; IM, inner membrane; $\Delta\psi$, membrane potential; Hsp70, Hsp90, cytosolic ATP-dependent chaperones; Tom40, pore-forming component of the TOM complex; Tom20, Tom22, Tom70, receptors of the TOM complex; porin/VDAC, voltage-dependent anion channel; Tim22, core component of the TIM22 translocase; Tim18, Sdh3 (succinate dehydrogenase 3), Tim54, auxiliary subunits of the yeast TIM22 translocase; Tim29, AGK (acylglycerol kinase), auxiliary subunits of the human TIM22 translocase.

Mitochondrial carriers of the MCF/SLC25 family are the eponymous substrates of the TIM22 carrier translocase pathway [12,13,17,19] (Figure 1). The best studied carrier is the ADP/ATP carrier AAC (yeast)/ANT (human; adenine nucleotide translocator) that has been employed both as a model substrate to study carrier biogenesis and for the analysis of MCF structure and transport mechanism [4,17,18,21–23]. Mitochondrial carriers of the MCF/SLC25 family have a tripartite organization, with three homologous repeats consisting of two transmembrane segments each. They uniformly possess six transmembrane segments and expose both their N- and C-termini to the intermembrane space (Figure 2) [4,12,17,19,24]. Mitochondrial carriers transport substrates by enabling alternate access of the substrate(s) to the matrix and the intermembrane space while maintaining membrane impermeability for non-substrates [4,25–28]. Divergent members of the MCF with a differing number of TM segments are localized in the outer membrane and have acquired functions distinct from metabolite transport [4,29,30].

Interestingly, the components of the heterodimeric mitochondrial pyruvate carrier (MPC) have recently been discovered as further substrates of the TIM22 pathway (Figure 1) [31,32]. In contrast to the classical mitochondrial carriers, they are related to sugar transporters of the eukaryotic sugars will eventually be exported transporter (SWEET) and prokaryotic semiSWEET families [33,34]. SWEET transporters possess seven TM segments that are arranged into two triple-helix bundles connected by another α -helix. SemiSWEETs instead consist of one triple-helix bundle and assemble to dimers, forming a six TM functional unit like the SWEETs. MPC subunits MPC2 (mammals) as well as Mpc2 and Mpc3 (yeast) have three TM segments (Figure 2). For MPC1/Mpc1, the topology is not entirely clear: It has been suggested that they have only two TM segments with both termini in the matrix, or alternatively that they share the same topology as Mpc2/Mpc3 [6,7,35–37] (Figure 2).

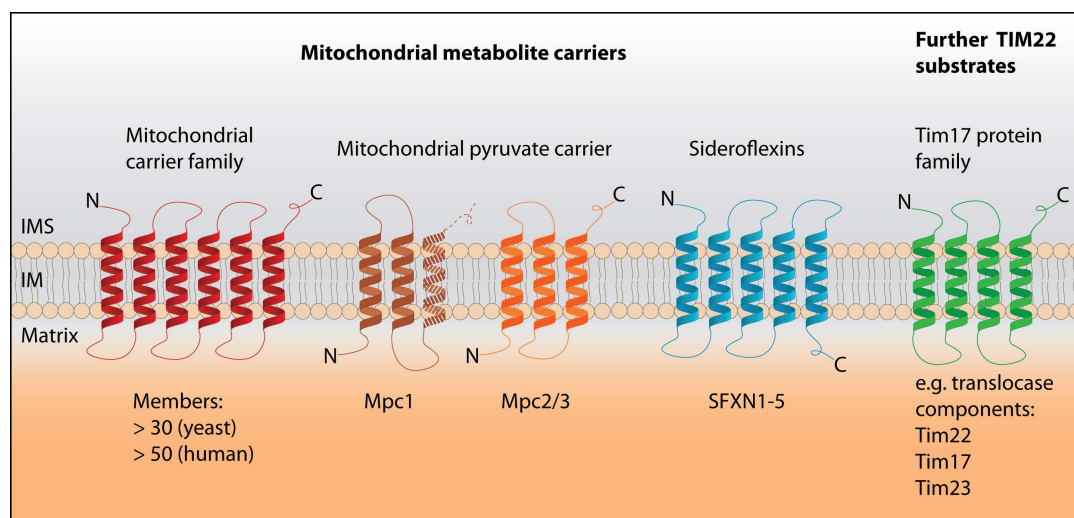


Figure 2. Substrates of the TIM22 carrier import pathway. Mitochondrial carriers of the mitochondrial carrier family (MCF)/SLC25 family (**red**), the components of the mitochondrial pyruvate carrier (**brown, orange**), as well as sideroflexins (**blue**) are imported into mitochondria via the TIM22 carrier pathway. MCF/SLC25 proteins have a uniform topology with 6 transmembrane segments [4,12,17,19,24]. In contrast, Mpc2/Mpc3 has only 3 TM segments, and Mpc1 has 2 or 3 TM segments [6,7,35–37]. The third unique family of metabolite carriers, the sideroflexins, has 5 TM domains with the N-terminus in the intermembrane space (IMS) [8,38,39]. Aside from metabolite carriers, the TIM22 pathway also imports the members of the Tim17 protein family including the translocase components Tim17, Tim22 and Tim23 (**green**). IMS, intermembrane space; IM, inner membrane.

Additionally, recent studies indicate that the sideroflexins, with five transmembrane segments and the N-terminus in the intermembrane space (IMS), also depend on the TIM22 carrier pathway for their biogenesis [38,39] (Figure 2). Thus, the mitochondrial pyruvate carrier components

and the sideroflexins with their unique topologies have challenged long-held views of the structural requirements for TIM22 substrates.

2. Carrier Recognition at the TOM Complex

Due to their hydrophobic nature, mitochondrial carrier precursors in the cytosol are bound by chaperones to prevent their aggregation (stage I). Since carrier import takes place post-translationally, the soluble stage can be distinguished from stage II that consists in precursor targeting to the translocase of the outer membrane (Figure 1, Table 1) [13,14,17,19]. The TOM complex is the main entry gate by which almost all precursor proteins destined to the different mitochondrial compartments gain access to the organelle [12,14,40,41]. It forms dimers *in vivo* and consists of the Tom40 β -barrel pore and six α -helical membrane proteins: Tom5, Tom6, Tom7 as well as the receptors Tom22, Tom20 and Tom70 [42–44]. Aggregation of the highly hydrophobic carrier precursors in the cytosol is prevented by molecular chaperones. In yeast, carriers are chaperoned mainly by Hsp70, whereas in mammalian cells both Hsp70 and Hsp90 participate in carrier biogenesis, along with several co-chaperones [14,45–49]. Recognition of precursors at the TOM complex is mediated by the receptors Tom20 and Tom70. They can functionally substitute for each other sufficiently well for single deletions to be viable, however Tom20 preferentially recognizes precursors that contain a presequence, while Tom70 preferentially binds precursors with internal targeting sequences including carrier proteins such as the ADP/ATP carrier or the phosphate carrier [12,13,49–60]. Tom70 not only interacts with the precursor, but also with the associated chaperone(s) via tetratricopeptide repeats (TPR) that bind the C-termini of Hsp70 or Hsp90 chaperones [14,46,49,61]. Moreover, one tripartite carrier precursor of the MCF/SLC25 family can recruit three Tom70 dimers, with each of the repeats participating in the interaction [21]. Thus, the interactions of Tom70 with the precursor-chaperone complex likely contribute to prevention of its aggregation. Import of carriers can be stalled at stage II by depletion of ATP (Table 1). ATP binding to Hsp70 triggers substrate release from Hsp70, the carrier precursor is handed over to the central receptor Tom22, and individual helix-loop-helix modules are threaded into the Tom40 pore in a hairpin-like conformation [21,62]. It is currently unclear how mitochondrial pyruvate carrier precursors with their distinct topology are handled by the TOM complex, although it is tempting to speculate that at least the two C-terminal TM segments of Mpc2/Mpc3 may be recognized in a fashion similar to classical carriers. Interestingly, even during translocation through the TOM complex, carriers follow a different route than presequence precursors, involving the distal regions of the Tom40 dimer and the N-terminal extension of Tom40 [42,44]. It was proposed that translocation through TOM is aided by interaction of positively charged regions in the precursors with the negatively charged inner surface of the Tom40 β -barrel [63], which is consistent with the previously reported head-first insertion of helix-loop-helix modules by their positively charged loops [21].

The efficiency of carrier recognition at the TOM complex is subject to metabolic regulation. Tom70 is phosphorylated by protein kinase A specifically during non-respiratory growth of yeast on glucose, resulting in an impaired interaction with Hsp70 and concomitantly reduced carrier import [64]. Thus, the efficiency of carrier biogenesis can be adjusted to the metabolic requirements of respiratory versus non-respiratory growth.

Table 1. Stages of carrier biogenesis via the TIM22 carrier import pathway.

TIM22 Carrier Import Pathway	Characteristics of Individual Stages in Carrier Biogenesis
Stage I	The carrier precursor is bound to cytosolic chaperones upon its synthesis, forming a soluble complex not associated with mitochondria.
Stage II	The precursor-chaperone complex is recognized by the Tom70 receptor of the TOM complex and can be arrested on the mitochondrial surface by ATP depletion. ATP binding triggers dissociation of Hsp70 chaperones and progression of the precursor.
Stage III IIIa:	The carrier precursor is translocated through the TOM complex into the IMS and concomitantly bound by soluble TIM chaperones (mainly Tim9-Tim10 in yeast, Tim9-Tim10a in humans).
IIIb:	The carrier precursor is handed over to the TIM22-bound TIM chaperones (Tim9-Tim10-Tim12 in yeast, Tim9-Tim10a-Tim10b in humans), resulting in tethering to the inner membrane.
Stage IV	In the presence of a low membrane potential, the carrier precursor is transferred to TIM22 and inserted into the inner membrane as a docked precursor.
Stage V	Formation of the mature, inner-membrane integrated carrier and release from TIM22 requires the presence of a higher membrane potential.

3. En Route through the Intermembrane Space

Unlike the TIM23 translocase that imports presequence proteins into the matrix or the inner membrane, the translocation of carrier precursors through the TOM complex is apparently not tightly coupled to integration into the inner membrane by the TIM22 carrier translocase [12,17,65,66]. Instead, once a carrier precursor has traversed the Tom40 pore and reached the IMS, it is bound by small TIM chaperones to prevent aggregation during its transit through the aqueous IMS environment to the inner membrane (stage III) [67–73] (Figure 1, Table 1). Translocation through the TOM complex is coupled to TIM chaperone binding [71]. The small TIM chaperones form ring-like hetero-hexameric complexes that bind carriers in an extended conformation [73–75]. The predominant TIM chaperone complex consists of alternating Tim9 and Tim10 subunits (Tim9 and Tim10a in humans) and is required for carrier import; the alternative Tim8-Tim13 complex (Tim8a or Tim8b and Tim13 in humans) has partially redundant substrate specificity [73,75–79]. Mutations in Tim8a cause the deafness–dystonia syndrome called Mohr–Tranebjærg syndrome [80], however, novel evidence suggests that the underlying molecular mechanism reflects a new function of Tim8a in cytochrome c oxidase maturation rather than a defective TIM22 carrier pathway [79]. The small TIM chaperones interact with the N-terminal extension of Tom40 that participates in carrier translocation, so they are ideally positioned to receive their cargo from the TOM complex [21,42,44,71]. Stage III of carrier import can be further subdivided, where stage IIIa denotes carriers bound to soluble TIM chaperones that may be associated with TOM or soluble in the IMS (Table 1) [17,19]. A recent comprehensive study demonstrated that an MCF carrier with six TM segments is bound by two TIM chaperone hexamers, and the precursor is chaperoned by interacting with a conserved hydrophobic cleft between the two tentacle-like α -helices of the small TIM proteins [73]. This conserved substrate binding region is also required for chaperoning of the structurally unrelated mitochondrial pyruvate carrier [31]. The soluble TIM complexes transfer carrier precursors to a separate TIM chaperone complex that is associated with the TIM22 carrier translocase of the inner membrane. This membrane-bound TIM hexamer consists of Tim9/Tim10/Tim12 (yeast) or Tim9/Tim10a/Tim10b (human) [67,81–86] (Figure 1). Carrier precursors bound to the membrane-associated TIM chaperones represent stage IIIb of the carrier import pathway where the precursor is tethered to the inner membrane, but not yet inserted (Table 1) [17,19]. Since this is

the last step that is independent of the membrane potential $\Delta\psi$, precursors accumulate in stage III upon dissipation of the membrane potential. The dependence of carrier import on TIM chaperones also allows to experimentally distinguish this import pathway into the inner membrane from the presequence pathway where import into a protease-protected environment depends on $\Delta\psi$ due to the coupling of TOM and TIM23 [65,66].

Unexpectedly, transport of carriers to the TIM22 carrier translocase is also aided by porin/voltage-dependent anion channel (VDAC), the major metabolite channel of the outer membrane (Figure 1) [87–90]. In addition to interacting with TIM chaperones as well as carrier precursors, porin recruits the TIM22 translocase and thereby brings the outer and inner membrane in close proximity, which may enhance carrier biogenesis [88,89]. Since porin, unlike the protein translocases, is significantly upregulated upon respiratory growth [91], this novel physiological role may support the higher levels of protein import required for metabolic remodeling of the mitochondria. While a contribution of VDACs to carrier biogenesis in human mitochondria has not been studied directly, they were found to interact with TIM22 [92,93].

4. Membrane Integration by the TIM22 Carrier Translocase

The TIM22 translocase consists of the Tim22 protein, several auxiliary subunits that have roles in assembly and stabilization of the complex, and TIM chaperones. In yeast, the additional subunits comprise Tim54, Sdh3, which also interacts with Sdh4 as part of the succinate dehydrogenase complex, and Tim18, a homolog of Sdh4 [12,17,19,20,94–100] (Figure 1A). Until recently, the only known membrane integral TIM22 component in humans was Tim22 itself, however, several studies have discovered two new subunits (Figure 1B). The metazoan-specific subunit Tim29, which like Tim54 is exposed to the IMS and can be crosslinked to TIM chaperones, is required for TIM22 assembly and efficient import of some substrates [92,101]. Moreover, Tim29 interacts with Tom40, indicating that there may be coupling between TOM and TIM22 in human cells [92], in contrast to yeast. The most recently identified subunit of human TIM22 is acylglycerol kinase (AGK) that phosphorylates glycerides to generate lysophosphatidic acid or phosphatidic acid [102–104]. AGK has a dual role in human mitochondria: It is required for TIM22 stability and carrier import independently of its lipid kinase activity, and loss of AGK results in TCA (tricarboxylic acid) cycle defects; however, kinase deficiency causes aberrant mitochondrial ultrastructure and concomitantly reduced respiration [103,104]. Mutations in AGK cause the mitochondrial disease Sengers syndrome [105,106], and its novel role as part of the TIM22 translocase appears to account for the disease phenotype [103]. Aside from AGK, mutations in Tim22 that impair carrier import were also recently reported to result in human pathology with neuromuscular defects [32,107]. Interestingly, human TIM22 interacts with the mitochondrial contact site and cristae organizing system (MICOS) [93], an inner membrane protein complex that is crucial for native cristae architecture and that forms contact sites between the two mitochondrial membranes [108–110]. Upon MICOS disruption, carrier import is specifically impaired, indicating that MICOS-mediated membrane contact sites might support efficient carrier biogenesis in human cells [93].

The TIM22 complex is a voltage-gated preprotein translocase that is thought to insert one helix—matrix loop—helix repeat at a time in a hairpin conformation into the inner membrane [19,20,86,97]. At least a low membrane potential is required for transfer of a precursor from the TIM chaperones to TIM22. Precursors can be trapped experimentally at this stage IV by reducing the membrane potential with ionophores (Table 1) [20]. In the presence of a higher membrane potential as well as of an internal targeting sequence, TIM22 integrates the protein into the inner membrane by an unknown mechanism involving lateral release, and the carrier reaches the mature stage V [20].

The modular topology of mitochondrial carriers of the MCF/SLC25 family—with repeats of helix-loop-helix domains, the termini facing the IMS and positively charged loops in the matrix—was long assumed to be a requirement for substrates of the TIM22 carrier pathway. This pathway also imports members of the Tim17 protein family that includes Tim22 itself as well as the TIM23

translocase components Tim23 and Tim17, all of which have four TM segments but otherwise share the topology of classical carriers [73,75–77,111–113] (Figure 2). As mentioned, both TOM and TIM22 translocases act on paired helices during import of classical carriers, including the dicarboxylate carrier, the ADP/ATP carrier and the phosphate carrier, as well as during import of Tim22-related proteins [21,70,77,114–116], in contrast to the linear import of other mitochondrial proteins. Until recently, multi-spanning inner membrane proteins apart from the MCF and Tim17 families were thought to be imported into mitochondria by the other translocases of the inner membrane: By the TIM23 translocase [11–13,65,66,117], by the oxidase assembly (OXA) translocase that is responsible for the membrane integration of mitochondrially encoded proteins [118,119] or by a combination of both machineries [120–122]. Moreover, truncated variants of carrier proteins are no longer recognized as substrates of the TIM22 pathway and instead are imported by TIM23 or remain in the intermembrane space [115,116]. However, recent work has identified the mitochondrial pyruvate carrier proteins with their divergent topology as substrates of the TIM22 pathway [31,32]. What is more, the unrelated sideroflexins also rely on the TIM22 carrier translocase for their biogenesis [38,39]. Of the MPC components, at least Mpc2 and Mpc3 have unpaired TM helices and none of the MPC proteins possess more than three TM segments [6,7,35–37], while the sideroflexins also have an uneven number of TM segments and yet another topology [8,39] (Figure 2). Thus, multiple recent studies have revealed a surprising versatility of the TIM22 pathway. The mechanistic differences in the handling of substrates with 4 or 6 TM segments (classical TIM22 substrates) versus 2/3 (MPC subunits) or 5 TM segments (sideroflexins) are still unclear. The C-terminal helix-loop-helix domain of Mpc2 and Mpc3 might conceivably be treated similarly as a typical carrier repeat, since they share the topology and positively charged matrix loop. In addition, MPC subunits were reported to have an N-terminal α -helix whose function is unknown [37]. For the human TIM22 translocase a differential requirement of the auxiliary subunits for different substrate classes has been reported: AGK is required for efficient carrier import and dispensable for the import of Tim22 and related proteins [103,104], whereas the opposite is the case for Tim29 [92]. Interestingly, sideroflexins, like classical carriers, rely on AGK, while Tim29 is dispensable [38]. It will be very interesting to learn how TIM22 adapts its function to import this range of structurally distinct substrates.

5. Perspectives

The biogenesis of mitochondrial metabolite carriers is still not fully understood despite the fact that the TIM22 import pathway has been under scientific investigation for decades. The recent discovery of two human TIM22 components and the very limited insight into the mechanism of membrane integration by the carrier translocase exemplify how much fundamental information is still lacking. Novel findings indicate that carrier import may benefit from contact sites between the outer and inner membranes after all. Moreover, the TIM22 pathway has turned out to be unexpectedly versatile regarding its substrate requirements. Finally, it seems likely that the biogenesis of proteins with such a central role in mitochondrial physiology is regulated at different steps. While there is precedent for this notion from yeast, the human TIM22 pathway still awaits characterization of regulatory factors. Thus, the biogenesis of mitochondrial metabolite carriers remains an exciting field of study that is expected to generate important insights into mitochondrial physiology.

Funding: This work was supported by the Excellence Initiative/Strategy of the German Federal and State Governments (EXC 2189 CIBSS Project ID 390939984).

Acknowledgments: We thank Nils Wiedemann and Nikolaus Pfanner for discussion and helpful suggestions. Work included in this study has been performed in partial fulfillment of the requirements for the doctoral thesis of P.H.

Conflicts of Interest: The authors declare no conflict of interest.

References

1. Palmieri, F.; Monné, M. Discoveries, metabolic roles and diseases of mitochondrial carriers: A review. *Biochim. Biophys. Acta* **2016**, *1863*, 2362–2378. [CrossRef] [PubMed]
2. Taylor, E.B. Functional Properties of the Mitochondrial Carrier System. *Trends Cell Biol.* **2017**, *27*, 633–644. [CrossRef] [PubMed]
3. Ogunbona, O.B.; Claypool, S.M. Emerging Roles in the Biogenesis of Cytochrome c Oxidase for Members of the Mitochondrial Carrier Family. *Front. Cell Dev. Biol.* **2019**, *7*, 3. [CrossRef]
4. Ruprecht, J.J.; Kunji, E.R.S. The SLC25 Mitochondrial Carrier Family: Structure and Mechanism. *Trends Biochem. Sci.* **2020**, *45*, 244–258. [CrossRef] [PubMed]
5. Palmieri, F.; Scarcia, P.; Monné, M. Diseases caused by mutations in mitochondrial carrier genes SLC25: A review. *Biomolecules* **2020**, *10*, 655. [CrossRef] [PubMed]
6. Bricker, D.K.; Taylor, E.B.; Schell, J.C.; Orsak, T.; Boutron, A.; Chen, Y.-C.; Cox, J.E.; Cardon, C.M.; Van Vranken, J.G.; Dephoure, N.; et al. A mitochondrial pyruvate carrier required for pyruvate uptake in yeast, *Drosophila*, and humans. *Science* **2012**, *337*, 96–100. [CrossRef] [PubMed]
7. Herzig, S.; Raemy, E.; Montessuit, S.; Veuthey, J.-L.; Zamboni, N.; Westermann, B.; Kunji, E.R.S.; Martinou, J.-C. Identification and functional expression of the mitochondrial pyruvate carrier. *Science* **2012**, *337*, 93–96. [CrossRef]
8. Kory, N.; Wyant, G.A.; Prakash, G.; Uit de Bos, J.; Bottanelli, F.; Pacold, M.E.; Chan, S.H.; Lewis, C.A.; Wang, T.; Keys, H.R.; et al. SFXN1 is a mitochondrial serine transporter required for one-carbon metabolism. *Science* **2018**, *362*, eaat9528. [CrossRef]
9. Azzi, A.; Glerum, M.; Koller, R.; Mertens, W.; Spycher, S. The mitochondrial tricarboxylate carrier. *J. Bioenerg. Biomembr.* **1993**, *25*, 515–524. [CrossRef]
10. Cunningham, C.N.; Rutter, J. 20,000 picometers under the OMM: Diving into the vastness of mitochondrial metabolite transport. *EMBO Rep.* **2020**, *21*, e50071. [CrossRef]
11. Neupert, W. A Perspective on Transport of Proteins into Mitochondria: A Myriad of Open Questions. *J. Mol. Biol.* **2015**, *427*, 1135–1158. [CrossRef]
12. Wiedemann, N.; Pfanner, N. Mitochondrial Machineries for Protein Import and Assembly. *Annu. Rev. Biochem.* **2017**, *86*, 685–714. [CrossRef]
13. Hansen, K.G.; Herrmann, J.M. Transport of Proteins into Mitochondria. *Protein J.* **2019**, *38*, 330–342. [CrossRef]
14. Becker, T.; Song, J.; Pfanner, N. Versatility of Preprotein Transfer from the Cytosol to Mitochondria. *Trends Cell Biol.* **2019**, *29*, 534–548. [CrossRef] [PubMed]
15. Zara, V.; Palmieri, F.; Mahlke, K.; Pfanner, N. The cleavable presequence is not essential for import and assembly of the phosphate carrier of mammalian mitochondria but enhances the specificity and efficiency of import. *J. Biol. Chem.* **1992**, *267*, 12077–12081. [PubMed]
16. Zara, V.; Dolce, V.; Capobianco, L.; Ferramosca, A.; Papatheodourou, P.; Rassow, J.; Palmieri, F. Biogenesis of eel liver citrate carrier (CIC): Negative charges can substitute for positive charges in the presequence. *J. Mol. Biol.* **2007**, *365*, 958–967. [CrossRef] [PubMed]
17. Ferramosca, A.; Zara, V. Biogenesis of mitochondrial carrier proteins: Molecular mechanisms of import into mitochondria. *Biochim. Biophys. Acta Mol. Cell Res.* **2013**, *1833*, 494–502. [CrossRef] [PubMed]
18. Ryan, M.T.; Müller, H.; Pfanner, N. Functional staging of ADP/ATP carrier translocation across the outer mitochondrial membrane. *J. Biol. Chem.* **1999**, *274*, 20619–20627. [CrossRef]
19. Rehling, P.; Brandner, K.; Pfanner, N. Mitochondrial import and the twin-pore translocase. *Nat. Rev. Mol. Cell Biol.* **2004**, *5*, 519–530. [CrossRef]
20. Rehling, P.; Model, K.; Brandner, K.; Kovermann, P.; Sickmann, A.; Meyer, H.E.; Kühlbrandt, W.; Wagner, R.; Truscott, K.N.; Pfanner, N. Protein insertion into the mitochondrial inner membrane by a twin-pore translocase. *Science* **2003**, *299*, 1747–1751. [CrossRef]
21. Wiedemann, N.; Pfanner, N.; Ryan, M.T. The three modules of ADP/ATP carrier cooperate in receptor recruitment and translocation into mitochondria. *EMBO J.* **2001**, *20*, 951–960. [CrossRef] [PubMed]
22. Klingenberg, M. The ADP and ATP transport in mitochondria and its carrier. *Biochim. Biophys. Acta Biomembr.* **2008**, *1778*, 1978–2021. [CrossRef]

23. Ruprecht, J.J.; King, M.S.; Zögg, T.; Aleksandrova, A.A.; Pardon, E.; Crichton, P.G.; Steyaert, J.; Kunji, E.R.S. The Molecular Mechanism of Transport by the Mitochondrial ADP/ATP Carrier. *Cell* **2019**, *176*, 435–447. [CrossRef] [PubMed]
24. Palmieri, F. Mitochondrial carrier proteins. *FEBS Lett.* **1994**, *346*, 48–54. [CrossRef]
25. Klingenberg, M. The ADP, ATP shuttle of the mitochondrion. *Trends Biochem. Sci.* **1979**, *4*, 249–252. [CrossRef]
26. Indiveri, C.; Tonazzi, A.; Palmieri, F. The reconstituted carnitine carrier from rat liver mitochondria: Evidence for a transport mechanism different from that of the other mitochondrial translocators. *Biochim. Biophys. Acta* **1994**, *1189*, 65–73. [CrossRef]
27. Monné, M.; Palmieri, F. Antiporters of the Mitochondrial Carrier Family. *Curr. Top. Membr.* **2014**, *73*, 289–320.
28. Ruprecht, J.J.; Kunji, E.R.S. Structural changes in the transport cycle of the mitochondrial ADP/ATP carrier. *Curr. Opin. Struct. Biol.* **2019**, *57*, 135–144. [CrossRef]
29. Coonrod, E.M.; Karren, M.A.; Shaw, J.M. Ugo1p is a multipass transmembrane protein with a single carrier domain required for mitochondrial fusion. *Traffic* **2007**, *8*, 500–511. [CrossRef]
30. Hoppins, S.C.; Horner, J.; Song, C.; McCaffery, J.M.; Nunnari, J. Mitochondrial outer and inner membrane fusion requires a modified carrier protein. *J. Cell Biol.* **2009**, *184*, 569–581. [CrossRef]
31. Rampelt, H.; Sucec, I.; Bersch, B.; Horten, P.; Perschil, I.; Martinou, J.-C.; van der Laan, M.; Wiedemann, N.; Schanda, P.; Pfanner, N. The mitochondrial carrier pathway transports non-canonical substrates with an odd number of transmembrane segments. *BMC Biol.* **2020**, *18*, 2. [CrossRef]
32. Gomkale, R.; Cruz-Zaragoza, L.D.; Suppanz, I.; Guiard, B.; Montoya, J.; Callegari, S.; Pacheu-Grau, D.; Warscheid, B.; Rehling, P. Defining the Substrate Spectrum of the TIM22 Complex Identifies Pyruvate Carrier Subunits as Unconventional Cargos. *Curr. Biol.* **2020**, *30*, 1119–1127. [CrossRef] [PubMed]
33. Xu, Y.; Tao, Y.; Cheung, L.S.; Fan, C.; Chen, L.-Q.; Xu, S.; Perry, K.; Frommer, W.B.; Feng, L. Structures of bacterial homologues of SWEET transporters in two distinct conformations. *Nature* **2014**, *515*, 448–452. [CrossRef] [PubMed]
34. Feng, L.; Frommer, W.B. Structure and function of SemiSWEET and SWEET sugar transporters. *Trends Biochem. Sci.* **2015**, *40*, 480–486. [CrossRef]
35. Bender, T.; Pena, G.; Martinou, J.-C. Regulation of mitochondrial pyruvate uptake by alternative pyruvate carrier complexes. *EMBO J.* **2015**, *34*, 911–924. [CrossRef] [PubMed]
36. Vanderperre, B.; Cermakova, K.; Escoffier, J.; Kaba, M.; Bender, T.; Nef, S.; Martinou, J.-C. MPC1-like Is a Placental Mammal-specific Mitochondrial Pyruvate Carrier Subunit Expressed in Postmeiotic Male Germ Cells. *J. Biol. Chem.* **2016**, *291*, 16448–16461. [CrossRef]
37. Tavoulari, S.; Thangaratnarajah, C.; Mavridou, V.; Harbour, M.E.; Martinou, J.-C.; Kunji, E.R.S. The yeast mitochondrial pyruvate carrier is a hetero-dimer in its functional state. *EMBO J.* **2019**, *38*, e100785. [CrossRef]
38. Jackson, T.D.; Hock, D.; Palmer, C.S.; Kang, Y.; Fujihara, K.M.; Clemons, N.J.; Thorburn, D.R.; Stroud, D.; Stojanovski, D. The TIM22 complex regulates mitochondrial one-carbon metabolism by mediating the import of sideroflexins. *bioRxiv* **2020**. [CrossRef]
39. Acoba, M.G.; Alpergin, E.S.S.; Renuse, S.; Fernández-del-Río, L.; Lu, Y.-W.; Clarke, C.F.; Pandey, A.; Wolfgang, M.J.; Claypool, S.M. The mitochondrial carrier SFXN1 is critical for complex III integrity and cellular metabolism. *bioRxiv* **2020**. [CrossRef]
40. Endo, T.; Yamano, K. Transport of proteins across or into the mitochondrial outer membrane. *Biochim. Biophys. Acta* **2010**, *1803*, 706–714. [CrossRef]
41. Kang, Y.; Fielden, L.F.; Stojanovski, D. Mitochondrial protein transport in health and disease. *Semin. Cell Dev. Biol.* **2018**, *76*, 142–153. [CrossRef] [PubMed]
42. Shiota, T.; Imai, K.; Qiu, J.; Hewitt, V.L.; Tan, K.; Shen, H.-H.; Sakiyama, N.; Fukasawa, Y.; Hayat, S.; Kamiya, M.; et al. Molecular architecture of the active mitochondrial protein gate. *Science* **2015**, *349*, 1544–1548. [CrossRef] [PubMed]
43. Bausewein, T.; Mills, D.J.; Langer, J.D.; Nitschke, B.; Nussberger, S.; Kühlbrandt, W. Cryo-EM Structure of the TOM Core Complex from *Neurospora crassa*. *Cell* **2017**, *170*, 693–700. [CrossRef] [PubMed]
44. Araiso, Y.; Tsutsumi, A.; Qiu, J.; Imai, K.; Shiota, T.; Song, J.; Lindau, C.; Wenz, L.-S.; Sakaue, H.; Yunoki, K.; et al. Structure of the mitochondrial import gate reveals distinct preprotein paths. *Nature* **2019**, *575*, 395–401. [CrossRef]

45. Komiya, T.; Rospert, S.; Schatz, G.; Mihara, K. Binding of mitochondrial precursor proteins to the cytoplasmic domains of the import receptors Tom70 and Tom20 is determined by cytoplasmic chaperones. *EMBO J.* **1997**, *16*, 4267–4275. [CrossRef]
46. Young, J.C.; Hoogenraad, N.J.; Hartl, F.U. Molecular chaperones Hsp90 and Hsp70 deliver preproteins to the mitochondrial import receptor Tom70. *Cell* **2003**, *112*, 41–50. [CrossRef]
47. Bhangoo, M.K.; Tzankov, S.; Fan, A.C.Y.; Dejgaard, K.; Thomas, D.Y.; Young, J.C. Multiple 40-kDa heat-shock protein chaperones function in Tom70-dependent mitochondrial import. *Mol. Biol. Cell* **2007**, *18*, 3414–3428. [CrossRef]
48. Opaliński, Ł.; Song, J.; Priesnitz, C.; Wenz, L.-S.; Oeljeklaus, S.; Warscheid, B.; Pfanner, N.; Becker, T. Recruitment of Cytosolic J-Proteins by TOM Receptors Promotes Mitochondrial Protein Biogenesis. *Cell Rep.* **2018**, *25*, 2036–2043.e5.
49. Avendaño-Monsalve, M.C.; Ponce-Rojas, J.C.; Funes, S. From cytosol to mitochondria: The beginning of a protein journey. *Biol. Chem.* **2020**, *401*, 645–661. [CrossRef] [PubMed]
50. Hines, V.; Brandt, A.; Griffiths, G.; Horstmann, H.; Brüttsch, H.; Schatz, G. Protein import into yeast mitochondria is accelerated by the outer membrane protein MAS70. *EMBO J.* **1990**, *9*, 3191–3200. [CrossRef] [PubMed]
51. Söllner, T.; Pfaller, R.; Griffiths, G.; Pfanner, N.; Neupert, W. A mitochondrial import receptor for the ADP/ATP carrier. *Cell* **1990**, *62*, 107–115. [CrossRef]
52. Steger, H.F.; Söllner, T.; Kiebler, M.; Dietmeier, K.A.; Pfaller, R.; Trülzsch, K.S.; Tropschug, M.; Neupert, W.; Pfanner, N. Import of ADP/ATP carrier into mitochondria: Two receptors act in parallel. *J. Cell Biol.* **1990**, *111*, 2353–2363. [CrossRef] [PubMed]
53. Brix, J.; Dietmeier, K.; Pfanner, N. Differential recognition of preproteins by the purified cytosolic domains of the mitochondrial import receptors Tom20, Tom22, and Tom70. *J. Biol. Chem.* **1997**, *272*, 20730–20735. [CrossRef] [PubMed]
54. Brix, J.; Rüdiger, S.; Bukau, B.; Schneider-Mergener, J.; Pfanner, N. Distribution of binding sequences for the mitochondrial import receptors Tom20, Tom22, and Tom70 in a presequence-carrying preprotein and a non-cleavable preprotein. *J. Biol. Chem.* **1999**, *274*, 16522–16530. [CrossRef] [PubMed]
55. Abe, Y.; Shodai, T.; Muto, T.; Mihara, K.; Torii, H.; Nishikawa, S.; Endo, T.; Kohda, D. Structural basis of presequence recognition by the mitochondrial protein import receptor Tom20. *Cell* **2000**, *100*, 551–560. [CrossRef]
56. Saitoh, T.; Igura, M.; Obita, T.; Ose, T.; Kojima, R.; Maenaka, K.; Endo, T.; Kohda, D. Tom20 recognizes mitochondrial presequences through dynamic equilibrium among multiple bound states. *EMBO J.* **2007**, *26*, 4777–4787. [CrossRef]
57. Yamano, K.; Yatsukawa, Y.-I.; Esaki, M.; Hobbs, A.E.A.; Jensen, R.E.; Endo, T. Tom20 and Tom22 share the common signal recognition pathway in mitochondrial protein import. *J. Biol. Chem.* **2008**, *283*, 3799–3807. [CrossRef]
58. Yamamoto, H.; Fukui, K.; Takahashi, H.; Kitamura, S.; Shiota, T.; Terao, K.; Uchida, M.; Esaki, M.; Nishikawa, S.I.; Yoshihisa, T.; et al. Roles of Tom70 in import of presequence-containing mitochondrial proteins. *J. Biol. Chem.* **2009**, *284*, 31635–31646. [CrossRef]
59. Yamamoto, H.; Itoh, N.; Kawano, S.; Yatsukawa, Y.I.; Momose, T.; Makio, T.; Matsunaga, M.; Yokota, M.; Esaki, M.; Shodai, T.; et al. Dual role of the receptor Tom20 in specificity and efficiency of protein import into mitochondria. *Proc. Natl. Acad. Sci. USA* **2011**, *108*, 91–96. [CrossRef]
60. Backes, S.; Hess, S.; Boos, F.; Woellhaf, M.W.; Gödel, S.; Jung, M.; Mühlhaus, T.; Herrmann, J.M. Tom70 enhances mitochondrial preprotein import efficiency by binding to internal targeting sequences. *J. Cell Biol.* **2018**, *217*, 1369–1382. [CrossRef]
61. Balchin, D.; Hayer-Hartl, M.; Hartl, F.U. In vivo aspects of protein folding and quality control. *Science* **2016**, *353*, aac4354. [CrossRef] [PubMed]
62. van Wilpe, S.; Ryan, M.T.; Hill, K.; Maarse, A.C.; Meisinger, C.; Brix, J.; Dekker, P.J.; Moczko, M.; Wagner, R.; Meijer, M.; et al. Tom22 is a multifunctional organizer of the mitochondrial preprotein translocase. *Nature* **1999**, *401*, 485–489. [CrossRef] [PubMed]
63. Tucker, K.; Park, E. Cryo-EM structure of the mitochondrial protein-import channel TOM complex at near-atomic resolution. *Nat. Struct. Mol. Biol.* **2019**, *26*, 1158–1166. [CrossRef]

64. Schmidt, O.; Harbauer, A.B.; Rao, S.; Eyrich, B.; Zahedi, R.P.; Stojanovski, D.; Schönfisch, B.; Guiard, B.; Sickmann, A.; Pfanner, N.; et al. Regulation of Mitochondrial Protein Import by Cytosolic Kinases. *Cell* **2011**, *144*, 227–239. [CrossRef] [PubMed]
65. Moulin, C.; Caumont-Sarcos, A.; Ieva, R. Mitochondrial presequence import: Multiple regulatory knobs fine-tune mitochondrial biogenesis and homeostasis. *Biochim. Biophys. Acta Mol. Cell. Res.* **2019**, *1866*, 930–944. [CrossRef] [PubMed]
66. Callegari, S.; Cruz-Zaragoza, L.D.; Rehling, P. From TOM to the TIM23 complex – handing over of a precursor. *Biol. Chem.* **2020**. [CrossRef] [PubMed]
67. Sirrenberg, C.; Endres, M.; Fölsch, H.; Stuart, R.A.; Neupert, W.; Brunner, M. Carrier protein import into mitochondria mediated by the intermembrane proteins Tim10/Mrs11 and Tim12/Mrs5. *Nature* **1998**, *391*, 912–915. [CrossRef]
68. Koehler, C.M.; Jarosch, E.; Tokatlidis, K.; Schmid, K.; Schweyen, R.J.; Schatz, G. Import of mitochondrial carriers mediated by essential proteins of the intermembrane space. *Science* **1998**, *279*, 369–373. [CrossRef]
69. Koehler, C.M.; Merchant, S.; Oppliger, W.; Schmid, K.; Jarosch, E.; Dolfini, L.; Junne, T.; Schatz, G.; Tokatlidis, K. Tim9p, an essential partner subunit of Tim10p for the import of mitochondrial carrier proteins. *EMBO J.* **1998**, *17*, 6477–6486. [CrossRef]
70. Endres, M.; Neupert, W.; Brunner, M. Transport of the ADP/ATP carrier of mitochondria from the TOM complex to the TIM22.54 complex. *EMBO J.* **1999**, *18*, 3214–3221. [CrossRef]
71. Truscott, K.N.; Wiedemann, N.; Rehling, P.; Müller, H.; Meisinger, C.; Pfanner, N.; Guiard, B. Mitochondrial Import of the ADP/ATP Carrier: The Essential TIM Complex of the Intermembrane Space Is Required for Precursor Release from the TOM Complex. *Mol. Cell. Biol.* **2002**, *22*, 7780–7789. [CrossRef] [PubMed]
72. Curran, S.P.; Leuenberger, D.; Oppliger, W.; Koehler, C.M. The Tim9p-Tim10p complex binds to the transmembrane domains of the ADP/ATP carrier. *EMBO J.* **2002**, *21*, 942–953. [CrossRef] [PubMed]
73. Weinhäupl, K.; Lindau, C.; Hessel, A.; Wang, Y.; Schütze, C.; Jores, T.; Melchionda, L.; Schönfisch, B.; Kalbacher, H.; Bersch, B.; et al. Structural Basis of Membrane Protein Chaperoning through the Mitochondrial Intermembrane Space. *Cell* **2018**, *175*, 1365–1379.e25.
74. Webb, C.T.; Gorman, M.A.; Lazarou, M.; Ryan, M.T.; Gulbis, J.M. Crystal Structure of the Mitochondrial Chaperone TIM9•10 Reveals a Six-Bladed α -Propeller. *Mol. Cell* **2006**, *21*, 123–133. [CrossRef]
75. Beverly, K.N.; Sawaya, M.R.; Schmid, E.; Koehler, C.M. The Tim8–Tim13 Complex Has Multiple Substrate Binding Sites and Binds Cooperatively to Tim23. *J. Mol. Biol.* **2008**, *382*, 1144–1156. [CrossRef]
76. Paschen, S.A.; Rothbauer, U.; Káldi, K.; Bauer, M.F.; Neupert, W.; Brunner, M. The role of the TIM8-13 complex in the import of Tim23 into mitochondria. *EMBO J.* **2000**, *19*, 6392–6400. [CrossRef]
77. Curran, S.P.; Leuenberger, D.; Schmidt, E.; Koehler, C.M. The role of the Tim8p–Tim13p complex in a conserved import pathway for mitochondrial polytopic inner membrane proteins. *J. Cell Biol.* **2002**, *158*, 1017–1027. [CrossRef]
78. Davis, A.J.; Alder, N.N.; Jensen, R.E.; Johnson, A.E. The Tim9p/10p and Tim8p/13p complexes bind to specific sites on Tim23p during mitochondrial protein import. *Mol. Biol. Cell* **2007**, *18*, 475–486. [CrossRef]
79. Kang, Y.; Anderson, A.J.; Jackson, T.D.; Palmer, C.S.; De Souza, D.P.; Fujihara, K.M.; Stait, T.; Frazier, A.E.; Clemons, N.J.; Tull, D.; et al. Function of hTim8a in complex IV assembly in neuronal cells provides insight into pathomechanism underlying Mohr-Tranebjærg syndrome. *eLife* **2019**, *8*, e48828. [CrossRef]
80. Koehler, C.M.; Leuenberger, D.; Merchant, S.; Renold, A.; Junne, T.; Schatz, G. Human deafness dystonia syndrome is a mitochondrial disease. *Proc. Natl. Acad. Sci. USA* **1999**, *96*, 2141–2146. [CrossRef]
81. Adam, A.; Endres, M.; Sirrenberg, C.; Lottspeich, F.; Neupert, W.; Brunner, M. Tim9, a new component of the TIM22.54 translocase in mitochondria. *EMBO J.* **1999**, *18*, 313–319. [CrossRef] [PubMed]
82. Mühlenbein, N.; Hofmann, S.; Rothbauer, U.; Bauer, M.F. Organization and Function of the Small Tim Complexes Acting along the Import Pathway of Metabolite Carriers into Mammalian Mitochondria. *J. Biol. Chem.* **2004**, *279*, 13540–13546. [CrossRef] [PubMed]
83. Gebert, N.; Chacinska, A.; Wagner, K.; Guiard, B.; Koehler, C.M.; Rehling, P.; Pfanner, N.; Wiedemann, N. Assembly of the three small Tim proteins precedes docking to the mitochondrial carrier translocase. *EMBO Rep.* **2008**, *9*, 548–554. [CrossRef] [PubMed]
84. Lionaki, E.; de Marcos Lousa, C.; Baud, C.; Vougioukalaki, M.; Panayotou, G.; Tokatlidis, K. The essential function of Tim12 in vivo is ensured by the assembly interactions of its C-terminal domain. *J. Biol. Chem.* **2008**, *283*, 15747–15753. [CrossRef] [PubMed]





85. Weinhäupl, K.; Wang, Y.; Hessel, A.; Brennich, M.; Lindorff-Larsen, K.; Schanda, P. Architecture and subunit dynamics of the mitochondrial TIM9-10-12 chaperone. *bioRxiv* **2020**. [CrossRef]
86. Qi, L.; Wang, Q.; Guan, Z.; Wu, Y.; Cao, J.; Zhang, X.; Yan, C.; Yin, P. Cryo-EM structure of the human mitochondrial translocase TIM22 complex. *bioRxiv* **2019**. [CrossRef]
87. Mertins, B.; Psakis, G.; Essen, L.-O. Voltage-dependent anion channels: The wizard of the mitochondrial outer membrane. *Biol. Chem.* **2014**, *395*, 1435–1442. [CrossRef]
88. Ellenrieder, L.; Dieterle, M.P.; Doan, K.N.; Mårtensson, C.U.; Floerchinger, A.; Campo, M.L.; Pfanner, N.; Becker, T. Dual Role of Mitochondrial Porin in Metabolite Transport across the Outer Membrane and Protein Transfer to the Inner Membrane. *Mol. Cell* **2019**, *73*, 1056–1065.e7. [CrossRef]
89. Grevel, A.; Becker, T. Porins as helpers in mitochondrial protein translocation. *Biol. Chem.* **2020**, *401*, 699–708. [CrossRef]
90. Becker, T.; Wagner, R. Mitochondrial Outer Membrane Channels: Emerging Diversity in Transport Processes. *Bioessays* **2018**, *40*, e1800013. [CrossRef]
91. Morgenstern, M.; Stiller, S.B.; Lübbert, P.; Peikert, C.D.; Dannenmaier, S.; Drepper, F.; Weill, U.; Höß, P.; Feuerstein, R.; Gebert, M.; et al. Definition of a High-Confidence Mitochondrial Proteome at Quantitative Scale. *Cell Rep.* **2017**, *19*, 2836–2852. [CrossRef] [PubMed]
92. Kang, Y.; Baker, M.J.; Liem, M.; Loubser, J.; McKenzie, M.; Atukorala, I.; Ang, C.-S.; Keerthikumar, S.; Mathivanan, S.; Stojanovski, D. Tim29 is a novel subunit of the human TIM22 translocase and is involved in complex assembly and stability. *eLife* **2016**, *5*, e17463. [CrossRef]
93. Callegari, S.; Müller, T.; Schulz, C.; Lenz, C.; Jans, D.C.; Wissel, M.; Opazo, F.; Rizzoli, S.O.; Jakobs, S.; Urlaub, H.; et al. MICOS-TIM22 Association Promotes Carrier Import into Human Mitochondria. *J. Mol. Biol.* **2019**, *431*, 2835–2851. [CrossRef] [PubMed]
94. Sirrenberg, C.; Bauer, M.F.; Guiard, B.; Neupert, W.; Brunner, M. Import of carrier proteins into the mitochondrial inner membrane mediated by Tim22. *Nature* **1996**, *384*, 582–585. [CrossRef] [PubMed]
95. Koehler, C.M.; Murphy, M.P.; Bally, N.A.; Leuenberger, D.; Oppliger, W.; Dolfini, L.; Junne, T.; Schatz, G.; Or, E. Tim18p, a new subunit of the TIM22 complex that mediates insertion of imported proteins into the yeast mitochondrial inner membrane. *Mol. Cell. Biol.* **2000**, *20*, 1187–1193. [CrossRef] [PubMed]
96. Kerscher, O.; Sepuri, N.B.; Jensen, R.E. Tim18p is a new component of the Tim54p-Tim22p translocon in the mitochondrial inner membrane. *Mol. Biol. Cell* **2000**, *11*, 103–116. [CrossRef] [PubMed]
97. Kovermann, P.; Truscott, K.N.; Guiard, B.; Rehling, P.; Sepuri, N.B.; Müller, H.; Jensen, R.E.; Wagner, R.; Pfanner, N. Tim22, the essential core of the mitochondrial protein insertion complex, forms a voltage-activated and signal-gated channel. *Mol. Cell* **2002**, *9*, 363–373. [CrossRef]
98. Hwang, D.K.; Claypool, S.M.; Leuenberger, D.; Tienson, H.L.; Koehler, C.M. Tim54p connects inner membrane assembly and proteolytic pathways in the mitochondrion. *J. Cell Biol.* **2007**, *178*, 1161–1175. [CrossRef]
99. Wagner, K.; Gebert, N.; Guiard, B.; Brandner, K.; Truscott, K.N.; Wiedemann, N.; Pfanner, N.; Rehling, P. The Assembly Pathway of the Mitochondrial Carrier Translocase Involves Four Preprotein Translocases. *Mol. Cell. Biol.* **2008**, *28*, 4251–4260. [CrossRef]
100. Gebert, N.; Gebert, M.; Oeljeklaus, S.; von der Malsburg, K.; Stroud, D.A.; Kulawiak, B.; Wirth, C.; Zahedi, R.P.; Dolezal, P.; Wiese, S.; et al. Dual Function of Sdh3 in the Respiratory Chain and TIM22 Protein Translocase of the Mitochondrial Inner Membrane. *Mol. Cell* **2011**, *44*, 811–818. [CrossRef]
101. Callegari, S.; Richter, F.; Chojnacka, K.; Jans, D.C.; Lorenzi, I.; Pacheu-Grau, D.; Jakobs, S.; Lenz, C.; Urlaub, H.; Dudek, J.; et al. TIM29 is a subunit of the human carrier translocase required for protein transport. *FEBS Lett.* **2016**, *590*, 4147–4158. [CrossRef] [PubMed]
102. Bektas, M.; Payne, S.G.; Liu, H.; Goparaju, S.; Milstien, S.; Spiegel, S. A novel acylglycerol kinase that produces lysophosphatidic acid modulates cross talk with EGFR in prostate cancer cells. *J. Cell Biol.* **2005**, *169*, 801–811. [CrossRef] [PubMed]
103. Kang, Y.; Stroud, D.A.; Baker, M.J.; De Souza, D.P.; Frazier, A.E.; Liem, M.; Tull, D.; Mathivanan, S.; McConville, M.J.; Thorburn, D.R.; et al. Sengers Syndrome-Associated Mitochondrial Acylglycerol Kinase Is a Subunit of the Human TIM22 Protein Import Complex. *Mol. Cell* **2017**, *67*, 457–470.e5. [CrossRef] [PubMed]
104. Vukotic, M.; Nolte, H.; König, T.; Saita, S.; Ananjew, M.; Krüger, M.; Tatsuta, T.; Langer, T. Acylglycerol Kinase Mutated in Sengers Syndrome Is a Subunit of the TIM22 Protein Translocase in Mitochondria. *Mol. Cell* **2017**, *67*, 471–483.e7. [CrossRef] [PubMed]

105. Mayr, J.A.; Haack, T.B.; Graf, E.; Zimmermann, F.A.; Wieland, T.; Haberberger, B.; Superti-Furga, A.; Kirschner, J.; Steinmann, B.; Baumgartner, M.R.; et al. Lack of the mitochondrial protein acylglycerol kinase causes Sengers syndrome. *Am. J. Hum. Genet.* **2012**, *90*, 314–320. [CrossRef] [PubMed]
106. Haghghi, A.; Haack, T.B.; Atiq, M.; Mottaghi, H.; Haghghi-Kakhki, H.; Bashir, R.A.; Ahting, U.; Feichtinger, R.G.; Mayr, J.A.; Rötig, A.; et al. Sengers syndrome: Six novel AGK mutations in seven new families and review of the phenotypic and mutational spectrum of 29 patients. *Orphanet J. Rare Dis.* **2014**, *9*, 119. [CrossRef]
107. Pacheu-Grau, D.; Callegari, S.; Emperador, S.; Thompson, K.; Aich, A.; Topol, S.E.; Spencer, E.G.; McFarland, R.; Ruiz-Pesini, E.; Torkamani, A.; et al. Mutations of the mitochondrial carrier translocase channel subunit TIM22 cause early-onset mitochondrial myopathy. *Hum. Mol. Genet.* **2018**, *27*, 4125–4144. [CrossRef]
108. Rampelt, H.; Zerbes, R.M.; van der Laan, M.; Pfanner, N. Role of the mitochondrial contact site and cristae organizing system in membrane architecture and dynamics. *Biochim. Biophys. Acta* **2017**, *1864*, 737–746. [CrossRef]
109. Wollweber, F.; von der Malsburg, K.; van der Laan, M. Mitochondrial contact site and cristae organizing system: A central player in membrane shaping and crosstalk. *Biochim. Biophys. Acta* **2017**, *1864*, 1481–1489.
110. Kozjak-Pavlovic, V. The MICOS complex of human mitochondria. *Cell Tissue Res.* **2017**, *367*, 83–93. [CrossRef]
111. Káldi, K.; Bauer, M.F.; Sirrenberg, C.; Neupert, W.; Brunner, M. Biogenesis of Tim23 and Tim17, integral components of the TIM machinery for matrix-targeted preproteins. *EMBO J.* **1998**, *17*, 1569–1576. [CrossRef]
112. Davis, A.J.; Ryan, K.R.; Jensen, R.E. Tim23p contains separate and distinct signals for targeting to mitochondria and insertion into the inner membrane. *Mol. Biol. Cell* **1998**, *9*, 2577–2593. [CrossRef] [PubMed]
113. Žárský, V.; Doležal, P. Evolution of the Tim17 protein family. *Biol. Direct* **2016**, *11*, 54. [CrossRef] [PubMed]
114. Brandner, K.; Rehling, P.; Truscott, K.N. The carboxyl-terminal third of the dicarboxylate carrier is crucial for productive association with the inner membrane twin-pore translocase. *J. Biol. Chem.* **2005**, *280*, 6215–6221. [CrossRef]
115. Vergnolle, M.A.S.; Sawney, H.; Junne, T.; Dolfini, L.; Tokatlidis, K. A cryptic matrix targeting signal of the yeast ADP/ATP carrier normally inserted by the TIM22 complex is recognized by the TIM23 machinery. *Biochem. J.* **2005**, *385*, 173–180. [CrossRef] [PubMed]
116. Yamano, K.; Ishikawa, D.; Esaki, M.; Endo, T. The phosphate carrier has an ability to be sorted to either the TIM22 pathway or the TIM23 pathway for its import into yeast mitochondria. *J. Biol. Chem.* **2005**, *280*, 10011–10017. [CrossRef]
117. Reinhold, R.; Kruger, V.; Meinecke, M.; Schulz, C.; Schmidt, B.; Grunau, S.D.; Guiard, B.; Wiedemann, N.; van der Laan, M.; Wagner, R.; et al. The Channel-Forming Sym1 Protein Is Transported by the TIM23 Complex in a Presequence-Independent Manner. *Mol. Cell. Biol.* **2012**, *32*, 5009–5021. [CrossRef] [PubMed]
118. Hell, K.; Neupert, W.; Stuart, R.A. Oxa1p acts as a general membrane insertion machinery for proteins encoded by mitochondrial DNA. *EMBO J.* **2001**, *20*, 1281–1288. [CrossRef]
119. Bonnefoy, N.; Fiumera, H.L.; Dujardin, G.; Fox, T.D. Roles of Oxa1-related inner-membrane translocases in assembly of respiratory chain complexes. *Biochim. Biophys. Acta* **2009**, *1793*, 60–70. [CrossRef]
120. Bohnert, M.; Rehling, P.; Guiard, B.; Herrmann, J.M.; Pfanner, N.; van der Laan, M. Cooperation of Stop-Transfer and Conservative Sorting Mechanisms in Mitochondrial Protein Transport. *Curr. Biol.* **2010**, *20*, 1227–1232. [CrossRef]
121. Stiller, S.B.; Höpker, J.; Oeljeklaus, S.; Schütze, C.; Schrempp, S.G.; Vent-Schmidt, J.; Horvath, S.E.; Frazier, A.E.; Gebert, N.; van der Laan, M.; et al. Mitochondrial OXA Translocase Plays a Major Role in Biogenesis of Inner-Membrane Proteins. *Cell Metab.* **2016**, *23*, 901–908. [CrossRef]
122. Park, K.; Botelho, S.C.; Hong, J.; Osterberg, M.; Kim, H. Dissecting Stop Transfer versus Conservative Sorting Pathways for Mitochondrial Inner Membrane Proteins in Vivo. *J. Biol. Chem.* **2013**, *288*, 1521–1532. [CrossRef] [PubMed]



Review

Physiopathology of the Permeability Transition Pore: Molecular Mechanisms in Human Pathology

Massimo Bonora ^{1,*}, Simone Patergnani ¹, Daniela Ramaccini ¹, Giampaolo Morciano ^{1,2}, Gaia Pedriali ^{1,2}, Asrat Endrias Kahsay ¹, Esmā Bouhamida ¹, Carlotta Giorgi ¹, Mariusz R. Wieckowski ^{3,†} and Paolo Pinton ^{1,2,*,†}

¹ Department of Medical Sciences, Laboratory for Technologies of Advanced Therapies (LTTA), University of Ferrara, 44121 Ferrara, Italy; simone.patergnani@unife.it (S.P.); rmcdnl@unife.it (D.R.); mrcgpl@unife.it (G.M.); pdrgai@unife.it (G.P.); asratendrias.kahsay@unife.it (A.E.K.); bhmsme@unife.it (E.B.); grgclt@unife.it (C.G.)

² Maria Cecilia Hospital, GVM Care & Research, Via Corriera 1, Cotignola, 48033 Ravenna, Italy

³ Laboratory of Mitochondrial Biology and Metabolism, Nencki Institute of Experimental Biology of the Polish Academy of Sciences, 3 Pasteur Str., 02-093 Warsaw, Poland; m.wieckowski@nencki.edu.pl

* Correspondence: bnmsm1@unife.it (M.B.); pnp@unife.it (P.P.)

† These authors share senior authorship.

Received: 9 June 2020; Accepted: 2 July 2020; Published: 4 July 2020

Abstract: Mitochondrial permeability transition (MPT) is the sudden loss in the permeability of the inner mitochondrial membrane (IMM) to low-molecular-weight solutes. Due to osmotic forces, MPT is paralleled by a massive influx of water into the mitochondrial matrix, eventually leading to the structural collapse of the organelle. Thus, MPT can initiate outer-mitochondrial-membrane permeabilization (MOMP), promoting the activation of the apoptotic caspase cascade and caspase-independent cell-death mechanisms. The induction of MPT is mostly dependent on mitochondrial reactive oxygen species (ROS) and Ca^{2+} , but is also dependent on the metabolic stage of the affected cell and signaling events. Therefore, since its discovery in the late 1970s, the role of MPT in human pathology has been heavily investigated. Here, we summarize the most significant findings corroborating a role for MPT in the etiology of a spectrum of human diseases, including diseases characterized by acute or chronic loss of adult cells and those characterized by neoplastic initiation.

Keywords: mitochondrial permeability transition; apoptosis; necrosis; ischemia/reperfusion; cancer; neurodegeneration; cyclosporin A

1. Introduction

Mitochondrial permeability transition (MPT) remains one of the most unusual and poorly characterized aspects of mitochondrial biology. This phenomenon was first reported in the late 1970s and was originally considered an artefact due to the experimental conditions required to investigate isolated mitochondria. However, (as better described below) MPT is triggered by the accumulation of Ca^{2+} in the mitochondrial matrix that occurs in isolated mitochondria exposed to a $[\text{Ca}^{2+}]$ significantly higher than that in the cytoplasm. The development of techniques to measure Ca^{2+} within different compartments later demonstrated that mitochondria can actively uptake Ca^{2+} even in living cells, prompting the investigation of MPT in cell pathophysiology.

1.1. Mitochondrial Routes of Cell Death

Mitochondria actively participate in multiple forms of regulated cell death (RCD) through different routes, all involving major alterations in the outer mitochondrial membrane (OMM) and/or

inner mitochondrial membrane (IMM). Activation of the mitochondrial pathway of RCA causes the redistribution of mitochondrial proteins into the cytoplasm, which activates cell-death effectors, or the dramatic impairment of cell bioenergetics, which ultimately leads to death of the affected cells. These mechanisms are, in general, categorized into two types that function under different conditions: those involving only outer-mitochondrial-membrane permeabilization (MOMP) and those in which there is also a long-lasting increase in IMM permeability, the MPT. MOMP is due to the formation of a pore composed of the protein B-cell lymphoma (Bcl-2) protein family members Bax and Bak. In response to some apoptotic signals, Bax re-localizes from the cytosol into distinct foci on the OMM. There, Bax oligomerizes into specific structures, such as rings and arc-shaped structures, which can create large-conductance pores in the OMM [1–3]. Similarly, Bak (which is mostly constitutively located in the OMM) can homo-oligomerize (Figure 1).

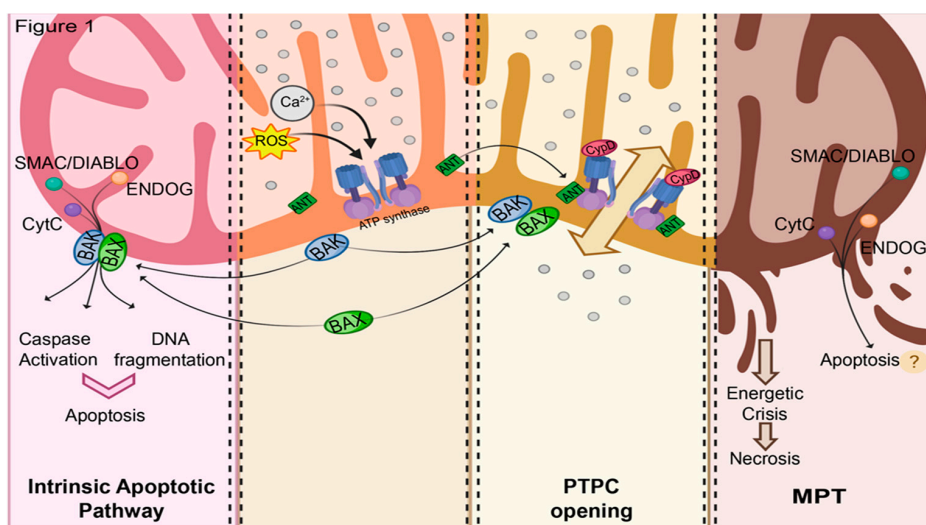


Figure 1. Major molecular paths in mitochondria-related regulated cell death (RCD). Mitochondrial calcium overload and ROS levels can trigger either the activation of intrinsic apoptotic pathway (left side) through the recruitment of Bcl-2 family proteins at the mitochondria, or permeability transition pore complex (PTPC) formation which could lead to mitochondrial outer membrane permeabilization (MOMP), energetic imbalance, and subsequent release of proapoptotic cofactors from the inter membrane space, such as SMAC/DIABLO, CytC, and ENDOG (right side).

Because of the permeabilization of the OMM, many proteins normally localized within the intermembrane space (IMS) are simultaneously released into the cytosol; these proteins are involved in the effector phase of apoptosis. In particular, (i) cytochrome *c* (CytC) mediates the organization of the apoptosome and then the activation of the caspase cascade [4]; (ii) apoptosis-inducing factor, (iii) mitochondria-associated, 1 (AIF) induces chromatin condensation; (iv) HtrA serine peptidase 2 (HTRA2) and Diabolo IAP-Binding Mitochondrial Protein (SMAC/DIABLO) bind inhibitor of apoptosis (IAP), preventing the inhibition of procaspases; and endonuclease G (ENDOG) mediates DNA fragmentation [5] (Figure 1).

Investigation of the Bcl-2-mediated control of RCD revealed a role of Ca^{2+} -mobilization signals. Indeed, several signals can induce RCD by the selective transfer of Ca^{2+} from the endoplasmic reticulum (ER, which acts as a store) to mitochondria [6–8]. When mitochondria are exposed to a pathological overload of Ca^{2+} , MPT is triggered [9]. MPT is associated with the opening of the mitochondrial permeability transition pore complex (PTPC), a voltage-dependent, high-conductance channel assembled at the interface between the IMM and the OMM [10]. PTPC opening leads to the redistribution of small solutes (<1.5 kDa). The dramatic osmotic influx of water into the mitochondrial matrix during MPT collapses mitochondrial membrane potential ($\Delta\psi_m$) and all related activities (including ATP recycling), and is followed by structural collapse (swelling). It results in the release of mitochondrial proteins

from IMS which triggers the apoptotic pathway. Alternatively, the incapability of the affected cell to sustain ATP production leads to the irreversible deterioration of ion homeostasis, ultimately resulting in cell death with a necrotic morphology [11] (Figure 1).

It is believed that Ca^{2+} is the only trigger for PTPC opening, while other factors manipulate the threshold of $[\text{Ca}^{2+}]$ required for the occurrence of the event. These include sensitizers (e.g., low $\Delta\psi_m$, ROS, high matrix pH, long-chain fatty acids, atractyloside, and carboxyatractyloside) [12–17] and desensitizers (Mg^{2+} , ADP, ATP, acidic matrix pH) [11]. Among the many desensitizing factors, the best characterized is cyclosporine A (CsA). This small molecule can inhibit the mitochondrial peptidyl-prolyl isomerase cyclophilin D (CypD) and to date has been considered the gold standard for evaluating the involvement of MPT in pathophysiology.

1.2. Current Hypotheses on PTPC Structure

The structure of the PTPC has been investigated for decades and is still not well characterized. Original studies on isolated proteins and reconstituted liposomes proposed the voltage-dependent anion channel (VDAC) on the OMM and the ADP/ATP translocase (ANT) on the IMM. The inclusion of ANT in the model is important as it possibly represents the inhibition site for ADP/ATP or the activation site for atractyloside. Notably, both proteins could be isolated in a complex containing CypD. Murine CypD is coded by the gene *Ppif*. The investigation of *Ppif*-KO mice (then ablated for CypD) robustly confirmed the involvement of CypD in PTPC composition [18]; in contrast, the genetic deletion of VDAC failed to do so. Indeed, when cells from VDAC1^{-/-}; VDAC3^{-/-} mice were treated with siRNA targeting VDAC2, they displayed comparable sensitivity to MPT [19].

A similar approach was conducted to investigate ANT. The knockout (KO) of the three mouse isoforms of ANT indeed showed that PTPC requires a large amount of Ca^{2+} to open, and that the inhibitory effect of ADP was lost [20]. Interestingly, in cells from ANT triple-KO animals, MPT was still sensitive to CsA, and in CypD-KO cells, MPT was still responsive to ADP [18]. The combined deletion of ANTs and CypD in a quadruple-KO model conferred resistance of MPT to $[\text{Ca}^{2+}]$ as high as 5 mM (which is considerably high), potentially indicating that the PTPC did not manifest. These experiments confirmed a role for ANT in the PTPC, but also implied that some other partners of CypD participate in the formation of the PTPC.

Recently, a new candidate was proposed as a pore-forming member of the PTPC—mitochondrial F1/FO ATP synthase (hereafter referred to as ATP synthase). Indeed, (i) genetic manipulation of ATP synthase subunits markedly affected MPT; (ii) isolated ATP synthase, or its C subunit, reconstituted in artificial bilayers generated PTPC-like currents after Ca^{2+} stimulation; (iii) ATP synthase interacts with CypD; and (iv) molecules that target ATP synthase impair MPT [21–23]. Furthermore, the mutagenesis of the beta subunit (β -subunit) and the oligomycin-sensitivity-conferring protein (OSCP) of ATP synthase impaired the effects of Ca^{2+} and acidic pH, respectively, on the PTPC [24,25]. ATP synthase is usually arranged in dimers that further cluster with oligomers on the IMM. PTPC-derived currents were obtained from monomers or dimers in different experimental settings, opening a debate on which portions of the complex are required [26,27]. Despite this, it was demonstrated that MPT is mediated by the rupture of ATP synthase dimers and that it was preventable by mutagenesis of the C subunit, altering the C-ring conformation [21]. CRISPR/Cas9-mediated deletion of the ATP synthase C or B subunits was still detectable, suggesting that ATP synthase might not be directly involved in the pore formation [28,29]. Later studies in cells devoid of the C subunit revealed that conductance of PTPC was significantly reduced and that the remaining current could still be inhibited by CsA or compounds targeting ANT (ADP and bongkrelic acid) [30]. Multiple hypothesis are now under evaluation to explain these apparently conflicting results: (i) ATP synthase might only indirectly regulate PTPC, by controlling crista structure and ADP levels, (ii) ATP synthase and ANT might form two independent pores among the IMM and, (iii) ANT and ATP synthase (which can interact in the so-called ATP synthasome) might be synergistically required for the proper formation of the PTPC pore.

1.3. Involvement of MPT in RCD Subroutines

Studies on *Ppif*-KO mice demonstrated that CypD-dependent MPT is fundamental for the activation of RCD with necrotic features. Indeed, CypD-deficient cells are resistant to necrotic cell death induced by reactive oxygen species (ROS) and Ca^{2+} overload, while stimuli that activate MOMP are insensitive to a lack of CypD [31,32]. Additionally, neuronal cell lines stably overexpressing CypD in mitochondria were prone to necrotic cell death after MPT induction, and were instead more resistant to apoptosis induced by nitric oxide (NO) or staurosporine [33]. This evidence suggests that MPT ultimately results in necrosis and does not induce other forms of cell death (Figure 1). As apoptotic cell death is an active, energy-demanding process, this conclusion is logical for all those conditions in which a marked PTPC opening is triggered, reaching the non-return point of energy depletion that engages the mechanism described above. Nevertheless, some deviation from this model should be considered. Indeed, different reports have shown that in several experimental models, different stimuli that increase intracellular ROS elicit markers of intrinsic apoptotic pathways that can be inhibited by CsA, including mitochondrial proapoptotic protein release, phosphatidylserine exposure, and DNA fragmentation [34–48]. This suggests that, at least under selected experimental conditions, submaximal MPT might represent an alternative path for apoptosis activation.

Furthermore, proteins that regulate MOMP are strictly connected to MPT. Several direct protein–protein interactions between Bcl-2 family members and constitutive mitochondrial proteins involved in MPT, such as ANT, VDAC, and ATP synthase, have been confirmed. Bax and Bak are also required for PTPC-dependent necrotic cell death; in fact, the loss of Bax/Bak resulted in resistance to mitochondrial calcium overload and swelling [49]. The confirmation of MPT control by these interactions was demonstrated by the evidence of Bax- and Bak-induced loss of $\Delta\psi_m$, mitochondrial swelling, and CytC release through a Ca^{2+} - and CsA-dependent mechanism [50]. In addition, it was demonstrated that tBID induced transient openings of the PTPC associated with a conspicuous remodeling of mitochondrial cristae through a Bak-independent but CsA-inhibitable process [51]. ANT function is under the control of Bcl-xL expression: growth-factor-deprived cells avoid apoptosis via an efficient exchange of ADP for ATP promoted by Bcl-xL, permitting mitochondria to adapt to changes in metabolic demand [52]. Furthermore, Bcl-2 positively regulates ANT activity, while Bax inhibits it by disrupting its interaction with Bcl-2 [53].

Necroptosis is a form of regulated necrosis recently discovered under conditions in which the apoptotic pathway was inhibited, and it presents morphological features of both apoptosis and necrosis. The key upstream kinases involved in the activation of necroptosis are RIPK1 [54], RIPK3, and the substrate MLKL [55], which can be inhibited either through genetic or pharmacological methods to block this type of programmed cell death [56].

RIPK3, which is essential for TNF α -induced necrosis, can inhibit the ADP/ATP exchange mediated by ANT [57], which coincides with the loss of the CypD–ANT interaction, reduced ATP, and the induction of necrotic cell death, suggesting a role of the ANT–CypD interaction in necroptosis [58]. Bax and Bak have also been defined as mediators of necroptosis [59]; in fact, the elimination of Bax/Bak or the overexpression of Bcl-xL leads to the inhibition of the necroptotic process [60]. Furthermore, necroptosis is associated with mitochondrial CytC release and is partly sensitive to CsA inhibition [61].

The investigation of MPT over the years has revealed its importance in multiple subroutines of RCD, prompting investigation into its involvement in human pathology. In the present manuscript, we review the most recent literature discussing the role of the PTPC in human diseases caused by the dysregulation of cell death.

2. PTPC in Acute Conditions

2.1. MPT during Ischemia

Ischemia and consequent reperfusion injury (RI) are pathological manifestations in which the involvement of MPT has been robustly confirmed. Ischemia is characterized by the reduced oxygenation

of a portion of a tissue (hypoxia), which results in the loss of tissue functions and eventually the activation of multiple forms of RCD. Ischemia impacts multiple organs, especially those that are more susceptible to hypoxia, such as the heart, brain, and kidney. Interestingly, not all tissues share the same susceptibility to ischemia/RI. In fact, the severity of the injury largely depends on how different types of cells, and therefore tissues, can survive under hypoxic conditions [62,63].

Mechanistically, a lack of oxygenation translates into reduced activity of the electron transport chain (ETC), and hence results in the blockage of oxidative phosphorylation (OXPHOS) and a consequent reduction in ATP recycling. In this scenario, to meet energy demands, cells upregulate anaerobic glycolysis, producing lactic acid and hydrogen ions, which results in intracellular acidosis. By neutralizing pH via the activation of Na^+/H^+ antiporter (NHE), the cell undergoes sodium accumulation that is counterbalanced by the reverse activity of $\text{Na}^+/\text{Ca}^{2+}$ exchanger (NCX). Concomitantly, the reduction in available ATP depresses the activity of Na^+/K^+ ATPase, plasma membrane calcium ATPase (PMCA), and sarco-/endoplasmic reticulum Ca^{2+} -ATPase (SERCA), which ultimately results in an overload of cytosolic Ca^{2+} [64]. Additionally, the reduced pO_2 causes the accumulation of electrons among different respiratory complexes, leading to the production of ROS. The concomitant increase in intracellular Ca^{2+} and ROS and the decrease in $\Delta\psi_m$ favors the induction of MPT. This mechanism has been demonstrated in cultured neonatal rat cardiomyocytes [65], hepatocytes [66], and immortalized cells [67].

Among all tissues, the brain exhibits high sensitivity to ischemia due to its glucose-dependent metabolisms [68]. Rapid and CsA-dependent mitochondrial depolarization is reported to occur early during experimental stroke in the mouse somatosensory cortex in vivo [69]. Additionally, CsA protects the retinal ganglion from cell death during acute intraocular pressure (IOP) elevation, a peculiar inducer of ischemia [70]. Furthermore, CsA administration attenuates hypoxic–ischemic brain injury in newborn rats induced by unilateral carotid artery ligation [71].

Despite this, MPT is commonly believed to occur to a minimal extent during ischemia. Indeed, as described, hypoxia leads to the accumulation of protons and ADP, which are strong inhibitors of PTPC. During ischemia, the manifestation of MPT depends on the subtle equilibrium between PTPC inducers (Ca^{2+} and ROS) and inhibitors (protons and ADP), which accumulate as a result of impaired mitochondrial respiration and excess glycolysis (Figure 2). Furthermore, the adaptive response to hypoxia-mediated by HIF1a affects PTPC opening by regulating hexokinase II (HKII) levels [72], another reported PTPC regulator. Indeed, when HIF1a is stabilized (e.g., following hypoxia or GSK360A administration), HKII protein expression significantly increases in the mitochondrial fraction, and this is directly involved in the cytoprotective effect started by HIF1a stabilization. Genetic depletion of HKII completely abolished this path even in the presence of an activated HIF1a [72]. Nevertheless, HKII is considered an inhibitor of the PTPC only when bound to the OMM (especially to VDAC), rather than when generally overexpressed in mitochondria.

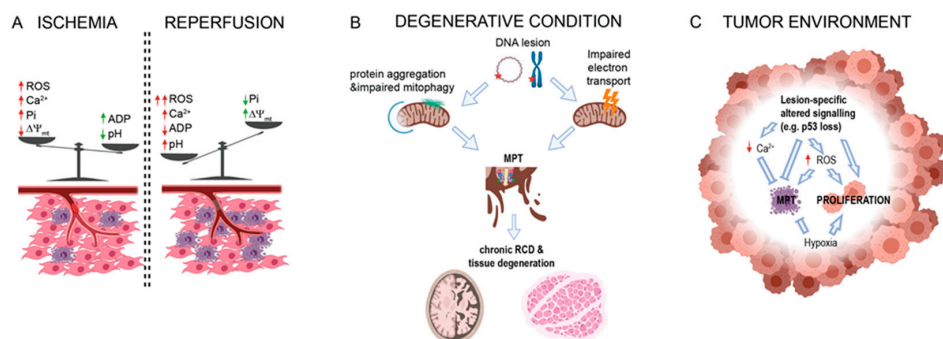


Figure 2. MPT alterations in human diseases. (A) Effect of ischemia and reperfusion in levels of MPT-regulating factor in insurgence of RCD (purple cells). (B) Schematic representation of the effect of mutations in mitochondrial or nuclear DNA (represented by circular DNA or chromosome, respectively) in human diseases characterized by degeneration of neuronal or muscular tissue. (C) Representation of major alterations in MPT regulators detected in tumor microenvironment.

Nevertheless, under this condition, Ca^{2+} overload may induce MPT-independent cell death as a result of the excessive activation of Ca^{2+} -dependent enzymes such as phospholipases, proteases, and endonucleases [73,74]. Noticeably, during myocardial infarction, the activation of calpains, Ca^{2+} -dependent cysteine proteases, results in myofibril disruption, thus promoting hypercontracture in the heart, which consists of sustained shortening and stiffening of the myocardium [75,76].

2.2. Role of MPT in Reperfusion Injury

The situation dramatically changes during tissue reperfusion. Indeed, the restoration of pO_2 recovers respiration, ATP synthesis, and the activity of plasma membrane pumps, which re-equilibrate intracellular pH. As a result, the inhibition of MPT by ADP and protons is removed, lowering the threshold for PTPC opening. In addition, reperfusion stimulates ROS production by multiple sources [77]. At the mitochondrial level, succinate is observed to accumulate in the mitochondrial matrix during ischemia and it was proposed to stimulate ROS production from complex I through reverse electron transport (RET), at the time of reperfusion [78]. Other pieces of evidence suggest that ETC conditions are not favorable for RET at the beginning of reperfusion, and that a burst of ROS production only occurs after a first wave of MPT. Besides mitochondria, reperfusion induces ROS via other enzymes including (but not limited to) xanthine oxidase, NADPH oxidase, and nitric oxide synthase [77]. These are believed to further stimulate ROS generation in the mitochondria, forming a vicious cycle and making mitochondria de facto the largest ROS source during reperfusion [79,80]. The elevated superoxide anion (O_2^-) reacts with nitric oxide (NO), producing the highly reactive peroxynitrite. This leads to a reduction in the availability of NO (which is a potent vasodilator) and causes the accumulation of neutrophils [77]. Furthermore, oxidative damage causes lipid peroxidation, DNA damage, and enzyme denaturation and activates the innate anti-inflammatory response, aggravating reperfusion injury (RI) [81].

The occurrence of MPT during the reperfusion phase was demonstrated by the experiments of Griffith and Halestrap in 1995. They showed that mitochondrial accumulation of radioactive deoxy glucose (hot-dog), which can pass through the IMM only during MPT, did not occur in isolated hearts undergoing ischemia, but was significantly induced (and inhibitable by CsA) during reperfusion [82].

In the past decade, several in vitro and in vivo studies have confirmed the involvement of MPT in ischemia/RI [83]. The administration of CsA (as well as its analog FK506) has been shown to protect against ischemia/RI in multiple animal models and in multiple tissues, including cardiac and skeletal muscle, brain, kidney, liver, lungs, and testis [84–89]. *Ppif*-KO mice are significantly protected from ischemia/RI in both cardiac muscle and the brain, in terms of both tissue function and survival rates [31,32,90]. In addition to CypD manipulation, genetic interference in mechanisms of Ca^{2+} homeostasis proved the importance of MPT in ischemia/RI. Cardiac-specific ablation of NCX significantly decreased ischemia/RI in isolated hearts [91]. Similarly, mice overexpressing *Bcl2* have reduced $[\text{Ca}^{2+}]_m$ accumulation and are therefore protected from myocardial ischemia/RI [92]. Accordingly, tissue-specific overexpression of the mitochondrial $\text{Na}^+/\text{Ca}^{2+}$ exchanger (TER-NCLX) in cardiac muscle accentuates the extrusion of Ca^{2+} from mitochondria to the cytosol and then suppresses $[\text{Ca}^{2+}]_m$, decreasing the sensitivity of cardiomyocytes to PTPC opening. Hearts from TER-NCLX mice also display protection from left coronary artery ligation-induced ischemia/RI [93]. Additionally, impairing mitochondrial calcium uniporter (MCU), using the inhibitor Ru360 [94] or in MCU-KO mice [95], lowers the uptake of mitochondrial Ca^{2+} and is correlated with increased brain and heart function. We recently demonstrated that inhibiting ATP synthase via N,N-dicyclohexylcarbodiimide (DCCD) partially recovered contractility of isolated heart exposure to ischemia/RI by Langendorff apparatus. Most interestingly, we observed that serum levels of the C subunit in patients with ST-segment elevation myocardial infarction (STEMI) correlated to several surrogate markers of myocardial reperfusion [96].

2.3. Role of MPT in Acute Kidney Injury

Renal tissue is also known to be affected by MPT in multiple conditions. Acute kidney failure (mostly known as acute kidney injury, AKI) is often characterized by extensive necrosis. The protective effect of CsA or CypD inactivation on experimental ischemia/RI has been largely reported in kidneys, as previously stated. Atherosclerotic renal artery stenosis (ARAS) is probably the most frequent cause of ischemia/RI-related AKI. The outcomes of experimental ARAS are significantly improved by exposure to the mitochondrial-targeted peptide Elamipretide. This peptide displays multiple protective functions, including the buffering of ROS and the stabilization of the structural mitochondrial lipid cardiolipin. Specifically, in experimental ARAS, the protective effect of Elamipretide is believed to be mediated by desensitization to PTPC opening [97].

Renal tissue can also undergo, at nominal pO_2 , conditions resembling manifestation of RI and that appear to be dependent on MPT. For example, an important cause of AKI with extended necrosis is exposure to drugs (e.g., FANS or chemotherapy) and crystal nephropathies. The etiology of these ischemic-like conditions is not yet fully comprehended, although it is proposed to act through excess ROS production, which ultimately triggers PTPC opening. In support of this model, under conditions of oxidative stress, glycogen synthase kinase-3 β (GSK3 β), an interactor and regulator of the putative PTPC, translocates from the cytosol to mitochondria in a VDAC2-dependent manner, promoting PTPC opening [98]. Inhibition of GSK3 β promotes resistance to MPT in mice undergoing paraquat- or diclofenac-induced nephrotoxicity [99,100]. Interestingly, it is now well recognized that cell death during AKI is significantly dependent on necroptosis, a finding largely confirmed by investigations on *Mkl1*-KO and *Ripk3*-KO animals [101]. Cisplatin-induced AKI is protected by the inactivation of both *Ripk3* and *CypD*. *Ripk3/Ppif*-double-KO models are more protected than the models with either KO [102], suggesting that MPT and *Ripk3* contribute to RCD by independent but concomitant pathways. A recent study by Mulay et al. using *CypD*-KO and *Mkl1*-KO mice showed that experimental conditions mimicking acute oxalosis (crystal nephropathy characterized by sudden increases in serum oxalate levels) resulted in kidney failure with necroptotic features that was strongly dependent on MPT [103]. That study, however, did not report significant differences among the *Ppif*-KO, *Mkl1*-KO and *Ppif/Mkl1*-double-KO mice in terms of protection from cell death.

3. PTPC in Degenerative Conditions

Degenerative disorders are human diseases characterized by the chronic loss of fully differentiated cells, which leads to the progressive impairment of the structure and/or function of the affected tissue/organ. Among the most frequent and probably most investigated degenerative disorders are conditions that affect the CNS or the skeletal or cardiac muscle. As previously mentioned, these organs all require large amounts of energy; therefore, it is not surprising that the mutations most frequently associated with degenerative disorders are linked to mitochondria. Intriguingly, many of these conditions share impaired mitochondrial respiration and ATP production, increased ROS production, and altered PTPC sensitivity. The involvement of MPT in these disorders appears to be more complex than the involvement of MPT in ischemia/RI in terms of molecular and cellular interactions. We therefore summarize the major observations made in different degenerative conditions.

3.1. Role of the PTPC in Protein-Aggregation-Related Neurodegenerative Diseases (NDs)

The primary features of neurodegeneration are the abnormal presence and accumulation of mutant and/or damaged proteins. Protein aggregation is the main cause of changes in the intracellular environment such as oxidative status, impaired protein quality control system, transcriptional alteration, and mitochondrial dysfunction. All these variations critically contribute to the pathogenesis of NDs and culminate in neuronal cell death. Among the diverse types of proteins that aggregate, amyloid-beta ($A\beta$), Tau, and alpha-synuclein (α Syn) are the most commonly studied and represent the primary

cause of sporadic and familial Alzheimer's disease (AD) and Parkinson's disease (PD), the most prevalent NDs.

Interestingly, A β , Tau protein, and α Syn are found in the mitochondria of patients affected by AD or PD [104–106] or their related animal models [107–109]. In particular, these protein aggregates have been observed to colocalize or directly interact with multiple partners of the PTPC, such as CypD, VDAC, ANT, and ATP synthase [104,107,109,110].

Additionally, A β exposure in cultured cortical neural progenitor cells induces PTPC opening [111]. In particular, short A β exposure led to decreased cell proliferation. However, when the exposure and thus PTPC opening were prolonged, CsA-inhibitable necrotic RCD was activated. Consistent with this result, intravital multiphoton imaging of AD mouse models demonstrated that near senile A β plaques, mitochondria showed severe structural and functional abnormalities, suggesting that senile plaques are the main source of toxicity in vivo [112]. A β plaques and phosphorylated Tau interact with VDAC, leading to mitochondrial dysfunction [105]. Similarly, a specific Tau fragment (NH2-26-44 fragment) affects OXPHOS and mitochondrial dynamics by interacting with ANT and impairing PTPC regulation [113].

Furthermore, α Syn oligomers move into mitochondria and colocalize with ATP synthase, inducing its oxidation concomitantly with increased PTPC opening, mitochondrial swelling, and necrosis activation [114]. Additionally, a PD mouse model characterized as having a mutant human α Syn (Thy1-h α Syn-A53T tg mice) proved that α Syn associates with neuronal mitochondria and interacts with VDAC and CypD in vivo [115]. This work directly linked motor abnormalities and neuropathology to the PTPC.

The study of rare inherited mutations in PD has provided insight into the molecular mechanisms of mitophagy, the regulated delivery of dysfunctional mitochondria to lysosomes via autophagic machinery. Multiple PD-related genes have been identified, among which the mitochondrial kinase PINK1 and the cytosolic E3 ubiquitin ligase Parkin are the most characterized. The PTPC may be involved in mitophagy-mediated quality control processes, which play a critical role in conserving neuronal health and function. Indeed, it has been suggested that the opening of the PTPC regulates mitochondrial depolarization and subsequent mitochondrial degradation in autophagosomes. Furthermore, CsA and its analogs block autophagosome formation, and the alteration of PTPC opening has been unveiled in models lacking PINK1, Parkin, and DJ1, which are components of the best-characterized stress-induced mitophagy pathways [116,117]. Consistently, the downregulation of PINK1 in mouse neurons resulted in altered mitochondrial morphology and function, ROS production, and finally PTPC opening. All these events were accompanied by the induction of mitochondrial autophagy [118].

Similarly, PINK1-deficient neurons showed selective increases in mitochondrial Ca²⁺, PTPC opening, and defective mitochondrial respiration. In addition, the inhibition of PTPC opening was found to be sufficient to rescue the mitochondrial impairments observed in *Pink1*^{-/-} cells [119]. ROS production and PTPC opening were increased in primary mouse embryonic fibroblasts (MEFs) and brains from *Park7*^{-/-} (the gene coding for DJ-1) mice compared with wild-type (WT) samples. In contrast, antioxidant molecules decreased ROS levels and PTPC opening. Interestingly, in contrast to *Pink1*^{-/-} cells, the lack of DJ-1 did not affect mitochondrial respiration and Ca²⁺ dynamics, suggesting that DJ-1 has a possible antioxidant role. Finally, Parkinsonian toxins (such as 6-hydroxydopamine and neurotoxin1-methyl-4-phenyl-1,2,3,6-tetrahydropyridine) are widely employed as in vivo and in vitro chemical models of PD and have been found to be potent activators of both PTPC and mitophagic processes [120,121]. Notably, both VDAC and ANT were demonstrated to be required for proper mitophagy [122,123]. Finally, recent pieces of evidence demonstrated that human samples obtained by AD-affected patients displayed inhibited damaged mitochondrial clearance [124] and that mitophagy activation diminished insoluble A β and Tau hyperphosphorylation to revert cognitive impairments in an AD mouse model [125,126] (Figure 2).

Taken together, these findings suggest that the mitochondrial accumulation of disease-specific protein aggregates might favor MPT via direct interactions or mitophagy impairment, which leads to the accumulation of mitochondria prone to PTPC opening and RCD (Figure 2).

3.2. Amyotrophic Lateral Sclerosis (ALS) and PTPC

ALS is the most common neuromuscular degenerative disease affecting adults. While several works have suggested a protein-aggregation origin, this progressive and severely disabling fatal neurological disease is generally considered to have multifactorial causes. Currently, there are no cures or effective treatments for ALS, and the molecular pathogenesis of ALS is poorly understood.

Recent findings show that mitochondrial perturbations are implicated in the pathogenesis and progression of ALS. Altered fission–fusion dynamics, altered mitochondrial Ca^{2+} homeostasis, excessive oxidative stress, reduced OXPHOS activity, and decreased proapoptotic factor release have been found in ALS models in vitro and in vivo. Additionally, the PTPC is emerging as a critical player in ALS. In a transgenic model of ALS (G93Ahigh), a profound alteration in mitochondrial structures with increased PTPC activity was observed [127]. Interestingly, dendritic mitochondria from the same ALS animal model displayed increased contact sites between the IMM and OMM. This conformation might favor the formation of the PTPC. Furthermore, the deletion of CypD delayed disease onset and extended the survival of transgenic ALS mice [127]. Consistent with this finding, the exposure of two independent ALS murine models to the novel PTPC inhibitor GNX-4728 protected against motor neuron degeneration and mitochondrial impairment and promoted their survival nearly 2-fold [128].

Preclinical studies have shown that olesoxime, a member of the cholesteroloxime family, improves the survival of neural cells and reduces the effects of oxidative stress by modulating the PTPC. In particular, this compound concentrates in mitochondrial compartments, where it binds the PTPC interactors VDAC and mitochondrial translocator protein (TSPO). Following olesoxime binding, the PTPC was desensitized, leading to neural cell protection both in vitro and in vivo [129,130]. Accordingly, the potent antioxidant and inhibitor of PTPC edaravone (Radicut™) has been approved for the treatment of ALS [131]. Compounds derived from cinnamic anilides such as GNX-4728 and GNX-4975 also represent an MPT-based treatment of ALS. In a murine model of ALS, these compounds delayed the onset of symptoms, increased lifespan, and reduced the inflammatory response [128].

3.3. Multiple Sclerosis (MS) and PTPC

MS is the most common primary demyelinating disease of the brain. MS is an inflammatory T-cell-mediated autoimmune disease characterized by progressive demyelination, gliosis (scarring), and neuronal loss [132]. Recently, mitochondrial dysfunction has been increasingly linked to the pathogenesis of MS. Additionally, impaired mitochondrial enzyme complex activity [133,134], increased oxidative stress [135], altered mitochondrial DNA [136], impaired quality control systems [137,138], and abnormal mitochondrial number and morphology have been described in MS patients [133] and in vivo MS mouse models [139,140]. In this context, it was discovered that the PTPC might also contribute to MS; indeed, CypD-KO mice with experimental autoimmune encephalomyelitis (EAE), a commonly used animal model for MS, recovered from their induced disabilities. Furthermore, axonal damage was decreased, and the mitochondria of cultured CypD-KO neurons accumulated higher levels of Ca^{2+} and were more resistant to oxidative stress compared to WT [141]. Subsequent studies confirmed this finding and demonstrated that the selective inhibition of PTPC exerted neuroprotective effects on the EAE model by increasing mitochondrial function, reducing oxidative stress, and blocking mitochondrial swelling and Ca^{2+} -mediated PTPC formation [142]. The p66Shc protein may also modulate the mitochondrial dynamics and PTPC opening that occur during neurodegeneration in EAE. P66Shc is a product of the ShcA gene normally localized in the cytoplasm. However, once phosphorylated by protein kinase C-Beta and following interaction with PIN1, P66Shc moves to the mitochondria, where it regulates distinct cellular processes such as apoptosis and autophagy [143,144]. Furthermore, in the mitochondrial compartment, p66Shc works as a ROS amplifier by generating

mitochondrial ROS to induce PTP opening. Consistent with this function, when EAE was induced in p66Shc-KO (*p66Shc*^{-/-}) mice, the clinical symptoms (manifested as limb weakness and paralysis) of these model mice were less severe than those of WT mice [145]. The fact that the onset and development of EAE in p66Shc/Cyc-D-double-KO mice were identical to those observed in *p66Shc*^{-/-} mice validates the role of the p66Shc-PTPC pathway in neurodegeneration and confirms that once activated, p66Shc interacts with PTPC to promote its opening [146].

3.4. PTPC in Muscular Dystrophies (MDs)

MDs refer to a clinically and genetically heterogeneous group of degenerative muscle diseases, manifested primarily as the progressive weakness and degeneration of skeletal muscles that control movement, resulting in severe pain, disability, and ultimately death. Some forms of MD also affect cardiac muscle [147,148]. Current therapies to treat muscle degenerative diseases are still limited by poor targeting, although promising new therapeutic directions remain [149].

The most common and severe form of human muscular dystrophy is Duchenne MD (DMD), which is an X-linked recessive genetic disorder associated with respiratory complications and cardiac dysfunction [150]. The disease is caused by a genetic defect—the absence of the cytoskeletal protein dystrophin, the primary function of which is to link the myofiber cytoskeleton to the extracellular matrix, stabilizing the sarcolemma [151–153]. Although the gene underlying the disorder was identified in 1987 [154], the pathophysiology leading to disease remains unclear. Numerous mitochondrial alterations are correlated with dystrophic conditions, including impaired ATP production, substrate handling, Ca²⁺ buffering capacity, and elevated ROS production. The mitochondria in muscular fibers from dystrophic mdx mice (a murine model of DMD) displayed a significantly shorter time to MPT induction in response to Ca²⁺ than WT mice [155]. In *C. elegans* and zebrafish models of DMD, mitochondrial fragmentation is detectable before overt signs of muscular degeneration, and CsA feeding delays muscle degeneration [156]. Cyclosporine also inhibits calcineurin, a signaling protein involved in skeletal muscle, and its inhibition was found to worsen muscular dystrophy in an mdx mouse model [157,158]. Nonetheless, the deletion of *Ppif* and the administration of Debio-025 (a CsA inhibitor with no effect on calcineurin) prevented dystrophic conditions in mdx and d-sarcoglycan-KO (*Scgd*^{-/-}) animals [159,160]. Additionally, several lines of evidence have shown that *Ppif* deletion is protective in *Col6a1*^{-/-} mice [161].

Mutations of collagen VI (ColVI) genes encoding the extracellular matrix protein, which is abundant in skeletal muscle, cause three muscle diseases in humans: Ullrich congenital muscular dystrophy (UCMD), Bethlem myopathy (BM), and the recently identified myosclerosis myopathy (MM) [162,163]. These collagen VI myopathies are inherited muscle diseases that share mitochondrial dysfunction due to altered PTPC opening [164]. Mouse models lacking collagen VI (*Col6a1*^{-/-}) display an early onset myopathic phenotype correlated with ultrastructure defects in mitochondria and the sarcoplasmic reticulum (SR), altered mitochondria caused by eventual inappropriate PTPC opening, and elevated muscle fiber apoptosis [161,165,166]. In addition, the absence of ColVI led to a marked decrease in the expression of proapoptotic Bcl-2, which may synergize with calcium to enhance the opening of the PTPC and eventually promote the release of mitochondrial proapoptotic factors [167].

In light of this fact, the altered expression of collagen in *Col6a1*^{-/-} mice and in BM and UCMD patients correlates with enhanced PTPC opening, resulting in the functional and ultrastructural deficiency of mitochondria, followed by impaired autophagy, [168]. As such, autophagy is altered in MDs, and autophagy activation due to low amino acid intake improved the skeletal muscle phenotype of a DMD mouse model (mdx), [169]. Consistently, pharmacological treatment with CsA has been reported to dramatically recover myofiber degeneration in a *Col6a1*^{-/-} mouse model and UCMD patients [161,166]. Additionally, it has been demonstrated that mitochondria-mediated cell death can be reduced by CsA in Ullrich congenital muscular dystrophy models [167].

4. Mitochondrial Disorders

Mitochondrial diseases are a clinically heterogeneous group of disorders that arise because of mitochondrial respiratory chain dysfunction. These diseases are caused by mutations in nuclear DNA (nDNA) and in mitochondrial DNA (mtDNA). Although mitochondrial diseases can involve any organ or tissue, they characteristically involve multiple systems, typically affect organs that are highly dependent on aerobic metabolism and are often relentlessly progressive with high morbidity and mortality. Like other degenerative diseases, the involvement of MPT in mitochondrial diseases has been proposed.

Mutations in mtDNA are responsible for the etiology of the most frequent mitochondrial diseases, especially Leber's hereditary optic neuropathy (LHON); neurogenic muscle weakness, ataxia, and retinitis pigmentosa (NARP); mitochondrial encephalomyopathy, lactic acidosis, and stroke-like episodes (MELAS); and myoclonic epilepsy with ragged red fibers (MERRF). These alterations most frequently involve single-base mutations in genes encoding components of respiratory complex I, ATP synthase, transfer RNA, and DNA polymerase, but also may be caused by large deletions of mtDNA. Hybrids carrying mtDNA mutations associated with LHON, NARP, MELAS, and MERRF displayed poor resistance to oxidative stress, which could be prevented by the administration of CsA or the deprivation of extracellular Ca^{2+} [170]. Accordingly, many of these mutations lower the threshold for PTPC opening in response to Ca^{2+} and ROS [171,172].

Mutations in nDNA associated with mitochondrial diseases have also been also related to alterations in MPT activity. Mutations in *leucine-rich pentatricopeptide repeat containing (LRPPRC)*, a protein involved in the maturation and stability of mitochondrial RNA [173], cause the French-Canadian variant of Leigh syndrome. Loss of LRPPRC results in defects in the assembly of respiratory complexes IV and V, leading to severe metabolic alterations. Fibroblasts isolated from patients presenting LRPPRC inactivation displayed multiple types of mitochondrial dysfunction, including a reduced threshold for Ca^{2+} -induced MPT [174]. Interestingly, all the mitochondrial alterations mentioned so far are often associated with impaired or unstable assembly of ATP synthase, providing significant clues to its involvement in MPT. Direct investigations of ATP synthase alterations and MPT in the etiology of mitochondrial disease have not been performed. Other significant nuclear genes relating mitochondrial diseases to MPT are optic atrophy 1 (OPA1) and Spastic paraplegia 7 (SPG7). OPA1 is an essential protein involved in the fusion and cristae arrangement of the IMM. Its mutations manifest clinically as optic atrophy, ataxia, and deafness [175]. SPG7 (paraplegin) is an ATP-dependent zinc metalloprotease located in the mitochondrial matrix, and its mutations are associated with chronic progressive ophthalmoplegia [176]. Interestingly, both proteins positively regulate the MPT threshold in response to Ca^{2+} induction, and their inactivation significantly inhibits PTPC opening [177,178]. Mechanisms by which OPA1 and SPG7 act on PTPC are still to be defined. While the role of OPA1 seems to be dependent on its control of crista morphology [179], SPG7 appears to regulate the amount of Ca^{2+} available for MPT via regulation of mitochondrial calcium uniporter assembly [180]. Taken together, this evidence indicates that PTPC might be a significant target for mitochondrial disease; however, the mechanism by which MPT influences these diseases is still poorly understood and might differ among syndromes, calling for further investigations in more complex experimental models.

5. PTPC in Nonalcoholic Fatty Liver Disease

Nonalcoholic fatty liver disease (NAFLD) is among the most prevalent chronic liver diseases in both children and adults, and is predicted to be the primary cause for liver transplants by 2020 [181]. NAFLD is characterized by an accumulation of fat (steatosis) in the liver, which can progress to inflammatory NASH and into more severe stages: fibrosis, cirrhosis, and hepatocellular carcinoma [182]. The prevalence of NAFLD has risen rapidly in Western societies, particularly in most of the European countries, due to an increase in mass consumption of highly processed ready-made food, which is rich in fructose and saturated fat. NAFLD has risen rapidly in parallel with the recent surge in metabolic-related diseases such as obesity and type 2 diabetes mellitus (T2DM),

which have been indicated as risk factors for the prevalence and progression of NAFLD. Despite the attempts of the liver to recover from fat accumulation, in the long run, mitochondrial adaptation is insufficient to prevent lipotoxicity due to continuous FFA accumulation [183]. At this later time point, mitochondria present alterations in the OXPHOS complexes, mitochondrial membrane potential, reduced ATP synthesis, and induced PTPC opening [183]. Opening of the PTPC may be the basis of the steatosis-induced apoptosis of hepatocytes observed *in vitro*, and may be related to the steatosis in NAFLD of human beings [184]. It has been postulated that stimulated PTPC opening in a rat model of NAFLD is the result of increased Bax expression and aberrant Bcl-2/Bax ratio. This seems to be an important mechanism of the mitochondrial damage in hepatocytes that occurs in NAFLD [185]. Wang et al. proposed that the overexpression of mitochondrial hepatic CypD induced mitochondrial stress and could be an early event that leads to the liver steatosis [186]. They found that overexpression of CypD is manifested in mitochondrial swelling and increased mitochondrial ROS production. Such mitochondrial perturbations provoke ER stress through Ca^{2+} /p38 MAPK activation, finally resulting in the increase of SREBP1c-mediated synthesis of triglycerides. Interestingly, in mice fed with a high-fat diet, the increased level of CypD was observed earlier than triglyceride accumulation in the liver. Moreover, Wang et al. speculated that CypD knockout or pharmacological inhibition of CypD could ameliorate triglyceride accumulation in HFD-fed mice [186]. On the other hand, the observations of Lazarin et al. indicated that mitochondria isolated from livers of monosodium l-glutamate obese rats were less susceptible to the opening of PTPC by calcium [187]. Regardless of several pieces of evidence for the involvement of the MPT in the NAFLD animal models, there is no direct evidence supporting the role of PTPC and especially CypD in NAFLD in humans.

6. PTPC in Cancer

One of the earliest established hallmarks of cancers is the resistance of transformed cells to RCD. Considering the discussed role of MPT in RCD, it is straightforward to hypothesize that the alteration of the PTPC machinery is involved in the establishment of neoplasia. According to this hypothesis, MPT is predicted to have a tumor-controlling mechanism, and its suppression is required for tumor development. It is harder to prove that a phenomenon does not occur than it is to prove that it does occur. Indeed, strong direct evidence confirming or confuting this hypothesis is lacking. Experiments based on the genetic manipulation of CypD for the other disease types discussed should provide significant evidence, but nothing of this kind has yet to be reported. Still, reduced MPT in transformed cells could be predicted by a large number of findings, as discussed below.

Another significant hallmark of cancer is metabolic rewiring, especially the abnormal increase in the glycolytic rate at almost normal pO_2 (Warburg effect). This large glucose consumption causes the significant conversion of pyruvate into lactate, resulting in intracellular acidification and leading to PTPC desensitization similar to that observed in ischemia [6]. Furthermore, many solid tumors develop a hypoxic area that, analogous to ischemic tissue, also promotes Hif1 α accumulation and HKII-mediated desensitization of PTPC. The Warburg effect then allows the hypoxic tumor to limit Pi and Ca^{2+} accumulation, similarly to ischemia, favoring the inhibitory effect of low pH. If, by analogy to ischemia, an increase in $[\text{Ca}^{2+}]$ could be expected, it is true that transformed cells have lower intracellular Ca^{2+} (Figure 2). Indeed, it has been shown that H-RAS-driven transformation is concomitant with a progressive reduction in the amount of intracellular Ca^{2+} [188]. Bcl-xL has been shown to negatively regulate PTPC opening by directly interacting with VDAC [189]. Additionally, Bcl-xL can interact with the β subunit of ATP synthase to promote its synthase activity and inhibit PTPC [190].

Furthermore, many other oncogenes and oncosuppressor genes regulate Ca^{2+} . Among the most characterized is Bcl-2, which can impair $[\text{Ca}^{2+}]$ in the ER lumen and its transfer to mitochondria via multiple proposed mechanisms [191]. Additionally, many tumors show alterations in the PI3K pathway. Members of this pathway, AKT and PTEN, can localize at mitochondrion-ER contact sites, especially with Ip3R, to alter its activity [192–196]. This effect is coordinated by the oncosuppressor PML [197–199]. Loss of PML or PTEN and activation of AKT (conditions prototypical of multiple

tumor types) lead to the inactivation of IP3R, which also limits the Ca^{2+} available to mitochondria. Additionally, AKT phosphorylates GSK3 β (altered in several cancer types), resulting in its inactivation and, as discussed, PTPC desensitization [200]. Finally, the master oncosuppressor p53 interacts with SERCA to maintain a high level of ER [Ca^{2+}]. Loss or inactivation of p53 (one of the most common alterations in cancer) impairs [Ca^{2+}] and results in reduced sensitivity to MPT-mediated RCD [201–205]. In addition, p53 can localize to mitochondria and interact with CypD to favor MPT and necrosis.

Interestingly, a network of chaperones seems to interact with CypD (which could be considered a chaperone itself) to modulate PTPC. In particular, HSP90, HSP60, and DnaJC15, which are often overexpressed in tumors, have been shown to interact with CypD, leading to their inhibition (then mimicking CsA) and suppressing RCD initiation [206–208]. These findings are supportive of the hypothesis, but contradict other strong evidence. First, transformed cells often have increased levels of ROS, not of a significant increase in multiple scavenging systems. It is currently accepted that elevated ROS can act as a mitogenic signal in tumors to support proliferation [209,210]. In addition, studies in cancer cell lines and tumor models have shown that different PTPC members are overexpressed, especially TSPO, VDAC, and ANT, possibly to favor their specific metabolic condition [16,211–217]. We can, therefore, speculate that tumor cells can survive pressure selection by the highly regulated suppression of MPT, which allows the maintenance of MPT-related features with potential mitogenic effects (Figure 2).

7. Potential of PTPC Targeting and Concluding Remarks

Because of the presented evidence (and much more), MPT has been investigated for the treatment of human disease in multiple clinical trials. CsA entered a trial procedure that lasted 15 years and ended with failure at phase III in cardiac RI. Indeed, the CIRCUS [218] and CYCLE [42] trials consisting of a single intravenous bolus of CsA (2.5 mg/kg) before revascularization had no effect on ST-segment resolution or cardiac enzymes and did not improve clinical outcome. These findings were reconsidered by a study by Piot et al., who saw hope in the use of CsA to treat RI. Similarly, TSPO targeting by 3,5-Seco-4-nor-cholestan-5-one oxime-3-ol (TRO40303) was tested in clinical trials, due to promising cardioprotective effects on a rat model of cardiac ischemia. However, the desensitization of PTPC opening seemed to be secondary to its remarkable antioxidant properties [219]. Indeed, studies on TSPO-KO mice showed that the protein was dispensable in models of ischemia/RI [220]. However, the safety and efficacy of this drug were evaluated a few years later in patients undergoing percutaneous coronary intervention (PCI). This multicenter, double-blinded, phase II study (MITOCARE) showed the inefficacy of the compound in reducing or limiting RI [221]. Additionally, an oral version of CsA was tested for the treatment of LHON but failed to reach the primary endpoint of the study, although it delayed the onset of the disease. [222]. There are multiple reasons that CsA-based trials have failed to reproduce the protection reported in preclinical studies, but a discussion of these failures is not the purpose of this review. The investigation of novel compounds able to target the PTPC is ongoing, and many investigations have already yielded promising results in preclinical studies. Most of these are designed to be more potent and specific inhibitors of CypD, including the small molecules C-9, C-19, and C-31, which have already been proven to be protective in models of AD, acute pancreatitis, and hepatic injury [223–225].

Library screening has also identified ML-404 [226] and N-phenylbenzamide [227] as CypD-independent, offering the possibility to combine their use with CsA to limit its side effects. It is of interest that ATP synthase is now the subject of investigation in these terms. Oligomycin and DCCD, which target the C subunit, displayed powerful MPT inhibition *in vitro*, but they also depleted mitochondrial ATP, causing an additional injury [21].

We recently generated a library of small molecules that target the C subunit by modifying the functional core of oligomycin and obtained new patented compounds able to notably reduce reperfusion damage in animal models of global ischemia without interfering with ATP production [22]. Finally, the natural hormone melatonin is of great interest. This hormone can act as an antioxidant

and can modulate the PTPC, although its exact mechanism is currently under investigation [228,229]. Currently, melatonin is considered the safest drug that can be used as a PTPC inhibitor, and we will probably see an increasing number of investigations on this molecule in the future.

Funding: P.P. is grateful to Camilla degli Scrovegni for continuous support. The Signal Transduction Laboratory is supported by the Italian Association for Cancer Research (AIRC: IG-23670 to P.P. and IG-19803 to C.G.), A-ROSE, Telethon (GGP11139B to P.P.), Progetti di Rilevante Interesse Nazionale (PRIN2017E5L5P3 to P.P. and PRIN20177E9EPY to C.G.), the Italian Ministry of Health (GR-2013-02356747 to C.G.), the European Research Council (ERC, 853057-InflaPML to C.G.), local funds from the University of Ferrara to P.P. and M.B. S.P. was supported by Fondazione Umberto Veronesi. MRW was supported by the National Science Centre, Poland (UMO-2018/29/B/NZ1/00589). Moreover, MRW gratefully acknowledge the financial support from the FOIE GRAS and mtFOIE GRAS projects. These projects received funding from the European Union's Horizon 2020 Research and Innovation program under the Marie Skłodowska-Curie Grant Agreement No. 722619 (FOIE GRAS) and Grant Agreement No. 734719 (mtFOIE GRAS).

Conflicts of Interest: The authors declare no conflict of interest.

References

1. Dejean, L.M.; Martinez-Caballero, S.; Guo, L.; Hughes, C.; Teijido, O.; Ducret, T.; Ichas, F.; Korsmeyer, S.J.; Antonsson, B.; Jonas, E.A.; et al. Oligomeric Bax is a component of the putative cytochrome c release channel MAC, mitochondrial apoptosis-induced channel. *Mol. Biol. Cell* **2005**, *16*, 2424–2432. [CrossRef] [PubMed]
2. Dejean, L.M.; Martinez-Caballero, S.; Manon, S.; Kinnally, K.W. Regulation of the mitochondrial apoptosis-induced channel, MAC, by BCL-2 family proteins. *Biochim. Biophys. Acta* **2006**, *1762*, 191–201. [CrossRef] [PubMed]
3. Salvador-Gallego, R.; Mund, M.; Cosentino, K.; Schneider, J.; Unsay, J.; Schraermeyer, U.; Engelhardt, J.; Ries, J.; Garcia-Saez, A.J. Bax assembly into rings and arcs in apoptotic mitochondria is linked to membrane pores. *EMBO J.* **2016**, *35*, 389–401. [CrossRef] [PubMed]
4. Kantrow, S.P.; Piantadosi, C.A. Release of cytochrome c from liver mitochondria during permeability transition. *Biochem. Biophys. Res. Commun.* **1997**, *232*, 669–671. [CrossRef]
5. Galluzzi, L.; Vitale, I.; Aaronson, S.A.; Abrams, J.M.; Adam, D.; Agostinis, P.; Alnemri, E.S.; Altucci, L.; Amelio, I.; Andrews, D.W.; et al. Molecular mechanisms of cell death: Recommendations of the Nomenclature Committee on Cell Death 2018. *Cell Death Differ.* **2018**, *25*, 486–541. [CrossRef] [PubMed]
6. Bonora, M.; Pinton, P. The mitochondrial permeability transition pore and cancer: Molecular mechanisms involved in cell death. *Front. Oncol.* **2014**, *4*, 302. [CrossRef]
7. Giorgi, C.; Danese, A.; Missiroli, S.; Patergnani, S.; Pinton, P. Calcium Dynamics as a Machine for Decoding Signals. *Trends Cell Biol.* **2018**, *28*, 258–273. [CrossRef] [PubMed]
8. Giorgi, C.; Marchi, S.; Pinton, P. The machineries, regulation and cellular functions of mitochondrial calcium. *Nat. Rev. Mol. Cell Biol.* **2018**, *19*, 713–730. [CrossRef]
9. Gunter, T.E.; Pfeiffer, D.R. Mechanisms by which mitochondria transport calcium. *Am. J. Physiol.* **1990**, *258*, C755–C786. [CrossRef]
10. Kroemer, G.; Galluzzi, L.; Brenner, C. Mitochondrial membrane permeabilization in cell death. *Physiol. Rev.* **2007**, *87*, 99–163. [CrossRef]
11. Bonora, M.; Wieckowski, M.R.; Chinopoulos, C.; Kepp, O.; Kroemer, G.; Galluzzi, L.; Pinton, P. Molecular mechanisms of cell death: Central implication of ATP synthase in mitochondrial permeability transition. *Oncogene* **2015**, *34*, 1475–1486. [CrossRef] [PubMed]
12. Schroers, A.; Kramer, R.; Wohlrab, H. The reversible antiport-uniport conversion of the phosphate carrier from yeast mitochondria depends on the presence of a single cysteine. *J. Biol. Chem.* **1997**, *272*, 10558–10564. [CrossRef] [PubMed]
13. Petronilli, V.; Cola, C.; Bernardi, P. Modulation of the mitochondrial cyclosporin A-sensitive permeability transition pore. II. The minimal requirements for pore induction underscore a key role for transmembrane electrical potential, matrix pH, and matrix Ca²⁺. *J. Biol. Chem.* **1993**, *268*, 1011–1016. [PubMed]
14. Takeyama, N.; Matsuo, N.; Tanaka, T. Oxidative damage to mitochondria is mediated by the Ca(2+)-dependent inner-membrane permeability transition. *Biochem. J.* **1993**, *294*, 719–725. [CrossRef]
15. Wieckowski, M.R.; Brdiczka, D.; Wojtczak, L. Long-chain fatty acids promote opening of the reconstituted mitochondrial permeability transition pore. *FEBS Lett.* **2000**, *484*, 61–64. [CrossRef]

16. Brenner, C.; Grimm, S. The permeability transition pore complex in cancer cell death. *Oncogene* **2006**, *25*, 4744–4756. [CrossRef]
17. Kowaltowski, A.J.; Castilho, R.F.; Vercesi, A.E. Opening of the mitochondrial permeability transition pore by uncoupling or inorganic phosphate in the presence of Ca²⁺ is dependent on mitochondrial-generated reactive oxygen species. *FEBS Lett.* **1996**, *378*, 150–152. [CrossRef]
18. Basso, E.; Fante, L.; Fowlkes, J.; Petronilli, V.; Forte, M.A.; Bernardi, P. Properties of the permeability transition pore in mitochondria devoid of Cyclophilin, D. *J. Biol. Chem.* **2005**, *280*, 18558–18561. [CrossRef]
19. Baines, C.P.; Kaiser, R.A.; Sheiko, T.; Craigen, W.J.; Molkentin, J.D. Voltage-dependent anion channels are dispensable for mitochondrial-dependent cell death. *Nat. Cell Biol.* **2007**, *9*, 550–555. [CrossRef]
20. Karch, J.; Bround, M.J.; Khalil, H.; Sargent, M.A.; Latchman, N.; Terada, N.; Peixoto, P.M.; Molkentin, J.D. Inhibition of mitochondrial permeability transition by deletion of the ANT family and CypD. *Sci. Adv.* **2019**, *5*, eaaw4597. [CrossRef]
21. Bonora, M.; Morganti, C.; Morciano, G.; Pedriali, G.; Lebiecinska-Arciszewska, M.; Aquila, G.; Giorgi, C.; Rizzo, P.; Campo, G.; Ferrari, R.; et al. Mitochondrial permeability transition involves dissociation of F1FO ATP synthase dimers and C-ring conformation. *EMBO Rep.* **2017**, *18*, 1077–1089. [CrossRef] [PubMed]
22. Morciano, G.; Preti, D.; Pedriali, G.; Aquila, G.; Missiroli, S.; Fantinati, A.; Carocchia, N.; Pacifico, S.; Bonora, M.; Talarico, A.; et al. Discovery of Novel 1,3,8-Triazaspiro[4.5]decane Derivatives That Target the c Subunit of F1/FO-Adenosine Triphosphate (ATP) Synthase for the Treatment of Reperfusion Damage in Myocardial Infarction. *J. Med. Chem.* **2018**, *61*, 7131–7143. [CrossRef] [PubMed]
23. Giorgio, V.; von Stockum, S.; Antoniel, M.; Fabbro, A.; Fogolari, F.; Forte, M.; Glick, G.D.; Petronilli, V.; Zoratti, M.; Szabo, I.; et al. Dimers of mitochondrial ATP synthase form the permeability transition pore. *Proc. Natl. Acad. Sci. USA* **2013**, *110*, 5887–5892. [CrossRef] [PubMed]
24. Giorgio, V.; Burchell, V.; Schiavone, M.; Bassot, C.; Minervini, G.; Petronilli, V.; Argenton, F.; Forte, M.; Tosatto, S.; Lippe, G.; et al. Ca(2+) binding to F-ATP synthase beta subunit triggers the mitochondrial permeability transition. *EMBO Rep.* **2017**, *18*, 1065–1076. [CrossRef]
25. Antoniel, M.; Jones, K.; Antonucci, S.; Spolaore, B.; Fogolari, F.; Petronilli, V.; Giorgio, V.; Carraro, M.; Di Lisa, F.; Forte, M.; et al. The unique histidine in OSCP subunit of F-ATP synthase mediates inhibition of the permeability transition pore by acidic pH. *EMBO Rep.* **2018**, *19*, 257–268. [CrossRef]
26. Mnatsakanyan, N.; Llaguno, M.C.; Yang, Y.; Yan, Y.; Weber, J.; Sigworth, F.J.; Jonas, E.A. A mitochondrial megachannel resides in monomeric F1FO ATP synthase. *Nat. Commun.* **2019**, *10*, 5823. [CrossRef]
27. Urbani, A.; Giorgio, V.; Carrer, A.; Franchin, C.; Arrigoni, G.; Jiko, C.; Abe, K.; Maeda, S.; Shinzawa-Itoh, K.; Bogers, J.F.M.; et al. Purified F-ATP synthase forms a Ca(2+)-dependent high-conductance channel matching the mitochondrial permeability transition pore. *Nat. Commun.* **2019**, *10*, 4341. [CrossRef]
28. He, J.; Carroll, J.; Ding, S.; Fearnley, I.M.; Walker, J.E. Permeability transition in human mitochondria persists in the absence of peripheral stalk subunits of ATP synthase. *Proc. Natl. Acad. Sci. USA* **2017**, *114*, 9086–9091. [CrossRef]
29. Carroll, J.; He, J.; Ding, S.; Fearnley, I.M.; Walker, J.E. Persistence of the permeability transition pore in human mitochondria devoid of an assembled ATP synthase. *Proc. Natl. Acad. Sci. USA* **2019**, *116*, 12816–12821. [CrossRef]
30. Neginskaya, M.A.; Solesio, M.E.; Berezhnaya, E.V.; Amodeo, G.F.; Mnatsakanyan, N.; Jonas, E.A.; Pavlov, E.V. ATP Synthase C-Subunit-Deficient Mitochondria Have a Small Cyclosporine A-Sensitive Channel, but Lack the Permeability Transition Pore. *Cell Rep.* **2019**, *26*, 11–17. [CrossRef]
31. Baines, C.P.; Kaiser, R.A.; Purcell, N.H.; Blair, N.S.; Osinska, H.; Hambleton, M.A.; Brunskill, E.W.; Sayen, M.R.; Gottlieb, R.A.; Dorn, G.W.; et al. Loss of cyclophilin D reveals a critical role for mitochondrial permeability transition in cell death. *Nature* **2005**, *434*, 658–662. [CrossRef] [PubMed]
32. Nakagawa, T.; Shimizu, S.; Watanabe, T.; Yamaguchi, O.; Otsu, K.; Yamagata, H.; Inohara, H.; Kubo, T.; Tsujimoto, Y. Cyclophilin D-dependent mitochondrial permeability transition regulates some necrotic but not apoptotic cell death. *Nature* **2005**, *434*, 652–658. [CrossRef] [PubMed]
33. Li, Y.; Johnson, N.; Capano, M.; Edwards, M.; Crompton, M. Cyclophilin-D promotes the mitochondrial permeability transition but has opposite effects on apoptosis and necrosis. *Biochem. J.* **2004**, *383*, 101–109. [CrossRef] [PubMed]

34. Zhang, J.; Han, Y.; Shi, H.; Chen, J.; Zhang, X.; Wang, X.; Zhou, L.; Liu, J.; Zhang, J.; Ji, Z.; et al. Swine acute diarrhea syndrome coronavirus-induced apoptosis is caspase- and cyclophilin D- dependent. *Emerg. Microbes Infect.* **2020**, *9*, 439–456. [CrossRef]
35. Garcia-Alvarado, F.; Govoni, G.; de Pascual, R.; Ruiz-Ruiz, C.; Munoz-Montero, A.; Gandia, L.; de Diego, A.M.G.; Garcia, A.G. Otilonium and pinaverium trigger mitochondrial-mediated apoptosis in rat embryo cortical neurons in vitro. *Neurotoxicology* **2019**, *70*, 99–111. [CrossRef]
36. Lee, Y.J.; Lee, C. Porcine deltacoronavirus induces caspase-dependent apoptosis through activation of the cytochrome c-mediated intrinsic mitochondrial pathway. *Virus Res.* **2018**, *253*, 112–123. [CrossRef]
37. Wang, H.; Chen, Y.; Zhai, N.; Chen, X.; Gan, F.; Li, H.; Huang, K. Ochratoxin A-Induced Apoptosis of IPEC-J2 Cells through ROS-Mediated Mitochondrial Permeability Transition Pore Opening Pathway. *J. Agric. Food. Chem.* **2017**, *65*, 10630–10637. [CrossRef]
38. Naserzadeh, P.; Ansari Esfeh, F.; Kaviani, M.; Ashtari, K.; Kheirbakhsh, R.; Salimi, A.; Pourahmad, J. Single-walled carbon nanotube, multi-walled carbon nanotube and Fe₂O₃ nanoparticles induced mitochondria mediated apoptosis in melanoma cells. *Cutan. Ocul. Toxicol.* **2018**, *37*, 157–166. [CrossRef]
39. Xie, Z.; Wang, J.; Liu, M.; Chen, D.; Qiu, C.; Sun, K. CC-223 blocks mTORC1/C2 activation and inhibits human hepatocellular carcinoma cells in vitro and in vivo. *PLoS ONE* **2017**, *12*, e0173252. [CrossRef]
40. Yang, M.; Wang, B.; Gao, J.; Zhang, Y.; Xu, W.; Tao, L. Spinosad induces programmed cell death involves mitochondrial dysfunction and cytochrome C release in *Spodoptera frugiperda* Sf9 cells. *Chemosphere* **2017**, *169*, 155–161. [CrossRef]
41. Liu, G.; Zou, H.; Luo, T.; Long, M.; Bian, J.; Liu, X.; Gu, J.; Yuan, Y.; Song, R.; Wang, Y.; et al. Caspase-Dependent and Caspase-Independent Pathways Are Involved in Cadmium-Induced Apoptosis in Primary Rat Proximal Tubular Cell Culture. *PLoS ONE* **2016**, *11*, e0166823. [CrossRef] [PubMed]
42. Ottani, F.; Latini, R.; Staszewsky, L.; La Vecchia, L.; Locuratolo, N.; Sicuro, M.; Masson, S.; Barlera, S.; Milani, V.; Lombardi, M.; et al. Cyclosporine A in Reperfed Myocardial Infarction: The Multicenter, Controlled, Open-Label CYCLE Trial. *J. Am. Coll. Cardiol.* **2016**, *67*, 365–374. [CrossRef]
43. Fakharnia, F.; Khodagholi, F.; Dargahi, L.; Ahmadiani, A. Prevention of Cyclophilin D-Mediated mPTP Opening Using Cyclosporine-A Alleviates the Elevation of Necroptosis, Autophagy and Apoptosis-Related Markers Following Global Cerebral Ischemia-Reperfusion. *J. Mol. Neurosci.* **2017**, *61*, 52–60. [CrossRef] [PubMed]
44. Ou, Z.; Jiang, T.; Gao, Q.; Tian, Y.Y.; Zhou, J.S.; Wu, L.; Shi, J.Q.; Zhang, Y.D. Mitochondrial-dependent mechanisms are involved in angiotensin II-induced apoptosis in dopaminergic neurons. *J. Renin. Angiotensin Aldosterone Syst.* **2016**, *17*, 1470320316672349. [CrossRef] [PubMed]
45. Dong, Y.Y.; Zhuang, Y.H.; Cai, W.J.; Liu, Y.; Zou, W.B. The mitochondrion interfering compound NPC-26 exerts potent anti-pancreatic cancer cell activity in vitro and in vivo. *Tumour Biol.* **2016**, *37*, 15053–15063. [CrossRef] [PubMed]
46. Chen, Y.; Li, M.; Li, Z.; Gao, P.; Zhou, X.; Zhang, J. Bufalin induces apoptosis in the U2OS human osteosarcoma cell line via triggering the mitochondrial pathway. *Mol. Med. Rep.* **2016**, *13*, 817–822. [CrossRef]
47. Borutaite, V.; Jekabsone, A.; Morkuniene, R.; Brown, G.C. Inhibition of mitochondrial permeability transition prevents mitochondrial dysfunction, cytochrome c release and apoptosis induced by heart ischemia. *J. Mol. Cell. Cardiol.* **2003**, *35*, 357–366. [CrossRef]
48. Precht, T.A.; Phelps, R.A.; Linseman, D.A.; Butts, B.D.; Le, S.S.; Laessig, T.A.; Bouchard, R.J.; Heidenreich, K.A. The permeability transition pore triggers Bax translocation to mitochondria during neuronal apoptosis. *Cell Death Differ.* **2005**, *12*, 255–265. [CrossRef]
49. Karch, J.; Kwong, J.Q.; Burr, A.R.; Sargent, M.A.; Elrod, J.W.; Peixoto, P.M.; Martinez-Caballero, S.; Osinska, H.; Cheng, E.H.; Robbins, J.; et al. Bax and Bak function as the outer membrane component of the mitochondrial permeability pore in regulating necrotic cell death in mice. *eLife* **2013**, *2*, e00772. [CrossRef]
50. Narita, M.; Shimizu, S.; Ito, T.; Chittenden, T.; Lutz, R.J.; Matsuda, H.; Tsujimoto, Y. Bax interacts with the permeability transition pore to induce permeability transition and cytochrome c release in isolated mitochondria. *Proc. Natl. Acad. Sci. USA* **1998**, *95*, 14681–14686. [CrossRef]
51. Scorrano, L.; Ashiya, M.; Buttler, K.; Weiler, S.; Oakes, S.A.; Mannella, C.A.; Korsmeyer, S.J. A distinct pathway remodels mitochondrial cristae and mobilizes cytochrome c during apoptosis. *Dev. Cell* **2002**, *2*, 55–67. [CrossRef]

52. Vander Heiden, M.G.; Chandel, N.S.; Schumacker, P.T.; Thompson, C.B. Bcl-xL prevents cell death following growth factor withdrawal by facilitating mitochondrial ATP/ADP exchange. *Mol. Cell* **1999**, *3*, 159–167. [CrossRef]
53. Belzacq, A.S.; Vieira, H.L.; Verrier, F.; Vandecasteele, G.; Cohen, I.; Prevost, M.C.; Larquet, E.; Pariselli, F.; Petit, P.X.; Kahn, A.; et al. Bcl-2 and Bax modulate adenine nucleotide translocase activity. *Cancer Res.* **2003**, *63*, 541–546. [PubMed]
54. Degterev, A.; Hitomi, J.; Germscheid, M.; Ch'en, I.L.; Korkina, O.; Teng, X.; Abbott, D.; Cuny, G.D.; Yuan, C.; Wagner, G.; et al. Identification of RIP1 kinase as a specific cellular target of necrostatins. *Nat. Chem. Biol.* **2008**, *4*, 313–321. [CrossRef] [PubMed]
55. Sun, X.; Lee, J.; Navas, T.; Baldwin, D.T.; Stewart, T.A.; Dixit, V.M. RIP3, a novel apoptosis-inducing kinase. *J. Biol. Chem.* **1999**, *274*, 16871–16875. [CrossRef]
56. Degterev, A.; Huang, Z.; Boyce, M.; Li, Y.; Jagtap, P.; Mizushima, N.; Cuny, G.D.; Mitchison, T.J.; Moskowitz, M.A.; Yuan, J. Chemical inhibitor of nonapoptotic cell death with therapeutic potential for ischemic brain injury. *Nat. Chem. Biol.* **2005**, *1*, 112–119. [CrossRef]
57. Kokoszka, J.E.; Waymire, K.G.; Levy, S.E.; Slight, J.E.; Cai, J.; Jones, D.P.; MacGregor, G.R.; Wallace, D.C. The ADP/ATP translocator is not essential for the mitochondrial permeability transition pore. *Nature* **2004**, *427*, 461–465. [CrossRef]
58. Temkin, V.; Huang, Q.; Liu, H.; Osada, H.; Pope, R.M. Inhibition of ADP/ATP exchange in receptor-interacting protein-mediated necrosis. *Mol. Cell. Biol.* **2006**, *26*, 2215–2225. [CrossRef]
59. Kroemer, G.; Galluzzi, L.; Vandenabeele, P.; Abrams, J.; Alnemri, E.S.; Baehrecke, E.H.; Blagosklonny, M.V.; El-Deiry, W.S.; Golstein, P.; Green, D.R.; et al. Classification of cell death: Recommendations of the Nomenclature Committee on Cell Death 2009. *Cell Death Differ.* **2009**, *16*, 3–11. [CrossRef]
60. Irrinki, K.M.; Mallilankaraman, K.; Thapa, R.J.; Chandramoorthy, H.C.; Smith, F.J.; Jog, N.R.; Gandhirajan, R.K.; Kelsen, S.G.; Houser, S.R.; May, M.J.; et al. Requirement of FADD, NEMO, and BAX/BAK for aberrant mitochondrial function in tumor necrosis factor alpha-induced necrosis. *Mol. Cell. Biol.* **2011**, *31*, 3745–3758. [CrossRef]
61. Tischner, D.; Manzl, C.; Soratroi, C.; Villunger, A.; Krumschnabel, G. Necrosis-like death can engage multiple pro-apoptotic Bcl-2 protein family members. *Apoptosis* **2012**, *17*, 1197–1209. [CrossRef] [PubMed]
62. Weiner, H. A medicine of human relationships. *Pharos. Alpha Omega Alpha Honor Med. Soc.* **1989**, *52*, 2–6. [PubMed]
63. Krawczak, M.; Bockel, B. The formal analysis of multilocus DNA fingerprints. *EXS* **1993**, *67*, 249–255. [PubMed]
64. Bonora, M.; Wieckowski, M.R.; Sinclair, D.A.; Kroemer, G.; Pinton, P.; Galluzzi, L. Targeting mitochondria for cardiovascular disorders: Therapeutic potential and obstacles. *Nat. Rev. Cardiol.* **2019**, *16*, 33–55. [CrossRef] [PubMed]
65. Wei, C.; Li, H.; Wang, Y.; Peng, X.; Shao, H.; Li, H.; Bai, S.; Xu, C. Exogenous spermine inhibits hypoxia/ischemia-induced myocardial apoptosis via regulation of mitochondrial permeability transition pore and associated pathways. *Exp. Biol. Med. (Maywood)* **2016**, *241*, 1505–1515. [CrossRef]
66. Zahrebelski, G.; Nieminen, A.L.; al-Ghoul, K.; Qian, T.; Herman, B.; Lemasters, J.J. Progression of subcellular changes during chemical hypoxia to cultured rat hepatocytes: A laser scanning confocal microscopic study. *Hepatology* **1995**, *21*, 1361–1372.
67. Fang, Y.D.; Xu, X.; Dang, Y.M.; Zhang, Y.M.; Zhang, J.P.; Hu, J.Y.; Zhang, Q.; Dai, X.; Teng, M.; Zhang, D.X.; et al. MAP4 mechanism that stabilizes mitochondrial permeability transition in hypoxia: Microtubule enhancement and DYNLT1 interaction with VDAC1. *PLoS ONE* **2011**, *6*, e28052. [CrossRef]
68. Soares, R.O.S.; Losada, D.M.; Jordani, M.C.; Evora, P.; Castro, E.S.O. Ischemia/Reperfusion Injury Revisited: An Overview of the Latest Pharmacological Strategies. *Int. J. Mol. Sci.* **2019**, *20*, 5034. [CrossRef]
69. Liu, R.R.; Murphy, T.H. Reversible cyclosporin A-sensitive mitochondrial depolarization occurs within minutes of stroke onset in mouse somatosensory cortex in vivo: A two-photon imaging study. *J. Biol. Chem.* **2009**, *284*, 36109–36117. [CrossRef]
70. Adachi, M.; Takahashi, K.; Nishikawa, M.; Miki, H.; Uyama, M. High intraocular pressure-induced ischemia and reperfusion injury in the optic nerve and retina in rats. *Graefes Arch. Clin. Exp. Ophthalmol.* **1996**, *234*, 445–451. [CrossRef]

71. Hwang, J.H.; Lee, J.H.; Lee, K.H.; Bae, E.J.; Sung, D.K.; Chang, Y.S.; Park, W.S. Cyclosporine A attenuates hypoxic-ischemic brain injury in newborn rats. *Brain Res.* **2010**, *1359*, 208–215. [CrossRef] [PubMed]
72. Ong, S.G.; Lee, W.H.; Theodorou, L.; Kodo, K.; Lim, S.Y.; Shukla, D.H.; Briston, T.; Kiriakidis, S.; Ashcroft, M.; Davidson, S.M.; et al. HIF-1 reduces ischaemia-reperfusion injury in the heart by targeting the mitochondrial permeability transition pore. *Cardiovasc. Res.* **2014**, *104*, 24–36. [CrossRef] [PubMed]
73. Chatterjee, P.K.; Brown, P.A.; Cuzzocrea, S.; Zacharowski, K.; Stewart, K.N.; Mota-Filipe, H.; McDonald, M.C.; Thiemeermann, C. Calpain inhibitor-1 reduces renal ischemia/reperfusion injury in the rat. *Kidney Int.* **2001**, *59*, 2073–2083. [CrossRef] [PubMed]
74. Kalogeris, T.; Baines, C.P.; Krenz, M.; Korthuis, R.J. Ischemia/Reperfusion. *Compr. Physiol.* **2016**, *7*, 113–170. [PubMed]
75. Shintani-Ishida, K.; Yoshida, K. Mitochondrial m-calpain opens the mitochondrial permeability transition pore in ischemia-reperfusion. *Int. J. Cardiol.* **2015**, *197*, 26–32. [CrossRef] [PubMed]
76. Piper, H.M.; Meuter, K.; Schafer, C. Cellular mechanisms of ischemia-reperfusion injury. *Ann. Thorac. Surg.* **2003**, *75*, S644–S648. [CrossRef]
77. Granger, D.N.; Kviety, P.R. Reperfusion injury and reactive oxygen species: The evolution of a concept. *Redox Biol.* **2015**, *6*, 524–551. [CrossRef]
78. Chouchani, E.T.; Pell, V.R.; Gaude, E.; Aksentijevic, D.; Sundier, S.Y.; Robb, E.L.; Logan, A.; Nadtochiy, S.M.; Ord, E.N.J.; Smith, A.C.; et al. Ischaemic accumulation of succinate controls reperfusion injury through mitochondrial ROS. *Nature* **2014**, *515*, 431–435. [CrossRef]
79. Zorov, D.B.; Juhaszova, M.; Sollott, S.J. Mitochondrial reactive oxygen species (ROS) and ROS-induced ROS release. *Physiol. Rev.* **2014**, *94*, 909–950. [CrossRef]
80. Chen, Y.R.; Zweier, J.L. Cardiac mitochondria and reactive oxygen species generation. *Circ. Res.* **2014**, *114*, 524–537. [CrossRef]
81. Barzyc, A.; Lysik, W.; Słyk, J.; Kuszewski, M.; Zarebinski, M.; Wojciechowska, M.; Cudnoch-Jedrzejska, A. Reperfusion injury as a target for diminishing infarct size. *Med. Hypotheses* **2020**, *137*, 109558. [CrossRef] [PubMed]
82. Griffiths, E.J.; Halestrap, A.P. Mitochondrial non-specific pores remain closed during cardiac ischaemia, but open upon reperfusion. *Biochem. J.* **1995**, *307*, 93–98. [CrossRef] [PubMed]
83. Morciano, G.; Bonora, M.; Campo, G.; Aquila, G.; Rizzo, P.; Giorgi, C.; Wieckowski, M.R.; Pinton, P. Mechanistic Role of mPTP in Ischemia-Reperfusion Injury. *Adv. Exp. Med. Biol.* **2017**, *982*, 169–189. [PubMed]
84. Upadhaya, S.; Madala, S.; Baniya, R.; Subedi, S.K.; Saginala, K.; Bachuwa, G. Impact of cyclosporine A use in the prevention of reperfusion injury in acute myocardial infarction: A meta-analysis. *Cardiol. J.* **2017**, *24*, 43–50. [CrossRef] [PubMed]
85. Pottecher, J.; Kindo, M.; Chamaroux-Tran, T.N.; Charles, A.L.; Lejay, A.; Kemmel, V.; Vogel, T.; Chakfe, N.; Zoll, J.; Diemunsch, P.; et al. Skeletal muscle ischemia-reperfusion injury and cyclosporine A in the aging rat. *Fundam. Clin. Pharmacol.* **2016**, *30*, 216–225. [CrossRef] [PubMed]
86. Uchino, H.; Minamikawa-Tachino, R.; Kristian, T.; Perkins, G.; Narazaki, M.; Siesjo, B.K.; Shibasaki, F. Differential neuroprotection by cyclosporin A and FK506 following ischemia corresponds with differing abilities to inhibit calcineurin and the mitochondrial permeability transition. *Neurobiol. Dis.* **2002**, *10*, 219–233. [CrossRef] [PubMed]
87. Konukoglu, D.; Tasci, I.; Cetinkale, O. Effects of cyclosporin A and ibuprofen on liver ischemia-reperfusion injury in the rat. *Clin. Chim. Acta* **1998**, *275*, 1–8. [CrossRef]
88. Li, J.; Yan, Z.; Fang, Q. A Mechanism Study Underlying the Protective Effects of Cyclosporine-A on Lung Ischemia-Reperfusion Injury. *Pharmacology* **2017**, *100*, 83–90. [CrossRef]
89. Yazdani, I.; Majdani, R.; Ghasemnejad-Berenji, M.; Dehpour, A.R. Comparison of multiple doses of cyclosporine A on germ cell apoptosis and epididymal sperm parameters after testicular ischemia/reperfusion in rats. *Exp. Mol. Pathol.* **2019**, *110*, 104271. [CrossRef]
90. Ruiz-Meana, M.; Inserte, J.; Fernandez-Sanz, C.; Hernandez, V.; Miro-Casas, E.; Barba, I.; Garcia-Dorado, D. The role of mitochondrial permeability transition in reperfusion-induced cardiomyocyte death depends on the duration of ischemia. *Basic Res. Cardiol.* **2011**, *106*, 1259–1268. [CrossRef]
91. Imahashi, K.; Pott, C.; Goldhaber, J.I.; Steenbergen, C.; Philipson, K.D.; Murphy, E. Cardiac-specific ablation of the Na⁺-Ca²⁺ exchanger confers protection against ischemia/reperfusion injury. *Circ. Res.* **2005**, *97*, 916–921. [CrossRef] [PubMed]

92. Imahashi, K.; Schneider, M.D.; Steenbergen, C.; Murphy, E. Transgenic expression of Bcl-2 modulates energy metabolism, prevents cytosolic acidification during ischemia, and reduces ischemia/reperfusion injury. *Circ. Res.* **2004**, *95*, 734–741. [CrossRef] [PubMed]
93. Luongo, T.S.; Lambert, J.P.; Gross, P.; Nwokedi, M.; Lombardi, A.A.; Shanmughapriya, S.; Carpenter, A.C.; Kolmetzky, D.; Gao, E.; van Berlo, J.H.; et al. The mitochondrial Na⁺/Ca²⁺ exchanger is essential for Ca²⁺ homeostasis and viability. *Nature* **2017**, *545*, 93–97. [CrossRef] [PubMed]
94. Zhao, Q.; Wang, S.; Li, Y.; Wang, P.; Li, S.; Guo, Y.; Yao, R. The role of the mitochondrial calcium uniporter in cerebral ischemia/reperfusion injury in rats involves regulation of mitochondrial energy metabolism. *Mol. Med. Rep.* **2013**, *7*, 1073–1080. [CrossRef]
95. Luongo, T.S.; Lambert, J.P.; Yuan, A.; Zhang, X.; Gross, P.; Song, J.; Shanmughapriya, S.; Gao, E.; Jain, M.; Houser, S.R.; et al. The Mitochondrial Calcium Uniporter Matches Energetic Supply with Cardiac Workload during Stress and Modulates Permeability Transition. *Cell Rep.* **2015**, *12*, 23–34. [CrossRef]
96. Campo, G.; Morciano, G.; Pavasini, R.; Bonora, M.; Sbrana, L.; Biscaglia, S.; Bovolenta, M.; Pinotti, M.; Punzetti, S.; Rizzo, P.; et al. Fo ATP synthase C subunit serum levels in patients with ST-segment Elevation Myocardial Infarction: Preliminary findings. *Int. J. Cardiol.* **2016**, *221*, 993–997. [CrossRef]
97. Eirin, A.; Li, Z.; Zhang, X.; Krier, J.D.; Woollard, J.R.; Zhu, X.Y.; Tang, H.; Herrmann, S.M.; Lerman, A.; Textor, S.C.; et al. A mitochondrial permeability transition pore inhibitor improves renal outcomes after revascularization in experimental atherosclerotic renal artery stenosis. *Hypertension* **2012**, *60*, 1242–1249. [CrossRef]
98. Tanno, M.; Kuno, A.; Ishikawa, S.; Miki, T.; Kouzu, H.; Yano, T.; Murase, H.; Tobisawa, T.; Ogasawara, M.; Horio, Y.; et al. Translocation of glycogen synthase kinase-3beta (GSK-3beta), a trigger of permeability transition, is kinase activity-dependent and mediated by interaction with voltage-dependent anion channel 2 (VDAC2). *J. Biol. Chem.* **2014**, *289*, 29285–29296. [CrossRef]
99. Bao, H.; Ge, Y.; Zhuang, S.; Dworkin, L.D.; Liu, Z.; Gong, R. Inhibition of glycogen synthase kinase-3beta prevents NSAID-induced acute kidney injury. *Kidney Int.* **2012**, *81*, 662–673. [CrossRef]
100. Wang, Z.; Ge, Y.; Bao, H.; Dworkin, L.; Peng, A.; Gong, R. Redox-sensitive glycogen synthase kinase 3beta-directed control of mitochondrial permeability transition: Rheostatic regulation of acute kidney injury. *Free Radic. Biol. Med.* **2013**, *65*, 849–858. [CrossRef]
101. Linkermann, A.; De Zen, F.; Weinberg, J.; Kunzendorf, U.; Krautwald, S. Programmed necrosis in acute kidney injury. *Nephrol. Dial. Transplant. Off. Publ. Eur. Dial. Transpl. Assoc. Eur. Ren. Assoc.* **2012**, *27*, 3412–3419. [CrossRef] [PubMed]
102. Linkermann, A.; Brasen, J.H.; Darding, M.; Jin, M.K.; Sanz, A.B.; Heller, J.O.; De Zen, F.; Weinlich, R.; Ortiz, A.; Walczak, H.; et al. Two independent pathways of regulated necrosis mediate ischemia-reperfusion injury. *Proc. Natl. Acad. Sci. USA* **2013**, *110*, 12024–12029. [CrossRef] [PubMed]
103. Mulay, S.R.; Honarpisheh, M.M.; Foresto-Neto, O.; Shi, C.; Desai, J.; Zhao, Z.B.; Marschner, J.A.; Popper, B.; Buhl, E.M.; Boor, P.; et al. Mitochondria Permeability Transition versus Necroptosis in Oxalate-Induced AKI. *J. Am. Soc. Nephrol.* **2019**, *30*, 1857–1869. [CrossRef] [PubMed]
104. Du, H.; Guo, L.; Fang, F.; Chen, D.; Sosunov, A.A.; McKhann, G.M.; Yan, Y.; Wang, C.; Zhang, H.; Molkentin, J.D.; et al. Cyclophilin D deficiency attenuates mitochondrial and neuronal perturbation and ameliorates learning and memory in Alzheimer’s disease. *Nat. Med.* **2008**, *14*, 1097–1105. [CrossRef]
105. Manczak, M.; Reddy, P.H. Abnormal interaction of VDAC1 with amyloid beta and phosphorylated tau causes mitochondrial dysfunction in Alzheimer’s disease. *Hum. Mol. Genet.* **2012**, *21*, 5131–5146. [CrossRef]
106. Devi, L.; Raghavendran, V.; Prabhu, B.M.; Avadhani, N.G.; Anandatheerthavarada, H.K. Mitochondrial import and accumulation of alpha-synuclein impair complex I in human dopaminergic neuronal cultures and Parkinson disease brain. *J. Biol. Chem.* **2008**, *283*, 9089–9100. [CrossRef]
107. Yao, J.; Du, H.; Yan, S.; Fang, F.; Wang, C.; Lue, L.F.; Guo, L.; Chen, D.; Stern, D.M.; Gunn Moore, F.J.; et al. Inhibition of amyloid-beta (Abeta) peptide-binding alcohol dehydrogenase-Abeta interaction reduces Abeta accumulation and improves mitochondrial function in a mouse model of Alzheimer’s disease. *J. Neurosci.* **2011**, *31*, 2313–2320. [CrossRef]
108. Liu, G.; Zhang, C.; Yin, J.; Li, X.; Cheng, F.; Li, Y.; Yang, H.; Ueda, K.; Chan, P.; Yu, S. alpha-Synuclein is differentially expressed in mitochondria from different rat brain regions and dose-dependently down-regulates complex I activity. *Neurosci. Lett.* **2009**, *454*, 187–192. [CrossRef]

109. Zhu, Y.; Duan, C.; Lu, L.; Gao, H.; Zhao, C.; Yu, S.; Ueda, K.; Chan, P.; Yang, H. alpha-Synuclein overexpression impairs mitochondrial function by associating with adenylate translocator. *Int. J. Biochem. Cell Biol.* **2011**, *43*, 732–741. [CrossRef]
110. Tillement, L.; Lecanu, L.; Yao, W.; Greenson, J.; Papadopoulos, V. The spirostenol (22R, 25R)-20alpha-spirost-5-en-3beta-yl hexanoate blocks mitochondrial uptake of Abeta in neuronal cells and prevents Abeta-induced impairment of mitochondrial function. *Steroids* **2006**, *71*, 725–735. [CrossRef]
111. Hou, Y.; Ghosh, P.; Wan, R.; Ouyang, X.; Cheng, H.; Mattson, M.P.; Cheng, A. Permeability transition pore-mediated mitochondrial superoxide flashes mediate an early inhibitory effect of amyloid beta1-42 on neural progenitor cell proliferation. *Neurobiol. Aging* **2014**, *35*, 975–989. [CrossRef] [PubMed]
112. Xie, H.; Guan, J.; Borrelli, L.A.; Xu, J.; Serrano-Pozo, A.; Bacskai, B.J. Mitochondrial alterations near amyloid plaques in an Alzheimer’s disease mouse model. *J. Neurosci.* **2013**, *33*, 17042–17051. [CrossRef] [PubMed]
113. Atlante, A.; Amadoro, G.; Bobba, A.; de Bari, L.; Corsetti, V.; Pappalardo, G.; Marra, E.; Calissano, P.; Passarella, S. A peptide containing residues 26–44 of tau protein impairs mitochondrial oxidative phosphorylation acting at the level of the adenine nucleotide translocator. *Biochim. Biophys. Acta* **2008**, *1777*, 1289–1300. [CrossRef] [PubMed]
114. Ludtmann, M.H.R.; Angelova, P.R.; Horrocks, M.H.; Choi, M.L.; Rodrigues, M.; Baev, A.Y.; Berezhnov, A.V.; Yao, Z.; Little, D.; Banushi, B.; et al. Alpha-synuclein oligomers interact with ATP synthase and open the permeability transition pore in Parkinson’s disease. *Nat. Commun.* **2018**, *9*, 2293. [CrossRef] [PubMed]
115. Martin, L.J.; Semenkov, S.; Hanaford, A.; Wong, M. Mitochondrial permeability transition pore regulates Parkinson’s disease development in mutant alpha-synuclein transgenic mice. *Neurobiol. Aging* **2014**, *35*, 1132–1152. [CrossRef] [PubMed]
116. Giaime, E.; Yamaguchi, H.; Gautier, C.A.; Kitada, T.; Shen, J. Loss of DJ-1 does not affect mitochondrial respiration but increases ROS production and mitochondrial permeability transition pore opening. *PLoS ONE* **2012**, *7*, e40501. [CrossRef]
117. Gandhi, S.; Wood-Kaczmar, A.; Yao, Z.; Plun-Favreau, H.; Deas, E.; Klupsch, K.; Downward, J.; Latchman, D.S.; Tabrizi, S.J.; Wood, N.W.; et al. PINK1-associated Parkinson’s disease is caused by neuronal vulnerability to calcium-induced cell death. *Mol. Cell* **2009**, *33*, 627–638. [CrossRef]
118. Cui, T.; Fan, C.; Gu, L.; Gao, H.; Liu, Q.; Zhang, T.; Qi, Z.; Zhao, C.; Zhao, H.; Cai, Q.; et al. Silencing of PINK1 induces mitophagy via mitochondrial permeability transition in dopaminergic MN9D cells. *Brain Res.* **2011**, *1394*, 1–13. [CrossRef]
119. Gautier, C.A.; Giaime, E.; Caballero, E.; Nunez, L.; Song, Z.; Chan, D.; Villalobos, C.; Shen, J. Regulation of mitochondrial permeability transition pore by PINK1. *Mol. Neurodegener.* **2012**, *7*, 22. [CrossRef]
120. Dagda, R.K.; Das Banerjee, T.; Janda, E. How Parkinsonian toxins dysregulate the autophagy machinery. *Int. J. Mol. Sci.* **2013**, *14*, 22163–22189. [CrossRef]
121. Rasheed, M.Z.; Tabassum, H.; Parvez, S. Mitochondrial permeability transition pore: A promising target for the treatment of Parkinson’s disease. *Protoplasma* **2017**, *254*, 33–42. [CrossRef] [PubMed]
122. Geisler, S.; Holmstrom, K.M.; Skujat, D.; Fiesel, F.C.; Rothfuss, O.C.; Kahle, P.J.; Springer, W. PINK1/Parkin-mediated mitophagy is dependent on VDAC1 and p62/SQSTM1. *Nat. Cell Biol.* **2010**, *12*, 119–131. [CrossRef] [PubMed]
123. Hoshino, A.; Wang, W.J.; Wada, S.; McDermott-Roe, C.; Evans, C.S.; Gosis, B.; Morley, M.P.; Rathi, K.S.; Li, J.; Li, K.; et al. The ADP/ATP translocase drives mitophagy independent of nucleotide exchange. *Nature* **2019**, *575*, 375–379. [CrossRef] [PubMed]
124. Castellazzi, M.; Patergnani, S.; Donadio, M.; Giorgi, C.; Bonora, M.; Bosi, C.; Brombo, G.; Pugliatti, M.; Seripa, D.; Zuliani, G.; et al. Autophagy and mitophagy biomarkers are reduced in sera of patients with Alzheimer’s disease and mild cognitive impairment. *Sci. Rep.* **2019**, *9*, 20009. [CrossRef] [PubMed]
125. Du, F.; Yu, Q.; Yan, S.; Hu, G.; Lue, L.F.; Walker, D.G.; Wu, L.; Yan, S.F.; Tieu, K.; Yan, S.S. PINK1 signalling rescues amyloid pathology and mitochondrial dysfunction in Alzheimer’s disease. *Brain* **2017**, *140*, 3233–3251. [CrossRef] [PubMed]
126. Fang, E.F.; Hou, Y.; Palikaras, K.; Adriaanse, B.A.; Kerr, J.S.; Yang, B.; Lautrup, S.; Hasan-Olive, M.M.; Caponio, D.; Dan, X.; et al. Mitophagy inhibits amyloid-beta and tau pathology and reverses cognitive deficits in models of Alzheimer’s disease. *Nat. Neurosci.* **2019**, *22*, 401–412. [CrossRef] [PubMed]

127. Martin, L.J.; Gertz, B.; Pan, Y.; Price, A.C.; Molkentin, J.D.; Chang, Q. The mitochondrial permeability transition pore in motor neurons: Involvement in the pathobiology of ALS mice. *Exp. Neurol.* **2009**, *218*, 333–346. [CrossRef]
128. Martin, L.J.; Fancelli, D.; Wong, M.; Niedzwiecki, M.; Ballarini, M.; Plyte, S.; Chang, Q. GNX-4728, a novel small molecule drug inhibitor of mitochondrial permeability transition, is therapeutic in a mouse model of amyotrophic lateral sclerosis. *Front. Cell Neurosci.* **2014**, *8*, 433. [CrossRef]
129. Weber, J.J.; Clemensson, L.E.; Schioth, H.B.; Nguyen, H.P. Olesoxime in neurodegenerative diseases: Scrutinising a promising drug candidate. *Biochem. Pharmacol.* **2019**, *168*, 305–318. [CrossRef]
130. Bordet, T.; Berna, P.; Abitbol, J.L.; Pruss, R.M. Olesoxime (TRO19622): A Novel Mitochondrial-Targeted Neuroprotective Compound. *Pharmaceuticals.* **2010**, *3*, 345–368. [CrossRef]
131. Okada, M.; Yamashita, S.; Ueyama, H.; Ishizaki, M.; Maeda, Y.; Ando, Y. Long-term effects of edaravone on survival of patients with amyotrophic lateral sclerosis. *eNeurologicalSci* **2018**, *11*, 11–14. [CrossRef] [PubMed]
132. Patergnani, S.; Fossati, V.; Bonora, M.; Giorgi, C.; Marchi, S.; Missiroli, S.; Rusielewicz, T.; Wieckowski, M.R.; Pinton, P. Mitochondria in Multiple Sclerosis: Molecular Mechanisms of Pathogenesis. *Int. Rev. Cell Mol. Biol.* **2017**, *328*, 49–103. [PubMed]
133. Mahad, D.; Ziabreva, I.; Lassmann, H.; Turnbull, D. Mitochondrial defects in acute multiple sclerosis lesions. *Brain* **2008**, *131*, 1722–1735. [CrossRef] [PubMed]
134. Inarrea, P.; Alarcia, R.; Alava, M.A.; Capablo, J.L.; Casanova, A.; Iniguez, C.; Iturralde, M.; Larrode, P.; Martin, J.; Mostacero, E.; et al. Mitochondrial complex enzyme activities and cytochrome C expression changes in multiple sclerosis. *Mol. Neurobiol.* **2014**, *49*, 1–9. [CrossRef] [PubMed]
135. Bonora, M.; De Marchi, E.; Patergnani, S.; Suski, J.M.; Celsi, F.; Bononi, A.; Giorgi, C.; Marchi, S.; Rimessi, A.; Duszynski, J.; et al. Tumor necrosis factor-alpha impairs oligodendroglial differentiation through a mitochondria-dependent process. *Cell Death Differ.* **2014**, *21*, 1198–1208. [CrossRef]
136. Tranah, G.J.; Santaniello, A.; Caillier, S.J.; D’Alfonso, S.; Martinelli Boneschi, F.; Hauser, S.L.; Oksenberg, J.R. Mitochondrial DNA sequence variation in multiple sclerosis. *Neurology* **2015**, *85*, 325–330. [CrossRef]
137. Castellazzi, M.; Patergnani, S.; Donadio, M.; Giorgi, C.; Bonora, M.; Fainardi, E.; Casetta, I.; Granieri, E.; Pugliatti, M.; Pinton, P. Correlation between auto/mitophagic processes and magnetic resonance imaging activity in multiple sclerosis patients. *J. Neuroinflammation* **2019**, *16*, 131. [CrossRef]
138. Patergnani, S.; Castellazzi, M.; Bonora, M.; Marchi, S.; Casetta, I.; Pugliatti, M.; Giorgi, C.; Granieri, E.; Pinton, P. Autophagy and mitophagy elements are increased in body fluids of multiple sclerosis-affected individuals. *J. Neurol. Neurosurg. Psychiatry* **2018**, *89*, 439–441. [CrossRef]
139. Barcelos, I.P.; Troxell, R.M.; Graves, J.S. Mitochondrial Dysfunction and Multiple Sclerosis. *Biology* **2019**, *8*, 37. [CrossRef]
140. Su, K.; Bourdette, D.; Forte, M. Mitochondrial dysfunction and neurodegeneration in multiple sclerosis. *Front. Physiol.* **2013**, *4*, 169. [CrossRef]
141. Forte, M.; Gold, B.G.; Marracci, G.; Chaudhary, P.; Basso, E.; Johnsen, D.; Yu, X.; Fowlkes, J.; Rahder, M.; Stem, K.; et al. Cyclophilin D inactivation protects axons in experimental autoimmune encephalomyelitis, an animal model of multiple sclerosis. *Proc. Natl. Acad. Sci. USA* **2007**, *104*, 7558–7563. [CrossRef] [PubMed]
142. Warne, J.; Pryce, G.; Hill, J.M.; Shi, X.; Lenneras, F.; Puentes, F.; Kip, M.; Hilditch, L.; Walker, P.; Simone, M.I.; et al. Selective Inhibition of the Mitochondrial Permeability Transition Pore Protects against Neurodegeneration in Experimental Multiple Sclerosis. *J. Biol. Chem.* **2016**, *291*, 4356–4373. [CrossRef] [PubMed]
143. Pinton, P.; Rimessi, A.; Marchi, S.; Orsini, F.; Migliaccio, E.; Giorgi, M.; Contursi, C.; Minucci, S.; Mantovani, F.; Wieckowski, M.R.; et al. Protein kinase C beta and prolyl isomerase 1 regulate mitochondrial effects of the life-span determinant p66Shc. *Science* **2007**, *315*, 659–663. [CrossRef] [PubMed]
144. Patergnani, S.; Marchi, S.; Rimessi, A.; Bonora, M.; Giorgi, C.; Mehta, K.D.; Pinton, P. PRKCB/protein kinase C, beta and the mitochondrial axis as key regulators of autophagy. *Autophagy* **2013**, *9*, 1367–1385. [CrossRef]
145. Su, K.G.; Savino, C.; Marracci, G.; Chaudhary, P.; Yu, X.; Morris, B.; Galipeau, D.; Giorgi, M.; Forte, M.; Bourdette, D. Genetic inactivation of the p66 isoform of ShcA is neuroprotective in a murine model of multiple sclerosis. *Eur. J. Neurosci.* **2012**, *35*, 562–571. [CrossRef]
146. Savino, C.; Pelicci, P.; Giorgi, M. The P66Shc/mitochondrial permeability transition pore pathway determines neurodegeneration. *Oxidative Med. Cell. Longev.* **2013**, *2013*, 719407. [CrossRef]
147. Burr, A.R.; Molkentin, J.D. Genetic evidence in the mouse solidifies the calcium hypothesis of myofiber death in muscular dystrophy. *Cell Death Differ.* **2015**, *22*, 1402–1412. [CrossRef]

148. Emery, A.E. The muscular dystrophies. *Lancet* **2002**, *359*, 687–695. [CrossRef]
149. Tabebordbar, M.; Wang, E.T.; Wagers, A.J. Skeletal muscle degenerative diseases and strategies for therapeutic muscle repair. *Annu. Rev. Pathol.* **2013**, *8*, 441–475. [CrossRef]
150. Emery, A.E. Population frequencies of inherited neuromuscular diseases—a world survey. *Neuromuscul. Disord.* **1991**, *1*, 19–29. [CrossRef]
151. Durbeej, M.; Campbell, K.P. Muscular dystrophies involving the dystrophin-glycoprotein complex: An overview of current mouse models. *Curr. Opin. Genet. Dev.* **2002**, *12*, 349–361. [CrossRef]
152. Ervasti, J.M.; Campbell, K.P. A role for the dystrophin-glycoprotein complex as a transmembrane linker between laminin and actin. *J. Cell Biol.* **1993**, *122*, 809–823. [CrossRef] [PubMed]
153. Jung, C.; Martins, A.S.; Niggli, E.; Shirokova, N. Dystrophic cardiomyopathy: Amplification of cellular damage by Ca²⁺ signalling and reactive oxygen species-generating pathways. *Cardiovasc. Res.* **2008**, *77*, 766–773. [CrossRef] [PubMed]
154. Hoffman, E.P.; Monaco, A.P.; Feener, C.C.; Kunkel, L.M. Conservation of the Duchenne muscular dystrophy gene in mice and humans. *Science* **1987**, *238*, 347–350. [CrossRef]
155. Dubinin, M.V.; Talanov, E.Y.; Tenkov, K.S.; Starinets, V.S.; Mikheeva, I.B.; Sharapov, M.G.; Belosludtsev, K.N. Duchenne muscular dystrophy is associated with the inhibition of calcium uniport in mitochondria and an increased sensitivity of the organelles to the calcium-induced permeability transition. *Biochim. Biophys. Acta Mol. Basis Dis.* **2020**, *1866*, 165674. [CrossRef]
156. Giacomotto, J.; Brouilly, N.; Walter, L.; Mariol, M.C.; Berger, J.; Segalat, L.; Becker, T.S.; Currie, P.D.; Gieseler, K. Chemical genetics unveils a key role of mitochondrial dynamics, cytochrome c release and IP3R activity in muscular dystrophy. *Hum. Mol. Genet.* **2013**, *22*, 4562–4578. [CrossRef]
157. Stupka, N.; Gregorevic, P.; Plant, D.R.; Lynch, G.S. The calcineurin signal transduction pathway is essential for successful muscle regeneration in mdx dystrophic mice. *Acta Neuropathol.* **2004**, *107*, 299–310. [CrossRef]
158. Chakkalakal, J.V.; Harrison, M.A.; Carbonetto, S.; Chin, E.; Michel, R.N.; Jasmin, B.J. Stimulation of calcineurin signaling attenuates the dystrophic pathology in mdx mice. *Hum. Mol. Genet.* **2004**, *13*, 379–388. [CrossRef]
159. Reutenauer, J.; Dorchies, O.M.; Patthey-Vuadens, O.; Vuagniaux, G.; Ruegg, U.T. Investigation of Debio 025, a cyclophilin inhibitor, in the dystrophic mdx mouse, a model for Duchenne muscular dystrophy. *Br. J. Pharmacol.* **2008**, *155*, 574–584. [CrossRef]
160. Millay, D.P.; Sargent, M.A.; Osinska, H.; Baines, C.P.; Barton, E.R.; Vuagniaux, G.; Sweeney, H.L.; Robbins, J.; Molkentin, J.D. Genetic and pharmacologic inhibition of mitochondrial-dependent necrosis attenuates muscular dystrophy. *Nat. Med.* **2008**, *14*, 442–447. [CrossRef]
161. Palma, E.; Tiepolo, T.; Angelin, A.; Sabatelli, P.; Maraldi, N.M.; Basso, E.; Forte, M.A.; Bernardi, P.; Bonaldo, P. Genetic ablation of cyclophilin D rescues mitochondrial defects and prevents muscle apoptosis in collagen VI myopathic mice. *Hum. Mol. Genet.* **2009**, *18*, 2024–2031. [CrossRef] [PubMed]
162. Lampe, A.K.; Bushby, K.M. Collagen VI related muscle disorders. *J. Med. Genet.* **2005**, *42*, 673–685. [CrossRef] [PubMed]
163. Merlini, L.; Martoni, E.; Grumati, P.; Sabatelli, P.; Squarzoni, S.; Urciuolo, A.; Ferlini, A.; Gualandi, F.; Bonaldo, P. Autosomal recessive myosclerosis myopathy is a collagen VI disorder. *Neurology* **2008**, *71*, 1245–1253. [CrossRef] [PubMed]
164. Bernardi, P.; Krauskopf, A.; Basso, E.; Petronilli, V.; Blachly-Dyson, E.; Di Lisa, F.; Forte, M.A. The mitochondrial permeability transition from in vitro artifact to disease target. *FEBS J.* **2006**, *273*, 2077–2099. [CrossRef] [PubMed]
165. Bonaldo, P.; Braghetta, P.; Zanetti, M.; Piccolo, S.; Volpin, D.; Bressan, G.M. Collagen VI deficiency induces early onset myopathy in the mouse: An animal model for Bethlem myopathy. *Hum. Mol. Genet.* **1998**, *7*, 2135–2140. [CrossRef]
166. Irwin, W.A.; Bergamin, N.; Sabatelli, P.; Reggiani, C.; Megighian, A.; Merlini, L.; Braghetta, P.; Columbaro, M.; Volpin, D.; Bressan, G.M.; et al. Mitochondrial dysfunction and apoptosis in myopathic mice with collagen VI deficiency. *Nat. Genet.* **2003**, *35*, 367–371. [CrossRef]
167. Angelin, A.; Tiepolo, T.; Sabatelli, P.; Grumati, P.; Bergamin, N.; Golfieri, C.; Mattioli, E.; Gualandi, F.; Ferlini, A.; Merlini, L.; et al. Mitochondrial dysfunction in the pathogenesis of Ullrich congenital muscular dystrophy and prospective therapy with cyclosporins. *Proc. Natl. Acad. Sci. USA* **2007**, *104*, 991–996. [CrossRef]

168. Tagliavini, F.; Sardone, F.; Squarzoni, S.; Maraldi, N.M.; Merlini, L.; Faldini, C.; Sabatelli, P. Ultrastructural changes in muscle cells of patients with collagen VI-related myopathies. *Muscles Ligaments Tendons J.* **2013**, *3*, 281–286. [CrossRef]
169. De Palma, C.; Morisi, F.; Cheli, S.; Pambianco, S.; Cappello, V.; Vezzoli, M.; Rovere-Querini, P.; Moggio, M.; Ripolone, M.; Francolini, M.; et al. Autophagy as a new therapeutic target in Duchenne muscular dystrophy. *Cell Death Dis.* **2012**, *3*, e418. [CrossRef]
170. Wong, A.; Cortopassi, G. mtDNA mutations confer cellular sensitivity to oxidant stress that is partially rescued by calcium depletion and cyclosporin A. *Biochem. Biophys. Res. Commun.* **1997**, *239*, 139–145. [CrossRef]
171. Haroon, M.F.; Fatima, A.; Scholer, S.; Gieseler, A.; Horn, T.F.; Kirches, E.; Wolf, G.; Kreutzmann, P. Minocycline, a possible neuroprotective agent in Leber’s hereditary optic neuropathy (LHON): Studies of cybrid cells bearing 11,778 mutation. *Neurobiol. Dis.* **2007**, *28*, 237–250. [CrossRef]
172. Cotan, D.; Cordero, M.D.; Garrido-Maraver, J.; Oropesa-Avila, M.; Rodriguez-Hernandez, A.; Gomez Izquierdo, L.; De la Mata, M.; De Miguel, M.; Lorite, J.B.; Infante, E.R.; et al. Secondary coenzyme Q10 deficiency triggers mitochondria degradation by mitophagy in MELAS fibroblasts. *FASEB J.* **2011**, *25*, 2669–2687. [CrossRef] [PubMed]
173. Cui, J.; Wang, L.; Ren, X.; Zhang, Y.; Zhang, H. LRPPRC: A Multifunctional Protein Involved in Energy Metabolism and Human Disease. *Front. Physiol.* **2019**, *10*, 595. [CrossRef] [PubMed]
174. Burelle, Y.; Bemeur, C.; Rivard, M.E.; Thompson Legault, J.; Boucher, G.; Consortium, L.; Morin, C.; Coderre, L.; Des Rosiers, C. Mitochondrial vulnerability and increased susceptibility to nutrient-induced cytotoxicity in fibroblasts from leigh syndrome French canadian patients. *PLoS ONE* **2015**, *10*, e0120767. [CrossRef] [PubMed]
175. MacVicar, T.; Langer, T. OPA1 processing in cell death and disease—The long and short of it. *J. Cell Sci.* **2016**, *129*, 2297–2306. [CrossRef]
176. Pfeffer, G.; Gorman, G.S.; Griffin, H.; Kurzawa-Akanbi, M.; Blakely, E.L.; Wilson, I.; Sitarz, K.; Moore, D.; Murphy, J.L.; Alston, C.L.; et al. Mutations in the SPG7 gene cause chronic progressive external ophthalmoplegia through disordered mitochondrial DNA maintenance. *Brain* **2014**, *137*, 1323–1336. [CrossRef]
177. Piquereau, J.; Caffin, F.; Novotova, M.; Prola, A.; Garnier, A.; Mateo, P.; Fortin, D.; Huynh le, H.; Nicolas, V.; Alavi, M.V.; et al. Down-regulation of OPA1 alters mouse mitochondrial morphology, PTP function, and cardiac adaptation to pressure overload. *Cardiovasc. Res.* **2012**, *94*, 408–417. [CrossRef]
178. Shanmughapriya, S.; Rajan, S.; Hoffman, N.E.; Higgins, A.M.; Tomar, D.; Nemani, N.; Hines, K.J.; Smith, D.J.; Eguchi, A.; Vallem, S.; et al. SPG7 Is an Essential and Conserved Component of the Mitochondrial Permeability Transition Pore. *Mol. Cell* **2015**, *60*, 47–62. [CrossRef]
179. Zhang, D.; Lu, C.; Whiteman, M.; Chance, B.; Armstrong, J.S. The mitochondrial permeability transition regulates cytochrome c release for apoptosis during endoplasmic reticulum stress by remodeling the cristae junction. *J. Biol. Chem.* **2008**, *283*, 3476–3486. [CrossRef]
180. Hurst, S.; Baggett, A.; Csordas, G.; Sheu, S.S. SPG7 targets the m-AAA protease complex to process MCU for uniporter assembly, Ca(2+) influx, and regulation of mitochondrial permeability transition pore opening. *J. Biol. Chem.* **2019**, *294*, 10807–10818. [CrossRef]
181. Wong, R.J.; Cheung, R.; Ahmed, A. Nonalcoholic steatohepatitis is the most rapidly growing indication for liver transplantation in patients with hepatocellular carcinoma in the U.S. *Hepatology* **2014**, *59*, 2188–2195. [CrossRef] [PubMed]
182. Gastaldelli, A.; Kozakova, M.; Hojlund, K.; Flyvbjerg, A.; Favuzzi, A.; Mitrakou, A.; Balkau, B.; Investigators, R. Fatty liver is associated with insulin resistance, risk of coronary heart disease, and early atherosclerosis in a large European population. *Hepatology* **2009**, *49*, 1537–1544. [CrossRef] [PubMed]
183. Teodoro, J.S.; Rolo, A.P.; Duarte, F.V.; Simoes, A.M.; Palmeira, C.M. Differential alterations in mitochondrial function induced by a choline-deficient diet: Understanding fatty liver disease progression. *Mitochondrion* **2008**, *8*, 367–376. [CrossRef] [PubMed]
184. Chen, D.F.; Wang, C.H. The relationship between the opening of mitochondrial permeability transition pores of cultured hepatocytes with their apoptoses in a non-alcoholic fatty liver disease model. *Chin. J. Hepatol.* **2007**, *15*, 837–839.
185. Kang, M.; Li, S.; Zhong, D.; Yang, Z.; Li, P. Hepatocyte apoptosis and mitochondrial permeability transition pore opening in rats with nonalcoholic fatty liver. *J. South. Med Univ.* **2013**, *33*, 1062–1066.

186. Wang, X.; Du, H.; Shao, S.; Bo, T.; Yu, C.; Chen, W.; Zhao, L.; Li, Q.; Wang, L.; Liu, X.; et al. Cyclophilin D deficiency attenuates mitochondrial perturbation and ameliorates hepatic steatosis. *Hepatology* **2018**, *68*, 62–77. [CrossRef]
187. Lazarin Mde, O.; Ishii-Iwamoto, E.L.; Yamamoto, N.S.; Constantin, R.P.; Garcia, R.F.; da Costa, C.E.; Vitoriano Ade, S.; de Oliveira, M.C.; Salgueiro-Pagadigorria, C.L. Liver mitochondrial function and redox status in an experimental model of non-alcoholic fatty liver disease induced by monosodium L-glutamate in rats. *Exp. Mol. Pathol.* **2011**, *91*, 687–694. [CrossRef]
188. Rimessi, A.; Marchi, S.; Patergnani, S.; Pinton, P. H-Ras-driven tumoral maintenance is sustained through caveolin-1-dependent alterations in calcium signaling. *Oncogene* **2014**, *33*, 2329–2340. [CrossRef]
189. Arbel, N.; Ben-Hail, D.; Shoshan-Barmatz, V. Mediation of the antiapoptotic activity of Bcl-xL protein upon interaction with VDAC1 protein. *J. Biol. Chem.* **2012**, *287*, 23152–23161. [CrossRef]
190. Alavian, K.N.; Li, H.; Collis, L.; Bonanni, L.; Zeng, L.; Sacchetti, S.; Lazrove, E.; Nabili, P.; Flaherty, B.; Graham, M.; et al. Bcl-xL regulates metabolic efficiency of neurons through interaction with the mitochondrial F1FO ATP synthase. *Nat. Cell Biol.* **2011**, *13*, 1224–1233. [CrossRef]
191. Bittremieux, M.; Parys, J.B.; Pinton, P.; Bultynck, G. ER functions of oncogenes and tumor suppressors: Modulators of intracellular Ca(2+) signaling. *Biochim. Biophys. Acta* **2016**, *1863*, 1364–1378. [CrossRef] [PubMed]
192. Marchi, S.; Marinello, M.; Bononi, A.; Bonora, M.; Giorgi, C.; Rimessi, A.; Pinton, P. Selective modulation of subtype III IP(3)R by Akt regulates ER Ca(2)(+) release and apoptosis. *Cell Death Dis.* **2012**, *3*, e304. [CrossRef] [PubMed]
193. Marchi, S.; Rimessi, A.; Giorgi, C.; Baldini, C.; Ferroni, L.; Rizzuto, R.; Pinton, P. Akt kinase reducing endoplasmic reticulum Ca2+ release protects cells from Ca2+-dependent apoptotic stimuli. *Biochem. Biophys. Res. Commun.* **2008**, *375*, 501–505. [CrossRef] [PubMed]
194. Papa, A.; Wan, L.; Bonora, M.; Salmena, L.; Song, M.S.; Hobbs, R.M.; Lunardi, A.; Webster, K.; Ng, C.; Newton, R.H.; et al. Cancer-associated PTEN mutants act in a dominant-negative manner to suppress PTEN protein function. *Cell* **2014**, *157*, 595–610. [CrossRef]
195. Bononi, A.; Bonora, M.; Marchi, S.; Missiroli, S.; Poletti, F.; Giorgi, C.; Pandolfi, P.P.; Pinton, P. Identification of PTEN at the ER and MAMs and its regulation of Ca(2+) signaling and apoptosis in a protein phosphatase-dependent manner. *Cell Death Differ.* **2013**, *20*, 1631–1643. [CrossRef]
196. Bononi, A.; Agnoletto, C.; De Marchi, E.; Marchi, S.; Patergnani, S.; Bonora, M.; Giorgi, C.; Missiroli, S.; Poletti, F.; Rimessi, A.; et al. Protein kinases and phosphatases in the control of cell fate. *Enzym. Res.* **2011**, *2011*, 329098. [CrossRef]
197. Missiroli, S.; Bonora, M.; Patergnani, S.; Giorgi, C. Novel function of the tumor suppressor PML at ER-mitochondria sites in the control of autophagy. *Oncotarget* **2017**, *8*, 81723–81724. [CrossRef]
198. Missiroli, S.; Bonora, M.; Patergnani, S.; Poletti, F.; Perrone, M.; Gafa, R.; Magri, E.; Raimondi, A.; Lanza, G.; Tacchetti, C.; et al. PML at Mitochondria-Associated Membranes Is Critical for the Repression of Autophagy and Cancer Development. *Cell Rep.* **2016**, *16*, 2415–2427. [CrossRef]
199. Giorgi, C.; Ito, K.; Lin, H.K.; Santangelo, C.; Wieckowski, M.R.; Lebedzinska, M.; Bononi, A.; Bonora, M.; Duszynski, J.; Bernardi, R.; et al. PML regulates apoptosis at endoplasmic reticulum by modulating calcium release. *Science* **2010**, *330*, 1247–1251. [CrossRef]
200. Luo, J. Glycogen synthase kinase 3beta (GSK3beta) in tumorigenesis and cancer chemotherapy. *Cancer Lett.* **2009**, *273*, 194–200. [CrossRef]
201. Giorgi, C.; Bonora, M.; Missiroli, S.; Morganti, C.; Morciano, G.; Wieckowski, M.R.; Pinton, P. Alterations in Mitochondrial and Endoplasmic Reticulum Signaling by p53 Mutants. *Front. Oncol.* **2016**, *6*, 42. [CrossRef] [PubMed]
202. Giorgi, C.; Bonora, M.; Sorrentino, G.; Missiroli, S.; Poletti, F.; Suski, J.M.; Galindo Ramirez, F.; Rizzuto, R.; Di Virgilio, F.; Zito, E.; et al. p53 at the endoplasmic reticulum regulates apoptosis in a Ca²⁺-dependent manner. *Proc. Natl. Acad. Sci. USA* **2015**, *112*, 1779–1784. [CrossRef] [PubMed]
203. Bonora, M.; Giorgi, C.; Pinton, P. Novel frontiers in calcium signaling: A possible target for chemotherapy. *Pharmacol. Res.* **2015**, *99*, 82–85. [CrossRef]
204. Giorgi, C.; Bonora, M.; Pinton, P. Inside the tumor: p53 modulates calcium homeostasis. *Cell Cycle* **2015**, *14*, 933–934. [CrossRef] [PubMed]

205. Giorgi, C.; Bonora, M.; Missiroli, S.; Poletti, F.; Ramirez, F.G.; Morciano, G.; Morganti, C.; Pandolfi, P.P.; Mammano, F.; Pinton, P. Intravital imaging reveals p53-dependent cancer cell death induced by phototherapy via calcium signaling. *Oncotarget* **2015**, *6*, 1435–1445. [CrossRef]
206. Kang, B.H.; Plescia, J.; Dohi, T.; Rosa, J.; Doxsey, S.J.; Altieri, D.C. Regulation of tumor cell mitochondrial homeostasis by an organelle-specific Hsp90 chaperone network. *Cell* **2007**, *131*, 257–270. [CrossRef]
207. Ghosh, J.C.; Siegelin, M.D.; Dohi, T.; Altieri, D.C. Heat shock protein 60 regulation of the mitochondrial permeability transition pore in tumor cells. *Cancer Res.* **2010**, *70*, 8988–8993. [CrossRef]
208. Sinha, D.; D’Silva, P. Chaperoning mitochondrial permeability transition: Regulation of transition pore complex by a J-protein, DnaJC15. *Cell Death Dis.* **2014**, *5*, e1101. [CrossRef]
209. Aggarwal, V.; Tuli, H.S.; Varol, A.; Thakral, F.; Yerer, M.B.; Sak, K.; Varol, M.; Jain, A.; Khan, M.A.; Sethi, G. Role of Reactive Oxygen Species in Cancer Progression: Molecular Mechanisms and Recent Advancements. *Biomolecules* **2019**, *9*, 735. [CrossRef]
210. Giorgi, C.; Marchi, S.; Simoes, I.C.M.; Ren, Z.; Morciano, G.; Perrone, M.; Patalas-Krawczyk, P.; Borchard, S.; Jedrak, P.; Pierzynowska, K.; et al. Mitochondria and Reactive Oxygen Species in Aging and Age-Related Diseases. *Int. Rev. Cell Mol. Biol.* **2018**, *340*, 209–344.
211. Fulda, S.; Galluzzi, L.; Kroemer, G. Targeting mitochondria for cancer therapy. *Nat. Rev. Drug Discov.* **2010**, *9*, 447–464. [CrossRef] [PubMed]
212. Shinohara, Y.; Ishida, T.; Hino, M.; Yamazaki, N.; Baba, Y.; Terada, H. Characterization of porin isoforms expressed in tumor cells. *Eur. J. Biochem.* **2000**, *267*, 6067–6073. [CrossRef] [PubMed]
213. Beinlich, A.; Strohmeier, R.; Kaufmann, M.; Kuhl, H. Relation of cell proliferation to expression of peripheral benzodiazepine receptors in human breast cancer cell lines. *Biochem. Pharmacol.* **2000**, *60*, 397–402. [CrossRef]
214. Maaser, K.; Hopfner, M.; Jansen, A.; Weisinger, G.; Gavish, M.; Kozikowski, A.P.; Weizman, A.; Carayon, P.; Riecken, E.O.; Zeitz, M.; et al. Specific ligands of the peripheral benzodiazepine receptor induce apoptosis and cell cycle arrest in human colorectal cancer cells. *Br. J. Cancer* **2001**, *85*, 1771–1780. [CrossRef] [PubMed]
215. Faure Vigny, H.; Heddi, A.; Giraud, S.; Chautard, D.; Stepien, G. Expression of oxidative phosphorylation genes in renal tumors and tumoral cell lines. *Mol. Carcinog.* **1996**, *16*, 165–172. [CrossRef]
216. Rempel, A.; Mathupala, S.P.; Griffin, C.A.; Hawkins, A.L.; Pedersen, P.L. Glucose catabolism in cancer cells: Amplification of the gene encoding type II hexokinase. *Cancer Res.* **1996**, *56*, 2468–2471.
217. Gudnason, V.; Ingvarsson, S.; Jonasdottir, A.; Andresdottir, V.; Egilsson, V. Isoenzyme pattern and subcellular localization of hexokinases in human breast cancer and nonpathological breast tissue. *Int. J. Cancer* **1984**, *34*, 63–66. [CrossRef]
218. Cung, T.T.; Morel, O.; Cayla, G.; Rioufol, G.; Garcia-Dorado, D.; Angoulvant, D.; Bonnefoy-Cudraz, E.; Guerin, P.; Elbaz, M.; Delarche, N.; et al. Cyclosporine before PCI in Patients with Acute Myocardial Infarction. *New Engl. J. Med.* **2015**, *373*, 1021–1031. [CrossRef]
219. Schaller, S.; Paradis, S.; Ngoh, G.A.; Assaly, R.; Buisson, B.; Drouot, C.; Ostuni, M.A.; Lacapere, J.J.; Bassissi, F.; Bordet, T.; et al. TRO40303, a new cardioprotective compound, inhibits mitochondrial permeability transition. *J. Pharmacol. Exp. Ther.* **2010**, *333*, 696–706. [CrossRef]
220. Sileikyte, J.; Blachly-Dyson, E.; Sewell, R.; Carpi, A.; Menabo, R.; Di Lisa, F.; Ricchelli, F.; Bernardi, P.; Forte, M. Regulation of the mitochondrial permeability transition pore by the outer membrane does not involve the peripheral benzodiazepine receptor (Translocator Protein of 18 kDa (TSPO)). *J. Biol. Chem.* **2014**, *289*, 13769–13781. [CrossRef]
221. Atar, D.; Arheden, H.; Berdeaux, A.; Bonnet, J.L.; Carlsson, M.; Clemmensen, P.; Cuvier, V.; Danchin, N.; Dubois-Rande, J.L.; Engblom, H.; et al. Effect of intravenous TRO40303 as an adjunct to primary percutaneous coronary intervention for acute ST-elevation myocardial infarction: MITOCARE study results. *Eur. Heart J.* **2015**, *36*, 112–119. [CrossRef] [PubMed]
222. Leruez, S.; Verny, C.; Bonneau, D.; Procaccio, V.; Lenaers, G.; Amati-Bonneau, P.; Reynier, P.; Scherer, C.; Prundean, A.; Orssaud, C.; et al. Cyclosporine A does not prevent second-eye involvement in Leber’s hereditary optic neuropathy. *Orphanet J. Rare Dis.* **2018**, *13*, 33. [CrossRef] [PubMed]
223. Valasani, K.R.; Vangavaragu, J.R.; Day, V.W.; Yan, S.S. Structure based design, synthesis, pharmacophore modeling, virtual screening, and molecular docking studies for identification of novel cyclophilin D inhibitors. *J. Chem. Inf. Modeling* **2014**, *54*, 902–912. [CrossRef] [PubMed]

224. Shore, E.R.; Awais, M.; Kershaw, N.M.; Gibson, R.R.; Pandalaneni, S.; Latawiec, D.; Wen, L.; Javed, M.A.; Criddle, D.N.; Berry, N.; et al. Small Molecule Inhibitors of Cyclophilin D To Protect Mitochondrial Function as a Potential Treatment for Acute Pancreatitis. *J. Med. Chem.* **2016**, *59*, 2596–2611. [CrossRef]
225. Panel, M.; Ruiz, I.; Brillet, R.; Lafdil, F.; Teixeira-Clerc, F.; Nguyen, C.T.; Calderaro, J.; Gelin, M.; Allemand, F.; Guichou, J.F.; et al. Small-Molecule Inhibitors of Cyclophilins Block Opening of the Mitochondrial Permeability Transition Pore and Protect Mice From Hepatic Ischemia/Reperfusion Injury. *Gastroenterology* **2019**, *157*, 1368–1382. [CrossRef]
226. Roy, S.; Sileikyte, J.; Schiavone, M.; Neuenswander, B.; Argenton, F.; Aube, J.; Hedrick, M.P.; Chung, T.D.; Forte, M.A.; Bernardi, P.; et al. Discovery, Synthesis, and Optimization of Diarylisoazole-3-carboxamides as Potent Inhibitors of the Mitochondrial Permeability Transition Pore. *ChemMedChem* **2015**, *10*, 1655–1671. [CrossRef]
227. Roy, S.; Sileikyte, J.; Neuenswander, B.; Hedrick, M.P.; Chung, T.D.; Aube, J.; Schoenen, F.J.; Forte, M.A.; Bernardi, P. N-Phenylbenzamides as Potent Inhibitors of the Mitochondrial Permeability Transition Pore. *ChemMedChem* **2016**, *11*, 283–288. [CrossRef]
228. Tarocco, A.; Caroccia, N.; Morciano, G.; Wieckowski, M.R.; Ancora, G.; Garani, G.; Pinton, P. Melatonin as a master regulator of cell death and inflammation: Molecular mechanisms and clinical implications for newborn care. *Cell Death Dis.* **2019**, *10*, 317. [CrossRef]
229. Zhou, H.; Zhang, Y.; Hu, S.; Shi, C.; Zhu, P.; Ma, Q.; Jin, Q.; Cao, F.; Tian, F.; Chen, Y. Melatonin protects cardiac microvasculature against ischemia/reperfusion injury via suppression of mitochondrial fission-VDAC1-HK2-mPTP-mitophagy axis. *J. Pineal Res.* **2017**, *63*, e12413. [CrossRef]



© 2020 by the authors. Licensee MDPI, Basel, Switzerland. This article is an open access article distributed under the terms and conditions of the Creative Commons Attribution (CC BY) license (<http://creativecommons.org/licenses/by/4.0/>).

Review

Diseases Caused by Mutations in Mitochondrial Carrier Genes *SLC25*: A Review

Ferdinando Palmieri ^{1,*}, Pasquale Scarcia ¹  and Magnus Monné ^{1,2,*} 

¹ Department of Biosciences, Biotechnologies and Biopharmaceutics, Laboratory of Biochemistry and Molecular Biology, University of Bari Aldo Moro, via E. Orabona 4, 70125 Bari, Italy; pasquale.scarcia@uniba.it

² Department of Sciences, University of Basilicata, via Ateneo Lucano 10, 85100 Potenza, Italy

* Correspondence: ferdpalmieri@gmail.com (F.P.); magnus.monne@unibas.it (M.M.); Tel.: +39-0805443323 (F.P.)

Received: 27 March 2020; Accepted: 17 April 2020; Published: 23 April 2020

Abstract: In the 1980s, after the mitochondrial DNA (mtDNA) had been sequenced, several diseases resulting from mtDNA mutations emerged. Later, numerous disorders caused by mutations in the nuclear genes encoding mitochondrial proteins were found. A group of these diseases are due to defects of mitochondrial carriers, a family of proteins named solute carrier family 25 (SLC25), that transport a variety of solutes such as the reagents of ATP synthase (ATP, ADP, and phosphate), tricarboxylic acid cycle intermediates, cofactors, amino acids, and carnitine esters of fatty acids. The disease-causing mutations disclosed in mitochondrial carriers range from point mutations, which are often localized in the substrate translocation pore of the carrier, to large deletions and insertions. The biochemical consequences of deficient transport are the compartmentalized accumulation of the substrates and dysfunctional mitochondrial and cellular metabolism, which frequently develop into various forms of myopathy, encephalopathy, or neuropathy. Examples of diseases, due to mitochondrial carrier mutations are: combined D-2- and L-2-hydroxyglutaric aciduria, carnitine-acylcarnitine carrier deficiency, hyperornithinemia-hyperammonemia-homocitrillinuria (HHH) syndrome, early infantile epileptic encephalopathy type 3, Amish microcephaly, aspartate/glutamate isoform 1 deficiency, congenital sideroblastic anemia, Fontaine progeroid syndrome, and citrullinemia type II. Here, we review all the mitochondrial carrier-related diseases known until now, focusing on the connections between the molecular basis, altered metabolism, and phenotypes of these inherited disorders.

Keywords: disease; error of metabolism; mitochondrial carrier; mitochondrial carrier disease; mitochondrial disease; mitochondrial transporter; membrane transport; mutation; SLC25.

Contents

1. Introduction
2. Characteristic features of mitochondrial carriers (MCs)
3. Diseases caused by mutations in MCs
 - 3.1. General information
 - 3.2. SLC25A1 (citrate carrier, CIC) deficiency
 - 3.3. SLC25A3 (phosphate carrier, PiC) deficiency
 - 3.4. SLC25A4 (ADP/ATP carrier 1, AAC1) deficiency
 - 3.5. SLC25A10 (dicarboxylate carrier, DIC) deficiency

- 3.6. SLC25A12 (aspartate-glutamate carrier 1, AGC1, aralar) deficiency
 - 3.7. SLC25A13 (aspartate-glutamate carrier 2, AGC2, citrin) deficiency
 - 3.8. SLC25A15 (ornithine carrier 1, ORC1) deficiency
 - 3.9. SLC25A16 deficiency
 - 3.10. SLC25A19 (thiamine pyrophosphate carrier, TPC) deficiency
 - 3.11. SLC25A20 (carnitine-acylcarnitine carrier, CAC) deficiency
 - 3.12. SLC25A21 (oxodicarboxylate carrier, ODC) deficiency
 - 3.13. SLC25A22 (glutamate carrier 1, GC1) deficiency
 - 3.14. SLC25A24 (ATP-Mg²⁺/phosphate carrier 1, APC1) deficiency
 - 3.15. SLC25A26 (S-adenosylmethionine carrier, SAMC) deficiency
 - 3.16. SLC25A32 deficiency
 - 3.17. SLC25A38 (glycine carrier, GlyC) deficiency
 - 3.18. SLC25A42 (CoA and PAP carrier) deficiency
 - 3.19. SLC25A46 deficiency
4. Multigenic diseases with mutations in MCs
 5. Concluding remarks

1. Introduction

Mitochondrial diseases are caused by mutations in either the mitochondrial or nuclear genome. Out of about 1500 proteins comprising the mitochondrial proteome, only 13 proteins, plus 2 ribosomal RNAs and 22 transfer RNAs, are encoded by the mitochondrial DNA (mtDNA) and all the rest by the nuclear DNA. Until now, more than 350 mutations have been identified as causing mitochondrial disorders [1,2]. The mutations in the nuclear genes are inherited in a Mendelian fashion, whereas those of the multi-copy mtDNA follow a maternal pattern of inheritance.

Mitochondrial diseases are a very heterogeneous group of pathologies in many aspects. The clinical features of these disorders manifest differently in various tissues and cell types but typically involve the brain, muscle, heart, kidney, liver, and retina—organs with high energy demands [3]. The age of onset of these disorders ranges from very early in the neonatal period to late in adulthood, and the symptoms are sometimes triggered by environmental factors and may occur suddenly or develop progressively.

The disease-causing mutations in the mtDNA primarily involve core subunits of the respiratory chain and oxidative phosphorylation complexes as well as gene products involved in mitochondrial translation. These defects give rise to, for example, Leigh syndrome, LHON (Leber hereditary optic neuropathy), MELAS (mitochondrial myopathy, encephalopathy, lactic acidosis, and stroke-like episodes syndrome), MERRF (myoclonic epilepsy with ragged fibers), and NARP (neurogenic muscle weakness ataxia and retinitis pigmentosa) [3,4]. The pathogenic nuclear mutations affect mitochondrial proteins involved in many important processes, such as the respiratory chain, oxidative phosphorylation, metabolism, cofactor biosynthesis, transport, replication, transcription, translation, iron homeostasis, cell signalling, organelle dynamics, protein biogenesis, and complex assembly [5]. Among the mitochondrial diseases caused by mutations in nuclear genes are: Friedreich's ataxia, dominant optic atrophy, Barth syndrome, Rett syndrome, spastic paraplegia, coenzyme Q10 deficiency, and progressive external ophthalmoplegia [3,4]. Furthermore, mutations in both nuclear and mitochondrial DNA play a role in diabetes, obesity, autism, Alzheimer's disease, Parkinson's disease, Huntington's disease, cancer, and aging [6].

This review focusses on the subgroup of mitochondrial diseases that are caused by mutations in the genes encoding members of the mitochondrial carrier family SLC25. Particular emphasis is given to the location and relevance of the mutations within the structure of the transporters and to the pathogenic mechanisms underlying the symptoms characteristic of the diseases.

2. Characteristic Features of Mitochondrial Carriers

Mitochondrial carriers (MCs) constitute a protein family also called the solute carrier family 25 (SLC25). It is the largest of the transporter families, its 53 human members are named from SLC25A1 to SLC25A53, and it is widely distributed in all eukaryotes [7–9]. The sequences of MCs contain three repeated domains, each of which consists of about 100 residues and includes two transmembrane segments that are linked by a signature motif sequence (SMS): PX[DE]XX[KR]X[KR]X20–30[DE]GXXXX[WYF][KR]G (PROSITE PS50920, PFAM PF00153 and IPR00193) [10,11]. These highly conserved sequence features are specific for MCs and have been used for the identification of family members in genomic sequences. The substrates transported by most MCs in *Homo sapiens*, *Saccharomyces cerevisiae* and *Arabidopsis thaliana*, have been identified by the EPRA method: recombinant expression of MC genes, purification of the proteins, and their reconstitution into liposomes that are subjected to direct transport assays [12–14]. By this means, it has been shown that MCs transport a great variety of substrates: nucleotides (e.g., ATP, ADP and dNTPs), cofactors (e.g., thiamine pyrophosphate, S-adenosylmethionine (SAM), coenzyme A (CoA) and NAD⁺), metabolites with carboxylic groups (e.g., malate, 2-oxoglutarate and citrate), amino acids (e.g., aspartate, glutamate, ornithine and arginine), and inorganic ions (e.g., phosphate and sulfate). The transport of the substrates across the inner mitochondrial membrane, i.e., between the intermembrane space/cytoplasm and the mitochondrial matrix and vice versa, is mediated by specific MCs. Consequently, MCs play numerous important roles in energy, nucleotide, fatty acid, and amino acid metabolism as well as in providing cofactors for enzymes and precursors for replication, transcription, and translation in mitochondria. The great majority of MCs catalyze an exchange (antiport) of substrates, but some also catalyze the unidirectional transport (uniport) of substrates, like the phosphate carrier, carnitine carrier, and UCP1 [9,15]. MC superfamily members that have the same or very similar substrate specificity form subfamilies, which are also characterized by distinctive structural and transport features [16,17]. At variance with all the other MCs, the aspartate-glutamate and ATP-Mg/phosphate carrier subfamilies have N-terminal extensions containing EF-hand Ca²⁺-binding motifs and are regulated by Ca²⁺ [18–20]. It is noteworthy that not all the characterized MCs are localized in the mitochondrial inner membrane; some are located in other organelles such as chloroplasts and peroxisomes [16,17]. MCs are synthesized on cytosolic ribosomes and imported usually into the inner mitochondrial membrane. Unlike most nuclear-encoded mitochondrial proteins, the targeting information is contained in their mature sequence. Only a few of them possess short cleavable presequences, which, however, are not essential for import, although those of phosphate and citrate carriers improve correct targeting [21–24].

In the atomic 3D-structures of the only MC family member determined until now, the ADP/ATP carrier (AAC), the six transmembrane segments form a bundle of α -helices (H1–H6) around a central cavity, which constitutes the substrate translocation pore, whereas the 20–30 less conserved residues in the middle of the SMSs form three α -helices almost parallel to the membrane on the matrix side [25–27]. Two conformations of AAC are trapped by the inhibitors carboxyatractyloside and bongkrekic acid that lock the protein with the substrate translocation pore alternatively closed towards the matrix or intermembrane space by a matrix (m) gate or a cytosolic (c) gate, respectively [28,29]. These two conformations (named c-state and m-state) are thought to correspond approximately to the carrier (in the absence of the inhibitors) that is open to receive the substrate from the intermembrane space or from the mitochondrial matrix, respectively. In the c-state, the matrix gate is formed by the three initial stretches of the SMS (PX[DE]XX[KR]), where the prolines kink H1, H3, and H5 and the two charged residues are involved in salt-bridges interconnecting these three helices. In the m-state, this salt-bridge relay is broken and a similar (but less conserved) salt-bridge network is formed by the c-gate residues [DE]XX[KR] located close to the intermembrane space on H2, H4, and H6. The structures [25–27] strengthen the hypothesized “single binding center-gating pore” transport mechanism for MCs, which was initially deduced from studies of the inhibitors carboxyatractyloside and bongkrekic acid and their competition with the transported substrates of AAC [28,29]. As indicated by the name of this mechanism there is a single substrate binding site centrally located in the pore of the protein, and

its access to the substrate is regulated by the alternating opening and closing of the c- and m-gates. It is believed that the binding of the substrate to the active site when entering from the open side of the pore (either from the outside or matrix side) triggers conformational changes leading to the closure of the open gate, the opening of the opposite closed gate and the release of the substrate on the opposite side of the membrane with respect to where it entered the carrier; then another (or the same) substrate is translocated in the opposite direction to complete the exchange reaction. The central binding site has been suggested to be determined by residues of H2, H4, and H6 located in positions called contact points I, II, and III, respectively, approximately at the same level in the middle of the membrane [30–32]. Indeed, the properties of the residues in contact point II co-vary with the kind of substrate; the motifs G[IVLM], R[QHNT] and R[DE] are conserved at this location in carriers for nucleotides, carboxylates, and amino acids, respectively. The residues in the other contact points and in their proximity contribute to the particular substrate specificity of each MC [17,30,33,34].

3. Diseases Associated with Mutations in MCs

3.1. General Information

Since 1997, mutations in 18 different MCs have been reported to cause diseases (Table 1) [35–37]. They are all rare diseases (errors of metabolism) and, with a few exceptions, follow a recessive pattern of inheritance. At the biochemical level, these MC mutations give rise to the reduction or elimination of their respective substrate transport, which leads to accumulating metabolites and dysfunctional cellular metabolism. In common with other mitochondrial diseases, that are caused by mutations in mitochondrial proteins, many of the MC-associated pathologies often manifest with different forms of myopathy, encephalopathy, and neuropathy, and a few of them present loss of mitochondrial DNA as a secondary effect [38]. When MCs directly linked to oxidative phosphorylation (i.e., the ADP/ATP carrier and the Pi carrier) are altered, the organ-specific symptoms are due to the activities of heart, muscle, and other tissues requiring particularly high energy demands and therefore being highly dependent on mitochondrial function. Otherwise, the symptomatology of the MC-related diseases depends on several factors such as the specific metabolism affected, its relevance in specific tissues, the tissue distribution of the affected carrier, and the presence in the same tissues of isoforms or other MCs that can compensate, at least partly, the function(s).

Table 1. Diseases caused by mutations in mitochondrial carrier genes.

Affected MC	Phenotype	OMIM/Inheritance	Mutations/Patients	References of First Reported Case
SLC25A1, citrate carrier (CIC)	Combined D-2- and L-2-hydroxyglutaric aciduria Congenital myasthenic syndrome 23	615182/AR 618197/AR	24/40	(Edvardson et al., 2013) (Nota et al., 2013) (Chaouch et al., 2014)
SLC25A3, phosphate carrier (PiC)	Mitochondrial phosphate carrier deficiency	610773	4/7	(Mayr et al., 2007)
SLC25A4, ADP/ATP carrier 1 (AAC1)	Autosomal dominant progressive external ophthalmoplegia with mitochondrial DNA deletions 2 (AdPEO2) Mitochondrial DNA depletion syndrome (MTDPS) 12B (cardiomyopathic type) Mitochondrial DNA depletion syndrome (MTDPS) 12A (cardiomyopathic type)	609283/AD 615418/AR 617184/AD	5/9? 6/7 3/5	(Kaukonen et al., 2000) (Palmieri et al., 2005) (Thompson et al., 2016)
SLC25A10, dicarboxylate carrier (DIC)	Intractable epileptic encephalopathy with complex I deficiency	AR	3/1	(Punzi et al., 2018)
SLC25A12, aspartate/glutamate carrier 1 (AGC1)	Early infantile epileptic encephalopathy 39 (AGC1 deficiency)	612949/AR	3/4	(Wibom et al., 2009)
SLC25A13, aspartate/glutamate carrier 2 (AGC2)	Adult-onset citrullinemia type II (CTLN2) Neonatal-onset citrullinemia type II (NICCD)	603471/AR 605814/AR	117/>600	(Saheki and Kobayashi, 2002) (Kobayashi et al., 1999)
SLC25A15, ornithine carrier 1 (ORC1)	Hyperornithinemia-hyperammonemia-homocitrullinemia (HHH) syndrome	238970/AR	38/91	(Camacho et al., 1999)
SLC25A16	Fingernail dysplasia	AR	1/9	(Khan et al., 2018)
SLC25A19, thiamine pyrophosphate carrier (TPC)	Amish microcephaly Thiamine metabolism dysfunction syndrome 4 (progressive polyneuropathy type)	607196/AR 613710/AR	1/? 5/8	(Rosenberg et al., 2002) (Spiegel et al., 2009)
SLC25A20, carnitine/acylcarnitine carrier (CAC)	Carnitine-acylcarnitine translocase deficiency (CAC deficiency)	212138/AR	38/43?	(Huizing et al., 1997)
SLC25A21, oxodicarboxylate carrier (ODC)	Mitochondrial DNA depletion and spinal muscular atrophy-like disease	618811	1/1	(Boczonadi et al., 2018)
SLC25A22, glutamate carrier 1 (GC1)	Early infantile epileptic encephalopathy 3 (EIEE3)	609304/AR	11/17	(Molinari et al., 2005)
SLC25A24, ATP-Mg/phosphate carrier 1 (APC1)	Fontaine progeroid syndrome	612289/AD	2/11	(Ehmke et al., 2017) (Witzl et al., 2017)
SLC25A26, S-adenosylmethionine carrier (SAMC)	Combined oxidative phosphorylation deficiency 28	616794/AR	4/3	(Kishita et al., 2015)
SLC25A32	Riboflavin-responsive exercise intolerance	616839/AR	3/2	(Schiff et al., 2016)
SLC25A38, glycine carrier (GlyC)	Congenital sideroblastic anemia 2 (pyridoxine-refractory)	205950/AR	25/39	(Guernsey et al., 2009)
SLC25A42, CoA and PAP carrier	Recurrent metabolic crises with variable encephalomyopathic features and neurologic regression	618416/AR	2/15	(Shamseldin et al., 2015)
SLC25A46	Hereditary motor and sensory neuropathy type VIB	616505/AR	16/25	(Abrams et al., 2015)

AD, autosomal dominant; AR autosomal recessive.

Most of the disease-causing mutations in MCs are single nucleotide substitutions (over 200). However, also insertions, deletions, and insertion/deletions (more than 70) of a varying number of nucleotides have been found (Table S1). It is possible to map the 166 disease-causing single nucleotide missense mutations (Figure 1) onto 100 different positions in the structures of AAC (Figure 2) due to the specific conserved sequence features of MCs, which makes structural alignments very reliable. Only 15% of these mutations are conservative mutations, i.e., substitutions with residues with similar chemical properties. Quite a large portion of the single-nucleotide missense mutations is found in the conserved residues of the SMSs (16%), in the contact point residues (10%), and 45% in the substrate translocation pore (Figure 2B,D). Of all the mutations, 25% are in lipid-exposed positions, 10% in buried positions within the protein, and the remaining 20% in mainly solvent-exposed positions (Figure 2A,C with all the positions outside the substrate translocation pore). Not surprisingly, these numbers suggest that the point mutations in the substrate translocation pore are the most common pathogenic missense mutations. Considering that only about 20% of the MC residues face the inside of the pore, 63% of these residue positions have at least one disease-causing point mutation. The corresponding numbers for the buried, lipid bilayer- and solvent-exposed positions are 29%, 30%, and 18%, respectively. Thus, it is clear that the substrate translocation pore residues are hotspots for disease-causing mutations.

All the diseases and respective phenotypes (23 until now), that have been associated to 18 MCs, are described below following the order of the SLC25 numbers.

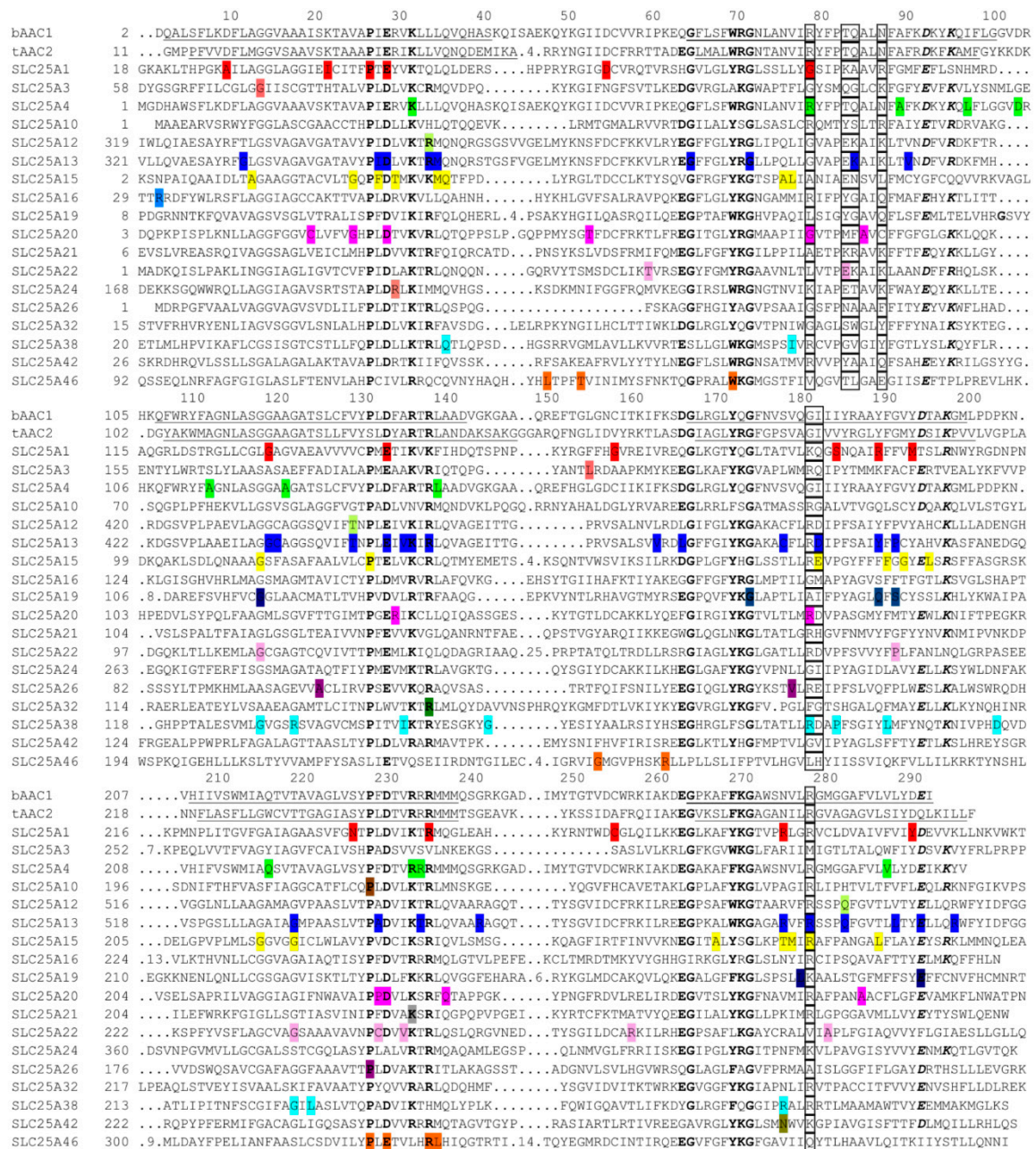


Figure 1. Multiple sequence alignment of mitochondrial carriers showing the position of disease-causing point mutations. The protein sequences of the 18 MCs found to have disease-causing point mutations are aligned against the sequences of bovine AAC1 (bAAC1 with numbering) and *Thermothelomyces thermophila* AAC2 (tAAC2) whose 3D-structures have been determined (Figure 2). Sequences of the transmembrane helices are underlined, the conserved residues of the SMSs are in bold, the charged residues of the cytoplasmic gate are in italics, and the contact points I, II, and III residues on the first, second, and third row of the alignment, respectively, are boxed. The numbers inside the alignment indicate missing residues. One color for each MC indicates the positions of the single point mutations associated with disease, and the top color in each position in the alignment corresponds to the colored positions in Figure 2.

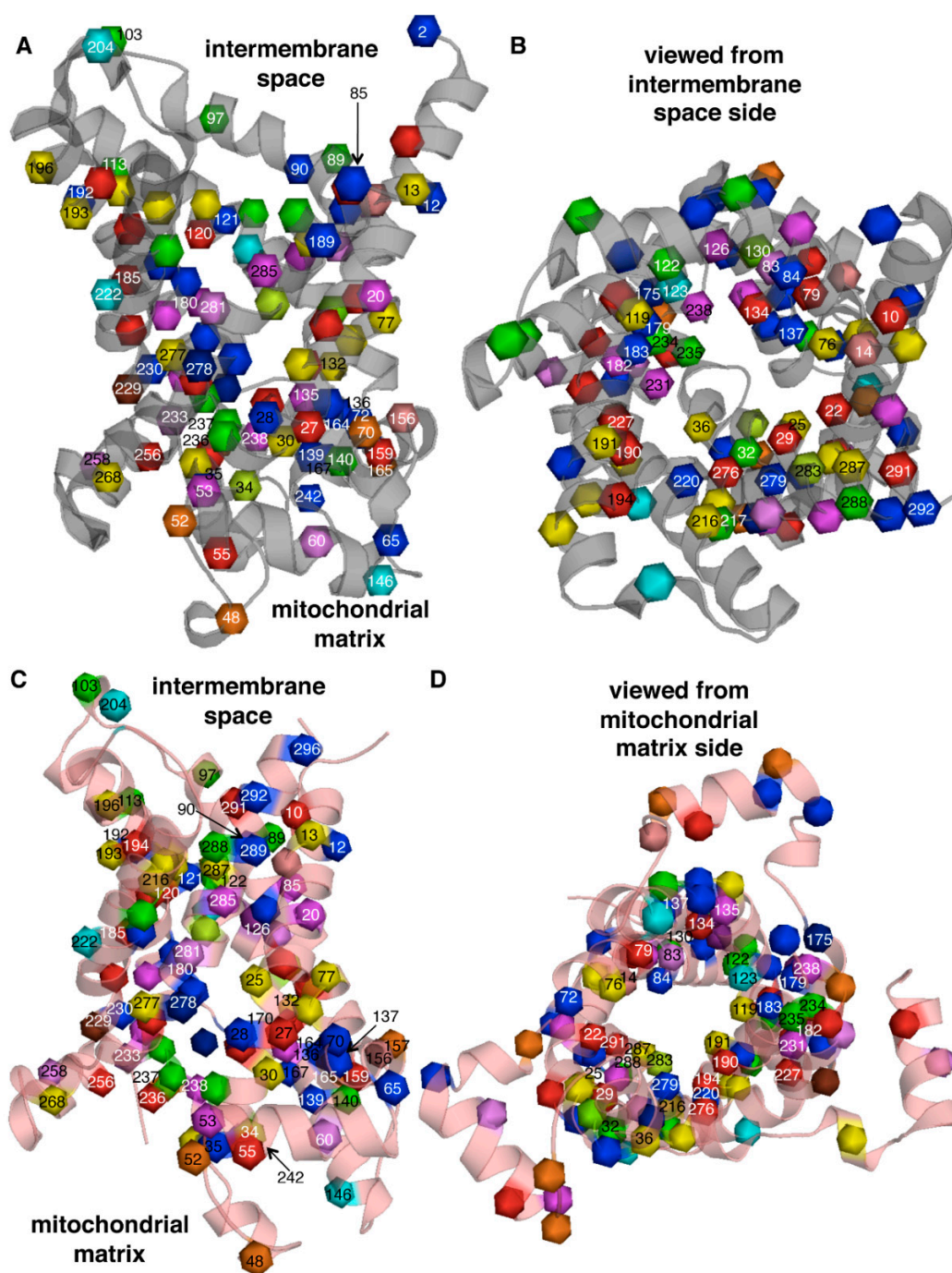


Figure 2. Structural positions of disease-causing point mutations in mitochondrial carriers. The bovine AAC1 structure (in the c-state, gray) and the thermophile AAC2 structure (in the m-state, pink) are viewed from the membrane plane (A,C) and the intermembrane space side (B,D). In all the panels, the α -carbons of the mutated positions are indicated as spheres colored as the top color of the mutations in the same position shown in the alignment of Figure 1. The numbering is that of bovine AAC1 (Figure 1) with the residue side chains exposed to the substrate translocation pore in B and D or outside the pore in A and C.

3.2. *SLC25A1* (Citrate Carrier, CIC) Deficiency

Since 2013 until now, 24 mutations in *SLC25A1* have been found in 27 patients suffering from combined D-2- and L-2-hydroxyglutaric aciduria [39–45] (Table 1 and Table S1). *SLC25A1* deficiency

patients exhibit lower levels of citrate and isocitrate in the urine as compared to controls. In contrast, the urinary excretion of the tricarboxylic acid (TCA) cycle intermediates 2-oxoglutarate, succinate, fumarate, and malate, besides that of D/L-2-hydroxyglutaric acids, is higher. SLC25A1 deficiency is generally characterized by a severe neurodevelopmental phenotype, including neonatal encephalopathy, respiratory insufficiency, developmental delay, hypotonia, seizures, and early death. Ventriculomegaly, congenital heart defects, lactic acidosis and mitochondrial respiratory chain deficiency have also been described in some patients. The genetic trait of the disease follows a recessive pattern of inheritance with patients presenting alleles with combinations of missense, nonsense, and frameshift mutations. Moreover, two mutations (p.Asp69Tyr and p.Arg247Gln) causing SLC25A1 deficiency are associated with congenital myasthenic syndromes and mild intellectual disability [41]. In addition, few patients manifested combined D-2- and L-2-hydroxyglutaric aciduria and diGeorge syndrome caused by a SLC25A1 mutation on one allele and a microdeletion of 22q11.2, which contains SLC25A1 and two other genes, on the homologous chromosome [45].

On the basis of its substrate specificity and other transport measurements, it has been suggested that the SLC25A1 gene product CIC catalyzes the electroneutral exchange of cytoplasmic malate²⁻ for mitochondrial citrate²⁻ or isocitrate²⁻ formed in the TCA cycle (Figure 3) [46–49]. In the cytoplasm citrate is important in the regulation of glycolysis through a feedback mechanism and in the production of acetyl-CoA which is needed for the synthesis of fatty acids, sterols, prostaglandins, dolichol and coenzyme Q (CoQ), and for histone acetylation. The CIC-catalyzed export of mitochondrial isocitrate plays a role in a shuttle that supplies cytosolic NADPH [49]. These transport functions are of central importance in most cell types, as CIC expression has been detected in a wide range of tissues with the highest mRNA levels in the liver, kidney, pancreas, and heart [50].

Several approaches have been used to assess the effects of missense mutations associated with SLC25A1 deficiency on CIC activity. The *S. cerevisiae* homologue of CIC, Ctp1p, harboring three corresponding human disease-causing mutations was reconstituted in liposomes for transport assays with radioactive citrate [39,41]. Another method utilized isotope-labeled glucose fed to fibroblasts from seven patients or to fibroblasts deficient of CIC and containing plasmids expressing 17 disease-causing point mutations, and the cellular efflux of isotope-labeled citrate formed was quantified [40,51]. A third approach employed mutant versions of human CIC expressed in *Lactococcus lactis*, and their transport activities in plasma membrane-fused liposomes were measured with radioactive citrate [52]. These studies show that the mutations causing D-2- and L-2-hydroxyglutaric aciduria affect citrate transport activity of CIC to various degrees, and that, with a few exceptions, the relative transport activities obtained by the different approaches for a specific CIC mutant are similar. The importance of the position of the mutations in the CIC structural homology model is generally in agreement with their relevance for the CIC activity: mutations in the vicinity of the substrate binding site and in the SMS residues lining the substrate translocation pore (Figure 2B,D, at positions 29, 79, 134, 190, and 276) almost deplete transport activity, whereas other mutations localized in the pore of the protein (Figure 2, at positions 10, 22, 194, and 291) or outside the pore retain partial activity (Figure 2A,C, at positions 27, 120, 159, 185, 236, and 256). Pop et al. (2018) have suggested correlations between the measured activity of single CIC mutants and the functional/structural importance of the original residue, as evaluated by analyses of the strength of the evolutionary selection in that amino acid position [53], as well as between the calculated average CIC activity of the two-allele mutations found in the patients and the severity of the disease [51]. Furthermore, zebrafish has been used as a model for exploring the morphological effects of CIC dysfunction; knockout of SLC25A1 causes mitochondrial loss, a decrease in brain size, and cardiac dysfunction [54], whereas the expression of mild, moderate, and severe CIC mutants in the knockout animal shows progressive morphological abnormalities and defective neuromuscular junction formation [41].

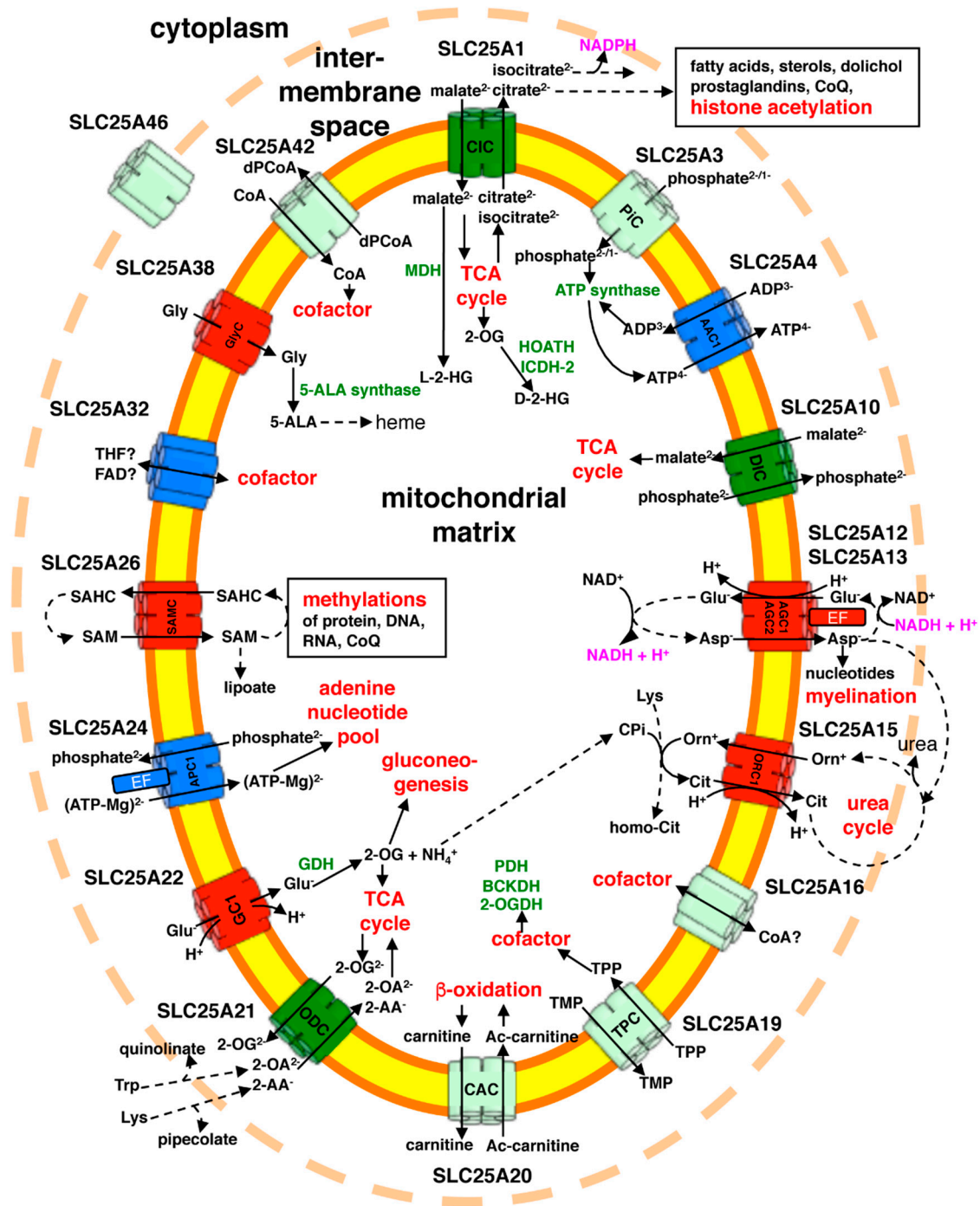


Figure 3. Metabolic roles of the mitochondrial carriers associated with diseases. When known, the substrate species transported by the carriers are shown. The carriers for carboxylates, amino acids, and nucleotides are colored in green, red, and blue, respectively, whereas the remaining MCs are colored in light lime. Enzymes are abbreviated in green. Other abbreviations are: 2-OA, 2-oxoacid; 2-AA, 2-aminoadipate; 2-OA, 2-oxoadipate; 2-OG, 2-oxoglutarate; 2-OGDH, 2-oxoglutarate dehydrogenase; 5-ALA, 5-aminolevulinic acid; Ac, acyl; BCKDH, branched chain ketoacid dehydrogenase; CPi, carbamoylphosphate; D-2HG, D-2-hydroxyglutarate; dPCoA, dephospho-CoA; EF, EF hand Ca²⁺-binding domains; GDH, glutamate dehydrogenase; HOATH, hydroxy-oxoacid transhydrogenase; ICDH-2, isocitrate dehydrogenase 2; L-2-HG, L-2-hydroxyglutarate; MDH, malate dehydrogenase; PDH, pyruvate dehydrogenase; SAHC, S-adenosylhomocysteine; SAM, S-adenosylmethionine; TCA, tricarboxylic acid; THF, tetrahydrofolate; TMP, thiamine monophosphate; TPP, thiamine pyrophosphate.

The connections between reduced CIC activity and the clinical symptoms of combined D-2- and L-2-hydroxyglutaric aciduria are not totally clear. It is likely that the reduced activity of the CIC mutants reduces citrate and isocitrate efflux from mitochondria, and, subsequently, from cells, which in turn leads to reduced urine levels of these metabolites. In contrast, the increased mitochondrial citrate and isocitrate levels, due to their diminished export, and the loss of glycolysis feedback inhibition by cytosolic citrate could increase the concentrations of other TCA cycle intermediates which may be exported from the mitochondria by other MCs and eventually diffuse into the urine. The accumulation of mitochondrial 2-oxoglutarate is partly converted to D-2-hydroxyglutarate by the action of hydroxy-oxoacid transhydrogenase or isocitrate dehydrogenase 2, and that of malate into L-2-hydroxyglutarate by malate dehydrogenase (Figure 3). It is known that mutations in other enzymes (L-2-hydroxyglutarate dehydrogenase, D-2-hydroxyglutarate dehydrogenase and isocitrate dehydrogenase 2) cause L-2-hydroxyglutaric aciduria or D-2-hydroxyglutaric aciduria type 1 or type 2 [55] and not a combined excretion of these two hydroxyacids. All three of these diseases manifest neurodevelopmental symptoms reminiscent of those found in combined D-2- and L-2-hydroxyglutaric aciduria. High levels of D/L-2-hydroxyglutarate have been suggested to inhibit 2-oxoglutarate-dependent enzymes, cause oxidative stress, and have neurotoxic effects [55]. Furthermore, it is likely that the reduced cytoplasmic acetyl-CoA concentration, leading to defective lipid anabolism and histone acetylation, contributes to the severe neurodevelopmental symptoms of combined D-2- and L-2-hydroxyglutaric aciduria.

3.3. *SLC25A3 (Phosphate Carrier, PiC) Deficiency*

The mitochondrial phosphate carrier PiC, encoded by *SLC25A3*, provides phosphate for oxidative phosphorylation and several other matrix processes as well as facilitates the transport of other substrates across the inner mitochondrial membrane by acting as a counter-substrate of other MCs (Figure 3). Due to the alternative splicing of exons III-A and III-B of *SLC25A3*, two isoforms of PiC are produced: isoform A, expressed in the heart and muscle, and isoform B that is expressed at much lower levels in all tissues [56–58]. PiC transports phosphate + H⁺ across the mitochondrial membrane. In particular, in studies with isolated rat-liver mitochondria, where virtually only isoform B is present, PiC was shown to transport both phosphate¹⁻ and phosphate²⁻ in symport with an equivalent amount of H⁺ [59].

Four mutations in *SLC25A3* have been found in seven individuals with PiC deficiency from four different families [60–62] (Table 1). In six patients, two homozygous mutations were found in exon 3A affecting isoform A only: the point mutation p.Gly72Glu, which is located in the substrate translocation cavity at position 14 and may interfere with substrate binding (Figure 2B) [62], and a splice site substitution (Table S1). The seventh patient was compound heterozygous with two mutations affecting both isoform A and B: a deletion-insertion located in the matrix helix between H5 and H6, and a single amino acid substitution (p.Leu200Trp of PiC isoforms A and p.Leu199Trp of isoform B), which is located in position 156 on the matrix side (Figure 2A,C) and probably restricts conformational changes [62]. All the patients displayed hypertrophic cardiomyopathy, skeletal myopathy, and often lactic acidosis. In the severe cases, the affected patients did not survive the first year of life, whereas other patients overcame the pre- or neo-natal symptoms to develop almost normally but with skeletal myopathy and exercise intolerance. The physiological effects of not having functional heart PiC have been reproduced in mice with inducible cardiac-specific deletion of *SLC25A3* [63]. These mice developed a cardiac phenotype reminiscent of *SLC25A3* deficiency and (see Section 3.4) the recessive forms of *SLC25A4* deficiency, that both involve altered transport of substrates and/or products of oxidative phosphorylation. Isolated cardiac mitochondria from *SLC25A3* knockout mice displayed a reduced ATP synthesis rate, although phosphate transport capacity was not completely abolished, as seen by measuring the uptake of radioactive phosphate. The latter observation may be explained by the fact that there are other MCs capable of transporting phosphate, such as the ATP-Mg²⁺/phosphate carriers (APCs), dicarboxylate carrier (DIC), and various uncoupling proteins (UCP2, UCP5, and UCP6) [19,64–70]. Furthermore, in *SLC25A3* deficiency patients who have mutations only in PiC

isoform A, also PiC isoform B may partly compensate for the defective phosphate transport. Until now, the transport activity of the disease-causing PiC mutations has not been investigated in reconstituted liposomes using the EPRA method.

3.4. *SLC25A4* (ADP/ATP Carrier 1, AAC1) Deficiency

Mutations in the *SLC25A4* gene, encoding AAC1, one of the four human AACs [71], have been reported to cause three different diseases: adult-onset autosomal-dominant progressive external ophthalmoplegia 2 (AdPEO2) [72] and recessive and dominant early-onset mitochondrial myopathy/cardiomyopathy assigned as mitochondrial DNA depletion syndrome (MTDPS) type 12B [73–76] and 12A, respectively [77] (Table 1). AAC1 is expressed mainly in heart and skeletal muscle, where it is the predominant AAC isoform, and has the key role in cellular energy metabolism of exchanging cytosolic ADP³⁻ for matrix ATP⁴⁻ electrophoretically to provide the substrate and export the product of ATP synthase (Figure 3) [29]. All three diseases associated to *SLC25A4* mutations are characterized by multiple deletions in mitochondrial DNA as well as a reduced respiratory chain and oxidative phosphorylation capacity. AdPEO2 has usually an onset in early adulthood and displays numerous ragged-red fibers in muscle biopsy, ptosis, and progressive muscle weakness, especially of the external eye muscle [72]. Other forms of AdPEO are caused by mutations in subunits of the mitochondrial DNA helicase (AdPEO3), polymerase (AdPEO1 and AdPEO4), and ribonucleotide reductase (AdPEO5), suggesting that AAC1 also has a role in the mitochondrial replication that lies beneath the mitochondrial DNA deletions. How AAC1 malfunction is connected to mitochondrial replication is not known, but it has been suggested to be through the disequilibrium of mitochondrial nucleotide pools or increased reactive oxygen species production [72]. The patients with MTDPS-12B (recessive) manifest muscle ragged-red fibers, mild myopathy with exercise intolerance, and lactic acidosis, but no ophthalmoplegia [73–76]. Recently, a new phenotype of recessive MTDPS-12B has been reported that, besides hypertrophic cardiomyopathy, lactic acidosis, and exercise intolerance, also displays elevated L-2-hydroxyglutarate urine levels and no mitochondrial DNA deletions [78]. It was speculated by the same authors that the increased L-2-hydroxyglutarate excretion may be a secondary effect of NADH accumulation in the mitochondrial matrix. The symptoms of the 12A variant of MTDPS (dominant) are more severe because hypotonia is apparent already after birth, in infancy respiratory insufficiency, requiring mechanical ventilation, and poor motor development leads to death in many cases [77].

It is striking that AdPEO is caused by single point mutations located outside the central translocation pore (p.Ala90Asp, p.Leu98Pro, p.Asp104Gly, and p.Ala114Pro at positions 89, 97, 103, and 113, respectively, in Figure 2A,C) with the exception of p.Val289Met (Figure 2B, at position 288), which is a conservative mutation located in the pore between the substrate binding area and the residues of the c-gate. By contrast, MTDPS-12B is caused by the deletion, frame shift, and point mutations close to the binding site (p.Ala123Asp and p.Gln218Pro at positions 122 and 217 in Figure 2) or the m-gate (p.Leu141Phe and p.Arg236Pro at positions 140 and 235); and MTDPS-12A is caused by mutations in contact point I (p.Arg80His at position 79) or in translocation pore SMS residues (Figure 1, p.Lys33Gln and p.Arg235Gly in Figure 2 at positions 33 and 234, respectively). Transport measurements have shown that the AdPEO point mutations outside the translocation pore have 24–56% activity as compared to that of the wild-type, whereas MTDPS-12B mutations p.Ala123Asp and p.Arg236Pro virtually abolish activity and the MTDPS-12A mutations p.Lys33Gln, p.Arg80His, and p.Arg235Gly have 0%, 24%, and 3% activity, respectively [73,77,79]. It appears, therefore, that the severity of the late-onset dominant AdPEO with respect to both MTDPS-12B and MTDPS-12A (which are more severe) correlates with the type of mutations, their position within the carrier structure, and the measured residual transport activity. In contrast, such a correlation between MTDPS-12B and MTDPS-12A is not clear.

3.5. *SLC25A10 (Dicarboxylate Carrier, DIC) Deficiency*

One patient with a severe neurodegenerative disorder, characterized by epileptic encephalopathy, complex I deficiency, and mitochondrial DNA depletion in skeletal muscle was shown to possess mutations in the gene *SLC25A10* [80]. The heterozygous mutations of the patient (a silent and an intron mutation in one allele and a frame shift mutation in the other, Table S1) resulted in reduced RNA quantity and malfunctional splicing, leading to the absence of the dicarboxylate carrier DIC (encoded by *SLC25A10*). Mammalian DIC was shown to transport dicarboxylates such as malate and succinate as well as inorganic anions such as phosphate, sulfate, and thiosulfate by a strict electroneutral counter-exchange (Figure 3) [64,67,68,81–84]. As shown by transport experiments with isolated mitochondrial membranes from patient fibroblasts fused with liposomes, the malate/phosphate exchange was dramatically reduced [80]. It was also observed that the ratios of NADPH/NADP⁺ and GSH/GSSG were decreased. The connection between the transport function of DIC and the disease phenotype is not clear but its roles in the transport of reducing equivalents, anaplerotic Krebs cycle intermediates or components of sulfur metabolism could contribute to increased sensitivity to oxidative stress. Oxidative damage may lead to the loss of mitochondrial DNA and, subsequently, to the symptoms observed. It might be that, in some tissues, other MCs that transport certain DIC substrates partly compensate for the lack of *SLC25A10* activity: PiC and APCs transport phosphate [19,58,85]; the oxoglutarate carrier transports malate and succinate [86–89]; UCP2 transports malate, phosphate, and sulfate [69]; and UCP5 and UCP6 transport malate, succinate, phosphate, sulfate, and thiosulfate [70].

3.6. *SLC25A12 (Aspartate-Glutamate Carrier 1, AGC1, Aralar) Deficiency*

Three children with arrested psychomotor development, hypotonia, seizures, global hypomyelination, and reduced levels of N-acetylaspartate in the cerebral hemispheres were found to have missense mutations in the gene *SLC25A12* of the aspartate-glutamate carrier AGC1 [90,91]. The two human AGC isoforms AGC1 and (see Section 3.7) AGC2 consist of two domains: an N-terminal soluble domain and a C-terminal MC catalytic domain [18]. Both proteins transport aspartate and glutamate by an obligatory electrophoretic exchange of (glutamate[−] + H⁺)_{out} for aspartate[−]_{in}, and are regulated by their N-terminal Ca²⁺-binding domains which protrude into the intermembrane space [18,92,93]. Their main physiological function is being key components of the malate-aspartate shuttle (together with the oxoglutarate carrier, *SLC25A11*, OGC) to catalyze the transfer of reducing equivalents of NADH from the cytosol to the mitochondrial matrix [49,94]. Another function of AGC1 and AGC2 is the mitochondrial export of aspartate that is a precursor for protein and nucleotide biosynthesis (Figure 3). In some tissues of AGC1 deficiency patients, the transfer of reducing equivalent of NADH may be maintained by AGC2 or the glycerol-3-phosphate shuttle, and the mitochondrial export of aspartate may be compensated, at least partly, by AGC2 or UCP2. In fact, the symptoms of *SLC25A12* deficiency are mainly associated with alterations in the central nervous system and muscle, where AGC1 is the predominantly expressed AGC isoform [18].

The effects of the pathogenic mutations in *SLC25A12* have been studied in some detail. Skeletal muscle mitochondria from an AGC1 deficiency-affected child with the homozygous disease-causing mutation p.Gln590Arg (located in the substrate translocation pore at position 283, Figure 2B,D) displayed much reduced ATP production, and recombinant reconstituted protein harboring the mutation had no transport activity [90]. Two other patients, two siblings with the homozygous mutation p.Arg252Gln (found in the SMS at position 34, Figures 1 and 2A,C, outside the pore) exhibited similar symptoms as the previous one; and the activity of the mutated protein was dramatically reduced but not completely abolished [91]. Recently, another disease-causing mutation, p.Thr444Ile (Figure 2B,D, at position 130), has been found in the substrate translocation pore (Table S1), but the transport activity of this AGC1 variant has not been investigated [95].

The link between defective AGC1 and hypomyelination is probably due to the protein contribution to mitochondrial export of aspartate, which is needed for the formation of N-acetylaspartate necessary for myelin biosynthesis. In fact, mice lacking AGC1 display growth retardation, an impaired

central nervous system function, and reduced brain levels of N-acetyl-aspartate [96]. Moreover, AGC1 depletion in neurons (Neuro2A cells) and oligodendrocytes (precursor cells) inhibits proliferation and N-acetylaspartate synthesis [97,98]. It is noteworthy that (i) single nucleotide polymorphisms in AGC1 have been suggested to be associated with multi-factorial disorders, such as autism [99], and (ii) a mutation in AGC1 of Dutch shepherd dogs causes reduced transport activity of aspartate and glutamate in reconstituted liposomes as well as inflammatory myopathy [100]. The clinical conditions, psychomotor development, and myelination were markedly improved in an AGC1 deficiency child by introducing a ketogenic diet through the gradual increase of the ratio of fat to protein and carbohydrates [101]. This finding suggests a direction of future treatments of AGC1 deficiency.

3.7. *SLC25A13 (Aspartate-Glutamate Carrier 2, AGC2, Citrin) Deficiency*

The second human isoform of the aspartate-glutamate carrier AGC2 (SLC25A13) is expressed ubiquitously, especially in the liver. As AGC1, the aspartate-glutamate isoform 2 (AGC2) is an important component of the malate-aspartate shuttle which transfers reducing equivalents of NADH from the cytosol to the mitochondrial matrix and provides aspartate in the cytosol that is needed, among other things, for the urea cycle (Figure 3) [18,49,102]. In the *SLC25A13* gene, 117 different mutations causing AGC2 deficiency have been identified, and the patients, most of them from East and South Asia, are classified into two clinical phenotypes: neonatal intrahepatic cholestasis caused by citrin deficiency (NICCD, also classified as neonatal-onset citrullinemia type II) and adult-onset type II citrullinemia (CTLN2) (Table 1 and Table S1) [103,104]. In Japan, the observed prevalence of NICCD and CTLN2 is about 1:17 000 and 1:100 000–1:230 000, respectively [105]. The observed prevalence of NICCD is close to the calculated one based on heterozygous carrier frequency, which is about 1:65 in Japan and China [104,106]. In addition to transient intrahepatic cholestasis, NICCD patients present hepatomegaly, citrullinemia, ketotic hypoglycemia, aminoacidemias, hypoproteinemia, and growth retardation. Other dysfunctional liver-related symptoms may also occur, such as hepatitis, jaundice, reduction of coagulation factors and hemorrhagic diathesis. The NICCD symptoms are generally not severe and gradually disappear during the first years of life. NICCD is treated by a lactose-free and medium-chain-triglyceride diet supplemented with fat-soluble vitamins. Some of the NICCD subjects may suddenly develop CTLN2 as adults (usually between 20–50 years of age). CTLN2 patients have an aversion to carbohydrate-rich food and are unable to consume alcohol. In contrast, they have a liking for foods rich in protein and fat, that are energy sources less dependent on the malate-aspartate shuttle. As a matter of fact, alcohol and sugar intake as well as medication and surgery may provoke the symptoms. On top of citrullinemia, CTLN2 is characterized by fatty liver and repeated episodes of hyperammonemia, which lead to encephalopathy. CTLN2 is often associated with neuropsychiatric symptoms, such as nocturnal delirium, aggression, irritability, hyperactivity, delusions, disorientation, restlessness, drowsiness, loss of memory, flapping tremor, convulsive seizures, and coma. Treatments of CTLN2 consist of lactose-restricted low-carbohydrate diets supplemented with medium-chain-triglycerides [107]. Recently, from mice model studies, a combined supplement of ornithine with alanine or aspartate to reduce ammonium levels in blood has been suggested [108]. Liver transplantation is a resolute remedy.

Among the many different AGC2 deficiency mutations identified, the pathogenic variant c.851-854del is the most common in Japan and China [105]. Besides the 68 more deleterious mutations (insertion, deletion, insertion/deletion, non-sense truncation, splicing, and frame shift mutations), 50 point mutations have been identified: 12 are found in the N-terminal soluble regulatory domain that harbours EF-hand Ca^{2+} -binding motifs and 36 in the C-terminal mitochondrial carrier domain (Figure 1 and Table S1). Out of the latter group of mutations, fourteen are found in conserved motifs (Figure 1) and about half in the substrate translocation pore (Figure 2, at positions 29, 84, 130, 134, 137, 179, 182, 190, 220, 276, 279, 283, and 292).

3.8. SLC25A15 (Ornithine Carrier 1, ORC1) Deficiency

The ornithine carrier ORC1 is responsible for an important transport step in the urea cycle by catalyzing the electroneutral exchange of cytoplasmic ornithine⁺ for matrix citrulline + H⁺ (Figure 3) [49,102,109–111]. Mutations in the ORC1 gene, *SLC25A15*, have been identified to cause hyperornithinemia, hyperammonemia, and homocitrullinuria (HHH) syndrome in more than 100 patients, the majority of which lives in Canada, Italy, or Japan (Table 1) [112,113]. Besides the alterations underlined in the name of the disease, the metabolic features of HHH syndrome include elevated levels of polyamines, glutamine, and alanine as well as increased amounts of orotic acid and uracil in urine. Among the highly variable clinical symptoms of HHH syndrome are: in the acute phase, hepatitis-like attacks of vomiting, liver failure, confusion, and coma; and in the chronic phase lethargy, seizures, mental retardation, spastic paraplegia, cerebellar ataxia, learning difficulties, coagulation factor defects, and aversion to protein-rich food. Lethargy and coma are the most common early-onset symptoms, whereas movement and behaviour dysfunction are usually associated with late-onset or progressed stages of disease. Patients with HHH syndrome are treated in the acute phase with intravenous glucose, abolished protein intake, and ammonia scavengers such as benzoate and phenylbutyrate, and in the chronic phase with low-protein diets supplemented with citrulline or arginine. The development of HHH syndrome in patients under treatment is very variable from cases with only mild manifestations, compatible with an almost normal life, to cases with severe disability.

ORC1 deficiency reduces the rate of the urea cycle and hence leads to hyperammonemia, similarly to other genetic diseases associated with the urea cycle and ammonia-related metabolism (including AGC2 deficiency, Section 3.7). The ammonia toxicity is thought to be responsible for the neurological symptoms, which are in common to these diseases [114]. ORC1 deficiency also causes the build-up of ornithine in the cytosol and, subsequently, hyperornithinemia, increased levels of polyamines (which originate from cytosolic ornithine), and a secondary creatine deficiency, due to arginine-glycine amidotransferase inhibition by an excess of ornithine. Homocitrullinuria and increased excretion of orotic acid in urine are explained by an increase in carbamoyl-phosphate, which either condensates with lysine (forming homocitrulline) or enters the pyrimidine pathway (Figure 3).

Among the 38 different mutations found to cause HHH syndrome, the most common are p.Phe188del and p.Arg179*, which are found in 45% of the patients. The effects of many disease-causing mutations on ORC1-catalyzed transport have been assessed in reconstituted liposomes by the EPRA method and by in vitro cell culture studies, which have shown that, with very few exceptions, the mutations are deleterious for activity [111,115–117]. Some of the mutations (p.Glu180Lys, p.Arg275Gly and p.Arg275Gln at positions 183 and 279) (Figure 2B,D) are in the contact points (Figure 1), changing residues that were proved experimentally to participate directly in substrate binding [31]. Most point mutations are located along the substrate translocation pore (at positions 25, 36, 76, 119, 183, 191, 216, 220, 276, 279, and 287), but others have their residue side chains outside the pore of ORC1 (at positions 13, 28, 30, 35, 77, 132, 193, 196, 268, and 277).

3.9. SLC25A16 Deficiency

SLC25A16 was called Graves' disease carrier protein because it was picked up in an immunoscreen with antisera from patients with Graves' disease [118,119]. However, its association to Graves' disease has never been clarified, although there are some clues about its function; SLC25A16 was shown to complement the lack of its yeast homologue Leu5p, which is implicated in mitochondrial CoA transport [120], and, furthermore, SLC25A16 is closely related to human SLC25A42, which was shown to transport CoA, dephospho-CoA, adenosine 3',5'-diphosphate (PAP) and some other adenine nucleotides [121]. Recently, a mutation in SLC25A16 (p.Arg31Leu, located just before H1, Figure 1, at position 2 in Figure 2A) has been associated with autosomal recessive isolated fingernail dysplasia in members of a Pakistani family [122]. The affected members displayed a severe form of onychodystrophy, a hyperkeratotic nail bed, a thickened and dystrophic nail plate, and digits with mild erythema and swelling close to the proximal nail folds, whereas the toenails were normal. The link between the nail

malformation phenotype and the role of SLC25A16 in the mitochondrial CoA transport (if this is the role of this transporter) is yet unclear.

3.10. *SLC25A19 (Thiamine Pyrophosphate Carrier, TPC) Deficiency*

Patients suffering from the disorder Amish microcephaly have severe congenital microcephaly, 2-oxoglutaric aciduria, and often premature death. The traits of this disease were traced back in many generations of Amish families in Lancaster County (Pennsylvania) and linked to a mutation in *SLC25A19* causing the substitution p.Gly177Ala in its gene product [123]. Later, eight patients aged 3–20 years with less severe symptoms, such as increased lactate levels in cerebrospinal fluid or serum, chronic progressive polyneuropathy and fever-triggered acute episodes of flaccid paralysis and encephalopathy with bilateral striatal necrosis, were associated with five other mutations in *SLC25A19* [124–127]. This form of *SLC25A19* deficiency was classified as thiamine metabolism dysfunction syndrome 4 (progressive polyneuropathy type).

SLC25A19 encodes the thiamine pyrophosphate carrier TPC1 that transports thiamine pyrophosphate, thiamine monophosphate, and deoxynucleotides [123,128,129] as its homologue in *S. cerevisiae* Tpc1p [130]. The knockout of *SLC25A19* in the mouse causes depletion of mitochondrial thiamine pyrophosphate, embryonic lethality, brain malformations, and anemia [129]. It is therefore likely that the major symptoms of *SLC25A19* deficiency are due to lack of mitochondrial import of thiamine pyrophosphate, which is formed in the cytoplasm from thiamine absorbed in the intestine, in exchange for intramitochondrial thiamine monophosphate (Figure 3). Mitochondrial thiamine pyrophosphate is an essential cofactor of three mitochondrial enzymes: pyruvate dehydrogenase, branched chain ketoacid dehydrogenase and 2-oxoglutarate dehydrogenase. The deficit of mitochondrial thiamine pyrophosphate causes reduced 2-oxoglutarate dehydrogenase activity, leading to the accumulation of 2-oxoglutarate and 2-oxoglutaric aciduria, and probably reduced pyruvate dehydrogenase activity, leading to the accumulation of lactate. Oral thiamine treatment has been reported to improve the conditions of some of the patients suffering from thiamine metabolism dysfunction syndrome 4 phenotype [125,127]. The severe phenotype-causing mutation p.Gly177Ala affects a highly conserved residue of the second part of the SMS (Figure 1, Figure 2B,D, at position 175); and the recombinant protein harboring this mutation was found to display a markedly reduced transport activity in isolated liposomes by the EPRA method [123,129]. In contrast, the mutations of the less severe phenotype may be less harmful to the activity because p.Gly125Ser and p.Gln192His (at positions 119 and 190, respectively), although located inside the substrate translocation pore, are not affecting conserved residues, and p.Ser194Pro and p.Leu290Gln (at positions 192 and 278, respectively) are outside the pore. However, p.Glu304Lys, which replaces a negative charge of the cytoplasmic gate (Figure 1, Figure 2B,C, at position 292) and therefore is expected to affect transport substantially, is also among the mutations causing the less severe phenotype. Unfortunately, the impact of the latter mutations on the transport function of *SLC25A19* has not been investigated yet.

3.11. *SLC25A20 (Carnitine-Acylcarnitine Carrier, CAC) Deficiency*

The carnitine-acylcarnitine carrier CAC catalyzes the uptake of carnitine-linked long fatty acids into the mitochondria in exchange for free carnitine. This reaction is part of the carnitine cycle which allows the entry of fatty acids from the cytosol into the mitochondrial matrix where they are degraded by the β -oxidation pathway (Figure 3) [131,132]. Patients with CAC deficiency had been discovered before [133] the CAC gene (*SLC25A20*) was sequenced and the first disease-causing mutation was identified [35,134]. There are two clinical types of CAC deficiency: a neonatal-onset severe form and an infancy-onset milder form. Both phenotypes are characterized by lethargy, seizures, vomiting, fasting-induced coma, hypotonia, cardiomyopathy, muscle weakness, liver dysfunction and respiratory distress. Metabolic alterations include hypoglycemia, hypoketosis, hyperammonemia, dicarboxylic aciduria, increased long-chain acyl-carnitines, transaminases, and creatine kinase, whereas free carnitine is decreased. Fasting and illness may lead to brain damage, coma and ultimately death,

even in the milder form. It is likely that the symptoms, with major effects on the liver, muscle, and brain, are due to accumulation of long-chain fatty acids and acyl-carnitines that cannot be oxidized or form ketone bodies. Similar symptoms are caused by mutations in the genes of β -oxidation enzymes. Mild form CAC deficiency patients usually respond well to a dietary treatment consisting of frequent, high-carbohydrate and low-fat meals supplemented with polysaturated fatty acids.

Only 12 out of the 38 CAC deficiency mutations are missense mutations, whereas the great majority are insertion, deletion, nonsense, frame shift, and splicing mutations (Table S1). Five of the CAC missense mutations are found in the substrate translocation pore (Figure 2B,D, at positions 25, 29, 79, 182, and 231), of which two are in the conserved SMS residues and two are in the contact point residues (Figure 1). The remaining missense mutations are outside the pore (Figure 2A,C, at positions 20, 53, 85, 135, 230, 238, and 285). Several approaches have been used to investigate the impact of the SLC25A20 mutations on the CAC transport. In the first method, indirect CAC activity was determined in fibroblasts by supplementing ^{14}C -labeled fatty acids and measuring the rate of fatty acid oxidation as $^{14}\text{CO}_2$ evolved/hr x mg cell protein [135]. All the other methods are based on the expression of the CAC variants in *Escherichia coli* [135,136] or in appropriate strains of *S. cerevisiae* [137] and *Aspergillus nidulans* [136,138].

3.12. SLC25A21 (Oxodicarboxylate Carrier, ODC) Deficiency

A homozygous missense mutation in *SLC25A21*, giving rise to the p.Lys232Arg replacement in the oxodicarboxylate carrier ODC, segregated with a patient with spinal muscular atrophy-like disease and mitochondrial myopathy associated with reduced mitochondrial DNA copy number (Table 1 and Table S1) [139]. ODC mainly transports 2-oxoadipate and 2-aminoadipate, that are produced from lysine and tryptophan degradation in the cytosol and are transported into the mitochondrial matrix, where they are oxidized and fed into the TCA cycle (Figure 3) [140,141]. It has been suggested by the same authors that the ODC-catalyzed mitochondrial import of these two metabolites occurs via an exchange for matrix 2-oxoglutarate [142]. Although the disease-causing p.Lys232Arg substitution is a conservative mutation, it affects an SMS residue (Figure 1) of the matrix salt bridge network (Figure 2B,D, at position 234), and renders SLC25A21 inactive [139]. In the SLC25A21-deficient patient, the urinary excretion of pipercolic and quinolinic acid, which are intermediates or by-products of the lysine and tryptophan degradation pathways, was observed together with that of 2-oxoadipate (Figure 3). The altered concentrations of these substances in the body are supposed to be toxic and lead to the reduction in mitochondrial DNA and cause mitochondrial dysfunction and spinal motor neuron abnormalities.

3.13. SLC25A22 (Glutamate Carrier 1, GC1) Deficiency

Initially, two mutations in *SLC25A22* were shown to cause severe neonatal epileptic encephalopathy with suppression bursts (NEESB) [143,144]. More recently, other eight mutations giving rise to similar symptoms have been identified in the same gene (all but one reviewed in [145]). This genetic disease is now classified as early infantile epileptic encephalopathy type 3 (EIEE3) (Table 1), and is characterized by early-onset myoclonic seizures, severe hypotonia, microcephaly, suppression burst pattern, severe developmental delay and often brain atrophy. A further mutation in *SLC25A22* caused hypotonia and developmental delay as in EIEE3, but also migrating partial seizures in infancy (MPSI) without suppression bursts [146]. Therefore, SLC25A22 deficiency patients present phenotypes spanning from very severe cases, with intractable epilepsy, no motor acquisition, vegetative state and early death, to moderate cases with tractable epilepsy, some motor acquisition, no microcephaly or suppression bursts [145].

SLC25A22 encodes the glutamate carrier GC1, which imports glutamate by proton co-transport into the mitochondrial matrix [147] where it is transformed into ammonium ions and 2-oxoglutarate by glutamate dehydrogenase (Figure 3). The ammonium enters the urea cycle for clearance of excess nitrogen, whereas 2-oxoglutarate is used in gluconeogenesis (in liver and kidney) or oxidized in TCA

cycle for ATP production (in non-hepatic tissues). SLC25A22 is highly expressed in most tissues including the brain, especially in areas associated with motor coordination and in astrocytes, that control the uptake of extracellular neurotransmitter glutamate [147,148]. It is likely that extracellular glutamate levels in brain are dysregulated in SLC25A22 deficiency patients [143] because it was shown that (i) reduced expression of SLC25A22 in glial cells leads to intracellular glutamate accumulation [148], and (ii) aberrant glutamate catabolism in astrocytes is associated with altered clearance of extracellular (synaptic) glutamate and early epileptic encephalopathy [149]. Moreover, some patients with SLC25A22 deficiency manifest hyperprolinemia [150], which might be explained by assuming that dysfunctional GC1 activity diminishes or abolishes the export of proline-derived glutamate from mitochondria leading to accumulation of proline in the body.

Out of ten point mutations in SLC25A22, two are in the first part of the third SMS, two in the same residue in contact point I (Figure 1), some are inside the substrate translocation pore (Figure 2, at positions 83, 119, and 220), and the rest outside the pore (at positions 60, 192, 230, 233, 258, and 281). It is noteworthy that patients with severe forms of SLC25A22 deficiency (severe EIEE3 and MPSI) have homozygous point mutations in residues with side chains protruding into the substrate translocation pore (with the exception of p.Pro206Leu), whereas milder forms exhibit the homozygous, or at least one of the heterozygous, mutations outside the pore. Moreover, GC1 variants of the most severe cases assessed in reconstituted liposomes by the EPRA method, exhibited negligible transport activity in vitro [143,144,146].

3.14. SLC25A24 (ATP-Mg²⁺/Phosphate Carrier 1, APC1) Deficiency

Gorlin–Chaudhry–Moss and Fontaine–Farriaux syndromes are rare dysmorphic genetic disorders manifested with similar symptoms: aged appearance with loose or wrinkled skin, short stature, hypertrichosis, skull deformities with craniosynostosis or brachycephaly, and a characteristic facial appearance of a depressed nasal bridge, low hairline, and microphthalmia [151]. Other common symptoms include digit and nail anomalies, cardiovascular abnormalities, umbilical hernia, and hypoplastic genital system. Whereas for some patients, early death has been reported, others display normal or nearly normal developmental outcomes. Given that both syndromes are caused by an autosomal dominant mutation in SLC25A24, either de novo p.Arg217Cys or p.Arg217His mutation [152,153], the two syndromes are now designated with a common name: Fontaine progeroid syndrome. Until now, 11 cases, which were confirmed to have one of the two above mentioned mutations, have been reported with this disease [151].

SLC25A24 encodes the ATP-Mg²⁺/phosphate carrier APC1, which, besides the MC domain that transports ATP, ATP-Mg²⁺, ADP, AMP, and phosphate (Figure 3), has a regulatory N-terminal domain containing EF-hand Ca²⁺ binding sites activating transport when cytosolic Ca²⁺ increases [19,154,155]. This carrier is one of the four human isoforms and is involved in regulating the matrix adenine nucleotide pool through its capacity to transport adenine nucleotides in exchange for intra- or extra-mitochondrial phosphate [19]. The corresponding residue of APC1 Arg217 in the AAC structures is also an arginine located in a non-conserved position in the first part of the first SMS (Figure 1) on the matrix side of H1 (Figure 2A, at position 30). In the c-state, this arginine is buried in the structure and forms hydrogen bonds with residues of H2 and H3, while in the m-state it is positioned at the entrance of the substrate translocation pore and does not participate in any apparent interaction (Figure 2C). Therefore, it may be that the interactions of Arg217 play a role in the m-gate and neither its substitution with cysteine nor with histidine have the ability to form the same hydrogen bonds. Until now, the effects of the disease-causing mutations on the transport activity of APC1 are not known.

The connection between the mutations in SLC25A24 and the symptoms of Fontaine progeroid syndrome is not clear. However, there are some clues: it was shown that fibroblasts from patients and cells expressing disease-causing mutant proteins have altered mitochondrial morphology, decreased proliferation rate, oxygen consumption, and mitochondrial ATP content, whereas mitochondrial membrane potential and oxidative stress sensitivity are increased [152,153]. These results may suggest that the above mentioned SLC25A24 mutations cause impaired energy metabolism, mitochondrial

dysfunction, and a mitochondrial ATP deficit, which lead to the imbalanced proliferation and differentiation of progenitor cells involved in the development of skeletal and connective tissues [152,153]. Whether these consequences are due to APC1 haplo-insufficiency or active dominant effects of the mutated proteins remains to be answered.

3.15. *SLC25A26 (S-Adenosylmethionine Carrier, SAMC) Deficiency*

SLC25A26 encodes mitochondrial S-adenosylmethionine carrier SAMC, which imports cytosol-synthesized S-adenosylmethionine (SAM) in exchange for matrix S-adenosylhomocysteine (Figure 3) [156], as its homologues in *S. cerevisiae* [157] and *A. thaliana* [158]. Matrix SAM is used as a methyl group donor in the methylation of DNA, RNA, proteins and coenzyme Q, and in the biosynthesis of lipoic acid. Therefore, it is not surprising that the three unrelated patients identified with *SLC25A26* deficiency exhibited reduced intra-mitochondrial methylation of RNA and proteins, reduced translation and diminished coenzyme Q and lipoic acid levels [159]. The consequent mitochondrial dysfunction and defective respiratory chain activity may explain the clinical features found in patients suffering from this disorder, i.e., respiratory insufficiency, lactic acidosis, acute episodes of cardiopulmonary failure, and progressive muscle weakness.

The levels of transport activity of the recombinant SAMC variants harboring the three missense mutations associated with *SLC25A26* deficiency seem to be related to their position in the SAMC homology model. p.Ala102Val and p.Pro199Leu, which cause almost depleted transport activity compared to the wild-type carrier protein and are found inside the substrate translocation pore (Figure 2, at position 126) and in the third SMS (at position 229, outside the pore), respectively, and p.Val148Gly, which causes a marked decrease in activity (15% of the wild-type protein), is found outside the pore (at position 180) [159]. Interestingly, the homozygous patient with the latter mutation displayed milder manifestations of the symptoms with respect to the heterozygous patient having the two first-mentioned mutations. Furthermore, the most severe case, which had a homozygous splice site mutation resulting in undetected protein product, died of respiratory and multiple organ failure in the first days of life. Therefore, the development and severity of the disease seem to be related to the transport activities of the mutated proteins and the allele composition of the patients.

3.16. *SLC25A32 Deficiency*

Two cases of *SLC25A32* deficiency have been reported. One patient had recurrent late-onset exercise intolerance and abnormalities in the acyl-carnitine profile, which are characteristic features of multiple acyl-CoA dehydrogenase deficiency [160]. Later, another patient with more severe neuromuscular phenotype was identified presenting early onset ataxia, myoclonia, dysarthria, altered levels of organic acids and acylcarnitines in plasma and urine, muscle weakness, and exercise intolerance [161]. The state of both patients was improved upon treatment with riboflavin, which is a precursor of the cofactor FAD. The less severely affected patient had a truncation and a conservative p.Arg147His mutation (in the second positively charged residue of the second SMS (Figure 1) at position 139 outside the pore (Figure 2A,C)) in her two *SLC25A32* alleles, respectively; the more severe case had a homozygous oligonucleotide insertion/deletion mutation (Table S1), probably leading to the complete absence of the *SLC25A32* protein. Until now, it has not been shown that *SLC25A32* transports FAD and/or folate by direct transport assays. However, experiments have been performed suggesting that its *S. cerevisiae* homologue Flx1p (and also *SLC25A32*) transport FAD and/or folate (Figure 3) [162–164]. Furthermore, the missense mutation p.Arg147His of *SLC25A32* introduced in a yeast Flx1 deletion strain complements the growth defect only partly. This may suggest that the mutant protein retains some activity [160] or the function of *SLC25A32* is partially compensated by some other MC. It is known, for example, that the yeast NAD⁺ carrier transports FAD to some extent [165]. In addition, the physiological importance of *SLC25A32* has been emphasized by gene-trap inactivation experiments of *SLC25A32* in mice displaying neural tube defects and embryonal death [166]. One might speculate that

both reduced mitochondrial FAD and folate transports would lead to mitochondrial defects underlying the symptoms of malfunctioning SLC25A32.

3.17. SLC25A38 (Glycine Carrier, GlyC) Deficiency

Mutations in *SLC25A38* cause autosomal recessive nonsyndromic congenital sideroblastic anemia, which is characterized by ringed sideroblasts with accumulated iron deposits in mitochondria [167,168]. The onset of SLC25A38-associated sideroblastic anemia, which is usually microcytic, is within the first years of life. If untreated, toxic iron deposits build up in organs, such as heart and liver, causing cardiomyopathy and hepatic fibrosis, which lead to heart failure, chronic liver damage, and endocrine disorders, and subsequently can result in failure to thrive and death. The patients are treated with recurrent blood transfusions with the risk of increasing the iron overload even further. Therefore, much attention is focused on assessment and monitoring the iron levels. Thus, the transport function of SLC25A38 is associated with heme biosynthesis, and reconstituted GlyC (the protein product of *SLC25A38*) and its yeast homolog Hem25p were shown to transport glycine, which needs to enter the mitochondrial matrix to be converted into the heme precursor 5-aminolevulinic acid [169]. Mutations in mitochondrial 5-aminoluvelinic synthase 2, i.e., the enzyme catalyzing this reaction, also cause an X-linked form of nonsyndromic congenital sideroblastic anemia. Out of the 25 pathogenic mutations found in *SLC25A38* so far, fifteen are single residue missense mutations (Figure 1 and Table S1). About half of the latter are found inside the substrate translocation pore (at positions 36, 119, 123, 191, 220, 276) and two precisely in the same residue of contact point II (at position 182, Figures 1 and 2B,D).

3.18. SLC25A42 (CoA and PAP Carrier) Deficiency

A single nucleotide mutation in *SLC25A42* (causing the substitution p.Asn291Asp in its protein product) was found in 14 homozygous individuals of Arabic descent, who presented variable degrees of severity of symptoms such as mitochondrial myopathy with muscle weakness, lactic acidosis, encephalopathy, developmental regression, and epilepsy [170–172]. Recently, also a homozygous splice site mutation was found in a patient with similar clinical features [172]. As additional evidence of the pathogenic effects of certain *SLC25A42* mutations, a comparable phenotype with severe muscle disorganization and weakness was observed in the zebrafish knockdown of this gene [170]. *SLC25A42* encodes a MC that transports CoA, dephospho-CoA, adenosine 3',5'-diphosphate (PAP), and some other adenine nucleotides [121]. The point mutation of Asn291 (Figure 2, at position 276) is localized inside the pore of the carrier structure in the vicinity of the substrate binding site and may therefore interfere with substrate binding. The main physiological function of SLC25A42 was suggested to be the import of CoA in exchange for PAP [121]. The possibility of external CoA and internal dephospho-CoA exchange was also considered [121]. In the mitochondrial matrix, CoA is an essential cofactor in many major processes, such as the TCA cycle, urea cycle, β -oxidation, heme biosynthesis, branched-chain amino acid oxidation, and protein acetylation. Moreover, in the mammalian mitochondrial matrix, PAP is formed when CoA donates its phosphopantetheine moiety to the acyl carrier protein for the synthesis of lipoic acid and long chain fatty acids. In *Drosophila melanogaster*, the main role of SLC25A42 has been suggested to be the export of mitochondrial dephospho-CoA [173]. At any rate, the disease-causing mutations affecting SLC25A42 transport activity probably give rise to a mitochondrial myopathy, which subsequently leads to the symptoms described above. Yet, it is difficult to comprehend the clinical heterogeneity and wide spectrum of severity of SLC25A42 deficiency even among patients with the same mutation in the same family.

3.19. SLC25A46 Deficiency

The clinical phenotypes resulting from mutations in *SLC25A46* are quite heterogeneous; they include axonal peripheral neuropathy, cerebellar, and optic atrophy found in patients diagnosed with congenital pontocerebellar hypoplasia, autosomal recessive cerebellar ataxia, Charcot–Marie–Tooth disease type 2 and optic atrophy spectrum disorder, Ramsay-Hunt or Leigh syndrome [174–180].

The severity and onset of the symptoms also vary, from death shortly after birth to mild manifestations appearing in adulthood. Unlike the other MCs, the SLC25A46 protein is localized in the outer mitochondrial membrane [174] and no transport activity has been associated with it so far. Instead, SLC25A46 has been suggested to play a role in mitochondrial fusion and fission because its overexpression and knockdown in cell lines lead to the fragmentation and hyperfusion of mitochondria, respectively [175]. In agreement to the symptoms observed in SLC25A46 deficiency patients, *SLC25A46* knockdown in zebrafish gives rise to defects in mitochondrial network maintenance, fission and cristae dynamics, and causes a dysfunctional neurodevelopment phenotype [174]. Notably, mutations in other genes involved in the regulation of the mitochondrial shape cause similar clinical features as those found in SLC25A46 deficiency patients [174]. Furthermore, it has been suggested that (i) the pathogenic SLC25A46 mutations affect the stability of the protein and interfere with protein–protein interactions important in mitochondrial morphology dynamics, and (ii) the degree of the protein destabilization and interference effects determine the severity of the disease [181]. Five of the pathogenic point mutations are located in different matrix helices (Figure 2A,C, at positions 48, 52, 70, 157, and 165) and they could be involved in protein-protein interactions; the other four are all in the SMS of H5 (Figure 1).

4. Multigenic Diseases with Mutations in MCs

There is clear evidence that mutations in MC genes cause the disorders described in Section 3. However, there are other diseases that are caused by mutations in several genes including MC genes or depend strongly on additional genetic and environmental factors. For example, it is noteworthy that polymorphisms in *SLC25A8* (encoding UCP2) and *SLC25A9* (UCP3) are associated with obesity and type 2 diabetes [182,183]; mutations in *SLC25A8* and other genes may lead to hyperinsulinism [184]; and a single nucleotide variation in *SLC25A40* (a carrier of unknown function) is linked to hypertriglyceridemia [185]. Furthermore, *SLC25A11* (encoding the oxoglutarate carrier OGC) is a tumor-suppressor gene (together with some genes encoding TCA cycle enzymes), i.e., mutations of *SLC25A11* confer a predisposition to metastatic paragangliomas [186]. In addition, genetic variants of several MCs have also been linked to complex multifactorial disorders such as autism [99,187,188].

5. Concluding Remarks

In the past decades, remarkable advances have been made in defining the molecular and genetic basis of different types of mitochondrial diseases, including those associated with MCs. Progress has been achieved despite the fact that many mitochondrial diseases are extremely heterogeneous clinically, biochemically, and genetically, and many of them are multi-system disorders affecting several organs [5]. As shown in this review, the number and understanding of the diseases associated with MCs is rapidly growing, and the connections between the mutations, defective transport, altered metabolism, and pathogenic mechanisms underlying the symptoms start to be better comprehended. This advance gives hope for improved, more rapid, and earlier diagnostics such as clinical observations, genetic counselling, prenatal diagnosis, and newborn screening, as well as for novel therapeutic strategies. However, this development is still hampered by the lack of knowledge about many MCs in terms of the substrates transported and their physiological roles in vivo in tissues and specialized cells. Future investigations are warranted along these lines of research to tackle and better comprehend the metabolic disorders associated with MCs.

Mitochondrial medicine aimed at correcting the mitochondrial defects is very challenging. Several complementary approaches, which include methods of general and personalized precision medicine, may be applied for efficient treatment. General approaches to improve and facilitate mitochondrial function utilize compounds such as antioxidants, factors that stimulate mitochondrial biogenesis (through signaling pathways and transcription factors), or clearance of defective mitochondria by autophagy and lysosomal removal [2,5]. For some of the MC-associated diseases, appropriate diets often supplemented with specific metabolites or cofactors are being used or are undergoing clinical trials. In principle, gene therapy is the resolute approach that can cure the

defects caused by specific gene alterations. Nowadays, viral vectors and/or CRISPR-Cas-based editing mutated DNA or RNA are available to accomplish gene therapy. These therapies aiming at correcting mutations in mtDNA are encountering many technical and physiological difficulties, such as a lack of mitochondrial vectors, multiple copies of mtDNA, and no systems for mtDNA recombination and repair. However, gene therapies for mitochondrial disorders caused by mutations in the nuclear DNA, such as the MC-associated diseases, may be developed in a relatively near future.

Supplementary Materials: The following are available online at <http://www.mdpi.com/2218-273X/10/4/655/s1>, Table S1: Disease-causing mutations in mitochondrial carriers.

Funding: Research in the authors' laboratories was supported by grants from the Ministero dell'Istruzione, dell'Università e della Ricerca (MIUR), Centre of Excellence "Genomics: genes involved in pathophysiological processes in the biomedical and agricultural fields" (CEGBA), Comitato Telethon Fondazione Onlus No. GGP11139, Italian Human ProteomeNet, and PRIN 2017 (2017PAB8EM_004).

Acknowledgments: The authors thank Prof. Yuang-Zong Song for his valuable comments on AGC2 deficiency. Research in the authors' laboratories has been made possible by the talent of students, fellows, and collaborators.

Conflicts of Interest: The authors declare no conflict of interest.

Abbreviations

CoA: coenzyme A; CoQ, coenzyme Q; EPRA, expression-purification-reconstitution-transport-assay; MC, mitochondrial carrier; SAM, S-adenosylmethionine; SLC25, solute carrier family 25; SMS, signature motif sequence; TMP, thiamine monophosphate; TPP, thiamine pyrophosphate; and UCP, uncoupling protein.

References

1. McCormick, E.M.; Zolkipli-Cunningham, Z.; Falk, M.J. Mitochondrial disease genetics update: Recent insights into the molecular diagnosis and expanding phenotype of primary mitochondrial disease. *Curr. Opin. Pediatr.* **2018**, *30*, 714–724. [CrossRef] [PubMed]
2. Rahman, J.; Rahman, S. Mitochondrial medicine in the omics era. *Lancet* **2018**, *391*, 2560–2574. [CrossRef]
3. Davis, R.L.; Liang, C.; Sue, C.M. Mitochondrial diseases. *Handb. Clin. Neurol.* **2018**, *147*, 125–141. [PubMed]
4. Dard, L.; Blanchard, W.; Hubert, C.; Lacombe, D.; Rossignol, R. Mitochondrial functions and rare diseases. *Mol. Aspects Med.* **2020**, *71*, 100842. [CrossRef]
5. Viscomi, C.; Zeviani, M. Strategies for fighting mitochondrial diseases. *J. Intern. Med.* **2020**. (In press) [CrossRef]
6. Wallace, D.C. Mitochondrial genetic medicine. *Nat. Genet.* **2018**, *50*, 1642–1649. [CrossRef]
7. Palmieri, F.; Agrimi, G.; Blanco, E.; Castegna, A.; Di Noia, M.A.; Iacobazzi, V.; Lasorsa, F.M.; Marobbio, C.M.T.; Palmieri, L.; Scarcia, P.; et al. Identification of mitochondrial carriers in *Saccharomyces cerevisiae* by transport assay of reconstituted recombinant proteins. *Biochim. Biophys. Acta* **2006**, *1757*, 1249–1262. [CrossRef]
8. Picault, N.; Hodges, M.; Palmieri, L.; Palmieri, F. The growing family of mitochondrial carriers in Arabidopsis. *Trends Plant Sci.* **2004**, *9*, 138–146. [CrossRef]
9. Palmieri, F. The mitochondrial transporter family SLC25: Identification, properties and pathophysiology. *Mol. Asp. Med.* **2013**, *34*, 465–484. [CrossRef]
10. Saraste, M.; Walker, J.E. Internal sequence repeats and the path of polypeptide in mitochondrial ADP/ATP translocase. *FEBS Lett.* **1982**, *144*, 250–254. [CrossRef]
11. Palmieri, F. Mitochondrial carrier proteins. *FEBS Lett.* **1994**, *346*, 48–54. [CrossRef]
12. Fiermonte, G.; Walker, J.E.; Palmieri, F. Abundant bacterial expression and reconstitution of an intrinsic membrane-transport protein from bovine mitochondria. *Biochem. J.* **1993**, *294*, 293–299. [CrossRef] [PubMed]
13. Palmieri, F.; Indiveri, C.; Bisaccia, F.; Iacobazzi, V. Mitochondrial metabolite carrier proteins: Purification, reconstitution, and transport studies. *Methods Enzymol.* **1995**, *260*, 349–369. [PubMed]
14. Palmieri, F.; Monné, M. Discoveries, metabolic roles and diseases of mitochondrial carriers: A review. *Biochim. Biophys. Acta* **2016**, *1863*, 2362–2378. [CrossRef]
15. Monné, M.; Palmieri, F. Antiporters of the mitochondrial carrier family. *Curr. Top. Membr.* **2014**, *73*, 289–320.
16. Palmieri, F.; Pierri, C.L. Mitochondrial metabolite transport. *Essays Biochem.* **2010**, *47*, 37–52.
17. Palmieri, F.; Pierri, C.L.; De Grassi, A.; Nunes-Nesi, A.; Fernie, A.R. Evolution, structure and function of mitochondrial carriers: A review with new insights. *Plant J.* **2011**, *66*, 161–181. [CrossRef]

18. Palmieri, L.; Pardo, B.; Lasorsa, F.M.; del Arco, A.; Kobayashi, K.; Iijima, M.; Runswick, M.J.; Walker, J.E.; Saheki, T.; Satrústegui, J.; et al. Citrin and aralar1 are Ca(2+)-stimulated aspartate/glutamate transporters in mitochondria. *EMBO J.* **2001**, *20*, 5060–5069. [CrossRef]
19. Fiermonte, G.; De Leonardis, F.; Todisco, S.; Palmieri, L.; Lasorsa, F.M.; Palmieri, F. Identification of the mitochondrial ATP-Mg/Pi transporter. Bacterial expression, reconstitution, functional characterization, and tissue distribution. *J. Biol. Chem.* **2004**, *279*, 30722–30730. [CrossRef]
20. Del Arco, A.; Satrústegui, J. Identification of a novel human subfamily of mitochondrial carriers with calcium-binding domains. *J. Biol. Chem.* **2004**, *279*, 24701–24713. [CrossRef]
21. Zara, V.; Palmieri, F.; Mahlke, K.; Pfanner, N. The cleavable presequence is not essential for import and assembly of the phosphate carrier of mammalian mitochondria but enhances the specificity and efficiency of import. *J. Biol. Chem.* **1992**, *267*, 12077–12081. [PubMed]
22. Palmieri, F.; Bisaccia, F.; Capobianco, L.; Dolce, V.; Fiermonte, G.; Iacobazzi, V.; Zara, V. Transmembrane topology, genes, and biogenesis of the mitochondrial phosphate and oxoglutarate carriers. *J. Bioenerg. Biomembr.* **1993**, *25*, 493–501. [CrossRef] [PubMed]
23. Zara, V.; Ferramosca, A.; Palmisano, I.; Palmieri, F.; Rassow, J. Biogenesis of rat mitochondrial citrate carrier (CIC): The N-terminal presequence facilitates the solubility of the preprotein but does not act as a targeting signal. *J. Mol. Biol.* **2003**, *325*, 399–408. [CrossRef]
24. Zara, V.; Ferramosca, A.; Robitaille-Foucher, P.; Palmieri, F.; Young, J.C. Mitochondrial carrier protein biogenesis: Role of the chaperones Hsc70 and Hsp90. *Biochem. J.* **2009**, *419*, 369–375. [CrossRef] [PubMed]
25. Pebay-Peyroula, E.; Dahout-Gonzalez, C.; Kahn, R.; Trézéguet, V.; Lauquin, G.J.-M.; Brandolin, G. Structure of mitochondrial ADP/ATP carrier in complex with carboxyatractyloside. *Nature* **2003**, *426*, 39–44. [CrossRef]
26. Ruprecht, J.J.; Hellowell, A.M.; Harding, M.; Crichton, P.G.; McCoy, A.J.; Kunji, E.R.S. Structures of yeast mitochondrial ADP/ATP carriers support a domain-based alternating-access transport mechanism. *Proc. Natl. Acad. Sci. USA* **2014**, *111*, E426–E434. [CrossRef]
27. Ruprecht, J.J.; King, M.S.; Zögg, T.; Aleksandrova, A.A.; Pardon, E.; Crichton, P.G.; Steyaert, J.; Kunji, E.R.S. The Molecular Mechanism of Transport by the Mitochondrial ADP/ATP Carrier. *Cell* **2019**, *176*, 435–447. [CrossRef]
28. Klingenberg, M. The ADP, ATP shuttle of the mitochondrion. *Trends Biochem. Sci.* **1979**, *4*, 249–252. [CrossRef]
29. Klingenberg, M. The ADP and ATP transport in mitochondria and its carrier. *Biochim. Biophys. Acta* **2008**, *1778*, 1978–2021. [CrossRef]
30. Robinson, A.J.; Kunji, E.R.S. Mitochondrial carriers in the cytoplasmic state have a common substrate binding site. *Proc. Natl. Acad. Sci. USA* **2006**, *103*, 2617–2622. [CrossRef]
31. Monné, M.; Miniero, D.V.; Daddabbo, L.; Robinson, A.J.; Kunji, E.R.S.; Palmieri, F. Substrate specificity of the two mitochondrial ornithine carriers can be swapped by single mutation in substrate binding site. *J. Biol. Chem.* **2012**, *287*, 7925–7934. [CrossRef] [PubMed]
32. Monné, M.; Palmieri, F.; Kunji, E.R.S. The substrate specificity of mitochondrial carriers: Mutagenesis revisited. *Mol. Membr. Biol.* **2013**, *30*, 149–159. [CrossRef] [PubMed]
33. Marobbio, C.M.T.; Giannuzzi, G.; Paradies, E.; Pierri, C.L.; Palmieri, F. α -Isopropylmalate, a leucine biosynthesis intermediate in yeast, is transported by the mitochondrial oxalacetate carrier. *J. Biol. Chem.* **2008**, *283*, 28445–28553. [CrossRef] [PubMed]
34. Tonazzi, A.; Console, L.; Giangregorio, N.; Indiveri, C.; Palmieri, F. Identification by site-directed mutagenesis of a hydrophobic binding site of the mitochondrial carnitine/acylcarnitine carrier involved in the interaction with acyl groups. *Biochim. Biophys. Acta* **2012**, *1817*, 697–704. [CrossRef]
35. Huizing, M.; Iacobazzi, V.; Ijlst, L.; Savelkoul, P.; Ruitenbeek, W.; van den Heuvel, L.; Indiveri, C.; Smeitink, J.; Trijbels, F.; Wanders, R.; et al. Cloning of the human carnitine-acylcarnitine carrier cDNA and identification of the molecular defect in a patient. *Am. J. Hum. Genet.* **1997**, *61*, 1239–1245. [CrossRef]
36. Palmieri, F. Diseases caused by defects of mitochondrial carriers: A review. *Biochim. Biophys. Acta* **2008**, *1777*, 564–578. [CrossRef]
37. Palmieri, F. Mitochondrial transporters of the SLC25 family and associated diseases: A review. *J. Inherit. Metab. Dis.* **2014**, *37*, 565–575. [CrossRef]
38. Rusecka, J.; Kaliszewska, M.; Bartnik, E.; Tońska, K. Nuclear genes involved in mitochondrial diseases caused by instability of mitochondrial DNA. *J. Appl. Genet.* **2018**, *59*, 43–57. [CrossRef]

39. Edvardson, S.; Porcelli, V.; J alas, C.; Soiferman, D.; Kellner, Y.; Shaag, A.; Korman, S.H.; Pierri, C.L.; Scarcia, P.; Fraenkel, N.D.; et al. Agenesis of corpus callosum and optic nerve hypoplasia due to mutations in SLC25A1 encoding the mitochondrial citrate transporter. *J. Med. Genet.* **2013**, *50*, 240–245. [CrossRef]
40. Nota, B.; Struys, E.A.; Pop, A.; Jansen, E.E.; Fernandez Ojeda, M.R.; Kanhai, W.A.; Kranendijk, M.; van Dooren, S.J.M.; Bevova, M.R.; Sistermans, E.A.; et al. Deficiency in SLC25A1, encoding the mitochondrial citrate carrier, causes combined D-2- and L-2-hydroxyglutaric aciduria. *Am. J. Hum. Genet.* **2013**, *92*, 627–631. [CrossRef]
41. Chaouch, A.; Porcelli, V.; Cox, D.; Edvardson, S.; Scarcia, P.; De Grassi, A.; Pierri, C.L.; Cossins, J.; Laval, S.H.; Griffin, H.; et al. Mutations in the Mitochondrial Citrate Carrier SLC25A1 are Associated with Impaired Neuromuscular Transmission. *J. Neuromuscul. Dis.* **2014**, *1*, 75–90. [CrossRef] [PubMed]
42. Prasun, P.; Young, S.; Salomons, G.; Werneke, A.; Jiang, Y.-H.; Struys, E.; Paige, M.; Avantaggiati, M.L.; McDonald, M. Expanding the Clinical Spectrum of Mitochondrial Citrate Carrier (SLC25A1) Deficiency: Facial Dysmorphism in Siblings with Epileptic Encephalopathy and Combined D,L-2-Hydroxyglutaric Aciduria. *JIMD Rep.* **2015**, *19*, 111–115. [PubMed]
43. Smith, A.; McBride, S.; Marcadier, J.L.; Michaud, J.; Al-Dirbashi, O.Y.; Schwartzentruber, J.; Beaulieu, C.L.; Katz, S.L.; FORGE Canada Consortium; Majewski, J.; et al. Severe Neonatal Presentation of Mitochondrial Citrate Carrier (SLC25A1) Deficiency. *JIMD Rep.* **2016**, *30*, 73–79.
44. Cohen, I.; Staretz-Chacham, O.; Wormser, O.; Perez, Y.; Saada, A.; Kadir, R.; Birk, O.S. A novel homozygous SLC25A1 mutation with impaired mitochondrial complex V: Possible phenotypic expansion. *Am. J. Med. Genet. A.* **2018**, *176*, 330–336. [CrossRef] [PubMed]
45. Eguchi, M.; Ozaki, E.; Yamauchi, T.; Ohta, M.; Higaki, T.; Masuda, K.; Imoto, I.; Ishii, E.; Eguchi-Ishimae, M. Manifestation of recessive combined D-2-, L-2-hydroxyglutaric aciduria in combination with 22q11.2 deletion syndrome. *Am. J. Med. Genet. A.* **2018**, *176*, 351–358. [CrossRef]
46. Palmieri, F.; Stipani, I.; Quagliariello, E.; Klingenberg, M. Kinetic study of the tricarboxylate carrier in rat liver mitochondria. *Eur. J. Biochem.* **1972**, *26*, 587–594. [CrossRef] [PubMed]
47. Bisaccia, F.; De Palma, A.; Palmieri, F. Identification and purification of the tricarboxylate carrier from rat liver mitochondria. *Biochim. Biophys. Acta* **1989**, *977*, 171–176. [CrossRef]
48. Bisaccia, F.; De Palma, A.; Dierks, T.; Krämer, R.; Palmieri, F. Reaction mechanism of the reconstituted tricarboxylate carrier from rat liver mitochondria. *Biochim. Biophys. Acta* **1993**, *1142*, 139–145. [CrossRef]
49. Palmieri, F. The mitochondrial transporter family (SLC25): Physiological and pathological implications. *Pflug. Arch.* **2004**, *447*, 689–709. [CrossRef]
50. Huizing, M.; Ruitenbeek, W.; van den Heuvel, L.P.; Dolce, V.; Iacobazzi, V.; Smeitink, J.A.; Palmieri, F.; Trijbels, J.M. Human mitochondrial transmembrane metabolite carriers: Tissue distribution and its implication for mitochondrial disorders. *J. Bioenerg. Biomembr.* **1998**, *30*, 277–284. [CrossRef]
51. Pop, A.; Williams, M.; Struys, E.A.; Monné, M.; Jansen, E.E.W.; De Grassi, A.; Kanhai, W.A.; Scarcia, P.; Ojeda, M.R.F.; Porcelli, V.; et al. An overview of combined D-2- and L-2-hydroxyglutaric aciduria: Functional analysis of CIC variants. *J. Inherit. Metab. Dis.* **2018**, *41*, 169–180. [CrossRef] [PubMed]
52. Majd, H.; King, M.S.; Smith, A.C.; Kunji, E.R.S. Pathogenic mutations of the human mitochondrial citrate carrier SLC25A1 lead to impaired citrate export required for lipid, dolichol, ubiquinone and sterol synthesis. *Biochim. Biophys. Acta* **2018**, *1859*, 1–7. [CrossRef]
53. Pierri, C.L.; Palmieri, F.; De Grassi, A. Single-nucleotide evolution quantifies the importance of each site along the structure of mitochondrial carriers. *Cell. Mol. Life Sci.* **2013**, *71*, 349–364. [CrossRef] [PubMed]
54. Catalina-Rodriguez, O.; Kolukula, V.K.; Tomita, Y.; Preet, A.; Palmieri, F.; Wellstein, A.; Byers, S.; Giaccia, A.J.; Glasgow, E.; Albanese, C.; et al. The mitochondrial citrate transporter, CIC, is essential for mitochondrial homeostasis. *Oncotarget* **2012**, *3*, 1220–1235. [CrossRef] [PubMed]
55. Kranendijk, M.; Struys, E.A.; Salomons, G.S.; Van der Knaap, M.S.; Jakobs, C. Progress in understanding 2-hydroxyglutaric acidurias. *J. Inherit. Metab. Dis.* **2012**, *35*, 571–587. [CrossRef]
56. Dolce, V.; Iacobazzi, V.; Palmieri, F.; Walker, J.E. The sequences of human and bovine genes of the phosphate carrier from mitochondria contain evidence of alternatively spliced forms. *J. Biol. Chem.* **1994**, *269*, 10451–10460.
57. Dolce, V.; Fiermonte, G.; Palmieri, F. Tissue-specific expression of the two isoforms of the mitochondrial phosphate carrier in bovine tissues. *FEBS Lett.* **1996**, *399*, 95–98. [CrossRef]

58. Fiermonte, G.; Dolce, V.; Palmieri, F. Expression in Escherichia coli, functional characterization, and tissue distribution of isoforms A and B of the phosphate carrier from bovine mitochondria. *J. Biol. Chem.* **1998**, *273*, 22782–22787. [CrossRef]
59. Palmieri, F.; Quagliariello, E.; Klingenberg, M. Quantitative correlation between the distribution of anions and the pH difference across the mitochondrial membrane. *Eur. J. Biochem.* **1970**, *17*, 230–238. [CrossRef]
60. Mayr, J.A.; Merkel, O.; Kohlwein, S.D.; Gebhardt, B.R.; Böhles, H.; Fötschl, U.; Koch, J.; Jaksch, M.; Lochmüller, H.; Horváth, R.; et al. Mitochondrial phosphate-carrier deficiency: A novel disorder of oxidative phosphorylation. *Am. J. Hum. Genet.* **2007**, *80*, 478–484. [CrossRef]
61. Mayr, J.A.; Zimmermann, F.A.; Horváth, R.; Schneider, H.-C.; Schoser, B.; Holinski-Feder, E.; Czermin, B.; Freisinger, P.; Sperl, W. Deficiency of the mitochondrial phosphate carrier presenting as myopathy and cardiomyopathy in a family with three affected children. *Neuromuscul. Disord.* **2011**, *21*, 803–808. [CrossRef]
62. Bhoj, E.J.; Li, M.; Ahrens-Nicklas, R.; Pyle, L.C.; Wang, J.; Zhang, V.W.; Clarke, C.; Wong, L.J.; Sondheimer, N.; Ficicioglu, C.; et al. Pathologic Variants of the Mitochondrial Phosphate Carrier SLC25A3: Two New Patients and Expansion of the Cardiomyopathy/Skeletal Myopathy Phenotype With and Without Lactic Acidosis. *JIMD Rep.* **2015**, *19*, 59–66. [PubMed]
63. Kwong, J.Q.; Davis, J.; Baines, C.P.; Sargent, M.A.; Karch, J.; Wang, X.; Huang, T.; Molkenin, J.D. Genetic deletion of the mitochondrial phosphate carrier desensitizes the mitochondrial permeability transition pore and causes cardiomyopathy. *Cell Death Differ.* **2014**, *21*, 1209–1217. [CrossRef] [PubMed]
64. Palmieri, F.; Prezioso, G.; Quagliariello, E.; Klingenberg, M. Kinetic study of the dicarboxylate carrier in rat liver mitochondria. *Eur. J. Biochem.* **1971**, *22*, 66–74. [CrossRef] [PubMed]
65. Bisaccia, F.; Indiveri, C.; Palmieri, F. Purification and reconstitution of two anion carriers from rat liver mitochondria: The dicarboxylate and the 2-oxoglutarate carrier. *Biochim. Biophys. Acta* **1988**, *933*, 229–240. [CrossRef]
66. Indiveri, C.; Capobianco, L.; Krämer, R.; Palmieri, F. Kinetics of the reconstituted dicarboxylate carrier from rat liver mitochondria. *Biochim. Biophys. Acta* **1989**, *977*, 187–193. [CrossRef]
67. Indiveri, C.; Dierks, T.; Krämer, R.; Palmieri, F. Kinetic discrimination of two substrate binding sites of the reconstituted dicarboxylate carrier from rat liver mitochondria. *Biochim. Biophys. Acta* **1989**, *977*, 194–199. [CrossRef]
68. Fiermonte, G.; Palmieri, L.; Dolce, V.; Lasorsa, F.M.; Palmieri, F.; Runswick, M.J.; Walker, J.E. The sequence, bacterial expression, and functional reconstitution of the rat mitochondrial dicarboxylate transporter cloned via distant homologs in yeast and *Caenorhabditis elegans*. *J. Biol. Chem.* **1998**, *273*, 24754–24759. [CrossRef]
69. Vozza, A.; Parisi, G.; De Leonardi, F.; Lasorsa, F.M.; Castegna, A.; Amorese, D.; Marmo, R.; Calcagnile, V.M.; Palmieri, L.; Ricquier, D.; et al. UCP2 transports C4 metabolites out of mitochondria, regulating glucose and glutamine oxidation. *Proc. Natl. Acad. Sci. USA* **2014**, *111*, 960–965. [CrossRef]
70. Gorgoglione, R.; Porcelli, V.; Santoro, A.; Daddabbo, L.; Vozza, A.; Monné, M.; Di Noia, M.A.; Palmieri, L.; Fiermonte, G.; Palmieri, F. The human uncoupling proteins 5 and 6 (UCP5/SLC25A14 and UCP6/SLC25A30) transport sulfur oxyanions, phosphate and dicarboxylates. *Biochim. Biophys. Acta Bioenerg.* **2019**, *1860*, 724–733. [CrossRef]
71. Dolce, V.; Scarcia, P.; Iacopetta, D.; Palmieri, F. A fourth ADP/ATP carrier isoform in man: Identification, bacterial expression, functional characterization and tissue distribution. *FEBS Lett.* **2005**, *579*, 633–637. [CrossRef] [PubMed]
72. Kaukonen, J.; Juselius, J.K.; Tiranti, V.; Kytälä, A.; Zeviani, M.; Comi, G.P.; Keränen, S.; Peltonen, L.; Suomalainen, A. Role of adenine nucleotide translocator 1 in mtDNA maintenance. *Science* **2000**, *289*, 782–785. [CrossRef] [PubMed]
73. Palmieri, L.; Alberio, S.; Pisano, I.; Lodi, T.; Meznaric-Petrusa, M.; Zidar, J.; Santoro, A.; Scarcia, P.; Fontanesi, F.; Lamantea, E.; et al. Complete loss-of-function of the heart/muscle-specific adenine nucleotide translocator is associated with mitochondrial myopathy and cardiomyopathy. *Hum. Mol. Genet.* **2005**, *14*, 3079–3088. [CrossRef]
74. Echaniz-Laguna, A.; Chassagne, M.; Ceresuela, J.; Rouvet, I.; Padet, S.; Acquaviva, C.; Nataf, S.; Vinzio, S.; Bozon, D.; Mousson de Camaret, B. Complete loss of expression of the ANT1 gene causing cardiomyopathy and myopathy. *J. Med. Genet.* **2012**, *49*, 146–150. [CrossRef]

75. Körver-Keularts, I.M.L.W.; de Visser, M.; Bakker, H.D.; Wanders, R.J.A.; Vansenne, F.; Scholte, H.R.; Dorland, L.; Nicolaes, G.A.F.; Spaapen, L.M.J.; Smeets, H.J.M.; et al. Two Novel Mutations in the SLC25A4 Gene in a Patient with Mitochondrial Myopathy. *JIMD Rep.* **2015**, *22*, 39–45.
76. Tosserams, A.; Papadopoulos, C.; Jardel, C.; Lemièrre, I.; Romero, N.B.; De Lonlay, P.; Wahbi, K.; Voermans, N.; Hogrel, J.-Y.; Laforêt, P. Two new cases of mitochondrial myopathy with exercise intolerance, hyperlactatemia and cardiomyopathy, caused by recessive SLC25A4 mutations. *Mitochondrion* **2018**, *39*, 26–29. [CrossRef]
77. Thompson, K.; Majd, H.; Dallabona, C.; Reinson, K.; King, M.S.; Alston, C.L.; He, L.; Lodi, T.; Jones, S.A.; Fattal-Valevski, A.; et al. Recurrent De Novo Dominant Mutations in SLC25A4 Cause Severe Early-Onset Mitochondrial Disease and Loss of Mitochondrial DNA Copy Number. *Am. J. Hum. Genet.* **2016**, *99*, 860–876. [CrossRef]
78. Von Renesse, A.; Morales-Gonzalez, S.; Gill, E.; Salomons, G.S.; Stenzel, W.; Schuelke, M. Muscle Weakness, Cardiomyopathy, and L-2-Hydroxyglutaric Aciduria Associated with a Novel Recessive SLC25A4 Mutation. *JIMD Rep.* **2019**, *43*, 27–35.
79. King, M.S.; Thompson, K.; Hopton, S.; He, L.; Kunji, E.R.S.; Taylor, R.W.; Ortiz-Gonzalez, X.R. Expanding the phenotype of de novo SLC25A4-linked mitochondrial disease to include mild myopathy. *Neurol. Genet.* **2018**, *4*, e256. [CrossRef] [PubMed]
80. Punzi, G.; Porcelli, V.; Ruggiu, M.; Hossain, M.F.; Menga, A.; Scarcia, P.; Castegna, A.; Gorgoglione, R.; Pierri, C.L.; Laera, L.; et al. SLC25A10 biallelic mutations in intractable epileptic encephalopathy with complex I deficiency. *Hum. Mol. Genet.* **2018**, *27*, 499–504. [CrossRef] [PubMed]
81. McGivan, J.D.; Klingenberg, M. Correlation between H⁺ and anion movement in mitochondria and the key role of the phosphate carrier. *Eur. J. Biochem.* **1971**, *20*, 392–399. [CrossRef] [PubMed]
82. Crompton, M.; Palmieri, F.; Capano, M.; Quagliariello, E. The transport of sulphate and sulphite in rat liver mitochondria. *Biochem. J.* **1974**, *142*, 127–137. [CrossRef] [PubMed]
83. Crompton, M.; Palmieri, F.; Capano, M.; Quagliariello, E. The transport of thiosulphate in rat liver mitochondria. *FEBS Lett.* **1974**, *46*, 247–250. [CrossRef]
84. Crompton, M.; Palmieri, F.; Capano, M.; Quagliariello, E. A kinetic study of sulphate transport in rat liver mitochondria. *Biochem. J.* **1975**, *146*, 667–673. [CrossRef]
85. Bisaccia, F.; Palmieri, F. Specific elution from hydroxylapatite of the mitochondrial phosphate carrier by cardiolipin. *Biochim. Biophys. Acta* **1984**, *766*, 386–394. [CrossRef]
86. Palmieri, F.; Quagliariello, E.; Klingenberg, M. Kinetics and specificity of the oxoglutarate carrier in rat-liver mitochondria. *Eur. J. Biochem.* **1972**, *29*, 408–416. [CrossRef] [PubMed]
87. Bisaccia, F.; Indiveri, C.; Palmieri, F. Purification of reconstitutively active alpha-oxoglutarate carrier from pig heart mitochondria. *Biochim. Biophys. Acta* **1985**, *810*, 362–369. [CrossRef]
88. Indiveri, C.; Palmieri, F.; Bisaccia, F.; Krämer, R. Kinetics of the reconstituted 2-oxoglutarate carrier from bovine heart mitochondria. *Biochim. Biophys. Acta* **1987**, *890*, 310–318. [CrossRef]
89. Runswick, M.J.; Walker, J.E.; Bisaccia, F.; Iacobazzi, V.; Palmieri, F. Sequence of the bovine 2-oxoglutarate/malate carrier protein: Structural relationship to other mitochondrial transport proteins. *Biochemistry* **1990**, *29*, 11033–11040. [CrossRef]
90. Wibom, R.; Lasorsa, F.M.; Töhönen, V.; Barbaro, M.; Sterky, F.H.; Kucinski, T.; Naess, K.; Jonsson, M.; Pierri, C.L.; Palmieri, F.; et al. AGC1 deficiency associated with global cerebral hypomyelination. *N. Engl. J. Med.* **2009**, *361*, 489–495. [CrossRef]
91. Falk, M.J.; Li, D.; Gai, X.; McCormick, E.; Place, E.; Lasorsa, F.M.; Otieno, F.G.; Hou, C.; Kim, C.E.; Abdel-Magid, N.; et al. AGC1 Deficiency Causes Infantile Epilepsy, Abnormal Myelination, and Reduced N-Acetylaspartate. *JIMD Rep.* **2014**, *14*, 77–85.
92. Lasorsa, F.M.; Pinton, P.; Palmieri, L.; Fiermonte, G.; Rizzuto, R.; Palmieri, F. Recombinant expression of the Ca(2+)-sensitive aspartate/glutamate carrier increases mitochondrial ATP production in agonist-stimulated Chinese hamster ovary cells. *J. Biol. Chem.* **2003**, *278*, 38686–38692. [CrossRef] [PubMed]
93. Thangaratnarajah, C.; Ruprecht, J.J.; Kunji, E.R.S. Calcium-induced conformational changes of the regulatory domain of human mitochondrial aspartate/glutamate carriers. *Nat. Commun.* **2014**, *5*, 5491. [CrossRef] [PubMed]
94. Indiveri, C.; Krämer, R.; Palmieri, F. Reconstitution of the malate/aspartate shuttle from mitochondria. *J. Biol. Chem.* **1987**, *262*, 15979–15983.

95. Pfeiffer, B.; Sen, K.; Kaur, S.; Pappas, K. Expanding Phenotypic Spectrum of Cerebral Aspartate-Glutamate Carrier Isoform 1 (AGC1) Deficiency. *Neuropediatrics* **2020**, *51*, 160–163. [CrossRef] [PubMed]
96. Jalil, M.A.; Begum, L.; Contreras, L.; Pardo, B.; Iijima, M.; Li, M.X.; Ramos, M.; Marmol, P.; Horiuchi, M.; Shimotsu, K.; et al. Reduced N-acetylaspartate levels in mice lacking aralar, a brain- and muscle-type mitochondrial aspartate-glutamate carrier. *J. Biol. Chem.* **2005**, *280*, 31333–31339. [CrossRef]
97. Profilo, E.; Peña-Altamira, L.E.; Corricelli, M.; Castegna, A.; Danese, A.; Agrimi, G.; Petralla, S.; Giannuzzi, G.; Porcelli, V.; Sbano, L.; et al. Down-regulation of the mitochondrial aspartate-glutamate carrier isoform 1 AGC1 inhibits proliferation and N-acetylaspartate synthesis in Neuro2A cells. *Biochim. Biophys. Acta Mol. Basis Dis.* **2017**, *1863*, 1422–1435. [CrossRef]
98. Petralla, S.; Peña-Altamira, L.E.; Poeta, E.; Massenzio, F.; Virgili, M.; Barile, S.N.; Sbano, L.; Profilo, E.; Corricelli, M.; Danese, A.; et al. Deficiency of Mitochondrial Aspartate-Glutamate Carrier 1 Leads to Oligodendrocyte Precursor Cell Proliferation Defects Both In Vitro and In Vivo. *Int. J. Mol. Sci.* **2019**, *20*, 4486. [CrossRef]
99. Napolioni, V.; Persico, A.M.; Porcelli, V.; Palmieri, L. The mitochondrial aspartate/glutamate carrier AGC1 and calcium homeostasis: Physiological links and abnormalities in autism. *Mol. Neurobiol.* **2011**, *44*, 83–92. [CrossRef]
100. Shelton, G.D.; Minor, K.M.; Li, K.; Naviaux, J.C.; Monk, J.; Wang, L.; Guzik, E.; Guo, L.T.; Porcelli, V.; Gorgoglione, R.; et al. A Mutation in the Mitochondrial Aspartate/Glutamate Carrier Leads to a More Oxidizing Intramitochondrial Environment and an Inflammatory Myopathy in Dutch Shepherd Dogs. *J. Neuromuscul. Dis.* **2019**, *6*, 485–501. [CrossRef]
101. Dahlin, M.; Martin, D.A.; Hedlund, Z.; Jonsson, M.; von Döbeln, U.; Wedell, A. The ketogenic diet compensates for AGC1 deficiency and improves myelination. *Epilepsia* **2015**, *56*, e176–e181. [CrossRef] [PubMed]
102. Monné, M.; Vozza, A.; Lasorsa, F.M.; Porcelli, V.; Palmieri, F. Mitochondrial Carriers for Aspartate, Glutamate and Other Amino Acids: A Review. *Int. J. Mol. Sci.* **2019**, *20*, 4456. [CrossRef]
103. Kobayashi, K.; Sinasac, D.S.; Iijima, M.; Boright, A.P.; Begum, L.; Lee, J.R.; Yasuda, T.; Ikeda, S.; Hirano, R.; Terazono, H.; et al. The gene mutated in adult-onset type II citrullinaemia encodes a putative mitochondrial carrier protein. *Nat. Genet.* **1999**, *22*, 159–163. [CrossRef]
104. Saheki, T.; Kobayashi, K. Mitochondrial aspartate glutamate carrier (citrin) deficiency as the cause of adult-onset type II citrullinemia (CTLN2) and idiopathic neonatal hepatitis (NICCD). *J. Hum. Genet.* **2002**, *47*, 333–341. [CrossRef] [PubMed]
105. Saheki, T.; Song, Y. Citrin Deficiency. In *GeneReviews®-NCBI Bookshelf*; University of Washington: Seattle, WA, USA, 2017.
106. Tabata, A.; Sheng, J.-S.; Ushikai, M.; Song, Y.-Z.; Gao, H.-Z.; Lu, Y.-B.; Okumura, F.; Iijima, M.; Mutoh, K.; Kishida, S.; et al. Identification of 13 novel mutations including a retrotransposal insertion in SLC25A13 gene and frequency of 30 mutations found in patients with citrin deficiency. *J. Hum. Genet.* **2008**, *53*, 534–545. [CrossRef] [PubMed]
107. Hayasaka, K.; Numakura, C.; Yamakawa, M.; Mitsui, T.; Watanabe, H.; Haga, H.; Yazaki, M.; Ohira, H.; Ochiai, Y.; Tahara, T.; et al. Medium-chain triglycerides supplement therapy with a low-carbohydrate formula can supply energy and enhance ammonia detoxification in the hepatocytes of patients with adult-onset type II citrullinemia. *J. Inherit. Metab. Dis.* **2018**, *41*, 777–784. [CrossRef] [PubMed]
108. Saheki, T.; Moriyama, M.; Kuroda, E.; Funahashi, A.; Yasuda, I.; Setogawa, Y.; Gao, Q.; Ushikai, M.; Furuie, S.; Yamamura, K.-I.; et al. Pivotal role of inter-organ aspartate metabolism for treatment of mitochondrial aspartate-glutamate carrier 2 (citrin) deficiency, based on the mouse model. *Sci. Rep.* **2019**, *9*, 4179. [CrossRef]
109. Indiveri, C.; Tonazzi, A.; Palmieri, F. Identification and purification of the ornithine/citrulline carrier from rat liver mitochondria. *Eur. J. Biochem.* **1992**, *207*, 449–454. [CrossRef]
110. Indiveri, C.; Tonazzi, A.; Stipani, I.; Palmieri, F. The purified and reconstituted ornithine/citrulline carrier from rat liver mitochondria: Electrical nature and coupling of the exchange reaction with H⁺ translocation. *Biochem. J.* **1997**, *327*, 349–355. [CrossRef]
111. Fiermonte, G.; Dolce, V.; David, L.; Santorelli, F.M.; Dionisi-Vici, C.; Palmieri, F.; Walker, J.E. The mitochondrial ornithine transporter. Bacterial expression, reconstitution, functional characterization, and tissue distribution of two human isoforms. *J. Biol. Chem.* **2003**, *278*, 32778–32783. [CrossRef]

112. Camacho, J.A.; Obie, C.; Biery, B.; Goodman, B.K.; Hu, C.-A.; Almashanu, S.; Steel, G.; Casey, R.; Lambert, M.; Mitchell, G.A.; et al. Hyperornithinaemia- syndrome is caused by mutations in a gene encoding a mitochondrial ornithine transporter. *Nat. Genet.* **1999**, *22*, 151–158. [CrossRef] [PubMed]
113. Martinelli, D.; Diodato, D.; Ponzi, E.; Monné, M.; Boenzi, S.; Bertini, E.; Fiermonte, G.; Dionisi-Vici, C. The hyperornithinemia-hyperammonemia-homocitrullinuria syndrome. *Orphanet J. Rare Dis.* **2015**, *10*, 29. [CrossRef] [PubMed]
114. Matsumoto, S.; Häberle, J.; Kido, J.; Mitsubuchi, H.; Endo, F.; Nakamura, K. Urea cycle disorders-update. *J. Hum. Genet.* **2019**, *64*, 833–847. [CrossRef] [PubMed]
115. Camacho, J.A.; Mardach, R.; Rioseco-Camacho, N.; Ruiz-Pesini, E.; Derbeneva, O.; Andrade, D.; Zaldivar, F.; Qu, Y.; Cederbaum, S.D. Clinical and functional characterization of a human ORNT1 mutation (T32R) in the hyperornithinemia-hyperammonemia-homocitrullinuria (HHH) syndrome. *Pediatr. Res.* **2006**, *60*, 423–429. [CrossRef]
116. Tessa, A.; Fiermonte, G.; Dionisi-Vici, C.; Paradies, E.; Baumgartner, M.R.; Chien, Y.-H.; Loguercio, C.; de Baulny, H.O.; Nassogne, M.-C.; Schiff, M.; et al. Identification of novel mutations in the SLC25A15 gene in hyperornithinemia-hyperammonemia-homocitrullinuria (HHH) syndrome: A clinical, molecular, and functional study. *Hum. Mutat.* **2009**, *30*, 741–748. [CrossRef]
117. Ersoy Tunali, N.; Marobbio, C.M.T.; Tiryakioğlu, N.O.; Punzi, G.; Saygılı, S.K.; Onal, H.; Palmieri, F. A novel mutation in the SLC25A15 gene in a Turkish patient with HHH syndrome: Functional analysis of the mutant protein. *Mol. Genet. Metab.* **2014**, *112*, 25–29. [CrossRef]
118. Zarrilli, R.; Oates, E.L.; McBride, O.W.; Lerman, M.I.; Chan, J.Y.; Santisteban, P.; Ursini, M.V.; Notkins, A.L.; Kohn, L.D. Sequence and chromosomal assignment of a novel cDNA identified by immunoscreening of a thyroid expression library: Similarity to a family of mitochondrial solute carrier proteins. *Mol. Endocrinol.* **1989**, *3*, 1498–1505. [CrossRef]
119. Fiermonte, G.; Runswick, M.J.; Walker, J.E.; Palmieri, F. Sequence and pattern of expression of a bovine homologue of a human mitochondrial transport protein associated with Grave’s disease. *DNA Seq.* **1992**, *3*, 71–78. [CrossRef]
120. Prohl, C.; Pelzer, W.; Diekert, K.; Kmita, H.; Bedekovics, T.; Kispal, G.; Lill, R. The yeast mitochondrial carrier Leu5p and its human homologue Graves’ disease protein are required for accumulation of coenzyme A in the matrix. *Mol. Cell Biol.* **2001**, *21*, 1089–1097. [CrossRef]
121. Fiermonte, G.; Paradies, E.; Todisco, S.; Marobbio, C.M.T.; Palmieri, F. A novel member of solute carrier family 25 (SLC25A42) is a transporter of coenzyme A and adenosine 3’,5’-diphosphate in human mitochondria. *J. Biol. Chem.* **2009**, *284*, 18152–18159. [CrossRef]
122. Khan, S.; Ansar, M.; Khan, A.K.; Shah, K.; Muhammad, N.; Shahzad, S.; Nickerson, D.A.; Bamshad, M.J.; Santos-Cortez, R.L.P.; Leal, S.M.; et al. A homozygous missense mutation in SLC25A16 associated with autosomal recessive isolated fingernail dysplasia in a Pakistani family. *Br. J. Dermatol.* **2018**, *178*, 556–558. [CrossRef]
123. Rosenberg, M.J.; Agarwala, R.; Bouffard, G.; Davis, J.; Fiermonte, G.; Hilliard, M.S.; Koch, T.; Kalikin, L.M.; Makalowska, I.; Morton, D.H.; et al. Mutant deoxynucleotide carrier is associated with congenital microcephaly. *Nat. Genet.* **2002**, *32*, 175–179. [CrossRef] [PubMed]
124. Spiegel, R.; Shaag, A.; Edvardson, S.; Mandel, H.; Stepensky, P.; Shalev, S.A.; Horovitz, Y.; Pines, O.; Elpeleg, O. SLC25A19 mutation as a cause of neuropathy and bilateral striatal necrosis. *Ann. Neurol.* **2009**, *66*, 419–424. [CrossRef] [PubMed]
125. Ortigoza-Escobar, J.D.; Alfadhel, M.; Molero-Luis, M.; Darin, N.; Spiegel, R.; de Coo, I.F.; Gerards, M.; Taylor, R.W.; Artuch, R.; Nashabat, M.; et al. Thiamine deficiency in childhood with attention to genetic causes: Survival and outcome predictors. *Ann. Neurol.* **2017**, *82*, 317–330. [CrossRef] [PubMed]
126. Bottega, R.; Perrone, M.D.; Vecchiato, K.; Taddio, A.; Sabui, S.; Pecile, V.; Said, H.M.; Faletra, F. Functional analysis of the third identified SLC25A19 mutation causative for the thiamine metabolism dysfunction syndrome 4. *J. Hum. Genet.* **2019**, *64*, 1075–1081. [CrossRef]
127. Gowda, V.K.; Srinivasan, V.M.; Jehta, K.; Bhat, M.D. Bilateral Striatal Necrosis with Polyneuropathy with a Novel SLC25A19 (Mitochondrial Thiamine Pyrophosphate Carrier OMIMI*606521) Mutation: Treatable Thiamine Metabolic Disorder—A Report of Two Indian Cases. *Neuropediatrics* **2019**, *50*, 313–317. [CrossRef]

128. Dolce, V.; Fiermonte, G.; Runswick, M.J.; Palmieri, F.; Walker, J.E. The human mitochondrial deoxynucleotide carrier and its role in the toxicity of nucleoside antivirals. *Proc. Natl. Acad. Sci. USA* **2001**, *98*, 2284–2288. [CrossRef]
129. Lindhurst, M.J.; Fiermonte, G.; Song, S.; Struys, E.; De Leonardis, F.; Schwartzberg, P.L.; Chen, A.; Castegna, A.; Verhoeven, N.; Mathews, C.K.; et al. Knockout of Slc25a19 causes mitochondrial thiamine pyrophosphate depletion, embryonic lethality, CNS malformations, and anemia. *Proc. Natl. Acad. Sci. USA* **2006**, *103*, 15927–15932. [CrossRef]
130. Marobbio, C.M.T.; Vozza, A.; Harding, M.; Bisaccia, F.; Palmieri, F.; Walker, J.E. Identification and reconstitution of the yeast mitochondrial transporter for thiamine pyrophosphate. *EMBO J.* **2002**, *21*, 5653–5661. [CrossRef]
131. Indiveri, C.; Iacobazzi, V.; Tonazzi, A.; Giangregorio, N.; Infantino, V.; Convertini, P.; Console, L.; Palmieri, F. The mitochondrial carnitine/acylcarnitine carrier: Function, structure and physiopathology. *Mol. Aspects Med.* **2011**, *32*, 223–233. [CrossRef]
132. Stanley, C.A.; Palmieri, F.; Bennett, M.J. Disorders of the Mitochondrial Carnitine Shuttle. In *Online Molecular and Metabolic Basis of Inherited Disease*; Valle, D., Vogelstein, B., Kinzler, K., Antonarakis, S., Ballagio, A., Gibson, K., Mitchell, G., Eds.; McGraw Hill: New York, NY, USA, 2013.
133. Stanley, C.A.; Hale, D.E.; Berry, G.T.; Deleuw, S.; Boxer, J.; Bonnefont, J.P. Brief report: A deficiency of carnitine-acylcarnitine translocase in the inner mitochondrial membrane. *N. Engl. J. Med.* **1992**, *327*, 19–23. [CrossRef]
134. Indiveri, C.; Iacobazzi, V.; Giangregorio, N.; Palmieri, F. The mitochondrial carnitine carrier protein: CDNA cloning, primary structure and comparison with other mitochondrial transport proteins. *Biochem. J.* **1997**, *321*, 713–719. [CrossRef]
135. Iacobazzi, V.; Invernizzi, F.; Baratta, S.; Pons, R.; Chung, W.; Garavaglia, B.; Dionisi-Vici, C.; Ribes, A.; Parini, R.; Huertas, M.D.; et al. Molecular and functional analysis of SLC25A20 mutations causing carnitine-acylcarnitine translocase deficiency. *Hum. Mutat.* **2004**, *24*, 312–320. [CrossRef]
136. De Lucas, J.R.; Indiveri, C.; Tonazzi, A.; Perez, P.; Giangregorio, N.; Iacobazzi, V.; Palmieri, F. Functional characterization of residues within the carnitine/acylcarnitine translocase RX2PANAXF distinct motif. *Mol. Membr. Biol.* **2008**, *25*, 152–163. [CrossRef]
137. IJlst, L.; van Roermund, C.W.; Iacobazzi, V.; Oostheim, W.; Ruiten, J.P.; Williams, J.C.; Palmieri, F.; Wanders, R.J. Functional analysis of mutant human carnitine acylcarnitine translocases in yeast. *Biochem. Biophys. Res. Commun.* **2001**, *280*, 700–706. [CrossRef]
138. Pérez, P.; Martínez, O.; Romero, B.; Olivas, I.; Pedregosa, A.M.; Palmieri, F.; Laborda, F.; Ramón De Lucas, J. Functional analysis of mutations in the human carnitine/acylcarnitine translocase in *Aspergillus nidulans*. *Fungal Genet. Biol.* **2003**, *39*, 211–220. [CrossRef]
139. Boczonadi, V.; King, M.S.; Smith, A.C.; Olahova, M.; Bansagi, B.; Roos, A.; Eyassu, F.; Borchers, C.; Ramesh, V.; Lochmüller, H.; et al. Mitochondrial oxodicarboxylate carrier deficiency is associated with mitochondrial DNA depletion and spinal muscular atrophy-like disease. *Genet. Med.* **2018**, *20*, 1224–1235. [CrossRef]
140. Fiermonte, G.; Dolce, V.; Palmieri, L.; Ventura, M.; Runswick, M.J.; Palmieri, F.; Walker, J.E. Identification of the human mitochondrial oxodicarboxylate carrier. Bacterial expression, reconstitution, functional characterization, tissue distribution, and chromosomal location. *J. Biol. Chem.* **2001**, *276*, 8225–8230. [CrossRef]
141. Palmieri, L.; Agrimi, G.; Runswick, M.J.; Fearnley, I.M.; Palmieri, F.; Walker, J.E. Identification in *Saccharomyces cerevisiae* of two isoforms of a novel mitochondrial transporter for 2-oxoadipate and 2-oxoglutarate. *J. Biol. Chem.* **2001**, *276*, 1916–1922. [CrossRef]
142. Scarcia, P.; Palmieri, L.; Agrimi, G.; Palmieri, F.; Rottensteiner, H. Three mitochondrial transporters of *Saccharomyces cerevisiae* are essential for ammonium fixation and lysine biosynthesis in synthetic minimal medium. *Mol. Genet. Metab.* **2017**, *122*, 54–60. [CrossRef]
143. Molinari, F.; Raas-Rothschild, A.; Rio, M.; Fiermonte, G.; Encha-Razavi, F.; Palmieri, L.; Palmieri, F.; Ben-Neriah, Z.; Kadhom, N.; Vekemans, M.; et al. Impaired mitochondrial glutamate transport in autosomal recessive neonatal myoclonic epilepsy. *Am. J. Hum. Genet.* **2005**, *76*, 334–339. [CrossRef] [PubMed]
144. Molinari, F.; Kaminska, A.; Fiermonte, G.; Boddaert, N.; Raas-Rothschild, A.; Plouin, P.; Palmieri, L.; Brunelle, F.; Palmieri, F.; Dulac, O.; et al. Mutations in the mitochondrial glutamate carrier SLC25A22 in neonatal epileptic encephalopathy with suppression bursts. *Clin. Genet.* **2009**, *76*, 188–194. [CrossRef] [PubMed]

145. Lemattre, C.; Imbert-Bouteille, M.; Gatinois, V.; Benit, P.; Sanchez, E.; Guignard, T.; Tran Mau-Them, F.; Haquet, E.; Rivier, F.; Carme, E.; et al. Report on three additional patients and genotype-phenotype correlation in SLC25A22-related disorders group. *Eur. J. Hum. Genet.* **2019**, *27*, 1692–1700. [CrossRef] [PubMed]
146. Poduri, A.; Heinzen, E.; Chitsazzadeh, V.; Lasorsa, F.; LaCoursiere, C.; Martin, E.; Yusakaitis, C.; Hill, R.; Elhosary, P.; Atabay, K.; et al. SLC25A22 is a novel gene for migrating partial seizures in infancy. *Ann. Neurol.* **2013**, *76*, 873–882. [CrossRef]
147. Fiermonte, G.; Palmieri, L.; Todisco, S.; Agrimi, G.; Palmieri, F.; Walker, J.E. Identification of the mitochondrial glutamate transporter. Bacterial expression, reconstitution, functional characterization, and tissue distribution of two human isoforms. *J. Biol. Chem.* **2002**, *277*, 19289–19294. [CrossRef]
148. Goubert, E.; Mircheva, Y.; Lasorsa, F.M.; Melon, C.; Profilo, E.; Sutera, J.; Becq, H.; Palmieri, F.; Palmieri, L.; Aniksztejn, L.; et al. Inhibition of the Mitochondrial Glutamate Carrier SLC25A22 in Astrocytes Leads to Intracellular Glutamate Accumulation. *Front. Cell. Neurosci.* **2017**, *11*, 149. [CrossRef]
149. Trabelsi, Y.; Amri, M.; Becq, H.; Molinari, F.; Aniksztejn, L. The conversion of glutamate by glutamine synthase in neocortical astrocytes from juvenile rat is important to limit glutamate spillover and peri/extrasynaptic activation of NMDA receptors. *Glia* **2017**, *65*, 401–415. [CrossRef]
150. Reid, E.S.; Williams, H.; Anderson, G.; Benatti, M.; Chong, K.; James, C.; Ocaña, L.; GOSgene; Hemingway, C.; Little, D.; et al. Mutations in SLC25A22: Hyperprolinaemia, vacuolated fibroblasts and presentation with developmental delay. *J. Inher. Metab. Dis.* **2017**, *40*, 385–394. [CrossRef]
151. Ryu, J.; Ko, J.M.; Shin, C.-H. A 9-year-old Korean girl with Fontaine progeroid syndrome: A case report with further phenotypical delineation and description of clinical course during long-term follow-up. *BMC Med. Genet.* **2019**, *20*, 188. [CrossRef]
152. Ehmke, N.; Graul-Neumann, L.; Smorag, L.; Koenig, R.; Segebrecht, L.; Magoulas, P.; Scaglia, F.; Kilic, E.; Hennig, A.F.; Adolphs, N.; et al. De Novo Mutations in SLC25A24 Cause a Craniosynostosis Syndrome with Hypertrichosis, Progeroid Appearance, and Mitochondrial Dysfunction. *Am. J. Hum. Genet.* **2017**, *101*, 833–843. [CrossRef]
153. Writzl, K.; Maver, A.; Kovačič, L.; Martinez-Valero, P.; Contreras, L.; Satrustegui, J.; Castori, M.; Faivre, L.; Lapunzina, P.; van Kuilenburg, A.B.P.; et al. De Novo Mutations in SLC25A24 Cause a Disorder Characterized by Early Aging, Bone Dysplasia, Characteristic Face, and Early Demise. *Am. J. Hum. Genet.* **2017**, *101*, 844–855. [CrossRef] [PubMed]
154. Harborne, S.P.D.; Ruprecht, J.J.; Kunji, E.R.S. Calcium-induced conformational changes in the regulatory domain of the human mitochondrial ATP-Mg/Pi carrier. *Biochim. Biophys. Acta* **2015**, *1847*, 1245–1253. [CrossRef] [PubMed]
155. Monné, M.; Daddabbo, L.; Giannossa, L.C.; Nicolardi, M.C.; Palmieri, L.; Miniero, D.V.; Mangone, A.; Palmieri, F. Mitochondrial ATP-Mg/phosphate carriers transport divalent inorganic cations in complex with ATP. *J. Bioenerg. Biomembr.* **2017**, *49*, 369–380. [CrossRef] [PubMed]
156. Agrimi, G.; Di Noia, M.A.; Marobbio, C.M.T.; Fiermonte, G.; Lasorsa, F.M.; Palmieri, F. Identification of the human mitochondrial S-adenosylmethionine transporter: Bacterial expression, reconstitution, functional characterization and tissue distribution. *Biochem. J.* **2004**, *379*, 183–190. [CrossRef]
157. Marobbio, C.M.T.; Agrimi, G.; Lasorsa, F.M.; Palmieri, F. Identification and functional reconstitution of yeast mitochondrial carrier for S-adenosylmethionine. *EMBO J.* **2003**, *22*, 5975–5982. [CrossRef]
158. Palmieri, L.; Arrigoni, R.; Blanco, E.; Carrari, F.; Zanor, M.I.; Studart-Guimaraes, C.; Fernie, A.R.; Palmieri, F. Molecular identification of an Arabidopsis S-adenosylmethionine transporter. Analysis of organ distribution, bacterial expression, reconstitution into liposomes, and functional characterization. *Plant Physiol.* **2006**, *142*, 855–865. [CrossRef]
159. Kishita, Y.; Pajak, A.; Bolar, N.A.; Marobbio, C.M.T.; Maffezzini, C.; Miniero, D.V.; Monné, M.; Kohda, M.; Stranneheim, H.; Murayama, K.; et al. Intra-mitochondrial Methylation Deficiency Due to Mutations in SLC25A26. *Am. J. Med. Genet.* **2015**, *97*, 761–768. [CrossRef]
160. Schiff, M.; Veauville-Merllié, A.; Su, C.H.; Tzagoloff, A.; Rak, M.; Ogier de Baulny, H.; Boutron, A.; Smedts-Walters, H.; Romero, N.B.; Rigal, O.; et al. SLC25A32 Mutations and Riboflavin-Responsive Exercise Intolerance. *N. Engl. J. Med.* **2016**, *374*, 795–797. [CrossRef] [PubMed]

161. Hellebrekers, D.M.E.I.; Sallevelt, S.C.E.H.; Theunissen, T.E.J.; Hendrickx, A.T.M.; Gottschalk, R.W.; Hoeijmakers, J.G.J.; Habets, D.D.; Bierau, J.; Schoonderwoerd, K.G.; Smeets, H.J.M. Novel SLC25A32 mutation in a patient with a severe neuromuscular phenotype. *Eur. J. Hum. Genet.* **2017**, *25*, 886–888. [CrossRef]
162. Tzagoloff, A.; Jang, J.; Glerum, D.M.; Wu, M. FLX1 codes for a carrier protein involved in maintaining a proper balance of flavin nucleotides in yeast mitochondria. *J. Biol. Chem.* **1996**, *271*, 7392–7397. [CrossRef]
163. Titus, S.A.; Moran, R.G. Retrovirally mediated complementation of the glyB phenotype. Cloning of a human gene encoding the carrier for entry of folates into mitochondria. *J. Biol. Chem.* **2000**, *275*, 36811–36817. [CrossRef] [PubMed]
164. Spaan, A.N.; Ijlst, L.; van Roermund, C.W.T.; Wijburg, F.A.; Wanders, R.J.A.; Waterham, H.R. Identification of the human mitochondrial FAD transporter and its potential role in multiple acyl-CoA dehydrogenase deficiency. *Mol. Genet. Metab.* **2005**, *86*, 441–447. [CrossRef]
165. Todisco, S.; Agrimi, G.; Castegna, A.; Palmieri, F. Identification of the mitochondrial NAD⁺ transporter in *Saccharomyces cerevisiae*. *J. Biol. Chem.* **2006**, *281*, 1524–1531. [CrossRef]
166. Kim, J.; Lei, Y.; Guo, J.; Kim, S.-E.; Wlodarczyk, B.J.; Cabrera, R.M.; Lin, Y.L.; Nilsson, T.K.; Zhang, T.; Ren, A.; et al. Formate rescues neural tube defects caused by mutations in Slc25a32. *Proc. Natl. Acad. Sci. USA* **2018**, *115*, 4690–4695. [CrossRef] [PubMed]
167. Guernsey, D.L.; Jiang, H.; Campagna, D.R.; Evans, S.C.; Ferguson, M.; Kellogg, M.D.; Lachance, M.; Matsuoka, M.; Nightingale, M.; Rideout, A.; et al. Mutations in mitochondrial carrier family gene SLC25A38 cause nonsyndromic autosomal recessive congenital sideroblastic anemia. *Nat. Genet.* **2009**, *41*, 651–653. [CrossRef]
168. Le Rouzic, M.-A.; Fouquet, C.; Leblanc, T.; Touati, M.; Fouyssac, F.; Vermylen, C.; Jäkel, N.; Guichard, J.-F.; Maloum, K.; Toutain, F.; et al. Non syndromic childhood onset congenital sideroblastic anemia: A report of 13 patients identified with an ALAS2 or SLC25A38 mutation. *Blood Cells. Mol. Dis.* **2017**, *66*, 11–18. [CrossRef]
169. Lunetti, P.; Damiano, F.; De Benedetto, G.; Siculella, L.; Pennetta, A.; Muto, L.; Paradies, E.; Marobbio, C.M.T.; Dolce, V.; Capobianco, L. Characterization of Human and Yeast Mitochondrial Glycine Carriers with Implications for Heme Biosynthesis and Anemia. *J. Biol. Chem.* **2016**, *291*, 19746–19759. [CrossRef]
170. Shamseldin, H.E.; Smith, L.L.; Kentab, A.; Alkhalidi, H.; Summers, B.; Alsedairy, H.; Xiong, Y.; Gupta, V.A.; Alkuraya, F.S. Mutation of the mitochondrial carrier SLC25A42 causes a novel form of mitochondrial myopathy in humans. *Hum. Genet.* **2016**, *135*, 21–30. [CrossRef]
171. Almannai, M.; Alasmari, A.; Alqasbi, A.; Faqeih, E.; Al Mutairi, F.; Alotaibi, M.; Samman, M.M.; Eyaid, W.; Aljadhai, Y.I.; Shamseldin, H.E.; et al. Expanding the phenotype of SLC25A42-associated mitochondrial encephalomyopathy. *Clin. Genet.* **2018**, *93*, 1097–1102. [CrossRef]
172. Iuso, A.; Alhaddad, B.; Weigel, C.; Kotzaeridou, U.; Mastantuono, E.; Schwarzmayr, T.; Graf, E.; Terrile, C.; Prokisch, H.; Strom, T.M.; et al. A Homozygous Splice Site Mutation in SLC25A42, Encoding the Mitochondrial Transporter of Coenzyme A, Causes Metabolic Crises and Epileptic Encephalopathy. *JIMD Rep.* **2019**, *44*, 1–7.
173. Voza, A.; De Leonardis, F.; Paradies, E.; De Grassi, A.; Pierri, C.L.; Parisi, G.; Marobbio, C.M.T.; Lasorsa, F.M.; Muto, L.; Capobianco, L.; et al. Biochemical characterization of a new mitochondrial transporter of dephosphocoenzyme A in *Drosophila melanogaster*. *Biochim. Biophys. Acta* **2017**, *1858*, 137–146. [CrossRef]
174. Abrams, A.J.; Hufnagel, R.B.; Rebelo, A.; Zanna, C.; Patel, N.; Gonzalez, M.A.; Campeanu, I.J.; Griffin, L.B.; Groenewald, S.; Strickland, A.V.; et al. Mutations in SLC25A46, encoding a UGO1-like protein, cause an optic atrophy spectrum disorder. *Nat. Genet.* **2015**, *47*, 926–932. [CrossRef]
175. Wan, J.; Steffen, J.; Yourshaw, M.; Mamsa, H.; Andersen, E.; Rudnik-Schöneborn, S.; Pope, K.; Howell, K.B.; McLean, C.A.; Kornberg, A.J.; et al. Loss of function of SLC25A46 causes lethal congenital pontocerebellar hypoplasia. *Brain J. Neurol.* **2016**, *139*, 2877–2890. [CrossRef]
176. Janer, A.; Prudent, J.; Paupe, V.; Fahiminiya, S.; Majewski, J.; Sgarlato, N.; Des Rosiers, C.; Forest, A.; Lin, Z.-Y.; Gingras, A.-C.; et al. SLC25A46 is required for mitochondrial lipid homeostasis and cristae maintenance and is responsible for Leigh syndrome. *EMBO Mol. Med.* **2016**, *8*, 1019–1038. [CrossRef]
177. Hammer, M.B.; Ding, J.; Mochel, F.; Eleuch-Fayache, G.; Charles, P.; Coutelier, M.; Gibbs, J.R.; Arepalli, S.K.; Chong, S.B.; Hernandez, D.G.; et al. SLC25A46 Mutations Associated with Autosomal Recessive Cerebellar Ataxia in North African Families. *Neurodegener. Dis.* **2017**, *17*, 208–212. [CrossRef]

178. Nguyen, M.; Boesten, I.; Hellebrekers, D.M.E.I.; Mulder-den Hartog, N.M.; de Coo, I.F.M.; Smeets, H.J.M.; Gerards, M. Novel pathogenic SLC25A46 splice-site mutation causes an optic atrophy spectrum disorder. *Clin. Genet.* **2017**, *91*, 121–125. [CrossRef]
179. Sulaiman, R.A.; Patel, N.; Alsharif, H.; Arold, S.T.; Alkuraya, F.S. A novel mutation in SLC25A46 causes optic atrophy and progressive limb spasticity, with no cerebellar atrophy or axonal neuropathy. *Clin. Genet.* **2017**, *92*, 230–231. [CrossRef]
180. Braunisch, M.C.; Gallwitz, H.; Abicht, A.; Diebold, I.; Holinski-Feder, E.; Van Maldergem, L.; Lammens, M.; Kovács-Nagy, R.; Alhaddad, B.; Strom, T.M.; et al. Extension of the phenotype of biallelic loss-of-function mutations in SLC25A46 to the severe form of pontocerebellar hypoplasia type I. *Clin. Genet.* **2018**, *93*, 255–265. [CrossRef]
181. Abrams, A.J.; Fontanesi, F.; Tan, N.B.L.; Buglo, E.; Campeanu, I.J.; Rebelo, A.P.; Kornberg, A.J.; Phelan, D.G.; Stark, Z.; Zuchner, S. Insights into the genotype-phenotype correlation and molecular function of SLC25A46. *Hum. Mutat.* **2018**, *39*, 1995–2007. [CrossRef]
182. Walder, K.; Norman, R.A.; Hanson, R.L.; Schrauwen, P.; Neverova, M.; Jenkinson, C.P.; Easlick, J.; Warden, C.H.; Pecqueur, C.; Raimbault, S.; et al. Association between uncoupling protein polymorphisms (UCP2-UCP3) and energy metabolism/obesity in Pima indians. *Hum. Mol. Genet.* **1998**, *7*, 1431–1435. [CrossRef]
183. Esterbauer, H.; Schneitler, C.; Oberkofler, H.; Ebenbichler, C.; Paulweber, B.; Sandhofer, F.; Ladurner, G.; Hell, E.; Strosberg, A.D.; Patsch, J.R.; et al. A common polymorphism in the promoter of UCP2 is associated with decreased risk of obesity in middle-aged humans. *Nat. Genet.* **2001**, *28*, 178–183. [CrossRef]
184. Ferrara, C.T.; Boodhansingh, K.E.; Paradies, E.; Fiermonte, G.; Steinkrauss, L.J.; Topor, L.S.; Quintos, J.B.; Ganguly, A.; De Leon, D.D.; Palmieri, F.; et al. Novel Hypoglycemia Phenotype in Congenital Hyperinsulinism Due to Dominant Mutations of Uncoupling Protein 2. *J. Clin. Endocrinol. Metab.* **2017**, *102*, 942–949. [CrossRef] [PubMed]
185. Rosenthal, E.A.; Ranchalis, J.; Crosslin, D.R.; Burt, A.; Brunzell, J.D.; Motulsky, A.G.; Nickerson, D.A.; NHLBI GO Exome Sequencing Project; Wijsman, E.M.; Jarvik, G.P. Joint linkage and association analysis with exome sequence data implicates SLC25A40 in hypertriglyceridemia. *Am. J. Hum. Genet.* **2013**, *93*, 1035–1045. [CrossRef] [PubMed]
186. Buffet, A.; Morin, A.; Castro-Vega, L.-J.; Habarou, F.; Lussey-Lepoutre, C.; Letouzé, E.; Lefebvre, H.; Guilhem, I.; Haissaguerre, M.; Raingeard, I.; et al. Germline Mutations in the Mitochondrial 2-Oxoglutarate/Malate Carrier SLC25A11 Gene Confer a Predisposition to Metastatic Paragangliomas. *Cancer Res.* **2018**, *78*, 1914–1922. [CrossRef] [PubMed]
187. Liu, J.; Mo, W.; Zhang, Z.; Yu, H.; Yang, A.; Qu, F.; Hu, P.; Liu, Z.; Wang, S. Single Nucleotide Polymorphisms in SLC19A1 and SLC25A9 Are Associated with Childhood Autism Spectrum Disorder in the Chinese Han Population. *J. Mol. Neurosci.* **2017**, *62*, 262–267. [CrossRef] [PubMed]
188. Köse, M.D.; Kagnici, M.; Özdemir, T.R.; Erdur, C.B.; Erdemir, G.; Karakoyun, M.; Guzin, Y.; Ceylaner, S.; Genel, F. Clinical findings in five Turkish patients with citrin deficiency and identification of a novel mutation on SLC25A13. *J. Pediatr. Endocrinol. Metab.* **2020**, *33*, 157–163. [CrossRef]



© 2020 by the authors. Licensee MDPI, Basel, Switzerland. This article is an open access article distributed under the terms and conditions of the Creative Commons Attribution (CC BY) license (<http://creativecommons.org/licenses/by/4.0/>).

MDPI
St. Alban-Anlage 66
4052 Basel
Switzerland
Tel. +41 61 683 77 34
Fax +41 61 302 89 18
www.mdpi.com

Biomolecules Editorial Office
E-mail: biomolecules@mdpi.com
www.mdpi.com/journal/biomolecules



MDPI
St. Alban-Anlage 66
4052 Basel
Switzerland

Tel: +41 61 683 77 34
Fax: +41 61 302 89 18

www.mdpi.com



ISBN 978-3-0365-3409-1